

\sim			
Co	nt	en	11.5

0011	COLICO		
7548:	Photoni 7548A: 7548B:	c Therapeutics and Diagnostics VI Photonics in Dermatology and Plastic Surgery Urology: Diagnostics, Therapeutics, Robotics,	2
	7548C:	Minimally Invasive, and Photodynamic Therapy Advanced Technology and Instrumentation in Otolaryngology: Lasers, Optics, Radio Frequency,	9
	7548D:	and Related Technology	19
	73400.	Light in Cardiology	29
	7548E:	Optical Techniques in Neurosurgery, Brain Imaging, and Neurobiology	
	7548F: 7548G:	Optics in Bone Biology and Diagnostics	39
7549:	Lasers i	in Dentistry XVI	
7550:	Ophtha	Imic Technologies XX	52
	Optical	Methods for Tumor Treatment and Detection: iisms and Techniques in Photodynamic Therapy XIX 7	
7550.		issms for Low-Light Therapy V8	
			2
1 553:	_	s in Pathogen Detection: From Nanosensors to 8	39

7554:	Coherence Domain Optical Methods and Optical Coherence Tomography in Biomedicine XIV96
7555:	Advanced Biomedical and Clinical Diagnostic Systems VIII \dots 120
7556:	Design and Quality for Biomedical Technologies III
7557:	Multimodal Biomedical Imaging V
7558:	Endoscopic Microscopy V
7559:	Optical Fibers and Sensors for Medical Diagnostics and Treatment Applications X
7560:	Biomedical Vibrational Spectroscopy VI: Advances in Research and Industry
7561:	Optical Biopsy VIII
7562:	Optical Interactions with Tissues and Cells XXI
7563:	Dynamics and Fluctuations in Biomedical Photonics VII 200
7564:	Photons Plus Ultrasound: Imaging and Sensing 2010 207
7565:	Biophotonics and Immune Responses V238
7566:	Optics in Tissue Engineering and Regenerative Medicine IV \dots 244
7567:	Design and Performance Validation of Phantoms used in Conjunction with Optical Measurement of Tissue
7568:	Imaging, Manipulation, and Analysis of Biomolecules, Cells, and Tissues VIII
7569:	Multiphoton Microscopy in the Biomedical Sciences X 273
7570:	
7571:	Single Molecule Spectroscopy and Imaging III
7572:	
7573:	Biomedical Applications of Light Scattering IV
7574:	Nanoscale Imaging, Sensing, and Actuation for Biomedical Applications VII
7575:	Colloidal Quantum Dots for Biomedical Applications V 346
7576:	Reporters, Markers, Dyes, Nanoparticles, and Molecular Probes for Biomedical Applications356
7577:	Plasmonics in Biology and Medicine VII

Technical Abstract Summaries

Conferences + Courses: 23-28 January 2010 BiOS Exhibition: 23-24 January 2010

Photonics West Exhibition: 26-28 January 2010

The Moscone Center San Francisco, California, USA







Saturday-Sunday 23-24 January 2010 • Part of Proceedings of SPIE Vol. 7548 Photonic Therapeutics and Diagnostics VI

7548A-01, Session

Multiphoton microscopy of engineered dermal substitutes: assessment of 3D collagen matrix remodeling induced by fibroblasts contraction

A. Pena, C. Olive, J. Michelet, J. Galey, D. Fagot, F. Leroy, L'Oréal Recherche (France); J. Martin, Ecole Polytechnique (France); A. Colonna, L'Oréal Recherche (France); M. Schanne-Klein, Ecole Polytechnique (France)

One of the main functions of dermal fibroblasts is the generation of mechanical forces within their surrounding extracellular matrix. Investigating molecules that could modulate fibroblast contraction and act as potent anti aging ingredients requires the development of dermal substitutes and of three-dimensional in situ imaging methodologies. Here we use multiphoton microscopy in order to investigate the fibroblast-induced collagen matrix reorganization in engineered dermal tissue and to evaluate the effect of fibroblast contraction inhibitors.

For that purpose, we studied dermal substitutes composed of fibroblast-populated collagen gel. We visualized these tissues by taking advantage of the intrinsic multiphoton signals from collagen (second harmonic generation) and from fibroblasts (endogenous cellular two-photon excited fluorescence). We compared dermal substitutes whose culture medium contained an inhibitor (Y-27632,a RhoA-kinase inhibitor,Calbiochem-688001) for fibroblast contraction with control substitutes cultured in the same conditions. The samples were analyzed at 3 different time sets: 1)T0, 2)T+24h and 3)T+48h after contraction had been induced by removing the gel from the well borders. At T+24h the culture medium containing the inhibitor was removed and replaced with a control medium in order to verify whether the inhibitor effect was reversible.

We observed that fibroblast contraction induced a 3D remodeling of collagen matrix. In control samples, collagen fibrils rearranged around fibroblast with increasing density, whereas collagen fibrils showed no remodeling at T+24h in the samples containing the inhibitor. Moreover, at T+48h, the dermal substitutes with the inhibitor presented the same 3D reorganization as control samples, which indicates that the inhibitor effects are reversible.

In conclusion, our study demonstrates the relevance of multiphoton microscopy to visualize three-dimensional remodeling of the matrix induced by fibroblast contraction.

7548A-02, Session

Ablative fractional resurfacing drug delivery for aminolevulinic acid photodynamic therapy (ALA-PDT)

F. H. Sakamoto, M. Wanner, A. G. Doukas, W. A. Farinelli, R. R. Anderson, Wellman Ctr. for Photomedicine, Massachusetts General Hospital (United States)

Background and Objective: Ablative fractional resurfacing (AFR) creates holes with micro-thermal zones of injury (MTZ). We tested the hypothesis that AFR could facilitate topical ALA delivery. Study Design/Materials and Methods: In pigs, AFR using a CO2 laser prototype was tested using 400, 200 and 100 MTZ/cm2, at 100 and 50 mJ per pulse. 20% ALA was applied for 3 hours, followed by PDT (635-nm, 200 J/cm2, 110 mW/cm2). Skin response, fluorescence photographs, fluorescence microscopy, histology, immunohistochemistry and viability assays were assessed before and after PDT. Results were compared to appropriate controls.

Results: Absence of porphyrin fluorescence within each MTZ was observed. AFR at 100 mJ, 400 MTZ/cm2 caused absence or reduced fluorescence compared with ALA alone. ALA applied after 200 and 100 MTZ/cm2 showed significantly higher epidermal fluorescence than ALA alone. Although increased pulse energy caused increased depth of thermal ablation, deep porphyrin fluorescence was not increased. At 400 MTZ/cm2 +ALA-PDT, epidermis and superficial dermis were severely damaged, moreso than for AFR or ALA-PDT alone. At 200 and 100 MTZ/ cm2 + ALA-PDT, there was more epidermal damage than with ALA-PDT alone. Conclusions: Within each MTZ, thermal denaturation appears to inhibit ALA metabolism. AFR at relatively low MTZ density increased porphyrin in the adjacent epidermis, but there was no evidence for enhanced deeper uptake. AFR at high MTZ density reduced ALA-induced fluorescence, but there was enhanced injury from this combination. This preliminary study suggests that low-density AFR may be useful for increased epidermal delivery of topical PDT agents or other drugs.

7548A-03, Session

Evaluation of cryo-preserved skin tissues using two-photon microscopy

I. Riemann, A. Beier, M. Schwarz, D. Doerr, F. Stracke, H. Zimmermann, Fraunhofer-Institut für Biomedizinische Technik (Germany)

If no fresh skin samples can be obtained or used, it is important for research and industries to have models and stored tissue samples as close to the native state as possible at disposal. One way to preserve tissues for a longer timeframe is to use deep freezing cryo-techniques. Unfortunately much damage can be induced during the cooling and the thawing processes like disruption of cells and extra-cellular matrices due to the formation of ice crystals. This could lead to a disturbance of the united cell structure up to the point of a loss of cell viability. Two-photon microscopy is able to gather information about cells and tissue components via excitation of the autofluorescence deep inside the sample with a high resolution in both, frozen and thawed states. It is possible to monitor the samples before and after and, important, observe events during the freezing process like the formation of ice crystals.

To determine the state of skin tissues after slow rate freezing and the quick process of vitrification, the samples were examined with two-photon microscopy. To establish an optimized freezing-protocol for skin tissues, morphological changes, changes in autofluorescence of endogenous fluorophores (NADH, keratin, flavins, elastin) or changes in second harmonic generation of collagen fibres could provide information about the quality of the used freezing parameters and protective additives and lead to an optimized freezing-protocol with a new set of parameters to obtain mostly intact tissue samples. Multiphoton microscopy has been established as a useful tool for optical in situ quality control of frozen tissues.

7548A-04, Session

Effect of vacuum and thermal shock on laser treatment of trichophyton rubrum (toenail fungus)

G. Aguilar, F. Sun, P. Carlier, E. Young, D. Hennings, Univ. of California, Riverside (United States)

In recent years, the eradication of Trichophyton Rubrum (toenail fungus) has been attempted via laser irradiation. Researchers have recognized that this approach could result advantageous relative to oral, mechanical and chemical therapies. However, anticipating that



the fluences required to achieve the necessary thermal effects on this fungus could unintentionally damage the underlying toe dermal layer, we have explored two auxiliary approaches: (a) vacuum pressure, and (b) rapid-cooling followed by laser heating (thermal shock). For both, we assess viability and regrowth of toenail fungus. The rationale behind these two approaches is that at low pressures, the temperature necessary to achieve necrotic thermal effects, e.g., water evaporation/ boiling, is significantly reduced, thus reducing the laser fluence. Similarly, a thermal shock induced by a cryogen-cooled tip followed by laser irradiation may require much lower fluences to achieve the same thermal effect. Our study includes numerical simulations, where we use a three layer (toenail, fungus, and toe) model to compute photon distribution during laser irradiation via a widely used Monte Carlo code (MCML and CONV). Its output is fed into a custom-made finite difference code to compute heat generation and diffusion through the layered model. For the experiments we use a Cooltouch, 1320 nm laser and an adapted Petri dish to perform the laser irradiation tests under controlled vacuum pressure. A thermoelectric cooler thermally attached to another Petri dish from underneath along with a miniature thermocouple are used during the thermal shock experiments to simulate the rapid cooling procedure and for temperature tracking, respectively.

7548A-05, Session

In vivo multiphoton excitation spectra of skin fluorophores

H. G. Breunig, H. Studier, JenLab GmbH (Germany); K. König, Saarland Univ. (Germany) and JenLab GmbH (Germany)

Multiphoton tomography of skin allows in-vivo non-invasive imaging with sub-cellular resolution and provides a valuable insight into tissue structure. The technique is based on the spatially resolved excitation and detection of autofluorescence signals from various endogenous fluorophores such as NAD(P)H, flavoproteins, keratin, lipofuscin, elastin, collagen, melanin, and metal-free porphyrins as well as on second harmonic generation (SHG) by collagen fibers induced by nonlinear optical excitation. We investigated the spectral intensity dependence of endogenous cellular fluorophores of human skin measured in vivo with the commercially available clinical multiphoton tomograph Dermalnspect (JenLab GmbH). The Dermalnspect images horizontal sections with subcellular resolution up to a depth of 200 m inside the skin and allows additionally time correlated single photon counting for each pixel and provides spectral information with the use of appropriate filters. High-resolution multiphoton images at different depths inside the skin were recorded with in the red and near infrared range spectrally tunable femtosecond-excitation pulses in dependence on wavelength and pulse duration. Variation of the excitation wavelength allows to excite different endogenous fluorophores with partially overlapping two-photon absorption spectra with varying efficiency and therefore in principle to distinguish them. The effect of the pulse duration on twophoton excited fluorescence and SHG signals is also discussed. The measurements are supplemented by measurements of the signal decay curves which allow in particular separating SHG from autofluorescence signals. Characteristics of the Dermalnspect and the spectral-intensity dependencies of endogenous cellular fluorophores measured in-vivo at different depths inside the skin will be presented.

7548A-06, Session

A blue-LED-based device for selective photocoagulation of superficial abrasions: theoretical modeling and in vivo validation

F. Rossi, R. Pini, Istituto di Fisica Applicata Nello Carrara, CNR (Italy); G. De Siena, D. Massi, F. S. Pavone, Univ. degli Studi di Firenze (Italy); D. Alfieri, Light4tech Firenze srl (Italy); G. Cannarozzo, Univ. degli Studi di Firenze (Italy)

The blue light (~400 nm) emitted by high power Light Emitting Diodes

(LED) is selectively absorbed by the haemoglobin content of blood and then converted into heat. This is the basic concept in setting up a compact, low-cost, and easy-to-handle photohaemostasis device for the treatment of superficial skin abrasions. Its main application is in reducing bleeding from superficial capillary vessels during laser induced aesthetic treatments, such as skin resurfacing, thus reducing the treatment time and improving aesthetic results (reduction of scar formation). In this work we firstly present the preliminary modeling study: a Finite Element Model (FEM) of the LED induced photothermal process was set up, in order to estimate the optimal wavelength (405 nm) and treatment time (30 s), by studying the temperature dynamics in the tissue. Then, a compact, handheld illumination device has been designed: commercially available high power LEDs emitting in the blue region were mounted in a suitable and ergonomic case. The prototype was tested in the treatment of dorsal excoriations in rats. Thermal effects were monitored by an infrared thermocamera, experimentally evidencing the modest and confined heating effects and confirming the modeling predictions. Objective observations and histopathological analysis performed in a follow-up study showed no adverse reactions and no thermal damage in the treated areas and surrounding tissues. The device was then used in human patients, in order to stop bleeding during Erbium laser skin resurfacing procedure. By inducing LED-based photocoagulation, the overall treatment time was shortened and scar formation was reduced, thus enhancing esthetic effect of the laser procedure.

7548A-07, Session

Imaging of human skin lesions with the multispectral dermoscope

D. Kapsokalyvas, N. Bruscino, V. De Giorgi, G. Cannarozzo, T. Lotti, F. S. Pavone, Univ. degli Studi di Firenze (Italy); D. Alfieri, Light4Tech Firenze Srl (Italy)

A novel Multispectral Dermoscope based on LED illumination and subsequent image processing, has been developed. The principle of operation is similar to that of a common Dermoscope. Major differences, however, are the use of high power LEDs emitting at three distinct spectral regions, 470 nm(blue), 530 nm(green) and 630 nm(red) as light source, a polarizer for the illumination and an analyzer for the detection. These spectral regions target on the major absorbers of the skin (hemoglobin and melanin). The lesion is illuminated with each spectral region at two different positions of the analyzer, one parallel (0°) to the polarizer and one orthogonal (90°). In the former case single and multiple photons are detected while in the latter only multiple scattered photons, from deeper layers of the skin, are detected. Subsequent processing of the images reveals information, on the localization of melanin, hemoglobin, collagen and structures with different scattering properties than the adjacent skin.

Several skin lesions have been examined. The revelation of blood vessel morphology in the superficial layers of the dermis is demonstrated and their destruction after Pulse Dye Laser treatment is assessed. The capability of indicating the level of proliferation of melanocytes in the dermis is demonstrated thus offering a result specific to melanoma in situ. Additionally the processed images offer high contrast for highly scattering structures inside the skin, a result which is useful for visualizing the skin surface morphology and monitoring the changes of scars in the skin.

7548A-08, Session

Photochemical predictive analysis of photodynamic therapy in dermatology

F. Fanjul-Vélez, I. Salas-García, Univ. de Cantabria (Spain); M. López-Escobar, Univ. Hospital Marqués de Valdecilla (Spain); N. Ortega-Quijano, J. L. Arce-Diego, Univ. de Cantabria (Spain)

Photodynamic Therapy (PDT) is a recent treatment modality that allows malignant tissue destruction. The technique provides a localized effect



and good cosmetic results. The application of PDT is based on the inoculation of a photosensitizer and the posterior irradiation by an optical source. This radiation chemically activates the drug and provokes reactions that lead to tissue necrosis.

Nowadays there are fixed clinical PDT protocols that make use of a particular optical dose and photosensitizer amount. These parameters are independent of the patient and the lesion. In this work we present a PDT model that tries to predict the effect of the treatment on the skin. First the results of a clinical study in the Dermatology Department of the Marqués de Valdecilla University Hospital are presented. The most common lesions and some unsuccessful cases are stated. The predictive model proposed is based on a 3D optical propagation of radiation by a Monte Carlo approach. Once the optical energy is obtained, a complex photochemical model is employed. This model takes into account the electronic transitions between molecular levels and particles concentrations. As the process of generation of photosensitizer is not homogeneous, the photosensitizer distribution is also taken into account. The optical power of the source, the exposition time and the optochemical characteristics of the tissue can be varied. This implies that these parameters could be adjusted to the particular pathology we are dealing with, so the unsuccessful cases could be better treated.

7548A-09. Session

Use of spectral imaging for documentation of skin parameters in face lift procedure

E. C. Ruvolo, Jr., P. R. Bargo, Johnson & Johnson CPPW (United States); T. Dietz, R. Scamuffa, K. Shoemaker, Ethicon Endo-Surgery, Inc. (United States); B. DiBernardo, New Jersey Plastic Surgery (United States); N. Kollias, Johnson & Johnson CPPW (United States)

In Rhytidectomy the postoperative edema (swelling) and ecchymosis (bruising) can influence the cosmetic results. Evaluation of edema has typically been performed by visual inspection by a trained physician using a four-level or, more commonly, a two-level grading. Few instruments capable of quantitatively assess edema and ecchymosis in skin exist. Here we demonstrate that edema and ecchymosis can be objectively quantitated in vivo by a multispectral clinical imaging system (MSCIS). Five patients undergoing rhytidectomy were recruited for a clinical study and multispectral images were taken at days 0, 1, 3, 5, 7, 10, 14, 21 and 30. Apparent concentrations of oxy-hemoglobin, deoxy-hemoglobin (ecchymosis), melanin, scattering and water (edema) were calculated for each pixel of a spectral image stack. These chromophore maps are twodimensional quantitative representations of the involved skin areas that demonstrated characteristics of the recovery process of the patient after the procedure. We conclude that multispectral imaging can be a valuable noninvasive tool in the study of edema and ecchymosis and can be used to document these chromophores in vivo and determine the efficacy of treatments in a clinical setting.

7548A-10, Session

Intravital multiphoton tomography as a novel tool for non-invasive in vivo analysis of human skin affected with atopic dermatitis

V. Huck, Westfälische Wilhelms-Univ. Münster (Germany); C. Gorzelanny, Ruprecht-Karls-Univ. Heidelberg (Germany); K. Thomas, T. A. Luger, Westfälische Wilhelms-Univ. Münster (Germany); K. König, JenLab GmbH (Germany); S. W. Schneider, Ruprecht-Karls-Univ. Heidelberg (Germany)

Atopic Dermatitis (AD) is an inflammatory disease of human skin. Its pathogenesis is still unknown; however, dysfunctions of the epidermal barrier and the immune response are regarded as key factors for the development of AD.

In our study we applied intravital multiphoton tomography (5D-IVT), equipped with a spectral-FLIM module for in-vivo and ex-vivo analysis of human skin affected with AD.

In addition to the morphologic skin analysis, FLIM technology gain access to the metabolic status of the epidermal cells referring to the NADH specific fluorescence lifetime. We evaluated a characteristic 5D-IVT skin pattern of AD in comparison to histological sections and detected a correlation with the disease activity measured by SCORAD. FLIM analysis revealed a shift of the mean fluorescence lifetime (taum) of NADH, indicating an altered metabolic activity.

Within an ex-vivo approach we have investigated cryo-sections of human skin with or without barrier defects. Spectral-FLIM allows the detection of autofluorescent signals that reflect the pathophysiological conditions of the defect skin barrier. In our study the taum value was shown to be different between healthy and affected skin.

Application of the 5D-IVT allows non-invasive in-vivo imaging of human skin with a penetration depth of 150 μm . We could show that affected skin could be distinguished from healthy skin by morphological criteria, by FLIM and by spectral-FLIM. Further studies will evaluate the application of the 5D-IVT technology as a diagnostic tool and to monitor the therapeutic efficacy.

7548A-11, Session

Imaging spectroscopy of thermal and electrical burs

J. C. Ramella-Roman, A. Basiri, T. Nguyen, The Catholic Univ. of America (United States)

Today it is still clinical practice to determine burns wounds and their depth by visual inspection. However, it was recently shown that burns develop differently from their initial grade depending on the contact time of the source. As this contact time varies it is difficult to assess the burn severity relaying only on a naked eye. Parameters such as oxygen saturation, hematocrit, water presence, and perfusion, can offer a more quantitative approach to wound assessment hence improving diagnosis and treatment. These parameters can be obtained with spectroscopic and flow sensitive techniques techniques. We propose a study of burns dynamic using a combination of spectroscopic and Doppler techniques. A multi-aperture camera based on a lenslet array architecture was used to obtain 18 images of the skin, each lenslet was interfaced with a narrow-band filter hence 18 spectrally sensitive images were obtained. 500g aluminum branding iron heated in a water bath to 100 degree Celsius was used for inducing thermal burns on anesthetized rat while electrical burns were obtained with a shock model. In this paper the results of the study are presented.

7548A-12, Session

Rapid hyperspectral characterization of skin

L. L. Randeberg, Norwegian Univ. of Science and Technology (Norway); T. V. Haavardsholm, Norwegian Defense Research Establishment (Norway); A. Aksnes, Norwegian Univ. of Science and Technology (Norway); T. Skauli, Norwegian Defense Research Establishment (Norway); L. O. Svaasand, Norwegian Univ. of Science and Technology (Norway)

Hyperspectral imaging provides a powerful tool for skin characterization. However, fast and efficient data analysis is required for the technique to be relevant for clinical in vivo diagnosis. This is challenging due to the large amounts of data collected in each scan. In this study, in vivo data (400-1000 nm) were collected from human skin using a pushbroom-scanning hyperspectral camera (VNIR 1600, Norsk Elektro Optikk AS) with 1600 spatial pixels in each scan line. The scan duration was 5 to 20 seconds, depending on the size of the object and the chosen focal length of the camera. The presented results were collected from skin regions approximately 10 cm in size. Image data were fed directly into a



real-time processing software which enables immediate visualization of results. Multiple processing algorithms can be applied in an essentially simultaneous manner as needed. Results are presented for simple band ratio metrics as well as more complex statistical image analysis methods applied during scanning. The algorithms enable visualization of skin structures like vasculature and chromophore distributions, as well as detection of skin anomalies. The real-time analysis is proven to be an efficient and flexible way to treat large amounts of data, and is believed to have a large potential for in vivo characterization of skin.

7548A-13, Session

Automated measurement of epidermal thickness from optical coherence tomography by image analysis using a region growing technique

J. de la Cruz, J. Weissman, K. W. Gossage, Unilever HPC USA (United States)

Optical Coherence Tomography (OCT) is a non-invasive imaging modality that acquires cross sectional images of tissue in-vivo. It accelerates skin diagnosis by eliminating invasive biopsy and laborious histology in the process. Dermatologists have widely used it for looking at morphology of skin diseases such as psoriasis, dermatitis, basal cell carcinoma etc. Skin scientists have also successfully used it for looking at differences in epidermal thickness and its underlying structure with respect to age, body sites, ethnicity, gender, and other related factors.

Similar to other in-vivo imaging systems, OCT images suffer from a high degree of speckle and noise content, which hinders examination of tissue structures. Most of the previous works in OCT segmentation of skin were done manually. This compromised the quality of the results by limiting the analyses to a few frames per area.

In this paper, we discuss a region growing method for automatic identification of the upper and lower boundaries of the epidermis in living human skin tissue. This image analysis method utilizes images obtained from a frequency-domain OCT. This system is high-resolution and high-speed, and thus capable of capturing volumetric images of the skin in short time. The three-dimensional (3D) data provides additional information that is used in the segmentation process to help compensate for the inherent noise in the images. This method not only provides a better estimation of the epidermal thickness, but also generates a 3D surface map of the epidermal-dermal junction, from which underlying topography can be visualized and further quantified.

7548A-14, Session

Multiphoton microscopic imaging of human keloid scar

J. Chen, Fujian Normal Univ. (China)

Keloid is characterized by the deposition of excessive extracellualar matrix components by abnormal fibroblasts in response to cutaneous injury. It occurs at areas of cutaneous injury that do not regress or contract and continue to grow and extend beyond the confine of the original wound. The most important question is that keloid scars have very high recurrence rate after surgical removal in clinic. In this study, morphology and amount of collagen and elastin were described and analyzed quantitatively in the dermis of keloid scar and compared to normal skin based on multiphoton microscopy. Our results showed that these two extracellular matrix components have a completely different behavior and characteristics in superficial and deep dermis. This study can help us better understand formation process of keloid scar and may lead to development of new therapeutic approach.

7548A-15, Session

Linking visual appearance of skin to the underlying optical properties using multispectral imaging

N. Choudhury, R. Samatham, S. Jacques, Oregon Health & Science Univ. (United States)

Visual appearance of human skin varies not only among individuals but also between various spatial locations in an individual. Hence, in order to study the underlying optical properties linked to human skin appearance we have used a multispectral camera system to obtain skin optical properties. Using the multispectral system we obtain a 2D reflectance image R(x,y) at various wavelengths. The data is combined to get a 3D data cube R(x,y,). From the data cube one can get the reflectance spectrum, R(), at a given location (x,y) of the imaged skin sample. The analysis of the reflectance spectrum involves a library of known absorption spectra from the literature for melanin, oxyhemoglobin, deoxyhemoglobin, and water. The analysis models the wavelength dependent nature of scattering by a combination of Rayleigh scattering (varies as $\,$ -4) and Mie scattering (varies as \sim -1). A one dimensional light transport model is used. By using our analysis on the reflectance spectra we specify the melanin content M (volume fraction of melanosome in the pigmented epi-dermis), the blood content B (average volume fraction of whole blood in skin), oxygen saturation level S, water content W (average volume fraction of water in tissue) and the reduced scattering µ's500 at 500 nm. The spatial map of the optical properties can now be linked to the visual appearance of the skin. We also studied the effects various parameters on the reflectance spectra and related visual appearances.

7548A-16, Session

Carbon nanotube assisted photothermal therapy of skin cancers - pilot proof-of-principle study in a murine model

N. Huang, H. Wang, J. Zhao, The BC Cancer Research Ctr. (Canada); H. Lui, The Univ. of British Columbia (Canada); M. Korbelik, H. Zeng, The BC Cancer Research Ctr. (Canada)

Single-wall carbon nanotubes (SWNTs) are a new type of nanomaterial with strong optical absorption. SWNTs also have intense Raman signals that facilitate convenient monitoring of their location within tissue thereby enabling non-invasive pharmacokinetic study. We hypothesize that SWNTs can absorb 785-nm laser light and generate significant local hyperthermia to destroy cancer cells and eradicate tumors.

In this study a 785-nm diode laser is used for both Raman excitation and photothermal therapy. SWNTs are made water-soluble by functionalizing with polyethylene glycol (PEG) and administrated by intratumoral injection. C3H/HeN mice were injected subcutaneously with 2 million mouse squamous cell carcinoma (SCCVII) cells to create the tumor model. We conducted experiments with 100 mice divided into 10 different groups: control, SWNT only, 100 mW/cm2 laser irradiation only, 200 mW/cm2 laser irradiation only, and 6 treatment groups with different drug and light dose combinations (SWNTs 0.1, 0.5. 1 mg/ml, laser 100 and 200 mW/cm2). The treatment time was 10 minutes. The temperatures of the tumors irradiated by laser were monitored by an IR thermometer. Mice survival was observed for 45 days.

The study revealed that the temperature within the tumors increased in a light- and drug-dose dependent manner. The optimized light and drug dose combinations (1 mg/ml + 120 J/cm²) resulted in tumor temperature elevation of 18.5°C and successful eradication of the tumors. This light dose is moderate and is as low as 1/10 of other published studies using nanomaterials. The Raman spectroscopy measurements suggest that SWNTs persisted within the tumor tissue for months.



7548A-17, Session

Fine scale alignment of skin images for acne detection and tracking over time

G. O. Cula, Johnson & Johnson CPPW (United States); S. K. Madan, Texas Instruments Inc. (United States); K. J. Dana, Rutgers, The State Univ. of New Jersey (United States); N. Kollias, Johnson & Johnson CPPW (United States)

It is known that effectiveness of acne treatment increases when the lesions are detected earlier, before they could progress into mature wound-like lesions, which lead to scarring and discoloration. However, little is known about the evolution of acne from early signs until after the lesion heals. In this work we attempt to computationally characterize the evolution of inflammatory acne lesions, based on analyzing crosspolarized images that document acne-prone facial skin over time. Taking skin images over time, and being able to follow skin features in these images present serious challenges, due to change in the appearance of skin, difficulty in repositioning the subject, inherent movement due breathing. Consequently, we have developed a practical robust algorithm to align face regions using skin texture with mostly indistinct micro level features, which are considered to be constant over time. Our method approximates the face surface as a collection of guasi-norm for estimation of spatially varying homographies. Moreover, a computational technique for automatic detection of lesions by separating the background normal skin from the acne lesions based on fitting Gaussian distributions to the intensity histograms is also presented. In order to track and quantify the evolution of lesions, in terms of the degree of progress or regress of the lesion we designed a study to register and analyze facial skin images of 21 young individuals, followed over the course of 2 months at 6 different time points. We found that early variation in appearance of lesions is a strong cue for characterizing the lesion as developing or healing. By following the appearance of the lesion over time, we document which lesions are more likely to develop post-inflammatory hyper-pigmentation (PIH). The detection technique we propose for inflammatory lesions correlates well with visual inspection of acne lesions by trained graders.

7548A-18, Session

5-ALA induced fluorescence image analysis of actinic keratosis

Y. Cho, Y. Bae, E. Choi, B. Jung, Yonsei Univ. (Korea, Republic of)

Actinic keratosis (AK) has been considered as a precursor of nonmelanoma skin cancer (NMSC), especially squamous cell carcinoma (SCC). 5-aminolevulinic acids (5-ALA) as a photosensitizing precursor has been used for non-invasive photodynamic therapy (PDT) of AK lesions. 5-ALA is converted into efficient photosensitizer, protoporphyrin IX (PpIX), by enzymatic conversion in exogenous heme biosynthetic pathway. The PpIX is preferentially accumulated in cancerous tissue lesion than normal skin. The PpIX has a broad absorption spectrum centered at 405nm and a fluorescence emission with a dominant peak at 635nm. After 5-ALA application on AK lesion including partly normal skin sites, broadband 2D fluorescent emission images were obtained with a hyper-spectral and a fluorescent color imaging system by exciting 5-ALA applied lesion using a UVA light source and processed to differentiate selectively the AK lesion. This study confirmed that the accumulation of 5-ALA photosensitizer in AK lesions can be more specifically evaluated by analyzing the fluorescent signal with hyper-spectral imaging system than fluorescent color image.

7548A-19, Session

Multimodal confocal mosaicing microscopy: an emphasis on squamous cell carcinoma

N. W. Chen, A. Ardeshiri, A. Blanchard, S. Jacques, D. Gareau, Oregon Health & Science Univ. (United States)

Mohs surgery, for the removal of Basal Cell Carcinomas (BCCs), involves the sequential examination of frozen histology to screen for the presence of residual tumor. The creation of a frozen histology is precise but slow. Our previous study reported a sensitivity of 96.6% and a specificity of 89.2% in detecting BCCs when nuclei were stained with acridine orange (1 mM) in 5-9 minutes, opposing 20-45 for frozen histology. Good contrast was found over the background dermis and submicron (diffraction limited) resolution over a cm field of view. Squamous Cell Carcinomas (SCCs) are more difficult to detect than BCCs due to less obvious atypical morphology. Surgeons screen for anaplasia, hyperkeratinization and pleomorphism. Infiltrative BCCs remain difficult due to smaller clusters of cancerous cells. Pathology can be achieved by utilizing both acridine orange (1 mM) and eosin (1 mM), which stains proteins for cytoplasm contrast. We found that the peak fluorescent excitation for eosin staining in tumor is near the 532 nm wavelength, and showed for physiological conditions(i.e. bound to DNA), the peak absorption wavelength for acridine orange lowers to approximately 488 nm. A second laser added to our previous design independently detects eosin fluorescence. Eosin displays dermis inconsistently, so a third mode shows collagen in reflectance. This study will use fluorescence confocal mosaicing to attempt to show good tumor contrast in SCC and infiltrative BCC by staining with both eosin and acridine orange. This study will also present sensitivity and specificity in multimodal confocal microscopy using eosin, acridine orange, and reflectance.

7548A-20, Session

Evaluation of basal and squamous cell carcinomas with combined Raman spectroscopy: optical coherence tomography (RS-OCT)

C. A. Patil, H. Krishnamoorthi, Vanderbilt Univ. (United States); M. Guo, Vanderbilt Univ. Medical Ctr. (United States); D. L. Ellis, Vanderbilt Univ. Medical Ctr. (United States) and Veterans Affairs Tennessee Valley Healthcare System (United States); T. van Leeuwen, Univ. of Amsterdam (Netherlands) and Univ. of Twente (Netherlands); A. Mahadevan-Jansen, Vanderbilt Univ. (United States)

Optical spectroscopy and imaging have shown promise for performing rapid non-invasive detection and diagnosis of skin cancers in vivo. Specifically, Raman Spectroscopy (RS) has demonstrated the ability to perform diagnosis of skin cancers with excellent overall classification accuracy based on its inherent biochemical specificity, but has a limited ability to relate features of skin morphology. Optical Coherence Tomography (OCT), on the other hand, has demonstrated the ability to perform real-time, high-resolution, cross-sectional imaging of the microstructural characteristics of skin disease, but typically lacks molecularly specific information that can assist in positively classifying pathology. We present the design, development, and characterization of a combined Raman Spectroscopy-OCT (RS-OCT) system for evaluating the both the structural and biochemical composition of skin lesions. The 785 nm Raman laser and 1310 nm OCT source, along with the detection hardware for both modalities, are housed in a portable cart for clinical convenience. The RS and OCT sampling beams are co-aligned in a handheld sampling probe that either continuously acquires OCT images or pauses OCT to acquire a Raman spectra from the central axis of the OCT image frame. We are currently enrolling patients in a pilot study aimed at identifying the morphological features of basal and squamous cell carcinomas with OCT as well as developing direct multi-class Bayesian classification algorithms to characterize the Raman spectra.



We plan to present the clinical results, evaluate the system performance, and assess the added value RS and OCT can provide, in combination, for non-invasive analysis of skin lesions.

7548A-22, Session

In vivo comparative documentation of skin hydration by confocal Raman microscopy, skin sensor, Skicon and NovaMeter

G. Zhang, A. Papillon, E. C. Ruvolo, Jr., P. R. Bargo, N. Kollias, Johnson & Johnson CPPW (United States)

The stratum corneum provides a vital physical barrier that protects against external insults and excessive internal water loss. Water activity is thought as a key factor to maintain proper skin barrier integrity via regulating enzyme activities and lipid phase behavior. Consequently, maintenance of an optimal hydration level in SC becomes an important clinical and cosmetic concern.

The objective methods to assess SC hydration are based on either electrical or optical properties of the SC. Electrical techniques used in the current study include high frequency conductance (Skicon), impedance (Nova DPM) and DC I-V curve (skin sensor). Confocal Raman Microscopy was utilized to document water profile versus depth, and this technique is based on inelastic scattering of monochromatic light from different chemical species of skin.

Water patches were applied on the 14 subjects' forearm for 20 minutes and 1.5 hrs. Skin hydration levels for individuals were documented by utilizing the mentioned above instruments in vivo. Results show that patterns of water profiles upon the hydration are significantly different among the individuals and these differences may be related to skin barrier function integrity. The intrinsic water content and water absorption upon the hydration were summed corresponding to different depths (3-m and 15-m) from the data obtained by confocal Raman microscopy. These results were correlated to the readings from electrical approaches. Results show that the NovaMeter is not sensitive to SC hydration changes. Neither superficial (3-m) nor deeper layer (15-m) water contents correlated well with the reading from Skicon and Skin Sensor among individuals. There is strong correlation between the data acquired with Skicon and Skin sensor.

7548A-23, Session

New multimodal multiphoton imaging and spectroscopy apparatus for dermatology

A. Lee, H. Wang, Y. Yu, J. Zhao, The BC Cancer Research Ctr. (Canada); S. Tang, H. Lui, D. I. McLean, The Univ. of British Columbia (Canada); H. Zeng, The BC Cancer Research Ctr. (Canada)

As skin cancers continue to be the most highly diagnosed form of cancer worldwide, there is an urgent need for non-invasive, non-destructive diagnostic tools for examining the skin. We present the construction of a new multimodal, multiphoton spectroscopic and imaging instrument for in vivo patient use. The instrument is designed with a large clearance to permit access to body sites where skin cancer is most commonly found. Utilizing a tunable femtosecond laser, we are able to simultaneously acquire two-photon excited fluorescence, second harmonic generation, and confocal reflectance images at video rates, while concurrently acquiring the two-photon excited fluorescence spectrum. We are also able to acquire the two-photon excitation emission matrix. Control of our scanning optics allows us to carefully control our 2D and 3D regions of interest. Thus, we can provide clinicians with imaging tools for visualizing tissue morphology, and spectroscopic analysis for biochemical specificity. We present preliminary results using this instrument on a subcutaneous murine tumour model.

7548A-24, Session

Assessment of microcirculation frequency components through functional diffuse reflectance spectroscopy: a promising tool for noninvasive skin diagnosis

P. R. Bargo, I. Seo, N. Kollias, Johnson & Johnson CPPW (United States)

Measurement of cutaneous microcirculation is of great importance for clinical evaluations as many biological processes (i.e. inflammation) activate superficial vessels. Diffuse Reflectance Spectroscopy (DRS) is a widely used method to assess cutaneous microcirculation since it is based on the spectral characteristics of skin chromophores, particularly the strong absorption bands of blood in visible spectral range. However, the DRS system only provides a snapshot of the blood content in tissue from the reflectance detected at a single exposure time, and it fails to demonstrate dynamic changes of blood flow inside the tissues. In the present study, a prototype system for functional DRS (fDRS) has been developed for the sequential acquisition of multiple reflectance spectra in the visible range at sub-second intervals. Twelve healthy subjects with skin phototype I-III were recruited for an UV skin phototest where the subject's back was exposed to an increasing dose of solar simulated irradiation at a maximum of 3 minimum erythema dose (MED). Evaluations included conventional DRS, functional DRS, and a laser Doppler flowmeter/imaging system. In a frequency analysis results, there were two distinctive frequency components. A low-frequency component was found near 0.03-0.1 Hz, and another high-frequency component near 0.9-1.2 Hz which is synchronous with heart pulsations. The magnitude of the high-frequency and the steady-state components of the fDRS signal increased with increase in exposure dose. These results demonstrate the potential of this technique for noninvasive assessment of cutaneous microcirculation.

7548A-25, Session

Monitoring chemically enhanced transdermal delivery of zinc oxide nanoparticles by using multiphoton microscopy

W. Lo, National Taiwan Univ. (Taiwan) and National Cheng Kung Univ. (Taiwan); C. Hsu, National Taiwan Univ. (Taiwan); T. Kuo, National Taiwan Normal Univ. (Taiwan); S. Chiang, Academia Sinica (Taiwan); S. Lin, National Taiwan Univ. Hospital (Taiwan); S. Chen, National Cheng Kung Univ. (Taiwan); C. Chen, National Taiwan Normal Univ. (Taiwan); C. Dong, National Taiwan Univ. (Taiwan)

In this work, we used multiphoton autofluorescence (AF) and scond harmonic generation (SHG) microscopy for monitoring the transdermal delivery pathway of ZnO NPs. Since the noncentrosymmetric structure renders ZnO nanoparticles effective in generating the second harmonic signals, therefore, the morphology of SC and the distribution of ZnO NPs can be spectrally resolved by detecting multiphoton excited AF and SHG respectively. We quantitatively analyzed the SHG intensity of ZnO NPs in skin with different chemical enhancers: oleic acid (OA), ethanol (EtOH) and oleic acid-ethanol (OA-EtOH). This investigation may help to understand the mechanisms of these chemical enhancements in transdermal delivery. The microtransport properties of ZnO NPs were quantified to reveal the enhancements of the vehicle-to-skin partition coefficient (K), the SHG intensity gradient (G) and the effective diffusion path length (L). The results showed that OA, EtOH and OA-EtOH were all capable of enhancing the transdermal delivery of ZnO NPs by increasing the intercellular lipid fluidity or extracting lipids from the SC.



7548A-26, Session

Automated detection of unequivocal malignant melanoma

R. Hennessey, D. S. Gareau, S. Jacques, Oregon Health & Science Univ. (United States)

In vivo reflectance confocal images can reveal malignant morphologies to detect melanoma. Because the application of confocal in the dermatology clinic is relatively new, establishing the sensitivity and specificity of the technique is key. Until recently, the hallmarks identified to indicate melanoma with adequate sensitivity and specificity have been recognized only by a handful of the top clinicians. Here, we present methods to automate the same feature recognition. As a first step to prove the technique on unequivocal lesions, the automated algorithm was tweaked to correctly classify malignant melanomas and benign nevi. These were melanomas that show pagetoid spread (the spreading of melanocytes in the epidermis) and dramatic breakdown of the dermal epidermal junction, the two traits that possess the highest diagnostic accuracy. The performance of the QR factorization method and Levenberg-Marquardt method were compared for specifying the axial decay of the confocal reflectance signal. The surface of melanin was identified and the stratum corneum and epidermis were digitally stripped to reveal the diagnostic region of interest. With future work to bring the performance of this pattern recognition technique to the level of the clinicians on difficult lesions, melanoma diagnosis could be brought to primary care facilities and save many lives by improving early diagnosis.

7548A-27, Poster Session

Delineating the region of localized human skin cancer (basal cell carcinoma) using polarization sensitive optical coherence tomography (PS-OCT)

A. Ortega, M. Wong, S. Islam, C. Oh, H. Park, Univ. of California, Riverside (United States)

Nonmelanoma skin cancer is a common condition that can occur with excess exposure to ultraviolet (UV) light, usually from the sun. Deformation of collagen due to dimerization of thymine from UV radiation allows non-invasive assessment of basal cell carcinoma using polarization-sensitive OCT. Previous studies demonstrated differentiation of BCC from normal skin by observing the differences in their collagenderived birefringence characteristics in single images. We expand on these preliminary findings using volumetric imaging to analyze and determine the location and boundaries of these cancerous tissues. Early results show favorable correlation between PS-OCT and histological images, pointing to potential future application as a screening tool for BCC's or as an aid in surgical guidance for their resection.

7548A-31, Poster Session

Yellow light in photodynamic therapy (PDT): the use of sodium light

I. M. Zich, C. Philipp, H. Berlien, Elisabeth Klinik (Germany)

Systemic PDT is an important treatment of tumor diseases. Severe side effects of PDT are acute and delayed photosensibilisation including undisired areas remote from the tumor site due to terrestric or artificial light. Sodium light sources (589nm) are used to spare patients and hospital personal from "dark-room detention". Aim of our work was to investigate the influence of yellow light sources during PDT specifically. Using the in vivo CAM-assay we evaluated the phototoxic effect of vellow light in the presence of photosensibilisators. In addition we meassured the singulet oxygen generation of several light sources using ESR. Wave lengths of regular commercial and frequently used in the OR halogen - illumination overlap with the absorbtion spectra of many photosensibilisators. Sodium light sources have a small absorption overlapp with common photosensitizers. Thus surgery under yellow light source might reduce side effects due to erratic, unspecific photodynamic effects at remote areas improving PDT tolerability and subsequently patient complience.



Saturday-Sunday 23-24 January 2010 • Part of Proceedings of SPIE Vol. 7548 Photonic Therapeutics and Diagnostics VI

7548B-32, Session 1

Near-infrared spectroscopy of the bladder: a new technique for studying lower urinary tract function in health and disease

B. Shadgan, K. Afshar, L. Stothers, A. J. Macnab, Univ. of British Columbia (Canada)

Near infrared spectroscopy (NIRS) is a non-invasive optical technique for monitoring tissue oxygenation and hemodynamics. The purpose of this study was to assess the feasibility of bladder NIR spectroscopy in children and to correlate the findings with uroflowmetry and cystometrogram results in both healthy and subjects with lower urinary tract symptoms (LUTS). Using a wireless NIRS system, changes of chromophores oxygenated, deoxygenated and total hemoglobin (O2Hb, HHb and tHb) of bladder detrusor in 20 male and female subjects 4-17 yrs were evaluated during voiding.

These included 5 healthy subjects and 15 patients with non-neurogenic lower urinary tract dysfunction (14 patients) and urethral stricture (1 patient). Simultaneous uroflow or cystometrogram was done as well. The NIRS probe was secured to the abdominal wall 2 cm above the symphysis pubis with a full bladder. NIRS data collection started 10-15 seconds before permission to void and continued for 30 seconds following termination of voiding. Chromophore changes were compared to standard urodynamic pressure tracings in all cases. Comparison of patients with abnormal bladder function with healthy subjects revealed two reproducible differences: lack of initial increase in detrusor O2Hb concentration following permission to void and steady increase in HHb level during detrusor contraction. Changes of NIRS chromophores were also observed during overactive detrusor contractions during filling cystometry. Our preliminary results are showing that NIRS is technically feasible in children and able to differentiate between normal and abnormal lower urinary tract function. Further studies are under way for confirming these qualitative findings and measuring them quantitatively.

7548B-33, Session 1

Multidimensional two-photon imaging and spectroscopy of fresh human bladder biopsies

R. Cicchi, A. Crisci, G. Nesi, A. Cosci, S. Giancane, M. Carini, F. S. Pavone, Univ. degli Studi di Firenze (Italy)

Two-photon fluorescence (TPEF) microscopy is a powerful tool to image human tissues up to 200 microns depth without any exogenously added probe. TPEF can take advantage of the autofluorescence of molecules intrinsically contained in a biological tissue, as such NADH, elastin, collagen, and flavins. Two-photon microscopy has been already successfully used to image several types of tissues, including skin, muscles, tendons, intestine. Nevertheless, its usefulness in imaging bladder tissue has not been deeply investigated yet. In this work we have used combined two-photon excited fluorescence (TPEF), second harmonic generation microscopy (SHG), fluorescence lifetime imaging microscopy (FLIM), and multispectral two-photon emission detection (MTPE) to investigate different kinds of human ex-vivo fresh biopsies of bladder. Morphological and spectroscopic analyses allowed to characterize both healthy mucosa and carcinoma in-situ (CIS) samples in a good agreement with common routine histology. Cancer cells have shown different morphology with respect to the corresponding healthy cells: they have appeared more elongated and with a larger nucleus to cytoplasm ratio. From the spectroscopic point of view, we found differences between the two tissue types in both spectral emission and fluorescence lifetime distribution. Even if further analysis, as well as a

more significant statistics on a large number of samples would be helpful to discriminate between low, mild, and high grade cancer, our method is a promising tool to be used as diagnostic confirmation of histological results, as well as a diagnostic tool in a multiphoton endoscope or cystoscope to be used in in-vivo imaging applications.

7548B-34, Session 1

Endoscopic probe for in vivo Raman spectroscopy of the urinary bladder: initial results

M. C. M. Grimbergen, R. O. P. Draga, Univ. Medical Ctr. Utrecht (Netherlands); C. F. P. van Swol, St. Antonius Ziekenhuis Nieuwegein (Netherlands); R. M. Verdaasdonk, R. J. H. L. Bosch, Univ. Medical Ctr. Utrecht (Netherlands)

Raman spectroscopy has proven to enable bladder cancer diagnosis with high specificity in-vitro. A customized Raman probe was developed in collaboration with EMVision LLC for in-vivo endoscopic application.

The materials of the Raman probe are in compliance with Dutch medical device directive and allowed for both EtO and Sterrad(R) sterilization. The external shielding of the probe comprises multiple layers to block any external light as required in the operating room. The Raman probe is connected to a custom build suspended Raman spectroscopy cart that allows safe transport between OR and lab, and different hospitals. The centrally located single-mode fiber of the Raman probe is connected to the FC/APC interfaced optical isolator of the Cheetah DFB laser (Sacher, Germany) producing 100mW output at 785nm. The 6 collection fibers are connected to a Hollolab 5000 (Kaiser Optical Systems, USA) spectrograph and a 256BR (PI-Acton, USA) deep depletion CCD camera.

Patients with known bladder cancer were informed of the study and consent was obtained in 40 cases. Lesions of interest were found by means of standard white light endoscopy and with fluorescence spectroscopy.

A total of 342 spectra were obtained in 40 patients. The first results show adequate S/N Raman spectra for further analysis with integration times above 2 seconds. Preliminary spectral analysis allows for discrimination of superficial and exophytic lesions in pathology subclasses. Normal tissue could be discriminated from dysplastic and CIS., Non-muscle invasive and muscle-invasive bladder cancer could also be discriminated, showing the potential for this technique.

7548B-35, Session 1

Quantitative analysis of urinary stone composition with micro-Raman spectroscopy

Y. Huang, National Yang-Ming Univ. (Taiwan); H. K. Chiang, National Yang-Ming Univ. (Taiwan) and Taipei City Hospital (Taiwan); Y. Chiu, National Yang-Ming Univ. (Taiwan); Y. H. J. Chou, Taipei City Hospital (Taiwan); S. Lu, Taipei City Hospital (Taiwan) and National Yang-Ming Univ. (Taiwan); A. W. Chiu, National Yang-Ming Univ. (Taiwan)

Urolithiasis is a common, disturbing disease with high recurrent rate (60% in five years). Accurate identification of urinary stone composition is important for treatment and prevention purpose. Our previous studies have demonstrated that micro-Raman spectroscopy (MRS)-based approach successfully detects the composition of tiny stone powders after minimal invasive urological surgery. But quantitative analysis of urinary stones was not established yet. In this study, human urinary stone



mixed with two compositions of COM, HAP, COD, and uric acid, were analyzed quantitatively by using a 633 nm Raman spectrometric system.

This quantitative analysis was based on the construction of calibration curves of known mixtures of synthetically prepared pure COM, HAP, COD and uric acid. First, the various concentration (mole fraction) ratio of binary mixtures including COM and HAP, COM and COD, or COM and uric acid, were produced. Second, the intensities of the characteristic bands at 1462cm -1(IRCOM), 1477cm-1(IRCOD), 960cm-1(IRHAP) and 1037cm-1(IRuric acid), for COD, COM, HAP and uric acid were used respectively for intensity calculation. Various binary mixtures of known concentration ratio were recorded as the basis for the quantitative analysis. The ratios of the relative intensities of the Raman bands corresponding to binary mixtures of known composition on the inverse of the COM concentration yielded a linear dependence. Third, urinary stone fragments collected from patients after management were analyzed with the use of the calibration curve and the quantitative analysis of unknown samples was made by the interpolation analysis. We successfully developed a MRS-based quantitative analytical method for measuring two compositions of mixed human urinary stones.

7548B-36, Session 1

Ex vivo imaging of human bladder and kidney with multiphoton microscopy

S. Mukherjee, J. S. Wysock, G. Wang, M. Lee, J. A. Sterling, M. Akhtar, M. A. Rubin, F. R. Maxfield, Weill Cornell Medical College (United States); W. R. Zipfel, W. W. Webb, Cornell Univ. (United States); D. S. Scherr, Weill Cornell Medical College (United States)

Our group is developing Multiphoton microscopy (MPM) of human tissues and organs as a tool for early cancer diagnosis and surgical margin assessment. Since the goal of this project is clinical translation of MPM, our emphasis is on imaging fresh, unstained tissue immediately after excision. Signals utilized include broadband autofluorescence (from cells, elastin and fat globules) and second harmonic generation (from tissue collagen). Immediately upon completion of a Multiphoton microscopy session, the specimens are submitted for histopathology workup. The Multiphoton images are subsequently compared with the current diagnostic gold standard, hematoxylin/eosin labeled thin sections. In this conference session last year, we presented data demonstrating our ability to obtain diagnostic quality images from fresh, unstained human bladder biopsies. In those studies, the interest was to obtain MPM images at low magnification for the assessment of local tissue architecture, and at higher magnification to study detailed cellular morphology, and then assess the extent to which the MPM images correlate with histopathology. We have now extended this approach to image: (1) bisected radical or partial cystectomy specimens with the urothelium under the objective, (2) transmural sections through the cystectomy specimens, and (3) radical and partial nephrectomy specimens, with the goal of recapitulating all known histological features in an organ using MPM. This should allow us to locate a tumor in the context of the surrounding structures, assess surgical margins, and eventually help in the translation of this methodology to Medical Multiphoton Microscopic Endoscopes, which will allow real time "optical biopsy."

7548B-37, Session 2

Near-infrared optical properties of prostate tissue using oblique-incidence reflectometry

S. Chitchian, N. M. Fried, The Univ. of North Carolina at Charlotte (United States)

Introduction: The optimal wavelength for deep penetration of near-infrared light into prostate tissue for optical imaging (e.g. optical coherence tomography) has yet to be determined. This study measures and compares optical properties of canine prostate tissue at several common near-IR laser wavelengths.

Methods: A simple, inexpensive technique for measuring tissue optical properties in their native state without fixation was developed. Oblique-incidence reflectometry with a normal-detector scanning system was designed to resolve the spatial distribution of diffuse reflectance. Using a Levenberg-Marquardt algorithm, the absorption and reduced scattering coefficients were calculated by fitting the experimental data to the modified dipole source diffusion-theory model. The absorption coefficient, µa, and reduced scattering coefficient, µ's, were measured for fresh canine prostate samples (n=10), ex vivo, at near-IR wavelengths of 1064, 1307, and 1555 nm.

Results: Using mean values for μ a and μ 's, the effective attenuation coefficient, μ eff, measured 2.00, 2.28, and 2.78 cm-1 at 1064, 1307, and 1555 nm, respectively, corresponding to an optical penetration depth of 0.50, 0.44, and 0.36 cm for canine prostate tissue. At longer near-IR wavelengths, increased water absorption appears to outweigh decreased scattering in the tissue, resulting in an overall reduction in optical penetration depth.

Conclusion: The optimal wavelength for deepest imaging of the canine prostate is at approximately 1064 nm. Studies on optical coherence tomography of the prostate may be improved by substitution of commonly used 1310 nm light sources with 1064 nm sources.

7548B-38, Session 2

Imaging of dog prostate tissue by a Stokes polarimetry imaging system

J. Kim, Northwestern Univ. (United States); W. K. Johnston III, NorthShore Univ. Health System (United States); J. T. Walsh, Northwestern Univ. (United States)

Prostate cancer is the second leading cause of death in United States and 190,000 new cases are reported with 2700 deaths in 2009. Today, removal of the prostate is the most common treatment option chosen. During prostate surgery for prostate cancer, all prostate tissue (both benign and cancerous) must be removed. The goal is to limit the removal of adjacent tissue that contains nerves and muscles that are important for the return of potency and continence, respectively. By improving differentiation of prostate tissue from adjacent tissue, a surgeon could improve cancer removal while reducing injury to adjacent nerves and

To improve visualization during prostate surgery, a novel Stokes polarimetry imaging (SPI) system was developed and evaluated using a dog prostate specimen in order to examine the feasibility of the system to differentiate prostate from bladder. The degree of linear polarization (DOLP) image maps from linearly polarized light illumination at different visible wavelengths (475, 510 and 650 nm) were constructed.

The SPI system provided the polarization property of the prostate tissue. Due to the differences in tissue character, the DOLP with visible filters allowed advanced differentiation by providing smooth muscle orientation of prostate from bladder. The DOLP image at 650 nm effectively differentiated prostate and bladder by strong DOLP in bladder.

SPI system has the potential to improve surgical outcomes in open or robotic-assisted laparoscopic removal of the prostate. Further in vivo testing is warranted.

7548B-39, Session 2

Real-time 3-D tactile elasticity imaging of prostate

A. Nehra, Mayo Clinic (United States); A. Sarvazyan, Artann Labs., Inc. (United States)

Prostate Mechanical Imager (PMI) provides real-time 3D reconstruction of prostate capturing its geometrical and elastic characteristics, as well as presence, size/location of tissue abnormalities. Using principles similar to palpation PMI utilizes intrarectal measurements of surface stress patterns using a pressure sensor array analogous to that sensed by the



physician's finger palpating the prostate during DRE. The changes in surface stress patterns as a function of pressure and time are closely related to elastic composition and geometry of the prostate and provide objective and quantitative information on the structure of the gland. Once recorded, the PMI data can be stored and used in subsequent examinations to track changes in geometry and mechanical properties of a given prostate. Clinical validation study has demonstrated the PMI capability to reliably reconstruct and produce a three dimensional image of the prostate. The technological advances of PMI may allow it to potentially be a cost effective and diagnostic tool for the evaluation of prostate abnormalities.

Sarvazyan A. Mechanical Imaging: A new technology for medical diagnostics. - Int. J. Med. Inf., 1998, 49, 195-216.

Egorov V, Ayrapetyan S, Sarvazyan A. Prostate mechanical imaging: 3-D image composition and feature calculations. IEEE Transactions on Medical Imaging 2006; 25(10): 1329-40.

Weiss R, Egorov V, Ayrapetyan S, Sarvazyan N, Sarvazyan A: Prostate mechanical imaging: a new method for prostate assessment. Urology 2008 Mar; 71(3):425-9.

7548B-40, Session 2

Real-time magnetic resonance imaging texture characterization of necrosis during laser interstitital thermotherapy procedures

N. Betrouni, R. Lopes, C. Pierre, S. Mordon, INSERM, Ctr. Hospitalier Regional Univ. de Lille (France)

Interest in interstitial thermotherapy procedures as laser-induced interstitial thermotherapy for the thermal coagulation of solid tumor such as liver metastases and T2b prostate cancers is growing. Cancer cells necrosis is produced by the selective, localized, moderate heating of tumor with a laser source.

One of the key points for the success of these therapies is the conformation of the lesion produced to the tumor volume. Many parameters (presence of vessels, optical parameters,...) can significantly influence the size and shape of the lesions. Monitoring of the treatment by imaging is achieved to reach this purpose. Ultrasound imaging is widely used to realize this monitoring.

In this study, we attempted to correlate the local temperature changes to the texture heterogeneities using the fractal geometry.

7548B-41, Session 2

Advantages of cross-polarization endoscopic optical coherence tomography in diagnosis of bladder neoplasia

N. Gladkova, E. Zagaynova, O. Streltsova, E. Kiseleva, M. Karabut, L. Snopova, E. Yunusova, E. Tararova, Nizhny Novgorod State Medical Academy (Russian Federation); V. Gelikonov, Institute of Applied Physics, RAS (Russian Federation)

Earlier research demonstrated the efficiency of the standard OCT for endoscopic diagnosis of bladder neoplasia. OCT diagnostics of bladder today faces some problems which include verification of OCT images: scar/cancer; cancer/cystic ulcer; simple hyperplasia/hyperplasia with dysplasia 2, metaplasia/ keratinizing metaplasia (leikoplakia). We call the version of cross-polarization OCT (CP OCT) focused on comparison of images resulting from cross-polarization and co-polarization scattering simultaneously. This technique provides information about mictostructural and biochemical alterations in depolarizing tissue components (collagen). We present results obtained using a endoscopic two-channel portable device for CP OCT based on polarization-maintaining fiber, designed at the Institute of Applied Physics. The CP OCT imaging was done for 158 patients during cystoscopy with suspicion on urothelial neoplasia (benign conditions - 61 patients, and dysplasia or carcinoma - 97 patients). CP

OCT images were compared with histological data. Special staining - Sirius Red for collagen types was applied. We found, that only mature collagen type I, gave the strong signal in the orthogonal polarization. CP OCT images of benign inflammatory processes always feature signal in orthogonal polarization, with layers and borders persisting to be well defined. In the presence of precancer alterations, such as hyperplasia, dysplasia 2-3, urothelial metaplasia, signal in orthogonal polarization is available in the image but it is irregular, disappearing in some areas. Image depth may be different in this case. CP OCT image of bladder cancer in orthogonal polarization either shows no signal at all or a weak signal with vertically oriented zones.

7548B-42, Session 3

Visualization strategies to study the ablation mechanism of BPH lasers with tissue and imaging absolute temperature distributions inside tissue

R. M. Verdaasdonk, S. Been, T. de Boorder, J. Klaessens, Univ. Medical Ctr. Utrecht (Netherlands)

The ablation mechanism and effectiveness of various laser systems used for BPH treatment is not fully understood. We developed various visualization strategies to obtain a better understanding of the contribution of the processes involved.

In a vitro setup, homogeneous biological tissues and transparent tissues were positioned underneath water in a transparent container. The tissue was irradiated with laser energy emitted from a fiber that was translated at a constant speed (~2mm /s) just above the tissue surface. The laser sources used were: A. 60 W 810 nm Diode, B. 60 W, 2.1 μm pulsed Holmium, 60 W, C. 2.0 μm cw Thulium and D. 80 W, 532 nm KTP laser.

The tissue ablation process was imaged through the wall of the container in close-up from the side at the level of the tissue surface. The imaging modalities used were: A. high speed imaging with frame rates up to 10.000 fr/s. B. Infra-Red thermal imaging using a IR transparent window (ZincSelenide) as wall of the container to image the absolute temperatures underneath the surface. C. Color Schlieren Imaging showing the temperature gradients in a tissue phantom. The imaging provided a good understanding of the ablation mechanism as to thermo dynamics and mechanical stresses. For the diode and KTP laser, tissue carbonization shows to be the driving mechanism, as is (explosive) water vapour for the 2 μm lasers.

New visualisation strategies prove to be useful to obtain a better understanding of the ablation mechanism of various lasers and will contribute to the safety and the optimal settings for BPH treatment.

7548B-43, Session 3

Five-year therapeutic efficacy of photoselective vaporization of prostate

C. Arum, P. Romundstad, J. Mjønes, St. Olavs Hospital (Norway)

OBJECTIVES: We evaluated the long term therapeutic efficacy of 80 watt photo-selective vaporization of the prostate (PVP) in patients suffering from lower urinary tract symptoms (LUTS) secondary to prostatic obstruction.

MATERIAL & METHODS: 150 unselected patients at the average age of 73 (range 51-92) and a mean American Society of Anesthesiologists score of 2.4 (median 2.0), of whom 33% were medicated with acetylsalicylic acid and 5% were anticoagulated with warfarin. Inclusion/exclusion criteria were the same as for TUR-P at our institution. First patient was operated March 2004 and yearly follow-up of all patients has been attempted for 5 years. Follow-up variables have included yearly creatinine, PSA, IPSS, ØOL, post-void residual urin and maximum/average urine flow rate.

RESULTS: At 12 and 24 months postoperatively, the following parameters

TEL: +1 360 676 3290 · +1 888 504 8171 · customerservice@spie.org



were significantly (p<0.001) improved: trans-rectal ultrasound, international prostate symptom score, quality of life score, post-void residual urine volume, flow max/average, opening pressure, pressure @ flow-max, and micturition resistance. At 48 and 60 months creatinine, PSA, IPSS, ØOL, post-void residual urin and maximum/average urine flow rates where still significantly (p<0.001) improved compared to preoperative values.

CONCLUSION: Up to 5 year follow-up reveals that 80 watt PVP provides significant and stable symptom relief as well as objective improvement in residual urine and flowmetric outcomes.

7548B-44, Session 3

MRI-guided trans-perineal laser ablation of locally recurrent prostate adenocarcinoma

L. A. Mynderse, E. F. McPhail, A. Kawashima, M. R. Callstrom, K. R. Gorny, T. D. Atwell, M. T. Gettman, K. K. Amrami, D. A. Woodrum, Mayo Clinic (United States)

Introduction: Biochemical recurrence of prostate cancer (PAC) after definitive therapy with radical prostatectomy (RRP) is known to occur between 25-30%. We present the first known cases of MRI guided ablation using laser interstitial thermal therapy (LITT) for locally recurrent PAC following RRP. Two patients who previously underwent RRP for Gleason 4+3 and 3+4, pT3a PAC with extraprostatic extension presented with rising PSA. Pre-treatment PSA's were 6.0 and 8.6 ng/ml. PSA remained undetectable for approximately 1.6 and 5.7 years post-operatively but then rose to 1.6 and 1.3 ng/ml. Endorectal coil 3T DCE MRI demonstrated enhancing 1.6-cm and 1.1-cm masses at the vesicourethral anastomosis. U/S guided biopsy demonstrated recurrent Gleason 4+3 and 3+4 PAC.

Methods: Both patients elected to undergo MRI-guided LITT of the PAC using an FDA-approved MRI compatible, 980nm, 15W laser. A MRI compatible urethral cooling catheter was placed to prevent urethral thermal damage. Using T2 weighted MRI (3.0T General Electric or 1.5T Siemens) imaging, two and three laser applicators were placed via transperineal approach. Multiple cycles of laser energy ablated the tumors guided by MR thermometry.

Results: Intra-procedural temperature mapping allowed continuous monitoring and guidance on adequacy of ablation and protective cooling by urethal catheter. Post-ablation gadolinium and T2 MR imaging demonstrated an ablation defect with no residual hyper-enhancing nodules. Early clinical follow-up show no post therapy incontinence, rectal damage or other associated treatment morbidity.

Conclusion: This represents the first known, successful, MRI-guided, LITT procedures at 3.0T and 1.5T for locally recurrent PAC following RRP.

7548B-45, Session 3

Photoselective vaporization of the prostate: outcomes and adverse events of 220 consecutive patients

E. J. Mueller, The Univ. of Texas Health Science Ctr. at San Antonio (United States)

Purpose: To evaluate the short term outcomes of the 532nm KTP greenlight photoselective vaporization of the prostate (PVP) procedure and to evaluate and categorize the adverse events associated with the procedure.

Materials and Methods: A total of 220 patients with symptomatic benign prostatic obstruction were treated with KTP photoselective vaporization of the prostate. Evaluation measures included the AUA/QOL score, peak urinary flow rate, post void residual urine and adverse events.

Results: Symptoms were evaluated at 3 months and adverse events at 1 and 3 months postop. 181 patients returned for their 1 month visit and 152 returned for their 3 month visit. AUA symptom score decreased

from 21.8 to 6.7. The QOL score decreased from 3.8 to 0.7. The PVR decreased from 262cc to 105cc. Most common adverse events lasting more than 10 days were: mild hematuria-45%, dysuria-32% and urgency/frequency-31%.

Conclusion: These results confirm, in a large series of patients, that photoselective vaporization of the prostate (PVP) is a safe and effective therapy for benign prostatic obstruction. However, there is frequent, but mild hematuria and irritative voiding symptoms during the early postoperative period.

7548B-46, Session 4

Incorporation of fiber optic beam shaping into a laparoscopic probe for laser stimulation of the cavernous nerves

S. Tozburun, The Univ. of North Carolina at Charlotte (United States); G. A. Lagoda, A. L. Burnett, Johns Hopkins Hospital (United States); N. M. Fried, The Univ. of North Carolina at Charlotte (United States)

Introduction: The cavernous nerves (CN) course along the prostate surface and are responsible for erectile function. Improved identification and preservation of CN's may result in increased sexual function after prostate cancer surgery. Noncontact laser nerve stimulation (LNS) of the CN's was recently demonstrated in an experimental rat model as a potential alternative to electrical nerve stimulation (ENS) for identification of CN's during prostate surgery. The therapeutic window for LNS is narrow, so design of the fiber optic delivery system is critical for safe, reproducible stimulation. This study describes modeling, assembly, and testing of LNS probe for delivering a small, collimated, and flat-top, laser beam to CN's for uniform stimulation.

Methods: Thulium fiber laser radiation (wavelength=1870 nm) was delivered through a 200-micron fiber, with distal fiber tip chemically etched to convert Gaussian to flat-top beam profile. The laser beam was collimated with a 1-mm-diameter spot using an aspheric lens. Computer simulations of fiber optic light propagation were used to optimize probe design. The probe was tested in four rats, in vivo.

Results: Consistent optical stimulation of the CN's was achieved with an average intracavernosal pressure (ICP) response of 39 mmHg, a 2:1 ratio to baseline ICP, at pulse energies of 3.7 mJ (0.4 J/cm2), 1-mm-diameter spot, 5-ms pulse duration, and pulse rate of 20 Hz for 60 s.

Conclusions: Fiber optic beam shaping was incorporated into a laparoscopic probe, providing a constant laser fluence at the nerve surface for safe, reproducible stimulation of the cavernous nerves.

7548B-47, Session 4

Enhancing laser tissue ablation with various compounds

M. Beck, E. Koullick, J. Crank, H. W. Kang, American Medical Systems (United States)

Laser tissue ablation using the wavelength at 532 nm, which corresponds to one of the hemoglobin absorption peaks, has been considered to be an efficient treatment for benign prostate hyperplasia (BPH). This laser therapy is capable of providing rapid and abundant tissue removal in a short and uncomplicated procedure when compared to other treatments. However, there is still a desire to ablate tissue at a faster rate to expedite the time the patient has to spend in the OR. In this study we want to determine if incorporating dyes and/or small molecules into prostatic tissue will increase the rate of tissue ablation faster than tissue without compounds. Utilizing the 532 nm wavelength that the GreenLight HPS system generates we tested several compounds (the plant compound amaranth, hemoglobin and carbon nanoparticles) that seem to absorb this wavelength. All compounds were injected into canine prostates in vitro using either a high pressurized jet injection method or needle



injections. We tested tissue with compounds at 60W and 80W and compared that to tissue without compounds at 120W using a side firing fiber that was 1mm above the tissue and moving at 3 mm/s. The amaranth performed marginally better than tissue treated at 120W without compounds. The carbon nanoparticles significantly increased total ablation whereas hemoglobin performed best of all compounds by doubling the amount of tissue ablated. These results demonstrate that by injecting a dye or small molecule it may be possible to increase the speed of tissue ablation while decreasing the total procedure time for the patient.

7548B-48, Session 4

Comparison between two time-resolved approaches for prostate cancer diagnosis: high rate imager vs. photon counting system

J. Boutet, L. Herve, M. Debourdeau, Commissariat à l'Énergie Atomique (France); J. Dinten, Lab. d'Electronique de Technologie de l'Information, CEA (France)

Finding a way to combine ultrasound and fluorescence optical imaging on an endorectal probe may improve early detection of prostate cancer. The ultrasound provides morphological information about the prostate while the optical system detects and locates fluorophore marked tumors.

A trans-rectal probe adapted to fluorescence diffuse optical tomography measurements was developed by our team. This probe is based on a pulsed NIR laser source, an optical fiber network and a time-resolved detection system. A reconstruction algorithm was used to help locate and quantify fluorescent prostate tumors.

In this study, two different kinds of time-resolved detectors are compared: High Rate Imaging system (HRI) and a photon counting system. The HRI is based on an intensified multichannel plate and a CCD Camera. The temporal resolution is obtained through a gating of the HRI. Despite a low temporal resolution (300ps), this system allows a simultaneous acquisition of the signal from a large number of detection fibers.

In the photon counting setup, 4 photomultipliers are connected to a Time Correlated Single Photon Counting (TCSPC) board, providing a better temporal resolution (0.1 ps) at the expense of a limited number of detection fibers (4).

At last, we show that the limited number of detection fibers of the photon counting setup is enough for a good localisation and dramatically improves the overall acquisition time. The photon counting approach is then validated through the localisation of fluorescent inclusions in a prostate-mimicking phantom and on small animals bearing mammary tumors.

7548B-49, Session 4

Investigation of wavelength-dependent tissue ablation: visible (lambda=532 nm) vs IR (lambda=2.01 µm)

H. W. Kang, A. Nemeyer, S. Peng, American Medical Systems (United States)

Laser prostatectomy with various lasers has been shown to be effective in the treatment of benign prostate hyperplasia. However, the impact of laser parameters on tissue ablation is still in question. The aim of this study is to experimentally characterize laser-tissue interactions as a function of wavelength by comparing visible (λ =532nm) and infrared (λ=2.01μm) spectra. Porcine kidney tissue was used as it has thermal properties and glandular structure similar to human prostatic tissue. Q-switched 532nm (GreenLightTM HPS) and CW 2.01µm (custom-made Tm:YAG) lasers were employed to remove soft tissue under various settings (power, working distance, and treatment speed). For both laser systems, ablation volume increased with power and decreased with

treatment speed. The 532 nm laser generated approximately 10% larger ablation volume than the IR laser (60.2 vs. 52.9mm3 at 100W for 2.5sec; p<0.005). Another difference was found in the dimensions of laserinduced craters: the IR laser created higher aspect ratio (=depth/width) craters than the 532nm laser (1.8 vs 1.5 at 100W). Owing to constant heating due the CW mode, the IR laser induced 15% thicker coagulation depth than the 532nm (0.95 vs 0.8mm at 100W; p<0.005). Histology also confirmed coagulation depth in response to each wavelength. Due to light absorption in aqueous environment, the IR laser exhibited a dramatic decrease in power transmission and ablation volume with increasing working distance whereas the 532nm laser maintained relatively constant features. In conclusion, the characteristics of tissue ablation were contingent upon the applied wavelengths due to optical properties and laser parameters.

7548B-50. Session 4

Effect of an optical clearing agent on canine scrotal skin, ex vivo

C. M. Cilip, The Univ. of North Carolina at Charlotte (United States); A. E. Ross, J. P. Jarow, Johns Hopkins Hospital (United States); N. M. Fried, The Univ. of North Carolina at Charlotte (United States)

Introduction: Our laboratory is developing noninvasive laser vasectomy. Preliminary results with this technique demonstrated reduced frequency and severity of scrotal skin burns as compared to previous therapeutic ultrasound vasectomy studies, however, skin burns still remain a concern. This study assesses the effect of application of an optical clearing agent to scrotal skin upon efficacy and scrotal skin burns during laser vasectomy.

Methods: A medical grade optical clearing agent, dimethyl sulfoxide, was injected into canine scrotal skin, ex vivo, and transmission of near-IR laser radiation (wavelength = 1075 nm) through the skin was monitored over time. For vas occlusion, an average laser power of 7 W, 500-ms pulse duration, pulse rate of 1 Hz, and 3-mm-diameter spot was synchronized with cryogen spray cooling of scrotal skin surface for 60-s treatment time. Successful thermal vas occlusion was judged with burst pressure measurements.

Results: A 35% temporary increase in transmission was observed 15-20 min after application of chemical agent. Successful noninvasive laser vasectomy was performed at a reduced average power of 7 Watts with chemical clearing agent, in comparison to 11 Watts previously reported without agent. The vasa were successfully occluded in 9/9 samples without skin burns, as indicated by burst pressures of 260 \pm 64 mmHg, compared to previous measured pressures of 295 ± 72 mmHg without agent, and normal physiological ejaculation pressures of 136 ± 29 mmHg.

Conclusions: Application of an optical clearing agent to scrotal skin significantly reduces laser power needed to thermally occlude the vas, safely, without skin burns.

7548B-51, Session 4

Noninvasive laser vasectomy: acute in vivo canine studies

C. M. Cilip, The Univ. of North Carolina at Charlotte (United States); A. E. Ross, J. P. Jarow, Johns Hopkins Medical School (United States); N. M. Fried, The Univ. of North Carolina at Charlotte (United States)

Introduction: Male sterilization has a higher success rate, lower complication rate, is less expensive, and is easier to perform than female sterilization. Despite these advantages female sterilization is more commonly performed, due to male fear of vasectomy complications (bleeding, infection, scrotal pain). Our previous studies in an ex vivo canine tissue model demonstrated successful noninvasive thermal occlusion of the vas. This study explores a similar approach to

TEL: +1 360 676 3290 · +1 888 504 8171 · customerservice@spie.org



noninvasive laser vasectomy in an acute in vivo canine model.

Methods: A standard vasectomy ring clamp was used to percutaneously separate the vas from surrounding tissue below the skin surface. Ytterbium fiber laser radiation with a wavelength of 1075 nm, average power of 11.2 W, 500-ms pulse duration, pulse rate of 1 Hz, and 3-mm diameter spot was synchronized with cryogen spray cooling of the scrotal skin surface for a treatment time of 60 s. Experiments were performed bilaterally in four dogs. The vasa were then excised following the procedure, and their burst pressures compared to previously reported ejaculation pressures.

Results: The vasa were successfully thermally occluded in 8/8 samples, as indicated by average burst pressures of 283 \pm 34 mmHg, significantly greater than ejaculation pressures of 136 \pm 29 mmHg. Very minor skin burns were observed on 4/8 sites but were resolved by the next day.

Conclusions: Noninvasive laser thermal occlusion of the vas was achieved in 100% of the samples. Chronic studies are needed to evaluate permanent closure of the vas.

7548B-52, Session 5

Optimal laser dosimetry for efficient Ho:YAG lithotripsy

J. Qiu, The Univ. of Texas at Austin (United States); J. M. H. Teichman, Univ. of British Columbia (Canada); T. Wang, D. Gamez, The Univ. of Texas at Austin (United States); R. Glickman, Univ. of Texas Health Science Ctr. at San Antonio (United States); B. Knudsen, The Ohio State Univ. (United States); K. F. Chan, Fourier Biotechnologies (United States); T. E. Milner, The Univ. of Texas at Austin (United States)

Over the last decade, the free running Ho:YAG laser has been the gold standard for laser lithotripsy as its clinical application produces small debris and fragments all stone compositions. We test stone phantoms and human stones for optimal ablation efficiency (defined as mass loss per condition) using a clinically available Ho:YAG laser. Optical coherence tomography (OCT) is used to determine ablation crater volume for single pulse ablation using multiple pulse widths(0.3-1ms), pulse energy(0.2-3J) and fiber diameters(272 um and 365 um). Experiments are repeated (n>10) on stone phantoms and human urinary calculi of known composition to generate statistically relevant data. Stone retropulsion in single pulse and free-running modes is measured for stone phantoms. Pulse energy in free running mode is varied at different frequencies to maintain constant power. From the above experiments we report laser dosimetry that produces optimal fragmentation but minimal retropulsion under the constraint of constant power.

7548B-53, Session 5

Use of a tapered distal fiber tip for thulium fiber laser lithotripsy

R. L. Blackmon, The Univ. of North Carolina at Charlotte (United States); P. B. Irby, Carolinas Medical Ctr. (United States); N. M. Fried, The Univ. of North Carolina at Charlotte (United States)

Introduction: Tapered fibers have been used in laser lithotripsy on the proximal fiber end for more efficient coupling of the large, multimode, holmium:YAG laser beam into surgical fibers. However, use of a tapered distal fiber tip for expanding the laser beam during lithotripsy has not been studied. The excellent beam profile of the thulium fiber laser has previously been shown to allow coupling of high power laser radiation (up to 60 W) into small, 150-micron-core fibers. This study explores use of a short taper for expanding the thulium fiber laser beam at the distal fiber tip of a small-core fiber.

Methods: Thulium fiber laser radiation with a wavelength of 1908 nm, pulse rate of 10 Hz, 70 mJ pulse energy, and 1-ms pulse duration was delivered through a 2-m-length fiber with 150-micron-input-end,

300-micron-output-end, and 5-mm-length taper, in contact with human uric acid (UA) and calcium oxalate monohydrate (COM) stones, ex vivo (n=10 each).

Results: After delivery of 1800 pulses, mass loss measured 12.7 \pm 2.6 mg for UA and 7.2 \pm 0.8 mg COM stones. These results are comparable to mass loss measured using non-tapered, 100-micron-core fibers (12.6 \pm 2.5 mg for UA and 6.8 \pm 1.7 mg for COM stones) with the same laser treatment parameters.

Conclusion: Use of a short tapered distal fiber tip allows expansion of the laser beam, resulting in less fiber tip damage and less dependence on fiber-stone contact than conventional small-core fibers, without compromising stone vaporization efficiency or irrigation rates.

7548B-54, Session 5

Holmium: Yag versus thulium fiber laser lithotripsy

R. L. Blackmon, The Univ. of North Carolina at Charlotte (United States); P. B. Irby, Carolinas Medical Ctr. (United States); N. M. Fried, The Univ. of North Carolina at Charlotte (United States)

Introduction: The holmium:YAG laser is currently the most clinically popular laser lithotripter. However, recent experimental studies have demonstrated that the thulium fiber laser is also capable of vaporizing urinary stones. The high-temperature water absorption coefficient for the thulium wavelength (µa=160 cm-1 at 1908 nm) is significantly higher than for the holmium wavelength (µa=28 cm-1 at 2120 nm). We hypothesize that this should translate into more efficient laser lithotripsy using the thulium fiber laser. This study compares stone vaporization rates for holmium and thulium fiber lasers.

Methods: Holmium laser radiation pulsed at 3 Hz with 70 mJ energy and 220- μ s pulse duration was delivered through a 100- μ m-core silica fiber in contact with human uric acid (UA) and calcium oxalate monohydrate (COM) stones, ex vivo (n=10 each). Thulium fiber laser radiation pulsed at 10 Hz with 70 mJ energy and 1-ms pulse duration was also coupled into a 100- μ m fiber for the same sets of 10 stones.

Results: For the same number of laser pulses and total energy (126 J) delivered to each stone, UA mass loss averaged 2.4 ± 0.6 mg for the holmium laser and 12.6 ± 2.5 mg for the thulium fiber laser. COM stone mass loss measured 0.7 ± 0.2 mg and 6.8 ± 1.7 mg, respectively.

Conclusion: UA and COM stone mass loss for the thulium fiber laser averaged 5-10 times higher than for the holmium laser. With further development, the thulium fiber laser may represent an alternative to the holmium laser for more efficient laser lithotripsy.

7548B-55, Session 5

Evaluation of six holmium: YAG optical fibers for ureteroscopy: What's new in 2009?

B. E. Knudsen, The Ohio State Univ. Medical Ctr. (United States); J. M. H. Teichman, The Univ. of British Columbia (Canada)

Purpose: Prior study has shown that holmium:YAG laser fiber performance differs among manufacturers. This study was designed to determine the performance and threshold for failure of six newly available holmium:YAG laser fibers from Cook Medical and Fibertech Gmbh.

Materials and Methods: Six different commercial available fibers were evaluated: two were supplied by Fibertech and have core sizes of 272 and 365 microns respectively with non-tapered connectors. Four fibers were supplied by Cook Medical (OptiLite) and have core sizes of 150, 200, 273, and 365 microns respectively. The OptiLite 150 and 200 micron fibers have tapered connectors, while the 273 and 365 micron fibers have non-tapered connectors. All fibers were evaluated for flexibility, threshold for failure during bend testing with laser activation, and true fiber diameter. Flexibility was measured by maximally deflecting a Stryker FlexVision U-500 ureteroscope with the fiber in the working



channel. The diameter of each fiber was measured by digital micrometer. Failure threshold was assessed by bending the fibers to 180 degrees beginning with a radius of 1.25cm. A Lumenis VersaPulse 100W holmium:YAG laser was operated at 1.2J and 10Hz for 1 minute or until fiber fracture. The bend radius was reduced in 0.25 cm increments and the testing repeated until a minimum bend radius of 0.5 cm was reached or until the fiber failed. Baseline energy transmission was measured by recording the mean of 50 pulses (0.5J, 10Hz) prior to bend testing and repeated after each bend test trial. Three fibers samples of each model were tested for a total of 18 fibers.

Results: The Cook OptiLite 150 had lower energy transmission compared to all other fibers tests (p<0.01) but was the most flexible. The remaining five fibers demonstrated no difference in energy transmission at initial testing. Baseline deflection of the endoscope with no fiber in the channel was 265°. The OptiLite 150 was the most flexible fiber and deflected 262°, followed by the OptiLite 200 (255°), the OptiLite 273 (240°), the FiberTech 272 (236°), the FiberTech 365 (188°) and the OptiLite 365 (186°). The OptiLite 273 did not fail during bend testing with laser activation while the OptiLite 365 failed at the largest bend radius (1.25 cm) (p<0.01). Comparing fibers of similar core size, the Cook OptiLite 273 was smaller in diameter, more flexible, and less likely to fail when activated in a bent configuration (p<0.01) compared to the FiberTech 272. Conversely, the FiberTech 365 was smaller in diameter, more flexible, and failed at a tighter bend radius (p<0.01) as compared to the Cook OptiLite 365.

Conclusion: Commercially available holmium: YAG laser fibers continue to differ significantly in their performance characteristics. The Cook OptiLite 150 had the worst energy transmission suggesting loss at the connector.

7548B-56, Session 5

Comparative evaluation of inertial forces generated by ultrasonic lithotriptors

B. E. Knudsen, The Ohio State Univ. Medical Ctr. (United States)

Purpose: Prior study has shown that handheld ultrasonic lithotriptors differ in performance. The Boston Scientific (BSci) LithoClast® Ultra, BSci LithoClast® Select with Vario handpiece, and the Olympus/ACMI Cyberwand are amongst the latest generation of ultrasonic lithotriptors. This study tests the hypothesis that inertial forces (g-force) vary amongst different ultrasonic handpieces when evaluated with an accelerometer.

Materials and Methods: Eight handpieces were evaluated including two US3 (LithoClast® Ultra) handpieces, three Vario handpieces (LithoClast® Select) and three Cyberwand handpieces using a simulated lithotripsy fixture incorporated a Bego stone phantom. An accelerometer was placed under the stone phantom and measurements recorded with data acquisition hardware as the ultrasound device was brought into contact with the stone. The US3 and Vario handpieces were tested using a LithoClast® Select generator set at 100% power and 100 duty. Only the ultrasound mode was tested. The Cyberwand handpiece was tested on a Cyberwand generator using the "large stone" setting. Three trials were performed for each handpiece.

Results: The overall mean inertial force generated by the handpieces was greatest for the Vario (64.04 g), followed by the US3 (56.01 g) and the Cyberwand (20.25 g). There was variability amongst the different samples of each handpieces. The two US3 handpieces each generated a mean inertial force of 56.01 and 60.41 g's respectively. The three Vario handpieces tested each generated a mean inertial force of 56.25, 66.17, and 68.34 g's respectively. The three Cyberwand handpieces generated a mean inertial force of 14.76, 16.48, and 20.30 g's respectively. All values are statistically significant (p < 0.01).

Conclusions: The US3, Vario, and Cyberwand ultrasonic handpieces differed in the inertial forces generated during fragmentation of a Bego stone phantom. Individual handpieces within the same model line also varied in performance. The Vario handpiece generated the greatest mean inertial force, followed by the US3 handpiece, and then the Cyberwand handpiece.

7548B-57, Session 6

Characterization of the positive sites by high magnification cystoscopy during fluorescence cystoscopy with Hexvix

B. Lovisa, Ecole Polytechnique Fédérale de Lausanne (Switzerland); D. Aymon, P. Jichlinski, Ctr. Hospitalier Univ. Vaudois (Switzerland); H. van den Bergh, G. A. Wagnières, Ecole Polytechnique Fédérale de Lausanne (Switzerland)

Fluorescence detection of early superficial bladder cancer has been well established over the last years. This technique exploits the selective production and accumulation within cancerous tissues of photoactivable porphyrins (PaP), mainly protoporphyrin IX (PpIX), after the instillation of hexaminolevulinic acid (Hexvix®) in the bladder. Although the selective production of PpIX and the sensitivity of this procedure are outstanding, its specificity can be improved due to false positive (FP) lesions. Therefore, our current research focuses on the characterization of positive sites by high magnification cystoscopy. Cancerization process often combines with changes in vascular architecture. It is likely that the visualization of these modifications should allow us to differentiate false and true positive (TP). New methods, using high magnification (HM) endoscopy, are being investigated by our group, and hopefully resulting in a reduced number of biopsies. In this study, we are using a dedicated rigid cystoscope, allowing conventional magnification during "macroscopic" white light and fluorescence observation, as well as image acquisition with HM when the endoscope is in contact with the tissue. This is realized by an optical setup directly integrated in the cystoscope. Vascular patterns (oedema, small loops, tortuous or disorganized network...) were highlighted with various spectral bands and classified thereafter with a dedicated algorithm. Data from 60 patients will be presented.

7548B-58, Session 6

Responses to hexyl 5-aminolevulinateinduced photodynamic treatment in rat bladder cancer model

C. Arum, St. Olavs Hospital (Norway); O. Gederas, E. Larsen, L. Randeberg, Norwegian Univ of Science and Technology (Norway); C. Zhao, St. Olavs Hospital (Norway)

OBJECTIVES: We evaluated histologically the effects of hexyl 5-aminolevulinate-induced photodynamic (HAL-PDT) treatment in a rat bladder cancer model.

MATERIAL & METHODS: Fischer-344 female rats were divided into 2 groups, half of which were orthotopically implanted with AY-27 urothelia1 rat bladder cancer cells and half sham implanted. 14 days post implantation 6 rats from each group were treated with HAL-PDT (8mM HAL and light fluence of 20 J/cm2). Additional groups of animals were only given HAL instillation, only light treatment, or no treatment. All animals were sacrificed 7 days after the PDT/only HAL/only light or no treatment. Each bladder was removed, embedded in paraffin and stained with hematoxylin, eosin, and saferin for histological evaluation at high magnification for features of tissue damage by a pathologist blinded to the sample source.

RESULTS: In all animals that were AY-27 implanted and not given PDT treatment, viable tumors were found in the bladder wall. In the animals treated with HAL-PDT only 3 of 6 animals had viable tumour. In the 3 animals with viable tumour it was significantly reduced in volume compared to the untreated animals. It was also noted that in the PDT treated animals there was a significantly increased inflammatory response (lymphocytic and mononuclear cell infiltration) in the peri-tumour area compared to implanted animals without complete HAL-PDT.

CONCLUSION: Our results suggest that HAL-PDT in a rat bladder cancer model involves both direct effects on cell death (necrosis and apoptosis) and indirect effects to evoke the host immune-response, together contributing to tumour eradication.

15

Return to Contents TEL: +1 360 676 3290 · +1 888 504 8171 · customerservice@spie.org

7548B-59, Session 6

Study on photochemical inactivation of cell-associated and cell-free human immunodeficiency virus in vitro

H. Yin, Y. Li, Tianjin Medical Univ. (China); Y. Zheng, Kunming Institute of Zoology, CAS (China); Z. Zou, Tianjin Medical Univ. (China)

To explore a potential treatment of AIDS--Photodynamic therapy by detecting the photoinaction on hunman immunodeficiency virus (HIV) in vitro. Method: Mixed the photosensitizes hematoporphyrin monomethyl ether or methylene blue by a series of dilute strengths with the host cells MT4, C8166 or H9/HIV-1 B or the virus HIV-1 B for 2 hours incubation, followed by irradiation by a 630nm semiconductor laser with energy density 0.3J/cm2. After certain time, the activites against HIV-1 B were assayed by determining the syncytial formation under the inverted microscope or MTT and measuring the p24 antigen expression level in supernatant by ELISA. Results: PDT inhibited the cell-cell fusion (inhibition rate, HMME-PDT64.68%, MB-PDT61.56%) and virus-cell fusion (inhibition rate, HMME-PDT 85%, MB-PDT 73.64%)induced by HIV-1 B significantly, and had an intensive inactivation on the cell-free HIV-1 B especially the inhibition rate up to 100%. However, PDT had no effect on the replication course 2 hours after cute infection or chronic infection of HIV-1 B. Conclusion:PDT has outstanding inhibition on cellfree HIV-1 B and fusion induced by HIV-1 B, which prompts PDT may be a new treatment of AIDS in future.

7548B-60, Session 6

The feasibility of real-time bladder mapping using a stereotactic navigational system

R. Draga, H. J. Noordmans, T. M. W. Lock, M. M. Grimbergen, R. J. L. H. Bosch, Univ. Medical Ctr. Utrecht (Netherlands)

Stereotactic navigational devices have been implemented in neurosurgery, orthopedics and ear-nose-throat to improve surgical accuracy. However, the feasibility of navigating inside the bladder has not yet been investigated. Occasionally, transurethral resections of bladder tumors (TURBTs) are impeded by bleeding and cloudiness inside the bladder and, consequently, the bladder lesions are not found back easily. In addition, bladder lesions are often concealed when viewed with the camera some distance away from the bladder wall. The aim of the study is to investigate the feasibility of real-time bladder mapping using the Medtronic Stealthstation system, without the use of pre-operative images. Ten patients were scheduled for a TURBT and were included in the study. During the TURBT procedure, the spatial coordinates of the bladder lesions were recorded two times independently, after filling the bladder with a fixed volume of 390 ml. The distance between the spatial coordinates of two consecutive measurements, in millimeters, was calculated. We found that bladder lesions can be found back using the navigational system with an accuracy of less than 12 mm. Real-time bladder navigation is feasible without the necessity of pre-operative images or calibration. If the coordinates are directly superimposed on the video image this could facilitate the retrieval of bladder lesions during TURBT. This system could reduce the stress for the surgeon and decrease the operating time. Furthermore, it could improve the success rate of the operation, reduce the recurrence rates, improve the patient's outcome and save overall treatment costs.

7548B-61, Session 7

Photodynamic action of the Hypericum Perforatum L. methanolic extracted fraction after short intravesical instillation and white light photoactivation in orthotopic implantation of transitional cell carcinoma AY-27 cells in rat bladder

I. Tsimaris, N. E. Stavropoulos, A. Ntemou, I. Tsironis, Hatzikosta General Hospital (Greece); D. Skalkos, Univ. of Ioannina (Greece); U. O. Nseyo, North Florida Foundation for Research and Education, Inc. (United States)

PDT is an alternative therapy for superficial transitional cell carcinoma of the urinary bladder. Short intravesical instillation of PMF and white light photoactivation induces high rates of apoptosis in an orthotopic transitional cell carcinoma bladder tumor model as presented by our group (SPIE 2007, 6427-11, section 3). There was no tumor eradication due to the bulking tumors produced by the applied cancer model. In this setting we managed to reproduce flat urethelial lesions, namely dysplasia. After catheterization, the bladder mucosa was mildly disrupted using a 15-sec wash with 0.4 ml of 0.1 N HCl, followed by neutralization with same quantity and strength of NaOH. AY-27 cells in a concentration 106 cells in 0,5 ml of PBS, were instilled intravesically in 20 female Wistar rats for one hour. After 10 days there were divided in two groups. One was treated with 15 minutes of intravesical instillation of PMF diluted in normal saline, containing 250 µg/ml hypericins. The bladder was washed out with normal saline. An optic fiber was inserted intravesically and Photodynamic Treatment with white light performed. The PMF was photoactivated with energy of 700 J/cm2. The second group of animals served as control and underwent photoactivation with the same quantity of energy without PMF instillation. After 30 days 5 rats of each group were sacrificed, their bladders removed, cut in 3µm sections and stained with hematoxylin/eosin. The same procedure was followed for the rest of the animals 90 days after the PDT. Dysplasia was noted in the bladder of all untreated animals. Complete lack of urothelium was apparent 30 days after PDT. The urothelium was regenerated 90 days in all animals after PDT. None of the rats treated had dysplasia. The Hypericum Perforatum L. extract, mainly its Polar Methanolic Fraction, is a potent photosensitizer that deserves further evaluation for its use in PDT.

7548B-62, Session 7

GreenLight laser prostatectomy: a safe and effective treatment for bladder outflow obstruction by prostate cancer

G. Muir, F. Liberale, S. Chandrasekara, K. Walsh, King's College Hospital (United Kingdom)

Most men with progressive prostate cancer will have some LUTS which may be minor or a dominant issue affecting quality of life: LUTS commonly leads to urinary retention in patients with relapsed prostate

While channel TURP has for years been the standard for palliation of men with this problem, there are few large series attesting to its safety. In those reports which do exist the incidence of bleeding, incontinence and post-operative failure to void are all much higher than one would expect in BPH series.

We report on a series of 41 prostate cancer patients treated for LUTS (32%) or urinary retention (68%) with 532nm GreenLight laser prostate vaporisation. 79% of patients had hormonally relapsed disease, the others (21%) having a mixture of refractory LUTS or previous radiation therapy. The mean age was 72,5 (54-96 years). Mean prostate volume was 76,2 cm3 (13-246 cm3) and mean pre-operative PSA was 125,4 g/ml (0.1-2000 g/ml), time from initial diagnosis to symptomatic local progression being 2.8 years (0-13 ys).



Operating time was 42 minutes, mean energy delivered 150,000 joules (31 patients were treated with the 80 watt PV machine and 12 with the HPS system).

Mean post-op hospital stay was 9.6 hours (range 2-36 hours, median 9,2 hours). 32 patients (74.4%) were admitted for less than 24 hours. Twelve patients (28%) had no post operative catheter, mean post-op catheter times was 22 hours.

All patients were able to void without a catheter within three days of surgery, with one (2%) having early stress incontinence. There were no post op transfusions or TUR syndrome, although three patients (7%) required simple bladder washout (without cystoscopy) for secondary haemorrhage.

At three months, 41/42 evaluable patients were voiding, and wherepre-op values were available there was a significant improvement in peak flow and symptom score.

With mean follow up of 22 months four (10%) patients had had redo laser therapy and three (7%) developed further retention and did not wish further surgery.

GreenLight laser prostate vaporisation is a safe non-invasive method of treating locally obstructing prostate cancer which minimises time in hospital and has medium term efficacy and complications at least equivalent to those reported with channel TURP.

7548B-63, Session 7

Multicentre prospective analysis of safety and efficacy of GreenLight HPS laser prostatectomy

G. Muir, F. Gómez Sancha, A. Bachmann, B. Choi, E. Collins, J. J. de la Rosette, O. Reich, S. Tabatabeh, H. Woo, King's College Hospital (United Kingdom)

240 patients treated sequentially at 9 centres had data prospectively collected for laser energy used, per-operative and post-operative complications and clinical effectiveness. Follow up was at three months with ongoing follow up at one year.

Data was obtained at all points for: IPSS and Quality of Life scores , Urine flow and/or ability to void without catheter, Residual urine volume, PSA and Prostate Volume, Morbidity and Mortality

One year data collection is ongoing but will be complete by the date of the conference. Early data show excellent safety with transfusion rates less than one percent, no stress incontinence and no early post-operative deaths or TUR syndrome. Energy use was approximately 4.5 kJ/cm3 of prostate tissue measured by transrectal ultrasound.

At all post op time points peak flow rate was improved by over 100%, while IPSS and residual volume had reduced to less than 50% of baseline. PSA reduction was significant and related to the size of the gland.

Recommendations on technique and energy use to achieve standardised results will be shown.

7548B-64, Session 7

Problems with assessing new technologies in surgery: assessing the evidence and new study design

G. Muir, King's College Hospital (United Kingdom)

There has been a trend in recent years to strive for level one evidence in all areas of medicine, and to ignore anything less. In practice this will usually mean that good evidence is available for medical interventions sponsored by major international pharmaceutical companies but for little else.

Surgery, and in particular assessment of new surgical technologies,

has particular difficulty. We recently published an assessment of RCT's in urological and other surgical techniques where it was shown that compliance with the accepted basic level of reporting for RCT's (CONSORT) was so poor as to make the great majority of published RCT's in surgery unsuitable for proper critical analysis. There are several reasons for these problems, none of which includes surgeons being too stupid to do the studies, since the same investigators are often experienced and active pharmaceutical triallists.

For the typical surgical RCT, a minimally invasive approach for a common condition is evaluated, often with minimal financial support. Usually, a single centre RCT is set up. Much more rarely multi-centre studies are set up. Hopefully (but rarely) some level of ensuring that surgical skills in the new procedure are equivalent to the existing procedure will have been attempted .

Randomisation may occurs yet blinding is very difficult. Inevitably there may be some subconscious bias towards one technology (kudos, private practice, conflict of interest with the company.)

Almost invariably the trial reports with small numbers and will only demonstrate rough equivalence. For very major differences a significant difference may be seen, although in a small study this would have been obvious from the start (you do not need to be randomised to know if a punch on the nose will hurt more than not being punched!).

I will discuss the problems inherent in surgical RCT's relating to funding , crossover errors, bias, reproducibility and technological obsolescence of new technology.

Some alternative cost- effective options will be proposed and discussed.

7548B-65, Poster Session

IR absorption spectra of dried urine samples in case of any deviation in urine composition and with the presence pathological salts

O. Z. Drobchak, O. Bordun, Ivan Franko National Univ. of L'viv (Ukraine)

Statistical review of nephrolithiasis diseases draws the following results: 5% of females and 12% of males have abovementioned diseases. It should be mentioned that average age of peoples with this disorder has sharply decreased. One of the negative characteristics of the nephrolithiasis is the fact that, as a rule, it is diagnosed on the posterior stages when the person needs either medication treatment or invasive interruption. In this case the problem of early diagnostics of kidney stone diseases is of the greatest importance. The IR spectroscopy might be promising in the aspects of enlarging the field of early medical diagnostics in nephrolithiasis.

IR absorption spectra of the following samples were studied: urea, dried urine samples in case of any deviation in urine composition and with the presence pathological salts in spectral range 500-8000 cm-1. The shifting of stretching vibrations frequency of carbonyl group C=O assert this fact that the pathological salt molecules join to urea molecules via oxygen atom of urea. IR absorption bands of pathological salts are identified. Obtained results may be used for developing of new methods of early nephrolithiasis diagnostics.

Return to Contents TEL: +1 360 676 3290 · +1 888 504 8171 · customerservice@spie.org



7548B-66, Poster Session

Anticancer effect of the Hypericum Perforatum L. extract in high grade T24 human bladder cancer cells after white light photoactivation

I. Tsimaris, N. E. Stavropoulos, Hatzikosta General Hospital (Greece); S. Mbellou, D. Skalkos, Univ. of Ioannina (Greece); U. O. Nseyo, North Florida Foundation for Research and Education, Inc. (United States)

The polar methanolic fraction (PMF) of the Hypericum perforatum L. extract has recently been developed and tested as a novel, natural photosensitizer to be used in the photodynamic therapy (PDT), and photodynamic diagnosis (PDD). It has significant photocytotoxicity against human bladder cancer cells after excitation with a 630 nm laser light. In this study we investigate its photodynamic action after photoactivation with white light. Bladder cancer cells T24 (2×104/well) were plated in 96-well tissue culture plates in DMEM containing 10% FBS and 1% pen/strep in a final volume of 0.1 mL. The culture plates were incubated with PMF at a concentration of 40µg/ml or 80µg/ml. Twenty-four hours later, replacement of the medium was replaced by fresh DMEM supplemented with 10%FCS and 1% pen/strep. Exposure to white light followed either under low-pressure mercury discharge lamp (TL-D Super 80 New generation, Philips) with a light dose of 310, 620, 1240 and 4650 J/cm2 or under a Halogen Storz cystoscope lamp with a light dose of 300, 600 and 900 J/cm2. Cells were incubated at 37°C for 48h. Cell viability was evaluated by 3-(4, 5-dimethylthiazol-2-yl)-2, 5-diphenyltetrazolium bromide (MTT) (Sigma, San Louis, MO, USA) assay. The photosensitizer exhibited significant photocytotoxicity at a concentration of 80µg/ml, with 1240 J/cm2 light dose (delivered from the low-pressure mercury discharge lamp) and with 600 J/cm2 light dose (delivered from the halogen cystoscope lamp), resulting in cell destruction in 98% and 96% respectively. At the concentration of 40µg/ml the PMF exhibited significant photocytotoxicity resulting in 96% cell death with 4650 J/cm2 (mercury lamp) and 95% cell death with 600 J/cm2 (halogen lamp) respectively. PMF was not active in either concentration when photoactivated with 310 or 620 J/cm2 delivered from low-pressure mercury discharge lamp. The apparent differences in the amount of the delivered light energy needed in order to achieve significant photocytotoxicity are due to the different emission spectra of the lamps. The halogen lamp has an emission spectrum that resembles closely the absorption spectrum of the PMF. The reported significant photocytotoxicity and the known selective localization, natural abundance, easy, and inexpensive preparation, underscore that the PMF extract hold the promise of being a novel, effective PDT photosensitizer.



Saturday-Sunday 23-24 January 2010 • Part of Proceedings of SPIE Vol. 7548 Photonic Therapeutics and Diagnostics VI

7548C-67, Session 1

Our experience with optical diagnostics of the head and neck

C. Hopper, Univ. College London Hospitals NHS Foundation Trust (United Kingdom); W. K. Jerjes, T. Upile, Univ. College Hospital (United Kingdom)

No abstract available.

7548C-68, Session 1

Wide-field and high-resolution optical imaging for early detection of oral neoplasia

M. C. Pierce, K. Rosbach, D. M. Roblyer, T. Muldoon, Rice Univ. (United States); M. D. Williams, A. K. El-Naggar, A. M. Gillenwater, The Univ. of Texas M.D. Anderson Cancer Ctr. (United States); R. R. Richards-Kortum, Rice Univ. (United States)

Current procedures for oral cancer screening typically involve visual inspection of the entire tissue surface at risk under white light illumination. However, pre-cancerous lesions can be difficult to distinguish from many benign conditions when viewed under these conditions. We incorporated cross-polarization, narrowband reflectance, and fluorescence imaging modes in a portable, robust, wide-field imaging device to reduce specular glare, enhance vascular contrast, and detect disease-related alterations in tissue autofluorescence.

We have also developed a portable system to enable high-resolution evaluation of cellular features within the oral mucosa in situ. This system is essentially a wide-field epi-fluorescence microscope coupled to a 1 mm diameter, flexible fiber-optic imaging bundle, capable of imaging nuclear size and nuclear-to-cytoplasmic ratio following topical application of a fluorescent labeling solution. Proflavine solution was used to specifically label cell nuclei, enabling the characteristic differences in N/C ratio and nuclear distribution between normal (b) and cancerous (d) oral mucosa to be quantified.

This presentation will discuss the technical design and performance characteristics of these complementary imaging systems. We will also present data from ongoing clinical studies aimed at evaluating diagnostic performance of these systems for detection of oral neoplasia in high- and low-prevalence populations.

7548C-69, Session 1

The detection of oral cancer using differential pathlength spectroscopy

H. J. C. M. Sterenborg, Univ. Medisch Ctr. Rotterdam (Netherlands)

No abstract available.

7548C-70, Session 1

Raman spectroscopy of lymph nodes in the head and neck

L. Orr, C. A. Kendall, J. C. Hutchings, M. Isabelle, J. Horsnell, N. Stone, Gloucestershire Royal Hospital (United Kingdom)

The development of lymphadenopathy in the neck has many causes, in children it is often found in relation to infection and in a small but significant number it is the first presentation of lymphoma. In adults neoplastic causes predominate for example, lymphoma, squamous cell carcinoma and adenocarcinoma. The treatment modalities and prognosis for these conditions varies enormously and in the case of squamous cell carcinoma an excision biopsy can lead to significant morbidity. A major prognostic factor for the response to treatment for example in lymphoma is the extent of the disease at presentation. Pre-treatment accurate diagnosis is imperative and is a compelling argument for investment in the development of accurate, sensitive and minimally invasive diagnostic techniques, such as Raman spectroscopy.

This work seeks to investigate the abilty of Raman spectroscopy to differentiate between the major neoplastic diseases of lymph nodes presenting within the neck. Raman spectroscopy at 830nm has been used to extensively study lymph nodes from the head and neck and pathology related spectral signatures have been identified.

7548C-72, Session 1

Assessment of suspicious oral lesions using optical coherence tomography

Z. Hamdoon, W. K. Jerjes, T. Upile, Univ. College Hospital (United Kingdom); G. P. McKenzie, Michelson Diagnostics Ltd. (United Kingdom); A. Jay, G. J. Thomas, Univ. College Hospital (United Kingdom); C. Hopper, Univ. College London Hospitals NHS Foundation Trust (United Kingdom)

No abstract available.

7548C-73, Session 1

Assessment of tumour resection margins using optical coherence tomography

Z. Hamdoon, W. K. Jerjes, T. Upile, Univ. College Hospital (United Kingdom); G. P. McKenzie, Michelson Diagnostics Ltd. (United Kingdom); A. Jay, G. J. Thomas, Univ. College Hospital (United Kingdom); C. Hopper, Univ. College London Hospitals NHS Foundation Trust (United Kingdom)

No abstract available.

TEL: +1 360 676 3290 · +1 888 504 8171 · customerservice@spie.org



7548C-74, Session 1

Quantitative analysis of head and neck resection margins using optical coherence tomography: Imperial-UCL work

Z. Hamdoon, W. K. Jerjes, T. Upile, Univ. College Hospital (United Kingdom); G. P. McKenzie, Michelson Diagnostics Ltd. (United Kingdom); A. Jay, Univ. College Hospital (United Kingdom); A. Sandison, Imperial College London (United Kingdom); C. Hopper, Univ. College London Hospitals NHS Foundation Trust (United Kingdom)

No abstract available.

7548C-75, Session 1

Real-time volumetric optical coherence tomography OCT imaging with a surgical microscope

G. Hüttmann, J. Probst, Univ. zu Lübeck (Germany); T. Just, H. W. Pau, Univ. Rostock (Germany); S. Oelckers, MÖLLER-WEDEL GmbH (Germany); D. Hillmann, P. Koch, Thorlabs GmbH (Germany); E. M. Lankenau, Univ. zu Lübeck (Germany)

Optical coherence tomography is a unique technique to visualize subsurface tissue structures with a resolution below 10 μm during microsurgery without tissue contact. Since it was introduced more than 15 years ago imaging speed was boosted by more than three orders of magnitude, from less than 100 to more than 300,000 A-scans per second. Instead of taking only still images of anatomical structures, the increased speed of OCT allows now to image volumes nearly in real time. This enables not only the scanning of larger tissue surfaces, but also opens new application beyond simple diagnosis. A noncontact volumetric imaging with less than 15 μm resolution can guide microsurgery at the eye, in Otolaryngology (ENT) and in other medical disciplines.

Here we present an ultrahigh speed OCT system with more than 200.000 A-scans/second integrated into a surgical microscope (MÖLLER Hi-R 1000, Möller-Wedel GmbH, Wedel, Germany), which is capable of processing, rendering and displaying more than 7 volumes with 12 million pixel per second by using a PC with a high performance graphics accelerator card. Best performance was reached by distributing the calculation of the A-scans to the four cores of the PC, whereas the preprocessing and rendering was done in real-time with dedicated software on graphic processing unit (GPU).

Possible applications of the system are OCT guided microsurgery in the middle ear or tumor surgery of the vocal fold.

7548C-168, Session 1

Design, conduct and challenges of a clinical trial utilizing elastic light scattering spectroscopy in thyroid lesions

J. E. Rosen, H. Suh, S. Lee, O. M. Aamar, I. J. Bigio, Boston Univ. (United States)

Thyroid cancer is the most common endocrine malignancy. The standard of care in the management of a patient with a thyroid nodule is fine-needle aspiration biopsy (FNA) with cytological evaluation. While 5-10% of nodules are malignant, 10-25% of FNAs are indeterminate. Consequently, about twice as many patients undergo surgery for a suspicious lesion that turns out to be benign as undergo surgery for a known malignant lesion. A more accurate molecular and ultrastructural based algorithm would be useful to improve diagnostic accuracy.

Noninvasive optical tissue diagnosis mediated by fiber-optic probes can be used to perform non-invasive, or minimally-invasive, real-time assessment of tissue pathology in-situ. Elastic light-scattering spectroscopy (ESS) is a point spectroscopic measurement technique, which is sensitive to cellular and subcellular morphological features. Normal and abnormal tissues can generate different spectral signatures as a result of changes in nuclear size, density, and other sub-cellular features, the optical-spectroscopy equivalent of histopathological readings. ESS is optimal for use in the small-volume area as found in thyroid FNA. An important advantage of ESS is that it provides an objective and quantitative assessment of tissue pathology that may not require on-site special expertise and subjective image interpretation as in conventional histopathology. Here we will describe our experience in the clinical application of elastic scattering spectroscopy in the thyroid.

7548C-174, Session 1

Current Munich status concerning invivo optical coherence tomography for differentiating lesions of the upper aerodigestive tract

V. Volgger, H. G. Stepp, Ludwig-Maximilians-Univ. München (Germany); W. K. Jerjes, T. Upile, Univ. College Hospital (United Kingdom); A. Leunig, Ludwig-Maximilians-Univ. München (Germany); C. Hopper, Univ. College London Hospital (United Kingdom); C. S. Betz, Ludwig-Maximilians-Univ. München (Germany)

No abstract available.

7548C-76, Session 2

Automatic segmentation of clinical OCT images for the determination of epithelial thickness changes in laryngeal lesions

H. Wisweh, L. Martinez Mateu, Laser Zentrum Hannover e.V. (Germany); M. Kraft, Kantonsspital Aarau (Switzerland); A. Krüger, H. Lubatschowski, Laser Zentrum Hannover e.V. (Germany)

Automated classification of laryngeal lesions using optical coherence tomography data be helpful in making a faster and safer diagnosis. A change in the epithelial layer thickness seems to be an effective indicator for laryngeal cancer and its precursors.

Lesions with different grades of malignity were scanned with a time domain OCT system during microlaryngoscopy. Every diagnosis was confirmed by performing a biopsy. Each OCT image was separately segmented, manually by an expert and automatically by a segmentation algorithm. Values for the maximal and average epithelial thickness as well as the standard deviations were compared for both segmentations.

The results show a thickening of the epithelium from normal over dysplastic to cancerous tissue. The values for the automatic segmentation are in good agreement with expert segmentation.

In conclusion, automatic segmentation can be used for epithelial thickness measurements as a promising indicator for laryngeal cancer. It would also be possible to extract other characteristics like standard deviation or signal attenuation within the segments. Thus, we laid the foundation for computer-aided diagnosis of laryngeal lesions.



7548C-77, Session 2

Ultrahigh-resolution 3D full-field optical coherence micropscopy of the pulmonary airways ex vivo

L. Liu, W. Oh, B. E. Bouma, Wellman Ctr. for Photomedicine, Massachusetts General Hospital (United States) and Harvard Medical School (United States); S. M. Rowe, The Univ. of Alabama at Birmingham (United States); G. J. Tearney, Wellman Ctr. for Photomedicine, Massachusetts General Hospital (United States) and Harvard Medical School (United States)

Visualizing the respiratory mucosa in pulmonary airways at the sub-cellular level could yield new insights into pathogenesis of many important diseases. However, current imaging modalities to study the respiratory mucosa lack the required resolution to visualize critical subcellular detail such as nuclei and respiratory epithelial cilia. Full-field optical coherence microscopy (FFOCM) is an emerging technique capable of providing reflectance images in situ with high spatial resolution in all three dimensions.

We have developed a FFOCM with an axial sectioning thickness of 1 μm and a high transverse resolution of 0.6 μm . The three-dimensional field of view was 256 (H) x 256 (W) x 400 (D) μm . Three-dimensional images of formalin-fixed, sectioned porcine bronchial segments were obtained immediately ex vivo. Images were compared to H&E stained histology at corresponding sites. Pilot images on fixed human airways from individuals with cystic fibrosis (CF) and Chronic Obstructive Pulmonary Disease (COPD) were also acquired.

Individual epithelial cells and goblet cells, including their subcellular morphologies, were easily seen. Cross-sectional views showed gland ducts containing mucus, cilia, the periciliary layer (PCL), and nuclei. Three-dimensional rendering of the trachea showed the presence of mucus droplets directly above non-ciliated goblet cells, tethered to the surface of these cells by a thin adherent mucus strand.

Our results demonstrate the potential of FFOCM to provide detailed microstructural imaging of pulmonary airways without administration of a contrast medium. The future development of a probe for in vivo monitoring of mucociliary transport, gland function, and airway surface liquid (ASL) depth could provide new avenues for improving our understanding of respiratory mucosal pathophysiology and enable longitudinal assessment of the response to novel drugs.

7548C-78, Session 2

High-speed three-dimensional imaging of the pulmonary alveoli

E. Namati, Harvard Medical School (United States) and Wellman Ctr. for Photomedicine, Massachusets General Hospital (United States); C. Unglert, Harvard Medical School (United States) and Massachusets General Hospital (United States) and Air Liquide (France); B. E. Bouma, G. J. Tearney, Harvard Medical School (United States) and Wellman Ctr. for Photomedicine, Massachusets General Hospital (United States)

Investigating the structure and function of pulmonary alveoli in vivo is crucial for understanding the normal and diseased lung. In particular, understanding the three-dimensional geometry and relationship of the terminal alveoli to their neighboring alveoli, alveolar ducts and acini during respiration would be a major advance. However, the lung is an inherently difficult organ to image in vivo and the peripheral lung has many compounding challenges not limited to its highly scattering micro architecture, large motion artifacts and difficult access through the bronchial tree.

In this study, we image the alveoli of fixed pig lungs using a high-speed high-resolution optical frequency domain imaging (OFDI) system that is endoscopically compatible for future in vivo imaging of human alveoli.

Core imaging components include a rapidly swept wavelength source centered at 1310nm resulting in an A-line depth scan rate of 62,500 Hz, a polarization diverse dual balanced receiver, and a high speed data acquisition system. Whole lungs were excised from normal piglets and inflation fixed at 15 cm H2O pressure using a modified Heitzman fixation technique. Lungs were air dried in a heated oven and sectioned into 500 µm slices. Three-dimensional datasets were acquired from lung slices with 512x512x1024 voxels and a voxel dimension of 5x5x8µm. Datasets were acquired at 122 frames per second and 0.23 volumes per second - indicating the potential to acquire a three-dimensional volume within a single human respiratory cycle.

OFDI images reveal clear delineation of alveolar septal walls, demonstrating that high-speed three-dimensional visualization of air filled alveoli is feasible. The fixed lung data provides a strong foundation for investigating the 3D structure and function of alveoli in vivo and suggests great promise for advancing our knowledge of the functional unit of the lung.

7548C-79, Session 2

Reflectance microscopy techniques for 3D imaging of the alveolar structure

C. Unglert, Wellman Ctr. for Photomedicine, Massachusetts General Hospital (United States) and Harvard Medical School (United States) and Air Liquide R&D Medical Gases (France); E. Namati, L. Liu, Wellman Ctr. for Photomedicine, Massachusetts General Hospital (United States) and Harvard Medical School (United States); H. Yoo, D. Kang, B. E. Bouma, Wellman Ctr. for Photomedicine, Massachusetts General Hospital (United States); G. Tearney, Wellman Ctr. for Photomedicine, Massachusetts General Hospital (United States) and Harvard Medical School (United States)

Lung disease involving the alveoli and distal bronchioles are poorly understood and most commonly studied indirectly via lung function tests. Available imaging tools for the non-destructive assessment of the alveolar structure include X-ray computed tomography, intra-vital fluorescence microscopy and Optical Coherence Tomography, which are either limited by long acquisition time, inadequate resolution and contrast, or shallow imaging depth.

In this study, we investigated the potential of two high-resolution reflectance microscopy imaging techniques, Spectrally Encoded Confocal Microscopy (SECM; $1\mu m$ (x) x $1\mu m$ (y) x $5\mu m$ (z) resolution) and Full Field Optical Coherence Microscopy (FFOCM; $1\mu m$ (x) x $1\mu m$ (y) x $1\mu m$ (z) resolution), for imaging alveolar microstructural detail. 2 mouse lung samples were imaged with both SECM and FFOCM. The specimens were inflation-fixed using a modified Heitzman fixation technique at 20 cm H2O pressure. They were cut in 500 mm thick slices and water immersed for imaging. Images were obtained and analyzed to determine whether or not the resolution and contrast of these techniques are sufficient to visualize the fine structures of the alveolar wall.

Alveolar microstructure could be resolved in three dimensions in images obtained by both technologies. Alveolar septal walls from multiple layers could be clearly identified while sub-cellular structures such as nuclei were also visible in the SECM technique. In conclusion, we have demonstrated that two imaging technologies provide important subcellular detail that is required to study alveolar microstructure. Future research to develop these imaging modalities further so that they may be used in vivo is merited.



7548C-80, Session 2

Three-dimensional microscopy of the human bronchial mucosa

M. J. Suter, Harvard Medical School (United States) and Wellman Ctr. for Photomedicine, Massachusetts General Hospital (United States); D. R. Riker, Lahey Clinic Medical Ctr. (United States); B. E. Bouma, Harvard Medical School (United States) and Wellman Ctr. for Photomedicine, Massachusetts General Hospital (United States); J. F. Beamis, Jr., Lahey Clinic Medical Ctr. (United States); G. J. Tearney, Harvard Medical School (United States) and Wellman Ctr. for Photomedicine, Massachusetts General Hospital (United States)

Introduction: Lung cancer is the leading cause of cancer related death, and despite recent efforts to reduce the mortality associated with the disease, patient prognosis remains poor with the current 5-year survival rate under 15%. Detection and diagnosis of lesions arising in the bronchial mucosa remains problematic and as a result they are typically well advanced upon discovery.

Methods: We are currently conducting a clinical study aimed at using optical frequency domain imaging (OFDI) to interrogate the bronchial mucosa of patients with the suspicion of lung cancer. During bronchoscopic evaluation, regions of interest suspicious for cancer or precursor lesions were identified and imaged, in addition to regions of normal appearing mucosa. Following OFDI imaging, mucosal biopsies were obtained for histopathologic analysis. Spiral cross-sectional OFDI images were obtained at a rate of 50 frames/sec using a 2.4 Fr catheter (frame size: 1536×1024 ; image resolution: $8 \ \mu m \times 23 \ \mu m \times 100 \ \mu m$).

Results/Conclusions: The layered structure of the normal bronchial mucosa was clearly visualized in the OFDI images including the identification of the epithelium, lamina propria, smooth muscle, perichondrium and cartilage layers. In addition, features such as mucosal vasculature, glands, ducts and alveoli were observed. Various features associated with airway disease were also observed including the presence of fibrous debris, airway inflammation, and lymphatic and blood vasculature remodeling. Based on these preliminary results we anticipate that OFDI imaging of the pulmonary airways will enable the early detection of airway features associated with the development of cancer. When used as a screening tool in high-risk patients we hope that early detection of airway associated cancer with OFDI will result in a decrease in patient mortality.

Acknowledgements: Olympus Corporation, K99 CA134920

7548C-81. Session 2

Endoscopic ICG perfusion imaging for flap transplants: technical development

H. G. Stepp, Ludwig-Maximilians-Univ. München (Germany) No abstract available.

7548C-82, Session 2

Endoscopic ICG perfusion imaging for flap transplants: clinical results

C. S. Betz, Ludwig-Maximilians-Univ. München (Germany) No abstract available. 7548C-83, Session 2

In vivo monitoring of Foscan-mediated photodynamic therapy in clinical head and neck procedures using optical spectroscopy

S. C. Kanick, Univ. Medisch Ctr. Rotterdam (Netherlands); B. Karakullukcu, Antoni van Leeuwenhoek Hospital, Netherlands Cancer Institute (Netherlands); R. L. van Veen, H. J. C. M. Sterenborg, Univ. Medisch Ctr. Rotterdam (Netherlands); I. Bing, Antoni van Leeuwenhoek Hospital, Netherlands Cancer Institute (Netherlands); M. J. Witjes, Univ. Medical Ctr. Groningen (Netherlands); A. Amelink, D. J. Robinson, Univ. Medisch Ctr. Rotterdam (Netherlands)

Photodynamic therapy with m-THPC (Foscan) is as established treatment for superficial squamous cell carcinoma and is also being considered for treatment of larger head and neck tumors. Recently, clinical implementation of Foscan-mediated PDT in the head and neck has not been optimal; a subset of patients has experienced incomplete response. It is well-understood that sufficient quantities of light, drug and oxygen must be present in the targeted tissue in order to deliver sufficient damage. This requirement is complicated by variations in the tissue optical properties and in the photosensitizer uptake rates; however, most clinical protocols do not measure the affect of these factors on the PDT dose delivered to individual patients. This study represents a first step toward incorporating optical techniques developed to monitor PDT treatments in pre-clinical models into the clinical treatment of head and neck cancer.

This clinical study incorporates reflectance and fluorescence spectroscopic measurements are into the PDT-treatment protocol. Spectral analysis allows the extraction of Foscan concentrations and the quantitative determination of tissue physiological parameters that are important to the PDT-delivered dose (e.g. blood volume and hemoglobin saturation). The study identifies the practical and technical challenges of translating these techniques into the clinical setting. Moreover, the data presented here contribute to understanding the link between these optical measurements and the PDT-dose delivered to individual patients during treatment.

7548C-167, Session 2

Fiber-based microendoscopic multiphoton imaging

G. Liu, Beckman Laser Institute and Medical Ctr., Univ. of California, Irvine (United States); B. J. Wong, Univ. of California, Irvine (United States); Z. Chen, Beckman Laser Institute and Medical Ctr., Univ. of California, Irvine (United States)

No abstract available.

7548C-175, Session 2

Multimodality bronchoscopic imaging of airway abnormalities

S. D. Murgu, H. G. Colt, Y. Ahn, M. Brenner, Univ. of California, Irvine (United States)

No abstract available.



7548C-176, Session 2

Utilizing 5-aminolevulinic acid and pulsed dye laser for photodynamic therapy of oral leukoplakia: pilot study

G. Shafirstein, Univ. of Arkansas for Medical Sciences (United States); W. Baeumler, Univ. Clinics Regensburg (Germany); E. Sigel, C. Fan, E. Vural, B. Stack, J. Y. Suen, Univ. of Arkansas for Medical Sciences (United States)

No abstract available.

7548C-177, Session 2

Emerging applications for OCT in the head and neck

M. Rubinstein, J. Kim, W. B. Armstrong, H. R. Djalilian, Univ. of California, Irvine (United States); Z. Chen, B. J. Wong, Beckman Laser Institute and Medical Ctr., Univ. of California, Irvine (United States)

Objectives: To describe the current and promising new applications of the Optical Coherence Tomography (OCT) as a helpful tool when imaging the different sites in the head and neck. Using the OCT Niris system, which is the first commercially available OCT device for applications outside the field of ophthalmology.

Methods: We obtained OCT images of normal, benign, premalignant and malignant lesions in different areas of the head and neck. The OCT imaging system has a tissue penetration depth of approximately 1-2mm, a scanning range of 2mm and a spatial depth resolution of approximately 10-20 m. Imaging was performed using a flexible probe in two different situations, the outpatient clinic and the operating room.

Results: High-resolution cross-sectional images from the larynx were obtained with the patient awake, without the need of general anesthesia. The OCT probe was inserted through the nasal cavity and placed in slightly contact with the laryngeal tissue, under direct visualization with a flexible fiberoptic. Images of other sites, such as the oral cavity, nasal cavity, and ears were also obtained in various settings.

Conclusions: This system is non invasive and easy to incorporate into the operating room as well as to the outpatient clinic. It requires minimal set-up and requires only one person to operate the system. OCT has the distinctive capability to obtain high-resolution images, where the microanatomy of different sites can be observed. OCT technology has the potential to offer a quick, efficient and reliable imaging method to help the surgeon not only in the operating room but also in the clinical setting to guide surgical biopsies and aid in the decision making of different head and neck pathologies, especially those arising form the larynx.

7548C-178. Session 2

Measurement of epithelial thickness within the oral cavity using optical coherence tomography (OCT)

S. Prestin, C. S. Betz, M. Kraft, State Hospital Aarau (Switzerland) and Ludwig-Maximilian Univ. Hospital München (Germany)

No abstract available.

7548C-179, Session 2

Towards early dental caries detetion with OCT and polarized Raman spectroscopy

L. Choo-Smith, National Research Council Canada (Canada)
No abstract available.

7548C-84, Session 3

Feedback controlled laser system for safe and efficient reshaping of nasal cartilage

E. Sobol, A. Sviridov, N. Vorobieva, Institute of Laser and Information Technologies (Russian Federation); V. Svistushkin, Vladimirskiy Research and Clinical Institute of Moscow Region (Russian Federation)

In 1992, we identified laser-induced stress relaxation in cartilage. This led to the development of a new laser application in otolaryngologyhead and neck surgery for the non-ablative reshaping of cartilage. Laser septochondrocorrection is non-invasive, bloodless, painless procedure which takes only 10 minutes to complete and can be performed in outpatient settings.

The efficacy and safety of this technology can be guarantied with the feed back control system measuring temperature and stress distribution in the course of laser treatment. The paper presents recent results of the research and clinical applications of the technology and equipment for laser reshaping of cartilage in the ENT. The new equipment LSC-701 (Arcuo Medical Inc., USA) for laser reshaping of nasal cartilage includes an Erbium doped glass fiber laser (1.56 micrometers in wavelength), special instrument and feedback control system which allow to correct laser settings in the course of laser treatment and to stop the laser when the procedure is completed. The laser technology and equipment are certificated by the Federal Service on Surveillance in Healthcare and Social Development of Russian Federation. The laser septocorrection using LSC-701 has been performed for 120 patients at the ENT Clinics of the Sechenov Medical Academy of Moscow and at the Vladimirskiy Research and Clinical Institute of Moscow Region (MONIKI). The positive results were obtained for 95 percent of the patients in two years follow up. No age limitation (for the patients from 12 until 68 years), no complications and negative secondary effects were observed.

7548C-85, Session 3

Methods for evaluating changes in cartilage stiffness following electromechanical reshaping

A. Lim, D. E. Protsenko, B. J. Wong, Beckman Laser Institute and Medical Ctr. (United States)

One component of several otolaryngological surgeries is the reshaping of cartilage. Several previous studies have demonstrated the efficient achievement of this procedure through electromechanical reshaping (EMR), a technique that involves the direct application of voltage to cartilage mechanically deformed in a jig. Two main parameters, voltage and application time, may be varied to achieve varying degrees of shape change. Both maximized shape change and minimized intrinsic tissue damage determine the ideal parameters for EMR. In preceding research, EMR parameters were correlated with degree of shape change. However, it remains necessary to correlate the same parameters with the degree of change in the mechanical properties of tissue. This study satisfies this need by providing comprehensive data on the pre- and post-EMR stiffness of both septal and auricular cartilage over a range of voltages with constant application time (2-8V, 2min, and 2-8V, 3min, respectively). EMR was applied using flat platinum electrodes to one of two 15 mm X 5 mm samples obtained from the same cartilage specimen, while

23

Return to Contents TEL: +1 360 676 3290 · +1 888 504 8171 · customerservice@spie.org



the second sample was maintained as a control. Following a 15 min rehydration period, the Young's modulus of the tissue was calculated for both the control and experimental sample from data obtained through a uniaxial tension test. A general reduction in stiffness was observed from beginning at 3V, with the magnitude of reduction increasing at 6V.

7548C-86, Session 3

Using optical coherence tomography to monitor effects of electromechanical reshaping in septal cartilage

H. Chen, Univ. of Southern California (United States) and University of California, Irvine (United States); L. Yu, C. Manuel, B. J. Wong, University of California, Irvine (United States)

Electromechanical reshaping (EMR) of cartilage is a promising noninvasive technique with potential for broad application in reconstructive surgery. EMR involves applying direct current electrical fields to localized stress regions and then initiating a series of oxidationreduction reactions, thus effecting a shape change. Previous EMR studies have focused on macroscopic structural measurements of the shape change effect or monitoring of electrical current flow. Only limited investigation of structural changes in the tissue at the histologic level have been performed, and not in real time. This study is the first to use optical coherence tomography (OCT) to examine structural changes in cartilage during EMR. Two platinum needle electrodes were inserted into fixed rectangular rabbit nasal septal cartilage specimens. The spectral domain OCT probe was then positioned above the anode needle. A constant voltage of 6V was applied for 3 minutes, and images were obtained (8 frames/second). OCT was also performed in specimens undergoing dehydration under ambient conditions and during pH changes produced by the addition of HCl, as both processes accompany EMR. The OCT data identified distinct findings among the three conditions, suggesting that EMR causes a much greater degree of reshaping on a molecular level than dehydration or a change in pH alone. OCT provides a means to gauge structural changes in the tissue matrix during EMR. The application of OCT to image the EMR process will add to our understanding of the mechanisms of action involved and potentially facilitate optimization of this process.

7548C-87, Session 3

Comparison of bend angle measurements in fresh cryopreserved cartilage specimens after electromechanical reshaping

K. Karimi, D. Protsenko, E. Wu, A. Foulad, C. Manuel, B. J. Wong, Beckman Laser Institute and Medical Ctr. (United States)

Cryopreservation of cartilage has been investigated for decades and is an established protocol. However, the reliability and application of cryopreservation of cartilage for use in electromechanical reshaping (EMR) has not been studied exclusively. A system to cryopreserve large amounts of tissue provides a steady source of similar quality cartilage for future experimentation. This will reduce error that may arise from different cartilage stock, and have the potential to maximize efficiency under time constraints. Our study utilizes a unique methodology to cryopreserve septal cartilage for use in electromechanical reshaping studies. Septal cartilages were extracted and placed in one of three solutions (Saline, PBS, and 10% DMSO by volume in PBS) for four hours in a cold room. Then, each cartilage specimen was vacuumed and sealed in an anti-frost plastic bag and placed in freezer for 1 to 3 week durations. EMR was performed using 2 volts for 2 minutes to create a bend. Bend angle measurements of the cryopreserved cartilage specimens were compared to the bend angles of fresh cartilage which underwent EMR using the same parameters. Results demonstrate that Saline, PBS, and DMSO were effective in cryopreservation, and indicated no significant differences in bend angle measurements. Our methodology to cyropreserve cartilage specimens provides a successful approach for use in electromechanical reshaping studies.

7548C-88, Session 3

Monitoring of electrical current in rabbit and porcine cartilage tissue during electromechanical reshaping

C. Manuel, A. Foulad, D. Protsenko, B. J. Wong, Beckman Laser Institute, Univ. of California, Irvine (United States)

Electro Mechanical Reshaping (EMR) with platinum needle electrodes has been recently developed to shape cartilage without conventional cut and suture surgery. This study investigates the relationship between the voltage applied, the electrical current measured during EMR with platinum needles, and the resulting shape. Monitoring the electrical current provides information to model the electro-chemistry, which will aid in determining the onset of shape stabilization. Rabbit septal, rabbit auricular, porcine auricular, and porcine costal grafts were bent into a 90° angle using a moulage. Platinum needle electrodes were then placed in contact with the cartilage and a constant voltage was applied for a set time. The electrical current was measured during the process and total charge transferred was calculated. The cartilage specimen was then removed from the jig and photographed after one minute in order to determine the resulting bend angle. Results show that a higher current in tissue is produced with increasing applied voltage. Each current trace is unique and is dependent on tissue thickness and inter-electrode distances. Understanding the electrical current process ultimately leads to optimizing EMR and feedback control. Voltage, for example, could be varied in real-time during EMR to produce a constant chemical reaction rate and potentially reduce total tissue dehydration in contact with electrodes. In conclusion, electric current traces provide information about chemical kinetics during EMR that depend on exposure settings, and monitoring these traces is an important step in optimizing the reshaping process.

7548C-89, Session 3

Numerical analysis of costal cartilage warping after laser modification

A. Foulad, C. Manuel, B. J. Wong, Beckman Laser Institute, University of California Irvine (United States)

Grafts obtained from peripheral regions of costal cartilage have an inherent tendency to warp over time. Laser irradiation provides a potential method to control the warping process, thus yielding stable grafts for facial reconstructive surgery. In our current study, we propose a simple and well-fitting model that numerically describes the degree of warping of laser irradiated costal cartilage grafts. Using an Nd:YAG laser (lambda=1.32 μm) at various exposure settings, grafts harvested from the peripheral regions of porcine costal cartilage were irradiated. The resulting graft geometry was fitted to a curve using a quadratic regression model. The coefficient of determination demonstrated a very strong fit for all grafts modeled. A quadratic regression is simple to perform and results in a single numerical value that appropriately describes the degree of cartilage warping. Our proposed model is valuable in assessing the effect of laser irradiation on the warping process of costal cartilage.

7548C-90, Session 3

A laser device for fusion of nasal mucosa

M. C. Larson, V. Sooklal, J. McClure, L. Hooper, J. Sieber, Univ. of Colorado at Colorado Springs (United States)

A patent pending device has been created, and successfully used, to fuse tissue membranes as an alternative to sutures or staples. The joining, or coaptation, is accomplished through the controlled application of laser heating to induce protein denaturation and subsequent renaturation across the interface. Lasers have been used by a number of researchers to close wounds in controlled laboratory tests over the



last 15 years. Many encouraging results have been obtained; however, no commercial delivery systems are currently available. This is due primarily to two factors: requiring an inordinate amount of experience on the part of the operator to detect changes in tissue appearance, and attempting to achieve general applicability for multiple tissue systems. The present device overcomes these barriers as it is tailored for the particular application of septal laser fusion, namely for the coaptation of mucoperichondrial membranes.

The important parameters involved in fusing biological tissues using radiation from laser sources are identified. The development of the device followed from computational modeling of the fusion process based on engineering first-principles from heat transfer, fluid dynamics and optics, and from experimental results on a particular tissue system. The experiments were designed and analyzed using orthogonal arrays, employing a subset of the relevant parameters, i.e., laser irradiance, dwell time and spot size, for a range of wavelengths. The in vitro fusion experiments employed 1cm by 1cm sections of equine nasal mucosa having a nominal thickness of 1mm.

7548C-91, Session 4

Ten years of experience with photodynamic therapy of early oral cavity and oropharynx cancers: a retrospective report of 170 patients

B. Karakullukcu, K. van Oudanaarde, M. Wildeman, M. Klop, B. Tan, A. van Leeuwenhoek, The Netherlands Cancer Institute (Netherlands)

No abstract available.

7548C-92, Session 4

The role of photodynamic therapy in the management of oral dysplasia

C. Hopper, Univ. College London Hospitals NHS Foundation Trust (United Kingdom); W. K. Jerjes, Z. Hamdoon, T. Upile, Univ. College Hospital (United Kingdom)

No abstract available.

7548C-93, Session 4

Photodynamic therapy of laryngeal cancers

M. A. Biel, Virginia Piper Cancer Institute, Abbott Northwestern Hospital (United States)

Carcinoma of the larynx accounts for 25-30 percent of all carcinomas of the head and neck. Early carcinomas of the larynx (Tis or T1) and severe dysplasia are presently treated with either radiation therapy or surgery alone. Radiation therapy, however, has significant disadvantages including mucositis during and for potential prolonged periods after therapy, permanently altered voice quality, dysphagia, chondroradionecrosis of the larynx and trachea, and the extensive length of therapy (6-7 weeks). Surgical therapy for early carcinomas of the larynx includes performing a partial cordectomy or hemilaryngectomy. Although cure rates are high, surgical removal of portions of the vocal cord or hemilarynx results in significant alteration of the quality of voice.

Photodynamic therapy has been demonstrated to be effective in the treatment of early carcinomas of the larynx, Tis and T1, with cure rates of 90% with followup to 236 months. The advantage of PDT therapy for early carcinomas of the larynx is the ability to preserve normal endolaryngeal tissue while effectively treating the carcinomas. This results in improved laryngeal function and voice quality. Furthermore, PDT requires a short duration of therapy as compared to radiation

therapy, is repeatable and carries less risk than surgical therapy and is performed as an outpatient noninvasive treatment. Importantly, the use of PDT does not preclude the use of radiotherapy or surgery in the future for new primary or recurrent disease.

7548C-94, Session 4

Ultrasound-guided interstitial photodynamic therapy for deeply seated pathologies: assessment of outcome

J. Osher, W. K. Jerjes, T. Upile, Z. Hamdoon, F. Nhembe, R. Bhandari, S. Mackay, P. Shah, Univ. College Hospital (United Kingdom); C. A. Mosse, Univ. College London (United Kingdom); S. Morley, Univ. College Hospital (United Kingdom); C. Hopper, Univ. College London Hospitals NHS Foundation Trust (United Kingdom)

No abstract available.

7548C-180, Session 4

Photochemical internalization

W. K. Jerjes, T. Upile, Univ. College Hospital (United Kingdom); C. A. Mosse, M. R. Austwick, Univ. College London (United Kingdom); Z. Hamdoon, D. Carnell, Univ. College Hospital (United Kingdom); K. Berg, Oslo Univ. Hospital (Norway); A. Høgset, PCI Biotech AS (Norway); S. G. Bown, C. Hopper, National Medical Laser Ctr. (United Kingdom)

No abstract available.

7548C-184, Session 4

Non-invasive measurement of photosensitiser concentration using fluorescence differential path-length spectroscopy: validation for different liposomal formulations of m-THPC: Foscan, Foslip and Fospeg

S. A. de Visscher, M. J. Witjes, Univ. Medical Ctr. Groningen (Netherlands); S. Kascáková, D. J. Robinson, H. J. C. M. Sterenborg, Univ. Medisch Ctr. Rotterdam (Netherlands); J. L. N. Roodenburg, Univ. Medical Ctr. Groningen (Netherlands); A. Amelink, Univ. Medisch Ctr. Rotterdam (Netherlands)

As previously described, Fluorescence differential path length spectroscopy (FPDS) can determine chromophore concentrations non-invasively after injection with m-THPC (Foscan) in the rat liver (1). Our first aim is to validate FDPS for two other, liposomal formulations of m-THPC; pegylated liposomes (Fospeg) and conventionel liposomes (Foslip), and compare them to Foscan. As a proof of principle we use the highly vascularised, optically homogenous liver of the rat (1). Validation of the FDPS-measurements was done by chemical extraction of the same liver (2).

Our second aim is to validate FDPS measurements of the tongue, which is optically less homogenous, but clinically more relevant. After successful validation in both liver and tongue tissue, the pharmacokinetic-profile in other tissue types could be assessed by FDPS alone. Therefore, FDPS can lower the need for labour-intensive chemical extraction.

Fifty-four male Wistar rats were intravenously injected with one of the three formulations of m-THPC; eighteen rats for each formulation. All rats were injected with 0.15 mg kg m-THPC. FDPS measurements

TEL: +1 360 676 3290 · +1 888 504 8171 · customerservice@spie.org



were performed on liver, palate, tongue, spleen and kidney 2, 4, 8, 24, 48, and 96 h after m-THPC administration. For validation of our FDPS measurements, liver and tongue were harvested for chemical extraction (2). Concentration estimates in liver and tongue measured by FDPS are here compared with chemical extraction.

At the HNODS-meeting we will present the results of our first step in the validation of FDPS; the correlation of FDPS measurements with chemical extraction for the three different formulations in the liver.

- 1. In vivo quantification of chromophore concentration using fluorescence differential path length spectroscopy. Kruijt B, Kascakova S, de Bruijn HS, van der Ploeg-van den Heuvel A, Sterenborg HJ, Robinson DJ, Amelink A. J Biomed Opt. 2009 May-Jun;14(3):034022.
- 2. Ex vivo quantification of mTHPC concentration in tissue: influence of chemical extraction on the optical properties. Kascáková, S; Kruijt, B; de Bruijn, HS; van der Ploeg-van den, Heuvel A; Robinson, DJ; Sterenborg, HJ; Amelink, A. J Photochem Photobiol B. 2008 May 29;91(2-3):99-107. Epub2008 Feb 19.

7548C-71, Session 5

An optical coherence tomography study for imaging the round window niche and the promontorium tympani

T. Just, Univ. Rostock (Germany); E. M. Lankenau, G. Hüttmann, Univ. zu Lübeck (Germany); H. W. Pau, Univ. Rostock (Germany)

Tympanosclerosis may involve the tympanic membrane, the ossicles, as well as the oval and round window niche, respectively. The surgical treatment of the obliterated oval window niche is most challenging. Beside stapesplasty, vibroplasty with coupling the floating mass transducer (FMT) onto the round window niche and into a new, socalled third window is indicated. In the latter situation, drilling a hole into the promontorium is necessary to couple the FMT close to the membranous endosteum. Any damage of the membranous inner ear needs to be avoided. The question was whether OCT is useful to identify the endosteum and to provide microanatomical information about the round window niche. OCT was carried out on human temporal bone preparations in which a third window was drilled, while leaving the membranous labyrinth and the fluid-filled inner ear intact and removing the overhang of the round window niche. A specially equipped operating microscope with integrated OCT prototype (spectral-domain-OCT) was used. The OCT images and 3D reconstructions demonstrate the usefulness of OCT to measure the drilling cavity, to visualize the inner ear structures, and to obtain microanatomical information about the round and oval window niche. These findings may have an impact on stapes surgery, on cochlea implantation, and on vibroplasty with coupling the FMT onto the round and third window. OCT-guided drilling allows identification of the intact inner ear more precisely.

7548C-96, Session 5

Photodynamic therapy as the "last hope" for tongue-based carcinoma

W. K. Jerjes, T. Upile, Z. Hamdoon, F. Nhembe, R. Bhandari, S. Mackay, Univ. College Hospital (United Kingdom); C. A. Mosse, Univ. College London (United Kingdom); S. Morley, Univ. College Hospital (United Kingdom); C. Hopper, Univ. College London Hospitals NHS Foundation Trust (United Kingdom)

No abstract available.

7548C-97, Session 5

The effect of PDT on H. influenza biofilm in vivo

C. Rhee, S. Chang, P. Chung, J. Jung, J. Ahn, M. Suh, Dankook Univ. Hospital (Korea, Republic of)

Biofilm formation has been demonstrated for many mucosal pathogens such as Haemophilus influenzae. The presence of mucosal biofilms with chronic otitis media with effusion (COME) suggests that bacteria do not clear by antibiotics. Aim: To test the effect of photodynamic therapy (PDT) on H. influenzae induced biofilm in vivo. Methods: Sixteen bullae of 8 gerbils were injected with 200µl (107CFU/ml) of H. influenza and formation of biofilms in the bullae was obtained by 5 days. The bullae were divided into control, laser, photofrin, and PDT groups. The control group received no treatment. For laser group, 120 J/cm2 (100 mw x 20 min) of 632 nm LD laser was irradiated into the bullae by a fiber inserted directly into the bullae. For photofrin group, photofrin 40µl (1mg/ ml) were injected into the bullae. For PDT group, photofrin same as in photofrin group was injected into the bullae and LD laser was irradiated into the bullae same way as in laser group. The mucosal tissues in bullae were examined by H/E staining, and SEM. Results: The control, laser, and photofrin groups have shown well formed biofilm. Two third of the PDT group bullae have shown well resolved biofilm while 1/3 of the bullae have shown incompletely resolved biofilms. Conclusion: The results of this study demonstrated that PDT appears to be effective to treat experimental H. influenzae induced biofilms in vivo. Further trial in different dose combinations of photosensitizer and laser needs to be tried for better results in PDT group. Clinical implication: PDT may be an alternative to antiobiotic treatment on otitis media with biofilm formation.

7548C-98, Session 5

Toward endoscopic ultrafast laser microsurgery of vocal folds

A. Ben-Yakar, C. L. Hoy, W. N. Everett, The Univ. of Texas at Austin (United States); J. Kobler, Massachusetts General Hospital (United States)

Vocal fold scarring can arise from disease or post-surgical wound healing and is one of the predominant causes of voice disorders. Focused ultrafast laser pulses have been previously demonstrated to create tightly confined sub-surface ablation in a variety of tissue, including vocal folds. Here, we demonstrate how we can take advantage of this unique ability of ultrafast laser ablation to create sub-surface vocal fold microsurgeries with a goal for eventually creating a plane in tough sub-epithelial scar tissue into which biomaterials can be injected. Specifically, we create sub-epithelial ablations in vocal fold tissue in under 1 minute using subμJ pulses from a compact, commercially available amplified ultrafast laser system from Raydiance Inc., operating at a 500 kHz repetition rate. The use of relatively high repetition rates, with a small number of overlapping pulses, is critical to achieving ablation in reasonable amounts of time while still avoiding significant heat deposition. Additionally, we use multiphoton fluorescence of the ablation region and SHG imaging of collagen fibers to obtain visual feedback of tissue structure and confirm successful ablation. Lastly, we demonstrate microsurgery using amplified ultrafast laser pulses delivered through over 1 meter of air-core photonic crystal fiber to a laser scanning microsurgery probe, illustrating the feasibility of developing an ultrafast laser surgical laryngoscope. We aim to further develop this clinical tool through demonstration of laryngeal microsurgery using a compact laser system in conjunction with a larynxspecific fiber-based surgery probe.



7548C-99, Session 5

Femtosecond laser microstructuring and bioactive nanocoating of titanium surfaces in relation to chondrocyte growth

J. F. R. Ilgner, S. Biedron, Univ. Hospital Aachen (Germany); E. Fadeeva, B. Cichkov, Laser Zentrum Hannover e.V. (Germany); D. Klee, RWTH Aachen (Germany); A. Loos, E. Sowa-Soehle, Medizinische Hochschule Hannover (Germany); M. Westhofen, Univ. Hospital Aachen (Germany)

Introduction: Titanium implants can be regarded as the current gold standard for restoration of sound transmission in the middle ear following destruction of the ossicular chain by chronic inflammation. Many efforts have been made to improve prosthesis design, while less attention had been given to the role of the interface. We present a study on chemical nanocoating on microstructured titanium contact surface with bioactive protein.

Materials and Methods: Titanium samples of 5mm diameter and 0,25mm thickness were structured by means of a Ti:Sapphire femtosecond laser operating at 970nm with parallel lines of 5µm depth, 5µm width and 10µm inter-groove distance. In addition, various nanolayers were applied to PVDF foils, while bone matrix protein 7 (BMP-7) was linked to the outer coating layer.

Results: Chondrocytes could be cultured on microstructured surfaces without reduced rate of vital / dead cells compared to native surfaces. Chondrocytes also showed contact guidance by growing along ridges particularly on 5µm lines. On PVDF foils, chondrocyte growth was doubled in contact with BMP-7 compared to hydrogel layer or native surface. Discussion: According to these results, relative preference for cell growth on titanium prosthesis contact surfaces compared to non-contact surfaces (e.g. prosthesis shaft) can be achieved by nanocoating. Relative selectivity induced by microstructures for growth of chondrocytes compared to fibrocytes is subject to further evaluation.

7548C-100, Session 5

Laser hearing aids

G. I. Wenzel, Medizinische Hochschule Hannover (Germany); H. H. Lim, Medizinische Hochschule Hannover (Germany) and Univ. of Minnesota (United States); K. Zhang, Laser Zentrum Hannover e.V. (Germany); S. Balster, Medizinische Hochschule Hannover (Germany); O. Massow, H. Lubatschowski, Laser Zentrum Hannover e.V. (Germany); G. Reuter, T. Lenarz, Medizinische Hochschule Hannover (Germany)

Visible light is a source of energy known to activate the visual system through absorption by photoreceptors in the eye. When the so-called stress-confinement condition is fulfilled, laser light can induce an acoustic signal through an optoacoustic effect. We sought to assess, if visible light with parameters that induce an optoacoustic effect (i.e., 532 nm, 10 ns pulses) could be used to stimulate the peripheral hearing organ at ear drum and middle ear level.

Auditory brainstem responses (ABRs) were recorded preoperatively in anesthetized guinea pigs to confirm normal hearing. After opening the bulla, a 50-µm core-diameter optical fiber was positioned first in the outer ear canal directed towards the tympanic membrane and then within the bulla directed towards the bony structures within the middle ear as well as towards the round window membrane.

Optically-induced ABRs (OABRs), similar in shape to those of acoustic stimulation, were elicited with single pulses after stimulation within the outer as well as the middle ear. The OABR peaks increased with energy level (0.6-23 µJ/pulse) but varied in magnitude depending on the location of stimulation

Our findings demonstrate that visible light can be used to activate the peripheral hearing organ when applied at the ear drum level or on bony

structures within the middle ear that can transmit vibrations to the cochlea or inner ear.

We propose that this novel, non-contact laser stimulation method could be used to improve implantable and non-implantable hearing aids as well as for research purposes.

7548C-101, Session 5

CO2 laser myringoplasty using a handheld waveguide

D. M. Kaylie, J. Miller, Duke Univ. Medical Ctr. (United States)

Introduction: Eustachian tube dysfunction is very common and is the predominant cause of otitis media with effusion. Negative middle ear pressure generated by Eustachian tube dysfunction can cause deformation of the collagen layer in the ear drum. Collagen becomes stretched and looses its orderly array. Over time, deep retraction pockets form. If left untreated, the tympanic membrane becomes prone to cholesteatoma formation. CO2 laser energy interacts with collagen and causes it to return to its natural configuration.

Objective: To describe and review our results treating tympanic membrane retraction pockets using laser myringoplasty with a novel hand-held flexible photonic band gap fiber CO2 laser.

Methods: A hand-held flexible fiber CO2 laser system (Omniguide BeamPath) was used to treat tympanic membrane retraction pockets. The fiber tip was held approximately 3mm from the membrane surface producing a spot size of 570 microns at the setting of 2 watt per 100 millisecond pulse. Pulses were administered until the desired level of membrane contraction was achieved. A tympanostomy tube was then placed in the affected ear.

Results: We reviewed our results with this procedure on 22 patients (40 ears). The average pre-operative air bone gap (ABG) pure-tone average (PTA) was 15 dB. The average post-operative ABG PTA was 6 dB (p=0.002). All patients had satisfactory contraction of the atelectatic segment. There were no adverse events recorded.

Conclusion: Laser myringoplasty using the Omniguide hand-held flexible fiber CO2 laser provides immediate hearing improvement and eardrum contraction. Long-term results are pending.

7548C-102, Session 5

The use of CO2 laser in tumour resection of the oropharyngeal region

T. Upile, W. K. Jerjes, Z. Hamdoon, Univ. College Hospital (United Kingdom); C. Hopper, Univ. College London Hospitals NHS Foundation Trust (United Kingdom)

No abstract available.

7548C-103, Session 5

CO2 laser ablation of oropharyngeal dysplasia

T. Upile, W. K. Jerjes, Z. Hamdoon, Univ. College Hospital (United Kingdom); C. Hopper, Univ. College London Hospitals NHS Foundation Trust (United Kingdom)

27

No abstract available.

Return to Contents TEL: +1 360 676 3290 · +1 888 504 8171 · customerservice@spie.org



7548C-169, Session 5

CO2 laser transoral laser microsurgery of head and neck cancer: lessons learned over ten years

W. B. Armstrong, Univ. of California, Irvine (United States); M. Rubinstein, Beckman Laser Institute and Medical Ctr., Univ. of California, Irvine (United States)

No abstract available.

7548C-171, Session 5

Lasers, a tool for soft cochleostomies

A. J. Fishman, Feinberg School of Medicine, Northwestern Univ. (United States) and National Naval Medical Ctr. (United States); L. E. Moreno, Feinberg School of Medicine, Northwestern Univ. (United States); A. Rivera, National Naval Medical Ctr. (United States); C. Richter, Feinberg School of Medicine, Northwestern Univ. (United States) and National Naval Medical Ctr. (United States)

Advancements in implantable auditory prostheses now demand preservation of residual auditory function following the surgery. Atraumatic cochleostomy formation is essential to this goal. Clinically reported hearing outcomes in human implantation are still quite variable in this regard. The objective of the study was to determine whether a CO2 laser operated with a handheld hollow waveguide can consistently produce cochleostomies without damaging the residual auditory function.

Human temporal bones were used to present a novel method creating a cochleostomy and adult guinea pigs were used to test whether cochlear function will be affected by the procedure. Baseline cochlear function was determined by recording compound action potential thresholds evoked by acoustic tone pips. Measurements were conducted at 6 steps per octave and 5 octaves starting at 50 kHz. The sound level as attenuated from 0 to 80 dB in steps of 5 dB.

The human temporal bones were mounted and a standard approach through the facial recess was used to access the cochlea. The lateral bone was thinned at the basal turn with a motorized drill (Anspach Effort®, Palm Beach Gardens, FL, USA). Care was taken not to open the cochlea. The final opening of scala tympani was made with the handheld CO2 laser fiber (BeamPath® OTO-S, OmniGuide® Inc., Cambridge, MA, USA) and a Sharplan 20C CO2 laser (Lumenis®, Yokneam, Israel).

In addition to describing the surgical approach, our experiments have demonstrated that for a careful selection of the laser's power, the safety range for the laser is superior to the safety range of drilling. Particularly important is the finding that multiple laser pulses through the same cochleostomy do not further increase the initial compound action potential (CAP) threshold elevation. Moreover, multiple laser pulses at different locations of the cochlea do not further increase the initial CAP threshold elevation observed after the first laser pulse. When opening the inner ear, safe laser settings would be up to 4 W, at pulse durations of 100 ms in single pulse mode.

7548C-181, Session 5

Treatment planning for interstitial photodynamic therapy for head and neck cancer

R. L. P. van Veen, D. J. Robinson, H. J. C. M. Sterenborg, Univ. Medisch Ctr. Rotterdam (Netherlands); J. B. Aans, Erasmus MC (Netherlands); I. B. Tan, F. Hoebers, Het Nederlands Kanker Instituut (Netherlands); M. J. Witjes, Univ. Medisch Ctr. Groningen (Netherlands); P. C. Levendag, Erasmus MC (Netherlands)

No abstract available.

7548C-182, Session 5

Laser interactive thermal therapy for head and neck lesions

G. Shafirstein, G. Richter, L. Buckmiller, J. Y. Suen, Univ. of Arkansas for Medical Sciences (United States)

No abstract available.



Conference 7548D: Diagnostic and Therapeutic Applications of Light in Cardiology

Saturday 23 January 2010 • Part of Proceedings of SPIE Vol. 7548 Photonic Therapeutics and Diagnostics VI

7548D-104, Session 1

Contour mapping of the chemical composition within human coronary artery via intravascular Raman spectroscopy

J. Nazemi, J. F. Brennan III, Prescient Medical, Inc. (United States); G. M. Sangiorgi, Univ. of Modena and Reggio Emilia (Italy); A. Mauriello, Univ. of Rome Tor Vergata (Italy)

The concentrations of lipids in human coronary artery can be estimated accurately with high wavenumber-shifted Raman spectra, which can be measured through a single optical fiber. Building upon these findings, we developed an intravascular catheter system that can measure spectra from the full lumen of a given coronary artery. These spectra can be processed to produce maps of chemical concentrations, such as cholesterol and esterified cholesterol, within an arterial wall. To assess this catheter system, we gathered spectra during pullback procedures in several coronary artery segments and correlated the mappings with histology. Human coronary artery segments were dissected from donor hearts within 24 hours after death, snap-frozen, and stored at -80 °C until use. After the segments were thawed, an intravascular Raman diagnostic catheter was positioned distally within an artery segment, and then the sensors were illuminated. The initial sensor position was marked with ink, and the catheter was withdrawn at 0.5 mm/s, sampling the artery every 250 um along its length and at 8 locations spaced circumferentially around the artery. The spectra were processed according to previouslyestablished algorithms to estimate the concentrations of cholesterol, esterified cholesterol, triglycerides, and protein, and the information was displayed as contour maps of chemical concentrations within arterial segments. The coronary segments were sectioned at fixed intervals and examined by a pathologist to determine the tissue morphology. We compared the Raman-derived contour maps to the artery morphology and found that the locations of plagues correlated well with increased concentrations of cholesterol and cholesterol esters.

7548D-105, Session 1

A steerable IVUS guided multimodal catheter for in vivo time-resolved fluorescence spectroscopy

H. Xie, D. N. Stephens, Y. Sun, Y. Sun, L. Marcu, Univ. of California, Davis (United States)

This study is to develop a multi-modal intravascular diagnostic technique integrating time-resolved fluorescence spectroscopy (TRFS) and intravascular ultrasonography (IVUS) to provide combined compositional and structural characterization of atherosclerotic plaques. We demonstrate the design of a prototype catheter (5.4 Fr) combining a 400 µm side-viewing optical fiber (SVOF) with 3.2 Fr 30 MHz IVUS probe. The hybrid catheter can locate a fluorophore mounted on a stent in vivo vessel wall, perform water flushing in flowing blood, and acquire consistent TRFS emission induced with pulsed UV laser excitation. The steering capability of the catheter allows for the co-registration of the site location of the TRFS measurement with the IVUS image plane. The performance of the catheter were evaluated in pig arteries in vivo (n=3) for the intravascular investigation. The resulting fluorescence spectrums from the pig arteries were proved to be consistent with the pig arterial wall composition and the retrieved average lifetime is relatively independent of blood interference. Co-registration of aligning the IVUS image plane and the SVOF beam was evaluated successfully by using a 0.8 mm fluorophore mounted on a 7 mm billiary stent, resulting in a guiding precision of 0.23 ± 0.12 mm to the site location on the pig arterial wall. A catheter pull-back procedure in vivo is also demonstrated using

real-time TRFS acquisition method, suggesting that TRFS measurement can be obtained in vivo at distances from the arterial wall up to 0.5 mm. Current results support the conclusion that this multi-modal catheter can be applied to clinical diagnosis of the intravascular atherosclerotic plaque under IVUS guidance.

7548D-106, Session 1

Endoscopic FLIM images of carotid plaque: an automated classification method

J. E. Phipps, N. Hatami, Y. Sun, R. Saroufeem, L. Marcu, Univ. of California, Davis (United States)

The objective of this study is to develop an automated algorithm which uses fluorescence lifetime imaging microscopy (FLIM) images of human carotid atherosclerotic plaque to provide quantitative and spatial information regarding compositional features related to plaque vulnerability such as collagen degradation, lipid accumulation, and macrophage infiltration. Images from human carotid plaques have been acquired through a flexible fiber imaging bundle with intravascular potential at three wavelength bands optimal to recognize markers of vulnerability: f1: 377/55 nm, f2: 460/50 nm, and f3: 510/80 nm (center wavelength/bandwidth). An automated algorithm segments groups of similar pixels then calculates ratios of spectroscopic parameters derived from the FLIM measurements to determine chemical composition. Correlations with histopathology are analyzed and statistical significance is calculated with an ANOVA analysis. For example (results given as mean +/- standard error), calculating a ratio of average fluorescence lifetimes from f1 and f2 distinguishes elastin-rich (1.60 +/- 0.1) from lipid-rich regions (1.30 +/- 0.1); a ratio of fluorescence intensity from f1 and f3 distinguishes collagen-rich (0.60 +/- 0.12) from lipid-rich regions (1.05 +/- 0.05); a ratio of a deconvolution parameter from f1 and f3 distinguishes collagen-rich (0.90 +/- 0.05) from lipid-rich regions (1.10 +/-0.06). The algorithm finally displays a false-color image with each pixel representative of varying amounts of elastin, collagen, and lipid content. The capability of this algorithm to use FLIM images to quickly determine the chemical composition of atherosclerotic plaque, particularly related to vulnerability, further enhances the potential of this system for implementation as an intravascular diagnostic modality.

7548D-107, Session 1

Raman spectroscopy for atherosclerotic plaque characterization

A. H. Chau, Massachusetts Institute of Technology (United States) and Massachusetts General Hospital (United States); J. A. Gardecki, B. E. Bouma, G. J. Tearney, Massachusetts General Hospital (United States) and Harvard Medical School (United States)

Raman spectroscopy is a promising technique for evaluating atherosclerotic plaque composition, yielding detailed information about the chemical composition of the arterial wall. While most biological applications of Raman spectroscopy have been performed in the "fingerprint" region (Raman shifts between 400 and 1800 1/cm), the high wavenumber region (2700-3100 1/cm) offers distinct technical advantages, including increased Raman signal relative to the fluorescent background and potentially less fiber background. However, the high wavenumber region may yield different molecular information and thus have different diagnostic capability. In this talk, we present a benchtop Raman system capable of acquiring Raman spectra in both wavenumber regions. In contrast to previous work, which focused on

Conference 7548D: Diagnostic and Therapeutic Applications of Light in Cardiology



plaque characterization based on the Raman spectrum from a single site within the plaque, our system utilizes a line scanning paradigm, in which Raman spectra are acquired at fixed intervals across the full cross-section of the plaque. Using the benchtop Raman system, we have acquired a database of Raman line scans and corresponding histology for over sixty plaque specimens. Using this database and a chemical basis spectra model, we compare the diagnostic capability of fingerprint and high wavenumber Raman spectroscopy for plaque characterization. By examining fit coefficient profiles for Raman line scans, it is possible to determine the presence and size of an atherosclerotic lesion.

7548D-108, Session 1

Non-thermal ablation technology for arrhythmia therapy: acute and chronic electrical conduction block with photosensitization reaction

A. Ito, H. Matsuo, T. Suenari, T. Kajihara, Keio Univ. (Japan); T. Kimura, S. Miyoshi, Keio Univ. School of Medicine (Japan); T. Arai, Keio Univ. (Japan)

We have examined the possibility of non-thermal ablation technology for arrhythmia therapy with photosensitization reaction, in which photochemically generated singlet molecular oxygen may induce myocardial electrical conduction block. In the most popular energy source for arrhythmia catheter ablation; radiofrequency current, the thermal tissue injury causes electrophysiological disruption resulting in electrical isolation of ectopic beats. The temperature-mediated tissue disruption is difficult to control because the tissue temperature is determined by the heating and thermal conduction process, so that severe complications due to excessive heat generation have been the problem in this ablation. We demonstrated the electrical conduction block of surgically exposed porcine heart tissue in vivo with photosensitization reaction. The acute myocardial electrical conduction block was examined by the stimulation and propagation set-up consisting of a stimulation electrode and two bipolar measurement electrodes. Fifteen to thirty minutes after the injection of 5-10 mg/kg water-soluble chlorin photosensitizer, talaporfin sodium (NPe6, LS11), the laser light at the wavelength of 663 nm with the total energy density of 50-200 J/cm2 was irradiated several times with 3 mm in spot-size to make electrical block line in myocardial tissue across the conduction pathway between the bipolar measurement electrodes. The propagation delay time of the potential waveform increased with increasing the irradiated line length. The observation of Azan-stained specimens in the irradiated area two weeks after the procedure showed that the normal tissue was replaced to the scar tissue, which might become to be permanent tissue insulation. These results demonstrated the possibility of non-thermal electrical conduction block for arrhythmia therapy by the photosensitization reaction.

7548D-109, Session 1

Monitoring and guidance of cardiac radiofrequency ablation using optical coherence tomography

C. P. Fleming, H. Wang, Z. Hu, Case Western Reserve Univ. (United States); K. J. Quan, Metro Health Medical Ctr. (United States); A. M. Rollins, Case Western Reserve Univ. (United States)

Radiofrequency ablation (RFA) is now the standard of care for treatment of many arrhythmias. The objective of epicardial ablation for ventricular tachycardia is ablation of the surviving myocardium that supports the arrhythmia by created linear lines of ablation. A major complication that arises is ablating close to a coronary vessel and ablation in the presence of epicardial fat limits the success of this procedure. We hypothesized that Optical Coherence Tomography (OCT) can provide real time

guidance to identify normal structures.

1600 images from freshly excised swine ventricular wedges were acquired using microscope integrated Fourier domain OCT system with linear in k spectrometer, 11µm axial and 10µm lateral resolutions and 40,000 A-line rate. A decision tree model was developed for automatic classification of the normal epicardium, epicardium with coronary vessels, and epicardial fat for guidance of epicardial ablation. Principle component analysis was used to reduce five analysis parameters (light attenuation, backscattering, imaging depth, tissue heterogeneity, and gradient intensity) to three principle components. A three tiered decision tree model resulted in a 5.7% misclassification rate. RFA linear lesions were subsequently created on ventricular wedges and imaged with to identify gaps within ablation lines. Gaps of viable myocardium had a characteristic birefringence band between two ablation lesions and correlated with triphenyltetrazolium chloride staining to identify viability and necrosis

We have demonstrated OCT has great potential for monitoring and guidance of RFA therapy. A direct image by OCT can guide the precise application of energy and provide real-time formation of successful lesions.

7548D-110, Session 2

Impact of the beam distortion on the quantitative coronary artery optical coherence tomography analysis

N. Suzuki, H. Yamamoto, S. Ishikawa, Y. Shiratori, A. Miyazawa, K. Kozuma, T. Isshiki, Teikyo Univ. (Japan)

Introduction: In the field of interventional cardiology, quantitative optical coherence tomography (OCT) analysis is about to be relevant for the correct assessment of appropriate coronary artery stent apposition. Nevertheless, the pseudo stent struts (PS)are sometimes seen at odd positions in the lumen and locate at the same distance from the image wire as a true strut. PS may be produced by the distorted beam and interfere accurate analysis. Our aim was to investigate the incidence of PS. Methods: We created a simple phantom model (2.5 mm-CypherTM apposed in 8Fr sheath filled with saline) was created. OCT pullback images at 1 mm/sec were obtained with an eccentric imagewire position. The strut location was recognized by locating the strong signal inside the sheath. Of these, PS was defined as: an irregularity of the alignment of strut reflections; the difference in the strut-wire distance with one of the adjacent struts is within 20 micron. Strut contour with and without PS were delineated by semi-automated dedicated beta-version software (OCT system software B.0.1, Light Lab Inc., Westford, MA) with cubic spline interpolation, and symmetry index (= Min/Max diameter) was calculated. Results: Of the 252 optimal frames, a pseudo strut reflection was observed in 10 (4.0%). The symmetry index was significantly higher in strut contours without pseudo strut (0.93±0.05 versus 0.87±0.08, p=0.001). Conclusion: PS may mislead to the wrong data of clinical OCT analysis, although it is infrequently observed. This artifact can be recognized by checking the wire location.

7548D-111, Session 2

Toward the development of an automatic image processing algorithm for initiating and terminating intracoronary OFDI pullback

L. P. Hariri, B. Bouma, G. J. Tearney, Massachusetts General Hospital (United States)

Intracoronary optical frequency domain imaging (OFDI) is a high-resolution, three-dimensional, catheter-based cross-sectional imaging technique that requires a non-occlusive saline/contrast purge through a guide catheter to displace blood and provide clear views of arterial wall. Recent studies utilized manual pullback initiation/termination based on real-time image observation. Automated pullback initiation/

Conference 7548D: Diagnostic and Therapeutic Applications of Light in Cardiology



termination, accomplished by conducting real-time OFDI signal analysis would enable simplified operation and more efficient data acquisition. We evaluated the use of the images' first and second moments to 1) differentiate diagnostic-quality, clear artery wall versus blood-obstructed fields and 2) determine whether the catheter's imaging segment was within an artery or within the guide catheter. Algorithms were tested retrospectively and prospectively using two data sets: 1) intracoronary OCT human data obtained from a previously conducted clinical study and 2) intracoronary OFDI swine data. In the prospective analysis, the sensitivity and specificity of the ratio of the second and first moments for distinguishing clear artery wall were 99.6% (95% CI: 99.4-99.8%) and 97.2% (96.3-98.1%), respectively. For determination of guide catheter, the second moment had a sensitivity and specificity of 98.1% (97.2-99.0%) and 99.8% (99.7-99.9%), respectively. These results indicate that the algorithm may be utilized with intracoronary OFDI for initiating and terminating automated pullback and digital data recording.

7548D-112, Session 2

Optimizing flushing parameters in intracoronary optical coherence tomography: an in vivo swine study

M. J. Suter, S. K. Nadkarni, K. A. Gallagher, N. Asanani, Harvard Medical School and Wellman Ctr. for Photomedicine (United States); G. B. Conditt, A. Tellex, K. Milewski, G. L. Kaluza, J. F. Granada, Cardiovascular Research Foundation (United States); B. E. Bouma, G. J. Tearney, Harvard Medical School and Wellman Ctr. for Photomedicine (United States)

Introduction: Intracoronary OCT requires the displacement of blood, a highly scattering media, for clear visualization of the arterial wall. Optically transparent radiographic contrast agents have been found to be highly effective at displacing blood in clinical OCT studies however, when coupled with relatively large doses administered during standard percutaneous coronary intervention, may increase the risk of contrast-induced nephropathy. The goal of this study was to determine the optimal flushing parameters necessary to reliably perform high quality intracoronary OCT while reducing the volume of administered radiographic contrast.

Methods: 14 days prior to imaging, bare metal stents were placed in 3 coronary arteries of 3 swine (9 arteries total). At day 14, OFDI imaging was performed in each vessel. Both 2 and 3 cc/sec flush rates were tested with a number of media including Lactated Ringers solution, 5% Dextran 40 in sodium chloride, and increasing concentrations of routinely used contrast agents including low-osmolar Omnipaque 350 and iso-osmolar Visipaque 320. A total of 144 OFDI pullbacks were acquired together with synchronized EKG and intracoronary pressure wire recordinas.

Results/Conclusion: Flushing media with viscosities that were closely matched to that of whole blood resulted in rapid and efficient blood displacement. Media with lower viscosities such as the Lactated Ringers solution or the diluted contrast solutions resulted in increased mixing or dilution of the blood rather than displacement therefore reducing the length of the OFDI imaging segment obtained. Intracoronary pressure wire readings were utilized to ensure that flushing variances were not attributed to guide catheter displacement. 100% Visipaque 320 routinely outperformed the other flushing media in terms of blood clearance rate and duration, however 5% Dextran 40 in sodium chloride was found to give highly comparable results. Given that Dextran 40 has been used for the prevention of nephrotoxicity associated with radiographic contrast media we recommend that it be used as the preferred OCT flushing media particularly in patients with decreased kidney function.

Acknowledgements: Merck, R01 HL076398, K99 CA134920.

7548D-113, Session 2

Durable phantoms of atherosclerotic arteries for optical coherence tomography

C. Bisaillon, M. L. Dufour, G. Lamouche, National Research Council Canada (Canada)

We previously reported a method to fabricate phantoms of coronary arteries. This method allows the deposition of multiple layers on a tubular structure, each layer replicating optical and mechanical properties of coronary artery layers. We now report further improvements to this method to produce phantoms of arteries affected by atherosclerosis. Different strategies used to add features such as intimal thickening, lipid pools, calcifications, and thin cap fibroatheroma to multilayered coronary artery phantoms will be presented. The phantoms can be used in training personnel to use OCT systems and to diagnose different conditions. They can also be used to develop and test procedures without requiring human or biological samples. Since they are highly durable, they can also serve as a reference for comparing results between different systems, or one system over time.

7548D-114, Session 3

Clinical studies of frequency domain optical coherence tomography in the coronary arteries: the first 200 patients

C. Petersen, D. C. Adler, J. M. Schmitt, LightLab Imaging, Inc. (United States)

We report clinical study results of three-dimensional (3D) in vivo imaging of human coronary arteries using frequency domain optical coherence tomography (FD-OCT). Over 200 patients at over 10 study sites were imaged between August 2007 and July 2009 using FD-OCT systems and disposable fiberoptic catheters developed by LightLab Imaging Inc. The first commercial versions of the system was introduced in Europe in May 2009. The system operates at 50,000 axial lines/s, performing a 50 mm spiral pullback in 2.5 seconds with a rotational frame rate of 100 Hz. The commercial system employs a proprietary micro-cavity swept laser, developed jointly with AXSUN Technologies Ltd., which enables highresolution imaging of vessel diameters up to 10 mm. Study data indicates that FD-OCT is being used for post-intervention imaging of deployed coronary stents in 42% of cases. High-resolution 3D imaging of stent geometry immediately following deployment enables detection of stent malapposition, which can increase the risk of thrombosis. Longer term follow-up imaging of stented vessels can detect thrombus formation, which can be treated pharmacologically, and neointimal growth, which may require angioplasty or re-stenting. FD-OCT is being used for preintervention imaging of stenotic lesions in 58% of cases. Here FD-OCT is used to measure the minimum lumen area and to identify calcified and lipid lesions, side branches, or other vascular structures that could interfere with the stenting procedure. Overall, FD-OCT continues to be adopted at an increasing rate and has provided clinicians with a powerful tool for pre- and post-intervention assessment of the coronary arteries.

7548D-115, Session 3

OCT catheterization of healthy and diseased artery models

M. D. Hewko, G. Lamouche, M. Dufour, M. Smith, B. Gauthier, E. Kohlenberg, S. Bascaramurty, S. Vergnole, C. Bisaillon, L. Choo-Smith, C. Ko, C. Padioleau, F. D'Amours, E. Pellerin, M. Sowa, National Research Council Canada (Canada)

An intravascular OCT catheter was developed and tested with both time-domain and swept-source OCT platforms. Intravascular imaging was initially conducted in a healthy porcine modified Langendorff heart

Conference 7548D: Diagnostic and Therapeutic Applications of Light in Cardiology



model. The left anterior descending coronary artery was catheterized and imaged with both OCT platforms. Imaged arterial sections were then harvested and prepared for histology. The co-registered OCT images and histology sections were compared for OCT image quality and penetration depth.

While the porcine heart model allowed for refinement of the catheterization procedure, the morphology was limited to healthy non-diseased tissue. Myocardial infarction prone Watanabe heritable hyperlipidemic (WHHL-MI) rabbits were selected as a model of atherosclerotic disease to allow for imaging of diseased arterial tissue. The aorta of the rabbit was catheterized with an intravascular OCT probe and images were collected along the aorta from the descending arch to the abdominal region. Coronal histological sections were collected from matched OCT regions and compared for morphological similarities. Thereafter, several remaining lengths of aortic tissue were cut longitudinally and the lumen surface was re-mapped with a microscopy style OCT system for comparison with catheter performance. The exposed luminal surface was also mapped with Raman spectroscopy and imaged by laser scanning nonlinear optical microscopy to provide information on the tissue biochemistry for comparison with both histology and the morphology of the OCT images.

7548D-116, Session 3

Increase of retrograde blood flow in the early quail embryonic vitelline artery after acute hypoxic exposure

S. Gu, M. W. Jenkins, L. M. Peterson, M. Watanabe, Y. Doughman, A. M. Rollins, Case Western Reserve Univ. (United States)

During vertebrate embryonic development, hypoxic heterogeneity contributes to normal development of the cardiovascular system. Perturbation of the oxygen concentration can cause abnormal development of the cardiovascular system. Previous studies focused on hypoxia's long-term effect on heart morphology, vessel patterning and gene expression during development. However, it has been recently demonstrated that mechanical forces exerted by blood flow play an important role in early development. We hypothesize that short-term exposure to hypoxia could affect these mechanical forces, and in turn the cardiovascular system. Using optical coherence tomography (OCT), we obtained M-mode Doppler images of the right-side vitelline artery of quail embryos at stage 20 (70-72 hours after incubation). OCT can provide high spatial (10 micrometer) and temporal resolutions (34 microsec), which enables us to accurately measure the flow pattern and detect even the smallest variations. A mild hypoxia (15% O2) was applied to an ex ovo culture for 1 hour, and significant increases of relative retrograde blood flow to the forward flow was observed after 5-10 minutes of exposure (0.9% under normoxic conditions to 3.0% under hypoxic conditions). It gradually recovered to baseline within 1 hour, demonstrating the ability of the embryo to adapt to this adverse condition. Embryos pre-treated with chetomin, an inhibitor of hypoxia-inducible factor 1 (HIF-1), can still adapt to hypoxia within 1 hour, suggesting a HIF-independent mechanism. Further exploration between acute changes in flow pattern and structural changes in the long-term could elucidate mechanisms leading to congenital heart disease in humans, especially in cases of placental insufficiency.

This work is supported by NIH grants R01HL083048, T32EB007509, and C06RR12463-01 $\,$

7548D-117, Session 3

Clinical experience with intracoronary optical frequency domain imaging for visualization of coronary artery microstructure

G. J. Tearney, Massachusetts General Hospital (United States); S. Waxman, Lahey Clinic (United States); M. Suter, M. Shishkov, B. Vakoc, Massachusetts General Hospital (United States); A. Maehara, C. Castellanos, Columbia Univ. Medical Ctr. (United States); M. Freilich, Lahey Clinic (United States); M. Rosenberg, Massachusetts General Hospital (United States); G. Weisz, J. Moses, M. Leon, Columbia Univ. Medical Ctr. (United States); B. Bouma, Massachusetts General Hospital (United States)

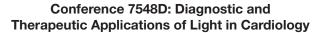
Optical Frequency Domain Imaging (OFDI) is second-generation form of optical coherence tomography (OCT) that enables the volume visualization of long segments of coronary artery microstructure following a brief, non-occlusive saline purge. Here, we report the first studies conducted with intracoronary OFDI in human patients. Volumetric OFDI images were obtained in twenty patients following intracoronary stent deployment. Images were acquired in all three coronary arteries using non-occlusive saline/radiocontrast purge rates ranging from 3-4 ml/s, and for purge durations of 3-4 seconds. Good visualization of artery wall was obtained in all cases, with lengths of clear viewing averaging 6.0 cm at pullback rates at 20 mm/s. A diverse range of microscopic features were identified in two- and three-dimensions, including thincapped fibroatheromas, calcium, macrophages, cholesterol crystals, bare stent struts, and stents with neointimal hyperplasia. Our results demonstrate that OFDI is a viable method for comprehensively imaging the microstructure of long coronary segments in patients and indicate that this technology will be very useful for studying human coronary pathophysiology and as a clinical tool for guiding the management of coronary artery disease.

7548D-118, Session 4

Assessment of peripheral tissue perfusion by dynamic optical imaging and nonlinear regression modeling

Y. Kang, J. Lee, Korea Advanced Institute of Science and Technology (Korea, Republic of); K. Kwon, Ewha Womans Univ. (Korea, Republic of); C. Choi, Korea Advanced Institute of Science and Technology (Korea, Republic of)

Accurate measurement of peripheral tissue perfusion is necessary but challenging in diagnosing peripheral vascular insufficiency. Deep tissue penetration of near-infrared (NIR) wave has enabled in vivo NIR fluorescence imaging. The purpose of this study is to estimate the peripheral tissue perfusion rates from time-series analysis of distribution and elimination kinetics of a clinically proven NIR fluorescence probe, indocyanine green (ICG). We developed a new method, dynamic ICG perfusion imaging technique to evaluate peripheral tissue perfusion that employs planar imaging with a CCD digital imaging system and timeseries analysis of the spatiotemporal dynamics (150s) of intravenously injected ICG by using nonlinear regression and differential evolution methods. Six parameters (, , s, d, m; parameters which depend on an arterial input function (AIF) into a lower extremity and p; perfusion rates in the lower extremity) were estimated by the nonlinear regression modeling method. We have confirmed the validity of our new method by applying the method to a normal control and a patient with peripheral arterial occlusive disease (PAOD). Recirculation time was estimated around 80 to 90 sec after detection of first ICG fluorescence signal in the normal control. In contrast, PAOD patient showed an unique AIF curve pattern, which was caused by collateral blood flow passing through the narrowing major artery. The lower extremity tissue perfusion rate of the PAOD patient was estimated as 12% to 20% of those of normal values. These results indicate that ICG perfusion imaging method is sensitive enough to diagnose PAOD and capable of diagnosing functional arterial diseases.





7548D-119, Session 4

Assessment of permeation of lipoproteins in human carotid tissue

K. V. Larin, M. Ghosn, Univ. of Houston (United States)

Cardiovascular disease is among the leading causes of death in the United States. Specifically, atherosclerosis is an increasingly devastating contributor to the tally and has been found to be a byproduct of arterial permeability irregularities in regards to lipoprotein penetration. To further explore arterial physiology and molecular transport, the imaging technique of Optical Coherence Tomography (OCT) was employed. With OCT, the permeation of glucose (MW = 180 Da), low density lipoprotein (LDL; MW = 2.1 x 106 Da), and high density lipoprotein (HDL; MW = 2.5 x 105 Da) in human carotid tissue was studied in vitro to determine the effect of different molecular characteristics on permeation in atherosclerotic tissues. The permeability rates calculated from the diffusion of the molecular agents into the abnormal carotid tissue samples is compared to those of normal, healthy tissue. The results show that in the abnormal tissue, the permeation of agents correlate to the size constraints. The larger molecules of LDL diffuse the slowest, while the smallest molecules of glucose diffuse the fastest. However, in normal tissue, LDL permeates at a faster rate than the other two agents, implying the existence of a transport mechanism that facilitates the passage of LDL molecules. These results highlight the capability of OCT as a sensitive and specific imaging technique as well as provide significant information to the understanding of atherosclerosis and its effect on tissue properties.

7548D-120, Session 4

Intraoperative assessment of acute revascularization effect on ischemic muscle perfusion and oxygenation

Y. Shang, Univ. of Kentucky (United States); Y. Zhao, Univ. of Kentucky (United States) and Tianjin Univ. (China); R. Cheng, L. Dong, S. P. Saha, G. Yu, Univ. of Kentucky (United States)

Peripheral arterial disease (PAD), a manifestation of lower extremity atherosclerosis, may result in tissue ischemia, causing intermittent claudication, rest pain and limb loss. Arterial revascularization can improve macro-circulation via bypass grafts or percutaneous transluminal angioplasty (PTA), thus potentially improving microcirculation and tissue oxygenation. A novel flow-oximeter based on near-infrared diffuse correlation spectroscopy (see another submitted abstract) has been developed for simultaneous measurement of the relative change of calf blood flow (rBF), oxy- and deoxy- hemoglobin concentration (Δ [HbO2] and Δ [Hb]) during revascularization. Nine legs out of eight PAD patients underwent low leg revascularization (2 PTAs, 6 bypass grafts, 1 PTA with bypass graft) have been studied. Two sterilized fiber-optic probes were taped respectively on the calf muscles in both legs before surgery. Calf muscle blood flow and oxygenation were continuously monitored throughout the revascularization. The post-revascularization values were averaged for 20 minutes and compared to the 10-minute averaged pre-revascularization baseline. The optical measurements demonstrated high sensitivity to dynamic physiological events (e.g., arterial clamping and releasing). Significant improvements in calf rBF [\pm 49.5 \pm 13.5% (mean \pm SE), p = 0.006] in the surgical legs were observed after revascularization whereas acute revascularization effects in tissue oxygenation were not evident ($\Delta[HbO2] = -1.0\pm1.7 \mu Mol$ and $\Delta[Hb] =$ +2.77±1.49 μMol, p>0.05). Further investigations are being conducted to correlate these acute effects with long-term clinical outcomes. This first pilot study suggests a role for the novel diffuse optical technologies in intraoperative evaluation of acute effects of revascularization on ischemic muscle perfusion and oxygenation.

7548D-121, Session 4

Optical frequency domain imaging for intracoronary blood flow measurements

G. J. Tearney, M. Suter, B. Vakoc, M. Shishkov, S. Nadkarni, B. Bouma, Massachusetts General Hospital (United States)

Interventional cardiologists measure intracoronary blood flow using an ultrasound Doppler guide wire to evaluate coronary vascular function and guide percutaneous coronary intervention (PCI). However, Doppler ultrasound requires a separate, standalone instrument and is difficult to use because the Doppler signal is dependent on the orientation of the transducer's tip. Optical Frequency Domain Imaging (OFDI), a new intracoronary imaging technique that enables the volume visualization of long segments of coronary artery microstructure, is currently on the verge of widespread clinical adoption. If intracoronary blood flow could be measured using an OFDI system and catheter, then imaging and functional perfusion measurements could be conducted easily, rapidly, and without additional cost above and beyond that of an OFDI device. In this abstract, we report a preliminary feasibility study to determine the capability of OFDI to measure blood flow in coronary arteries of living swine. For this study, a 2.4F OFDI catheter was inserted in a swine coronary artery in vivo, blood allowed to freely flow through the vessel, and OFDI data obtained while catheter optics were stationary. The OFDI data was processed to produce a flow waveform. Comparison of the OFDI flow waveform to EKG and pressure waveforms, obtained simultaneously with the OFDI data, demonstrated a high degree of correlation between the different measurements. These results indicate that OFDI may be utilized to obtain both structural and functional intracoronary flow measurements in vivo.



Conference 7548E: Optical Techniques in Neurosurgery, Brain Imaging, and Neurobiology

Saturday 23 January 2010 • Part of Proceedings of SPIE Vol. 7548 Photonic Therapeutics and Diagnostics VI

7548E-122, Session 1

Multichannel time-resolved spectroscopic system for TBI/stroke monitoring: preliminary study

J. J. Selb, Massachusetts General Hospital (United States); M. Mujat, D. X. Hammer, N. Iftimia, Physical Sciences, Inc. (United States)

We have developed a compact multi-channel time-resolved near-infrared spectroscopic (TR-NIRS) instrument for topographic brain imaging with depth sensitivity. The device is based on three time-multiplexed pulsed laser diodes (690, 800, and 830 nm), whose combined output is injected through an optical switch to 15 source fibers. The time-correlated single photon counting (TCSPC) detection uses 8 photo-multiplier tubes (PMTs). A neutral density filter of variable attenuation is positioned in front of each detector and can be adjusted to the light level. This versatile device can accommodate various mono- or bi-hemispheric head probe geometries. The device interface enables real-time monitoring of blood volume and oxygenation: it displays 2D maps of oxy- and deoxy-hemoglobin variations, obtained from the integrated CW signal, as well as maps of mean time of flight, or pulse width at each wavelength. Further data analysis for characterization of the baseline optical properties, or imaging with depth reconstruction are performed off-line. We have characterized the instrument on phantoms, and have performed preliminary in-vivo testing. We will now apply the device to measuring absolute cerebral blood volume and oxygenation on healthy adult subjects, as well as to performing functional imaging during cerebral activation to characterize the system depth sensitivity in-vivo. We will then translate the instrument to the hospital to perform bi-hemispheric measurements on stroke and traumatic brain injury patients and assess baseline brain oxygenation in these subjects, as well as their variations during clinical procedures.

7548E-123, Session 1

Functional Doppler optical coherence tomography for cortical blood flow imaging

L. Yu, G. Liu, E. Nguyen, B. Choi, Z. Chen, Beckman Laser Institute and Medical Ctr., Univ. of California, Irvine (United States)

Optical methods have been widely used in basic neuroscience research to study the cerebral blood flow dynamics in order to overcome the low spatial resolution associated with magnetic resonance imaging and positron emission tomography. Although laser Doppler imaging and laser speckle imaging can map out en face cortical hemodynamics and columns, depth resolution is not available. Two-photon microscopy has been used for mapping cortical activity. However, flow measurement requires fluorescent dye injection, which can be problematic. The noninvasive and high resolution tomographic capabilities of optical coherence tomography make it a promising technique for mapping depth resolved cortical blood flow.

Here, we present a functional Doppler optical coherence tomography (OCT) imaging modality for quantitative evaluation of cortical blood flow in a mouse model. Fast, repeated, Doppler OCT scans across a vessel of interest were performed to record flow dynamic information with a high temporal resolution of the cardiac cycles. Spectral Doppler analysis of continuous Doppler images demonstrates how the velocity components and longitudinally projected flow-volume-rate change over time, thereby providing complementary temporal flow information to the spatially distributed flow information of Doppler OCT. The proposed functional Doppler OCT imaging modality can be used to diagnose vessel stenosis/ blockage or monitor blood flow changes due to pharmacological

agents/neuronal activities. Non-invasive in-vivo mice experiments were performed to verify the capabilities of function Doppler OCT.

7548E-124, Session 1

Optically based quantification of absolute cerebral metabolic rate of oxygen (CMRO2) with high spatial resolution in rodents

M. A. Yaseen, V. J. Srinivasan, S. Sakad?ić, Massachusetts General Hospital (United States); S. A. Vinogradov, Univ. of Pennsylvania (United States); D. A. Boas, Massachusetts General Hospital (United States)

Measuring oxygen delivery in brain tissue is important for identifying the pathophysiological changes associated with brain injury and various diseases such as cancer, stroke, and Alzheimer's disease.

We have developed a multi-modal imaging system for minimally invasive measurement of cerebral oxygenation and blood flow in small animals with high spatial resolution. The system allows for simultaneous measurement of blood flow using Fourier-domain optical coherence tomography, and oxygen partial pressure (pO2) using either confocal or multiphoton phosphorescence lifetime imaging with exogenous porphyrin-based dyes sensitive to dissolved oxygen.

Here we present the changes in pO2 and blood flow in superficial cortical vessels of Sprague Dawley rats in response to conditions such as hypoxia, hyperoxia, and functional stimulation. pO2 measurements display considerable heterogeneity over distances that cannot be resolved with more widely used oxygen-monitoring techniques such as BOLD-fMRI. Large increases in blood flow are observed in response to functional stimulation and hypoxia.

Our system allows for quantification of cerebral metabolic rate of oxygen (CMRO2) with high spatial resolution, providing a better understanding of metabolic dynamics during functional stimulation and under various neuropathologies. Ultimately, better insight into the underlying mechanisms of neuropathologies will facilitate the development of improved therapeutic strategies to minimize damage to brain tissue.

7548E-125, Session 1

Long-term monitoring cerebrovascular response in focal traumatic and ischemic brain injuries

Y. Jia, A. Gruber, N. Alkayed, R. K. Wang, Oregon Health & Science Univ. (United States)

Inadequate cerebral blood flow (CBF) is an important contributor to neurological disorder after brain injuries. Restoration of local blood flow in post-traumatic or post-ischemic brain plays a critical role in rescuing damaged neurons and long-term functional recovery. Therefore, in clinical, increasing attention has been focused on potential strategies of promoting cerebrovascular response in the area of insult for recovery of blood flow supply.

Optical Micro-AngioGraphy (OMAG), capable of resolving 3D distribution of dynamic blood perfusion at the capillary level within microcirculatory beds in vivo, has been developed recently. The goal of this study is to develop and implement OMAG for simultaneously in vivo measuring hemodynamic properties, such as CBF and volume (CBV) and imaging vascular remodeling, i.e. neovascularization in small rodent animal models of focal traumatic brain injury (fTBI) and focal ischemic brain injury (fIBI). Firstly, we used flow phantoms to verify the reliability of

Conference 7548E: Optical Techniques in Neurosurgery, Brain Imaging, and Neurobiology



this novel microvascular imaging system in vitro, and then tested its feasibility to evaluate localized CBF in normal mice by comparing with autoradiography. Then we detected its feasibility to image the fluctuation of CBF and vascular remodeling in these two animal models. Separately, the performance of OMAG will be verified by conventional immunohistochemistry.

7548E-126, Session 2

Four-dimensional multi-site two-photon excitation

V. R. Daria, C. Stricker, The Australian National Univ. (Australia); R. Bowman, Univ. of Glasgow (United Kingdom); H. Bachor, S. Redman, The Australian National Univ. (Australia)

We use high-speed programmable holograms to project threedimensional (3D) optical field patterns suitable for multi-site non-linear photostimulation in four-dimensions. Holographic splitting of a collimated femtosecond-pulse laser transforms an incident beam into optical field patterns characterized by several intensity maxima or focal spots. Each spot can be used for multi-site photostimulation via non-linear two-photon absorption. To meet the speed requirements, we use a straightforward derivation of the hologram with no iterative optimization procedure. We further optimize the speed by taking advantage of the parallel computing capability of a graphics accelerator board. Since no iterative optimization procedure is utilized during the generation of the hologram, we theoretically analyse the efficiency, fluctuations in peak intensities, and aberrations as the spots are projected around the focal volume. For quantitative two-photon response, we show that fluctuations from interference effects and device parameters can be minimized with random spot configurations and can be accurately modelled using optical theory. We further show that the various excitation spots have sufficient energy and spatiotemporal photon density for localized two-photon absorption. The multiple spots allow for user-defined multi-site non-linear photostimulation within the focal volume of a lens. The applications of our system point to 3D non-linear microscopy, volume holographic storage, microfabrication and nano-surgery. In neuroscience, our system allows for realistic simulation of integrating simultaneous synaptic signals from multiple sites within the 3D dendritic trees of a neuron. Photo-stimulation of neurotransmitters at arbitrary sites provides fundamental answers to the mechanisms of information processing in the human brain.

7548E-127, Session 2

A modified MPEG2 algorithim for HD and 3D medical imaging

W. J. Picard, Picard Internet Products (Canada)

The worlds economy now feeds off of promoting problems that often have simple cures if thinking beyond the envelope is used. This paper describes novel cures to cancer detection and cure through compression based vision algorithms described for medical robots to reduce the high cost of medical care. A cure for computer eyestrain and fatigue using a \$100 laptop terminal with a more vision friendly 3D LCD screen display algorithm described in detail. Finally a solution to the world's monetary crisis by pegging the US dollar to Federal Reserve Bank real estate mortgages instead of precious metals to promote confidence. An oatmeal breakfast made with tea cures world hunger due to poverty and the car based US economy could be saved by promoting large cars and energy conservation simultaneously through car pools of 4 or more occupants. A survey of home and work postal codes among interested parties would be a good start. Termite stomach bacteria could turn straw into liquid gold (oil) and hydrogen from seawater is possible using silver chloride which is light sensitive like silver oxide for film in a photographic process with a nickel catalyst

7548E-128, Session 2

Semantic deficit in Chinese dyslexia: a NIRS study

J. Sun, J. Zhai, T. Li, Z. Zhang, H. Gong, Huazhong Univ. of Science and Technology (China)

The phonologic and orthographic pathways during semantic processing in Chinese dyslexic children were evaluated using the stroop paradigm with near-infrared spectroscopy (NIRS). The NIRS instrument is a portable, continuous-wave system and can measure concentration changes of hemodynamic parameters (including oxy-/deoxyhemoglobin). Considering better sensitivity, the deoxy-hemoglobin (deoxy-Hb) measured by NIRS in prefrontal cortex was chosen to indicate Stroop interference effect and evaluate semantic process. Thirty-one Chinese primary school children (14 with developmental dyslexia and 17 with normal reading abilities) were recruited to participate in this study. They were instructed to judge the presented color of color irrelevant words, color homophone words, and color words, corresponding to control task, phonological task and semantic task respectively. Stroop interference effect was reflected as longer response time and more deoxy-Hb activation than control task. Both behavioral and deoxy-Hb data showed evident color Stroop effect, but no homophone effect for normal and dyslexic children. The color Stroop effect was significantly larger than homophone effect for normal children, but not for the dyslexics. Further, deoxy-Hb revealed that color Stroop effect and activation difference between semantic task and phonological task of the dyslexics was significantly smaller than normal children. These findings suggest dyslexic children have deficit in semantic processing and that might be caused by their deficit in processing orthographic information. The results show that NIRS can be used to study semantic process.

7548E-129, Session 2

Causality of cerebral hemodynamic responses to whisker stimulation in the rat brain using NIRS

S. Lee, D. Koh, Korea Univ. (Korea, Republic of); Y. Jung, C. Im, Yonsei Univ. (Korea, Republic of): B. Kim, Korea Univ. (Korea, Republic of)

Causality (effective causal connectivity), originated from economics, is one of the powerful tools in understanding the neurovascular connection of the brain during brain activation. Recently, the theory of causality has been applied to explore functional pathways in neurological pathologic conditions such as epilepsy, schizophrenia and dementia. In this study, we estimated the effective causal connectivity of cerebral hemodynamic responses to whisker stimulation in the rat brain using the near-infrared spectroscopy (NIRS) with the Granger Causality (GC) method. Our results show that the effective causal connectivity from primary somatosensory cortex (SI) and secondary somatosensory cortex (SII) to primary motor cortex (MI) regions can be identified during whole whisker stimulation. Also, it shows consistent pattern with electrical causal connectivity result. We propose that the NIRS with the GC can be a useful tool for investigating a functional network of the brain.

7548E-130, Session 3

Dynamic contrast enhanced magnetic resonance imaging (DCE-MRI) for the assessment of Pc 4-sensitized photodynamic therapy of a U87-derived glioma model in the athymic nude rat

A. Anka, P. Thompson, E. Mott, R. Sharma, R. Zhang, N. Cross, J. Sun, C. A. Flask, N. L. Oleinick, D. Dean, Case Western

Conference 7548E: Optical Techniques in Neurosurgery, Brain Imaging, and Neurobiology



Reserve Univ. (United States)

Introduction: Dynamic Contrast-Enhanced-Magnetic Resonance Imaging (DCE-MRI) may provide a means of tracking the outcome of Pc 4-sensitized photodynamic therapy (PDT) in deeply placed lesions (e.g., brain tumors). We previously determined that 150 uL of gadolinium (Gd) is an optimal dose for U87-derived intracerebral tumors in an athymic nude rat glioma model. We wish to determine how consistently DCE-MRI enhancement will detect a statistically significant increase in Gd enhancement signal following Pc 4-PDT. Methods: We injected 2.5 x 10^5 U87 cells into the brains of 5 athymic nude rats. After 8-9 days peri-tumor DCE-MRI images were acquired on a 7.0T microMRI scanner before and after administration of 150 uL Gd. DCE-MRI scans were repeated following Pc 4-PDT on Day 11. Results: Useful DCE-MRI data were obtained for 3 animals before (i.e., Day 8-9) and after (i.e., day 11) PDT. Before PDT (i.e., Day 8-9), approximately 30-90 seconds after Gd administration, an average, normalized peak Gd enhancement was observed in the tumor region that was 1.298 over baseline (0.029 Standard Error [SE]). The average normalized peak Gd enhancement in the tumor region in the scan following PDT (i.e., Day 11) was 1.598 (0.080 SE) over baseline, a statistically significant increase in enhancement (p < 0.0247) over the pre-PDT level. Discussion: The 150 uL Gd dose appears to provide an unambiguous increase in signal indicating Pc 4-PDTinduced necrosis of the U87-derived tumor region. This protocol may allow the development of a clinically robust (i.e., unambiguous) technique for the assessment of PDT outcome.

7548E-131, Session 3

Development of an autofluorescent probe designed to help brain tumour removal: study on an animal model

R. Siebert, CNRS, Univ. Paris-Sud 11 (France); B. Leh, Univ. Paris-Sud 11 (France); M. Collado-Hilly, F. Monnet, INSERM (France); P. Varlet, Hopital Sainte Anne (France); Y. Charon, Univ. Paris 7 (France); M. Duval, Univ. Evry (France); L. Menard, Univ. Paris 7 (France)

The issue of guided brain tumour resection, especially in case of glioblastoma, is to improve the patient life quality and prognosis. A way to differentiate healthy from tumorous tissues is autofluorescence spectroscopy. This modality of detection needs to define a fluorescence intensity indicator of cancerous tissues.

A probe composed of optical fibres is developed to measure fluorescence intensity. The first prototype consists of only 2 fibres, one transferring the excitation light to the tissue, the other collecting the fluorescent light coming from the tissue thereafter analyzed by a spectrometer.

To get inside potential discriminating signals between normal and cancerous tissues, we started first measurements on an animal model. C6 cells (rat Glioblastoma) are injected in the right striatum of the rat. After a few weeks of tumour development, the animal is sacrificed and the fresh (not-perfused) brain is cut into slices for autofluorescence and histopathological analysis. Several excitation wavelengths are tested. As a first result, several endogenous fluorophores likely to contribute to the signal are identified: e.g. the flavins, the lipopigments and the porphyrins. The intensity of these peaks differs according to the nature of the brain tissue (white matter, grey matter and healthy or tumourous tissues). After subsequent fixation (formalin-zinc) of the slices a histopathological analysis has been done. Autofluorescence and histological results are compared and a correlation between the current state of the tissue (cerebral tissue type, tumoral or not, different levels of tumour cell concentration) and the autofluorescence spectrum has been carried out.

7548E-132, Session 3

Bypassing the blood brain barrier: delivery of therapeutic agents by macrophages.

H. Hirschberg, Beckman Laser Institute and Medical Ctr. (United States); G. Gulsen, Y. J. Kwon, Univ. of California, Irvine (United States); S. J. Madsen, Univ. of Nevada, Las Vegas (United States)

Cells migrating out from malignant brain tumors have the ability to insinuate themselves seamlessly and extensively into normal neural tissue. They are therefore protected by the blood brain barrier (BBB) which prevents the delivery and limits the effects of anti-tumor agents. For a therapeutic agent delivery system to be successful at preventing glioma recurrence, some means of bypassing the BBB is necessary. Tumor-associated macrophages (TAMs) are frequently found in and around glioblastomas in both experimental animals and patient biopsies. Intravenously injected macrophages loaded with iron oxide nanoparticles have been shown to target experimental brain tumors. This would indicate local synthesis of chemo attractive factors in gliomas and that inflammatory cells can pass through an intact BBB. Monocytes or macrophages loaded with drugs, nanoparticles or photosensitizers could therefore be used to target tumors. In this context the ability to increase macrophage migration into brain tumors is a critical factor. We have investigated photodynamic therapy (PDT) as a method to increase the number of inflammatory cells in experimental brain tumors in rats. PDT was highly effective in locally opening the BBB and inducing macrophage migration into the irradiated portions of normal brain. In addition PDT at low fluence levels could significantly increase the number of TAMs in treated brain tumors in rats. Experiments to determine the ability of PDT to increase the number of iv injected nanoparticle loaded macrophages into C6 tumors in rodents is presently ongoing.

7548E-133, Session 3

Near-infrared-activated gold nanoshells for thermal ablation of macrophages in vitro

S. J. Madsen, A. R. Makkouk, Univ. of Nevada, Las Vegas (United States); H. M. Gach, Nevada Cancer Institute (United States); H. Hirschberg, Beckman Laser Institute and Medical Ctr. (United States)

The diffuse and infiltrative nature of glioblastoma multiforme (GBM) is a primary factor for its resistance to therapeutic interventions. Therefore, one of the challenges in brain tumor therapy is maintaining an elevated concentration of therapeutic agents at the tumor site in order to prevent the spread of tumor cells into healthy tissue. In this context, cell-based vectorization of therapeutic agents has significant potential. The use of circulating cells, such as macrophages, presents several features of interest in the case of brain tumors. Specifically, studies in rat brain tumor models have found high concentrations of macrophages within the tumor and near the tumor periphery. Therefore, macrophages may serve as a vector for the delivery of therapeutic agents such as gold-coated anoshells

Uptake of both nanoshells and iron oxide particles by rat macrophages was investigated in vitro using inductively coupled plasma atomic emission spectroscopy (ICP-AES) and transmission electron microscopy (TEM). The rationale for using iron oxide particles is that, unlike nanoshells, they can be visualized on magnetic resonance images thus providing a means for imaging macrophage distributions in vivo. The results clearly demonstrated the ability of this macrophage line to internalize both types of particles. Significant cell death was observed following exposure of nanoshell-laden macrophages to near-infrared (810 nm) light, corresponding to the absorption peak of these particles. Collectively, the in vitro results suggest that photothermal ablation of GBM may be possible via macrophage-mediated delivery of nanoshells.

Conference 7548E: Optical Techniques in Neurosurgery, Brain Imaging, and Neurobiology



7548E-134, Session 3

RF hyperthermia using conductive nanoparticles

M. Gach, T. Nair, Nevada Cancer Institute (United States)

Specific absorption rate (SAR) heating using radiofrequency (RF) waves is affected by the RF frequency and amplitude, and the conductivity of the tissue. Recently, conductive nanoparticles were demonstrated to induce hyperthermia in vitro and in vivo upon irradiation with an external 13.56 MHz RF field. The addition of conductive nanoparticles was assumed to increase the tissue conductivity and SAR. However, no quantitative studies have been performed that characterize the conductivities of biocompatible nanofluids or tissues containing nanoparticles, and relate the conductivity to SAR.

The complex permittivities of nanofluids containing single-wall carbon nanotubes (SWCNTs) in normal saline were measured for different nanoparticle concentrations (0 to 93 mM for carbon) and RF frequencies (20 MHz to 1 GHz) using a dielectric probe and RF impedance analyzer. The nonionic surfactant Pluronic F108 was added to the solutions to minimize aggregation of the nanotubes. The conductivities of the nanofluids were derived from the imaginary component of the permittivity and corrected for the dipolar nature of water. The conductivities of the nanofluids rose linearly with carbon concentration and RF frequency. The dielectric of the nanofluids also rose linearly with carbon concentration above a percolation threshold of 5 mM but decreased with increasing RF frequency.

The nanofluids were placed inside a Bruker 7T/20 magnetic resonance (MR) imaging (MRI) system and irradiated at 300 MHz using a high duty cycle pulse sequence. The temperature changes were measured directly using fiber-optic thermometers and indirectly using MR thermometry and spectroscopy. Temperature changes were consistent with the nanofluid conductivities.

7548E-135, Session 4

Using the blood oxygenation level dependent signal utilizing spectral-domain optical coherence tomography

E. Freeman, Y. Wang, M. S. Islam, C. M. Oh, A. Ortega, B. H. Park, Univ. of California, Riverside (United States)

While a number of imaging technologies, such as fMRI and diffuse optical imaging, have successfully utilized the blood oxygenation level dependent (BOLD) signal to image neural activity, the exact mechanisms underlying this signal remain largely unknown. Current thinking hypothesizes that the BOLD signal is caused by some combination of changes in overall blood flow and localized oxygen consumption as observed through the ratio of oxygenated to deoxygenated hemoglobin. However, previously utilized techniques have largely lacked the appropriate spatiotemporal resolution necessary to elucidate a detailed sequence of events from neural activation through detection of the various components in the BOLD signal. The aim of this study is assess the feasibility of spectral-domain optical coherence tomography to study the BOLD signal. In particular, the results of optical Doppler tomography and spectroscopic OCT imaging of porcine blood in a microfluidic chamber designed to mimic neural architecture will be presented.

7548E-136, Session 4

Diffuse reflectance spectroscopy on cerebral cortex of pediatric patients with tuberous sclerosis complex

S. Oh, Miami Children's Hospital (United States) and Florida International Univ. (United States); T. Stewart, S. Bhatia, J.

Ragheb, I. Miller, Miami Children's Hospital (United States); W. Lin, Miami Children's Hospital (United States) and Florida International Univ. (United States)

Patients with tuberous sclerosis complex (TSC) often suffer from spontaneous recurrent seizures. One of most effective treatment for these patients is surgical resection of the epileptogenic cortical tubers. This study reports on the use of intraoperative diffuse reflectance spectroscopy on the cerebral cortex associated with tuberous sclerosis in vivo as a method of surgical guidance during tuberectomy.

A pilot clinical study on three pediatric patients with TSC who underwent tuberectomy for seizure control was conducted by using a diffuse reflectance spectroscopy with a fiber-optic probe.

Diffuse reflectance spectra were intraoperatively collected from the surface of cortex above tuber, the surface of normal cortex, and directly on the tuberous sclerosis tissue.

Significant findings from the pilot clinical study are that the cortex above the tuber has less cerebral blood volume as well as lower hemoglobin oxygenation, compared to the normal cortex. Also this cortex has the combined optical properties of the normal cortex and the tuber. One reason for this may be that the measurement on the cortex above tuber has some portion of normal cortex as well as tuber.

Proper interpretation and understanding of diffuse reflectance spectroscopy data from the cortex above tuber is important in making a clinical decision for the surgical plan. The findings in this study suggest the value of optical spectroscopy for aiding the surgical guidance in cases of tuberectomy for seizure control.

7548E-137, Session 4

Neuroendovascular optical coherence tomography Imaging: Clinical feasibility and applications.

M. S. Mathews, Univ. at Buffalo (United States); J. Su, E. Heidari, Beckman Laser Institute and Medical Ctr. (United States); M. E. Linskey, Univ. of California, Irvine (United States); L. N. Hopkins, Univ. at Buffalo (United States); Z. Chen, Beckman Laser Institute and Medical Ctr. (United States)

Optical Coherence Tomography (OCT) is a high resolution in vivo imaging modality that has found wide clinical application for retinal imaging. More recent work has found it to be feasible and useful for luminal imaging (such as gut and respiratory) as well as for coronary vascular imaging. However there has been very little work demonstrating its safety, feasibility, and applicability for intracranial use. The authors report on a clinical series of intracranial OCT imaging using neuroendovascular techniques. OCT imaging was carried out in patients using groin access under fluoroscopic visualization, with approval from the Institutional Review Board. Clinical imaging findings were correlated with cadaveric specimen imaged with OCT and then visualized histologically using a trichrome stain. Safety was evaluated using pre- and post-procedure clinical examination and post-procedure Magnetic Resonance Imaging in some cases. There was no clinical or radiographic evidence of postprocedure complications. OCT findings correlated well with histology. The study demonstrated that clinical neuroendovascular OCT imaging is safe and feasible. Potential applicability for visualization of intracranial pathology such as intracranial aneurysms, arteriovenous malformations, plagues, and dissections will be discussed.

7548E-138, Session 4

Brain connectivity study of joint attention using frequency-domain optical imaging technique

U. Chaudhary, V. Sharma, A. Godavarty, Florida International

TEL: +1 360 676 3290 · +1 888 504 8171 · customerservice@spie.org

Conference 7548E: Optical Techniques in Neurosurgery, Brain Imaging, and Neurobiology



Univ. (United States)

Autism is a socio-communication brain development disorder. It is marked by degeneration in the ability to respond to joint attention skill task, from as early as 12 to 18 months of age. This trait is used to distinguish autistic from non-autistic. In this study, diffuse optical imaging is being used to study brain connectivity for the first time to probe the Joint Attention experience in normal adults. The prefrontal region of the brain was non-invasively imaged using a frequency-domain based optical imager, Imagent. The imaging studies were performed on 11 normal right-handed adults and optical measurements were acquired in response to joint-attention based video clips. While the intensity-based optical data provides information about the hemodynamic response of the underlying neural process, the time-dependent phase-based optical data has the potential to explicate the directional information on the activation of the brain. Thus brain connectivity studies are performed by computing covariance/correlations between spatial units using these optical measurements (intensity and phase). The preliminary results indicate that the extent of synchrony and directional variation in the pattern of activation varies in the left and right prefrontal regions of the brain. The result has significant implication for research in neural pathways associated with autism, which can be mapped using diffuse optical imaging tools.

7548E-139, Session 4

Dynamic differential imaging of intrinsic optical responses in the retina

X. Yao, Y. Li, L. Liu, The Univ. of Alabama at Birmingham (United States)

Different eye diseases, such as glaucoma, diabetic retinopathy, macular degeneration, etc., can target different retinal neurons. Because of the complexity of retinal structure, high resolution examination of stimulusevoked retinal neural activities is important for accurate identification of localized retinal dysfunction, and thus provide improved disease diagnosis and treatment evaluation. Fast intrinsic optical signals (IOSs) have time courses comparable to electrophysiological kinetics of the retina, and thus near infrared light imaging of fast IOSs holds promise for high resolution imaging of retinal function. However, practical application of fast IOSs has been challenged by low specificity, i.e., unclear sources and mechanisms, of IOSs. Recently, we demonstrated dynamic differential recording of IOSs correlated with photoreceptor and post-photoreceptor responses. Both conventional microscope and home-built confocal imager were employed to investigate transmitted and reflected light IOSs in frog retinas activated by variable stimuli. Highspeed (1000 Hz) differential imaging disclosed rapid IOS, which might relate to early photoreceptor response, immediately after the onset of the stimulus. Moreover, both fast IOSs and simultaneous electrophysiological responses could follow high frequency flicker stimuli up to at least 6 Hz. It is well known that different retinal neurons, such as cone and rod systems, have different critical fusion frequency (CFF), which is the maximal frequency of stimulation that can be perceived as flickering. Further development of dynamic differential imaging of fast IOSs correlated with retinal flicker stimuli may provide selective evaluation of different retinal neurons.





Saturday 23 January 2010 • Part of Proceedings of SPIE Vol. 7548 Photonic Therapeutics and Diagnostics VI

7548F-140, Session 1

Potential of Raman spectroscopy to evaluate bone quality in postmenopausal osteoporosis patients.: first results of a perspective study

G. S. Mandair, F. W. Esmonde-White, A. M. Swick, Univ. of Michigan (United States); M. P. Akhter, Creighton Univ. (United States); J. Kreider, S. A. Goldstein, Univ. of Michigan (United States); R. R. Recker, Creighton Univ. (United States); M. D. Morris, Univ. of Michigan (United States)

As part of our ongoing assessment of bone tissue composition and structure, we report the first results of a prospective study to investigate the potential of using Raman spectroscopy to diagnose and predict skeletal fragility in postmenopausal osteoporosis patients. This multicenter study will assess several potential spectroscopic and X-ray based diagnostic techniques. One hundred and twenty participants will be enrolled in this five year study and the investigators will be blinded to information concerning patient history and status. They are given iliac crest bone biopsy specimens with no identifying information except a patient study number. Our research centers will use micro-computed tomography (micro-CT) to identify regions of interest in both cortical and trabecular bone from specimens delivered to us. Raman imaging will be performed using a line-focused 785 nm laser in order to obtain local and averaged values on several spectroscopic metrics of bone quality. These metrics include mineral crystallinity, carbonate/phosphate ratio, and mineral/matrix ratio. Results from the initial set of biopsies will be presented. Protocols for obtaining measurements will be discussed, with emphasis on the challenges presented by the use of fixed and polymer embedded specimens.

7548F-141, Session 1

Stereo digital image correlation for charaterization of fresh bone

M. E. Bland, Univ. of Michigan (United States); M. Cortes, Western New England College (United States); K. J. Solt, M. Siadat, L. X. Yang, Oakland Univ. (United States)

In this study a whole field, non-contact optical method, Stereo Digital Image Correlation (SDIC), was used to determine the strain distribution and mechanical properties of fresh bone in Phosphate Buffered Saline (PBS) solution. Knowing the whole-surface strain distribution of bone is useful for understanding the effects of normal physiological loading, disease, drugs and aging. In addition, knowing the mechanical properties of bone will aid in the design of new biomaterials. Although there currently are methods for measuring the mechanical properties of bone, these methods have some limitations. Many current methods are only able to characterize material properties at select points. These methods may miss areas of strain concentration, especially because of the inhomogeneous nature of bone. Digital speckle pattern interferometry is a whole surface method but is restricted to small displacement measurements. It is also difficult to measure fresh bone with a complex surface. SDIC overcomes these limitations by being able to precisely measure whole-surface 3D contour and strain of samples in solution over a wide range of deformations. In this study, SDIC was used to measure the axial and transverse strain of fresh chicken tibia. A setup which has the capability to apply force axially or transversely was designed. This paper describes the methodology of SDIC for measuring fresh bone in a PBS solution. The effect of drying time on strain distribution was investigated. The usefulness of the SDIC system is demonstrated by examples of deformation and strain measurements for different chicken tibia in PBS solution.

This study was supported by NSF/NIH 0552707.

7548F-142, Session 1

Polarized Raman spectroscopy of bone tissue: watch the scattering

M. Raghavan, N. D. Sahar, R. H. Wilson, M. Mycek, Univ. of Michigan (United States); N. Pleshko, Temple Univ. (United States); D. H. Kohn, M. D. Morris, Univ. of Michigan (United States)

Polarized Raman spectroscopy is widely used in the study of molecular composition and orientation in synthetic and natural polymer systems. Here, we describe the use of Raman spectroscopy to extract quantitative orientation information from bone tissue. Bone tissue poses special challenges to the use of polarized Raman spectroscopy for measurement of orientation distribution functions because the tissue is turbid and birefringent. Standard polarized Raman theory assumes that the medium is completely transparent. However, multiple scattering in turbid media depolarizes light and is potentially a source of error. In this work, we aim to characterize these multiple scattering effects on the polarized bone Raman spectra.

Using a Raman microprobe, we show that repeating the measurements with a series of objectives of differing numerical apertures can be used to assess the contributions of sample turbidity and depth of field to the calculated orientation distribution functions. With this test, an optic can be chosen to minimize the systematic errors introduced by multiple scattering events. We also measure the elastic light scattering properties of several different types of bones such as human specimens, genetically modified mouse bones and deuterium oxide equilibrated mouse bones. With knowledge of the optical properties of these bone tissues, we can determine if elastic light scattering affects the polarized Raman measurements.

7548F-143, Session 1

Raman spectroscopic evidence of crystalline phosphate precursor to bone apatitic mineral

J. P. McElderry, Q. Yang, G. S. Mandair, R. T. Franceschi, M. D. Morris, Univ. of Michigan (United States)

Bone is a highly specialized connective tissue comprised of cross-linked collagen fibers interspersed with apatitic mineral crystallites of various sizes, shapes, orientation, and composition. However, the nucleation, growth, and propagation of mineral crystallite into the collagenous matrix are not clearly understood. By using a research grade inverted microscope fitted with a line-shaped 830 nm laser and spectrograph, we show that the Raman scatter from mineralizing cell cultures in an incubation chamber can be collected and monitored directly through the bottom of the well-plates over a period of 24 hours. In our studies, murine-derived MC3T3 cells were incubated at 37°C in the presence of 5% CO₂ and 95% humidity. Preliminary results show the presence of a crystalline phosphate precursor to the stable bone apatite which diminished over the first 6 hours of mineralization. This transient phase caused a gradual shift in the phosphate 1 apatitic band center (950-955 cm⁻¹). The phosphate ₁ apatitic band width also narrowed with time. To quantify the amount of crystal growth in vivo, we used a calibration curve derived from X-ray powder diffraction and Raman studies performed on a series of synthetic carbonated apatites and deproteinated mouse femoral specimens.

Conference 7548F: Optics in Bone Biology and Diagnostics



7548F-144, Session 2

Results of CO2 robotic laser oseotomy in surgery with motion compensation

H. Mönnich, D. Stein, Univ. Karlsruhe (Germany)

This paper presents a visual servoing application with and without motion compensation and a fixed visual servoing configuration for CO2 laser osteotomy. A multi camera system from ART is used to track the position of the robot and a skull via marker spheres that are attached to both. A CT scan from the skull is performed and segmented to acquire a 3D model. Inside the model the position for the robot for the laser ablation is planned. The accuracy of the lightweight robot is increased with the additional supervision of an optical tracking system. Accuracy improvement was measured with an FARO measurement arm. A visual servoing control schema is presented. The demonstrator shows a working visual servoing application for laser osteotomy. To improve the error resulting mainly from the delay to acquire the data from the devices a motion compensation algorithm is introduced based on iterative learning and a normalized Least Mean Square (nLMS) filter. The results during the simulation and the experimental setup are shown. The system was then evaluated with the CO2 laser system OsteoLas X10 from Caesar - Bonn, Germany. Different cuts are performed in a static case and with breathing motion with the robot. For the breathing motion a robotic breathing simulator is used. The reached accuracy and the cutting results on bone are shown in both cases.

7548F-145, Session 2

Maturity of human bone estimated by FTIR spectroscopy analysis: implications for ostheoporosis

I. Salas-García, L. Buelta-Carrillo, F. Fanjul-Vélez, N. Ortega-Quijano, Univ. de Cantabria (Spain); M. Rada-Arias, ICANE (Spain); J. L. Arce-Diego, Univ. de Cantabria (Spain)

The knowledge about bone structure is important in several pathologies, like osteopetrosis or osteomalacia. The process of hidroxiapatite deposition on collagen structure is specially relevant in ostheoporosis. This pathology affects 1 out of 3 women and 1 out of 12 men over 50 years old.

There are several works that deal with the amount of mineral and organic components in bones. They show the existence of changes in these components of the bone tissue with the patient's age and pathology. Most of them are based on homogenized bone, so they do not consider the spatial heterogeneity of the bone.

Fourier Transform Infrared spectroscopy (FTIR) is an optical technique that allows the study of spatial bone properties. In this work the variations of the properties of mineral and organic bone components depending on anatomical position and patient's age are studied. Autopsies of healthy human iliac crest are analyzed by means of FTIR. Patients of different ages and different anatomical positions in trabecular bone are included. The maturity of the bone is estimated by means of spectra analysis, particularly phosphate and carbonate bands. Several quantitative coefficients are calculated, like the maturity index or the carbonate to phosphate ratio.

The results show a tendency in the spatial distribution of mineral and collagen maturity in most of samples, with a strong dependence on age. The results could be important in the study, prevention and treatment of ostheoporosis.

7548F-146, Session 2

Treatment feasibility study of osteoporosis using minimal invasive laser needle system

D. Kang, C. Ko, Y. Ryu, S. Park, H. Kim, B. Jung, Yonsei Univ. (Korea, Republic of)

Low level laser therapy (LLLT) has been suggested as a treatment method of osteoporosis because of its effectiveness in bone cell proliferation and bone consolidation of fracture. The clinical efficacy of LLLT is mainly limited by the light scattering property of tissue, which reduces the laser photon density at target bone sites. Minimal invasive laser needle system (MILNS) was developed to address partially the problem. MILNS stimulates directly the target bone sites by employing fine hollow needles which guides 100um optical fibers. The clinical feasibility of the system was investigated by evaluating the therapeutic efficacy for osteoporosis induced ICR female mice. Mice were divided into two groups: the SHAM-group was only stimulated by fine needle and the LASER-group was stimulated both laser and fine needle. After treatment, in-vivo micro-CT images were obtained over all mice. Three dimensional (3D) structural parameters and vBMD(volume bone mineral density, q/cm3) in the trabecular bone were measured. After 2weeks of treatment, the vBMD, BV/TV, Tb.Th and Tb.N in LASER group were significantly higher than SHAM group and the Tb.Sp, SMI and tb.Pf lower than SHAM group(p<0.05). This study implies that the MILNS might have clinically effective for osteoporosis treatment.

7548F-147, Session 2

Exposed and transcutaneous measurement of musculoskeletal tissues using fiber optic coupled Raman spectroscopy

F. W. L. Esmonde-White, K. A. Esmonde-White, M. D. Morris, Univ. of Michigan (United States)

Raman spectroscopic measurement of bone composition has shown promise as a medical diagnostic by measuring the molecular composition of the bone mineral and matrix. We previously demonstrated proof-ofprinciple transcutaneous Raman spectroscopy bone measurements. In this paper, we discuss further optimization of the instrumental configuration for efficient collection of bone signal using contact fiberoptic probe designs. To optimize collection of Raman signal through overlaying soft tissue, novel geometrically-accurate tissue phantoms were prepared. MRI and CT images of the human cadaveric specimens were used to create solid tissue phantoms with accurate geometric dimensions. In these tissue phantoms, optical properties were varied systematically. Raman spectra of the prepared tissue phantoms were used to optimize the positions of the fibers in the fiber optic system, and the laser illumination sequence in the measurements. Three fiber optic probes were developed and tested with both novel tissue phantoms and human cadaveric specimens. The contact fiber optic probes were developed for arthroscopic measurements of joints, for transcutaneous measurements of bone in situ, and for contact measurements of exposed bone. By coupling the fiber optic probe to an imaging spectrograph, spectra were collected simultaneously at many positions on the tissue. Furthermore, spectra were collected with several different excitation laser patterns to enhance the effective spatial resolution of the measurements. Finally, a series of improvements were made in the data preprocessing to improve the recovered spectral signal. Together, these modifications improve signal-to-noise and spatial resolution.

Conference 7548F: Optics in Bone Biology and Diagnostics



7548F-148, Session 2

Dynamic photophysical processes in laser irradiated human cortical skull bone measured by means of modulated luminescence and infrared photothermal radiometry

A. Mandelis, Univ. of Toronto (Canada); C. H. Kwan, University of Toronto (Canada); A. Matvienko,

Modulated luminescence (LUM) and photothermal radiometry (PTR) were used to analyze photophysical processes in the cortical layer of human skull bones. The theoretical interpretation of the results was based on the optical excitation and decay rate equations of the fluorophore and on the molecular interaction parameter with the photon field density in the matrix of the bone. Using comparisons of the theory with the frequency response of dental LUM it was concluded that the optically active molecular species (fluorophore) in the bones is hydroxyapatite. An effective relaxation lifetime of skull cortical bone was derived theoretically and was found to depend on the intrinsic fluorophore decay lifetime, on the photon field density, and on the thickness of the bone.

The photophysical theory was based on the optical excitation and decay rate equations of the fluorophore and on the molecular interaction parameter with the photon field density in the matrix of the bone. These results show that quantitative LUM and PTR can be used as a powerful and sensitive method to measure optical properties of the active fluorophore in cortical skull bones and the optical-field-induced molecular interaction parameter, the average of the excitation and decay coupling coefficients between the active lower and upper energy states E1 and E2 participating in the optical interaction and the molecular fluorophore (hydroxyapatite) which undergoes an optical field photon absorption (B12) or luminescence photon emission (B21) event. When calibrated vs. laser intensity, modulated luminescence can also be used to measure human skull thickness. These traits can be applied to monitor the bone mineral density (BMD) and, ultimately can be used as potential markers of bone health or disease, such as osteoporosis or bone cancer.

7548F-149, Session 3

Optical analysis of physical and biochemical properties of murine calvaria with combined Raman spectroscopy optical coherence tomography

H. Krishnamoorthi, C. A. Patil, D. S. Perrien, E. C. O'Quinn, G. E. Gutierrez, J. S. Nyman, A. Mahadevan-Jansen, Vanderbilt Univ. (United States)

Analysis of murine calvaria is important to the study of bone formation and development, involving the regulation of osteoblasts, the bone forming cells, and the physiochemical properties of the bone matrix. Bone biologists typically rely on histology, as well as micro computed tomography (micro-CT), to measure physical properties, namely calvarial thickness and mineral density. However, these techniques are either time-consuming (micro-CT) or destructive (histology). Multi-modal optical characterization can overcome these disadvantages and provide a faster and more detailed method than these current techniques for calvarial analysis. Optical coherence tomography is an emerging imaging modality that is capable of generating 3D volumes of data in real-time similar to micro-CT. Raman spectroscopy assesses the molecular composition of tissue, such as the mineral and collagen phases in bone. Here, we demonstrate the potential of combined Raman Spectroscopy-Optical Coherence Tomography (RS-OCT) to perform non-destructive characterization of both the structural and biochemical properties of calvaria. OCT images of dissected calvaria provided quantitative measurements of calvarial thickness, volume, and surface area. Raman spectra taken across the calvaria surface were analyzed to assess mineralization, crystallinity, and carbonate substitution. We validate

the performance of OCT in bone by correlation with both histology and micro-CT. We intend to show that RS-OCT is a potential tool for providing rapid analysis of bone formation assays as well as detecting phenotypic changes involved in genetic mouse models of bone physiology and disease.

7548F-150, Session 3

Photothermal radiometry and modulated luminescence examination of demineralized and remineralized dental lesions

A. Mandelis, Univ. of Toronto (Canada); A. Hellen, Univ. of Toronto (Canada) and Univ. of Toronto, Dept. of Dentistry (Canada); Y. Finer, University of Toronto (Canada)

Background: Dental caries is a bacterial disease manifested as a dynamic equilibrium between cycles of mineral loss (demineralization) originating in the outer tooth shell, enamel, and mineral recovery from ions in saliva to restore lost mineral (remineralization). The mechanisms governing demineralization have been well-established; however debate over physicochemical factors governing remineralization still exists. Enamel remineralization can be described as being controlled by ion diffusion through a mineralized surface layer or by diffusion through bulk enamel. As an emerging non-destructive methodology, photothermal radiometry and modulated luminescence (PTR-LUM) has shown promise in measuring changes in tooth mineral content. Objectives: 1) To identify the relationship between transverse microradiography (TMR) parameters, mineral loss and lesion depth, and PTR-LUM signals. 2) To evaluate kinetics of demineralization and remineralization and develop a photothermal diffusion model to explain signal evolution. Methods: The PTR-LUM setup consisted of two laser diodes (659 nm, 120 mW; 830 nm, 100 mW), with a beam size of 5.60 mm to ensure a one-dimensional photothermal field, a mercury-cadmium-telluride (MCT) infrared detector for PTR and photodiode for LUM. Sterilized (gamma irradiated, 4 kGy) human teeth (n=36) were subjected to demineralization (10 days) in 0.1M lactic acid gel (pH 4.5), followed by random assignment to no treatment group (n=6) or incubation in a remineralizing solution with either 0, 1 or 1000 ppm fluoride (n=10/group) for 4 weeks. Teeth mounted on LEGO® were coated in acid-resistant varnish, excluding the treated lingual surfaces and scanned intermittently during demineralization and remineralization with PTR-LUM frequency scans (1-1000 Hz). TMR analysis followed the conclusion of all treatments. Results/Conclusion: Monotonic changes with treatment time in PTR and LUM amplitude and phase signals during demineralization are consistent with an increased scattering coefficient in the demineralized enamel lesion. Remineralization produced further monotonic shifts in PTR amplitude and phase, with notable decreases in phase lag and shift of phase peaks to lower frequencies. This is consistent with the formation of a layer with lower thermal diffusivity or a layer growing in thickness as remineralization proceeded. A dense, compact mineralized layer at the enamel surface, as determined by TMR, may arrest lesion progression and arrest enamel porosities created during demineralization, thus preventing subsurface enamel remineralization. These results reveal the potential for PTR-LUM to non-invasively detect and longitudinally monitor enamel caries.

7548F-151, Session 3

Evaluation of laser ablation of knee cartilage as an alternative to microfracture surgery: pilot investigations

E. Su, B. J. F. Wong, H. Sun, T. Juhasz, Univ. of California, Irvine (United States)

An emerging clinical treatment option for articular cartilage injury includes bone marrow stimulation techniques, such as microfracture, which has grown increasingly popular among athletes. During the microfracture procedure, the surgeon penetrates the subchondral bone with an awl

Conference 7548F: Optics in Bone Biology and Diagnostics



and creates "microholes" deep enough to ensure bleeding from the bone marrow. This procedure triggers a spontaneous repair response that results in the formation of fibrocartilaginous repair tissue. The study aimed to evaluate the potential use of femtosecond lasers and Er:YAG lasers as alternatives to microfracture surgery of the knee by assessing the effects of ablation on bovine femoral condyles. Bovine femoral condyles were obtained and blocks (8mm) were extracted. The specimen were ablated with various laser dosimetry parameters and observed under a dissecting microscope to examine the effects of the lasers. Further imaging with a scanning electron microscope and conventional histology (hematoxylin and eosin staining) were done to provide more accurate information. Preliminary results show some carbonization but demonstrate little thermal damage to surrounding tissues. The femtosecond laser offers a more precise and efficient ablation than the Er:YAG laser, but both are demonstrated to be possible alternatives to the surgical-skill dependent microfracture procedure.

7548F-170, Session 3

In vivo detection of osteoarthritis in the hand with three-dimensional photoacoustic tomography

Y. Sun, E. S. Sobel, H. Jiang, Univ. of Florida (United States)

This paper presents a pilot clinical study in detecting osteoarthritis (OA) in the hand using three-dimensional (3D) photoacoustic tomography (PAT). Distal interphalangeal (DIP) finger joints from OA patients and healthy volunteers were imaged with our 3D PAT system in a spherical scanning configuration. Absorption coefficient images of the joint tissue were obtained using our finite element based photoacoustic image reconstruction algorithm coupled with the photon diffusion equation. The recovered quantitative photoacoustic images revealed significant differences in the absorption coefficient of the joint cavity (cartilage and synovial fluid) between the OA and healthy joints. Quantitative analysis of the joints also indicated an apparent difference in the recovered joint spacing between OA and healthy subjects, which is in agreement with the clinical observations. This study suggests that 3D PAT has the potential to become a useful tool for diagnosis of osteoarthritis.

Conference 7548G: Photons and Neurons II



Monday 25 January 2010 • Part of Proceedings of SPIE Vol. 7548 Photonic Therapeutics and Diagnostics VI

7548G-152, Session 1

Non-contact detection of functionally stimulated nerve activity using spectral domain optical coherence tomography

M. S. Islam, E. G. Freeman, Y. Wang, C. Oh, A. R. Ortega, B. H. Park, Univ. of California, Riverside (United States)

Current technology largely limits the analysis of neuronal processing to single or small clusters of neurons using different varieties of electrodes or the introduction of exogenous contrast agents and most of these techniques are invasive in some ways. Optical Coherence Tomography (OCT) is capable of noninvasively achieving very high resolution cross sectional images of the tissue structure in submicron level. Recent developments in spectral domain optical coherence tomography (SD-OCT) enable us to detect very small transient structural changes in nerves during action potential propagation in a non-contact minimallyinvasive manner. We demonstrate here the optical detection of the nerve activity by using a multi-functional SD-OCT system. In our experiments, rather than using electrical stimulation, the nerve sample taken from the eye of Limulus polyphemus is functionally stimulated by light and the detection of neural activity is achieved using endogenous mechanisms. Our experimental results show that we are able to detect and quantitatively measure slight changes in phase difference between the upper and lower surfaces of nerve bundles caused by a transient swelling that accompanies neural spike propagation. Importantly, these changes have a similar temporal length to the electrical signal that propagates through the nerve bundle at that time. In addition, these results require no averaging over multiple trials, indicating the ability to detect each single nerve impulse. This study might serve as the basic ground work for future experiments and will hopefully have an overall revolutionary impact on functional neuroimaging.

7548G-153, Session 1

Quantitative assessment of peripheral nerve damaging using polarization-sensitive optical coherence tomography

Y. Wang, C. M. Oh, M. S. Islam, E. G. Freeman, A. Ortega, B. H. Park, Univ. of California, Riverside (United States)

The necessity for surgical intervention for peripheral nerve damage often depends on the severity of the injury. The overall length of the repaired nerve is critical, and so such surgeries often involve differentiation of viable from damaged nerve by observation of scar formation, intraoperative electrophysiology, or imaging modalities such as computed tomography and magnetic resonance myelography. While these well-established techniques have led to great improvements in the field of acute nerve repair, they are not without flaw; waiting for scar formation introduces a delay before surgical intervention, intraoperative electrophysiology yields only bulk conduction properties of a nerve bundle with no cross-sectional differentiation, and CT and MR myelography can image only gross morphologies. Polarization-sensitive optical coherence tomography (PS-OCT) can provide a non-destructive quantitative optical assessment of nerve myelination by taking advantage of the higher degree of birefringence of myelin compared to the rest of a peripheral nerve. PS-OCT can provide rapid volumetric imaging of nerve microstructure with a resolution on the order of 2-5 microns. We present results of an animal study using data acquired from rat sciatic nerve that demonstrate the ability to non-destructively assess the viability of the peripheral nervous system through examination of structural features. A comparison of this image-derived data to electrical conduction and quantitative assessment of histological processing after Wallerian degeneration in response to controlled injury will be presented.

7548G-154, Session 2

Fast two-photon neuronal imaging and control using a spatial light modulator and ruthenium compounds

D. Peterka, V. Nikolenko, E. Fino, R. Araya, Columbia Univ. (United States); R. Etchenique, Univ. de Buenos Aires (Argentina); R. Yuste, Columbia Univ. (United States)

The ability to monitor and control neurons is critical in understanding the activity of the brain. While non-linear microscopic methods have given detailed views of structure and function, the traditional laser scanning methods typically suffer from relatively poor temporal resolution because of the serial scanning of each pixel. To increase the imaging speed, we have developed a spatial light modulator (SLM) based microscope that uses diffraction to shape the incoming two photon laser source to any arbitrary light pattern. This allows the simultaneous imaging or photostimulation of different regions of a sample with three-dimensional precision at high frame rates. Additionally we have combined this microscope with a new class of two photon active neuromodulators with Ruthenium BiPyridine (RuBi) based cages that offer great flexibility for neuronal control. We demonstrate the functionality of this system in brain slices by imaging action potentials in neuronal populations at 60Hz, and by stimulating individual neuronal spines and firing (or suppressing) action potentials in pyramidal neurons with single cell precision.

7548G-155, Session 2

Optical devices for neural imaging: an analysis of light source noise

E. A. Munro, Univ. of Toronto (Canada); T. D. O'Sullivan, Stanford Univ. (United States); K. So, H. Levy, X. Jin, Univ. of Toronto (Canada); J. S. Harris, Jr., Stanford Univ. (United States); O. Levi, Univ. of Toronto (Canada)

Intrinsic optical signal imaging (IOSI) is widely used to measure neural activation on the surface of the brain. Our group strives to integrate IOSI components into a miniature, implantable device so that images can be taken continuously in freely behaving subjects. To accomplish this, we are fabricating lasers and photodiodes in close proximity on a semiconductor substrate. Preliminary in vivo studies using a camera indicate that VCSEL (vertical cavity surface emitting laser) sources, which we desire for their high intensity, directionality, and smaller device footprint, exhibit higher noise than LEDs due to coherence effects, effectively limiting the magnitude of neural signal that can be extracted. These studies aim to quantify and reduce coherence related noise.

We implemented a novel switching circuit which acquires images sequentially using any two light sources. The switching mechanism eliminates trial to trial variability so that spatial and temporal noise between sources can be directly compared at speeds of up to 9Hz. We evaluated a red 630nm LED and a red 670nm VCSEL. In vitro measurements on a brain phantom show that the single mode VCSEL exhibits up to 10x more noise than the LED. We found that by operating the VCSEL in multimode or by using diffusing elements, the laser noise could be reduced to within a factor of 2 of the LED. Preliminary in vivo rat studies of cortical spreading depression (our chosen neural model) show that an observable optical change is measurable with both sources.



7548G-156, Session 3

Plasma membrane permeabilization by ultrashort electric pulses in nueroblastoma cells

B. L. Ibey, Air Force Research Lab. (United States); F. M. Andre, V. V. Nesin, Old Dominion Univ. (United States); G. J. Wilmink, W. P. Roach, Air Force Research Lab. (United States); A. G. Pakhomov, Old Dominion Univ. (United States)

Draft Publically Releaseable Document. Publication upon approval by Dr. Bennett Ibey

Cellular exposure to ultrashort electrical pulses (USEP) has been shown to create small pores or nanopores within the plasma membrane of mammalian cells. While too small to allow diffusion of large molecules (DNA, proteins, propidium iodide), nanopores allow ion flows into and out of the cell. It is unclear what impact USEP exposure will have on neural tissue, specifically stimulation and propagation of action potentials. As a first step in this direction, we studied the impact of USEP exposure on cultured neuroblastoma cells. Whole-cell voltage-clamp recordings and fluorescent microscopy of cells exposed to USEP showed an increase in membrane conductance and influx of thallium ions. Such results suggest that USEP may induce sufficient ion flow across excitable cell membranes to initiate action potentials.

7548G-157, Session 3

Thermographic and oxygenation imaging system for non-contact skin measurements to determine the effects of regional block anesthesia

J. H. Klaessens, M. Landman, R. de Roode, H. J. Noordmans, R. M. Verdaasdonk, Univ. Medical Ctr. Utrecht (Netherlands)

Regional anesthetic blocks are performed on patients who will undergo hand surgery. In this study, thermal and oxygenation imaging techniques were applied to observe the region affected by the peripheral block as a fast objective, non-contact, method compared to the standard pinpricks or cold sensation tests. The temperature images were acquired with an IR thermal camera (FLIR ThermoCam SC640). The data were recorded and analyzed with the ThermaCamTM Researcher software. Concentration changes of oxygenated and deoxygenated hemoglobin in the dermis of the skin were calculated using the modified Lambert Beer equation using images at selected wavelengths obtained with a CCD camera either combined with a Liquid Crystal Tunable Filter (420-730 nm) or a tunable multi wavelength LED light source ((450-880nm). In 5 patients an anesthetic block was set by administering 30-40 ml Naropin 7,5 mg/ ml around the plexus brachialis. The anesthetic block of the axillary, ulnar, median and radial nerve causes dilatation of the blood vessels inducing an increase of blood flow and, consequently, an increase of the skin temperature and skin oxygenation in the lower arm. Both imaging methods showed distinct oxygenation and temperature differences at the surface of the skin of the lower arm and hand with a good correlation with the areas with or without nerve blocks. The oxygenation imaging using a CCD camera with selected LED wavelengths might be a relative inexpensive method to observe the effectiveness of regional blocks.

7548G-158, Session 3

Noninvasive optical measurements of spatially resolved electrical activity in the mouse retina

H. C. Hendargo, R. Herrmann, B. A. Bower, V. Y. Arshavsky, J. A. Izatt, Duke Univ. (United States)

We describe development and initial results of optical imaging technology for non-invasive functional mapping of neural activity in the mouse retina. The only currently available methodology for functional mapping of the retina is electroretinography (ERG), which integrates electrical signals from all layers of retinal neurons but cannot isolate responses from individual layers. Optical coherence tomography (OCT) is capable of sectioning both in time and in depth changes that occur in the retina under visual stimulation and has been used primarily for structural imaging of the retina. However, OCT is also sensitive to minute changes in the reflectivity and index of refraction as a function of tissue depth. Such changes have been shown to accompany the activation and inactivation of retinal neurons as they process visual information. While retinal reflectivity measurements using OCT have recently been reported by others in rats, rabbits, and humans, they have not been obtained in the optically more challenging but genetically more versatile mouse model. We demonstrate the ability of OCT to detect distinct reflectivity changes in the photoreceptor and inner plexiform layers of the mouse retina in vivo in response to a bright flash stimulus. By using selective pharmacological agents and transgenic mice bearing knockouts of key retinal proteins, we will correlate the optical signals with characteristic ERG responses to isolate activity from individual retinal layers. The application of OCT to functional interrogation of the retina may open opportunities for early non-invasive diagnostics of diseases that often remain asymptomatic before irreversible visual loss takes place.

7548G-159, Session 4

Combined optical and electrical stimulation of neural tissue in vivo

A. R. Duke, J. Cayce, J. Malphrus, P. Konrad, A. Mahadevan-Jansen, D. Jansen, Vanderbilt Univ. (United States)

The recent discovery of low-intensity, pulsed infrared light for neural activation provides a novel neural stimulation modality that circumvents many of the fundamental limitations of electrical stimulation; namely the necessity of contact, presence of a stimulation artifact and relatively limited spatial selectivity. However, infrared neural stimulation (INS) is limited by an approximately 2:1 range of damaging radiant exposures to stimulation threshold radiant exposures at 2 Hz in the rat sciatic nerve. In an effort to mitigate the risk of thermally-induced tissue damage, we have developed a novel stimulation modality which delivers a sub-threshold electrical stimulus concomitantly with INS. We have shown that INS threshold is reduced by a factor of nearly 4 with hybrid stimulation, thus extending the range of radiant exposures that are both safe and effective for neural stimulation. The results of this study indicate that the relationship between the electrical stimulus (expressed as a percentage of electrical stimulation threshold) and the additional optical energy required to achieve stimulation (expressed as a percentage of INS threshold) is nonlinear. The change in INS threshold was shown to decrease linearly as the INS pulse is increasingly delayed relative to the electrical pulse. Finally, we have shown that the spatial selectivity attributed to INS is maintained when combined with a sub-threshold electrical stimulus. This novel hybrid stimulation modality is expected to facilitate the development of INS applications and to provide a new tool for elucidating the underlying mechanism of infrared neural stimulation.

7548G-160, Session 4

A comparison between infrared neural and electrical stimulation in the rat brain

J. M. Cayce, R. Friedman, E. D. Jansen, A. Mahadevan-Jansen, P. Konrad, Vanderbilt Univ. (United States)

Infrared neural stimulation has been well characterized as a novel method to stimulate peripheral nerves without causing damage or inducing a stimulation artifact. Recently, our group has shown that INS can be used to produce intrinsic optical images of the intact brain in response to INS that follow established time courses for intrinsic responses to tactile stimulation of the forepaw and whisker. While tactile stimulation is a good

Conference 7548G: Photons and Neurons II



method for identifying areas activated cortex and to test functionality of the cortex after INS, it is not a direct method of stimulating cortex. The goal of this study was to compare the optical signals (intrinsic and flavoprotein imaging) generated by INS to the signals generated by electrical stimulation. INS and electrical stimulation was performed in the somatosensory cortex corresponding to the forepaw and barrel cortex. INS was performed at 1.94 m and 1.875 m light using repetition rates between 10 - 250 Hz for pulse trains ranging between 500 ms to 1000 ms. Electrical stimulation was performed between 10 - 250 Hz at amplitudes ranging between 0.5 to 200 A through a tungsten electrode inserted 100 m into cortex. Optical images were collected at 10 Hz for 8 secs under 632 nm illumination (intrinsic) and 450 nm illumination/ >490 nm emission (flavoproteins). The resulting images were compared for signal amplitude, spatial precision, and temporal precision.

7548G-161, Session 4

Investigating the effects of infrared neural stimulation in the Aplysia californica

A. R. Duke, M. A. Gault, Vanderbilt Univ. (United States); J. Eckert, H. Lu, M. Jenkins, Case Western Reserve Univ. (United States); E. D. Jansen, Vanderbilt Univ. (United States); H. J. Chiel, Case Western Reserve Univ. (United States)

Due to advantages over traditional electrical methods of neural activation, infrared neural stimulation (INS) has guickly become the target of numerous promising research efforts seeking to apply this contact-free, artifact-free and spatially precise method of neural stimulation. However, attempts at uncovering the mechanism of INS have not progressed as quickly. Here we present an invertebrate model, the marine mollusk Aplysia californica, which offers the ability to investigate INS at the cellular level. The Aplysia is advantageous due to its large cell bodies (10-100 µm in diameter) and well-characterized axonal network. It is particularly exciting for INS as it allows for simultaneous acquisition of intracellular, extracellular and nerve bundle potentials. Here we show changes in intracellular and extracellular potentials, as well as the propagating action potentials associated with INS. In the ex vivo buccal ganglion we have demonstrated that INS is not only able to produce a suprathreshold depolarization in some cells, but also inhibit firing in other cells through the generation of a hyperpolarizing intracellular current with each pulse. We have also shown that in a single cell, stimulation at low repetition rates results in summation of the sub-threshold depolarization stemming from each INS pulse - ultimately leading to action potential initiation. The Aplysia is exciting as a new invertebrate model for studying the effects of INS at a cellular level. This system also demonstrates INS as a new spatially selective, noncontact and artifact-free tool for the neuroscience and neurobiology communities to use for high precision stimulation of a neural network.

7548G-162, Session 5

An optogenetic neural stimulation platform for concurrent induction and recording of neural activity in neurons

B. McGovern, P. Degenaar, N. Grossman, R. Berlinguer-Palmini, M. Neil, E. Drakakis, Imperial College London (United Kingdom)

The precise control of neural activity afforded by the use of light sensitive ion channels such as Channel Rhodopsin (ChR2) offers neuroscientists the means to devise new experiments not previously possible. A pulse of blue light, at a suitable intensity and wavelength results in the generation of an action potential by the illuminated neuron. In this paper we present the Optogenetic Neural Stimulation (ONS) platform which enables complex in-vitro or ex-vivo investigation of neural activity. The platform is based on the use of thousands of micro-meter sized Light Emitting Diodes (LEDs) integrated onto a single Gallium Nitrite chip. Mounted onto a microscope system, this system can be used to carry out experiments on networks of cells, or on sub-cellular regions of a neuron. We show

how the ONS enables many cells to be stimulated in parallel with millisecond timing and micrometer resolution. The resulting activity of the cells is measured using Ca2+ fluorescent imaging, patch clamping and Micro electrode arrays (MEA) recording.

7548G-163, Session 5

Transdermal Stimulation of Neural Receptors using a Nanosecond-pulsed Laser

N. M. Jindra, Air Force Research Lab. (United States)

Laser stimulation of nerves is one of the newest and fastest growing areas of the photonics industry. However, much of the studies in this field are on direct stimulation of nerves or deal with beam pulses of several milliseconds or more, likely relying on thermal constraints for nerve activation. The objective of this study was to determine if action potentials could be elicited through stimulation of skin receptors using nanosecond pulsed lasers; parameters that lie within the stress confinement region. Measurements of laser stimulated action potentials in the sciatic nerve of hairless rats (Rattus norvegicus) were made using 1540 nm and 1064 nm wavelengths. The dorsal sides of the rat's hind limbs were exposed to pulses of 15ns (Nd:YAG laser) and 55ns (Er:Glass laser) at three separate spot sizes: 2 mm, 3 mm, and 4 mm. Energy density thresholds were determined for eliciting an action potential at each experimental condition. Results from these exposures showed similar evoked potential threshold results for both wavelengths. The 2-mm diameter spot sizes yielded action potentials at much higher radiant exposure levels than those seen with the 4-mm beam size. Just as importantly, the data showed action potential thresholds well below the skin damage threshold, demonstrating the potential of using these laser parameters for neural stimulation applications.

7548G-164, Poster Session

Plasticity of climbing fibers after laseraxotomy

A. L. Allegra Mascaro, Univ. degli Studi di Firenze (Italy); P. Cesare, Fondazione Santa Lucia (Italy); L. Sacconi, Univ. degli Studi di Firenze (Italy); G. Grasselli, P. Strata, Fondazione Santa Lucia (Italy); F. S. Pavone, Univ. degli Studi di Firenze (Italy)

In the adult nervous system, different population of neurons corresponds to different regenerative behavior.

Although previous works show that olivocerebellar fibres are capable of axonal regeneration in a suitable environment as a response to injury, we have hitherto no details about the real dynamics of fiber regeneration.

Recently, two photon imaging has been coupled to laser-induced lesions to perform in vivo multiphoton nanosurgery in the Central Nervous System (CNS) of living mice expressing fluorescent proteins.

We exploited this innovative technique to investigate the reparative properties of Climbing Fibers (CFs) in the adult CNS, following the time evolution of this plastic process in vivo.

The nanosurgery technique is applied to the distal portion of a CF; 3D reconstructions of the imaged fiber through the days after this point disruption are then used to detect morphological changes in time.

Time lapse imaging of the same region over the following days shows that there may be a structural rearrangement of the dissected neuron itself or of the surrounding fibers.

According to our preliminary results, the regeneration comes not from the damaged end but from adjacent portions, suggesting that some molecules may be released and recall a reorganization of the surroundings in order to compensate for the lost afference.

The great potential of long-term two photon imaging, coupled to genetic manipulation, opens great opportunities to further investigate the dynamic properties of neurons and their rearrangement following an injury.



7548G-165, Poster Session

Sensitivity map to photostimulation of pyramidal neurons with femtosecond laser pulses

X. Liu, S. Zeng, Britton Chance Ctr. for Biomedical Photonics (China)

Abstract Specifically Induction of a neuron with light is a new method to probing neural activities. Pyramidal neurons are depolarized and fire action potentials irradiated by high intensity mode-locked infrared light. We activated of pyramidal neurons using a femtosecond laser at different locations of the cell, and simultaneously recorded their membrane potentials under the current clamp mode. According the strength of the electronic response to the photostimulation, sensitivity geography of pyramidal neurons was mapped. Through all the parts of pyramidal neurons, the axon initial segments have the highest sensitive to the photostimulation with femtosecond laser pulses.

7548G-166, Poster Session

In vivo optical microscopy of axonal myelination in chronic EAE using polarization sensitive-optical coherence tomography (PS-OCT)

C. M. Oh, Y. Wang, M. S. Islam, E. Freeman, A. Ortega, H. Park, Univ. of California, Riverside (United States)

Multiple Sclerosis is an incurable autoimmune condition in which the immune system attacks the CNS. Resulting demyelination of nerves causes progressive levels of physical and cognitive disability. This project utilizes recent advances in optical imaging to quantitatively assess nerve myelination as myelin exhibits a greater degree of birefringence than axons. Using polarization-sensitive optical coherence tomography (PS-OCT), we are capable of imaging nerves and quantitatively assessing the degree of myelination. Preliminary results indicate a direct correlation of histological parameters with birefringence values obtained from PS-OCT images which allows for a statistically significant method of quantifying axonal myelination. We applied this approach using chronic experimental autoimmune encephalomyelitis (EAE) in rodents.

By means of direct histological correlation, the ability of PS-OCT to evaluate and quantify axonal myelination/demyelination in a non-destructive, in vivo manner was assessed for this disease model.



Sunday 24 January 2010 • Part of Proceedings of SPIE Vol. 7549 Lasers in Dentistry XVI

7549-02, Session 1

Near-IR imaging of thermal changes in dental enamel during drilling with a high-speed CO2 laser and the dental hand-piece

L. H. Maung, C. S. Lee, D. Fried, Univ. of California, San Francisco (United States)

No abstract available.

7549-03, Session 1

Analysis of dental abfractions by optical coherence tomography

E. T. Demjan, C. Marcauteanu, C. Sinescu, M. Negrutiu, R. Lighezan, L. Vasile, F. Topala, Univ. de Medicina si Farmacie Victor Babes, Timisoara (Romania); M. Hughes, A. Bradu, G. Dobre, A. G. Podoleanu, Univ. of Kent (United Kingdom)

Aim and objectives. Abfraction is the pathological loss of cervical hard tooth substance caused by biomechanical overload. High horizontal occlusal forces result in large stress concentrations in the cervical region of the teeth. These stresses may be high enough to cause disruption of the bonds between the hydroxyapatite crystals, eventually resulting in the loss of cervical enamel. The present study proposes the microstructural characterization of this cervical lesions by optical coherence tomography (OCT).

Material and methods: 31 extracted bicuspids were investigated using OCT. 24 teeth derived from patients with active bruxism and laterotruzive/mediotruzive interferences; they presented deep buccal abfractions and variable degrees of occlusal pathological attrition. The other 7 bicuspids were not exposed to occlusal overload and had a normal morphology of the dental crowns.

The dental samples were investigated using a OCT device operating at 1300 nm (B-scan and C-scan mode). The system penetrates 2,5 mm in air. OCT images were compared with histological sections.

Results. The OCT investigation of bicuspids with a normal morphology revealed a homogeneous structure of the buccal cervical enamel. The C-scan and B-scan images obtained from the occlusal overloaded bicuspids visualized the wedge-shaped loss of cervical enamel and damage in the microstructure of the underlying dentin. The high occlusal forces produced a characteristic pattern of large cracks, which reached the tooth surface.

Conclusions: Optical Coherence Tomography is a promising imaging method for dental abfractions and it may offer some insight on the etiological mechanism of these noncarious cervical lesions.

7549-04. Session 1

Evaluation of a SS-OCT versus a TD-OCT system for early caries assessment

L. Choo-Smith, S. Vergnole, National Research Council Canada (Canada); J. Li, Univ. of Manitoba (Canada); M. Dufour, M. Hewko, G. Lamouche, M. Sowa, National Research Council Canada (Canada)

Optical coherence tomography (OCT) is being developed for the detection and monitoring of early dental caries. Our previous studies have shown that OCT imaging is a non-destructive method that reveals high resolution morphological details as well as regions of demineralization in early caries development. Furthermore, we have demonstrated the utility of acquiring OCT images of teeth (ex vivo) using

fibre optic probes. For this tool to be viable in a clinical setting, a system that provides rapid high-resolution imaging is required. Using a subset of extracted human teeth containing incipient lesions and other clinical features of interest, paired matched OCT images were collected from a swept-source OCT (SS-OCT) system and a time-domain OCT (TD-OCT) system both operating at ~1310 nm. Data were acquired using a rotating OCT catheter probe. The images were compared to determine which system would be more suitable for future pre-clinical studies in vivo. Results will be presented regarding the image signal-to-noise and contrast-to-noise ratios as well as parameters regarding resolution, depth penetration, measurement time and suitability for further image analyses methods involving denoising and segmentation. Based on these findings, an appropriate setup is selected for continuing OCT studies in vivo.

7549-05, Session 1

Near-IR and PS-OCT imaging of secondary caries lesions

J. Stahl, H. Kang, C. L. Darling, D. Fried, Univ. of California, San Francisco (United States)

No abstract available.

7549-06, Session 1

Selective near-UV ablation of dental calculus: measurement of removal rates

J. E. Shoenly, W. Seka, Univ. of Rochester (United States); P. Rechmann, Univ. of California, San Francisco (United States)

No abstract available.

7549-07, Session 1

High-speed scanning ablation of dental hard tissues with an I=9.3-µm CO2 laser: heat accumulation and peripheral thermal damage

D. Nguyen, M. Staninec, C. S. Lee, D. Fried, Univ. of California, San Francisco (United States)

No abstract available.

7549-08. Session 1

Laser brackets debonding: Tm:YAP and ClarityTM SL self-ligating appliance system

T. Dostalova, Charles Univ. in Prague (Czech Republic); H. Jelinkova, J. Sulc, Czech Technical Univ. in Prague (Czech Republic); P. Michalik, Charles Univ. in Prague (Czech Republic); P. Koranda, M. Nemec, M. Jelínek, M. Fibrich, Czech Technical Univ. in Prague (Czech Republic); M. Miyagi, Sendai National College of Technology (Japan)

The study demonstrates the possibility of Tm:YAP laser radiation application for ceramic brackets removing. The amount of enamel loss and residual resin on teeth has been evaluated. A diode pumped continuously running Tm:YAP microchip laser with the output power 4 W generating at wavelength 2 um was used for this debonding purposes. Interacting time and the output power were changed from 30 up to 60 sec and from 1 to 4 W, respectively, with the aim to obtain

47

Return to Contents TEL: +1 360 676 3290 · +1 888 504 8171 · customerservice@spie.org



the optimization of the debonding process. Quantitative measurements were made for visualization of the enamel surface before and after self-ligating bonding technique. The temperature rise measurement during the debonding procedure brought the possibility to find the safe value of used power and time interaction for the most rapid debonding. The whole set of debonding tooth was checked in CCD camera and scanning electron microscope to proof the damage of tooth surface.

From the measurements it is possible to conclude that continuously running, compact, diode pumped Tm:YAP microchip laser having the output power 1W applied for 60 sec can remove the ceramic bracket without enamel iatrogenic damage.

7549-09, Session 1

Er:YAG laser debonding of porcelain veneers

C. Moforth, N. C. H. Buu, F. C. Finzen, A. B. Sharma, Univ. of California, San Francisco (United States)

No abstract available.

7549-16, Poster Session

The impact of antimicrobial photodynamic therapy on streptococcus mutans in an artificial biofilm model

M. Schneider, G. Kirfel, F. Krause, O. Brede, M. Frentzen, A. Braun, Univ. Bonn (Germany)

The aim of the study was to assess the impact of laser induced antimicrobial photodynamic therapy on the viability of Stretococcus mutans cells employing an aritificial biofilm model.

Employing sterile chambered coverglasses, a salivary pellicle layer formation was induced in 19 chambers. Streptococcus mutans cells were inoculated in a sterile culture medium. Using a live/dead bacterial viability kit, bacteria with intact cell membranes stain fluorescent green. Test chambers containing each the pellicle layer and 0.5 ml of the bacterial culture were analyzed using a confocal laser scan microscope within a layer of 10 μm at intervals of 1 μm from the pellicle layer. A photosensitizer was added to the test chambers and irradiated with a diode laser (wavelength: 660 nm, output power: 100 mW, Helbo) for 2 min each.

Comparing the baseline fluorescence (median: 13.8 [U], min: 3.7, max: 26.2) with the values after adding the photosensitizer (median: 3.7, min: 1.1, max: 9), a dilution caused decrease of fluorescence could be observed (p<0.05). After irradiation of the samples with a diode laser, an additional 48 percent decrease of fluorescence became evident (median: 2.2, min: 0.4, max: 3.4) (p<0.05). Comparing the samples with added photosensitizer but without laser irradiation at different times, no decrease of fluorescence could be measured (p>0.05).

The present study indicates that antimicrobial photodynamic therapy can reduce live bacteria within a layer of 10 μ m in an artificial biofilm model. Further studies have to evaluate the maximum biofilm thickness that still allows a toxic effect on microorganisms.

7549-17, Poster Session

Evaluation of the antimicrobial effect of photodynamic antimicrobial therapy in dentin caries: a pilot in vivo study

F. M. C. Borges, J. P. M. L. Lima, M. A. S. Melo, Federal Univ. of Ceara (Brazil); M. Nobre-dos-Santos, Piracicaba Dental School -State University of Campinas (Brazil); L. K. A. Rodrigues, I. C. J. Zanin, Federal Univ. of Ceara (Brazil)

Previous in vitro and in situ studies have demonstrated that the Photodynamic antimicrobial therapy (PACT) are effective in reducing Streptococcus mutans population in artificially carious dentin. Therefore, the purpose of this pilot in vivo study was to evaluate the antimicrobial effect of PACT using toluidine blue O (TBO) and a light-emitting diode in carious dentin lesions. Five healthy adults aged 19-36 yr, with 4 active carious cavities each, participated in this study. Teeth of each volunteer were randomly divided into four groups: 1-without TBO and light; 2with TBO and without ligh; 3- without TBO and LED with 94.J cm2 and 4- with TBO and LED with 94 J.cm2. Each cavity was divided into two halves. The baseline carious dentine sample was collected from half of each cavity. Following, the treatments were performed using a random distribution of tooth into treatments. Then, the second collection of carious dentin samples was performed. Before and after treatments, carious dentine samples were analyzed with regard to the counts of total viable microorganisms, total streptococci, mutans streptococci, and lactobacilli. The data were statitically analysed by Kruskal-Wallis and Student-Newman-Keuls tests (=5%). Log reductions ranged from -0.12 to 2.68 and significant reductions were observed for PACT (group 4) when compared to the other groups (1, 2, and 3) for total streptococci and mutans streptococci. In Conclusion, PACT was effective in killing oral microorganisms present in vivo carious dentine lesions and may be a promising useful technique for eliminating bacteria from dentine before restoration.

7549-18, Poster Session

Wavelength effect in temporomandibular joint pain

A. M. C. Marques, C. M. de Carvalho, M. J. P. Ramalho, L. M. P. Ramalho, A. L. Barbosa Pinheiro, Univ. Federal da Bahia (Brazil)

Temporomandibular Disorders (TMDs) are common painful multifactorial conditions affecting the temporomandibular joint (TMJ) whose treatment depends on the type and symptoms. Initially it requires pain control. Laser-phototherapy (LPT) have been used on the treatment of pain of several origins, including TMDs. This study reports the treatment of a selected group of 74 patients treated at Laser Center of Federal University of Bahia between 2003 and 2008. Following standard anamneses, clinical and imaginologic examination and with the diagnosis of any type of TMD, the patients were set for LPT. No other intervention was carried out during the treatment. Treatment consisted of three sessions a week during six weeks. Prior irradiation, the patients were asked to score their pain using a VAS. 780, 790 or 830nm and or 660, 680nm lasers were used on each session (30/40mW; ~ 3mm; mean dose per session of 14.2 ± 6.8 J/cm²; and mean treatment dose of 170 ± 79.8 J/cm2). Eighty percent of the patients were female (~46 years old). At the end of the 12 sessions the patients were again examined and scored their pain using the VAS. The results were statistically analyzed and showed that 64% of the patients were asymptomatic or improved after treatment and that the association of the both wavelengths was statistically significant (p = 0.02) on the asymptomatic group. It is concluded that the association of red and IR laser light was effective on pain reduction on TMJ disorders of several origins.

7549-10. Session 2

Influence of photodynamic therapy on dental plaque of oral biofilm of artificial dental caries

Z. Zou, Y. Li, H. Yin, Tianjin Medical Univ. (China)

Objective: To build an artificial caries model consistent with the physiological environment and used it in PDT anti- caries experiments. To discuss the effects of PDT on the mainly oral cariogenic biofilm bacteria

Methods: An artificial caries model was built consistent with the physiological environment with Streptococcus mutans. Hematoporyrin monomethyl Ether was selected for photosensitizer. 635nm diode laser was used for irradiation, with delivered power 10mW and energy density 12.47 J/cm2. Fifty enamel blocks after recovery and breeding of



Streptococcus mutans, collection of the saliva, preparation of enamel blocks, acquired membrane of saliva, were formed artificial caries models. Separated them into five groups random, ten blocks each group: 1. Group of HMME; 2. Group of laser; 3. Group of PDT; 4. Positive control group of 0.05% chlorhexidine; 5.Negative control group of 0.9% saline. The influence of on dental plaque oral biofilm of artificial dental caries was observed according to plate counting of bacteria method.

Results: Compared to Negative control group, the number of Streptococcus mutans (CFU/ml) of oral biofilm in artificial caries model of HMME group was not significant difference (P>0.05), with the bactericidal rate only 0.05%; laser irradiation and 0.05% chlorhexidine made the number of Streptococcus mutans (CFU/ml) of oral biofilm in artificial caries model significantly reduced (P<0.05), with the bactericidal rate 59.94% and 58.52% separately; after PDT treatment against dental caries, the number of Streptococcus mutans (CFU/ml) of oral biofilm in artificial caries model significantly reduced (P<0.05), the bactericidal rate up to 99.36%.

Conclusions: HMME-PDT was an effective method in eliminate Streptococcus mutans of oral biofilm for artificial caries model. It provided an new effective approach for dental caries prevention.

7549-11, Session 2

Effects of 980 diode laser treatment combined with scaling and root planing on periodontal pockets in chronic periodontitis patients

A. Fallah,

Objective: This study compared the effect of 980 Diode laser + scaling and root planing (SRP) versus SRP alone in the treatment of chronic periodontitis.

Method: 21 healthy patients with moderate periodontitis with a probing depth of at least 5mm were included in the study. A total of 42 sites were treated during 6weeks with a combination of 980 Diode laser and SRP (21 sites) or SRP alone (21 sites). We used 980nm diode laser with 2.5W, continuous mode, 400nm fiber, and 3 mm/sec sweeping motion from the depth of pocket upward to the margin. The whole laser process was done twice with a 2 minutes gap. Every 7days for 5 weeks (total 6 dental treatment session) the laser treatment on the test group was performed on the same site. The whole laser process was performed as sham for the control group during the 6 weeks. The gingival index (GI), probing pocket depth (PPD) and bleeding on probing (BOP) were examined at the baseline and 6 weeks after the start of treatment.

Results: Both groups showed statistically significant improvements in GI, BOP and PPD after treatment. The results also showed significant improvement from laser+ SRP group to SRP alone group.

Conclusion: The present data suggest that treatment of chronic periodontitis with either 980 Diode laser + SRP or SRP alone results in statistically significant improvements in the clinical parameters. The combination of 980 Diode laser irradiation in the gingival sulcus and SRP, was significantly better as compared to SRP alone.

7549-12, Session 2

Connective tissue attachment regeneration effect of new integrated biostimulation/soft tissue laser and the reduction of periodontal pockets

R. Gougaloff, Redondo Beach Dental Group (United States) and Loma Linda Ctr. for Implantology (United States); N. Marquina, USA Laser Biotech Inc. (United States)

Aims. Measured the effects of a new dental laser that integrates biostimulation and soft tissue laser technologies in the regeneration

of connective tissue attachments and the reduction of periodontal pockets. The study measured the clinical effectiveness as an adjunct to conventional scaling and root planning (SRP) periodontal therapy.

Materials and Methods. Each of the 50 subjects in the study had at least two periodontally compromised sites on different teeth. Laser treatments were rendered using one of three lasers: (1) conventional soft tissue diode (830 nm), (2) Nd:YAG or (3) the new laser device (wavelength 805 nm, peak power 120W, maximum adjustable average power 10.5W). All subjects received SRP. Clinical Attachment Level, Bleeding on Probing, Plaque Index, and Radiographic Bone Levels were used to compare the three laser groups.

Results. The clinical results suggest that the regeneration of connective tissue attachments respond well to laser energy delivered in short bursts (low duty cycles) of high intensity laser pulses.

Conclusions. Applications of a new laser with integrated biostimulation and soft tissue laser technologies are effective in the reduction of periodontal pockets as adjunct to conventional SRP periodontal therapies.

7549-13, Session 2

Color analysis of the mucogingival tissues depending on abutment type using hyperspectral imaging

H. J. Noordmans, M. Cune, R. v. Brakel, R. Verdaasdonk, Univ. Medical Ctr. Utrecht (Netherlands)

In dentistry, titanium implant abutments cause blue-grayish shimmering of the overlying mucogingival tissues, giving an unhealthy appearance. White, zirconia abutments are supposedly advantageous from a biological and aesthetic perspective. To determine the effect on optical appearance, we measured the reflected spectrum through the mucogingival tissues covering zirconia and titanium abutments as a function of the soft-tissue thickness using hyper-spectral imaging.

Fifteen implants in 11 patients were provided with zirconia and titanium abutments (within-subject comparison) and imaged with a hyper-spectral camera mounted on a surgical microscope. Each hyper-spectral image (720x576 pixels, 70 wavelengths from 440 to 720 nm) was captured in 30 seconds, spatially and spectrally normalized, and motion corrected using GPU based image registration software. Reflection spectra were extracted from the image along the midline on the implant starting 1 mm before the mucogingival margin, and continuing 3 mm apically. Mucogingival thickness was measured on plaster casts.

Results show that zirconia implant abutments influence the reflection spectrum up to a soft-tissue thickness of 2 mm. As expected from theory, after reflection at the zirconia abutment, the longer wavelengths (red) dominate the spectrum of the back scattered light. Hemoglobin peaks are clearly visible in the reflection spectrum and may be an indicator of mucogingival health. By blinking between zirconia and titanium abutments images, it becomes clear that the difference in light reflection is the major reason why zirconia implants appear healthier. Hyperspectral imaging shows to be a practical and promising method to study the condition of oral mucogingival tissues.

7549-14, Session 2

Compositional and crystallographic changes on enamel when irradiated by Nd:YAG or Er,Cr:YSGG lasers and its resistance to demineralization when associated with fluoride

D. M. Zezell, P. A. Ana, Instituto de Pesquisas Energéticas e Nucleares (Brazil); L. Bachmann, Univ. de São Paulo (Brazil); F. G. Albero, Instituto de Pesquisas Energéticas e Nucleares (Brazil); C. Tabchoury, J. A. Cury, Faculdade de Odontologia de Piracicaba-



UNICAMP (Brazil)

This study investigated the compositional and crystallographic changes on enamel when irradiated by Er, Cr:YSGG (=2.78µm, 85J/cm2) or Nd:YAG ((=1064nm, 84.9J/cm2 associated with black coating), its resistance to demineralization when irradiation is associated with fluoride (APF-gel), and CaF2 formation and retention. Sample surfaces were analyzed by ATR-FTIR (4000-650cm-1, 4cm-1) resolution. Irradiation with Er,Cr:YSGG laser promoted a significant decrease on carbonate content of enamel. After Nd:YAG irradiation, it was observed a significant decrease of carbonate and amides I and II. X-ray diffraction showed that both laser irradiations promoted formation of -tricalcium phosphate and tetracalcium phosphate, and a significant increase on the crystal growth of the enamel apatite. (ANOVA, p<0.05 was used for all analysis). These changes can explain the improved resistance of enamel to demineralization observed in the second part of the study, in which 240 enamel slices divides in 8 groups, received 4 min of professional fluoride gel (APF-gel 1.23%F-) applied before or after irradiation. After treatments, the formation of calcium fluoride (CaF2) was determined. The remaining slabs of each group were submitted to a 10-day pH-cycling model and, subsequently, enamel demineralization was evaluated by cross-sectional microhardness. Both lasers significantly reduced enamel demineralization (ANOVA, p<0.05), and the previous APF-gel application followed by laser showed the higher reduction of enamel demineralization. CaF2 formed before pH-cycling was significantly higher in groups were APF was associated with laser irradiation. After demineralization, these groups also presented higher CaF2 retention in respect to isolated treatments (only APF or only laser), suggesting its anticaries potential.

7549-15, Session 2

Assessment of the effect of the use of laser light or Dantrolen® on facial muscle under occlusal wear: a Raman spectroscopic study in a rodent model

A. L. Barbosa Pinheiro, M. V. Lisboa, Univ. Federal da Bahia (Brazil); C. B. Lopes, R. Rocha, Univ. do Vale do Paraíba (Brazil); T. A. Ramos, I. D. Abreu, M. C. T. Cangussú, J. N. dos Santos, Univ. Federal da Bahia (Brazil)

The aim of the present study was to use Raman spectroscopy to measure levels of CaPi on muscles under occlusal wear and treated with LLLT and/or muscle relaxant therapy on rodents. The etiology of temporomandibular disorders is multifactorial. Malocclusion may influence the masticatory muscles causing fatigue. A major type of fatigue is the metabolic, caused by the increased accumulation of metabolites such as inorganic phosphate. Raman spectroscopy allows nondestructive analysis of the biochemical composition tissues. Animals and methods: 40 male Wistar rats were randomly divided into 4 groups: control (GI), Occlusal wear (GII), occlusal wear + LLLT (GIII), and occlusal wear + muscle relaxant (GIV). Controls had no treatment. Under intraperitoneal general anesthesia animals of groups II, III and IV had unilateral amputation molar cusps to simulate an occlusal wear situation. The masseter muscle of GIII received LLLT (830nm, 4J/cm2, 40mW, 2mm) after the procedure and repeated at every other day during 14/30 d. Animals of GIV were treated with a daily injection of Dantrolene® (2.5 mg/Kg in 0.5 ml of H2O) beginning 24 hours after cusp removal. Animals were killed by an overdose of general anesthetics at days 14th and 30 after cusps removal and the ipsilateral masseter muscle was excised and divided into 2. One part was routinely processed and underwent histological analysis the other was kept in Liquid nitrogen for Raman spectroscopy. The mean value of the intensity of the peak 958 cm_1 was determined. No morphological changes were seen. Raman Analysis showed significant differences between G1 and G3 (P<0.05) and between G2 and G3 (P<0.05) at day 30. Conclusion: Fatigue did not caused morphologic alterations on masseter muscle under fatigue but resulted on changes on the level of CaPi that were less compromising when the laser light was used.

7549-20, Poster Session

Do the parameters of the Er:Yag laser influences the apical sealing?

A. M. C. Marques, J. N. dos Santos, A. L. B. Pinheiro, Univ. Federal da Bahia (Brazil)

Failures on the sealing of the tooth apex is responsible for most the failures of apical surgeries. The Er:YAG laser has been proposed as an alternative for the use of rotator instruments on surgical endodontics. 12 human extracted canines without previous endodontic treatment, anatomically normal roots, free from apical lesions and disinfected were sectioned at the crown-root junction and submitted to routine endodontic treatment and randomly distributed into 2 groups. Group I, apicectomy was performed with the Er:YAG laser (250mJ/15Hz). Apical cut was performed of perpendicular mode with 3mm from the apical foramen. On Group II, the same procedures and the same sequence as above was used and 400mJ/6Hz. The specimens were divided into groups and fixed, by the cervical third, on wax. The roots were immersed in a 2% methylene blue solution and placed in a bacteriological oven for 48 h and were sagittally split into 2 parts. Apical staining was measured by 3 calibrated examiners. Group I showed the greatest level of dye leakage. There was a significantly difference between the groups (p = 0.001). it is concluded that the apicectomies carried out with 400mJ/6Hz showed the smallest infiltration value.

7549-21, Poster Session

Secondary caries detection with an oral fluorescence based camera system in vitro

O. Brede, C. Wilde, F. Krause, A. Braun, M. Frentzen, Univ. Bonn (Germany)

The aim of the study was to compare the ability of a fluorescence based optical system to detect secondary caries.

The optical detecting system (VistaProof®) illuminates the tooth surfaces with blue light emitted by high power GaN-LEDs at 405 nm. Employing this almost monochromatic excitation, fluorescence is analyzed using a RGB camera chip and encoded in color graduations (blue - red - orange - yellow) by a software (DBSWIN®), indicating the degree of caries destruction. 31 freshly extracted teeth with secondary caries were clened, excavated and refilled (Grandio®). 19 of them were filled and refilled with amalgam and 12 with a composite resin. Each step was analyzed with the respective software and analyzed statistically. Differences were considered as statistically significant at p<0.05.

There was no difference between measurements at baseline and after cleaning (Mann Whitney, p>0,05). There was a significant difference between baseline measurements of the teeth primarily filled with composite resins and the refilled situation (Mann Whitney, p=0.014). There was also a significant difference between the non-excavated and the excavated group (Mann Whitney Composite p=0.006, Amalgam p=0.018).

The in vitro study showed, that the fluorescence based system allows detecting secondary caries next to composite resin fillings but not next to amalgam restorations. Cleaning of the teeth is not necessary, if there is no visible plaque. Further studies have to show, whether the system shows the same promising results in vivo.



7549-22, Poster Session

Dental hard tissue investigation after Er:YAG laser-assisted treatment

C. C. Todea, C. Balabuc, C. Sinescu, Univ. de Medicina si Farmacie Victor Babes, Timisoara (Romania); C. Locovei, C. Demian, A. Raduta, Politehnica Univ. of Timisoara (Romania); A. Bradu, A. Podoleanu, Univ. of Kent (United Kingdom)

Purpose: To investigate the dental hard tissues morphology after Er:YAG laser-assisted treatment using en-face Optical Coherence Tomography (OCT) and Scanning Electron Microscopy (SEM) analysis.

Material and Methods: Thirty single- and multi-rooted freshly extracted human teeth free of caries were used in this study. All teeth were randomly divided into two study groups, group I (laser) and group II (control). In group I, the dental hard tissues were prepared using Er:YAG laser. The laser parameters used were VSP mode, 40-320 mJ and 10-20 Hz. In group II, the dental hard tissues were prepared using conventional methods. The dental hard tissues were first investigated using enface Optical Coherence Tomography prototype, based on transverse scanning and operating at 1300 nm. Then the samples were sectioned transversally and submitted to SEM analysis.

Results: Both investigation methods demonstrated qualitatively the surface morphology after Er:YAG laser-assisted treatment, which was considerably more suitable for filling as compared to the control group, in which the dental hard tissues were prepared conventionally.

Conclusion: The en-face OCT method provided a superior non-invasive, in depth and real time investigation method, while the SEM analysis offered more accurate surface information. Moreover, based on the results of both investigation methods, it may be concluded that Er:YAG laser-assisted treatment provides an improved surface morphology of the dental hard tissues.

7549-23, Poster Session

An in vitro study of the effect of a pulsed 10.6 µm CO2 laser and fluoride on the reduction of caries lesions progression in bovine root dentin

T. M. Parisotto, P. A. Sacramento, Faculdade de Odontologia de Piracicaba (Brazil); M. C. Alves, Educational Instistution for Agriculture-ESALQ (Brazil); M. B. D. Gavião, R. M. Puppin-Rontani, M. Nobre dos Santos, Faculdade de Odontologia de Piracicaba (Brazil)

The aim of the present study was to evaluate in vitro the combined effects of a pulsed 10.6 µm CO2 laser and fluoride on the reduction of caries lesions progression in root dentin. Sixty five slabs of previously demineralized bovine root dentin were assigned into five groups (n=13): control (no treatment), acidulated phosphate fluoride gel 1.23% (FFA), CO2 Laser (L), FFA+L, L+FFA. The lased groups were irradiated with 4.0 J/cm2. After a 7 days pH cycling regime, the knoop hardness number (KHN) was determined by cross-sectional microhardness testing (5g, 5s, 10-60 μm , 10 μm interval). The data was analyzed by ANOVA and Student t-test (= 0.05). A significant effect between KHN and the depths that indentations were made was found (p<0.05). At 10-20 µm, FFA+L (KHN: 12.12±0.95/13.07±1.03) inhibited caries progression when compared to control (KHN: 8.76±0.95/9.50±1.03) (p<0.05) and did not differ from groups L and FFA (p>0.05). At 30 µm, only in the group FFA (KHN: 15.35±1.16) the KHN was significantly higher than the control. At 40 µm, the groups FFA, L and L + FFA were capable of inhibiting significantly caries progression, however they did not differ each other (p>0.05). At depths of 50-60 μm, L alone (KHN: 17.05±1.29/18.26±1.30) was the only group that differed statistically from the control (KHN: 13.43±1.24/13.81±1.25), but did not from the other groups. In conclusion, CO2 laser alone was capable of inhibiting caries progression in the deepest layers. However, no synergic effect was obtained when FFA application and CO2 laser irradiation were combined.

7549-24, Poster Session

In vitro near-IR imaging of occlusal caries lesions using a germanium enhanced CMOS camera

C. S. Lee, C. L. Darling, D. Fried, Univ. of California, San Francisco (United States)

No abstract available.

7549-25, Poster Session

Near-IR polarization imaging of sound and carious dental hard tissues

C. L. Darling, J. J. Jiao, C. S. Lee, H. Kang, D. Fried, Univ. of California, San Francisco (United States)

No abstract available.

7549-26, Poster Session

Imaging early demineralization with PS-OCT

H. Kang, J. J. Jiao, C. S. Lee, D. Fried, Univ. of California, San Francisco (United States)

No abstract available.

7549-27, Poster Session

Measurement of the severity of occlusal caries lesions with near-IR imaging and PS-OCT

S. M. Douglas, D. Fried, C. L. Darling, Univ. of California, San Francisco (United States)

No abstract available.



Saturday-Monday 23-25 January 2010 • Part of Proceedings of SPIE Vol. 7550 Ophthalmic Technologies XX

7550-01, Session 1

Three-dimensional multimodal microscopy of rabbit cornea after cross-linking treatment

A. Krueger, Laser Zentrum Hannover e.V. (Germany); M. Hovakimyan, Univ. Rostock (Germany); D. F. Ramirez, R. Lorbeer, Laser Zentrum Hannover e.V. (Germany); M. Kröger, O. Stachs, A. Wree, R. F. Guthoff, Univ. Rostock (Germany); H. Lubatschowski, A. Heisterkamp, Laser Zentrum Hannover e.V. (Germany)

A novel clinical treatment of keratoconus is cross-linking of the cornea with Riboflavin and UV-A radiation. In spite of the positive clinical track record, the complex wound healing process is still unclear. The objective of this study was to evaluate the wound healing process in the cornea after cross-linking using various microscopic imaging techniques for complementary information on changes in morphology and physiology. Rabbit eyes were investigated in vivo using confocal cw-laser scanning microscopy in reflective mode, ex vivo with an femtosecond-laser based imaging platform integrating second harmonic generation laser scanning microscopy in forward and backward detection mode, two photon excited laser scanning microscopy of NAD(P)H and reflective confocal laser scanning microscopy. The corneae were also fixated and processed for histology and immunohistochemistry. Results: No corneal swelling after one week, fast regeneration of the epithelial layer (in process after 1 week, fully after 5 weeks), no noticeable differences in lamellar structure of collagen fibres. The anterior stroma lacked cell nuclei after one week, after 5 weeks there was still a lower abundance of metabolic active keratocytes in the anterior stroma. In the reflective confocal images, the anterior stroma constantly showed a high abundance of cell-shaped scattering structures but with features differing from normal keratocytes. Conclusion: The combination of various microscopic imaging techniques provides insight into the complex cellular and extracellular structures and processes in the cornea during the wound healing after cross-linking. Additional investigative attention should be paid on the recovery of stromal keratocytes after cross-linking.

7550-02, Session 1

Internal limiting membrane layer visualization and vitreoretinal surgery guidance using a common-path OCT integrated microsurgical tool

X. Liu, The Johns Hopkins Univ. (United States); P. Gehlbach, Johns Hopkins Univ. School of Medicine (United States); J. U. Kang, The Johns Hopkins Univ. (United States)

Contemporary retinal microsurgery is performed by skilled surgeons through operating microscopes, utilizing free hand techniques and manually operated precision micro-instruments. One technically challenging procedure involves incising the Internal Limiting Membrane (ILM) while minimizing damage to the underlying retina. One strategy for minimizing damage is to improve visualization of the ILM layer. Here we present a preliminary evaluation of a prototype tool that integrates an Ultra High Resolution Fourier Domain Common Path OCT (FD CP-OCT) into a single mode fiber probe that is integrated with a microsurgical pick. The tool provides OCT guided visualization of the ILM layer at the point of tissue contact by the microsurgical pick.

The CP-OCT system consists of a broadband SLD source (central wavelength 800nm; 3dB bandwidth 106nm), a 2x2 coupler, a spectrometer and a single mode fiber probe incorporated with a 25 gauge surgical needle (0.5mm OD). The distal end of the fiber was cleaved at a right angle, therefore the Fresnel reflection at the fiber tip provides reference light.

We have evaluated the imaging properties of this system in an enucleated

ex vivo fish eye model. Our results indicate that the ILM layer of retina was clearly visible. The current maximum imaging depth and the sensitivity of our CP-OCT was 1.4mm and 91dB respectively. We have achieved an experimental axial resolution of 3µm in air and this appears sufficient to both identify the ILM and to perform surgical maneuvers.

7550-03, Session 1

On-line visualization of retinal photocoagulation by OCT: Ex-vivo experiments

H. H. Müller, K. Schlott, T. Bonin, E. Lankenau, M. Bever, R. Brinkmann, Univ. of Lübeck (Germany); G. Hüttmann, Univ. zu Lübeck (Germany)

Photocoagulation is one of the most successful laser therapy in medicine. By irradiation of the retina with cw-laser, tissue damage is produced, which spans from the RPE to the superficial parts of the neural retina. Recently an interest in more selective retinal treatments is observed. With microsecond irradiation or near threshold coagulation, a damage confined to the RPE is possible.

Optical coherence tomography (OCT) is the only non-invasive imaging modality, which can visualize the layered structure of the retina. Though post operatively OCT images showed changes in tissue morphology due to the photocoagulation, the direct response of the tissue during and shortly after irradiation is still not known. Aim of the study was to show, that Fourier-Domain OCT is able the follow the morphological tissue changes during and immediately after coagulation.

Tissue effects of photocoagulation were visualized by OCT in enucleated pig eyes. Changes in tissue scattering were observed during and after coagulation. Whereas an initial decrease in signal intensity was caused by fringe wash-out during thermal changes of the tissue, increased scattering in parts of the retina after coagulation is caused by the the coagulation of the tissue, which ophthalmologically gives white lesions in the retina. A more sensitive marker for the onset of tissue changes are phase changes of the back scattered light which can be visualized by Doppler-OCT.

7550-04, Session 1

Bioluminescent reporters of retinal response to sub-lethal thermal stress

M. A. Mackanos, Stanford Univ. (United States); H. Nomoto, Stanford Univ. School of Medicine (United States); C. Sramek, Stanford Univ. (United States); C. H. Contag, D. Palanker, Stanford Univ. School of Medicine (United States)

It has been debated whether retinal laser therapy requires destruction of some cells or whether sub-lethal thermal stress can trigger cellular responses leading to beneficial therapeutic outcomes. Sub-lethal thermal stress does not produce ophthalmoscopically visible changes, and lack of effective means of detection cellular responses to sub-lethal irradiation has precluded the objective testing of these distinct approaches. Here we present a quantitative technique for imaging and analysis of responses to sub-lethal thermal stress in the retina using a bioluminescent reporter gene expressed from the promoter of the 70 kilodalton heat shock protein (hsp70) gene. A Nd:YAG laser (532 nm, 100 ms pulse duration, 400 um beam diameter, 6 spots per eye) was used to treat the retina in transgenic reporter mice. An increase of bioluminescence was measured at seven hours post laser treatment using a Sirius Luminometer with the Promega luciferase assay kit. Damage thresholds of photoreceptors and RPE were assessed using ophthalmoscopic visibility of the lesions, Fluorescein Angiography (FA), and fluorescent live/dead assay of the RPE whole-



mount preparation. We bracketed the retinal damage thresholds with powers ranging from 20 to 125 mW. It was determined that the threshold for induction of the hsp70 promoter was ~40% below the RPE damage as determined by live/dead assay (25 mW vs. 45 mW, respectively). Using ophthalmoscopic visibility of the lesions for titration, and decreasing the laser power accordingly, one could apply sub-lethal thermal stress to the retina, and study its response to laser retinal treatments.

7550-05, Session 1

Automatic dosimetry control for gentle retinal photocoagulation

R. Brinkmann, K. Schlott, L. Ptaszynski, J. Langejürgen, M. Bever, Univ. zu Lübeck (Germany); S. Koinzer, J. Roider, Univ. Schleswig-Holstein (Germany); R. Birngruber, Univ. zu Lübeck (Germany)

Purpose:

The extent of retinal laser coagulations depend on the temperature increase at the fundus and the time of irradiation. Due to light scattering within the eye and variable fundus pigmentation the induced temperature increase and therefore the extent of the lesions cannot be predicted solely from the laser parameters. We use optoacoustics to monitor the temperature rise in real-time and to automatically control the coagulation onto a preselected strength for each individual spot, relieving the ophthalmologists from any manual dosimetry.

Methods:

A Q-switched Nd:YLF-laser (523nm, 75ns, 1kHz) is used to probe the temperature increase during photocoagulation. The excited thermoelastic pressure waves from the retina are detected with an ultrasonic transducer embedded in the contact lens. The probe pulses are transmitted via the same slitlamp and fiber as the treatment laser radiation (cw Nd:YAG-laser, 532 nm). Experiments are performed on enucleated porcine eye globes and rabbits in vivo.

Results:

The coagulations in rabbits rise about proportional in diameter from 220 to 340 μm with an irradiation time of 300 ms when increasing the laser power from 40 to 60 mW, respectively. Using an automatic Arrhenius-correlated laser shut-off, lesions with similar diameter are generated. Automatic switch-off times vary between 59 and 87 ms for a spot diameter of 110 μm , exemplary, in the above mentioned power range.

Conclusions:

The temperature/time course during laser photocoagulation can be determined non-invasively by optoacoustics. The preliminary results are very promising towards realization of an automatic feedback controlled irradiation with adjustable coagulation strength.

7550-06. Session 2

Measurement of vibrations induced on the surface of crystalline eye lens using PhS-SDOCT

K. V. Larin, N. Sudheendran, Univ. of Houston (United States); S. Y. Emelianov, The Univ. of Texas at Austin (United States)

Studying stiffness of a crystalline eye lens can help in understanding several ocular diseases. Studies have shown that stiffness of the eye lens increases with age that might contribute to loss of accommodation. The stiffness of the lens could be assessed by measuring mechanically induced surface waves propagating on its surface. Here we present preliminary results on measurements of the vibrations induced on surface of an eye lens with phase sensitive spectral domain optical coherence tomography (PhS-SDOCT). The system shows an axial resolution of 8 µm, phase sensitivity of 0.01 radians, imaging depth of up to 3.4 mm in air and a scanning speed of 29 kHz for a single A-line. The results

indicate that the system could detect vibrations as small as 0.45 μm induced on the crystalline lens, and hence, PhS-SDOCT could be potentially used to assess stiffness of a crystalline lens.

7550-07, Session 2

Onset of oxidative stress in clear lenses using dynamic light scattering

R. R. Ansari, NASA Glenn Research Ctr. (United States); M. B. Datiles III, National Institutes of Health (United States)

We evaluated 52 eyes of young normal volunteers 22 years old and younger to determine the amount of alpha crystallin protein levels using a fiber-optic dynamic light scattering device. We find a variable amount of alpha crystallins in young clear lenses, suggesting possible predisposition of some individuals to develop cataracts sooner in life due to lower protection from oxidative stress.

7550-08, Session 2

Femto-disruption of the crystalline lens for presbyopia and cataract surgery: history and new advancements

R. R. Krueger, The Cleveland Clinic Foundation (United States); R. Naranjo Tackman, Univ. Nacional Autonoma de Mexico (Mexico); J. Villar Kuri, APEC Hospital (Mexico); R. Frey, LensAR, Inc. (United States)

Purpose: To outline the history and recent advancements of femtosecond laser use in the crystalline lens

Methods: The first concept of femtosecond laser disruption of the lens for presbyopia was published ten years ago and since that time research and investigation has led to progress in the treatment of femtosecond laser assisted presbyopia correction and cataract surgery, including comparative, contralateral studies of laser vs conventional capsulorhexis (85 eyes) and laser assisted vs. phaco-fragmentation of LOCS grade 2 cataracts (54 eyes) at the APEC hospital in Mexico City following IRB and Mexican Regulatory approval.

Results: The first of several companies in this area, LensAR, has designed a spatial localization system for precise femtosecond laser delivery within the crystalline lens. Precision capsulotomy was easily created and removed with a mean achieved diameter difference of 0.183 ±0.246mm for the laser group vs. 0.456 ±0.735mm for the manual capsulorhexis group (p=0.001). Laser cubing for nucleus fragmentation required a median cumulative dispersed energy (CDE) of 3.82 (range from 2.25 to 14.22) for the laser group vs. 7.23 (range from 2.73 to 42.35) for conventional phacoemulsification. Both groups had equivalent visual outcomes

Conclusion: Femtosecond lasers can be effectively delivered transcorneally into the crystalline lens to significantly enhance the precision of capsulotomy and reduce by 50% the CDE in breaking up nuclear fragments for cataract extraction. This technology holds promise for femto-lens surgery as the next new application of femtosecond lasers in ophthalmology.

7550-10, Session 2

Extended depth of focus intra-ocular lens: A solution for presbyopia and astigmatism

Z. Zalevsky, Bar-Ilan Univ. (Israel); A. Zlotnik, I. Raveh, S. Ben Yaish, Xceed Imaging Ltd. (Israel); O. Yehezkel, M. Belkin, Tel-Aviv Univ. (Israel)

Purpose: Subjects after cataract removal and intra-ocular lens (IOL)



implantation lose their accommodation capability and are left with a monofocal visual system. The IOL refraction and the precision of the surgery determine the focal distance and amount of astigmatic aberrations. We present a design, simulations and experimental bench testing of a novel, non-diffractive, non-multifocal, extended depth of focus (EDOF) technology incorporated into an IOL that allows the subject to have astigmatic and chromatic aberrations-free continuous focusing ability from 35cm to infinity as well as increased tolerance to IOL decentration.

Methods: The EDOF element was engraved on a surface of a monofocal rigid IOL as a series of shallow (less than one micron deep) concentric grooves around the optical axis. These grooves create an interference pattern extending the focus from a point to a length of about one mm providing a depth of focus of 3.00D with negligible loss of energy at any point of the focus while significantly reducing the astigmatic aberration of the eye and that generated during the IOL implantation. The EDOF IOL was tested on an optical bench simulating the eye model. In the experimental testing we have explored the characteristics of the obtained EDOF capability, the tolerance to astigmatic aberrations and decentration.

Results: The performance of the proposed IOL was tested for pupil diameters of 2 to 5mm and for various spectral illuminations. The MTF charts demonstrate uniform performance of the lens for up to 3.00D at various illumination wavelengths and pupil diameters while preserving a continuous contrast of above 25% for spatial frequencies of up to 25 cycles/mm. Minimal sensitivity to decentration of up to 0.75mm and capability of correcting astigmatism of up to 1 Diopter was measured.

Conclusions: The proposed EDOF IOL technology was tested by numerical simulations as well as experimentally characterized on an optical bench. The new lens is capable of solving presbyopia and astigmatism simultaneously by providing focus extension of 3.00D under various illumination conditions, wavelengths, pupil diameters and decentrations of the implanted lens without loss of energy at any of the relevant distances.

Proprietary interest: Dr. Zalevsky is a consultant to Xceed imaging and has a financial interest in the presented technology.

7550-100, Session

Technology needs for the development of the accommodative intraocular lens

O. Nishi, Nishi Eye Hospital (Japan)

No abstract available.

7550-12, Session 3

Measuring the rate of hypoxic swelling of individual layers in human cornea with high-speed ultrahigh-resolution optical coherence tomography

K. K. Bizheva, D. C. Hyun, A. A. Moayed, J. Eichel, S. Shakeel, L. Sorbara, T. Simpson, N. Hutchings, Univ. of Waterloo (Canada)

Hypoxia induced corneal swelling was observed and evaluated in healthy human volunteers by use of high speed, ultrahigh resolution optical coherence tomography (UHROCT). Two dimensional corneal images were acquired at a speed of 47,000 A-scans/s with 4.3μm x 10μm (axial x lateral) resolution in corneal tissue. The UHROCT tomograms showed clear visualization of all intra-corneal layers and allowed for evaluation of hypoxia induced swelling by measuring the thickness of individual corneal layers over time. Results from this study show that the response to hypoxia is different in the various corneal layers, with anisotropic swelling and recovery rates for the epithelium, epithelium-Bowman's complex and stroma.

7550-13, Session 3

Rapid line-scan confocal imaging of retinal activation

Y. Li, X. Yao, The Univ. of Alabama at Birmingham (United States)

Intrinsic optical signal (IOS) imaging promises a new method for high resolution study and diagnosis of retinal function. We have used a transmitted light microscope to demonstrate the feasibility of high resolution imaging of fast IOSs in isolated amphibian retinas. Transmitted light imaging provides important application for the study of isolated retinas, but reflected light recording is required for potential in vivo application of IOSs. Here, we demonstrate a rapid, high-sensitive confocal imager to achieve reflected light imaging of IOSs. In this imager, a cylindrical lens based line-scanner is employed to provide parallel illumination, and a high-speed (68,000 Hz) linear CCD camera is used to achieve simultaneous confocal detection of IOSs from multiple (1024) retinal points. The rapid line-scan confocal imager provides frame-to-frame and line-to-line imaging modalities. While the frameto-frame imaging allows dynamic visualization of IOSs with a frame speed up to 500 Hz; the line-to-line recording can provide ultrafast (68,000 Hz) monitoring of a fixed line area of the retina. In coupling with concurrent electrophysiological measurement, a series of experiments was conducted to characterize reflected IOSs in frog retinas. Our experiments indicate that fast IOSs have time courses comparable to electrophysiological kinetics. Because of effective rejection of out-offocus background light, fast confocal imaging typically discloses fast IOSs with magnitude peak > 20% dl/l, where dl is dynamic optical change and I is background light intensity. We anticipate that further development of the IOS imaging technology will pave the way toward noninvasive, high resolution evaluation of retinal function.

7550-14, Session 3

High-sensitive blood flow imaging of the retina and choroid by using double-beam optical coherence angiography

S. Makita, M. Yamanari, Univ. of Tsukuba (Japan) and Computational Optics and Ophthalmology Group (Japan); M. Miura, Tokyo Medical Univ. (Japan) and Computational Optics and Ophthalmology Group (Japan); Y. Yasuno, Univ. of Tsukuba (Japan) and Computational Optics and Ophthalmology Group (Japan)

Wide-field and high-sensitive Doppler optical coherence angiography of the posterior human eye has been demonstrated. High-sensitive phase-resolved spectral-domain optical coherence tomography using the superluminescent diode with the central wavelength of 840 nm and bandwidth of 50 nm (FWHM) is developed. Two OCT signals with a time separation are acquired simultaneously with double sampling beams divided by using a Wollaston prism and a polarization-sensitive spectrometer consisting of two line scan cameras. The total power of two beams on the cornea is 700 uW. The line scan rate of cameras is 27 kHz and each OCT channel has the sensitivity of 93 dB.

The two sampling beams are separated by approximately 162 um on the retina. The scanning of the beams is applied along the plane consisting of them. A single position on the sample is scanned twice with these two beams. High-contrast and high-sensitive phase-resolved blood flow image is obtained with these two OCT signals. Since the two signals are highly correlated, the decorrelation noise is small. In addition to that, this method does not require dense lateral sampling comparing to the lateral resolution which is demanded for previous phase-sensitive flow imaging. High-speed and high-sensitive blood flow imaging is enabled. The retinal and choroidal vasculature images with the area of 7.7 x 7.7 mm (512 x 256 axial scans) are obtained within 5 s.



7550-15, Session 3

Flicker stimulated retinal perfusion changes assessed with high-speed Doppler tomography

T. Schmoll, C. Blatter, Medizinische Univ. Wien (Austria); M. L. Villiger, C. Pache, T. Lasser, Ecole Polytechnique Fédérale de Lausanne (Switzerland); R. A. Leitgeb, Medizinische Univ. Wien (Austria)

We developed a high speed Doppler tomography system together with flow extraction algorithms that provide a flexible tool to assess retinal perfusion. The aim of the present study is to stimulate perfusion by flickering with light of adjustable color and to measure changes depending on light frequency and flicker location. We observed relative changes in arterial flow velocity during flicker stimulation up to 50%. An increase in arterial vessel diameter by 11% has been measured. We found in arteries close to the optic nerve head the highest flicker response at a frequency of 10Hz. We believe that a multi-modal functional imaging concept is of high value for an accurate and early diagnosis and understanding of retinal pathologies and pathogenesis.

7550-16, Session 3

True velocity mapping using joint spectral and time domain optical coherence tomography

I. Grulkowski, M. Szkulmowski, D. Bukowska, S. Tamborski, I. Gorczynska, A. A. Kowalczyk, M. Wojtkowski, Nicolaus Copernicus Univ. (Poland)

In this contribution we present both axial and transverse components estimation using joint Spectral and Time domain Optical Coherence Tomography (STdOCT) method. Whereas axial component of velocity vector can be determined from the time-dependent Doppler beating frequency, the transverse component can be assessed by the analysis of the broadening of flow velocity profiles (Doppler bandwidth). This enables us to quantitatively determine the absolute value of the velocity vector. The accurate analyses are performed using well-defined flow of Intralipid solution in the glass capillary. This enables performing in vivo imaging and allows to calulate velocity maps of the retinal vasculature.

7550-17, Session 3

Perfusion measures from dynamic ICG scanning laser ophthalmoscopy

S. Larkin, Lickenbrock Technologies, LLC (United States);
A. Invernizzi, Univ. of Milan (Italy); D. Beecher, Lickenbrock
Technologies, LLC (United States); G. Staurenghi, Univ. of Milan
(Italy); T. J. Holmes, Lickenbrock Technologies, LLC (United States)

Movies acquired from fundus imaging using Indocyanine Green (ICG) and a scanning laser ophthalmoscope provide information for identifying retinal vascular abnormalities. A limitation of this modality is the necessity of esoteric training for interpretation for certain disease conditions and treatments. A straightforward interpretation of these movies by objective measurements would help to eliminate this problem.

A software program has been prototyped that produces and visualizes 2D maps of perfusion measures. The program corrects for eye motion - both rigid misalignment and warp. The movie is further corrected by removing intensity flicker, vignetting and shading artifacts. Each pixel in the corrected movie is least-squares fit with a spline function to yield a smooth time-intensity function. From these smoothed curves, several perfusion measures are calculated. These include a metric that represents the amount of time required for a vessel to fill with dye and

a metric representing relative blood flow. Changes due to disease-condition progression or response to treatment are seen by comparing a baseline movie and a movie from a later date.

Preliminary test cases were studied where these measures were compared to the evaluations by standard clinical means. The measures agreed with these standard evaluations by showing increased or decreased perfusion, respectively, when the pathologic lesion was progressing or responding to treatment, respectively.

7550-18, Session 4

Corneal topography and pachymetry using high-speed swept source OCT

K. M. Karnowski, M. Gora, B. J. Kaluzny, Nicolaus Copernicus Univ. (Poland); R. A. Huber, Ludwig-Maximilians-Univ. München (Germany); M. Szkulmowski, Nicolaus Copernicus Univ. (Poland); S. Marcos, Consejo Superior de Investigaciones Científicas (Spain); A. A. Kowalczyk, M. Wojtkowski, Nicolaus Copernicus Univ. (Poland)

We present applicability of the high speed swept-source optical coherence tomography for quantitative corneal analysis, including corneal topography, pachymetry and elevations maps. The accuracy and repeatability of the measurements preformed using OCT, Oculus - Pentacam and standard corneal topographer are assessed. Simple model of the cornea as well as the human cornea in vivo are examined. An influence of a misalignment of measured cornea with respect to the instrument are estimated.

7550-19, Session 4

Extraction of clinical refractive parameters from spectral domain optical coherence tomography of the cornea

M. Zhao, A. Kuo, S. Farsiu, J. A. Izatt, Duke Univ. (United States)

Accurate determination of parameters such as curvature and power are important in the clinical diagnosis and management of processes affecting corneal refraction. Unlike Placido ring based systems [1], spectral domain-optical coherence tomography (SDOCT) offers the ability to image both the anterior and posterior refractive surfaces of the cornea for the determination of these parameters and offers higher resolution than that found in photographic imaging techniques. To produce SDOCT representations of the cornea sufficiently accurate for extraction of refractive parameters, any artifacts due to minute scanning mechanism imperfections, 3D refraction in the patient's cornea, and patient motion during SDOCT acquisition must be eliminated. We present here algorithms correcting for non-telecentric scan deformation and 3D refraction correction in the cornea, as well as a trial scan acquisition protocol designed to reduce patient motion artifact. The implemented algorithms were then used to correct SDOCT volumes of a contact lens phantom and of corneas of five healthy volunteers. Clinical parameters including radii of curvature, central power, and thickness were extracted. For the contact lens phantom, we were able to accurately recover the reference parameters. For volunteer subjects, our values varied from those of other available clinical imaging systems by approximately 2 diopters. These discrepancies are possibly due to the use of an adjusted corneal refractive index used by other systems. Incomplete removal of patient motion artifacts may also have contributed to observed discrepancies.



7550-20, Session 4

Change in peripheral refraction during acommodation: myopes vs. emmetropes

A. Ho, S. Delgado, A. Martinez, P. Sankaridurg, Institute for Eye Research Ltd. (Australia)

No abstract available.

7550-21, Session 4

Imaging distortions of the isolated crystalline lens posterior surface during optical coherence tomography

D. Borja, S. R. Uhlhorn, R. Urs, F. Manns, Bascom Palmer Eye Institute, Univ. of Miami Miller School of Medicine (United States) and Univ. of Miami (United States); J. A. Parel, Bascom Palmer Eye Institute, Univ. of Miami Miller School of Medicine (United States) and Univ. of Miami (United States) and Vision Cooperative Research Ctr. (Australia)

Purpose: To characterize the effect optical distortions on the curvature and asphericity of the posterior lens surface in OCT imaging of the isolated crystalline lens. Methods: A TD-OCT system (12µm axial and 60µm lateral resolution and a 10.0 mm axial scan length) with telecentric beam delivery and a flat scan field was used to image the complete sagittal profile of the isolated lens immersed in a preservation medium. OCT images were acquired with the anterior lens surface up and the posterior surface up on isolated human (n=8, pmt = 66±25hrs, age: 6 to 90 years) and cynomolgus monkey lenses (n = 6, pmt<24 hrs, age: 5 to 7 years). Undistorted cross-sectional shadowgraph images were obtained using an optical comparator. The posterior lens radius curvature (Rp) and asphericity (Qp) values obtained from the OCT and shadowgraph images were compared. Results: The difference between Rp measurements obtained from the two OCT images was 0.05 \pm 0.43mm and 0.02 \pm 0.20mm for the human and the cynomolgus monkey. The difference between the Rp values obtained from the shadowgraph and OCT images were 0.23 ± 0.46 (mm) and -0.19 ± 0.18 mm for the human and cynomolgus. A Bland Altman analysis showed no systematic differences between the OCT and the shadowgraph images. Conclusions: The effects of the distortions induced from the lens refractive properties are less than the resolution of our experimental OCT system. OCT can provide accurate biometric measurements of isolated lenses without the need for distortion correction.

7550-22, Session 4

A novel scanning method in anterior segment OCT to be used in imaging the radial 3-mm section of the crystalline lens

R. Yadav, Univ. of Rochester (United States); G. Yoon, Univ. of Rochester Eye Institute (United States) and Univ. of Rochester (United States)

A novel sample scanning method for an anterior segment optical coherence tomography (AS-OCT) system has been described. This scanning method has been designed for imaging the entire anterior segment of the eye (from cornea to posterior surface of the crystalline lens) at a time. The imaging of the entire anterior segment is crucial in analyzing various physiological properties of the eye.

In a traditional scanning system the beam is shined straight into the eye parallel to the optical axis. For anterior segment imaging, larger scan area leads to increase in the angle of incidence on the ocular surfaces; this causes the reduction in signal collected from regions further from the optical axis. This loss in signal combined with loss in signal due to

coherence makes it impossible to image off axis portions of the deeper surfaces of the eye, thus making it very difficult to image the entire anterior segment, where optical depth penetration of 10mm is required.

In this study we have developed a design, which achieves close to normal incidences at all the lateral locations on the ocular surfaces within 3mm from the optical axis; this way we increase the amount of light scattered back to the system. To achieve normal incidence on all the surfaces we have designed two focusing systems, one of them optimized for cornea and the front surface of the crystalline lens, while other for the back surface of the crystalline lens. The two systems are combined together into just one system by cutting the optical elements into semicircles and then gluing them together.

To evaluate the performance of our design we imaged model eye using our scanning design and compared the images obtained with the images obtained by traditional scan. Two different model eyes were used for evaluating the two optical systems. In the images obtained for the model eyes we observed significantly stronger signal (SNR improvement by a factor of 4) from our scanning design than from the traditional scan.

7550-23, Session 4

Directionality of the retinal reflection as measured with optical coherence tomography

W. Gao, Indiana Univ. (United States); B. Cense, Utsunomiya Univ. (Japan); O. P. Kocaoglu, Q. Wang, R. S. Jonnal, D. T. Miller, Indiana Univ. (United States)

The directional component of the retinal reflection, known as the optical Stiles-Crawford effect (SCE), results from the waveguiding properties of photoreceptors. The SCE is of clinical interest as normal directionality requires normal morphology of the photoreceptors and extracellular space. Uncertainty, however, remains as to the portion of the fundus reflections that is waveguided and how this may vary with retinal location. To address these questions, we have developed a spectral-domain optical coherence tomography (SD-OCT) instrument that is tailored for measuring the optical SCE over a wide range of retinal locations. The instrument systematically translates the beam across the pupil with B-scans of the retina acquired at pupil intervals of 0.5 mm. From the B-scans, the magnitude of the primary retinal reflections were extracted and fitted to a parabolic function using a least-squares method. Results show that reflections from the inner/outer segment junction (IS/OS) and posterior tips of outer segment (POS) were highly sensitive to beam entry position, whereas that of the RPE were noticeably less so. Directionality of the POS reflection was consistently stronger than that of the IS/ OS reflection regardless of retinal location with directionality of both increasing with retinal eccentricity. In comparison, directionality of the RPF was observed weak and less sensitive to retinal location.

7550-24, Session 5

Polarization sensitive corneal and anterior segment swept-source optical coherence tomography

Y. Lim, M. Yamanari, Y. Yasuno, Univ. of Tsukuba (Japan) and Computational Optics and Ophthalmology Group (Japan)

Corneal and anterior segment optical coherence tomography (CAS-OCT) is a non contact and noninvasive cross-sectional imaging tool for measuring anterior eye segment in vivo. A conventional OCT that measures only the backscattering intensity is often difficult to discriminate the tissues of the anterior eye segment, namely conjunctiva, sclera, and trabecular meshwork. Polarization-sensitive OCT (PS-OCT) has been used to visualize birefringence of the fibrous tissues, including sclera and trabecular meshwork, for better tissue discrimination. Since the PS-OCT has the advantage of tissue discrimination, and thus may be important in a clinic, we develop a compact polarization-sensitive CAS-OCT (PS-CAS-OCT) for the purpose of the routine clinical use.



Our PS-CAS-OCT also has the purpose for evaluating the usefulness of PS-OCT, and enabling large scale studies in the tissue properties of normal and diseased eyes using the benefits of the PS-OCT. To achieve our purposes, the dimensions of detection arm and reference arm were reduced to a 19 inch box in order to make the system to be portable, and a position adjustable scanning head is well-equipped for high usability.

Our PS-CAS-OCT was used to simultaneously acquire intensity and birefringence images of the anterior eye segment successfully. The system is considered to have potential to be an imaging tool for anterior eye segment which discriminates tissues by its optical properties not only by its anatomy. Using this system, we will evaluate the performance of PS-OCT as a diagnostic tool for corneal and anterior eye segment.

7550-25, Session 5

Tissue discrimination in anterior eye using three optical parameters obtained by polarization sensitive optical coherence tomography

A. Miyazawa, M. Yamanari, S. Makita, Univ. of Tsukuba (Japan) and Computational Optics and Ophthalmology Group (Japan); M. Miura, Tokyo Medical Univ. Kasumigaura Hospital (Japan) and Computational Optics and Ophthalmology Group (Japan); K. Kawana, Univ. of Tsukuba (Japan) and Computational Optics and Ophthalmology Group (Japan); K. Iwaya, National Defense Medical College (Japan) and Tokyo Medical Univ. (Japan); H. Goto, Tokyo Medical Univ. (Japan); Y. Yasuno, Univ. of Tsukuba (Japan) and Computational Optics and Ophthalmology Group (Japan)

Identification of tissue types in optical coherence tomography (OCT) were important for the diagnosis of disease. In anterior eye, because scattering property of tissues are not so different, tissue segmentation based on structural information is hard to be applied. In this presentation we demonstrate our tissue classification algorithm which is not using a levelset algorithm but based on classification of the optical properties of tissue obtained by polarization sensitive OCT (PS-OCT). We measured 4 eyes of 4 subjects by PS-OCT and calculated 3 optical property values, which were intensity, extinction coefficient and birefringence. These properties were used as features of tissue and each pixel has a set of 3 feature values which is referred to as three dimensional (3D) feature vector. All pixels were discriminated to the types of tissues according to the positions of feature vectors in the feature space. Feature distributions of 5 tissues (conjunctiva, sclera, trabecular meshwork (TM), cornea and uvea) were well separated in the 3D feature space. In 4 eyes of 4 subjects, the 5 tissues were successfully segmented. A TM-line as observed by a gonioscopy can be observed in 3D volume. According to the distance between the TM and the surface of the iris, we can intuitively asses the angle structures. Our method is useful to investigate the narrow angle and because the OCT is non-contact measurement method, this method may have a potential for a large population screening of angleclosure glaucoma.

7550-26, Session 5

Thickness and birefringence measurement of retinal nerve fiber layer tissue using polarization-sensitive optical coherence tomography and adaptive optics

Q. Wang, B. Cense, O. P. Kocaoglu, W. Gao, R. S. Jonnal, D. T. Miller, Indiana Univ. (United States)

Early detection of retinal nerve fiber layer (RNFL) loss is a critical step towards effective treatment of glaucoma and other ocular diseases that destroy this anterior layer. Change in RNFL birefringence has been

suggested to be a sensitive indicator of RNFL health and to precede clinically detectable vision loss. Here we investigate the utility of a polarization-sensitive optical coherence tomography (PS-OCT) system endowed with adaptive optics (AO) for measuring RNFL birefringence across a wide range of RNFL thicknesses. AO provides several performance advantages for PS-OCT, including increased signal to noise, higher lateral resolution, and smaller speckle size. AO-PS-OCT B-scans were acquired at multiple locations of a 61-year-old volunteer with a known arcuate RNFL defect. Results show that the double pass phase retardation per unit depth varies greatly across the retina (0.13 deg/um to 0.89 deg/um) with the thin RNFL tissue of the arcuate defect being the most birefringent.

7550-27, Session 5

Quantification of retinal lesions by polarization sensitive optical coherence tomography

C. K. Hitzenberger, B. Baumann, E. Götzinger, M. Pircher, H. Sattmann, C. Ahlers, C. Schütze, F. Schlanitz, U. Schmidt-Erfurth, Medizinische Univ. Wien (Austria)

Segmentation of retinal structures and lesions is an important step for quantitative diagnostic applications of optical coherence tomography (OCT) in ophthalmology. Previous algorithms are essentially based on variations of backscattered intensity between layers or at the boundaries of layers. Intensity based algorithms are, however, sensitive to various factors like illumination conditions, presence of vessels, or phase washout caused by ocular motions.

Polarization sensitive (PS) OCT provides additional information on tissue, allowing direct tissue identification by intrinsic contrast mechanisms. E.g., the retinal nerve fiber layer is birefringent while the retinal pigment epithelium (RPE) act as depolarizers, i.e. scramble the polarization state. We recently used the latter effect to develop improved algorithms for RPE segmentation. We now report on further extensions of this technique to segment and quantify retinal lesions. We used a spectral domain PS-OCT/SLO system for the measurements. The instrument operates at a wavelength of 840 nm and records 20000 A-scans/s. Three parameters can be measured simultaneously: reflectivity, retardation, and optic axis orientation. In addition, spatially resolved Stokes vectors can be measured from which the degree of polarization uniformity (DOPU) can be derived, a quantity closely related to the degree of polarization known from classical polarization optics.

Up to now, we used PS-OCT to image more than 600 eyes of patients with various retinal disorders like age related macular degeneration (AMD), diabetic retinopathy (DR), glaucoma, choroidal tumors, and others. Segmentation and quantification of several retinal lesions like drusen, geographic atrophy, and subretinal fluids will be presented.

7550-28, Session 6

Irreversible electroporation for non-chemical sterilization of eye drops

M. Belkin, Tel Aviv Univ. (Israel); A. Golberg, B. Rubinsky, The Hebrew Univ. of Jerusalem (Israel)

Purpose: Testing Irreversible Electroporation (IRE) as a method for nonchemical sterilization of topical eye medications.

Methods: Hylo-Comod® preservative-free eyedrop solution was contaminated with 106 CFU/mL Escherichia coli bacteria. Electroporation parameters for sterilization were investigated by comparing electrical fields of 5.4, 7.2, and 10 kV/cm, delivered as 100-µs square pulses at 1 Hz in sequences of 10 pulses, 20 pulses, or 20 pulses delivered as four sets of five pulses with 1-min intervals between each set. Pour plate counting method was used to determine microorganism survival. Effects of the treatment on temperature and pH were recorded.

Results: Twenty pulses delivered as four separate sets resulted in three



orders of magnitude reduction in bacterial load (to 0.14% \pm 0.03%). The solution remained at pH 7.5 and the temperature rose to 35.6° \pm 0.2C° when these IRE parameters were used.

Conclusions: IRE seems to be a simple method for sterilization of drugs in solution to regulatory requirements, making the use of toxic preservatives such as benzalkonium chloride and thimerosal unnecessary. The method is potentially applicable to any non-solid drug, contact lens solutions, drinks and foods.

7550-29, Session 6

Ultrashort pulse laser surgery on healthy and oedematous cornea and sclera

K. Plamann, D. A. Peyrot, F. Deloison, C. Crotti, Ecole Nationale Supérieure de Techniques Avancées (France); M. Savoldelli, J. Legeais, Hôpital Hôtel Dieu (France); F. Morin, F. Druon, M. Hanna, P. Georges, Institut d'Optique Graduate School (France)

Ultrashort pulse laser surgery on the anterior segment of the eye is an established and very successful technique in re-fractive surgery. However, present day systems are of limited use on scattering tissue: the strong degradation of the beam quality makes it difficult to use them on pathological cornea for corneal grafting. Glaucoma surgery which would neces-sitate interventions in the volume of the sclera is not possible.

Basic considerations in tissue optics and earlier experimental work suggest that the use of longer laser wavelengths will greatly improve the penetration depth and incision quality in these cases.

We present near-field and far-field theoretical modelling of the scattering process and experimental measurement of the direct and diffuse transmission of human cornea and sclera. We compare the results of these measurements to surgical experiments on tissue performed as a function of the wavelength using a broadly tuneable Optical Parametric Amplifier, an Optical Parametric Generator and a compact fibre laser source specially designed for surgery of the anterior segment of the eye. The experimental results confirm the validity of the approach and demonstrate an improvement at least of a factor of three of the laser penetration depth in pathological, strongly scattering tissue when using wavelengths within the optical transmission window between 1.6 µm and 1.8 µm. Histological and ultrastructural analysis of the tissue using transmission electron microscopy reveal the absence of any appreciable thermal or other side effects.

7550-30, Session 6

Visualizing of fs laser pulse induced microincisions inside crystalline lens tissue

O. Stachs, Univ. Rostock (Germany); S. Schumacher, Laser Zentrum Hannover e.V. (Germany); M. Kröger, Univ. Rostock (Germany); H. Hoffmann, M. Fromm, A. Heisterkamp, H. Lubatschowski, Laser Zentrum Hannover e.V. (Germany); R. F. Guthoff, Univ. Rostock (Germany)

Purpose: One strategy for restoring accommodation and overcoming lens stiffening is to use fs laser pulses either to separate the collagen fibrils by microbubbles or to induce micro-incisions inside the lens. The aim of the study was to evaluate a method for visualizing fs laser pulse induced microincisions inside crystalline lens tissue.

Method: Lenses removed from porcine eyes were modified ex vivo by fs laser pulses (wavelength 1040 nm, pulse duration 306 fs, pulse energy 1.0-2.5 $\mu J_{\rm J}$ repetition rate 100 kHz) to create defined planes at which lens fibers separate. The fs laser pulses were delivered by a 3D scanning unit and transmitted by focusing optics into the lens tissue. Lens fiber orientation and fs laser-induced micro-incisions were examined using a confocal laser scanning microscope based on a Rostock Cornea Module attached to a Heidelberg Retina Tomograph II.

Results: Normal lens fibers showed a parallel pattern, with diameters

between 3 μ m and 9 μ m, depending on scanning location. Micro-incision visualization revealed different cutting effects depending on fs laser pulse energy, ranging from altered tissue scattering properties with all fibers intact through to definite fiber separation with a wide gap. Pulse energies that were too high or overlapped too tightly produced an incomplete cutting plane due to extensive micro-bubble generation.

Conclusions: 3D CLSM permits visualization and analysis of fs laser pulse induced microincisions inside crystalline lens tissue. Avoidance of invasive tissue preparation offers a method for studying the outcome of fs laser pulse treatment without artifacts.

7550-31, Session 6

Improved safety of retinal photocoagulation with a shaped beam

C. Sramek, J. Brown, Stanford Univ. (United States); Y. Paulus, H. Nomoto, D. V. Palanker, Stanford Univ. School of Medicine (United States)

Laser photocoagulation has long been the standard of care for several retinopathies. A recent innovation, patterned scanning laser photocoagulation, simplifies and accelerates the treatment by producing multiple retinal lesions in a single step with shorter exposures. Pulses of 20 ms in duration have been found to reduce inner retinal damage and subsequent scarring, while minimizing pain, compared to conventional 100 ms treatment. However, the safe therapeutic window (defined as a ratio of power for producing a rupture to that of mild coagulation) has been found to decrease with shorter exposures.

A ring-shaped beam produces lower peak temperature in the center of the laser spot during coagulation due to optimized heat diffusion in the irradiated area. This reduces the threshold of rupture and thus improves safety of short pulse photocoagulation. A finite-element computational model of retinal photocoagulation and rupture was used to predict the expected improvement in therapeutic window for a ring-shaped beam. Sizes of the damage zone were quantified in porcine RPE explants using a fluorescent viability assay in vitro, and coagulation and rupture thresholds were measured in rabbit eyes in vivo. A 20 - 40% increase in therapeutic window relative to top-hat beam was observed for 5 - 50 ms pulse durations, potentially allowing for safe photocoagulation two times faster than with a top-hat beam. For a retinal beam size of 130 μm in diameter, the limit of safe pulse duration can be decreased from 20 ms down to 10 ms.

7550-32, Session 6

Selective retinal therapy with a continuous line scanning laser

Y. M. Paulus, A. Jain, R. F. Gariano, Stanford Univ. (United States); H. Nomoto, Stanford Univ. School of Medicine (United States); G. Schuele, Optimedica Corp. (United States); C. Sramek, R. Charalel, Stanford Univ. (United States); D. V. Palanker, Stanford Univ. School of Medicine (United States)

Many macular diseases are initiated by dysfunction of the retinal pigment epithelium (RPE), suggesting the need for RPE-specific treatments. Microsecond pulse lasers, as well as rapidly scanning continuous lasers, can selectively treat RPE cells. We evaluate the selectivity and safety of a continuous line scanning laser, as well as healing of the resulting retinal lesions.

A 532 nm laser (PASCAL) with retinal beam diameters of 40 and 66 μm and dwell times ranging from 15 to 60 μs was applied to 30 pigmented rabbits. Lesions were acutely assessed ophthalmoscopically, with fluorescein angiography (FA), and with live-dead fluorescent assay (LD). Histological analysis was performed at 7 time points from 1 hour to 2 months

FA and LD yielded similar thresholds of RPE damage. Histological



analysis demonstrated that ophthalmoscopic visibility (OV) of the lesions corresponded to photoreceptor damage. Safety and selectivity (the ratios of the thresholds of rupture and OV to FA visibility) increased with decreasing duration and beam size, but did not improve with repetitive scanning. Above the threshold of OV, histology at one day showed RPE damage and drop-out of photoreceptors. By one week, RPE proliferation and photoreceptor migration from adjacent areas restored continuity of the photoreceptor and RPE layers. By 1 month, photoreceptors appeared normal.

Retinal therapy with a fast scanning continuous laser can provide selective targeting of the RPE and, at higher power, of the photoreceptors, and allows for treatment of large areas in a short time. The safety window and selectivity increases with decreasing exposure time.

7550-33, Session 6

Experimental retinectomy with a 6.1 µm Q-switched Raman-shifted alexandrite laser

K. M. Joos, R. Prasad, J. A. Kozub, B. L. Ivanov, A. Agarwal, J. Shen, Vanderbilt Univ. (United States)

Purpose: A wavelength at 6.1 µm produced by an experimental Free Electron Laser as capable of ablating tissue, including retina, with a minimal amount of collateral damage. We hypothesize that 6.1 µm produced by a portable laser, likewise, would be useful to perform retinectomy in detached retina with extensive proliferative vitreoretinopathy.

Methods: An alexandrite laser system, which provides a high-intensity Q-switched pulse (780 nm, 50-100 ns duration, 10 Hz), is wavelength-shifted by a two-stage stimulated Raman conversion process into the 6-7 µm range (Light Age, Inc.). Fifteen fresh cadaver porcine retinas were quartered. They were lased with 6.1 µm with a 200 µm diameter spot at 0.6 - 1.8 mJ/pulse after removal of the vitreous. Specimens were examined grossly and prepared for histological examination.

Results: The Raman-shifted alexandrite laser produced a smooth Gaussian profile. A narrow spectrum was produced at 6.1 μm making it well-suited for future efficient coupling into a hollow-glass waveguide beam delivery system. The laser was capable of producing retinal incisions at 0.6 mJ. However, more uniform incisions were obtained with an output of 1.8 mJ and a 300 $\mu m/sec$ scanning speed.

Conclusions: The 6.1 µm mid-infrared energy produced by a portable laser is capable of incising retinas with minimal thermal damage. Further experiments will explore different cutting parameters as well as delivery of the energy through a surgical probe.

7550-34, Session 7

Integrated eye tracking and wide-field imaging for adaptive optics SLO

R. D. Ferguson, D. X. Hammer, Physical Sciences Inc. (United States); Z. Zhong, S. A. Burns, Indiana Univ. School of Optometry (United States)

We have developed a new adaptive optics (AO) patient interface module design and implementation incorporating a wide-field line-scanning ophthalmoscope (LSO) and a closed-loop optical retinal tracker. AO SLO or OCT scans and rasters are deflected by the tracker mirrors so that direct AO stabilization is automatic during tracking lock. The wide-field imager and dual mirror optical interface design enable placement of the AO image field at any retinal coordinates of interest in the >30 deg field. Several normal adult volunteers were image at IU. High quality AO images with a diagonal raster size of approximately 1 deg were obtained over a large angular range in the eye exhibiting a number of fine scale anatomical features Tracking was initiated during AO imaging and was compared to non-tracking sequences. During small saccades with fixating subjects, the tracking system successfully locks and maintains

the field of view. Small transients during eye accelerations may cause averaged images to loose contrast over longer duration imaging, but significant fine scale details survive. Without tracking, eye motions often exceed the raster size resulting in total loss even of reference features that might be used for post-processing image registration. Long-term tracking does not yet perform at the single cone level, yet still preserves spatial information at the cone scale. The new AO interface has the potential to address the practical limitation of AO in the clinic, and may lead to more wide-spread use of high-resolution imaging technology by ophthalmologist, optometrist, and vision researchers.

7550-35, Session 7

Multimodal adaptive optics for depth enhanced high-resolution ophthalmic imaging

D. X. Hammer, M. Mujat, N. V. Iftimia, R. D. Ferguson, Physical Sciences Inc. (United States)

Age-related macular degeneration (AMD) is a leading cause of blindness and is characterized by drusen followed by photoreceptor and retinal pigment epithelium (RPE) atrophy (geographic atrophy, GA) or the development of choroidal neovascular membranes (CNV). FDOCT systems at 1-µm have been previously developed to enhance depth penetration and these may be well suited to image AMD initiation and progression in the photoreceptor, RPE, and choriocapillaris layers. We have constructed a compact, clinical-prototype, multimodal AO retinal imaging system specifically designed to image the deeper retinal layers with long wavelength illumination. The instrument acquires AO-corrected SLO and FDOCT images. It is comprised of a 1-µm swept source Fourier domain OCT imager, a 750-nm scanning laser ophthalmoscope (SLO), and an 830-nm wide-field line scanning ophthalmoscope (LSO). The system design also includes a dual deformable mirror configuration and retinal tracker, which will be implemented in a latter stage of the project. An initial human subject investigation is underway to characterize and optimize the multimodal AO retinal imager. We will present results from normal human eyes for all imaging modes and discuss novel strip and montage scanning schemes. Future clinical studies are planned on subjects with AMD and other retinal disease (glaucoma, retinitis pigmentosa, etc.).

7550-36. Session 7

Retinal imaging with a combined adaptive optics optical coherence tomography and adaptive optics scanning laser ophthalmoscopy system

R. J. Zawadzki, UC Davis Medical Ctr. (United States); S. M. Jones, Lawrence Livermore National Lab. (United States); S. Pilli, UC Davis Medical Ctr. (United States); D. Kim, UC Davis Medical Ctr. (United States); S. S. Olivier, Lawrence Livermore National Lab. (United States); J. S. Werner, UC Davis Medical Ctr. (United States)

We describe retinal imaging results with a novel instrument that combines adaptive optics - Fourier-domain optical coherence tomography (AO-OCT) with an adaptive optics scanning laser ophthalmoscope (AO-SLO). One of the benefits of combining Fd-OCT with SLO includes automatic co-registration between the two imaging modalities and the potential for correcting lateral and transversal eye motion resulting in motion artifact-free volumetric retinal imaging. Additionally this allows for direct comparison between retinal structures that can be imaged with both modalities (e.g., photoreceptor mosaics or microvasculature maps). This dual imaging modality provides insight into some retinal properties that could not be accessed by a single imaging system. Additionally, extension of OCT and SLO beyond structural imaging may open new avenues for diagnostics and testing in ophthalmology. In particular, non-invasive vasculature mapping with these modalities holds promise



of replacing fluorescein angiography in vascular identification. Several new improvements of our system including results of testing a novel 97-actuator deformable mirror and wavefront sensor, as well as AO-SLO light intensity modulation, will also be presented.

7550-37, Session 7

Imaging retinal nerve fiber bundles at ultrahigh speed and ultrahigh resolution using OCT with adaptive optics

O. P. Kocaoglu, Indiana Univ. (United States); B. Cense, Utsunomiya Univ. (Japan); Q. Wang, J. Bruestle, J. Besecker, W. Gao, R. S. Jonnal, D. T. Miller, Indiana Univ. (United States)

Ultrahigh speed line scan detectors based on CMOS technology have been recently demonstrated in ultrahigh resolution spectral-domain optical coherence tomography (UHR-SD-OCT) for retinal imaging. While successful, fundamental tradeoffs exist been image acquisition time, image sampling density, and sensitivity, all of which impact the extent of motion artifacts, visualization of fine spatial detail, and detection of faint reflections. Here we investigate these tradeoffs for imaging retinal nerve fiber bundles (RNFBs) using UHR-SD-OCT with adaptive optics (AO). Volume scans of 3°x3° and 1.5°x1.5° were acquired at retinal locations of 3° nasal and 6° superior to the fovea on a healthy subject. Dynamic AO compensation across a 6 mm pupil provided near-diffraction-limited performance. The acquisition rates were was 22.5k lines/s and 125k lines/s with A-lines spaced at 0.9 microns and 1.8 microns and B-scans at 1.8 microns and 9 microns. Focus was optimized for visualizing the RNFBs, therefore maximizing its signal. En face projection and crosssectional views of the RNFBs were extracted from the volumes and compared to images acquired with an established CCD-based line-scan camera. The projection view was found highly sensitive to eye motion artifacts, yet could only be partially compensated with coarser sampling, since fine sampling was necessary to observe the microscopic features in the RNFBs. For the cross-sectional view, speckle noise rather than eye motion artifacts limited bundle clarity. The highest B-scan density (1.8 microns spacing) coupled with B-scan averaging proved the best combination. Regardless of view, the higher line rate provided better RNFB clarity.

7550-38, Session 8

Adaptive optics for the correction of eye aberrations

A. Hansen, M. K. Khattab, R. Lorbeer, Laser Zentrum Hannover e.V. (Germany); R. R. Krueger, The Cleveland Clinic Foundation (United States); H. Lubatschowski, Laser Zentrum Hannover e.V. (Germany)

In ophthalmology, femtosecond laser tissue transections (photodisruption) which do not provoke any damage to the retina are currently limited to the cornea or lens. In order to not harm the retina during laser application, the laser focus needs to be either a safe distance apart from the retina or the threshold energy for the tissue interaction needs to be low enough to not destruct any peripheral tissue. For surgery in the direct vicinity of the retina the threshold energy has to be reduced to a safe level. However, the aberrations of the anterior elements of the eye cause a distortion of the wavefront and therefore a raised threshold energy when focussing into the posterior segment and thus prevent an application with minimized threshold energy. We present an optical system that allows for correcting aberrations in eyes using adaptive optics consisting of a deformable mirror and a Hartmann-Shack-Sensor with a novel light source. If combined with femtosecond laser pulses this system offers the possibility for minimally invasive laser surgery in the posterior eye segment with minimized threshold energy. This offers a new approach for e.g. the treatment of tractional retinal detachment as a minimally invasive alternative to the current invasive standard vitrectomy which is very traumatic and in most cases causes

complications like cataract formation which could be avoided with laser surgery.

7550-39, Session 8

Novel applications of an adaptive optics visual simulator in the clinical setting

R. R. Krueger, K. Maia Rocha, The Cleveland Clinic Foundation (United States)

Purpose: To evaluate the clinical benefit of using an adaptive optics visual simulator (AOVS) for assessing aberration specific changes in visual acuity (VA) and depth of focus (DoF).

Methods: An AOVS (Imagine Eyes, Orsay, France) was used to optically introduce individual aberrations of different magnitude in 9 normal eyes for assessing VA change (Group 1), 10 cyclopleged eyes for assessing the ocular DoF with a fixed letter size at various distances (Group 2), and to optically correct 20 highly aberrated eyes (12 keratoconus and 8 symptomatic post refractive) in order to assess the gain in recorded visual acuity and improved visual perception (Group 3).

Results: Group 1: The correction of normal HOAs (up to 4th order) improved the best corrected VA by a mean of one line (-0.1 LogMAR), while the introduction of individual HOAs of 0.3 μm (5 mm pupil) or more reduced the VA by ~1.5 lines (+0.15 LogMAR). Group 2: The DoF was most enhanced (~2.0 D) with the introduction of 0.6 μm of spherical aberration, and worse at 0.9 μm (6 mm pupil). Group 3: The correction of highly aberrated HOAs improved keratoconus BCVA by a mean of 2 lines and post-refractive BCVA by 1.5 lines. The visual perception was markedly improved.

Conclusion: The AOVS defines the degree of VA compromise vs DoF benefit with HOAs induced in normal eyes, which is useful in designing optimal corneal or IOL shapes. It also defines the degree of improvement with HOAs corrected in highly aberrated eyes, which is useful in patient counseling.

7550-40, Session 8

Binocular adaptive optics visual simulator: understanding the impact of aberrations in real vision

E. J. Fernandez, P. Prieto, P. Artal, Univ. de Murcia (Spain)

A novel adaptive optics system is presented for the integral study of vision. The apparatus is capable for binocular operation. The binocular adaptive optics visual simulator permits measuring and manipulating ocular aberrations of the two eyes simultaneously. Aberrations can be corrected, or modified, while the subject performs visual testing under binocular vision. One of the most remarkable features of the apparatus consists on the use of a single correcting device, and a single wavefront sensor. Both the operation and the total cost of the instrument largely benefit from this attribute. The correcting device is a liquid-crystal-onsilicon (LCOS) spatial light modulator. Aberrations from the two eyes are measured with a Hartmann-Shack sensor. The basic performance of the visual simulator consists in the simultaneous projection of the two eyes' pupils onto both the corrector and sensor. Several examples of the potential of the apparatus for the study of the impact of the aberrations under binocular vision are presented. Measurements of contrast sensitivity with modified spherical aberration are showed. Different binocular combinations of spherical aberration were explored through focus. Special attention was paid on the simulation of monovision, where one eye is corrected for far vision while the other is focused at near distance. The results suggest complex binocular interactions in presence of aberrations. The apparatus can be dedicated to the better understanding of the vision mechanism, which might have an important impact in developing new protocols and treatments for presbyopia. The technique and the instrument might contribute to search optimized ophthalmic corrections.



7550-41, Session 8

Hybrid adaptive optics visual simulator

C. Canovas, S. Manzanera, P. Prieto, P. Artal, Univ. de Murcia (Spain)

Visual simulators are useful tools both to study new aspects of the visual system functioning and to design and develop new ophthalmic optics elements. We present a new Adaptive Optics system for Visual Simulation which comprises two phase manipulating elements based on diverse technologies. The Hybrid Adaptive Optics Visual Simulator synergistically combines a liquid crystal programmable phase modulator, which is ideal for static generation of abrupt or discontinuous phase profiles, with a membrane deformable mirror that can be operated to compensate ocular aberrations in real time. As a proof of concept, we present results for a trifocal phase element structured in six radial sectors with discontinuities between them. Image quality as a function of defocus was objectively measured and the experimental results were in very good agreement with the theoretical expectations, both for the trifocal profile alone and in presence of a real subject's ocular aberrations. The Hybrid Adaptive Optics Visual Simulator combines advantages from the two types of active elements currently available for adaptive optics. The device has a wide range of applications but it is specially intended as a tool for designing and developing new ophthalmic optics elements, reducing the costs of the process and eventually leading to better solutions.

7550-42, Session 9

Small animal ocular biometry using optical coherence tomography

M. Ruggeri, O. P. Kocaoglu, S. R. Uhlhorn, D. Borja, R. Urs, T. Chou, Bascom Palmer Eye Institute, Univ. of Miami Miller School of Medicine (United States) and Univ. of Miami (United States); V. Porciatti, Bascom Palmer Eye Institute, Univ. of Miami Miller School of Medicine (United States); J. A. Parel, Bascom Palmer Eye Institute, Univ. of Miami Miller School of Medicine (United States) and Univ. of Miami (United States) and Vision Cooperative Research Ctr. (Australia); F. Manns, Bascom Palmer Eye Institute, Univ. of Miami Miller School of Medicine (United States) and Univ. of Miami (United States)

An OCT system was built for imaging the whole eye in small animal models of disease. We developed a software tool for ocular biometry measurements that allows semi-automatic segmentation and conic function fitting of the main ocular structure boundaries, making the acquired data suitable for quantitative information extraction. The system was used to quantify age-related changes in the biometry of healthy C57BL/6J mice and DBA/2J mouse model of glaucoma. The algorithm for ocular biometry measurement was applied to extract the radius of curvature of the anterior and posterior cornea in three normal mice at the same age. The preliminary measurements compared well with biometric data reported in literature.

7550-43, Session 9

Ultrahigh speed imaging of the rat retina using ultrahigh resolution spectral/Fourier domain OCT

J. J. Liu, Massachusetts Institute of Technology (United States); B. M. Potsaid, Massachusetts Institute of Technology (United States) and Thorlabs, Inc. (United States); Y. Chen, Massachusetts Institute of Technology (United States); I. M. Gorczynska, Massachusetts Institute of Technology (United States) and Tufts Medical Ctr. (United States) and New England

Eye Ctr. (United States); V. J. Srinivasan, Massachusetts General Hospital (United States); J. S. Duker, Tufts Medical Ctr. (United States) and New England Eye Ctr. (United States); J. G. Fujimoto, Massachusetts Institute of Technology (United States)

We performed OCT imaging of the rat retina at 70,000 axial scans per second with ~3 µm resolution. Three-dimensional OCT (3D-OCT) data sets of the rat retina are acquired. The high speed and high density data sets enable improved en face visualization by reducing eye motion artifacts and improve Doppler OCT measurements. Minimal motion artifacts are visible and the OCT fundus images offer more precise registration of individual OCT images to retinal fundus features. Projection OCT fundus images show features such as the nerve fiber layer, retinal capillary networks and choroidal vasculature. Doppler OCT images and quantitative measurements show pulsatility in retinal blood vessels. In sum, 3D-OCT data sets obtained at high speed show reduced motion artifacts, enabling improved en face OCT fundus imaging. Doppler OCT provides non-invasive in vivo quantitative measurements of retinal blood flow properties and may benefit studies of diseases such as glaucoma and diabetic retinopathy. Ultrahigh speed imaging using ultrahigh resolution spectral / Fourier domain OCT promises to enable novel protocols for measuring small animal retinal structure and retinal blood flow. Furthermore, this non-invasive imaging technology is a promising tool for monitoring disease progression in rat and mouse models to characterize ocular disease pathogenesis and response to treatment.

7550-44, Session 9

Glaucoma models in tree shrew and rat imaged with 3D 1050-nm optical coherence tomography

A. R. Tumlinson, P. Samsel, V. Vorobyov, K. Kapoor, W. Drexler, J. E. Morgan, Cardiff Univ. (United Kingdom)

Tree shrew and rat models of glaucoma were investigated. Elevated ocular pressure (IOP) was induced by either sclerosis of the episcleral drainage vessels or injection of 5 micron magnetic beads directed to occlude the trabecullar meshwork. Preliminary work with postmortem tissues has demonstrated thinning of the nerve fiber layer and characteristic cupping of the optic discs. Preparatory to analysing in vivo changes in the glaucoma models, 3D spectral-domain optical coherence tomograms of optic nerve heads have been collected from anesthetized rat and tree shrew. In vivo tomograms appear to be favorably comparable to published data for the same species at 800nm center wavelength while showing deeper penetration beyond the retina into scleral tissue.

Please see attached 2 page extended abstract.

7550-45, Session 9

An adaptive-optics scanning laser ophthalmoscope for imaging murine retinal microstructure

C. Alt, D. P. Biss, Wellman Ctr. for Photomedicine (United States); N. Tajouri, Schepens Eye Research Institute (United States); T. C. Jakobs, Massachusetts Eye and Ear Infirmary (United States); C. P. Lin, Massachusetts General Hospital (United States)

In vivo retinal imaging is an outstanding tool to observe biological processes unfold in real-time. The ability to image microstructure in vivo can greatly enhance our definition of retinal microanatomy and normal function. Transgenic mice are frequently used for mouse models of retinal diseases. However, commercially available retinal imaging instruments lack the optical resolution necessary to visualize detail.

We developed an adaptive optics scanning laser ophthalmoscope (AO-SLO) specifically for mouse eyes. Rather than using adaptive optics correction with a Shack Hartmann wavefront sensor and a beacon laser,



our AO-SLO increases confocal signal intensity to correct for wavefront aberrations introduced by the mouse eye. The instrument employs a stochastic parallel gradient descent algorithm to modulate a deformable mirror, ultimately improving image sharpness after the confocal pinhole.

The resulting resolution allows detailed observation of retinal microstructure, such as microglia, ganglion cells with their axons and microvasculature. Our AO-SLO can resolve the moving processes microglia, demonstrating that microglia are highly motile, constantly probing their immediate environment. Similarly, we observe the slow cell death of retinal axons in models of retinal disease. We begin to study in vivo in real time how different cell populations interact to maintain or defend retinal structure and function.

7550-46, Session 9

Imaging of mouse embryonic eye development using optical coherence tomography

K. V. Larin, S. Syed, Univ. of Houston (United States)

Congenital eye defects can damage vision or even lead to blindness and account for 3.68/10,000 newborns globally. Early diagnosis is vital in the treatment, understanding and prevention of eye malformations such as irreversible blindness caused by congenital glaucoma. Some of the most common congenital eye malformations include congenital cataract, microphthalmia, anophthalmia, coloboma, corneal opacity, and congenital glaucoma. It was shown recently that Optical Coherence Tomography can be used to study cardiovascular development in cultured mice embryos. In this study, we utilized Swept Source Optical Coherence Tomography (SS-OCT) to image live mice embryos between the ages of 12.5 to 18.5 dpc through the uterus. OCT depth penetration allowed us to image whole embryonic eye globe at these stages. Our data shows that OCT can be used to image morphological growth of the ocular tissue including formation of the eyelids, lens, retina and growth of the globe with a resolution of up to 8 m. The overall growth of the eye was tracked using volume measurements of the globe. These results show that OCT imaging of the embryonic eye can establish a normal model of embryonic eye development and become a useful technique to monitor, detect and deeper understand abnormalities that could arise in the mice embryonic eye development.

7550-47, Session 9

Structural and biochemical characterization of the rat retina with combined Raman spectroscopy optical coherence tomography

C. A. Patil, Vanderbilt Univ. (United States); J. Kalkman, Academisch Medisch Ctr. (Netherlands); D. J. Faber, Univ. van Amsterdam (Netherlands); J. S. Penn, Vanderbilt Univ. (United States); T. A. G. van Leeuwen, Univ. van Amsterdam (Netherlands) and Univ. Twente (Netherlands); A. Mahadevan-Jansen, Vanderbilt Univ. (United States)

Optical Coherence Tomography (OCT) has become an established tool in ophthalmic evaluation due to its ability to perform non-invasive, high-resolution, cross-sectional imaging of the retina in real-time. However, conventional OCT provides no information as to the molecular composition of tissue. The fact that molecular changes can precede structural in the progression of retinal pathology has motivated alternative OCT system implementations with molecular contrast. An alternative approach is to develop a multi-modal instrument capable of augmenting OCT images with co-registered molecularly sensitive data sets. We present the development of a dual-modal combined Raman Spectroscopy-OCT (RS-OCT) instrument for evaluating both structural and biochemical composition of the retina. RS probes biomolecules at the vibrational level, producing tissue spectra with features associated with nucleic acids, proteins, lipids, etc. The biochemical sensitivity of RS

has been demonstrated to improve the specificity of disease diagnosis in epithelial tissues, and could assist in determining early stage retinal disease based on biochemical features that arise before structural changes become evident. The RS-OCT system here is based on a spectral domain OCT backbone at 850 nm and a 785 nm RS source, which facilitates the use of a common spectrometer. Raman spectra are registered to the central axis of the OCT image, arise from the full retinal thickness, and are collected while OCT imaging is disabled. We plan to present the system design and development, along with a feasibility study that will assess the potential for RS-OCT to track pathological progression in rat pups with oxygen induced retinopathy.

7550-48, Session 10

Multimodal multiphoton imaging of unstained cornea

N. Olivier, Ecole Polytechnique (France); F. Aptel, Ecole Nationale Supérieure de Techniques Avancées (France); A. Deniset-Besseau, Ecole Polytechnique (France); J. Legeais, Hôpital Hôtel Dieu (France); K. Plamann, Ecole Nationale Supérieure de Techniques Avancées (France); M. Schanne-Klein, E. Beaurepaire, Ecole Polytechnique (France)

Non-invasive optical methods that enable in situ visualization of tissue components are of particular relevance in ophthalmology. Commonly used techniques such as optical coherence tomography (OCT) and reflectance confocal imaging provide three-dimensional cell-scale information, based on spatial variations of refractive indices. Multiphoton imaging appears as a promising alternative method for obtaining virtual biopsies with additional contrast. We evaluated three modalities of multiphoton microscopy for imaging the anterior segment of intact human eye tissue: third-harmonic generation (THG), second-harmonic generation (SHG), and two-photon-excited fluorescence (2PEF). Imaging was performed on a custom-built laser scanning THG-SHG-2PEF microscope[1]. The three modalities provide complementary information over the entire thickness of the cornea and in the trabecular meshwork. THG imaging reveals the tissue morphology, including the epithelium and endothelium structure with sub-cellular resolution. SHG imaging probes the distribution of stromal collagen lamellae organization. 2PEF imaging reveals the elastic component of the extra-cellular matrix and the distribution of fluorescent organelles in epithelial, stromal and endothelial cells. Multimodal imaging therefore provides a detailed description of several key corneal components. We note that coherent nonlinear images (THG and SHG) rely on specific contrast mechanisms, and that their interpretation requires a careful analysis. We discuss the contrast mechanisms in these images, based on our previous studies[1]. Our data show that combined THG-SHG-2PEF microscopy is a very effective method for evaluating corneal microstructures in intact tissue, which should prove appropriate for studying corneal and glaucoma physiopathologies.

[1] Débarre et al, Nat Methods 2006.

7550-49, Session 10

Real-time mapping of the corneal subbasal nerve plexus by in vivo laser scanning confocal microscopy

R. F. Guthoff, A. Zhivov, O. Stachs, Univ. Rostock (Germany)

PURPOSE: To produce two-dimensional reconstruction maps of the living corneal sub-basal nerve plexus by in vivo laser scanning confocal microscopy in real time.

METHODS: Confocal microscopy (Heidelberg Retinal Tomograph II Rostock Cornea Modul (HRTII-RCM)) of the sub-basal nerve plexus was performed in normal and LASIK eyes. Source data (frame rate 30Hz) was used to create large-scale maps of the scanned area by means of automatic real time composite mode. The algorithm attempts to



align single live image into the mapped composite image by means of landmark feature based image processing. As a result of this spatial image transformation the same corneal structure is at the same pixel location in the transformed live image and in the composite image. Initially a single live image is used as the first instance of the composite image. The transformed live image is added to the composite image and a pixel by pixel averaging was performed in the overlap area to reduce noise in the final image.

RESULTS: Real-time mapping of the sub-basal nerve plexus was performed in large-scale up to a size of 1.6mm x 1.6mm in healthy subjects and after LASIK. Mapping quality is depending on the subject's compliance and the examiner's experience.

CONCLUSIONS: The presented method enables a real-time in vivo mapping of the sub-basal nerve plexus which is stringently necessary for statistically firmed conclusions about morphometric plexus alterations. The developed method can be used for large-scale mapping of several two-dimensional structures which is imaged by using the HRTII - RCM laser scanning system.

7550-50, Session 10

Fully automated analysis of specular microscopy images within a large range of endothelial cell densities

C. P. Bucht, St Erik's Eye Hospital (Sweden); G. Manneberg, Royal Institute of Technology (Sweden); P. G. Söderberg, Uppsala Univ. (Sweden)

No abstract available.

7550-51, Session 10

Ultrahigh-resolution corneal microstructure and tear film imaging with FDOCT at 100.000 scans/sec

R. A. Leitgeb, T. Schmoll, C. Kolbitsch, Medizinische Univ. Wien (Austria); T. Le, A. Stingl, FEMTOLASERS Produktions GmbH (Austria)

We present high-speed ultra-high resolution FDOCT providing 1.6µm axial resolution at 100.000 A-scans per second. For the first time it is possible to resolve the corneal tear film of $8.6\pm1.6\mu m$ with OCT. This is a pre-requisite for dynamic tear film studies such as film breakage. The system acquires full 3D corneal tomograms with high transverse sampling of 1000×100 Pixels within a single second thus substantially reducing motion artifacts. Applying edge detection algorithms we extract the epithelium and Bowman layer with $1\mu m$ -precision and determine their respective thicknesses as $48.7\pm1.07\mu m$ and $17.43\pm2\mu m$ over a 4mm disk.

7550-52, Session 11

low-cost, high resolution scanning laser ophthalmoscope for the clinical environment

P. Soliz, VisionQuest Inc. (United States); S. Barriga, VisionQuest Biomedical (United States) and University of New Mexico (United States); A. Larichev, Moscow State Univ. (Russian Federation)

Researchers have sought to gain greater insight into the mechanisms of the retina and the optic disc at high spatial resolutions that would enable the visualization of structures (less than 10 micrometers) such as capillary beds, photoreceptors, and nerve fiber bundles. The sources of retinal image quality degradation are aberrations within the human eye, which limit the achievable resolution and the contrast of small image details. To

overcome these fundamental limitations, researchers have been applying adaptive optics (AO) techniques to correct for the aberrations. Today, deformable mirror based adaptive optics devices have been developed to overcome the limitations of standard fundus cameras, but at prices that are typically outside affordability for most clinics.

The objective of our research was to demonstrate clinically a commercially viable, low-cost, high-resolution fundus camera that: is easy to use, i.e., consistent with the operation of current fundus cameras; has a field of view (FOV) that is typical of current fundus cameras; and has a factor of five or more improvement in resolution as compared to existing clinical instruments. This is not an adaptive optics device in the traditional sense in that it does not use deformable optics. Our low-cost fundus camera removes low-order aberrations, focus and astigmatism. We have shown that removal of low-order aberrations results in significantly better resolution images. Our optical compensator has been integrated into a low-cost scanning laser ophthalmoscope (SLO). This integrated retinal imager produces retinal and optic disc images that have up to five times better resolution when compared to today's commercial fundus cameras.

7550-53, Session 11

Spectrally encoded confocal scanning laser ophthalmoscope

Y. K. Tao, J. A. Izatt, Duke Univ. (United States)

Fundus imaging has become an essential clinical diagnostic tool in ophthalmology. Current generation scanning laser ophthalmoscopes (SLO) offer advantages over conventional fundus photography and indirect ophthalmoscopy in terms of light efficiency and contrast. As a result of the ability of SLO to provide rapid, continuous imaging of retinal structures and its versatility in accommodating a variety of illumination wavelengths, allowing for imaging of both endogenous and exogenous fluorescent contrast agents, SLO has become a powerful tool for the characterization of retinal pathologies. However, common implementations of SLO, such as the confocal scanning laser ophthalmoscope (CSLO) and line-scanning laser ophthalmoscope (LSLO), require imaging or multidimensional scanning elements which are typically implemented in bulk optics placed close to the subject eye. Here, we apply a spectral encoding technique in one dimension combined with single-axis lateral scanning to create a spectrally encoded confocal scanning laser ophthalmoscope (SECSLO) which is fully confocal. This novel implementation of the SLO allows for high contrast, high resolution in vivo human retinal imaging with image transmission through a single-mode optical fiber. Furthermore, the scanning optics are similar and the detection engine is identical to that of current-generation spectral domain optical coherence tomography (SDOCT) systems, potentially allowing for a simplistic implementation of a joint SECSLO-SDOCT imaging system.

7550-54, Session 11

In vivo investigation of human cone photoreceptors with high-speed high-resolution SLO/OCT

M. Pircher, B. Baumann, H. Sattmann, H. Prokesch, E. Goetzinger, T. Schmoll, R. A. Leitgeb, C. K. Hitzenberger, Medizinische Univ. Wien (Austria)

We use a recently developed SLO/OCT imaging system to investigate the human cone photoreceptors in vivo. The instrument operates at a frame rate of 40fps with a field of view of 1x1 degree. Hardware based axial eye tracking and a software based algorithm to correct for transverse eye motion are implemented to the system in order to eliminate all eye motion artifacts. The unique pattern of the cone mosaic can be used to observe exactly the same location on the retina over time. Bright reflections of unknown origin can be observed in the recorded 3D volumes within the outer segments of cone photoreceptors (between the inner-outer



photoreceptor segments junction and the end tips of the photoreceptors). These reflections are investigated at different eccentricities from the fovea.

7550-55, Session 11

Improved clinical performance in OCT using 1060 nm

M. Esmaeelpour, B. Hermann, B. Povozay, B. Hofer, V. Kajic, N. Sheen, R. V. North, W. Drexler, Cardiff Univ. (United Kingdom)

Introduction: Retinas of subjects with significant cataracts are difficult to image with conventional 800 nm OCT and visible light fundus photography. Additionally, visualisation of choroidal structures in emmetropic and hyperopic eyes is difficult using 800nm OCT systems.

Aims: To demonstrate the performance of the 1060nm 3D OCT it was used to measure choroidal thickness and to visualise retinal structures when cataract is present.

Methods: 3D UHR OCT at 1060nm was performed over about 36 degree centred on the fovea with 6-8 µm axial resolution and 47 kA-scans/ second, resulting in up to 70 frames/second (512 A-scans/frame). 30 subjects (age range 19-80yrs) with emmetropia or ametropia, but otherwise healthy eyes were selected. Axial eye length (cornea-RPE) was measured using optical biometry (IOL Master Zeiss, Germany). Colour coded choroidal thickness maps were segmented manually from three dimensional stacks (Figure 1). Choroidal thickness was determined between retinal pigment epithelium and the choroidal-scleral interface at central (C), nasal (N), temporal (T), superior (S), and inferior (I) locations ~7.5° off-centre. Another 15 subjects with cataract were graded by the Lens Opacities Classification System III (LOCS III) and imaged at 1060 and 800nm OCT. Imaging was performed in an area of 20 degrees centred around the fovea. Excluded criteria included pseudo-aphakia, no cataracts, or subjects who lacked the ability to fixate the target during imaging. A fundus photograph with a 45° photographic angle was taken (CR-DGi Non-Mydriatic retinal Camera, Canon, Inc., USA) from all

Results: Mean \pm SD ChTs were 317 \pm 100 μ m (C), 252 \pm 100 μ m (N), 298 \pm 90 μ m (T), 316 \pm 102 μ m (S), and 297 \pm 105 μ m (I). Axial lengths were negatively correlated with ChTs for five transversal locations (R²C=0.47, R²N=0.36, R²T=0.4, R²S=0.4, R²I=0.41, P<0.001 for all). Among 15 subjects, 25 eyes had cataract. From all 25 eyes with cataract, 48% were successfully imaged by the 800nm OCT and 88% by the 1060nm device. Remaining images were altered by diffuse shadowing that prevented viewing of retinal and choroidal structures on tomograms (Figure 2). Image quality was not altered in subjects with high fundus pigmentation.

Conclusion: The results demonstrate feasibility of 1060nm OCT imaging at the posterior pole. It is possible to penetrate the retinal pigment epithelium and visualise the choroid, while signal deterioration due to scattering caused by cataract are significantly reduced.

7550-56, Session 11

Ultrahigh-speed volumetric OCT ophthalmic imaging at 800 nm and 1050 nm

B. M. Potsaid, Massachusetts Institute of Technology (United States) and Thorlabs Inc. (United States); J. Liu, Massachusetts Institute of Technology (United States); Y. Chen, I. Gorczynska, Massachusetts Institute of Technology (United States) and Tufts Medical Ctr. (United States) and New England Eye Ctr. (United States); V. J. Srinivasan, Massachusetts General Hospital (United States); S. Barry, J. Y. Jiang, A. Cable, Thorlabs Inc. (United States); V. Manjunath, New England Eye Ctr. (United States) and Tufts Medical Ctr. (United States); J. S. Duker, Tufts Medical Ctr. (United States) and New England Eye Ctr. (United States); J. G. Fujimoto, Massachusetts Institute of Technology (United States)

We demonstrate ultrahigh speed OCT research instrumentation for acquiring high density volumetric data sets at speeds of 100,000-250,000 axial scans per second at 850nm for high axial resolution and 47,000-250,000 axial scans per second at 1050nm for deep image penetration. Motion artifacts are reduced at these ultrahigh imaging speeds and high transverse sampling densities decrease the possibility of missing focal point disease. Novel scan protocols that collect auxiliary registration data are used in post processing algorithms to generate motion corrected volumetric renderings which represent the true retinal morphology over large areas. The dense transverse sampling within the volume also enables en face visualization of individual retinal layers, revealing nerve fiber bundles, retinal capillary networks, choroid vasculature, and pores within the lamina cribrosa. Ultrahigh speed improves visualization of small features, allowing en face visualization of individual cone photoreceptors and retinal capillaries. These techniques may enable novel methods for assessing disease progression and promise to reduce the time over which retinal changes and response to therapy can be quantified. High speed imaging also allows rapid repeated imaging along a single line. Averaging of the images obtained from the same location increases contrast and reduces speckle. The results of this study suggest that ultrahigh speed OCT used to acquire dense volumetric data sets can achieve a significant improvement in performance for ophthalmic imaging. This promises to have a powerful impact in clinical applications, improving early diagnosis, reproducibility of quantitative measurements and enabling more sensitive assessment of disease progression or response to therapy.

7550-57, Session 11

Clinical application of the high-penetration optical coherence tomography using 1060-nm wavelength

Y. Ikuno, K. Sayanagi, Osaka Univ. Medical School (Japan); Y. Yasuno, Univ. of Tsukuba (Japan); S. Usui, K. Nakai, M. Sawa, M. Tsujikawa, F. Gomi, Osaka Univ. Medical School (Japan)

Purpose: Recent advances of imaging technologies have revealed the involvement of the choroid in various posterior eye diseases, which increasingly requires imaging the whole choroidal status. To evaluate the usefulness of high-penetration optical coherence tomography (HP-OCT) using a long wavelength (1060nm) in various ophthalmic pathologies originated from the choroid.

Methods: Prototype swept-source HP-OCT (50,000 A-scan/s) was applied in patients with vision-threatening and challenging diseases such as age-related macular degeneration (AMD, 26 eyes), polypoidal choroidal vasculopathy (PCV, 46 eyes), central serous chorioretinopathy (CSC, 16 eyes), Vogt-Koyanagi-Harada (VKH, 10 eyes) disease, normal tension glaucoma (NTG, 18 eyes), pathological myopia (PM, 45 eyes). Healthy volunteers (105 eyes) were also scanned as controls. Scan protocol was 512 x 255 A-scans covering 6 x 6 mm. The macula was scanned in the macular diseases, and optic nerve head in NTG patients. Choroidal thickness was measured manually by the original measuring software.

Results: Mean subfoveal choroidal thickness was 354 mm in healthy eyes. Pathologies beneath the retinal pigment epithelium (RPE) were clearly visualized in all of the subjects. Abnormal vascular tissue, choroidal polyps, and Bruch's membrane were clearly visualized inside the RPE detachment in PCV. Disappearance of the choroidal meshwork-like tissue and loss of small vessels were visualized in VKH disease, and choroidal vessels dilation in CSC. Choroidal thinning was recognized in NTG and PM.

Conclusions: HP-OCT seems to be useful to detect choroidal changes in various ocular pathologies.



7550-11, Poster Session

Non-invasive measurements of flicker vertigo

M. G. Masi, L. Peretto, Univ. degli Studi di Bologna (Italy); L. Rovati, Univ. degli Studi di Modena (Italy); R. Ansari, NASA Glenn Research Ctr. (United States)

A light flickering at a frequency of 4-20 flashes per second can produce flicker vertigo leading to convulsions, nausea, or unconsciousness. This has been a cause for several aviation accidents. Flicker vertigo can occur when a pilot is looking through a slow moving propeller toward the sun or flying with strobes light through fog and clouds.

In this paper we present a new non-invasive measurement device based on the evaluation of the pupil size variation under flicker light conditions of changing amplitude, frequency and color. The preliminary measurements were conducted in volunteer subjects of various age and gender. Two complimentary techniques (near-infrared spectroscopy or NIRS) and laser Doppler flowmetry are also being used to compare the results. Results will also be presented on the evaluation of the effect of alcohol use ("bottle-to-throttle rule) and subjects' level of fatigue and impairment.

7550-58, Poster Session

Characterization of corneal edema by forward and backward second harmonic generation microscopy

C. Hsueh, W. Lo, H. Tan, C. Dong, National Taiwan Univ. (Taiwan)

The purpose of this study is to image and quantify the structural changes of corneal edema by second harmonic generation (SHG) microscopy. Bovine cornea was used as an experimental model for characterization of structural alterations in edematous corneas. Forward SHG (FWSHG) and backward SHG (BWSHG) signals were simultaneously collected from normal and edematous bovine corneas to reveal their morphological differences. For edematous cornea, the uneven expansion in lamellar interspacing and increased lamellar thickness in posterior stroma (depth > 200 m) were identified, while the anterior stroma composed of interwoven collagen architecture remained unaffected. Our work demonstrate the capability of SHG imaging in providing morphological information for the investigation of corneal edema biophysics and that this approach may be applied in the evaluation of advancing corneal edema in vivo.

7550-59, Poster Session

Automated image classification applied to reconstituted human corneal epithelium for the early detection of toxic damage

G. F. Crosta, C. Urani, Univ. degli Studi di Milano-Bicocca (Italy); B. De Servi, M. Meloni, VitroScreen Srl (Italy)

Reconstituted human corneal epithelium (HCE) consists of immortalized cells which, when grown in vitro, give rise to a 3D layered structure resembling, by morphology and marker expression, the human corneal tissue. HCE is a model in ophthalmic toxicology. Corneal injury can be caused by a variety of agents including benzalkonium chloride (BAK). Increasing BAK concentrations reduce epithelial thickness and increase the number of necrotic cells. This investigation aims at quantitatively assessing HCE damage on a purely morphological basis by means of image recognition. The latter involves two functions: feature extraction by the spectrum enhancement algorithm and classification by principal components (PC) analysis. Four types of treatments were carried out: H1) HCE grown in standard conditions for 24h, the negative control, H2) HCE exposed to 0.1% BAK for 24h, the positive control, H3) HCE grown in standard conditions for 48h and H4) HCE exposed to 0.01% BAK for

24h. Tissues slices were stained and imaged by white light microscopy. Classifier training and validation were carried out through H1 and H2 and were rated by the confusion matrix. Images of H3 and H4, not used before, were submitted to a trained classifier. H1 and H2 have been discriminated, H3 has been recognized as morphologically identical to H1, whereas the morphology of H4, featuring the onset of damage, has been positioned in between those of H1 and H2. These results provide a proof of principle for the automated classification of HCE by means of the spectrum enhancement algorithm.

7550-60, Poster Session

Segmentation of ophthalmic optical coherence tomography images using graph cuts

S. Farsiu, X. Li, C. A. Toth, J. A. Izatt, Duke Univ. (United States)

We report on the development of an automatic method for segmenting morphological and pathological ophthalmic structures in images captured via high speed spectral domain optical coherence tomography (SDOCT). The proposed algorithm is based on the graph theory formulation of grouping, which for long has been used by for a variety of image segmentation applications. However, it was only very recently that D. Tolliver, et al. [ARVO, 2008] incorporated graph cuts for segmenting morphological structures seen on retinal SDOCT images. Unlike the said method, which relies on the mathematically complex spectral rounding solution of the grouping problem, we have based our solution on the normalized cut formulation of Shi-Malik [PAMI, 2000]. Moreover, for many practical ophthalmic segmentation problems, our approach can benefit from Dijkstra's algorithm, which facilitates incorporating prior knowledge about the structure of interest in algorithmic implementation. The rational for proposing our alternative algorithm is that, even if technically possible, it is a cumbersome task for many clinical research groups (that may not have access to the high-level image processing expertise) to customize the complex spectral rounding technique for their particular segmentation need. Alternatively, our relatively simple segmentation framework takes advantage of standard MATLAB function and toolboxes. We believe that even with low-level expertise in image processing, this framework can be customized to efficiently segment different ophthalmic structures. Experimental results on segmenting retinal layers of premature infants, as well as segmenting low-quality corneal images, are included, which attest to the effectiveness of the proposed technique.

7550-61, Poster Session

Multimodal imaging of retina tissue with enhanced contrast by multifunctional microbubbles and nanobubbles

L. Zhang, J. S. Xu, J. Huang, C. J. Roberts, R. X. Xu, The Ohio State Univ. (United States)

Purpose:

Oxygen and perfusion play an important role in the development of several retinal diseases, such as age-related macular degeneration and diabetic retinopathy. However, current techniques can not measure retina tissue oxygen and perfusion with accuracy. Therefore, we are developing multimodal imaging systems and contrast agents for quantitative imaging of retina tissue oxgen and perfusion.

Methods:

A) Contrast agent fabrication. Indocyanine Green dye (ICG) was encapsulated in biodegradable poly (lactic-co-glycolic acid) (PLGA) microbubbles and nanobubbles by a modified double emulsion process. Biomolecular markers can be conjugated with microbubbles and nanobubbles for disease targeting or oxygen sensing.

B) Multimodal imaging. The following imaging techniques are explored for tissue oxygen and perfusion imaging: (1) multispectral imaging, (2) ultrasound imaging of disease targeting microbubbles and nanobubbles,



(3) fluorescence imaging, (4) photoacoustic imaging.

Results:

A) The size distribution of microbubbles and nanobubbles are 3.4±1.8um and 400±100nm respectively. The PLGA shell effectively protected ICG from aggregation and molecular interaction. Therefore the contrast agents showed consistent absorption and emission peaks in water and in plasma. PLGA surface has also been modified to conjugate with disease specific biomarkers.

B) ICG microbubbles and nanobubbles have been tested in various imaging modalities such as multispectral imaging, ultrasound imaging, fluorescence imaging, and photoacoustic imaging.

Conclusions:

Multimodal imaging with contrast enhancement by multifunctional microbubbles and nanobubbles have the potential for quantitative imaging of retina tissue oxygen and perfusion.

7550-62, Poster Session

In vivo dual-modality imaging of eye in small animal models: optical coherence tomography and photoacoustic microscopy within a single instrument

B. Rao, L. Li, S. Hu, K. Maslov, L. V. Wang, Washington Univ. at St. Louis (United States)

Optical Coherence Tomography (OCT) has great impact on in vivo human eye imaging as one of major clinic diagnostic technologies in ophthalmology. By combining the optical scattering contrast and Doppler contrast with optical coherence gating, OCT has demonstrated high spatial resolution imaging of tissue anatomy structure and blood flow in human eye. Alternatively, photo-acoustic imaging method utilizes the optical absorption contrast that is complement to OCT to form tomography image. Recent development of photo-acoustic microscopy (PAM) has demonstrated in vivo microvasculature imaging with high spatial resolution. Previous work has revealed the potential of a dualmodality instrument that employs both OCT and transmission mode PAM. In this work, we combined contrasts of both OCT and PAM in a single reflection-mode instrument for the potential applications of diagnosing, monitoring and management of human eye diseases. We demonstrated in vivo dual-modality eye imaging in small animal models with endogenous contrasts.

7550-63, Poster Session

Early cataract detection by dynamic light scattering with sparse Bayesian learning

S. Nyeo, National Cheng Kung Univ. (Taiwan); R. R. Ansari, NASA Glenn Reseach Ctr. (United States)

Experimental data are statistical in nature and necessarily require a probabilistic analysis tool. For early cataract detection by dynamic light scattering (DLS), the probabilistic sparse Bayesian learning (SBL) algorithm is introduced for analyzing DLS data of ocular lenses. The algorithm is used to reconstruct the most-probable size distribution of alpha-crystallin and their aggregates in an ocular lens. The performance of the algorithm is studied by analyzing simulated correlation data from known distributions and DLS data from the ocular lenses of humans so as to establish the required efficiency of the SBL algorithm for clinical studies.

7550-64, Poster Session

Label-free structural characterization of mitomycin C modulated wound healing after photorefractive keratectomy by the use of multiphoton microscopy

W. Lo, National Taiwan Univ. (Taiwan) and National Cheng Kung Univ. (Taiwan); T. Wang, Taipei Medical Univ. (Taiwan) and National Taiwan Univ. (Taiwan) and National Taiwan Univ. College of Medicine (Taiwan); C. Hsueh, National Taiwan Univ. (Taiwan); S. Chen, National Cheng Kung Univ. (Taiwan); F. Hu, National Taiwan Univ. Hospital (Taiwan) and National Taiwan Univ. College of Medicine (Taiwan); C. Dong, National Taiwan Univ. (Taiwan)

In this work, we investigate post surgery wound healing process from photorefractive keratectomy (PRK) using label-free, multiphoton autofluroescence and second harmonic generation microscopy. The effectiveness of mitomycin C (MMC) in modulating collagen regeneration and keratocyte activation is qualitatively and quantitatively evaluated. We found that MAF imaging shows that re-epithelialization is accomplished in 1 week in corneas with and without MMC treatment and reveals that keratocyte activation peaks at Week 2 after PRK procedure. However, we found that keratocyte activation is highly reduced in MMC treated corneas. In addition, there is positive, linear correlation between active keratocyte density in MAF imaging and myofibroblasts in IHC observation. In addition, SHG microscopy shows that MMC treatment effectively reduced structurally irregular collagen deposition. Our results demonstrate that MAF and SHG imaging can be utilized to monitor keratocyte activation and SHG regeneration in corneal wound healing process. Moreover, MMC effectively reduces myofibroblast formation and suppresses collagen regeneration in post-PRK wound healing processes.

7550-65, Poster Session

In vivo monitoring of outer retinal damage in a rat retina model with high-resolution OCT

S. Hariri, A. Akhlagh Moayed, C. Hyun, S. Shakeel, Univ. of Waterloo (Canada); A. Ali-Ridha, St. Michaels Hospital (Canada); K. Bizheva, Univ. of Waterloo (Canada); S. Boyd, St. Michaels Hospital (Canada)

A high speed (47,000 A-scan/second), high resolution FD-OCT system, operating in the 1060nm wavelength range was used to acquire in-vivo 3D images of normal and damaged rat retinas and to monitor non-invasively outer retinal degeneration over time. The OCT system provided 3µm axial resolution in the rat eye and ~102dB sensitivity at 1.3 mW power of the imaging beam. Images of the normal rat retinas show clear visualization of all retinal layers, as well as the capillary network of the inner and mid-retina. Images acquired from the degenerated retinas show partial or full disintegration of the external limiting membrane (ELM), inner and outer segments (IS/OS) of the photoreceptor layer and damage to the retinal pigment epithelial (RPE) layer.

7550-66, Poster Session

Spectral characterization of an ophthalmic fundus camera

C. Miller, T. Holmes, Lickenbrock Technologies, LLC (United States); C. J. Bassi, Univ. of Missouri, St. Louis (United States); D. Brodsky, St. Louis Ophthalmic Equipment Co. (United States)

A fundus camera is an optical system that is carefully designed to uniformly illuminate and image the retina while minimizing stray light and backreflections. Modifying such a system requires characterization of the optical path in order to meet the new design goals and avoid the



introduction of problems. This work describes measurements made to characterize one system, the Topcon TRC-50F, necessary for converting this camera from color film photography to spectral imaging with a CCD sensor. This conversion consists of replacing the camera's original flash tube with a monochromatic light source and the film back with a CCD array. Two main aspects of the camera must be understood in order to appropriately choose the new light source and CCD camera, as well as predict the performance of the modified device. First, the transmission efficiency of the camera's illumination optical path, from the flash tube's condenser lens to the retina, is required as a function of wavelength. Similarly, the efficiency of the imaging optics from the retina to the CCD plane is required. Combining these results with existing knowledge of the eye's reflectance and transmission allows for a prediction of the available light levels at the CCD for imaging. The second aspect examined here, which also impacts efficiency, is correct optical coupling of the new light source to the camera. The goal is to maximize throughput without introducing artifacts such as non-uniformities in the illumination of the retina. Measurements to achieve this characterization are described here, along with their results.

7550-67, Poster Session

Image processing algorithms for ocular fundus reflectometry

N. Palanisamy, M. Bonaiuti, L. Rovati, Univ. degli Studi di Modena e Reggio Emilia (Italy); C. E. Riva, Univ. degli Studi di Bologna (Italy)

Ocular fundus reflectometry is a technique aimed at the in-vivo measurement of the reflectance of the tissues on the ocular fundus. Studies have demonstrated a correlation between optical and physiological properties of such tissues in humans and the existence of a control mechanism, called neuro-vascular coupling (NC), that adjusts local blood perfusion to support vision-induced neural activity. We developed an instrument for functional imaging of the neural tissues of the ocular fundus based on reflectance measurements to study the NC. The images acquired with the instrument need processing to work out reflectance time-courses. The out of focus and eye blinking images are removed before aligning. The algorithms exploited previously requires long computational time, poor discrimination of objects and need manual intervention. We have developed fully automatic algorithms optimized for the processing of the images of the ocular fundus with reduced computational time. The good images are separated from the database with the help of a software developed using maximum count algorithm. The separated images are aligned by exploiting template matching algorithm. The template matching algorithm is reasonably efficient to determine relative translational displacement (translation and rotation) between the images and also remove the geometric distortion. Depending upon this measurement, a high speed image registration algorithm is obtained by combining the linear transformation model with the template matching technique. Simulation results performed on the fundus images shows that template matching image registration reduces computational times upto one third of the time required by the general purpose algorithm, and better alignment precision.

7550-68. Poster Session

Use of a cyanine dye probe to estimate the composition of the vitreous body after enzymatic treatment

I. G. Panova, Koltsov Institute of Developmental Biology (Russian Federation); A. S. Tatikolov, Emanuel Institute of Biochemical Physics (Russian Federation); N. P. Sharova, Koltsov Institute of Developmental Biology (Russian Federation)

The aim of this work was to study the effect of enzymes such as proteinase K, trypsin, collagenase with hyaluronidase, as well as a mixture of these enzymes, on albumin and collagens incorporated in

the vitreous body, using a cyanine dye probe. We studied the vitreous body of the eyes of 19/20-week human fetuses, in which, as we showed earlier, the concentration of albumin in the vitreous body is sufficiently high. Proteinase K steeply decreased the albumin content in the vitreous body, whereas trypsin and hyalonidase with collagenase had no effect on the albumin content. Collagen was not subjected to proteinase K. Enzymatic digestion of collagen occurred under the action of collagenase with hyalonidase. The content of albumin and collagen sharply decreased in the system after treatment of the vitreous body with mixture of all enzymes. Hence, the results obtained showed that, even being in the mixture, these enzymes have a selective effect on albumin and collagens. The possibility to study the dose-dependent character of enzymatic vitreolysis using a cyanine dye probe has been shown in the work. The spectral-fluorescent probe for albumin and collagens proved to be useful for experimental approaches at screening the enzymatic mixtures possessing the selective action. The study performed is considered as a preclinical trial, and the method presented as promising for the further research in this field. The effect of the enzymes used for therapeutic purposes on the functional conditions of the vitreous body should be studied. The work was supported by RFFI (09-04-01054).

7550-69, Poster Session

Oxygen saturation imaging of human retinal vessels and measurement in eye disease patient for clinical application

D. Nakamura, N. Matsuoka, K. Tatsuguchi, M. Ogata, Y. Yoshinaga, Kyushu Univ. (Japan); H. Enaida, Kyushu Medical Ctr. (Japan); T. Okada, T. Ishibashi, Kyushu Univ. (Japan)

We have proposed a new automatic visualization procedure based the ratio of optical densities (ODs) obtained at different wavelength for the oxygen saturation imaging in human retinal vessels. This method utilized the morphological processing and the line convergence index filter to estimate the reflection image of outside vessels and extract the vessel structure from retinal image, respectively. In the experimental measurement, clear difference between retinal arteries and veins has been observed. In this time, disease eyes were investigated using the method and the change of OD ratio as a relative indicator of oxygen saturation was obtained at the disease area.

7550-70, Poster Session

Blood flow measurement and slow flow detection in retinal vessels with joint spectral and time domain method in ultrahigh-speed OCT

I. M. Gorczynska, M. Szkulmowski, I. Grulkowski, A. Szkulmowska, D. Szlag, Nicolaus Copernicus Univ. (Poland); J. G. Fujimoto, Massachusetts Institute of Technology (United States); A. Kowalczyk, M. Wojtkowski, Nicolaus Copernicus Univ. (Poland)

Purpose: To utilize the Joint Spectral and Time domain OCT (STdOCT) method for detection of wide range of flows in the retinal vessels in the optic disk, macula and capillary network. To utilize ultrahigh speed spectral/Fourier domain OCT (SOCT) imaging for development of scan protocols for Doppler signal analysis.

Methods. Retinal imaging in normal eyes was performed using ultrahigh speed (200 000 axial scans/s) SOCT instrument with CMOS camera. The imaging resolution was 4.3 µm axially and 10 µm transversally. Various raster scan protocols were implemented for investigation of flow in different retinal regions. Data analysis was performed using the method of STdOCT.

Results. We will show three dimensional imaging of the retinal vasculature in normal eyes. Flow in the region of the optic disc and in the macular



region will be shown and correlated with structural imaging of the vessels in projection OCT fundus images. Enhanced visualization of capillary network will be demonstrated.

Conclusions. Detection of blood flow velocities ranging from several tens of mm/s to several tenths of mm/s is possible in the retinal vessels with various scan protocols. It is possible to utilize the blood flow as a contrast not only for imaging of large vessels but also for the detection of capillary network. If the goal is the velocity measurement, design of advanced scan protocols is required. Scan methods should specifically target Doppler shift frequencies characteristic of blood flow in given retinal regions. Implementation of such protocols is possible with ultrahigh speed OCT imaging.

7550-71, Poster Session

High-resolution wide field of view blood perfusion maps for retina and choroid with optical micro angiography

L. An, R. Wang, Oregon Health & Science Univ. (United States)

In this presentation, we present the high resolution and wide field of view retina and choroid blood perfusion maps, which are obtained through optical micro-angiography (OMAG) technology. Based on the special frequency analysis, OMAG is able to visualize the vascular perfusion map down to the capillary level resolution. We used an 840 nm, 27 kHz FDOCT system to capture 16 OCT data sets in a sequential order, which could provide wide field blood field (~7.4mm×7.4mm) information of posterior part of a human volunteer. For each of these data sets, we eliminated the bulk motion artifacts through phase compensation method, which is based on the histogram bulk motion phase estimation. The displacements occurred between adjacent frames in one data set were compensated through 2 dimensional cross correlation of two adjacent OMAG flow images. Compared with the FA and ICGA images results, the OMAG results of blood perfusion map of retina and choroid demonstrate a very good agreement with them.

7550-72, Poster Session

Near-infrared receiver for advanced opthalmology

R. A. Myers, Radiation Monitoring Devices, Inc. (United States); Y. Zhang, Univ. of Alabama at Birmingham (United States); G. Derderian, Dipole Engineering, Inc. (United States); F. Robertson, Radiation Monitoring Devices, Inc. (United States); A. Roorda, Univ. of California, Berkeley (United States)

Some of the most useful tools for diagnosis and understanding of blinding retinal diseases rely on the use of spectral reflectance. Improvements to these tools, especially over the past decade, have greatly advanced our ability to achieve extremely high-resolution images of the human retina. In particular, scanning laser ophthalmoscopy (SLO) has proven to be an important technique for studies of microperimetry, psychophysics and visual neuroscience by imaging the cone mosaic while simultaneously delivering stimuli to single cones.

Due to the unprecedented resolution now achieved during retinal imaging, there is an increasing need for using longer wavelength light that is invisible or imperceptible to the human eyes. Bounded by human eye response and increased optical absorption, the use of wavelengths between 1000 and 1100 nm is the most suitable solution. Unfortunately, while there are several venders providing decent light sources across this wavelength range there are no suitable photodetectors.

We will present results of a research effort to develop an avalanche photodiode (APD) module with exceptional response from 800 nm to 1050 nm that is compatible with established scanning laser ophthalmoscopes. This will include the discussion of a novel fabrication process to enhance the APD's responsivity to near-infrared radiation. We will present initial results of experiments to utilize the module for visual

threshold testing and the recording of retinal images with illumination wavelengths longer than presently applied.

7550-73, Poster Session

Retinal oximetry with a multi-aperture camera

P. Lemaillet, J. C. Ramella-Roman, The Catholic Univ. of America (United States); A. Lompado, Polaris Sensor Technologies, Inc. (United States); Q. Nguyen, Johns Hopkins Medical Institutions (United States)

Measurement of oxygen saturation of the retina vessels has proven to be paramount in monitoring diabetic retinopathy (DR), a disease that can lead diabetic patient to blindness. Assessment of the oxygen saturation is difficult because of the layered structure of the eye and the eye saccadic movements. This last difficulty can be circumvented by using spectroscopic snapshot image acquisition. We present the development of a retinal oximeter that can acquire nine wavelengthdependent sub-images of the patient fundus in a single snapshot. The setup is composed of a regular fundus ophthalmoscope and a CCD. The fundus image is projected on the detector by an array of nine lenses and wavelength selection is provided by a filter array. Hence, nine wavelength-dependent images are involved in the estimation of the oxygen saturation. Higher wavelength images help establishing melanin absorption which is further extrapolated to shorter wavelength and subtracted from the absorption images. The remaining shorter wavelength sub-images are used to fit oxy- and deoxy-hemoglobin absorption curves and assess the oxygen saturation in the retina. The setup was calibrated with calibrated standards a well as optical phantoms of know optical properties. USAF registration targets were used in the image registration procedure.

We present the results of a clinical trial conducted at The Wilmer Eye Institute of Johns Hopkins University on thirty healthy and diabetic patients.

7550-74, Poster Session

Quantitative analysis of thermally induced alterations of corneal stroma by second-harmonic generation imaging

P. Matteini, F. Ratto, F. Rossi, Istituto di Fisica Applicata Nello Carrara (Italy); R. Cicchi, D. Kapsokalyvas, F. S. Pavone, Univ. degli Studi di Firenze (Italy); R. Pini, Istituto di Fisica Applicata Nello Carrara (Italy)

Thermal modifications induced in the corneal stroma were investigated with the use of second harmonic generation imaging (SHGI). Whole fresh cornea samples were heated in a water bath at temperatures in the 35-90°C range for a 4-min time. SHG images of the structural modifications induced at each temperature value were acquired from different areas of cross-sectioned corneal stromas by using a 880 nm linearly- and circularly-polarized excitation light from a mode-locked Ti-sapphire laser. The SHG images were then analyzed both by using an empirical approach and by applying a 2D-model for extrapolating relevant physiological parameters. The proposed analysis provided a detailed description of the changes in the structural architecture of the cornea up to a sub-micron level and at different hierarchical levels of the stromal collagen. The results allowed to depict a temperature-dependent biochemical model for the progressive destructuration occurring to the collagen fibrils and to the non-collagen components of the stroma. In conclusion, the multifaceted analysis carried out on the SHG images made it possible 1) to achieve a fine and simple quantification of the thermally-induced tissue damage and 2) to gain insight into the structural behavior of the stromal components in the 35-90 °C temperature range. Similar analytical methods could be proposed to track the modifications in the normal architecture of connective tissues during surgical procedures based on heating treatments.



7550-76, Poster Session

Availability of fluorescence spectroscopic in the accompaniment of formation of corneal cross-linking

M. M. Costa, Sr., Univ. de São Paulo (Brazil); C. Kurachi, Univ. de São Paulo (Brazil) and The Univ. of Texas M.D. Anderson Cancer Ctr. (United States); V. S. Bagnato, S. J. d. F. Souza, L. Ventura, Univ. de São Paulo (Brazil)

The corneal cross-linking is a method that associates riboflavin and ultraviolet light to induce a larger mechanical resistance at cornea. This method has been used for the treatment of Keratoconus. Since crosslinking is recent as treatment, there is a need to verify the effectiveness of the method. Therefore, the viability of the fluorescence spectroscopy technique to follow the cross-linking formation at cornea was studied. Corneas were divided in two groups: G1 (cornea plus riboflavin), and G2 (cornea plus riboflavina plus light irradiation, 370nm). For fluorescence measurements, a spectrofluorimeter was used, where several wavelengths were selected (between 320nm and 370nm) for cornea excitation. Several fluorescence spectra were collected, at 10 min-interval, during 60 min. Spectra allowed one to observe two very well defined bands of fluorescence: the first one at 400nm (collagen), and the second one at 520nm (riboflavin). After spectra analyses, a decrease of collagen fluorescence was observed for both groups. For riboflavin, on the other hand, there was a fluorescence increase for group G1, and a decrease for group G2. Thus, it is possible to conclude that it this technique is sensitive for the detection of tissue structural changes during cross-linking treatment, encouraging subsequent studies on quantification of cross-linking promotion in tissue.

7550-77, Poster Session

Long term observation of low power diode laser welding after penetrating keratoplasty in human patients

F. Rossi, P. Matteini, R. Pini, Istituto di Fisica Applicata Nello Carrara (Italy); L. Menabuoni, I. Lenzetti, Unita Operativa Oculistica (Italy)

Low power diode laser welding is a recently developed technique used as a support tool for conventional suturing in ophthalmic surgery. The main application is in penetrating keratoplasty: in the last four years (2005-2009), clinical trials were performed at the Ophthalmology Department of Prato (Italy). In penetrating keratoplasty, diode laser welding is used to assure the transplanted corneal button in its final position. The donor tissue is positioned in the recipient eye and 8-16 single stitches are apposed. The surgical wound is then stained with a saturated (10% w/w) sterile water solution of Indocyanine Green (ICG), it is washed with sterile water and then a diode laser (810 nm, 13 W/cm2) is used to induce the welding effect. The laser light induces a thermal effect, localized in the stained tissue. In vivo and ex vivo studies in animal models evidenced that welding induces a modification of the architecture of the corneal collagen through the wound walls, thus enabling a short healing time and a good restoration of the tissue. In this study on human subjects, we confirmed the results evidenced in animal models, by morphological observations. In two cases out of 60, transplant rejection was observed. It was thus possible to study the efficacy of laser welding in the closure of the wound one year after implant. Direct morphological observation evidenced good strengthness of the welded tissue. Microscopy pointed out a good restoration of the regular collagen architecture at the external perimeter of the corneal button, where laser welding was performed, showing the occurrence of a correct and effective wound healing process.

7550-78, Poster Session

Ultraviolet analysis on in vitro corneas following tissue removal

V. A. C. Lincoln, L. Ventura, S. J. de Faria e Sousa, Univ. de São Paulo (Brazil)

Even short exposition to ultraviolet (UV) radiation can cause several damages to the human eye. Continuous exposure the ultraviolet rays may cause corneal swelling, lens opacity (cataract), problems in the retina and pterygium. The purpose of this work is the study of the alteration of the corneal tissue and its UV natural protection in different scenarios, with a portable equipment previously developed, which provides measurements of corneal transmittance in the UV range. The opto-electronics consists of ultraviolet source and detector, digital processing and visualization of results in real time. This equipment provides also an additional tool to assist eye banks on preliminary analysis of corneas for transplantation regarding limits for its UV protection. The dual beam system, one for reference and other for the sample analysis, provides tissue UV transmission with accuracy of 0.25%. A protocol has been established for testing the UV protection on the cornea, as well as performing the removal of the corneal tissue, simulating refractive keratotomy. We have observed that it's evident that each corneal layer has influence in the UV absorbance, the results show the little influence of the epithelial and endothelium layers (~10µm depth) and the stroma was the most important layer (~350µm depth). Preliminary studies on 42 human corneas lead to demonstrate that as the stromal layer is reduced, there is significant loss of the natural UV protection of the cornea, sometimes presenting a very restricted protection.

7550-79, Poster Session

Zernike modes from anisotropic material and noncircular plate deformations for adaptive optical applications

C. Ou, Hsiuping Institute of Technology (Taiwan)

Adaptive optics is promising and feasible technique to enhance the performance of optical systems by compensating the aberrations or produced specific wavefront-illuminating patterns. It uses a spatial light modulator (SLM) to change or to correct the wavefront from an illuminated object, such that the image qualities or illuminating condition of specific object can be improved or modified. Commercialized deformable mirror using tens to hundreds of electrodes to control the deformation modes of the membrane. In spite of these advantages and attractive features, the problem is that these devices are quite expensive, therefore, there are research team works on low cost approach for several years. They study the deformations of simpler membrane structures and evaluate the optical effects for these devices, and try to reduce the cost of whole system. Therefore, it becomes a practical approach to study the performance for membrane/plate like structures, even though it might with only limited controllability on the wavefront modulation. This report studies the wavefront modulation capabilities and the optical performance of a simple circular plate structures, with different boundary conditions (clamped edge, simply support), loading types (uniform distribution and concentrated loading) and the anisotropic material properties. This device can induce or correct part of the aberrations through the correlation with Zernike coefficients, and complicated Zernike modes can be introduced in very simple way.

7550-80, Poster Session

Simultaneous correction of large LOA and HOA with a new deformable mirror technology.

F. Rooms, S. Camet, J. Curis, ALPAO (France)



A new technology of deformable mirror will be presented. Based on magnetic actuators, these deformable mirrors feature record stroke (more than +/- $45\mu m$ of astigmatism and focus correction) with an optimized temporal behaviour. Furthermore, the development has been made in order to have a large density of actuators within a small clear aperture (typically 52 actuators within a diameter of 9.0mm). We will present the key benefits of this technology for vision science: simultaneous correction of low and high order aberrations, AO-SLO image without artifacts due to the membrane vibration, optimized control, etc.

Furthermore, using recent papers published by Dobble, Thibos and Miller, we will show the performances that can be achieved by various configurations using statistical approach. The typical distribution of wavefront aberrations (both LOA and HOA) have been computed and the correction applied by the mirror. The correction of the wavefront estimation has been estimated for 1000 maps. We will compare two configurations of deformable mirrors (52 and 97 actuators) and highlight the influence of the number of actuators on the fitting error, the photon noise error and the effective bandwidth of correction.

7550-81, Poster Session

Measurement of the tearfilm and anterior chamber by confocal microscopy

K. K. Buttenschoen, J. Girkin, Durham Univ. (United Kingdom); C. G. Wilson, Univ. of Strathclyde (United Kingdom); D. J. Daly, Lein Applied Diagnostics Ltd. (United Kingdom)

We report on the development of a novel low-cost non-contact optical instrument based on scanning confocal microscopy that permits the recording of precision depth profiles through the anterior segment of the eye. We have measured the axial distances first within an artificial eye with a precision of 1 micrometer and later in human patients through to the rear of the lens at rates of up to 10Hz. The instrument has sufficient resolution to resolve the central tear film and results will be presented that show the thinning of the tear film before blinking. Further results show the influence of agents for treating dry eye syndrome on the tear film and the cornea and natural changes in the cornea during the day. The presentation will also discuss the use of the instrument for tracking drugs within the aqueous chamber of the eye. We believe that the instrument will have a clinical role to play in assessing the efficacy of ophthalmic drugs and also for the accurate and rapid measurement of corneal thickness which is of increasing significance in relation to glaucoma diagnosis.

7550-82, Poster Session

Characterization of transverse chromatic aberration of electro-optic ophthalmic lens

G. Li, Univ. of Missouri/St. Louis (United States)

Transverse chromatic aberration causes lateral smearing or blurring of the images on retina due to color dependent magnification, and it is an important performance parameter for ophthalmic lens. The transverse chromatic aberration is usually characterized by the prism diopters and the Abbe number of the lens material, which involves the refractive indices at wavelengths 589.3 nm, 486.1 nm and 656.3 nm, and the latter two wavelengths are away from the photopic peak. Here a new parameter, called effective Abbe number is introduced and used to characterize the transverse chromatic aberration. The measurement is performed at 543 nm and 594 nm, which are close to the photopic peak and available with commercial tunable He-Ne laser. It requires only the laser beam displacements due to the angular deviation imparted by the lens. Other parameters such as the lens power, the distance of the measurement location from the center of the lens, and the distance from the lens to the camera are not required. The effective Abbe number gives a much better indication of visual performance than the actual Abbe number. Using this method, experimental results for the electro-optic ophthalmic lens will be reported.

7550-83, Poster Session

Non-toric extended depth of focus contact lenses for astigmatism and presbyopia correction

Z. Zalevsky, Bar-Ilan Univ. (Israel); S. Ben Yaish, A. Zlotnik, Xceed Imaging Ltd. (Israel); O. Yehezkel, M. Belkin, Tel Aviv Univ. (United States)

Purpose: Testing whether the extended depth of focus technology embedded on non-toric contact lenses is a suitable treatment for both astigmatism and presbyopia. Methods: The extended depth of focus pattern consisting of micron-depth concentric grooves was engraved on a surface of a mono-focal soft contact lens. These grooves create an interference pattern extending the focus from a point to a length of about 1mm providing a 3.00D extension in the depth of focus. The extension in the depth of focus provides high quality focused imaging capabilities from near through intermediate and up to far ranges. Due to the angular symmetry of the engraved pattern the extension in the depth of focus can also resolve regular as well as irregular astigmatism aberrations. Results: The contact lens was tested on a group of 8 astigmatic and 13 subjects with presbyopia. Average correction of 0.70D for astigmatism and 1.50D for presbyopia was demonstrated. Conclusions: The extended depth of focus technology in a non-toric contact lens corrects simultaneously astigmatism and presbyopia. The proposed solution is based upon interference rather than diffraction and thus it is characterized by high energetic efficiency to the retina plane as well as reduced chromatic aberrations.

7550-84, Poster Session

Software for keratometry measurements using portable devices

J. G. S. De Groote, Univ. de Ribeirão Preto (Brazil); L. Ventura, C. M. Iyomasa, Univ. de São Paulo (Brazil)

In this work we present an image processing software for automatic astigmatism measurements developed for a hand held keratometer. The system projects 36 light spots, from LEDs, displayed in a precise circle at the lachrymal film of the examined cornea. The displacement, the size and deformation of the reflected image of these light spots are analyzed providing the keratometry. The purpose of this project was to develop a software that performs fast and precise calculations in mainstream mobile devices. In another words, a software that can be implemented in portable computer systems, which could be of low cost and easy to handle. This project allows portability for keratometers and is a previous work for a portable corneal topographer.

7550-86, Poster Session

Age-related model of the human crystalline lens during simulated accommodation

D. D. Nankivil, D. Borja, Bascom Palmer Eye Institute (United States); V. Nath, L. V. Prasad Eye Institute (India); E. Arrieta-Quintero, Bascom Palmer Eye Institute (United States); M. Taneja, L. V. Prasad Eye Institute (India); N. M. Ziebarth, Bascom Palmer Eye Institute (United States); A. Mohamed, L V Prasad Eye Institute (India); A. Ho, Institute for Eye Research Ltd. (Australia); F. Manns, J. A. Parel, Univ. of Miami (United States)

Purpose: To examine the age dependency of the optical power of the human crystalline lens during simulation of accommodation in a lens stretcher.

Methods: Post-mortem human eyes (n=109; age: 0 - 85 years) were dissected leaving intact the lens, zonules, ciliary body, hyaloid



membrane, anterior vitreous and a scleral rim. The lens was mounted in an optomechanical lens stretching system and stretched 2mm radially in a step-wise fashion. The lens power was measured at each step and the unstretched power, stretched power and change in power were quantified and examined as a function of age.

Results: The unstretched power, stretched power and change in power as a function of age were fit with quadratic functions as follows: y = $(0.0061\pm0.0003) \times 2 - (0.714\pm0.031) \times + (42.0\pm0.7)$, y = $(0.0035\pm0.0004) \times 2 - (0.384\pm0.033) \times + (31.6\pm0.7)$, y = $(0.0020\pm0.0002) \times 2 - (0.282\pm0.014) \times + (9.8\pm0.3)$. Using the roots of these equations, the minimum unstretched power of 21.0±2.4D occurs at 58.6±3.5years, the minimum stretched power of 21.0±2.2D occurs at 55.2±4.2years, and the change in power reaches 0±1.45D at 58.9±19.8years.

Conclusion: The unstretched power and stretched power of the human lens decrease with age until 50-60 years, and the change in power of the human lens decreases with age, reaching zero between 40 and 80 years. Increases in the unstretched and stetched power of older lenses may represent a period when physical changes in lens curvatures overcome the decrease in refractive index of the lens.

Supported by: NIH grant EY14225-01, NIH center grant P30 EY14801, NIH F31EY015395, Vision CRC, Sydney, Australia, Florida Lions Eye Bank, Research to Prevent Blindness, Henri and Flore Lesieur Foundation (JMP).

The authors do not have any proprietary or financial interest in any of the devices or results presented herein.

7550-87, Poster Session

Surfaces geometry and optical aberrations of ex vivo isolated human crystalline lenses

J. M. Bueno, C. Schwarz, Univ. de Murcia (Spain); E. Acosta, Univ. de Santiago de Compostela (Spain); P. Artal, Univ. de Murcia (Spain)

Aberrations of the crystalline lens result from both the shape of their surfaces and the refractive index distribution. The shape of the anterior and posterior surfaces of isolated (fully accommodated) human crystalline lenses was measured with a shadow photography technique. Lenses were immersed in a chamber filled with culture medium that was positioned on a micrometric rotation stage. They were back-illuminated and a CCD camera with a telecentric objective recorded shadow-images of meridians 10° apart. Hyperbolas produced the best fitting to the anterior surface whereas the posterior surface showed a tendency to be well fitted by circumferences or ellipses. The radii of curvature of both surfaces, as well as the central lens thickness were also determined. The back-focal distance and the lens aberrations were calculated by ray-tracing from the measured geometrical shape data (3D-fitted) when assuming a constant refractive index (1.42) or a gradient refractive index (GRIN). Measured and simulated back-focal length agreed well. The actual wavefront aberrations were measured in monochromatic light (633nm) using two different techniques: a Hartmann-Shack sensor and point-diffraction interferometry. During the measurements all lenses were immersed in a chamber filled with culture medium with good opticalquality parallel plates as covers. Spherical aberration and astigmatism were the dominant terms. The measured aberrations were not accurately predicted from the geometrical data by the ray-tracing approach. This is may be due to resolution in the surface measurements, the fitting procedure, the refractive index assumptions or the experimental measurement noise.

7550-88, Poster Session

Monochromatic aberrations estimated from single-pass point spread functions of a physical model eye by computational phase retrieval

R. C. Bakaraju, K. Ehrmann, E. B. Papas, A. Ho, Institute for Eye Research Ltd. (Australia) and Vision Co-operative Research Ctr. (Australia) and The Univ. of New South Wales (Australia)

To explore the optical performance of vision correction devices, such as spectacles, contact and intra-ocular lenses, an anatomically and optically equivalent physical model eye had been constructed and presented previously1. Extracting quantitative wavefront information from the model eye with use of an aberrometer set-up would need frequent repositioning of the apparatus and could sometimes be time-consuming if numerous measurements with different pupils, corrective lenses, and/or accommodative states are involved. Here, we investigate for a useful, quick and reliable alternative option, if possible.

Phase retrieval (PR) is defined as a technique that determines the shape of a wavefront of an optical system from intensity measurements at the focal plane. This current work describes the use of a computational PR algorithm to obtain the exit pupil wavefront from the single-pass point spread functions at the retinal plane of the model eye. The results obtained by using this technique are verified against the gold-standard double-pass Hartmann-shack measures (COAS aberrometer). This technique of using intensity patterns at multiple planes parallel to the focal region for recovering the monochromatic aberrations is a viable alternative for reporting the quality of the optical system.

References

1. Bakaraju RC, Ehrmann K, Falk D, Papas E & Ho A. Proceedings of SPIE, 7163: 16: 1-9.

7550-89, Poster Session

Toward an anatomically correct solid eye model with volumetric representation of retinal morphology

R. J. Zawadzki, UC Davis Medical Ctr. (United States); T. S. Rowe, Rowe Technical Design (United States); A. R. Fuller, B. Hamann, Univ. of California, Davis (United States); J. S. Werner, UC Davis Medical Ctr. (United States)

An accurate solid eve model (with volumetric retinal morphology) is likely to have numerous applications in the field of ophthalmology, including the evaluation of ophthalmic instruments as well as optometry/ ophthalmology training. We present a method that uses volumetric Optical Coherence Tomography (OCT) retinal data sets to create an anatomically correct representation of three-dimensional (3D) retinal layers. This information is exported to a laser scan system to re-create it with solid eye retinal morphology to be used in OCT testing. A solid optical model eye is constructed from PMMA acrylic, with equivalent optical power (~58D) and axial length to that of the human eye. Although the index of refraction of PMMA is not a close match to that of any of the ocular tissues its dispersion Abbe values are (d = 57.4)1. A Coddington style pupil provides for an apparent 8 mm clear aperture, large enough for easy imaging by any ophthalmic instrument. It has one refracting surface and one scanning surface. The scanning surface is slightly aspherical, mirroring the curve of best focus over a 50 degree internal field of view, with a base curvature of 12 mm, nearly equivalent to the nominal human eve's retinal curvature2. The optical focus curve was designed to be 300-500 µm anterior to the actual scanning surface. To test the accuracy of this method we compare OCT volumetric data sets acquired with the solid eye model and those acquired from human retina imaged in vivo.



Conference 7551: Optical Methods for Tumor Treatment and Detection: Mechanisms and Techniques in Photodynamic Therapy XIX

Saturday-Sunday 23-24 January 2010 • Part of Proceedings of SPIE Vol. 7551 Optical Methods for Tumor Treatment and Detection: Mechanisms and Techniques in Photodynamic Therapy XIX

7551-01, Session 1

Early cellular effects of photodynamic therapy

D. H. Kessel, Wayne State Univ. (United States)

Early responses to PDT mediated by the release of reactive oxygen species (ROS) include loss of anti-apoptotic Bcl-2 family functions and/ or release of lysosomal enzymes, the latter leading to activation of the pro-apoptotic protein Bid. We have found that enhanced formation of hydrogen peroxide and OH radical can promote apoptosis and cell death, although these ROS have been reported unable to independently initiate apoptosis. An additional factor is an early PDT-induced inhibition of endocytic pathways, regardless of the initial site of photodamage: mitochondria, ER or lysosomes. This effect could amplify cell-death signals. Photodamage to cellular organelles is known to lead to autophagy as cells attempt to repair injuries. An additional factor in the appearance of autophagy is the loss of Bcl-2 function. At this point, autophagy appears to be mainly functioning as a survival mechanism unless it becomes excessive. There are reports that autophagy can lead to apoptotic death, but in the context of PDT, a more likely result appears to be the appearance of non-viable cells filled with autophagic vacuoles.

7551-02, Session 1

Molecular markers of cell and tumor response to photodynamic therapy

N. L. Oleinick, Case Western Reserve Univ. (United States)

PDT produces oxidative damage to cells and tissues which results in a variety of responses, including protein oxidative changes, activation of stress gene expression, and induction of cell death pathways. A variety of molecular changes in the treated cells have been studied for their ability to report on the extent of damage. Some of these have been studied in terms of their ability to elucidate mechanisms and to monitor PDT response.

7551-03, Session 1

Combination treatments with PDT are enhanced by co-encapsulation of PDT agents and biologics in targeted nanoconstructs

T. Hasan, Wellman Ctr. for Photomedicine (United States)

Photodynamic Therapy (PDT) is most effective when the photosensitizer (PS) can selectively accumulate in the target tissue in sufficient quantities, thereby limiting the phototoxic effects to the tumor alone and reducing collateral damage to "normal" tissue. Nanotechnology provides an exciting opportunity to develop multi-functional constructs carrying a targeting moiety, high payloads of therapeutic and imaging agents. Combining nanotechnology with PDT provides a potentially powerful tool for selective destruction of diseased cells and tissues. We have synthesized targeted polymeric nanoparticles loaded with PS and biologics such as Avastin and Cetuximab. Targeting is achieved using aptamers, antibodies or peptides that recognize receptors overexpressed on these cells. Such nano-constructs allow for detection of disease followed by tailored release of the therapeutic to selectively destroy it. Our studies demonstrate significant enhancement in treatment outcomes when nanoconstruct-based PDT is combined with Avastin,

Cetuximab, or small molecule inhibitors of receptor tyrosin kinase. In addition, these studies establish for the first time, the intracellular delivery of a cell-impermeant antibody that targets proteins present inside the cells. Results and implications of these early experiments will be presented and discussed.

7551-04, Session 2

Vitamin D as a potential enhancer of aminolevulinate-based photodynamic therapy for nonmelanoma skin cancer

E. V. Maytin, S. Anand, N. Atanaskova, C. Wilson, Cleveland Clinic Lerner Research Institute (United States)

Vitamin D3 is a hormone essential for normal bone and cardiovascular health, and may also participate in preventing malignancies such as nonmelanoma skin cancers (NMSC). Initially synthesized in the skin (catalyzed by sun exposure), Vit D3 is subsequently hydroxylated in the liver and kidney to create the active form, 1,25 dihydroxyD3 ("calcitriol"). We previously showed that calcitriol is a potent inducer of protoporphyrin IX (PpIX) in skin keratinocytes grown in 3-D organotypic cultures. Currently, we are investigating the ability of Vit D to enhance PpIX levels within skin tumors in vivo. Squamous papillomas and carcinomas are generated by chemical carcinogenesis in mice (topical DMBA/TPA; 20 weeks). Tumors are pretreated for 3 days with topical calcitriol. Then 5-aminolevulinic acid is applied topically, and PpIX levels measured by noninvasive fluorimetry, and in biopsied tissue. Calcitriol pretreatment results in a 3- to 4-fold elevation of PpIX in tumors, relative to no pretreatment. Enhanced tumor destruction is demonstrable following illumination with treatment light. For deep tumors, topical calcitriol may not penetrate sufficiently. We are therefore exploring the possibility that systemic Vit D3, given short-term (3 days), might elevate PpIX within NMSC. Following injection of defined amounts of calcitriol in mice, an ELISA assay is used to measure calcitriol levels in serum and tissues; these levels are then correlated with PpIX in a deep NMSC model (A431 cells, implanted subcutaneously). The approach could prove attractive. Since most Americans are currently Vitamin D deficient, an increase in calcitriol may be possible without risk of hypercalcemia.

7551-05, Session 2

In vivo detection of time-resolved singlet oxygen luminescence under PDT relevant conditions

B. Röder, J. Schlothauer, S. Hackbarth, J. Lademann, Humboldt-Univ. zu Berlin (Germany)

Singlet oxygen (102) is the main mediator of PDT induced effects. It also is being generated during normal cell activity. Thus kinetics of 102 has been of great interest since its discovery. However, extremely low quantum yields of radiative deactivation, especially in biological environments, hinder a direct observation. Very recent developments now allow precise determination of 102 kinetics in vitro analysing the characteristic NIR-luminescence [1]. Attempts to measure the 102 kinetics in vivo have not yet been successful.

For the fist time worldwide we report high amplitude NIR-Luminescence signals, measured in vivo. The measurements are achieved with a recently developed setup that was shown to provide superior



performance for 102 luminescence detection in vitro [2]. This setup has been adapted to allow now the detection of singlet oxygen signals in vivo. Pig ears were used for first measurements as a widely accepted in vivo model for human skin. A major drawback of singlet oxygen luminescence detection from tissues is a high noise signal, which makes it difficult to discriminate between the singlet oxygen signal and noise if the SNR is low.

By contrast, in our luminescence signals singlet oxygen could be identified as the main contribution. Additionally, the characteristics of the background signals were analysed regarding the variance between samples and spectral parameters. Using this knowledge we identified the singlet oxygen signals from our samples. The high SNR allows determination of the 102 kinetics. Our in vivo experiments clearly show an interaction of singlet oxygen with the tissue. A definite dependence of rise and decay of the 102 signal with irradiation time was observed.

[1] Steffen Hackbarth, Jan Schlothauer, Annegret Preuß, Beate Röder. Singlet oxygen kinetics inside living cells: observation of endogenous quencher consumption and consequences for the spatial resolution in time-resolved measurements. Proc. SPIE 7380, 2009, in print.

[2] Jan Schlothauer, Steffen Hackbarth, and Beate Röder. A new benchmark for time-resolved detection of singlet oxygen luminescence - revealing the evolution of lifetime in living cells with low dose illumination. Laser Phys. Lett., 3:216-221, 2009.

7551-06, Session 2

Effects of Verteporfin-PDT on tumor microenvironment

T. M. Busch, A. L. Maas, S. L. Carter, M. Yuan, The Univ. of Pennsylvania Health System (United States); X. Xing, Univ. of Pennsylvania (United States)

Combining photodynamic therapy (PDT) with pharmaceuticals that either augment PDT cytotoxicity or abrogate the effects of pro-survival factors induced by PDT have demonstrated much potential in preclinical investigations. The design of such combination therapies is informed by knowledge of PDT effects on tumor microenvironment, e.g. its stand-alone effects on tumor vascular damage, hypoxia creation, and production of angiogenic factors. We plan combinations of Verteporfinmediated PDT with molecular-targeting pharmaceuticals that will alter tumor microenvironment, and toward this goal have undertaken evaluation of how Verteporfin-PDT itself affects local tumor physiology. PDT conditions studied include short drug-light intervals, e.g. 15 min, which target primarily the tumor vasculature, and longer drug-light intervals, e.g. 3 h, which are reported to cause less of a vascular effect. For these conditions, PDT-mediated cytotoxicity, including vascular damage, is being quantified, as well as treatment-induced angiogenic response. Pilot studies examining combinations of PDT with antiandiogenic agents are in progress.

7551-07, Session 2

Explicit dosimetry for photodynamic therapy: macroscopic singlet oxygen modeling

K. K. Wang, T. Busch, J. C. Finlay, T. C. Zhu, Univ. of Pennsylvania (United States)

Singlet oxygen (102) is the major cytotoxic agent during photodynamic therapy (PDT), defining the most fundamental treatment efficacy. It has been a long-term issue to correlate/quantify the amount of 102 with tumor death in PDT field. The production of 102 involves the complex reactions among light, oxygen molecule, and photosensitizer. From an universal macroscopic kinetic equations describing the photochemical processes of PDT, the reacted 102 concentration, [102]rx with cell target can be expressed in a form related to time integration of the product of 102 quantum yield and the PDT dose rate. The light propagation in tumor tissue is described by the diffusion equation. A simple term

describing the macroscopic oxygen supply phenomena is introduced in the equation set. Incorporating all these physiological and photochemical mechanisms, the spatially and temporally-resolved [102]rx can be numerically calculated within a fairly short computational time. To apply this model as a clinical dosimetry, it is urgent to have the modeling ability being able to predict treatment outcome. Parallel to the simulation work, a series of interstitial Photofrin-PDT experiments have been conducted, spanning sufficiently wide treatment regime, and the measurable necrosis distance are observed. In this work, an optimization routine is developed to fit the calculated [102]rx profile to the measured necrosis distance by adjusting the modeling parameters. We expect that this 102 model can be used as an explicit dosimetry to optimize/predict the treatment efficacy, using the modeling parameters extrapolated from the fitting for the particular photosensitizer of interest.

7551-08, Session 2

Spectroscopic evaluation of photodynamic therapy of the intraperitoneal cavity

J. C. Finlay, A. Dimofte, K. Cengel, T. C. Zhu, Univ. of Pennsylvania (United States)

We present the results of spectroscopic measurements of diffuse reflectance and fluorescence before and after photodynamic therapy of healthy canine peritoneal cavity. Animals were treated intra-operatively after iv injection of the benzoporphyrin derivative (BPD). The small bowel was treated using a uniform light field projeced by a microlens-tipped fiber. The cavity was then filled with scattering medium and the remaining organs were treated using a moving diffuser. Diffuse reflectance and fluorescence measurements were made uding a multifiber optical probe positioned on the surface of various tissues within the cavity before and after illumination. The measured data were analyzed to quantify hemoglobin concentration and oxygenation and sensitizer concentration.

7551-09, Session 3

To be announced

C. J. Gomer, Childrens Hospital Los Angeles (United States) No abstract available.

7551-10, Session 3

A fast heterogeneous algorithm for light fluence rate for prostate PDT

C. Chang, T. C. Zhu, The Univ. of Pennsylvania Health System (United States)

To accurately calculate light fluence rate distribution in prostate photodynamic therapy (PDT), optical heterogeneity has to be taken into account. Previous study has shown that a kernel based on analytic solution of the diffusion equation can perform the calculation with accuracy comparable to Finite-element method. An assumption is made that light fluence rate detected at a point in the medium is affected primarily by the optical properties of points (or elements) on the line between the source and the point. The exponential decay term of the light fluence rate is expressed as an integral of effective attenuation coefficient of each point along the line. The kernel method is first developed for a point source and then extended for a linear source. A linear source is considered being composed of multiple point sources and light fluence rate is summation of the fluence rates generated by the point sources. In this study, we have implemented a fast ray-trace algorithm to substantially speed up the calculation. The kernel calculation is compared with FEM calculation and is examined with light fluence rate measurements. The examination with clinical measurement data shows that calculated fluence rates present similar features in distribution as the measurement, with errors of 30%-70% for the peak fluence rates. We

Return to Contents TEL: +1 360 676 3290 · +1 888 504 8171 · customerservice@spie.org



concluded that our heterogeneous algorithm is potentially valuable for light fluence rate optimization during interstitial PDT.

7551-11, Session 3

A treatment planning system for pleural PDT

J. Sandell, C. Chang, T. C. Zhu, The Univ. of Pennsylvania Health System (United States)

Uniform light fluence distribution for patients undergoing photodynamic therapy (PDT) is critical to ensure predictable PDT outcome. However, common practice uses a point source to deliver light to the pleural cavity. To improve the uniformity of light fluence rate distribution, we have developed a treatment planning system using an infrared camera to track the movement of the point source. This study examines the light fluence (rate) delivered to chest phantom to simulate a patient undergoing pleural PDT. Fluence rate (mW/cm2) and cumulative fluence (J/cm2) was monitored at 7 different sites during the entire light treatment delivery. Isotropic detectors were used for in-vivo light dosimetry. Light fluence rate in the pleural cavity is also calculated using the diffusion approximation with a finite-element model. We have established a correlation between the light fluence rate distribution and the light fluence rate measured on the selected points based on a spherical cavity model. Integrating sphere theory is used to aid the calculation of light fluence rate on the surface of the sphere as well as inside tissue assuming uniform optical properties. The resulting treatment planning tool can be valuable as a clinical guideline for future pleural PDT treatment.

7551-12, Session 3

Comparative study of diffuse reflectance data analysis algorithms

J. Sandell, J. C. Finlay, Univ. of Pennsylvania (United States)

Diffuse reflectance spectroscopy has been shown to allow quantification of the hemoglobin saturation and concentration as well as the concentration of sensitizers and other photo-active drugs, making it an ideal modality for the determination of the parameters that contribute to photodynamic therapy dosimetry. A number of different algorithms have been published for the analysis and interpretation of diffuse reflectance spectra obtained from human tissue. We present the results of a comparison of several of these algorithms using a modular fitting software platform to analyze a standard set of spectra from phantoms of known composition as well as in -vivo data obtained from animals and humans. The strengths and weaknesses of each algorithm with respect to quantification of absorption and scattering coefficients, sample composition, and spatial heterogeneity. Special attention is given to the parameters relevant for photodynamic therapy.

7551-13, Session 3

A heterogeneous optimization algorithm for the optimization of reacted singlet oxygen for interstitial PDT

T. C. Zhu, M. D. Altschuler, Y. Hu, K. Wang, J. C. Finlay, A. Dimofte, K. Cengel, S. M. Hahn, The Univ. of Pennsylvania Health System (United States)

Singlet oxygen (102) is the major cytotoxic agent for type II photodynamic therapy (PDT). The production of 102 involves the complex reactions among light, oxygen molecule, and photosensitizer. From universal macroscopic kinetic equations which describe the photochemical processes of PDT, the reacted 102 concentration, [102] rx, with cell target can be expressed in a form related to time integration of the product of 102 quantum yield and the PDT dose rate. The object of this study is to develop optimization procedures that account for the

optical heterogeneity of the patient prostate, the tissue photosensitizer concentrations, and tissue oxygenation, thereby enable delivery of uniform reacted singlet oxygen to the gland. We use the heterogeneous optical properties measured for a patient prostate to calculate a light fluence kernel. Several methods are used to optimize the positions and intensities of CDFs. The Cimmino feasibility algorithm, which is fast, linear, and always converges reliably, is applied as a search tool to optimize the weights of the light sources at each step of the iterative selection. Maximum and minimum dose limits chosen for sample points in the prostate constrain the solution for the intensities of the linear light sources. The study shows that optimization of individual light source positions and intensities is feasible for the heterogeneous prostate during PDT. To study how different photosensitizer distributions as well as tissue oxygenation in the prostate affect optimization, comparisons of light fluence rate were made with measured distribution of photosensitizer in prostate under different tissue oxygenation conditions.

7551-14, Session 3

In vivo PDT dosimetry: singlet oxygen emission and photosensitizer fluorescence

S. Lee, K. L. Galbally-Kinney, B. A. Murphy, S. J. Davis, Physical Sciences Inc. (United States); T. Hasan, B. Spring, Y. Tu, Massachusetts General Hospital (United States); B. W. Pogue, J. A. O'Hara, Dartmouth College (United States)

Photodynamic therapy (PDT) is a light activated chemotherapy that is dependent on three parameters: photosensitizer (PS) concentration; oxygen concentration; and light dosage. Due to highly variable treatment response, the development of accurate dosimetry to optimize PDT treatment outcome is an important requirement for practical application. Singlet oxygen is an active species in PDT, and we are developing two instruments, ultra-sensitive singlet oxygen point sensor and 2D imager, for PDT researchers with the goal of a real-time dosimeter. The 2D imaging system can visualize spatial maps of both the singlet oxygen production and the location of the PS in a tumor during PDT. We have detected the production of singlet oxygen during PDT treatments with both in-vitro and in-vivo studies. Effects of photobleaching have also been observed. These results are promising for the development of the sensor as a real-time dosimeter for PDT which would be a valuable tool for PDT research and could lead to more effective treatment outcome.

7551-15, Session 4

Targeting cytochrome C oxidase in mitochondria with Pt(II)-porphyrins for photodynamic therapy

M. Börsch, Univ. Stuttgart (Germany); H. Zimmermann, Albert-Ludwigs-Univ. Freiburg (Germany)

Mitochondria are the power house of living cells, where the synthesis of the chemical energy currency adenosine triphosphate (ATP) occurs. Oxidative phosphorylation by a series of membrane protein complexes I to IV, that is, the electron transport chain, is the source of the electrochemical potential difference of protons across the inner mitochondrial membrane required for ATP production. Destroying cytochrome C oxidase (COX; complex IV) in photodynamic therapy (PDT) is achieved by the cationic photosensitizer Pt(II)-TMPyP. Electron microscopy revealed the disruption of the mitochondrial christae as a primary step of PDT. Time resolved resonance energy transfer imaging identified COX as the binding site for Pt(II)-TMPyP in living HeLa cells. As this photosensitizer competed with cytochrome C binding to COX, destruction of COX might not only disturb ATP synthesis but could expedite the release of cytochrome C to the cytosol inducing apoptosis.



7551-16, Session 4

Absolute fluence rate quantification in a three-dimensional volume for interstitial photodynamic therapy using multisensor fluorescence probes

B. Lai, Ontario Cancer Institute (Canada) and Univ. of Toronto (Canada); L. Lilge, Ontario Cancer Institute (Canada)

The efficacy of photodynamic therapy (PDT) on superficial lesions has recommended its use for various indications such as the esophagus and skin. However, for conditions requiring an interstitial approach (IPDT) such as deep-seated tumors of the lung, brain and prostate, efficacy appears to be reduced even when using otherwise effective and clinically approved photosensitizers such as Photofrin. One of the efficacy-determining factors of IPDT and other light-based therapies is the distribution of treatment light fluence rate within the clinical treatment volume (CTV). One major challenge of IPDT of solid tumors is to provide sufficient photon fluence to ensure destruction of the target cells, yet avoid overexposure of organs at risk and normal surrounding tissue. The current standard tools for light quantification are the scattering tip or cut-end fiber, which allow only single position measurements. Multisensor fiber-based fluorescent probe (MSP) has been demonstrated as an alternative tool for spatially resolved fluence rate measurements. These MSPs are embedded with fluorescent sensors that use the PDT treatment light for excitation. The sensors' emission intensities are therefore correlated to the localized treatment light intensity, effectively transforming spatial information into the spectral domain. Presented in this work is a fluence rate quantification system capable of employing up to 12 MSPs to simultaneously measure the absolute fluence rate distribution throughout a treatment volume. The system features: components for sensor calibration, data acquisition, and weighted leastsquares processing designed to allow localized fluence rate information to be computed in real-time.

7551-17, Session 4

3D ovarian cancer models: imaging and therapeutic combinations

J. P. Celli, I. Rizvi, Wellman Ctr. for Photomedicine (United States); F. Xu, Brigham and Women's Hospital (United States); C. Evans, A. Abu-Yousif, Wellman Ctr. for Photomedicine (United States); S. Moon, Brigham and Women's Hospital (United States); J. F. deBoer, Vrije Univ. Amsterdam (Netherlands); U. Demirci, Brigham and Women's Hospital (United States); T. Hasan, Wellman Ctr. for Photomedicine (United States)

The vast majority of ovarian cancer (OvCa) patients present with advanced disseminated disease with treatment options limited primarily to surgery and chemotherapy and a dismal survival rate that has shown only marginal improvements. In order to reliably and efficiently evaluate new combination treatment strategies for this lethal form of the disease, there is a critical need to create laboratory models that recapitulate key aspects of the biology and biophysics of micrometastatic OvCa including: cellular adhesion, motility, communication with stromal partners, and influence of matrix rheology during tumor growth and in response to cytotoxic insults. We are exploring a physical-science based approach to understanding cellular behavior using an innovative cell printing technology to create multicellular tumor arrays as a highthroughput reporter of treatment efficacy. These OvCa models approach the complexity of in vivo systems by restoring key biological and material interactions that are absent from traditional monolaver cultures. However, in contrast to time intensive and costly animal models, these 3D tumor arrays provide the opportunity for high-throughput in situ monitoring of tumor development and response to novel therapeutic strategies. Using high-throughput image processing routines to analyze size and cytotoxic efficacy with this platform we are able to quantitatively characterize growth and differential response to PDT, chemotherapy and EGFR

inhibition treatments in heterogeneous distributions of thousands of acini simultaneously. We utilize analysis of nodule-size dependent treatment response and patterns of cell death to inform combination regimens with enhanced efficacy. This presentation will discuss recent results and implications from our laboratory.

7551-18, Session 4

Three-dimensional visualization of the structure and treatment dynamics of ovarian tumor models following photodynamic therapy

C. L. Evans, A. Abu-Yousif, I. Rizvi, J. Celli, Wellman Ctr. for Photomedicine (United States); J. F. de Boer, Vrije Univ. Amsterdam (Netherlands); T. Hasan, Wellman Ctr. for Photomedicine (United States)

Ovarian epithelial cancer has a high morbidity due to its propensity to metastasize onto surfaces in the abdomen. In order to effectively treat these metastatic lesions with photodynamic therapy (PDT), it is critical to understand the detailed dynamics of the PDT response. 3D in vitro models of ovarian cancer are a promising system for studying the response to PDT of these lesions, as they replicate the size, appearance, and characteristics of metastatic disease observed in the clinic. An ideal approach capable of non-purturbative, 3D imaging of this model is optical coherence tomography (OCT). An ultrahigh resolution time-lapse OCT system was developed to visualize the photodynamic therapeutic response in the hours and days following treatment. Tumor nodules were observed to experience rapid cell death within the first 24 hours post-treatment using benzophorphyrin derivative monoacid A (BPD), characterized by structural breakdown of the model nodules. Highly scattering cells were observed with OCT contrast to form in the tumor nodules. These highly scattering moieties were identified as apoptotic bodies, indicating that OCT is capable of tracking the PDT-induced apoptosis in real-time without the need for labels. A size-dependent response was observed, with small ovarian nodules found to be more susceptible to treatment. To test if this effect is due to hypoxia, we compared PDT with BPD, which is primarily a type-II photosensitizer, with EtNBS, a primarily type-I photosensitzer that is less dependent of oxygen. Multiplexed viability assays were conducted alongside OCT measurements to study the PDT treatment response following these treatments.

7551-19, Session 5

Photodynamic therapy for gastrointestinal cancers

K. K. Wang, Mayo Clinic (United States)

Photodynamic therapy in the United States for gastrointestinal malignancies is confined to the esophagus and involves the use of sodium porfimer which is associated with long term photosensitivity. In addition, this photosensitizer appears to be unable to clinically treat patients with p16 abnormalities. We established this is a prospective randomized study of 148 pts mean age 63 ± 12 (range 22-88) with 129 males. 74 were randomized to PDT with 2 mg/kg of sodium porfimer given intravenously 48 hours prior to photoradiation with a diode laser at a wavelength of 630nm. Photoradiation was conducted with a 5 cm long cylindrical diffusing fiber at a power output of 400 mW/cm fiber and a total dose of 200 J/cm fiber. 74 were randomized to control. We assessed ploidy status as well as genetic status using FISH for Her2, c-myc, p53, p16, and their respective centromeric markers. Patients were assessed for their response to PDt at 3 months. P16 abnormalities, either losses or gains were associated with a significantly decreased response to PDT. We have recently begun to investigate the use of HPPH for the treat of esophagus, biliary, and pancreatic lesions. This agent produced 96% cell death in cholangiocarcinoma cell lines, 97% in pancreatic cancer cell lines, and 89% in Barrett's cell lines at a concentration of .25 ug/



ml. This was significantly more effective than sodium porfimer at similar concentrations and light dosages.

7551-20, Session 5

PDT for locally advanced pancreatic cancer: early clinical results

S. P. Pereira, N. S. Sandanayake, S. G. Bown, Univ. College London (United Kingdom)

Pancreatic adenocarcinoma ranks as the sixth commonest cause of cancer death in the UK and USA. Patients usually present late with advanced disease, limiting curative surgery to 10% of cases. Overall prognosis is poor with one-year survival rates of less than 10% with palliative chemotherapy and/or radiotherapy. Photodynamic therapy (PDT) may have a role in local tumour debulking. In preclinical PDT studies in hamster models, necrosis in normal pancreas and stomach was observed, which healed without serious adverse effects. PDT has been shown to achieve tumour necrosis in chemically induced pancreatic tumours transplanted into rats and hamsters, complicated on occasion by duodenal sealed perforation or stenosis, but no significant damage to the liver, bile duct or major blood vessels. Our group demonstrated a survival advantage in a randomised controlled study of PDT in pancreatic tumours transplanted into hamsters. We also conducted the first clinical study of pancreatic interstitial PDT published in 2002 (Bown et al Gut 2002), using meso-tetrahydroxyphenyl chlorin (mTHPC) in 16 patients with unresectable locally advanced pancreatic adenocarcinoma. All patients had evidence of tumour necrosis on follow-up imaging, with a median survival from diagnosis of 12.5 (range 6-34) months. In patients with locally advanced pancreatic cancer, we are currently conducting a phase I dose-escalation study of verteporfin single fibre PDT followed by standard gemcitabine chemotherapy. Randomised controlled studies are also planned.

7551-21, Session 5

Photodynamic therapy of head and neck malignancies

M. A. Biel, Virginia Piper Cancer Institute, Abbott Northwestern Hospital (United States)

Photodynamic therapy has been successfully used to treat various cancers of the head and neck. Four hundred fifty two patients with neoplastic diseases of the larynx, oral cavity and pharynx have been treated with PDT with follow-up to 238 months. Those patients with primary or recurrent carcinoma in situ and T1 carcinomas obtained a complete response after one PDT treatment and 88% remain free of disease. Patients with T2 and T3 carcinomas treated with PDT obtained a complete response but in most cases they recurred locally, many with normal overlying mucosa. This is due to the inability to adequately deliver laser light to the depths of the tumor despite aggressive use of interstitial implantation. Intraoperative adjuvant PDT was used in 19 patients with recurrent head and neck cancers and only two developed local recurrences.

PDT is effective for the curative treatment of early carcinomas of the head and neck. It may also be of benefit as an adjuvant intraoperative treatment of large recurrent tumors.

7551-22, Session 6

Interstitial Doppler optical coherence tomography vascular monitoring and quantification during photodynamic therapy of prostatic carcinoma: a preclinical in vivo study

B. A. Standish, Ryerson Univ. (Canada) and Ontario Cancer Institute (Canada); K. K. Lee, X. Jin, A. Mariampillai, N. R. Munce, M. Wood, B. C. Wilson, I. A. Vitkin, Ontario Cancer Institute (Canada); V. X. Yang, Ryerson Univ. (Canada) and Ontario Cancer Insitute (Canada)

We have tested the feasibility of real-time localized blood flow measurements, obtained with interstitial Doppler optical coherence tomography (IS-DOCT), as a predictive measure of photodynamic therapy (PDT)-induced tumor necrosis deep within solid Dunning rat prostate tumors.

IS-DOCT was used to quantify the PDT-induced microvascular shutdown rate in subcutaneous Dunning prostate tumors (n=28). Photofrin® (12.5 mg/Kg) was administered 20-24 h prior to tumor irradiation, with 635nm surface irradiance rates of 8-133 mW/cm2 for 25 minutes. High frequency ultrasound (HFUS) was used to locate the echogenic IS probe, where treatment efficacy was estimated by percent tumor necrosis within the DOCT imaging region as quantified by H&E staining, and correlated to the measured microvascular shutdown rate during the PDT treatment.

IS-DOCT measured significant PDT-induced vascular shutdown within the imaging region in all tumors. A strong relationship (R^2=0.723) exists between the percent tumor necrosis at 24 hours post treatment and the vascular shutdown rate: slower shutdown corresponded to higher treatment efficacy, i.e. more necrosis. Controls (needle + light, no drug, n=3) showed minimal microvascular changes or necrosis (4 \pm 1%).

To our knowledge this is the first study that has correlated a biological endpoint with a direct localized measurement of PDT-induced microvascular changes, suggesting a potential clinical role of on-line, real-time microvascular monitoring for optimizing treatment efficacy in individual patients.

7551-23, Session 6

Laser-induced photoacoustic imaging for breast cancer detection using multivariate image analysis

Y. H. El-Sharkawy, Cairo Univ. (Egypt)

Time-resolved photoacoustic imaging has been used to characterize breast tissue for the purpose of discriminating between normal and maligned areas of the tissue. Ultrasonic thermoelastic waves were generated in breast tissue by the absorption of nanosecond laser pulses at 193 nm produced by Q-switched Excimer laser in conjunction with a Michelson interferometer used to detect the thermoelastic waves and reconstruct the signal in 3-D image through IR- CCD. The concepts behind the use of photo-acoustic techniques for off-line detection of breast cancer tumor features were presented in earlier research papers [1][2]. This paper illustrates the application of multivariate image analysis (MIA) techniques to detect the presence of tumor features of breast cancer. MIA is used to rapidly detect the presence and quantity of common tumor features as they scanned by an RGB camera. Multiway principal component analysis is used to decompose the acquired threechannel tumor images into a two dimensional principal components (PC) space. Masking score point clusters in the score space and highlighting corresponding pixels in the image space of the two dominant PCs enables isolation of tumor defect pixels based on contrast and color information. The technique provides a qualitative result that can be used for early tumor detection. The proposed technique can potentially be used on-line to prescreen the existence of tumors through vision based systems.



7551-24, Session 6

Optical characteristics of hematoporphyrin monomethyl ether (HMME): a new PDT photosensitizer

G. Glazner, S. Pendyala, T. Lei, Univ. of Colorado, Denver (United States); X. Wang, H. Wang, Shanghai Skin Diseases and STD Hospital (China); F. Hetzel, Z. Huang, Univ. of Colorado, Denver (United States)

Hematoporphyrin monomethyl ether (HMME) is a new photosensitizer in photodynamic therapy (PDT). It is currently being used in vascular targeted PDT to treat port-wine stain (PWS) birthmarks in clinical trials in China, and alternatively may be suitable for ocular PDT. However, to date, the optical properties, either one photon or two photon excitation, of HMME have not been fully studied and published data are inconsistent. In this study, we characterized this photosensitizing drug on the basis of one photon absorption and studied its fluorescence emission profiles. In addition, two photon cross sections were measured for a set of wavelengths. The effects of photobleaching were probed to characterize decay kinetics, which indirectly indicates the production of singlet oxygen and its therapeutic effect. We also examined the relation between the treatment temperature and fluorescence/photobleaching characteristics of the drug, since temperature change may cause reversible conformational changes. This thermal effect may be of use in modifying treatment modalities. We further characterized two photon fluorescence lifetimes of HMME using fluorescence lifetime imaging microscopy (FLIM) in various solvents and with certain biological molecules. In addition, we performed a comparative study using other porphyrin photosensitizers (e.g. Photofrin, protoporphyrin IX). In this presentation we will report our evaluation on the optical properties of HMME under both one- and twophoton excitations.

7551-25, Session 6

EGF targeted fluorescence molecular tomography as a predictor of PDT outcomes in pancreas cancer models

K. S. Samkoe, S. C. Davis, S. Srinivasan, J. A. O'Hara, Dartmouth College (United States); T. Hasan, Wellman Ctr. for Photomedicine (United States); B. W. Pogue, Dartmouth College (United States)

Verteporfin photodynamic therapy (PDT) is a promising adjuvant therapy for pancreas cancer and investigations for its use are currently underway in both orthotopic xenograft mouse models and in human clinical trials. The mouse models have been studied extensively using magnetic resonance (MR) imaging as a measure of surrogate response to verteporfin PDT and it was found that tumor lines with different levels of aggression respond with varying levels to PDT. MR imaging was successful in determining the necrotic volume caused by PDT but there was difficultly in distinguishing inflamed tissues and regions of surviving tumor. In order to understand the molecular changes within the tumor immediately post-PDT we propose the implementation of MR-guided fluorescence molecular tomography (FMT) in conjunction with an exogenously administered fluorescently labeled epidermal growth factor (EGF-IRDye800CW, LI-COR Biosciences). We have previously shown that MR-guided FMT is feasible in the mouse abdomen when multiple regions of fluorescence are considered from contributing internal organs. In this case the highly aggressive AsPC-1 (+EGFR) orthotopic tumor was implanted in SCID mice, interstitial verteporfin PDT (1mg/kg, 20J/cm) was performed when the tumor reached ~60mm3 and both tumor volume and EGF binding were followed with MR-guided FMT. It was found that the increase in tumor volume of the PDT treated group was delayed as compared to the control group, and that EGF fluctuations corresponded with this growth pattern. Currently, further investigations into the identical treatment with a Panc-1 (-EGFR) tumor line are being carried out to determine growth factor effect on treatment success.

7551-26, Session 6

Novel visible light activated Type 1 Photosensitizers

R. Rajagopalan, A. Poreddy, A. Karwa, P. Lusiak, K. Srivastava, R. B. Dorshow, Covidien (United States)

As part of our program directed toward promising phototherapeutic agents, we have focused our efforts on the development of novel photosensitizers that operate via Type 1 mechanism. In contrast to Type 2 process (PDT), Type 1 process has not, surprisingly, received much attention despite its considerable potential. The latter process has a distinct advantage over the former in that Type 1 process does not require oxygen for inducing tissue damage. In order to establish feasibility, we have prepared and tested in vitro several classes of molecules containing fragile bonds that will produce reactive intermediates such as radicals and nitrenes upon photoexcitation with visible light. These include azido, oxaza, and diaza. In vitro cell viability experiments were carried out with U937 leukemia cell lines. The cells were first incubated with the photosensitizer at various concentrations range depending on the compound. Thereafter, the cells were illuminated for 5, 10, and 20 minutes. The corresponding control conditions are: (a) no photosensitizer, no light; (b) no photosensitizer, light; and (c) photosensitizer, no light. The results show that all compounds caused selective cell death compared to the controls when exposed to both the photosensitizers and light.

7551-27, Session 7

In vitro biological effects of novel Type I photosensitizers and their mechanism of action

A. Karwa, A. Poreddy, P. Lusiak, K. Srivastava, R. B. Dorshow, R. Raiagopalan. Covidien (United States)

Phototherapy has been demonstrated to be a safe and effective treatment procedure for various cancerous and non-cancerous lesions. However the majority of photodynamic therapy research has focused on developing Type 2 photosenstizers (PS), and not on Type 1 PS despite its considerable potential. Unlike Type 2 compounds that generate singlet oxygen, Type1 process generates reactive intermediates that directly interact with cellular components. Several classes of novel Type 1 compounds were synthesized and screened for their effect on the viability of U937 cells. The compounds were incubated at different concentrations with U937 and exposed to different amount of visible light. The presentation will discuss the effects of photofragmentation and the possible mechanism of action of these compounds in inducing cell death. Compounds selected from the primary screen of U937 cell were then evaluated in different cancer cells. An important aspect of this program is to develop targeted approach for enhanced drug delivery of these compounds. The presentation will discuss in detail the conjugation of these compounds to different targeting vectors and selective and enhanced cell death caused in different cell lines.

7551-28, Session 7

Noninvasive assessment of tissue distribution and tumor pharmacokinetics of Pc 181: a silicon phthalocyanine analogue in mice

L. Bai, J. Guo, Univ. of Pittsburgh Cancer Institute (United States) and Univ. of Pittsburgh (United States); D. Clausen, Univ. of Pittsburgh Cancer Institute (United States); J. Eiseman, Univ. of Pittsburgh Cancer Institute (United States) and Univ. of Pittsburgh (United States)

Objective: In in vitro photodynamic therapy, the LD50 of Pc 181 has

TEL: +1 360 676 3290 · +1 888 504 8171 · customerservice@spie.org



been reported to be 7-8 times lower than silicon phthalocyanine 4 (Pc 4) because of the greater uptake of Pc 181 into MCF-7c3 cells. The Optical Pharmacokinetic System (OPS) can be used to measure photosensitizer concentrations non-invasively. In this study, we used OPS to evaluate the tumor pharmacokinetics of Pc 181 in mice bearing MDA-MB-231 and SCC-15 xenografts and the tissue drug distribution.

Methods: Following iv administration of 2.5 mg/kg Pc 181 to mice bearing MDA-MB-231 or SCC-15 xenografts, OPS measurements were taken on tumor and tissues between 5 and 4320 min in vivo or in situ. The tissues were collected for HPLC analysis.

Results: Large variations in tumor Pc 181 concentrations were observed among mice. In MDA-MB-231 tumor, the Pc 181 concentration decreased for the first hour then gradually increased with time. Tumor Pc 181 concentration was approximately half of the tumor Pc 4 concentration at an equimolar dose. Pc 181 concentrations were the highest in liver, followed by spleen, and kidney. Pc 181 concentrations in SCC-15 tumors peaked at 24 h following administration. Skin and underlying tissue Pc 181 concentrations appeared to be higher than tumor concentrations at all time points examined.

Conclusions: This first Pc 181 pharmacokinetics study described a similar tissue Pc 181 distribution to that of Pc 4. However, tumor Pc 181 concentrations were lower than those of Pc 4 at an equimolar dose.

7551-29, Session 7

Plasmonic gold nanoparticle enhanced photodynamic therapy

S. Chen, Chalmers Univ. of Technology (Sweden); B. Bauer, Univ. of Gothenburg (Sweden); L. Gunnarsson, A. Dimitriev, M. Käll, Chalmers Univ. of Technology (Sweden); M. Ericson, Univ. of Gothenburg (Sweden)

In photodynamic therapy, the photosensitizer (PS), light and oxygen must be co-localized in order for the treatment to work. By using plasmonic nanoparticles, the localization and the effectiveness of the treatment could be improved. The purpose of this work is to examine the possibility to enhance the photosensitization effect of the PS by adding plasmonic gold nanoparticles with strong light absorption at the irradiation wavelength. Human A431 cell line was incubated with protoporphyrin IX and nanoparticles before illumination with red low power LED lamp. The cells were colored by trypan blue death stain and counted afterwards. We found that less illumination time and increased cell death is observed when nanoparticles were used together with the photosensitizer. When cells were only illuminated with nanoparticles, no cell death was observed therefore excluded the heating effect as in photo thermotherapy. To isolate that it is indeed due to an increased singlet oxygen effect we have used uric acid as a singlet oxygen reporter in a model system which only involves protoporphyrin IX and phosphatidylcholine vesciles and nanoparticle.

7551-30, Session 7

Photodynamic inactivation of psuedomonas aeruginosa in burned skin in rats

A. Hirao, Keio Univ. (Japan); S. Sato, D. Saitoh, N. Shinomiya, H. Ashida, National Defense Medical College (Japan); M. Obara, Keio Univ. (Japan)

Control of local infection in wounds is critically important to avoid transition to sepsis; however, recent rise of drug-resistant bacteria makes it difficult. Thus, antimicrobial photodynamic therapy (APDT) has recently received considerable attention. In this study, we examined methylene blue (MB)-mediated photodynamic inactivation of Psuedomonas aeruginosa in rat burned skin. Deep dermal burn with a 20% total body surface area was made on the back of a rat and a suspension of Ps. aeruginosa was applied to the wound surface at 24 h post-burn. Two days after infection, the wound surface was contacted with a MB

solution at different concentrations for 2 h and thereafter, the wound was irradiated with cw 665-nm light at a constant power density of 250 mW/cm2 for different time durations. After illumination, tissue was biopsied and the number of bacteria was counted on the basis of colony forming assay. We observed a two orders in magnitude decrease in the number of bacteria by PDT with 0.5-mM MB solution and 480-J/cm2 illumination, demonstrating the efficacy of PDT against infection with Ps. aeruginosa in wounds. However, our in vivo photoacoustic monitoring of photosensitizer showed a limited diffusion of MB in the tissue, i.e., 0.2 - 0.3 mm in depth, indicating that contact delivery of photosensitizer is not sufficient to treat infection in deeper tissue.

7551-31, Session 7

Patient specific integrating spheres for the improvement of dosimetry in skin PDT

D. L. Glennie, McMaster Univ. (Canada); T. J. Farrell, M. S. Patterson, J. E. Hayward, Juravinski Cancer Ctr. (Canada) and McMaster Univ. (Canada); G. Sawesky, Juravinski Cancer Ctr. (Canada)

The treatment of superficial skin cancers with photodynamic therapy (PDT) relies on uniformly covering the treatment target with sufficient light fluence using an externally applied source.

Inhomogeneities in the irradiance as well as specular and diffuse reflectance of light from the patient's skin can introduce dose uncertainties that prevent an optimum treatment. These can be reduced by incorporating an integrating sphere into the treatment delivery.

A patient-specific irradiation device has been developed, consisting of a micro-lens tipped optical fiber coupled to an integrating sphere. The integrating sphere is both easy and inexpensive to build and consists of a large irradiation port matched to the lesion size on the skin as well as an optical fiber-based detection port which allows online spectroscopy in real time.

A prototype irradiation device was built, consisting of an integrating sphere measuring 10 cm in diameter with a 5 cm wide treatment port located directly across from the source fiber. Using an isotropic probe, the radial and depth dependence of the fluence rate were measured in a series of tissue-simulating liquid phantoms.

Initial results showed an increase in surface fluence rate (compared to the open beam) as well as improved depth penetration and uniformity across the port opening. Monte Carlo simulations of the experiment support the experimental data and can be used to determine the optimum ratio of the sphere radius to the illumination port radius.

7551-32, Session 7

Gold nanoparticle assisted light activation of heat-sensitive nanobubbles for photothermal therapy

S. Xu, J. Huang, R. Xu, The Ohio State Univ. (United States)

Background: Gold nanoparticles, on account of the phenomenon of surface plasmon resonance, are emerging contrast agent for photothermal cancer therapy. The unique photophysical properties of gold nanoparticle make it tunable to fit the exciting light from visible to near infrared, and highly efficient for the light-heat conversion as well. However, broad clinical use of gold nanoparticles is hindered by several limitations, such as no real-time dosage feedback and chemical reactions of nanoparticle bioconjugates in physiological environments. We conjugated gold nanoparticles with poly-lactic-co-glycolic acid (PLGA) nanobubbles for targeted thermotherapy and dosage control.

Method: PLGA nanobubbles has perfluorocarbon core and can be activated by the exposure of heat. These heat-sensitive nanobubbles were fabricated by an emulsion evaporation method. Gold nanoparticles were conjugated on the PLGA bubble surface. Light was illuminated



nanobubbles in aqueous solution or in a tissue simulating phantom. The nanobubble expansion process was monitored by microscopy or ultrasound

Result: Light was demonstrated to be able to active the nanobubbles by heating gold nanoparticles and followed to form microbubbles, either in the aqueous solution or the phantom. The size of bubble before and after activation changed more than 10 times. For the phantom, the ultrasound contrast was significantly enhanced after light activation.

Conclusion: The activation of gold nanoparticles by light illumination will offer a real-time ultrasound monitoring during the photothermal therapy. The light active heat-sensitive nanobubbles will potentially overcome the limitations of gold nanoparticles, and greatly enhance the therapy efficiency.

7551-33, Poster Session

Photodynamic therapy with 5-ALA in the treatment of condyloma by human pappilomavirus: clinical protocol, device development, and application

N. M. Inada, C. Kurachi, O. Guimarães, M. Costa, S. Quintana, W. Lombardi, V. Bagnato, Univ. de São Paulo (Brazil)

Photodynamic Therapy (PDT) is useful in the treatment of condyloma by human papillomavirus (HPV) however is necessary to improve the instrumentation and the clinical protocol to make this technique feasible. In this work we present the development of the "PDT Flex Use", a brazilian PDT device specifically designed for the treatment of vulvar and vaginal lesions induced by HPV. This equipment is optically based in 640 nm LED (Light Emitting Diodes) arrays and the illumination probes were anatomically designed for specific site applications: vulvar, vaginal, anal and perianal condyloma. The consequence of multiple surgical procedures can be vulvar disfigurement and loss of sexual function and laser therapy has the advantage of preservation of vulvar architecture, but again, recurrence rates are high. The aminolevulinic acid cream (20%; wt/wt) is incorporated in an emollient cream and topically placed over the lesions and 4-6 hours after the application the illumination is performed. The presence of protoporphyrin IX in the lesions were analyzed with diagnostic system based on fluorescence using other brazilian homemade device. The illumination time is set depending on the chosen probe and treatment area to achieve a fluence of 200 J/cm2. As expect, PDT is not equally effective for all subgroups: was observed that in two specific cases, the PDT showed rapid and better results: in young woman and non-cigarette smoker.

7551-34, Poster Session

Return to Contents

Vibrational spectroscopy characterization of low-level laser therapy on mammary culture cells: an micro-FTIR study

T. D. Magrini, N. V. dos Santos, G. Cerchiaro, N. A. Daghastanli, H. d. Silva Martinho, Univ. Federal do ABC (Brazil)

Low level laser therapy (LLLT) is an emerging therapeutic approach for pain treatment, wound healing; tuberculosis; temporomandibular joint disorders; and several musculoskeletal conditions. The clinical effects induced by LLLT presumably go from the photobiostimulation/photobionibition at cellular level. However, the detailed mechanism underlying this effect is obscure. The present work is dedicated to quantify some relevant aspects of LLLT related to cell proliferation and apoptosis of. This goal was attached by exposing malignant breast cells (MCF7) to spatially filtered light of a He-Ne laser (633 nm). The parameters of the study were the laser power density (0.32, 0.65 and 0.97 mW/cm2), treatment time (1 minute), and cell adaptation time 6-24h. The cell viability was evaluated by microscopic observation using Triplan Blue. The vibrational spectra of each experimental group (micro-FTIR technique on dry cells) was used to identify the relevant biochemical

alterations occurred in the process. It was found necrotic and apoptotic characteristic signals wich had statistically correlation to the high fluence experimental group.

7551-35, Poster Session

Color image reconstruction of oral cavity for abnormal tissue detection

H. Wang, H. Zih, F. Hsu, National Chung Cheng Univ. (Taiwan); C. Chiang, National Taiwan Univ. (Taiwan); F. Cheng, Chung Hua Univ. (Taiwan)

Early identification of high-risk disease could greatly reduce both mortality and morbidity due to pathological changes of oral tissue. We have shown that there is significant color difference between normal and abnormal tissue in the oral cavity, owing to difference in the spectrum of reflected with a special light emitting device. We describe an algorithm of color reconstruction, which preserves this color difference, enabling optimal delineation of normal and abnormal areas. With our method, we evaluate the perceived tissue reflectance in the each pixel of image and color reproduction with different illuminated spectra. Our approach to enhancement of visually perceived color difference between normal and abnormal oral tissue involves optimization of illumination and observation conditions by allowing a significant optical contrast of illuminated spectrum to reach the observer's eyes. For the observer, this method would involve using a light emitting diode with a color filter by the physician to observe tissue reflectance.

7551-36, Poster Session

Reconstruction of optical properties using a linear source model for interstitial diffuse optical tomography

K. K. Wang, T. C. Zhu, Univ. of Pennsylvania (United States)

The therapeutic efficacy of photodynamic therapy (PDT) significantly depends on the quantification of light fluence rate distribution. An interstitial diffuse optical tomography (iDOT) system with multiple cylindrical linear sources and isotropic detectors has been developed to quantify the light distribution of prostate gland during PDT. For our continuous-wave (CW) iDOT system with the incorporation of linear sources, the optical measurements for the entire prostate can be made within 30 seconds for up to 16 linear sources. With such prompt system, it will be a significant improvement to real-time PDT light dosimetry with corresponding fast optical properties reconstruction. An inverse model with an adjoint method based on the CW diffusion equation is developed for the iDOT system, and three dimensional optical properties for a series of prostate slices can be accomplished within fairly short computational time. However, it is generally known that optical property reconstruction is an ill-conditioned problem especially for the clinical condition where measured data points are less than the reconstructed nodes. To best evaluate the necessary detector numbers for a successful interstitial reconstruction, a mathematical phantom is used. In this study, a linear source model with finite length sources is used and the forward calculated data is used for the subsequent inverse computation. Several scenarios of source and detector configurations are examined in this study. We expect through this study, the linear source and detector numbers can be optimized, and the results will have direct impact on the clinical study.

79

TEL: +1 360 676 3290 · +1 888 504 8171 · customerservice@spie.org

etion:

Conference 7551: Optical Methods for Tumor Treatment and Detection: Mechanisms and Techniques in Photodynamic Therapy XIX

7551-37, Poster Session

Pre-clinic study of uniformity of light blanket for intraoperative photodynamic therapy

Y. Hu, K. K. Wang, T. C. Zhu, Univ. of Pennsylvania (United States); B. C. Wilson, Univ. of Toronto (Canada)

A light blanket composed of a series of parallel cylindrical diffusing fibers (CDF) is designed to substitute the hand-held point source in the PDT treatment of the malignant pleural or intraperitoneal diseases. It achieves more uniform light delivery and less operation time in operating room. The blanket is designed and fabricated with multiple fiber bundles CDFs to produce a large treatment area. The characteristics of the water-proof and sterilization are considered and achieved. The distribution of light field is scanned using the isotropic detector and the motorized platform. The output average and deviation are 7.4 mW/cm2/W and 1.1 mW/ cm2/W respectively with 0.2% intralipid layer. With the more efficient (more than 60%) beamsplitter and attenuation system, the computerized modulation of light fluence distribution is performed by adjusting the power distribution to individual CDFs on the light blanket. The actual mean spacing between the CDFs and intralipid concentration are also adjusted to find the optimal distances combined with the intralipid concentration for the uniform light fluence distribution. Light fluence rate between the light blankets and a moving point source for different tissue-simulating phantom of flat and curved shapes are compared to investigate the uniformity of light distribution within the appropriate light fluence level used in clinic. The light blanket produces a reasonably uniform field for effective light coverage and is flexible to conform to anatomic structures in intraoperative PDT. Taking the advantage of large coverage and flexible conformity, it will have great potential value for superficial PDT treatment of uneven surface.

7551-38, Poster Session

The online optimal motion planning of robotic multichannel platform for photodynamic therapy

Y. Hu, J. C. Finlay, T. C. Zhu, Univ. of Pennsylvania (United States)

A compact robotic platform is designed for simultaneous multichannel motion control for light delivery and dosimetry during interstitial photodynamic therapy (PDT). Movements of light sources and isotropic detectors are controlled by individual motors along different catheters. A multi-channel servo motion controller and micro DC motors, each with high resolution optical encoder, are adopted to control the motions of up to 16 channels independently. Each channel has a resolution of 0.1mm and a speed of 5cm/s. The online optimal motion planning, composed of the pre-alignment, source stepping optimization, rapid operational scheme and adaptive control strategy, is adopted to control the robotic platform for light delivery and dosimetry. With the capability of allowing arbitrary positioning of light sources and detectors in each catheter, the pre-alignment can be easily achieved for the profiles of each scan. The characteristic of high speed and coordinating motion will make it possible to use short linear sources (e.g., 1- cm) to deliver uniform PDT treatment to a bulk tumor within reasonable time by multiple source stepping optimized simultaneously. Operational schemes with various combinations of source and detector are adopted to greatly reduce the data acquisition time to 30s. The adaptive control strategy determines whether making retraction and retry or aborting the delivery, in case of excessive force on any channel cased by the resistance of fiber bending or transmission mechanism. The optimal motion planning of robotic platform is fully adaptable for the clinical environment and procedure to improve the light delivery and dosimetry in interstitial PDT.

7551-40, Poster Session

Dependence of light fluence on treated depth with photosensitization reaction shortly after photosensitizer injection in rabbit myocardial tissue in vivo

T. Suenari, H. Matsuo, A. Ito, Keio Univ. (Japan); S. Miyoshi, Keio Univ. School of Medicine (Japan); T. Arai, Keio Univ. (Japan)

We investigated experimentally dependence of light fluence on treated depth with photosensitization reaction shortly after photosensitizer injection in rabbit myocardial tissue in vivo. In this particular photosensitization reaction scheme, the photosensitizer accumulation characteristics for target region is not available. Meanwhile, the photosensitizer dose and hospitalization period under restricted light circumstance might be reduced. Since both photosensitizer and oxygen supply are governed by blood flow, this photosensitization reaction is influenced significantly by blood flow variation in particular blood vessel occlusion. We employed the myocardial tissue to keep tissue blood flow during the photosensitization reaction because vessel blood flow speed in myocardial tissue is fast to resist vascular occlusion. Surgically exposed rabbits myocardial tissues were irradiated with the light fluence ranging 25-100 J/cm2 by a 663 nm diode laser 30 min after the injection of 2 mg/kg water soluble chlorin photosensitizer, Talaporfin sodium. Two weeks after the irradiation, the rabbits were sacrificed and the histological specimens of the irradiated area were made to measure scar layer thickness. The scar layer tissue thickness of 0.2-3 mm was observed microscopically by the light fluence ranging 25-100 J/cm2. The scarring threshold in the deposit light fluence was estimated to 15-25 J/cm3 based on the above mentioned relation assuming constant and uniform myocardial effective attenuation coefficient of 0.72 mm-1. The estimated scarring threshold in the deposit light fluence was lower than the threshold of conventional PDT. Large variation of the estimated threshold value might be attributed to unconsidered PDT parameter such as flow rate inhomogeneity in the myocardial tissue. These results suggested that the photosensitization reaction investigated in this study would be available to apply arrhythmia therapy such as atrial fibrillation.

7551-43, Poster Session

Light dosimetry for pleural PDT

A. Dimofte, T. C. Zhu, J. C. Finlay, M. Cullighan, J. S. Friedberg, K. A. Cengel, S. M. Hahn, Univ. of Pennsylvania (United States)

This study examines the light fluence (rate) delivered to patients undergoing pleural PDT as a function of treatment time, treatment volume and surface area. The accuracy of treatment delivery is analyzed as a function of the calibration accuracies of each isotropic detector and the calibration integrating sphere. The patients studied here are enrolled in a Phase I clinical trial of HPPH-mediated PDT for the treatment of nonsmall cell lung cancer with pleural effusion. Patients are administered 4mg per kg body weight HPPH 48 hours before the surgery. Patients undergoing photodynamic therapy (PDT) are treated with light therapy with a fluence of 15-60 J/cm2 at 661nm. Fluence rate (mW/cm2) and cumulative fluence (J/cm2) is monitored at 7 different sites during the entire light treatment delivery. Isotropic detectors are used for in-vivo light dosimetry. The anisotropy of each isotropic detector was found to be within 15%. The mean fluence rate delivery and treatment time are recorded. A correlation between the treatment time and the treatment volume will be established. The result can be used as a clinical guideline for future pleural PDT treatment.



7551-44, Poster Session

In vivo sampling of Verteporfin uptake in pancreas cancer xenograft models: comparison of surface, oral, and interstitial measurements

M. E. Isabelle, J. A. O'Hara, K. S. Samkoe, P. J. Hoopes. Dartmouth College (United States); S. Mosse, S. P. Pereira, Univ. College London (United Kingdom): T. Hasan, Wellman Ctr. for Photomedicine, Massachusetts General Hospital (United States); B. W. Poque, Dartmouth College (United States) and Wellman Ctr. for Photomedicine, Massachusetts General Hospital (United States)

Photodynamic therapy (PDT) mediated with verteporfin is being investigated as a pancreatic cancer treatment in the cases for nonsurgical candidates. Interstitial PDT treatment is the method being carried out in phase 1 trials, and sampling of the photosensitizer through the treatment fiber syringe is ongoing, as is sampling from oral tissues. While the data set is limited, we can assess the quality of this data through parallel pre-clinical studies. Interstitial photodynamic therapy (IPDT) is administered to internal tumors using light delivered via fibers inserted percutaneously and guided by ultrasound imaging.

In this study, an orthotopic pancreatic cancer model (PANC-1) was implanted in SCID mice and treated with the liposomal form of the photosensitizer, Verteporfin. Verteporfin uptake and distribution was analyzed by measuring its fluorescence in oral tissues, liver, pancreas and tumor in vivo, using an Aurora Optics Inc. PDT fluorescence dosimeter. Probe measurements were made using a surface probe and an interstitial needle probe before and up to one hour after tail injection of the photosensitizer.

Ten dosimetry measurements were made on each tissue at different time points for mice in the interstitial and superficial groups. Tissue distribution of the photosensitizer in relation to perfused tumor vasculature was determined by using the fluorescent carbocyanine dye, DiOc7, on frozen tissue sections taken from the tumor which stains cells immediately adjacent to blood vessels.

Photosensitizer fluorescence in tissue elevated rapidly in the first minutes after administration and continued to rise during 1-hour post injection. The study demonstrates the challenges that solid tumors play on the implementation of minimally invasive interstitial PDT and PDT dosimetry determination, but that careful interpretation of pre-clinical models might help inform clinical decisions.

7551-45, Poster Session

Analytic modeling of in vivo drug delivery: comparison of antibody versus vesiclemediated delivery to tumor cells

B. W. Poque, S. Srinivasan, Dartmouth College (United States); P. R. Rai, Z. Mai, T. Hasan, Wellman Ctr. for Photomedicine (United

Understanding the potential benefits and optimization of new drug delivery methods could be significantly enhanced by development of accurate quantitative models that predict delivered concentration in vivo, and are used to independently examine the sensitivity of each parameter. This work focuses on an analytic description of the uptake of antibody targeting to cancer cells, and compares the relative uptake from native form ligand, versus ligand delivered through a vesicle particle. The computational model uses three interlined pieces, including (1) a vascular supply with known clearance rate, (2) a Krogh cylinder diffusion approximation for interstitial transport, and (3) an antibody-antigen binding kinetic model, to predict the consumption of ligand at the site of delivery. This approach is outlined in rate equation terminology and analytic approximations are used to estimate the temporal and spatial kinetics of the drug delivery. It is shown that high affinity of the antibody will lead to limited penetration in the tumor, whereas encapsulated vesicle delivery provides an essentially unlimited diffusion in space. Yet the Diffusion coefficient and the clearance rate in the blood, both can lead to reduction in the overall concentration across the tumor. Finally, the tradeoff between site of delivery and binding versus the concentration is very interesting. Vesicle-based delivery has the potential to deliver to intracellular sites, and so even if the overall concentration is lower, the higher rate of binding can lead to higher intracellular concentrations than the native delivery approach. This is because the native delivery approach is limited in terms of spatial delivery by the consumption along the pathway. This modeling Is the first step in a more complete analysis of how the interplay between (1) pharmacokinetics, (2) interstitial relocation by diffusion, and (3) ligand binding all contribute to the overall efficacy of delivery of photosensitizer to tumor cells in vivo.

TEL: +1 360 676 3290 · +1 888 504 8171 · customerservice@spie.org

Conference 7552: Mechanisms for Low-Light Therapy V



Saturday 23 January 2010 • Part of Proceedings of SPIE Vol. 7552 Mechanisms for Low-Light Therapy V

7552-01, Session 1

Fundamental mechanisms of phototherapy

T. Hode, Immunophotonics, Inc. (United States) and Irradia USA (United States); P. Jenkins, Irradia USA (United States); L. Hode, Swedish Laser-Medical Society (Sweden)

Many studies have been published about the mechanisms of phototherapy, both with regard to primary mechanisms and secondary mechanisms. In the case of primary mechanisms there are primarily two key processes that have gained the most attention, both of which are connected to photon absorption in mitochondria: 1) Increased ATP formation and 2) formation of reactive oxygen species that trigger transcription factors, which in turn upregulates the expression of a large number of genes. The secondary mechanisms are commonly referred to as the cascade of processes that are triggered by the primary mechanisms, and include tissue regeneration, nerve stimulation or inhibition, and modulation of the cytokine environment that in turn affects the immune system. However, despite these efforts, not much attention has been given to the fundamental photochemical and photophysical reactions that give rise to the increased ATP production and formation of ROS in the first place.

There are many factors that could contribute to the observed phototherapy effects, for example, chromophore relaxation times vs. photon absorption rates, two-photon effects, release of nitric oxide, lasing effects in tissue, speckle formation and microthermal effects, rotation of chromophore molecules in the host enzyme, photolysis, and more. Furthermore, it is possible that the increased ATP production and the formation of ROS are two fundamentally different processes, where the modulated ATP production could be a result of, for example, photoreduction of Cytochrome c Oxidase, whereas ROS production may be caused by reactions between molecular oxygen and photoexcited states of the photoreceptor molecules.

7552-02, Session 1

The importance of pulsing illumination parameters in low-level light therapy

D. Barolet, RoseLab Skin Optics Lab. (Canada) and McGill Univ. (Canada)

The use of Low Level Light Therapy (LLLT) in an ever growing number of clinical indications is constantly evolving. The large number of illumination parameters now available add to the medical applicability but also to its complexity. The influence of emission parameters on cellular response is not yet fully understood. In the present study, we investigated the impact of visible to near infrared (NIR) light continuous wave (CW) emission and various pulse illumination structures (msec vs µsec, duration, interval, pulse per train, pulse train interval) on collagen production in vitro using human primary fibroblasts in culture. Type 1 procollagen levels were measured at baseline and 72 hours post illumination. Results showed that specific pulsing patterns contrasted with the CW mode in the ability of fibroblasts to produce collagen de novo. Current evidence suggests that the cascade of events leading to photobiomodulation effects by red to NIR illumination is initiated by the antenna molecule mitochondrial cytochrome c oxidase. Respiration in the mitochondria can be inhibited by nitric oxide (NO) binding to cytochrome c oxidase which competitively displaces oxygen and affect cell metabolism. Excess NO binding is associated with cell damage and apoptosis. Light absorption dissociates NO allowing cellular respiration to resume and normalization of cell activity, ultimately triggering biomolecular processes leading to collagen production. Pulse light delivery might favourably enhance this cellular strategy. Short and intermittent light emission might enhance NO dissociation therefore augmenting mitochondrial energy production and cellular activity. These findings could be relevant to clinical applications of LLLT.

7552-03, Session 1

The effects of laser phototherapy device design and treatment technique on the optical properties of tissue, and the clinical implications thereof

P. A. Jenkins, Irradia LLC (United States) and SpectraVET, Inc. (United States) and SpectraMedics Pty, Ltd. (United States); T. Hode, ImmuoPhotonics, Inc. (United States) and Irradia LLC (United States)

An investigation into the effects of various physical and functional characteristics of laser devices, and their practical application, on the optical properties of living tissue, and the implications thereof for researchers, clinicians and laser device manufacturers.

When a laser beam interacts with soft tissue, varying proportions of the incident light will be reflected, scattered, transmitted and absorbed. In a clinical sense, the most important of these are transmission and absorption.

Various treatment techniques can be employed by the practitioner to maximize transmission of laser energy into deeper tissues, the most effective of which is to maintain contact and firm pressure between the laser applicator and the skin. However, not all laser devices can be safely used in such a manner, and others may not, by the nature of their design, be capable of providing maximal benefit.

The technique by which laser energy is applied to the tissue can greatly influence the efficacy of laser phototherapy treatments, and contact with pressure is probably the most important of these, especially for the treatment of deeper tissues.

Further, the physical design of a laser delivery system can determine which techniques are available to the practitioner and influence their efficacy, which has implications for the design and selection of laser devices for clinical use.

Most importantly, however, application technique greatly affects the relationship between the incident dose and the actual dose received in the tissue, with significant implications for researchers and clinicians.

7552-04, Session 1

Role of the circulation in the systemic effects of low-light therapy

M. Dyson, King's College London (United Kingdom)

Systemic photon-induced changes in the circulation may be involved in the reduction of pain and the acceleration of tissue repair by low-light therapy (LLT) including low level laser therapy (LLLT). Pain reduction and tissue repair acceleration follow the absorption of photons by cells either resident in, or in transit through, the skin and underlying tissues provided that the correct treatment parameters are used. These cells include immune cells and stem cells. Photon absorption can lead to an increase in ATP synthesis and the release of reactive oxygen species that can activate specific transcription factors resulting in changes in synthesis of the enzymes needed for nitric oxide synthesis, protein synthesis and secretion, molecular and cellular movement, and cell proliferation. Amplification of the effects of photon absorption increases the range and duration of LLT. This may be caused in part by indirect effects initiated, in cells that have not absorbed photons, by regulatory proteins secreted by resident cells that have absorbed photons. Photons may also induce changes in immune cells and stem cells in transit through the dermal capillaries. The peripheral location of these capillaries and other vessels of the microcirculation makes their contents readily accessible to photons. The longer the duration of treatment, the greater will be the number of cells in transit that can be affected by photons. For

Conference 7552: Mechanisms for Low-Light Therapy V



a treatment to be clinically effective, its duration as well as its power may therefore be important.

Direct and indirect photon-induced increases in the microcirculation and macrocirculation reported recently will be described, together with their clinical significance in the reduction of pain and acceleration of delayed tissue repair by LLT. For example, local and systemic increases in the dermal circulation have been observed in healthy volunteers following exposure to polychromatic visible light; it was concluded that these increases were due to activation of nitric oxide synthesis in the irradiated region which produced both local (direct) and distant (indirect) microcirculatory effects [1]. Macrocirculatory effects have been demonstrated following the application of LLLT to the temporomandibular joint (TMJ). A significant increase in vessel diameter and in blood flow through the superficial temporal artery (STA) were found on the treated side, a direct effect, and also on the untreated contralateral side, an indirect effect. The increases in vessel diameter and blood flow in both the ipsilateral STA (on the side of the treated TMJ) and contralateral STA (on the side of the untreated TMJ) may be caused by a vasodilator reflex via the hypothalamic thermostat, a further indication that photons can have a systemic effect[2]. Increase in blood flow has also been found in the central retinal artery following the irradiation of either the stellate ganglion or the common carotid artery in healthy volunteers with nearinfrared LLT [3], another example of an indirect effect of photons.

It is suggested that some of the local and systemic clinical effects of exposure of the scalp to LLT may be related to photon-induced changes in blood flow. The veins of the scalp, the cranial diploe and the intracranial venous sinuses are linked by emissary veins that traverse cranial foramina. The valveless nature of the emissary veins permits transport from the scalp of blood containing cells that have absorbed and been directly affected by photons to cranial and intracranial structures where they can induce indirect effects. The emissary veins may also act as conduits for photons, conducting them through the scalp into the cranium and intracranial structures where they may produce direct effects on the cells that absorb them.

References:

- 1. Samoilova KA, Zhevago NA, Petrishchev NN, Zimim AA. Photomed Laser Surg 2008; 26(5):443-9.
- 2. Makiara E, Masumi S. Nihon Hotetsu Shika Gakkhai Zasshi 2008; 52(2):167-70.
- 3. Mii S, Kim C, Matsui H, Oharazawa H, Shiwa T, Takahashi H, Sakamoto A. J Nippon Med Sch 2007: 74(1):23-9.

7552-05, Session 1

Will LLLT be an alternative treatment for traumatic brain injury?

Y. Huang, Q. Wu, A. C. Chen, M. R. Hamblin, Massachusetts General Hospital (United States)

Low level laser (or light) therapy (LLLT) has been clinically applied for many indications in medicine that require the following processes: protection from cell and tissue death, stimulation of healing and repair of injuries, and reduction of pain, swelling and inflammation. One area that is attracting growing interest is the use of LLLT to treat traumatic brain injury. The fact that near-infrared light can penetrate into the brain allows non-invasive treatment to be carried out with a low likelihood of treatment-related adverse events. LLLT may have beneficial effects in the acute treatment of brain damage injury. LLLT works, in part, by increasing respiration in the mitochondria - an effect that continues long after the light is removed - causing activation of transcription factors leading to cellular effects such as increased brain antioxidant capacity, reduction of key inflammatory mediators, and inhibition of apoptosis. It is proposed that red and NIR light is absorbed by chromophores in the mitochondria of cells leading to increased ATP production, nitric oxide release, and formation of low levels of reactive oxygen species. All these mediators can alter gene transcription and upregulate proteins involved in cell survival, antioxidant production, collagen synthesis, reduction of chronic inflammation and cell migration and proliferation. With no broad agreement on many of these parameters, it will require much more research before LLLT ever becomes an alternative therapy to TBI.

7552-06, Session 1

Molecular mechanisms of the antiinflammatory effect on rheumatoid arthritis by low level laser irradiation

Y. Abiko, Nihon Univ. (Japan)

A number of studies have attempted to elucidate the mechanism of the anti-infla- mmatory effect of low-level laser irradiation (LLLI), however, the molecular basis of the mechanism remains obscure.

Bioinformatics has become an integral part of research and useful in biomedical sciences. Now it has an essential role in deciphering genomic, transcriptomic and proteomic approach generated by high through put technologies. Thus, there is a great potential for laser science and medical clinical development to take this advantage of bioinformatics study. Recently, signal pathway database systems, for querying, visualization and analysis, should support formats in bioinformatics research. Novel computational approaches, using the Ingenuity Pathway Analysis (IPA) to mapping gene onto signaling pathways, have well developed and constructed to take advantage functional genomic study.

Rheumatoid arthritis rats were generated by immunization with type-II collagen and showed significant swelling of foot paw and knee joints. LLLI (SuperLizer; Tokyo Iken; Panalas 2000, Panasonic) significantly reduced these swellings, suggesting these LLLI are effective to reduce inflammations. To elucidate the molecular mechanism using cell culture system, human rheumatoid synoviocytes (MH-7) were challenged with IL-1 and monitored mRNA levels using Affimetrix GeneChip system (47,000 genes). LLLI altered many genes expression of cytokine, chemokine, growth factor and signal transduction factor. The signal pathway database vary widely in coverage and representation of biological processes, however, making their use is extremely difficult.

IPA analysis results revealed the cellular mechanisms for understanding the anti-inflammatory effect of LLLI. LI kept the MH7A to the normal state after IL-1 treatment due to suppress mRNA levels of IL-8, IL-1 , CXC1, NFkB1, FGF13 enhanced by IL-1 as same as dexamethasone (DEX) did, however, certain gene expressions were different between LLLI and DEX. IPA analysis results suggest that LLLI altered useful gene expressions, whereas DEX randomly altered many gene expressions including the unwanted genes for anti-inflammation. Thus, genome based gene expression monitoring provide unprecedented access to elucidate the mechanism of biostimulatory effects by LI.

7552-07, Session 2

In vitro suppression of metabolic activity in malignant human brain cancer and normal human fibroblast due to extremely low frequency pulsed electric potential exposures

D. B. Tata, U.S. Food and Drug Administration (United States); A. Schlichting, Marquette Univ. (United States); R. W. Waynant, U.S. Food and Drug Administration (United States)

The role of low (repetition) frequency pulsed electric potential was investigated in suppressing the metabolic activities of aggressive human glioblastoma (Glios) and normal human fibroblast (NHF) cells. The cells were exposed in sterile 60mm Petri-dishes (within their respective growth medium with 10% fetal bovine serum) to the following electric potential exposure parameters: pulse repetition frequency = 150Hz, pulse duration = 250 micro-secs, Peak voltage amplitude = 80 volts. A time course exposure (0 - 5 mins) study revealed a robust production of hydrogen peroxide (as determined via Amplex Red assay) within both (cell-free) growth media at the end of the 5 min exposure. The cellular metabolic activity for various duration of exposure was determined through the colorimetric MTS assay, 24Hrs after the pulsed E-field exposures. Comparatively, 24Hrs post exposure, the Glios were found to be highly sensitive to the pulsed 5 mins electric potential exposures, retaining only 1.5 % of their metabolic activity (relative to control) as opposed to



35% for the NHF's metabolic activity. The pulsed electric field induced hydrogen peroxide concentration dose response curves revealed the Glios to be approximately 45 times more sensitive in the reduction of 50% metabolic activity (relative to the control) than the NHFs. Taken together, these in-vitro findings suggest a "window of therapeutic opportunity" in the obliteration of Glio's metabolic activity through selective low frequency pulsed electric field exposures.

7552-08, Session 2

Dermal papilla cell activation by low level light irradiation

Y. Sheen, National Taiwan Univ. Hospital (Taiwan) and National Taiwan Univ. College of Medicine (Taiwan); S. Lin, National Taiwan Univ. Hospital (Taiwan); M. S. Fan, National Taiwan Univ. (Taiwan); C. Chan, S. Jee, National Taiwan Univ. Hospital (Taiwan)

Hair cycles are maintained by perpetual dermal-epidermal interaction between dermal papilla cells (DPC) and above lying keratinocytes. Anything that disrupts the balance will lead to hair loss. Light emitting diode (LED), when designed as a low level light therapy (LLLT), is well tolerated by biological tissues. Recently, related products are proven to be beneficial in promoting hair growth, without knowing the actual working mechanism.

In this research, we aim to investigate the mechanisms underlying the growth promotion associated with LED irradiation. Primary DPC harvested from rat vibrissa follicle were irradiated with LED with specific wavelength. In comparison with the untreated group, irradiated DPC have a distinct higher rate of proliferation and enhanced cellular viability. We found a high proportion of DPC in S/G2M phase in irradiated group. The levels of ERK and Akt phosphorylation increased significantly. The addition of either PD98059 or LY294002 reversed the growth increase induced by LLL, which showed that LLL affects the growth of DPC specifically through both the ERK and the Akt signaling pathways. The number of outer root sheath keratinocytes (ORSK) co-cultured with irradiated DPC was significantly higher than that of the direct-irradiated and control group. The increased growth of ORSK in the co-culture system would be explained by indirect action through increased DPC activation in turn mediating ORSK proliferation. We suggest that LLL irradiation simulates the growth of DPC. Furthermore, DPC may increase ORSK proliferation via secreting soluble factors and then modulate hair follicle epithelial-mesenchymal interaction.

7552-09, Session 2

Activation of transcription factors by low level light in different cell types

A. C. Chen, Y. Huang, M. R. Hamblin, Massachusetts General Hospital (United States)

Discoveries are rapidly being made in multiple laboratories that shed "light" on the fundamental molecular and cellular mechanisms underlying the use of low level light therapy (LLLT) in vitro, in animal models and in clinical practice. Increases in cellular levels of respiration, in cytochrome c oxidase activity, in ATP levels and in cyclic AMP are found. Increased expression of reactive oxygen species and release of nitric oxide have also been shown. In order for these molecular changes to have a major effect on cell behavior, it is likely that various transcription factors will be activated, possibly via different signal transduction pathways. This presentation will compare and contrast the effects of LLLT in vitro on murine embryonic fibroblasts, primary cortical neurons and bone-marrow derived dendritic cells. The effects of red and near-infra-red light will be compared, and the effects of low and high fluences will be addressed. Reactive oxygen species generation, nitric oxide release, transcription factor activation and ATP increases will be reported.

7552-10, Session 2

Effect of low-level laser on hair cell regeneration following gentamicin induced ototoxicity in postnatal organotypic culture of rat cochlea

C. Rhee, M. Suh, P. He, J. Ahn, Dankook Univ. Hospital (Korea, Republic of)

Aim

To investigate effects of low level laser (LLL) on hair cell regeneration following gentamicin exposure in organotypic culture of rat cochlea.

Organotypic culture of cochlea in culure medium was allowed to grow for 17 days (C group). The organotypic culture was irradiated with 808 nm, at 28.8 J/cm2(L group). The cochlea were exposed to 1 mM of gentamicin for 48 hr and allowed to recover (G group) or allowed to recover in the culture medium with daily irradiation (GL group) of LLL (28.8 J/cm2). The cochleae were stained with FM1-43. The number of hair cells was counted in each group serially for 17 days.

Results

While the C group kept on losing hair cells in vitro culture, the hair cells remained rather stationary in the L group. The number of hair cells revealed significantly larger number of hair cells in the L group compared to the C group (p=0.05). And the group \times time interaction was also significant (p=0.04). That is, the number of hair cells in the C group showed decreasing tendency which was significantly different from the L group.

In G group, the initial number of hair cells decreased to 37.2% of that of the gentamicin non-exposed groups. While the G group kept on losing hair cells, the number of hair cells increased in the GL group. The number of hair cells revealed significantly larger in the GL group (p=0.01) compared to G group. And the group \times time interaction was also significant (p=0.01). Also, the number of hair cells in the GL group showed increasing tendency which was significantly different from the G group

Conclusion

These results suggest that LLL promotes hair cell regeneration following gentamicin damage in cochlear explants.

7552-11, Session 2

Optimization of dose and power density for 980 nm and 810 nm light based on mitochondrial activity

I. Erbele, X. Wu, H. Moges, Uniformed Services Univ. of the Health Sciences (United States); B. Pryor, LiteCure (United States); J. Anders, Uniformed Services Univ. of the Health Sciences (United States)

BACKGROUND: Low level light therapy has been shown to promote wound healing, but the optimal frequency, dose, and power density are unknown. The aim of this in vitro study was to compare the effects of altering dose and power densities of 810nm and 980nm light on the mitochondrial activity of human fibroblasts. METHODS: Human fibroblasts were irradiated with combinations of three parameters: 810nm or 980nm light; doses of 0.2, 1, or 5 J/cm2; and power densities of 10, 25, or 50 mW/cm2. The cells were irradiated three times, with 120 minutes between exposures. At forty minutes after each irradiation, mitochondrial dehydrogenase activity was determined by an MTS assay. RESULTS: The greatest statistically significant increases in enzyme activity occurred with 810nm light at doses of 1 and 5 J/cm2 and a power density of 50 mW/cm2 after two exposures (40 % above control). For 980nm light, the greatest statistically significant increase in enzyme activity occurred with 5 J/cm2 and 10 mW/cm2 after two

Conference 7552: Mechanisms for Low-Light Therapy V



exposures (11.2% above control). CONCLUSIONS: These data provide convincing evidence that specific combinations of dose, power density, and wavelength are necessary to cause a significant alteration in cellular function and that the power density used is of major importance. It is interesting that 980 nm light was most effective at a lower power density compared to 810 nm light. The quantitative differences in the enzyme activity between the wavelengths may indicate either a need for further optimization of the 980nm light or a different mechanism of action.

7552-12, Session 3

NIR treatment delays the progression of parkinson's disease model in A53T transgenic mice

H. T. Whelan, Medical College of Wisconsin (United States); K. Desmet, Univ. of Wisconsin, Milwaukee (United States); E. Buchmann, M. Henry, Medical College of Wisconsin (United States); J. T. Eells, Univ. of Wisconsin, Milwaukee (United States)

Transgenic mice expressing the A53T alpha-synuclein mutation driven by the mouse prion protein gene promoter develop a rapid, severe motor phenotype that is linked to the accumulation of alpha-synuclein containing aggregates (Giasson et al, 2002). One hundred percent of homozygous A53T transgenic mice from the M83 line develop the motor phenotype within 8-16 months of age (Giasson et al., 2002). A53T transgenic mice (M83 line) were utilized as an in vivo model of PD to determine the effectiveness of NIR treatment at delaying disease progression. By 20 months of age, 95% of non-NIR treated A53T transgenic mice developed the motor phenotype associated with this alpha-synuclein mutation. In contrast, only 85% of NIR treated A53T transgenic mice developed the motor phenotype by 20 months of age. The average age of phenotype onset was 458 days for non-NIR treated mice and 524 days for NIR treated mice. NIR treatment effectively delayed the progression of disease such that at 500 days the group of mice treated with NIR light had significantly less mice display the motor phenotype (p=0.0005) as well as succumbing to the disease (p=0.0054). NIR treatment increased dopamine concentrations in the striatum by 153% (p<0.001). NIR treatment increases BcI-2 and decreases Bax and Caspase-9 apoptotic protein expression (<0.05).

7552-13, Session 3

Low-power light effects on rat hearts after ischemia of myocardium

V. A. Monich, Nizhny Novgorod State Medical Academy (Russian Federation)

Total ischemia of myocardium has been simulated on isolated hearts of rats. Effects of a low-power HeNe laser (λ =632.8 nm) and a fiber optic photo-luminescent radiation source of red light (λ of the spectral peak is equal to 630 nm) on isolated heart contractile function characteristics and on lipid peroxidation (LPO) level in myocardium tissues have been investigated. The internal pressure in the left ventricle and its first derivation were registered by an automatic recorder based on a straingauge transducer. The LPO level was evaluated according to content of molecular products of lipid peroxidation in cardiac muscle tissues. Two groups of the specimens have been irradiated with red light during the postischemia (reperfusion) period of time. The first group has been treated with laser light and the second one with the luminescent radiation (lumir) with 0.18 J/cm2 at a fluence rate 0.2 mW/cm2 and 1.35 J/cm2 at a fluence rate 1.5 mW/cm2 correspondingly. More rapid restoration of the speed of contraction, of the force of contraction, of the relaxation speed and of the heart rate with respect to the data of the control group has been observed in both experimental groups. Contents of diene conjugates (DC) and triene conjugates (TC) after red light irradiation decreased with respect to the control group data by more than 300% and 150% correspondingly. The similar tendency was observed in the laser treated specimens. The effects of fibrillation of myocardium of

isolated hearts irradiated by low-power He-Ne laser light were observed. These effects could be caused by the local light fluence rate excess in the interference pattern of laser light diffracted on the heart muscle structures.

7552-14, Session 3

LASER and LED photobiomodulation in the prevention and treatment of oral mucositis after chemotherapy: experimental study in hamsters

M. d. R. S. Freire, R. Prehatney, A. M. C. Marques, L. M. P. Ramalho, V. A. Sarmento, Federal Univ. of Bahia (Brazil)

Oral mucositis is a common side effect in patients receiving chemotherapy and until now researchers looking for methods to minimize it. These clinical and histomorphometric investigation proposes to evaluate effects of chemotherapy with 5-FU (Sonis model), Lasers GaAlAr (MMOptics, São Carlos, SP, Brazil), wavelenght of 660nm, the output power was 40mW,CW, with the spot size of 4mm, 20J/cm and GaAllnP (MMOptics, São Carlos, SP, Brazil), wavelenght of 780nm, total power was 40mW,CW, with the spot size of 4mm, 20J/cm (MMOptics, São Carlos, SP, Brazil,); and Leds (Kondortech, São Carlos, SP, Brazil), emitting red light (670nm), with the output power of 16mW, CW, spot size of 16mm, with the total energy of 8J, 4J/cm2 and emitting infraredlight (880nm), output power of 50mW, CW, spot of 16mm, total energy of 4J irradiations, in hamster cheek pouch mucosa. Preventive groups (I, II) started one day before the drug administration, every 48 hours for fifteen days and the therapeutic groups (III, IV) started on the fifth day; and two control groups (V, VI), with and without chemotherapy. Primary results indicated loss of body mass and allopecia, the healing of mucositis in different degrees. Histologically, was observed epithelial atrophy, hyperemia, fibroblasts proliferation, angiogenesis and collagen fibers at different intervals.

7552-15, Session 3

Raman spectroscopy validates the use of fluorescence readings of the Diagnodent® as a method of optical biopsy of tibial fractures treated or not with laser phototherapy, BMPs, guided bone regeneration and internal rigid fixation

A. L. Barbosa Pinheiro, Univ. Federal da Bahia (Brazil); C. B. Lopes, Univ. do Vale do Paraíba (Brazil); M. T. T. Pacheco, A. Brugnera Junior, Unicastelo (Brazil); F. A. A. Zanin, Instituto Brugnera & Zanin (Brazil); M. C. T. Cangussú, Univ. Federal da Bahia (Brazil); L. Silveira Junior, Unicastelo (Brazil)

Fractures have different etiology and treatment and may be associated or not to bone losses. LLLT has been shown to improve bone healing. We aimed to assess through Raman spectroscopy and fluorescence the levels of CHA (958cm-1) and lipids and proteins (1447cm-1) on complete fractures treated with IRF treated or not with LLLT and associated or not to BMPs and GBR. Tibial fractures were created on 15 animals and divided into 5 groups. LLLT started immediately after surgery, repeated at 48 h interval. Animal death occurred after 30 days. Raman spectroscopy and fluorescence were performed at the surface. Diagnodent data of Group IRF + L + B showed similar readings to the ones on the group IRF_NBL. Significant differences were seen between groups IRF + L + B and IRF + L; IRF + L + B and IRF + B and between IRF + L + B and IRF. CH groups of lipids and proteins readings evidenced decreased level of organic components on subjects treated with the association of LLLT, biomaterial and GBR. Pearson Correlation showed that fluorescence readings of CHA correlated negatively with the Raman data. Using the



data of CH groups of lipids and proteins Raman we found significant positive correlation. The use of both methods indicates that the use of the biomaterial associated to IR LLLT resulted on a more advanced and of quality bone repair on fractures treated with miniplates and that the Diagnodent® may be used to perform optical biopsy on bone.

7552-16, Session 3

The photobiomodulation in the bone repair after radiotherapy: experimental study in rats

M. d. R. S. Freire, Federal Univ. of Bahia (Brazil); D. de Almeida, Federal Univ. of Reconcavoi Baiano (Brazil); J. N. dos Santos, V. A. Sarmento, Federal Univ. of Bahia (Brazil)

This research evaluated the effect of the lasertherapy in the healing of surgical wounds produced in Wistar rats femurs, few days before the beginning of the radiotherapy. For this, an orifice was artificially produced in the femur bone of the rats and they had been submitted to an external radiotherapy with a radioactive source of cobalt in the dosage of 3000 cGys. The experimental group received additionally seven sessions of 780 mm, 40 mW, 100 J/cm2, 5 J/cm2 in four points around the surgical wound, at each 48 h, initiated at the day of the surgery. These animals had been sacrificed in three and five weeks. The results were based on the clinical and hystologic analyses. Clinically, even though the rats had gained body mass with elapsing of the experiment (p< 0,05), those who has been submitted to the lasertherapy presented cutaneous inflammatory reactions. Regarding the hystologic findings, the number of osteocits (p< 0,0001) and Harvers channels (p< 0,0001) was significantly larger in the groups that had been radiated with laser, during the experiment.

7552-17, Session 3

Prevention of bloodstream infections by photodynamic inactivation of multiresistant pseudomonas aeruginosa in burn wounds

M. C. E. Hashimoto, R. A. Prates, D. J. Toffoli, L. C. Courrol, M. S. Ribeiro, Instituto de Pesquisas Energéticas e Nucleares (Brazil)

Bloodstream infections are potentially life-threatening diseases. They can cause serious secondary infections, and may result in endocarditis, severe sepsis or toxic-shock syndrome. Pseudomonas aeruginosa is an opportunistic pathogen and one of the most important etiological factors responsible for nosocomial infections, mainly in immuno-compromissed hosts, characteristic of patients with severe burns. Its multiresistance to antibiotics produces many therapeutic problems, and for this reason, the development of an alternative method to antibiotic therapy is needed. Photodynamic inactivation (PDI) may be an effective and alternative therapeutic option to prevent bloodstream infections in patients with severe burns. In this study we report the use of \overrightarrow{PDI} to prevent bloodstream infections in mice with third-degree burns. Burns were produced on the back of the animals and they were infected with 109 cfu/mL of multi-resistant (MR) P. aeruginosa. Fifteen animals were divided into 3 groups: control, PDT blue and PDT red. PDT was performed thirty minutes after bacterial inoculation using 10µM HB:La+3 and a 400mW light-emitting diode (LED) emitting at =460nm±20nm and a 10mW LED emitting at =630nm±20nm for 180s. Blood of mice were colected at 7h, 10h, 15h, 18h and 22h pos-infection (p.i.) for bacterial counting. Control group presented 1x104 cfu/mL in bloodstream at 7h p.i. increasing to 1x106 at 22h, while mice PDT-treated did not present any bacteria at 7h; only at 22h p.i. they presented 1x104cfu/mL. These results suggest that HB:La+3 associated to blue LED or red LED is effective to delay and diminish MR P.aeruginosa bloodstream invasion in third-degree-burned mice.

7552-18, Session 4

Review of technology development and clinical trials of low level light therapy for acute stroke treatment

B. E. Catanzaro, CFE Services (United States); J. Streeter, L. de Taboada, Photothera (United States)

Stroke is the one of the leading cause of mortality in the United States, claiming 600,000 lives each year. Evidence suggests that infrared illumination has beneficial effects on a variety of cells when these cells are exposed to adverse conditions. Among these conditions are the hypoxic state produced by acute ischemic stroke. To demonstrate the impact Low Level Light Therapy (LLLT) has on ischemic stroke in humans, a series of double blind clinical trials were designed using the NeuroThera Laser System (NTS). The NTS was developed to treat subjects non-invasively using near-infrared (808 nm) illumination. LLLT as it applies to stroke therapy and the NTS will be described. The results of the two clinical trials will be reviewed and discussed.

7552-19, Session 4

Laser therapy for the treatment of arthritic knees: a clinical study

F. Kahn, L. Perrin, F. Saraga, Meditech International, Inc. (Canada)

Arthritis results in the deterioration of the joints through the process of chronic inflammation. The most common form is osteoarthritis and degenerative joint disease which is estimated to affect 80% of the population by the age of 65. Osteoarthritis most commonly affects the hands, feet, spine and the large weight bearing joints such as the hips and knees. The lifetime risk of developing osteoarthritis of the knee has been estimated at 40%. Recent studies have shown that patients with this condition are unlikely to benefit from arthroscopic surgery. On the other hand, clinical trials have indicated that laser therapy for osteoarthritis of the knees alleviates pain to a significant degree, along with the restoration of normal function and the quality of the patient's life. In a follow-up clinical study to our previously published 2006 SPIE conference proceeding, we analyzed a cross-section of patients treated for a variety of knee conditions that present at our Meditech Clinics on a daily basis.

Of the 98 knee patients included in this study, 65% presented with osteoarthritis of a knee. On average, 11 treatments were administered for each patient over a duration of 30 minutes and this program resulted in a significant improvement rate in excess of 92%.

Duration of treatment and positioning of the treatment arrays and laser probe are crucial in the process of achieving an optimal therapeutic effect. Our experience indicates that the knee is best treated in a relatively flexed position in order for penetration of the photon stream to the posterior aspect of the patella and the patellar compartment. Laser therapy is active at both the cellular and systemic levels through a variety of mechanisms including collagen production, DNA synthesis, improved microcirculation and the anti-inflammatory effect.

7552-20, Session 4

Transcranial high-intentsity LED therapy for cognitive dysfunction in chronic mild traumatic brain injury: two case reports

M. Naeser, Boston Univ. School of Medicine (United States); A. Saltmarche, MedX Health Corp. (Canada)

Objective: Transcranial, low-level laser therapy research has shown significant benefit for acute stroke in humans1 and acute traumatic brain injury (TBI) in mice2. Two chronic, mild TBI (mTBI) cases are presented,

Conference 7552: Mechanisms for Low-Light Therapy V



where cognitive function improved following treatment with transcranial, high-intensity light emitting diode (LED) therapy.

Methods and Procedures: P1 (age 59) had closed-head injury from motor vehicle accident (MVA) with no loss of consciousness, normal MRI. Unable to return to work as development specialist for Internet marketing due to cognitive dysfunction. At 7 Yr. post-MVA, began transcranial, LED treatment with cluster heads (2.1" diameter with 61 diodes each - 9x633nm, 52x870nm; 12-15mW per diode; total 500mW; 22.2 mW/cm2) on bilateral frontal, temporal, parietal, occipital areas (13.3 J/cm2 at scalp, estimated 0.4 J/cm2 to brain cortex3). Treated weekly at office; then daily at home. P2 had series of closed-head injuries related to military training; 10-20 years later, scored below average on attention and executive function; unable to work (age 52). MRI scan was abnormal with widespread cortical atrophy. Performed daily transcranial, LED home treatments.

Results: P1: Prior to transcranial LED, focused time on computer was 20 minutes. After 2 months of weekly, transcranial LED, increased to 3 hours; formed a small business. Has continued nightly home treatments, 4.5 years; if stops treating for 2-7 weeks, regresses. P2: After 4 months of nightly home treatments with transcranial LED, can return to part-time work. Continues with home treatments.

Conclusions: Transcranial LED may help treat cognitive dysfunction in mTBI. Controlled research is necessary.

References

- 1. Zivin JA, Albers GW, Bornstein N, Chippendale T, Dahlof B, Devlin T, Fisher M, Hacke W, Holt W, Ilic S, Kasner S, et al. Effectiveness and Safety of Transcranial Laser Therapy for Acute Ischemic Stroke. Stroke 2009;40:1359-1364.
- 2. Oron A, et al. Low level laser therapy applied transcranially to mice following traumatic brain injury significantly reduces long-term neurological deficits. J Neurotrauma 2007; 24:651-656.
- 3. Wan S, Parrish JA, Anderson RR, Madden M. Transmittance of nonionizing radiation in human tissues. Photochemistry and Photobiology, 1981;34:679-681.

7552-21, Session 4

Return to Contents

The effects of infrared laser therapy and weightbath traction hydrotherapy as a component of complex physical treatment in disorders of lumbar spine: a controlled pilot study with follow-up

C. Oláh, B. Demeter, V. Páll, Borsod County Univ. Teaching Hospital (Hungary); M. Oláh, Hungarospa Health Resort (Hungary); Z. Jancsó, Debrecen Medical Univ. (Hungary); T. Bender, St. John of God Hospital (Hungary)

Introduction: The therapeutic modalities available for the conservative management of chronic lumbar pain included infrared laser therapy and underwater traction , which usefulness is not universally acknowledged. This study was intended to ascertain any beneficial impact of infrared laser therapy and weightbath treatment on the clinical parameters and quality of life of patients with lumbar discopathy.

Material and methods: The study population comprised 54 randomised subjects. I. group of 18 patents received only infrared laser therapy to lumbar region and painful Valley points. II. group of 18 subjects each received underwater traction therapy of lumbar spine with add-on McKenzie exercise and iontophoresis. The remaining III. group treated with exercise and iontophoresis, served as control.

VAS, Oswestry index, SF36 scores, range of motion, neurological findings and thermography were monitored to appraise therapeutic afficacy in lumbar discopathy. A CT or MRI scan was done at baseline and after 3 moths follow-up.

Result:Infrared laser therapy and underwater traction for discopathy achieved significant improvement of all study parameters, which was evident 3 months later. Among the controls, significant improvement of

only a single parameter was seen in patients with lumbar discopathy. Conclusions: Infrared laser therapy and underwater traction treatment effectively mitigate pain, muscle spasms, enhance joint flexibility, and improve the quality of life of patients with lumbar discopathy.

7552-23, Session 4

Syntonic phototherapy

R. Gottlieb, College of Syntonic Optometry (United States)

This presentation will describe syntonics, an optometric phototherapy applied to the eyes used to treat children and adults with learning, reading and attention disabilities, brain injury, eye pathology, strabismus, headache and more. In a darkened room the patients view a glowing dot of colored light, 50mm in diameter at about 50cm away. A 50w, 115v incandescent bulb (powered at 145V to increase color temperature) illuminates absorption filters and is then focused to the eyes through a frosted collimating lens. The light may be flashed or constant. There are a dozen syntonic filters covering the visual spectrum. These are typically prescribed in pairs to narrow the bandwidth or steepen cut off slope. Treatments last 20 minutes, one per day for a minimum of three consecutive days per week, usually for 20 sessions. Syntonic prescribing is based on medical and birth history, past and present symptoms, and visual measures. Patients typically have poor eye motility, accommodation, visual discrimination, binocularity, weak pupil responses and contracted visual fields caused by brain trauma from head injury, stroke, high fever, hypoxia, toxicity, fatigue or high stress. Data is recorded in the initial diagnostic workup and checked after 6-8 treatments, at the last treatment and six weeks later. Typically progress exams show larger fields, improved objective findings and the symptoms and signs of visual dysfunction and underachievement improve permanently. Theory and possible research will be discussed.

7552-24. Poster Session

Polarized light improves cutaneous healing on diabetic rats

L. M. P. Ramalho, P. C. Oliveira, A. M. C. Marques, A. L. Barbosa Pinheiro, Univ. Federal da Bahia (Brazil)

The aim of this study was to evaluated the healing of 3rd degree burn on diabetic rats submitted or not to treatment with Polarized Light (400-2000nm, 20 or 40J/cm2, 40mW; 2.4J/cm2/min; ± 5.5 cm). Diabetes melitus was induced on 45 rats and a burn was created in the dorsum under general anesthesia. Phototherapy (Polarized Light source -Bioptron®, 20J/cm2 or 40J/cm2 per session) stared immediately and repeated at every other day during 21 days. Specimens were taken, cut, processed to wax, and stained with H&E, Sirius Red, and imunnomarked with CK AE1/AE3 antibody. The animals submitted to phototherapy (20J/cm2) showed significant differences on regards revascularization and epithelialization. Despite the illuminated group (40J/cm2) showed stimulation of fibroblastic proliferation as isolated feature, no other the laling of third degree buns on diabetic animals at both early and late stages of the repair.

7552-25, Poster Session

Assessment of laser photobiomodulation and polarized light on the healing of cutaneous wounds on euthyroid and hypothyroid induced rats

L. M. P. Ramalho, B. M. P. Weyll, M. D. M. da Costa Lino, M. J. P. Ramalho, A. L. Barbosa Pinheiro, Univ. Federal da Bahia (Brazil)

Thyroid hormone deficiency impairs healing. Laser and polarized light are

87

TEL: +1 360 676 3290 · +1 888 504 8171 · customerservice@spie.org

Conference 7552: Mechanisms for Low-Light Therapy V



therapies that can speed up healing. 40 rats were divided into euthyroid and hypothyroid groups and subdivided into Laser (l660nm, 30mW, f 3mm) or Polarized Light (l400-2000nm, 40mW, f 10mm) with 20 or 40J/cm²: Standardized wounds were created and left without suturing and irradiation or illumination was carried out every 48 h (7d). Animals were killed at the 8th day and underwent histological examination (H/E and Sirius Red). Hypothyroids showed delayed healing, reduced wound contraction (p=0.0276), poor re-epithelization and incipient formation of disorganized collagen fibers, when compared to the euthyroids The use of both therapies increased the number of fibroblasts and the amount and thickness of collagen fibers, especially in the L 20J/cm² group. Euthyroid rats showed more regular collagen fibers than the hypothyroids, which showed irregular fiber distribution. It was concluded that hypothyroidism delays wound healing and that both polarized light and laser light improved the healing process mostly at the dose of 20j/cm².

7552-28, Poster Session

The antinociceptive effects of monechma ciliatum and changes in EEG waves following oral and intrathecal administration in rats

A. B. Meraiyebu, Bingham Univ. (Nigeria) and University of Jos (Nigeria); A. B. Adelaiye,

The research work was carried out to study the effect of Oral and Intrathecal Monechma Ciliatum on Antinociception and EEG readings in Wistar Rats. Traditionally the extract is given to women in labour believed to reduce pain and ease parturition, though past works show that it has oesteogenic and oxytotic effects. The rats were divided into 5 major groups, Group 1 and 2 served as oral control and Intrathecal Controls respectively and were treated with dextrose. Group 3 and 4 served as experimental groups and were treated with 500mg/kg and 1000mg/kg respectively. Group 5 served as intrathecal experimental group treated with Monechma Ciliatrum intrathecally. The antinociceptive effect was analysed using an aesthesiometer to take series of Tail Flick Latencies (TFL). Monechma Ciliatum showed significant antinociceptive effect both orally and intrathecally, although it had a greater effect orally and during the first 15 minutes of intrathecal administration. EEG readings were also taken for all the groups and there was a decrease in amplitude and an increase in frequency for experimental groups and they produced 13-14 waves per second as seen in relaxed persons (beta waves) and had a symmetrical distribution, similarly accentuated by sedative-hypnotic drugs.

7552-31, Poster Session

Transcranial near infrared laser treatment (NILT) improves clinical performance in embolized rabbits: correlation with increased cortical adenosine-5'-triphosphate (ATP) content

P. A. Lapchak, Univ. of California, San Diego (United States); L. H. De Taboada, PhotoThera, Inc. (United States)

Background and Purpose: Transcranial near-infrared laser therapy (NILT) is currently under investigation in a pivotal clinical trial because laser therapy has been shown to improve clinical outcome in preclinical stroke models and in stroke patients. However, nothing is known about the mechanisms responsible for the behavioral improvements. The purpose of the present study was to determine the physiological effects of NILT in embolized rabbits and elucidate mechanisms involved in NILT-induced neuroprotection.

Methods: First, we determined the effects of post-embolization treatment with NILT on behavioral function in rabbits using a treatment duration of 2 minutes and a wavelength of 808 nm. For the studies, we used the rabbit small clot embolic stroke model (RSCEM), a multiple infarct ischemia model with a well-defined behavioral endpoint, which allows us to construct quantal analysis curves to define the amount of microclots (mg) that produce neurologic dysfunction in 50% of a group of animals (P50). A separate quantal analysis curve is generated for each treatment condition. For these studies, behavior including motor function was measured daily for 3 weeks following embolization. For this we treated embolized rabbits with NILT initiated 3-12 hours following embolization and measured behavior 48 hours following embolization. Second, it has been proposed that mitochondrial energy production may underlie a response to NILT, but this has not been demonstrated using an in vivo embolic stroke model. Thus, we evaluated the effect of NILT on cortical ATP content using the RSCEM. Following embolization, rabbits were exposed to NILT, which was driven to output either continuous wave (CW), or pulsed wave modes (PW). Three hours later, the cerebral cortex was excised and processed for the measurement of ATP content using a standard luciferin-luciferase assay. NILT-treated rabbits were directly compared to sham-treated embolized rabbits and naïve control rabbits.

Results: In this study, NILT significantly (p<0.05) increased motor function and the P50 value to 2.21 ± 0.54 mg (n=28) when administered 3 hours following embolization, compared to the control group (P50=0.97\pm0.19 mg, n=23). Moreover, NILT increased behavioral function when administered 6 hours following embolization (P50=2.06\pm0.59, n=29). The effects of NILT are durable and can last up to 21 days post-treatment. However, NILT was ineffective when applied 12 hours following embolization. Embolization decreased cortical ATP content in ischemic tissue by 45% compared to naive rabbits, a decrease that was attenuated by CW NILT which resulted in a 41% increase in cortical ATP content compared to the embolized group (p>0.05 compared to either the naïve or sham-EMBO group). However, following PW NILT, which delivered 5 (PW1) and 35 (PW2) times more energy than CW, we measured a 157% increase (PW1 p=0.0032) and 221% increase (PW2 p=0.0001) in cortical ATP content, respectively.

Conclusion: In the rabbit embolic stroke model, NILT administration significantly improved behavioral function when administered up to 6 hours following embolization. Based upon biochemical measurements of cortical ATP content, we demonstrated that embolization can decrease ATP content in rabbit cortex and that NILT significantly increases cortical ATP content in embolized rabbits, an effect that is correlated with cortical fluence and the mode of NILT delivery. The data provides new insight into the molecular mechanisms associated with clinical improvement following NILT.



Saturday-Monday 23-25 January 2010 • Part of Proceedings of SPIE Vol. 7553 Frontiers in Pathogen Detection: From Nanosensors to Systems

7553-01, Session 1

Photonic crystal-enhanced fluorescence

B. T. Cunningham, Univ. of Illinois at Urbana-Champaign (United States)

Optical resonances produced by photonic crystal surfaces can be designed to substantially amplify the electric field excitation of fluorophores while at the same time increasing the collection efficiency of emitted photons. Because PC surfaces can be produced inexpensively over large areas by replica molding, they offer an effective means for increasing sensitivity for broad classes of surface-based fluorescent assays. In this talk, the design and fabrication of photonic crystal surfaces and detection instrumentation for fluorescent enhancement will be described, along with demonstrated applications in gene expression microarrays and protein biomarker microarrays.

7553-02, Session 1

Real-time small molecule binding detection using a label-free optical biosensor

Y. Guo, J. Y. Ye, Univ. of Michigan (United States); B. Huang, D. McNerny, The Michigan Nanotechnology Institute for Medicine and Biological Sciences (United States); T. P. Thomas, Univ. of Michigan (United States); J. R. Baker, Jr., The Michigan Nanotechnology Institute for Medicine and Biological Sciences (United States); T. B. Norris, Univ. of Michigan (United States)

We have developed a novel label-free optical biosensor using a one-dimensional photonic crystal structure in a total-internal-reflection geometry (PC-TIR). This sensor has a narrow resonance width (~1 nm) and high bulk solvent refractive index sensitivity (~1500 nm/RIU), which enable sensitive measurements for the presence of analytes on the sensing surface, and at the same time perform real-time measurements of biomolecular binding as it employs an open sensing surface. Moreover, by measuring the differential intensity ratio during binding, ultralow detection limits have been obtained: $6\times10^{\circ}(-5)$ nm for analyte layer thickness, $7\times10^{\circ}(-8)$ RIU for bulk refractive index, and 20 fg/mm2 for protein mass density.

In this report, we further demonstrate the capability of the PC-TIR sensor for small-molecule detection. The well-studied biotin-streptavidin system is chosen in order to calibrate the detection limit. Streptavidin is immobilized on the silica sensing surface. Then analyte molecules - a series of biotin-conjugated molecules of various molecular weights - are detected in real time with specific binding to the sensing surface. The binding of the smallest molecule investigated, D-Biotin (MW 244Da), is easily experimentally observed with a high signal to noise ratio. The PC-TIR sensor thus promises to be a high-sensitivity, high-accuracy sensing platform for biomolecular binding analysis.

7553-03, Session 1

Microcavities in photonic crystal waveguides for biosensor applications

S. Pal, E. Guillermain, B. L. Miller, P. M. Fauchet, Univ. of Rochester (United States)

In this study, resonant microcavities in photonic crystal (PhC) waveguides are investigated for biosensing applications. The device architecture consists of a PhC waveguide with a defect line for guiding the transmission of light. Resonant microcavities created by changing

the radius of a hole adjacent to the defect line are coupled to the PhC waveguide. Detection is based on shifts in the resonance wavelength observed in the transmission spectra. The PhC waveguide device is fabricated on silicon-on-insulator (SOI) wafers using electron beam lithography and reactive-ion etching (RIE). Receptor molecules are attached to the defects in the device by standard amino-silane and glutaraldehyde crosslinking chemistry. Preliminary results demonstrate successful detection of human IgG molecules as the target at large concentration levels of 500 $\mu \text{g/ml}$. Such PhC waveguide devices are advantageous for medical diagnostics and biosecurity applications as they allow rapid, label-free, and sensitive detection of multiple analytes in a single platform.

7553-04, Session 1

Single virus detection with optical mircocavities

F. Vollmer, Harvard Univ. (United States); S. Arnold, Polytechnic Institute of NYU (United States)

Virus nano-particles are a major cause for human disease, and their early detection is of added urgency since modern day travel has enabled these disease agents to be spread through populations across the globe. Fast and early detection on site of an outbreak requires biosensors where ideally individual nano-particles produce a quantitative signal. We present an optical technique that provides such ultimate sensitivity towards detection of label-free virions. The high sensitivity relies on the re-circulation of the probing light in high-Q microcavities, examples for which are silica microspheres and defects in silicon photonic crystals. We establish the technique by detecting single polystyrene nanoparticles from resonance-wavelength fluctuations in spherical microcavities. We find that the magnitude of the wavelength-shift signal follows a reactive mechanism with inverse dependence on mode volume, providing a means to increase sensitivity by reducing the size of the microsphere. We then optimize the approach and demonstrate detection of single Influenza A virus particles. The mass (5.2 x 10(-16) gram) and size (47 nm) of single virions is determined directly from the magnitude of the wavelength shift, demonstrating a label-free approach towards identification of an unknown virus without the need for antibodies. Furthermore, we introduce a novel approach for trapping and accumulation of virus particles directly at the microcavity-sensor-region by using light-force exerted in evanescent field gradients.

7553-05, Session 2

Colorimetric-resonant-reflection and imagecorrelation sensing with sub-wavelength lowindex-contrast aperiodic gratings

S. V. Boriskina, S. Lee, A. Gopinath, Boston Univ. (United States); J. A. Amsden, J. Mondia, D. Kaplan, F. Omenetto, Tufts Univ. (United States); L. Dal Negro, Boston Univ. (United States)

We investigate light scattering from aperiodic low-refractive-index gratings and discuss their potential applications as multiplexed platforms for label-free optical biosensing. We demonstrate color localization in aperiodic gratings by using dark field microscopy measurements, and reveal the physical mechanism of the colorimetric signatures formation via rigorous full-wave numerical simulations based on the generalized multi-particle Mie theory. Unlike periodic gratings, which scatter light into well-defined grating orders, aperiodic arrays feature a broad-band frequency response with a wide angular intensity distribution governed by the Fourier properties of the aperiodic lattice. We demonstrate a



possibility of the label-free detection with aperiodic lattices both by monitoring the shift of the resonant scattering (or reflection) peaks in their spectra and by performing the image correlation analysis of the gratings colorimetric signatures. Broadband spectral characteristics of aperiodic gratings make possible obtaining enhanced resonant reflection at several widely separated wavelengths by adjusting the angle of light incidence, which paves the way for realization of wavelength- or angle-multiplexed sensors. We also show that broadband fluorescence sensors can be realized with aperiodic nano-patterned structures.

7553-06, Session 2

The design of a microfluidic biochip for the rapid multiplexed detection of food-borne pathogens by surface plasmon resonance imaging

M. D. Zordan, M. G. Grafton, K. Park, J. F. Leary, Purdue Univ. (United States)

The rapid detection of food-borne pathogens is increasingly important due to the rising occurrence of contaminated food supplies. We have previously demonstrated the design of a hybrid optical device that has the capability to perform real-time surface plasmon resonance (SPR) and epi-fluorescence imaging. We now present the design of a microfluidic biochip consisting of a two-dimensional array of functionalized gold spots. The spots on the array have been functionalized with capture peptides that specifically bind E. coli O157:H7 or Salmonella enterica. This array is enclosed by a PDMS microfluidic flow cell. A magnetically pre-concentrated sample is injected into the biochip, and whole pathogens are bound to the capture array. The previously described optical device was used to detect the presence and identity of captured pathogens using SPR imaging. This detection occurs in a label-free manner, and does not require the culture of bacterial samples. Molecular imaging can also be performed using the epi-fluorescence capabilities of the device to determine pathogen state, or to validate the identity of the captured pathogens using fluorescently labeled antibodies. We demonstrate the real-time screening of a sample for the presence of E. coli O157:H7 and Salmonella enterica. Additionally the mechanical properties of the microfluidic flow cell are assessed. The effect of these properties on pathogen capture is examined. The device is portable and can be taken to the site of either food origin or processing for rapid multiplexed testing for food pathogens.

7553-07, Session 2

A microflow cytometer on a chip

J. P. Golden, J. Kim, G. Anderson, N. Hashemi, R. Eitel, F. Ligler, Naval Research Lab. (United States)

A rapid, automated, multi-analyte Microflow Cytometer is being developed as a portable, field-deployable, rapid sensor for on-site diagnosis of biothreat agent exposure and environmental monitoring. The technology relies on a unique method for ensheathing a sample stream in continuous flow past an interrogation region. Optical fibers provide excitation and collect emission from the interrogation region. This microfluidic approach avoids clogging by complex samples and provides for subsequent separation of the core and sheath fluids in order to capture the target for orthogonal confirmatory assays and recycling of the sheath fluid. Flow channels have been constructed in PDMS and PMMA. Coded microspheres provide the capability for highly multiplexed assays in a few minutes. Optical analysis at four different wavelengths identified six sets of coded microspheres and quantified target bound by the presence of phycoerythrin tracer. The Microflow Cytometer detected fluorescence from the phycoerythrin that correlated to antibodies conjugated to microsphere sets recognizing Escherichia coli, Listeria, and Salmonella as well as cholera toxin, staphylococcal enterotoxin B (SEB), and ricin. Through the formation of an additional layer of phycoerythrin on the microspheres, signal amplification was performed and provided

improvement in limits of detection (E. coli: 10^3 cfu/mL; Listeria: 10^5 cfu/mL; Salmonella: 10^5 cfu/mL; cholera toxin: 1.6 ng/mL; SEB: 0.064 ng/mL; ricin: 8.0 ng/mL). The results provided sensitivity comparable to assays performed on a Luminex commercial benchtop detection system. Automated sample processing is being incorporated with the assays.

7553-08, Session 2

Programmable nano-bio-chip sensor systems: toward next-generation pathogen detectors

J. T. McDevitt, Rice University (United States)

Diagnostic tools are critical to the delivery of effective healthcare, yet current in vitro diagnostic (IVD) devices are incapable of keeping pace with the explosive growth of information in the genomics, proteomics, metabolomics and glycomics areas. With US annual per capita healthcare costs now above \$7,400, and rising 7 to 8 percent per year, it is clear that the current trends can't be sustained. A key factor in determining health care costs is clinical specimen testing. While the ability to process large amounts of information at the point-of-need is common in the field of electronics, the capacity to process complex molecular disease signatures at the point-of-care has not yet been fully demonstrated. However, the electronics industry provides inspiration for cost reductions while at the same time producing ever increasing performance. The marriage of micro-fabrication and in vitro diagnostic devices may play a key role in developing the next generation diagnostic devices that can be affordable and accessible for all humanity. This presentation will review our advances made in the area of nano-bio-chip sensor systems that are suitable for a variety of human medical, homeland defense, pathogentoxin detection and humanitarian applications. Here integrated lab-on-achip sensor systems have been developed into a series of cost effective and programmable sensor modules that can service a broad range of applications areas.

7553-09, Session 3

Design of nanoscale interfaces for optical biosensors

A. Chilkoti, Duke Univ. (United States)

I will describe two examples from my laboratory on the design of nanoscale interfaces for optical biosensors. In the first example, I will describe our efforts in the design of a chip-based, label-free sensor that exploits the local surface plasmon resonance effect exhibited by noble metal nanostructures. The development of a sensor that measures the ensemble averaged spectral response of a large collection of particles as well as recent efforts in detecting binding at the single particle level will be described. The second example will describe the redesign of a conventional, antibody sandwich fluoroimmunoassay in an array format where we have focused on abolishing an important source of "chemical" noise in the assay by preventing the non-specific binding of proteins. We have developed a new method for the in situ synthesis of nanometer thick brushes of an oligoethyleneglycol-functionalized polymer on glass by surface-initiated polymerization. These polymer brushes show extraordinary resistance to proteins with a total adsorption from serum of less than 1 ng/cm2. At the same time, these polymer brushes can be physically printed with antibodies to enable stable binding of analytes and capture antibodies for fluoro-immunoassays and protein microarrays. I will show that decreasing the adventitious binding of proteins enables detection of a cytokine, IL-6, down to the femtomolar limit in whole blood, which is orders of magnitude better than commercially available fluorescence based microarrays.



7553-10, Session 3

Rapid and sensitive homogenous detection of the Ibaraki virus NS3 cDNA using magnetic modulation biosensing system

A. Danielli, Tel-Aviv Univ. (Israel); N. Porat, Univ. of Illinois at Chicago (United States); A. Arie, M. Ehrlich, Tel-Aviv Univ. (Israel)

Rapid and sensitive detection of specific DNA sequences is a well known challenge in many biological applications. For example, changes in the sequence of particular genes of human pathogens such as anthrax (Bacillus anthracis) can serve as biomarkers for early detection and response in the event of bioterrorism. Orbiviruses, such as EHDV2-Ibaraki, represent an acute threat to the bovine and ovine industries. Furthermore, similarly to other veterinary viruses, the relevant site of detection and action has the potential to differ considerably from laboratory settings, a fact that in conjecture with the need to perform a large number of assays, in a short period of time, underscore the need for an accurate, fast and sensitive detection technique, involving minimal enzymatic manipulation. In this work we experimentally demonstrate magnetic modulation biosensing system for rapid and homogeneous detection of the Ibaraki virus NS3 cDNA. A novel fluorescent resonance energy transfer (FRET)-based probe discriminates the target DNA from the control. When detection is made, the FRETbased probe is cleaved using Taq-polymerase activity and fluorescent light is produced. The biotinylated probes are attached to streptavidin coupled superparamagnetic beads and are maneuvered into oscillatory motion by applying an alternating magnetic field gradient through two electromagnetic poles. The beads are condensed into the detection area and their movement in and out the orthogonal laser beam produces a periodic fluorescent signal that is demodulated using synchronous detection. 1.9 picomolar of the Ibaraki virus NS3 cDNA was detected in homogeneous solution within 18 minutes without separation or washing

7553-11, Session 3

Detection of food-borne pathogens by nanoparticle technology coupled to a lowcost fluorescence cell reader

I. Noiseux, J. Bouchard, INO (Canada); H. Cao, S. Chen, Univ. of Guelph (Canada); R. Johnson, Public Health Agency of Canada (Canada); M. Vernon, O. Mermut, INO (Canada)

The detection, identification and quantification of different pathogenic microorganisms simultaneously and at low cost are of great interest to the agro-food industry. We have developed a simple, rapid, sensitive, and specific method for detection of foodborne pathogens based on use of nanoparticles alongside a low cost fluorescence cell reader for the bioassay. The nanoparticles are coupled with selected antibodies which allow specific recognition of the targeted foodborne pathogen bacteria in either a liquid or food matrix. The bioconjugated nanoparticles contain thousands of dye molecules binding to each individual bacterial cell, enabling significant amplification of the fluorescent signal emitted from each bacterium. The developed fluorescence cell reader is an LED-based reader coupled with suitable optics and a camera that uses image processing algorithms to improve the signal-to-noise ratio compared to that of commercial readers. The cell reader acquires high resolution images of the entire sample surface containing bacteria. The algorithm treats all the images acquired from the sample allowing the counting of each individual nanoparticles-fluorescent bacterial cell, thus enabling highly sensitive reading. Since only the targeted foodborne pathogens are fluorescent, only those are imaged with the fluorescent cell reader. Thus, sample preparation is simple and no separation of non targeted bacteria is required. Results of bioconjugated nanoparticles used to specifically target Listeria monocytogenes (responsible for a large amount of foodborne illness every year) will be presented. The combination of nanoparticle technology with a compatible optical cell reader is presented as a low cost solution for the detection of food-born pathogens.

7553-12, Session 3

Advanced laser spectroscopy approaches for sensing surface contaminants on medical devices

X. Tan, I. Ilev, U.S. Food and Drug Administration (United States)

Surface contamination is commonly encountered for medical devices, such as molecular contaminants from manufacturing, packaging, and sterilizing residues, trace heavy metals on dental crowns, protein pathogens on surgical instruments, and bacterial biofilms on implants. Currently applied clinical methods based on swab/wipe sampling and subsequent ex-situ detection suffer from inaccuracy and inefficiency. More sophisticated and sensitive techniques such as surface plasmon resonance (SPR), X-ray photoelectron spectroscopy (XPS), and time-offlight secondary ion mass spectrometry (ToF-SIMS) are too expensive and complex to handle for in-situ analysis. New technologies for rapidly assessing the presence and identification of surface contaminants are in pressing need. Laser spectroscopy with fiber-optic sensing technology fills the void by offering the advantage of being non-invasive, sensitive, and efficient with the potential to be miniaturized for in-situ applications. In the present work, we develop label-free detection approaches based on Fourier Transform Infrared and dispersive Raman vibrational spectroscopy, and fiber-optical sampling for sensing surface contamination. Contaminants to be examined first are carcinogenic and endocrine disrupting plasticizers such as the phthalates (DBP, DEHP) which are most commonly used in food, cosmetics, and medical device industries. The study includes validation of the developed technologies and characterization of the designed sensing systems in terms of chemical specificity, sensitivity, sample processing and analysis. We will extend the investigation on contamination validation and analysis to the more complex protein pathogens and biofilms by exploring advanced sampling and data analysis as well as system design and integration for real-time in-situ detection.

7553-13, Session 4

Engineered photonic-plasmonic aperiodic surfaces for optical biosensing

L. Dal Negro, The Boston Univ. Photonics Ctr. (United States)

In this talk, I will discuss our approaches towards the engineering of Surface Enhanced Raman Scattering (SERS) chips and colorimetric biosensors based on light localization in Deterministic Aperiodic Nano Structures (DANS). DANS are generated by the mathematical rules of L-systems and number theory, manifest unique light localization and transport properties, and can be fabricated using conventional nano-lithographic techniques. When combined with metal-dielectric nanostructures, DANS give rise to strongly localized field states with large fluctuations of the photonic mode density - essential attributes to achieve spatio-temporal energy localization and enhanced light-matter coupling for broadband optical biosensing. In this paper, I will discuss electromagnetic coupling, resonant light scattering, structural color localization and SERS detection from two-dimensional metal-dielectric arrays of different-shaped/different sized nanoparticles arranged in deterministic aperiodic sequences. All the arrays have been fabricated using Electron-Beam Lithography (EBL) on transparent quartz substrates. Experimental results on chemical reporters and different bacteria will be presented, along with the discussion of specific engineering design rules. Finally, I will discuss optical sensing by spectral color localization in photonic-plasmonic nano-hole arrays and gold nanoparticles on quartz substrates. Spectrally resolved correlation analysis and enhanced backscattering measurements were performed on the arrays revealing distinctive colorimetric signatures (color localization patterns). Using BSA protein monolayers as our biological target, we designed, fabricated and optimized different aperiodic structures and demonstrated for the first time that structural color localization in lithographically defined photonicplasmonic DANS can be utilized as a highly sensitive colorimetric method for on-chip protein detection and optical biosensing applications.



7553-14, Session 4

Biological sensing using SERS on metallized ultra-thin porous silicon membranes

K. Shome, C. Hoeppener, M. Kavalenka, L. Novotny, P. M. Fauchet, Univ. of Rochester (United States)

Ultra-thin porous silicon membranes provide a novel platform for label free detection and identification of biological samples using SERS. A 10 nm thin gold metal film is deposited on top of a 30 nm thick porous silicon membrane to form a thin porous metal film. 3D FDTD simulations show EM field enhancement inside the holes together with increased scattering and extinction cross sections, making this structure a novel SERS substrate.

7553-15, Session 4

Colorimetric signatures on photonicplasmonic surfaces for biosensing

Y. K. S. Lee, Boston Univ. (United States); J. Amsden, Tufts Univ. (United States); S. Boriskina, A. Gopinath, Boston Univ. (United States); D. Kaplan, F. Omenetto, Tufts Univ. (United States); L. Dal Negro, Boston Univ. (United States)

In this study, we investigate optical sensing by spectral color localization in photonic-plasmonic nanostructured surfaces. Aperiodic arrays consisting of chromium nanoparticles and nanoscale air holes on quartz substrates with minimum interparticle separations ranging from 50nm to 200nm were fabricated using electron beam lithography and nanoimprinting pattern transfer fabrication techniques. Silk protein thin films, in different concentrations, were deposited on the arrays and their scattering spectra were experimentally measured by dark-field spectroscopy under white light illumination. Colorimetric signatures (color localization patterns) on the aperiodic arrays were analyzed with the spectrally resolved correlation analysis and compared with rigorous multiple scattering semi-analytical calculations based on the Generalized Mie Theory. Using silk protein as our target, we designed, fabricated and optimized different aperiodic structures, which provide broadband electric field enhancement and mode localization for enhanced biological sensing. Our results demonstrate for the first time that the characteristic color localization patterns observed in lithographically defined aperiodic photonic-plasmonic structures can be directly utilized as highly sensitive colorimetric signatures for protein detection and employed in optical biosensing applications in the future.

7553-16, Session 4

Ultrasensitive Raman sensor based on a highly scattering non-absorbing porous structure

V. V. Yakovlev, Univ. of Wisconsin-Milwaukee (United States)

Analytical methods capable of in situ monitoring of water quality have been in high demand for environmental safety, the identification of minute impurities and fundamental understanding of potential risks of these molecular species. Raman spectroscopy, which provides 'fingerprint' information about molecular species in the excitation volume, is a powerful tool for in vivo diagnostics. However, due to a relatively weak Raman signal (~ 1 out of 1014 incident photons produces the useful signal) there is a need to significantly (by many orders of magnitude) enhance this signal, to raise the detection sensitivity of this technique.

Traditionally, surface enhanced Raman spectroscopy is employed to dramatically increase the local field intensity and substantially improve the efficiency of Raman scattering. However, the above enhancement occurs only in "hot spots", which represent only a small percent of the total surface are of the substrate. Plasmonic nanostructures are also

found to be hard to manufacture in large quantities with the desired degree of reproducibility and to be unable to handle high laser power.

We propose and experimentally demonstrate a new type of approach for ultrasensitive Raman sensing. It is based on manufacturing a random porous structure of high-index material, such as GaP, and use the effect of light localization to help improving the detection sensitivity of such sensor. The desired structure was manufactured using electrochemical etching of GaP wafers. The observed Raman signal amplitudes are favorably compared to the best known plasmonic substrates.

7553-17, Session 5

Spectral reflectance imaging for a multiplexed, high-throughput, label-free, and dynamic biosensing platform: protein, DNA and virus detection

M. S. Ünlü, E. Ozkumur, C. Lopez, A. Yalcin, Boston Univ. (United States); M. Chiari, C.N.R. (Italy); S. Ahn, G. Daaboul, A. Reddington, M. Monroe, R. Vedula, J. H. Connor, Boston Univ. (United States)

Optical resonance is one of the key properties of light enabling important devices such as interference filters and lasers. We have utilized basic principles of optical interference and resonance in biological applications demonstrating label-free sensing of protein binding in a high-throughput micro-array format.

Direct monitoring of primary molecular binding interactions without the need for secondary reactants would markedly simplify and expand applications of high-throughput label-free detection methods. We developed a simple interferometric technique - Spectral Reflectance Imaging Biosensor (SRIB) - that monitors the optical phase difference resulting from accumulated biomolecular mass. Dynamic measurements were made at ~3 pg/mm2 sensitivity. We have also demonstrated simultaneous detection of antigens and antibodies in solution using corresponding probes on the SRIB surface as well as label-free measurements of DNA hybridization kinetics.

A primary advantage of label-free detection methods over fluorescent measurements is its quantitative detection capability, since an absolute measure of adsorbed material facilitates kinetic characterization of biomolecular interactions. We demonstrated quantified and calibrated measurements for protein and DNA assays.

Using our label-free technique, we observed a linear dependence over 4 orders of magnitude.

Finally, we have demonstrated evidence towards single virus detection promising a highly multiplexed platform for pathogen sensing.

7553-18, Session 5

Multiplex detection of disease marker proteins with arrayed imaging reflectometry

B. L. Miller, A. Yadav, R. Sriram, Univ. of Rochester (United States)

Arrayed Imaging Reflectometry, or "AIR", is a new label-free optical technique for detecting proteins that relies on binding-induced changes in the response of an antireflective coating on the surface of a silicon chip. Thus far, we have demonstrated the use of AIR for the detection of pathogenic E. coli, and for multiplex detection of a broad range of proteins in human serum. This lecture will discuss the current state of development of AIR, including recently developed quantitative models for sensor response. These models allow direct correlation of reflective intensity and solution protein concentration, as a function of the dissociation constant of the capture molecule on the array.



7553-19, Session 5

LED-based spectral reflectance imaging biosensor for label-free high-throughput multi-analyte and single-pathogen detection

G. Daaboul, R. S. Vedula, A. Reddington, E. Ozkumur, C. Lopez, J. Connor, H. Fawcett, S. Ünlü, Boston Univ. (United States)

Field clinics lack a rapid and robust methodology for diagnosis of viral infections. The general consensus among doctors and researchers in infectious disease detection is that there is an immediate need for a tool that provides rapid and multiplexed detection. A new detection technique, Spectral Reflectance Imaging Biosensor (SRIB) has proven to be a powerful, high-throughput, label-free immunoassay platform for detecting biomolecular binding interactions on reflective, layered silicon substrates with a thick oxide top layer, eliminating the need for multi-step reagents and labeling processes used in ELISA and PCR systems. In its original form, SRIB uses a tunable laser and multiple intensity images on a CCD camera to acquire a cycle of periodic spectral reflectance signature to determine the profile of the surface in the entire field of view simultaneously with pm accuracy. A change in the surface profile indicates binding of target molecules to the specific probes spotted on the substrate. While external cavity diode lasers provide a compact and bright light source at a precise wavelength, they have limited tuning range requiring a thick oxide layer to capture a full period of spectral oscillation. To maintain the visibility of the spectral interference, a small collection is used necessitating a low lateral resolution. In case of detecting binding of analytes on probe molecules (ligands) in large spots, low lateral resolution is not a handicap. However, in case of whole virus detection, it is desirable to reduce the imaging spot to increase the effective interference signature of a single pathogen. In this paper, an inexpensive and compact LED-based SRIB is presented that uses LEDs with wavelengths in the visible range to illuminate the Si/SiO2 substrate and acquire the spectral reflectance data. The LED platform not only has the high-throughput capability of the laser based SRIB and but also allows for single pathogen detection through high magnification/resolution interferometric imaging. Initial data will be presented on the label-free detection of single Vesicular Stomatitis and flu viruses captured on the surface at clinically relevant detection limits (106 PFUs) with future work demonstrating multiplexed label-free detection capabilities. The longterm impact of these results is the future development of a commercial optical immunoassay technology that will address the need for highthroughput disease diagnostics and ultra-sensitive virus detection.

7553-20, Session 5

Hybrid nanoporous silicon optical biosensor architectures for biological sample analysis

L. A. DeLouise, Univ. of Rochester Medical Ctr. (United States); L. M. Bonanno, Univ. of Rochester (United States)

A major focus in advancing health care alternatives is on developing rapid point-of-care (POC) biosensors. Considerable effort has centered on developing label-free optical sensors exploiting the unique properties of nanomaterials including quantum dots, plasmonic metal nanoparticles and thin films. A major emphasis in developing state-of-the-art biosensor technology is on achieving unprecedented target detection sensitivity (subfemtomolar). However, what is practically required for POC applications is a low cost technology capable of detecting target at physiological relevant levels (nano to micromolar) in the complex milieu of a biological sample using convenient assay protocols. Over the past 10 years, research has shown that electrochemically synthesized nanoporous silicon (PSi) holds great promise as an emergent POC biosensor technology. PSi possesses many characteristics ideal for this application including its inexpensive fabrication, precise control of pore morphology (pore diameter and porosity), intrinsic filtering capability (molecular size selection), high surface area (>100 m2/gm), versatile surface chemistry, capacity for label-free colorimetric readout by eye, and compatibility with high throughput array and microfluidic technologies.

This talk will highlight recent advances in PSi device fabrication including the manipulation of operational protocols and the development of a promising new hybrid device architecture that employs target responsive hydrogels to control the target detection sensitivity range particularly for analysis of small molecules (<1000 MW) which typically pose unique challenges for optical transducers. Results from our recent efforts to conduct translational studies using PSi sensors to detect IgG levels in whole blood and to screen test clinical urine samples for drugs of abuse will also be presented.

7553-21, Session 6

Enhancement of diffraction-based biosensing using porous structures and electromagnetic surface states

J. E. Sipe, Univ. of Toronto (Canada); S. Weiss, Vanderbilt Univ. (United States); M. Liscidini, Univ. degli Studi di Pavia (Italy)

Diffraction-based biosensors are often based on the adsorption of a target material on a grating made of thin layers, where the adsorption is detected by a modification of the diffracted signal. In this communication we discuss two strategies for enhancing this detection process. The first is based on the use of grating structures made of porous elements, where sensing is based on target molecules penetrating into the elements and modifying their effective index of refraction. The second is a resonant process where the effectiveness of the grating is enhanced by the coupling to surface electromagnetic states, in particular Bloch surface waves that exist at the interface between a homogeneous medium and a photonic crystal.

7553-22, Session 6

Photonic molecules as ultrasensitive and tunable devices for mass and fluorescence spectroscopy

S. V. Boriskina, Boston Univ. (United States)

Optical and light-matter interaction in coupled optical microcavities (photonic molecules) give rise to amazingly rich physics and can be harnessed for a variety of practical applications, including chip scale integrated bio(chemical) sensing systems. I will show that coupled-cavity configurations provide additional degrees of freedom for detecting, capturing and manipulating biological nano-objects over isolated optical resonators. Sharp and asymmetric Fano resonance features in spectral characteristics of photonic molecules translate into a higher sensitivity to environment-induced resonant frequency shifts. Furthermore, photonic molecules can be designed to support collective multi-cavity resonances that provide better overlap of the modal field with the analyte accompanied by the dramatic increase of their quality factors. Performance improvement offered by the photonic molecule sensors for the detection of the changes in the ambient refractive index or presence of nano-particles over sensors based on individual microcavities with comparable Q-factors will be demonstrated. Finally, I will discuss the strategies for mechanical and optical tuning of photonic molecule spectra and for engineering tunable interaction of light forces generated by photonic molecules with small biological objects, which paves the way to the development of ultra-sensitive devices for mass, size and orientation spectroscopy.

[1]. S.V. Boriskina, "Photonic Molecules and Spectral Engineering," in Microresonator Research & Applications, to be published, Springer, 2009.



7553-23, Session 6

Sensitivity analysis of polymer-cladded porous silicon waveguide for small molecule detection

Y. Jiao, S. M. Weiss, Vanderbilt Univ. (United States)

Waveguides fabricated in porous materials have recently attracted much attention for biosensing applications. The large available surface area and strong field confinement in the porous waveguides significantly enhance the detection sensitivity of these sensors compared to planar waveguide and surface plasmon resonance sensors, especially for small molecule detection. In this work, we theoretically and experimentally demonstrate a polymer-cladded porous silicon membrane waveguide based on a 1.5 um thick porous silicon membrane coated on one side with a low loss polymer. The sensor operates in the Kretchmann configuration, which is amenable to microfluidics integration, with a high index cubic zirconia prism. Light incident in the prism couples into the porous silicon waveguide through the polymer cladding. Strong field confinement in the waveguide is achieved based on the large refractive index contrast between the high index porous silicon film and low index polymer. We show through experiments and complimentary calculations how the cladding thickness and porosity of the porous silicon film directly impact the small molecule detection sensitivity of the sensor. For example, a 60% porosity porous silicon membrane waveguide exhibits a detection sensitivity of 30 degrees/RIU for the detection of 0.8 nm silane molecules and nanomolar detection of DNA molecules while measurements performed using a 30% porosity waveguide reveal a more than two times increase in detection sensitivity. Calculations predict that careful tuning of the porous silicon membrane and polymer cladding parameters will lead to further improvement of the detection sensitivity.

7553-24, Session 6

Detection of biologicals with functional porous nanostructures

M. J. Sailor, Univ. of California, San Diego (United States)

Porous Si possesses several properties that make it advantageous for biosensor applications, including low toxicity,[1, 2] a high surface area[3] and tunable pore sizes and volumes.[3] Chemical modification[4] provides a means to adjust the specificity of the material towards many analytes of interest. Probably the most commonly employed porous Si-based sensors are those that involve the passive optical properties of porous Si, measured using various reflectance spectroscopies. Porous Si sensors based on optical reflectivity typically utilize spectral interference that occurs within a thin film or a multilayered porous Si structure. These sensors are essentially refractive index sensors, responding to the introduction of a chemical or biochemical species within the porous film that causes a net change in the refractive index of the entire matrix. [5-17] High sensitivity detection of both solvent vapors and biological compounds has been demonstrated using these methods. [14, 18-20]

The chemistry and electrochemistry of nanoporous silicon can be manipulated to allow the material to collect, concentrate, and detect chemical and biological material. The pore dimensions are controlled by the current used in the etch [21], allowing the construction of stratified "nanoreactors" in which enzyme compartmentalization [19], reagent delivery [22], protein separation [12], and reactant heating [23] can be performed. This presentation will discuss these various aspects of porous silicon and other porous nanostructures relevant to detection of pathogens in aqueous environments.

References

- [1] L. T. Canham, Adv. Mater. 1995, 7, 1033.
- [2] J. L. Coffer, M. A. Whitehead, D. K. Nagesha, P. Mukherjee, G. Akkaraju, M. Totolici, R. S. Saffie, L. T. Canham, Phys. Status Solidi A-Appl. Mat. 2005, 202, 1451.
- [3] X. G. Zhang, J. Electrochem. Soc. 2004, 151, C69.
- [4] J. M. Buriak, Chem. Rev. 2002, 102, 1272.

- [5] C. L. Curtis, V. V. Doan, G. M. Credo, M. J. Sailor, J. Electrochem. Soc. 1993, 140, 3492.
- [6] V. S.-Y. Lin, K. Motesharei, K. S. Dancil, M. J. Sailor, M. R. Ghadiri, Science 1997, 278, 840.
- [7] S. Chan, P. M. Fauchet, Y. Li, L. J. Rothberg, B. L. Miller, Phys. Status Solidi A-Appl. Res. 2000, 182, 541.
- [8] S. Zangooie, M. Schubert, C. Trimble, D. W. Thompson, J. A. Woollam, Appl. Optics 2001, 40, 906.
- [9] B. E. Collins, K.-P. Dancil, G. Abbi, M. J. Sailor, Adv. Funct. Mater. 2002, 12, 187.
- [10] L. A. DeLouise, B. L. Miller, C. Haidaris, J. Invest. Dermatol. 2004, 122, A136.
- [11] H. Ouyang, M. Christophersen, R. Viard, B. L. Miller, P. M. Fauchet, Adv. Funct. Mater. 2005, 15, 1851.
- [12] C. Pacholski, M. Sartor, M. J. Sailor, F. Cunin, G. M. Miskelly, J. Am. Chem. Soc. 2005, 127, 11636.
- [13] C. Pacholski, C. Yu, G. M. Miskelly, D. Godin, M. J. Sailor, J. Am. Chem. Soc. 2006, 128, 4250.
- [14] M. M. Orosco, C. Pacholski, G. M. Miskelly, M. J. Sailor, Adv. Mater. 2006, 18, 1393.
- [15] J. Salonen, J. Tuura, M. Bjorkqvist, V. P. Lehto, Sens. Actuator B-Chem. 2006, 114, 423.
- [16] K. A. Kilian, T. Bocking, L. M. H. Lai, S. Ilyas, K. Gaus, M. Gal, J. J. Gooding, Int. J. Nanotechnol. 2008, 5, 170.
- [17] M. M. Orosco, C. Pacholski, M. J. Sailor, Nature Nanotech. 2009, 4, 255.
- [18] M. J. Sailor, in Properties of Porous Silicon, Vol. 18 (Ed: L. Canham), Institution of Engineering and Technology, London 1997, 364.
- [19] J. C. Thomas, C. Pacholski, M. J. Sailor, Lab Chip 2006, 6, 782.
- [20] K. A. Kilian, T. Böcking, K. Gaus, M. Gal, J. J. Gooding, ACS Nano 2007, 1, 355.
- [21] V. Lehmann, R. Stengl, A. Luigart, Mater. Sci. Eng., B 2000, B69-70, 11.
- [22] J. R. Dorvee, A. M. Derfus, S. N. Bhatia, M. J. Sailor, Nature Mater. 2004, 3, 896.
- [23] J.-H. Park, A. M. Derfus, E. Segal, K. S. Vecchio, S. N. Bhatia, M. J. Sailor, J. Am. Chem. Soc. 2006, 128 7938.

7553-25, Poster Session

Suspended photonic crystal slabs for biosensing

M. El Beheiry, Univ. of Toronto (Canada); V. Liu, S. Fan, Stanford Univ. (United States); O. Levi, Univ. of Toronto (Canada) and Stanford Univ. (United States)

Photonic crystal (PC) slabs support in-plane guided resonances that easily couple to external radiation. The evanescent field tail normal to the slab can be used for index of refraction sensing, similar to surface plasmon resonance biosensors. Index of refraction changes due to analyte binding to PC slab surfaces subscribe to changes in the guided resonance frequency.

We propose a novel suspended PC slab-based biosensing approach. Our design consists of a high-index PC slab (SiNx) suspended in a microfluidic environment. Suspended PC slabs provide enhanced sensitivity compared to PC structures lying directly on a substrate due to index change overlap with the field on both the top and bottom PC slab surfaces. Our design consists of parameters (slab thickness, lattice constant, hole radius, and selection of even/odd guided modes) which allow accommodation of fabrication constraints and excitation sources.

It has been demonstrated that the quality factor (Q) for odd (TM-like) guided resonances in PC slabs can be significantly higher (>20x) than those of even (TE-like) resonances for the same structure, resulting in easier detection of resonance peak shifts during biosensing. We show





that Q values of the lowest frequency even (Q \sim 100-300) and odd guided resonances (Q>2000) are largely invariable between suspended PC slab and slab-on-substrate designs. In our slab-on-substrate design, similar sensitivities (\sim 240-270 nm/RIU) were calculated for both odd and even guided resonances. However, the potential enhancement in sensitivity for a suspended slab design can be nearly three-fold over the slab-on-substrate design. We have designed and are currently fabricating suspended PC slabs for increased biosensing sensitivity.

7553-26, Poster Session

New sensitive ammonia gas sensor based on the Fabry-Perot properties of the layer-bylayer assembly films

W. Lin, K. Xu, Tianjin Univ. (China)

In recent years, poly(acrylic acid) (PAA) films have attracted attention in the field of active materials for the ammonia sensing applications, because the carboxyl groups in PAA can be specific sites for ammonia molecule absorption. In this work, poly(vinyl pyrrolidone) (PVPON) and poly(acrylic acid) (PAA) have been alternately deposited onto a substrate by the Layer-by-Layer assembly technique to fabricate an ammonia gas sensor. The absorption spectrum of a PVPON/PAA multilayer film displays Fabry-Perot fringes through the UV, visible, and near-IR wavelength, which are generated by the light interference between the air-film and film-substrate interfaces. The ammonia sensitive responses were determined by the change of Fabry-Perot fringes when the PVPON/ PAA multilaver films are exposed to ammonia gas. The ionization of weak polyacids was characterized to evaluate the adsorption properties of ammonia on the PVPON/PAA multilayer films. An additional feature of this sensitive material is that as PVPON/PAA films are exposed to ammonia, the Fabry-Perot fringes give instant response, making the hydrogen bonded Layer-by-Layer PVPON/PAA film a suitable sensor material and a potential breath ammonia diagnostic method in Helicobacter pylori infection. The same rationale can be extended to assembly films with sensitive components which display Fabry-Perot fringes.



Monday-Wednesday 25-27 January 2010 • Part of Proceedings of SPIE Vol. 7554

Optical Coherence Tomography and Coherence Domain Optical Methods in Biomedicine XIV

7554-01, Session 1

Optical frequency domain imaging for studying the natural history of coronary atherosclerotic plaques

G. J. Tearney, Massachusetts General Hospital (United States); S. Waxman, Lahey Clinic (United States); M. J. Suter, M. Shishkov, B. J. Vakoc, Massachusetts General Hospital (United States); A. Maehara, C. Castellanos, Columbia Univ. Medical Ctr. (United States); M. I. Freilich, Lahey Clinic (United States); M. Rosenberg, Massachusetts General Hospital (United States); G. Weisz, J. W. Moses, M. B. Leon, Columbia Univ. Medical Ctr. (United States); B. E. Bouma, Massachusetts General Hospital (United States)

Even though coronary atherosclerosis is a leading cause of death in the US, relatively little is known about how coronary plaques progress over time to lead to acute coronary events and myocardial infarction. Many methods have been proposed to image these lesions over time to uncover this information, but only optical coherence tomography (OCT) has the resolution that is sufficient to identify the arterial microstructure relevant to the progression of coronary artery disease.

Initiated in 2007, we have conducted a multicenter clinical trial to utilize OFDI to study the natural history of coronary atherosclerotic lesions in vivo. Patients undergoing percutaneous coronary intervention (PCI) were imaged with OFDI at baseline and at 12-18 month follow-up. Images were acquired in all three main coronary arteries using non-occlusive saline/radiocontrast purges through a guide catheter. To date, a total of 20 patients have been imaged at baseline and 4 at follow-up. Good visualization the artery wall (> 5.0 cm pullback lengths) has been achieved in over 90% of cases. A diverse range of microscopic features were identified in two- and three-dimensions, including thin-capped fibroatheromas, calcium, macrophages, cholesterol crystals, bare stent struts, and stents with neointimal hyperplasia. Follow-up data has shown OCT neointimal coverage in bare and drug-coated stents, late stent thrombus formation, plaque progression, rupture, and regression.

Our results demonstrate that OFDI is a viable method for studying plaque progression. This information will be critical for improving our understanding of this disease and for guiding clinical management on a per-patient basis.

7554-02, Session 1

System design and image processing algorithms for frequency domain optical coherence tomography in the coronary arteries

D. C. Adler, C. Xu, C. L. Petersen, J. M. Schmitt, LightLab Imaging Inc. (United States)

We report on the design of a frequency domain optical coherence tomography (FD-OCT) system, fiber optic imaging catheter, and image processing algorithms for in vivo clinical use in the human coronary arteries. This technology represents the third generation of commercially-available OCT system developed at LightLab Imaging Inc. over the last ten years, enabling three-dimensional (3D) intravascular imaging at unprecedented speeds and resolutions for a commercial system. The FD-OCT engine is designed around a proprietary micro-cavity swept laser that was co-developed with AXSUN Technologies Ltd. The laser's unique combination of high sweep rates, broad tuning ranges, and narrow linewidth enable imaging at 50,000 axial lines/s with an axial resolution of < 16 μm in tissue at ranging depths up to 7.5 mm in air. The disposable

2.7 French (0.9 mm) imaging catheter provides a spot size of $<30~\mu m$ at a working distance of 2 mm. The catheter is rotated at 100 Hz and pulled back 50 mm at 20 mm/s to conduct a high-density spiral scan in 2.5 s. Image processing algorithms have been developed to address clinically relevant needs such as lumen area measurements, 3D visualization of deployed stents, and neointimal thickness estimates. This system has been used in over 200 procedures since August 2007 at over 10 clinical sites, providing clinical users with an advanced tool for 3D assessment of the coronary arteries.

7554-03, Session 1

Optical coherence tomography forward imaging catheter for real-time monitoring of cardiac radiofrequency ablation lesion formation

C. P. Fleming, H. Wang, Z. Hu, W. Kang, Case Western Reserve Univ. (United States); K. J. Quan, MetroHealth Medical Ctr. (United States); A. M. Rollins, Case Western Reserve Univ. (United States)

Radiofrequency ablation (RFA) is now the standard of care for treatment of many arrhythmias. However, there is no direct method to monitor RFA lesion formation in real-time. We hypothesized that Optical Coherence Tomography (OCT) can provide real time monitoring of RFA lesion formation.

RFA lesions are formed most efficiently when the ablation catheter is in contact with the tissue and is perpendicular to the tissue surface. A forward scanning OCT catheter was prototyped that provides contact, circular imaging with no metal, $30\mu m$ lateral resolution and 2mm scan diameter. Real-time ablative lesion formation was demonstrated in vitro, using ventricular wedges from a swine heart. The OCT forward imaging probe was bound to the RFA catheter. During the application of RF energy real-time imaging of ablation lesion formation was conducted at 10 frames per second, with 4000 A-scans per frame with a Fourier domain OCT system with an $11\mu m$ axial resolution and linear in wavenumber spectrometer.

During the application of RF energy, the mean intensity and backscattering increased nearly linearly with time. Samples were thereafter submerged in heparanized blood, where an image of the myocardium was obtained when the catheter was in direct contact with the tissue, displacing the blood.

We have demonstrated that OCT has great potential for real time monitoring of cardiac ablation lesion formation, and imaging in the presence of blood. A direct image by OCT has the potential to guide the precise application of energy and provide real-time formation of successful lesions.

7554-04, Session 1

Catheter motion tracking in intracoronary optical frequency division imaging

J. Ha, M. Shishkov, M. Colice, W. Y. Oh, L. Liu, G. Tearney, B. Bouma, Havard Medical School (United States)

A novel method for compensating motion artifacts due to cardiac motion is demonstrated with a heterodyne Doppler interferometer with the use of a modified angled ball lens for intracoronary optical frequency domain imaging (OFDI). To track the relative motion of a catheter with regard to the vessel, a motion tracking system is incorporated with a standard OFDI system by using wavelength division multiplexing



(WDM) techniques. Without affecting the imaging beam, dual WDM monochromatic beams are utilized for tracking the relative radial and longitudinal velocities of a catheter-based fiber probe. The velocity of the tracking beam is obtained from measurements of the Doppler shift. Our results demonstrate that tracking instantaneous velocity can be used to compensate for distortion in the images due to motion artifacts, thus leading to accurate reconstruction and volumetric measurements of endoscopic imaging.

7554-05, Session 1

Investigations of the intravascular backscattering distribution of light in optical coherence tomography

P. Cimalla, J. Walther, E. Koch, Technische Univ. Dresden (Germany)

The inhomogeneous backscattering distribution of low-coherent light in blood vessels, which appears as waisted double fan-shaped intensity pattern in optical coherence tomography, is investigated in an in vivo mouse model. A high resolution spectral domain imaging system operating in the 1.3 µm wavelength region is applied to obtain structural and functional Doppler tomograms of the murine saphenous artery and vein. Based on a predicted orientation of the red blood cells towards the laminar flow, an angular modulation of the corresponding backscattering cross-section inside the blood vessels is assumed. In combination with the signal attenuation in depth by absorption and scattering, a simple model of the intravascular intensity modulation along a circular path centered at the vessel midpoint is derived. In a first step, the suitability of the model is demonstrated by analyzing images of the saphenous artery during different states of the heart cycle which were recorded at an A-scan rate of 12 kHz and an exposure time of 79.4 µs. The obtained data and the predicted model show good correspondence to each other which leads to the conclusion that the orientation of the red blood cells seems to be the reason for the observed intensity distribution inside the blood vessels. Therefore, the analysis of the intravascular intensity pattern might be useful for the evaluation of flow characteristics. Additional investigations at different A-scan rates in the artery and the vein as well as in phantoms with well known flow characteristics have to be employed for further model refinement and validation.

7554-06, Session 1

Return to Contents

Scanning the cardiac functions of live drosophila with optical coherence tomography

M. Tsai, National Taiwan Univ. (Taiwan) and Chang Gung Univ. (Taiwan); C. Lee, T. Chi, J. Wu, L. Lin, C. Yang, National Taiwan Univ. (Taiwan)

Drosophila has emerged as a powerful model system for a number of human diseases such as diabetes and cancer. However, it is difficult to study cardiomyopathy in the post-developmental heart due to the inability to phenotype normal and abnormal cardiac function and the structure in the adult drosophila. Functional studies of the adult drosophila heart have been difficult, and in vivo cross-sectional imaging has been essentially impossible. For such a study, time-domain optical coherence tomography (OCT) has been used to provide real-time images of drosophila heart. However, with time-domain OCT, it is difficult to real-time observe the diastole and systole of the whole area of heart due to the limitation of imaging speed. In this paper, we use a swept-source OCT (SS-OCT) system to obtain the real-time B-mode and M-mode images of live drosophila heart. With the higher imaging speed of SS-OCT, successive B-mode images can be obtained and the diastole and systole of the whole area of the heart can be observed. Through gene manipulation, we can identify the different heart functions between normal and abnormal drosophilae. In addition to the structural information of heart chamber during heart beats, the flow velocity of

heart fluid in the heart chamber can be quantified by using the optical Doppler tomography technique. The results prove that the drosophila can be used as a good model to explore the role of novel human mutation in the development of dilated cardiomyopathy.

7554-07, Session 2

In vivo early detection of smoke-induced airway injury using 3D swept source optical coherence tomography

J. Yin, G. Liu, J. Zhang, L. Yu, S. Mahon, D. Mukai, Beckman Laser Institute and Medical Ctr. (United States); M. Brenner, Beckman Laser Institute and Medical Ctr. (United States) and Irvine Medical Ctr., Univ. of California, Irvine (United States); Z. Chen, Univ. of California, Irvine (United States) and Beckman Laser Institute and Medical Ctr. (United States)

We report the feasibility of rapid, high resolution, 3-dimensional swept source optical coherence tomography (3D SSOCT) to detect early airway injury changes following smoke inhalation exposure in a rabbit model. The SSOCT system obtained 3-D helical scanning using a microelectromechanical system (MEMS) motor based endoscope. Realtime 2-D data processing and image displaying at the speed of 20 frames per second was achieved by adopting the technique of shared-memory parallel computing. Longitudinal images were reconstructed via an image processing algorithm to remove motion artifacts caused by ventilation and pulse. We demonstrated the ability of the SSOCT system to detect increases in tracheal and bronchial airway thickness that occurs shortly after smoke exposure.

7554-08, Session 2

Multiscale imaging of human thyroid pathologies using integrated optical coherence tomography (OCT) and optical coherence microscopy (OCM)

C. Zhou, Massachusetts Institute of Technology (United States); Y. Wang, Beth Israel Deaconess Medical Ctr. (United States); A. D. Aguirre, T. Tsai, Massachusetts Institute of Technology (United States); D. W. Cohen, J. L. Connolly, Beth Israel Deaconess Medical Ctr. (United States); J. G. Fujimoto, Massachusetts Institute of Technology (United States)

We evaluate the feasibility of optical coherence tomography (OCT) and optical coherence microscopy (OCM) for imaging of benign and malignant thyroid lesions ex vivo using intrinsic optical contrast. Thirty four thyroid gland specimens were imaged from 17 patients, covering a spectrum of pathology, ranging from normal thyroid to neoplasma and benign disease.

The integrated OCT and OCM imaging system allows seamlessly switching between low and high magnifications, in a way similar to traditional microscopy. Good correspondence was observed between optical images and histological sections. The results provide a basis for interpretation of future OCT and OCM images of the thyroid tissues and suggest the possibility of future in vivo evaluation of thyroid pathology.

97

TEL: +1 360 676 3290 · +1 888 504 8171 · customerservice@spie.org



7554-09, Session 2

Three-dimensional swine esophageal imaging in vivo using spectral-domain optical coherence tomography

W. Kang, H. Wang, Case Western Reserve Univ. (United States); Y. Pan, Thorlabs, Inc. (United States); M. W. Jenkins, Case Western Reserve Univ. (United States); G. Isenberg, A. Chak, D. Agrawal, Case Western Reserve Univ. (United States) and Univ. Hospital Case Medical Ctr. (United States); Z. Hu, A. Rollins, Case Western Reserve Univ. (United States)

Optical coherence tomography (OCT) obtains micron-scale, crosssectional structural images to depths exceeding 1mm in the human esophagus. The first generation of Endoscopic OCT systems scanned slowly due to the time-domain OCT configuration and was designed for spot examination of focal lesion. We present a high-speed spectraldomain endoscopic OCT system which utilizes a linear-k spectrometer and can visualize long segment of esophageal wall. The system permits imaging at 47k A-lines/s. The effective imaging range is 4.2 mm, which is needed to image esophageal lumens with various diameters and avoid complex conjugate artifact. The plastic sheath used to enclose the fiber probe, torsion cable and to support the balloon works like a concave cylindrical lens that introduces significant astigmatism. By using a GRIN lens and a cylinder rod lens, we corrected the astigmatism which results in resulted in a round focal spot with a FWHM diameter of 30 µm and a focal length of 9.5 mm. A urethane low durometer balloon with a diameter of 18 mm and length of 25 mm is bound to the distal end of the catheter, which enters the fiber probe in the esophageal lumen. A fiber rotary joint rotates the catheter probe at 9.5 revolution/s and a handheld pullback device pulls the probe at 800 µm/s, which allows the beam scans helically on the esophageal wall. We were able to obtain comprehensive swine esophageal images in vivo. 3D reconstruction of a 25mm long section of swine esophagus will be shown.

7554-10, Session 2

Optical frequency domain imaging of the biliary tree: a pilot clinical study

M. J. Suter, W. Warger, M. Shishkov, P. S. Yachimski, D. Forcinone, W. Brugge, B. E. Bouma, G. J. Tearney, Harvard Medical School and Wellman Ctr. for Photomedicine (United States)

Current methods for the assessment and diagnosis of biliary stricture malignancies involve an endoscopic retrograde cholangiopancreatography (ERCP) imaging procedure together with tissue sampling via forceps biopsy or brush cytology. Unfortunately, the diagnostic yields of these tests are low, are difficult to obtain, and may be associated with a high risk of complications. The goal of this research is to comprehensively image the entire biliary duct of patients using optical frequency domain imaging (OFDI) to diagnose malignant strictures and cholangiocarcinoma. We have designed and developed a custom 1.67 mm OFDI catheter to image the billiary duct. The catheter was designed for use through the accessory channel of a standard duodenoscope during an ERCP procedure. The distal optics were based on a ball lens design and provided a 30 μm spot size at a focal distance of 2 mm. The catheter's optical core was encased in a single use sheath with a distal guide wire provision to facilitate placement in patients with narrow strictures. The OFDI imaging system acquired spiral cross-sectional images at a rate of 20 frames per second (frame size: 2048 x 2048). To date we have successfully imaged the biliary duct of 5 patients in segments up to 10 cm in length without complication. Features including the epithelium, lamina propria, dense connective tissue layer, glands and vasculature were visualized. In addition, regions of adenocarcinoma were identified on the OFDI images. We anticipate that OFDI imaging of the biliary tree will provide useful diagnostic information to complement current ERCP procedures including the diagnosis of biliary stricture

malignancies and cholangiocarcinoma. OFDI imaging may additionally prove beneficial in determining tumor-free margins in the surgical resection of biliary duct malignancies.

7554-11, Session 2

Differentiating different carcinogenesis stages of oral lesions with optical coherence tomography

M. Tsai, Chang Gung Univ. (Taiwan); C. Lee, T. Chi, K. Yang, H. Chen, C. Chiang, Y. Wang, C. Yang, National Taiwan Univ. (Taiwan)

A swept-source optical coherence tomography (SS-OCT) system is used to clinically scan oral lesions in different oral carcinogenesis stages, including normal control, mild dysplasia (MiD), moderate dysplasia (MoD), early-stage squamous cell carcinoma (ES-SCC), and well-developed SCC (WD-SCC), for diagnosis purpose. Based on the analyses of the SS-OCT images, the stages of dysplasia (MiD and MoD) and SCC (ES-SCC and WD-SCC) can be differentiated from normal control by evaluating the depth-dependent standard deviation (SD) values of lateral variations. Due to the higher density of connective tissue papillae in the ES-SCC stage, the SD values of the slowly-varying lateral scan profiles in the ES-SCC samples are significantly larger than those in the WD-SCC sample. Also, ES-SCC can be differentiated from WD-SCC by comparing the exponential decay constants of averaged A-mode scan profiles.

7554-12, Session 2

Resonant fiber scanning endoscope for highspeed three-dimensional and en face OCT imaging

L. Huo, J. Xi, Y. Wu, X. Li, The Johns Hopkins Univ. (United States)

A miniaturized endoscope based on a resonant fiber scanner was developed for high-speed three-dimensional and en face optical coherence tomography (OCT) imaging. The resonant frequency of conventional resonant fiber scanner was slowed down to 62.5 Hz by using 20-mm fiber cantilever and extra weight on the fiber cantilever tip. The overall size of the endoscope was 2.4 mm in diameter including the housing tube. When interfaced with a 40-kHz FDML swept source OCT, axial-priority scanning sequence was performed and three-dimensional volumetric data could be collected in a single en face scan.

7554-13, Session 3

Adaptive optics spectral domain optical coherence tomography with one-micrometer light source

K. Kurokawa, K. Sasaki, S. Makita, Y. Yasuno, Univ. of Tsukuba (Japan)

Adaptive optics (AO) retinal imaging provide high lateral resolution retinal images by correcting dynamic ocular aberration. Adaptive optics spectral domain optical coherence tomography (AO SD-OCT) with one-micrometer broadband light source ($c=1027\,$ nm, $\Delta=106\,$ nm, Superlum) was developed for the in vivo investigation of cellular level anatomical alterations caused by cone-rod dystrophy and optic nerve neuropathies from glaucoma, which is expected to provide high isotropic resolution retinal images with high penetration depth. In our system, theoretical axial resolution was 3.4 micrometer in tissue, and the ocular aberration was corrected by a single deformable mirror (Mirao52, Imagine Eyes). A left eye of normal subject was examined, and the results showed OCT signal gain with the AO correction. Lateral



resolution was not significantly improved compared to AO scanning laser ophthalmoscope.

The residual RMS wavefront error was reduced to be 0.07 micrometer, which is corresponding with the lateral resolution of 3.5 micrometer on the retina.

The incident beam was focused on the nerve fiber layer and photoreceptors by adding the additional defocus. Each nerve fiber bundle and hyper scattering spots of photoreceptors were visualized. Owing to the high penetration of one-micrometer lights, a strong signal was observed at the choroid even though the probing beam was focused on the nerve fiber layer.

7554-14, Session 3

Real-time intraoperative spectral domain optical coherence tomography for vitreoretinal surgery

Y. K. Tao, C. A. Toth, J. A. Izatt, Duke Univ. (United States)

Vitreoretinal surgery visualization is inherently limited by the ability to distinguish between tissues with subtle contrast, and to judge the location of an object relative to other retinal substructures. Inherent issues in visualizing thin translucent tissues, in contrast to underlying semitransparent ones, require the use of stains such as indocyanine green, which is toxic to retinal tissue. Spectral domain optical coherence tomography (SDOCT) has demonstrated strong clinical success in retinal imaging, enabling high-resolution, motion-artifact-free cross-sectional imaging and rapid accumulation of volumetric macular datasets. Current generation SDOCT systems achieve <5 µm axial resolutions in tissue, and have been used to obtain high resolution datasets from patients with various retinopathies. While OCT imaging has been considered for various intrasurgical applications, it is uniquely suited for vitreoretinal surgery where multiple layers of the retinal structure are readily accessible, and where high resolution cross-sectional viewing would immediately change the steps of surgery as they are performed today. Real-time cross-sectional OCT imaging would also provide critical information relevant to the location and deformation of structures that may shift during surgery. Here, we demonstrate opto-mechanical designs for an intraoperative microscope-mounted OCT system (MMOCT) and preliminary in vivo human retinal imaging in a test subject. By adapting a Leica Binocular Indirect Opthalmo-Microscope with SDOCT scanning and relay optics, we have demonstrated real-time cross-sectional imaging of multiple layers of the retinal structure, allowing for SDOCT augmented intrasurgical microscopy for intraocular visualization.

7554-15, Session 3

Simultaneous visualization of retinal structure and function in vivo in healthy and diseased rat retina with a combined UHROCT and ERG system

A. Akhlagh Moayed, S. Hariri, Univ. of Waterloo (Canada); T. W. Kraft, The Univ. of Alabama at Birmingham (United States); B. Doran, Diagnosys, LLC (United States); S. Boyd, St. Michael's Hospital (Canada) and Univ. of Toronto (Canada); K. Bizheva, Univ. of Waterloo (Canada)

A combined Ultra High Resolution Optical Coherence Tomography (UHROCT) and Electroretinography (ERG) system was designed to probe in-vivo and simultaneously, the structure and functional response to light stimulation of normal and damaged rodent retina. The UHROCT system operates in the 1060 nm wavelength region and provides 3 µm axial resolution leading to better visualisation of retinal and choroidal features than can shorter wavelength systems. The ERG system is used to determine the electrochemical activity of the retina resulting from light stimulation. An animal model was used to simulate photoreceptor

degeneration characteristic to retinal degenerative diseases such as retinitis pigmentosa or age-related macular degeneration. Data collected with the combined ERG and UHROCT system in normal and damaged rat retina shows correlation between retinal structure and function for different stages of the photoreceptor degeneration.

7554-16, Session 3

Choroidal neovascularization imaging in a laser-induced mouse model using phase contrast swept-source optical coherence tomography at 1050 nm

R. S. Motaghiannezam, D. Koos, California Institute of Technology (United States); S. He, D. R. Hinton, Keck School of Medicine, The Univ. of Southern California (United States); S. E. Fraser, California Institute of Technology (United States)

We report preliminary results of phase contrast imaging with a highspeed swept source optical coherence tomography (SS-OCT) system in a mouse laser-induced model of choroidal neovascularization (CNV). We developed a 1050 nm swept laser source with ~90 nm tuning range and 0.1 nm instantaneous line width at 50 kHz. To generate a 2D phase contrast image of a mouse retina, five B-scans of a single slice through retina were acquired in 25 ms at 50 kHz A-line rate. The statistical variance of the phase differences between two successive B-scans at each depth was calculated in order to construct an image over a 2 mm transverse scan range. Three dimensional phase sensitive OCT data sets were collected by acquiring several neighboring B-scans over a 2mm x 2mm field of view (FOV). We show that phase contrast OCT is able to visualize retinal and choroidal microvasculature as well as the flat vessel beds perpendicular to illumination beam. For studying CNV mouse model using phase contrast SS-OCT, one diode laser photocoagulation (75- m spot size, 0.1-second duration, 140 mW) burns were delivered to the retina lateral to the optic discs of both eyes of an adult C57BL/6J mouse. By performing phase contrast SS-OCT 10 after laser surgery, we were able to visualize 3D volume of CNV lesion as well as leaking fluid in the mouse model. This method highlights its potential application to visualize growth of new abnormal vessels and leaking fluids in CNV lesion.

7554-17, Session 3

In vitro retinal imaging with full field swept source optical coherence tomography

J. R. Fergusson, B. Povazay, B. Hofer, W. Drexler, Cardiff Univ. (United Kingdom)

The retina of a tree shrew has been imaged in vitro with full field swept source optical coherence tomography, visualising multiple intraretinal layers. Combining a frequency stepped SLD light source centred at 850nm with a 50.8nm bandwidth with custom written software and image speckle reduction, we have achieved ~8µm of axial resolution and 4µm of transversal resolution with a measured signal to noise ratio of 75dB. Volumetric tomograms of retinal tissue with dimensions of 1248x936x678µm3 (horizontal x vertical x axial) were recorded in two seconds (equivalent of 153,600 A-scans per second). Various intraretinal layers can be distinguished in the tomograms including the Ganglion cell layer, Inner/outer photoreceptor junction and the top of the choroid as well as the retinal pigment epithelium and nerve fibre layers. En face images show nerve fibre bundles and choroidal layer structure. From the 5mW of SLD optical power available, 720µW illuminates the sample, giving a power per pixel of 4.6nW - ten times less then that used in standard FDOCT systems. Additionally, due to the diffuse nature of the illumination beam, the safe limit for the optical power that can be applied to an in vivo eye is higher than that for the focussed beams used in FDOCT, potentially allowing access to higher SNR levels.

TEL: +1 360 676 3290 · +1 888 504 8171 · customerservice@spie.org



7554-18, Session 3

Variable lateral size imaging of the human retina in vivo by combined confocal/en face optical coherence tomography with closed loop OPD-locked low coherence interferometry based active axial eye motion tracking

R. G. Cucu, Univ. of Kent (United Kingdom); M. Hathaway, OTI/ Opko Instrumentation (Canada); A. Podoleanu, Univ. of Kent (United Kingdom); R. Rosen, New York Eye and Ear Infirmary (United States)

We have reported an active tracking device based on white light coherence ranging using a spectrally interrogated Michelson interferometer, which was used to monitor and correct for the axial displacement of the eye and head of the subject in a confocal scanning ophthalmoscope/ en face OCT system (SLO/OCT) by tracking the axial position of the eye fundus. Both the tracking and imaging interferometers share the eye interface optics and the sample and also an optical path (OPD) changing device in the reference (fast voice coil mounted retroreflector), that keeps them locked at constant OPD values. As a consequence, the sensitivity of the tracking interferometer is not affected by the spectrometer sensitivity roll-off with increased OPD and mirror term ambiguity tracking errors close to OPD = 0 are eliminated. Moreover, the axial tracking range is only limited by the voice coil stage travel range and the tracking system has an update time better than 5 ms. We investigate the potential of the new configuration for acquiring volumetric data free of axial eye motion artifacts. Sets of SLO and en face OCT images at progressive depths in the retina are simultaneously acquired for two lateral sizes, 25 deg x 25 deg and 2.5 deg x 2.5 deg, revealing interesting details of the retinal morphology.

7554-19, Session 3

Ultrahigh-speed full range complex spectral domain optical coherence tomography for volumetric imaging at 140,000 A scans per second

H. Subhash, L. An, R. Wang, Oregon Health & Science Univ. (United States)

We demonstrate an ultra-high speed full rang spectral domain optical coherence tomography system based on CMOS camera at 140,000 A-scans per second. By implementing beam-offset method, a constant modulation frequency is introduced into each B-scan that enables the reconstruction of the full range complex SDOCT images from in vivo biological specimens. To make use of the full acquisition capacity of detection camera used in the system, we developed system control software that streams the raw spectral fringe data directly into the computer memory. The feasibly of our high speed full range SDOCT system is demonstrated for imaging the dynamics of anterior segment of human eye in vivo.

7554-20, Session 3

Keratometric optical coherence tomography using fast distributed scan patterns

R. P. McNabb, Duke Univ. (United States); A. Kuo, Duke Univ. Eye Ctr. (United States); M. Zhao, J. A. Izatt, Duke Univ. (United States)

Accurate quantitative imaging of the cornea is critical for predictable outcomes in corneal based surgical interventions. While long the

standard, reflection based corneal topography to assess corneal curvature and refractive power is insufficient in an era when surgical manipulation of the corneal shape is routine and undermines the basis of reflection topography. Laser refractive surgery is one particular corneal intervention that has revealed current inadequacies in measuring the cornea. Over 7 million people in the United States have had some form of laser refractive surgery to reduce their dependence on corrective eye wear. The corneal reshaping that occurs from laser refractive surgery results in excellent visual results for the patient, but renders current technologies incapable of accurately measuring the power of the reshaped cornea. Accurate measurement of corneal power is critical in applications such as the prediction of intraocular lens power needed after cataract surgery, an event which this group of patients will invariably encounter as they age into late adulthood. We present a novel concept for motion corrected high-speed keratometric spectral domain optical coherence tomography (SDOCT) based on a high-speed distributed scan approach in which patient motion up to ~100Hz is encoded into high spatial frequency image content which is then eliminated via low-pass spatial filtering. In order to achieve the <1ms large-angle beam steering required for this approach, we introduce a novel non-inertial 2D acoustooptic SDOCT scanner which includes a diffractive optical element for negative chromatic dispersion compensation.

7554-21, Session 4

Shear stress in the developing heart tube

M. W. Jenkins, M. Gargesha, L. M. Peterson, S. Gu, B. M. Webb, Case Western Reserve Univ. (United States); K. K. Linask, Univ. of South Florida (United States); M. Watanabe, D. L. Wilson, A. M. Rollins, Case Western Reserve Univ. (United States)

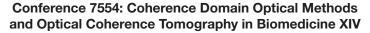
Here, we present the first shear stress measurements in the embryonic avian heart using OCT. Image-based gated imaging enabled us to collect a 4-D Doppler data set. The Doppler data was unwrapped using a Goldstein algorithm and corrected for angle of incidence. The unwrapping allowed us to make measurements (pulsed Doppler and shear stress) at several locations within the heart tube simultaneously to assess regions of interest. Orthogonal planes to the flow were selected at critical locations along the heart tube and an automated shear stress algorithm allowed us to calculate the shear stress on the endocardium at the selected orthogonal planes. A maximum forward velocity of 24.3 mm/s occurred in the outflow portion of the heart tube, while the maximum shear stress of 10 Pa was produced by regurgitant blood flow (max velocity = 34.7 mm/s). The maximum shear stress region coincides with the cardiac cushions, which is where heart valves will eventually form. A technique to map shear stresses on the endocardium in 3-D would allow investigations into the role of shear in gene regulation and how abnormal blood flow may lead to congenital heart defects.

7554-22, Session 4

Mutant and wild type cell chemotaxis in 3D and 4D with ultrahigh-resolution optical coherence tomography

S. M. Rey, B. Povazay, B. Hofer, A. Unterhuber, A. Harwood, W. Drexler, Cardiff Univ. (United Kingdom)

Conventionally, cell chemotaxis is studied on two-dimensional (2D) transparent surfaces due to limitations in optical and image data-collection techniques. However, substrates which more closely mimic the natural environment of cells are often opaque or three-dimensional (3D). The non-invasive label-free imaging technique of frequency domain optical coherence tomography (OCT) has high axial and transverse resolution of $>\!\!4\mu m$, comparatively high penetration depth and the ability to acquire full volumes in a few seconds, therefore offering the potential to visualize moving cells in 3D (2D+time) and 4D (3D+time). Cell migration is demonstrated in 3D on opaque surfaces, and in 4D within an agarose gel.





3D images of 256x256x2048 voxels showed that the speed and directionality of wild type (Ax2) cell movement is comparable on agar and nitrocellulose filter substrates. This compared well with previous data from Ax2 cells, although cell movement was slower, probably because these surfaces are rougher than glass. 4D images were acquired with 800x800x2048 voxels. Differences can be clearly seen in the character of 4D cell movement between Ax2 and myosin knockout (mhcA-) ~10µm Dictyostelium discoideum cells within 0.5% agarose gel, using frequency domain ultrahigh resolution OCT with 800nm central wavelength. The Ax2 cells develop normally and move up to and stream along the surface, while the mhcA- are unable to move within the agarose. OCT is therefore shown to be a useful technique for the study of cell migration.

7554-23, Session 4

Structural and functional imaging of live rat embryos with OCT

K. V. Larin, Univ. of Houston (United States); I. Larina, Baylor College of Medicine (United States); R. Behringer, The Univ. of Texas M.D. Anderson Cancer Ctr. (United States)

The rat has long been considered an excellent system to study mammalian embryonic cardiovascular physiology, but has lacked the extensive genetic tools available in the mouse to be able to create single gene mutations. However, the recent establishment of rat embryonic stem cell lines facilitates the generation of new models in the rat embryo to link changes in physiology with altered gene function to define the underlying mechanisms behind congenital cardiovascular birth defects. Along with the ability to create new rat genotypes there is a strong need for tools to analyze phenotypes with high spatial and temporal resolution. OCT has been previously used for 3-dimensional structural analysis and blood flow imaging in other model species. In this work, Swept Source OCT was used for live imaging of early post-implantation rat embryos. Structural imaging was used for 3D reconstruction of embryo morphology and dynamic imaging of the beating heart and vessels. This work demonstrates that Swept Source OCT can provide essential information about dynamics of early rat embryos and serve as a basis for a wide range of studies on functional evaluation of rat embryo physiology.

7554-24, Session 4

A heterodyne Mach-Zehnder interferometer employing dynamic phase demodulation technique to investigate live-cell dynamics

S. Joseph, Stokes Research Institute (Ireland); J. Gineste, European Commission Joint Research Ctr (Italy); M. Whelan, European Commission Joint Research Ctr. (Italy); D. Newport, Stokes Research Institute (Ireland)

In the present study a demodulation technique is reported which can be employed to extract dynamic phase information. A Mach-Zehnder heterodyne interferometer, integrated to a microscope is used for visualizing and capturing live-cell changes. Two frequency locked acousto-optical devices were used to obtain two laser beams with an optical frequency difference of 238 Hz. When temporal phase shifting technique is used for measuring dynamic phase changes, the continuous wave (CW) signal reaching the detector is a like phase modulated (PM) signal. To extract the dynamic phase, at first the instantaneous frequency of the phase modulation is determined, which is then integrated with respect to time to obtain time-varying phase. The instantaneous frequency of the PM modulated signal can be obtained by taking a ratio between the time derivative of its analytic signal and the complex signal itself. The algorithm is used to extract a time varying phase, caused by a stimulated vibration at 30 Hz and 200 nm amplitude. CCD camera with an acquisition rate of 1000 Hz is used to acquire the data. Higher frequency phase changes could also be evaluated using this method, but the acquisition rate should be higher than the Nyquist frequency of the phase change. For live cell imaging, a 3T3 Fibroblast cell is used as the

sample. Heterodyne phase extraction method is used to obtain the phase image of the cell. The reported demodulation technique and set-up could be used for extracting functional states of cells.

7554-25, Session 4

Visualization of damage in mouse models of muscular dystrophy by three-dimensional optical coherence tomography

B. R. Klyen, D. Gerstmann, T. Shavlakadze, H. G. Radley, M. D. Grounds, D. D. Sampson, The Univ. of Western Australia (Australia)

Biological tissue from animal models is routinely assessed in pre-clinical experiments of therapies for muscular dystrophy. This paper reports the application of three-dimensional optical coherence tomography (3D-OCT) for the imaging of mouse skeletal muscle tissue from exerciseinduced damage models of inflammation and dystropathology in human Duchenne muscular dystrophy. 3D-OCT scans of ex vivo samples of the hindlimb muscles from the mdx mouse were acquired with a timedomain OCT system with center wavelength of 1320nm and resolution of ~11µm in the axial and lateral dimensions. Samples underwent subsequent histological preparation, and custom visualization software was used to match the optical 2D OCT images with the H&E-stained sections. Commercial software was also used to perform segmentation and visualize 3D images of the muscle structure and pathology. We present 2D and 3D images of skeletal muscle tissue showing fibers and connective tissue, and regions of dystropathology. Muscle fibers and dystrophic lesions, containing inflammation and necrosis, were visible in 2D OCT images and validated in the corresponding H&E-histology. Volumes of damage could be segmented from the surrounding intact tissue based on intensity-level mapping methods and visualized in 3D images. These results show the ability of OCT to image the structure of skeletal muscle tissue and identify pathology in 3D volumes, and demonstrate its suitability as a modality for small-animal imaging studies of human muscular dystrophy.

7554-26, Session 4

Spectral characterization of individual biological cells and microparticles via spectroscopic optical coherence tomography

J. Yi, X. Li, Northwestern Univ. (United States)

Empowered by spatially resolved spectra, spectroscopic optical coherence tomography (SOCT) has drawn significant research attention. The recent development of high resolution SOCT system intrigues great interest on the investigations of micro-scale structures, spectrally modified by exdogeneous or endogenous contrast agents. In this paper, we demonstrate the feasibility of recovering visible light range spectral features from individual micro-scale structures. SOCT measurements have been conducted in two phantom experiments containing red blood cells and fluorescent microspheres, respectively. Spectra at 500-630nm from individual red blood cells were reconstructed and fitted with our analytical model to spectrally estimate oxygen saturation based on the absorption feature of hemoglobin. We further calibrate our estimation with that from diffuse reflectance spectroscopy. Our microparticle phantom is composed of 6 micron fluorescent spheres and 3 micron polystyrene spheres in 1% intralipid solution. We analyzed the spectra from fluorophore-containing microspheres and associated the spectra to the chemical-dependent absorption spectrum. In that means we developed an algorithm to discriminate the fluorescent microspheres from non-absorbing ones in 3D volume, based on the distinguished absorbing feature. The effectiveness of the algorithm was confirmed by en face fluorescence image.



7554-27, Session 4

In vivo optical coherence tomography of percutaneous implants in hairless mice

S. Donner, Laser Zentrum Hannover e.V. (Germany); F. Witte, I. Bartsch, CrossBIT (Germany); F. Petraglia, Univ. of Pittsburgh (United States); O. Massow, M. Heidrich, H. Lubatschowski, A. Heisterkamp, A. Krueger, Laser Zentrum Hannover e.V. (Germany)

Optical Coherence Tomography (OCT) was applied to visualize and enable quantification of the local skin anatomy around percutaneous implants in an animal model using hairless mice. In order to investigate their biocompatibility titanium devices with different coatings were implanted into a percutaneous location at the side caudal the costal arch of the mice. OCT is a contact less non destructive imaging technique having a µm resolution allowing the analysis of the on going process of marsupialisation. In vivo three dimensional OCT scans of the tissue around the implant were taken on the seventh and 21st day after the implantation and ex vivo in situ after inflammation of the skin around the implant occurred. Additionally B-Scans at different angular positions all crossing each other at the middle of the implant were taken. These scans enabled investigation of the implant-tissue interface at different locations at the interface during the postoperative phase. Compared to a reslice of the 3D stack a decrease of artifacts caused by axial sample movement within one B-Scan could be achieved by this scanning scheme. Automatic image segmentation was performed and a depth correction according to the refractive index of tissue was done. The thickness of the tissue above the implant, epithelia thickness and epithelia downgrowth were measured. Qualitatively the OCT B-Scans were in a good agreement with the histological sections and therefore can be regarded as a non destructive in vivo alternative.

7554-28, Session 4

Characterizing matrix remodeling in collagen gels using optical coherence tomography

D. Levitz, M. T. Hinds, S. R. Hanson, S. L. Jacques, Oregon Health & Science Univ. (United States)

Optical coherence tomography (OCT) has shown promise at nondestructively characterizing engineered tissues such as collagen gels. However, as the collagen gels develop, the OCT images lose contrast of structures as the gels develop, making visual assessment difficult. Our group proposed quantitatively characterizing these gels by fitting the optical properties from the OCT signals. In this paper, we imaged collagen gels seeded with smooth muscle cells (SMCs) over a 5-day period and used the data to measure their optical properties. Our results showed that over time, the reflectivity of the samples increased 30fold, corresponding to a decrease in anisotropy factor g, without much change in the scattering coefficient mu_s. Overall, the optical properties appeared to be dominated by scattering from the collagen matrix, not the cells. However, SMCs remodeled the collagen matrix, and this collagen remodeling by the cells is what causes the observed changes in optical properties. Moreover, the data showed that the optical properties were sensitive to the activity of matrix metalloproteinases (MMPs), enzymes that break down local collagen fibrils into smaller fragments. Blocking MMPs in the SMC gels greatly impeded both the remodeling process and change in optical properties at 5 d. Treating 1 d old acellular with MMP-8 for 3 hr managed to partially reproduce the remodeling observed in SMC gels at 5 d. Altogether, we conclude that matrix remodeling in general, and MMPs specifically, greatly affect the local optical properties of the sample, and OCT is a unique tool that can assess MMP activity in collagen gels both non-destructively and label free.

7554-85, Poster Session

In vivo 3D FD OCT of subpleural lung parenchyma in the intact thorax

S. Meissner, C. Schnabel, L. Knels, E. Koch, Technische Univ. Dresden (Germany)

In vivo determination of three-dimensional and dynamic geometries of alveolar structures with adequate resolution is essential to help developing numerical models of the lung. A thorax window was prepared in anesthetized rabbits by removal of muscle tissue between 3rd and 4th rib without harming the parietal pleura. The transparent parietal pleura allows contact-free imaging by intra-vital microscopy (IVM) and 3D optical coherence tomography (3D-OCT). We have demonstrated that it is possible to acquire the identical region in the inspiratory and expiratory phase, and that OCT in this animal model is suitable for generating 3D geometry of in vivo lung parenchyma. The 3D data sets of the fine structure of the lung beneath the pleura could provide a basis for the development of three-dimensional numerical models of the lung.

7554-86, Poster Session

Optical Doppler tomography and spectral Doppler imaging of localized ischemic stroke in a mouse model

L. Yu, Univ. of California, Irvine (United States)

We present a combined optical Doppler tomography and spectral Doppler imaging modality to quantitatively evaluate the dynamic blood circulation and artery blockage characteristics before and after a localized ischemic stroke in a mouse model. Spectral Doppler imaging (SDI) provides the temporal blood flow information, which is complementary to the spatially distributed flow information of optical Doppler tomography (ODT). Fast ODT scans across a vessel of interest were performed in order to record flow dynamic information with a high temporal resolution of the cardiac cycles. Spectral Doppler analysis of continuous Doppler images demonstrates how the velocity components and longitudinally projected flow-volume-rate change over time for scatters within the imaging volume using spectral Doppler waveforms. Vascular conditions can be further quantified with various Doppler-angle-independent flow indices. Non-invasive in-vivo mice experiments were performed to verify the proposed imaging modality.

7554-87, Poster Session

Monitoring of sutured flexor tendons using Fourier domain optical coherence tomography

C. M. B. Tay, Nanyang Technological Univ. (Singapore); M. He, W. A. Gan, National Univ. Hospital (Singapore); T. Chow, B. Ng, Nanyang Technological Univ. (Singapore); K. A. Chong, National Univ. Hospital (Singapore); S. Gulam Razul, Nanyang Technological Univ. (Singapore)

Flexor tendons, found in the hand connecting muscle to bone, govern digital motion as well as share load in joints. Torn or injured tendons, which can cause a significant loss of motion and pain, are often repaired with surgical sutures. The material behaviour of tendons is important in healing models as mechanical trauma to the tendon during surgery and subsequent collagen growth abnormalities during the healing process compromises the mechanical strength of the tendon. Furthermore digital motion may become limited due to the formation of fibrous growths at the suture site. The objective of this work is to investigate the use of Fourier domain optical coherence tomography (FD-OCT) as a depth resolved, non-destructive optical imaging technique for the monitoring of injured flexor tendons and its behaviour under load. Flexor tendons from



New Zealand white rabbits were severed and then sutured back together. OCT images of normal and sutured tendons were taken under different loading conditions for comparison. The tendons were subjected to loads varying from 0 g to 500 g, in steps of 50 g. Average crimp periods in normal tendons were observed to increase as the load increases, but the crimp periods in sutured tendons were constrained at the suture site and features like differential loading and crimp compression were observed. This imaging technique will eventually be used to monitor tendon healing at the suture site.

CP-OCT, our proposed PS-OCT could provide depth-resolved images, which reflect tissue birefringence. One of the problems that still limit PS-OCT applications in clinics is that it is somewhat cumbersome to use the fiber-based system. Multiple input polarizations have to be supplied to the system to determine the polarization state of the light reflected from the tissue, which can be problematic since longer data acquisition times are needed. Solving these problems will increase the utility of PS-OCT in clinical diagnosis and this can be considered in further studies.

7554-88, Poster Session

Preliminary optical coherence tomography investigation of the temporo-mandibular joint disc

C. Marcauteanu, E. T. Demjan, C. G. H. Sinescu, M. Negrutiu, A. Motoc, R. Lighezan, C. Clonda, Univ. de Medicina si Farmacie Victor Babes, Timisoara (Romania); M. R. Hughes, A. Bradu, G. Dobre, A. G. Podoleanu, Univ. of Kent (United Kingdom)

Aim and objectives. The morphology and position of the temporomandibular disc are key issues in the diagnosis and treatment of arthrogenous temporo-mandibular disorders. Magnetic resonance imaging and arthroscopy are used today to identify: flattening of the pars posterior of the disc, perforation and/or adhesions in the pars intermedia of the disc and disk displacements. The present study proposes the investigation of the temporo-mandibular joint disc by optical coherence tomography (OCT).

Material and methods 8 human temporo-mandibular joint discs were harvested from dead subjects, under 40 year of age, and conserved in formalin. They had a normal morphology, with a thicker pars posterior (2,6 mm on the average) and a thinner pars intermedia (1mm on the average). We investigated the disc samples by two OCT systems: a time domain OCT device, working at 1300 nm (C-scan and B-scan mode) and a Fourier spectral OCT device, working at 840nm (B-scan mode).

Results. The OCT investigation of the temporo-mandibular joint discs revealed a homogeneous microstructure. Time domain OCT offers a higher penetration depth (2,5 mm in air), which is important for the analysis of the pars posterior, while spectral OCT is much faster.

Conclusions: OCT is a promising imaging method for the microstructural characterization of the temporo-mandibular disc.

7554-89, Poster Session

A study on the qualitative morphological features of the muscle and subcutaneous shapes in vivo using Fourier-domain common path OCT

C. Song, Chonbuk National Univ. (Korea, Republic of) and The Johns Hopkins Univ. (United States)

We have developed a high-resolution and minimally invasive imaging system for monitoring and diagnosing subcutaneous based on common path optical coherence tomography using near infrared broadband light source at 0.8µm. Qualitative control of polarizations of the light beam by paddled wave plates can enhance the imaging characteristics that are relying on the collagenous figures of dermal tissue with intrinsic or form birefringence. The efficacy of the system for pre-medical applications was evaluated by using fresh beef and in vivo rat samples to observe fine dermal structures, and differentiate tissues such as fat and muscle which differ in scattering properties. The result shown the ability to delineate muscle with high resolution of 9µm and 6µm in both axial and lateral directions, respectively. Preliminary results using fresh beef and in vivo rat show that we can visualize the birefringence effect of the tissue collagen fibers in the samples for better image contrast and sensitivity for detection of hidden dermal structures. Compared to conventional

7554-90, Poster Session

Clinical optical coherence tomography combined with multiphoton tomography of patients with skin diseases

K. König, M. Speicher, JenLab GmbH (Germany); H. Studier, R. Bückle, JenLab Gmbh (Germany); J. Reckfort, JenLab GmbH (Germany); G. P. McKenzie, Michelson Diagnostics Ltd. (United Kingdom); J. Welzel, General Hospital Augsburg (Germany); M. J. Koehler, P. Elsner, M. Kaatz, Friedrich-Schiller-Univ. Jena (Germany)

We report on the first clinical study based on optical coherence tomography (OCT) in combination with multiphoton tomography (MPT) and dermoscopy. 47 patients with a variety of skin diseases and disorders such as skin cancer, psoriasis, hemangioma, connective tissue diseases, pigmented lesions, and autoimmune bullous skin diseases have been investigated with (i) state-of-the-art OCT systems for dermatology including multibeam swept source OCT, (ii) the femtosecond laser multiphoton tomograph, and (iii) dermoscopes. Dermoscopy provides two-dimensional color images of the skin surface. OCT images reflect modifications of the intratissue refractive index whereas MPT is based on nonlinear excitation of endogenous fluorophores and second harmonic generation. A stack of cross-sectional OCT "wide field" images with a typical field of view of 5x2 mm2 gave fast information on the depth and the volume of the lesion. Multiphoton tomography provided 0.36x0.36 mm2 horizontal/diagonal optical sections within seconds of a particular region of interest with superior submicron resolution down to a tissue depth of 200 µm. The combination of OCT and MPT provides a unique powerful optical imaging modality for early detection of skin cancer and other skin diseases as well as for the evaluation of the efficiency of treatments.

7554-91, Poster Session

Pulse analyzer system using optical coherence tomography for oriental medical application

N. Cho, U. Jung, M. Jeon, C. Lee, Kyungpook National Univ. (Korea, Republic of); C. S. Na, Dongshin Univ. (Korea, Republic of); J. Song, J. Kim, Kyungpook National Univ. (Korea, Republic of)

In oriental medicine, pulse wave at region of radial artery is one of the important diagnostic parameters. The skin above the artery radial has an important role because oriental medicine practitioners put their finger tips on the area to diagnose a patient's health condition by feeling the pulsation of the arterial contraction. There are three different clinically important areas called chon, gwan, and chuk, near the wrist where the arteria radialis reaches close to the skin surface. The finger tip diagnostic method relies on the subjective opinion of the practitioner, and there is a need to develop an objective diagnostic modality. The goal of this study is to demonstrate the feasibility of using a time domain optical coherence tomography (TD-OCT) to detect pulsation of the arterial contraction. A software algorithm is developed to extract four different parameters from the OCT image. The parameters include the pulse speed, amplitude, intensity, and irregularity of the pulse. Analysis study is also performed to



relate the parameters and the clinical evaluation, and more than 68% of specificity can be achievable. The performance of the system is graded and compared with that of oriental medicine practitioners. The results suggest the system may provide objective and robust evaluation on those parameters. The TD-OCT based pulse monitoring system may provide an objective approach to diagnostics in oriental medicine.

mental stress is applied to a volunteer, and it is more useful for evaluation of activity of the sympathetic nerve. Furthermore, the MIP imaging has been proposed for quick 3-D imaging of the spiral lumen of sweat glands. Using time-sequential MIP images with the frame spacing as short as 1.4 sec, several sweat glands can be tracked simultaneously to quantify sweating stimulated by a mental stress.

7554-92, Poster Session

Spectral domain polarization sensitive optical coherence tomography for imaging the nerve fiber layer at 1 micron

B. Elmaanaoui, J. C. Dwelle, The Univ. of Texas at Austin (United States); A. B. McElroy, Volcano Corp. (United States); A. Paranjape, L. Luck, H. G. Rylander III, T. Milner, The Univ. of Texas at Austin (United States)

We report a fiber-based spectral-domain polarization-sensitive optical coherence tomography system (SD-PSOCT) at 1.06 m for in-vivo high resolution real time imaging of the retinal nerve fiber layer (RNFL) about the optic nerve head (ONH). Change in RNFL birefringence about the ONH may be used to clinically track glaucoma progression. The hypothesis for this approach is that birefringence in the RNFL of earlystage glaucomatous eyes will diminish because the vitality of retinal ganglion cell axons in the RNFL is diminished and structural orientation of the neurotubules that gives rise to birefringence is lost. The A-scan rate of the SD-PSOCT system is 34 KHz and uses a tunable laser source centered at 1064nm with a FWHM of 55nm and 3mW average power. A bulk electro-optic modulator was constructed to input multiple polarization states into the interferometer. Using a balanced detection scheme horizontal and vertical polarization channels are acquired linearly in k-space and do not require any post-processing to balance dispersion. Using Intensity and phase information from the two channels we construct high resolution thickness, retardation, and birefringence maps of the RNFL of human subjects.

7554-93, Poster Session

Morphometric analysis of the optic nerve head with optical coherence tomography

M. Young, S. Lee, Simon Fraser Univ. (Canada); K. Hsu, Micron Optics (United States); M. F. Beg, Simon Fraser Univ. (Canada); P. J. Mackenzie, Univ. of British Columbia (Canada); M. V. Sarunic, Simon Fraser Univ. (Canada)

Optical Coherence Tomography is a powerful tool for diagnostic imaging of the ocular posterior chamber. Recent advances in OCT technology have facilitated acquisition of high resolution volumetric images of the retina and optic nerve head. In this report, we investigate the optic nerve head imaging in humans using home-built laboratory OCT systems at 830nm and at 1060nm. We also introduce the development of computational models of the optic nerve heard morphology in order to study physiological changes which may be associated with elevated intra-ocular pressure.

7554-94, Poster Session

Dynamic analysis of mental sweating by optical coherence tomography

M. Ohmi, M. Tanigawa, H. Saigusa, A. Yamada, Y. Ueda, M. Haruna, Osaka Univ. (Japan)

In the dynamic OCT of mental sweating, we have found internal mental sweating without ejection of excess sweat from the spiral lumen to the skin surface. Internal sweating occurs more often in the case where

7554-95, Poster Session

Minimal invasive localization of the germinal disc in ovo for subsequent chicken sexing using optical coherence tomography

A. Burkhardt, S. Geissler, P. Cimalla, J. Walther, E. Koch, Technische Univ. Dresden (Germany)

Reason for using optical coherence tomography (OCT) to locate the germinal disc is the questionable and ethically alarming killing of male layer chickens because for the layer line only the females are necessary. To avoid this and to protect the animal rights, the sex of the fertilized chicken egg has to be determined as early as possible in the unincubated state. Because the information whether the chick becomes male or female can be found in the germinal disc an accurate localization is essential for sexing. The germinal disc is located somewhere on top of the yolk and has a diameter of approximately 4 - 5 mm. Different imaging methods like ultrasonography, 3D-X-ray micro computed tomography and magnetic resonance imaging were used for localization until now, but found to be impractical. The goal of this study is to prove if OCT can be a moderate approach for the precise in ovo localization. The suitability of SD OCT to image the germinal disc in an open egg was proven in a preliminary study. Because the eggshell is an impenetrable barrier for OCT and to minimize the penetration of germs a very small hole is placed in the eggshell and a fan-shaped optical scanning pattern is used. The design of the new 3D scanner head allows imaging through a hole with a diameter of approximately 1 mm and then sector scanning can be performed by rotating the focussed OCT beam around a virtual point in the centre of the hole.

7554-96, Poster Session

High-speed concatenation of frequency ramps using sampled grating distributed Bragg reflector laser diode sources for OCT resolution enhancement

D. J. Derickson, B. J. George, California Polytechnic State Univ., San Louis Obispo (United States)

Wavelength tunable sampled grating distributed Bragg reflector (SG-DBR) lasers used for telecommunications applications have previously demonstrated the ability for linear frequency ramps covering the entire tuning range of the laser at 100 kHz repetition rates1. An individual SG-DBR laser has a typical tuning range of 50 nm. The InGaAs/InP material system often used with SG-DBR lasers allows for design variations that cover the 1250 to 1650 nm wavelength range. This paper addresses the possibility of concatenating the outputs of tunable SGDBR lasers covering adjacent wavelength ranges for enhancing the resolution of OCT measurements. This laser concatenation method is demonstrated by combining the 1525 nm to 1575 nm wavelength range of a "C Band" SG-DBR laser with the 1570nm to 1620 nm wavelength coverage of an "L-Band" SG-DBR laser. Measurements show that SGDBR lasers can be concatenated with a transition switching time of less than 50 ns with undesired leakage signals attenuated by 50 dB.



7554-97, Poster Session

Tunable semiconductor laser based on interaction between strongly mismatched Fabry-Perot interferometer and waveguide modes

A. A. Moiseev, V. M. Gelikonov, G. V. Gelikonov, Institute of Applied Physics (Russian Federation); E. A. Mashcovitch, Nizhny Novgorod State Univ. (Russian Federation)

The new method of spectral selection, based on interaction between strongly mismatched waveguide and Fabri - Perot interferometer modes has been proposed. It was shown, that in certain circumstances in spectrum, reflected from Fabri - Perot interferometer, narrowband lines, typical for spectrum of transmitted through Fabri - Perot light, are appear.

System consists of waveguide and Fabri - Perot cavity, made of concave mirrors, with partly mismatched modes has been examined, using conversion coefficient approach. Has been discovered, that in some circumstances, if waveguide mode and mode of Fabri - Perot interferometer are strongly mismatched, conversion coefficient for Fabri - Perot interferometer mode, coupling back to the waveguide mode will be more than ten times bigger, than for reflected from front mirror radiation. Thus, spectrum, reflected from Fabri - Perot interferometer back to the waveguide mode, has the same distinguishing feature as a spectrum of transmitted through Fabri - Perot light. This effect has been used for wavelength selection in tunable semiconductor laser with tuning range 25 nm at central wavelength 1290 nm.

7554-98, Poster Session

MEMS scanner based swept-source laser for optical coherence tomography

K. Totsuka, K. Isamoto, T. Sakai, A. Morosawa, C. Chong, Santec Corp. (Japan)

We developed a swept source laser using a micro electro mechanical systems(MEMS) scanner mirror, and demonstrated optical coherence tomography. The laser is composed of a fiber based ring cavity with a tunable filter. A semiconductor optical amplifier is used as a gain medium. A tunable optical filter is composed of a MEMS scanner mirror and a diffraction grating which is arranged in Littrow configuration. In general, it is difficult to fabricate a MEMS scanner which has a fast scanning speed while maintaining a large scanning angle. To overcome this trade-off, a concept of two degree of freedom(2-DOF) MEMS mirror is introduced. 2DOF operation makes it possible to achieve an optical scan angle over 20 degree at a resonant frequency of 17.9 kHz with a 1mm aperture. The laser has a wavelength range of 143 nm, center wavelength of 1304 nm, peak power of 16 mW. OCT measurements are performed at a rate of 17.9 kHz and doubled 35.9 kHz at unidirectional and bidirectional sweeps, respectively. We confirmed that the both upward and downward wavelength sweeps can generate images with almost equivalent quality, and can be used to integrate into a single image which has a double A-line number.

7554-99, Poster Session

Measurement of the coherent transfer function

M. L. Villiger, C. Pache, T. Lasser, Ecole Polytechnique Fédérale de Lausanne (Switzerland)

It is important to characterize and quantify the imaging performance of optical coherence tomography (OCT) and especially optical coherence microscopy (OCM) systems. The axial resolution and dispersion can easily be measured on a flat reflector. To assess the lateral resolution, microspheres embedded in a gel or resin are often used. The size and

refractive index of the microspheres, their concentration in the gel, and the temporal stability of this gel are critical parameters. Instead of measuring the point spread function (PSF), we suggest using a simple rubber surface, presented to the setup at different focal positions, to characterize the system's coherent transfer function (CTF). Rubber is a nearly perfect scatterer and produces a fully developed speckle pattern. The speckle size and shape are directly defined by the system's aperture and hence reveal its CTF. The rubber surface is scanned in both lateral directions. Isolating the interference term by background subtraction and Hilbert transformation, a two dimensional speckle pattern for each wavenumber k of the spectrometer is obtained. Taking the two-dimensional Fourier transform of this pattern uncovers the spatial frequency spectrum which was transmitted through the optical system. Since this information is available in function of the wavelength, chromatic variations and aberrations can be analyzed. Changing the focal position of the rubber completes the characterization of the system. The CTFs of an OCM with three different illumination and detection aperture combinations were analyzed and compared to the theoretical results to validate our approach.

7554-100, Poster Session

Real-time display on SD-OCT using a linearin-wavenumber spectrometer and a graphics processing unit

Y. Watanabe, T. Itagaki, Yamagata Univ. (Japan)

Fourier domain optical coherence tomography (FD-OCT) requires resampling of spectrally resolved depth information from wavelength to wavenumber, and the subsequent application of the inverse Fourier transform. The display rates of OCT images are much slower than the image acquisition rates, due to processing speed limitations on most computers. We demonstrated a real-time display of processed OCT images using a linear-in-wavenumber (linear-k) spectrometer and a graphic processing unit (GPU). We used the linear-k spectrometer with optimal combination of a diffractive grating with 1200 lines/mm and a F2 equilateral prism in the 840 nm spectral region, to avoid calculating the re-sampling process. The calculations of the FFT (fast Fourier transform) were accelerated by the low cast GPU (Nvidia, GeForce GTX 280, processor clock of 1296 MHz, memory clock of 2214 MHz, 240 stream processors, and memory 1 Gbytes) with many stream processors, which realized highly parallel processing. We used NVIDIA's CUDA (compute unified device architecture) architecture, which could be programmed in only a C language environment to implement the processing power of the GPUs The computing time on the GPU was about 28 times faster than that on the CPU, and only 17% of the interval time of the line scan camera was used. A display rate of 27.9 frames per second for processed images (2048 axial pixels × 1000 lateral A-scans) was achieved in our OCT system.

7554-101, Poster Session

Frequency domain optical coherence tomography with subsequent depth resolved spectroscopic image analysis

C. Kasseck, Ruhr-Univ. Bochum (Germany); V. Jaedicke, Georg Agricola Univ. of Applied Sciences (Germany); N. C. Gerhardt, Ruhr-Univ. Bochum (Germany); H. Welp, Georg Agricola Univ. of Applied Sciences (Germany); M. R. Hofmann, Ruhr-Univ. Bochum (Germany)

We present an analysis method to obtain additional depth resolved spectroscopic information from standard frequency domain optical coherence tomography (FDOCT) images. The postprocessing analysis utilizes Fourier transforms of signal peaks within the complex FDOCT depth profiles to extract depth resolved spectroscopic information. By varying the interval length of the Fourier transformed peaks, a



trade-off can be made between spectroscopic resolution itself and spectroscopic depth resolution. Larger depth intervals imply better spectroscopic resolution due to a higher number of data points and worse spectroscopic depth resolution due to the extended depth intervals. In any case, the depth resolution of the backscattering profile is not influenced by the spectroscopic analysis due to the subsequent analysis process. For verification of the depth resolved spectroscopic image analysis method, theoretical simulations as well as experimental studies are demonstrated. The simulation results clearly show the numerical ability of the method to reconstruct transmission spectra from a simulated three layer sample. Measurements were performed on multilayer samples with four different transmission spectra. All transmission spectra can be reconstructed accurately and thus validate the simulation results. Furthermore, the accurate depth resolved spectroscopic reconstruction enables a depth allocation of material specific transmission spectra due to absorption or scattering. In a further analysis step, the spectral patterns of specific depth regions can be compared to spectral material patterns and colored according to their correlation, thus allowing an automated spectral pattern recognition. This analysis tool improves the image contrast and allows image mapping of material specific spectral characteristics for optical histology.

7554-102, Poster Session

Adaptive filtering of optical coherent tomography fringe data with ensemble empirical mode decomposition

G. Liu, J. Zhang, L. Yu, Z. Chen, Beckman Laser Institute and Medical Ctr. (United States)

Empirical mode decomposition (EMD) is a new adaptive data analysis method in which the analyzed data is decomposed into a limited number of intrinsic mode functions (IMFs) through a sifting process. One problem with EMD is mode mixing, which is defined as a single IMF either consisting of signals of widely disparate scales or a signal of a similar scale residing in different IMF components. The mode mixing phenomenon has been solved by Wu et al using ensemble EMD (EEMD). In this paper, we applied the EEMD method to data acquired from optical coherence tomography (OCT) to improve the image quality. First, the original OCT fringe data is converted from linear wavelength to linear frequency through a calibration process. Second, the calibrated data is decomposed into different IMFs by EEMD. Third, the physical meaning of different IMFs was analyzed. Fourth, IMFs that represented noise were removed from the calibrated fringe data. The noise removed fringe data was then Fourier transformed to get depth information. EEMD was found to be able to separate different frequency noise into different IMFs. The signal to noise ratio of OCT image was improved by removing the IMFs that represent noise from the acquired fringe data.

7554-103, Poster Session

High-speed full-range imaging with harmonic detection swept-source optical coherence tomography

K. A. Peterson, C. Huang, Southwest Sciences, Inc. (United States); A. B. Vakhtin, Vista Photonics (United States)

Fourier domain optical coherence tomography (FDOCT) has become an attractive technology for high-resolution biomedical imaging due to its high sensitivity and fast imaging speeds. However, a major drawback of FDOCT is the complex conjugate ambiguity due to real Fourier transforms. The image is symmetric to the zero plane, and only half of the theoretical imaging depth range is used in practice. In this paper, harmonic detection, which we have previously demonstrated with a video rate, line scan camera-based FDOCT, is combined with swept source optical coherence tomography (SSOCT) to obtain the complex interferogram. This removes the complex conjugate ambiguity, allowing use of the full imaging range and providing flexibility of zero plane

position. This harmonic detection SSOCT system exhibits micrometer axial resolution, 110dB sensitivity, 40 dB dynamic range, and can operate at the full sweep rate of the 16 kHz swept source laser.

7554-104, Poster Session

Signal processing with unequally spaced data in Fourier-domain optical coherence tomography

S. Vergnole, D. Lévesque, National Research Council Canada (Canada); S. S. Sherif, Univ. of Manitoba (Canada); G. Lamouche, National Research Council Canada (Canada)

Two different algorithms for performing Fourier transforms with unequally sampled data in wavenumber space for Fourier-domain optical coherence tomography are considered. The efficiency of these algorithms is evaluated from point-spread functions (PSF) evaluated as a function of depth with a swept-source optical coherence tomography system. The amplitude of the PSF, the width of the PSF, and the processing time are discussed. The performance of the proposed algorithms is compared to the usual combination of interpolation and fast Fourier transform. Although more processing intensive, these algorithms provide better sensitivity at large depth without impacting the width of the PSF. Additionally, these algorithms are applied to simulated data with different level of nonlinearity in wavenumber space. This provides better understanding of the source of improved sensitivity provided by the proposed algorithms.

7554-105, Poster Session

Evaluation of complex conjugate artifact removal methods used in spectrometer based Fourier-domain optical coherence tomography systems: a comparative study

D. Y. Kim, J. S. Werner, R. J. Zawadzki, Univ. of California, Davis (United States)

We evaluated several, previously published, complex conjugate artifact removal methods and algorithms that were implemented in Fd-OCT. To ensure comparable conditions, only one OCT system was used, but with modified data acquisition schemes, depending on each method/algorithm's requirements. This limited our evaluation to single spectrometer based Fd-OCT approaches. The suppression ratio of mirror complex artifact images was assessed for all tested methods. Several other metrics were also used for comparison, including a list of additional hardware requirements (beyond standard Fd-OCT components), total data acquisition time, and image processing time (tested in Labview). Finally potential problems and limitations connected with different data acquisition schemes and data processing algorithms will be discussed.

7554-106, Poster Session

Three-dimensional speckle suppression in optical coherence tomography based on the curvelet transform

L. Yu, Z. Jian, B. Rao, B. J. Tromberg, Z. Chen, Univ. of California, Irvine (United States)

Optical coherence tomography is an emerging non-invasive technology that provides high resolution, cross-sectional tomographic images of internal structures of specimens. It holds great potentials for a wide variety of applications, especially in the field of biomedical imaging. OCT images, however, are usually degraded by significant speckle noise. Here we report a 3D approach to attenuating speckle noise in OCT images.



This approach is based on the 3D curvelet transform, and is conveniently controlled by a single parameter that determines the threshold in the curvelet domain. Unlike 2D approaches which only consider information in individual images, 3D processing, by analyzing all images in a volume simultaneously, has the advantage of also taking the information between images into account. This, coupled with the curvelet transform's nearly optimal sparse representation of curved edges that are common in OCT images, provides a simple yet powerful platform for speckle attenuation. We show the approach suppresses a significant amount of speckle noise, and in the mean time preserves and thus reveals many subtle features that could get attenuated in other approaches.

7554-107, Poster Session

Multi-beam resolution video rate swept source optical coherence tomography (OCT) provides endogenous contrast for in vivo blood flow independent of flow direction

F. Bazant-Hegemark, S. Hattersley, J. Holmes, Michelson Diagnostics Ltd. (United Kingdom)

The capillary network provides functional information that can be used for research, diagnosis of disease, prognosis on treatment options, and monitoring intervention. Optical coherence tomography (OCT) allows non-invasive imaging of sub-surface structures in vivo, ideally without a need for target preparation. In conventional OCT, the contrast for blood vessels depends on a variety of factors and can be challenging. Speckle variance has been recognised as a method to enhance contrast for blood flow without the application of contrast agents in OCT images.

Here, we demonstrate the possibility of extracting blood flow information from volumetric OCT datasets that were obtained routinely from human participants. We used a commercially available CE-marked system for clinical use. The light source has a central wavelength of 1310 nm. Using multi-beam technology, the system achieves an isometric resolution of better than 7.5 μm in tissue over the entire imaging depth of around 1 mm. At 1 mm image width, 21 frames (B-scans) per second can be imaged.

We used the speckle variance in order to enhance the contrast for blood vessels in vivo. This method allowed us determining the presence and depth of blood flow within the 1 mm penetration depth, without dependence on direction or orientation of the blood flow with respect to the scanning beam.

7554-108, Poster Session

Focusing light through living tissue

I. M. Vellekoop, C. M. Aegerter, Univ. of Zürich (Switzerland)

Tissues such as skin, fat or cuticle are non-transparent because inhomogeneities in the tissue scatter light. We demonstrate experimentally that it is possible to focus light through turbid layers of living tissue, in spite of scattering. Our method is based on the fact that coherent light forms an interference pattern, even after hundreds of scat-tering events. This interference pattern can be changed by spatially shaping the wavefront of the incident laser beam. For a specific configuration of the incident wa-vefront, the transmitted scattered light focuses to a point. We used this principle to focus laser light through living pupae of the Drosophila melanogaster. In contrast to earlier experiments, where light was focused through solid objects, the body of the pupa is mainly fluid. In living tissue, microscopic movements of scattering particles cause the interference pattern to change with time. A dynamic wavefront shaping algorithm was used to follow these changes in real time. We relate the performance of the algorithm to the measured timescale of the changes in the speckle pattern and ana-lyze our experiment in the light of Laser Doppler flowmetry. Finally, we discuss applications in particle tracking in turbid tissue, imaging, and thermal manipulation.

7554-109, Poster Session

Coherent noise compensation improvement in spectral-domain optical coherence tomography

P. A. Shilyagin, V. M. Gelikonov, G. V. Gelikonov, I. V. Kasatkina, D. A. Terpelov, Institute of Applied Physics (Russian Federation)

An efficient technique of the coherent noise separation of and compensation for in spectral-domain optical coherence tomography (SD-OCT) is proposed and validated. The coherent noise is separated during one exposure by modulating the relative delay of the signal and reference waves by a certain waveform. It is shown that the influence of internal motions in an object on the coherent noise separation quality can be reduced by increasing of modulation frequency. The technique has been numerically and experimentally validated with the help of an optical coherence tomography (OCT) setup with a radiation source operating at a wavelength of 1277 nm and a width of the recorded spectrum of about 100 nm.

7554-110, Poster Session

Effective bandwidth in spectral-domain OCT

M. Jiang, S. Jiao, The Univ. of Southern California (United States)

We found that the bandwidth in the formula calculating the depth resolution of OCT is usually not the same as the bandwidth of the light source because the effective spectral profile for the interfering signal is determined not only by the spectrum of the light source but also by the dot product of the electric vectors of the light field in the two interfering arms. We thus introduced a new concept: the effective bandwidth in spectral-domain OCT (SD-OCT) to calculate the depth resolution of the optical-fiber based SD-OCT more accurately. Through theoretical analyses we found that the effective bandwidth is a function of both the polarization matching conditions (PMC) and the path length difference (PLD) between the sample and reference arms. We investigated the two factors separately through experiments. The variation of the effective bandwidth with PMC for partially polarized light is a universal phenomenon for both time-domain and spectral-domain OCT, which comes from the fact that PMC varies across the spectrum when the degree of polarization (DOP) is less than one. The variation of the effective bandwidth with PLD is a special phenomenon for SD-OCT, which comes from the fixed element size (or sampling interval) of the array detector in the spectrometer. Since the spatial frequency of the interference pattern along the linear array detector varies with wavelength (higher frequency for shorter wavelength, lower frequency for longer wavelength), the signal drop off with PLD is more severe for shorter wavelength.

7554-111, Poster Session

Comparison of time domain vs. frequency domain high-speed full-field optical coherence tomography with low NA

T. Bonin, M. Hagen-Eggert, Univ. zu Lübeck (Germany); P. Koch, Thorlabs HL AG (Germany); G. Hüttmann, Univ. zu Lübeck (Germany)

In ultrahigh-speed Fourier domain OCT systems, the commonly used galvanometric scanners have almost reached their limits in terms of speed. As the acquisition speed of 2D cameras increased over the last years, full-field OCT may lead to significantly higher imaging speed bypassing the need to scan the area of interest. The parallel illumination of the full field of view also allows for higher light powers when applied to biological tissue. The first implementations of full-field OCT, which used thermal light sources with low spatial and temporal coherence in combination with a high NA objective and a time domain detection

107

Return to Contents TEL: +1 360 676 3290 · +1 888 504 8171 · customerservice@spie.org



scheme, demonstrated high image quality.

Although in these cases no transversal scanning is necessary, there still are moving parts because either the reference mirror or the sample has to be translated. To overcome this and to benefit from the advantage in SNR by detecting all photons, the use of swept-sources to setup time encoded frequency domain full-field OCT systems was demonstrated.

In this paper, we will experimentally compare the performance of time domain and frequency domain full field OCT in an identical setup with a lower NA of 0.1 and a fast camera with 1000 frames/s and a spatially coherent light source

Fast swept-sources are laser based and therefore have a high degree of spatial coherence. This will introduce significant crosstalk between adjacent image points in scattering samples. Therefore, different mechanisms of crosstalk reduction for spatially coherent light sources are investigated and compared to a TD full-field OCT with a thermal light source.

7554-112, Poster Session

Speckle imaging by combination of mathematical morphology and contrast ratio

Z. Li, S. Cai, L. Fan, H. Li, Fujian Normal Univ. (China)

This paper presents a novel speckle imaging that combines mathematical morphology with contrast ratio. We apply this technique to visualize laterally localized inhomogeneities embedded within a highly scattering sample. The speckle images are obtained by intensity polarized parallel to incident beam minus those polarized perpendicular. The speckle image is decomposed into a series of component images by the mathematical morphology, whose a recursive decomposition algorithm consists of successive opening operations with disc of increasing radii as structuring elements. We demonstrate that the position and size of the two objects are accurately reconstructed in the component image for the greatest structuring element. Furthermore, contrast ratio of a series of component images are related to the optical properties of objects, which distinguish objects buried in turbid media from the background. Finally, the results also show that granulometry in the field of mathematical morphology could be useful for characterizing the optical properties of background media. Thus, this technique could be a potential tool for medical diagnosis in the future.

7554-29, Session 5

Multimodal imaging with integrated photoacoustic microscopy and optical coherence tomography

S. Jiao, Univ. of Southern California (United States); H. F. Zhang, Z. Xie, Univ. of Wisconsin-Milwaukee (United States)

We have developed a multimodal imaging technique by integrating photoacoustic microscopy and spectral-domain optical coherence tomography to provide simultaneous volumetric microscopic imaging of both optical absorption and scattering contrasts in biological tissues. In the integrated system, the two imaging modalities share the same optical scanning and delivery mechanisms after their probing and illumination light beams are combined. By further synchronizing the image acquisitions, the images from the two modalities are intrinsically registered. The capabilities of this novel technique were demonstrated by imaging both the microanatomy and microvasculature in mouse ears in vivo.

7554-30, Session 5

Optimizing penetration depth, contrast, and resolution in 3D dermatologic OCT

A. Aneesh, B. Povžay, B. Hofer, Cardiff Univ. (United Kingdom); S. Popov, Imperial College (United Kingdom); W. Drexler, Cardiff Univ. (United Kingdom)

High speed, three-dimensional optical coherence tomography (3D OCT) at 800nm, 1060nm and 1300nm with approximately 4µm, 7µm and 6µm axial and less than 15µm transverse resolution is demonstrated to investigate the optimum wavelength region for in vivo human skin imaging. The imaging speed is 20 kHz for the 800nm OCT system and 47 kHz for 1060nm and 1300nm systems. The wavelength-dependent components of the handheld probe such as collimator and objective lens were selected appropriately, so that each system was comparable in terms of transverse resolution and depth of field. Signal to noise ratios of all the three OCT systems were made comparable and images obtained from same locations of the skin in vivo using these three systems is compared in terms of resolution, contrast, penetration depth and dynamic range. Penetration depth was better for 1300nm system, while images obtained at 800nm were better in terms of contrast and speckle noise. 1060nm region was a compromise between 800nm and 1300nm in terms of penetration depth and image contrast. The availability of ultra-broadband sources in all investigated wavelength regions in conjunction with high resolution spectrometers with accurate numeric non-linearity correction and dispersion management helps to accomplish high quality depth-resolved images with up to 1.5mm penetration into the skin. Unprecedented visualization of three-dimensional morphology at 10 µm resolution across areas of more than 50 mm² of glabrous and non-gölabrous skin, moles and scars could be demonstrated with an optimized high speed OCT system at all the three wavelengths.

7554-31, Session 5

Noninvasive assessment of biofilm growth in the middle ear using a portable low-coherence interferometry system

S. A. Boppart, C. T. Nguyen, H. Tu, E. J. Chaney, Univ. of Illinois at Urbana-Champaign (United States); C. N. Stewart, Blue Highway, LLC (United States)

Otitis media (OM) is the most common illness in children in the United States. Three-fourths of children under the age of three have OM at least once. Children with chronic OM, including OM with effusion and recurrent OM, will often have conductive hearing loss and communication difficulties, and need surgical treatment. Recent clinical studies state that almost all chronic OM cases are accompanied by a bacterial biofilm behind the tympanic membrane (eardrum). Biofilms are typically very thin, making them difficult to recognize using a regular otoscope. However, low coherence interferometry (LCI) is capable of detecting and quantifying this microstructure. Our goal was to design a portable system integrating LCI with a standard video otoscope to detect the presence of biofilms and provide quantitative information of the middle ear to assist physicians in diagnosing middle ear infections. In the future, it is expected such quantitative information will direct and monitor treatment protocols. The system uses a super luminescent diode centered at 940 nm with a bandwidth of 60 nm and the axial resolution of ~ 4.5 µm in tissue. Axial scans are acquired in vivo at the rate of 2 kHz, and classified according to microstructural features to provide statistical determination for OM status. Preliminary results are described in a rat OM model and in humans



7554-32, Session 5

Design of a dual-modality imaging system using optical coherence tomography and fluorescence lifetime imaging for oral cancer detection

S. Shrestha, B. E. Applegate, P. Pande, J. A. Jo, Texas A&M Univ. (United States)

We have developed a combined Optical Coherence Tomography (OCT) and Fluorescence Lifetime Imaging (FLIM) system to provide high-speed coregistered microanatomical and biochemical images. The OCT/FLIM system is capable of a maximum A-line rate of 59 kHz for OCT and a maximum pixel rate of 200 kHz for FLIM. A 40 nm bandwidth 830 nm SLED provides 7.6 mm axial resolution for OCT. A pulse picked frequency doubled tunable femtosecond Ti:Sapph laser (350-500 nm) was used for the FLIM excitation. The OCT sample light and FLIM excitation co-propagate through a galvo mirror pair and ultrawide bandwidth achromatic objective lens to provide lateral scanning with 15 mm and 40 mm lateral resolution for OCT and FLIM, respectively. A multispectral time-resolved fluorescence detection system enables the simultaneous high-speed acquisition of time resolved emission from three wavelength bands. Each 2-D galvo scan results in the acquisition of three timeresolved fluorescence emission images and an OCT volume. Once optimized the OCT/FLIM system will be capable of rapid acquisition and processing enabling near real time diagnosis. Future applications of this technology include the early detection and diagnosis of oral cancer and atherosclerotic vulnerable plaque detection.

7554-33, Session 5

Diagnosis of oral submucous fibrosis with optical coherence tomography

C. Lee, National Taiwan Univ. (Taiwan); M. Tsai, Chang Gung Univ. (Taiwan); H. Lee, H. Chen, C. Chiang, Y. Wang, T. Chi, K. Yang, C. Yang, National Taiwan Univ. (Taiwan)

The epithelium (EP) thickness and the standard deviation (SD) of A-mode scan intensity in the laminar propria (LP) layer are used as effective indicators for the diagnosis of oral submucous fibrosis (OSF) based on the noninvasive clinical scanning of a swept-source optical coherence tomography (OCT) system of ~6 micron in axial resolution (in tissue) and 103 dB in sensitivity. Compared with the corresponding parameters in healthy oral mucosal mucosa, in OSF mucosa the EP thickness becomes smaller and the SD of A-mode scan intensity in the LP layer (LP SD) also becomes smaller. The LP SD can also be used for effectively differentiating OSF (small LP SD) from lesion (large LP SD). This application is particularly useful in the case of a lesion without a clear surface feature. Meanwhile, the use of the SD of A-mode scan intensity in the EP layer (EP SD) can further help in differentiating OSF (medium EP SD) from healthy oral mucosal (small EP SD) and lesion (large EP SD) conditions. Compared with the conventional method of maximum mouth opening measurement, the use of the proposed OCT scanning results can be a more effective technique for OSF diagnosis.

7554-34, Session 5

Return to Contents

Guidance of hard tissue ablation by forwardviewing optical coherence tomography

P. J. L. Webster, B. Y. Leung, Queen's Univ. (Canada); V. X. D. Yang, Ryerson Univ. (Canada); J. M. Fraser, Queen's Univ. (Canada)

A key issue in laser surgery is the inability for the human operator to stop the laser irradiation in time while cutting/ablating delicate tissue layers. In the present work, we forward-image through the laser machining

front in complex biological tissue (bovine cortical bone) to monitor the incision's approach to subsurface interfaces in real-time (47 kHz line rate). Feedback from imaging is used to stop the drilling process within 150 micron of a targeted interface. This is accomplished by combining the high temporal and spatial resolution of infrared optical coherence tomography (OCT) with a robust, turn-key, high brightness fiber laser. The high sensitivity of the imaging system (98 dB) permit imaging through the rapidly changing beam path even with the additional scattering caused by the thermal cutting process. Line rates of 47 kHz and 10 microseconds camera integration time provide access to fast morphology changes within the system, including thermal relaxation after cutting. In spectral-domain OCT, the imaging acquisition period is easily locked to the machining laser exposure. Though motion-induced artifacts reduce interface contrast, they do not introduce incorrect depth measurements as found in other OCT variants. Standard tomography imaging of the tissue (B-scans) is also recorded in situ before and after laser processing to highlight morphology changes.

7554-35, Session 6

Speckle variance OCT tracking of tumor angiogenesis and response to vascular targeted photodynamic therapy

A. Mariampiilai, M. T. Jarvi, M. K. Leung, K. K. C. Lee, B. C. Wilson, I. A. Vitkin, Univ. of Toronto (Canada); V. X. Yang, Ryerson Univ. (Canada)

We have recently demonstrated a simple new functional extension of OCT known as speckle variance OCT (SV-OCT) that has a significantly improved sensitivity to microvasculature over the more traditional Doppler OCT imaging techniques. Using confocal fluorescence microscopy and an optimized SV-OCT acquisition scheme we were able to confirm that SV-OCT is capable of visualizing capillaries with a diameter as small as 6um over large fields of view (5mm x 5mm). SV-OCT was used to longitudinally monitor 3-Dimensional vascular changes induced by tumor angiogenesis in the dorsal skin-fold window chamber model. Subsequent treatment of tumors with vascular targeted photodynamic (PDT) therapy demonstrated the ability of SV-OCT to monitor transient changes during PDT treatments (minutes) with subsequent vascular shutdown and revascularization over longer time periods (days). Methods and metrics used to quantify these vascular changes will be presented. The ability to longitudinally track vascular changes without the use of exogenous contrast agents, in real-time and with high sensitivity provides exciting opportunities for studying vascular changes in tumors and the effects of vascular targeted therapies.

7554-36, Session 6

Optical micro-angiography detects angiogenesis in brain trauma

Y. Jia, R. Wang, Oregon Health & Science Univ. (United States)

Angiogenesis following brain trauma is crucial to the post-traumatic repair process. In this study, using Optical Micro-AngioGraphy (OMAG), a volumetric imaging method capable of in vivo mapping localized blood perfusion with capillary level resolution, we demonstrated a substantial increase in angiogenesis following brain injury and investigated dynamic growth of the trauma-induced angiogenesis on the mouse brain. The result suggests that OMAG has the potential to be used for in vivo detecting post-traumatic angiogenesis during rehabilitation process.

109

TEL: +1 360 676 3290 · +1 888 504 8171 · customerservice@spie.org



7554-37, Session 6

Influence of blood optical inhomogeneity on Doppler OCT signals

D. Bukowska, A. Szkulmowska, Nicolaus Copernicus Univ. (Poland); R. A. Leitgeb, Medizinische Univ. Wien (Austria); M. Szkulmowski, I. Grulkowski, S. Tamborski, A. A. Kowalczyk, M. Wojtkowski, Nicolaus Copernicus Univ. (Poland)

In this paper we would like to report that optical inhomogenity of human blood have an influence on Doppler OCT measurements. To confirm this phenomenon various experiments with different materials and different well controlled experimental configurations was carried out. Imaging was performed using SOCT instrument with CCD camera. Data analysis was performed using STdOCT.

The results show that more detailed analysis of velocity data reveals the presence of Doppler signals coming from scattering steady medium place underneath the capillary while optically inhomogeneous particles flow throughout the capillary. In the case of homogeneous flowing particles like intralipid results are negative. Concluding those observations we can confirm that Doppler signal coming from the scattering steady medium is caused by the dynamic changes of the refractive index which can strongly influence the Doppler readout causing significant broadening of Doppler profiles and the same errors. There can be also an impact of this effect into a reconstruction of flow in small capillaries. Additionally we realized that better understanding of the optical inhomogenity of blood is important for the correct measurement of the blood flow. Hence, a detailed investigation of the optical properties of hemoglobin and whole blood using SOCT is needed.

7554-38, Session 6

BM-mode scanning with parabolic phase modulation for full range Doppler optical tomography

F. Jaillon, S. Makita, Y. Yasuno, Univ. of Tsukuba (Japan)

Monitoring vessel flow properties may aid the screening and the treatment of pathologies such as age related macular degeneration, glaucoma or diabetic retinopathy. Although, Spectral Domain OCT (SDOCT) has become an advantageous method with respect to time domain OCT due to its high speed acquisition and large sensitivity, an intrinsic problem is linked to SDOCT: the complex ambiguity. A solution to this problem has been brought by the B-M-mode scanning method. But the latter fails to remove mirror image for high flow regions. We propose here to solve this issue in changing the linear phase modulation (along the B-scan direction) used in the standard method to a parabolic phase modulation. Indeed the shift generated by this parabolic phase modulation in the spatial frequency domain is related to the acceleration of the structure and not to its velocity. Consequently, the shift is much smaller and enables to keep the signal within the filter bandwidth used to remove the mirror image. We first tested the proposed method utilizing a loudspeaker as sample in a 1 um SDOCT system. This simple experiment enables to demonstrate, for different sample axial velocities, a better mirror image removal efficiency of the proposed technique. Moreover, we acquired phase-resolved Doppler images of human eye retina using the parabolic phase modulation technique. We observed, with respect to the standard BM mode scanning method, the suppression of mirror image artifacts due to high blood flow.

7554-39, Session 6

Real-time bulk motion insensitive flow segmentation algorithm for Doppler spectral optical coherence tomography

M. Szkulmowski, A. Szkulmowska, D. Szlag, I. Grulkowski, A. Kowalczyk, M. Wojtkowski, Nicolaus Copernicus Univ. (Poland)

We present a simple and efficient numerical technique for segmentation retinal and choroidal blood vasculature with bulk motion correction in functional Doppler Spectral Optical Coherence Tomography (Doppler SOCT). The technique uses local variance of velocity tomogram which is higher in the areas of the tomogram with internal flow. The resulting variance map reveals the position of vessels. This can be used either for vessel segmentation purposes or for masking the vessels on velocity tomograms. The remaining velocity information is connected only with static structure velocity offset. As only Fourier transformations are used in calculations the algorithm removes the bulk motion from velocity tomograms and provides images of segmented vessels with speed of 200 000 lines/s. When combined with basic structural and velocity tomogram reconstruction techniques that generate 150 000 lines/s, this speed allows for real-time creation of bulk-motion free velocity tomograms. The algorithm is shown to work with velocity tomograms obtained either by phase-resolved Doppler SOCT or by joint Spectral and Time domain OCT (STdOCT).

7554-40, Session 6

High-resolution wide-field of view blood perfusion maps for retina and choroid with optical micro angiography

L. An, D. Wilson, R. Wang, Oregon Health & Science Univ. (United States)

In this presentation, we present the high resolution and wide field of view retina and choroid blood perfusion maps, which are obtained through optical micro-angiography (OMAG) technology. Based on the special frequency analysis, OMAG is able to visualize the vascular perfusion map down to the capillary level resolution. We used an 840 nm, 27 kHz FDOCT system to capture 16 OCT data sets in a sequential order, which could provide wide field blood field (~7.4mm×7.4mm) information of posterior part of a human volunteer. For each of these data sets, we eliminated the bulk motion artifacts through phase compensation method, which is based on the histogram bulk motion phase estimation. The displacements occurred between adjacent frames in one data set were compensated through 2 dimensional cross correlation of two adjacent OMAG flow images. Compared with the FA and ICGA images results, the OMAG results of blood perfusion map of retina and choroid demonstrate a very good agreement with them.

7554-41, Session 7

FDML based multi-spot OCT at 4,100,000 A-scans and 4 Gvoxels per second

W. Wieser, B. R. Biedermann, C. M. Eigenwillig, T. Klein, R. A. Huber, Ludwig-Maximilians-Univ. München (Germany)

We demonstrate OCT imaging at 4.1M A-scans per second. The system uses a Fourier domain mode locked laser with a sweep repetition rate of 1028kHz at a sweep range of 106nm centered at 1320nm. A 4 spot parallel detection system with a power of 4x7.8mW on the sample achieves a measured sensitivity of 101dB, resulting in good image quality. With an effective rate of more than 4Gvoxels/s, this system represents a 2x speed improvement over the fastest, previously demonstrated OCT setups. The system design, data acquisition solution and limitations are discussed.



7554-42, Session 7

Coherent transfer functions and extended depth of field

M. L. Villiger, C. Pache, Ecole Polytechnique Fédérale de Lausanne (Switzerland); R. A. Leitgeb, Medizinische Univ. Wien (Austria); T. Lasser, Ecole Polytechnique Fédérale de Lausanne (Switzerland)

To preserve the speed advantage of Fourier Domain detection in Optical Coherence Microscopy (OCM), extended depth of field is needed. With a narrow probing volume that extends over a long axial range, tissue could be measured in vivo and at cellular resolution. To assess and improve the DOF and the lateral resolution, we analyzed the coherent transfer function (CTF) of OCM. Both the illumination and detection optics contribute equally to the overall imaging performance. In the Fourier domain detection, each pixel of the spectrometer has its specific CTF, sampling a different region of the object's spatial frequency spectrum. For classical optics and increasing numerical apertures these regions start to overlap and bend, which limits the depth of field. Annular apertures, created with Bessel-like beams produced by axicon lenses or phase filters, circumvent these detrimental effects, but introduce strong side lobes. Decoupling the detection and the illumination apertures is needed to provide the flexibility in engineering a CTF that optimizes the lateral resolution and the DOF at the same time all while reducing these side lobes

We evaluated different combinations of Gaussian and Bessel-like illumination and detection optics, both theoretically and experimentally. Using Bessel-like beams as well in the illumination as in the detection paths, but with annular apertures of different lobe radii, we obtained a lateral resolution of 1.3 µm and an extended depth of field of more than 300 µm, which was completely decoupled from the numerical aperture and scalable to high lateral resolution.

7554-43, Session 7

Multichannel optical coherence tomography using a high-power telescope-less polygon-based swept laser in dual amplifier configuration

M. K. K. Leung, A. Mariampillai, Univ. of Toronto (Canada); B. A. Standish, Ryerson Univ. (Canada); K. K. C. Lee, N. R. Munce, I. A. Vitkin, Univ. of Toronto (Canada); V. X. D. Yang, Ryerson Univ. (Canada)

A major component of swept-source optical coherence tomography is the light source. Here, we report a high-power wavelength-swept laser and demonstrate its use for multichannel optical coherence tomography (MOCT) imaging. The main benefit of MOCT is faster image acquisition rates without a corresponding increase in the tuning speed, which tends to decrease the performance of the laser and may be limited mechanically. The wavelength-swept laser was constructed using a compact telescope-less polygon-based filter in Littman arrangement. It consists of a diffraction grating, a polygon scanning mirror, and an end reflector mirror. High output power, necessary for MOCT, is achieved by incorporating two serial semiconductor optical amplifiers in the laser cavity in Fourier domain mode-locked configuration. The measured wavelength tuning range of the laser is 111 nm centered at 1329 nm, coherence length of 5.5 mm, and total average output power of 131 mW at a 43 kHz sweeping rate. To demonstrate the applicability of the laser for MOCT, a six-channel imaging system was constructed. The imaging arm consists of a multi-fiber push-on connector mounted on a galvanometer-based scanner. All channels were focused at the same depth using an achromatic doublet. Six-channel OCT imaging to achieve 258 kHz scan rate is demonstrated. The increase in effective frame rate using multichannel acquisition may be beneficial for 3-dimensional invivo imaging where bulk tissue motion can adversely affect the image quality.

7554-44, Session 7

Design and performance of a novel sample arm for dynamic optical coherence elastography

B. F. Kennedy, T. R. Hillman, R. A. McLaughlin, B. C. Quirk, D. D. Sampson, The Univ. of Western Australia (Australia)

3 page summary attached

7554-45, Session 7

Large field OCT by optical movement tracking of a single point probe

G. Hüttmann, B. Martensen, E. M. Lankenau, Univ. zu Lübeck (Germany)

OCT measures subsurface tissue structures by interferometric analysis of depth in which broad band irradiation is scattered. For lateral sampling of the tissue the beam is scanned or the whole optics is moved over the tissue. The second approach which is used in endoscopic OCT offers in principle unrestricted field of view. Scanning is done in a predictable way by actuators in order to construct B- and C-scans. For some applications a deliberate scan of the tissue by moving the OCT optics by the physician would be advantageous. Large tissue areas could be imaged with minimal technical complexity by a small size and lightweight OCT probe. With this principle skin could be imaged at a difficult location, a simple OCT probe could be inserted in the working channel of an endoscope and moved over suspicious lesions by the surgeon. However, to get a geometrical correct image of tissue structures, displacement or velocity of the OCT probe has to be traced. The lateral movement is either measured by an optical sensor or calculated directly from the speckle pattern in the image. Also, good quality images of skin through a high NA objective with several millimeters field of view were demonstrated. This opens a way for a simple combination of multiphoton imaging with fast OCT of large areas using the same objective. An OCT probe consisting of a high NA microscope objective, which shall be used for combined multiphoton and OCT imaging, was build with an optical mouse sensor.

7554-46, Session 7

Integrated photonic circuit in silicon on insulator for Fourier domain optical coherence tomography

G. Yurtsever, P. Dumon, W. Bogaerts, Univ. Gent (Belgium) and IMEC (Belgium); R. Baets, Univ. Gent (Belgium)

Optical Coherence Tomography (OCT) is an emerging optical imaging technology with growing number of applications. OCT enables micron scale cross-sectional imaging of subsurface microstructures by analyzing the backscattered light from subsurface layers of the materials. Current OCT imaging systems are fiber or free space optics based and they are table-top portable systems. Through implementation of OCT subsystems in photonic lightwave circuits both their size and price can be reduced. Silicon on insulator (SOI) is a versatile platform for CMOS compatible, wafer scale integrated photonic circuit fabrication. On this material system, passive components such as waveguides, splitters, filters and active components like lasers, photodetectors and modulators has already been demonstrated. We present, a planar lightwave circuit on SOI for Fourier domain OCT. The integrated photonic circuit consists of grating couplers, single mode waveguides, a multi-mode interference splitter, a reference arm and a broadband reflector. The grating couplers are used to couple the light from an external light source in and to couple the interference signal out to a spectrometer. The center wavelength of operation is designed to be 1550 nm, supporting 30 nm of 3 dB



bandwidth. Currently the device has 6 dB insertion loss per grating coupler, resulting in total of 24dB loss. However, with different processing methods this can be eventually reduced to the level of fiber connector losses. Integrated photonics on silicon offers significant miniaturization possibilities to optical system design for optical coherence tomography and possible integration with electronics on the same die.

7554-47, Session 7

Novel continuous-wave supercontinuum light source with stable, broadband, and highpower spectrum for spectrally sampled OCT

E. J. Jung, Pusan National Univ. (Korea, Republic of); J. Lee, The Univ. of Seoul (Korea, Republic of); H. S. Lee, M. Y. Jeong, C. S. Kim, Pusan National Univ. (Korea, Republic of)

We present a novel scheme of continuous-wave (CW) supercontinuum light source for spectrally-sampled optical coherence tomography (OCT). Instead of conventional short-pulse pumping method, the implemented all-fiberized light source exhibits CW high-power of 500 mW and flat and stable 3-dB spectral bandwidth of ~110 nm covering 1560 ~ 1670 nm. From the experimental comparison of point spread functions between conventional continuous spectral source and suggested multi-wavelength source, the advantage of spectrally-sampled OCT is clearly demonstrated for the enhancement of dynamic range of cross sectional OCT image using the same average optical power level.

7554-48. Session 7

Linear OCT system with multiple carrier frequency encoded reference beams for a discontinuous measurement range

G. Hüttmann, V. Hellemanns, Univ. zu Lübeck (Germany); P. Koch, Thorlabs GmbH (Germany)

Time domain OCT systems can be build with a linear detector array (linear OCT or L-OCT), which makes them are simple and robust. However, the measurement range is limited by the number of pixel. For some applications a discontinuous measurement range is advantageous. E.g. for the measurement of the refracting surfaces of the eye the totally needed measurement range is quite high though the rough position of each surface is known. Here we present the theory of a linear OCT with several reference arms of different length which each use different carrier frequencies. Thereby a unique measurement of non-continuous structures is possible. Experimental results with two reference arms are presented.

7554-49, Session 8

Frequency comb swept lasers for optical coherence tomography

T. Tsai, C. Zhou, D. C. Adler, J. G. Fujimoto, Massachusetts Institute of Technology (United States)

We demonstrate a frequency comb (FC) swept laser and a frequency comb Fourier domain mode locked (FC-FDML) laser for applications in optical coherence tomography (OCT). A frequency comb filter in the cavity of swept lasers causes the lasers to generate a series of frequency steps. The narrow bandwidth of the frequency comb filter enables a -1.2dB sensitivity roll off over ~3mm range, while conventional swept source and FDML lasers have -10dB and -5dB roll offs respectively. Measurements at very long ranges are possible with minimal sensitivity loss, however reflections from outside the principal measurement range of 0-3mm appear aliased back into the principal range. In addition, the frequency comb outputs from the lasers are equally spaced in frequency.

7554-50, Session 8

Compact ultrafast reflective Fabry-Perot tunable lasers for OCT imaging applications

M. Kuznetsov, W. Atia, B. Johnson, D. C. Flanders, Axsun Technologies Inc. (United States)

We demonstrate novel reflective Fabry-Perot tunable lasers (RFPTL) for fast swept-source OCT imaging applications. This external cavity semiconductor laser uses silicon micro-electro-mechanical system (MEMS) tunable Fabry-Perot filter in a novel reflective mode of operation. The laser is packaged in a compact 25x15 mm fiber-pigtailed butterfly package. Lasers at 1060 and 1300 nm wavelengths have been demonstrated with tuning ranges up to 140 nm, fast scan rates of 100 kHz, and coherence lengths greater than 13 mm. We also describe OCT imaging with these lasers. RFPTL lasers with 1-2 μ m wavelengths and tuning ranges of 250 nm have also been demonstrated for a wide range of applications.

7554-51, Session 8

High-frequency driving vs. buffering: scaling the sweep speed of Fourier domain mode locked (FDML) lasers

B. R. Biedermann, W. Wieser, C. M. Eigenwillig, T. Klein, R. A. Huber, Ludwig-Maximilians-Univ. München (Germany)

The sweep rate of FDML lasers is limited by the mechanical response of the intra-cavity bandpass filter. We investigate two different approaches to push the sweep speed of the laser beyond 700kAscans/sec and demonstrate high quality OCT imaging. The first method is to choose a higher filter drive frequency, away from its mechanical resonance. The second method is to increase the filter drive amplitude and to time multiplex the sweep ("buffering"). For both techniques, OCT relevant parameters like coherence, sensitivity and noise are measured, compared and discussed. OCT imaging with sweep durations of 1.3µs/A-scan and 110nm sweep range is demonstrated.

7554-52, Session 8

Fiber-based swept source at 1060 nm using a tapered amplifier

S. Marschall, C. Pedersen, P. E. Andersen, O. B. Jensen, Technical Univ. of Denmark (Denmark); K. Hsu, Micron Optics, Inc. (United States); B. Sumpf, K. Hasler, G. Erbert, Ferdinand-Braun-Institut für Höchstfrequenztechnik (Germany)

Swept source-OCT at 1060 nm has become a valuable tool especially for ophthalmology. Conventional semiconductor optical amplifiers, the preferred gain media for swept sources, can only provide low saturation power in this wavelength range. As an alternative, we propose the use of a tapered amplifier, a semiconductor gain medium with a narrow waveguide section where a single-mode light field is generated and a slowy broadening section that subsequently boosts the output power while maintaining the mode-profile. These devices can provide high output power and good beam quality, and are hence suitable to be integrated in a fiber-based light source. We demonstrate the feasibility of a tapered amplifier in a fiber-based frequency-swept laser. Using a device with an ASE bandwidth of 22 nm, sweep operation with a range of 25 nm is possible at a repetition rate of 1 kHz with an average output power of 12 mW. If required, the power can be increased by coupling a larger fraction of light out of the resonator. Point spread functions generated in a Michelson interferometer show a slow sensitivity roll-off of 8 dB for 15 mm probing depth, which makes this light source interesting for applications that require a long depth range. The proof of principle looks promising, and further investigations will address tapered amplifiers



with broader gain bandwidth in order to increase the depth resolution for OCT applications, as well as optimization of the laser cavity for higher sweeping speeds.

7554-53, Session 8

Ultrabroadband Fourier domain mode locked swept source based on dual SOAs and WDM couplers

J. Zhang, G. Liu, Z. Chen, Univ. of California, Irvine (United States)

A high-speed, ultra-broad band wavelength swept source based on Fourier domain mode-locking (FDML) technique at center wavelength of 1310 nm was demonstrated. Two semiconductor optical amplifiers combined with wavelength-division multiplexing (WDM) couplers were used as the gain media. The laser is capable of FWHM tuning range of more than 180 nm and the edge-to-edge scanning range of more than 220 nm at 100 kHz sweeping rate. With the built swept source, an ultra high resolution FDOCT system was developed.

7554-54, Session 8

Multiband swept laser source for frequency domain optical coherence tomography

J. Jiang, Tianjin Univ. (China); R. Hui, The Univ. of Kansas (United States)

We demonstrated a multiband frequency-swept laser based on wavelength division multiplexing (WDM) and parallel signal processing. Utilizing the periodical spectral lines of an FPI, multiband simultaneous optical frequency scanning can be realized. The laser is constructed with a fiber ring configuration, in which an optical demultiplexer/ multiplexer pair is used to divide the signal wavelength into N wavelength bands, and the width of each band is v. Each wavelength band has a dedicated amplifier to provide the optical gain and avoid the crosstalk between bands. A scanning fiber FPI is used for wavelength selection sweeping. The ring laser output is fed to the interferometer for OCT operation. In order to separate optical signals from different wavelength bands, two identical optical DEMUXs are used such that signal from each wavelength band is detected by a balanced optical receiver. After electrical amplification and digitizing, the data from all wavelength bands are combined for signal processing. For calibration and synchronization purpose, a small portion of the optical signal is taped from a wavelength band and its frequency is monitored by a fixed Mach-zehnder interferometer and a photo detector.

The proposed technique opens the possibility of significantly improved OCT spatial resolution due to the increases optical bandwidth. It also allows parallel signal processing and thus reduces the speed requirement on the ADC and increases the measureable optical path difference between the two interference arms of OCT. In order to demonstrate the feasibility of the proposed WDM-OCT, a proof of concept demonstration was conducted.

7554-55, Session 8

Imaging with novel swept-source OCT system based on integrated thermo-optic tunable laser chip

J. D. Cho, E. J. Jung, M. Y. Jeong, C. S. Kim, Pusan National Univ. (Korea, Republic of); Y. Noh, Chemoptics Inc. (Korea, Republic of); H. Lee, ChemOptics Inc. (Korea, Republic of); M. Oh, ChemOptics Inc. (Korea, Republic of) and Pusan National Univ. (Korea, Republic of)

We experimentally demonstrated OCT images using a swept-source OCT based on novel tunable laser chip. Based on the thermo-optic tuning of a polymer waveguide Bragg reflector, a cost-effective and microminiaturized integrated chip is demonstrated for wavelength swept laser. The photonic integrated chip laser shows more than 19 nm of bandwidth centered at 1532 nm, 0.06 nm instantaneous linewidth, and 5 mW peak output power. The linear response of thermo-optic effect induces continuously corresponding sweep of output lasing wavelength by tuning the repeatedly applied voltage on the micro heater. Utilizing repeated sweeps, each A-line rate is available for cross-sectional OCT imaging from the Fourier domain detection of the interferometric signal through the sample. The bandwidth and repetition rate will be enhanced with better performance of optical emitting source and integrated heating component, respectively.

7554-56, Session 8

Wavelength swept amplified spontaneous emission source at 1060 nm with Yb doped fiber post-amplification

C. M. Eigenwillig, T. Klein, B. R. Biedermann, W. Wieser, R. A. Huber, Ludwig-Maximilians-Univ. München (Germany)

We present a rapidly wavelength swept light source for Optical Coherence Tomography (OCT) at 1060nm. Light alternately passes a cascade of several different amplification elements and optical bandpass filters. A phase-shifted control of the two filters compensates for light transit time. As a last post-amplification step we use a diode pumped Yb doped fiber setup providing improved gain performance. 11 mW average output power are demonstrated for a sweep rate of 2x55 kHz (62 nm full sweep range) and 2x160 kHz (50 nm full sweep range).

7554-57, Session 9

Polarization sensitive optical coherence tomography of melanin provides tissue inherent contrast based on depolarization

B. Baumann, Medical Univ. of Vienna (Austria); S. O. Baumann,

T. Konegger, Vienna Univ. of Technology (Austria); M. Pircher,

E. Götzinger, H. Sattmann, Medical Univ. of Vienna (Austria); M. Litschauer, Vienna Univ. of Technology (Austria); C. K. Hitzenberger, Medical Univ. of Vienna (Austria)

Polarization sensitive optical coherence tomography (PS-OCT) was used to investigate the polarization properties of melanin. Measurements in samples with varying melanin concentrations revealed polarization scrambling, i.e. depolarization. The results indicate that the depolarizing appearance of pigmented structures like, for instance, the retinal pigment epithelium (RPE) is likely to be caused by the melanin granules contained in these cells.

7554-58, Session 9

Full range polarization-sensitive sweptsource optical coherence tomography at 1 um with polarization modulation and BMmode scan

M. Yamanari, S. Makita, Y. H. Lim, Y. Yasuno, Univ. of Tsukuba (Japan) and Computational Optics and Ophthalmology Group (Japan)

We demonstrate full range imaging of polarization-sensitive swept-source optical coherence tomography (PS-SS-OCT) at 1 um wavelength to



measure intensity and phase retardation images of retina without mirror images. Continuous source polarization modulation and BM-mode scan are applied. Since the axes of these modulations are orthogonal, these methods can be applied simultaneously.

The incident state of polarization is modulated by electro-optic modulator sinusoidally at a frequency of 40 MHz during sweeping the wavelength by a light source at a rate of 30 kHz. In addition, BM-mode scan is applied along the transversal scan on the sample using a phase modulator in the reference arm with a phase step of pi/2. Horizontally and vertically polarized components of the interference between the reference and sample beams are detected by two photoreceivers individually and digitized at 100 MS/s.

The measured spectra are demultiplexed for the polarization modulation in the signal frequency domain for each A-scan. Subsequently, the complex conjugate ambiguity is removed using BM-mode scan in the spatial frequency domain. As a result, we obtain all elements of the Jones matrix of the sample without complex conjugate ambiguity. Full range intensity and phase retardation images of retina are demonstrated. Our method can extend the measurable depth range and improve the image quality of polarization-sensitive imaging of retina.

7554-59, Session 9

Single camera polarization sensitive spectral domain OCT by spatial frequency encoding

T. Schmoll, E. Götzinger, M. Pircher, C. K. Hitzenberger, R. A. Leitgeb, Medizinische Univ. Wien (Austria)

Recent developments in polarization sensitive OCT gave important insights into retinal and cardio vascular pathologies. In order to retrieve retardation and optical axis orientation, it is necessary to use amplitude as well as phase information. In the present work we introduce a method that allows for parallel acquisition of orthogonally polarized spectra with a single detector and an electro-optic modulator (EOM). If the EOM is illuminated with linear polarized light at an angle of 45deg with respect to fast axis of the EOM crystal, any modulation introduced by the EOM will only effect the phase of the polarization component that is parallel to the fast axis. The orthogonal component will not be affected by the modulation. Viewing this modulation as spatial carrier frequency we obtain a separation of the spatial spectra of both polarization components. Retardation and optical axis orientation are reconstructed using the relations where illumination of the sample with circularly polarized light is assumed. Such reconstruction allows for a parallel recording of orthogonally polarized signal channels. Proof-of principle using a chromatic quarter wave plate designed for 1300nm as a sample and acquisitions of a piece of borealis, a highly birefringend plastic is provided. Results of the method for in-vivo imaging of a fingertip are presented.

7554-60, Session 9

Polarization-sensitive optical frequency domain imaging based on depolarized light

K. H. Kim, Pohang Univ. of Science and Technology (Korea, Republic of); C. Kerbage, Neuroptix Corp. (United States); B. H. Park, Univ. of California, Riverside (United States); Y. Tu, W. Y. W. Oh, T. Hasan, Wellman Ctr. for Photomedicine (United States); J. F. de Boer, Vrije Univ. Amsterdam (Netherlands)

We present a new method for polarization-sensitive optical frequency domain imaging (PS-OFDI). In this method, a sample is probed with depolarized light, which is composed of two polarization states separated by 180° in the Poincaré sphere with an enough path length difference between them, and the reflected sample states are acquired simultaneously based on the frequency multiplexing scheme. This simultaneous acquisition of two reflection states enables to use depolarized light, because the phase information between the two

polarization states is available, and the full Jones matrix of the sample and the output path can be obtained. The new PS-OFDI system ran at 31K axial scans/s with 3072 pixels per spectrum, and its sensitivity was 98dB. Images of the chicken leg muscle, human finger tip are presented. Lastly a mouse cancer model was imaged to demonstrate that PS-OFDI provides a good contrast to distinguish the cancer and normal tissues.

7554-61, Session 9

High-speed spectral domain polarizationsensitive OCT using a single InGaAs line-scan camera and an optical switch

S. Lee, H. Jeong, B. Kim, Korea Univ. (Korea, Republic of)

We demonstrate high-speed spectral domain polarization-sensitive optical coherence tomography (SD-PS-OCT) using a single InGaAs line-scan camera and a 1 x 2 optical switch. The SD-PS-OCT system was constructed by free-space optics. The horizontal and vertical polarization light rays split by polarization beam splitter were delivered and detected via an optical switch to a single spectrometer by turns instead of dual spectrometers. The SD-PS-OCT system has an axial resolution of 8.2 um, a sensitivity of 101.5 dB, and an acquisition speed of 23,496 A-lines/s.

7554-62, Session 9

Ultrahigh-resolution fiber-based polarization sensitive spectral domain optical coherence tomography

E. Götzinger, B. Baumann, M. Pircher, C. K. Hitzenberger, Medizinische Univ. Wien (Austria)

We developed a fiber based ultra high resolution polarization sensitive spectral domain optical coherence tomography system. The system is based on polarization maintaining fibers and retrieves the backscattered intensity, birefringence and optic axis orientation with only one A-scan per measurement location. In addition a light source with a bandwidth of 100nm was implemented. The setup was used to image the polarization properties of the human retina.

7554-63, Session 10

From controlling the shape of Talbot bands' visibility to improving the sensitivity decay with depth in FD-OCT

A. G. Podoleanu, M. R. Hughes, A. Bradu, D. Woods, Univ. of Kent (United Kingdom)

We present theoretical and experimental studies on the sensitivity variation versus optical path difference (OPD) in Fourier domain spectral interferometry using configurations which produce Talbot bands. Such configurations require that the two interfering beams use different parts of the diffraction grating in the interrogating spectrometer. We show that by manipulating the power distribution within the two interfering beams, the OPD value where maximum sensitivity is achieved can be conveniently tuned, as well as the sensitivity variation with OPD. Furthermore, creating a gap between the two beams leads to adjustment of the minimum detectable OPD value, while the widths of the beams determine the maximum detectable OPD value. These features cannot be explained by theoretical models involving spectrometer resolution elements only. Improvement in the sensitivity variation with depth is demonstrated experimentally.



7554-64, Session 10

Performance of reduced bit-depth acquisition for optical frequency domain imaging

B. D. Goldberg, B. J. Vakoc, Wellman Ctr. for Photomedicine, Massachusetts General Hospital (United States) and Harvard-MIT Div. of Health Sciences and Technology (United States); W. W. Oh, M. J. Suter, Wellman Ctr. for Photomedicine, Massachusetts General Hospital (United States); S. Wasman, M. I. Freilich, Lahey Clinic (United States); B. E. Bouma, G. J. Tearney, Wellman Ctr. for Photomedicine, Massachusetts General Hospital (United States) and Harvard-MIT Div. of Health Sciences and Technology (United States)

High-speed optical frequency domain imaging (OFDI) has enabled wide-field microscopic imaging in the biological laboratory and clinical medicine. The imaging speed of OFDI, and therefore the field of view, of current systems is limited by the rate at which data can be digitized and archived rather than the system sensitivity or laser performance. One solution to this bottleneck is to digitize OFDI signals at reduced bit depths. However, the implications of reduced bit-depth acquisition on image quality have not been studied. In this paper, we use simulations and empirical studies to evaluate the effects of reduced depth acquisition on OFDI image quality. We show that image acquisition at 8-bit depth allows high system sensitivity with only a minimal drop in the signal-to-noise ratio compared to higher bit-depth systems. Images of a human coronary artery acquired in vivo at 8-bit depth are presented and compared with images at higher bit-depth acquisition.

7554-65, Session 10

Sonification of optical coherence tomography data and images

A. Ahmad, S. G. Adie, Y. Wang, S. A. Boppart, Univ. of Illinois at Urbana-Champaign (United States)

Sonification is the process of representing data parameters with audio signals or waveforms. In this manuscript, we describe the auditory presentation of OCT data and images. This conversion will be especially valuable in time-sensitive surgical or diagnostic procedures where it may not be possible to visually interpret or analyze the image-based data in real-time. In these scenarios, auditory feedback can complement visual data without requiring the surgeon to constantly monitor the screen. In this paper we present techniques to translate OCT data and images into sound based on the extracted spatial and Fourier domain properties from the OCT data. Results obtained from parametric mapping sonification of human adipose and tumor tissues are presented which indicate that audio feedback of OCT data may be used for interpretation of OCT images.

7554-66, Session 10

Return to Contents

Non-harmonic analysis for high-resolution optical coherence tomography

C. Chong, A. Morosawa, K. Totsuka, T. Suzuki, Santec Corp. (Japan); X. Cao, S. Hirobayashi, Univ. of Toyama (Japan)

A new processing technique called Non-Harmonic Analysis (NHA) is proposed for OCT imaging. Conventional Fourier-Domain OCT relies on the FFT calculation which depends on the window function and length. Axial resolution is counter-proportional to the frame length of FFT that is limited by the swept range of the swept source in SS-OCT, or the pixel counts of CCD in SD-OCT degraded in FD-OCT. However, NHA process is intrinsically free from this trade-offs; NHA can resolve high frequency without being influenced by window function or frame length of sampled data, i.e. wavelength range in the case of SS-OCT. In this study, NHA

process is explained and applied to SS-OCT imaging and compared with OCT images based on FFT. We apply the nonlinear equation process to convey the calculation of OCT signal using NHA. In order to validate the benefit of NHA in OCT, we carried out OCT imaging based on NHA with three different sample, onion-skin, pig-eye, human skin. The results show that NHA process can realize image quality equivalent to 100nm swept range by only using less than half-reduced wavelength range, and it also implies the potential of ultra-high resolution imaging capability without the need of an ultra-broadband source.

7554-67, Session 10

Resolution improvement in optical coherence tomography by step-frequency encoding

E. Bousi, I. Charalambous, C. Pitris, Univ. of Cyprus (Cyprus)

A novel technique for axial resolution improvement of Optical Coherence Tomography (OCT) systems is presented. The technique is based on step-frequency encoding of the OCT signal, using frequency shifting. A resolution improvement by a factor of ~ 7 is achieved without the need for a broader bandwidth light source. This method exploits a combination of two basic principles: the appearance of beating, when adding two signals of slightly different carrier frequencies, and the resolution improvement of OCT images by deconvolution of the interferogram with the encoded source autocorrelation function. In OCT, step-frequency encoding can be implemented by performing two A-scans, with different carrier frequencies and subsequently adding them to create the encoded signal. Deconvolution of the resulting interferogram, using appropriate kernels, results in a narrower resolution width when the frequency steps are appropriately selected.

7554-68, Session 10

Twofold improvement in axial resolution of optical coherence tomography by four-pass sample probing

M. Sylwestrzak, E. A. Kwiatkowska, P. Targowski, Nicolaus Copernicus Univ. (Poland)

In this contribution a proof of concept for the alternate way of twofold increasing the axial resolution of Optical Coherence Tomography systems is shown. On the contrary to expanding the bandwidth of the light source, the number of passes of light between sample and the Michelson interferometer is increased. In two simplified novel configurations of Spectral OCT devices designed for this research, the interferometer is equipped with polarization controlling elements in order to force light to pass the distance from the beam splitter to the sample four times: during the first pass the initial liner polarization of the probing beam is converted to the perpendicular component and on return to the interferometer deflected by the polarization sensitive beam splitter towards the additional mirror reflecting it back to the sample. After the second pass the state of polarization is changed again and restored to the initial one in order to interfere with the reference beam. As a result in both set-ups optical paths difference between both arms of the Michelson interferometer is twofold longer comparing to the standard system. This results in two times smaller axial calibration coefficient and finally twofold increase of an effective axial resolution for the same coherence length of the light source. In the paper the experimental evidences are given and limitations of the method discussed.

115

TEL: +1 360 676 3290 · +1 888 504 8171 · customerservice@spie.org



7554-69, Session 11

Magnetomotive optical coherence tomography for in vivo molecular imaging of mammary tumors using targeted magnetic nanoprobes

R. John, R. Rezaeipoor, S. G. Adie, E. J. Chaney, B. P. Sutton, M. Marjanovic, A. Oldenburg, S. A. Boppart, Univ. of Illinois at Urbana-Champaign (United States)

In this study, we report for the first time, in vivo imaging of functionally targeted magnetic iron oxide nanoparticles (MNPs) using magnetomotive optical coherence tomography (MM-OCT) in a rat mammary tumor model. These specially engineered super paramagnetic iron oxide nanoprobes have multifunctional capabilities enabling them to be used as molecular agents in magnetic resonance imaging (MRI), MM-OCT, and magnetic drug targeting applications. The dextran-coated iron oxide nanoparticles were functionalized with anti-epidermal growth factor receptor type 2 (anti-HER2) antibody to target the HER2 receptor, which is over expressed in about 30% of human invasive breast carcinomas. In vivo imaging using MM-OCT demonstrates accumulation of antibodyconjugated nanoparticles in only mammary tumors, whereas nontargeted nanoparticles show a weak biodistribution in lungs and liver and do not show any specific accumulation in mammary tumors. In vivo MRI of the rats performed before and after injection of targeted iron oxide nanoparticles show changes in T2* contrast, confirming the accumulation and multimodal imaging of these iron oxide nanoparticles. Biodistribution studies confirm the accumulation of targeted nanopartcles in tumors with sizes up to ~1.5 cm.

7554-70, Session 11

The development of pump-probe optical coherence microscopy

Q. Wan, B. R. Applegate, Texas A&M Univ. (United States)

We have developed a novel subcellular molecular imaging technique based on the fusion of Pump-Probe absorption spectroscopy and Optical Coherence Microscopy (OCM). Pump-probe absorption spectroscopy is a well established tool in molecular physics for measuring the spectrum and dynamics of molecular species which are poor fluorophores. OCM combines the scattered light rejection of low coherence interferometry with confocal microscopy to enable subcellular resolution deep in highly scattering tissue. Their fusion, Pump-Probe Optical Coherence Microscopy (PPOCM), is able to image chromophores with subcellular resolution deep in highly scattering tissue. The PPOCM signal is detected as an amplitude modulation of the OCM signal hence each scan results in the acquisition of two images, the reflectance (OCM) image and the molecular (PPOCM) image. We have demonstrated the prototype system on a fixed human skin sample containing a nodular melanoma. The results indicate that PPOCM can clearly provide strong contrast between the melanotic and amelanotic regions. Potential applications of PPOCM imaging of melanin include the early diagnosis of melanoma and the mapping of tumor margins during excision. While we have demonstrated the prototype PPOCM system on melanin the technique may in general be applied to any biological chromophore with a known absorption spectrum.

7554-71, Session 11

Magnetomotive optical coherence elastography for relating lung structure and function in cystic fibrosis

R. K. Chhetri, J. Carpenter, R. Superfine, S. H. Randell, A. L. Oldenburg, The Univ. of North Carolina at Chapel Hill (United States)

Cystic fibrosis is a genetic defect in the cystic fibrosis transmembrane conductance regulator protein and is the most common life-limiting genetic condition affecting the Caucasian population. It is an autosomal recessive, monogenic inherited disorder characterized by failure of airway host defense against bacterial infection, which results in bronchiectasis, the breakdown of airway wall extracellular matrix (ECM). Using externally controlled magnetic nanoparticles as force transducers, magnetomotive optical coherence elastography (MMOCE) is employed to study the internal microscopic deformations associated with bronchiectasis. We hypothesize that several factors contribute to ECM breakdown which are linked to bacterial colonization, including the excretion of microbial proteases, activation and migration of neutrophils and their production of neutrophil activating factors and matrix metalloproteinase (MMP) activity by the epithelial cells. To non-invasively access ECM remodeling, we use in vitro models consisting of human tracheo-bronchial-epithelial (hBE) cells grown on porous supports at an air-liquid interface. It is shown that MMOCE can reveal the elastic properties of the electrospun in vitro scaffolds, and that OCT can visualize the epithelial cell cultures similar to histology but non-destructively. Correlative studies using OCT examined the morphology of ex vivo CF and non-CF lung tissues. These studies will result in improved understanding of the major pathologic changes in CF lung structure and function, and may lead to new in vivo imaging and elastography methods to monitor disease progression and treatment.

7554-72, Session 11

Overcoming barriers in topical administration of gold nanoparticles for optical coherence tomography using multimodal delivery

C. S. Kim, P. Wilder-Smith, Y. Ahn, L. L. Liaw, Z. Chen, Beckman Laser Institute and Medical Ctr. (United States); Y. J. Kwon, Univ. of California, Irvine (United States)

Optical coherence tomography (OCT) is a non-invasive imaging modality with higher resolution than other conventionally practiced diagnostic techniques. However, its low achievable contrast level in biological tissues limits the use of OCT in detecting early-stage cancer with pinpointed accuracy, which can be improved by employing optical contrast agents. Gold nanoparticles (Au NPs) can be a promising contrast agent because they are easy to synthesize into a desired size and shape and possess optical properties suitable for OCT, such as high light scattering and surface plasmon resonance (SPR) effects, which could help differentiate early-stage cancer lesions from normal tissue. While topical delivery of Au NPs offers many advantages, including significantly lower systemic toxicity and dosage, poor penetration and distribution of Au NPs in tissue are major barriers, which were attempted to be overcome in this study. It is hypothesized that Au NPs are able to penetrate through micropassages created by microneedles and distributed by ultrasound afterwards (multi-modal delivery). Enhanced penetration and distribution of Au NPs via multi-modal topical delivery were proven to overcome two major barriers in topically administering Au NPs using an in vivo oral dysplasia hamster models (overall 150% enhanced contrast). This talk will also present an expanded progress on a highly efficient and versatile Au NP-releasing microneedle platform for multi-modal delivery of Au NPs.

7554-73, Session 11

Tissue differentiation in human lymph nodes using parameterized optical coherence tomography

R. A. McLaughlin, L. Scolaro, The Univ. of Western Australia (Australia); P. Robbins, PathWest Lab. Medicine WA (Australia); C. Saunders, Sir Charles Gairdner Hospital (Australia) and The Univ. Western Australia (Australia); S. L. Jacques, Oregon Health & Science Univ. (United States); D. D. Sampson, The Univ. of Western Australia (Australia)



This paper presents a method to construct parametric images from a 3D-OCT data set. By modeling the rate of signal attenuation within an A-scan, the algorithm estimates the local tissue attenuation coefficient. Calculating this value automatically for each A-scan, it is possible to construct a 2D parametric en-face image, where the parameter value indicates the underlying tissue type. The algorithm is demonstrated on ex vivo human lymph nodes, both normal and cancerous, and validated against a histological gold standard. Results demonstrate variation in attenuation between adipose, lymph cortex and stroma, and between cancerous and healthy tissue.

7554-74, Session 11

Reconstruction of absorption profiles of indocyanine green using spectral OCT

S. Tamborski, D. Bukowska, M. Szkulmowski, I. Grulkowski, A. Kowalczyk, M. Wojtkowski, Nicolaus Copernicus Univ. (Poland)

In Spectral Optical Coherence Tomography (SOCT) in-depth information about the object structure is encoded in a spectral fringe signal produced at the output of an interferometer system and collected by a spectrometer with a multipixel photodetector. By taking advantage of high imaging speed, high sensitivity and high resolution of this technique it has been already successfully applied to structural imaging of the anterior eye and retina in three dimensions. Moreover, the OCT fringe signal enables diverse functional analysis of biomedical objects. Since now, functional OCT research have been conducted mostly in the field of flow analysis. Another important issue for functional studies is depth resolved extinction which can provide information about relative variation of the chemical content in measured tissue and thereby be useful for example in determination of the blood oxidization level. Joint Spectral and Time domain OCT method proposed by our group enables simultaneous calculation of flow velocity and depth and wavelength dependent extinction from the same measurement outcome. Moreover, in particular experimental setup the method shows potential to distinguish between absorption and scattering contributions to extinction. This information can be relatively easily derived when the OCT signal is constructed with light reflected from the surfaces within the sample. Far more complex case is when light is just scattered by the object, as it is usual when the latter is turbid biological tissue. This contribution contains the detailed description of the method dealing with this problem followed by the demonstration and comments on experimental results.

7554-75. Session 11

Monitoring small changes in blood hematocrit using phase sensitive spectral domain optical coherence tomography

K. V. Larin, V. G. R. Manne, Univ. of Houston (United States)

A new method for monitoring ultra-small changes in blood hematocrit (~0.2%) based on measurement of refractive index changes in vitro using Phase Sensitive Spectral Domain Optical Coherence Tomography modality (PhS-SDOCT) is introduced. The developed system has an axial resolution of ~8 μm , phase sensitivity of ± 0.01 radians, imaging depth of 3.4 ± 0.01 mm in air, and image acquisition speed of 29 kHz. The experimental accuracy for monitoring refractive index changes as a function of hematocrit level in blood is found to be $\pm 1.5 \times 10^{-4}$ ($\pm 0.2 \%$). Obtained results indicate that the PhS-SDOCT can be used to monitor ultra-small changes in the hematocrit and in vitro and, potentially, in tissue blood vessels in vivo.

7554-77, Session 12

Dark-field optical coherence microscopy

C. Pache, M. L. Villiger, T. Lasser, Ecole Polytechnique Fédérale de Lausanne (Switzerland)

Over the past years, many solutions have been proposed to produce phase quantitative images of biological cell samples. Among these, Spectral Domain Phase Microscopy combines the fast imaging speed and high sensitivity of Optical Coherence Microscopy (OCM) in the Fourier domain with the high phase stability of common-path interferometry. We report on a new illumination scheme for OCM that enhances the sensitivity for backscattered light and detects the weak sample signal, otherwise buried by the signal from specular reflection. With the use of a Bessel-like beam, a dark-field configuration was realized. Sensitivity measurements for three different illumination configurations were performed to compare our method to standard OCM and extended focus OCM. Using a well-defined scattering and reflecting object, we demonstrated an attenuation of -40 dB of the DC-component and a relative gain of 30 dB for scattered light, compared to standard OCM. In a second step, we applied this technique, referred to as darkfield Optical Coherence Microscopy (dfOCM), to living cells. Chinese hamster ovarian cells were applied in a drop of medium on a coverslide. The cells of ~15 µm in diameter and even internal cell structures were visualized in the acquired tomograms.

In conclusion, this work demonstrates that Bessel-like beams can find application in OCM not only for extended depths of field but also to improve the sensitivity. With dfOCM, tomograms of backscattered light from living cells were obtained, revealing internal cell structures and providing complementary information to the optical path length measurements of common phase microscopy methods.

7554-78, Session 12

Ultrahigh-speed phase mapping at 512,000 A-scan rate with line field Fourier domain optical coherence tomography

B. Grajciar, Medical Univ. of Vienna (Austria); Y. Lehareinger, ETH Zurich (Switzerland); A. F. Fercher, R. A. Leitgeb, Medical Univ. of Vienna (Austria)

We present a new ultra high speed parallel (line-field) FD-OCT method for phase mapping employing 2D CMOS detector technology operating at equivalent 512,000 Hz. A single tomogram is captured in one single exposure with no additional lateral scanning device and therefore the structure is free of any motion artifacts and we can observe excellent transversal phase stability. The high speed is exploited by phase sensitive assessment changes of refractive indices of solutions by ultra fast recording of injection processes for observing the mixing and interaction between phases and/or particles of different liquids.

7554-79, Session 12

Crosstalk rejection in full-field optical coherence tomography using spatially incoherent illumination with a partially coherent source

A. Z. Dhalla, J. Migacz, J. A. Izatt, Duke Univ. (United States)

The recent advent of ultra high frame rate cameras gives rise to the possibility of constructing swept source full-field OCT systems with achievable volume rates approaching 10Hz and net A-scan rates approaching 10MHz. Unfortunately, when illuminated with partially coherent light, full-field OCT in turbid media suffers resolution and SNR degradation from coherent multiple scattering, a phenomenon commonly referred to as crosstalk. As a result, most FFOCT systems

117

Return to Contents TEL: +1 360 676 3290 · +1 888 504 8171 · customerservice@spie.org



employ thermal sources, which provide spatially incoherent illumination to achieve crosstalk rejection. However, these thermal sources preclude the use of swept source lasers. In this work, we demonstrate the use of a carefully configured FFOCT system employing a multimode fiber in the illumination arm to reduce the spatial coherence of a partially coherent source. By reducing the coherence area below the system resolution, the illumination becomes effectively spatially incoherent and crosstalk is largely rejected. We compare FFOCT images of a USAF test chart positioned beneath both transparent and turbid phantoms using both illumination schemes.

7554-80, Session 12

Breast cancer surgery and full-field OCT in the operating room

B. Sigal-Zafrani, Institut Curie (France); S. Gigan, Ecole Supérieure de Physique et de Chimie Industrielles (France); B. De Poly, O. De Witte, LLTech (France); C. Brossollet, Ecole Supérieure de Physique et de Chimie Industrielles de la Ville de Paris (France); C. Boccara, Ecole Supérieure de Physique et de Chimie Industrielles (France)

Full Field OCT (FFOCT) images allow an easy comparison with histological sections, nevertheless they are limited to about 1mm2 whereas histological sections expand typically over 0.1 to 1 cm2. The pathologist being used to explore a large number of scales from cm down to μm in order to achieve realistic comparisons we stitched images to display a significant field of view.

"Virtual sectioning" of normal and cancerous tissues as well as the histological sections of the same samples have been performed on colons, breast tumors, lymph nodes etc. it appears that the same structures are easily identified in both kinds of images down to the cellular level.

We thus started to explore the FFOCT ability to become a useful complementary tool for pathologists working on breast cancer diagnostics.

Current per surgery tumor margins and sentinel breast lymph node analysis are usually performed in two steps: the pathologist makes a rapid "macroscopic" observation in the operating room; in parallel on one frozen tissue section a microscopic analysis is performed, leading to a first diagnosis concerning the presence of cancer cells. Then, in case of negative answer, the rest of the tumor or of the axillary nodes are preserved for serial sectioning and specific colorations for a careful search of cancer cells. In case of positive diagnosis (from 10 to 40 % of the cases) a re-operation is scheduled. Our program intends to reduce the re-operation rate by allowing the pathologist to get within a time interval of 15 minutes a cellular resolution view of the suspected areas. This FFOCT does not aim to replace the scheduled examinations but hopefully will complement efficiently the per-operatory diagnostic.

7554-81, Session 12

Low-coherence enhanced backscattering imaging with simultaneous multiple spatial filters

J. Liu, Z. Xu, Y. L. Kim, Purdue Univ. (United States)

In conventional optical coherence tomography and confocal microscopy, spatial gating such as low-coherence gating and optical-sectioning is the key element to eliminate background intensity caused by out-of-focus scattered light. To achieve an alternative yet effective approach for spatial gating without mechanical pinhole scanning, we take advantage of the intrinsic property of low spatial coherence illumination and the self-interference effect of low-coherence enhanced backscattering (LEBS). The unique combination of low spatial coherence illumination and differential angle imaging permits the implementation of multiple independent virtual pinholes into an imaging platform, which in turn offers

self-generated optical-sectioning to the subsurface in a relatively large area (our imaging approach is hereafter referred to as LEBS imaging). Indeed, resolution and contrast improvements in LEBS imaging have analogy with confocal (or pinhole) gating such that resolution and contrast obtained from confocal microscopy are better than those from conventional microscopy. We further make use of sensitivity of light scattering spectroscopy to capture subtle alterations in size and density of internal structures of samples. We demonstrate that our novel spectroscopic imaging platform substantially minimizes cross-talk among adjacent pixels, rejects the background light caused by out-of-plane scattered light, and thereby enhances image contrast and resolution. Given that LEBS is one of the most robust interference phenomena in light scattering, the key characteristics in LEBS spectroscopic imaging may have the potential for widespread utilization in tissue imaging and histopathological guidance. In addition, our approaches could potentially be used to develop wide-field optical coherence tomography for large tissue areas.

7554-82, Session 12

Double common-path phase microscopy for the use of high numerical aperture objective lens

J. S. Park, H. D. Kim, M. Y. Jeong, C. Kim, Pusan National Univ. (Korea, Republic of)

We demonstrate a novel phase-sensitive optical coherence microscopy system based on double common-path interferometer configuration. Conventional single common-path phase microscopes have suffered the spatial resolution problem by using low numerical aperture objective lens for the simultaneous focus of the sample and the reference reflector. We introduce new interferometer scheme to overcome those limitations by adding a tunable common-path optical delay line. Since our double common-path interferometer is flexible to change the distance between sample and reference reflector, it is easily permitted to use high numerical aperture microscope objectives. As it is also possible to enhance the spatial resolution and phase stability, we demonstrate the experimental comparison results of nanometer scale profiling of sample surface using the wavelength-swept light source and Fourier domain detection for rapid phase measurement. Displacement sensitive surface profile is experimentally measured using the sample of a U.S. Air Force resolution target. It will be possible to measure more accurate displacement sensitivity by using higher NA objectives and reducing detection noise further

7554-83, Session 12

The role of a detector dead time in phaseresolved Doppler analysis using spectral domain optical coherence tomography

J. Walther, P. Cimalla, E. Koch, Technische Univ. Dresden (Germany)

We have recently shown that for any oblique sample movement containing a transverse velocity component, the prevalent classic Doppler model assuming that the phase shift is proportional to the axial velocity component is erroneous for spectrometer-based FD OCT. While the previous derivation assumed a continuous integration of the photocurrent, we extend the new Doppler model for detectors with a shutter control by taking the detector dead time into account. Because an analytical solution for the new relation between phase shift and oblique sample displacement can not be given, numerically calculated universal contour plots, which are valid for any center wavelength and beam size, are presented for detector dead times ranging from 5% to 90%. The theoretical results were verified by using a flow phantom model. We have shown theoretically and experimentally that for small Doppler angles between the transverse and the flow direction and small detector dead times the discrepancy to the assumed linear relationship





may be dramatic. Compared to systems with a duty cycle of 100%, the average phase shift does not approach a constant value for large transverse displacements and high sample velocities. In contrast, at large detector dead times and with this small integration times, the numerically simulated phase shift corresponds almost to the assumed one according to the classic Doppler model for the investigated velocity range. With these findings, the question of whether a detector dead time at a constant A-scan rate will be beneficial for the Doppler flow measurement is addressed in this study.

7554-84, Session 12

Sub-cellular resolution imaging with Gabor domain optical coherence microscopy

P. Meemon, CREOL, The College of Optics and Photonics, Univ. of Central Florida (United States); K. Lee, The Institute of Optics, Univ. of Rochester (United States); S. Murali, CREOL, The College of Optics and Photonics, Univ. of Central Florida (United States) and General Optics (Asia) Ltd. (India); I. Kaya, CREOL, The College of Optics and Photonics, Univ. of Central Florida (United States); K. P. Thompson, Optical Research Associates (United States); J. P. Rolland, CREOL, The College of Optics and Photonics, Univ. of Central Florida (United States) and The Institute of Optics, Univ. of Rochester (United States)

To achieve an axially and laterally high resolution OCT image, Optical Coherence Microscopy (OCM) that used a high NA microscope objective in the sample arm was proposed. An increase in NA however leads to a dramatically decreased depth of focus (DOF) and hence shorten an imaging depth range so that high lateral resolution is maintained only within a small depth region close to the focal plane. Consequently, to increase the depth of imaging while keeping a high lateral resolution, dynamic-focusing (DF) was introduced. We have recently presented and quantified a solution for high invariant resolution imaging using a liquid lens embedded variable focusing element within a fixed optics handheld custom microscope. In this paper we demonstrate the details how the portions of the in-focus cross-sectional images can be extracted and fused to form an invariant lateral resolution image with multiple cross-sectional images acquired corresponding to a discrete refocusing step along depth enabled by the DF probe. The combination of the automatic C-mode acquisition accommodated by the DF objective optics and the sliding-window based fusing mechanism that builds on the Gabor transform is referred to as Gabor domain OCM (GD-OCM). We demonstrate sub-cellular resolution imaging of an African frog tadpole (Xenopus Laevis) taken from a 500 µm x 500 µm cross-sectional portion. The first skin in vivo image will be shown with high speed GD-OCM.



Sunday-Tuesday 24-26 January 2010 • Part of Proceedings of SPIE Vol. 7555 Advanced Biomedical and Clinical Diagnostic Systems VIII

7555-01, Session 1

Development of a multimodal tissue diagnostic system combining time-resolved fluorescence spectroscopy, high-resolution ultrasound, and photoacoustic imaging

Y. Sun, Y. Sun, D. N. Stephens, H. Xie, M. Lam, Univ. of California, Davis (United States); J. M. Cannata, Univ. of Southern California (United States); G. Farwell, Univ. of California, Davis (United States); K. Shung, Univ. of Southern California (United States); L. Marcu, Univ. of California, Davis (United States)

We report the research for development and validation of a multimodal tissue diagnostic technique, which combines three complementary techniques into one system: time-resolved fluorescence spectroscopy (TRFS), ultrasonic backscatter microscopy (UBM), and photoacoustic imaging (PAI). Distinct chemical, structural, and functional features of bio-systems can be simultaneously extracted by the fusion of these three methods. A novel compact combined probe was designed integrating a 3.5 µm single mode fiberoptic (excitation for PAI), a miniature 40 MHz angle ultrasound transducer (for UBM and PAI), and a multimode 600 µm fiberoptic (for TRFS). Fluorescence was induced with a nitrogen laser (337 nm, pulse width 800 ps, 2 µJ/pulse, 30 Hz), detected by a gated MCP-PMT, and recorded by an oscilloscope (20 Gs/s, bandwidth 2.5 GHz) with the overall time resolution of 300 ps. Ultrasonic backscatter signals were detected by the transducer, amplified with a low noise amplifier by 35 dB, and recorded by a fast digitizer (400 Ms/s). Photoacoustic signals were excited by a Nd:YAG laser (532 nm, pulse width 8 ns, 20 Hz), and acquired by the shared UBM receiving circuit, showing substantial contrast for the distribution of optical absorbers. The system performance was evaluated with multimodal physical and biological tissue phantoms, and in vivo hamster buccal pouch model of carcinoma induced by 7,12-Dimethylbenz[a]anthracene. The ability for the multimodal system to derive biochemical and microanatomical information from tissue and to evaluate the tumor angiogenesis, for the discrimination between healthy tissue, early lesion, and malignant tumor will be reported.

7555-02, Session 1

Clinically compatible instrumentation for accurate detection of fluorescence intensity and lifetime in turbid media

C. Chang, W. Lloyd, R. Wilson, Univ. of Michigan (United States); G. Gillispie, Fluorescence Innovations (United States); M. Mycek, Univ. of Michigan (United States)

Fluorescence wavelength-time matrices (WTMs) consist of fluorescence decay curves collected over a range of emission wavelengths. The information-rich nature of WTM data shows promise for a variety of biomedical optics applications. Here we report data collected with a specialized transient digitizer, high repetition rate microchip laser sources, and fiber optic light delivery and collection for rapid remote sensing in tissue-simulating phantoms. The instrumentation is highly suitable for eventual translation to a clinical setting owing to the speed of data acquisition and small footprint.

Tissue-simulating phantoms that replicate intrinsic optical properties in a controlled manner were used for quantitative studies of photon transport in turbid media. One set of phantoms was composed of varying concentrations of polystyrene microspheres embedded in a fluorescent gelatin matrix. A second set of phantoms was composed of varying concentrations of fluorescent microspheres embedded in a

collagen gel matrix. Ranges for data acquisition time and instrument sensitivity were determined by measuring WTMs from these phantoms for varying scattering and absorption coefficients. The accuracy of the instrumentation and the phantoms was determined by comparison of the collected WTMs with the results of Monte-Carlo simulations of time- and wavelength-resolved fluorescent light propagation in turbid media.

7555-03, Session 1

Using Raman spectroscopy to detect cervical dysplasia in minority populations

E. Vargis, Vanderbilt Univ. (United States); T. Byrd, Meharry Medical College (United States); D. Khabele, Vanderbilt Univ. (United States) and Meharry Medical College (United States); A. Mahadevan-Jansen, Vanderbilt Univ. (United States)

Cervical cancer is the second most common malignancy among women worldwide. When cervical cancers are detected early, they are highly curable. In fact, early detection of cervical dysplasia using Pap smears and colposcopies has played a central role in reducing the mortality associated with this disease in the US over the last 50 years. However, this trend is not observed across all areas of the US and in countries such as Zambia, where the mortality and prevalence rate of invasive cervical cancer is the second highest in the world. These places have less access to the resources necessary to perform Pap smears and colposcopies. An automated diagnostic method or a "See and Treat" protocol with adequate sensitivity and specificity would significantly improve the management of the disease in any low resource setting. Over the past few years, we have developed an instrument to acquire Raman spectra from the cervix, as well as a sophisticated algorithm to classify tissue as normal (benign or inflammatory), squamous metaplasia, lowgrade dysplasia, or high-grade dysplasia. Previous results on a primarily Caucasian population show that high-grade spectra classify correctly 95% of the time and low-grade classify correctly 74% of the time with a sensitivity of 98% and a specificity of 96%. This study details the results found by using this tool with patients from a more diverse background, with varying socioeconomic and ethnic/racial statuses, showing that this tool will greatly benefit areas where professional care is difficult to achieve, regardless of inherent patient variability.

7555-04, Session 1

Optical fiber guided needle insertion to localize epidural space in porcine

Y. Chang, National Yang-Ming University (Taiwan); C. K. Ting, M. Tsou, P. Chen, K. Chan, Taipei Veterans General Hospital (Taiwan)

Experiments of ex-vivo and in-vivo in porcine were performed to verify that the epidural space could be localized without assistance of additional guidance. In the ex-vivo study the optically reflective spectra of identified porcine tissues were firstly obtained. By which wavelengths of 650 nm and 532 nm were selected to differentiate epidural space and ligamentum flavum. A specially designed hollow stylet that contained optical fibers served for tissue illumination and receiving reflected light from tissue in the in-vivo experiment. The data was real-time displayed on an oscilloscope and stored for analysis. A total of 50 punctures from upper thoracic to lower lumbar regions of spin were done in four 20-kg pigs.

Two-way ANOVA for reflective lights of 650 and 532 nm indicates no significant difference at the different puncture sites for ligamentum flavum and epidural space (all p>0.05). Mean magnitudes for 650 nm and 532 nm and their ratio at epidural space and ligamentum flavum



were 3.565+/-0.194, 2.542+/-0.145, 0.958+/-0.172 and 3.842+/-0.191, 2.563+/-0.131, 1.228+/-0.244 respectively. Paired t test showed that significant differences occurred between epidural spaces and ligamentum flavum in both 650nm (p<0.001), 532nm (p=0.014) and their ratio (p<0.001). Optically feature extraction is the core technique in this study to distinguish different in-vivo tissues. Ultrasonograph has verified that the catheter for anesthetic drug delivery can be correctly placed in the epidural space by using this technique.

7555-05, Session 1

Development of an accurate 3D blood vessel searching system using NIR light

Y. Mizuno, T. Katayama, E. Nakamachi, Doshisha Univ. (Japan)

The health monitoring system (HMS) and the drug delivery system (DDS) requires accurate puncture for the automatic blood sampling. In this study, our objective is to develop a miniature and high accuracy automatic 3D blood vessel searching system. The size of detecting system is 40×25×10 mm. Our detecting systems use a Near-Infrared (NIR) LED light, CMOS camera modules and an image processing unit. We employ the stereo method for the searching system to determine 3D blood vessel location. The blood vessel visualization system adopts hemoglobin's absorption characterization of the NIR light. The NIR LED is set behind the finger and it irradiates Near Infrared light for the finger. CMOS camera modules are set in front of the finger and it captures clear blood vessel images. The two dimensional location of the blood vessel is detected by the luminance distribution of the image and its depth is calculated by the stereo method. A 3D blood vessel location is automatically detected by our image processing system. To examine the accuracy of our detecting system, we carried out experiments using finger phantoms with blood vessel diameters, 0.5, 0.75, 1.0mm, at the depths, 0.5 ~ 2.0 mm, under the artificial tissue surface. Experimental results of depth obtained by our detecting system showed good agreements with the given depths, and the availability of this system is confirmed.

7555-06, Session 2

Comparison of image cytometry and flow cytometry for detection of DNA ploidy abnormalities in Barrett's oesophagus

L. B. Lovat, J. M. Dunn, D. Oukrif, Univ. College London (United Kingdom); P. S. Rabinovitch, Univ. of Washington (United States); S. G. Bown, M. Novelli, Univ. College London (United Kingdom)

Introduction: DNA ploidy abnormalities (aneuploidy/tetraploidy) are strong predictors of future cancer risk in Barrett's oesophagus (BE) as measured by flow cytometry (FC). There is, however, variability in accuracy of diagnosis between laboratories, which may be explained by technical and sampling errors. Image cytometry (IC) is an optical technique allowing visualisation of abnormal nuclei and can be undertaken on archival tissue.

Aim: To compare the accuracy of IC versus FC to detect DNA ploidy abnormalities

Methods: 48 paraffin embedded blocks from 35 patients were retrieved. A nuclear suspension was prepared and separated for IC analysis at UCL and FC at UW. A nuclear monolayer was then prepared and scanned by an automated image cytometric analyzer, which consists of a Zeiss Axioplan 2 microscope, a 546-nm green filter, and a black-and-white, high-resolution digital camera. The digital images of nuclei of interest were stored individually and converted into a series of pixels that were quantified as the integrated optical density (IOD) value, representing the DNA content of the nucleus.

Results: 44 samples were analysed. 91% (40/44) were classified identically. 4 were not concordant;2 aneuploid at UW/diploid at UCL;1 aneuploid at UW/tetraploid at UCL; 1 diploid UW/ aneuploid UCL. Of the

matched cases 67% aneuploid, 9% tetraploid, 24% diploid. There was no significant difference in either the coefficient of variance for the diploid peak or the DNA index of the aneuploid peak between the two methods.

Conclusion: These data demonstrate IC is highly accurate for the detection of DNA ploidy abnormalities against the current gold standard of FC.

7555-07, Session 2

Imaging spectroscopy for substance identification in capillaries using dispersive gel grating Raman and absorption spectrometers

O. Pawluczyk, R. Pawluczyk, P&P Optica Inc. (Canada)

Advances in spectrometer design now allow imaging of separation mixtures directly in capillaries. A novel approach using capillary connected directly to the long entrance slit of a high performance, gel grating transmission spectrometer is described. The direct attachment to the entrance slit of the spectrometer permits very efficient collection of signal, in both Raman and absorption modes. The fluid under investigation enters a capillary and separation techniques such as electrophoresis or isoelectric focusing are used. The high performance, non-scanning spectrometer used for slit imaging permits to capture information regarding both the chemical and dynamic information of the substance under investigation.

A series of tests have been conducted to analyze fluids in capillaries. First, Raman spectroscopy at 785 nm excitation was used for the measurement of biological samples. The Raman spectra of proteins could be identified within the capillary. Spatial information regarding the location of the protein within the focused capillary was also obtained. The experiment showed high sensitivity in identification of similar proteins as both Raman and spatial information could be used. Furthermore, the use of absorption spectrometer for the same samples also provided additional information about the chemical composition.

7555-08, Session 2

Development of a hyperspectral laparoscope system for intraoperative diagnosis of intestinal ischemia

V. R. Sauvage, D. James, K. Koh, T. Wood, D. S. Elson, Imperial College London (United Kingdom)

Intestinal ischemia is characterized by a localized or well-spread insufficient blood supply to the small or large bowel. Spectroscopic techniques have been successfully used to diagnose ischemia by detecting hemoglobin during endoscopic procedures, one of the main constituents of blood and the strongest colon tissue absorber in the visible. However, they cannot easily detect the extent of the ischemic area as they are non-imaging devices. Current imaging techniques may acquire images of anatomic modifications resulting from ischemia but these changes can be caused by other pathologies. Furthermore, these techniques are time-consuming, limiting their intraoperative use. We present here a simple and compact system consisting of a CCD camera and liquid crystal tunable filter which allows for the acquisition of wavelength resolved diffuse reflection images between 400nm and 720nm. It can be easily attached to a standard rigid laparoscope or endoscope, with illumination provided by a Xenon lamp using the incorporated fiber bundle. The whole system is small enough to fit in the sterile sheath usually used to isolate the non-sterile camera of video laparoscopes. Hemoglobin concentrations and oxygen saturations were calculated on a pixel-by-pixel basis using a model which assumes that oxyhemoglobin and deoxyhemoglobin are the only absorbers and which accounts for the scattering properties of the colon. The ability of this hyperspectral laparoscope to image these variations from images acquired at different wavelengths is demonstrated in a) tissue phantoms



and b) in vivo in a porcine model under general anesthesia during an open and a laparoscopic abdominal surgical procedures.

7555-09, Session 2

Real-time hyperspectral endoscope for early cancer diagnostics

R. Kester, L. Gao, T. S. Tkaczyk, Rice Univ. (United States)

Hyperspectral imaging has tremendous potential to detect important early cancer molecular biomarkers such as NADH, FAD, oxy- and deoxy- hemoglobin based on their unique spectral signatures. Several drawbacks have limited their use for in vivo screening applications most notably their poor temporal and spatial resolution, high expense, and low optical throughput. We present the development of a new real-time hyperspectral endoscope capable of addressing these challenges. We call this device the image slicing endoscope or ISE as its principle is adapted from the image slicing technique used in astronomy. The ISE is the first real-time hyperspectral endoscope capable of collecting a 3D (x,y,l) datacube of 200x200x24 without scanning. The parallel, high optical throughput nature of this technique enables the device to operate at frame rates of 5-10 frames per second. The key component of the ISE is the imaging slicing element which is responsible for remapping the initial imaging onto the CCD detector to provide space for the spectral spread. For portability the ISE is designed to be compact using tiny mirrors (< 75 microns in width) for the slicing unit and a miniature array of amici prisms for spectral separation of the remapped image zones. Initial imaging results obtained with our first generation prototype system will be presented.

7555-11, Session 2

Molecular nanoprobes for breast cancer gene diagnostics

H. Wang, T. Vo-Dinh, Duke Univ. (United States)

No abstract available.

7555-12, Session 3

Extracting information from optical coherence tomography images of tissues: signal attenuation and fractal analysis of speckle pattern

D. P. Popescu, C. Flueraru, Y. Mao, S. Chang, M. G. Sowa, National Research Council Canada (Canada)

Although technological advances from the last decade have transformed intravascular optical coherence tomography (OCT) into a strong candidate to be used for guiding intravascular procedures and for assessing vascular conditions, there is still the need to develop reliable procedures for interpreting and extracting the maximum amount of information from OCT images of vascular structures.

In this project, images of rabbit and porcine arterial tissues are acquired using a swept-source Fourier-domain OCT that offers a high imaging speed. The system uses a commercially available fast swept laser with a scanning frequency of 20 kHz, a spectral range of 110 nm centered at 1320 nm and a source power of 10 mW. The setup has a resolution of 7 µm in the axial direction and a measured sensitivity of 107 dB.

The specificity of the OCT measurements is generally based on the variation of gray levels and the images obtained here could be used to identify various arterial anatomical features. Further differentiation of tissue types and structures is desirable and can be done by employing specific scattering properties of various tissue regions. A parameter used to differentiate among tissue types is the attenuation coefficient of the

OCT signal measured between different depth levels. Another parameter introduced in this analysis is the fractal roughness that characterises the texture of the OCT signal generated from various regions of interest. The correlation between the OCT signal attenuation and the texture of probed sample is further studied.

7555-13, Session 3

Full-field OCT and pathology diagnostics

C. Brossollet, Ecole Supérieure de Physique et de Chimie Industrielles (France); B. De Poly, LLTech (France); B. Slgal-Zafrani, Hopital Institut Curie (France); S. Gigan, Ecole Supérieure de Physique et de Chimie Industrielles (France); O. De Witte, LLTech (France); C. Boccara, Ecole Supérieure de Physique et de Chimie Industrielles (France)

We have achieved a large number of significant experiments on various normal and cancerous tissues. Our images allow an easy comparison with histological sections because we are able to explore the same field of view (0.1 to 1 cm2) with the same ultimate resolution (1 μm). Indeed the pathologist being used to explore a large number of scales from cm down to μm in order to achieve realistic comparisons we stitched images to display a significant field of view associated to a large zooming capability.

"Virtual sectioning" of normal and cancerous tissues as well as the histological sections of the same samples have been performed on colons, breast tumors, lymph nodes etc. it appears that the same structures are easily identified in both kinds of images down to the cellular level.

We thus started to explore the FFOCT ability to become a useful complementary tool for pathologists working on breast cancer diagnostics.

Current per surgery tumor margins are usually performed in two steps: a rapid "macroscopic" observation in the operating room leading to a first diagnosis. Then, in case of negative answer, the rest of the tumor is preserved for serial sectioning and specific colorations for a careful search of cancer cells. In case of positive diagnosis (from 10 to 40 % of the cases) a re-operation is scheduled.

Our research program intends to reduce the re-operation rate by allowing the pathologist to get within a time interval of 15 minutes a cellular resolution view of the suspected areas. This FFOCT does not aim to replace the scheduled examinations but hopefully will complement efficiently the per-operatory diagnostic.

We will show a number of demonstrative examples and describe our strategy that intends to make FFOCT a useful complementary tool to pathologists' diagnostic.

7555-14, Session 3

3D-OCT imaging of ex vivo human tissue using a novel rotating needle probe

B. C. Quirk, R. A. McLaughlin, L. Scolaro, The Univ. of Western Australia (Australia); P. Robbins, PathWest Lab. Medicine WA (Australia); C. Saunders, Sir Charles Gairdner Hospital (Australia) and The Univ. of Western Australia (Australia); D. D. Sampson, The Univ. of Western Australia (Australia)

Assessment of lymph node metastasis is the single most important prognostic marker in early breast cancer. Previous work has demonstrated the ability of optical coherence tomography (OCT) to image the micro-architectural structures present in lymph nodes. However, OCT is unable to image deep tissues because of a limited penetration depth of 2-3mm. We have developed a novel rotating OCT needle probe, and used this to acquire 3D images from deep within tissue. Optics for the probe consisted of a single mode fiber terminated with a section of no-core fiber to expand the beam, and multimode fiber to focus the beam. This



was encased in a 22-gauge hypodermic needle (outer diameter 0.71mm). The beam was deflected at 45 degrees by a highly polished copper mirror positioned within the needle, and passed through a small window etched into the needle wall. The probe was mounted on a stepper motor rotating at 2Hz, and a linear translation stage enabling insertion and retraction. The probe was attached to an OCT system with central wavelength of 1320nm and source bandwidth of 154nm. The system was used to image 5 ex vivo samples of human axillary lymph nodes. Fresh tissue was obtained from patients undergoing axillary clearance for breast cancer. Results demonstrated clear distinction between adipose and the lymphocyte-dense cortical tissue. Variations in backscatter within the lymph node body indicated the presence of stromal tissue. Individual fat cells could also be distinguished.

7555-15, Session 3

Quantitative tool for rapid disease mapping in OCT images of a mouse colorectal cancer model

A. M. Winkler, P. F. S. Rice, The Univ. of Arizona (United States); R. A. Drezek, Rice Univ. (United States); J. K. Barton, The Univ. of Arizona (United States)

Optical coherence tomography (OCT) may provide new insight into disease progression and therapy by enabling non-destructive, serial imaging in vivo of mouse cancer models. In previous studies, we have shown the utility of endoscopic OCT for identifying neoplasia in the AOM-treated mouse model of colorectal cancer and tracking disease progression over time. Due to improved imaging speed made possible through Fourier domain imaging, three-dimensional imaging of the entire mouse colon is possible. Increased data enable more accurate classification of tissue but require more time on the part of the researcher to perform manual grading. Here we present a tool based on Fourier domain endoscopic OCT imaging with quantitative software for automatically identifying diseased areas and creating a two-dimensional disease map from a three-dimensional dataset. Furthermore, this algorithm is sensitive to the presence of highly attenuating gold nanoshells and may facilitate functional imaging and therapeutic monitoring. Initial studies have shown the software to have 84% sensitivity and 69% specificity to adenoma, with histology as the gold standard.

7555-16, Session 4

Clinical multiphoton intravital tomography with submicron spatial resolution and spectral fluorescence lifetime imaging for the investigation of skin aging and atopic dermatitis

K. König, J. Müller, R. Bückle, M. Höfer, M. Weinigel, JenLab GmbH (Germany); V. Huck, Westfälische Wilhelms-Univ. Münster (Germany); C. Gorzelanny, Ruprecht-Karls-Univ. Heidelberg (Germany); K. Thomas, T. A. Luger, Westfälische Wilhelms-Univ. Münster (Germany); F. Fischer, Beiersdorf AG (Germany); I. Riemann, F. Stracke, M. Schwarz, Fraunhofer-Institut für Biomedizinische Technik (Germany); M. Kaatz, Friedrich-Schiller-Univ. Jena (Germany); S. W. Schneider, Ruprecht-Karls-Univ. Heidelberg (Germany)

5D intravital multiphoton tomographs with submicron spatial resolution, picosecond temporal resolution, and 10 nm spectral resolution have been developed and employed to investigate human in vivo skin affected with Atopic Dermatitis (AD). Atopic Dermatitis (AD) is an inflammatory disease of human skin. Its pathogenesis is still unknown; however, dysfunctions of the epidermal barrier and the immune response are regarded as key

factors for the development of AD.

Application of the 5D-IVT allowed to distinguish skin affected with AD in an early stage from healthy skin areas by morphological criteria based on two-photon autofluorescence/SHG signals and fluorescence lifetime imaging (FLIM). A characteristic FLIM pattern of AD in dependence on the disease activity measured by SCORAD was found.

Furthermore, young and aged ex vivo and in vivo skin has been studied. Criteria to characterize in vivo skin aging such as the spatially resolved ratio of elastin to collagen have been developed.

Further studies will evaluate the potential of 5D multiphoton tomographs as a diagnostic tool and to monitor the therapeutic efficacy.

7555-17, Session 4

Detection of rheumatoid arthritis in humans by fluorescence imaging

B. Ebert, T. Dziekan, C. Weissbach, J. Voigt, R. Macdonald, Physikalisch-Technische Bundesanstalt (Germany); M. L. Bahner, M. Mahler, M. Schirner, mivenion GmbH (Germany); M. Berliner, HELIOS Klinikum Berlin-Buch (Germany); B. Berliner, HELIOS Research Center (Germany); D. Bauer, HELIOS Klinikum Berlin-Buch (Germany)

Besides clinical parameters there are no imaging modalities with high spatial resolution except contrast enhanced MRI and US which support early diagnosis of rheumatoid arthritis (RA). The major disadvantage of conventional radiography, the most accepted method for the diagnosis of this disease, is its lack of sensitivity in detecting early changes. Typically, RA affects small joints first, and symptoms often appear bilaterally. Precise validation is crucial for treatment efficacy and prediction of therapy success.

In the present study we discuss first results of a prospective study including patients with rheumatoid arthritis and osteoarthritis as well as healthy volunteers. To increase the efficacy of the investigation an optical setup was applied which allowed the imaging of two hands simultaneously after intravenous administration of a bolus of indocyanine green (ICG). Subsequently, the imaging results obtained were compared with the disease activity score (DAS28) and partially with contrast enhanced MRI. Arthritis of the finger joints was classified semiquantitatively on a 4-point scale comparing joint and background signals. In addition, quantitative measurements were performed.

In conclusion, results of the study revealed that sensitive dynamic fluorescence imaging of the non-specific NIR contrast medium (ICG) may be used to differentiate rheumatoid arthritis from osteoarthritis and healthy joints. The temporal behavior as well as spatial distribution of fluorescence intensity are suited to differentiate healthy and inflamed

This work was supported by the European Regional Development Fund (EFRE) and by the Investitionsbank Berlin (IBB).

7555-18, Session 4

High-speed time- and wavelength-resolved fluorescence measurement for dynamic point spectroscopy and lifetime imaging

Y. H. Sun, Y. Sun, D. N. Stephens, H. Xie, J. Phipps, Univ. of California, Davis (United States); D. S. Elson, Imperial College London (United Kingdom); L. Marcu, Univ. of California, Davis (United States)

This work reports the development of simultaneous time- and wavelength-resolved fluorescence spectroscopy (STWRFS) with real-time data acquisition for dynamic tissue characterization ex vivo and in vivo. Different lengths of optical fibers acting as optical delays were combined with multiple dichroics and bandpass filters to produce a STWRFS



system that allows the near real-time acquisition of time-resolved fluorescence spectra using a single detector (sampling rate 20 GHz/s) and excitation laser (337nm/700ps/50Hz, or 355nm/30ps/1MHz). The recording of fluorescence decay profiles at three specified wavelength bands can be completed within microseconds. Using this technique, large human artery specimens (centimeters) were dynamically scanned for discriminating plaque from normal tissue. A dynamic tissue analysis in vivo with a pig artery model was approached using a hand-hold probe including a single optical fiber to deliver laser excitation and collect the fluorescence emission. These results demonstrate the capability of STWRFS as a clinical guiding tool for atherosclerosis diagnosis. Based on the high-speed simultaneous data acquisition, STWRFS also opens the potential for fast multi-color fluorescence lifetime imaging by coupling to a microscope scanning device.

7555-19, Session 4

Cancer diagnostics using spatially resolved fluorescence-based optical imaging

D. Strat, W. S. L. Strauss, R. Hibst, A. Kienle, Univ. Ulm (Germany)

3D reconstruction of position and concentration of fluorophores can be used in diagnostics made over investigation areas within a distance of up to several cm from the tissue surface. Fluorophores emitting between 700 nm and 1100 nm are ideal labels that may preferentially locate and become activated in the target areas. The fluorophores are excited according to the distribution of the incident photons fluence rate in the tissue. The tissue absorbs little and scatters most of the light in this wavelength range, exhibiting a high signal-to-noise ratio of the fluorescence signal. Optical imaging is impaired by the penetration depth of the excitation light and the geometrical restrictions of the detectors. Different wavelengths are dissimilarly scattered and absorbed, therefore offering higher depth resolved resolution than a single wavelength. The higher depth resolution from multiple wavelengths is achieved when at least one of the used wavelengths can penetrate deep enough in the tissue to extract information specific to the required depth.

Forward model: The steady state light propagation through tissue is determined analytically using the diffusion model approximation and the optical properties known a-priori [1].

Analytical solutions of the diffusion model approximation are available for parallelepiped geometry [2].

Inverse problem: Derives the locations of interest, i.e. the fluorophores, within the tissue. The reconstruction method uses the fluence rate distribution calculated with the model of a turbid parallelepiped medium [2]. The luminescent light source can be expressed as a linear combination of unit light sources positioned at each of the nodes in the 3D volume. The numerical 3D reconstruction algorithm extracts the exact locations of the fluorescing light sources by a single step linear calculation [3, 4]. For the simulations that produced the enclosed results, instead of fluorophores, embedded luminescent sources were assumed, with no external illumination. From the mathematical reconstruction point of view, this is no different than reconstructing fluorophores locations. The software program will be extended to use fluorescent light sources instead of luminescent light sources. The calculations will include in the future the reconstruction from a layered media and will be generalised using a Finite Element Model for more complex geometries found in the real environment.

7555-20, Session 4

Wide-field catadioptric system design for endoscopic autofluorescence imaging

R. Wang, Q. Fang, McMaster Univ. (Canada)

Fluorescence endoscopy of the GI system has been identified as a good potential diagnostic tool for dysplasia tissue due to the different fluorescence emission of the malignant areas compared with normal

areas that could indicate a structural change of the tissue. White light imaging based endoscopy is widely available on the market today, but only a handful has fluorescence imaging capabilities. Fluorescence endoscopy is a useful supplement to white light endoscopy since it could act as markers for automated screening of lengthy endoscopic video especially in the case of capsule endoscopy. The auto-fluorescence emission signals resulting from endogenous tissue such as collagen and NADH in the GI tract are very weak. We are currently investigating the feasibility of a wide field approach using catadioptric optics for autofluorescence endoscopy. Catadioptric wide field imaging may be able to provide wide coverage of the GI tract, decent light collection, as well as possible digitally reconstructed low distortion images using unwrapping algorithms specific to the mirror geometries. Our system would have a simultaneous forward looking view that would generate images similar to traditional endoscopy.

7555-21, Session 5

Forward focused scanning magneto-motive optical Doppler tomography

J. Kim, U. Jung, M. Jeon, Kyungpook National Univ. (Korea, Republic of); J. Oh, Pukyong National Univ. (Korea, Republic of); W. Jung, R. John, V. Crecea, S. A. Boppart, Univ. of Illinois at Urbana-Champaign (United States)

We report an upgraded magnetomotive optical Doppler tomography system which allows the application of an external focused magnetic field in the same direction as ODT light. The magnetic generator consists of a solenoid with a hollow cone-shaped ferrite core to increase the magnetic field strength (Bmax=1.5 T, |B|2=220 T2/m) at the tip of the core and focus the magnetic force on targeted samples. The hollow core, containing focusing optics, allows the ODT light to be delivered directly to the imaged sample exposed to the magnetic field. This upgraded system enables thick-tissue imaging, whereas a previous system was limited to only thin samples. We demonstrate novel contrast using magnetic iron oxide nanoparticles (average diameter ~ 100 nm) with magnetomotive optical Doppler tomography (MM-ODT), which combines an externallyapplied temporally-oscillating high-strength magnetic field with ODT to detect magnetic bio-conjugated nanoparticles targeted to cancer cells. Results suggest that MM-ODT may be a promising technique to enhance magnetic nanoparticle contrast for imaging bio-conjugated nanoparticles, particularly in biological fluids.

7555-22, Session 5

Step-FMCW signaling and target detection for ultrasound imaging systems with conformal transducer arrays

S. Natarajan, Univ. of California, Los Angeles (United States); R. S. Singh, Univ. of California, Santa Barbara (United States) and Univ. of California, Los Angeles (United States); M. Lee, B. P. Cox, Univ. of California, Los Angeles (United States); M. O. Culjat, Univ. of California, Los Angeles (United States) and Univ. of California, Santa Barbara (United States); H. Lee, Univ. of California, Santa Barbara (United States); W. S. Grundfest, Univ. of California, Los Angeles (United States)

This paper presents the use and evaluation of stepped frequency modulated continuous waves (FMCW) in a conformal ultrasound array-based medical imaging system currently in development. Conventional medical ultrasound systems featuring rigid transducer arrays are highly user-dependent and require manual rotation and translation to identify and image landmarks. Conformal ultrasound arrays have a larger aperture that can follow the surface curvature of the body, thereby enabling increased data capture without mechanical scanning. The complexity of image reconstruction in conformal ultrasound necessitates the use



of step-FMCW, since it directly captures the frequency space thereby enabling image reconstruction techniques to operate directly on the data, greatly simplifying and allowing for real-time performance. Further, FMCW is advantageous in general since it requires lower peak power and produces better receiver noise characteristics than conventional pulse-echo signaling.

In the proposed stepped FMCW signaling, packets of acoustic waves at stepped frequencies are emitted from transducers sequentially. Phase and magnitude information from each transmitter-receiver pair of the array are captured producing the frequency space representation of the conventional A-scan data.

The experimental results comprise of bistatic data produced by both pulse-echo and step-FMCW signaling methods, and obtained using the conformal ultrasound transducer on soft-tissue phantoms with stationary metal targets. Data from both sets of experiments were compared for target detection and signal-to-noise ratio (SNR). Due to the previously described advantages, step-FMCW exhibited higher SNR and gave accurate target detection, thereby demonstrating its viability in a conformal ultrasound array and imaging system. This signaling mode is also being investigated for volumetric imaging using conformal arrays.

7555-23, Session 5

Imaging fine vascular details with no contrast agent injection by the Retinal Function Imager

A. Grinvald, Weizmann Institute of Science (Israel); D. A. Nelson, D. Izhaky, Z. Burgansky-Eliash, A. Ruf, H. Barash, Optical Imaging Ltd. (Israel)

Purpose: Fluorescein Angiography (FA), is widely used to image the ocular vasculature after contrast agent injection. The goal here was to develop a Retinal Function Imager (RFI) that will be using the hemoglobin as an intrinsic contrast agent. We tested if this novel method can display detailed maps of the retinal vasculature, particularly capillaries, equivalent to the FA results, noninvasively.

Methods: Multiple retinal image series (8 images, 55 Hz) were acquired from all participants, after registration, pixel value distribution parameters in high spatial frequencies were analyzed to locate RBC motion, thus tracing microvasculature in fine detail.

Results: The RFI perfusion maps reveals microvascular detail, in as much and often greater detail than FA images. Areas of capillary non-perfusion and the foveal avascular zone are sharply delineated in the RFI map shown

Conclusions: The capillaries perfusion maps thus obtained offer a good anatomic capillary map that is at least equivalent to the FA images. The production of perfusion maps is noninvasive, comfortable and safe and therefore can be repeated as often as required for follow up of desease progression and treatment. This novel technique might serve as a non-invasive alternative to FA images for assessing perfusion abnormalities in patients with ischemic retinopathies in a large retinal area, simultaneously.

7555-24, Session 5

Hemodynamic analysis of patients in intensive care unit based on diffuse optical spectroscopic imaging system

Y. Hsieh, C. Wang, Y. Lin, National Chiao Tung Univ. (Taiwan); M. Chuang, China Medical Univ. Hospital (Taiwan); C. Chuang, J. Tsai, National Taiwan Univ. (Taiwan); C. Lu, Industrial Technology Research Institute (Taiwan); C. Sun, National Yang-Ming Univ. (Taiwan)

Diffuse optical spectroscopic imaging (DOSI) is a technique to assess the

spatial variation in absorption and scattering properties of the biological tissues and provides the measurement of changes in concentrations of oxy-hemoglobin and deoxy-hemoglobin. In this study, a continuous-wave DOSI system was built with double-wavelength laser diodes (LD) as near-infrared light sources. We hypothesized that monitoring the dynamic response to non-invasive measurement of tissue oxygenation during a venous occlusion test could characterize local metabolic rate and local tissue perfusion adequacy because O2 saturation recovery behavior would reflect pre-existing cardiovascular reserve. The muscle oxygenation in the human extremity was measured during vessel occlusion test in normal subjects and ICU patients with septic shock and heart failure as our preliminary results.

7555-25, Session 5

Fast coregistered breast imaging in vivo using a hand-held optical imager

S. J. Erickson, S. Martinez, J. DeCerce, L. Caldera, A. Godavarty, Florida International Univ. (United States)

Hand-held based optical imaging devices are currently developed towards the clinical breast cancer diagnostics. A hand-held optical device has been developed in our laboratory towards fast 2D imaging and 3D tomography for breast cancer detection and diagnosis. The device has the unique ability to contour to different tissue curvatures using a flexible probe face and is capable of performing fast 2D imaging by employing simultaneous over sequential source illumination, and augmented with self co-registration facilities towards (future) 3-D tomography. The objective of the current work is to demonstrate fast coregistered 2D imaging on breast tissue of healthy female subjects. Fluorescence imaging experiments are performed in-vitro and in-vivo to demonstrate coregistered imaging as well as the ability to detect deep targets from multiple surface scans. A 0.23-0.45 cc spherical target(s) filled with 1 µM indocyanine green is embedded at various depths of a cubical phantom filled with chicken breast (in-vitro models). For in-vivo studies, the fluorescent target is placed under the flap of the breast tissue to represent a tumor for fluorescence imaging. Multiple scans (fast continous-wave images of fluorescence intensity) are collected and coregistered at different locations on the breast tissue. The surface contour plots of fluorescence signal obtained from multiple scans are used to demonstrate the feasibility of fast 2D coregistered imaging as well as ability to detect deep targets (from in-vitro studies). This study demonstrates the potential of the hand-held optical device towards future in vivo surface imaging of breast cancer and tomographic imaging for 3D tumor localization.

7555-26, Session 6

Image guided intervention system for cancer diagnosis and therapy guidance

N. V. Iftimia, M. Mujat, D. Hammer, D. Ferguson, Physical Sciences Inc. (United States)

An advanced imaging system for cancer diagnosis and therapy guidance will be discussed. Optical Coherence Tomography (OCT) imaging and laser therapy were combined within the same instrument to provide the clinician with and advanced tool that could help to better manage patients with cancer lesions. Using backreflected light to visualize tissue microstructure, OCT can provide information on nuclear size and shape, nuclear-to-cytoplasmic ratio, and the organization and structure of glands. It can also provide functional information, like blood flow, tissue birefringence, etc. These capabilities could potentially be employed in three ways: as a primary diagnostic test to replace biopsy, as a screening tool to direct biopsy, and as a diagnostic tool to guide therapy and monitor therapy response. If a therapeutic tool, like laser hyperthermia is added to the same probe, the clinician has also the option to perform therapy on some lesions that might be treated in this way. OCT could be used to real-time monitor this therapeutic process and estimate its efficacy. However, since OCT has a relatively small field of view, it usually



has to be combined with other large field/lower resolution imaging modalities, like endoscopy, ultrasound imaging, fluorescence endoscopy, etc., to guide the OCT probe to a region of interest and collect complementary structural and functional information. All these aspects will be discussed in our paper.

7555-27, Session 6

A microfluidic-photonic-integrated device with enhanced excitation power density

B. R. Watts, McMaster Univ. (Canada); T. Kowpak, C. Xu, McMaster University (Canada)

Optical excitation power density of a microfluidic-photonic-integrated flow cytometer has been enhanced. The device integrates both optical and fluidic components into the same layer of an SU-8 photoresist on a glass wafer sealed by bonding a PDMS layer on the top. Device structures were optimized through simulation and its performance was tested.

Multi-modal waveguides, integrated with a complex 2-D lens system, focused all light within the large NA waveguide into the centre of a microfluidic channel. This lens system enhances the optical power density in the center of the microfluidic channel, improving the sign-to-noise ratio. Without it, light from the waveguide will spread across the channel resulting in low power density in the channel. Efforts were made to design an effective lens system and integrate it efficiently with the waveguides and microfluidic channel. The beam width in the channel center can be reduced from 86 m to ~10 m without introducing any processing complexity.

Beam shape was imaged by filling the channel with fluorescent dye excited by a HeNe laser coupled to the waveguide through a high NA objective. An obviously focused beam in the centre of the channel was obtained in agreement with simulation results. This achieved focusing of multi-modal light beams has practical meaning since high powered sources can be efficiently coupled into a channel, boosting signal-to-noise ratio. Furthermore, off-chip lasers can be replaced by an LED source integrated directly next to the waveguide on the same chip to further increase the portability of the device and reduce system costs.

7555-28, Session 6

Rapid optical heating of blood for clinical point of care diagnositics

B. E. Catanzaro, CFE Services (United States); M. Kotob-Yahfoufi, C. Johnson, K. Gandola, Accumetrics (United States)

Clinical testing of human blood requires adherence to a number of regulatory standards, including maintaining a temperature that is representative of the human body (e.g. 37 C). The economics of private and public healthcare drives blood assays to be conducted using low cost, disposable assay devices that also eliminate the possibility of cross contamination. Unfortunately, the materials that meet the economic and disposable constraints of the marketplace are thermal insulators, not ideal for rapid heating. We present a novel means of optically heating blood samples in plastic assay devices within a time period suitable for point of care use. The novel approach uses LED's in the red portion of the visible spectrum. The lower absorption of optical radiation in the visible spectrum enables the absorption of energy deep into the assay device. This produces even heating, avoiding the gradients that can occur by surface heating (conduction) or surface absorption (highly absorbing wavelengths). Analytical and computational models will be discussed. A specific application to a point of care blood assay instrument will be reviewed. In this application, optical heating was achieved using a small array of high brightness LED's. Experimental results will be discussed. The experimental results with this instrument validated the predictions.

7555-29, Session 6

Detection of endometriotic lesions by a polarization-based imaging system

J. Kim, J. T. Walsh, M. Milad, Northwestern Univ. (United States)

Endometriosis is one of the most common causes of chronic pelvic pain and infertility and is characterized by the presence of endometrial glands and stroma outside of the uterine cavity.

A novel laparoscopic polarization imaging system was designed to detect endometriosis by imaging endometrial lesions. Linearly polarized light with varying incident polarization angles illuminated endometrial lesions. Degree of linear polarization image maps of endometrial lesions were constructed by using remitted polarized light. The image maps were compared with regular laparoscopy image.

The degree of linear polarization map contributed to the detection of endometriosis by revealing structures inside the lesion. The utilization of rotating incident polarization angle (IPA) for the linearly polarized light provides extended understanding of endometrial lesions.

The developed polarization system with varying IPA and the collected image maps could provide improved characterization of endometrial lesions via higher visibility of the structure of the lesions and thereby improve diagnosis of endometriosis.

7555-30, Session 6

A near-infrared vessel imaging system, the VascuLuminator, to facilitate arterial puncture in young children

N. Cuper, J. C. de Graaff, C. J. Kalkman, R. M. Verdaasdonk, Univ. Medical Ctr. Utrecht (Netherlands)

A practical near-IR blood vessel imaging system, the 'VascuLuminator' (VL), was proven successful in decreasing puncture attempts and procedural time during blood withdrawal in young children.

In this study, the effectiveness of the VL was tested as an aid in arterial line placement (ALP) in children being prepared for surgery, which can be difficult and might require up to an hour of precious OR time and prolonged time of anesthesia.

In a group of 48 children up to 3 years of age, time to place an arterial line, number of punctures and puncture site were recorded. In the first 36 patients, ALP was performed without the VL. Consequently, the VL was used as an aid by pediatric anesthesiologists with approval from the Medical Ethics Committee.

Data is presented by median and interquantile range (IQR). The total number of punctures dropped from 6 (IQR 2-13) to 3 (IQR 1-4, P .11). In the non-VL group, 12/36 procedures exceeded 20 minutes, as compared to 2/12 procedures in the VL group. Total failure of ALP was 2 in the non-VL compared to 0 in the VL group. The number of punctures in the groin, which is often a last resort, was 15/36 for non-VL as opposed to 1/12 VL (P .04).

Already, in this small patient group, the 'Vasculuminator' has shown promising results on its effectiveness for arterial line placement and is well received by the pediatric anesthesiologists as a useful tool.

7555-31, Session 6

development of imaging system for use in real-time visualization of parathyroid glands in endocrine surgery

I. J. Pence, C. Paras, A. Mahadevan-Jansen, Vanderbilt Univ. (United States)

Complications from incomplete or accidental removal of the parathyroid glands are a major concern associated with endocrine surgery. Current



localization techniques are primarily preoperative and only applicable in select surgeries. The proximity of the various tissues encountered in the neck during surgery and the tendency of these tissues to blend together serve as confounding factors for surgeons. There is a need for a sensitive, real-time, intra-operative diagnostic tool to assist with anatomical guidance. Previous studies have shown the ability of nearinfrared (NIR) autofluorescence to differentiate between the parathyroid and the surrounding tissue based on the intrinsic optical properties. The parathyroid exhibits stronger fluorescence than all other tissues in the neck. Near-infrared imaging would provide spatial context as a more intuitive approach for the surgeon. Here we present the first application of an autofluorescence-based imaging system for real-time intra-operative use in endocrine surgery. A 785nm diode laser is used to excite the tissue and a converter tube is employed to detect the NIR fluorescence and render it in the visible wavelengths. The image is then captured by CCD and processed to apply a false color gradient for distinction between tissue types. We demonstrate the utility of the NIR fluorescence imaging system in vivo and in vitro. Preliminary results indicate that imaging is able to capture the higher level of autofluorescence exhibited by the parathyroid differentiating it from the surrounding tissue.

7555-32, Session 6

Development of an imaging fluorescence system applied on HPV condyloma treatment by photodynamic therapy

M. M. Costa, N. Inada, C. Kurachi, V. S. Bagnato, L. Ventura, Univ. de São Paulo (Brazil)

Photodynamic Therapy (PDT) is a useful technique for treatment of condyloma induced by human papillomavirus (HPV). However, it is necessary to improve instrumentation and clinical protocols to develop this technique. This study presents the development of an imaging fluorescence system designed to assess 5-aminolevulinic acid-induced protoporphyrin IX (PpIX) presence/photodegradation during PDT applications. Monitoring PpIX can improve applications by allowing one to know the approximate amount of the photosensitizer present in the tissue during treatment. This could help to avoid longer/shorter irradiation times than actually needed for the treatment, or to better establish the optimum time to start irradiation. To achieve this improvement, a portable system for visual PpIX fluorescence monitoring during HPV condyloma treatment by PDT was developed. The system is composed of a high intensity LED light source, with emission band between 400-460nm that allows for PpIX excitation, and filters that allow one to observe PpIX red fluorescence emission. For PDT application, 5-aminolevulinic acid cream (20%; wt/wt) was used. It was incorporated in an emollient cream and topically placed over the lesions, and PDT irradiation was performed 4-6 hours after application. Irradiation was performed using "PDT Flex Use", a Brazilian device anatomically designed specially for HPV condyloma treatments. Using the visual fluorescence monitoring system here presented, it was possible to monitor PpIX generation and degradation. This made possible to make the irradiation time shorter, and to verify the actual production of PpIX in the treated tissue. Such observations helped to make a more effective and comfortable PDT treatment.

7555-53, Poster Session

Percutaneous sensor platform for chronic biomarker monitoring in vivo

K. Liao, National Chung Hsing University (Taiwan); J. O'Kelly, Cedars-Sinai Medical Center (United States); L. Marcu, University of California Davis (United States); T. Hogen-Esch, F. Richmond, University of Southern California (United States): Y. Chou. National Chung Hsing University (Taiwan); P. Koeffler, Cedars-Sinai Medical Center (United States); G. Loeb, University of Southern California (United States)

In order to manage certain disease and conditions, it is important to make frequent measurements of specific biomarker over an extended period of time. These include diabetes, cancer chemotherapy treatment, and hormonal monitoring for fertility and pregnancy.

We are developing a sensor platform, which are disposable, minimally invasive, and can provide in vivo monitoring of various biomarkers for several weeks. The key element is a percutaneous optical fiber that permits reliable spectroscopic measurement to interrogate the analytes in situ. Chronic animal implantation studies have demonstrated good compatibility and durability for clinical applications.

The first application of the device senses interstitial glucose based on fluorescence resonance energy transfer (FRET) between fluorophores bound to betacyclodextrin and Concanavalin A in a polyethylene glycol (PEG) matrix, which is attached to one end of the fiber-optic sensor. Preliminary results indicate the potential of the glucose sensor to build an "artificial pancreas / beta cell", consisting of a chronic implantable sensor, an insulin pump and a close-loop algorithm for adjusting dosage continuously.

The second application of the platform technology is in the identification of effective chemotherapy treatment for solid tumors in individual patients. The sensor delivered the fluorescent agent locally, and detects apoptotic activity initiated by the anticancer treatment. Asymmetric scrambling of phosphatidylserine on cell membrane is one of the indications. The presence of phosphatidylserine on the external surface of apoptotic cells can be detected by increased fluorescence of the infused dye FM 1-43. Preliminary results indicate the capability of the apoptosis sensor to detect the drug-induced apoptotic activities both in vitro and in vivo.

7555-54, Poster Session

5D-intravital tomography as a novel tool for non-invasive in-vivo analysis of human skin affected with Atopic Dermatitis

K. König, JenLab GmbH (Germany); V. Huck, Westfälische Wilhelms-Univ. Münster (Germany); C. Gorzelanny, Medizinischen Fakultät Mannheim (Germany); K. Thomas, T. A. Luger, Westfälische Wilhelms-Univ Münster (Germany); S. W. Schneider, Medizinischen Fakultät Mannheim (Germany); H. Studier, JenLab GmbH (Germany)

For analysis of human skin affected with Atopic Dermatitis (AD) we applied intravital multiphoton tomography (5D-IVT).

We evaluated a characteristic 5D-IVT skin pattern of AD correlated with the disease intensity. We measured a shift of the mean fluorescence lifetime (taum) indicating an altered metabolic activity. Moreover, we investigated human skin with or without barrier defects.

Application of the 5D-IVT allows to distinguish skin affected with AD from healthy skin by morphological criteria and fluorescence lifetime. Further studies will evaluate its capacity as a diagnostic tool and to monitor the therapeutic efficacy.

7555-55, Poster Session

Signal-to-noise analysis for 3D luminescence imaging of hypoxia in deep tissues

R. S. Gurjar, M. Seetamraju, Radiation Monitoring Devices, Inc. (United States)

Non-invasive 3-D imaging of hypoxia in deep-tissue tumors is important in order to understand the progression of cancer to malignant forms. In our previous study [1] we have identified a biomarker, which targets endothelial cells specific to cancer angiogenesis, for measuring the oxygen tension in tumor tissue. The biomarker is an F3 peptide covalently bound to a polyacrylamide nanoparticle, which also encapsulates an oxygen sensitive NIR phosphor. The excited state



lifetime of the phosphor is related to oxygen concentration through the Stern-Volmer relation. We have developed a time-domain lifetime imaging diffuse optical tomography setup to optically excite and detect the phosphorescence from the oxygen-sensitive biomarker. Previous work demonstrated proof-of-principle by reconstructing images of a cylindrical tissue phantom with two embedded heterogeneities comprising of the nanoparticle biomarker at two different oxygen concentrations. In this work, we will present a detailed signal-to-noise analysis for molecular imaging of this contrast agent in deep tissues. A phantom tissue having homogeneous scattering and absorption coefficient of mu_s'

 $\sim 15\text{--}20$ cm-1 and mu_a ~ 2 cm-1 respectively, will be used and the phosphorescence signal strength and fitted lifetime to the decay signal will be studied as a function of luminophore's concentration, oxygen tension, inclusion size and its depth. Details on limits of spatial resolution, emitter concentration, oxygen tension and sources of systemic errors will be discussed.

1. Gurjar. R. et al, "Diffused Optical Tomography Using Oxygen-Sensitive Luminescent Contrast Agent," IEEE Proceedings of International Symposium on Biomedical Imaging: From Nano to Macro, ISBI 2009.

7555-56, Poster Session

The design and implementation of a windowing interface pinch force measurement system

T. Ho, Feng Chia University (Taiwan); Y. Chen, Ling Tung University (Taiwan)

This paper presents a novel windowing interface pinch force measurement system that is basically based on an USB (Universal Series Bus) microcontroller. The system includes a force sensor, instrumentation amplifier, voltage regulator, analog to digital converter, monitoring device, and a microcontroller. A small analog signal is generated from the force sensor resistor to which a force is applied. It is then amplified through the instrumentation amplifier and regulated for the input of analog/digital converter. This analog signal is converted to digital signal and processed by the USB controller. Finally, it is transmitted to the PC via a cable. The PC screen displays the data and curve trace of the corresponding applied force in the designed windowing human interface.

There are several functions designed in the windowing human interface for the pinch force measurement system, such as the selection of pinch force type, the value of the applied force and its corresponding curve trace, the transition of pinch force variations, zoom in and out of the curve trace, frequencies of the finger pinch. Because the value and curve trace of the applied force by a hand injured patient is displayed in real time on a monitoring screen, not only the physician can easily evaluate the effect of hand injury rehabilitation, but also the patients get more progressive during the hand physical therapy by interacting with the screen of pinch force measurement.

In order to facilitate the pinch force measurement system and make it friendly, the system is based on an USB controller so that it can be easily installed and communicated with any PC's via the function of plug and play. The detail hardware design and software programming flowchart is described in this paper. First of all, the relationship between the applying force and the FSR sensors are measured and verified. Later, the different type of pinch force measurements are verified by the oscilloscope and compared with the corresponding values and curve trace in the windowing interface display to obtain the consistency. Finally, a windowing interface pinch force measurement system based on the USB microcontroller is implemented and demonstrated. The experimental results show the verification and feasibility of the system.

7555-57, Poster Session

Label-free diagnosis of human hepatocellular carcinoma by multiphoton autofluorescence microscopy

T. Sun, C. Dong, National Taiwan Univ. (Taiwan)

Conventionally, the diagnosis of hepatocellular carcinoma (HCC) is performed by qualitative examination of histopathological specimens, which takes times for sample preparation. Our objective is to demonstrate an effective and efficient approach to apply multiphoton microscopy for imaging and characterizing HCC specimens. The imaging modality of multiphoton autofluorescence (MAF) was used for the qualitative imaging and quantitative analysis of HCC of different grades under ex-vivo. label-free conditions. We found that while MAF is effective in identifying cellular architecture in the liver specimens, and for obtaining quantitative parameters in characterizing the pathological tissue. Our results demonstrates the capability of using tissue quantitative parameters of multiphoton autofluorescence (MAF), the nuclear number density (NND), and nuclear-cytoplasmic ratio (NCR) for tumor discrimination and that this technology has the potential in clinical diagnosis of HCC and the in-vivo investigation of liver tumor development in animal models.

7555-58, Poster Session

Calibration protocol for Fourier-domain OCT using optical fiber gratings

T. J. Eom, Gwangju Institute of Science and Technology (Korea, Republic of); Y. Ahn, Univ. of California, Irvine (United States); B. Yu, Gwangju Institute of Science and Technology (Korea, Republic of); E. S. Choi, Chosun Unv. (Korea, Republic of); C. Kim, Pusan National Univ. (Korea, Republic of); Z. Chen, Univ. of California, Irvine (United States)

A spectrometer of Fourier-domain OCT (FD-OCT) requires very tight design conditions of light incidence angle into the diffraction grating, the diffraction angle, and the focal length between a focusing lens and CCD array. Moreover, advanced FD-OCT systems become more complex in their construction to increase functionality and performance. The additional complexities in these systems were necessary to acquire multifunctional images and to reduce the tailoff in OCT while reducing the computation time.

To alleviate these difficulties in alignment process and the evaluation of the spectrometer performance, we present a quantitative optimization protocol for FD-OCT using a long period fiber grating and fiber Bragg gratings. Three crucial design parameters of the spectrometer for FD-OCT are the light incident angle, the diffraction angle, and the focal length of the focusing lens between the diffraction grating and the CCD array. The choice of these three parameters ultimately determines the spectral resolution of the FD-OCT system. However, the evaluation of the performance of a custom-made spectrometer is rather challenging since we need to assess not only the spectral resolution but also the reduction of nonlinearity between the measured CCD pixel number and the matched wavelength.

In this paper, we have proposed the calibration protocol to get the alignment factors for a custom-made spectrometer for a SD-OCT system using optical fiber gratings. We have used 5 different FBGs covered the broadband source wavelength range with 0.05 nm spectral bandwidth and 92 % reflectivity to align the spectrometer and to obtain the nonlinear fitting function between the pixel domain of the CCD camera and the wavelength domain. The implemented FD-OCT followed the proposed protocol. We have achieved alignment factors of the incident angle, the diffraction angle, and the focal length and recalculated the spectral resolution of the OCT system. The proposed protocol is expected to alleviate difficulties in alignment process and the evaluate spectrometer performance for the multi-functional and specially designed FD-OCT system.



7555-59, Poster Session

Two-layer optical model of skin for diffuse reflectance spectroscopy

D. Yudovsky, L. Pilon, Univ. of California, Los Angeles (United States)

Analysis of light transfer through biological tissue is complicated by tissue heterogeneity. Skin is comprised of several layers which absorb and scatter incident light. The top layer (the epidermis) is characterized by strong absorption due to melanin. Beneath the epidermis is the dermis whose optical properties are affected by the presence of blood. Furthermore, blood exhibits drastically different absorption and scattering characteristics that vary with oxygen saturation.

Spectroscopic analysis of skin has been based on approximate models of light transfer such as Beer-Lambert's law or the diffusion approximation. Then, skin is treated as a semi-infinite and homogenous medium. Unfortunately, these methods provide an incomplete and often inaccurate assessment of light transfer through biological tissue. More complex, multilayered Monte Carlo models have been developed, but are too slow and computationally intensive to use with real-time spectroscopy or inverse method for non-invasive monitoring of skin.

In this study, a model of light transfer through skin, treated as a two-layer medium, is developed that is both realistic and computationally efficient. The model exhibits the accuracy of Monte Carlo simulations, but the simplicity and speed of the two-flux approximation. Furthermore, since skin reflectance is calculated taking into account optical and geometric properties of the epidermis and dermis individually, spectroscopic methods based on this model can retrieve layer specific information.

7555-68, Poster Session

In vivo Noninvasive Quantitative Evaluation of Human Skin

A. N. Yaroslavsky, E. Salomatina, Wellman Ctr. for Photomedicine (United States); V. Neel,

Recent advances in optical technologies have made quantitative subsurface imaging of human skin feasible. In this contribution, the evaluation of clinical polarization-enhanced reflectance and fluorescence imaging system (PERFIS) will be discussed in the context of real time noninvasive assessment of skin composition and structure. PERFIS provides wide-field imaging with lateral resolution of down to 8 µm. Linearly polarized monochromatic light in the spectral range from 390 to 750 nm is used for illumination. CCD camera and lenses are employed for image registration. Fourteen volunteers, eight men and six women, aged between 28 and 65 years, with the skin types I to IV (Fitzpatrick classification system) have completed the study. Several sun exposed locations on the head were imaged. Co- and cross polarized reflectance images were collected. Fluorescence emission and polarization was excited at 410 nm and registered between 435 and 650 nm. Automated thresholding algorithm was used for quantitative assessment of skin vascularization, collagen, and melanin. In vivo polarized reflectance images visualize subsurface skin layers, including epidermis, blood plexus, and dermis. Fluorescence emission and polarization images reveal prominent network-like collagen pattern in the older subjects. Quantitative analysis of the images enables noninvasive examination of the sizes and density of collagen bundles, blood vessels, as well as of melanin distribution.

7555-69. Poster Session

In vitro and in vivo SORS measurements for breast tumor surgical margin analysis

M. D. Keller, Lockheed Martin Aculight (United States) and Vanderbilt Univ. (United States); E. Vargis, Vanderbilt Univ (United States); N. Granja, I. Meszoely, M. Kelley, Vanderbilt Univ Medical Center (United States); A. Mahadevan-Jansen, Vanderbilt Univ (United States)

Raman spectroscopy has been widely applied for cancer diagnosis, but it only provides limited depth information in its traditional implementations. Spatially offset Raman spectroscopy (SORS) can probe deeper into tissues and can discriminate among multiple layers. Until recently, the primary biological application of SORS was in detecting hard tissues such as bone or calcifications through soft tissue. Using individual source and detector fibers at a number of spatial offsets, we previously demonstrated that two layers of soft tissue, specifically normal human breast tissue overlying human breast tumor tissue, can be discriminated as well. Based on these results and a series of Monte Carlo simulations, a multi-separation SORS probe was designed to be capable of detecting tumor signatures from below a maximum of 2 mm of normal breast tissue. This probe was used to acquire Raman spectra from frozenthawed normal breast and breast tumor samples in the laboratory, and a probabilistic classification scheme was developed to determine whether any tumor signature was present in the first 2 mm of tissue under the probe site. In a sample of 35 specimens, this discrimination was performed with sensitivity and specificity both greater than 90%. Measurements were then made on a small set of freshly excised breast specimens in the hospital to ensure the feasibility of translating this technique to the operating room.

7555-33, Session 7

Lung alveolar wall disruption in threedimensional space identified using secondharmonic generation and multiphoton excitation fluorescence

T. Abraham, J. Hogg, St. Paul's Hospital (Canada)

The structural remodeling of extracellular matrix (ECM) macromolecules is an important feature of the remodeling of the peripheral lung in chronic obstructive pulmonary disease (COPD). Such remodeling is inadequately characterized due to the lack of availability of non-invasive imaging methodologies which are capable of providing sufficient specificity, sensitivity and spatial resolution. Second harmonic generation (SHG) is a nonlinear optical phenomenon which exhibits several common characteristics of multi-photon excited fluorescence (MPEF) microscopy. These characteristics include the identical equipment requirements and the intrinsic capability of generating 3D high resolution images. Highly ordered ECM macromolecules such as the fibril-forming collagens produce SHG signal without the need for any exogenous label. On the other hand, ECM macromolecules such as the elastin fibers generate MPEF signal due to their endogenous auto-fluorescence characteristics. Both these signals can be captured simultaneously to provide spatially resolved 3D structural reorganization of ECM matrix. In this study, SHG and MPEF microscopy methods were used to examine structural remodeling of the ECM matrix in human lung alveolar walls undergoing emphysematous destruction. Flash frozen lung samples removed from a patient undergoing lung transplantation for very severe COPD were compared to similar samples from an unused donor lung that served as a control. Two samples from each lung types (n = 4) were first immobilized on the flat bottom of a small dish, immersed in phosphate buffed saline (PBS) solution and subsequently imaging operations were performed directly on these unfixed unstained tissue sections at least three different areas. Non-de-scanned detectors and spectral scanning mode both in the reflection geometry were used for generating the 3D images and for the spectra, respectively. An infrared ultra -short pulse laser tuned to 880-nm was used for generating SHG and MPEF images. The generated spatially resolved 3D images generally show the spatial distribution of collagen, elastin and other endogenously fluorescent tissue components such as the macrophages. These images are supplemented with the spectral data which show the specificity of the signals emerging from these alveolar components. The morphological features of multi-photon images and the spectral specificities of the signals are also validated using standard histo-chemical procedures such as Hematoxylin-Eosin and Verhoeff-Van Gieson methods. In the case of the control lung tissue, we found well ordered alveolar wall with composite type structure made



up of collagen matrix and relatively fine elastic fibers. In contrast, lung tissue undergoing emphysematous destructions was highly disorganized with increased alveolar wall thickness compared to the control. We conclude that these multi-dimensional and non-invasive imaging modalities provide spatially resolved 3-dimensional images with spectral specificities, that are sensitive enough to identity the early changes associated with emphysematous destruction in severe COPD.

7555-34, Session 7

Application of laser diodes and LEDs in new diagnostic tools for noninvasive transcutaneous bilirubinometry of neonatal jaundice

M. Hamza, Mansoura Univ. (Egypt); M. H. Sayed El-Ahl, A. M. Hamza, M. Y. Hamza, A. M. Hamza, Tabarak Children's Hospital (Egypt)

To prevent kernicterus in newborn infants, it is important to detect jaundice in its early stages. The standard clinical method for measuring serum bilirubin is by laboratory analysis. The accuracy and precision of the results obtained by these analyzers and other conventional meters have undesirable variability. In this paper the authors present the theory and design of new noninvasive transcutaneous bilirubin meters using laser diodes and LEDs. The choice of the wavelengths follows the principles of optical bilirubinometry. The differential absorption systems of the new diagnostic tools are designed to make use of the selective absorption characteristics of bilirubin taking into consideration the presence of other chromophores in the skin of the neonate. The new compact, small size and low cost transcutaneous bilirubin meter provides more accurate instrument for either screening or monitoring of serum bilirubin concentration in a diverse population of neonates.

7555-35, Session 7

Time-resolved near-infrared technique for bedside monitoring of absolute cerebral blood flow

M. Diop, K. M. Tichauer, J. Elliott, Lawson Health Research Institute (Canada); T. Lee, Lawson Health Research Institute (Canada) and Robarts Research Institute (Canada); K. St. Lawrence, Lawson Health Research Institute (Canada)

Neurological emergencies such as subarachnoid hemorrhage and stroke are associated with high morbidity and mortality in part because of the incidence of secondary ischemic injury. Consequently, a primary focus of intensive care is monitoring the injured brain to avoid harmful events that impair cerebral blood flow (CBF). Since current clinical methods only indirectly assess CBF, the goal of this research was to develop an optical technique for measuring CBF at the bedside. A time-resolved near-infrared (NIR) system was developed due to its superior depth sensitivity compared to continuous-wave NIR apparatus. A vascular tracer, indocyanine green (ICG), was intravenously injected and ICG concentration time curves in brain and arterial blood were simultaneously measured by the time-resolved NIR apparatus and dye densitometry, respectively. An in-house developed deconvolution algorithm was used to calculate CBF from the ICG data. Initial studies were conducted on newborn piglets to avoid errors associated with extra-cerebral contamination. Preliminary results from two animals at normo- and hyper-capnia demonstrated that the technique was sensitive to changes in CBF: average CBF was 138 \pm 14 and 220 \pm 40 ml/100g/min at normocapnia and hypercapnia, respectively. However, these values are approximately 50% greater than previous measurements acquired with a continuous-wave NIR system. The most likely cause is errors in the measured instrument response function, which is currently under investigation.

7555-36, Session 7

Broad-beam fluctuation spectroscopy for non-flow cytometry and clinical diagnostics

M. J. Levene, E. Olson, R. Torres, Yale Univ. (United States)

Fluorescence fluctuation spectroscopy (FFS), including fluorescence correlation spectroscopy (FCS), photon counting histograms (PCH) and their derivatives, have found wide-spread use in biophysics but have not expanded significantly into clinical applications. Many clinical blood diagnostics consist of measuring the concentration of cell types within the blood, and are therefore well-suited to FFS methods that make absolute concentration measurements. We present a novel scanning FFS system, which we term Broad-beam Scanning Fluctuation Spectroscopy (BSFS), for performing cytometry. BSFS scales up the dimensions of a typical FFS observation volume to ~100 microns, so that cells can act as the fluctuating particles rather than single molecules. BSFS is a viable alternative to flow cytometry for a wide variety of cell-based clinical diagnostics, but without the complications of a flow system. BSFS is less destructive to cells, enabling cytometry on the same sample over time.

7555-37, Session 8

Optical wire guided lumpectomy: measuring distance in breast tissue

A. Dayton, N. Choudhury, S. A. Prahl, Oregon Health & Science Univ. (United States)

In practice, complete removal of the tumor during a lumpectomy is rare. We have demonstrated the use of an optical wire to remove breast lesions in eight patients. The surgeon used an optical wire, which was an optical fiber attached to the standard metal wire used to localize breast lesions. The optical wire emitted light from the center of the lesion and successfully guided the surgeries. However, a quantitative way to orient the surgeon to the lesion was needed. To provide for negative margins and acceptable cosmesis, a spherical specimen centered around the lesion is desired. The proposed method may provide a practical means by which such resections can be achieved. A 195µm optical fiber is positioned in the lesion and coupled to a 638 nm diode laser which is sinusoidally modulated between 50 and 400 MHz by a network analyzer. A handheld optical probe is used to collect the modulated light and measure the phase lag. This data is used to calculate the distance the light has traveled from the emitting fiber tip to the probe. An array of polyurethane phantoms as well as prophylactic mastectomy specimens were used to validate the accuracy of the system. The phantoms had absorption coefficients of 0.05-0.1[1/mm] and reduced scattering coefficients of 0.5-2[1/mm]. The phase lag was measured in 5 mm increments up to 40 mm. Nine prophylactic mastectomy specimens were also tested. Each specimen was measured at six locations; for each location, three directions from the source to the probe were measured from 5 to 40 mm.

7555-38, Session 8

Do radio frequencies of medical instruments common in the operating room interfere with near-infrared spectroscopy signals?

B. Shadgan, B. Molavi, D. Reid, G. A. Dumont, A. J. Macnab, P. J. O'Brien, The Univ. of British Columbia (Canada)

The medical diagnostic application of near infrared spectroscopy (NIRS) in medicine especially in intra-operative events and intensive care units is increasing. Since the NIRS frequency of operation is within the optical range, radio frequency interference from instruments in the operating room (OR) is unlikely to significantly alter the NIRS signals. However, the NIRS output may be affected by various sources of interference within the OR. In order to pave the way for clinical applications of NIRS, it is



necessary to provide sufficient evidence that it can be reliably used in a clinical setting. In this study, we investigated the influence of 3 common OR instruments, namely electrical cautery, a battery-powered drill and a portable x-ray imaging system on NIRS signals of 17 patients who underwent ankle surgery. The exact moment of activation of each of the 3 devices were recorded during the surgeries. A total of 24 cautery points, 84 drilling points and 85 x-ray events were studied. In order to remove the effects of slow changing physiological variables, we first used a low pass FIR filter and then selected 3 windows with variable lengths around the moment of device onset. For each instant, the mean and variance (energy) of the signals in 3 windows were compared. The results show that there is no statistically significant change in the mean and variance of the NIRS signals (p < 0.01) for any of the 3 devices. This highlights the suitability of the NIRS device in clinical environments such as the OR.

7555-39, Session 8

THz imaging of skin hydration: motivation for the frequency band

R. Singh, Univ. of California, Santa Barbara (United States) and Univ. of California, Los Angeles (United States); Z. D. Taylor, Univ. of California, Santa Barbara (United States); P. Tewari, Univ. of California, Los Angeles (United States); M. O. Culjat, Univ. of California, Los Angeles (United States) and Univ. of California, Santa Barbara (United States); H. Lee, E. R. Brown, Univ. of California, Santa Barbara (United States); W. S. Grundfest, Univ. of California, Los Angeles (United States)

Terahertz imaging has been proposed for use in the detection and monitoring of various skin pathologies, and takes advantage of the hydration, specifically the dielectric constant, of skin. Terahertz is defined as the electromagnetic spectrum between 300 GHz and 3 THz. The optimal operational frequency band should provide the best tradeoff between atmospheric attenuation and robustness to scattering, spatial resolution and sensitivity to changes in skin hydration. In terms of atmospheric attenuation, there are broad absorption lines at 556 GHz and 750 GHz, and large transmission windows centered at 500 GHz, 650 GHz, and 870 GHz. The scattering of the reflected energy from the skin was shown that there was a significant decrease in the power fraction reflected in the specular direction as the frequency increased. The sensitivity to changes in water content, key to imaging of skin hydration, was determined that at 100 GHz is almost an order of magnitude higher than it is at 1 THz. Higher frequencies, as expected, have superior spatial resolution.

Taking the above criteria into account, it was shown that the 400-700 GHz band is effective for THz skin hydration imaging as this band mitigates scattering and atmospheric attenuation while providing sufficient hydration sensitivity and spatial resolution. In this paper, the motivation for using this band will be presented as well as overview of the challenges related THz imaging of skin and the description of a THz pulse reflective imaging system specifically designed for imaging and monitoring of skin abnormalities.

7555-40. Session 8

Optical model of skin for early, non-invasive detection of wound development on the diabetic foot

D. Yudovsky, Univ. of California, Los Angeles (United States); K. T. Schomacker, Hypermed, Inc (United States); A. Nouvong, Western Univ. of Health Sciences (United States); L. Pilon, Univ. of California, Los Angeles (United States)

Foot ulceration is a debilitating comorbidity of diabetes that may result in loss of mobility and amputation. Optical detection of cutanous tissue changes due to inflammation and necrosis at the preulcer site could

constitute a preventative strategy. A commercial hyperspectral oximetry system (OxyVu by HyperMed Inc., Burlington, MA) was used to measure reflectance of the feet of 256 diabetic patients at risk of developing foot ulcers. Measurements were performed during 7 visits over an 18-month period. During the course of the study, 24 foot ulcers formed. A predictive index based on hyperspectral tissue oximetry was developed. It was able to differentiate preulcer tissue from surrounding healthy tissue with a sensitivity of 92% and specificity of 80% (Q-value = 86%).

While this predictive index accurately determined the location of a preulcer, it did not quantify the degree of inflammation and/or necrosis associated with a forming ulcer. Thus, an optical skin model was developed treating skin as a two-layer medium and explicitly accounting for (i) melanin content and thickness of the epidermis, (ii) blood content and hemoglobin saturation of the dermis, and (iii) tissue scattering in both layers. The model exhibited the simplicity and speed of the two-flux approximation with the accuracy of Monte Carlo simulations for the range of optical properties of skin in the visible range. Using this forward model, an iterative inverse method was used to determine the skin properties from simulated diffuse reflectance measurements. These numerical results demonstrated the feasibility of such a method for invivo applications.

7555-41, Session 9

Gold thin layer assisted DNA immobilization for photoelectrochemical DNA sensor

S. Iwanaga, S. Suzuki, N. Hori, H. Kirimura, Sysmex Corp. (Japan)

Electrochemical biosensors have been developed recently due to the possibility to become a compact medical diagnostic method with the high sensitivity. We have developed a DNA sensor which measures photoelectrochemical signals (photocurrent) from the target DNA labeled with fluorescence dyes. We made transparent semiconductor films such as ITO, ATO (Antimony Tin Oxide) patterned on a quartz plate as an electrode and immobilized the probe DNA (~20bases) on the electrode. After hybridization with target DNA molecules labeled with fluorescence dyes, we measured the photocurrent by illuminating the laser light to the sample. To improve the photocurrent collection efficiency, we modified the immobilization method of the probe DNA. Au thin film with the thickness of less than 10nm was deposited on the semiconductor electrode and probe DNA molecules were immobilized on it by the thiol-Au binding. We also used an organic solvent including iodine and tetrapropyl-iodide as an electrolyte. Au thin layer was etched by iodine in the electrolyte and then DNA molecules immobilized on the Au film were directly attached to the electrode surface. The photocurrent obtained by this method became 10times higher compared to typical DNA immobilization technique using aminosilane coupling agent. We will also report the effect of excitation wavelength (from visible to near-infrared) in order to suppress the photocurrent due to the excitation of electrode and optimization of semiconductor films to reduce the dark current from the electrolyte.

7555-42, Session 9

Tissue differentiation by diffuse reflectance spectroscopy for automated oral and maxillofacial laser surgery: ex vivo pilot study

A. Zam, F. Stelzle, Friedrich-Alexander-Univ. Erlangen-Nürnberg (Germany); K. Tangermann-Gerk, BLZ Bayerisches Laserzentrum GmbH (Germany); W. Adler, Friedrich-Alexander-Univ. Erlangen-Nürnberg (Germany); M. Schmidt, BLZ Bayerisches Laserzentrum GmbH (Germany); E. Nkenke, A. Douplik, Friedrich-Alexander-Univ. Erlangen-Nürnberg (Germany)

Remote laser surgery lacks of haptic feedback during the laser ablation of tissue. Hence, there is a risk of iatrogenic damage or destruction of



anatomical structures like nerves or salivary glands. Diffuse reflectance spectroscopy provides a straightforward and simple approach for optical tissue differentiation. The results obtained show a potential for differentiating tissues as guidance for oral and maxillofacial laser surgery.

imaging approach to be implemented into our Raman trap system, which allows for hyperspectral Raman imaging of floating single cells within minutes. The system has been used to distinguish between normal and Jurkat T cells.

7555-43, Session 9

Fluorescence-free biochemical characterization of cells using modulated Raman spectroscopy

A. C. De Luca, M. Mazilu, A. Riches, C. S. Herrington, K. Dholakia, Univ. of St Andrews (United Kingdom)

A new modulation method of separating Raman scattering from fluorescence has been developed that uses the principle of multi-channel lock-in detection. The method allows a suppression of the fluorescent background and improves spectral quality of the Raman data. It can remove in real-time static background and render visible weak Raman features that are masked by the fluorescence background in the standard spectrum. In this paper, we present an application of this method to the biochemical characterization of cells for biomedical diagnosis and imaging. Importantly, by analyzing separate spectra from the membrane, cytoplasm and nucleus of single cells, we are able to identify characteristic Raman features associated with DNA, protein and lipid molecular vibrations for discriminating between different location inside the cell, away from interfering fluorescence background. In addition, our method avoids potential misinterpretation of the data due to the standard background subtraction procedure. Finally, using the Principal Component Analysis (PCA) for the interpretation and classification of the Raman data, we demonstrate that our modulated Raman spectroscopy facilitates spectral assignment and increases detection sensitivity, opening the way for biomedical imaging. In particular, the reduced background variability of modulated Raman spectra with respect to the standard Raman enhances the relative importance of pure Raman peaks in the PCA. This explains the improved PCA prediction efficiency of the modulated spectra versus the standard method. These results are particularly encouraging, as this method will enhance the use of Raman for biomedical applications, including disease diagnosis.

7555-44, Session 9

Development of a compact high-throughput laser trap Raman system for fully automated single cell analysis

R. Liu, T. Moritz, D. Taylor, D. L. Matthews, Ctr. for Biophotonics Science and Technology (United States); J. W. Chan, Lawrence Livermore National Lab (United States)

Laser tweezers Raman spectroscopy has proven to be an effective technique for single cell analysis and identification in suspension with minimal sample preparation. However, the commercialization and further development of this technique into Raman activated flow cytometer is impeded by the long acquisition times (~minutes), the cumbersome instrumentation, and the lack of necessary automation for sampling large numbers of cells. In this talk, we present our latest progress to address these limitations. A compact and microscope free laser trap Raman spectroscopy apparatus with a footprint of only 2 ft x 2 ft has been built. Several efforts to improve the optical throughput of the system will be discussed in the talk, such as combining a semi-confocal detection configuration with a lens-based high throughput spectrometer, detecting both forward and backward scattered Raman photons simultaneously, and developing a system with multiple optical traps. Raman spectra can be acquired from biological samples with reasonable SNR in less than 1 second with our compact system. A novel optical configuration that uses the backscattered laser light from the trapped objects as a trigger to acquire Raman spectra from the particle has been implemented into the system to enable fully automated acquisition of the Raman spectra. The use of a dual-beam optical trap configuration enables a slit-scan Raman

7555-45, Session 9

Assessment of the clinical application of near-infrared fluorescence for the detection of parathyroid glands

C. Paras, L. White, J. T. Broome, J. E. Phay, A. Mahadevan-Jansen, Vanderbilt Univ. (United States)

Endocrine surgery traditionally involves meticulous dissection and resection of diseased glands based on visual recognition by the surgeon. Complications such as postoperative hypocalcemia and hypo-parathyroidism can occur due to accidental or incomplete removal of parathyroid glands. Initial fiber probe measurements have shown that the parathyroid exhibits markedly higher levels of near-infrared autofluorescence in comparison to all other tissues in the neck. In addition, imaging experiments have demonstrated that is possible to image the NIR fluorescence produced by the parathyroid providing the same level of anatomic guidance while providing spatial context. The impact of disease state, gender and age on the peak intensities of the thyroid and parathyroid signals was examined with the point based spectra from the fiber probe study. Results indicate that the intensity of parathyroid fluorescence is consistently stronger than the surrounding tissues regardless of disease state and, moreover, that none of the factors evaluated have a significant impact on the fluorescence intensity. Additionally, we have performed protein analysis to determine the source of the near-infrared biological fluorescence.

7555-46, Session 10

The cyanide detoxification effects are dependent on cobinamide administration routes as demonstrated by near-infrared spectroscopy

J. G. Kim, J. Lee, D. Mukai, S. Mahon, Beckman Laser Institute and Medical Clinic (United States); G. R. Boss, W. Blackledge, Univ. of California, San Diego (United States); S. Patterson, Univ. of Minnesota (United States); O. Mohammad, V. S. Sharma, Univ. of California, San Diego (United States); B. J. Tromberg, Beckman Laser Institute and Medical Ctr. (United States); M. Brenner, Univ. of California, Irvine Medical Ctr. (United States) and Beckman Laser Institute and Medical Ctr. (United States)

In this study, we administered a novel CN antidote, cobinamide, to animals poisoned with CN via either intravenous or intramuscular routes and monitored CN poisoning and recovery in both the brain and the forearm muscle simultaneously using a non invasive near infrared spectroscopy (NIRS) to compare CN detoxification effectiveness of cobinamide depending on administration routes.

New Zealand male white rabbits (~4kg) were administered 10mg of NaCN in 60cc normal saline via the left femoral vein at a rate of 1cc/min. After CN infusion, 0.082mmoles of cobinamide was either administered IV (n=6) or by intramuscular injection into the muscle (n=6) while control animals (n=6) received inactive vehicles. A NIRS probe with 1.65cm source detector separation was placed on the forehead, and a second probe with 0.95cm separation was placed on the right forearm muscle. Changes in oxy- ([OHb]) and deoxyhemoglobin concentration ([RHb]) during CN infusion and recovery were measured from both brain and forearm muscles. Recovery rate was compared among groups by obtaining the slope during 10min of initial recovery.

[OHb] from both brain and forearm muscle increased while respective [RHb] decreased gradually during the CN infusion. Cobinamide



administration via both routes caused a much faster recovery of [OHb] and [RHb] compared to those from control animals. We also found that intravenous administration was more effective than intramuscular administration at the same dose.

These results show that NIRS can be a useful tool for monitoring CN poisoning and recovery, and also for optimizing the administration routes and the dose of novel drugs such as cobinamide in CN detoxification.

7555-47. Session 10

In vivo rabbit traumatic lung injury detected by noninvasive near-infrared spectroscopy

J. G. Kim, J. Lee, S. B. Mahon, B. J. Tromberg, Beckman Laser Institute and Medical Ctr. (United States); M. Brenner, Univ. of California, Irvine Medical Ctr. (United States) and Beckman Laser Institute and Medical Ctr. (United States)

In previous studies, we demonstrated the feasibility of a simple near infrared spectroscopy (NIRS) device for detection of traumatic lung injury using an ex vivo intact pig lung injury model. From the ex vivo pig model, we observed marked changes in reflectance spectra amongst normal in vivo, post sacrifice, and pneumothorax cases. Marked changes in reflectance between in vivo and post sacrifice conditions indicated that an in vivo animal model is necessary to determine whether one can detect and differentiate various classifications of pleural space injury. In this study, we have established an in vivo rabbit lung injury model to confirm results from the ex vivo pig model. Two incisions were made through the chest wall of the anesthetized rabbit to insert a trocar for laparoscopy and chest tube for simulation of pneumothorax, pleural effusion, and hemothorax by introducing air, 60ml of saline, and 60 ml of blood. Laparoscopy was performed to ensure proper induction of pneumothorax. With the rabbit laid on its side, the NIRS probe (source detector separation of 2.85cm) was placed on its dorsal side to perform a series of spectroscopic measurements. The reflectance spectra were normalized at 805nm to be compared amongst in vivo, pneumothorax, pleural effusion, and hemothorax. Results showed that a simple near infrared spectroscopy can differentiate the different types of lung injury in this in vivo model. These findings indicate the potential utility of NIRS in the battle field as a rapid non invasive diagnostic and monitoring tool.

7555-48, Session 10

Fiber spectroscopy of oxygen saturation of the gastric conduit during esophagectomy

D. S. Gareau, J. Hunter, S. L. Jacques, Oregon Health & Science Univ. (United States)

Esophagectomy replaces a cancerous esophagus with part of the stomach remodeled into a gastric conduit. To mobilize the stomach tissue that will become the conduit, the short gastric and left gastric arteries must be severed (ligated). Blood supply is decreased to the very tissue that must be fused to the opening left by esophagus removal. 20% of the cases fail and leak at the fusion site (anastamosis). Many factors influence the binary outcome of success or failure but we hypothesize that blood suppled oxygen (oxygen saturation) at the anastamosis is critical to success. Unfortunately, diagnostics are lacking and failures present too late for intervention.

We developed an intraoperative fiber probe that measures the total amount and oxygen saturation of blood in the tissue. Two sterilized 12' fibers deliver and collect light from the tip of the gastric conduit. The light travels about 1cm in the tissue and the transmission spectrum carries information about blood content and saturation. In 20 patients thus far, we observed a statistically significant drop in saturation with the left gastric artery ligation. Unfortunately, there was no correlation between patients left poorly saturated immediately after the surgery and failures one week later. Unseen dynamics play out in the days after surgery where secondary blood supply is either increasing capacity or not. This information could predict failures in time for intervention.

7555-49, Session 10

Integrated micro-total analysis system (mTAS) for biophotonic enzymatic detections

A. Chandrasekaran, M. Packirisamy, Concordia Univ. (Canada)

Lab-on-a-chip or Micro total analysis systems (mTAS) technologies offer a lot of potential applications for biosensing and biomedical detections. This paper presents the design, fabrication and characterization of a novel fully integrated silicon-polymer based biophotonic Micro-Total Analysis System for the real-time detection of enzymes and antigens. This device uses optical detection methods i.e optical absorption and Laser induced fluorescence techniques to detect the presence, concentration and the activity of biomolecules. The main components of the proposed system are microfluidic unit and micromechanical fluid actuation system, integrated with the optical detection systems. Echelle grating based Spectrometer-on-Chip on Silica-on-Silicon (SOS) is integrated with the opto-microfluidic assembly. One of the novelties of the present work is the wavelength specific configuration of the Spectrometer-on-Chip as against the arrangement of a standard spectrometer and herein, each output channel is designed for specific wavelength of tunable bandwidth targeting fluorescence of a particular band. In this way, simultaneous detection of multiple biomolecules is feasible, each fluorescing at specific wavelengths. On-Chip fabrication and integration of valveless micropump has been carried out in order to facilitate the transportation of fluid within the system.

The feasibility of absorption detection is demonstrated using enzymeantienzyme reaction and the fluorescence detection demonstrated through the detection of non-covalent interaction between antigen and fluorophore tagged antibody. The important advantages of the proposed mTAS are functional independence of each module of the system, simultaneous multi-analyte detection, rapid, precise and discriminating results, low background/high signal-to-noise ratio, lack of moving parts, robust, portability, and feasibility of bulk fabrication.

7555-50, Session 10

FCS measurement of von Willebrand Factor multimer distributions for coagulation disorder subtyping

R. Torres, M. J. Levene, Yale Univ. (United States)

Fluorescence correlation spectroscopy (FCS) has found wide-spread use in biophysics but has not expanded significantly into clinical applications. We present measurement of von Willebrand Factor (vWF) multimer distributions using FCS as an early example of its applicability to clinical laboratory diagnostics. The distribution of vWF multimers is critical for proper blood clotting. The most common heritable clotting disorder, von Willebrand's disease (vWD), is characterized by abnormalities in the vWF distribution. Thrombocytopenia purpura (TTP), a difficult-to-diagnose and critical condition, is also characterized by an abnormal distribution of vWF multimers. FCS provides a rapid and inexpensive method of measuring vWF distributions that can improve our ability to diagnosis, classify by sub-type, and manage vWD and TTP.

7555-51, Session 10

Correlation of morphological and molecular parameters for colon cancer

S. Yuan, Univ. of Maryland, College Park (United States); C. A. Roney, National Institutes of Health (United States); Q. Li, Univ. of Maryland, College Park (United States); J. Jiang, A. Cable, Thorlabs Inc. (United States); R. M. Summers, National Institutes of Health (United States); Y. Chen, Univ. of Maryland, College Park (United States)

TEL: +1 360 676 3290 · +1 888 504 8171 · customerservice@spie.org



Colorectal cancer is the second leading cause of cancer death in the United States. There is great interest in studying the relationship among microstructures and molecular processes of colorectal cancer during its progression at early stages. In this study, we use our multi-modality optical system that could obtain co-registered optical coherence tomography (OCT) and fluorescence molecular imaging (FMI) images simultaneously to study colorectal cancer. The over-expressed carbohydrate -L-fucose on the surfaces of polyps facilitates the bond of adenomatous polyps with UEA-1 and is used as biomarker. The UEA-1 conjugated contrast agent contains fluorescence dye Lissamine Rhodamine PE. Tissue scattering coefficient and adjusted standard deviation derived from OCT axial scan are used as quantitative values of structural information. Both structural images from OCT and molecular images show spatial heterogeneity of tumors. Correlations among those values are analyzed and demonstrate that scattering coefficients are positively correlated with FMI signals in conjugated samples and negatively in non- conjugated samples. In UEA-1 conjugated samples (8 polyps and 8 control regions), the correlation coefficient is ranged from 0.45 to 0.99; while in non-conjugated samples (16 polyps and 16 control regions), the correlation coefficient is ranged from -0.68 to -0.31. These findings indicate that the microstructure of polyps is changed during cancer progression and the change is well correlated with certain molecular process. Our study demonstrated that multi-parametric imaging is able to simultaneously detect morphology and molecular information and it can enable spatially and temporally correlated studies of structure-function relationships during tumor progression.

7555-52, Session 10

A non-contact optical measurement procedure for precise monitoring of respiration rate and flow

L. Scalise, P. Marchionni, Univ. Politecnica delle Marche (Italy)

In this paper we present a non-contact measurement procedure designed for precise monitoring of the respiration rate (RR), in terms of time intervals, and respiration flow (RF), in terms of L/min. It is based on the optical measurement of the chest wall movements induced by the inspiration and expiration. This procedure is based on the use of a laser Doppler vibrometer (LDVi) to access the velocity of displacement of the skin in correspondence of the chest wall and on special data processing to obtain the respiration rate and flow.

The method has been validated on in-vivo on a population of 30 subjects. We simultaneously operated our measurement with LDVi and a spyrometer (golden standard measurement method for RR and RF), in order to synchronously record the chest wall velocity, named optical VibroSpyrometer (VS) and the RR and RF signals from the spirometer. From both signals we have firstly extracted inspiration and expiration peaks (making use of Wavelet Analysis) and then compared respiration intervals (RR) series and RF values, from the two instruments, by Bland-Altman method.

Results show how the optical (VS) succeeds in computing precisely the RR (differences < 97%) and showed a good agreement for what concern the determination of the respiration flow.

References.

Tomasini E.P et al. Carotid artery pulse wave measured by a laser vibrometer. Proc SPIE, 3rd Int Conf on Vibration Measurements by Laser Techniques, Ancona, 1998; 3411: 611-616.

Morbiducci U et al. Optical vibrocardiography: a novel tool for optical monitoring of cardiac activity. Annals of Biomedical Engineering. 2007;35(1):45-58.

Scalise, L. and U. Morbiducci, Non-contact cardiac monitoring from carotid artery using optical vibrocardiography. Med Eng Phys, 2008. 30(4): p. 490-7.





Monday-Tuesday 25-26 January 2010 • Part of Proceedings of SPIE Vol. 7556 Design and Quality for Biomedical Technologies III

7556-01, Session 1

Development and analysis of a polarized endoscopic hyperspectral reflection and fluorescence imaging system

D. S. Elson, T. Wood, K. Koh, V. Sauvage, Imperial College London (United Kingdom)

One of the key areas of biomedical engineering is the development of new, low-cost non-invasive diagnostic techniques for the early stages of various diseases. For detecting superficial tissue pathologies, such as epithelial neoplasia or carcinomas, the primary in vivo tool is inspection under white light. However, point-based fluorescence spectroscopy can provide excellent information on the presence and relative abundance of a whole library of tissue constituent chemicals. Polarisation effects also provide a large amount of information, for instance, Mie theory calculations can give an indication of scatterer size in tissue, a good indicator for cancer. Such high-resolution point-based techniques can offer excellent determination of tissue pathology, but for such a limited region that diseased regions can be easily missed. To attempt to investigate these signals in a clinical setting, we have constructed an imaging platform based around commercially available components that is capable of performing hyperspectral fluorescence imaging, narrow-band reflectance imaging, and polarisation resolved imaging. The focus of this presentation is the experimental measurement and characterisation of the polarisation properties of two commercial rigid laparoscopes as a necessary calibration step to allow the input polarisation field to be reconstructed. We have applied this system to the investigation of scattering and fluorescence test samples as well as to freshly excised human tissue.

7556-02, Session 1

Polarimetric signature imaging of the anisotropic bio-medical tissues

S. H. Wu, National Yang-Ming Univ. (Taiwan); D. Yang, Taipei Veterans General Hospital (Taiwan); A. E. T. Chiou, S. F. Nee, T. Nee, National Yang-Ming Univ. (Taiwan)

The polarimetric imaging of Stokes vector (I, Q, U, V) can provide 4 independent signatures showing the linear and circular features of biological tissues and cells. It is useful for critical disease discrimination and medical diagnostics applications. Using a novel Stokes digital imaging system that we have recently developed, we measured the Stokes vector images of tissue samples from sections of rat livers containing normal portions and hematomas. The Mueller matrix determined from the measured Stokes signatures data are analyzed using our optical polarization theory of anisotropic bio-molecule and bio-medium. These results provide an option of biosensing technology to inspect the structures of tissue samples, particularly for discriminating tumor and non-tumor biopsy.

7556-03, Session 1

High count rate pseudo-random single photon counting system for time-resolved diffuse optical imaging

Q. Zhang, N. Chen, National Univ. of Singapore (Singapore)

Pseudo-random single photon counting (PRSPC) is a new timeresolved method combining the spread spectrum time-resolved optical measurement method with single photon counting. A continuous wave laser diode is modulated with a pseudo-random bit sequence, while a single photon detector is used to record the pulse sequence in response to the modulated excitation. Periodic cross-correlation is performed to retrieve the impulse response. Compared with conventional time-correlated single photon counting (TRSPC), PRSPC enjoys many advantages such as low cost and high count rate without compromising the sensitivity and time-resolution. In this paper, we report a PRSPC system that can be used for high speed acquisition of the temporal spread function of diffuse photons. It can reach a photon count rate as high as 3Mcps. Experimental work has been conducted to demonstrate the system performance.

7556-04, Session 1

Confocal microscopes for imaging skin cancers: translation from laboratory to clinic

M. Rajadhyaksha, Memorial Sloan-Kettering Cancer Ctr. (United States)

Recent translational advances demonstrate the potential of confocal microscopy for diagnosis of melanoma in vivo (sensitivity 91%, specificity of 69%), diagnosis of basal cell carcinoma in vivo (sensitivity 92%, specificity 97%), pre-operative mapping of lentigo maligna and amelanotic melanomas to guide precise surgery, and intra-operative imaging of residual basal cell carcinoma to guide accurate biopsy. Basal cell carcinoma is detected in Mohs surgically excised tissue ex vivo (sensitivity 96%, specificity 89%), showing the feasibility of rapid pathology-at-the-bedside. However, today's state-of-the-art confocal microscopes are based on point-scanning technology which remains relatively complex, expensive and confined to tertiary cancer healthcare settings. Toward creating low-cost technology for worldwide translation into primary healthcare settings, line-scanning, with the use of linear CMOS or CCD array detectors and FPGA-based control electronics, may offer simpler and lower-cost alternatives. Our laboratory prototypes consist of only 8-10 main optical components and cost \$15,000 each. Preliminary results with full-pupil and divided-pupil configurations show optical sectioning of 1-2 um, lateral resolution of 0.7-1.0 um and imaging of nuclear detail in human epidermis in vivo that is competitive with point-scanning microscopes. Pupil engineering allows trade-offs between optical sectioning, resolution and contrast in scattering tissue. Opportunities for and challenges to large-scale translation to the clinic include the ability to observe large volumes of tissue in real-time, image interpretation in grayscale without the benefit of contrast agents, strategies to improve specificity, image-guided pathology, screening of early precancers, development of low-cost and reliable technology, and determining new paradigms for clinical utility.

7556-05, Session 2

Low-cost, portable imaging systems for cancer detection

M. C. Pierce, K. Rosbach, N. Thekkek, Rice Univ. (United States); A. Gillenwater, MD Anderson Cancer Center (United States); S. Anandasabapathy, Mt Sinai Hospital (United States); R. Richards-Kortum, Rice Univ. (United States)

The incidence of cancer in developing countries is rising rapidly. By 2010, it is estimated that 60% of new cases worldwide will occur in the developing world. Providing access to objective screening tools at the point-of-care can have significant impact on cancer mortality and morbidity, by enabling early diagnosis when treatment is cheaper and more effective. Optical imaging technologies are well suited to fill this



need, based upon measuring changes in scattered or fluorescent signals from tissue due to the onset and progression of neoplasia.

Our group has developed both wide-field (macroscopic) and high-resolution (microscopic) optical imaging devices for cancer screening and diagnosis. We have recently developed low-cost, portable, battery-powered versions of these systems, targeting cancer screening and diagnosis in developing countries. This presentation will discuss the technical challenges involved in translating optical imaging systems to these unique settings, and present data from recent field trials at clinical sites in India and China.

7556-06, Session 2

Disposable low-cost video endoscopes for straight and oblique viewing direction with simplified integration

F. C. Wippermann, E. Beckert, P. Dannberg, Fraunhofer-Institut für Angewandte Optik und Feinmechanik (Germany); B. Messerschmidt, Grintech GmbH (Germany); G. Seyffert, Optikron GmbH (Germany)

Video endoscopes with an imager located at the distal end possess a simplified opto-mechanical layout compared to classical setups since an optical relay system is not required. Together with the availability of low price miniature CMOS imagers, this enables for building low cost devices for single usage avoiding the necessity of withstanding autoclaving which is one of the major drivers in both, system fabrication and operating cost. The optical layout has to take into account geometrical as well as opto-electronical aspects and is therefore a trade-off between system diameter, sensitivity and resolution. Consequently, the image circle should be as close as possible to the outer diameter for optimum performance in terms of resolution and sensitivity which goes along with large pixel size. We propose systems designs and prototypes for f/4, 3mm outer diameter endoscopes with 70° and 110° field of view using a CMOS imager with 650x650 pixels of 2.8µm pitch. The systems are based on a simplified and rugged integration using a single polymer lens made by injection molding, a GRIN lens and a dispensed lens made of UV curing material allowing for high performance paired with low fabrication cost. Additionally, a side view system angled at 30° is presented based on a tilting reflection prism requiring minimum construction space allowing for an outer diameter of 3mm.

7556-07. Session 2

Portable, battery-operated, fluorescent field microscope for the developing world

A. R. Miller, G. Davis, Beyond Traditional Borders, Rice University (United States); Z. M. Oden, R. Richards-Kortum, Department of Bioengineering, Rice University (United States)

In many areas of the world, current methods for diagnosis of infectious diseases such as malaria and TB, involve microscopic evaluation of a patient specimen. Advances in fluorescence microscopy can improve diagnostic sensitivity and reduce time and expertise necessary to interpret diagnostic results. However, modern researchgrade microscopes are neither available nor appropriate for use in many settings in the developing world, outside of centralized health centers. To address this need, we designed, fabricated and tested a portable, battery-powered fluorescent field microscope, optimized for infrastructural constraints of the developing world. The compact microscope (3x5x7 inches, <2 lbs) provides images in either brightfield or fluorescence mode at up to 1000X magnification. Illumination is provided using two battery-powered flashlights, incorporating a white (brightfield) or blue (fluorescence) LED. The cost of a single prototype was 480 USD, and we estimate a cost of less than 300 USD when produced in quantity. Tests using clinical specimens illustrate that the image resolution obtainable exceeds the minimum necessary to discern malaria parasites

and M. Tuberculosis bacilli using bright-field and fluorescent techniques, respectively. By using over-the-counter parts, such as a flashlight for the light source, the microscope is designed to be repairable in-country. A portable, battery-operated fluorescent field microscope provides an inexpensive tool for improved disease diagnosis and screening, for TB and malaria, particularly in developing world and rural areas where centralized health centers with microscopy services are difficult to access

7556-08, Session 2

Cost assessment of disposable endomicroscopic objectives for medical diagnostics

R. T. Kester, J. Sun, T. Tkaczyk, Rice University (United States)

Cost assessment of disposable endo-microscopic objectives for medical diagnostics.

7556-09, Session 3

In vivo Gabor-Domain Optical Coherence Microscopy

J. P. Rolland, P. Meemon, S. Murali, K. P. Thompson, K. Lee,

Optical Coherence Tomography (OCT) is an emerging technology capable of depth sectioning biological tissue at micrometer scale resolution. As a result of the large efforts put forth by the scientific and commercial community to develop larger and larger source bandwidth, OCT has achieved, since the mid 1990s, remarkable axial resolution. A remaining challenge is to simultaneously demonstrate micron-scale lateral resolution without scanning stages, because it is only then that we open a path for in vivo clinical applications seeking histology grade image quality. High speed imaging is an intrinsic stringent requirement for in vivo imaging. Here, we present and discuss a developing technology, Gabor-Domain Optical Coherence Microscopy (GD-OCM), whose innovation intrinsically builds on a recently reported liquid-lens based varifocal optical probe that delivers 2 µm invariant lateral resolution by design throughout a 2 mm cubic full-field of view. We shall report on how optical system design can enable innovation and we shall report on the automatic data fusion method developed to render in real-time an infocus high resolution image throughout the imaging depth of the sample. 2D and 3D images of an African frog tadpole (Xenopus laevis) and in vivo human skin imaged with the Gabor Domain OCM will be shown that demonstrate subcellular resolution without the need, for the first time, for either x-y translation stages, depth scanning, high-cost adaptive optics, or manual intervention.

7556-10, Session 3

Perspectives of optical scanning in OCT

V. Duma, Aurel Vlaicu Univ. of Arad (Romania); J. Rolland, Univ. of Rochester (United States); A. G. Podoleanu, Univ. of Kent (United Kingdom)

We present an overview of our contributions and directions of research in the domain of optical scanners, with regard to their perspectives of use in optical coherence tomography (OCT). The performances, advantages and drawbacks of the different types of scanning systems are summarized, in a comparative look. Both 1D and 2D scanners for various applications in OCT, from swept source filters to probe scan are considered. We present our developments of polygon mirror (PM) scanners both analitycally and experimentally. We study galvoscanners (GS) in order to increase their duty cycle even for high scan frequencies, and the limitations in reaching this goal are discussed. Based on these advancements, 2D scanners, i.e. the double GS and the PM+GS solutions are approached with





regard to their optimum driving functions. These 2D devices are finally compared to the Risley prism scanner, the best choice when compactity is of prime importance. A trade-off is thus accomplished between recent developments and requirements of scanning devices for OCT in order to achieve the most apropiate results for a certain application.

7556-11, Session 3

Full-range frequency domain Doppler optical coherence tomography

P. Meemon, College of Optics and Photonics, Univ. of Central Florida (United States); K. Lee, J. P. Rolland, Univ. of Rochester (United States)

Frequency domain optical coherence tomography (FD-OCT) systems achieve higher sensitivities compared to time domain OCT systems. However, one of the main challenges in FD-OCT is the obscuring object structure caused by the mirror image generated by the Fourier transform of the real spectrum. We have designed and developed a novel full range FD OCT system based on phase shifting method that we refer to as the dual-reference full-range FD-OCT (DR-FR-OCT), which enables doubling the imaging depth by removing the mirror image. The technique enables full range imaging without any loss of speed and is intrinsically less sensitive to movements of the subject since two spectral interference signals with a phase difference of $\pi/2$ are obtained simultaneously from two reference arms. In this paper, we applied the DR-FR-OCT to Doppler imaging. FD-OCT allows direct access to the phase component of the reflectivity profile and hence can be directly used to quantify the Doppler velocity. The application of DR-FR-OCT to Doppler imaging is straight forward and without loss in the velocity dynamic range since the phase information of the acquired spectra is preserved. Furthermore, the full range FD-OCT provides a superior signal-to-noise ratio (SNR) over the normal FD-OCT since the region around the zero delay, which is the most sensitive region, is used. Because the quality of Doppler imaging relies on the SNR of the system, the DR-FR-OCT Doppler imaging is investigated to achieve a superior performance when imaging the flow in weak backscattered flow sample or the flow in deep tissue.

7556-12. Session 3

Full-range k-domain linearization in spectral-domain optical coherence tomography

J. Kim, C. Lee, M. Jeon, U. Jung, Kyungpook National Univ. (Korea, Republic of); W. Jung, S. A. Boppart, Univ. of Illinois at Urbana-Champaign (United States)

We report a full bandwidth k-domain linearization method in spectraldomain optical coherence tomography (SD-OCT). The proposed method utilizes wavelength-pixel information provided by a rotating slit-based wavelength filter. For calibration purposes, the filter is located either after a broadband source or at the end of the sample path, and returns a filtered spectrum with a narrowed line width (~0.5 nm) to the line scanning camera in the detection path. The wavelength swept spectrums are co-registered with the pixel positions according to their center wavelengths, which can be automatically measured with an optical spectrum analyzer (OSA). To avoid using an OSA, the rotating slit pattern is specially designed to scan the wavelength linearly in the k-domain, and therefore, one can acquire the linear k information throughout all the pixels in the camera. During regular imaging sessions, the method does not require any filter or software recalibration algorithm, but simply resamples the OCT signal from the detected array without using rescaling or interpolation methods. The accuracy of k linearization is maximized by increasing the number of k linear positions, which is known to be a crucial parameter to maintain a narrow point spread function width in depth. The broadening effect is also studied by changing the number of k linear positions by under-sampling to search for the optimal value. However, the system provides more position information, surpassing the optimum without sacrificing imaging speed. As a result, the SD-OCT

system can benefit from hardware/software simplification, an increase in speed, and an improvement in axial image resolution by using this full range k-domain linearization method.

Key Words: Spectral Domain Optical Coherence Tomgoraphy, k domain linearization, wavelength sweeping filter.

7556-13, Session 3

Optical design of spectrometer and catheter probe in OCT

Z. Hu, A. M. Rollins, Case Western Reserve Univ. (United States)

This presentation will report the progresses and considerations of the optical designs of the spectrometer and catheter probe used in the optical coherence tomography (OCT) in the OCT group at Case Western Reserve University. The considerations in the design of the spectrometer include high spectra resolution, mechanical simplicity, high throughput, flat-top spectra response and spectra linearity with which OCT delivers less image fall-off, high imaging sensitivity, high axial resolution. It also leads to a low developing cost of building the spectrometer. The design considerations of the catheter probe include small size, short rigid length, astigmatism and chromatic dispersion compensations, high illuminating light return coupling efficiency and simple structure with which OCT delivers high image contrast, high lateral resolution and sensitivity, more imaging depth and insertion depth. It also leads to a low probe developing cost. In order to manufacture the optimally designed spectrometer and catheter probe, the optical design and mechanical design software were used in the development of the spectrometer and the probe in the OCT group at Case Western Reserve University. The detail will be demonstrated in the presentation.

7556-14, Session 4

Characterization and comparison of relative intensity noise in optical sources for optimizing performance of optical coherence tomography systems

S. Shin, Beckman Institute for Advanced Science and Technology (United States) and Univ. of Illinois at Urbana-Champaign (United States); U. Sharma, H. Tu, W. Jung, Beckman Institute for Advanced Science and Technology (United States); S. A. Boppart, Beckman Institute for Advanced Science and Technology (United States) and Univ. of Illinois Urbana-Chammpaign (United States)

System sensitivity and imaging speed are two of the most important parameters used to evaluate the performance of an OCT system. While it is possible to obtain A-scan rates up to several MHz, the increase in speed is often realized at the cost of reduced system sensitivity. Hence, a thorough understanding of all the noise sources is very critical to maximize the system sensitivity. Although the theory behind the origin of various noise sources including thermal noise, shot noise, quantization error, etc., is well understood, the existing prevalent theory for estimating RIN for various OCT light sources is questionable. Hence, this theory cannot be applied uniformly because the origin of noise in various light sources differs significantly owing to the different physical nature of photon generation. A careful characterization and understanding of RIN associated with various optical sources is essential for evaluating their comparative performance. In this study, we perform experimental characterization of RIN of several optical sources including several SLDs, bandwidth filtered SLDs, combined outputs from two SLDs, a supercontinuum source, and a wavelength-swept semiconductor laser. To the best of our knowledge, no systematic study has been performed to quantitatively measure the RIN contribution of various OCT light sources. These quantitative experimental results will be helpful in providing a better understanding of the contribution of RIN towards degradation of OCT system sensitivity, and subsequently aid in designing



optimized systems. Improved performance in system sensitivity could then enable imaging at even higher imaging speeds, potentially without compromise in image quality.

7556-15, Session 4

Fast-gated single-photon detectors boost dynamic range in NIR spectroscopy

A. Tosi, A. Dalla Mora, F. Zappa, S. Cova, D. Contini, L. Spinelli, A. Pifferi, A. Torricelli, R. Cubeddu, Politecnico di Milano (Italy)

We present a novel technology for wide dynamic range optical investigations, based on fast-gated silicon Single-Photon Avalanche Diodes (SPAD) in Time-Correlated Single-Photon Counting (TCSPC) setup. The detector is gated-on and off in less than 500ps and kept on for detecting photons only within short time slots. This technique is particularly useful in applications where a large amount of unnecessary photons precedes or follows the optical signal to detect, such as in time-resolved NIR spectroscopy, optical mammography, and optical molecular imaging.

In particular, in time-resolved reflectance spectroscopy, when the source-detector separation is decreased to improve performances, the detection electronics easily saturates. The reason being the huge amount of "early" photons, diffused by superficial layers. Our setup is able to reject these photons and detect only "late" photons, thus allowing to increase the injected power. We acquired diffusive curves of two phantoms with 95ps time resolution and dynamic range of 10^7 with a further strong improvement of three orders of magnitude in the measurement time. This approach allows to go beyond the limits of TCSPC technique which forces one to reduce the optical power to avoid the saturation of the detection electronics.

7556-16, Session 4

Spectral calibration of an AOTF hyperspectral imaging system

J. Katrašnik, F. Pernuš, B. Likar, Univ. of Ljubljana (Slovenia)

Near-infrared hyperspectral imaging is becoming a popular tool in pharmaceutical quality assurance and in biomedicine, especially in live cell microscopy, in detection and analysis of melanoma, and in the study of microcirculation. Acousto-optic tunable filter (AOTF) in combination with a near-infrared camera is one of the most cost-effective systems for near-infrared hyperspectral imaging. Unfortunately there is no accurate, low-cost and simple technique for spectral calibration of such an imaging system. Namely, calibration of AOTF filters is usually done by measuring AOTF parameters and calculating the tuning curve with the physical model. This approach is inaccurate and very complex, since all of the AOTF parameters have to be measured or known beforehand. Other calibration approaches either use two lasers or a spectrometer with a higher accuracy. The first approach is inaccurate, but low cost, while the latter is accurate, yet expensive and complex. In this paper an accurate, low cost and simple calibration method utilizing a mercury calibration lamp is presented. A mercury lamp is one of the best calibers for AOTF spectral calibration, as its emission spectrum is exactly defined, and because of its low cost. The algorithm is based on modeling the imaging system's response to the mercury lamp light spectrum and on automatically matching this model to the actual measured spectrum. The laser-based validation indicated that the method yields better results than calibration with the physical model and thus represent a practically feasible approach to efficient spectral calibration of AOTF hyperspectral imaging systems.

7556-17, Session 4

Geometrical calibration of an AOTF hyperspectral imaging system

Z. Spiclin, J. Katrasnik, M. Buermen, B. Likar, F. Pernus, Univ. of Ljubljana (Slovenia)

Optical aberrations present an important problem in optical measurements. Geometrical calibration of an imaging system is therefore of the utmost importance for achieving accurate optical measurements. In hyperspectral imaging systems, the problem of optical aberrations is even more pronounced because optical aberrations are wavelength dependent. Geometrical calibration must therefore be performed over the entire spectral range of the hyperspectral imaging system, which is usually far greater than that of the visible light spectrum. This problem is especially adverse in AOTF (Acousto-Optic Tunable Filter) hyperspectral imaging systems, as the diffraction of light in AOTF filters is dependent on both wavelength and angle of incidence. Geometrical calibration of the hyperspectral imaging system was preformed by stable caliber of known dimensions, which was imaged at different wavelengths over the entire spectral range. The acquired images were then automatically registered to the caliber model by rigid and non-rigid registration transformation based on B-splines and by minimizing normalized correlation coefficient. The calibration method was tested on an AOTF hyperspectral imaging system in the near infrared spectral range. The results indicated substantial wavelength dependent optical aberration that is especially pronounced in the spectral range closer to the infrared part of the light spectrum. The calibration method was able to accurately characterize the aberrations and produce transformations for efficient sub-pixel geometrical calibration over the entire spectral range, finally yielding better spatial resolution of hyperspectral imaging system.

7556-34, Poster Session

Development of portable health monitoring system device for automatic self-blood sugar level measurement

H. Kim, E. Nakamachi, M. Yusuke, M. Yoshihumi, Doshisha Univ. (Japan)

In this study, a new HMS (Health Monitoring System) device is developed for the diabetic patient. This device has features such as 1)3D blood vessel location search 2) laptop type, 3) puncturing a blood vessel by using a minimally invasive micro-needle, 4) very little blood sampling (10µl), and 5) automatic transfer and measurement blood sugar level. This compact SMBG (Self-Monitoring of Blood Glucose) device employs a syringe reciprocal type blood extraction mechanism because of its high accuracy, and a disposable syringe unit. The syringe unit consists of a syringe itself, a piston, a magnet, a ratchet and a titanium alloy microneedle, whose inner diameter is about 80µm. The body unit consists of body parts, a linear driven type stepping motor, a glucose enzyme sensor, and a slider for accurate positioning control. The body unit is all-in-one mechanism with a glucose enzyme sensor for compact size and stable blood transfer. On designing, required thrust force to drive the slider is designed to be greater than the value of the blood extraction force. Further, only one linear stepping motor is employed for blood extraction and transportation processes. The experimental results have shown more than 80% of volumetric efficiency under the piston speed 2.4mm/s. Further, the blood sugar level was measured successfully by using the glucose enzyme sensor. Finally, the availability of our device was confirmed.



7556-35, Poster Session

Homogeneous UVA system for corneal crosslinking treatment

F. R. Ayres Pereira, Univ. of Sao Paulo (Brazil); M. A. Stefani, J. A. Otoboni, E. H. Richter, Opto Eletronica SA (Brazil); L. Ventura, Univ. of Sao Paulo (Brazil)

The treatment of keratoconus and corneal ulcers by collagen crosslinking using ultraviolet type A irradiation, combined with photo-sensitizer Riboflavin (vitamin B2), has shown to be a promising technique. The standard protocol suggests instilling Riboflavin in the pre-scratched cornea by 5 minutes for 30min during the UVA (365nm) irradiation of the cornea at 3mW/cm² for 30 min. This process leads to an increase of the biomechanical strength of the cornea, stopping the progression, or sometimes, even reversing the Keratoconus. The collagen Cross-Linking can be achieved by many methods, but the utilization of UV-A light is ideal because of its possibility of a homogeneous treatment leading to an equal result along the treated area.

We have developed a system, to be clinically used for treatment of unhealthy corneas using this technique, which consists of an UV emitting device controlled by a closed loop system.

The UVA irradiation system presents a peak wavelength of 365nm with adjustable power (irradiance) output. The adjustable power output provides flexibility to be used in non-standard cases. The system consists of a hardware closed loop, which guarantees a 20% precision for the adjusted power output.

The optical system provides homogeneity of the UV beam for three selectable beam spots: 6, 8 and 10mm diameters. Tests show that the homogeneity varies only up to 4% along the UV beam.

The controlled emitting power and beam homogeneity ensure the best condition for a good performance treatment, even at room temperature gradients, system's aging and electromagnetically noisy interference from the environment.

7556-36, Poster Session

Quality of clinical therapeutic tools and instrumentation for neonatal jaundice and advanced technologies of Laser phototherapy

M. Hamza, Mansoura Univ (Egypt); M. H. Sayed El-Ahl, A. M. Hamza, M. Y. Hamza, A. M. Hamza, Tabarak Children's Hospital (Egypt)

Prevention of kernicterus has to be planned at a national level in the context of regionalization of neonatal care. Globally neonatal hyperbilirubinemia is a major cause of newborn death and disability. Evidence based recommendations for the prevention of neonatal hyperbilirubinemia aims at identification of neonates at risk and their prompt treatment with phototherapy or exchange transfusion when indicated. High quality intensive phototherapy of neonatal jaundice helps to reduce the need for exchange transfusion. The authors present their clinical experiences about the quality of conventional therapeutic tools and instrumentation for neonatal jaundice in addition to laser phototherapy to lower serum bilirubin levels in newborn infants. Home phototherapy helps to reduce the need for hospitalization with its negative impact on bonding and breast feeding. The authors present the design of high quality new mobile devices using the advanced technologies of laser diodes and light emitting diodes that are suitable for home phototherapy, easy to use, safe and cost effective.

7556-37, Poster Session

Hamiltonian metric for tumor detection

C. Ou, Hsiuping Institute of Technology (Taiwan)

There is always high qualities demand on the biomedical images for the diagnosis. Many researches already work on these topics. Among these research, new architecture, image reconstruction and noise reduction are the main topics. Techniques like pattern recognitions, filters, fusion and Wobulation are proposed to overcome and deal with the biomedical image degradation problems. Motion estimation, interpolation and edge detection are works together to improve these images for tumor detection. However, a good and fast metric is still under a high demand for fast estimating the overall-pixel-based qualities of the medical images. Pixels based metric must tell the essential difference of different platforms, not only the bulk properties like uniformity or contrast ratios, but also as a measurement for microscopic properties. During the formation of the medical images, one can always found that the images are different under the same bulk properties. The fabrication of the device and the usages of the platform will cause such problems.

In this report, metric based on the idea of the lattice gas Hamiltonian dynamics [5] is proposed to give a clear estimation of various transmitted images. Brief introduction on the calculation of the Hamiltonian and the application of this proposed metric to different kinds of imaging producing and transmission conditions are reveals. Simulations on the proposed Hamiltonian metric to these conditions are discussed for the tumor detection.

7556-38, Poster Session

Safe XML Software Standards

R. C. Leif, Newport Instruments (United States)

Introduction: Because the Digital Imaging and Communications in Medicine (DICOM) standard is a FDA Class II device, the safety of the software developed as part of a standard should be maximized. Readability, modularity, strong typing, and reuse are 4 software engineering principles that can and should be applied to XML schemas. This is possible with the use of the XML Schema Definition Language

Materials & Methods: The information and data-types present in an XML page prepared by a domain expert (not the author) were used to design a schema. New data-types were created and data-types from the other CytometryML schemas were reused. The XSDL schema was validated by XMLSpy and Stylus Studio. A new XML page was subsequently produced from the schema and then filled with the values from the original XML page, and validated.

Results: The new CytometryML schema, the XML page prepared by a domain expert, and the new XML page generated from that schema will be discussed and compared. The XML produced from the schemas was more compact and readable that the original, which was based upon DICOM semantics. The data values for the generated XML page could be validated by type checking; whereas, those in the original XML page

Conclusions: It has been possible with XSDL to maximize readability, create a modular structure and strongly typed as well as reusable datatypes. Maximizing reuse including reuse of designs and documentation besides increasing safety should significantly help to improve the US medical informatics infrastructure, which should produce a significant decrease in healthcare costs.



7556-39, Poster Session

The common-path optical frequency domain imaging for discriminating pearl's grading

M. J. Ju, S. Y. Ryu, J. Na, H. Y. Choi, B. H. Lee, Gwangju Institute of Science and Technology (Korea, Republic of)

We present the common-path optical frequency domain imaging (CP-OFDI) system, which uses a ready-to-ship scanning light source, for non-invasive evaluation of various pearls. By adopting the commonpath configuration, we could implement a compact and efficient optical probe with highly minimized polarization problem and group velocity dispersion (GVD) mismatch. Besides, this imaging system could image the whole circumference of a pearl without any scanning but with a sample rotating stage. The common path probe consists of a standard objective lens and a partial reflector operating as the reference arm in a conventional imaging system based on interferometer. The rotation stage is continuously operated with a 1 arcsec resolution. The average imaging depth reached up to 5 mm, which was deep enough to examine the internal structure of the pearl. The sensitivity of the system was experimentally determined to be 110 dB. Moreover, this CP-OFDI system is capable of real-time display of two-dimensional images. Based on the proposed CP-OFDI system, the nacreous thickness and nacreous laminated pattern were measured and analyzed simultaneously. In addition, we could check which kind of nucleus was inserted in the pearl as well as the presence of nucleus itself. Experimental results show that the CP-OFDI system has great potential for identifying and grading pearls and other jewelry with a non-invasive way.

7556-40, Poster Session

A practical approach to spectral calibration of short wavelength infrared hyperspectral imaging systems

M. Bürmen, F. Pernuš, B. Likar, Univ. of Ljubljana (Slovenia)

Near-infrared spectroscopy is a promising, rapidly developing, reliable and noninvasive technique, used extensively in the biomedicine and in pharmaceutical industry. With the introduction of acousto-optic tunable filters (AOTF) and highly sensitive InGaAs focal plane sensor arrays. real-time high resolution hyper-spectral imaging has become feasible for a number of new biomedical in vivo applications. However, due to the specificity of the AOTF technology and lack of spectral calibration standardization, long-term stability and compatibility of the acquired hyper-spectral images among different systems is still a challenging problem. Efficiently solving both is essential as the majority of methods for analysis of hyper-spectral images relay on a priori knowledge extracted from large spectral databases, serving as the basis for reliable qualitative or quantitative analysis of various biological samples. In this study, we propose and evaluate fast and reliable spectral calibration of hyper-spectral imaging systems in the short wavelength infrared spectral region. The proposed spectral calibration method is based on light sources and materials, exhibiting distinct spectral features, which enable robust non-rigid registration of the acquired spectra. The proposed calibration accounts for all of the components of a typical hyper-spectral imaging system such as AOTF, light source, lens and optical fibers. The obtained results indicated that practical, fast and reliable spectral calibration of hyper-spectral imaging systems is possible, thereby assuring long-term stability and inter-system compatibility of the acquired hyper-spectral images.

7556-18, Session 5

In situ optical property measurement in layered tissue: theoretical and experimental assessment of an unconstrained approach

Q. Wang, U.S. Food and Drug Administration (United States); K.

Shastri, Univ. of Virginia (United States); A. Agrawal, J. Pfefer, U.S. Food and Drug Administration (United States)

Accurate data on tissue optical properties (OPs) are essential for elucidating light-tissue interactions during optical spectroscopy-based detection of neoplasia in mucosal tissues such as those in the cervix and colon. We have developed and evaluated a diffuse-reflectancebased approach for in situ measurement of absorption coefficient (mua) and reduced scattering coefficient (mus') in top/epithelial (mua1, mus1') and bottom/mucosal (mua2, mus2') layers as well as the top layer thickness (L). Our approach requires no a priori knowledge of tissue chromophores and scatterers and is focused on UVA and visible wavelengths. Radially-resolved reflectance distributions were calculated for a wide variety of OPs and L combinations (mua from 1 to 22.5 1/ cm and mus' from 5 to 42.5 1/cm for both layers and L from 0.1 to 0.6 mm) using a condensed Monte Carlo (MC) model. These data were then used to train a neural network inverse model to estimate the OPs and L. Evaluation of this approach was performed using simulated data as well as multi-wavelength fiberoptic probe measurements from sixteen hydrogel phantoms. The experimental results show that the mean error for mua1, mus1', mua2, mus2' and L are 3.8 1/cm, 4.6 1/cm, 2.4 1/ cm, 6.8 1/cm and 0.12 mm, respectively. Theoretical simulations also indicate that additional detection fibers may enhance accuracy. Although our approach required extensive computational modeling, it has strong potential to provide accurate unconstrained measurements of OPs in two-layer mucosal tissue.

7556-19, Session 5

Assessment of pressure, angle, and temporal effects on polarization-gated spectroscopic probe measurements

S. Ruderman, V. Stoyneva, A. J. Gomes, J. D. Rogers, V. Backman, Northwestern Univ. (United States)

Noninvasive and real-time analysis of tissue properties, in particular, the quantitative assessment of blood content and light scattering properties of mucosa is useful in a wide variety of applications. However, the nature of interactions between contact fiber-optic probes and the tissue surface presents a challenging problem with respect to the variability of in vivo measurements, for example effects due to variations in the pressure and angle of the probe tip on the tissue surface. Previously, pressure and angle effects have been investigated for other modalities (i.e. diffuse reflectance and Raman spectroscopy). We present an evaluation of this variability, as well as the length of time in contact with tissue for polarization-gated spectroscopy. The evaluation is based on the quantification of mucosal blood content at superficial depths (within 100 to 200 microns of tissue surface) for ex-vivo measurements of colonic mucosa and in vivo measurements of oral mucosa. Measurements are presented for different pressures, angles and time scales and the variability due to these factors is assessed.

7556-20, Session 5

A fiber optic probe holder for optical spectroscopy and optical imaging

S. Oh, Miami Children's Hospital (United States) and Florida International Univ. (United States); A. Romero, Florida International Univ. (United States); J. Ragheb, S. Bhatia, W. Lin, Miami Children's Hospital (United States)

Currently fiber-optical probes in various biomedical optical systems are held by the investigator's hands during an in vivo data acquisition procedure. Inevitably, unintentional movements from the investigator alter the probe contact pressure against the target tissue. Ultimately these movements create noises or artifacts in the collected data. In addition, organs such as the heart and the brain possess rhythmic pulsations, which influence the probe contact pressure. Based on published



literature and reviews of our optical data from in vivo experiment, the inconsistent probe contact pressure induces detrimental optical intensity fluctuations and spectral profile change on the acquired optical data. Often, this type of data alternation reduces the accuracy of data analysis. To avoid this unwanted source of spectral alterations, it is crucial to maintain the probe pressure against the investigating sample, especially in vivo live tissue. This paper discloses the design of a fiber-optic probe holder with a damping mechanism which enables a steady probe contact pressure during an in vivo optical data acquisition procedure. The probe holder has two parallel axles and four springs incorporated for a damping mechanism on vertical movement. By utilizing this probe holder, time-dependent diffuse reflectance spectroscopy was acquired from cerebral cortex in vivo in a clinical study on a patient who underwent a craniotomy. In comparison to the optical data measured by hand held probe, motion artifact was efficiently reduced and the signal to noise ratio increased significantly. This demonstrates the clinical usefulness of the probe holder.

7556-21, Session 5

A 3D fluorescence imaging system incorporating structured illumination technology

L. Antos, Qioptiq-linos, Inc. (United States); P. Heneka, B. Luquette, B. McGee, Rochester Institute of Technology (United States); D. Nguyen, Rrochester Institute of Technology (United States); A. Phipps, D. B. Phillips, M. Helguera, Rochester Institute of Technology (United States)

A currently available 2-D high-resolution, optical molecular imaging system was modified by the addition of a structured illumination source to investigate the feasibility of providing depth resolution along the optical axis. The modification included additional optics as well as control and signal processing software. The objective of this effort is to evaluate the possibility of providing low-cost, non-invasive, functional imaging in three dimensions. In addition to the proposed system modifications, a calibration device has been developed to test the capabilities of the system in terms of range and resolution. Results from calibration experiments will be presented.

The modified system is capable of in focus projection of the Optigrid at different spatial frequencies, and supports the use of different lenses. A calibration process has been developed for the system to achieve consistent phase shifts of the Optigrid. Post processing has extracted depth information using depth of modulation analysis using a phantom block with fluorescent sheets at different depths.

7556-22, Session 6

A laser reflectometry technique for on-device coating thickness measurements

S. J. Morris, Nightingale-EOS, Ltd. (United Kingdom)

We demonstrate the use of Beam Profile Reflectometry (BPR) to measure coating thicknesses on small, highly curved devices such as cardiac stents. BPR has long been used in the semiconductor industry as a powerful technique for measuring the thickness and refractive index of transparent films. The method uses a diffraction-limited focused laser beam to provide light at multiple angles-of-incidence simultaneously within a sub-micron measurement area. By analyzing the reflected light as a function of angle-of-incidence and polarization, robust and deterministic measurements of film-thickness and refractive index can be obtained taking proper account of scatter, inhomogeneity and birefringence.

For the current work, the technique has been implemented in a compact desktop configuration suitable, for example, for the in-line monitoring of coating thickness and composition as part of a stent manufacturing process. Provision is made for the alignment and manipulation of the

small and fragile samples, and for the location of the measurement spot at the appropriate site on the stent's outer or inner surface.

Validation measurements on stent-like reference samples, comparing results from the technique with destructive measurements on the same samples, show correlation of better than 99% over a range of coating thicknesses and sample morphologies down to curvature radii of ~50µm.

The method is intrinsically scalable to other, larger medical devices, such as catheters or orthopedic prostheses.

7556-23, Session 6

A novel optical device for end tidal air sampling in breath analysis

C. Loccioni, Loccioni Health Care (Italy); L. Scalise, Univ. Politecnica delle Marche (Italy)

The ability to exchange carbon dioxide (CO2) is essential for most life forms, recently new CO2 monitoring systems for clinical purpose have been realised. One of the main limit is the lack of established sampling and measurement procedures causing increase variability, alter multivariate data patterns and hinder the comparison of data. Novel devices necessary to run standard operating protocols are presently under study by the scientific community.

The aim of this work is to present a novel optical breath sampling device, based on tuneable diode laser spectroscopy (TDLS), able to monitor CO2 and to precisely separate different fractions from breath.

The device can sample subject's breath into a bag and the preconcentration of analytes in an absorption tube is then performed off-line. The system integrates a flow meter and a CO2 measurement unit based on TDL spectroscopy. It allows the measurement of: either volume or CO2 concentrations, sampling of different breath fractions, breathby-breath calculation of the volume of anatomical dead space (Fowler's method) and end-tidal CO2 concentration values. Large sample volumes can be precisely sampled on multiple breaths with the advantages of increased reproducibility and higher concentrations of compounds.

The realised system show good prospective for the development of portable diagnostic instruments based on laser device (TDL spectroscopy) expanding the possibility of observing new species and decreasing costs.

References.

Schubert J K. Panel Discussion on Standardization Issues Breath Analysis Summit -Clinical Applications of Breath Testing (2006), Cleveland, OH, USA.

Werle P, A review of recent advances in semiconductor laser based gas monitors. Spectrochim. Acta A 54 197-236 (1999).

RA Dweik, A Amann, Exhaled breath analysis: the new frontier in medical testing, J. Breath Res. 2:1-3(2008)

7556-24, Session 6

Opto-physiological modeling for tomographical blood perfusion assessment

S. Hu, J. Zheng, V. Azorin Peris, A. Echiadis, P. Shi, Loughborough Univ. (United Kingdom)

This study aims to assess tomographical blood perfusion in a simplified yet comprehensive opto-physiological model through a biomedical photonics engineering setup. The research considered two aspects: 1) biomedical photonics engineering setup remotely operating a ring illumination source with resonant cavity light emitting diodes at 805nm, and capturing the backscattered photon images using a 10-bit CMOS camera; and 2) an opto-physiological engineering model mathematically quantifying the effect of optical properties on absorbance and scattering of tissue through numerical stimulation. The optimized parameters derived from the images captured by the engineering setup were used to access blood perfusion segments over a wide tissue area and different



tissue depths by means of the opto-physiological engineering model. The results reveal the pulse waveforms extracted from the images from the setup and exhibits comparable functionality characteristics with those from the conventional contact pulse waveform measurement, i.e. photoplethysmographic sensor in both time domain and frequency domain, also shows great reliability and stability in measuring cardiac-vascular components, e.g. heart beat and respiration rate. The mean amplitude of the pulsatile component was extracted from these images to map blood perfusion of human tissue in a 3-D format to bring a new insight in hemodynamic imaging and mapping. The recent work will greatly benefit clinical assessment and diagnosis to understand blood circulation in various segments of tissue, specially in burns, healing and transplant tissue areas, and could also be useful in remote sensing of vital signs for triage or sports purpose.

7556-25, Session 6

Research and development of an integrated multi-parameter quartz crystal microbalance and surface plasmon resonance system

Y. Lin, C. Chen, W. Yen, C. Lee, National Taiwan Univ. (Taiwan)

We developed a multi-parameter detection system that integrates both a quartz crystal microbalance (QCM) and surface plasma resonance (SPR) components. A QCM is known to possess the capabilities of measuring both mass loading (e.g. frequency shift) and stiffness (e.g. damping factor) of the adsorption layer. However, the measured mass from a QCM includes coupled water instead of only the true mass of the adsorption layer. On the other hand, a SPR is a well known technique which can be used to measure the true mass loading of the adsorption layer. By integrating these two techniques, we can simultaneously measure many properties, such as stiffness, conformation and mass loading of the adsorption layer.

To simplify the chip manufacturing procedures, this new detection system adopts a prism couple method which consists of a He-Ne laser, a prism, quartz and a power meter. In consideration of the light transmission issue, one side of the quartz was coated with ITO instead of gold. Preliminary results showed that this set-up can perform QCM and SPR techniques simultaneously. The experimental results match well with the theoretical predictions.

7556-33, Session 6

Solid state light engines support bioanalytical instruments and biomedical devices

C. B. Jaffe, S. M. Jaffe, Lumencor, Inc. (United States)

Lighting subsystems to drive 21st century bioanalysis and biomedical diagnostics face stringent requirements. Industrywide demands for speed, accuracy and portability mean illumination must be powerful as well as spectrally pure, switchable, stable, durable and inexpensive. Ideally a common lighting solution could service these needs for numerous research and clinical applications. Lumencor produces a customizable illumination subsystem or light engine that embodies the best traits of each of today's sources: lamps, lasers or LEDs.

For any given application, the analysis needs dictate the illumination specification. Most typically fluorescence signals are required. Lumencor's light engines can provide the requisite spectral purity, maximal spectral overlap between source output and fluor absorption, and low heat generation. White light of a predetermined color temperature is also in demand. Lumencor's solution allows for tuning that color temperature and meeting the chromaticity needs for most any requirement.

Lumencor's light engines produce outputs from a hybrid of solid state technologies. As many as seven discrete outputs or white light is generated. Optical subsystems with large and small étendue are available to satisfy the broad range of biomedical instrument designs and novel measurement tools. Several multicolor prototypes will be discussed

and their performance capabilities disclosed. Specifically, seven color output light engine data for fixed and live cell microscopy, white light for endoscopy, NIR illumination for minimally invasive surgery, field uniformity for demanding biochemical and fluidic arrays and multi-parametric data for high content screening will be highlighted.

7556-26, Session 7

Two-Photon Probes for Bioimaging

B. R. Cho, Korea Univ. (Korea, Republic of)

Two-photon microscopy (TPM), which uses two photons of lower energy as the excitation source, is growing in popularity among biologists because of several distinct advantages. Using TPM, researchers can image intact tissue for a long period of time with minimum interference from tissue preparation artifacts, self-absorption, and autofluorescence. To make TPM a more versatile tool in biology, researchers need a wider variety of two-photon (TP) probes for specific applications. In this context, we have developed a series of TP probes that can detect the intracellular free metal ions, acidic vesicles, lipid rafts, and cancer cells at 100-300 mm depth in live tissues. In this presentation, I will discuss the photophysical properties and bio-imaging applications of a few TP probes. With a TP calcium ion probe, we could visualize the spontaneous Ca2+ waves in the somas of neurons and astrocytes at ~120 micrometer depth in fresh hypothalamic slices for more than 1000 s. Moreover, a TP lysotracker could visualize the transport of the acidic vesicles along the axon in fresh rat hippocampal slices at ~120 micrometer depth. Further, a TP glucose tracer could monitor the glucose uptake in normal and colon cancer tissues from human patients and visualize the efficacy of anticancer agents in colon cancer tissues at a depth of 75-150 micrometer by TPM.

7556-27, Session 7

Direct cell writing 3D tissue-on-a-chip as an in vivo tissue analog in optical imaging

R. C. Chang, National Institute of Standards and Technology (United States)

In their normal in vivo matrix milieu, tissues assume complex wellorganized three-dimensional architectures. In situ cells are surrounded by other cells, where many extracellular ligands including many types of collagens, laminin, and other matrix proteins, not only allow attachments between cells and the basal membrane but also allow access to oxygen, hormones, and nutrients; removal of waste products and other cell types associated in tissues. Therefore, a primary aim in the tissue engineering design process is to fabricate an optimal analog of the in vivo scenario. This challenge can be addressed by applying emerging layered biofabrication approaches in which the precise configuration and composition of cells and bioactive matrix components can recapitulate the well-defined three-dimensional microenvironments that represent the natural context of tissues with cell-cell and cell-matrix interactions. Furthermore, the advent of and refinements in microfabricated systems presents physical and chemical cues to cells in a controllable and reproducible fashion unrealizable with conventional tissue culture, resulting in high-fidelity, high-throughput in vitro models capable of simulating both normal and pathological processes in vivo. The tissue model developed in this research involves the combinatorial setup of an automated syringe-based, layered direct cell writing process with micropatterning techniques to fabricate a microscale in vitro device housing a chamber of three-dimensional cell-encapsulated hydrogelbased tissue constructs in defined design patterns that biomimic the cell's natural microenvironment for enhanced performance and functionality. In order to assess the structural formability and biological feasibility of the tissue analog, reproducibly fabricated tissue constructs are biologically characterized for both viability and cell-specific function. In the proposed work, this three-dimensional tissue-based model subject to physiological perfusion flow will enable broad application as an in vitro testbed amenable to optical imaging methods for probing various



biological and disease phenomena that emerge from complex cellular processes.

7556-28, Session 7

Targeted delivery of cancer-specific multimodal contrast agents for intraoperative detection of tumor boundaries and therapeutic margins

R. X. Xu, J. S. Xu, J. Huang, C. Schmidt, S. P. Povoski, E. W. M. Martin, Jr., The Ohio State Univ. (United States)

Background:

Accurate assessment of tumor boundaries and intraoperative detection of therapeutic margins are important oncologic principles for minimal recurrence rates and improved long-term outcomes. However, many existing cancer imaging tools are based on preoperative image acquisition and do not provide real-time intraoperative information that supports critical decision-making in the operating room.

Method:

Poly lactic-co-glycolic acid (PLGA) microbubbles (MBs) and nanobubbles (NBs) were synthesized by a modified double emulsion method. The MB/ NB surfaces were conjugated with CC49 antibody to target TAG-72 antigen, a human glycoprotein complex expressed in many epithelial-derived cancers. Multiple imaging agents were encapsulated in MBs and NBs for multimodal imaging. Both one-step and multi-step cancer targeting strategies were explored. Active MBs/NBs were also fabricated for therapeutic margin assessment in cancer ablation therapies.

Results:

The multimodal contrast agents and the cancer-targeting strategies were tested on tissue simulating phantoms, LS174 colon cancer cell cultures, and cancer xenograft nude mice. Contrast enhanced multimodal imaging were demonstrated using fluorescence, ultrasound, and photoacoustic modalities. Active MBs/NBs appropriately estimated the therapeutic margin propagation.

Conclusion:

The cancer-specific multimodal contrast agents we developed have the potential for intraoperative detection of tumor boundaries and therapeutic margins.

7556-29, Session 8

Confirmation of uncontrolled flow dynamics in clinical simulated multi-infusion setups using absorption spectral photometry

A. Timmerman, B. Riphagen, J. Klaessens, R. M. Verdaasdonk, Univ. Medical Ctr. Utrecht (Netherlands)

Multi-infusion systems are used frequently at intensive care units to administer several liquid therapeutic agents to patients simultaneously. By passively combining the separate infusion lines in one central line, the number of punctures needed to access the patient's body, is reduced. So far, the mutual influence between the different infusion lines is unknown. Although the flow properties of single infusion systems have been investigated extensively, only a few research groups have investigated the flow properties of multi-infusion systems. Our previous study has shown that applying multi-infusion can lead to fluctuations in syringe pump infusions, resulting in uncontrolled and inaccurate drug administration. This study presents a performance analysis of multiinfusion systems as used in the Neonatology Intensive Care Unit. The dynamics between multiple infusion lines in multi-infusion systems were investigated by simulation experiments of clinical conditions. A newly developed real-time spectral-photometric method was used for the quantitative determination of concentration and outflow volume using a deconvolution method of absorption spectra of mixed fluids. The effects for three clinical interventions were studied: start-up, flow rate doubling and syringe replacement. Results showed mutual influence between the different infusion lines following these interventions. This mutual influence led to significant volume fluctuations up to 50%. These deviations could result in clinically dangerous situations. A complete analysis of the multi-infusion system characteristics is recommended in further research to estimate both the presence and severity of potential risks in clinical use.

7556-30, Session 8

Quantitative comparison of three electrosurgical smoke evacuation systems

T. de Boorder, S. Been, H. J. Noordmans, M. Grimbergen, R. Verdaasdonk, Univ. Medical Ctr. Utrecht (Netherlands)

Electrosurgical equipment used during surgery generate smoke consisting of particles, vapor, aerosols and potentially harmful biological agents. Smoke evacuation systems are used more commonly and various types are available. A special image enhancement technique was used to study the behavior of surgical smoke and the effectiveness of smoke evacuation systems.

Three different smoke evacuation systems were investigated. A back scatter illumination technique in combination with a high speed camera was applied to image the dynamics of a smoke plume generated by vaporizing a homogenous meat paste irradiated with the beam of a 10 W cw CO2 laser moving at a constant speed. The three different smoke evacuation systems with their individual nozzles, were held 2 cm above the smoke plume and were switched on and off at fixed intervals to mimic a clinical situation. For images analysis, software was developed to count 'smoke pixels' in the video frames as a quantification tool. For the observer's eye, there were no differences between the systems. However, images quantification showed significantly less 'smoke' for one of the systems. It is expected that the performance in a clinical situation is also influenced by additional conditions like nozzle design, airflow and noise level.

Contrast enhanced smoke visualization proved to be a useful method to quantify the effectiveness of smoke evacuation units and can be applied for strategic positioning and improvement of the nozzle.

7556-31, Session 8

Characterization of Intraocular lenses: a comparison of different measurement methods

I. Erichsen, J. Heinisch, S. Zilian, TRIOPTICS GmbH (Germany)

Nowadays one of the most commonly performed ophthalmic surgeries is the replacement of the eye lens by a synthetic intraocular lens (IOL), restoring eye sight.

Because of the trend to match the intraocular lens with the properties of the individual eye in which it is going to replace the eye lens, intricate designs for IOLs have been developed. Multifocal, diffractive as well as aspheric designs demand for elaborate measurement and analysis options.

Various measurement methods have evolved including techniques which analyze for example the image itself or the emerging wavefront. In order to understand the advantages of these different methods intraocular lenses of various designs have been measured and analyzed under miscellaneous conditions. These include dry and wet sample environment as well as in-situ measurement in the so called model eye.

Measurement results of this comparison will be presented.



7556-32, Session 8

Validation of arterial oxygen saturation data in neonatal intensive care unit

L. Scalise, P. Marchionni, V. Carnielli, Polytechnic Univ. of Marche (Italy)

The measurement of concentration of blood gases (in particular O2) is of extreme interest for the evaluation of efficiency of pulmonary gas exchange, adequacy of alveolar ventilation, mechanisms of blood-gas transport and tissue oxygenation. Invasive techniques, although still common in many clinical situations, present the limit to be necessary not continuous, time-delayed (typically 20-30 min), painful and with an associated risk. Such limitation becomes particularly severe in critical ill patients where close and frequent (continuous) monitoring of arterial blood gases is essential.

In this paper, we describe a real-time, novel measurement procedure to validate non-invasive arterial oxygen saturation (SO2) data measured by standard pulse-oxymeter. Such instrument, especially when used in intensive care units (ICU), can produce wrong data due to voluntary or involuntary motion artefacts or imperfect skin-sensor contact. We have monitored (sampling frequency: 1 Hz) in 14 preterm subjects and used the heart rate (HR) signal provided by the ECG (II-lead) and the same quantity provided by the SO2 sensor (SHR); such data have been used to validate the SO2 data. A dedicated algorithm has been developed in order to provided "most-probable" values in case of single or few not validated SO2 data.

Results show that less than 10% of the arterial oxygen saturation data are not validated, which means, in our case, 25 hours of data (out of 250 hours observed) are not validated. With the provided algorithm the still not validated data are reduced to less than 5%.

References.

Shyang-Yun P. At al. Validation of oxygen saturation monitoring in neonates. Am J Crit Care. 2007; 16(2): 168-178.

Conference 7557: Multimodal Biomedical Imaging V



Saturday 23 January 2010 • Part of Proceedings of SPIE Vol. 7557 Multimodal Biomedical Imaging V

7557-01, Session 1

Diffuse optical methods for cancer therapy monitoring in vivo

R. Choe, Univ. of Pennsylvania (United States)

No abstract available

7557-02, Session 1

Image reconstruction for time-domain diffuse optical tomography based on multi-level three-dimensional wavelet domain decomposition

F. Yang, P. Ruan, F. Gao, Tianjin Univ. (China)

It is generally believed that the inverse problem in diffuse optical tomography (DOT) is highly ill-posed and its solution is always underdetermined and sensitive to noise, because the number of boundary measurements data is generally far fewer than that of unknown parameters to be reconstructed. In this paper, we propose a method on image reconstruction for time-domain breast diffuse optical tomography based on panel detection and Finite-Difference Method, and we introduce an approach to reduce the number of unknown parameters in the reconstruction process. We propose a multi-level scheme to reduce the number of unknowns by parameterizing the spatial distribution of optical properties via three dimensional wavelet transform and then reconstruct the coefficients of this transform. Compared with previous direct full spatial domain algorithm, this method can efficiently improve the reconstruction quality. Numerical simulation results illustrate that the spatial resolution of reconstructed image is 4mm edge-to-edge.

7557-03, Session 1

Multispectral red-shifted fluorescent protein tomography with autofluorescence subtraction

N. C. Deliolanis, Helmholtz Zentrum München GmbH (Germany) and Massachusetts General Hospital (United States); T. Wurdinger, B. Tannous, Massachusetts General Hospital (United States); V. Ntziachristos, Helmholtz Zentrum München GmbH (Germany)

Fluorescent proteins (FPs) have revolutionized biological discovery by allowing a highly versatile visualization of otherwise invisible cellular and sub-cellular processes in-vivo. Ongoing research on FP development has resulted in a variety of constructs that operate in the far-red and near-infrared part of the spectrum. There is one major advantage veiling behind the development of these proteins, i.e. the ability to macroscopically visualize FP activity deep in tissues. We demonstrate herein a multispectral fluorescence tomography method that allowed the visualization of mCherry labeled glioma tumors in animal brains operating with two-orders of magnitude better sensitivity compared to imaging GFP. The method makes use of a novel spectral inversion scheme that integrates three-dimensional image reconstruction and auto-fluorescence correction that works seamlessly in the steep absorption transition from visible to near-infrared. The approach offers therefore the ability for tomographically visualizing the emerging new class of red-shifted fluorescent proteins though entire animals. We discuss how the detection sensitivity can be improved by at least an order of magnitude using further shifted FP's and the potential of the method for accelerating discovery associated with functional genomics, stem cell research and systems biology.

7557-04, Session 1

Free-space fluorescence tomography using adaptive spatial sampling based on anatomical information from microCT

X. Zhang, C. Badea, G. A. Johnson, Duke Univ. (United States)

Image reconstruction is one of the main challenges for fluorescence tomography. For in vivo experiments on small animals, in particular, the inhomogeneous optical properties and irregular surface of the animal make free-space image reconstruction challenging because of the difficulties in accurately modeling the forward problem and the finite dynamic range of the photodetector. These two factors are fundamentally limited by the currently available forward models and photonic technologies. Nonetheless, these limitations can be significantly eased using a signal processing approach. We have recently constructed a free-space panoramic fluorescence diffuse optical tomography system that uses co-registered microCT data acquired on the same animal. In this article, we present a data processing strategy that adaptively selects the optical sampling points in the raw 2-D fluorescent CCD images. Specifically, the general sampling area and sampling density are initially specified, which create a set of potential sampling points to sufficiently cover the region of interest. Based on 3-D anatomical information from microCT and the fluorescent CCD images, a data point is excluded from the set if it is located in an area either where the forward model is known to be problematic (e.g., large wrinkles on the skin) or where the signal is unreliable (e.g., saturated or low signal-to-noise ratio). Animal experiments were conducted on the cadavers of mice with artificial fluorescent inclusions. Using the presented sampling strategy, the reconstruction results were favorable compared to those using standard uniform sampling.

7557-44. Session 1

Time gated functional diffuse optical tomography based on Monte Carlo

J. Chen, V. Venugopal, X. Intes, Rensselaer Polytechnic Institute (United States)

No abstract available.

7557-05, Session 2

Image-guided surgery using diffuse near-infrared light

S. Gioux, Beth Israel Deaconess Medical Ctr. (United States)
No abstract available.

7557-06, Session 2

Development of a bi-modality XCT-fDOT instrument

A. Koenig, A. Planat-Chrétien, J. Coutard, L. Hervé, M. Brambilla, J. Dinten, Lab. d'Electronique de Technologie de l'Information (France)

Three dimensional fluorescence Optical Diffusion Tomography (fDOT) allows in vivo studies of tumor life. Coupling this imaging modality to X-ray computed tomography (XCT) ensures a co-registration of the tumor distribution with the animal anatomy.

Return to Contents TEL: +1 360 676 3290 · +1 888 504 8171 · customerservice@spie.org

Conference 7557: Multimodal Biomedical Imaging V



The fDOT instrument chain consists of a continuous wave laser source (690nm) coupled to a rotating stage, a CCD camera and filters for fluorescence detection. The excitation and emission wavelengths and the fluorophore are chosen to optimize transmission through the whole animal. The optical chain bulk has been optimized according to X-ray constraints. The XCT chain is placed perpendicularly to the optical path.

The acquisition geometry is cylindrical for both imaging modalities. XCT reconstruction is conducted using a Feldkamp algorithm. The XCT reconstructed volume is then meshed using finite volumes and used by an fDOT algorithm taking into account actual studied object boundaries and using Greens functions corrected from optical properties variations.

A study on cylindrical phantoms is conducted to evaluate our fDOT system. Different glass capillary tubes filled with Alexa 750 and/or absorbent solutions are placed in the phantom, separated in x/y plane and in z (cylinder axis) by various distances. In a second study mice with a capillary inserted in the oesophagus, are reconstructed with a good estimation of the capillary 3D position, an co-registered with XCT reconstructions: fDOT location of fluorophore distribution matches well with XCT reconstruction.

Future work will address the use of anatomical information (organs boundaries) provided by the X-ray data as a regularization factor in the optical reconstruction scheme.

7557-07, Session 2

A hybrid fluorescence tomography and x-ray CT system for small animal molecular imaging

Y. Lin, Univ. of California, Irvine (United States); W. C. Barber, DxRay Inc. (United States); H. Yan, Univ. of California, Irvine (United States); J. S. Iwanczk, E. Nygard, N. Malakov, N. E. Hartsough, T. Gandhi, DxRay Inc. (United States); W. W. Roeck, O. Nalcioglu, G. Gulsen, Univ. of California, Irvine (United States)

In vivo fluorescence tomography (FT) has becoming a popular molecular imaging tool recent years. However, quantitative FT is still difficult due to the ill-posedness of the inverse problem. In this study, we have developed a combined X-ray CT-FT small animal imager.

Both XCT and FT systems are mounted on a single rotating gantry with a common animal holder. In this setting, the FT provides the molecular information. Meanwhile, the XCT provides the anatomical information of the animal and uses that as a priori information to improve the FT reconstruction.

The FT images are acquired from multiple views using several source positions. The XCT image is acquired using a high-efficiency high-resolution flat panel detector. The animal/phantom is held by two carbon rods supported by black fabric thread. The DOT measurements are also taken in the same setting to provide optical background correction. The FT imaging slice is accurately localized on XCT image to ensure the perfect co-registration.

Phantom study has performed for validating this combined system. A multi-modality phantom with background optical heterogeneity is build. ICG is used as the fluorophore, and the clinical used iodine solution is added to different regions so that the structure of the phantom can be visible on XCT. The phantom study demonstrated that the concentration of a fluorescence inclusion deeply embedded inside a heterogeneous background can only be recovered accurately when the a priori information from both XCT and DOT is available.

We are currently evaluating the system with in vivo small animal studies.

7557-08, Session 2

A portable optical tissue flow-oximeter based on diffuse correlation spectroscopy

G. Yu, Y. Shang, Y. Zhao, R. Cheng, L. Dong, D. Irwin, Univ. of Kentucky (United States)

A near-infrared (NIR) diffuse correlation spectroscopy (DCS) has recently been developed for noninvasive measurement of blood flow in deep tissues. This novel technology has also been combined with a NIR diffuse reflectance spectroscope (DRS) for simultaneous measurements of tissue blood flow and oxygenation, thus directly probing tissue oxygen metabolism. The existing hybrid instrument (DCS+DRS) is large, complex and expensive. Thus, we sought to build and validate a portable, easyto-use and inexpensive optical device for bedside monitoring of deep tissue hemodynamics. We added a second laser diode to a portable DCS device and measured light intensities at two wavelengths (785 and 854 nm) to extract tissue oxygen information. The relative changes of oxy- and deoxy-hemoglobin concentrations were calculated based on the modified Beer-Lambert Law. We name this device the "DCS flowoximeter" as it measures both blood flow and oxygenation. For the validation purpose, calf muscle blood oxygenation during cuff inflation and deflation was measured concurrently using the DCS flow-oximeter and a commercial tissue-oximeter (Imagent, ISS Inc). Ten healthy volunteers participated in this study. The oxygenation traces from the two measurements exhibited similar dynamic response for each subject and data were highly correlated (rmean>0.9, p<10e-5, n=10). The DCS flow-oximeter employs a new design with significantly less cost (1/2) and smaller size (1/5) to achieve the same functions as the existing hybrid instrument (DCS+DRS), and is significantly simple in construction and operation. The portable, inexpensive, and easy-to-use DCS flowoximeter has promise for bedside monitoring of tissue blood flow and oxygenation in clinics.

7557-45, Session 2

A quantitative time domain functional imager for small animal studies

V. Venugopal, J. Chen, X. Intes, Rensselaer Polytechnic Institute (United States)

No abstract available.

7557-09, Session 3

A multimodal contrast agent for simultaneous magnetic resonance and optical imaging of small animal

M. B. Unlu, Y. Ling, Univ. of California, Irvine (United States); B. Grimmond, A. Sood, E. Uzgiris, GE Global Research (United States); O. Nalcioglu, G. Gulsen, Univ. of California, Irvine (United States)

Our goal is to assess the feasibility of a bifunctional contrast agent that is intravenously injected to an R3230 induced small animal breast tumor model. The MR/optical contrast agent was produced by GE Global Research, NY, and it was available in two different sizes, Dp20 and Dp71. We used a combined frequency domain diffuse optical tomography (DOT) and a 4T magnetic resonance (MR) scanner to simultaneously measure the kinetics of the contrast agent in vivo. Both systems detected the signal change in the tumor and the bladder. MR measurements served as a gold standard to validate the optical kinetics. We will present both MR and DOT dynamic curves as well as the reconstructed optical parameter maps.



7557-10, Session 3

Integrated intravascular optical coherence tomography (OCT) ultrasound (US) imaging system

J. Yin, Univ. of California, Irvine (United States); H. Yang, C. Hu, Q. Zhou, K. K. Shung, The Univ. of Southern California (United States); Z. Chen, Beckman Laser Institute and Medical Ctr. (United States)

Optical coherence tomography (OCT) and intravascular ultrasound (IVUS) are considered two complementary imaging techniques in the detection and diagnosis of atherosclerosis. OCT permits visualization of micronscale features of atherosclerosis plaque, and IVUS offers full imaging depth of vessel wall. Under the guidance of IVUS, minimal amount of flushing agent will be needed to obtain OCT imaging of the interested area. To the best of our knowledge, we have developed the first dualmodality OCT-US probe that integrates OCT optical components and ultrasound transducer. The OCT probe is mainly composed of a single mode fiber, a gradient index (GRIN) lens (0.35mm in diameter) for light beam focusing, and a right-angled prism for reflecting light almost perpendicular to biological tissue. A 40MHz side-viewing ultrasound transducer was fabricated to generate and receive ultrasonic pulse. It also provides a hollow-core cylindrical-shaped housing for the OCT probe. These components were integrated into a single probe, enabling both OCT and ultrasound imaging. In vitro OCT and ultrasound images of a rabbit aorta were obtained using this dual-modality imaging system. This study has demonstrated the feasibility of OCT-US system in intravascular imaging, which is expected to have a prominent impact on early detection and characterization of atherosclerosis.

7557-11, Session 3

An intra-arterial catheter for simultaneous optical frequency domain imaging and near-IR fluorescence imaging

H. Yoo, M. Shishkov, B. E. Bouma, Massachusetts General Hospital (United States) and Harvard Medical School (United States); G. Mallas, Massachusetts General Hospital (United States); F. A. Jaffer, G. J. Tearney, Massachusetts General Hospital (United States) and Harvard Medical School (United States)

Optical frequency domain imaging (OFDI) and fluorescence imaging are complementary techniques for obtaining microstructural and molecular information from artery walls, respectively. In this paper, we report a dual modality intra-arterial catheter system that simultaneously obtains co-registered OFDI and near-IR (NIR) fluorescence images. The catheter is comprised of a double-clad fiber (DCF), contained within a rotating cable and a transparent 1.0 mm diameter outer sheath. The single-mode inner core of the DCF transmits the OFDI beam (1310 nm), whereas the multi-mode inner cladding is utilized to excite (700-750 nm) and detect NIR fluorescence from the sample (780-850 nm). A side-viewing ball lens directs and focuses the OFDI and NIR light on the arterial wall. The lens was formed at the end of the DCF by splicing a short piece of the coreless fiber, melting the tip, and polishing the side. Single-mode OFDI and multi-mode NIR excitation and fluorescence emission light is combined at a custom optical rotary junction by use of a dichroic mirror. The rotary junction scans the fiber and optics along the artery wall in a helical pattern to obtain co-registered 3-D structural OFDI and 2-D fluorescence images. Images of phantoms and fluorescently labeled stents were obtained with the multimodality catheter system, demonstrating accurate overlap of the microstructural and fluorescence signals. The structural and molecular information obtained by this technology could provide valuable information on atherosclerosis, including characterizing coronary inflammation found in plaques at risk for causing heart attacks.

7557-12, Session 3

Localization of fluorescence marked prostate tumor with time-resolved diffuse optical tomography

L. Hervé, L. Guyon, M. Debourdeau, J. Boutet, J. Dinten, Lab. d'Electronique de Technologie de l'Information (France)

Prostate cancer diagnosis currently relies on random biopsies undertaken on suspicious patients. To obtain a better sensibility, we propose to add an optical molecular imaging modality to an ultrasound guided (US) biopsy tool to localize fluorophore marked tumors.

Because of the prostate high absorption (µa 0.3 cm-1, ten times more than breast), depth of fluorescent inclusions (till 3 cm) and high level of background signal due to the reflection geometry imposed by the diagnosis, the optical signal of interest is weak and special attention must be paid on the quality of measurements and data processing.

To maximize informational content provided by optical tissue exploration, a time-resolved acquisition chain is used. A 770 nm 25 mW femtosecond laser source is multiplexed into six optics fibers and the medium response is sampled by four detection fibers and analyzed simultaneously by a four channels Time Correlated Single Photon Counting (TCSPC) device.

We will show in the final paper that despite the small number of measurements, a sparse fluorescence concentration can be reconstructed by processing intensity and mean time of flight acquired from each source-detector time-resolved signal. We prove that mean time of flight is a valuable and essential piece of information for reflection geometry. The choice of features leads to non linear computations which are dealt by an iterative approach. Validation experiments are performed on a special phantom mimicking prostate tissues both on their optical and ultrasound properties with 2 cm deep multiple 5 μ l-ICG-inclusions to simulate a marked tumors.

7557-13, Session 3

Developing handheld real time multispectral imager to clinically detect early stage pressure ulcer in darkly pigmented skin

L. Kong, S. Sprigle, D. Yi, F. Wang, C. Wang, F. Liu, Georgia Institute of Technology (United States)

Pressure ulcers have been identified as a public health concern by the US government through the Healthy People 2010 initiative and the National Quality Forum (NQF). Currently, no tools are available to assist clinicians in erythema, i.e. the early stage pressure ulcer detection.

The results from our previous research (supported by NIH grant) indicate that erythema in different skin tones can be identified using a set of wavelengths 540, 577, 650 and 970nm.

This paper will report our recent work which is developing a handheld, point-of-care, clinically-viable and affordable, real time multispectral imager to detect erythema in persons with darkly pigmented skin. Instead of using traditional filters, e.g. filter wheels, generalized Lyot filter, electrical tunable filter or the methods of dispersing light, e.g. optic-acoustic crystal, a novel custom filter mosaic has been successfully designed and fabricated using lithography and vacuum multi layer film technologies. The filter has been integrated with CMOS and CCD sensors. The filter incorporates four or more different wavelengths within the visual to near-infrared range each having a narrow bandwidth of 30nm or less. Single wavelength area is chosen as 20.8µx 20.8µ. The filter can be deposited on regular optical glass as substrate or directly on a CMOS and CCD imaging sensor. This design permits a multispectral image to be acquired in a single exposure, thereby providing overwhelming convenience in multi spectral imaging acquisition.

The importance of the research and development work is they create a completely novel idea in constructing miniaturized, low cost real time multispectral imaging device. Innumerous fields which are using multi spectral imaging technology will certainly benefit from this innovation.

Conference 7557: Multimodal Biomedical Imaging V



7557-14, Session 3

Computed Radiography Imaging Based on High-Density 670 nm VCSEL Arrays

M. M. Dummer, K. Johnson, W. Hogan, M. Witte, M. K. Hibbs-Brenner, Vixar (United States)

Although vertical cavity surface emitting lasers (VCSELs) have traditionally found their place in high-speed communication links, recently VCSELs emitting in the visible spectrum have sparked interest for scanning and imaging applications. Compared to other lasers, VCSELs have many advantageous characteristics including compact size, low power requirements, low cost, and high reliability. VCSELs also offer the unique ability to be fabricated in one- or two-dimensional arrays, and thus can be used to replace a mechanically scanned beam in imaging applications. One such application is computed radiography (CR), which provides a low-cost, versatile solution for digitizing and electronically storing x-ray images. Such systems utilize a storage phosphor plate which is exposed and subsequently excited by a red laser scanner to acquire the image data.

This work presents the first CR scanner based on high-density VCSEL arrays. The new configuration potentially offers higher throughput and resolution than current CR readers, while improving the overall compactness and mechanical stability of the system. Our proof-of-concept demonstration consists of a 1-inch linear array of VCSELs on a 50 μm pitch. Using specialized tooling, multiple 96-VCSEL array chips are placed consecutively to achieve the full array length, while maintaining consistent pixel spacing with submicron accuracy. Greater than 5 mW/pixel has been demonstrated at $\lambda = 670$ nm. Cascaded laser drivers enable fast pulses of consecutive pixels to replicate a scanning beam. A GRIN lens array focuses each laser beam onto the phosphor plate to achieve a spot size <50 μm . Using this device, x-ray images have been successfully acquired.

7557-15, Session 4

X-Ray and near-infrared imaging: similarities, differences and combinations

B. W. Pogue, Dartmouth College (United States)

No abstract available.

7557-16, Session 4

Dual-modal quantitative imaging of wound tissue oxygenation and perfusion

S. Xu, J. Huang, J. Ewing, K. Huang, C. Sen, R. Xu, The Ohio State Univ. (United States)

Background: Accurate assessment of wound oxygenation and perfusion is important for evaluating wound healing/regression and guide followed therapeutic processes. However, many existing techniques and clinical practices are subjective and qualitative due to background bias, tissue heterogeneity, and inter-patient variations. To overcome this limitation, we developed a dual-modal imaging system for in vivo, non-invasive, real-time quantitative assessment of wound tissue oxygenation and perfusion.

Method: The imaging system integrated a broadband light source, a high resolution CCD camera, a highly sensitive infrared camera and a liquid crystal tunable filter. A user-friendly interface was developed to control all components systematically. Advanced algorithms were explored for reliable reconstruction of tissue oxygenation without interferences of blood concentration, tissue scattering, pigmentation and background absorption. Thermal images and hyperspectral visual/near infrared images were co-registered.

Result: The reliability of the algorithms was tested on a tissue-simulating homogeneous liquid phantom. The tissue perfusion was reconstructed

from the measurements of the dynamic changes of hemoglobin concentration and temperature distribution in response to vascular occlusion and reperfusion. A fused image that co-registered tissue morphology, oxygenation and perfusion maps was displayed in real-time. Clinical feasibility for quantitative imaging of tissue oxygenation and perfusion was also demonstrated on healthy human subjects.

Conclusion: The results show that the dual-modal imaging system is able to detect tissue oxygenation and perfusion in real-time with minimal bias introduced by tissue heterogeneity and background absorption. This imaging system will improve the accuracy of the quantitative assessment of chronic wounds.

7557-17, Session 4

Near-infrared spectroscopy with spectroscopic technique with wide range of wavelength information detects tissue oxygenation level clearly

H. Eda, The Graduate School for the Creation of New Photonics Industries (Japan) and Photonics Innovations Co., Ltd. (Japan); H. Aoki, S. Eura, The Graduate School for the Creation of New Photonics Industries (Japan)

Near-infrared spectroscopy (NIRS) calculates hemoglobin parameters, such as oxygenated hemoglobin (oxyHb) and deoxygenated hemoglobin (deoxyHb) using the near-infrared light around the wavelength of 800nm. NIRS is based on the modified-Lambert-Beer's law that indicates that changes in absorbance are proportional to changes in hemoglobin parameters. Majority of the conventional methods uses only two or more wavelengths, however, in this research, basic examination of NIRS measurement was performed by acquiring wide range of wavelength information.

Arterial occlusion test was performed by using the blood pressure cuff around the upper arm. Pressure of around 200mmHg was then applied for about 3 minutes. During the arterial occlusion, the absorption spectrum of the lower arm muscles was measured every 15 seconds, within the range of 600 to 1100nm. The secondary derivative spectrum was calculated from the spectrum. Arterial occlusion is a task which changes the oxygenation level of the tissue. The change can be regarded as the change of the spectrum form, not as the change of the baseline. Furthermore, it was found that other wavelength bands hold information correlating to this arterial occlusion task. Technique of improving the performance of NIRS measurement, using the above method, will be reported.

7557-18, Session 4

Breast cancer detection using frequencydomain diffuse optical tomography with single source detector pair

A. G. Orlova, Institute of Applied Physics (Russian Federation); A. V. Maslennikova, Nizhny Novgorod State Medical Academy (Russian Federation) and Institute of Applied Physics (Russian Federation); G. Y. Golubiatnikov, N. M. Shakhova, V. I. Plekhanov, V. A. Kamensky, I. V. Turchin, Institute of Applied Physics (Russian Federation)

An experimental setup for multicolor frequency-domain Diffuse Optical Tomography (FD DOT) was created to visualize neoplasia of breast tissue. The breast is scanned in the transilluminative configuration by a single source and detector pair. Illumination at three wavelengths (684 nm, 794 nm, and 850 nm) which correspond to different parts of the absorption spectrum in a therapeutic transparency window provides information about concentration of the main absorbers (oxygenated hemoglobin, deoxygenated hemoglobin, and fat/water). Source amplitude modulation

Conference 7557: Multimodal Biomedical Imaging V



at 140 MHz increases spatial resolution and provides separate reconstruction of scattering and absorption coefficients. The described FD DOT setup was applied for in vivo imaging of breast tissues. Eight volunteers without breast pathology and eight patients with breast carcinoma were involved in the investigation. In every case, ultrasonic examination of breast was performed before DOT to compare information obtained by different methods. Maps of 2D distributions of reconstructed absorption and scattering coefficients and concentration of hemoglobin were obtained. Normal breast tissues are characterized by uniform distribution and steady level of investigated parameters. In case of breast cancer, DOT images varied depending on the patient. We can conclude that the FD DOT setup allows for investigation of breast tissue, for detection of neoplastic changes and for obtaining additional information that cannot be provided by routine methods of breast cancer diagnostics.

7557-19. Session 4

Multi-spectral skin imaging by a consumer photo-camera

J. Spigulis, D. Jakovels, U. Rubins, Univ. of Latvia (Latvia)

The possibilities to perform multi-band spectral imaging by means of a simple consumer color CCD camera without any external filters have been studied. Images at up to 6-8 spectral bands may be available if appropriate signal pre-processing technology is applied. The proposed technique was clinically tested for advanced skin autofluorescence bleaching rate imaging and for skin chromophore (e.g. melanin, haemoglobin) mapping.

7557-20, Poster Session

A comparative investigation on linear inversion schemes in fluorescence lifetime tomography

F. Gao, Tianjin Univ. (China); P. Polulet, Lab d'Imagerie et de Neurosciences Cognitives (France); H. Zhao, L. Zhang, Tianjin Univ. (China); Y. Yamada, Univ. of Electro-Communications (Japan)

Fluorescence lifetime tomography (FLT) is an emerging imaging modality that seeks for recovering distributions of the fluorescent yield and lifetime inside in vivo tissues. This technique, mainly based on time-domain instrumentation, has found promising applications in small-animal imaging for studying tumor pathology and for drug development. As one of the model-based imaging methods, FLT can be finalized with inverting an underdetermined, ill-posed linear system with regard to both the parameters, for which several methods has been adopted. This paper concisely revises the main facts of three commonly-used linear inversions: algebraic reconstruction technique, truncated singular value decomposition and conjugate gradient descent, and presents a comparative investigation on these methods in terms of the image quality and noise robustness.

7557-21, Poster Session

A fiber-based non-contact scheme for timedomain diffuse fluorescence tomography: methodology and simulative investigation

F. Gao, Tianjin Univ. (China); P. Poulet, Univ. de Strasbourg (France)

Non-contact scheme is prevalent to diffuse fluorescence tomography (FDT) since it facilitates instrumentation as well as experimental procedure. Although non-contact FDT generally uses CCD camera as detectors to achieve high throughput of data collection, a fiber-based

implementation can make full use of well-established high-sensitive and time-resolved detection techniques. Therefore, a system that combines the fiber-based time-resolved detection and the non-contact geometry of optodes would be significantly attractive, which also means a more complex modeling of photon migration. This paper presents detailed computational aspects of fiber-based non-contact DFT, including the forward and inverse models. A pilot validation of the method is performed using simulated data.

7557-22, Poster Session

Improving performance of time-domain optical mammography by Jacobian scaling method

Y. Ma, F. Gao, F. Yang, H. Zhao, Tianjin Univ. (China)

Time-domain optical mammography can efficiently reconstruct optical parameter and that can diagnose early breast cancer. Nevertheless, the performance of reconstructed imaging is badly influenced by different Jacobian magnitudes of absorption coefficient and reduced scattering coefficient. With a relative data type based on generalized pulse spectrum technique, an efficient Jacobian scaling method is proposed. Our simulated and experimental reconstructions show that this Jacobian scaling method can efficiently enhancing the quality of reconstructed image.

7557-23, Poster Session

Reconstructing three-dimensional fluorescent parameters using time-resolved data based on transmittance and reflection measurements

L. Zhang, F. Gao, J. Li, H. Zhao, Tianjin Univ. (China)

As near infrared light can travel several centimeters in tissue, fluorescence diffuse optical tomography (FDOT) with the aid of specific fluorescent probes promises to open new pathways for the characterization of biological processes in living animals at cellular and molecular levels. Several approaches have been proposed for recovering the fluorescent yield and/or lifetime distributions based on finite light measurements collected at the tissue boundary. In FDOT, the yield imaging can provide the location information of biological fluorophores, while the lifetime one offers further chemical messages about the surroundings, such as pH, enzyme, and oxygen, etc. The time domain technique offers the potential advantages of directly measuring lifetime and has the favorite performances of simultaneously recovering of fluorescent yield and lifetime distributions, as well as resolving multiple components. Thus, it is necessary that FDOT modality be extended to time-domain.

We present a full three-dimensional algorithm for time-domain fluorescence molecular tomography. A pair of appropriate transformfactors is employed to extract the featured information on the temporal profiles for time-domain coupled diffusion equations. The linear inversions at two distinct transform-factors are solved with an algebraic reconstruction technique, and the normalized Born ratio is used used for its independence of the source intensity and less sensitivity to the systematic errors. In addition, it eliminates the requirement for accurate calibration of the temporal-origin in time-domain measurement. The simulate phantom is measured in reflection and transmittance modes by use of multi-channel time-correlation single photon counting system. We experimentally validate that the proposed scheme can achieve simultaneous three-dimensional reconstruction of the fluorescent yield and lifetime. The results show that for the positions, sizes and shapes of the targets, there are some deviation in reflection measurement, the quality in transmittance one is better and in the two-mode is more satisfied.



7557-24, Poster Session

Two-dimensional reconstruction of region boundaries and optical properties in shape-based diffuse optical tomography

P. Ruan, F. Yang, F. Gao, H. Zhao, M. Jin, Tianjin Univ. (China)

In this paper we apply the shape-based approach to diffuse optical tomography (DOT) reconstruction, which aims to simultaneously recover the smooth boundaries of the tissue regions and the constant coefficients within them. An advantage of shape-based solutions is the reduction of the unknown parameters, which is especially important for nonlinear ill-posed inverse problems. We introduce a Fourier series representation of the closed region boundaries and a boundary element method (BEM) for the forward model. For inverse problem the Levenberg-Marguardt optimization process is implemented here. The performance of the proposed method is evaluated by simulations at different noise levels and phantom experiment which is embedded a single cylinder target. We can get reasonable reconstruction from both Gauss noise and real noise in the experimental study. The results illuminate that the methodology is very promising and of global convergence, the boundaries and the optical coefficients can both be recovered with good accuracy from the noisy measurements.

7557-25, Poster Session

A finite-difference-method solution to radiative transfer equation with natural boundary condition

M. Jin, F. Gao, H. Zhao, Tianjin Univ. (China)

Accurate modeling of light propagation in turbid media of small-size is important for small-animal imaging. This issue is addressed here with a finite-difference-method (FDM) solution to time-independent Radiative Transfer Equation (RTE), where a natural boundary condition based on Fresnel's law is applied and improved, instead of the traditional scheme that forces zero inflow of the photons. For the validation of the modeling, we have compared the boundary flux of a two-dimensional scenario from the Monte-Carlo simulation and those from the FDM-RTE with both the natural and traditional boundary conditions, and demonstrated that that the nature boundary condition can more accurately depict the photon propagation in turbid media than the zero-inflow boundary condition.

7557-26, Poster Session

Fast reconstruction method based on graphic processing unit for fluorescence molecular tomography

G. Quan, Y. Deng, H. Gong, Q. Luo, Britton Chance Ctr. for Biomedical Optics, WNLO, Huazhong Univ. of Science and Technology (China)

Reconstruction accuracy is the spirit of Fluorescence Molecular Tomography (FMT), but better reconstruction accuracy requires more discrete points and more source-detector pairs. This will dramatically increase the time-consuming of reconstruction algorithm. In this paper we propose a fast FMT reconstruction algorithm based on Graphic Processing Unit (GPU), and we test the validity of the fast FMT reconstruction method with the experimental data. The result shows that the reconstruction algorithm based on Graphic Processing Unit (GPU) can be more than 10 times faster than traditional algorithm based on Center Processing Unit (CPU). In conclusion with the same time-consuming our method can get better accuracy than traditional method based on CPU.

7557-27, Poster Session

Determination of female breast tumor and its parameter estimation by thermal simulation

X. Chen, A. Xu, H. Yang, Y. Wang, S. Xie, Fujian Normal Univ. (China)

Breast tumor is one of the most fatal malignancies in females. Thermal imaging is an emerging method for breast tumor early detection. The main challenge for thermal imaging used in breast clinics is how to detect or locate the tumor and obtain its related parameters. The purpose of this study is to apply an improved method which combined a genetic algorithm with finite element thermal analysis to determine the breast tumor and estimate its parameters, such as the size, depth and metabolic heat generation. A finite element model for breast embedded a tumor was firstly presented, and it was used to investigate the temperature distribution of the breast changed with tumor metabolic heat generation, tumor location and tumor size. And then, the breast tumor related parameters were estimated by an improved genetic algorithm based on the temperature data from the thermography. The results show that thermal imaging is a potential detection tool for breast tumor, and the presented method may be helpful for the explanation of breast thermogram and its diagnosis.

7557-28, Poster Session

Regularization in fluorescence diffuse optical tomography using prior information on the medium optical properties

E. Pery, CREATIS-LRMN (France); L. Herve, J. Dinten, Lab. d'Electronique de Technologie de l'Information (France); F. Peyrin, CREATIS-LRMN (France)

Fluorescence diffuse optical tomography (FDOT) is new non-invasive functional imaging modality allowing the localization of fluorescent markers that can specifically signal tumoral tissue. Its principle is to measure the fluorescence light emerging at different positions of the surface when the biological media is excited with punctual sources in the near infra-red. The three-dimensional concentration of fluorescent markers has to be recovered by solving an inverse problem. However, this inverse problem is known to be ill posed and to require the knowledge of the optical properties of the studied medium, which is most often assumed to be homogeneous.

In this paper, we propose to investigate the regularization of the inverse problem by taking into account prior information on the optical properties of the studied medium. First, by a simulation study, we quantitatively evaluate the influence of the medium optical properties on the reconstruction of the fluorescence map. Second, we introduce a new method to estimate the optical properties of a non homogeneous medium, with a prior knowledge on the contour of its different constituents. Then we shall study the improvement in the fluorescent reconstruction when using this method. This prior shape information could come from a second non-invasive modality providing anatomical information such as ultrasound imaging, since this modality has been suggested to be beneficial to provide an anatomic reference to the optical image.

7557-29. Poster Session

Combined swept-source optical coherence tomography and fluorescence spectroscopy system

S. Y. Ryu, M. J. Ju, K. S. Park, J. B. Eom, B. H. Lee, Gwangju Institute of Science and Technology (Korea, Republic of)

We report a combined swept source optical coherence tomography

Conference 7557: Multimodal Biomedical Imaging V



(SSOCT) and fluorescence spectroscopy (FS) system for multimodal measurements of internal structure and biochemical information at the same time. The fiber optic FS probe composed of a double clad fiber (DCF) and DCF coupler is adopted into the single mode fiber (SMF) based SSOCT system. The DCF is specially designed to have the same core and cladding sizes with the ones of SMF but to have low index jacket, thus it can provide two concentric signal channels through its core and cladding. Through the core of DCF, the OCT and the FS excitation beam are guided and the fluorescence signal is effectively collected by the large area inner cladding of the DCF. In addition, since the DCF coupler is designed to couple only the inner cladding mode, the FS signal can be selectively detected via the cross port of the coupler. To show the performance of the SSOCT-FS multimodal system, we measured both OCT and fluorescence signal from biological sample. The optical characteristics of a photo-sensitizer are monitored by measuring the fluorescence signal from a cancerous region of an in-vivo rat and also the internal structure of the same region is tomographically imaged with a speed of 40 frames/sec. The experimental results show that the compact SSOCT-FS combined system can provide multimodal information for early detection of cancer or disease.

7557-30, Poster Session

A multidistance probe arrangement NIRS for detecting absorption changes in cerebral gray matter layer

T. Yamada, S. Umeyama, K. Matsuda, National Institute of Advanced Industrial Science and Technology (Japan)

We proposed a removal method of task-correlated artifacts on the functional near-infrared spectroscopy (fNIRS) in BiOS 2009. In this time, we give a further theoretical analysis and Monte Carlo simulations of the layered media in which both scattering and absorption changes occur. It shows that optimized multidistance probe arrangement can be effective in removing interferences by scattering and absorption changes in upper layers and extracting absorption change in the gray matter layer. Using newly designed probes, their holders and sources-detectors system, both conventional and proposed fNIRS measurements were implemented with non-functional (body and head movements and respiratory change) and functional (finger opposition) tasks. Artifacts, even which correlate with task sequence, were well reduced. Functional signals were well localized at lateralized cerebral functional area.

7557-31, Poster Session

Line scan CCD image processing for biomedical application

C. Lee, Kyungpook National Univ. (Korea, Republic of)

Positioning is one of the most important operations in computer vision for bio-medical systems. Line-scan CCD image sensor is widely used in inspection systems. In this paper, a complete set of algorithms is presented for image processing in blood cell positioning. Firstly, the line scan merging algorithm is proposed as a novel connected component labeling that can be applied on line scan ccd imaging system.

The line scan merging algorithm is a one-scan algorithm for labeling connected components. The advantages of this algorithm can be summarized as follows: (1) this algorithm can be directly applied to digital imaging system with line scan camera. (2) the algorithm scans the whole image only once which makes it suitable for real-time image processing.

Secondly, the direct ellipse-fitting algorithm is applied to position the blood cells by segmenting connected objects. From the processing result of line scan merging, the coordinates of end points of objects are stored as the representation of objects. The size of object and the overlap degree of connected objects are calculated to classify connected objects into single object.

The experimental results show the proposed algorithms can be

successful to position each blood cell. The test image has 521 single objects and 160 connected objects. The accuracy of finding center of blood cells for connected cells is over 96%. The proposed image processing algorithm can be applied to bio-medical imaging system.

7557-32, Poster Session

A comparative performance study characterizing breast tissue microarrays using standard RGB and multispectral imaging

X. Qi, W. Cukierski, D. J. Foran, Univ. of Medicine and Dentistry of New Jersey (United States)

The lack of clear consensus over the utility of multispectral imaging (MSI) for bright-field imaging prompted our team to investigate the benefit of using MSI on breast tissue microarrays (TMA). We have conducted performance studies to compare MSI with standard bright-field imaging in hematoxylin stained breast tissue. The methodology used in the experiments has three components. The first extracts a region of interest using adaptive thresholding and morphological processing. The second performs texture feature extraction. A local binary pattern was applied to extract rotation-invariant, uniform patterns for each specimen within each spectral channel. The third component performs feature selection and classification. For each spectral band, exhaustive feature selection was used to search for the combination of features that yields the best classification accuracy. AdaBoost with a linear perceptron leastsquare classifier was applied. The spectral bands carrying the greatest discriminatory power were automatically chosen and a majority vote was used to make the final classification. 92 breast TMA discs were included in the study. Sensitivity of 0.91 and specificity of 0.89 were achieved on the multispectral data, compared with sensitivity of 0.83 and specificity of 0.85 on RGB data. MSI consistently achieved better classification results than those obtained using standard RGB images. While the benefits of MSI for unmixing multi-stained specimens are well documented, this study demonstrated statistically significant improvements in the automated analysis of single stained bright-field images.

7557-33, Poster Session

Widefield reflectance and fluorescence imaging device and digital image processing for the detection of skin and oral cancer

S. Pratavieira, P. Santos, V. Bagnato, C. Kurachi, Univ. de São Paulo (Brazil)

The most common screening method for oral cancer is visual inspection and palpation of the mouth. Visual examination relies heavily on the experience and skills of the physician to identify and delineate early premalignant and cancer changes, which is not simple due to the similar characteristics of early stage cancers and benign lesions. Contrast between normal and neoplastic areas may be increased, distinct to the conventional white light, when using illumination and detection conditions. Reflectance imaging can detect local changes in tissue scattering and absorption and fluorescence imaging can probe changes in the biochemical composition. These changes have shown to be indicatives of malignant progression. Widefield optical imaging systems are interesting because they may enhance the screening ability in large regions allowing the discrimination and the delineation of neoplastic and potentially of occult lesions. Digital image processing allows the combination of autofluorescence and reflectance images in order to objectively identify and delineate the peripheral extent of neoplastic lesions in the skin and oral cavity. Combining information from different imaging modalities has the potential of increasing diagnostic performance, due to distinct provided information. A simple widefiled imaging device based on fluorescence and reflectance modes together with a digital image processing. The image processing procedure based



on the combination of fluorescence and reflectance data is proposed to enhance normal/abnormal discrimination. This image system and proposed image processing may improve the detection of occult lesions, delimitation of lesion margins, evaluation of treatment response, and screening of large areas at risk patients.

7557-34, Poster Session

A dual agent dynamic contrast-enhanced MRI-DOT study for improved breast tumor characterization

D. A. Thayer, B. Unlu, J. Chen, M. Su, O. Nalcioglu, G. Gulsen, Univ. of California, Irvine (United States)

Diffuse Optical Tomography (DOT) has been used, in conjunction with Magnetic Resonance Imaging (MRI), to characterize breast tumors with some success. Unfortunately the inherent contrast ratio between healthy and diseased tissue is somewhat low, between two and four for optical imaging. In order to improve optical contrast indocyanine green (ICG) has been used while gadolinium-DTPA has been used to improve MRI contrast. In this study, gadolinium-DTPA and ICG are used together for the first time to characterize breast tumors in vivo in the same setting. Dynamic phantom experiments have been conducted and a small-scale clinical study is being undertaken in breast cancer patients. Subjects will be imaged with a combined MRI-DOT system with both contrast agents administered sequentially. The resulting MRI images are used to detect and localize the tumor as well as to select an ROI for the DOT data. The motivation for using dual contrast agents comes from the size difference between the two agents. Gadolinium is a small agent and readily leaves the vasculature, whereas ICG binds to albumin and acts as a large agent which remains in the vasculature. Because of this size difference, the two agents provide complementary information that may improve MRI-DOT tumor characterization. The aim of the study is to show that the specificity of breast tumor characterization can be improved through the use of ICG in addition to gadolinium dynamic contrast enhancement.

7557-35, Poster Session

Bioluminescence tomography with structural and functional a priori information

H. Yan, B. Unlu, O. Nalcioglu, G. Gulsen, Univ. of California, Irvine (United States)

In bioluminescence tomography (BLT), a light emitting probe, such as luciferase is activated within a volume and the emitted signal at the boundary is measured from multiple views. Afterwards, the measurements are used to reconstruct the source distribution map. During the past years it has become generally recognized that both structural and functional a priori information, also known as anatomical and optical background information are needed for successful BLT reconstruction. Multi-spectral measurement scheme has also been adapted to cope with the underlying problem of non-uniqueness associated with non-spectrally resolved intensity-based bioluminescence technique. Thus it is of great desire to develop an imaging system that is capable of acquiring both structural and optical a priori information along with the multi-spectral bioluminescence data in the same setting. In the past, our group had successfully developed a bench-top system that combines both BLT and diffuse optical tomography (DOT) and tested it with phantom studies. In this paper we present a hybrid bioluminescence tomography system, which uses an X-ray micro CT system to obtain anatomical information and a DOT module to recover the optical background. A cooled CCD camera and a multi-wavelength laser unit required for optical measurements are mounted on the micro CT rotating gantry. Phantom experiments were undertaken to verify the accuracy, repeatability and resolution of the hybrid system. Currently we are undertaking animal studies to evaluate the performance of the hybrid BLT/DOT/CT system in vivo.

7557-36, Poster Session

The examination of an optimized video frequency with the visual stimulus experiment for fMRI

K. Kiyohara, The Graduate School for the Creation of New Photonics Industries (Japan) and Deep Brain Inc. (Japan); T. Ode, M. Kiyohara, Kiyohara Optics Inc. (Japan); H. Eda, The Graduate School for the Creation of New Photonics Industries (Japan) and Photonics Innovations (Japan)

The visual stimulus experiment with fMRI is now popular method in the brain research field. It can be often one of the major topics that researching of the sense of sight. Although people often discuss about output information as a result or a reaction, people don't discuss about input information what it is optimized frequent visual stimulus. This time, we would report the examination of an optimized video frequency with the visual stimulus experiment for fMRI.

So far, many researchers usually use a liquid crystal display (LCD) under control of the computer as a source or an output function of the visual stimulus. However, using LCD is a kind of unsuitable function to control the timing of visual stimulus, compared with a cathode-ray tube (CRT). Even though researchers use the same software to provide the visual stimulus, it would be hard to provide an accurate-timing control, if they wouldn't examine how they do the final output. This signifies that researchers might have different results, which they would choose LCD or CRT as the final output function for the visual stimulus. Furthermore, they couldn't compare the result or analysis without the same circumstances. Even if researchers would use CRT, there were still problems because CRT needs more space than LCD.

We tried experiments with some of visual stimulus system using the brain measurement light system.

Through those comparisons, we would like to discuss about the optimization of video frequency when people doing brain research with visual stimulus.

7557-37, Poster Session

Contrast and resolution analysis of angular domain imaging for iterative optical projection tomography reconstruction

E. Ng, The Univ. of Western Ontario (Canada); F. Vasefi, B. Kaminska, G. Chapman, Simon Fraser Univ. (Canada); J. J. L. Carson, The Univ. of Western Ontario (Canada)

Angular domain imaging (ADI) generates a projection image of an attenuating target within a turbid medium by employing a silicon micro-tunnel array to reject photons that have deviated from the initial propagation direction. In this imaging method, image contrast and resolution are position dependent. The objective of this work was to first characterize the contrast and resolution of the ADI system at a multitude of locations within the imaging plane. The system characterization was then applied to an iterative optical projection tomography reconstruction method. The ADI system consisted of a pulsed laser (100ps, 780nm, PicoTA, Picoquant) with a beam expander for illumination of the sample cuvette. At the opposite side of the cuvette, an Angular Filter Array (AFA) of 60 µm x 60 µm square-shaped tunnels 1 cm in length was used to reject the transmitted scattered light. Image-forming light exiting the AFA was detected by a gated camera (Picostar HR, LaVision) operating with a long gate time to mimic a CW system. Our approach was to translate a point attenuator (0.5 mm graphite rod) using a SCARA robot (Epson E2C351S) to cover a 100x100 matrix of grid points in the imaging plane within the 1x1 cm sample cuvette. At each grid point, a onedimensional point-spread distribution was collected. This process was repeated for varying levels of scattering media. After the ADI system was characterized, the robot was used to rotate the target to collect projection images at several projection angles. At low scattering levels,

Conference 7557: Multimodal Biomedical Imaging V



resolution was position independent and contrast degraded minimally as the target was moved farther from the AFA. At high scattering levels, the target was only discernable when placed within a few millimeters from the AFA. When compared to a filtered backprojection, the iterative method showed the most improvement with images collected at high scattering levels.

7557-38, Poster Session

Evaluation of a multiwavelength laser array with frequency-domain diffuse optical tomography

T. Zhou, M. Ghijsen, D. Thayer, Univ of California, Irvine (United States); G. Gulsen, Univ. of California, Irvine (United States)

Diffuse Optical Tomography (DOT) uses near-infrared light to recover the optical parameter maps of the medium under investigation. Moreover, multi-wavelength measurements allow the determination of the spatial distribution of a number of physiologically significant chromophores, mainly water, fat, oxy- and deoxy-hemoglobin. In fact, data with more wavelengths would reduce the error in the recovered chromophore concentrations. In continuous wave (CW) technique, DOT systems utilize a continuous light source. Therefore, a broadband white light source can be used to enrich the data content with CW systems. Alternatively, light sources with varying in intensity over time can be utilized for DOT. The latter approach can further be divided into two as frequency-domain and time-domain techniques. In the frequency-domain technique, the light source is modulated (~50MHz and above) and the additional phase shift information that is obtained with this technique enables separation of absorption and scattering coefficients, which is difficult with the CW technique. We have evaluated a multi-array laser array that has been developed by Praevium Research Incorporation, CA with our frequencydomain DOT system. This source provides more than 10mW of power at up to 12 wavelengths ranging from 659 to 908nm. The driver circuitry and the temperature controller unit for 12-laser module were constructed and it was integrated to the DOT system. Phantom experiments have been conducted to evaluate the performance of the multi-wavelength laser array.

7557-39, Poster Session

A multimodal based DOT system for in vivo small animal study

S. X. Yi, Technest Holdings, Inc. (United States)

This paper presents our desktop multi-spectral (two-channel) in-vivo DOT imaging system design. The innovative system is integrated with our full-field (360 degree) 3D surface imaging cameras. Data shows that, by using accurate three-dimensional (3D) geometric boundary conditions, the system has significantly enhanced the imaging capacity of diffuse optical tomography (DOT) technology, it also facilitates the multi-spectral image registration process. In recent years several methods have been developed to model photon propagation through diffuse media with complex boundaries using finite solutions of the diffusion or transport equation (finite elements or differences) or more recently analytical methods based on the tangent-plane method. To fully exploit the advantages of these sophisticated algorithms, accurate and full-field 3D boundary geometry of the subject has to be extracted in practical, realtime, and in vivo manner. To date, there is no known reported technique for extracting full-field 3D dimensional boundaries with fully automated, accurate and real-time in vivo performance.

Conference 7558: Endoscopic Microscopy V



Sunday-Monday 24-25 January 2010 • Part of Proceedings of SPIE Vol. 7558 Endoscopic Microscopy V

7558-01, Session 1

Spectrally encoded endoscopy through separated illumination and collection channels

D. Yelin, A. Abramov, Technion-Israel Institute of Technology (Israel)

In spectrally encoded endoscopy (SEE), a miniature lens-grating assembly at the distal end of a single optical fiber is used to illuminate one line on the sample, where each point is encoded by a different wavelength. The backscattered light is then collected through the same optical path and detected in a high speed spectrometer. Since no rapid distal scanning mechanism is required, SEE can be conducted through flexible, sub-millimeter endoscopic probes. The use of a single optical path for both illumination and collection imposes, however, some challenges associated with probe design and image quality, including high speckle noise, back-reflections from the probe's optics, and a need to use spatially coherent light sources. By replacing the single-mode fiber with a double clad fiber, image quality and depth of field were improved, however practical endoscopic imaging through the miniaturized SEE probes was challenging due to strong mode coupling, high back-reflections and high sensitivity to misalignment of the optics.

In this paper we present a scheme for separating the illumination channel from the collection channel, and demonstrate that two-dimensional spectrally encoded imaging is possible with only a single wavelength-encoded channel. Several bench-top setups were constructed in order to simulate different sample illumination configurations, including spectrally encoded incoherent illumination, external (not encoded) illumination, as well as wavelength-encoded imaging of a broadband sample luminescence. In addition, we demonstrate that the separated channels approach allow the use of low-cost white light, spatially incoherent illumination, and compare the resulting imaging characteristics with those obtained using spatially coherent sources.

7558-02, Session 1

Balloon catheter for comprehensive optical frequency domain imaging of the esophagus

H. Yoo, M. J. Suter, M. Shishkov, B. J. Vakoc, B. E. Bouma, Massachusetts General Hospital (United States) and Harvard Medical School (United States); N. S. Nishioka, Massachusetts General Hospital (United States); G. J. Tearney, Massachusetts General Hospital (United States) and Harvard Medical School (United States)

Optical frequency domain imaging (OFDI) is a second-generation form of optical coherence tomography (OCT) that enables comprehensive imaging of the entire distal esophageal wall in two minutes. Threedimensional OFDI is accomplished by scanning the probe's focused beam in a helical pattern (rotation + pullback). Because the diameter of the esophagus (25 mm) is much larger than the ranging depth of OFDI (6 mm) and the confocal parameter of the probe's optics, the optics of the catheter need to be centered in the esophageal lumen. In order to center the optics, we have developed an esophageal OFDI balloon catheter, designed to either be inserted through the accessory port of the endoscope or over a guide wire. The balloon catheter is comprised of an inner rotating cable enclosed by an outer 1.8 mm diameter transparent sheath. A 6.0 cm long PTE balloon (inflated diameter 25 mm) resides at the distal end of the transparent sheath. The sheath is flexible at the proximal end of the balloon and stiff within the imaging portion of the balloon, which reduces the eccentricity of the optics with respect to the balloon. The inner cable contains an optical fiber, terminated by distal optics that includes a glass ferrule, a glass spacer, a GRIN lens,

and a micro prism. Astigmatism induced by the transparent sheath is compensated by employing a cylindrical surface at the micro prism. We have fabricated this balloon probe and have measured a lateral resolution of ~40 μm in both directions, a depth of focus (confocal parameter) of 2.0 mm, and a working distance of 13 mm. We are utilizing this probe in a pilot clinical study (N=6) to compare standalone, over the wire balloon-catheter 3D esophageal imaging to balloon-catheter imaging through an endoscope accessory port. Our results, including an analysis of the relative merits of the two imaging modes, will be presented at the meeting.

7558-03, Session 1

Color imaging in spectrally encoded endoscopy

D. Kang, Massachusetts General Hospital (United States); D. Yelin, Technion-Israel Institute of Technology (Israel); B. E. Bouma, G. J. Tearney, Massachusetts General Hospital (United States)

Spectrally encoded endoscopy (SEE) is a recently-developed miniature endoscopy technology. In SEE, broadband light is dispersed by a diffraction grating at the tip of the probe to spectrally encode one transverse dimension of the sample. Previously, we demonstrated a 350-µm-diameter SEE probe that was successfully used for laparoscopic animal imaging in vivo through a 23-gauge needle. However, color information of the sample could not be acquired in SEE due to its use of the spectral bandwidth for spatial encoding. In this paper, we present a new method for acquiring color images in SEE (RGB-SEE). This technique uses three distinctive spectral bands of blue, green, and red colors that are incident on a diffraction grating at different angles. The incident angles are chosen so that the diffracted beams of the three spectral bands overlap with each other on the sample. By comparing the color gamut of the new method to that of sRGB, we determined that the effective color gamut of RGB-SEE for half of the FOV was similar to that of sRGB. A bench-top system was developed, which used three 525-µmdiameter beams (spectral bandwidth = 75 nm) and a 2400-lpmm grating. A resolution target, a color reference card, and an excised swine small intestine tissue were imaged to evaluate the color imaging capabilities of RGB-SEE. The RGB-SEE images showed qualitatively and quantitatively similar color appearances to those obtained by a conventional digital

7558-04, Session 1

Large luminal area imaging by spectrally encoded confocal microscopy

D. Kang, H. Yoo, P. A. Jillella, B. E. Bouma, G. J. Tearney, Massachusetts General Hospital (United States)

Spectrally encoded confocal microscopy (SECM) is a high-speed reflectance confocal microscopy technology that diffracts different wavelengths of light to distinct locations on the sample. The image can then be determined using a high-speed spectrometer that is located outside of the body, providing images that can be obtained 10-100 times faster than video rate. The high imaging speed of SECM makes it possible to automatically image entire luminal organs, such as the distal esophagus, by helical scanning of the probes' optics through a centering-catheter. One challenge with comprehensive luminal organ imaging is that the focal location of the objective lens must be continuously adjusted to accommodate decentering of the optics and an irregular luminal surface. In this paper, we present a new SECM centering probe, implemented as a bench top apparatus, that incorporates a high-speed autofocus mechanism to keep the focused beam within the tissue at all times. A



miniature translation actuator was used for adaptive focusing. The focal plane of the bench-top probe was tilted relative to the luminal surface of the sample to generate the feedback signal used in the adaptive focusing and also to obtain three-dimensional information over a depth of 50 μm . Images of a cylindrical tissue phantom (diameter = 20 mm; length = 20 mm) were obtained, demonstrating that the tissue surface height could be tracked and used to control the focal position of the objective lens at high speeds. Our results show that large luminal area imaging with SECM is feasible.

7558-05, Session 2

Wide-field fluorescence imaging in narrow passageways using scanning fiber endoscope technology

C. M. Lee, E. Seibel, Univ. of Washington (United States)

An ultrathin scanning fiber endoscope (SFE) has been developed for high resolution imaging of regions in the body that are commonly inaccessible. The SFE produces 500-line color images at 30-Hz frame rate while maintaining a 1.2-mm outer diameter. The distal tip of the SFE houses a 9-mm ridged scan engine attached to a highly flexible tether (minimum bend radius < 8-mm) comprised of optical fibers and electrical wires within a protective sheath. Unlike other ultrathin technologies, the unique physical characteristics of this system have allowed the SFE to navigate narrow passages without sacrificing image quality. To date, the SFE has been used for in vivo imaging of the bile duct, esophagus and peripheral airways. In this study, the standard SFE operation was tailored to capture wide field fluorescence images. Green (523-nm) and blue (440-nm) lasers were used as illumination sources, while the white balance gain values were adjusted to accentuate red fluorescence signal. To demonstrate wide field fluorescence imaging of small lumens, the SFE was inserted into a phantom model of a human pancreatic duct and navigated to a custom fluorescent target. Both wide field fluorescence and standard color images of the target were captured to demonstrate multimodal imaging.

7558-06, Session 2

Development of microactuators for improved spatial sampling in fiber bundle optical biopsy systems

M. R. Kyrish, R. Kester, R. Richards-Kortum, T. Tkaczyk, Rice Univ. (United States)

To reduce the number of biopsies performed for cancer diagnosis, we are developing two methods to improve the quality of in vivo tissue imaging by utilizing oversampling and image reconstruction. The first method utilizes an electromagnetic microactuator to laterally shift a fiber bundle which is part of a confocal microendoscope while the system observes a region of interest. Several images of the area are captured, each displaced from the others by a few micrometers, and are subsequently recombined using a custom algorithm to provide a high resolution image of the sample. The second method utilizes a rotational actuator to rotate the distal end of a fiber bundle microendoscope, which captures images while it spins. This method also allows high resolution images to be reconstructed which are not bound by the limitations of the fiber bundle. In both cases, the movement of the fiber bundles causes changes in the recorded images, which can be exploited through image processing to improve the quality beyond that which can be obtained with a stationary system. The two types of actuators were used in different systems to optimize the use of their functionality, to investigate improved spatial sampling in various applications, and to fulfill design constraints. Also, both systems to which the actuators were added were preexisting systems which had already been developed within the research group. This indicates the possibility of applying this technology to other systems, particularly ones used for in vivo imaging.

7558-07, Session 2

Foveated endoscope objective design to combine high resolution with wide field of view

J. D. Rogers, Northwestern Univ. (United States); T. S. Tkaczyk, Rice Univ. (United States); M. R. Descour, College of Optical Sciences, The Univ. of Arizona (United States)

There is always a tradeoff between resolution and Field of View (FOV) in an imaging system. This limit can be due to the number of pixels in the detector, however a fundamental limit also exists in any optical system called the Space Bandwidth Product (SBP) which scales as the FOV area divided by the area of the diffraction limited spot. The SBP can only be increased by increasing the size of the optical system. In applications where the size of the optical system is constrained such as endoscopes, the SBC will ultimately limit the resolution or FOV. However, there is a way to provide both high resolution and a wide FOV without changing the total number of pixels in the image. The technique is called foveated imaging because is mimics this characteristic of the human eye in which the fovea has a higher resolution at the center of the FOV than the surrounding retina. A similar effect can be achieved optically by introducing a large amount of barrel distortion in the lens design. The result is an effective increase in the magnification at the center of the FOV, and reduced resolution but larger angular sampling at the edge. The stretching effect of the distortion can be compensated for computationally to provide an onscreen display that is not distorted, but merely appears blurred at the edges. Such an objective will enable for endomicroscopy while still providing "peripheral vision" to allow endoscopists to navigate and locate regions of interest.

7558-08, Session 2

A multipoint scanner for high frame rate confocal microendoscopy

A. R. Rouse, H. Makhlouf, A. A. Tanbakuchi, A. F. Gmitro, The Univ. of Arizona (United States)

Slit-scanning geometries for confocal microendoscopy represent a compromise between acquisition rate and optical performance. Such systems provide high frame rates that freeze motion but recent Monte Carlo simulations show that scattered light severely limits the practical imaging depth for in vivo applications. A new multi-point scanning architecture for confocal microendoscopy has been developed. The new scanner is based on a relatively simple modification to the slitscanning geometry that results in a parallelized point-scanning confocal microendoscope that maintains the high frame rate of a slit-scanning system while providing optical performance close to that of a single point scanning system. The multi-point scanner has been incorporated into an existing multi-spectral slit-scanning confocal microendoscope. The new confocal aperture consists of a slit and a rotating low duty cycle binary transmission grating, which effectively produces a set of continuously moving widely-spaced illumination points along the slit. The design maintains the ability to rapidly switch between grayscale and multispectral imaging modes. The improved axial resolution of the multi-point scanning confocal microendoscope leads to significantly better confocal sectioning and deeper imaging, which greatly improves the diagnostic potential of the instrument.

7558-09, Session 2

Simultaneous optical coherence tomography and laser induced fluorescence imaging in rat model of ovarian carcinogenesis

L. P. Hariri, E. R. Liebmann, S. L. Marion, P. B. Hoyer, J. R. Davis, The Univ. of Arizona (United States); M. A. Brewer, Univ. of



Connecticut (United States); J. K. Barton, The Univ. of Arizona (United States)

Ovarian cancer is the most lethal gynecologic malignancy. The development of reliable ovarian cancer models could provide increased understanding of ovarian cancer pathogenesis, but appropriate tools are required to assess these models. Optical coherence tomography (OCT) and laser-induced fluorescence (LIF) spectroscopy are non-destructive optical imaging modalities. OCT provides architectural information at near histological resolutions and LIF provides biochemical information. We utilize combined OCT-LIF to image the ovaries of post-menopausal ovarian carcinogenesis rat models and controls to evaluate normal cyclic, acyclic, and neoplastic ovaries ex vivo. Eighty-three female Fisher rats were exposed to combinations of control sesame oil, vinylcyclohexidine diepoxide (VCD) inducing ovarian failure, and/or 7,12-dimethylbenz[a] anthracene (DMBA) inducing carcinogenesis. Three or six months posttreatment, 162 ovaries were harvested and imaged with OCT-LIF: 40 cyclic, 105 acyclic, and 17 Sertoli-Leydig cell tumors (SLCT). OCT was able to identify follicles of various developmental stages, corpora lutea (CL), CL remnants, and epithelial invaginations/inclusions and allowed for the characterization of both cystic and solid SLCT. Comparisons of signal attenuation in corpora lutea and solid SLCT revealed a statistically significant increase in signal attenuation among corpora lutea. LIF was able to characterize spectral differences among cyclic, acyclic, and neoplastic ovaries in fluorescence emission attributed to collagen, NADH/ FAD, and hemoglobin absorption. We present combined OCT-LIF imaging in rat ovarian carcinogenesis models, providing preliminary criteria for normal cyclic, acyclic, and SLCT ovaries which support the potential of combined OCT-LIF for evaluation of ovarian cancer pathogenesis. Future studies will aim to evaluate these animal models in vivo.

7558-10, Session 3

Real-time monitoring of esophageal laser thermal therapy

L. A. Bartlett, B. Vakoc, M. Shishkov, A. Soroka, G. Tearney, Wellman Ctr. for Photomedicine (United States); B. E. Bouma, Wellman Ctr. for Photomedicine (United States) and HST Division of Harvard and MIT (United States)

Laser-induced thermal injury of epithelial tissues has been investigated as an endoscopic therapeutic response to early neoplastic changes and intramucosal cancer. Controlling the depth of therapy and conforming the treated volume to a desired treatment plan could more accurately be achieved by methods for real-time monitoring of tissue response. Depthresolved interferometric imaging techniques have been demonstrated to detect unique dynamic changes in depth-resolved complex reflectivity profiles that arise within zones of active tissue denaturation. The depth of these phase and amplitude signatures is correlated with histological evidence of thermal injury. By simultaneously delivering two overlapping laser beams to porcine esophageal specimens ex vivo, one beam induces thermal injury, and the second beam of a distinct wavelength detects the tissue thermal response. By translating samples during irradiation, linear scans were performed to investigate a range of therapeutic-laser parameters and histology was subsequently performed to determine the depth of injury for each linear scan. At the depth of active thermal denaturation, the phase of the reflected monitoring beam exhibits a pronounced inflection, potentially arising from local microscopic deformation. Our data demonstrates that this signature is highly correlated with histologically determined injury depth (=0.96) and yields an accuracy of injury-depth detection of 50 µm for depths ranging from 200 to 900 µm. Additionally, the modulated speckle variations in the magnitude of the complex reflectivity profiles were analyzed quantitatively with standard time frequency analysis techniques. Further, we have confirmed the feasibility of conducting these measurements in living swine using a novel esophageal probe design.

7558-11, Session 3

Uniform illumination scheme for spiralscanning based fiber optic two-photon fluorescence endomicroscopy

L. Huo, Y. Wu, Y. Chen, X. Li, Johns Hopkins Univ. (United States)

An effective solution was demonstrated to combat the non-uniform illumination problem associated with spiral-scanning based fiber-optic two-photon endomicroscopy. The problem was manifested by a higher excitation power density in the central part than in the peripheral part of a circular field of view (FOV) and resulted in faster photobleaching of fluorescence signal as well as an increased risk of laser-induced damage of cells/tissues in the central portion of the FOV. An acousto-optic modulator (AOM), which was driven by a synthesized waveform and synchronized with the spiral beam scanning pattern, was used to achieve uniform illumination throughout the FOV by dynamically attenuating the excitation light when the scanning beam fell on the center. The image intensity was well calibrated with the modulated excitation power. The scheme was verified on a resonant fiber scanning two-photon fluorescence endomicroscope consisting of a double-clad fiber (DCF) cantilever, a focusing lens unit and a tubular lead zirconate titanate (PZT) actuator which vibrated the DCF cantilever in a spiral-scanning pattern. Cell viability experiments (with Skov-3 cells) were performed to demonstrate the need for a uniform illumination with reduced photo damage. It was found that cells in the center of the FOV died after ~35 min when an excitation power of ~40 mW was used without AOM modulation of excitation light intensity. When uniform illumination was applied by using an AOM with a maximal excitation power of ~40 mW and an extinction ratio of 3:1, cells were found still alive even after 75 min observation time.

7558-12, Session 3

Design, modeling, and pilot testing of a new prototype scanning CARS-based endoscope

P. Grenier, M. Fortin, P. Gallant, INO (Canada); R. S. Da Costa, B. C. Wilson, Univ. Health Network (Canada); E. J. Seibel, Univ. of Washington (United States); O. Mermut, J. Cormier, INO (Canada)

A nonlinear, multimodal Coherent Anti-Stokes Raman scattering endoscope would be of significant clinical value for improving diagnostic specificity for disease detection. However, developing this technology is challenging for many reasons. First, nonlinear techniques such as CARS are inherently single point measurement technique, thus requiring fast scanning for video rate imaging. Moreover, the intrinsic nonlinearity of this modality imposes several technical constraints and limitations, mainly related to pulse and beam distortions that occur within the optical fiber.

Here, we describe the design and report early results of modeling and experimental testing of a new miniature CARS optical probe. Our computational model accounts for pulse distortion in optical fibers. It also defines and evaluates a CARS signal generation efficiency parameter, and calculates an estimate of the optimal collection geometry based on the scattered CARS signal distribution in biological tissues using Monte Carlo modeling and Zemax optical design model.

A preliminary performance assessment of optical-fiber based CARS is also presented, based on reference samples containing Raman-active compounds. We present pilot results evaluating the compatibility of the CARS technology with a new and complementary spiral scanning-fiber endoscopic imaging technology developed at the University of Washington. This technology has ideal attributes for clinical use such as small footprint, adjustable field-of-view and high spatial-resolution. This new compact hybrid fiber-based endoscopic CARS imaging system is anticipated to have wide clinical applicability, particularly in the early detection of endoluminal cancers.



7558-13, Session 3

Double-clad fiber coupler for endoscopy

M. Rivard, S. Lemire-Renaud, D. Morneau, M. Strupler, N. Godbout, C. Boudoux, Ecole Polytechnique de Montréal (Canada)

Double-clad fibers (DCF) have been shown to enhance single-fiber endoscopy, such as spectrally encoded endoscopy (SEE), through improvements in speckle contrast, signal collection and depth of field. Here we present and demonstrate an all-fiber approach for DCF endoscopy allowing for robust and efficient light coupling into the DCF core while permitting efficient light collection and separation into single- and multi-mode signals. An achromatic double-clad fiber coupler (DCFC) was obtained by fusing and tapering two pieces of commercially available DCF (Nufern, SM-9/105/125-20A; Core diameter 10.5 microns, NA=0.12; Inner clad diameter 105 microns, NA=0.20). The DCFC ensured high throughput into the single-mode path by isolating the cores (-27.6dB of isolation) while statistically separating the inner clad modes into each branch (coupling ratios: -3.5dB and -2.6dB). To test the imaging characteristics of the DCFC, we integrated it into a rapid wavelength swept-source (lambda=1310 ±40nm) SEE imaging system. Light was efficiently launched into the DCFC single-mode core by splicing the coupler with a single-mode fiber having a similar mode field diameter. In comparison with the traditional free-space beam-splitter approach, the DCFC increased the single-mode path efficiency by >6dB, was less sensitive to back reflections and to misalignment. The DCFC was used to simultaneously obtain single-mode and multi-mode SEE images in real time (512x512pixels, 30 fps). Speckle-free (speckle contrast reduced by a factor 4.6) reflectance maps of in vivo samples were combined with 3D profiles, obtained from the interference between the single mode signal and a reference arm. With its improved efficiency and robustness to vibrations, this DCFC allows the transfer of DCF endoscopy to clinical settings. Future work includes translation of the technique to smaller diameter DCF for confocal endoscopy.

7558-14, Session 3

A novel imaging system of optical detection on cancers and tissues in gastrointestinal endoscope using high-chroma white and color tunable LEDs

T. Taguchi, Y. Uchida, S. Kurai, Yamaguchi Univ. (Japan); H. Yanai, Kanmon National Hospital (Japan); J. Nishikawa, S. Kiyotoki, T. Okamoto, S. Higaki, I. Sakaida, Graduate School of Medicine Yamaguchi Univ. (Japan)

Our prototype white LED upper digestive endoscope also allowed clear visualization of the early gastric cancer by close observation in the stomach. Indigo carmine chromoendscopy emphasized the redness of the lesion and delineated the demarcation between the cancerous and non-cancerous mucosa. The color tunable white LED endoscope also showed a flat lesion, which was located at the anterior wall of the midgastric body and had ill-defined margins accompanied by slightly reddish or focally pale mucosa.

7558-15, Session 4

Numerical analysis of cascaded GRIN lensbased imaging probes for endoscopic optical coherence tomography

W. Jung, W. Benalcazar, U. Sharma, A. Ahmad, H. Tu, S. A. Boppart, Univ. of Illinois at Urbana-Champaign (United States)

One of the major challenges faced in endoscopic OCT is the design of miniaturized beam-focusing optics to enable high lateral resolutions at

longer working distances (>6-8 mm) for circumferential imaging of large luminal organs such as the esophagus. While several research studies have achieved high-resolution endoscopic OCT images using single GRIN lens-based probes, these designs usually provide limited working distances (1-4 mm). In this study, we perform numerical analyses of single and cascaded GRIN lens-based imaging probes, compare their relative performance and derive optimal design parameters to obtain high lateral resolution at longer working distances. Our design model employs a complex beam parameter method and Gaussian beam theory to calculate the changes in working distance and beam waist size as a result of varying parameters such as spacing between components, spacing refractive index etc.. Numerical results show that a single GRIN lens- based probe can be optimized to provide a beam waist size of ~20 um with working distances of 2-4 mm. However, longer working distances (~10 mm) resulted in significant deterioration of lateral resolution (>60 um). In an optimized two GRIN lens-based design, the combination of the first GRIN lens and spacer can modify the divergence and confocal parameter of the incident beam, enabling efficient filling of the effective aperture of the second GRIN lens, thereby providing longer working distances (>8 mm) while still maintaining a smaller beam waist (~20 um). We also explore the effect of modifying enclosure tubing geometry to compensate for beam distortion.

7558-16, Session 4

Optical frequency domain imaging of the distal esophagus in Barrett's patients

M. J. Suter, P. A. Jillella, H. Yoo, M. Mino-Kenudson, G. Y. Lauwers, B. E. Bouma, N. S. Nishioka, G. J. Tearney, Harvard Medical School and Wellman Ctr. for Photomedicine (United States)

Introduction: Optical coherence tomography has been shown to accurately differentiate esophageal pathology relevant to screening and surveillance in Barrett's patients. With developments in both imaging technology and catheter designs we are currently conducting a clinical study aimed at performing comprehensive microscopy of the entire distal esophagus using optical frequency domain imaging (OFDI). The goal of the study is to compare the sensitivity of OFDI to endoscopy for the diagnosis of specialized intestinal metaplasia (SIM), using histopathology as the gold standard.

Methods: Using a custom balloon catheter (2.5 cm diameter, 6 cm imaging window) we have acquired OFDI images of the entire distal esophagus in 76 patients (frame rate: 10 frames/sec, frame size: 2048 x 4096, image resolution: 8 μ m x 18 μ m x 50 μ m). The treating endoscopist rendered a diagnosis at the time of the procedure based on the endoscopy images alone. The acquired OFDI images were interpreted offline by a blinded expert OFDI reader. Biopsies with jumbo forceps were acquired and processed according to current standard of care recommendations in place at the Massachusetts General Hospital gastrointestinal endoscopy department and were analyzed blinded by an expert gastrointestinal pathologist.

Results/Conclusions: >99% of the esophageal wall was visible throughout the 6cm extent of the catheter's imaging window and traversed the gastroesophageal junction in 95% of cases. There were 27 cases that were positive for SIM by histopathology. There were no SIM+ cases that were incorrectly diagnosed as negative for SIM by both OFDI and endoscopy. OFDI incorrectly gave a result of negative for SIM in 2 cases when endoscopy was positive for SIM and endoscopy mistakenly rendered a negative for SIM diagnosis in 6 cases when OFDI was positive for SIM (p=0.289). The study revealed a positive trend for superior OFDI sensitivity for detection of SIM when compared to endoscopy. With continued enrollment we anticipate that we will demonstrate a statistically significant increased sensitivity of OFDI for the detection of SIM.



7558-17, Session 4

Optical frequency domain imaging as a tool for assessing the tissue response to radiofrequency ablation therapy for Barrett's esophagus

P. A. Jillella, M. J. Suter, M. Shishkov, B. E. Bouma, N. S. Nishioka, G. J. Tearney, Massachusetts General Hospital (United States)

Monitoring the micro-structural response to radio-frequency (RF) ablation therapy is important for determining the efficacy of this endoscopic technique for eradicating Barrett's esophagus. Optical frequency domain imaging (OFDI) is a recently developed, high speed OCT technology that is capable of imaging the three dimensional architectural morphology of the esophageal wall. In this paper, we describe a 15-patient pilot study, where OFDI imaging was conducted at 3 time points (baseline, 3 month, and 6 month) on a patient to evaluate the tissue response following a BARRX radio-frequency ablation therapy. A 1.7mm diameter OFDI probe, inserted through the accessory port of an endoscope, was used to obtain 4 longitudinal (~5 cm length) volumetric image datasets spaced around the circumference of the esophagus. The OFDI images obtained during this study show 1) the presence of Barrett's prior to treatment, 2) heterogeneous generation of escar immediately following treatment, and 3) the presence of buried glands in the majority of cases at followup. These results demonstrate the potential of OFDI for evaluating the degree of injury associated with the therapeutic radiofrequency ablation techniques and efficacy of RF ablation for treating Barrett's esophagus.

7558-18, Session 4

Dual-beam functional FDOCT endoscope for phase stable imaging

C. Blatter, T. Schmoll, Medizinische Univ. Wien (Austria); A. Bachmann, T. Lasser, EPFL (Switzerland); R. A. Leitgeb, Medizinische Univ. Wien (Austria)

In FDOCT high phase stability between successive spectra is required, since any additional phase noise introduced by e.g. sample motion, beam scanning or in the case of handheld probes fiber bending, will cause signal degradation. To overcome this problem we are using a dual beam FDOCT endoscope with a reference reflex within sample arm inside the endoscope. As both reference and sample light share the same path we achieve much improved relative phase stability. The dual beam approach allows pre-delaying one of the two beams that illuminate the sample arm, such that the sample will always be within the coherence gate relative to the reference mirror. By introducing a phase modulation across the B-scan we realized a rigid angular scanning dual beam FDOCT endoscope, with the advantage of high phase stability, high speed, high resolution, and full range imaging. We discuss the drawback of the dual beam FDOCT approach that all light fields present within the unambiguous depth range of FDOCT are coherently summing up and contribute to the interference signal and therefore constrains the achievable dynamic range. However when applying FDOCT's functional extensions, such as Doppler FDOCT or polarization sensitive FDOCT to endoscopic measurements high phase stability is of essence. We show ex-vivo results of porcine esophagus as well as in-vivo measurements of the human oral cavity. To demonstrate the high phase stability we present endoscopic Doppler FDOCT measurements and PSOCT measurements inside the human oral cavity.

7558-19, Session 4

A dual modality fluorescence confocal and optical coherence tomography microendoscope

H. Makhlouf, College of Optical Sciences, The Univ. of Arizona (United States); A. R. Rouse, A. F. Gmitro, The Univ. of Arizona (United States)

We demonstrate the implementation of a Fourier domain optical coherence tomography (OCT) imaging system incorporated into the optical train of a fluorescence confocal microendoscope. The slit-scanning confocal system has been presented previously and achieves 3µm lateral resolution and 30µm axial resolution over a field of view of 430µm. Its multi-spectral channel captures images with an average spectral resolution of 6nm. To incorporate OCT imaging, a super luminescent diode and diffraction grating couple light into the microendoscope catheter. The infrared diode has a spectral bandwidth of 24nm allowing for an OCT axial resolution of 10µm. A common-path interferometer is made with a reference coverslip located at the distal end of the fiber bundle catheter. Light from the reference and sample combine to produce a spectral interferogram on the same 2D CCD camera used for confocal microendoscopic imaging, and OCT depth information is recovered by a Fourier transform along the spectral dispersion direction. Shutters and a scan mirror are appropriately activated to switch rapidly between confocal and OCT imaging modes. The OCT extension takes advantage of the slit-scanning geometry, so that a 2D image is acquired for each position of the scan mirror and a 3D view is reconstructed after a single scanning cycle. Combining confocal and OCT imaging modalities provides a more comprehensive view of tissue and the potential to improve disease diagnosis. A preliminary bench-top system design and imaging results are presented.

7558-20, Session 4

Endoscopic 3D-OCT reveals buried glands following radiofrequency ablation of Barrett's esophagus

C. Zhou, D. C. Adler, T. Tsai, H. Lee, Massachusetts Institute of Technology (United States); L. Becker, VA Healthcare System Boston (United States); J. M. Schmitt, LightLab Imaging Inc. (United States); Q. Huang, VA Healthcare System Boston (United States); H. Mashimo, VA Healthcare System Boston (United States) and Harvard Medical School (United States)

Barrett's esophagus (BE) with high-grade dysplasia is generally treated by endoscopic mucosal resection or esophagectomy. Radiofrequency ablation (RFA) is a recent treatment that allows broad and superficial ablation for BE. Endoscopic three-dimensional OCT (3D-OCT) is a volumetric imaging technique that is uniquely suited for followup surveillance of RFA treatment. 3D-OCT uses a thin fiberoptic imaging catheter placed down the working channel of a conventional endoscope. 3D-OCT enables en face and cross-sectional evaluation of the esophagus for detection of residual BE, neo-squamous mucosa, or buried BE glands. Patients undergone RFA treatment with the BARRX HALO90 system were recruited and imaged with endoscopic 3D-OCT before and after (3-25 months) RFA treatment. 3D-OCT findings were compared to pinch biopsy to confirm the presence or absence of squamous epithelium or buried BE glands following RFA. Gastric, BE, and squamous epithelium were readily distinguished from 3D-OCT over a large volumetric field of view (8mm x 20mm x 1.6mm) with less than 10 µm axial resolution. In all patients, neo-squamous epithelium (NSE) was observed in regions previously treated with RFA. A small number of isolated glands were found buried beneath the regenerated NSE and lamina propria. NSE is a marker of successful ablative therapy, while buried glands may have malignant potential and are difficult to detect using conventional video endoscopy and random biopsy. Buried glands were not observed with pinch biopsy due to their extremely sparse



distribution. These results indicate a potential benefit of endoscopic 3D-OCT for follow-up assessment of ablative treatments for BE.

7558-01, Session 5

In vivo brain imaging using miniaturized oneand two-photon fluorescence microscopes

M. J. Schnitzer, Stanford Univ. School of Medicine (United States)

An important aim of neuroscience research is to explain mammalian behavior in terms of underlying cellular dynamics. However, there has been a paucity of tools for visualizing the dynamics of individual cells in the brains of awake behaving mammals. I will describe recent progress in the development of miniaturized microscopes (1-4 grams) that are sufficiently small to be borne on the head of a freely behaving adult mouse. High-speed (100 Hz) fiber-optic epifluorescence microscopy now permits the visualization of intracellular calcium dynamics and of cerebral microcirculation within the brains of mice that are actively behaving. A complementary approach involves miniaturized, laser-scanning two-photon fluorescence microscopes, which have employed either resonant or non-resonant fiber-scanners, or microelectromechanical systems (MEMS) laser-scanning mirrors. The two approaches to fluorescence excitation have complementary advantages and limitations, and miniaturized microscopes of both types are likely to find key niches in neuroscience research, for studies of healthy animals and animal models of brain disease.

7558-02, Session 5

MEMS-devices for laser camera systems for endoscopic applications

C. Drabe, H. Schenk, T. Sandner, Fraunhofer Institute for Photonic Microsystems (Germany); R. A. James, Microvision, Inc. (United States)

In 2007 IPMS and MVIS presented the results of a full colour scanned beam imaging system. In this paper we will in addition give an update on the technological development since the last paper. The already small die size of 3000µm x 2300µm was further reduced to less than 2000µm x 2000µm. The new devices consist of a moveable frame oscillating at frequencies in the range of 700 Hz - 900 Hz and 1400 Hz - 1800 Hz carrying a mirror of 350 µm diameter in a gimbal mounting. The mirrors oscillate at frequencies in the range of 13-15 kHz. The characteristic mechanical amplitudes are 21° MSA (mechanical can angle) for the frame and 28° MSA for the mirror respectively. Voltages of less than 50 V for the frame and 100 V for the mirror were necessary to accomplish this. The improved MEMS device design is presented as well as the related measurement results. The images of various objects taken with an optical system using the former devices are presented revealing the excellent resolution of such a system and enabling an outlook on the possibilities of the new device.

7558-03. Session 5

In vivo 3D and Doppler OCT imaging using electrothermal MEMS scanning mirrors

J. Sun, L. Wu, H. Xie, Univ. of Florida (United States)

Most cancers occur inside human body, which requires high-resolution endoscopic imaging modalities. The paper reports in vivo endoscopic optical coherence tomography (OCT) imaging enabled by integrating rapid-scanning MEMS mirrors into a miniature imaging probe. The MEMS mirror has an aperture size of 1mm by 1mm and a chip size of 2mm by 2mm. The optical scan angle exceeds $\pm 25~$ at 6 Vdc. The outer diameter of the probe is only 5 mm. The axial resolution is about 10 μm and the imaging speed is 2.5 frames per second. Doppler OCT imaging has also been demonstrated.

7558-21, Session 5

Piezoelectric MEMS mirrors for forwardlooking endoscopic imaging

S. Grego, K. H. Gilchrist, RTI International (United States); R. P. McNabb, J. A. Izatt, Duke Univ. (United States)

A novel scanning mirror device consisting of a mm-sized microfabricated mirror actuated by a single piezoelectric cantilever is presented. The device was designed to provide wide-range rapid forwarding-looking scanning of a 500 um diameter optical beam at the distal end of a 3 mm catheter. The piezoelectric scanning mirror can be cascaded in a dual mirror system to allow 2D beam steering. Two-dimensional scanning MEMS mirrors are generally used in a side-looking configuration, however, forward-looking MEMS probes could be effectively used in imaging large hollow organs such as stomach, bladder and colon. The MEMS optical scanner provides a large ratio of mirror aperture to device size; optical angular displacements up to ±14 deg were demonstrated and resonance frequencies ranging from hundreds of Hz to kHz were measured for a set of different mirror sizes. The imaging capability of the piezoelectric scanner was demonstrated using a bench-top spectrometer based Fourier-Domain OCT system. The packaging approach to integrate the MEMS devices in a highly compact 2D scanning system will be discussed.

7558-22, Session 5

Dual-axes confocal microendoscopy of gastrointestinal tract

W. Piyawattanametha, NECTEC (Thailand) and Stanford Univ. (United States); M. Mandella, H. Ra, Stanford Univ. (United States); Q. Zhen, Univ. of Michigan (United States); K. Loewke, J. Liu, S. Frieland, G. Kino, R. Soetikno, Stanford Univ. (United States); T. D. Wang, Univ. of Michigan (United States); O. Solgaard, C. Contag, Stanford Univ. (United States)

We demonstrated a Dual-Axes Confocal (DAC) fluorescence microendope (785-nm-light-source) and obtained in vivo images of the human gastrointestinal (GI) tract. All optical components, including a MEMS scanner, are assembled in a 5.5-mm diameter stainless steel package equipped with a micromotor for vertical translation (z-axis). The endomicroscope delivers an excitation wavelength of 785 nm with a maximum laser output of 2.5 mW at the surface mucosa. Confocal images can then be collected at a scan rate of 4 frames/second with a 225 μ m \times 425 μ m FOV. Both axial and transverse resolutions are 5 μ m and lamina propria constituents can be visualized to a depth of 130 μ m.

While performing standard videocolonoscopy, the confocal images are simultaneously collected from the MEMS based endomicroscope that occupies the instrument channel. An Indocyanine Green (ICG) mixture is topically applied onto the mucosal surface 5 minutes before each image is obtained. Two distinct morphologies have been identified from the endomicroscope based on the in vivo subsurface crypt appearance. Normal crypt architecture is classically represented by ordered and regular crypt openings covered by a homogenous epithelial layer with visible goblet cells within the subcellular matrix. Dysplastic crypt architecture is represented by architectural disorder of the crypts characterized by ridge-lined epithelia.

This novel imaging instrument have potential for major clinical implications as it allows in vivo diagnosis of colonic intra/sub-epithelial neoplasia that can influence 'on table' management decisions.



7558-23, Session 5

A surgical confocal microscope utilizing a MEMS scanner and a GRIN relay lens for molecular image-guided brain tumor resection

J. T. C. Liu, M. J. Mandella, Stanford Univ. (United States); N. O. Loewke, Univ. of California, Los Angeles (United States); E. Garai, W. Piyawattanametha, H. Ra, H. Haeberle, O. Solgaard, G. S. Kino, C. H. Contag, Stanford Univ. (United States)

Numerous studies have indicated a correlation between the outcomes of brain tumor patients with the degree of surgical resection. Real-time image guidance is necessary to allow for complete resections in a larger proportion of patients, and to reduce the debilitating effects of overaggressive resections. Confocal microscopy, if modified for deep tissue imaging, allows one to image sub-surface cells that are in their natural undisturbed tissue microenvironment, where cell-surface proteins may accurately be labeled with exogenous contrast agents.

We have developed a surgical confocal microscope with a 2-mm diameter GRIN relay lens at the distal tip for in vivo histopathological guidance during brain tumor resection. The microscope we have developed utilizes a dual-axis confocal architecture to efficiently reject out-of-focus light for high-contrast optical sectioning within intact tissues. A biaxial MEMS scanning mirror is actuated at resonance along each axis to achieve a large field of view. We have developed a synchronized and calibrated waveform-generation and data-acquisition system to decode the unstable Lissajous pattern that results from actuating the orthogonal axes of the MEMS mirror at highly disparate resonance frequencies.

Imaging studies have been performed with tissues from a transgenic mouse (Ptc+/-p53-/- Math1-GFP) that spontaneously develops medulloblastoma with colocalized GFP expression. We are also developing fluorescent antibody- and peptide-contrast agents for delineating tumor margins in human patients. These techniques will allow surgeons to unambiguously distinguish between normal and cancerous tissues for chemically-specific and spatially-precise tumor debulking.

7558-04, Session 6

MEMS deformable mirrors for focus control in vital microscopy

D. L. Dickensheets, S. J. Lukes, E. Dunbar, J. Lutzenburger, Montana State Univ. (United States)

MEMS deformable mirrors can play an important role in beam focusing and wavefront correction in microscopy systems. The technology is especially well suited to endoscopic microscopy platforms where extreme miniaturization is required and any microscopy system where high speed focus control or focus scanning is necessary. MEMS deformable mirrors designed specifically for focus control and spherical aberration compensation can be made quite small and require only a few actuators, making them attractive for miniaturization for endoscopy applications. With control over primary spherical aberration, these mirrors can correct for depth-dependent spherical aberration that decreases image contrast and resolution when imaging into tissue using high NA. This paper describes recent progress toward our design goal to reach 200 microns of focus adjustment range with an NA=1.0 imaging system, typical of high NA confocal reflectance imaging. The mirrors are constructed as metalized polymer membranes ranging from 1-3 mm in diameter using the photo-cured epoxy SU-8. They are electrostatically actuated using three concentric electrodes to provide large displacement while minimizing mirror-induced aberration. A feedback control system maintains desired surface shape while maximizing the range of stable deflection of the mirror. The mirrors have resonant frequencies of several hundred Hertz, making them suitable for real-time x-z scanning confocal microscopy. Imaging examples will be presented to illustrate the mirror ability as a focusing element. Finally, limitations including residual

aberrations that are non-linearly dependent on focus will be discussed in the context of anticipated future performance of this class of deformable mirror for focus control in microscopy.

7558-05, Session 6

High-speed liquid lens with 2-ms response and 80.3-nm root-mean-square wave front error

H. Oku, M. Ishikawa, The Univ. of Tokyo (Japan)

High-speed focusing technology has been desired for decades. Here, a liquid lens with a novel structure using a liquid-liquid interface with a pinned contact line that can arbitrarily control the focal length in milliseconds and achieve practical imaging performance is reported.

The interface curvature is dynamically controlled by liquid volume change. The lens includes two immiscible liquids infused in two chambers, but they are interfaced at a circular aperture. One chamber is equipped with a deformable wall that is thrust by a piezostack actuator to change the chamber volume.

The vibrating interface behaves like a damped harmonic oscillator depending on the kinematic viscosity of the infused liquid. Based on the result of preliminary experiment, ultra pure water and poly-dimethylsiloxane (PDMS) with 5000 cSt were used as immiscible liquids to achieve high-speed response.

The pinned contact line should be a good circle in three dimensions to realize a good spherical interface. The largest deformation of the interface could be limited by the largest contact line deformation. By setting the acceptable vertical deformation of the contact line to be less than the quarter wave length, a machining accuracy of less than 1.95 um is required for the circular edge pinning the contact line.

A prototype achieved a refractive power range of 52 D, a 2 ms step response time and a minimum RMS wavefront error 80.3 nm. The potential applications of this device are axial focus scanning of microscopes, and focusing/zooming of camera lenses and machine vision systems.

7558-24, Session 6

Improved chromatic performance of endomicroscope optics for broadband imaging

G. C. Birch, College of Optical Sciences, The Univ. of Arizona (United States); B. McCall, T. S. Tkaczyk, Rice Univ. (United States); M. R. Descour, College of Optical Sciences, The Univ. of Arizona (United States)

Conventional miniature optical microscope systems are usually made from a single optical material and therefore have poor correction of chromatic focal shift (CFS, a.k.a., axial color). Typical Stokes shifts exceed the limited bandwidth of such single-material optics. This problem is compounded when using multiple fluorophores.

To demonstrate a solution, we have designed, fabricated, and tested an achromatic doublet made from optical polymers. Ten different common optical polymers were analyzed and doublet designs were evaluated for the most promising materials combination. Optical polymers were chosen for the range of available manufacturing options (e.g., diamond turning, milling, or injection molding), their low cost, and their ready availability. The final doublet design employs two common, off-the-shelf optical polymers: PMMA and polystyrene.

The all-polymer achromat doublet was manufactured using diamond milling and single point diamond turning (SPDT). Diamond milling differs from SPDT by employing a shaped diamond tool with the radius of the desired surface and the same semi-diameter as the desired clear aperture (e.g., 1.5 mm in our case). Advantages of this manufacturing technique will be discussed in detail.

Conference 7558: Endoscopic Microscopy V



The measurement of the doublet's residual CFS was made using a custom designed, multispectral Shack-Hartmann (SH) test setup. The SH test uses a lenslet array to locally sample the wavefront emerging from the test lens. The CFS measurements were simulated in ZEMAX to predict the results of evaluating the achromatic doublet design. The experimental performance of the achromatic doublet, as well as an example miniature microscope design based on doublets, will be presented.

7558-25, Session 6

Focused OCT and LIF endoscope

R. A. Wall, The Univ. of Arizona (United States) and College of Optical Sciences, The Univ. of Arizona (United States); G. T. Bonnema, D4D Technologies, LLC (United States); J. K. Barton, The Univ. of Arizona (United States)

Optical coherence tomography (OCT) is a non-invasive, interferometric imaging technique capable of imaging up to 2 mm deep in highly scattering tissue. Laser-induced fluorescence (LIF) has shown promise as a viable option for diagnostic tests in the gastrointestinal tract. Our in vivo work on the mouse colon with similar LIF techniques has shown high sensitivity and specificity in spectrophotometric analysis of distinguishing normal tissue from adenoma. Combining OCT and LIF in one endoscope shows a heightened sensitivity to early changes in tumor progression when compared to either modality alone.

Previously, we have built ultrahigh resolution (2-5 microns) OCT endoscopes with unfocused LIF and have demonstrated imaging of mouse colon serially over time. Our new design is a high-resolution endoscope 2 mm in diameter that can focus light from 325-1300 nm. A reflective design ball lens is employed that eliminates the difficulty of operating achromatically over a large range, while taking advantage of TIR at two faces and coating a third mirror face internally to focus the beams downwards. It is a 1:1 imaging system that obtains a theoretical diffraction-limited resolution for both the OCT (800-1300 nm) and LIF (greater than 325 nm) channels.

We have built the focused OCT-LIF endoscope and integrated it into an existing arrangement. In vivo and ex vivo images acquired using this focused OCT-LIF system suggest higher lateral resolution in both imaging modalities than those images collected with previous systems, allowing for heightened specificity and sensitivity in the detection of early changes in tumor progression.

7558-26, Session 6

High-resolution axicon based endoscopic FD OCT imaging with a large depth range

K. Lee, The Institute of Optics, Univ. of Rochester (United States); W. Hurley, Rochester Precision Optics (United States); J. P. Rolland, The Institute of Optics, Univ. of Rochester (United States)

Endoscopic imaging in tubular structures, such as the tracheobronchial tree, could benefit from imaging optics with an extended depth of focus (DOF). These optics could accommodate for varying sizes of tubular structures across patients and along the tree within a single patient. However, most small sized catheters cannot simultaneously achieve high lateral resolution and long depth of focus. In the paper we demonstrate extended DOF without sacrificing resolution showing rotational images in biological tubular samples with arbitrary cross-section through a custom designed axicon. The axicon microoptics (i.e.,<1 mm in diameter) achieves a measured invariant resolution of ~ 8 µm across a 4 mm DOF. The measured DOF and resolutions were compared to theoretical results from the quasi-Bessel beam simulation using parameters of the fabricated axicon and the profile of the incident beam on the axicon. A fabricated gold coated mirror (size: 1.4mm by 2.1mm) attached to a custom 45-degree-wedged ferrule was located after the axicon to put the 4 mm DOF in the tubular sample. To secure the 4 mm imaging depth with

the spectral resolution given by the spectrometer and broadband source in the FD OCT, the mirror image is suppressed using a piezoelectric fiber stretcher in the reference arm. In conclusion, a sub millimeter catheter design is presented for high resolution OCT over long DOF demonstrating OCT images of tubular biological samples with 2.5 μm axial resolution and 8 μm lateral resolution over a 4 mm depth range.

7558-27, Poster Session

Design of small confocal endo-microscopic probe working under multiwavelength environment

Y. D. Kim, M. K. Ahn, D. G. Gweon, KAIST (Korea, Republic of)

Recently, confocal microscope has been used to get the biomedical imaging so they can diagnose diseases comparing normal cell image to abnormal image. confocal microscope has high resolving power and its beam scanning method provide outstanding environment for biomedical research area. confocal microscope is divided to two types, fluorescence and reflectance(there are many kind of confocal microscope, except this two). Fluorescence microscope uses fluophor died in various color. And reflectance microscope use reflectance of each material in the sample.

In biomedical imaging, In-vivo imaging is very important so various diseases are diagnosed prior to occurrence. Many of researches have been being conducted in the world wide. In fiber-confocal reflectance microscope research, they demonstrated that doctors can diagnose epithelium cancer by reflectance image of human cervical biopsy. Other researches demonstrate the diagnosis of cancer in human body, using two-photon image of NADH in human cell. But many of these researches are restricted in two constraints. One is size and the other is light wave. Fiber confocal reflectance microscope has high NA and its size is small, but is use only one light wave so researchers get only reflectance image. And outer kind of microscope use various kind of light wave so that can use fluorescence and reflectance image together, has large size. Many of these large size probes cannot reach inside of human body.

In this research, I recommend the confocal microscope endoscopic probe, that can be used as a probe at the end of a normal endoscope and confocal microscope to take both fluorescence and reflectance image.

7558-28, Poster Session

360° endoscopy using panomorph lens technology

S. Thibault, Univ. Laval (Canada); R. Denis, Univ. de Montréal (Canada); P. Roulet, ImmerVision (Canada)

Minimally invasive surgical procedures or examinations required more and more sophisticated devices to explore the interior of the patient's body.

The new generation of medical endoscopes is taking advantage of the recent progress on imaging sensors and optics. The modern endoscope benefits of sensor miniaturization to increase their resolution up to 1.3Megapixel (HD).

Even in such high resolution, the endoscopic vision stays very different than a human vision, especially regarding the field of view.

The limited field of view produces a poor visualisation for the clinician and increases endoscope manipulations and procedure time. These drawbacks drive the industries to develop endoscope with larger field of view.

Several optical systems have been developed, convex mirror, prisms or wide angle lens to meet large field of view requirement. However most of these optical systems suffer from low resolution or poor quality. A particular concern in the optical design of this type of wide angle imager is the uniformity of the image quality.

This paper will present innovative wide angle panomorph lens dedicated

Conference 7558: Endoscopic Microscopy V



to the endoscope and dedicated visualisation software. This lens is based on the human vision which increases the resolution in the field of view of interest to meet the image quality requirement specific to endoscopic applications. We present a miniature rugged panomorph lens suitable for medical endoscope.

We show how the wide angle field of view, augmented resolution, close focus and distortion free visualisation software can improve endoscopic procedures.

7558-29, Poster Session

Endoscopic OCT for early lung cancer detection and diagnosis

A. Lee, The BC Cancer Research Ctr. (Canada) and Univ. of British Columbia (Canada); A. Mariampillai, B. Standish, Univ. of Toronto (Canada); A. Mauro, M. Harduar, Ryerson Univ. (Canada); M. Cardeno, P. Lane, The BC Cancer Research Ctr. (Canada); A. Vitkin, Univ. of Toronto (Canada); V. Yang, Ryerson Univ. (Canada); C. MacAulay, S. Lam, The BC Cancer Research Ctr. (Canada)

As lung cancer continues to be the leading cause of cancer death worldwide, there is considerable impetus to develop tools for early lung cancer detection and diagnosis. Coupled with a wide-area screening method such as autofluorescence bronchoscopy, Optical Coherence Tomography (OCT) is an ideal complementary technique to examine microscopic details of suspicious bronchial lesions. Measurement of the thickness of the bronchial epithelium has previously shown to be able to identify normal tissue from dysplastic tissue and cancerous lesions. Here, we present the development of a new OCT instrument for in vivo lung use.

The endoscopic fiber optic OCT probe presented here is designed specifically for use down the instrument channel of a standard bronchoscope. Using a swept-source laser, the side-looking circumferentially scanning probe with pullback capability is able to image large sections of the bronchial tree. Doppler functionality and speckle variance imaging are being implemented to explore their utility in imaging pulmonary vasculature. We are employing this OCT system in clinical trials to assess its ability to assist in lung cancer detection and diagnosis.



Saturday-Sunday 23-24 January 2010 • Part of Proceedings of SPIE Vol. 7559

Optical Fibers and Sensors for Medical Diagnostics and Treatment Applications X

7559-01, Session

Research on the FBG's high-temperature sustainability influenced by the doping process

F. Tu, Yangtze Optical Fibre and Cable Co., Ltd. (China)

The numerous potential applications of UV-induced fiber Bragg gratings (FBGs) in fiber optic sensing and telecommunications have generated a significant interest in this field in recent years. However, two major factors-the photosensitivity of the fiber in which the grating is written and the thermal stability of the grating-are of prime importance in terms of choosing the most appropriate fiber to use and of the long-term functionality of the grating over a wide range of temperatures. B/Ge-codoped fiber has been reported to give a much higher level of photosensitivity when compared with other fibers, and the technique of hydrogen loading can further enhance this property of the fiber, but the gratings written in these fibers, with or without pre-treatment or post-treatment, are reported to have a much poorer high-temperature stability.

Based on the plasma chemical vapor deposition (PCVD) process, the high Ge (Germanium) and Ge/B (Germanium/Boron) co-doped photosensitive fiber were developed. The photosensitive fiber with different doping composition and doping concentration have been studied. Based on the experimental results obtained from studies of several kinds of photosensitive fiber on both the photosensitivity and the temperature sustainability of the FBGs written into them, the so-called cation hopping model has been used to explain, in which the size of the cation responsible for the temperature sustainability.

7559-02, Session

Efficiency of integrated waveguide probes in the detection of fluorescence and backscattered light

N. Ismail, F. Sun, F. Civitci, K. Wörhoff, R. M. de Ridder, M. Pollnau, A. Driessen, Univ. of Twente (Netherlands)

Integrated optical probes for detecting backscattered light in, e.g., Raman spectroscopy show desirable characteristics compared to conventional optical fiber probes, although the latter ones may have better collection efficiency in many cases. Major advantages of integrated probes include reduced size; reduced background noise due to scattering in the probe because of reduced propagation length; potential for monolithic integration with filters and spectrometers; very small collection volume, providing high spatial resolution; and polarization maintenance. We demonstrate that in a practically relevant case where scattered light needs to be collected from a thin layer close to the probe surface, integrated probes can have better collection efficiency than fiber probes do.

We modeled a multimode integrated waveguide probe by adapting an analytical model that had been developed by Schwab et al. (1984) for fiber probes. The model was extended in order to account for arbitrary waveguide geometries and a low number of discrete waveguide modes compared to the quasi-continuum of modes in a typical multimode fiber. Using this model we compared the collection efficiencies of integrated and fiber probes for a thin scattering sample. We found that the integrated probe has a higher collection efficiency for scattering layer thickness and probe-to-layer distance both smaller than ~100 m.

Multi-waveguide integrated probes having rectangular waveguide cross-sections were fabricated in silicon oxynitride. For experimental convenience we measured fluorescence from a ruby rod that was excited through one probe channel, while fluorescent light was collected by the

other probe channels. The measurements confirmed the validity of our probe model.

7559-03, Session

Transmission properties of dielectriccoated hollow optical fibers based on silvercladding-stainless pipe

K. Iwai, Sendai National College of Technology (Japan); A. Hongo, Hitachi Cable, Ltd. (Japan); H. Takaku, M. Miyagi, Sendai National College of Technology (Japan); J. Ishiyama, Miyagi National College of Technology (Japan); Y. Shi, Fudan University (China); Y. Matsuura, Tohoku University (Japan)

Silver-cladding-stainless pipe is used as the supporting tube for the infrared hollow fiber to obtain high durability and strong mechanical strength. For the dielectric inner-coating layer, cyclic olefin polymer(COP) and silver iodide (Agl) are used to lower the transmission loss. The COP layer is formed by using liquid-phase coating method as it is done before. For the Agl layer, liquid-filling technique is developed to reduce the waste liquid of iodine solution. Rigid hollow fiber with optimized COP or Agl inner film thicknesses for CO2 laser light were fabricated and reasonable transmission losses for an output tip was demonstrated.

7559-04, Session

Time-resolved all fiber fluorescence spectroscopy system

A. Chen, F. Vanholsbeeck, The Univ. of Auckland (New Zealand); D. Tai, Institute of Bioengineering and Nanotechnology (Singapore); M. Svrcek, Brno Univ. of Technology (Czech Republic); B. Smaill, The Univ. of Auckland (New Zealand)

Fluorescence imaging is widely used in biomedical research to probe biological structure and function at the cellular and subcellular levels. For example, intracellular calcium ion concentration can be recorded with calcium indicators such as Indo-1, while membrane potential-sensitive dyes such as di-4-ANEPPS are employed to measure electrical activity in the heart and other excitable tissues. The fluorometric systems used within this context generally incorporate relatively complex free space optical assemblies. In this paper, we describe a simple fiber optic fluorescence spectrometry system with a wide variety of biomedical applications. This low-cost, all-fiber system is portable, robust and has the capacity to acquire fluorescence spectra at rates up to 1 kHz. We demonstrate the capabilities of the system by presenting experimental measurements of action potentials in the di-4-ANEPPS stained rat heart. Di-4-ANEPPS is a ratiometric dye and conventional method of obtaining the short and long wavelength signals is to use a dichroic mirror for spectral separation. Here we have the advantage of direct spectral decomposition which enables us to choose any spectral windows for recovering the action potential signals. By optimizing the boundaries of both the short and long wavelength windows the signal to noise ratio (SNR) of the recovered action potential can be improved. Moreover we perform a thorough spectral analysis of the motion artifact to show how it can be more effectively removed even in measurements taken without any form of motion suppression in the heart.

TEL: +1 360 676 3290 · +1 888 504 8171 · customerservice@spie.org



7559-24, Session

Progress toward inexpensive endoscopic high-resolution common-path OCT

J. U. Kang, The Johns Hopkins Univ. (United States)

A single-arm interferometer based optical coherence tomography (OCT) system known as common-path OCT (CPOCT) has been making rapid progress toward being a practical system. The common path makes the system design very simple, cost-effective and allows freedom to use any arbitrary length for the probe arm. Such system can image and identify tissue boundaries accurately and in real time, together with their respective distances from a surgical tool. In addition, it can provide information about the tissue distortion and optical spectral absorption changes due to the physiological changes in the tissue. Due to the simplicity and robustness of the CPOCT, various simple fiber optic probes can be easily integrated into small delicate surgical tools. The result of the marriage of CPOCT probes and functional tool tips is a "smart tool" that can enable surface topology, motion limiting and compensation for safer and enhanced surgical performance of the specific tool's function. Challenges and recent progress toward making CPOCT a practical and cost effective 3-D imaging and sensing system will be discussed in detail.

7559-05, Session

Hollow waveguide for urology treatment

H. Jelinková, M. Nemec, P. Koranda, Czech Technical Univ. in Prague (Czech Republic); J. Pokorny, O. Kohler, Central Military Hospital (Czech Republic); M. Miyagi, K. Iwai, Sendai National College of Technology (Japan); Y. Matsuura, Tohoku Univ. (Japan)

Mid-infrared laser radiation has a great potential in medical treatment. In urology the laser radiation from 2 to 3 um can be utilized for laser assisted lithotripsy or soft tissue incision. The main drawback is the laser radiation delivery to the place of interaction. For this purpose the proper hollow waveguides are one of the best choice. In our experimental study we have compared the effects of Ho:YAG (wavelength 2100 nm) and Er:YAG (wavelength 2940 nm) laser radiation both on human urinary stones (or compressed plaster samples which serve as a model) fragmentation and soft ureter tissue incision in vitro. For the effective Er:YAG laser radiation delivery we have utilized Cyclic Olefin Polymer - coated silver (COP/Ag) hollow glass waveguides with inner and outer diameters 700 and 850 um, respectively. The measured transmission for the wavelength 2940 nm was 80% for 1 m long waveguide. For urology treatment the hollow waveguide with the 10 cm length was used. To prevent any liquid to diminish and stop the transmission, the waveguide termination was utilized.

From our experiments it follows that Er:YAG laser radiation delivered by hollow waveguide is comparable with Ho:YAG laser (delivered by special fiber) in case of human urinary stones and compressed plaster samples perforation and fragmentation. In case of soft ureter tissue incision the system of Er:YAG laser is more effective than Ho:YAG laser. The sealed waveguide remain without damage through whole experiment.

7559-06, Session

A Raman cell based on hollow optical fibers for breath analysis

Y. Okita, T. Katagiri, Y. Matsuura, Tohoku Univ. (Japan)

A compact Raman cell based on the hollow optical fiber for high sensitivity breath analysis is reported. A silver-coated polycarbonate hollow optical fiber is used for both a gas cell and a Stokes collector. An excitation laser light at 780 nm is launched into the cell filled with analytes and the Stokes light collected in the cell is detected by the multichannel Raman spectrometer. A high-reflectivity mirror is placed

at the distal end of the cell to increase the effective interaction length between the excitation laser light and the analytes and reflect forward scattered Stokes light back into the cell. Although the cell is coiled into a multiple loop with a 3.3 cm radius for miniaturization, the Raman spectrum of major breath molecule (oxygen, carbon dioxide) is obtained without a serious decrease of the signal-to-noise ratio.

7559-07, Session

Low-temperature and UV curable solgel coatings for long lasting optical fiber biosensors

D. Otaduy, Tekniker (Spain); G. Beobide, E. Gorritxategi, R. Prado, A. Marcaide, Fundacion Tekniker (Spain)

The use of optical fibers as sensing element is increasing in clinical, pharmaceutical and industrial applications. Excellent light delivery, long interaction length, low cost and ability not only to excite the target molecules but also to capture the emitted light from the targets are the hallmarks of optical fiber as biosensors. In biosensors based on fiber optics the interaction with the analyte can occur within an element of the optical fiber. One of the techniques for this kind of biosensors is to remove the fiber optic cladding and substitute it for biological coatings that will interact with the parameter to sensorize. The deposition of these layers can be made by sol-gel technology.

The sol-gel technology is being increasingly used mainly due to the high versatility to tailor their optical features. Incorporation of suitable chemical and biochemical sensing agents have allowed determining pH, gases, and biochemical species, among others. Nonetheless, the relatively high processing temperatures and short lifetime values mean severe drawbacks for a successful exploitation of sol-gel based coated optical fibres. With regard to the latter, herein we present the design, preparation and characterization of novel solgel coated optical fibres. Low temperature and UV curable coating formulations were optimized to achieve a good adhesion and optical performance. The UV photopolymerizable formulation was comprised by methacryloxypropyltrimethoxysilane, TEOS and an initiator. While the thermoset coating was prepared by using 3-aminopropyltrimethoxysilane, glycidoxypropyltrimethoxysilane, and TEOS as main reagents. Low temperature and UV curable sol-gel coated fibres were analysed by FTIR, SEM and optical characterization.

7559-13, Session

Influence of polarization-gated probe geometry and scattering properties on penetration depth distributions in turbid media: a Monte Carlo and experimental analysis

A. J. Gomes, V. Turzhitzsky, S. Ruderman, J. Rogers, V. Backman, Northwestern Univ. (United States)

Biological tissue is organized into layers with different physiological and optical properties. Targeting the appropriate layer is crucial to accurately detect certain diseases. For example, precancerous changes are usually most apparent in the epithelium. Polarization-gated spectroscopy is one method to depth-selectively assess tissue optical properties. We have previously used Monte Carlo simulations to qualitatively describe how the penetration depth of polarization-gated spectroscopy depends on probe configuration parameters such as the illumination and collection geometry. We have extended this analysis and now present empirical equations based on Monte Carlo simulations that predict the average penetration depth for a given probe geometry and scattering medium. Inputs to the equation include the illumination/collection radius, collection angle, separation distance between illumination and collection areas, scattering mean free path, and anisotropy factor. In addition, using the equation, we have calculated the sensitivity of the average penetration



depth to the scattering properties of the medium. We have found that some geometries, such as one with a high collection angle, are relatively insensitive to changes in scattering properties and would therefore be ideal probe designs for absorption spectroscopy. This study will enable researchers to design fiber-optic probes with optimal penetration depth characteristics for their application of interest. Results comparing tissue phantom data and the Monte Carlo analysis will be discussed.

7559-34, Session

Skewmodes in specialty fibers with stepindex profiles

K. Klein, C. P. Gonschior, Fachhochschule Giessen-Friedberg (Germany); G. Hillrichs, Hochschule Merseburg (Germany); H. Poisel, M. Bloos, Univ. of Applied Sciences Nürnberg (Germany)

For medical, analytical and industrial applications, step-index specialty fibers are mainly used in combination with laser or LED-systems, from 200 nm (UV) up to 2300 nm (NIR). Depending on the application, different fibers are in operation; in addition, the light-transportation related to the input conditions of light beam has to be specific, too.

In step-index multimode-fibers, controlled excitation conditions are essential to achieve optimized transmission properties and control the output beam profile; especially with laser-light, this is important. Fiber properties are normally specified for meridional ray propagation, as proposed with the inverse far-field and near-field methods. In addition to these meridional rays (modes), skew modes can be selectively excited in step-index fibers, too. Mostly unknown, high-order skew rays can propagate with high stability and low losses, especially with excitation angles bigger in comparison to the numerical aperture of the fiber. Therefore, the propagation of skew rays has to be taken into account for application-dependent optimization of fiber-optic systems with large core

In this paper skew ray excitation and propagation will be studied in more detail, within the step-index fibers with different numerical aperture, cladding materials including currently developed microstructured fibers with high numerical aperture in the visible and near infrared wavelength region. The bending properties and mode-conversion on the near-field and far-field intensity distribution (output beam profile) are discussed.

In addition to the usage for more detailed characterization of specialty fibers, skew rays/modes are interesting for new sensor applications, too. For example, ATR-methods can be significantly improved with standard light-sources. First results of skew mode excitation using a supercontinuum light-source are very promising, too; however, the detection scheme is more complex.

7559-11, Session

Homogeneous catheter for esophagus highresolution manometry using fiber Bragg gratings

S. Voigt, Technische Univ. Chemnitz (Germany); M. Becker, M. Rothhardt, IPHT Jena (Germany); T. Lüpke, C. Thieroff, Kunststoff-Zentrum in Leipzig gGmbH (Germany); J. Mehner, Technische Univ. Chemnitz (Germany)

High resolution manometry for the in-vivo diagnosis of swallowing disorders is beginning to move from research into clinical practice. Hence there is a need for easy to use and patient friendly measurement methods. Besides established methods like solid state sensor manometry and perfusion manometry the use of optical fiber with fiber bragg gratings (FBGs) has gained interest in the medical field.

Working Principle: A wideband light source is selectively reflected by FBGs of chirped reflection wavelength. In case of the presented pressure sensor catheter the FBGs are sensitive to pressure and the characteristic wavelengths can be allocated to the place of applied pressure.

The advantages are the absence of electrical components, the feasibility of long time measurements, the non-bulky interrogation systems which allows the manometry in rather natural situations and the homogeneous surface which enables easy cleaning and disinfection.

The catheter presented consists of a 80 µm single mode optical fiber containing 30 chirped FBGs [5] with a spacing of 10 mm covered with a two layer thermoplastic silicone cover fabricated using a two step extrusion process. Different catheter diameters varying from 3 to 5 mm have been fabricated.

Experiments show detectable forces in the range of 10 mN which corresponds to an applied pressure of 1mbar at a catheter section of 10

This proved principle is promising to be applied beyond esophagus manometry such as the pancreas sphincter due to the fact that the sensor catheter can be moved trough the working channel of endoscopes.

7559-12, Session

Transverse mode analysis of optofluidic intracavity spectroscopy of canine hemangiosarcoma

W. Wang, D. H. Thamm, Colorado State Univ. (United States); D. W. Kisker, Eoptra LLC (United States); K. L. Lear, Colorado State Univ. (United States)

The label-free technique of optofluidic intracavity spectroscopy (OFIS) uses the optical transmission spectrum of a cellular body in a microfluidic optical resonator to distinguish cancerous and non-cancerous cells. Cancerous cells produce multimode transmission spectra while noncancerous cells create only weak transmission peaks between bare

Based on their distinctive characteristic transmission spectra, canine hemangiosarcoma (HSA) cancer cells and normal peripheral blood mononuclear cells (PBMCs) have been differentiated by the OFIS technique. A single characteristic parameter indicative of strong multitransverse-mode resonances was determined for each individual cell by forming a linear combination of the mean and standard deviation of the transmission spectra over one free spectral range excluding the residual peaks due to the passive Fabry-Pérot cavity without cells. The difference in the characteristic parameters of HSA cells and PBMCs was highly statistically significant with a p-value as low as 10^-6. A theoretical receiver operating characteristic (ROC) curve constructed from t-distributions fit to the HSA and PBMC transmission parameters showed that 95% sensitivity and 98% specificity can be achieved simultaneously, indicating potential clinical utility. This preliminary result indicates that such a diagnostic cancer test based on blood samples could lead to earlier detection and treatment, and provide dog owners with more certain prognosis at reduced cost when facing decisions on treatment of suspected HSA.

A cell lens model that combines Gaussian beam propagation method and cell lens assumption was employed to further understand and explain the transverse mode pattern in the transmission spectra of HSA cells.

7559-14, Session

Demonstration of the immunoassay using local evanescent array coupled biosensor

R. Yan, L. C. Kingry, R. A. Slayden, K. L. Lear, Colorado State Univ. (United States)

A Label-free optical waveguide immunosensor is investigated both theoretically and experimentally. The local evanescent array coupled (LEAC) biosensor is based on a local evanescent field shift mechanism, which differs from those of other evanescent waveguide sensors. Antigens specifically bound to the immobilized antibodies on the

TEL: +1 360 676 3290 · +1 888 504 8171 · customerservice@spie.org



waveguide surface increase the refractive index of the upper cladding of the waveguide, and hence shift the evanescent field distribution up. This local detection mechanism grants the LEAC sensor multi-analyte ability in a single optical path. Compared to traditional biosensors, including surface plasmon resonance and ring resonance biosensors, the non-resonant and temperature/wavelength insensitive properties of the LEAC biosensor relax its requirement on the optical source. It requires no off-chip instruments such as spectrometers, making it a chip-scale biosensing platform. The on-chip detection is accomplished by integrating buried polysilicon detector arrays into silicon nitride waveguide in a commercial complementary metal oxide semiconductor (CMOS) process. Bovine serum albumin (BSA) layers and IgG antibodyantigen interaction were used to test the LEAC biosensors. Beam propagation simulation method and chips with different geometric parameters were used to study the relationship between the sensitivity and structure of LEAC biosensor.

7559-27, Session

Dissociation constant measurement using combination tapered fiber optic biosensor (CTFOB) dip-probes

C. Wang, R. Kapoor, The Univ. of Alabama at Birmingham (United States)

We are proposing a new method to measure dissociation constant (k $_{\rm D}$) of an antigen and antibody interaction. Dissociation constant (k $_{\rm D}$) is defined as the ratio of dissociation rate constant (k $_{\rm d}$) and association rate constant (k $_{\rm a}$).

 $k_D = k_d/k_a$

The method was demonstrated by measuring dissociation constant (k D) of human Interleukin 6 (IL-6) and anti-IL-6 antibodies interaction. The measurements were done by using combination tapered fiber-optic biosensor (CTFOB) dip-probe. A sandwich immunoassay using two monoclonal antibodies, which recognize different epitopes on the antigen (IL-6), was used. The capture anti-IL-6 antibodies were first immobilized on the probe surface. The probes were subsequently incubated in the different concentrations of IL-6 prepared in 1mg/ml of egg albumin(EA) buffer solution. Finally these probes were submerged in detection anti-IL-6 antibodies labeled with Alex488 dye. Signal was recorded with the help of a CCD based fiber optic spectrometer (Ocean Optics, Inc.). A 476 nm diode laser was use as an excitation source. The background signal for each probes were recorded before incubated into labeled detection antibodies. The real signals were extracted by least square fitting method. Two kinds of negative control probes were used to assure that the signal is specifically from IL-6. The measured value of dissociation constant for IL-6 and capture anti-IL-6 (clone MQ2-13A5) antibodies at room temperature is $k_D = 317 \pm ,76 \text{ pM}.$

7559-10, Session

Experimental study on the durability of dielectric-coated silver hollow fibers for corrosive gas sensing

W. Shao, Q. Chen, B. Sun, X. Wu, Y. Shi, Fudan Univ. (China)

The possibility of spectroscopic gas sensing using infrared hollow fiber as the absorption cell was demonstrated. By optimizing the coating dielectric material and fiber structure parameters, hollow fiber obtains low-loss property at the absorption wavelength band of various gases. Using low-loss infrared hollow fiber as the gas absorption cell has the potential advantages of miniaturization, high sensitivity, small gas sample volume, and thus rapid response. Several kinds of dielectric-coated silver hollow fiber were fabricated and tested for corrosive gas sensing. The durability of the fibers, with inner coating film of silver and Agl, cyclic olefin polymer, SiO2, polycarbonate, as well as Ag tube, glass capillary were experimentally discussed. We used NH3, HCI, SO2, and

ammonia, hydrochloric acid as the corrosive gas or liquid. By flowing the corrosive material through the hollow fiber, durability of the fiber on these corrosives were measured. Experimental results showed that Agl/Ag and COP/Ag hollow fiber have high durability. Finally improved fabrication technique for high performance and durability Agl/Ag and COP/Ag hollow fibers were proposed and discussed.

7559-26, Session

Analysis of some substantial collimating lens functions in fiber optic confocal microscopy

D. Kim, I. K. Ilev, U.S. Food and Drug Administration (United States)

Fiber-optic confocal microscope can be designed in various configurations. It is a common practice to use two separate lenses, one for collimation and the other for focusing due to its flexibility in choosing two different types of lenses. Although critical for its overall performance, substantial functions of the collimating lens in this two-lens configuration have not been investigated extensively. The numerical aperture (NA) of the collimating lens and the degree of collimation determines the effective NA of the focusing lens which affects the confocal microscope imaging resolution.

In this study, we experimentally and theoretically investigated key functions of the collimating lens in fiber-optic confocal microscope designs. We have tested a fiber-optic confocal microscope approach using a high-NA (0.28) single-mode optical fiber in comparison with a conventional single-mode fiber (NA = 0.15) confocal configuration. The usage of high-NA fiber enabled us to utilize high-magnification lens for collimation, thus high-confocality and coupling efficiency can be achieved. Experimentally measured axial resolution was 6.24 µm when high-NA fiber and 10× and 60× objective lens was used for collimation and focusing, respectively. The obtained value is close to the theoretical limit. In addition, a ray-tracing simulation was used to theoretically demonstrate the relation between the NA of optical fiber and collimating lens as well as to calculate the effective NA of focusing lens depending on the degree of collimation. The obtained results confirm the strong dependence of the overall resolution of the confocal microscope system on the collimation of the input laser beam.

7559-28, Session

Quantitative estimation of IL-6 in serum/ plasma samples using a papid and costeffective fiber optic dip-probe

C. Wang, U. Manne, V. V. B. Reddy, R. Kapoor, The Univ. of Alabama at Birmingham (United States)

We could successfully detect presence of IL-6 in two serum samples, non-neoplastic autoimmune patient (lupus) sample (#1024) and lymphoma patient sample (#1027), using combination tapered fiber-optic biosensor (CTFOB) dip-probe. Sandwich assay was used for detection. Capture antibodies of IL-6 were immobilized on the probe surface while detection antibodies of IL-6 were labeled with Alexa 488 dye. The probes with immobilized capture antibodies were immersed in serum samples for one hour. After washing the probes were immersed in detection antibodies solution for another hour. A fluorescence signal, proportional to immobilized IL-6 on the probe surface, was generated by evanescent wave excitation technique. Signal was recorded by a CCD based spectrometer.

We also estimated concentration of IL-6 in both of these serum samples. Quantitative estimation needs a calibration curve. The calibration curve was obtained by recording signal from various known concentrations (5 pM - 500 pM) of IL-6 using identical fiber-optic dip-probes. Commercial IL-6 (Biolegend Inc.) was used for calibration curve.

The estimated amount of IL-6 in sample # 1024 was 4.8 ± 0.5 pM and in sample # 1027 was 1.8 ± 0.1 pM. Relative concentration of IL-6 in these



two serum samples were also measured using Luminex assay detections system. It was found that the concentration of IL-6 in sample # 1024 was about seven times more than the IL-6 concentration in sample # 1027. Both the results indicate that lupus serum sample contains higher concentration of IL-6 than lymphoma patient sample. It demonstrates that CTFOB dip-probe is capable of quantitative estimation of proteins in serum/plasma samples with high specificity.

7559-29, Session

New conducting telluride glasses for electrophoretic collection and IR sensing of proteins and viruses.

P. Lucas, Z. Yang, A. Wilhelm, M. Riley, K. Reynolds, The Univ. of Arizona (United States)

A new family of tellurium based glasses has been developed for use in electrophoretic IR sensors. These glasses combine high conductivity and an outstanding IR window down to more than 20 microns. ATR crystals built from these glasses have been simultaneously used as on optical element for IR sensing in the signature region of bio-molecule as well as an electrode for electrophoretic collection of charged particles such as proteins and viruses. These new glasses are based on a Terich composition from the Ge-As-Te system. The resulting glasses are good glassformer and can be cast into large rods for fabrication of ATR crystals. The high Te content provides an outstanding optical window towards long wavelength which includes selective protein vibrational modes. The resulting glass also has sufficiently high conductivity for application of a potential in an electrophoretic set up. The complete migration of protein solutions within a short time scale has been demonstrated. This aqueous detection method provides enough selectivity to differentiate between different protein molecules and

7559-30, Session

Optical microfrabrication of tapers in low-loss chalcogenide fibers for fiber evanescent-wave spectroscopy.

P. Lucas, Z. Yang, The Univ. of Arizona (United States); E. Lepine, The Univ. of Arizona (United States) and Univ. de Rennes 1 (France); J. Troles, X. Zhang, B. Bureau, Y. Gueguen, J. Sangleboeuf, Univ. de Rennes 1 (France)

A novel approach for the development of accurate tapers in chalcogenide glasses has been demonstrated. This method builds on the photofluidity effect which occurs in chalcogenide glasses under sub-bandgap irradiation. The glass can be fluidified at room temperature through a dynamic photoexcitation mechanism that is shown to be athermal. Careful plastic deformation of the glass can then be performed in order to produce fiber tapers. Fiber tapering of Ge-Se glass fibers irradiated with a Ti-sapphire laser has been demonstrated. Low-loss chalcogenide fibers have shown excellent potentials for remote IR spectroscopy through fiber evanescent wave collection due to their wide transparency in the infrared region which encompass most molecular vibrational modes. The fiber diameter reduction along the taper can increases the detection sensitivity by orders of magnitude. The use of optically fabricated tapers in a fiber evanescent wave spectroscopy set up is demonstrated with several target molecules.

7559-16, Session

Thin film thickness measurement change using dual LEDs and reflectometric interference spectroscopy modeling in a biosensor

Y. Ling, N. Wu, W. Wang, L. Farris, B. Kim, X. Wang, M. McDonald, Univ. of Massachusetts Lowell (United States)

The thin film thickness measurement is widely used in biosensors. But a costly effectively handheld device for thin film measurement is not yet available, because most of the previous researches use a spectrometer which is usually big and expensive. With the development of electronics and optics, especially the LED technique, this kind of small device has become feasible. In previous work, we employ dual LEDs with different wavelengths and a photodetector to build up the sensor measuring the thickness change of a transparent thin film. The thickness change is caused by a specific binding of ProteinG on the PMMA (Poly(methyl methacrylate)) layer coated on the silicon chip. However how much the thickness change was unknown.

In this paper, a mathematic model of reflectometric interference spectroscopy (RIfS) around the wavelengths of the dual LEDs is built, and the thickness change is derived from the experiment data of the reflected light intensity from the dual LEDs acquired by the photodetector. The derived results are compared with reference values ranging from 1 to 100nm. Although the peak wavelengths of the LEDs are shifted and the LEDs' wavelengths are not ideal ones, the comparison shows that the dual LEDs method and the model predict fairly good thickness change. By this method with the use of LEDs and a photodetector, the handheld device for transparent thin film measurement may become practical.

7559-18, Session

High-NA HPCS optical fibers for medical diagnosis and treatment

B. J. Skutnik, CeramOptec Industries, Inc. (United States)

Cladding technology has advanced greatly since the earliest hard plastic clad silica (HPCS) fibers were first introduced. New fibers have been drawn and characterized for their mechanical and spectral properties. Dynamic strength measurements as well as bending strength and static fatigue results are being made and will be presented. Pure silica cores are clad with lower index materials to provide optical fibers with numerical apertures (NA) of greater than 0.50. In contrast to older fibers with high NA, these fibers are as robust as normal NA HPCS, and have good spectral behavior. Standard 200 µm core fibers are used primarily to carry out the testing. Having robust lower cost optical fibers with very large NA, will permit better fiber optic diagnostics in many areas as well as provide enhanced uses for surgical applications. Having pure silica cores will mean less concerns about radiation damage. In the specialty field of fiber lasers, which show great promise for surgical applications, there is great possiblity of using this technology for high power fiber lasers, including increasing the power modes that can be safely contained in the pump lasing volume.

7559-19, Session

An effective design for the distal end of the fiber optic probes: a design concept with a generalized equation

S. Oh, Miami Children's Hospital (United States) and Florida International Univ. (United States)

Uses of optical spectroscopy with a fiber-optic probe are increasing exponentially in the research and clinical fields for various applications, e.g. tumor and cancer tissue detection. The fiber-optic probe design

167

Return to Contents TEL: +1 360 676 3290 · +1 888 504 8171 · customerservice@spie.org



is important to maximize the detection efficiency and to optimize the source-detector distance for the investigation depth of the optical spectroscopy system. Therefore, selection of the size, number of the fibers and geometrical configuration of optical fibers at the distal end of the fiber-optic probe is crucial to the probe design. This study proposes a technique for an effective design of the fiber-optic probe, specifically for the distal end of the probe that comes in contact with the target sample.

This technique encompasses optimized geometrical design concepts for the distal end of the fiber-optic probes as well as the general equation for both the size and the position of the optical fibers, given the distance from the center of the probe. The geometrical design concepts include:

1) a symmetric and concentric configuration; to evenly deliver the source light to the target sample, and 2) maintaining the optimized distance between the source and the detection fibers; to investigate the target tissue at a specific depth. Based on these concepts a general equation is derived for the size and the geometrical position of the optical fibers.

By applying these design concepts and the generalized equation, calculation for the size of the optical fiber and determine the geometrical configuration can be conveniently performed, and various probe designs are illustrated in the result section. Hence, this technique for designing an optical probe is useful and versatile. In addition, it is applicable to any type of fiber optic probe design.

7559-36, Session

Fabrication of Low Loss Alumina (Al2O3) Waveguides for Near-UV Biosensing Applications

M. M. Aslan, TUBITAK MAM Research Ctr. (Turkey); C. L. Byard, N. A. Webster, R. S. Wiederkehr, S. B. Mendes, Univ. of Louisville (United States)

An optical biosensor usually consists of three components: bioreceptor (molecular specie or biological system), transducer, and electronic interface. The most vital region is the transducer's surface where the bioreceptor is formed. The biocompatible surface is usually flat and it is prepared to create a biologically selective surface to react to the targeted analyte. Adsorption and desorption of the target analyte by bioreceptors on transducer surface at interface of transducer and cover medium alters the effective refractive index of optically guided modes (Neff,TE and Neff.TM) as well as thickness of the biolayer (tb) (coupling element + bioreceptor + analyte). Detection of these changes is possible with an optical system. Even though basic principles or configurations of the optical systems can vary, all are based on generating evanescent field on the transducer surface inside the cover medium where biological activity happens [1]. Depending on the optical configuration and the layers of the transducer surface plasmon or waveguide modes can be exited. One of the most widely used transducers is an integrated optical waveguide (IOW).

In this study, we fabricate and characterize integrated optical waveguides (IOW) that is a one-layer transducer for near-UV applications. Fabrication steps of alumina waveguides include surface cleaning of sample slides, spin-coating of photoresist film, holographic exposure, photomask development, reactive ion-etching, and vacuum deposition of a transparent thin-film optical waveguide. The slides (75 mm x 25 mm x 1 mm) of fused silica (from Plan Optik) are cleaned, spin-coated by a 160-nm of a 1:1 solution of Shipley 1805 photoresist and J.T. Baker BTS-220 thinner. In order to create grating pattern in the photoresist film, the slides are exposed by a 325-nm laser light for 3 seconds using a holographic Lloyd's mirror setup. Development of gratings is performed in a 1:4 solution of Shipley 351 Microposit developer and DI water. An STS Multiplex Etcher deep reactive-ion etching (DRIE) system is used to transfer the grating photo-pattern to the silica substrates.

Alumina was chosen as the waveguide material because of its low propagation loss from near-UV to near-IR. The fused silica substrates are coated with an alumina thin film by using a Savannah-100 ALD vacuum deposition system from Cambridge NanoTech Inc. In order to form an alumina thin film, the ALD deposition process consists of alternating the injection into the vacuum reactor chamber of trimethylaluminium (TMA

from Sigma Aldrich) and highly purified DI water. The TMA precursor was introduced into the reactor chamber for 25 milliseconds, then the reactor chamber was purged with N2 gas for 8 seconds, which was followed by the introduction of the H2O precursor into the process chamber also for 25 milliseconds, and finally the chamber was purged again with N2 (20 sccm) for another 8 seconds. Those steps complete a full cycle that forms approximately one atomic layer on the substrate surface; by replicating the cycle described above at a precise number of times one can deposit a desired film thickness. Surface quality of the silica substrates and alumina films are measured by AFM. Average surface RMS value is 4 Å. More details on the fabrication steps can be found in the literature [2, 3].

Both the spectral transmittance envelope technique and the waveguide mode technique are employed to determine the refractive index, loss, and thickness of the waveguides. Figure 1 shows refractive index and propagation loss of the waveguide. Our characterization results indicate that low loss alumina waveguide was fabricated; the measured propagation loss is below 4 dB/cm down to a wavelength as short as 250 nm. The alumina waveguides developed in this work can be used as a high performance optical transducer for biosensing applications in the near UV.

7559-09, Session

FT-IR based loss-spectrum measuring system for infrared hollow waveguides

C. Yang, H. Hua, W. Tan, Y. Shi, Fudan Univ. (China); K. Iwai, M. Miyagi, Sendai National College of Technology (Japan)

A loss-spectrum measuring-system for hollow waveguides was established based on the Fourier Transform infrared Spectrometer (FTIR). In order to obtain better repeatability, we designed and fabricated two couplers for the system. One is a silver-coated hollow tube with the same inner diameter as the measured hollow waveguide. The other is a silver-coated tapered coupler whose inner diameter of the output end is the same as the measured hollow waveguide. Characteristics of the measuring system were discussed theoretically and experimentally when using the two couplers. Several kinds of hollow waveguides were measured and the properties of the loss spectrum were discussed. The measured loss property showed that loss property depends on the output divergence angle of the coupler. Tapered coupler has a much larger output divergence than that of the hollow tube. Both of the couplers attains stable coupling with the hollow waveguides. Loss spectra were successfully measured for hollow waveguides with the length ranging from several centimeters to 3 meters. The possibility for gas sensing by using the system and hollow waveguides as the gas absorption cell were also demonstrated.

7559-21, Session

High-resolution SPR fiber sensing platform for in situ characterization of the deposition of nanoscale thickness polymer films

Y. Y. Shevchenko, M. Dakka, N. U. Ahamad, G. Galway, A. Ianoul, J. Albert, Carleton Univ. (Canada)

Surface plasmon resonance is recognized as a major sensing mechanisms for chemical analysis and characterization of biomolecular interactions1. The currently available Surface Plasmon Resonance (SPR) sensors based on either a prism configuration or a fiber optic platform suffer from temperature instabilities as well as from poor resolution resulting from wide resonances.

The SPR sensor presented in this study utilizes a single mode fiber with a Tilted Fiber Bragg Grating (TFBG) in its core and a gold film on the surface of the unmodified cladding2. The TFBG provides the sensor with an internal reference mechanism by means of a back-reflected core mode, which eliminates the temperature cross-sensitivity3 In addition the sensor is very compact, easy to manufacture and to operate.



The sensor has a measured bulk chemical sensitivity of 454 nm/r.i.u.. The sensor's performance was optimized for the best thickness of the gold layer and by using properly oriented linearly polarized light. For high resolution measurements, a methodology was developed to use individual cladding mode resonance amplitudes instead of wavelengths to infer SPR wavelength shifts at the picometer level. The sensor was applied to detect the consecutive adsorption of 30 polyelectrolyte monolayers, each 0.55 nm thick. Results indicate that sub-nm thickness changes can be detected with high repeatability using the amplitude transfer method. The SPR data was complemented by Atomic Force Microscopy (AFM) and by a model of the SPR coupling in order to evaluate the thickness and refractive index of the deposited material.

- [1] Homola J. 2003. Present and Future of Surface Plasmon Resonance Biosensors. Analytical. Bioanl. Chem., Vol. 377, no. 3, pp. 528-39.
- [2] Shevchenko Y.Y., and Albert J. 2007. Plasmon Resonances in Gold-Coated Tilted Fiber Bragg Gratings. Optics Letters, Vol. 32, no. 3, pp. 211-213.
- [3] Chen C. and Albert J. 2006. Strain-optic coefficients of the individual cladding modes of a single mode fiber: theory and experiment. Electron. Lett. Vol. 43, pp.21-22.

7559-22, Session

Accurate in vivo NIR measurement of muscle SO2 through fat

C. Jin, F. Zou, B. Peshlov, G. Ellerby, P. Scott, B. Soller, Univ. of Massachusetts (United States)

Noninvasive near infrared (NIR) spectroscopic measurement of muscle oxygenation requires the penetration of light through overlying skin and fat layers. We have previously demonstrated a dual-light source design and orthogonalization algorithm that corrects for interference from skin absorption and fat scattering. To achieve accurate muscle oxygen saturation (SmO2) measurement, one must select the appropriate sourcedetector distance (SD) to completely penetrate the fat layer. Methods: Six healthy subjects were supine for 15min to normalize tissue oxygenation across the body. NIR spectra were collected from the muscles of the calf, shoulder, lower and upper thigh with long SD distances of 30mm, 35mm, 40mm and 45mm. Spectral preprocessing with the short SD (3mm) spectrum preceded SmO2 calculation with a Taylor series expansion method. Three-way ANOVA was used to compare SmO2 values over varying fat thickness, subjects and SD distances. Overlying fat layers varied in thickness from 4.9mm to 19.6mm across all subjects. Results: SmO2 measured at the four locations were comparable for each subject (p=0.133), regardless of fat thickness and SD distance. SmO2 (mean±std dev) measured at calf, shoulder, lower and upper thigh were 62±3%, 59±8%, 61±2%, 61±4% respectively for SD distance of 30mm. In these subjects no significant influence of SD was observed (p=0.948). Conclusions: The results indicate that for our sensor design a 30mm SD is sufficient to penetrate through a 19mm fat layer and that orthogonalization with short SD effectively removed spectral interference from fat to result in a reproducible determination of SmO2. This study is supported by NSBRI through NASA NCC 9-58.

7559-23, Session

Real-time association rate constant measurement using combination tapered fiber optic biosensor (CTFOB) dip-probes

B. Simmonds, C. Wang, R. Kapoor, The Univ. of Alabama at Birmingham (United States)

We successfully measured association rate constant ($\rm k$ _a) of BSA and anti-BSA antibodies. All the measurements were done in real time using combination tapered fiber-optic biosensor (CTFOB) dip-probe. "Direct method" was used for detection; goat anti-BSA "capture" antibodies

were immobilized on the probe surface while the antigen (BSA) was directly labeled with Alexa 488 dye. The probes were subsequently submerged in 3 nM Labeled BSA in EA (1 mg/ml). The fluorescence signal, proportional to immobilized anti-BSA on the probe surface, was generated by evanescent wave excitation technique. Signal was recorded with the help of a CCD based fiber optic spectrometer (Ocean Optics, Inc.). Diode laser was use as an excitation source.

The probes were individually mounted in the signal detection setup and real-time acquisition was initiated with the OOIBase32 software (Ocean Optics, Inc.). Ten seconds before each acquisition, the signal was zeroed and the excitation laser was turned on for the signal to stabilize before recording. The laser was turned off promptly after each acquisition to prevent bleaching effect. Signal was recorded every 5 minutes for 2 hours. The negative control probes were not immersed in labeled BSA rather; they were put into labeled EA, a non-specific protein. They showed no change in background signal greater than their own background, demonstrating the specificity of the CTFOB. The measured value of association rate constant for BSA and anti-BSA at room temperature is k $_{\rm a}$ = (9.40 \pm 0.01)×10 $^{\rm 4}$ M $^{\rm -1}{\rm s}^{\rm -1}$.

7559-35, Session

Thermal imaging bundles for medical applications

I. Gannot, Tel Aviv Univ. (Israel); J. Harrington, C. M. Bledt, N. Syzonenko, Rutgers, The State Univ. of New Jersey (United States); U. Gal, M. Tepper, M. Ben-David, Tel Aviv Univ. (Israel)

Thermal imaging became an important tool for diagnostic medical imaging. This is due to the major improvement of thermal cameras from the point of view of temperature and spatial resolution, Real time capabilities and of course the size and the cost which are very much reduced.

We developed a thermal imaging bundle that can extend the potential of thermal imaging for within body cavities (ie. detection of tumors, vulnearble plaques). We developed also methods to make thermal imaging specific by adding nanoshells or rely on different absorption curves (i.e. oxy and de-oxy hemoglobin).

We will discuss in this presentation the waveguide fabrication processes, thermal and spatial resolution, transfer function and preliminary in vitro work applying the waveguides on tissue like phantoms.

7559-37. Session

Fiber-coupled organic plastic scintillator for on-line dose rate monitoring in 6 MV x-ray beam for external radiotherapy

L. R. Lindvold, Technical Univ. of Denmark (Denmark); A. R. Beierholm, C. E. Andersen, Risø National Lab. (Denmark)

Fiber-coupled organic plastic scintillators enable on-line dose rate monitoring in conjunction with pulsed radiation sources like linear medical accelerators (linacs). The accelerator, however, generates a significant amount of stray ionizing radiation. This radiation excites the long optical fiber (15-20 m), connecting the scintillator, typically with a diameter of 1 mm and 5 mm in length, with the optical detector circuit, causing parasitic luminescence in the optical fiber. In this paper we propose a method for circumventing this problem. The method is based on the use of an organic scintillator, 2-Naphthoic acid, doped in an optical polymer. The organic scintillator possesses a long luminescent lifetime (room temperature phosphorescence). The scintillator is molded onto the distal end of a polymer optical fiber. The luminescent signal from the scintillator is detected by a PMT in photon-counting mode.

The long lifetime of the scintillator signal facilitates a temporal gating of the dose rate signal with respect to the parasitic luminescence from the optical fiber. We will present data obtained using a solid water phantom irradiated with 6 MV X-rays from a medical linac at the Copenhagen



University Hospital. Also issues pertaining to the selection of proper matrix as well as phosphorescent dye will be presented in this paper.

7559-08, Session

Polymer-functionalized microspheres for immunosensing applications

S. Soria, F. Baldini, S. Berneschi, M. Brenci, F. Cosi, A. Giannetti, G. Nunzi conti, S. Pelli, G. C. Righini, IFAC-CNR Istituto di Fisica Applicata (Italy); B. Tiribilli, ISC-CNR, Istituto dei Sistemi Complessi (Italy)

Homogeneous polymeric thin layers have been used as functionalizing agents on silica microspherical resonators in view of the implementation of an immunosensor. A crucial step for producing reliable biosensors is the surface functionalization, or chemical modification of the transducer surface in order to bind the biological recognition element on it. This functional layer, however, has to be very thin, 10-100 nm and homogeneous, in order to preserve the high quality of the transducer and the interaction with the sensing layer and the whispering gallery modes.

Here we propose, characterise and compare polylactic-acid (a crystalline polymer) and Eudragit® L100 (anionic copolymer made of metacrylic acid and methyl methacrylate) as functionalising material alternative to 3-Aminopropyltrimethoxysilane. Polymer coated silica microspheres are proposed as an alternative to polymeric microresonators which have low Q factors in the infrared regime or possess high enough Q factors in the visible regime but need expensive and bulky experimental arrangements like optical tweezers. Further advantage of polymeric coatings is their extremely easy protocol of preparation.

It is shown that polymeric functionalization does not affect the high quality factor (Q greater than 107) of the silica microspheres, and that the Q factor is about 3x105 after chemical activation and covalent binding of immunogammaglobulin1. This functionalizing process of the microresonator constitutes a promising step towards the achievement of an ultra sensitive immunosensor.

[1] S. Soria, F. Baldini, S. Berneschi, F. Cosi, A. Giannetti, G. Nunzi Conti, S. Pelli, G.C. Righini, "High Q polymer coated microspheres for Immunosensing Applications" Opt. Express, accepted.

7559-17, Session

Characterization of UV single-mode and low-mode fibers

K. Klein, C. Gonschior, G. Hillrichs, T. Halim, Fachhochschule Giessen-Friedberg (Germany)

For medical and analytical applications, laser spectroscopy with optical silica-based fibers and diode-array spectrometer have been studied in the past.

However, there is an increasing demand for UV-singlemode fibers, too. Due to the small diameter, the coupling efficiency is extremely small, if broadband light-sources or LEDs with nearfield diameter in the order of approx. 500 µm are used. Therefore, UV-lasers are the requested candidates for high efficiencies. Although the power is in the order of several milliwatts, the intensities in the small fiber core are significantly high. Therefore, UV-damage plays a role, even in the wavelength region above 300 nm. The results of UV-damage will be discussed, especially in respect to applications requiring singlemode operation.

7559-20, Session

A multichannel fiber optic photoluminescence based biosensor

Z. Yi, Z. Zhong, K. Reardon, W. Wang, M. Katragadda, K. Lear, Colorado State Univ. (United States)

A multi-channel fiber optic photoluminescence based biosensor system was developed for real time, in-situ and continuous monitoring of chemical analytes using a low cost electronic multiplexed architecture. It allows multiple analyte sensing simultaneously on 8 equivalent channels. The system achieved the low cost objective by using a single photomultiplier tube and a dedicated LED instead of a laser as each channel's excitation optical source without optical multiplexing. The system is operated in time-division multiplexing by LabVIEW software, which provides easy reconfiguration of the operating parameters.

The biosensor system uses photoluminescence response of an oxygen or pH sensitive dye, which is integrated with genetically engineered enzyme. The system's ability to simultaneously sense different chemicals on different channels allows its application to detection of multiple toxic organic pollutants in contaminated ground water.

Characterization experiments on the multi-channel fiber optic photoluminescence based biosensor system with Ru based optodes led to a modified Stern-Volmer relationship between the dye's photoluminescence and the concentration of oxygen acting as a quencher. Deviations in the measured emission intensities from those theoretically predicted by the Stern-Volmer relationship have been explored as a function of optode dye concentration and system non-idealities. When the dye concentration is less than 1.5mg RuDPP in 0.5 ml of chloroform, the response ratio to different quencher concentrations behaves the same as the Stern-Volmer equation describes; however, such response ratio is reduced at high dye concentrations.

7559-25, Session

Highly specific detection of IL-8 protein using combination tapered fiber optic biosensor dip-probe

C. Wang, R. Kapoor, The Univ. of Alabama at Birmingham (United States)

We could successfully detect up to 60 pM of IL-8 concentration using combination tapered fiber-optic biosensor (CTFOB) dip-probe. Sandwich assay was used for detection. Capture antibodies of IL-8 were immobilized on the probe surface while the detection antibodies of IL-8 were labeled with Alexa 488 dye. The probes with immobilized capture antibodies were immersed in various concentrations (20 pM to 1 nM) of IL-8 for one hour. After washing the probes were immersed in detection antibodies solution for another two hours. After washing, a fluorescence signal, proportional to immobilized IL-8 (Biolegend Inc.) on the probe surface, was generated by evanescent wave excitation technique. Signals were recorded with the help of a CCD based spectrometer. We could detect signal from all the probes.

Two types of negative control probes were also prepared. Negative control-I is to check the amount of non specific binding of labeled antibodies to the probe. Capture antibody of IL-8 was immobilized on the negative control-I probe surface but it was not immersed in the sample (IL-8) solution, instead it was directly immersed in detection antibody solution. Negative control-II is to check non specific binding of IL-8 to the probe. Capture antibodies of bovine serum albumin (BSA) were immobilized on the negative control-II probe surface. The probe was first immersed in highest concentration (1nM) of IL-8 solution and then in labeled detection antibodies (of IL-8) solution.

Absence of any detectable signal on control probes confirms that signal in regular probes is due to specific binding of IL-8 to the probes.





7559-33, Session

Suppression of Modal Noise in a Multimode Fiber-Optic Delivery Output from an Ultra-Broadband Supercontinuum Light Source

D. Kim, I. K. Ilev, U.S. Food and Drug Administration (United States); K. Klein, Fachhochschule Giessen-Friedberg (Germany)

Because of their larger core diameter, multimode optical fibers (MMF) have advantage over its single-mode (SM) counterpart especially in terms of higher light-to-fiber coupling efficiency and easier coupling without complicated equipment and procedure. However, when coherent light source is coupled into an MMF at non-optimal coupling conditions, a modal noise can be introduced and the output spectrum can be significantly altered. Conventional non-coherent white-light sources do not suffer from this problem. However, recently developed supercontinuum light sources need extra caution when step-index MMFs are used for light delivery output because of fairly high coherence.

We have tested various methods for suppressing the modal noise in MMF output from an ultra-broadband supercontinuum light which is generated in a nonlinear photonic crystal fiber pumped with a 1.06-µmwavelength, subnanosecond-pulse-width, 8-kHz-rep-rate Nd:YAG laser source. Significant amount of modal noise including spectral fluctuations was observed when the output from the photonic crystal SM-fiber was directly coupled into different MMF. Standard methods such as mode scrambling and fiber stretching have been studied for modal noise suppression, however, the effect was minimal. We observed significant suppression of modal noise by expanding the output beam from the photonic crystal fiber and tightly focus into MMF using multiple lenses. The resulting spectra of the different MM-fibers are compared with the output from different single-mode fiber coupled to the supercontinuum source, which are necessary to cover the broadband range of the supercontinuum source over more than two decades, from 450 nm up to 2100 nm wavelength.



Saturday-Sunday 23-24 January 2010 • Part of Proceedings of SPIE Vol. 7560 Biomedical Vibrational Spectroscopy IV: Advances in Research and Industry

7560-02, Session 1

In vivo diagnosis of mammary adenocarcinoma using Raman spectroscopy: an animal model study

R. A. Bitar, Univ. Federal do ABC (Brazil); D. G. Ribeiro, M. A. d. S. Martins, E. A. P. dos Santos, K. K. Sakane, Univ. do Vale do Paraíba (Brazil); L. N. Z. Ramalho, F. S. Ramalho, Univ. de São Paulo (Brazil); A. A. Martin, Univ. do Vale do Paraíba (Brazil); H. d. S. Martinho, Univ. Federal do ABC (Brazil)

Breast cancer is the most frequent cancer type in women Worldwide. Unfortunately it still persists as the main induced-cancer deaths. Sensitivity and specificity of clinical breast examinations have been estimated from clinical trials to be approximately 54 % and 94 %, respectively. Further, approximately 95 % of all positive breast cancer screenings turn out to be false-positive. The optimal method for early detection should be both highly sensitive to ensure that all cancers are detected, and also highly specific to avoid the humanistic and economic costs associated with false-positive results. In vivo optical spectroscopy techniques, Raman in particular, have been pointed out as promising ways to improve the accuracy of screening mammography. The aim of the present study was to apply FT-Raman spectroscopy to discriminate normal and adenocarcinoma breast tissues of Sprague-Dawley female rats. The study was performed on 32 rats divided in the control (N=5) and experimental (N=27) groups. Histology analysis indicated that mammary hyperplasia, cribiforme, pappilary and solid adenocarcinomas were found in the experimental group subjects. The spectral collection (transcutaneously and open sky) was made using a commercial FT-Raman Spectrometer (Bruker RFS100) equipped with fiber-optic probe (RamProbe) and the spectral region between 500 and 2000 cm-1 was analyzed. Principal Components Analysis (PCA) and Linear Discriminant Analysis (LDA) were applied as spectral classification algorithm. As concluding remarks it is show that normal and adenocarcinoma tissues discriminations is possible (Sensibility = 83.3%, Specificity = 78.4 %). However, a conclusive diagnosis among the 4 lesion subtypes was not possible. Similar results were found for both transcutaneous and open sky methodology.

7560-03, Session 1

How specific are Raman spectroscopic models are: a comparative study between different cancers

S. P. Singh, Advanced Ctr. for Treatment Research and Education in Cancer (India); K. K. Kumar, M. V. P. Chowdary, K. Maheedhar, Manipal Univ. (India); C. M. Krishna, Advanced Ctr. for Treatment Research and Education in Cancer (India)

Optical spectroscopic methods are being considered as techniques which could be complementary or even alternative to biopsy and pathology. Several groups are pursuing diagnostic application of Raman-spectroscopy in cancers. We have developed Raman-spectroscopic-models for diagnosis of cancers like breast, oral, stomach etc. So far specificity and applicability of spectral- models has been limited to particular tissue origin. In this study we have explored explicity of spectroscopic-models among different cancers.

Spectra from standard spectral-models representing normal and malignant tissues of breast (46), cervix (52), colon (25), larynx (53), and oral (47) were analyzed. Specificity of models was evaluated by PCA using scores of factor, Mahalanobis distance, Spectral residuals as discriminating-parameters. Multiparametric limit test approach was also explored.

The preliminary unsupervised PCA of pooled data indicates that normal tissue types were always exclusive from their malignant counterparts. But when we consider tissue of different origin, heavy overlap among clusters was found. Supervised analysis by Mahalanobis distance and spectral residuals gave similar results. The 'limit test' approach where classification is based on both match and mis-match of the given spectrum against all the available spectra, has revealed that spectral models are very exclusive and specific. For example breast normal spectra matched only with breast normal spectral-model and mismatched to all other spectral-models. And pattern repeated for all the spectral models

Therefore, results of the study indicate the exclusiveness and efficacy of Raman spectroscopic-models. Prospectively, these findings open new application of Raman spectroscopic-models in identifying a tumor as primary or metastatic.

7560-11, Session 1

NIR Raman spectroscopy integrated with multimodal endoscopic imaging techniques for improving early diagnosis of gastric malignancies

Z. Huang, S. Teh, W. Zheng, K. Y. Ho, M. Teh, K. G. Yeoh, National Univ. of Singapore (Singapore)

We report an integrated Raman spectroscopy and wide-field imaging techniques (white-light reflectance, autofluorescence and narrow band) for early detection of gastric cancer. A special 1.8 mm endoscopic Raman probe with filtering modules is developed permitting effective elimination of interference of fluorescence background and silica Raman in fibers while maximizing tissue Raman collections. We demonstrated for the first time that high-quality in vivo Raman spectra of upper gastrointestinal tract can be acquired within 1s or subseconds under the guidance of wide-field endoscopic imaging modalities. Our recent clinical tests on 12 patients with gastric malignancies indicated that good differentiation (over 95% of diagnostic sensitivity and specificity) between cancer and normal gastric mucosal tissues in vivo can be achieved, suggesting that the integrated Raman spectroscopy and endoscopic imaging techniques can be clinically useful tool for improving in vivo diagnosis and detection of gastric malignancies during clinical gastroscopy.

7560-19, Session 1

Development of a Raman based endoscopic imaging probe utilizing SERS nanoparticles for detection of early stage colon cancer

E. Garai, J. T. C. Liu, M. J. Mandella, C. Zavaleta, Stanford Univ. (United States); I. Walton, Oxonica (United States); C. H. Contag, S. S. Gambhir, Stanford Univ. (United States)

Screening endoscopy has been very successful in decreasing the incidence of colorectal cancer over the past decade. However, with traditional endoscopic tools physicians still cannot efficiently and accurately distinguish between dysplastic (precancerous) and hyperplastic (benign) polyps without biopsy and subsequent histopathology. Moreover, it is difficult to even determine the location of flat lesions. In the colon, flat lesions are reported to be five times more likely to contain cancerous tissue than polyps detected during conventional colonoscopy.

We have developed a Raman endoscopic probe with a 5-mm outer



diameter for in vivo molecular screening of the lumen of the colon. This probe has been designed to be inserted into an endoscope and used to detect and quantify the presence of a multiplexed panel of tumor targeting surface-enhanced-Raman-scattering (SERS) nanoparticles. One of the key features of our Raman probe is that it has been designed for efficient use over a wide range of working distances from 0.5 to 1.5 cm. This is necessary to accommodate for imperfect centering of the probe within the colon, as well as variable working distances due to folds and bends within the colon.

Preliminary ex vivo experiments have shown the ability to detect 10 pM concentrations of SERS particles with an integration time of 10 ms (100 spectra/sec) and a working distance of approximately 1 cm. These tests utilized 20 mW of laser radiation, a 1 mm spot size. ANSI regulations will allow us to increase the laser illumination power to about 175 mW resulting in a detection limit of approximately 1 pM. These techniques could allow endoscopists to distinguish between normal and cancerous tissues instantly, as well as to identify flat lesions that are easily missed during conventional screening endoscopy.

7560-21, Session 1

In vivo characterization of lung cancers using endoscopic Raman spectroscoy: a pilot study

M. A. Short, S. Lam, A. McWilliams, H. Zeng, The BC Cancer Research Ctr. (Canada)

Our previous results from Raman spectroscopy studies on ex vivo human lung tissue showed the technique could easily differentiate between samples with different pathologies. We thus developed a fast dispersivetype near-infrared in vivo Raman system to test its efficacy as a tool to improve the clinical characterization of lung cancers and pre cancers. The 785 nm excitation, and the tissue Raman emission, were guided from the laser, and to the spectrometer respectively, by a 1.8 mm diameter fiber optic bundle which passed down the instrument channel of a bronchoscope. Two stages of optical filtering were used to substantially reduce the background light. The spectrometer itself consisted of one of two holographic gratings, and these, together with the optical filters, permitted measurements in two frequency ranges: 700 to 2000 cm-1 and 1500 to 3400 cm-1. The dispersed light was detected by a cooled 400 x 1340 pixel CCD array. The estimated spectral resolution of the system was approximately 9 cm-1. Initial results showed that clear real time in vivo Raman signals could be obtained with 1-2 seconds of excitation in both spectral ranges, although the 1500 to 3400 cm-1 range had a better signal to noise ratio because of the lower tissue fluorescence. So far we have measured spectra from 50 patients using the high frequency range. Principal component analyses followed by linear discrimination analyses on these data show that malignant and benign lesions can be separated with around 90% sensitivity and specificity using a leave-one-out crossvalidation process.

7560-26. Session 1

FTIR, Raman and CARS microscopic imaging for histopathologic assessment of brain tumors

C. Krafft, N. Bergner, Institute of Photonic Technology Jena e.V. (Germany); B. Romeike, R. Reichart, R. Kalff, Friedrich-Schiller-Univ. Hospital Jena (Germany); B. Dietzek, J. Popp, Institute of Photonic Technology Jena e.V. (Germany) and Friedrich-Schiller-Univ. Jena (Germany)

Objective: The contribution demonstrates how the molecular contrast of Fourier transform infrared (FTIR), Raman and coherent anti-Stokes Raman scattering (CARS) microscopic imaging can be applied for the histopathologic assessment of brain tumors.

Material and methods: Brain tissue specimens were obtained from patients undergoing neurosurgery. Thin sections of human gliomas, meningeomas and brain metastases were prepared on calciumfluoride windows which are appropriate substrates for data acquisition in transmission and reflection mode.

Results: All CARS images correlate well with the photomicrographs because the non-resonant signals provided significant morphological information. All CARS images also correlate well with the FTIR and Raman images. Whereas CARS images were collected within seconds, exposure times were minutes for FTIR imaging and hours for Raman imaging. CARS images near 2900 cm-1 mainly probed spectral contributions of lipids which are important diagnostic markers of brain tumors. Full spectral information could be extracted from Raman and FITR images which enabled to distinguish different tissue types and malignancy grades in brain tumors.

Conclusions: Based on the current results we suggest a complementary application of FTIR, Raman and CARS imaging. FTIR and Raman imaging defines spectral regions and spectral markers that are essential for tissue classification. CARS imaging at different Stokes shifts or in the multiplex mode probes these spectral descriptors at video-rate speed.

Acknowledgements: Financial support of the European Union via the Europäischer Fonds für Regionale Entwicklung (EFRE) and the "Thüringer Kultusministerium (TKM)" (Projects: B714-07037, B578-06001, 14.90 HWP) is highly acknowledged. B.D. thanks the Fond der Chemischen Industrie for financial support.

7560-05, Session 2

In situ cell cycle phase determination using Raman spectroscopy

Y. Oshima, Aoyama Gakuin Univ. (Japan) and RIKEN (Japan); T. Takenaka, Aoyama Gakuin Univ. (Japan); H. Sato, Kwanse Gakuin Univ. (Japan) and RIKEN (Japan); C. Furihata, Aoyama Gakuin Univ. (Japan)

Raman spectroscopy is a powerful tool for analysis of the chemical composition in living tissue and cells without destructive processes such as fixation, immunostaining, and fluorescence labeling. Microscopic Raman spectroscopic technique enables us to obtain a high quality spectrum from a single living cell. We demonstrated in situ cell cycle analysis with Raman spectroscopy and multivariate statistical analysis. Each of the cell cycle phases, G0/G1, S and G2/M were able to be identified in the present study. The result of in situ Raman analysis was evaluated with FASC analysis. The Raman spectra obtained from living cell have too much information to understand the spectral dissimilarity in cell cycle change as life phenomenon, but several Raman bands could be useful as markers for the cell cycle identification. A single cell analysis using Raman spectroscopy has capability to observe directly molecular dynamics intracellular organelles, in nucleus, mitochondrion, ribosomes, and so on. We also demonstrated Raman measurement in each of the cell fractions and quantitative analysis of molecular component based on the Raman peak intensities. Our current study focused on intracellular organelles and discussed how the Raman signals from cellular components contribute to the Raman spectral changes in cell cycle change, malignant alteration and differentiation of the human living cell.

7560-06, Session 2

A system for the rapid detection of bacterial contamination in cell-based therapeutica

C. Bolwien, C. Erhardt, S. Gerd, Fraunhofer IPM (Germany); H. Thielecke, R. Johann, Fraunhofer IBMT (Germany); M. Pudlas, H. Mertsching, S. Koch, Fraunhofer IGB (Germany)

Monitoring the sterility of cell or tissue cultures is of major concern, particularly in the fields of regenerative medicine and tissue engineering when implanting cells into the human body. Our sterility-control-system is based on a Raman micro-spectrometer and is able to perform fast sterility testing on microliters of liquid samples. In conventional sterility



control, samples are incubated for weeks to proliferate the contaminants to concentrations above the detection limit of conventional analysis. By contrast, our system filters particles from the liquid sample. The filter chip fabricated in microsystem technology comprises a silicon nitride membrane with millions of sub-micrometer holes to retain particles of critical sizes and is embedded in a microfluidic cell specially suited for concomitant microscopic observation. After filtration, identification is carried out on the single particle level: image processing detects possible contaminants and prepares them for Raman spectroscopic analysis. A custom-built Raman-spectrometer-attachment coupled to the commercial microscope uses 532nm or 785nm Raman excitation and records spectra up to 3400 wavenumbers. In the final step, the recorded spectrum of a single particle is compared to an extensive library of GMP relevant organisms, and classification is carried out based on a support vector machine (SVM). We present our latest results on the training of the SVM and the evaluation of the viability of the system using tissue engineering growth medium that has been randomly spiked with bacterial contaminants

7560-09, Session 2

Surface enhanced Raman spectroscopy for urinary tract infection diagnosis and antibiogram

E. Kastanos, Univ. of Nicosia (Cyprus); K. Hadjigeorgiou, A. Kyriakides, C. Pitris, Univ. of Cyprus (Cyprus)

Urinary tract infection (UTI) diagnosis and antibiotic sensitivity testing require a minimum of 48 hours using conventional clinical tests. This extensive waiting period results in ineffective treatments, chronic infections, increased health care costs, and, most importantly, increased bacterial resistance to antibiotics. In this work, Surface Enhanced Raman Spectroscopy (SERS) is used as a novel method for classifying bacteria and determining their sensitivity or resistance to an antibiotic. SERS spectra of five species of gram negative and gram positive bacteria, isolated from urine cultures, were classified after mixing bacterial samples with gold nanoparticles. The classification algorithm used for the analysis involved novel feature extraction and discriminant analysis and resulted in > 90% accuracy of classification. For antibiotic sensitivity testing, SERS spectra were collected just two hours after exposure to the antibiotics ciprofloxacin and amoxicillin. Analysis of the spectra showed clear separation between samples exposed to ciprofloxacin, to which the bacteria were sensitive, samples exposed to amoxicillin, to which they were resistant, and negative control samples. With the enhancement provided by SERS, the technique can be applied to small quantities of bacteria thus bypassing the need for urine cultures. The proposed method can become the basis for the development of new technology for UTI diagnosis and antibiogram with same day results and avoiding all undesirable consequences of current practice.

7560-28, Session 2

Raman spectroscopic characterization of single cells

J. Popp, Institute of Photonic Technology Jena e.V. (Germany) No abstract available.

7560-10, Session 3

Gender determination of birds by Fourier transform infrared spectroscopic imaging

G. Steiner, E. Koch, Technische Univ. Dresden (Germany); T. Bartels, Univ. Leipzig (Germany)

Birds are traditionally classified as male or female based on their

anatomy and plumage color as judged by the human eye. Knowledge of a bird's gender is important for the veterinary practitioner, the owner and the breeder. The accurate gender determination is essential for proper pairing of birds, and knowing the gender of a bird will allow the veterinarian to rule in or out gender-specific diseases. In particular the poultry industry is highly interested in fast, objective and inexpensive methods for sexing of day-old chicks. Several biochemical methods of gender determination have been developed for avian species where otherwise the gender of the birds cannot be determined by their physical appearances or characteristics. In this contribution, we demonstrate that FT-IR spectroscopic imaging is a suitable tool for a quick and objective determination of the bird's gender. The method is based on differences in chromosome size. Male birds have two Z chromosomes and female birds have a W chromosome and a Z chromosome. Each Z chromosome has approx. 75.000.000 bps whereas the W chromosome has approx. 260.00 bps. This difference can be detected by FT-IR spectroscopy. Spectroscopic images were recorded from germ cells obtained from the feather pulp of 60 turkey chicks. Principal component analysis (PCA) and soft independent models of class analogy (SIMCA) were use to analyzed and classified spectra as male or female. Significant changes between cells of male and female birds occur in the region of phosphate vibrations around 1080 and 1020 cm-1. The classification success rate of 98% demonstrates the potential of FT-IR spectroscopy to bird sexing.

7560-12, Session 3

In vitro characteristics of a mid-infrared continuous glucose sensor

C. Vrancic, C. Herrmann, N. Gretz, S. Hoecker, A. Pucci, W. Petrich, Univ. of Heidelberg (Germany)

The continuous monitoring of the concentration of glucose provides an essential tool for the improved glycemic control in diabetics. Most of the present approaches of transcutaneous, continuous glucose monitors are based on electrochemistry and require the insertion of reagents into the body. In contrast, we aim at the reagent-free measurement of glucose by means of mid-infrared spectroscopy without consumption of the analyte.

A quantum cascade laser provides narrow band radiation at wavelengths around the absorption bands of glucose (~10 μ m). At the same time, it yields sufficient energy to allow for a good signal-to-noise ratio in transmission measurements despite the strong "background" absorption of water.

We investigated various concepts for the sensor head based on the light-guiding properties and handling of materials such as AgCl/AgBr or silicon. In-vitro experiments were performed using a custom-made, temperature-stabilized measurement flow chamber. The detection limits for the quantification of glucose are given together with the impact of various additional analytes on the absorption measurement. In preparation for future in-vivo applications, we will present first results of biocompatibility tests of the fiber sensors.

7560-20, Session 3

Simultaneous observation of ultrafast ligand dissociation and docking-site trapping in heme proteins using upconversion infrared spectroscopy

P. Nuernberger, K. F. Lee, A. Bonvalet, A. Alexandrou, M. H. Vos, M. Joffre, Lab. d'Optique et Biosciences, Ecole Polytechnique, (France) and Institut National de la Santé et de la Recherche Médicale (France)

We report on ultrafast pump-probe spectroscopy of CO-liganded heme proteins employing our recently developed chirped-pulse upconversion technique. In the experiments, a visible pump laser pulse dissociates the ligand from the iron atom of the heme, and the induced dynamics are probed with a probe laser pulse in the mid-infrared spectral region. This



probe laser pulse is then transferred from the mid-infrared to the visible spectral region through a sum-frequency-mixing process with a chirped near-infrared laser pulse. A spectrometer with a CCD camera acts as a detector for the visible light, combining mid-infrared spectroscopy with the high resolution and high sensitivity of detectors in the visible spectral range.

We apply this technique to the spectroscopy of liganded heme proteins like carboxyhemoglobin in the mid-infrared. Commonly, the bleach signal due to photoinduced ligand dissociation and the incipient docking site absorption signal are studied individually, since their spectral signatures are about 200cm-1 apart and differ by more than an order of magnitude in absorptivity, necessitating both high resolution and sensitivity. We demonstrate that it is possible to monitor them simultaneously with the chirped-pulse upconversion technique, allowing a direct observation and a concurrent analysis of the initial processes after photoinduced ligand dissociation. These processes include the reorientation of the CO ligand and the formation of hot vibrational bands lasting for more than a hundred picoseconds in the docking site.

7560-04, Session 4

Evaluation of thyroid tissue by Raman spectroscopy

A. A. Martin, C. S. B. Teixeira, Univ. do Vale do Paraíba (Brazil); R. A. Bitar, Univ. Federal do ABC (Brazil); A. B. O. Santos, Univ. do Vale do Paraíba (Brazil); H. S. Martinho, Univ. Federal do ABC (Brazil); E. A. L. Arisawa, Univ. do Vale do Paraíba (Brazil)

The diagnosis of thyroid pathologies is usually made by cytologic analysis of the fine needle aspiration (FNA) material. However, this procedure has a low sensitivity presenting a variation of 2% to 37%. The application of optical spectroscopy in the characterization of alterations could result in the development of a minimally invasive and non-destructive method for the diagnosis of thyroid diseases. Thus, the objective of this work was to study the biochemical alterations of tissues and hormones (T3 and T4) of the thyroid gland by means of molecular vibrations of the FT-Raman spectra. Through the discriminative linear analysis of the Raman spectra of the tissue, it was possible to establish the correct classification index among the groups: goitre adjacent tissue, goitre nodular region, follicular adenoma, follicular carcinoma and papillary carcinoma. A relevant result was obtained in the analysis of the benign tissues (goitre and follicular adenoma) versus malignant tissues (papillary and follicular carcinomas), for which the index was 72.5% and considered good. It was also possible, by means of visual observation, to find similar vibrational modes in the hormones and pathologic tissues. In conclusion, it was possible to identify some biochemical alterations, represented by the FT-Raman spectra that could possibly be used to classify histologic groups of the thyroid.

7560-18, Session 4

Detecting changes during pregnancy with Raman spectroscopy

E. Vargis, Vanderbilt Univ. (United States); K. Robertson, A. Al-Hendy, Meharry Medical College (United States); J. Reese, A. Mahadevan-Jansen, Vanderbilt Univ. (United States)

Preterm labor is the second leading cause of neonatal mortality and leads to a myriad of complications like delayed development and cerebral palsy. Currently, there is no way to accurately predict preterm labor, making its prevention and treatment virtually impossible. While there are some at-risk populations (previous preterm birth or uterine/cervical abnormalities), over half of all preterm births do not fall into any highrisk category. This study seeks to predict and prevent preterm labor by using Raman spectroscopy to detect changes in the cervix during pregnancy. Results indicate that molecular and cellular changes that occur in precancerous tissues and as well as in benign conditions yield distinct Raman features. Since Raman spectroscopy has been used to

detect cancers in vivo in organs like the cervix and skin, it follows that spectra will change over the course of pregnancy. A study by Maul, et. al., showed that fluorescence decreased during pregnancy and increased during post-partum exams to pre-pregnancy levels. We believe similarly significant changes will occur in the Raman spectra obtained during the course of pregnancy. In this study, Raman spectra from the cervix of pregnant mice and women will be acquired. Specific changes that occur due to cervical softening or changes in hormonal levels will be observed and quantified to output a likelihood that a female mouse or a woman will enter labor. Any algorithm that can be developed to predict when a woman will enter labor will greatly benefit the outcome for pregnant women and their children.

7560-23, Session 4

Near infra-red Raman spectroscopic study of reactive gliosis and the glial scar in injured rat spinal cords

T. Saxena, B. Deng, K. Hoellger, E. Lewis-Clark, J. M. Hasenwinkel, J. Chaiken, Syracuse Univ. (United States)

Comparative Raman spectra of ex vivo, saline-perfused, injured and healthy rat spinal cord as well as experiments using enzymatic digestion suggest that proteoglycan over expression may be observable in injured tissue. Principal component analysis and comparison with authentic materials in vitro suggest the occurrence of side reactions between products of chondroitinase (cABC) treated cord that produce lactones and similar species. These species have distinct Raman features that are often not overlapped with Raman features from other chemical species. Since the glial scar is thought to be a biochemical and physical barrier to nerve regeneration this observation suggests the possibility of using near infrared Raman spectroscopy to study disease progression and potential treatments ex vivo. If potential treatments can be designed, it might be possible to monitor potential remedial treatments within the spinal cord in vivo.

7560-25, Session 4

Label free investigation of bio-molecules on the nanometer scale using tip-enhanced Raman spectroscopy

T. Deckert-Gaudig, M. Richter, R. Treffer, X. Lin, IPHT Jena (Germany); V. Deckert, IPHT Jena (Germany) and Friedrich-Schiller-Univ. Jena (Germany)

Tip enhanced Raman spectroscopy (TERS) enables a label free exploration of molecular structures at the nanometer scale. As the major theoretical and technical aspects of the methods are well understood, the focus is presently directed towards applications. A particular interesting field is the investigation of biological relevant structures or molecules. TERS provides limits-of-detection that allow the investigation of single peptides or DNA strands potentially leading towards a sequencing of such molecules. A major challenge is presently a reproducible sample preparation that does not interfere with the general properties of the molecules and still allows TERS measurements. We will present first steps towards this ultimate goal starting with a classification of TER spectra of immobilized amino acids. The obtained results provide the specific conformation of the amino acids when attached to an ultra flat and still transparent gold or silver crystal. In addition to the investigation of the specific amino acids we systematically investigated these gold and silver crystals and consider them as ideal substrates for TERS experiments. As a next step we investigated oxidised glutathione as an example for a short peptide. Markers for all three amino acid components could be assigned and in addition distinct shifts of the Raman bands also allow a hypothesis on how the molecule is attached to the surface. The results are very encouraging and will eventually lead to a TERS investigation of actual proteins.



7560-14, Session 5

Evaluation of intracoronary time-gated Raman spectroscopy

H. Wang, Boston Univ. (United States) and Massachusetts General Hospital (United States); J. A. Gardecki, B. E. Bouma, G. J. Tearney, Massachusetts General Hospital (United States) and Harvard Medical School (United States)

Raman spectroscopy is a powerful in situ tool for the chemical analysis and classification of atherosclerotic plaques. However, the performance may be limited by a low signal-to-noise ratio (SNR) due to high autofluorescence background from the native tissue. By using the different timescales for generation of spontaneous Raman and fluorescence, it may be possible to reduce the fluorescence background associated with a tissue Raman spectrum by temporally gating the Raman spectrum. In this presentation, we will evaluate the feasibility of using time-gated detection for biomedical Raman spectroscopy with the application focused on the detection of atherosclerotic plaques. We will describe a quantitative model that accounts for the effect of time gate width, fluorescence lifetime, and excitation wavelength on estimated fluorescence rejection factor. Measurements of the time-gated Raman spectra and fluorescence lifetime will be reported, and the fluorescence rejection factor will be calculated from experimental data for several atherosclerotic pathologies. A comparison of the experimental and theoretical rejection factors will be discussed.

7560-16, Session 5

Automated system for gathering elastic and inelastic scattering data from single cells

A. J. Berger, D. Shipp, Z. J. Smith, Univ. of Rochester (United States)

Raman spectroscopy can be combined with angularly-resolved elastic scattering measurements to create a multimodal platform for sample characterization. By performing these measurements through a microscope, single cells can be studied. An integrated Raman and angular-scattering microscope (IRAM) system in our group has been used to quantify morphogical and chemical differences between individual activated and non-activated immune cells (CD8+ T cells). The activation fractions agree with those deduced from fluorescence-activated cell sorting (FACS), but with IRAM no external contrast agents are required. The cells can also be studied at multiple time points each. We will present results from our ongoing tests on immune cells, discuss advances in automation that significantly improve the types of experiments that can be conducted, and indicate different illumination and detection schemes that could provide increased sensitivity to morphological changes.

7560-17, Session 5

A new strategy for noninvasive preclinical imaging in small animal models using Raman spectroscopy in conjunction with SERS nanoparticles

C. Zavaleta, K. Hartman, B. Smith, A. de la Zerda, Z. Cheng, Z. Liu, H. Dai, S. S. Gambhir, Stanford Univ. (United States)

Raman spectroscopy is a well established bioanalytical tool with many advantages including excellent sensitivity, multiplexing capabilities, and resistance to photobleaching. Although scientists have reported the use of Raman spectroscopy to image living cells and excised tissues, its inherently weak effect has limited its application to non-invasively assess preclinical models. However, with careful system design, we have developed a Raman microscope capable of non-invasive deep tissue imaging in small animals in conjunction with Raman nanoparticles.

The focus of this project was to evaluate the ability of our newly optimized non-invasive Raman microscope to image deep tissues and multiplex using various surface enhanced Raman scattering (SERS) nanoparticles, as well as localize functionalized single walled nanotubes (SWNTs) in small animal models.

For deep tissue imaging, mice were injected intravenously with either SERS nanoparticles or tumor-targeting SWNTs and imaged with our Raman microscope at various times post-injection to evaluate their localization

In this study we showed that our optimized Raman microscope has the ability to non-invasively image deep tissues, multiplex up to 10 SERS nanoparticles, and localize targeting of SWNTs conjugated with RGD in an integrin expressing tumor model.

These results have significant implications toward the development of a new noninvasive preclinical imaging modality with high sensitivity, and specificity to assess the efficacy of new diagnostic and therapeutic approaches in preclinical tumor models.

7560-15, Session 6

Optical fiber bundle coupling errors in Raman spectra: correction via data processing

K. A. Dooley, F. W. L. Esmonde-White, M. D. Morris, Univ. of Michigan (United States)

Light can be coupled into imaging spectrographs through the use of fiber-optic bundles. Ideally, the collected spectra from adjacent optical fibers should be resolved and independent. However, this assumption breaks down if a partial overlap of adjacent fibers on the detector CCD results from either diffraction or uncorrected monochromatic aberrations. In addition, spectral mixing can be caused by optical cross-talk among tightly packed fibers, particularly if the fiber-optic buffer has been removed in order to use the CCD area more efficiently and increase the linear fiber packing density. These coupling effects can become sources of systematic error, especially when fiber bundles are used to map composition of a sample or when branches of the fiber bundle are interrogating different samples. Coupling errors can prohibit local variations in composition from being detected and also can mix spectra from different spatial regions of the sample. In this paper, the mixing in fiber bundles of differing geometries will be assessed. Methods to resolve overlapped signals will be discussed, including the use of multivariate curve resolution to evaluate the illumination patterns arising from individual fibers and correct for the spectral mixing. Using data processing to correct for optical coupling errors, instead of physically changing the spacing between fibers in the bundle, allows for the efficient use of the limited spectrograph detector area by having a larger number of fibers.

7560-22, Session 6

Calibration of Raman systems for biomedical and clinical applications

H. Krishnamoorthi, A. Mahadevan-Jansen, Vanderbilt Univ. (United States)

Previous studies have demonstrated the potential utility of Raman spectroscopy as a diagnostic tool. Despite this, there has been little progress in the standardization of Raman calibration and processing of Raman spectra within the field. To obtain the most informative Raman spectra for biomedical application, three important tasks must be fulfilled: calibration of system response, determination of methods of processing and analysis, and relation of spectra to their bases. Current techniques of system response calibration are time-consuming and cumbersome, particularly when Raman spectroscopy is used in the clinical setting, where the patient would be better served by more efficient procedures. Here, we present the use of glass as a reliable intensity standard for system response, along with a comparison of the use of this standard with other common intensity standards. Different



practices of Raman processing can lead to differing interpretations of data, even shifts of Raman peaks, and here we present a comparison of various processing procedures to the analysis of Raman. Finally, proper understanding of spectroscopic data requires association of the spectra with its constituents, and here we present the application of our calibration and processing protocols to the analysis of tissue spectra and its basis molecules with a least-squares method. We demonstrate that a standardization of Raman calibration and processing would allow for stronger comparisons between different Raman systems and spectra.

7560-24, Session 6

Direct noninvasive observation of near infrared photobleaching of autofluorescence in human volar side fingertips in vivo

B. Deng, C. Wright, E. Lewis-Clark, Syracuse Univ. (United States); G. Shaheen, LighTouch Medical, Inc. (United States); R. Greier, J. Chaiken, Syracuse Univ. (United States)

Human transdermal in vivo spectroscopic applications for tissue analysis involving near infrared (NIR) light often must contend with broadband NIR fluorescence that, depending on what kind of spectroscopy is being employed, can degrade signal to noise ratios and dynamic range. NIR fluorescence is produced by many relatively weak sources and so is often referred to using the relatively inclusive term "autofluorescence". Blood tissues and various other endogenous materials associated with the static tissues in the irradiated volume are known to fluoresce but only differentiating between fluorescence from the blood vs. the static tissues has been previously accomplished. Results of recent experiments on human volar side fingertips in vivo are beginning to provide a more detailed relative ordering of the major contributions. Preliminary results involving the variation in a bleaching effect across different individuals suggest that for 830 nm excitation as much as 85% of the total fluorescence comes from the static tissues and remainder originates with the blood tissues, i.e. the plasma and the hematocrit. Of the NIR fluorescence associated with the static tissue, over half originates with products of well-known post-enzymatic glycation reactions, i.e. Maillard chemistry, in the skin involving glucose and other carbohydrates and skin proteins like collagen. We presume that the remainder originates with all other known sources such as vitamin A (carotene) and related molecules e.g. licopene, vitamin D and endogenous anti-oxidants and porphyrins.

7560-01, Poster Session

Influence of permanent magnetic field on dynamic aqueous glucose absorption

X. Zhang, C. M. Ting, GlucoStats System Pte, Ltd. (Singapore): W. Zhang, Mr (Singapore); J. H. Yeo, Nanyang Technological Univ. (Singapore)

Blood glucose level is an important parameter for doctors to diagnosis and treat Diabetes. Traditional way to measure blood sugar level needs to prick finger to get blood, which is painful, potentially dangerous and expensive to operate. In recent ten years many non-invasive methods have been developed to measure blood sugar level. The non-invasive methods are fast, painless, safe and convenient, but the measurement accuracy is still a barrier due to the weak signal from blood and interference of other blood components. The optical method is based on the light magnitude absorbed by glucose in blood, to enhance the blood glucose absorption is the key problem. The effect of magnetic field on aqueous glucose solution was reported in the range of 900-2000nm. In this paper we investigated the NIR absorption spectrum of aqueous glucose by using a FTIR spectrometer after glucose solution passing through a permanent magnetic field. When glucose solution flowing through the permanent magnetic field, some of the aqueous glucose molecules are magnetized and glucose absorption is enhanced in the NIR range of 1000-2500nm. The experimental results show that glucose absorbance in its combination region and first overtone region

is increased when the permanent magnetic field is introduced into the experiment. The increment of absorbance in first overtone region is greater than that in combination region.

7560-07, Poster Session

In vivo Raman spectroscopy biochemical changes of human skin for cosmetic application

M. G. Tosato, E. P. dos Santos, R. d. S. Alvez, L. Raniero, A. A. Martin, Univ. of Paraíba Valley (Brazil); O. Kruger, P. F. Menezes, C. E. d. O. Praes, O Boticário Franchising (Brazil)

The skin aging process is mainly accelerated by external agents such as sunlight, air humidity and surfactants action. Changes in protein structures and hydration during the aging process are responsible for skin morphological variations. In this work the human skin was investigated by in vivo Raman spectroscopy before and after the topical applications of a cosmetic on 17 healthy volunteers (age 60 to 75). In vivo Raman spectra of the skin were obtained with a Spectrometer SpectraPro- 2500i (Pi-Acton), CCD detector and a 785 nm laser excitation source, collected at the beginning of experiment without cream (T0), after 30 (T30) and 60 (T60) days using the product. The primary changes occurred in the following spectral regions: 935 cm-1 (CC), 1060 cm-1 (lipids), 1174 to 1201 cm-1 (tryptofan, phenylalanine and tyrosin), 1302 cm-1 (phospholipids), 1520 to 1580 cm-1 (C=C) and 1650 cm-1 (amide I). Simultaneously, there was an increase in the area around the 3250 cm-1 (OH) peak, which showed better hydration. These findings indicate that skin positive effects were enhanced by a continuous cream application.

7560-13, Poster Session

FT-IR microspectroscopy for rapid identification of bacteria in mixed culture

I. Fontoura, K. K. Sakane, M. A. G. Cardoso, S. Khouri, M. Uehara, R. Belo, L. Raniero, A. A. Martin, Univ. do Vale do Paraíba (Brazil)

Lately, it takes the conventional microbiological culture techniques 24 to 48 hours to identify a microorganism. However, in the last few years the FT-IR Microspectroscopy has been used for analysis in microbiology and applied successfully in pure microorganisms cultures in order to quickly identify strains of bacteria, yeasts and fungi.

The investigation and characterization of mixed microorganisms cultures is also of rising importance, especially in hospital environments where it is common the polimicrobial infection. However, few studies on this application can be found in the literature. Thus, the objective of this work was to apply the infrared spectroscopy to study the rapid identification of bacteria in this kind of culture.

The bacteria used in this study were obtained from the culture collection the Oswaldo Cruz Institute - Brazil. Echerichia coli ATCC 10799 and Staphylococcus aureus ATCC 14456, 3 inoculations were examined: Escherichia coli, Staphylococcus aureus, mixed culture of both.

The inocula were prepared according to the McFarland scale 0,5, incubated at 37°C for 6 hours, diluted in saline solution, put into CaF2 window and submitted to incubator to obtain biofilm. The samples were measured on Spectrum Spotlight 400 (Perkin-Elmer) on 4000-900 cm-1 with 32 scans done by transmittence.

The treated data were then used as input to cluster analysis, utilizing the first derivative and applying Ward's algorithm, and an excellent discrimination between pure and mixed culture was obtained.

Our preliminary result indicates that the FT-IR Microspectroscopy associated to the cluster analysis can be used to discriminate pure and mixed culture.



7560-27, Poster Session

Detecting early stage pressure ulcer on dark skin using multispectral imager

L. Kong, S. H. Sprigle, D. Yi, C. Wang, F. Wang, F. Liu, Georgia Institute of Technology (United States); J. Wang, F. Zhao, Bejing Bodian Optical Technology Co., Ltd. (China)

This paper introduces a novel idea, innovative technology in building multi spectral imaging based device. The benefit from them is people can have low cost, handheld and standing alone device which makes acquire multi spectral images real time with just a snapshot. The paper for the first time publishes some images got from such prototyped miniaturized multi spectral imager.

Conference 7561: Optical Biopsy VIII



Wednesday-Thursday 27-28 January 2010 • Part of Proceedings of SPIE Vol. 7561 Optical Biopsy VII

7561-39, Poster Session

Diagnosis of inflammatory fibrous hyperplasia of buccal mucosa by high-wavenumber FT-Raman spectroscopy

L. F. d. C. e. S. Carvalho, E. T. Sato, ABC Federal Univ. (Brazil); A. A. Martin, Vale do Paraíba Univ. (Brazil); J. D. Almeida, São Paulo State Univ. (Brazil); H. d. Silva Martinho, ABC Federal Univ. (Brazil)

Raman-based optical biopsy is a widely recognized potential technique for non-invasive real-time diagnosis. However, few studies had been devoted to the discrimination of very common subtle or early pathological states as inflammatory process which are always present on, e.g., cancer lesion border. In the present work, the water and lipids alterations between inflammatory fibrous hyperplasia (IFH) and normal tissues of buccal mucosa (NM) were probed by high intensity (2800 -3800 cm-1) FT-Raman spectra. Thirty spectra of IFH from 6 patients were compared to 30 spectra of NM from 6 patients. The average spectra of IFH and NM were deconvoluted to seven Lorentzian or Gaussian curves. The detailed analysis showed that seven peak regions are found in this region (2800 - 3800 cm-1), but only five peak regions get statistically significant differences (t-Student test) between the groups: 2854 (NM) / 2843 cm-1 (IFH); 2934 (NM /2937 cm-1 (IFH); 2991 (NM)/2977(IFH) cm-1 ; 3071(NM)/3060 (IFH) cm-1; and 3362 (NM)/ 3387(IFH) cm-1. Statistical analysis (Principal Components Analysis and Clustering) showed a clear separation of the spectra into NM and IFH clusters, which enabled the construction of a binary diagnosis model based on Logistic Regression. Compared to the It was concluded that this spectral region bands can give better differentiation among IFH and NM groups than the usual fingerprint region (500-1800 cm-1).

7561-40, Poster Session

Healing and evaluating guinea pig skin incision after surgical suture and laser tissue welding using in vivo Raman spectroscopy

A. Alimova, V. Sriramoju, R. Chakraverty, R. Muthukatti, R. Alfano, The City College of New York (United States)

The healing process in guinea pig skin following surgical incisions was evaluated at the molecular level, in vivo, by the use of Raman spectroscopy. The collagen deposition is one of the markers for healing process. The excess of collagen caused the scar formation which is unfavorable especially for incision healing after cosmetic surgery. Raman spectroscopy in vivo allowed not only evaluates the healing process, but also provided information regarding the internal structure of formed proteins. After the incisions were closed either by suturing or by laser tissue welding (LTW) the ratio of the Raman peaks of the amide III (1247 cm 1) band to a peak at 1326 cm 1 (the superposition of elastin and keratin bands) can be used to evaluate the progression of collagen deposition and respectively, the wound healing. Histopathology was used as the gold standard. LTW skin demonstrated better healing than sutured skin, exhibiting minimal hyperkeratosis, minimal collagen deposition, near-normal surface contour, and minimal loss of dermal appendages.

7561-41, Poster Session

Changes of collagen, elastin, and tryptophan fluorescence in laser welded porcine aorta tissues

C. Liu, W. Wang, V. Kartazaev, The City College of New York (United States); H. Savage, The New York Eye and Ear Infirmary (United States); R. R. Alfano, The City College of New York (United States)

The emission spectra of welded and non-welded (normal) porcine aorta tissues were measured on both sides of tunica intima and adventitia. The tunable Forsterite laser and Cr4+: YAG laser with wavelengths of 1250nm, 1455nm and 1460nm were used to weld porcine aorta tissue.

Three emission bands emitted from three fluorophores were studied under different welding and excitation conditions. The 395nm band is associated with the emission from the structural proteins of collagen type III and type I. The 445nm band obtained with excitation wavelength of 340nm is associated with the emission of the structural protein of elastin. The 350nm band recorded with excitation wavelength of 300nm is associated with the amino acid of tryptophan. The relative emission intensities of collagen, elastin and tryptophan at their fluorescence peaks were found changed with laser tissue welding wavelengths indicating the change of contents of those tissue molecules.

The ratio of emission peak intensity of collagen to that of elastin increases by 13% as compared to the normal aorta tissue at the tunica intima side. For the tunica adventitia side of aorta tissue, this ratio increases by 38% in comparison with the normal tissue. These changes indicate that content of collagen increases relative to elastin due to laser tissue welding. The peak fluorescence intensity of tryptophan for both sides of tunica intima and adventitia was found increase significantly in comparison with the normal tissue when the optimum laser welding wavelength of 1455 nm was used. These effects will be presented and discussed.

7561-42, Poster Session

Optical birefringence measurements of aorta tissues

G. C. Tang, W. B. Wang, Y. Pu, R. R. Alfano, Institute for Ultrafast Spectroscopy and Lasers (United States)

The optical birefringence of porcine aortic tissues including heated and non-heated tissues was measured using polarization technique. The orientation of the samples was set parallel to the direction of blood flow as the axis angle of zero degree. The aorta tissue sample was placed between a polarizer and an analyzer. The polarizer was rotated from 0 to 360 degrees relative to the polarization direction of analyzer to measure birefringence of the tissue with a fixed orientation of tissue.

For the non-heated porcine aortic tissue, the transmitted intensities showed oscillatory pattern with maxima and minima. The maxima are found shift to different polarizer angles when the orientation of the tissue was changed to 0, 22.5 45, 67.5 and 90 degrees, respectively. The result demonstrates that the aorta tissue shows similar properties as a birefringence crystal. This result is expected because of alignment of the elastin and collagen fiber structure. The aorta has a ordered structure of elastin and collagen fibers which produce a well defined optic axis. The fiber structure makes the aorta tissue behave like a birefringence crystal acausing optical birefringence. For the heated samples, the transmitted maximum intensities are located at a same angle of the rotating polarizer when the tissue orientation was changed. This result indicates that the heated tissues became denaturized and the order of the fibers and the native birefringence of tissue disappeared.

The measurements indicate that the birefringence status of tissue may

TEL: +1 360 676 3290 · +1 888 504 8171 · customerservice@spie.org

Conference 7561: Optical Biopsy VIII



have potential applications for measuring and monitoring changes of tissue structure due to burning, plastic surgery, laser tissue welding and wound healing.

7561-43, Poster Session

Development of optical mammography based on analysis of time-resolved photon path distribution

Y. Ueda, D. Yamashita, K. Yoshimoto, E. Ohmae, T. Suzuki, T. Yamanaka, Hamamatsu Photonics K.K. (Japan); H. Ogura, C. Teruya, H. Nasu, E. Imi, H. Sakahara, Hamamatsu Univ. School of Medicine (Japan); M. Oda, Y. Yamashita, Hamamatsu Photonics K.K. (Japan)

A diffused optical mammography composed of a 48-channel time-resolved spectroscopy system is being developed for breast cancer diagnosis. The system utilizes the time-correlated single photon counting method and the detector modules and the signal processing circuits were custom made to obtain a high signal to noise ratio and a high temperature stability with a high temporal resolution. Pulsed light generated by a Ti:Sapphire laser was irradiated to the breast, and the transmitted light was collected by the optical fibers placed on the surface of a hemisphere gantry filled with an optical matching fluid. The system acquires the time-resolved data with 12 picoseconds temporal resolution and the acquisition time for the both breasts was within 15 minutes.

Prior to the measurement of the patient's breast, the optical matching fluid without the breast were measured as a background data. These data were also used to correct for the influence of the system instrumental function (IF), cutting through the cumbersome procedure of IF measurements.

To reconstruct a 3D image of the breast, we employed a method using time-resolved photon path distribution (time-resolved PPD) based on the assumption that scattering and absorption are independent of each other. As it is not necessary to recalculate the PPD corresponding to change in the absorption, we can obtain the reconstructed image quickly.

The clinical research was started from January 2007. In a comparative study with conventional modalities, the breast cancers were detected as optically higher absorption regions. Moreover, it was suggested that the optical mammography is useful in monitoring the effect of chemotherapy.

7561-50, Poster Session

Application of NIR fluorescent markers to quantify expression level of HER2 receptors in carcinomas in vivo

V. V. Chernomordik, M. Hassan, S. Lee, R. Zielinski, J. Capala, A. H. Gandjbakhche, National Institutes of Health (United States)

HER2 overexpression has been associated with a poor prognosis and resistance to therapy in breast cancer patients. However, up to now, quantitative estimates of this important characteristic have been limited to ex vivo ELISA essays of tissue biopsies and/or PET-based analysis. We aim at developing a novel approach in optical imaging, involving specific probes that do not interfere with the binding of the therapeutic agents, thus, excluding competition between therapy and imaging. Affibody-based molecular probes seem to be ideal for in vivo analysis of HER2 receptors using near-infrared optical imaging. The fluorescence intensity distributions, originating from specific markers in the tumor area, can reveal the corresponding fluorophore concentration. Our approach is to use temporal changes of the signal detected from a fluorescence contrast agent, conjugated with HER2-specific Affibody molecules as a signature to monitor the in vivo status of the receptors in mice with different HER2 over-expressed tumor models. Developed kinetic model, taking into account potential saturation of the bound ligands in the tumor area due to HER2 receptor concentration, is

suggested to analyze relationship between tumor cell characteristics, i.e., HER2 overexpression, obtained by traditional ("golden standard") ex vivo methods (ELISA, FISH), and parameters, directly estimated from the series of images in vivo. Observed good correlation between these parameters and HER2 overexpression indicates that our approach can be potentially applied to quantification of HER2 receptors concentration in vivo.

7561-01, Session 1

Conjugated nanoparticle labeled threedimensional cellular imaging using multiphoton endomicroscope

H. Choi, S. Chen, Massachusetts Institute of Technology (United States); J. Moon, Florida International University (United States); M. L. Culpepper, P. T. C. So, Massachusetts Institute of Technology (United States)

We have developed a miniaturized multiphoton endomicroscope to assist the diagnosis of epithelial cancers in organs such as the skin. colon. esophagus, oral cavity and cervix. Cancers in these category is located a few hundred microns deep in the tissue and is optically accessible using multiphoton endomicroscope at the early stage of these diseases. The endomicroscope consists of a two axes MEMS-fabricated thermal actuator, a fiber resonator, a micro prism and a GRIN lens that are all assembled at the distal end of the endoscope for three dimensional volume scanning of the target. Near IR femtosecond Ti-Sa pulsed laser beam is delivered to the distal end through a double clad photonic crystal fiber of which the excitation beam is delivered through the single mode inner core and the fluorescence signal from the tissue is delivered back to the photon detector confined by the multimode inner cladding. The instrument field of view is measured to be 200 m in lateral and 100 m in depth directions respectively. While the endoscopic multiphoton imaging using the endogenous fluorophores such as NAD(P)H and protoporphyrin IX remains challenging due to the low two photon cross-section of these makers, we can increase the signal to noise ratio significantly with recently developed biocompatible conjugated polymer nanoparticles (CPNs) which have two photon cross-section that is comparable with quantum dots. Experimental demonstration is performed by imaging cancer cells labeled with CPNs targeting surface EGFR and folate acid receptors using the two-photon endomicroscope.

7561-02, Session 1

Visualization of epithelial morphology using autofluorescence microscopy under ultraviolet excitation

B. Lin, Univ. of California, Davis (United States); S. Urayama, R. M. G. Saroufeem, Univ. of California, Davis Medical Ctr. (United States); D. L. Matthews, Univ. of California, Davis (United States); S. G. Demos, Lawrence Livermore National Lab. (United States) and Univ. of California, Davis (United States)

Visualization of microscopic changes in epithelial tissue is critical for early carcinoma diagnosis. A significant limitation to traditional white light endoscopy is the inability to image cellular epithelial morphology. We have recently demonstrated that autofluorescence (AF) microscopy under ultra violet (UV) excitation provides a method to image epithelial microstructures without contrast agents, sectioning techniques, or tissue preparation. In this work, we explore the origin at the microscopic level of the AF signal that enables imaging of the epithelial cells and their organization. This knowledge supports the development of designing criteria for future implementation of this technology in vivo.

IRB-approved human tissue biopsy specimens were used to perform this work. Multispectral AF microscopy images were acquired with a prototype hyperspectral microscope system to better understand the



contribution and emission characteristics of the cellular components observed in the AF images. These results complemented spectroscopic measurements at the tissue level and suggest that the superficial propagation depth under UV excitation is the main reason for attaining visualization of epithelial cellular morphology using conventional widefield microscopy.

Image analysis results from biopsy specimens obtained from 60 patients suggest that this technology has the potential to provide information for in vivo diagnostics. Adaptation of UV AF microscopy into an endoscope probe for real-time in vivo imaging may be feasible if the UV exposure is kept below the MPE limit. To address this issue, a bench top microendoscope system was developed to test design criteria and operational parameters.

7561-03, Session 1

Advances in handheld spectral sensors and systems

J. M. Eichenholz, Ocean Optics, Inc. (United States)

Spectrometer system designs have evolved rapidly over the last decade after a major paradigm shift occurred as spectroscopy systems advanced from bulky lab based instruments to the modern compact, flexible, and portable instruments we see today. Previously, these complicated tabletop laboratory instruments required controlled conditions to function and were extremely expensive. We changed the paradigm by introducing a new class of fiber coupled spectrometers that combined innovative compact designs with low-cost detectors developed for high volume commercial applications like barcode scanners and fax machines. No longer did users have to carry the sample to the spectrometer, now they could take the spectrometer to the sample enabling thousands of new applications. This innovation has been particularly helpful to the field of biophotonics. Over time, the performance and benefits of these compact systems have improved. The recent development of CMOS sensors and extremely powerful compact microprocessors has enabled a new phase of even more compact spectroscopy systems. In this talk, we'll discuss our new handheld and portable miniature optical spectroscopy systems that are enabling several real world biomedical applications. We will also cover the future trends and directions in the next generation of ultracompact wireless spectral sensors including the new colorBUG sensor designed to wirelessly interface with the Apple iPhone.

7561-04, Session 1

Portable point-detection fluorescence spectroscopy system for brain cancer diagnostics

Q. Liu, J. Li, Duke Univ. (United States); S. Li, G. Grant, Duke Univ. Medical Ctr. (United States); T. Vo-Dinh, Duke Univ. (United States)

We report the use of a portable point-detection fluorescence spectroscopy system and corresponding data analysis algorithm for brain cancer diagnostics. Our system employs two compact cw diode lasers, one at 407 nm and the other at 446 nm, as the light source. The light beams from two lasers are coupled to the excitation channel of a custom built fiber-optic probe by use of a dichroic mirror. The lasers are pulsed so that background spectra can be taken when the laser is off and its effect can be removed from sample spectra. In this manner the system was immune to ambient light. The system was used to collect fluorescence spectra from both normal tissues and tumors in a rat brain tumor model. The spectra were analyzed using a spectral filtering modulation method developed by our group to derive hemoglobin concentration and oxygenation and fluorescence redox ratio. The results of this animal study demonstrated that this portable system can be potentially used in a brain tumor surgery to demarcate the boundary between brain tumor and surrounding normal tissue.

7561-05, Session 1

Spectral filtering modulation method for imaging hemoglobin concentration and oxygenation based on fluorescence ratios

Q. Liu, Nanyang Technological Univ. (Singapore); T. Vo-Dinh, Duke Univ. (United States)

We proposed a method to image hemoglobin concentration and oxygenation based on fluorescence ratios. This method consists of two steps. In the first step, total hemoglobin concentration is determined by comparing a ratio of fluorescence intensities at two emission wavelengths to a calibration curve. The second step is to estimate oxygen saturation by comparing a double ratio that involves three emission wavelengths to another calibration curve that is a function of oxygen saturation for known total hemoglobin concentration. Theoretical derivation shows that the ratio in the first step is linearly proportional to total hemoglobin concentrations and the double ratio in the second step is related to both total hemoglobin concentration and hemoglobin oxygenation for the chosen fiber-optic probe geometry. Experiments on synthetic fluorescent tissue phantoms, which included hemoglobin with both constant and varying oxygenation as the absorber, polystyrene spheres as scatterers and flavin adenine dinucleotide (FAD) as the fluorophore, were carried out to validate the theoretical prediction. Because our method only involves imaging at a few emission wavelengths, it is suitable for clinical measurements in which fast data acquisition and processing is critical.

7561-06, Session 1

UV extended supercontinuum source for fluorescence detection of biological and chemical molecules

R. R. Alfano, V. A. Kartazaev, I. S. Zeylikovich, B. B. Das, The City College of New York (United States)

The supercontinuum (SC) - a white light source due to the nonlinear laser interaction in materials covers the UV through mid-IR has many applications. It is ideal as an excitation and probe source for spectroscopy in biology, chemistry, and condensed matter physics; and for NLO multiphoton, CARS microscopy and medical imaging. In this report, we demonstrate that the bandwidth of the supercontinuum spectrum generated by femtosecond Ti:Sapphire laser in photonic crystal fiber (PCF) can be increased by using small core diameter PCF with ZD wavelength shorter 600nm into the UV. We generate flat spectrum that spans from 350 to 1000nm with modulation less than 10 dB and the maximum spectral intensity in the region 350 - 450nm. Spectral intensity in UV spectral region can be increased by employing dual-wavelength pumping using second harmonic of Ti:Sapphire laser as a second pumping wavelength for generating cross phase modulation. The SC was used here as an excitation source for spectroscopy.

Fluorescence spectra were detected from dye molecules and native molecules in tissues samples with excitation from wavelengths extracted from ultrafast SC light in the spectral range between 350 - 500nm using narrow bandpass filters and will be presented. A Streak Camera was used for time-resolved fluorescence measurements.

7561-07, Session 1

Multi-excitation fluorescence spectroscopy for analysis of non-alcoholic fatty liver disease

V. R. Sauvage, Imperial College London (United Kingdom); H. Nguyen Thanh, Imperial College London (United Kingdom) and Institut d'Alembert, École Normale Supérieure de Cachan (France); R. Hill, D. Concas, A. Levene, M. Thursz, R. Goldin. Q.



Anstee, D. S. Elson, Imperial College London (United Kingdom)

Non-alcoholic fatty liver disease (NAFLD) includes a broad spectrum of abnormalities including simple steatosis and non-alcoholic steatohepatitis (NASH), which can progress to cirrhosis and hepatocellular carcinoma. There is a need to identify those livers most prone to primary non-function, which is associated with steatosis and increased tissue oxidative stress. Blood tests and imaging studies are insensitive, nonspecific indicators of NAFLD-related liver damage, while liver biopsies are diagnostically sensitive but cannot distinguish NAFLD from other causes of fatty liver disease such as alcohol abuse. Recent studies have shown that autofluorescence spectroscopy is a powerful approach for real-time, minimally invasive liver function characterization. Among numerous endogenous fluorophores in the liver, NAD(P)H and vitamin A have been shown to provide autofluorescent information on the metabolic function. Three groups of 5 mice were compared: (A) male Db/Db mice fed Methionine/Choline deficient diet for 8 weeks (fibrosing steatohepatitis); (B) Db/Db mice fed normal chow (steatosis); (C) Db/m mice fed chow (normal liver). Animals were culled by exsanguination under general anesthesia and liver tissue harvested. Fluorescence spectra were recorded with a probe comprised of one excitation and six emission optical fibers (core diameter 200 µm, NA 0.22). Two laser diodes provided excitation light at 375 nm and 405 nm, and an imaging spectrograph system distinguishes the fluorescence spectra. At 375nm excitation, the mean 465nm:530nm fluorescence ratio was significantly lower in steatohepatitis than in steatosis or normal tissue (p<0.001). These data were correlated to histological, biochemical and TBARS measurements (p=0.004) of liver damage.

7561-08, Session 1

Optical spectroscopy approach for the predictive assessment of kidney functional recovery following ischemic injury

R. N. Raman, Lawrence Livermore National Lab. (United States); C. Pivetti, UC Davis Medical Ctr. (United States); A. Rubenchik, Lawrence Livermore National Lab. (United States); D. Matthews, C. Troppmann, UC Davis Medical Ctr. (United States); S. Demos, Lawrence Livermore National Lab. (United States)

Tissue that has undergone significant yet unknown amount of ischemic injury is frequently encountered in organ transplantation as well as trauma clinic. With no reliable real-time method of assessing the degree of injury incurred in tissue, surgeons generally rely on visual observation which is subjective. In this work, we investigate the use of optical spectroscopy methods as a potentially more reliable approach. Previous work by various groups was strongly suggestive that tissue autofluorescence from NADH obtained under UV excitation is sensitive to metabolic response changes. To test and expand upon this concept, we monitored autofluorescence and light scattering intensities of injured vs. uninjured rat kidneys via multimodal imaging under 355 nm, 325 nm, and 266 nm excitation as well as scattering under 500 nm illumination. 355 nm excitation was used to probe mainly NADH, a metabolite, while 266 nm excitation was used to probe mainly tryptophan to correct for non-metabolic signal artifacts. The ratio of autofluorescence intensities derived under these 2 excitation wavelengths was calculated and its temporal profile was fit to a relaxation model. Time constants were extracted, and longer time constants were associated with kidney dysfunction. Analysis of both the autofluorescence and light scattering images suggests that changes in microstructure tissue morphology, blood absorption spectral characteristics, and pH contribute to the behavior of the observed signal which may be used to obtain tissue functional information and offer predictive capability.

This work was performed under the auspices of the U.S. Department of Energy by Lawrence Livermore National Laboratory under Contract DE-AC52-07NA27344.

7561-09, Session 1

Rotational dynamics and polarization anisotropy of receptor-targeted contrast agents in cancerous and normal prostate tissues studied by time-resolved fluorescence polarization

Y. Pu, W. Wang, R. Alfano, Institute for Ultrafast Spectropscopy and Lasers (United States)

The dynamics of polarized fluorescence of the receptor-targeted Cybesin and Cytate, in prostate tissues was studied using time-resolved spectroscopy. An analytical model was introduced to describe the time-resolved polarized fluorescence kinetics of the contrast agents in prostate tissue. The time-resolved polarization anisotropy of light emitted from contrast agents in prostate tissues are denoted by two components: (1) a static component formed by the emission of the cell-bonded Cybesin (Cytate) molecules without rotation; and (2) a time-dependent component formed by the emission of the un-bonded molecules (with rotational motion) in the body liquid of prostate tissue.

The rotational times and fluorescence polarization anisotropies of the contrast agents in stained cancerous and normal prostate tissues were extracted using the analytical model with the measured time-resolved polarized fluorescence data. The differences of rotational time and static polarization anisotropy were observed for Cybesin in cancerous tissue by 1.4 times and 10 times larger than those in normal prostate tissue, respectively. This observation reflects the changes of micro-structures of cancerous and normal tissues, and much larger portion of conjugated contrast agents and tissue cells than that in normal tissue. These differences may be used to develop better optical methods for prostate cancer detection.

7561-11, Session 1

Stokes shift spectroscopy for breast cancer diagnosis

E. Jeyasingh, Jamal Mohamed College (India); A. Prakashrao, G. Singravelu, Anna Univ. (India)

The objective of this study is to assess the diagnostic potential of stokes shift (SS) spectroscopy (SSS) for normal and different pathological breast tissues such as fibroadenoma and infiltrating ductal carcinoma. The SS spectra were measured by simultaneously scanning both the excitation and emission wavelengths while keeping a fixed wavelength interval delta lambda between them. This SSS technique simplifies emission spectrum and provides more sharp spectral signatures of the endogenous fluorophores in the tissues. SS spectra were measured from 30 biopsies from 20 patients in vitro. In this study, SS spectra of normal (n=10), fibroadenoma (n=10) and infiltrating ductal carcinoma (n=10) were measured by scanning both excitation and emission wavelength simultaneously with a fixed wavelength of interval delta lambda = 20 nm. Characteristic, highly resolved peaks and significant spectral differences between normal and different pathological breast tissues were observed. The observed spectral peaks were tentatively identified from measured spectra of standard fluorophores. The SS spectra of normal, fibroadenoma and infiltrating ductal carcinoma of breast tissues shows the distinct peaks around 300, 350, 450, 500 and 600 nm may be attributed to tryptophan, collagen, NADH, flavin and porphyrin respectively. Using SSS technique one can obtain all the key fluorophores in a single scan and hence they can be targeted as a tumor markers in this study. To quantify the observed spectral differences between normal and different pathological diseased breast tissues are verified by statistical analysis. The detail experiment results of the SSS technique for breast cancer diagnosis and the results of the statistical analysis to be discussed.



7561-12, Session 2

Excitation energy transfer in photosynthesis: coherent or incoherent or both

G. Govindjee, Univ. of Illinois (United States)

Photosynthesis converts solar energy into chemical energy. It provides food and oxygen; and, in future, it could provide bio-alcohol and even hydrogen. To exploit such a highly efficient capture of energy requires an understanding of the fundamental physics. The process is initiated by photon absorption, followed by highly efficient and extremely rapid transfer and trapping of the excitation energy. We first review early fluorescence experiments on in vivo Energy Transfer by Lou Duysens, and later by one of us (G), which were undertaken to understand the mechanism of such efficient energy capture. A historical synopsis is given of experiments and interpretations by others that dealt with the question of how energy is transferred from the original location of photon absorption in the photosynthetic antenna system into the reaction centers, where it is converted into useful chemical energy. We conclude by examining some current models concerning the roles of coherent excitons and incoherent hopping in the exceptionally efficient transfer of energy into the reaction center.

7561-13, Session 2

Quantum effects in biological systems

M. Sarovar, Univ. of California, Berkeley (United States)

Identification of non-trivial quantum mechanical effects in the functioning of biological systems has been a long-standing and elusive goal in the fields of physics, chemistry and biology. Recent progress in control and measurement technologies, especially in the optical spectroscopy domain, have made possible the identification of such effects. I will review some recent experimental results and theoretical predictions, focussing on quantum effects in photosynthetic light harvesting systems. Recent exciting progress on the experiment and theory fronts suggest that non-trivial quantum mechanical effects are present, and moreover important, in the functioning of some biological structures.

7561-14, Session 2

Coherent excitons in the primary PS units

G. R. Fleming, Univ. of California, Berkeley (United States).

7561-15, Session 3

Multispectral imaging of tissue autofluorescence including UVB and UVC excitation

T. Renkoski, U. Utzinger, The Univ. of Arizona (United States)

Multispectral imaging for early detection of cancer in epithelial tissues will be discussed. Preclinical results and device details are presented on a multispectral tissue imager incorporating excitation light that is filter-selectable from 270 nm to 600 nm. UV-transmitting optics allow efficient autofluorescence imaging over this UV/VIS range using high-sensitivity CCD. Excitation in the UVB (320 nm - 280 nm) and UVC (280 nm - 100 nm) is necessary for targeting amino acids such as tryptophan, tyrosine, and phenylalanine, which have peak excitations in the 260 - 280 nm range. The ability to excite in this range is expected to bring gains in specificity and sensitivity when indentifying cancer and pre-cancer in tissues. Two computer-controlled filter wheels are used. One wheel filters excitation light, and a second filters the emission light. Interference filters have been selected according to known excitation and emission fluorescence peaks of tissue constituents. In addition to amino acids,

these include the metabolic cofactors NADH and FAD, collagens and elastin. The imaging system has been designed for use in the operating room during open surgery. Such use is facilitated by the housing of the system in a mobile cart, the placement of the camera on an extendable arm, and the use of fiber optic bundle for delivery of excitation light. Using ultraviolet light on living tissue can be damaging, and safety considerations such as exposure thresholds will be discussed. Plans for a clinical study using the multispectral imager to differentiate epithelial tissues in different disease stages will be explained.

7561-16, Session 3

Development of a multiview multispectral 3D tomographic small animal in vivo fluorescence imaging system

J. R. Mansfield, R. M. Levenson, C. M. Gardner, CRi (United States)

Fluorescence-based molecular imaging in small animals is having a major impact on drug development and disease research. There have been a number of stages in the development of imaging systems for in vivo fluorescence systems, ranging from simple monochrome epi-fluorescent imaging systems, to multispectral imaging systems which can separate fluorophores of interest from tissue autofluorescence, to systems which attempt to determine three-dimensional information about the distribution and concentration of fluorophores in mice. While useful in a range of experiments, epi-fluorescence imaging systems overemphasize the contributions of fluorophores near the surface and under-emphasize signals from deeper tissues. Transillumination methodologies can aid in the detection and quantitation of deeper signals, and there are a number of systems which utilize this. Multiple views of the animal can aid in the determination of the three-dimensional distribution of fluorophores and tomographic reconstructions. However, to date, no system combines multispectral imaging for both excitation and emission spectroscopy with an ability to image multiple views of the animal along with control of the direction of the excitation light. We describe here a multi-view, multispectral 3D tomographic small animal in vivo fluorescence imaging system that is designed around a multi-view mirror system which allows the simultaneous viewing of 4 sides of a mouse. The excitation light, under control of a digital micromirror device, can be directed onto any one of four sides of the animal. In addition, the system is equipped to to perform both excitation and emission imaging spectroscopy, resulting in an excitation-emission map of the animal at each pixel on each of the sides of the animal. These data are then combined with a sophisticated system for determining the position of the surface of the animal and a three-dimensional tomographic reconstruction of the distribution of fluorophores inside the animal.

7561-17, Session 3

Telegrapher-based model for fluorescence enhanced optical tomography in small volume

R. Roy, The Univ. of Texas-Pan American (United States)

Small animal optical tomography has potential for streamlining drug discovery and preclinical investigation of drug candidates. However, accurate modeling of photon propagation in small animals is critical to quantitatively obtain accurate tomographic images. The diffusion approximation to the Boltzmann transport equation is commonly used for biomedical optical diagnostic technique in large volumes. Unfortunately, this approximation has significant limitations to accurately predict radiative transport in turbid small media and also in a media where absorption is high compared to scattering systems. A radioactive transport equation that describes the density of photons as a function of position and direction is best suited for photon propagation in human tissues. However, such models are quite expensive computationally. To alleviate these difficulties, we use the telegrapher equation in the frequency domain for fluorescence-enhanced optical tomography

Conference 7561: Optical Biopsy VIII



problems in small geometries. The telegrapher-based model can accurately and efficiently predict ballistic as well as diffusion-limited transport regimes which could simultaneously exist in small animals. The accuracy of telegrapher-based model is tested by comparing with the diffusion based model using stimulated data in a small volume. The use of the telegrapher equation shows promise in solving small volume problems. Specifically, this model will allow using small source detector separation and media with high absorption and small scattering. For fluorescence-enhanced, optical tomography problems, this may allow the development of image reconstruction with a negligible computation time compared to the radiative transport equation. Our results provide a significant test of the applicability of the telegrapher equations in small volumes for fluorescence-enhanced optical tomography problems. This work demonstrates the use of the telegrapher-based model in small animals optical tomography problems.

7561-18, Session 3

Autofluorescence visualization of fallopian tube carcinogenesis

P. M. Lane, S. Au, BC Cancer Research Ctr. (Canada); J. McAlpine, University of British Columbia (Canada); B. Gilks, D. Miller, The Univ. of British Columbia (Canada); C. E. MacAulay, The BC Cancer Research Ctr. (Canada)

Each year ovarian cancer accounts for approximately 114,000 deaths worldwide. The overall 5-year survival rate for women with advanced staged disease is approximately 20-25% and despite advances in ovarian cancer biology, surgical technique, and chemotherapy, the survival rate has not changed significantly in the last three decades. Autofluorescence imaging is used clinically for the detection of precancers in the lung and oral cavity and may also be useful for the early detection of ovarian cancers. Several recent studies have implicated the fallopian tube in the pathogenesis of ovarian and/or peritoneal serous carcinoma. The lumen of the fallopian tube is accessible via endoscopy and is also a naturally occurring conduit to the ovaries and pelvic peritoneum. We present fluorescence images from freshly resected fallopian tubes with corresponding pathology to support the use of autofluorescence imaging for the early detection of intraepithelial lesions. We also present evidence implicating the fallopian tube in the pathogenesis of ovarian carcinoma.

7561-19, Session 3

Polarized fluorescence study in human cervical tissue: change in autofluorescence through different excitation wavelengths

R. Singh, K. K. S. Tomar, P. Shukla, A. Pradhan, Indian Institute of Technology Kanpur (India); R. Gupta, S. Jain, C. Pantola, A. Agarwal, K. Pandey, Ganesh Shanker Vidhyarthi Memorial Medical College (India)

This study aims towards applying the intrinsic fluorescence technique, extracted from polarized fluorescence, to detect subtle biochemical changes occurring during the progression of cancer from human cervical tissue samples. The efficacy of this technique, earlier validated through tissue phantoms, is tested in human cervical tissues by comparing the biochemical changes for diagnostic purpose at different wavelengths. It was observed that sensitivity and specificity of intrinsic fluorescence technique is high at 325 and 370nm for Collagen and NADH respectively in comparison to 350nm excitation wavelength. This information can provide a guiding path for designing a probe for clinical purpose.

In the current project a comparative study of co- & cross- polarized and intrinsic fluorescence in cervical tissues has been done by extracting intrinsic fluorescence spectra from polarized fluorescence spectra recorded for 325nm, 350 and 370nm excitation wavelengths. It was observed that better decoupling can be seen between collagen and

NADH peaks for 325nm excited intrinsic spectra in comparison to spectra extracted at 350nm excitation wavelength. In addition it was also observed that intrinsic fluorescence provides better sensitivity for collagen. Further investigations show that NADH is the dominant fluorophore with negligible effect of collagen, with 370nm excitation. Here the detection sensitivity is higher than that of 350nm excited NADH spectra. It is pertinent to note that the co- and cross-polarized fluorescence do not display the high sensitivity obtained through extracted intrinsic fluorescence.

It may be concluded that decoupled information at 325 and 370nm wavelengths for collagen and NADH respectively, through intrinsic fluorescence provides better diagnostic parameters for early detection of cervical dysplasia.

7561-20, Session 3

Near field scanning optical microscopy

A. Lewis, Hebrew Univ. of Jerusalem (Israel)
No abstract available.

7561-21, Session 4

Photoacoustic tomography: high-resolution in vivo imaging of optical contrast at new depths

L. V. Wang, Washington Univ. in St. Louis (United States)

Functional and molecular imaging has been developed by physically combining non-ionizing electromagnetic and ultrasonic waves via energy transduction. Key applications include early-cancer detection and functional imaging. Unfortunately, electromagnetic waves in the non-ionizing spectral region do not penetrate biological tissue in straight paths as x-rays do. Consequently, high-resolution pure optical imaging (e.g., confocal microscopy, two-photon microscopy, and optical coherence tomography) of biological tissue is limited to depths within one optical transport mean free path (~1 mm in the skin). Ultrasonic imaging, on the contrary, provides good image resolution but suffers from strong speckle artifacts as well as poor contrast in early-stage tumors. Ultrasound-mediated imaging modalities have been developed by combining electromagnetic and ultrasonic waves synergistically to overcome the above problems. In photoacoustic tomography (PAT), a pulsed laser beam illuminates the biological tissue and generates a small but rapid temperature rise, which causes the emission of ultrasonic waves as a result of thermoelastic expansion. The short-wavelength ultrasonic waves are then detected to form high-resolution tomographic images. Thermoacoustic tomography (TAT) is similar to PAT except that low-energy radio-frequency pulses, instead of laser pulses, are used. Although the long-wavelength radio-frequency waves diffract rapidly in the tissue, the short-wavelength ultrasonic waves provide high spatial resolution.

7561-22, Session 4

Longitudinal optical imaging of tumor metabolism and hemodynamics

M. C. Skala, A. Fontanella, L. Lan, J. Izatt, M. Dewhirst, Duke Univ. (United States)

An important feature of tumor hypoxia is its temporal instability, or "cycling hypoxia". The primary consequence of cycling hypoxia is increased tumor aggressiveness and treatment resistance beyond that of chronic hypoxia. Longitudinal imaging of tumor metabolic demand, hemoglobin oxygen saturation and blood flow would provide valuable insight into the mechanisms and distribution of cycling hypoxia in tumors. Fluorescence imaging of metabolic demand via the optical

Conference 7561: Optical Biopsy VIII



redox ratio (fluorescence intensity of FAD/NADH), absorption microscopy of hemoglobin oxygen saturation and Doppler optical coherence tomography (OCT) of vessel morphology and blood flow were combined to non-invasively monitor changes in oxygen supply and demand in the mouse dorsal skin fold window chamber tumor model every 6 hours for 36 hours. Biomarkers for metabolic demand, blood oxygenation and blood flow were all found to significantly change with time (p<0.05). These variations in oxygen supply and demand are superimposed on a significant (p<0.05) decline in metabolic demand with distance from the nearest vessel. Significant (p<0.05), but weak (r \leq 0.5) correlations were found between the hemoglobin oxygen saturation, blood flow and redox ratio. These results indicate that cycling hypoxia depends on both oxygen supply and demand, and that non-invasive optical imaging could be a valuable tool to study therapeutic strategies to mitigate cycling hypoxia, thus increasing the effectiveness of radiation and chemotherapy.

7561-23, Session 4

Multimodality optical imaging combining optical coherence tomography (OCT) and fluorescence lifetime imaging (FLIM) for morphological and biochemical tissue characterization

S. Shrestha, B. Applegate, P. Pande, J. A. Jo, Texas A&M Univ. (United States)

Here we report on our current efforts to simultaneously quantify both morphological and biochemical tissue information by combining optical coherence tomography (OCT) and fluorescence lifetime imaging (FLIM). The Fourier domain OCT module is built around a custom designed high speed spectrometer (bandwidth of 102 nm, 3 dB rolloff of 1.2 mm, lines rates of up to 59 kHz). A 40 nm bandwidth SLED centered at 830 nm provided an axial resolution of 7.6 um for OCT. The objective lens provided 10 um lateral resolution for OCT and 40 um for FLIM. Lateral OCT and FLIM beam scanning was accomplished using a set of galvo mirrors. The FLIM module excites and collects the fluorescence decay signal pixel by pixel coincident with OCT A-line collection. Each 2-D FLIM image has a corresponding coregistered OCT volume. Tunable excitation for FLIM (350-450 nm) was generated by a frequency doubled Ti:Al2O3 laser. The fluorescence signal was detected with a MCP-PMT coupled to a 1.5 GHz digitizer (250 ps temporal resolutions). In addition, simultaneous multispectral time-resolved fluorescence detection was achieved by separating the fluorescence emission in three bands using a series of dichroic mirrors and bandpass filters, and launching each band into three fibers of different lengths (providing a time delay of 50 ns among bands) focused onto the MCP-PMT. The multimodality OCT/FLIM imaging system has been validated on biological tissue. Future efforts include evaluating its potential for oral cancer diagnosis and intravascular detection of atherosclerotic vulnerable plaques.

7561-24, Session 4

Multispectral imaging techniques observing the dynamic changes in the hemoglobin concentrations as diagnostic tool for diseased tissues

J. H. Klaessens, H. J. Noordmands, R. de Roode, R. M. Verdaasdonk, Univ. Medical Ctr. Utrecht (Netherlands)

Tissue oxygenation imaging is a promising diagnostics tool to study the changes and dynamics of tissue perfusion reflecting pathologic and/or physiologic conditions of tissue. In clinical settings, imaging of local oxygenation or blood perfusion variations can be useful for e.g.; detection of skin cancer, detection of early inflammation, effectiveness of peripheral nerve block anesthesia, study of the process of wound healing or localization of the cerebral area causing an epileptic attack.

In this study, two oxygenation imaging methods based on multi-spectral techniques were evaluated: one system consisting of a CCD camera in combination with a Liquid Crystal Tunable Filter (420 - 730 nm) and a broad band (white) light source, while the second system was a CCD camera in combination with a tunable multi-spectral LED light source (450-890nm).

By collecting narrowband images at selected wavelengths, concentration changes of the different chromophores at the surface of the tissue (e.g. dO2Hb, dHHb and dtHb) could be calculated using the modified Lambert Beer equation. In vivo measurements were obtained during skin oxygen changes induced by temporary arm clamping to validate the methods and algorithms. Functional information from the tissue surface was collected, in non-contact mode, by imaging the hemodynamic and oxygenation changes just below that surface.

Both multi-spectral imaging techniques show promising results for detecting dynamic changes in the hemoglobin concentrations. The algorithms need to be optimized and the data collecting/processing has to be developed to real-time imaging method.

7561-25, Session 4

Fast hyperspectral imaging system based on Fourier transform spectroscopy incorporating a coherent fiber bundle for early detection of squamous cell carcinoma (SCC)

T. Tseng, W. Hsu, C. Chen, K. Sung, National Taiwan Univ. (Taiwan)

In recent years, researchers make lots of efforts in developing optical spectroscopy and microscopy techniques for early detection of cancer. There have been many delicate fiber optic probes integrated with optical spectroscopes or microscopes to obtain tissue optical properties or images respectively for clinical diagnosis. For efficient acquisition of spectral and imaging data simultaneously, we combine an imaging Fourier transform spectroscope developed in our laboratory with a fiber bindle to construct a hyperspectral imaging system which has the capability to map the spatial distribution of tissue optical properties obtained with reflectance or fluorescence spectroscopy. We investigate the effects of alterations in tissue properties on the measured tissue spectra using Monte Carlo simulation models. For example, dysplastic epithelium shows different scattering and absorption coefficients from normal tissue and shows higher autofluorescence, both of which increase variations in the spatial distribution of tissue spectral features. Tissue phantoms mimicking squamous epithelium are constructed and used to demonstrate the feasibility of the fiber-based hyperspectral imaging system to probe large tissue areas at multiple depths. We expect that the fiber-based hyperspectral imaging system could be successfully applied to in-vivo tissue spectroscopic measurement for clinically screening neoplasia, classifying SCC grades and precisely determining tumor boundary during surgical tumor removal in the future.

7561-26, Session 4

Tissue characterization by using narrow band imaging

K. Gono, Olympus Medical Systems Corp. (Japan)

Narrow band imaging (NBI) is an approach of "Image-Enhanced Endoscopy". Using spectrally narrowed illuminations of 415 nm and 540 nm highlight a capillary pattern within a superficial layer of mucosa. In addition, mucosal textures and micro morphologies are also enhanced. This talk will provide overviews of what signatures NBI highlights and its mechanisms. And we will discuss future directions of "Image-Enhanced Endoscopy".



7561-27, Session 4

Automated algorithm for breast tissue differentiation in optical coherence tomography images and its potential for breast biopsy guidance

M. Mujat, R. D. Ferguson, D. X. Hammer, C. Gittins, N. Iftimia, Physical Sciences Inc. (United States)

An automated algorithm for differentiating breast tissue types based on optical coherence tomography (OCT) data is presented. Eight parameters are derived from the OCT reflectivity profiles and their means and covariance matrices are calculated for each tissue type from a training set (48 samples) selected based on histological examination. A quadratic discrimination score is then used to assess the samples from a validation set. The algorithm results for a set of 89 breast tissue samples were correlated with the histological findings yielding specificity and sensitivity of 0.88. If further perfected to work in real time and yield even higher sensitivity and specificity, this algorithm would be a valuable tool for biopsy guidance and could significantly increase procedure reliability by reducing both the number of non-diagnostic aspirates and the number of false negatives. The application of the algorithm to automated interpretation of OCT data could have a significant impact on clinical translation of OCT. Even the reported level of accuracy in differentiating tissue types could increase the yield of the biopsy procedure if OCT is used as a guidance tool. With this simple technology the pathologist or clinician performing the biopsy will be able to guide the needle or the biopsy forceps to the most representative diagnostic area of the mass based on the instruments ability to determine the tissue type in real time. This will avoid unnecessary biopsy and increase the effectiveness of the procedure.

7561-28, Session 4

Lensless LEBS: a simplified geometry for lowcoherence enhanced backscattering (LEBS)

J. D. Rogers, V. Stoyneva, N. N. Mutyal, V. M. Turzhitsky, V. Backman, Northwestern Univ. (United States)

Low-coherence Enhanced Backscattering (LEBS) is a practical and sensitive method for measuring optical properties of scattering media. LEBS is a generalization of Enhanced Backscattering (EBS) where partial spatial coherence is used. The spatial coherence effectively limits the lateral separation of rays exiting the medium. LEBS can equivalently be described as the convolution of EBS peaks with the source function. LEBS is particularly suited to measurement of layered media such as tissue as it affords control of the signal's depth of penetration by limiting the lateral ray separation. A typical instrument for measuring LEBS incorporates a large number of lenses, apertures, and other optical components to deliver collimated, partially coherent illumination to the sample and collect and focus the angular profile of scattered light onto an imaging detector. Here we present a fascinating property of enhanced backscattering: phase conjugation of the incident wavefront. By considering LEBS as a phase conjugation, it is shown that much of the optical path is unnecessary and the phenomenon can be observed as a direct localization of light in three dimensions. This dramatic simplification in geometry can be applied to the design of a compact probe for in vivo measurements. Additionally, the spatial coherence of the illumination can be scanned by simply changing the distance to the object. The experimental observation of LEBS under a lensless geometry will be presented and the application to a probe design for in vivo measurements will discussed.

7561-29, Session 4

Diffuse reflectance spectroscopy of pre and post-treated oral submucous fibrosis: an in vivo study

S. Shanmugam, Anna Univ. (India); P. v. C, J. S, K. D, P. C, ; A. p, G. S, Anna Univ. (India)

Oral submucous fibrosis (OSF) is a high risk precancerous condition characterized by changes in the connective tissue fibers of the lamina propria and deeper parts leading to stiffness of the mucosa and restricted mouth opening, fibrosis of the lining mucosa of the upper digestive tract involving the oral cavity, oro- and hypo-pharynx and the upper two-thirds of the oesophagus. Optical reflectance measurements have been used to extract diagnostic information from a variety of tissue types, in vivo. We apply diffuse reflectance spectroscopy to quantitatively monitor tumour response to chemotherapy. Twenty patients with submucous fibrosis were diagnosed with diffuse reflectance spectroscopy and treated with the chemotherapy drug, Dexamethasone sodium phosphate and Hyaluronidase injection for seven weeks and after the treatment they were again subjected to the diffuse reflectance spectroscopy. The major observed spectral alterations on pre and post treated submucous fibrosis is an increase in the diffuse reflectance from 450 to 600 nm. And there is the red shift in the region of 530nm. Normal mucosa has showed lesser reflectance when compared to the pre and post-treated cases. The spectral changes were quantified and correlated to conventional diagnostic results viz., maximum mouth opening, tongue protrusion and burning sensation. The results of this study suggest that the diffuse reflectance spectroscopy may also be considered as complementary optical techniques to monitor oral tissue transformation.

7561-30, Session 4

Hyperspectral low-light camera for macroscopic imaging of biological samples

J. E. Hernandez, Norsk Elektro Optikk AS (Norway) and Univ. of Oslo (Norway); L. L. Randeberg, Norwegian Univ.of Science and Technology (Norway); T. Skauli, Norwegian Defence Research Establishment (Norway); I. Baarstad, T. Løke, Norsk Elektro Optikk AS (Norway)

Imaging spectroscopy, also known as hyperspectral imaging, is capable of collecting rich information from a wide variety of biological samples and processes. However, the quality of the spectral information depends on the amount of light available in each spectral band. Lowlight signals are degraded due to noise from the fundamental photon counting statistics as well as readout noise in the camera. Many imaging techniques, notably those based on fluorescence, inherently produce low-light signals leading to challenges in their adaptation to hyperspectral imaging. In an effort to extend the applicability of this technique, we have developed a camera capable of low-light hyperspectral imaging in the visible and near-infrared spectral range. An electron-multiplying CCD (EMCCD) detector has been integrated into the architecture of a hyperspectral camera system. Through its internal gain mechanism, the EMCCD effectively suppresses the readout noise and achieves a performance close to the fundamental photon noise limit. The size of the imaged area is on the order of centimeters, thus providing overview and context information as a complement to microscopic techniques. Such macroscopic imaging is useful for optical diagnostics and characterization of biological tissue samples. Data collected from biological samples are used to illustrate the camera performance under low light imaging conditions. The examples include e.g. autofluorescence imaging and low-light polarimetric imaging. The results show that hyperspectral imaging of low-light signals on the larger-than-microscopic scale has a clear potential for use in biomedical applications.



7561-31, Session 5

Medical diagnostics via optical biopsy with multiphoton microscopic endoscopy

W. W. Webb, Cornell Univ. (United States)

Medical Multiphoton Microscopic Endoscopy (M-MPM-E) can achieve real time in vivo diagnostics by application of MPM imaging, comprised of excitation of the tissue by femtosecond infrared laser pulse scanned illumination. MPM imaging of animal model tissues presenting both normal and diseased states provides comparison reference data. This often utilizes MPM imaging in transgenic mice. The MPM-excited fluorescence spectra and optical second and third harmonic generation form chromatic images of tissue structures including both cellular conformations and aggregations to provide the diagnostics. Official clinical reliance on M-MPM-E in human medical care depends on its correspondence with pathologists' diagnostics based on imaging of associated fixed stained tissues to create diagnostic imaging atlases. The photophysical designs of M-MPM-Endoscopes for human in vivo applications during surgery depend on the relevant organs to be imaged, thus requiring a diversity of capabilities and designs. For example, initial designs for internal bladder cancer detection and subsequent treatment monitoring are 3mm in maximum diameter, rigid for about 25cm and provide MPM laser illumination with in situ microscopic raster scanning at variable focal depths in tissue, collection pathways, and guidance imaging with white scattered light at low magnifications. Image reconstruction with selected bandpass filters at fluorescence and harmonic generation wavelength imaging in virtual real time guide the surgery. Some endoscope applications require long flexible endoscopes as in colon and intestines, or 1mm diameter Gradient Refractive Index (GRIN) needle lens imaging or spectroscopy, as for lung and thyroid glands.

7561-32, Session 5

Photonic approach to the selective inactivation of viruses with ultrashort pulsed lasers

K. Tsen, Arizona State Univ. (United States); S. D. Tsen, School of Medicine, Washington Univ. in St. Louis (United States); Q. Fu, S. M. Lindsay, K. Kibler, B. Jacobs, Arizona State Univ. (United States); J. G. Kiang, Uniformed Services Univ. of the Health Sciences (United States)

We report a photonic approach for selective inactivation of viruses with ultrashort pulsed (USP) lasers. We demonstrate that this method can selectively inactivate viral particles ranging from non-pathogenic viruses such as M13 bacteriophage, tobacco mosaic virus (TMV) to pathogenic viruses like human papillomavirus (HPV) and human immunodeficiency virus (HIV). At the same time sensitive materials like human Jurkat T cells, human red blood cells, and mouse dendritic cells remain unharmed. The laser technology targets the global mechanical properties of the viral protein shell, making it relatively insensitive to the local genetic mutation in the target viruses. As a result, the approach can inactivate both the wild and mutated strains of viruses. This intriguing property is particularly important in the treatment of diseases involving rapidly mutating viral species like HIV. Our photonic approach could be used for the disinfection of viral pathogens in blood products and for the treatment of blood-borne viral diseases in the clinic.

7561-33, Session 5

The importance of optical methods for noninvasive measurements in the skin care industry

G. N. Stamatas, Johnson & Johnson Consumer France (France)

Cosmetic and pharmaceutical industries are concerned with treating skin disease, as well as maintaining and promoting skin health. They are dealing with a unique tissue that defines our body in space. As such, skin provides not only the natural boundary with the environment inhibiting body dehydration as well as penetration of exogenous aggressors to the body, it is also ideally situated for optical measurements. A plurality of spectroscopic and imaging methods is being used to understand skin physiology and pathology and document the effects of topically applied products on the skin. The obvious advantage of such methods over traditional biopsy techniques is the ability to measure the cutaneous tissue in vivo and non-invasively. In this work, we will review such applications of various spectroscopy and imaging methods in industrial skin research. Examples will be given on the importance of optical techniques in acquiring new insights about acne pathogenesis and infant skin development.

7561-34, Session 5

Applications of biophotonics to point-of-care testing and clinical diagnosis

D. L. Matthews, UC Davis Medical Ctr. (United States)

I will present market studies on and biophotonics technology development for point-of-care testing and clinical diagnostics.

7561-35, Session 5

Industrial biophotonics: an overview of biomedical optics research at GE

S. Yazdanfar, GE Global Research (United States)

The General Electric Global Research Center has active programs in biophotonics, ranging from biomolecular kinetics to nonlinear microscopy to intraoperative fluorescence imaging. I will present ongoing research results in several of these programs. Our research in biophotonics can be summarized by spatial scale, ranging from molecular interactions up to the tissue scale.

At the smallest level, we are developing technologies to improve labelfree interaction analysis, i.e., the analysis of binding affinity, kinetics and selectivity of proteins and biomolecules, using surface plasmon resonance.

At the cellular and subcellular level, we have research programs in advanced microscopy. These include the development of an automated brightfield platform for digital pathology, multiplexed fluorescence microscopy for molecular pathology, and multiphoton microscopy of near infrared contrast agents.

Projects at the tissue and organ level primarily involve planar fluorescence imaging. For preclinical applications, we have developed a widefield instrument for imaging quantum dot fluorescence. Time-gating is used to discriminate quantum dots from background autofluorescence based on their relatively long fluorescence lifetime. Finally, we have constructed dual mode imaging systems, combining brightfield and fluorescence imaging for intraoperative guidance.

I will present highlights from these programs, emphasizing how the technology addresses unmet needs in medicine and life science.

7561-36, Session 5

Quantitative multispectral imaging of skin chromophores

J. M. Kainerstorfer, J. D. Riley, F. Amyot, M. Hassan, V. Chernomordik, National Institutes of Health (United States); C. K. Hitzenberger, Medical Univ. of Vienna (Austria); A. H. Gandjbakhche, National Institutes of Health (United States)

Conference 7561: Optical Biopsy VIII



Non-invasive, non-contact imaging modalities, which can assess blood volume and oxygenation as a measure of angiogenesis, would find great use in the clinical routine for characterization of skin lesions. The challenge is to make quantitative assessments of these chromophores in different layers of the skin. We are using diffuse multi-spectral imaging together with a two layered analytical skin model to address this problem. Light passing the first layer, the epidermis, is modeled by Lambert's law; light through the second layer, the dermis, is modeled by random walk theory of photon migration in diffuse media. Six images are being acquired in the near-infrared spectrum (700, 750, 800, 850, 900, and 1000nm) by a CCD camera, each image area being 10x10 cm2. When reconstruction for blood volume and oxygenation is performed, the epidermal thickness is assumed to be known and constant. However, this assumption might not always be valid and even small deviations from the real thickness shift the reconstruction results towards higher or lower values. Prior knowledge about the structure of the skin is therefore important for quantitative reconstruction of blood volume and oxygenation. To address this problem, we are introducing a combination of Optical Coherence Tomography (OCT) with multi-spectral imaging. Using the structural information obtained by OCT to determine the epidermal thickness, we will show the improvement of skin chromophore quantification.

7561-37, Session 5

Global convergence for inverse problems in optical tomography

M. V. Klibanov, The Univ. of North Carolina at Charlotte (United States)

Numerical methods for solving inverse problems, including ones for problems of Optical Tomography, are based on the minimization of least squares objective functionals. These functionals often suffer from the problem of local minima and ravines. The latter makes those algorithms locally convergent. In particular, sometimes only locations of small tumor-like abnormalities are imaged well. Whereas the contrasts are lowered. In this talk we will present our new results on globally convergent numerical methods for some inverse problems, including ones of optical tomography. These methods are independent on the availability of a good first guess. Co-authors of this presentation are: L. Beilina. J. Su, H. Shan, N. Pantong and H. Liu.

7561-38, Session 5

Differentiation of normal and cancerous lung tissues by multiphoton imaging

C. Wang, F. Li, W. Lin, S. Lin, C. Dong, National Taiwan Univ. (Taiwan)

In this work, we utilized multiphoton microscopy for the label-free diagnosis of non-cancerous, lung adenocarcinoma (LAC), and lung squamous cell carcinoma (SCC) tissues from human. Our results show that the combination of second harmonic generation (SHG) and multiphoton excited autofluorescence (MAF) signals may be used to acquire morphological and quantitative information in discriminating cancerous from non-cancerous lung tissues. Specifically, non-cancerous lung tissues are largely fibrotic in structure while cancerous specimens are composed primarily of tumor masses. Quantitative ratiometric analysis using MAF to SHG index (MAFSI) shows that the average MAFSI for non-cancerous and LAC lung tissue pairs are 0.55 ±0.23 and 0.87±0.15 respectively. In comparison, the MAFSIs for the non-cancerous and SCC tissue pairs are 0.50±0.12 and 0.72±0.13 respectively. Our study shows that nonlinear optical microscopy can assist in differentiating and diagnosing pulmonary cancer from non-cancerous tissues. With additional development, multiphoton microscopy may be used for the clinical diagnosis of lung cancers.



Monday-Wednesday 25-27 January 2010 • Part of Proceedings of SPIE Vol. 7562 Optical Interactions with Tissues and Cells XXI

7562-01, Session 1

Rapid analysis of spectral images using a simplified light transport model

S. L. Jacques, Oregon Health & Science Univ. (United States) No abstract available.

7562-02, Session 1

Molecular delivery into live cells using gold nanoparticle arrays fabricated by polymer mold guided near-field photothermal annealing

T. Wu, F. Xiao, M. A. Teitell, P. E. Chiou, Univ. of California, Los Angeles (United States)

A massively-parallel molecular delivery system for mammalian cells is demonstrated by pulsed-laser irradiation of a gold nanoparticle array situated below a cell monolayer. Upon irradiation by a short pulse laser, the nanoparticles create transient and localized explosive vapor bubbles, which disrupt part of the adjacent cell membrane, allowing exogenous molecules to be carried into the cell by fluid flow or thermal diffusion. This system is capable of high throughput and spatially-targeted delivery into desired areas of a cell culture by designing the laser irradiation pattern. To optimize delivery efficiency and cell viability, we systematically vary the gold nanoparticle size and density. Rapid fabrication of gold nanoparticle arrays over large areas (>1 mm2) is achieved by polymer mold guided near-field photothermal annealing. A PDMS phase shifting mask is placed in contact with a gold thin film. The PDMS mold spatially modulates the incident nanosecond laser pulse energy and creates an intensity-modulated near-field light pattern at the surface of the gold film. The molten gold driven by instability and thermocapillary force migrates from hot (high laser intensity) to cold (low laser intensity) areas and forms periodic gold nanolines or nanodots after resolidification. The gold nanoparticle density or period is defined by the period of the PDMS mold and the nanoparticle size can be controlled by the thickness of the pre-annealed gold film.

7562-03, Session 1

Spurious analyte calibration models from fluorescence quenched tissue Raman spectra

I. Barman, C. Kong, G. Singh, R. R. Dasari, M. S. Feld, Massachusetts Institute of Technology (United States)

A major challenge in quantitative biological Raman spectroscopy lies in overcoming the influence of the dominant fluorescence background. Furthermore, the prediction accuracy of a calibration algorithm can be severely compromised by the quenching of the endogenous fluorophores over the period of spectral acquisition due to the presence of spurious correlations between analyte concentrations and fluorescence levels. Apparently functional models can be obtained from such correlated samples, which can never be used successfully for prospective prediction. Typically, subtraction of best fit lower order polynomials and high pass filtering are used to eliminate the fluorescence background. However, these methods introduce artifacts to the true Raman spectrum and are unsuitable for quantitative studies.

In this work, we investigate the deleterious effects of photobleaching and the introduction of spurious correlations on prediction accuracy of explicit and implicit calibration algorithms. Numerical simulations are then employed to understand the efficacy of shifted excitation Raman difference spectroscopy (SERDS) as a correction methodology. SERDS studies are also performed on a set of tissue phantoms to validate our numerical findings.

We show that the prospective prediction error on a set of random samples can be as much as three times larger when the calibration algorithm is developed on correlated samples than on uncorrelated ones. This indicates that development of calibration algorithms, especially for diabetic people, via a glucose tolerance test is liable to yield incorrect results due to the photobleaching affected spurious correlations. Finally, we show that the application of SERDS removes the stated spurious correlation and reduces the prediction error for the correlated samples' case to that of the uncorrelated levels.

7562-04, Session 1

Second harmonic generation imaging microscopy of ovarian cancer

R. LaComb, O. Nadiarnykh, Univ. of Connecticut Health Ctr. (United States); M. Brewer, Neag Cencer Ctr. (United States); P. Campagnola, Univ. of Connecticut Health Ctr. (United States)

We report the integrated use of 3D Second Harmonic Generation (SHG) imaging microcopy and Monte Carlo simulation as a combined metric to quantifiably differentiate normal and malignant human ovarian biopsies. To achieve this we use a set of parameters comprising of SHG depth-dependent profiles and bulk optical parameters, where these are utilized collectively in a comparative method. We determined that the scattering coefficient, µs, and anisotropy is larger for malignant ovary over that of normal ovarian tissue. These results are likely due to higher collagen concentration and order observed in histological analysis. The underlying structural dissimilarities also lead to significant differences in the measured forward-backward (F/B) ratio We find the SHG from normal tissues is statistically more forward-directed than the malignant ovaries (93 vs 77%). Similar attenuation is observed in both, which arises from increased scattering and increased SHG brightness due to the more densely packed collagen. Monte Carlo simulations of the photon propagation based on the measured bulk optical parameters model the overall experimental trends. A more complete description requires consideration of the emission creation directionality as well. To this end, we apply our recently developed model using quasi-phase matching conditions to relate the SHG image intensities, and signal directionality to the respective collagen fibrillar assemblies. TEM analysis shows more closely packed collagen fibrils in cancer, lead to more efficient backward emission, consistent with our phase matching considerations.

7562-06, Session 1

A far-field superposition method for 3D FDTD simulations of light scattering from multiple biological cells

M. S. Starosta.

No abstract available.

TEL: +1 360 676 3290 · +1 888 504 8171 · customerservice@spie.org



7562-07, Session 2

Modeling fluorescent light distributions in layered media

K. G. Phillips, S. Jacques, Oregon Health & Science Univ. (United States)

We present a numerical procedure using the Pn-method to model fluorescent light distributions in layered tissue models. Two coupled steady state transport equations are used to model the problem. The first describes the propagation of excitation light from the tissue boundary to the fluorophore distribution which acts as an absorption inhomogeneity. The second transport equation models the propagation of the fluorescent emission to the layer surfaces. Wavelength dependent scattering and absorption are incorporated into the formalism to account for the optical properties of oxygenated and deoxygenated hemoglobin, water, and melanin and their role in frustrating fluorescent light propagation. This technique provides a quick means to explore the dependence of predicted boundary measurements on the tissue-light interaction, the optical properties, and the fluorophore depth.

7562-08, Session 2

Optical imaging of structures within highly scattering material using an incoherent beam and a spatial filter

N. Pfeiffer, G. H. Chapman, B. Kaminska, Simon Fraser Univ. (Canada)

Angular Domain Imaging (ADI) is a high resolution, ballistic imaging method that utilizes the angular distribution of photons to separate out multiply-scattered photons, which have a wide range of angles, from ballistic and quasi-ballistic photons which exit a scattering medium with a small distribution of angles around their original trajectory. An advantage of the ADI method is that it is suitable with a wide variety of light sources, as it is not sensitive to coherence or wavelength and does not require a pulsed source or a highly collimated beam. We extend the ADI method to transmissive imaging of scattering media using incoherent, collimated sources with a spatial filter comprised of a converging lens (focal distance of 50-100 mm) and pinhole aperture (diameter of 100-500 µm) giving acceptances angles of 0.06 to 0.6° to produce wide-beam, full-field images of planar, high contrast, phantom test objects through 5 cm thick scattering media at optical scattering depths of up to 14.5 (scattered to ballistic photon ratio > 2E6). Experimental images, obtained using a 12 mm diameter beam produced by a quartz-halogen incandescent source (beam divergence angle 0.52°, beam power < 10 mW), demonstrate the advantages of this combination of broadband, incoherent source and spatial filter: lack of interference artifacts seen with laser sources, ease of changing image magnification, simple correlation between system geometry and resolution, and ease of spectral filtration to obtain multispectral images. Monte Carlo simulation with angular tracking is used to validate the experimental results and determine system trade-

7562-09, Session 2

Angle-resolved diffused light spectroscopy using radial angular filter arrays

F. Vasefi, Simon Fraser Univ. (Canada) and Lawson Health Research Institute (Canada); M. Najiminaini, B. Kaminska, Simon Fraser Univ. (Canada); H. Zeng, The BC Cancer Research Ctr. (Canada); G. H. Chapman, Simon Fraser Univ. (Canada); J. J. Carson, Lawson Health Research Institute (Canada) and Univ. of Western Ontario (Canada)

This paper presents a novel optical filter called the Radial Angular

Filter Array (RAFA) for high resolution measurement of the angular and spectral distribution of scattered light exiting from a turbid medium. The RAFA consists of a radially-distributed series of 48 micro-channels micromachined into a silicon substrate. Each micro-channel was 80 μm wide, 80 μm deep, and 5 mm long resulting in an aspect ratio of 62.5:1 and providing a photon acceptance angle range of <1.29°. The micro-channels were positioned at steps of 2.5° with each 80 $\mu m \times$ 80 μm opening facing a common focal point 3.9 mm from the device edge.

To test the device, we propose to construct an angle-resolved spectroscopy system by integrating a wideband light source, the RAFA, and an imaging spectrometer. The collimated broadband light source will be configured to trans-illuminate a turbid sample over a wide range of wavelengths in the near infrared spectral region. The RAFA will be used to collect the angular distribution of light exiting the turbid sample. The imaging spectrometer will be used to decompose the output of the RAFA into hyperspectral images representative of scatter angle and wavelength. By scanning the RAFA and imaging spectrometer over the sample, a the intensity of the scattered light will be acquired as a function of location on sample surface, wavelength, and angle relative to the surface normal. With angle resolved spectroscopy it will be possible to characterize the optical properties of turbid samples such as tissue biopsy samples in great detail.

7562-10, Session 3

Optical phase conjugation by dynamic holography for wavefront restoration in turbid media

N. Ortega-Quijano, F. Fanjul-Vélez, I. Salas-García, Univ. de Cantabria (Spain); O. G. Romanov, D. V. Gorbach, A. L. Tolstik, Belarusian State Univ. (Belarus); J. L. Arce-Diego, Univ. de Cantabria (Spain)

Optical Phase Conjugation is a non-linear optical phenomenon that generates a phase conjugate replica of an incident beam. It has been widely used to suppress the effects of aberrations in optical systems such as resonators or image-transmitting optical fibers. In this work, the possibility of using optical phase conjugation as a means of suppressing the effect of scattering in turbid media is analyzed, with the final aim to apply it to biological tissues.

Firstly, light propagation through a slab representing a turbid sample was calculated by solving Maxwell's equations with the Finite-Difference Time-Domain method, in order to preserve all the information about the phase and coherence of the wavefront. The non-linear process that takes place within the phase conjugation mirror is described by coupled-wave theory. A set of simulations was performed, and the results confirm the feasibility of using this effect to compensate the effect of scattering in turbid media.

Subsequently, an experimental set-up was performed. In order to obtain a phase conjugation mirror, degenerate four-wave mixing was achieved by a real-time volume holography configuration. The pulsed laser source was a Nd3+:YAG laser at its second-harmonic (532nm). An ethanol solution of Rhodamine 6G was used as a non-linear medium. A lipid-based scattering sample was obtained by a solution of homogenized milk and distilled water, which provided us with an appropriate tissue phantom. The experimental results demonstrate scattering suppression, and constitute some preliminary measurements of an effect with a promising potential for a wide range of applications.

7562-11. Session 3

Spatiofrequency filters for imaging fluorescence in scattering media

P. B. Tsui, G. Chiang, G. H. Chapman, N. Pfeiffer, B. Kaminska, Simon Fraser Univ. (Canada)

Researchers have been using simple optics to image optically induced



fluorescence in tissues. We now apply the Angular Domain Imaging technique - accepting only photons within a small deviation angle from its original trajectory with a Spatiofrequency Filter, to image a fluorescing medium beneath a scattering layer. A Rhodamine 6 G dye fluorescing layer, under an interlipid scattering medium was excited by a 533nm Nd: Yag laser. Without ADI, phantom structures of 204-152µm lines/spaces placed between scattering and fluorescing layers become undetectable at Scattering Ratio of <3, ~0.55mm tissue depth. By applying ADI with acceptance angle of 0.17°, the structures are distinguishable at Scattering Ratio of 10, ~1.1mm tissue depth. It was established previously that as the acceptance angle decreases, the amount of scattered light/noise in the images decreases, however, the resolution also deteriorates. In these experiments, an excitation at 533nm generates an emission fluorescence wavelength at ~600nm for R6G, requiring specific color filters to eliminate the excitation wavelength. Note that the scattering coefficients decrease as the wavelength increases. Thus as the excitation beam going through the scattering medium (SR~14:1), photons are widely scattered before reaching the fluorescing layer, leading to a larger emitting area at this layer. The fluorescence emission going through the scattering medium (SR~10:1) undergoes less scattering due to the longer wavelength enabling greater resolution. This is done in preparation for the next stage of experiment using pig skin with the collagen as the fluorescing source excited between 340-470nm and emitting between 420-540nm.

7562-12, Session 3

Comparison of the near-infrared optical properties of excised and cultured human ocular tissues

B. G. Yust, D. K. Sardar, A. Tsin, The Univ. of Texas at San Antonio (United States)

The near infrared (NIR) optical properties of human retinal pigmented epithelial (RPE) cells were studied using a double-integrating sphere setup and a Cary14 spectrophotometer. The Inverse Adding-Doubling and Kubelka-Munk techniques were applied to obtain absorption and scattering coefficients. Retinal pigmented epithelial monolayers were cultured from an ARPE19 line in Nunc Opticell culture windows and were optically characterized as a function of wavelength and induced melanization. Newly excised human RPE cells were characterized in the same way. A comparison is made between the optical properties of the excised and cultured cells to determine any significant differences between samples of differing origin. Photo-induced damage to the live cultured RPE cells was studied as a function of dosage, wavelength, and induced melanization as well. The photo-induced "wounds" were characterized by size and the regenerative time it took for the cultures to reach confluence in the irradiated areas. Validity of the use of cultured tissues for determination of optical properties and damage thresholds will

This work was supported in part by the NSF sponsored Center for Biophotonics Science and Technology (CBST) at UC Davis under Cooperative Agreement No. PHY 0120999.

7562-13, Session 4

Determination of the optical property changes by photodynamic therapy using inverse Monte Carlo method between 350 nm and 1000 nm

N. Honda, T. Terada, T. Nanjo, K. Ishii, K. Awazu, Osaka Univ. (Japan)

Photodynamic therapy (PDT) is one of the treatments of malignancies, and a treatment modality based on the interaction of light, a photosensitizing drug, and oxygen. In PDT, the understanding the light propagation within the tissue is essential. Optical properties (absorption

coefficient μ a, scattering coefficient μ s and anisotropy factor g, etc.) help us understanding a light propagation. The understanding of relation between irradiation doses and optical property changes is important for treatment planning.

However, there are few reports about optical property changes of tumor tissues by photodynamic therapy. The objective of this study is to determine the optical property changes of tissues treated by PDT between 350 nm and 1000 nm during and after PDT operating. In this study, mouse tumor tissues obtained from subcutaneously implanted Lewis lung carcinoma cell line were treated by a normal photodynamic therapy procedure used a talaporfin sodium (5 mg/kg) as a photosensitizer and a laser diode with a wavelength of 664 nm. Average power density was 100 mW/cm2 and total light dose was 100 J/cm2. Transmittance and Reflectance of removed PDT-treated tissues were measured by double integrating sphere system. After that, we calculated the µa and µs' of PDT-treated tissues between 350 nm and 1000 nm using Inverse Monte Carlo method. During PDT, the absorption coefficient spectra were not changed, and the reduced scattering coefficient spectra were slightly decreased entirely. After PDT, the reduced scattering coefficient spectra were increased entirely with passage of time.

7562-14, Session 4

In vivo comparison of near infared laser lesions in the non-human primate retina using adaptive optics imaging

G. M. Pocock, J. W. Oliver, A. D. Shingledecker, K. Schuester, B. A. Rockwell, Air Force Research Lab. (United States)

Non-human primates that received retinal exposure to wavelengths between 1110 to 1319 nm were imaged using an Adaptive Optics enhanced Spectral Domain Optical Coherence Tomographer (AO SD-OCT). The progression of damage in retinal areas that received exposures below, greater than, and at threshold values for each respective wavelength are compared. Results show differences in lesion characteristics. * The animals involved in this study were procured, maintained, and used in accordance with the Federal Animal Welfare Act and the "Guide for the Care and Use of Laboratory Animals," prepared by the Institute of Laboratory Animal Resources - National Research Council.

7562-15, Session 4

Effect of coating material on uptake of indocyanine green-loaded nanocapsules by normal and cancerous lung cells

B. Jung, E. Lomeli, B. Anvari, Univ. of California, Riverside (United States)

Fluorescent molecular probes offer a potential for early cancer detection. Indocyanine green (ICG) is an FDA-approved near-infrared (NIR) fluorescent dye used in ophthalmic angiography and assessment of cardiac and hepatic functions. However, clinical applications of ICG remain very limited due to its rapid clearance from vascular circulation, unstable optical properties, non-specific vascular plasma binding and inability for localized targeting. To overcome these limitations, we have encapsulated ICG within nanoconstructs composed of poly(allylamine) hydrochloride and disodium hydrogen phosphate salt. Nanoencapsulated ICG can potentially be used in tumor-targeting by appropriate surface coating and or functionalization, as well as laser-mediated therapy of malformations. Our in-vivo preliminary results demonstrate that ICGloaded nanocapsules (ICG-NCs) coated with the composite magnetite and polyethylene glycol (PEG) material deposit in greater amounts within the lungs of healthy mice than nanocapsules coated with polylysine or dextran. To understand the effects of coating materials on the cellular distribution of the nanocapsules within the lungs, we measure the



uptake of ICG-NCs coated with various coating materials by normal and cancerous pulmonary cells such as bronchial epithelial cells in-vitro. Results of these studies provide important information for subsequent applications of ICG-NCs in optical and phototherapy of diseased pulmonary tissue.

7562-16, Session 4

Label-free optical control of arterial contraction

M. Choi, J. Yun, C. Choi, Korea Advanced Institute of Science and Technology (Korea, Republic of)

The diameters of blood vessels, especially in the brain, change dynamically over time to provide sufficient blood supply as needed. No existing technique allows noninvasive control of vascular diameter in vivo. Here, we report that label-free irradiation with a femtosecond pulsed laser can trigger blood vessel contraction in vivo. In response to laser irradiation, cultured vascular smooth muscle cells showed a rapid increase in calcium concentration, followed by cell contraction. In a murine thinned skull window model, laser irradiation focused in the arterial vessel wall caused localized vascular contraction, followed by recovery. The nonlinear nature of the pulsed laser allowed highly specific targeting of subcortical vessels without affecting the surrounding region. We believe that femtosecond pulsed laser irradiation will become a useful experimental tool in the field of vascular biology.

7562-43, Poster Session

Measurement of the temperature increase in the porcine cadaver iris during direct illumination by femtosecond laser pulses

H. Sun, R. M. Kurtz, T. Juhasz, Univ. of California, Irvine (United States)

Purpose: The IntraLase femtosecond laser (AMO Corp. Santa Ana, CA) has been approved by the US Food and Drug Administration for creation of corneal flaps in LASIK surgery. During normal operation, as we measured 50% of laser energy may pass beyond the cornea with potential effects on the iris. As a model for iris laser exposure during femtosectond corneal surgery, we quantified the temperature increase in porcine cadaver iris during direct illumination by the laser.

Methods: The temperature increase induced by laser energy deposited in porcine cadaver iris during femtosecond laser illumination was investigated in situ using an infrared thermal imaging camera (Fluke corp. Everett, WA). To model the geometry of the eye during the surgery, an excised porcine cadaver iris was placed 2.2 mm from the flat glass contact lens. The temperature field was observed in 20 cadaver iris with the infrared camera at energy levels ranging from 1 to 2 J.

Results: A maximum temperature increase of less than 1.5 0C was observed in the cadaver iris during laser scanning, with little variation between specimens in temperature profiles for the same laser energy illumination.

Conclusions: Our studies suggest that minimal iris heating occurs during femtosecond laser corneal surgery. It is a safe procedure for iris at normal surgery laser energy.

7562-44, Poster Session

Analytical continuous-wave diffuse optical tomography in cylindrical geometry

J. Ho, J. Dong, K. Lee, Nanyang Technological Univ. (Singapore)

Diffuse optical tomography (DOT) is an emerging non-invasive medical imaging modality that is especially suited for imaging of the breast and

brain. Especially in breast imaging, DOT offers many advantages over conventional X-ray mammography, such as using non-ionizing radiation and cost-effectiveness.

In recent years, system symmetry has been exploited by some researchers for image reconstruction. These include translational symmetry in a slab and rotational symmetry in a cylinder or sphere. When the computational volume is made into such simple shapes, one can reformulate the single 3-D matrix inversion into multiple 1-D matrix inversions, which improves the speed and efficiency in solving the inverse problem. In addition, for cylindrical and spherical geometries, acquiring data from various angles of projections also helps to contribute to image stability.

In this paper, we present an analytical DOT table-top experiment in cylindrical geometry. A non-contact, single-wavelength, continuous-wave DOT system will be built using a galvanometer-steered laser and a CCD camera. Targets with various shapes, sizes and optical contrast are positioned in the middle of a cylindrical container filled with highly scattering Intralipid solution. Surface intensity measurement data is then collected via CCD for various source positions at different projection angles, which can be used to reconstruct a 3D image of the absorption coefficient. Subsequently, system performance will be evaluated in terms of speed and resolution and compared with that of conventional numerical techniques such as the nonlinear conjugate gradient method.

7562-45, Poster Session

Analytic reconstruction of absorption and scattering properties in parallel plate diffuse optical tomography

K. Lee, J. H. Ho, J. Dong, Nanyang Technological Univ. (Singapore)

Various numerical methods have been developed for the inverse problem in diffuse optical tomography (DOT). Although quite a handful of them are relatively successful in terms of accuracy, they all share the common disadvantage of being computationally intensive in both memory and CPU usage when dealing with large data sets. Recently, an analytic image reconstruction method has been developed which is significantly less expensive in terms of computation. It makes use of the known mathematical form of the Green's function in simple geometries such as the slab geometry. It also deals with large data sets in Fourier space where the dimensional space of the inverse problem is reduced due to the symmetry inherent in the geometry.

In this paper, we present the results of a table-top phantom RF-DOT experiment and assess the quality of the images reconstructed by the analytic method in Fourier domain. In the experimental setup, we used a 70MHz-modulated laser source of 660 nm, along with a gain-modulated image intensifier attached to an electron-multiplying CCD camera. Next, using a homodyne method, we acquired phase-sensitive transmission images at multiple source positions on a grid, both with and without a target inside the diffuse medium. The resulting images were sampled and fitted to a sinusoidal wave to obtain the amplitude and phase for each virtual detector position. The resolution, contrast, and level of crosstalk between absorption and scattering are assessed, and future possible uses of this algorithm in real-time clinical imaging will be discussed.

7562-46, Poster Session

The accuracy of a commercially spectrophotometer with an integrating sphere for measuring optical properties of turbid sample

Y. Zhang, X. Wen, D. Zhu, Huazhong Univ. of Science and Technology (China)

A commercially spectrophotometer with an integrating sphere is



widely used to measure the spectra of transmittance and reflectance of turbid sample, and then the optical properties can be deduced by inverse adding-doubling algorithm. Unfortunately, the accuracy of the measurement is not been elucidated completely. What's more, for the system, there still exists some other limits, i.e., light's collimation is not well and size of light spot is too large compared with the sample port.

Thus, the purpose of this study is to evaluate the accuracy of the commercially spectrophotometer with an integrating sphere for measuring optical properties of tissue phantom. Two phantom materials, Intralipid and Evens Blue, or the mixture of this two, were chosen for the experiments.

The results show that the phantom measurement in conjunction with IAD algorithm enable the determination of scattering coefficient $\mu s'$ to better than 5% accuracy, absorption coefficient μa to better than 10% accuracy when the optical depth of sample is between 1 and 10, and the albedo is bigger than 0.4. For scattering of samples during 1-5 mm-1, the error of $\mu s'$ is smaller than 4%; whereas for absorbing of samples >0.4 mm-1, the maximum error is smaller than 8.3%. Therefore, spectrophotometer with an integrating sphere technique combined IAD algorithm is applicable for the measurements of optical properties for most tissue, and its repeatability and accuracy is high.

7562-47, Poster Session

Optical constants measurement of tissue for the laser coagulation by inverse Monte Carlo method

T. Terada, T. Nanjo, N. Honda, K. Ishii, K. Awazu, Osaka Univ. (Japan)

The laser coagulation is the effective method of treatment for retinal disease, hemostasis and benign prostatic hyperplasia. Currently, the irradiation conditions such as the intensity and the irradiation time are decided based on the experience of physicians in the laser coagulation. Therefore, there are problems that the curative effect is inadequate and the medical malpractices are caused by the excessive irradiation. It is necessary to evaluate the optical interaction with the tissue quantitatively. The optical interaction depends on the optical contents of the tissue. In this study, the optical contents of the tissue before and after the laser coagulation were measured by the double integrating sphere system. The absorption and scattering coefficients were calculated from the reflectance and the transmittance of the experiment by Inverse Monte Carlo Method. The absorption and scattering coefficients of the chicken breast were measured in the wavelength regions from 350 to 1000 nm. In all regions, the adsorption coefficients are reduced and the scattering coefficients are increased. It was considered that the reasons of these results were the change of proteins and hemoglobin.

7562-48, Poster Session

Return to Contents

LED light source and secondary optics design for the efficient energy delivering on plant growth and the matching of the chlorophyll/ PAR spectrum

C. Ou, Hsiuping Institute of Technology (Taiwan)

Recently, the LED lighting for the plant growth had been paid much attention. Due to the fact that the plant required particular spectrum compositions to produce the most efficient growing situation, this article study several types of the LED spectrum for plant growth, and the matching of the spectrum between the LED, the chlorophyll/PAR spectrum of different plant/cell and the optical components. As for the methodology, we study the energy efficiency of the LED device to the plant growth by consider several factors, which include the photosynthesis, the photoperiodism, the photo-morphogenesis, light intensity, light photoperiod, PAR, ASP and the Red/FR ratio. More than this, the discussion on the Etendues of the system and the plant

morphologies through the complicated integrations on the shape of the plant and the lighting devices are also report. Particular optical design is proposed to provide a more efficient energy delivering into the plant. Results suggest that the position or the light intensity of the LED lighting better be adaptive for each stage of the plant growth, and the controlling of the spectrum decomposition required precise.

7562-49, Poster Session

Near-infrared measurement of porcine tissue optical properties using a dual-integrated sphere system

C. A. Davis, N. Jindra, Air Force Research Lab. (United States)

The measurement of tissue optical properties is essential to understanding how lasers interact with the body in order to predict the effects of intentional and accidental laser exposures. The majority of safety standards are based on actual experimentation as well as theoretical damage calculations that use computer models. Those simulations incorporate optical properties to determine photon movement within each tissue. However, much of the optical data is taken from work which has been done with thin sections of excised samples. That data is then extrapolated to come up with a number for the full tissue. To date, there is little to no data available on the optical properties of fullthickness samples. This study used two integrating spheres to measure full-thickness skin and fat samples from Yorkshire pigs at 1064nm and 1313nm wavelengths. Results were obtained for the transmission and reflectance values and then an Inverse-Adding Doubling software program designed by Scott Prahl was run to determine the absorption and scattering coefficients of each sample.

7562-17, Session 5

THz in biology and medicine: toward quantifying and understanding the interaction of millimeter- and submillimeter-waves with cells and cell processes

P. H. Siegel, California Institute of Technology (United States); V. Pikov, Huntington Medical Research Institute (United States)

Careful evaluation of the impact and interactions of millimeter and submillimeter wavelength radiation on biological systems is becoming more relevant as high frequency communications, radar and imaging begin to make their way into commercial applications. Methods to identify and quantify the impact of this radiation on a microscopic scale are just beginning to emerge. In this overview presentation, a quick survey of ongoing research in this area is undertaken. The focus then shifts to three avenues of development we have been pursuing in our own laboratory: (1) an optical Raman technique for remotely monitoring the temperature of cells and cell media in-vitro and at depth using changes in the spectral shape of a stretch band of the hydroxyl group in liquid water at 3100 to 3700 cm-1; (2) a FRET (Forster resonance energy transfer) technique applied on eternal human lung cells transfected with GFP (green fluorescent protein) on the inner surface of the membrane to look at the non-destructive formation of nanopores on exposure to low levels of millimeter-wave (60 GHz) energy; and (3) membrane depolarization of GFP transfected neuronal cells in-vitro stimulated by low level millimeter-wave exposure. Current findings and future plans will be presented.

7562-18, Session 5

Metamaterial based devices for terahertz imaging

X. G. Peralta, The Univ. of Texas at San Antonio (United States)

193

TEL: +1 360 676 3290 · +1 888 504 8171 · customerservice@spie.org



The terahertz (THz) region has been shown to have considerable application potential for spectroscopic imaging, nondestructive imaging through nonpolar, nonmetallic materials and imaging of biological materials. These applications have all been possible due to the recent progress in sources, detectors and measurement techniques. However, only moderate progress has been made in developing passive and active devices to control and manipulate THz radiation, which can enhance current imaging capabilities. One promising approach for implementing passive and active devices at THz frequencies are metamaterials. Metamaterials are composite materials designed to have specific electromagnetic properties not found in naturally occurring materials. The most common implementation utilizes a metallic resonant particle periodically distributed in an insulator matrix where the periodicity is significantly smaller than the wavelength of operation. The resonator units can interact with either or both the incident electric and magnetic field, enabling tuning of the composite's permittivity and/or permeability.

We have designed and implemented three metamaterial based devices with potential applications to THz imaging. We present an electrically-driven active metamaterial which operates as an external modulator for a ~2.4 THz CW quantum cascade laser. We obtained a modulation depth of 50%. We also demonstrate a polarization sensitive metamaterial which can be used as a continuously variable attenuator and a quarter-wave plate. The THz quarter-wave plate may be useful for the development of THz phase contrast imaging.

Work performed at Sandia National Laboratories, a multiprogram laboratory operated by Sandia Corporation, a Lockheed Martin Company, for the US DoE's NNSA under Contract DE-AC04-94AL85000.

7562-19, Session 5

Measurement of the optical properties of skin using terahertz time-domain spectroscopic techniques

G. J. Wilmink, Air Force Research Lab. (United States); T. Tongue, Zomega Terahertz Corp. (United States); B. L. Ibey, Air Force Research Lab. (United States); B. Shulkin, Zomega Terahertz Corp. (United States); X. Peralta, The Univ. of Texas at San Antonio (United States); B. D. Rivest, E. C. Haywood, W. P. Roach, Air Force Research Lab. (United States)

Terahertz (THz) radiation is the part of the electromagnetic spectrum ranging in frequency from 0.1 to 10 THz or wavelengths from 30 to 3000 µm. Although the optical properties of biological tissues are wellcharacterized in neighboring spectral regions, few studies have been conducted to determine their properties in the THz range. In this study, we used THz time-domain spectroscopic (TDS) techniques to measure the optical properties of water, excised pig skin, adipose tissue, and striated muscle. Measurements were conducted on samples using the following preparation techniques: acute (~2 h post-excision), fresh (~15 h post-excision), and frozen (~2 d post excision). Here we used the THz-TDS technique to directly measure the effect that each sample material has on both the amplitude and phase of the THz waveform. After applying a Fourier transform to extract the frequency spectrum from the time-domain data, we then used these waveforms to determine the sample's index of refraction (n) and absorption coefficient (µa). The optical properties we measured using these techniques will be compared to those values we previously measured using pulsed photothermalradiometric techniques.

7562-20, Session 5

Determination of death thresholds and identification of terahertz (THz)-specific gene expression signatures

G. J. Wilmink, Air Force Research Lab. (United States); D. Roberson, The Univ. of Texas at San Antonio (United States); B.

L. Ibey, B. Rivest, W. P. Roach, Air Force Research Lab. (United States)

Terahertz (THz) radiation is increasingly being used for various imaging applications; however, the potential impact that this radiation has on biological systems is not well characterized. In addition, no empirically validated safety guidelines (e.g. cellular and tissue damage thresholds) exist for this range. In this study, we determined both the necrotic and apoptotic thresholds (ED50) for several human cell lines using MTS viability assays and flow cytometry techniques. In addition, we identified THz-specific gene expression signatures using transcriptomic and genomic analysis techniques. For the THz frequencies tested, we found that the cell death thresholds were both frequency and cell typedependent. We also found that each cell type exhibited THz-specific gene expression signatures. Both the specific genes and magnitude of expression were markedly different from those responses induced by judiciously selected positive-stress controls (e.g. genotoxic and hyperthermic stress). These results provide evidence for the specific effects that THz radiation has on human cells, and these results may contribute to the development of empirically-based safety guidelines. We speculate that the identified gene markers may serve as excellent candidate biomarkers for THz exposures.

7562-21, Session 5

Quantitative investigation of the bioeffects associated with terahertz radiation

B. D. Rivest, G. J. Wilmink, L. X. Cundin, J. Payne, B. L. Ibey, D. Mixon, W. P. Roach, Air Force Research Lab. (United States)

Terahertz (THz) radiation is increasingly being used for medical imaging and security screening applications. In support of this increased interest, our research group aims to explore the potential bioeffects across this frequency range. In this study, we examined the viability of cultured dermal fibroblasts exposed to 2.52 THz radiation (H: 37.3 mW/cm2, 0-80 minute exposure times). Using an IR camera and custom exposure chamber, a ~3°C temperature rise was detected over an 80 minute exposure, agreeing well with results from a finite difference time domain model. In addition, we exposed cells to a heated bath using identical exposure conditions (temperature and duration). For both exposures, we found that cells exhibited no significant changes in viability. Recent publications have suggested that THz radiation elicits genetic instability because intracellular biomolecules (e.g. DNA and protein) possess a host of rotational and vibrational resonances at THz frequencies. We found that cells exposed to hyperthermic stress and THz showed only minimal increases in the expression of stress and DNA sensing/repair genes. To validate this finding, we examined the genetic response of cells exposed UV radiation, a stressor known to activate DNA repair mechanism and promote genomic instability. These results provide evidence that 2.52 THz radiation does not activate DNA and protein repair mechanisms, suggesting that THz radiation is not preferentially absorbed by DNA and intracellular proteins.

7562-22, Session 5

Damage thresholds for terahertz radiation

D. R. Dalzell, R. Vincelette, B. Ibey, G. J. Wilmink, W. P. Roach, Air Force Research Lab (United States)

The interaction between terahertz frequencies (0.1 - 10 THz) and dermal tissue has remained poorly explored due to the lack of high power terahertz sources. Advances in technology have brought about new applications for terahertz, specifically active imaging for medical and security applications. To support deployment of such technologies for use within the general population, research must be performed that establishes proper safety standards. Our research goal was to determine the damage threshold, ED50, for excised porcine skin exposed to continuous-wave (CW), THz radiation. Experiments were performed using a SIFIR 50 THz radiation source, FLIR infrared camera, and a custom exposure set up.



7562-23, Session 5

TBA

H. L. Mosbacker, The Ohio State Univ. (United States)

No abstract available.

7562-24, Session 6

Interaction of temporal and spatial separated cavitation bubbles in water

N. Tinne, T. Ripken, H. Lubatschowski, Laser Zentrum Hannover e.V. (Germany)

The LASIK procedure is a well established laser based treatment in ophthalmology. Nowadays it includes a cutting of the corneal tissue bases on ultra short pulses which are focused below the tissue surface to create an optical breakdown and hence a dissection. The energy of the laser pulses is absorbed by nonlinear processes that result in an expansion of a cavitation bubble and rupturing of the tissue. Hence positioning of several optical breakdowns side by side generates an incision. Due to a reduction of the duration of treatment the current development of ultra short laser systems points to higher repetition rates in the range of hundreds of kHz or even MHz instead of tens of kHz. This in turn results in a probable occurrence of interaction between different optical breakdowns and respectively cavitation bubbles of adjacent optical breakdowns. While the interaction of one single laser pulse with biological tissue is analyzed reasonably well experimentally and theoretically, the interaction of several spatial and temporal following pulses is scarcely determined yet. We present a high-speed photography analysis of cavitation bubble interaction varying the laser pulse energy as well as the spatial and temporal distance. Depending on a change of these parameters different kinds of interactions such as a flattening and deformation of bubble shape or jet formation are observed. The results of this research can be used to comprehend and optimize the cutting effect of ultra short pulse laser systems with high repetition rates (> 1 MHz).

7562-25, Session 6

Analysis of the short-pulsed CO2 laser ablation process for optimizing the processing performance for cutting bony tissue

M. Mehrwald, J. Burgner, C. Platzek, C. Feldmann, J. Raczkowsky, H. Woern, Univ. Karlsruhe (Germany)

Recently we established an experimental setup for robot-assisted laser bone ablation using short-pulsed CO2 laser. Due to the comparable low processing speed of laser bone ablation the application in surgical interventions is not yet feasible. In order to optimise this ablation process, we conducted a series of experiments to derive parameters for a discrete process model. After applying single and multiple laser pulses with varying intensity onto bone, the resulting craters were measured using a confocal microscope in 3D. The resulting ablation volumes were evaluated by applying Gaussian function fitting. We then derived a logarithmic function for the depth prediction of laser ablation on bone.

In order to increase the ablation performance we conducted experiments using alternate fluids replacing the waterspray: pure glycerine, glycerine/water mixture, citric acid and caustic soda. Because of the higher boiling point of glycerine compared to water we had expected deeper craters through the resulting higher temperatures. Experimental results showed that glycerine or a glycerine/water mix do not have any effect on the depth of the ablation craters. Additionally applying the acid or base on to the ablation site does not show any benefits compared to water. Furthermore we preheated the chemicals with a low energy pulse prior to the ablation pulse, which also showed no effect. However, applying a longer soaking time of the chemicals induced nearly a doubling of the

ablation depth. Furthermore with this longer soaking time, carbonisation at the crater margins does not occur as it can be observed with conventional waterspray.

7562-26, Session 6

Selective mucosal ablation using CO2 laser for the development of novel endoscopic submucosal dissection: comparison of continuous wave and nanosecond pulsed wave

K. Ishii, S. Watanabe, Osaka Univ. (Japan); D. Obata, Kobe Univ. (Japan); H. Hazama, Osaka Univ. (Japan); Y. Morita, Y. Matsuoka, H. Kutsumi, T. Azuma, Kobe Univ. (Japan); K. Awazu, Osaka Univ. (Japan)

Endoscopic submucosal dissection (ESD) is accepted as a minimally invasive treatment technique for small early gastric cancers that allows en bloc resection of large sections of mucosa over 2 cm in diameter. Procedures are carried out using some specialized electrosurgical knifes (insulation-tipped knife (IT knife) and bipolar needle knife (B-knife) etc.). After injection of submucosal injection solution (glycerol and sodium hyaluronate acid solution etc.) into a submucosal layer, a circumferentia incision is made and submucosal dissection is performed endoscopically. However it is not widely used because its procedure is difficult. The objective of this study is to develop a novel ESD method which is safe in principle and widely used by using laser techniques. In this study, we used CO ₂ lasers with a wavelength of 10.6 µm for mucosal ablation. Two types of pulse, continuous wave and pulsed wave with a pulse width of 100 ns, were studied to compare their values. Porcine stomach tissues were used as a sample. Aqueous solution of sodium hyaluronate (MucoUp®) with 50 mg/ml sodium dihydrogenphosphate is injected to a submucosal layer. As a result, ablation effect by CO 2 laser irradiation was stopped because submucosal injection solution completely absorbed CO₂ laser energy in the invasive energy condition which perforates a muscle layer without submucosal injection solution. Mucosal ablation by the combination of CO₂ Laser and a submucosal injection solution is a feasible technique for treating early gastric cancers safely because it provides a selective mucosal resection and less-invasive interaction to muscle layer.

7562-27, Session 6

Selective cancer therapy via IR-laser-excited gold nanorods

J. Lin, Y. Hong, C. Chang, National Taiwan Univ. (Taiwan)

Phototherapy has been used for the treatment of cancers (tumors), where various sensitizing dyes were used to absorb the visible light (lasers or LED). This study evaluated the effectiveness of near infrared (NIR) laser-excited gold nanorods (GNRs) as the active target to selectively kill the cancer cells. The key laser and sample parameters to be measured include: the absorption coefficient (A), the penetration depth (D), the laser fluence (F) and irradiation time (t), the temperature increase (dT), and concentration of the GNR.

Solution with gold nanorods having aspect (length/width) ratio of R=(3.8-4.2) with a given concentration (C) was filled into a container which is irradiated by a continuous wave (CW) diode laser at NIR (760-850 nm) having a collimated spot size about 8.0 mm. The temperature increases of the laser-targeted solution near the surface (T1 at z=1.0 mm) and inside (T2 at z=6.0 mm) were measured by thermal probes and recorded in real time. Optimal laser operation for the surface and volume heating was achieved by a novel pulsed-train technique using an auto-controlled laser on-off to meet the desired T1 and T2. The measured dT is an increasing function of F, C and t, where typical value dT=100 C could be achieved for t=(50-10) seconds depending on laser F=(0.4-1.5) (W/cm2). Our measured data are predictable and consistent with analysis based on a volume heating heat diffusion equation which was solved numerically.



7562-28, Session 7

Nanorose and lipid detection in atherosclerotic plaque using dual-wavelength photothermal wave imaging

T. Wang, J. Qiu, L. L. Ma, J. Sun, S. Ryoo, The Univ. of Texas at Austin (United States); X. Li, The Univ. of Texas Health Science Ctr. at San Antonio (United States); K. P. Johnston, The Univ. of Texas at Austin (United States); M. D. Feldman, The Univ. of Texas Health Science Ctr. at San Antonio (United States); T. E. Milner, The Univ. of Texas at Austin (United States)

Atherosclerosis and specifically rupture of vulnerable plaques account for 23% of all deaths worldwide, far surpassing both infectious diseases and cancer. In atherosclerosis, macrophages can infiltrate plaques which are often associated with lipid deposits. Photothermal wave imaging is based on the periodic thermal modulation of a sample using intensity modulated light. Intensity modulated light enters the sample and is absorbed by targeted chromophores and generates a periodic thermal modulation. We report use of photothermal wave imaging to visualize nanoroses (taken up by macrophages via endocytosis) and lipids in atherosclerotic plaques. Two excitation wavelengths were selected to image nanoroses (800 nm) and lipids (1210 nm). Atherosclerotic plaque in a rabbit abdominal artery was irradiated (800 nm and 1210 nm) to generate photothermal waves at a frequency of 4 Hz. The radiometric temperature at the tissue surface was recorded by an infrared (IR) camera over a 10 second time period at the frame rate of 25.6 Hz. Extraction of images (256 × 256 pixels) at various frequencies was performed by Fourier transform at each pixel. Frequency amplitude images were obtained corresponding to 800 nm and 1210 nm laser irradiation. Computed images suggest that the distributions of both nanorose and lipid can be identified in amplitude images at a frequency of 4 Hz. Observation of high concentration of nanoroses in atherosclerotic plaque confirms that nanoroses are present at locations associated with lipid deposits.

7562-29, Session 7

Method for measuring ocular aberrations induced by thermal lensing in vivo

R. L. Vincelette, J. W. Oliver, G. Noojin, K. Schuster, A. D. Shingledecker, Air Force Research Lab. (United States); A. J. Welch, Univ. of Texas at Austin (United States)

An adaptive optics imaging system was used to qualitatively observe the types of aberrations induced by an infrared laser in a rhesus eye. Thermal lensing was induced with an infrared laser radiation wavelength of 1150-nm. The adaptive optics system tracked the temporal response of the aberrations at a frequency of 30 Hz for continuous-wave exposures. Results are compared against thermal lensing aberrations of an artificial eye.

7562-30, Session 7

New method to visualize subsurface absolute temperature distributions and dynamics during laser-tissue interactions using thermo cameras

S. Been, T. de Boorder, J. Klaessens, R. Verdaasdonk, Univ. Medical Ctr. Utrecht (Netherlands)

The visualization of temperature fields using thermal imaging has always been limited to the surface of a medium. We have developed a new strategy to look below the surface of biological tissue by viewing through a ZincSelenide window from the side to a block of tissue. When exposed from above with an energy source like a laser, the temperature

distribution below the surface can be observed through the window. This new method was compared to a technique to visualize temperature gradients in a transparent tissue model based on color-Schlieren imaging.

The thermo dynamics during laser tissue interaction of various medical laser systems were studied to obtain a better understanding of the working mechanism of medical laser interventions. Simultaneously with thermal imaging, normal close-up video footage was obtained to support the interpretation of the thermal imaging.

The basic temperature distribution and dynamics underneath the surface of chicken breast and steak were studied with various laser sources: 810 nm Diode, 1064 nm Nd YAG, 2.1 μm pulsed Holmium, 2.0 μm continuous thulium and 2.78 μm Er:YSGG. The laser source was either in a static position or scanned over the surface. The thermal imaging was compared to normal video and color-Schlieren images. The three imaging modalities showed to be both compatible and complementary showing the pro- and cons- of each modality.

The new subsurface thermal imaging method will give a better understanding of interaction of various lasers and RF devices and contribute to the safety and the optimal settings for various medical applications.

7562-31, Session 7

Effect of temperature on fluorescence: an animal study

A. J. Walsh, D. B. Masters, Vanderbilt Univ. (United States); A. J. Welch, The Univ. of Texas at Austin (United States); A. Mahadevan-Jansen, Vanderbilt Univ. (United States)

The fluorescence yield of collagen is known to be a function of the temperature of the collagen sample. In this study, we have evaluated the effect of temperature on the fluorescence properties of enucleated porcine eyes, excised porcine cornea, and rat skin. A pulsed nitrogen laser at 337 nm excitation was used for fluorescence measurements and a white light source was used for diffuse-reflectance measurements. Tissue temperature at the time of fluorescent measurement was acquired using a thermal camera. The samples were mounted in a saline bath and measurements were made as the tissue temperature was increased from -20°C to 70°C. Results indicate that temperature affects several fluorescence spectra characteristics: the peak height decreased as temperature increased; at temperatures above 60°C, the peak position shifted to lower wavelengths; and the signal to noise ratio decreased as temperature increased. Heating and cooling the cornea indicated that the process is reversible with heating to 50°C but irreversible past 60°C. The diffuse-reflectance spectra indicated a change in optical properties past 60°C. Prior to the denaturation temperature for collagen at 57°C, no change in optical properties was observed. This implies that the temperature-dependent decrease in fluorescence is a property of fluorescence and not a result of altering optical properties.

7562-32, Session 7

Collagen thermal denaturation study for thermal angioplasty based on modified kinetic model: relation between the artery mechanical properties and collagen denaturation rate.

N. Shimazaki, T. Hayashi, M. Kunio, T. Arai, Keio Univ. (Japan)

We have been developing the novel heating angioplasty in which sufficient artery lumen dilatation was attained with thermal softening of the collagen fiber in artery wall. In the present study, we investigated on the relation between the mechanical properties of heated artery and thermal denaturation rate of arterial collagen in ex vivo. We employed Lumry-Eyring model to estimate the temperature- and time-dependent thermal denaturation rate of arterial collagen fiber during heating.



We made kinetic model of arterial collagen thermal denaturation by adjustment of K and k in this model, those were the equilibrium constant of reversible denaturation and the rate constant of the irreversible denaturation. Meanwhile we demonstrated that the change of artery reduced scattering coefficient during heating reflected the reversible denaturation of arterial collagen. Based on this phenomenon, the K was determined experimentally by backscattered light intensity measurement (at 633nm) of extracted porcine carotid artery during temperature elevation and descending (25°C→70°C→25°C). Then, the reversible (irreversible) denaturation rate defined as reversible (irreversible) denatured collagen amount / total collagen amount was calculated by this model. Artery thermo-mechanical analysis was performed to compare the artery mechanical properties during heating with the calculated denaturation rate with the model. In any artery temperature condition in 70-80°0, the irreversible denaturation rate was estimated to be around 20% when the artery thermal shrinkage started. On the other hand, the estimated irreversible denaturation rate remained below 5% and reversible denaturation reached up to 20% while the artery softening occurred without shrinkage. We think that our model of arterial collagen thermal denaturation might be reasonable to estimate the artery mechanical properties during heating.

7562-33, Session 7

Effects of laser parameters on propagation characteristics of laser-induced stress wave for gene transfer

T. Ando, Keio Univ. (Japan); S. Sato, National Defense Medical College (Japan); M. Terakawa, Keio Univ. (Japan); H. Ashida, National Defense Medical College (Japan); M. Obara, Keio Univ. (Japan)

We have been demonstrating targeted gene transfection by laser-induced stress waves (LISWs) that are generated by irradiating a laser-absorbing material with high-power laser pulses. Advantages of this method include a capability of treating deep-located tissues, since LISWs can be efficiently propagated in tissue. However, maximum treatable tissue depth is not clear. In this work, we investigated effects of laser parameters on propagation characteristics of LISWs in tissue phantoms and depth-dependent properties of gene transfection. A rubber disk with a plastic sheet for plasma confinement was placed on a gel phantom mimicking acoustic characteristics of soft tissue and it was irradiated with a nanosecond Nd: YAG laser pulse. Temporal pressure profiles of LISWs were measured with a hydrophone and their propagation was visualized by shadowgraphy. The measurements showed that with a larger laser spot diameter, LISWs were propagated more efficiently with flat wavefront in phantoms. Gene delivery was attempted by applying LISWs that were propagated through phantoms. Phantoms with various thicknesses were placed on the rat dorsal skin that had been injected with plasmid DNA coding for reporter gene; LISWs were applied from the top of the phantom. Efficient gene expression was observed in the skin even under a 15 mm thick phantom at a laser fluence of 0.5 J/cm2 with a laser spot diameter of 6 mm; no remarkable damage was observed in the tissue. These results would be useful to determine appropriate laser parameters for noninvasive gene delivery to deep-located tissues based on transcutaneous application of LISWs.

7562-50, Session 7

Effects of temperature on fluorescence in human tissue

D. B. Masters, A. J. Walsh, Vanderbilt Univ. (United States); A. J. Welch, The Univ. of Texas at Austin (United States); A. Mahadevan-Jansen, Vanderbilt Univ. (United States)

The fluorescence properties of human tissue are known to be temperature dependent. The most apparent effect of this dependence is the inverse relationship between fluorescence yield and temperature. In

this study, we used fluorescence and diffuse-reflectance spectroscopy to investigate the effects of temperature on fluorescence yield, thermal coagulation, and tissue optical properties.

Human tissue from the breast and abdomen were examined in vitro, and human skin was examined in vivo using a fluorescence and diffuse-reflectance system to observe the effects of temperature on fluorescence and optical properties. Fluorescence measurements were carried out using a pulsed nitrogen laser at 337 nm for excitation and a thermal camera for temperature measurements. Thermal variation of the specimens was provided by a saline bath for the in vitro experiments and an ice pack and heat lamp for the in vivo experiments. In vitro temperatures were varied from -20°C to 70°C and in vivo temperatures ranged from 0°C to 40°C. Optical property measurements and Monte Carlo simulations were carried out on the in vitro samples for different levels of thermal exposure.

Results of both the in vivo and in vitro experiments indicate that optical properties of human tissue change at high temperatures due to increased scattering. In addition, the activation energy of certain internal processes contributed to a decrease in fluorescence yield with increasing temperature. Some of these effects were found to be reversible before a certain temperature threshold, while some effects of coagulation on fluorescence and optical properties were not reversible.

7562-34, Session 8

Picosecond laser tissue dissection with extended and multiple foci

I. Toytman, A. S. Silbergleit, Stanford Univ. (United States); D. Simanovski, Coherent, Inc. (United States); D. Palanker, Stanford Univ. (United States)

Ultrashort lasers are typically utilized for tissue dissection by sequential application of tightly focused beam along a scanning pattern. Each pulse creates a small (on the order of 1 micrometer) zone of multiphoton ionization (optical breakdown). At energies exceeding vaporization threshold cavitation bubble is formed around the focal volume. The rupture zones produced by separate bubbles coalesce and form a continuous cut. We present an alternative approach, in which an extended zone of tissue is cut by simultaneous application of laser energy in multiple foci. Simultaneous formation of multiple cavitation bubbles results in hydrodynamic interactions that can lead to significant extension of the rupture zone in tissue. Two simultaneously expanding bubbles compress and strain material between them, while simultaneously collapsing bubbles can produce jets towards each other.

We calculated and experimentally imaged the flow dynamics of expanding and collapsing bubbles and obtained maps of tissue deformation. With the measured tissue threshold strain, the deformation map allows predicting the rupture zone as a function of maximum bubble size and distance between the bubbles.

We also demonstrate an optical system producing 1 mm long dissection with a single laser pulse. Combination of a lens and an axicon produces a wire-like zone of optical breakdown, with aspect ratio 250:1. The subsequent cavitation bubble has aspect ratio 100:1 at early stage of expansion. We calculated an optimal laser beam intensity profile to create axially-uniform elongated ionization pattern.

7562-36, Session 8

Real-time OCT imaging of laser ablation of biological tissue

M. Ohmi, M. Ohnishi, D. Takada, M. Haruna, Osaka Univ. (Japan)

During laser ablation of a diseased area, the surrounding tissues and organs suffer serious damage. In order to optimize laser ablation of biological tissues, it is necessary to observe the laser ablation in situ. The real-time imaging of tissue laser ablation is realized in the fusion system of the YAG ablation laser and optical coherence tomography

Return to Contents TEL: +1 360 676 3290 · +1 888 504 8171 · customerservice@spie.org



(OCT). A swept-source OCT (SS-OCT) is combined with a YAG-laser ablation system. The SS-OCT consists of fiber-optic components, and the illuminating laser beam on the signal arm of the OCT interferometer is aligned with the YAG laser beam, using a dichroic mirror. The sweep frequency of the laser source is 20 kHz with 25 frames / s, where the imaging area is 1 x 1 mm.

In the human tooth, time variation of the crater depth is measured very precisely, with a standard deviation comparable to the coherence length of the SS-OCT, resulting in determination of the ablation rate with an accuracy below 0.01 mm / pulse. At the interface between enamel and dentine, the ablation rate changes drastically, as does the crater shape, because of the differences in hardness between these two media. On the other hand, during laser ablation of soft tissue, such as the aorta of a dog, thermal deformation of the crater is found that includes upheaval and removal of tissues.

7562-37, Session 8

Cavitation induced by CW lasers in liquids

J. C. Ramirez-San-Juan, E. Rodriguez-Aboytes, A. E. Martínez-Cantón, O. Baldovino-Pantaleón, Instituto Nacional de Astrofísica, Óptica y Electrónica (Mexico); S. Torres-Hurtado, Univ. de Sonora (Mexico); A. Robledo-Martinez, Univ. Autónoma Metropolitana (Mexico); R. Ramos-Garcia, Instituto Nacional de Astrofísica, Óptica y Electrónica (Mexico)

In this work we present novel results on thermocavitation in highly absorbing solutions using CW low power laser. Our experiments were realized using a continuous wave low power (200 mW) near infrared laser (980 nm) focused in a transparent container filled with a saturated copper nitrate saline solution. The solution shows a large absorption coefficient at the laser wavelength (150 cm-1) so the penetration length is short ~66 microns. As a result, the bubble is created near the beam's entrance wall and therefore asymmetric bubbles are created. We report the temporal dynamic of the cavitation bubble, which is much shorter than previously reported: it reaches its maximum radius in ~100 microsec and the collapse time is much faster occurring in 5-8 microsec. A strong shock wave is created at the bubble collapse whose amplitude depends on the radio's bubble. We found that the bubble's radius and amplitude of the shock wave escalate with the inverse of the beam power. Thermocavitation can be an useful tool for the generation of ultrasonic waves and controlled ablation for use in high-resolution lithography.

7562-38, Session 8

Photomechanical and thermomechanical response of nanosecond laser irradiated agar gel

F. G. Perez-Gutierrez, Univ. of California, Riverside (United States); R. Evans, S. Camacho-Lopez, Ctr. de Investigación Científica y de Educación Superior de Ensenada (Mexico); G. Aguilar, Univ. of California, Riverside (United States)

Nanosecond long laser pulses are used in medical applications where precise tissue ablation with minimal thermal and mechanical collateral damage is required. When a laser pulse is incident on a material, optical energy will be absorbed by a combination of linear and nonlinear absorption according to both: laser light intensity and material properties. In the case of water or gels, the first results in heat generation and thermoelastic expansion; while the second results in an expanding plasma formation that launches a shock wave and a cavitation/boiling bubble. Plasma formation due to nonlinear absorption of nanosecond laser pulses is originated by a combination of multiphoton ionization and thermionic emission of free electrons, which is enhanced when the material has high linear absorption coefficient. In this work, we present an analysis of pressure transients originated when 6 ns laser pulses are incident on agar gels with varying linear absorption coefficient using laser

radiant exposures above threshold for bubble formation. The underlying hypothesis is that pressure transients are composed of the superposition of both: shock wave originated by hot expanding plasma resulting from nonlinear absorption of optical energy and, thermoelastic expansion originated by heat generation due to linear absorption of optical energy. The objective of this work is to evaluate the relative contribution of each absorption mechanism to mechanical effects in agar gel. Real time pressure transients are recorded with PVDF piezoelectric sensors 10 mm away from focal point.

7562-39, Session 9

Retinal neuroprotection by intravitreal saline injections

M. Belkin, M. Belokopitov, S. Shulman, G. Dubinsky, M. Rosner, Tel Aviv University (Israel)

Purpose: Laser-induced retinal lesions are enlarged by secondary degeneration processes which damage tissues adjacent to the primary lesion. In the past we tested, neuroprotective modalities to limit the secondary degeneration and augment the healing processes, using intravitreal saline injections as controls. In this study, we evaluated the neuroprotective effect of intravitreal saline injection as a neuroprotective modality in itself.

Methods: Standard argon laser lesions (514 & 544 nm, 200 mm, 0.1 W, 0.05 sec) were created in 36 DA pigmented rats that received saline either by intravitreal (5µl) or intravenous (0.5 ml) injection seven days before the laser session. The intravitreal injection was performed with a 30-gauge needle of a Hamilton-syringe through the temporal posterior sclera and retina. The laser-induced lesions were evaluated histologically and morphometrically 3, 20 and 60 days after exposure to laser.

Results: At all the time-points examined, intravitreal injection of saline reduced the laser- induced cell-loss (P < 0.05) and decreased the lesion diameter (P < 0.05), as compared to intravenous treatment.

Conclusions: Pre-treatment by intravitreal saline injection has a neuroprotective effect in the rat retina. The mechanism of the preconditioning action should be evaluated and the clinical applicability of this effect, tested.

7562-40, Session 9

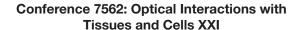
Artificial haze scotoma-induced visual disorders in sensory and perceptual tasks: serial vs. parallel processing

R. Brandeis, I. Egoz, D. Peri, J. Turetz, Israel Institute for Biological Research (Israel)

Macular scotomas, affecting visual functioning, characterize many eye and neurological diseases. In this work, we modeled foveal visual field defects, and evaluated their effects on fovially and parafovially-biased perceptual tasks.

The modeled occluding central scotomas were superimposed on the stimuli presented on the computer display, and were stabilized on the retina using a mono Purkinje Eye-Tracker. Each simulated scotoma was a round digital image, constructed of a dark central core, circumscribed by blur margins, thus making it a relative scotoma. Performance was evaluated on three tests: Visual Scanning and Color Blinded Test - Ishihara, performed through foveal vision, and Simultaneous Pattern Comparison, which may demand (depending on the subject's individual strategy), foveal or parafoveal vision.

Artificially generated, central haze scotomas impaired performance of all tasks. Reaction time was slowed significantly in a size dependent manner. In the Visual Scanning test, a slight decrease in accuracy as well as substantial alteration in search strategy, were also obtained. Deadlines increased considerably. A gender- segmentation showed that reaction time of male subjects was not sensitive to scotoma effect, in the Simultaneous Pattern Comparison test, while reaction time of female





subjects did increase significantly as a function of scotoma size. In contrast, no gender differences were shown in the two other tests.

These results support the hypothesis that subjects are sensitive to the effect of a central scotoma when using a serial, slow search strategy, known also as "vision with scrutiny". However, when using a parallel, automatic, preattentive strategy, subjects are able to overcome the central scotoma-induced visual disorders.

7562-41, Session 9

New methods in order to determine the extent of temporary blinding from laser and LED light and proposal how to allocate into blinding groups

H. Reidenbach, Cologne University of Applied Sciences (Germany); G. Ott, FIOSH/BAuA (Germany); M. Brose, BGETE (Germany); K. Dollinger, Cologne University of Applied Sciences (Germany)

Indirect effects arising from bright artificial optical sources like temporary blinding might result in serious incidents or even accidents due to accompanying alteration of visual functions like visual acuity, contrast sensitivity and color discrimination.

In order to determine the degree and duration of impairment resulting from dazzle, flash-blindness and afterimages, caused by a beam from a laser or lamp product, an investigation has been performed with the goal to improve the current knowledge as far as especially visual acuity recovery duration is concerned.

For this two different test set-ups were designed and engineered in order to be able to determine the time duration after which visual acuity returns to its previous value after temporary blinding from a laser or a LED and in addition to look for any functional relations as far as wavelength, optical power and exposure duration are concerned.

In addition to normal visual acuity measurements, which have been applied in order to determine the recovery time after irradiation with a high brightness LED with the aid of a modified binoptometer, a reading test was delivered to the subjects on a computer monitor in the case of laser irradiation.

As stimulating light sources laser with 632.8 nm and 532 nm and red, green, royal blue and white HB-LEDs were applied. The maximum optical power in a 7-mm aperture was 0.783 mW (laser) and 3 mW (LED). The exposure durations were chosen between 0.25 s and 20 s.

The visual acuity recovery time has been found to obey the following dose relationship:

 $t/s = 3.7 \times ln(energy/\mu J)$ - 16.2 in the case of a green HB-LED. The afterimage duration from a red laser beam was determined to be: $t/s = 50.6 \times ln[(P \times t \exp)/\mu J]$ - 13.4.

The results of the research project suggest classifying light sources like laser and LEDs into so-called blinding groups. In total 3 different groups which reflect the obtained results are proposed in order to fulfil the requirements of a special classification and might be regarded as an appropriate assistance to perform a risk analysis.



Saturday-Sunday 23-24 January 2010 • Part of Proceedings of SPIE Vol. 7563 Dynamics and Fluctuations in Biomedical Photonics VII

7563-02, Session 1

Tissue viability imaging for quantification of skin erythema and blanching

G. E. Nilsson, Linköping University (Sweden) and Wheelsbridge (Sweden); M. J. Leahy, Univ. of Limerick (Ireland)

Naked eye observation has up to recently been the main method of determining skin erythema (vasodilatation) and blanching (vasoconstriction) in skin testing. Since naked eye observation is a highly subjective and investigator-dependent method, it is difficult to attain reproducibility and to compare results reported by different researchers performing their studies at different laboratories. Consequently there is a need for more objective, quantitative and versatile methods in the assessment of alterations in skin erythema and blanching caused by internal and external factors such as the intake of vaso-actice drugs, application of agents on the skin surface and by constituents in the environment. Since skin microcirculation is sensitive to applied pressure and heat, such methods should preferably be noninvasive and designed for remote use without touching the skin. As skin microcirculation further possesses substantial spatial variability, imaging techniques are to be preferred before single point measurements. An emerging technology based on polarization digital camera spectroscopy - Tissue Viability Imaging (TiVi) - fulfills these requirements. The principles of TiVi and some of its early applications are addressed in this chapter.

7563-03, Session 1

tissue structural organization: measurement, interpretation, and modeling

D. D. Duncan, Oregon Health & Science Univ. (United States); D. G. Fischer, NASA/Glenn Research Center (United States); M. Daneshbod, University of New Mexico (United States); S. A. Prahl, Oregon Medical Laser Center (United States)

Analysis of the first and second order statistical properties of light is powerful means of establishing the properties of a medium with which the light has interacted. In turn, the first and second order statistical properties of the medium dictate the manner in which light interacts with the medium. The former is the inverse problem and the latter is the forward problem. Towards an understanding of the propagation of light through complex structures, such as biological tissue, one might choose to explore either the inverse or the forward problem. Fundamental to the problem, however, is a physical parametric model that relates the two halves; a model that allows prediction of the measured effect or prediction of the parameters based on measurements. This is the objective of our study.

As a means of characterizing the first and second order properties of tissue, we discuss measurements using differential interference contrast microscopy and a phase-stepping Mach-Zehnder interferometer. First and second order properties are characterized respectively in terms of scatter phase functions and spatial power spectral densities Results are shown for a number of representative tissue types. To explore the utility of such parametric tissue models, we report preliminary efforts at quantifying the effects of partial spatial coherence. These measurements are made on various biological media using a spatial light modulator within the Mach-Zehnder interferometer.

7563-04, Session 1

Image quality comparison of high-energy phase contrast x-ray images with low-energy conventional images: phantom studies

M. Wong, D. Zhang, H. Liu, Univ. of Oklahoma (United States)

A significant challenge in the field of mammography that has yet to be overcome involves providing adequate image quality for detection and diagnosis, while minimizing the radiation dose to the patient. An emerging x-ray technology, high energy phase contrast imaging holds the potential to reduce the patient dose without compromising the image quality, which would benefit the early detection of breast cancer. The purpose of this preliminary study was to compare the image quality of high energy phase contrast images to conventional x-ray images at typical mammography energies. The experimental settings were selected to provide similar entrance exposures for the high and low energy images. Several phantoms were utilized in this study in an effort to provide a comprehensive image quality comparison. The results indicate that similar image quality can be provided by the high energy phase contrast images at a lower patient dose.

7563-05, Session 1

Characterization of tissue scattering with speckle measurements under partial spatial coherence illumination

V. Turzhitsky, N. N. Mutyal, J. D. Rogers, V. Backman, Northwestern Univ. (United States)

The speckle phenomenon, although an impediment for some techniques, has been implemented into several useful technologies. Although conventional laser speckle typically has no relationship with the optical properties of a diffusely scattering media, recent work has shown that speckle contrast measurements under partial temporal coherence can be sensitive to the optical properties of the scattering media when the temporal coherence length is on the order of the width of the path length distribution of light through the media. In this work, we explore the role of spatial coherence on the resulting properties of the speckle pattern. For a single for single scattering random media such as ground glass or polished metal, the Fourier transform of the speckle pattern yields the square of the magnitude of the spatial coherence function when the illumination spot radius is greater than the spatial coherence length. In this work, the Fourier transform of the speckle pattern is measured from diffusely scattering samples to evaluate the effect of the scattering media on the spatial coherence function. Therefore, the Fourier transform of the speckle pattern after scattering through the media represents the propagated coherence function. The experiment is performed on samples with varying optical properties and the results are compared with published models that simulate the propagation of spatial coherence through turbid media. This application of speckle measurement allows for a simple and accurate study of the propagation of spatial coherence in turbid media with potential applications for characterizing tissue properties.



7563-06, Session 1

4D non-gated chicken embryo heart outflow imaging using spectral optical coherence tomography

A. Liu, Z. Ma, K. Thornburg, R. K. Wang, S. Rugonyi, Oregon Health & Science Univ. (United States)

4D imaging of chicken embryonic heart at early stage is challenging due to the small dimensions of the heart (e.g., typically<2mm) and the rapid cardiac motion (typically >2 heart beats per second). OCT with high resolution (~10um) can solve the first problem. Comparing with the rapid cardiac motion, imaging speed of OCT is however relatively slow. Here, we present a non-gated 4D imaging strategy combined with an efficient post-acquisition synchronization procedure that circumvents limitations on acquisition rate. Using the method, we reconstruct the cardiac outflow tract (OFT) of a chicken embryo, imaged with OCT at early stages of development (HH 18). We showed that the proposed synchronization procedure achieves efficiency without sacrificing accuracy, and that the reconstructed 4D images properly captured the dynamics of the OFT wall motion

7563-08, Session 1

Characterizing polarized autofluorescence of normal and benign tissues using singular value decomposition and wavelet transform

A. H. Gharekhan, C. U. Shah Science College (India); S. Arora, University of Oxford (United Kingdom); P. K. Panigrahi, Physical Research Laboratory (India) and Indian Institute of Science Education and Research (IISER) (India); A. Pradhan, Indian Institute of Technology (India)

A systematic investigation of the polarization characteristics of the autofluorescence of normal and benign human breast tissues is carried out complementing our earlier studies on normal and cancer tissues. Co- and cross-polarized auto-fluorescence are collected in the 500 to 700nm range through excitation at 488nm using laser as excitation source. A number of parameters, capturing spectral variations are extracted in the co- and cross-polarized channels through singular value decomposition and wavelet decomposition, which differentiate normal and benign tissues. The correlation matrix differs significantly in normal and benign tissues reflecting the presence of different fluorophores. The eigenvectors corresponding to the dominant eigenvalues reveal differences between tissue types. The co-polarized component being sensitive to intrinsic fluorescence shows different behavior for normal and benign tissues in the emission domain of known fluorophores. Interestingly, the benign tissue samples show correlation properties intermediate to malignant and normal cases. In the wavelet domain the standard deviation of percentage fluctuation reveal differences between tissues type. The correlation characteristics manifest prominently in the wavelet low pass (average) domain.

7563-12, Session 1

LED illumination effects on proliferation and survival of meningioma cellular cultures

E. Solarte, H. Urrea, W. Criollo, O. Gutierrez, Universidad del Valle (Colombia)

Generating controlled cellular effects by irradiating cell cultures is a subject of great interest, because these can be used to control the cellular growth, to improve the cellular proliferation and the implant adaptation, and to make the cellular regulation in chemical therapy possible. Special interest is devoted to tumoral and malignant cell cultures because of the importance of cancer treatment and therapy.

In this work, meningioma cell cultures were prepared from LN2 frozen cell samples following a two step protocol developed in our laboratories, once the primary culture reach 100% confluence, a set of secondary cultures were produced, in 96 wells culture plates, to study cell proliferation. Semiconductor light sources (LEDs) emitting in seven different wavelength ranges were used to illuminate the meningiomas' culture wells, and three different irradiation doses: 0.025J/ cm2, 0.05J/cm2, and 0.05J/cm2, were selected for each light source. Simultaneously, control cultures were processed in order to provide the comparison. Spectrophotometric quantification of cell proliferation, viability, and cytotoxicity were performed every 24 hours for 6 days, using the XTT colorimetric assay (Roche®). None of the irradiated cultures exhibit citotoxicity; nevertheless, the proliferation measurements, done in both irradiate and control cultures, shown that some proliferation inhibition occurs for a given LED color, and for a certain dose range. The larger proliferation was detected at a 0.05J/cm2 dose, almost independent of the light wavelength; but for the orange and violet LEDs generated the bigger proliferation rate. Results show the improvement of meningioma cell proliferation using illumination in some given wavelength ranges.

7563-01, Session

Photoacoustic microcopy of vasculature: functional volumetric imaging in vivo

L. V. Wang, Washington Univ. in St. Louis (United States)

Commercially available high-resolution 3D optical imaging modalities-including confocal microscopy, two-photon microscopy and optical coherence tomography-have fundamentally impacted biomedicine. Unfortunately, such tools cannot penetrate biological tissue deeper than the optical transport mean free path (~1 mm in the skin). Photoacoustic tomography, which combines strong optical contrast and high ultrasonic resolution in a single modality, has broken through this fundamental limitation and achieved high-resolution optical imaging at super-depths (depths beyond the optical transport mean free path). Based on intrinsic optical contrast, photoacoustic microscopy is able to provide 3D functional imaging with scalable spatial resolution and penetration limits.

7563-09, Session 2

Medical application-oriented nanostructure design: physical basics and limitations

L. D. Shvartsman, B. Laikhtman, The Hebrew Univ. of Jerusalem (Israel)

We present a theoretical overview of key physical limitations for application-oriented nanostructure design. We focus on such promising applications as: nanodot-assisted optical imaging, and photo-thermal therapy with the help of nanostructures. For these applications we consider the following nanostructures: metal-coated nanoshells and metal nanoparticles, semiconductor quantum dots. The actual design of relevant nanoobjects for particular applications must include consideration of such phenomena as: plasmon resonance, light scattering, light absorption, heating and heat dissipation, change of carrier spectrum resulting from size-quantization. These phenomena are considered for model systems of various designs for different parameters of radiation. Our model estimations are compared with experimental results when such results are available. The conclusions are formulated as a paradigm "desired vs. feasible".

7563-10, Session 2

Quantification of microbubbles in blood with phase-sensitive SSOCT

K. V. Larin, Univ. of Houston (United States)



We have developed phase stabilized swept source optical coherence tomography (PhS-SSOCT), that shows an axial resolution of 10 μm , phase sensitivity of 0.04 radians, imaging depth of up to 6 mm in air and a scanning speed of 20 kHz for a single A-line. In this paper, the PhS-SSOCT is applied to quantify gas microbubbles in blood. The results indicate that the system is able to detect bubbles of diameters greater than 10 μm using the structural image and the microbubbles of diameter less than 10 μm could be detected using the temporal phase response. Images of the bubbles of diameters 600 μm , 405 μm and 6 μm along with their phase responses are presented. Results indicate that, the PhS-SSOCT could be potentially used for rapid assessment of blood microbubbles in vivo that cause diseases associated with decompression sickness, venous and arterial gas emboli and barotraumas. Eventually, the PhS-SSOCT can be utilized as an early diagnostic tool for clinical purposes.

7563-11, Session 2

Optical microscopy for gold nanoparticles temperature and velocity field visualization

I. V. Fedosov, N.G. Chernyshevsky Saratov State Univ. (Russian Federation); I. S. Nefedov, Helsinki University of Technology (Finland); B. N. Khlebtsov, The Russian Academy of Sciences' Institute of Biochemistry and Physiology of Plants and Microorganis (Russian Federation); V. V. Tuchin, N.G. Chernyshevsky Saratov State Univ. (Russian Federation)

Optical microscopy based technique for nanoparticles dynamics studies has been developed. It includes the high contrast dark field nanoparticle imaging using the selective plane illumination with laser light and statistical particle tracking velocimetry based image processing. This technique allows for the visualization of water suspended gold nanoparticles dynamics. Distribution of particles temperature and velocity of their ordered motion could be obtained with up to 1 um spatial resolution. The proposed technique could be used for the studies of photothermal and photophorethic effects induced by laser irradiation in colloidal systems.

7563-13, Session 3

High-resolution wide field of view blood perfusion maps for retina and choroid with optical micro-angiography

L. An, D. Wilson, R. K. Wang, Oregon Health & Science Univ. (United States)

In this presentation, we present the high resolution and wide field of view retina and choroid blood perfusion maps, which are obtained through optical micro-angiography (OMAG) technology. Based on the special frequency analysis, OMAG is able to visualize the vascular perfusion map down to the capillary level resolution. We used an 840 nm, 27 kHz FDOCT system to capture 16 OCT data sets in a sequential order, which could provide wide field blood field (~7.4mm×7.4mm) information of posterior part of a human volunteer. For each of these data sets, we eliminated the bulk motion artifacts through phase compensation method, which is based on the histogram bulk motion phase estimation. The displacements occurred between adjacent frames in one data set were compensated through 2 dimensional cross correlation of two adjacent OMAG flow images. Compared with the FA and ICGA images results, the OMAG results of blood perfusion map of retina and choroid demonstrate a very good agreement with them

7563-14, Session 3

Laser Doppler flowmetry for assessment of tissue microcirculation: 30 years to clinical acceptance

M. J. Leahy, Univ. of Limerick (Ireland) and RCSI and NBIPI (Ireland); G. E. Nilsson, Linköping University (Sweden) and Wheelsbridge AB (Sweden)

Both LDPM and LDPI are relatively easy to use methods in the experimental as well as in the clinical situation. Basic knowledge about the skin microcirculation and its temporal and spatial variations is, however, required to correctly interpret the results. The measurement depth, which has been estimated by means of Monte Carlo simulation, can be modulated to some degree by separating the transmitting and receiving fibres in LDPM. No such mechanism is available for LDPI. In a practical situation, however, there is no a priori knowledge about the epidermal thickness and hence of the distance from the skin surface to the microvascular bed. Results obtained from different organs and even from skin sites at different parts of the body surface should therefore not be directly compared. Best results are generally obtained if the investigation includes some element of tissue challenging such as topical application of a vaso-active substance or heat.

In summary, both LDPM and LDPI are versatile methods for investigation of the microcirculation of the skin. True everyday clinical applications - after about 30 years of use - are however, still sparse with the possible exception of burn depth assessment and LDF has to be regarded as a laboratory rather than a clinical tool.

7563-15, Session 3

In vivo studies of skin blood microcirculation using dynamic light scattering

I. Meglinski, University of Otago (New Zealand); V. Kalchenko, A. Harmelin, Weizmann Institute of Science (Israel)

We combine diffusing wave spectroscopy and dynamic light scattering microscopy to simultaneous non-invasive imaging of skin blood microcirculation. We demonstrate that the local blood micro-flows and blood microcirculation can be observed and analyzed quantitatively at the the biological zero level, i.e. when the arterial and vein flows are completely stopped. We show that the biological zero signal arises from the local blood micro-flows can be observed postmortem up to 100 minutes. The high sensitivity

of diffusing correlation technique and the feasibility for non invasive measurement of skin blood microcirculation is thus demonstrated, and the potential for methodology can now be explored.

7563-16, Session 3

In vivo assessment of speed distribution of red blood cells based on laser-Doppler spectrum decomposition

S. Wojtkiewicz, A. Liebert, A. Zbiec, R. Maniewski, Institute of Biocybernetics and Biomedical Engineering (Poland)

A novel method for estimation of speed distribution of particles moving in an optically turbid medium was validated during in-vivo measurements. This technique is based on analysis of spectrum of AC component of laser-Doppler signal. Laser-Doppler spectrum can be represented as a linear combination of Doppler shift probability distributions which depend only on scattering angle distribution. That observation allows us to decompose laser-Doppler spectra for estimation of speed distribution of red blood cells (RBC) in microcirculation. Proposed technique can provide simultaneous information about RBC speed distribution in



absolute units and changes of concentration in arbitrary units. We reported previously on validation of the spectrum decomposition technique in series of Monte Carlo simulations and physical phantom

Self constructed laser-Doppler flowmeter with high signal to noise ratio was used for in-vivo measurements. Spectra of laser-Doppler signals measured on middle finger of healthy volunteers were collected during full occlusion, venous occlusion and thermal tests. It was observed that decomposed speed distributions are influenced by changes of speed of red blood cells and their concentration during the stimulation tests. Maxima of speed distributions are correlated with cuff pressure during venous occlusion test. During thermal tests reaction of speed distributions maxima and RBC concentration for heating and cooling can be observed.

7563-17, Session 4

Comparison of scanning beam and whole field laser Doppler perfusion imaging

W. Steenbergen, E. Hondebrink, T. G. Van Leeuwen, Univ. Twente (Netherlands); M. J. Draijer, Spaarne Hospital (Netherlands)

Currently, laser perfusion imaging (LDPI) is undergoing a technology shift from scanning beam perfusion imagers to whole field systems. The latter can be subdivided in laser Doppler methods systems based on high speed CMOS cameras, and laser speckle contrast analysis (LASCA) technologies using slow imaging arrays, mostly CCD-based.

In scanning beam systems, a collimated laser beam scans the tissue with diffusely back reflected light being captured with a single detector. In wide field systems a large tissue area is illuminated, and the reflected light is imaged onto an array and captured at once. Unlike scanning beam systems, both whole field methods enable perfusion imaging at

In this study we compare the scanning beam LDPI principle with whole field LDPI, from a theoretical point of view, but also experimentally on phantoms and in vivo. For the tissue phantoms, the Monte Carlo simulation technique will be used as a reference.

From measurements on Intralipid phantoms compared to Monte Carlo, we conclude that in whole field LDPI the flux image, representing the first order moment of the power spectrum of photocurrent fluctuations is much closer related to real perfusion than for scanning beam systems. This difference can be explained in terms of the different behaviour of dynamic speckle patterns generated in both methods, in response to varying tissue optical properties. This is partly confirmed by in vivo measurements where such a different behaviour was forced by local modulation of optical properties.

7563-18, Session 4

Architectural and functional imaging of the microcirculation

M. J. Leahy, University of Limerick (Ireland)

Even in the 600-1200 nm region scattering dominates absorption leading to the development of low coherence methods (e.g. OCT) to image tissue with only ballistic photons. Ballistic photons returning from depths of more than a few mm are so few, so that researchers are using diffuse light tomographic methods (DOT, PAT) for deeper tissue imaging with a ten-fold depth enhancement. Planar Doppler, absorption and fluorescence imaging have recently been merged with tomographic methods to provide exquisite 3D images of architecture and function. This paper will discuss these new developments and the path to clinical, FDA and ultimately commercial acceptance. We have compared the operation of laser Doppler perfusion imaging (LDPI), with the more recently available laser speckle and Tissue Viability (TiVi) imaging system in human skin tissue using well-established microvascular provocations. The work confirms laser Doppler's sensitivity to provocations affecting the bulk of the upper dermis, but not the most superficial nutritional

layers. Despite using the same lasing wavelength, the speckle (FLPI) images were dominated by the superficial papillary plexus as shown in its tracking of the inflammatory response to a topical analgesic where the LDPI had failed. The TiVi system, similarly tracked the inflammatory response as one might expect from a system designed specifically to track red blood cell concentration. However, TiVi differs from the other techniques in its response to occlusion of the brachial artery. Architectural imaging techniques such as OCT and PAT can be more readily compared via resolution and imaging depth. The addition of functional imaging, while having the potential to greatly aid diagnosis, it may present additional obstacles in getting clinical and FDA approval.

7563-19, Session 4

Noise analysis in laser speckle contrast imaging

S. Yuan, Univ. of Maryland, College Park (United States); R. D. Naphas, Y. Chen, University of Maryland (United States); A. K. Dunn, University of Texas at Austin (United States); D. A. Boas, Martinos Center for Biomedical Imaging (United States)

Laser speckle contrast imaging (LSCI) is becoming an established method for full-field imaging of blood flow dynamics in animal models. A reliable quantitative model with comprehensive noise analysis is necessary to fully utilize this technique in biomedical applications and clinical trials. In this study, we investigated several major noise sources in LSCI: periodic physiology noise, shot noise and statistical noise. (1) We observed periodic physiology noise in our experiments and found that its sources consist principally of motions induced by heart beats and/or ventilation. Several methods, including frequency filtering, background subtraction, motion restraining, and EKG triggering, were developed to reduce or eliminate periodic physiology noise. The signal-to-noise ratio increased by 30% - 100% after applying said methods. (2) We found that shot noise caused an offset of speckle contrast (SC) values, and this offset is directly related to the incident light intensity. A mathematical model was developed to estimate the offset of SC values. We found this model to be consistent with our phantom experiment results. (3) A mathematical model of statistical noise was also developed. The model indicated that statistical noise in speckle contrast imaging is related to the SC values and the total number of pixels used in the SC calculation. Our experimental results are consistent with theoretical predications, as well as with other published works.

7563-07, Session 5

Measuring temporal autocorrelation functions and dermal perfusion using laser speckle contrast with multiple exposures

O. B. Thompson, Industrial Research Ltd. (New Zealand) and Auckland Bioengineering Institute (New Zealand); M. K. Andrews, Industrial Research Ltd. (New Zealand)

Laser speckle contrast measurements provide effectively instantaneous maps of dermal perfusion, using easily obtainable hardware, but such maps are qualitative. Clinical applications of these techniques require a good theoretical and experimental foundation of understanding before relating speckle measurements to a physiologically significant quantitative perfusion value.

We have confirmed that multiple-exposure laser speckle methods produce the same spectral information as laser Doppler measurements when applied to targets such as human tissue with embedded moving scatterers. This confirmation is based on both computer simulation of laser speckle data and experimental measurements on Brownian motion and skin perfusion using a laser Doppler system and a multiple-exposure laser speckle system. The Power Spectral Density (PSD) measurements of the light fluctuations derived using both techniques are equivalent. Dermal perfusion can therefore be measured in exactly equivalent terms



by either laser speckle contrast or more laborious laser Doppler methods.

Most analyses relating laser speckle contrast to perfusion depend on assuming a particular temporal autocorrelation function for the light intensity fluctuations in biospeckle. Using multiple-exposure laser speckle allows the autocorrelation function to be measured rather than assumed. Measured autocorrelation functions for perfusion under a variety of conditions are presented, including measurements under arterial occlusion to establish a biological zero: the speckle blur relating to the remaining movement of tissue constituents when there is no net blood flow.

7563-23, Session 5

A gel-based skin and blood flow model for doppler optical coherence tomography (DOCT) imaging system

K. Lawlor, E. Jonathan, M. J. Leahy, University of Limerick (Ireland)

Since its discovery in 1842 by Christian Johann Doppler, the Doppler Effect has had many applications in the scientific world. In recent years, the phenomenon has been integrated with Optical Coherence Tomography (OCT) yielding Doppler Optical Coherence Tomography (DOCT), a technique that is useful for high-resolution imaging of skin microcirculation. However interpretation of DOCT images is rather challenging. Our study aims to aid understanding and interpretation of DOCT images with respect to parameters of microcirculation components such as blood vessel size, depth and angular position. We have constructed a gel-based tissue and blood-flow model for performing DOCT studies under well controlled conditions.

Our model consists of a series of glass capillary tubes of varying internal diameter suspended at a range of angles in a tank filled with an optically scattering gel (composed of gel, Intralipid and Indian ink). Human blood was pumped through the capillary tubes at various velocities from a commercial calibrated syringe pump, serving as a standard reference point for all velocity measurements. The velocity values were chosen to coincide with those found in the human vasculature. The blood was both infused and withdrawn to account for bidirectional flow.

Simultaneous DOCT images at different flow rates, vessel depths and vessel diameters allowed the capabilities and limitations of the DOCT system and technique to be analysed. Our results indicate a robust validation protocol which will aid all future research performed on this system.

References:

- 1. K.R. Forrester, J. Tulip, C. Leonard, C. Stewart and R.C. Bray. "A laser speckle imaging technique for measuring tissue perfusion", Biomedical Engineering, 2004, 51, Issue 11, Pages 2074-2084.
- 2. Brian W. Pogue, Michael S. Patterson. "Review of tissue simulating phantoms for optical spectroscopy, imaging and dosimetry" Journal of Biomedical Optics, 11(4) 041102 July/August 2006.

7563-27, Session 5

Three dimensional dynamics of temperature fields in phantoms and biotissue under IR laser photothermal therapy using gold nanoparticles and ICG dye.

G. G. Akchurin, A. G. Garif, M. L. Irina, S. A. Alexander, Jr., Saratov State University (Russian Federation); T. S. Georgy, Sr., First Veterinary Clinic (Russian Federation); B. N. Khlebtsov, Sr., Institute of Biochemistry and Physiology of Plants (Russian Federation); N. G. Khlebtsov, Institute of Biochemistry and Physiology of Plants and Microorganisms (Russian Federation); V. V. Tuchin, Saratov State University (Russian Federation)

We describe applications of silica(core)/gold(shell) nanoparticles and ICG dye to photothermal therapy of phantoms, biotissue and spontaneous tumor of cats and dogs. The laser irradiation parameters were optimized by preliminary experiments with laboratory rats. Three dimensional dynamics of temperature fields in tissue and solution samples was measured with a thermal imaging system. It is shown that the temperature in the volume region of nanoparticles localization can substantially exceed the surface temperature recorded by the thermal imaging system. We demonstrate effective optical destruction of cancer cells by local injection of plasmon-resonant gold nanoshells and ICG dye followed by continuous wave (CW) semiconductor laser irradiation at wavelength 808 nm.

7563-31, Session 5

Temperature dependence of the optical properties of skin in vivo

A. N. Yaroslavsky, Wellman Ctr. for Photomedicine (United States); E. Salomatina, Massachusetts General Hospital (United States)

No abstract available.

7563-20, Poster Session

Analysis and modification of estimate error in optical properties measurement with the double-integrating-spheres system

C. Li, Tianjin Univ. (China); Q. Wang, Z. Shi, Tianjin University (China); Y. Luo, Jinan Univ. (China); H. Zhao, Tianjin University (China); K. Xu, Tianjin Univ. (China)

The estimate of tissue optical properties is an important challenge in biomedical science. When the canceration arise, the chromophore in the tissue often changes in the early stage. In the research of precancerous diagnosis and glucose concentration detection, the accuracy of chromophore concentrations depends on the measurement of absorption coefficient. So determining the absorption coefficient accurately is crucial both in vivo and in vitro. The Double Integrating-spheres System (DIS) is widely used in measuring optical properties of tissue. But because of the effects of light losses of sample and cross talk between two integrating spheres, the estimating error of the optical properties increased, especially for the reconstruction of absorption coefficient. In the article we research the effects that cause the error in measurement of optical properties. Based on the DIS setup, the Monte Carlo simulation and principle of the integrating sphere were applied to investigate the effects of light loss and cross talk with various parameters, such as the sample port of integrating sphere, thickness and optical properties of the sample. According to the investigation of these factors, a fast correcting method was introduced to modify the measuring results. The method included experimental calibration and algorithm to adapt various situations. A calibration sample set was measured and employed to deduct the effect of light loss and cross talk when other samples were measured. The algorithm based on artificial neutral network was applied to modify the measurement of samples with different optical properties. The modified result showed that the reconstruction accuracy of absorption coefficient was fully improved compared with the uncorrected IAD results.

7563-21, Poster Session

Study of optical clearing effects by using tissue-like phantom

J. Jiang, W. Chen, Q. Qong, Tianjin Univ. (China); R. K. Wang, Orgen Health and Science University (United States); K. Xu, Tianjin Univ. (China)



Previous studies have focused on different tissue samples treated with biocompatible hyperosmotic agents, which showed delightful results of optical clearing on decreasing the scattering effects to some degree. However, the difference in tissue samples even in the same kind of tissue sample could lead to unreliable results, further could make it difficult to quantitatively control the dose of biocompatible hyperosmotic agents during tissue optical clearing. In this study, in order to study the effects of optical clearing, we induced tissue-like phantoms with stabile optical properties which are in accord with the characteristic of human tissues. Firstly, the preparation of tissue-like phantoms mimicking the optical properties of human skin was introduced. And then dimethyl sulfoxside (DMSO), replacing a certain amount of deionized water in tissue-like phantom, was used as enhancer for experimental study. Further experimental studies were performed to prove the optical clearing effects of tissue-like phantom induced by DMSO. With the increase concentration of DMSO being added in tissue-like phantom, the transmitted intensity presented an ascending of tissue-like phantoms with different DMSO concentration trend. Optical properties, obtained by using double integrating-spheres system and Inverse Adding-doubling(IAD) method, showed that DMSO led to a reduction in scattering of tissue-like phantoms as it did to porcine skin tissue in vitro. Results indicated that a robust tissue-like phantom could play an important role during quantitatively controlling optical clearing, thereby would facilitate the technique of optical clearing to be used in light-based non-invasive diagnostic and therapy.

7563-22, Poster Session

Design and development of an optimized TiVi light source for detection of oxygenated and deoxygenated haemoglobin

S. D. Mc Elligott, University of Limerick, Limerick (Ireland); P. M. McNamara, Univ. of Limerick (Ireland)

Assessment of the cutaneous microcirculation is of major importance in understanding the vascular effects of pathological conditions such as diabetes and also in fundamental physiology of the vasculature. Current technological methods for the assessment of the microcirculation suffer from many limitations such as reduced spatial and temporal resolution and awkward image interpretation [1].

Tissue Viability (TiVi) is a means of imaging tissue embedding the microcirculation by illuminating it by a Xenon light source. Backscattered light is projected onto a camera after passing through an orthogonally-oriented analyser [2] and undepolarised light is blocked. By elimination of the reflected light and imaging of only the backscattered light, subsurface structures (e.g. microcirculation) may be observed.

TiVi technology has been validated against other techniques such as capillary microscopy and intravital fluorescent microscopy, for its relevance and use in clinical monitoring [3]. However TiVi technology presents several shortcomings; one of these relates to real time detection of the oxygenated and deoxygenated state of haemoglobin. Thus, the primary limitation of the current TiVi apparatus is the light source that is being used. A ringlight structure composed of superbright LEDs of differing isobestic wavelengths has been designed, which illuminate in synchrony performing intravital stroboscopy preventing smearing of moving features. In doing so, the knowledge will present a quantitative means of determining the degree of haemoglobin oxygenation.

References

- [1] O'Doherty, J. Assessment of Tissue Viability by Polarised Light Spectroscopy. PhD Thesis, University of Limerick, 2007
- [2] Goedhart, P.T, et al. Sidestream Dark Field (SDF) imaging; a novel stroboscopic LED ring-based imaging modality for clinical assessment of microcirculation. Optics Express 2007; Vol. 15; No. 23
- [3] Milstein, D.M.J. et al. SDF imaging and image analysis of oral microcirculation under clinical conditions. Anaesthesia, Pain, Intensive Care and Emergency A.P.I.C.E.; Springer Milan 2006; 10.1007/88-470-0407-1_6; pp. 79-88

7563-24, Poster Session

Study of the structural dynamics of proteins by the method of energy transfer.

A. G. Melnikov, Saratov State University (Russian Federation)

In this work we investigate processes of radiation and radiationless deactivation of electronic excitation energy of the polar and nonpolar luminescent probes bound to immunoglobulin, human serum albumin (HSA) and human blood plasma albumin. We chose xanthene dyes such as eosin, erythrosine and others as polar luminescent probes and polycyclic aromatic hydrocarbons (PAH) such as anthracene, pyrene and others as nonpolar luminescent probes.

Delayed fluorescence (DF) and room temperature phosphorescence (RTP) of the probes bound to chosen proteins were observed in oxygenless solutions. Significant increase of the intensity DF and RTP of the dyes and their lifetime on going from aqueous solutions to proteins indicates that probes bound to proteins are immobilized. On the base of obtained results we concluded that efficiency of quenching of the xanthene dyes molecules bound to HSA globules by water-soluble compounds, containing heavy atoms, are determined by interactions of the dyes molecules with proteins. Triplet-triplet energy transfer (TET) of electronic excitation energy between xanthene dyes and anthracene both bound to chosen proteins was observed. So far as anthracen are insoluble in water, TET is possible only in the protein globule. Rate constants of the TET energy transfer were determined subject to localization of donor and acceptor molecules in the protein globules.

We found out that the rate constant of the energy transfer is sensitive to conformational changes of the protein globule under the action of surfactants. It is shown that triplet-triplet energy transfer method is applicable for registration of the intramolecular structural changes in protein globule.

7563-25, Poster Session

Characterization of renal blood flow regulation using the discrete wavelet transform

A. N. Pavlov, O. N. Pavlova, N.G. Chernyshevsky Saratov State Univ. (Russian Federation); E. Mosekilde, O. V. Sosnovtseva, Technical University of Denmark (Denmark)

The purpose of this study is to demonstrate the possibility of revealing new characteristic features of renal blood flow autoregulation in healthy and pathological states through application of discrete wavelet transforms to experimental time series for normotensive and hypertensive rats. We show how the coefficients of the discrete wavelet transform allow us to detect pathological changes in the renal blood flow dynamics that occur in hypertension. The aim of this study is to obtain a new information about the physiological processes using "a language" of wavelet coefficients. These coefficients characterize the variability of a signal associated with different time scales. Their dispersion or standard deviation can serve as a measure of the reaction of the cardiovascular system to the blood pressure. This reaction may be more important as a marker of the cardiovascular problems than the blood pressure itself and may characterize the level of flexibility of the cardiovascular system. An advantage of the considered approach over earlier used techniques consists in the possibility to analyze nonstationary processes with lowamplitude rhythmic components (comparable with the noise level). The latter situation creates difficulties for methods based on identification of rhythms. We show that a reduction of the variability of the waveletcoefficients in hypertension is observed at both the microscopic level of the blood flow in efferent arterioles of individual nephrons and at the macroscopic level of the blood pressure in the main arteries.



7563-28, Poster Session

Optical clearing of human dura mater by glucose solution

A. N. Bashkatov, E. A. Genina, Y. P. Sinichkin, V. V. Tuchin, N.G. Chernyshevsky Saratov State Univ. (Russian Federation)

We present experimental results of investigation on the optical properties of the human dura mater controlled by administration osmotically active chemical, such as 3M-glucose solution. Administration of the chemical agent induces diffusion of matter and as a result equalization of the refractive indices of collagen and ground material. Results of experimental study of influence of the osmotical liquid (glucose solution) on transmittance spectra of human dura mater are presented. The significant increase of transmittance of the human dura mater samples under action of the glucose solution was demonstrated. Glucose diffusion coefficient in human dura mater was estimated.

7563-29, Poster Session

OCT monitoring of diffusion of clearing agents within tooth dentin

N. A. Trunina, N.G. Chernyshevsky Saratov State Univ. (Russian Federation); V. V. Tuchin, University (Russian Federation); V. V. Lychagov, Saratov State University (Russian Federation)

Monitoring of agent diffusion within tooth tissues is important in a wide context of tooth therapy (diffusion of medicinal preparations) and cosmetics (chemical whitening agents). We report here the results of optical coherence tomography (OCT) monitoring of diffusion of water and glycerol as clearing agents in samples of human tooth tissue. The diffusion process is analyzed by monitoring the changes in the OCT signal slope and the depth-resolved amplitude of OCT signal from a sample. Slow temporal kinetics of the mean attenuation coefficient was measured to monitor a saturable optical clearing due to the diffusion of the agent. The average permeability coefficient was estimated by dividing the measured thickness of the selected region by the time it took for the agent to diffuse through. The experimental results demonstrate that OCT can be an efficient tool in the study of agent diffusion through hard tissues.

7563-30, Poster Session

Fat tissue staining and photodynamic/ photothermal effects

V. V. Tuchin, N.G. Chernyshevsky Saratov State Univ. (Russian Federation) and Insitute of Precise Mechanics and Control (Russian Federation); G. B. Altshuler, Palomar Medical Technologies, Inc. (United States); I. Y. Yanina, G. V. Simonenko, N.G. Chernyshevsky Saratov State Univ. (Russian Federation)

Because heat is required to initiate collagen and/or fat cells denaturation, it is apparent that the temperature developed by heating inside the tissue, e.g., at the subcutaneous fat layer level, was producing alterations in the subcutaneous skin layer. Adipocyte matrix properties manifested marked changes in their characteristics as membrane lysis decreases volume and thickening of their membrane.

The 100-150 m fat tissues slices were used in in vitro experiments. Water-ethanol solutions of indocyanine green (ICG) and brilliant green (BG) of 1 mg/ml and 6 mg/ml concentration, respectively, were used for fat tissue staining. CW laser diode (OPC-B015-MMM-FCTS, 805 nm) and dental diode irradiator Ultra Lume Led 5 (442 and 597 nm) were used for irradiation of tissue slices. Alterations of tissue morphology was studied using digital microscopy with a CCD camera and software allows for analysis of cell size and shape.

Using this method of combining photothermal and photodynamic treatments will lead to more effective removal of fat cells.

7563-32, Poster Session

Tissue Viability (TiVi) imaging: following effects of local occlusion on the volar forearm

P. M. McNamara, J. O'Doherty, M. O'Connell, B. W. Fitzgerald, C. D. Anderson, Univ. of Limerick (Ireland); G. E. Nilsson, Univ. Hospital Linköping (Sweden); R. Toll, M. J. Leahy, Univ. of Limerick (Ireland)

No abstract available.

7563-33, Poster Session

Quantitative optical evaluation of malignancy risk related to cutaneous phototype

E. G. Borisova, L. A. Avramov, Institute of Electronics (Bulgaria); P. E. Pavlova, Technical Univ. Sofia (Bulgaria); E. N. Pavlova, P. Troyanova, National Oncological Ctr. (Bulgaria)

No abstract available.





Sunday-Tuesday 24-26 January 2010 • Part of Proceedings of SPIE Vol. 7564 Photons Plus Ultrasound: Imaging and Sensing 2010

7564-01, Session 1

Transverse flow velocity measurement with photoacoustic Doppler bandwidth broadening

J. Yao, L. V. Wang, Washington Univ. in St. Louis (United States)

In photoacoustic (PA) imaging of microvascular networks, the transverse component of the blood flow that is perpendicular to the acoustic probing beam is usually dominant. We propose a new method to measure the transverse flow, based on the Doppler bandwidth broadening. The bandwidth broadening is determined by the geometry and center frequency of the ultrasound transducer, and proportional to the transverse speed. Because the photoacoustic signal in one A-scan has a wide band, multiple successive A-scans are used to estimate the relatively small variance of the Doppler-shifted frequency. Then the bandwidth broadening can be calculated from the frequency variance. By exploiting the pulse excitation and raster motor scanning, three-dimensional structural and flow information can be obtained simultaneously. From a flow of a suspension of carbon particles (diameter: 2-12 µm) in both clear (deionized water) and scattering (0.5 mm chicken breast tissue) media, transverse flow speeds from 0 to 3.5 mm/s were measured using an optical-resolution photoacoustic microscope. The bandwidth broadening at each speed was in good agreement with the theoretical prediction.

7564-03, Session 1

Combined photoacoustic and high-frequency power Doppler ultrasound imaging

Y. Jiang, T. Harrison, J. Ranasinghesagara, R. Zemp, Univ. of Alberta (Canada)

Photoacoustic imaging is a hybrid imaging technique which can provide high optical contrast and ultrasonic spatial resolution. Since it relies on optical absorption of tissues, photoacoustic imaging is particularly sensitive to vascular structures even at the micro-scale. Power Doppler ultrasound can be used to detect moving blood irrespective of Doppler angles. However, the sensitivity may be inadequate to detect very small vessels with slow flow velocities. In this work, we merge these two synergistic modalities and compare Power Doppler ultrasound images with high-contrast photoacoustic images. We would like to understand the advantages and disadvantages of each technique for assessing microvascular density, an important indicator of disease status. A combined photoacoustic and high-frequency ultrasound system has been developed. The system uses a swept-scan 25MHz ultrasound transducer with confocal dark-field laser illumination optics. A pulsesequencer enables ultrasonic and laser pulses to be interlaced so that photoacoustic and Doppler ultrasound images are co-registered. Signal processing methods and wall filters have been developed and tested on simulated and phantom data. Power Doppler experiments have been performed on flow phantoms using blood-mimicking fluid. Work in progress includes in vivo Color-Flow mapping. This combined system will be used to perform blood oxygen saturation and flow estimations, which will provide us with the parameters to estimate the local rate of metabolic oxygen consumption, an important parameter for many diseases.

7564-04, Session 1

Dynamic optical angiography of mouse anatomy using radial projections

R. A. Kruger, R. B. Lam, D. R. Reinecke, S. P. DelRio, OptoSonics, Inc. (United States); M. M. Thornton, P. A. Picot, T. G. Morgan, Endra, Inc. (United States)

We demonstrate optical angiography on live mice using a new photoacoustic tomography (CT) scanner. The scanner uses a sparse array of discrete ultrasound detectors geometrically arranged to capture 128 simultaneous radial "projections" through a 25-mm-diameter volume of interest. Denser sets of interleaved radial projections are acquired by rotating the sparse array continuously about its vertical axis during data acquisition. The device has been designed specifically for imaging laboratory mice, which remain stationary during data collection.

Angiographic data are acquired at a rate of 128 radial projections per second following a bolus injection of 1 mg/mL of indocyanine green (ICG). Additional sets of 128 interleaved radial projections are acquired every second, generating a complete set of 3840 uniformly-distributed radial projections within thirty seconds. This time span is sufficient to capture the dynamic flow of ICG (first pass) through the vascular system of a mouse.

We use Highly Constrained Back Projection Reconstruction (HYPR) algorithms to improve the signal-to-noise ratio of the reconstructed images for each sparsely-sampled set of 128 radial projections. The resulting set of thirty Photoacoustic images allows visualization of ICG flow through the vascular system with one second temporal resolution. The HYPR processing maintains the SNR of the complete set of 3840 projections.

7564-05, Session 1

Serial determination of HIF-mediated multistage angiogenesis and microvascular network elaboration using optical-resolution photoacoustic microscopy

S. Hu, S. Oladipupo, J. Yao, A. C. Santeford, K. Maslov, J. Kovalski, J. M. Arbeit, L. V. Wang, Washington Univ. in St. Louis (United States)

A major obstacle in studying angiogenesis is inability to noninvasively image microvascular network elaboration in real time in an individual animal. We applied optical-resolution photoacoustic microscopy (OR-PAM) to determine the kinetics of hypoxia-inducible factor-1 (HIF-1)-mediated angiogenesis in a switchable transgenic mouse model. During continued 60-day activation of HIF-1alpha, and 14-day ON and 14-day OFF transgene induction experiments, we used OR-PAM to monitor structural and cellular alterations in blood vessels in transgenic mice compared to non-transgenic mice. Our in vivo chronic imaging results were validated by FITC-lectin perfusion angiography and ear skin whole mounts. OR-PAM has demonstrated the potential to more precisely monitor antiangiogenic therapy of human cancers allowing for tailoring and rapid determinations of efficacy or resistance.

207

Return to Contents TEL: +1 360 676 3290 · +1 888 504 8171 · customerservice@spie.org



7564-06, Session 1

In vivo photoacoustic imaging of the vascular response to brain electrical stimulation

V. Tsytsarev, S. Hu, J. Yao, C. P. Favazza, K. I. Maslov, L. V. Wang, Washington Univ. in St. Louis (United States)

Photoacoustic microscopy (PAM) has rapidly emerged as a valuable tool for studying neurovascular coupling, allowing neural activity to be retrieved from hemodynamic properties-such as changes in local blood oxygenation and vessel diameter-of the surrounding vasculature. Here, we investigated microvascular responses to direct electrical stimulation on mouse cortical tissues by both acoustic-resolution photoacoustic microscopy (electrical stimulation was introduced through a small hole in the skull, and hemodynamic imaging was performed transcranially) and optical-resolution photoacoustic microscopy (through an open skull cranial window). Trains of the square pulses were used to provide electrical stimulation, with ten pulses per train at a frequency of 300 Hz, a pulse duration of 0.3 ms, and a current ranging from 100-400 μA. Stimuli were delivered through an intracortical glass insulated tungsten monopolar electrode. The experimental setup is capable of imaging individual vessels with diameters as small as 10 µm. We observed vascular responses of both types, vasoconstriction as well as vasodilation, as a result of electrical stimulation. The type of response was dependent on the parameters of stimulation and location of the vessel with respect to the electrode. We hypothesize that electrical stimulation is able to stimulate directly the pericites and muscular cells of the vessels that cause vasoconstriction. When vasodilation was observed, stimulation of neurons and astrocytes was prevalent, reflected in the release of vasodilators. The method described here could be very useful in understanding and studying disorders in the neurovascular system.

7564-77, Session 1

Ultrasound-array-based realtime photoacoustic microscopy for dynamic 3D imaging in both humans and small animals

L. Song, C. Kim, K. Maslov, Washington Univ. in St. Louis (United States); K. K. Shung, The Univ. of Southern California (United States); L. V. Wang, Washington Univ. in St. Louis (United States)

With a refined ultrasound-array-based realtime photoacoustic microscopy (UA-PAM) system, we demonstrated the feasibility of noninvasive in vivo imaging of human pulsatile dynamics, as well as 3D dynamic monitoring of sentinel lymph nodes (SLNs) in mice and rats. The system, capable of realtime B-scan imaging at 50 Hz and high-speed 3D imaging, was validated by imaging the subcutaneous microvasculature in rats and humans. After the validation, a human artery around the palm-wrist area was imaged, and its pulsatile dynamics, including the arterial pulsatile motion and changes in hemoglobin concentration, was monitored, with 20-ms B-scan imaging temporal resolution. In addition, noninvasive photoacoustic sentinel lymph node (SLN) mapping with high spatial resolution has the potential to reduce the false negative rate and eliminate the use of radioactive tracers in SLN identification. Upon intradermal injection of Evans blue, the system maps SLNs accurately in mice and rats. Furthermore, the ~6 s 3D imaging temporal resolution offers the capability to quantitatively and noninvasively monitor the dye dynamics in SLNs in vivo through sequential 3D imaging. The demonstrated capability suggests that high-speed 3D photoacoustic imaging should facilitate the understanding of the dynamics of various dyes in SLNs, and potentially help identify SLNs with high accuracy. With the results shown in this study, we believe that UA-PAM can potentially enable many new possibilities for studying functional and physiological dynamics in both preclinical and clinical imaging settings.

7564-07, Session 2

Integrated catheter for intravascular ultrasound and photoacoustic imaging

A. B. Karpiouk, B. Wang, S. Emelianov, The Univ. of Texas at Austin (United States)

The atherosclerosis is a complex of diseases characterized by atherosclerotic plagues built up into a wall of arteries. The successful treatment of the atherosclerosis requires the reliable information about both the morphology of the plagues and their vulnerability that is primarily determined by plague's composition. Recently, we introduced combined intravascular ultrasound (IVUS) and intravascular photoacoustic (IVPA) imaging to detect and characterize the atherosclerotic plagues. IVUS imaging is capable of providing the structural details of plagues while IVPA imaging is based on the mapping of optical properties of tissue thus suitable for assessment of plague's composition. The clinical application of the combined IVUS/IVPA imaging, however, requires an integrated IVUS/IVPA imaging catheter consisting of light delivery system and an ultrasound transducer. In current paper, we present a working prototype of the integrated IVUS/IVPA imaging catheter where the custom-designed light delivery system is integrated with an ultrasound transducer into a single device. Unlike the earlier prototypes reported previously, this integrated IVUS/IVPA imaging catheter, rotated inside of a stationary sample, is capable of 360-degree imaging of the vessel cross-section. In IVPA imaging, the vessel was irradiated from within the lumen using 5-7 ns laser pulses, and photoacoustic signal were detected using a singleelement ultrasound transducer operating at 12 MHz center frequency. In IVUS imaging, the same ultrasound transducer was used in pulse-echo mode. The combined IVUS/IVPA imaging catheter was tested in phantom studies and ex-vivo. The advantages and constrains of the catheter are analyzed.

7564-08, Session 2

Design and fabrication of an integrated intravascular ultrasound/photoacoustic scan head

B. Hsieh, National Taiwan Univ. (Taiwan); S. Chen, T. Ling, L. J. Kuo, Univ. of Michigan (United States); P. Li, National Taiwan Univ. (Taiwan)

The combination of intravascular ultrasound and intravascular photoacoustic imaging has been proposed. In this presentation, we will propose a design for the scan head that is sufficiently small to fit in the tip of the catheter. In addition, the design is also suitable for ultra high frame rate imaging. The scan head consists of a single element, ring-shape transducer for sideward ultrasound transmission. The transducer has a diameter of 3mm. On acoustic detection, we propose to use a polymer micro-ring array. For demonstration purposes, a single micro-ring is used with mechanical scanning in this study. For optical illumination, a multimode fiber with a cone-shaped mirror is used. Note that only a single ultrasound/laser pulse is required to acquire an ultrasound/photoacoustic image frame. We will present phantom imaging results, as well as methods to reduce distortion from unfocused ultrasound transmit beam.

7564-09, Session 2

Intravascular photoacoustic imaging of macrophages using molecular targeted gold nanoparticles: ex vivo study

B. Wang, V. Sapozhnikova, The Univ. of Texas at Austin (United States); J. Amirian, The Univ. of Texas Health Science Ctr. at Houston (United States); S. H. Litovsky, The Univ. of Alabama at Birmingham (United States); R. Smalling, The Univ. of Texas



Health Science Ctr. at Houston (United States); K. Sokolov, The Univ. of Texas at Austin (United States) and University of Texas M.D. Anderson Cancer Center (United States); S. Emelianov, The Univ. of Texas at Austin (United States)

Using contrast agents with desired targeting moiety and optical absorption, intravascular photoacoustic (IVPA) imaging can be used to identify various biomarkers expressed during the progression of atherosclerotic lesions. In this paper, we present IVPA imaging of macrophages in the atherosclerotic lesions using bioconjugated gold nanoparticles (Au NPs) as the contrast agent. Atherosclerotic lesions were created in the aorta of a New Zealand white rabbit subjected to a high cholesterol diet and balloon injury. The rabbit was injected with 20 nm spherical Au NPs conjugated with IgG antibodies - these NPs demonstrated a superior uptake by macrophages in experiments with cell cultures as compared to other types of coating. The macrophages with internalized Au NPs can be imaged using irradiation in the near infrared (NIR) range; this is possible because of plasmon resonance coupling between closely spaced Au NPs after uptake by macrophages. After 24 hours, the rabbit was sacrificed and the excised aorta was imaged. The multi-wavelength IVPA images of the cross-section of the diseased aorta were analyzed by intraclass correlation (ICC) method to identify the presence and location of Au NPs-labeled macrophages. Areas of high ICC coefficients were found in the intima layer of the diseased aorta suggesting the presence of NPs. High concentration of NPs within macrophages in the locations identified in IVPA-based ICC images was further confirmed by macrophage-specific RAM 11 staining and Au-specific silver staining of the tissue cross-section. The results of our study suggest that IVPA imaging can be used to image macrophages in the atherosclerosis.

7564-10. Session 2

Application of limited-view image reconstruction to intravascular photoacoustic tomography

Y. Sheu, C. Chou, B. Hsieh, P. Li, National Taiwan Univ. (Taiwan)

Intravascular photoacoustic (IVPA) reconstruction methods that aim to detect atherosclerotic plaques with differential composition will be studied numerically and experimentally. IVPA images are conventionally reconstructed by simply aligning photoacoustic signals followed by scan conversion. The scanning aperture in IVPA, in contrast to other photoacoustic imaging applications, is enclosed within the imaged object. Consequently, quantitative image reconstruction becomes infeasible as the data sufficiency condition for perfect image reconstruction is not satisfied in such a limited-view condition. However, useful information regarding certain plaque boundaries can still be reconstructed, which can facilitate plaque detection. In this study, strategies for limited-view reconstruction will be investigated for IVPA. Computer simulations were carried out to validate the proposed method, which will be also applied to experimental data.

7564-11, Session 2

Photoacoustic imaging of lipid rich plagues in human aorta

T. J. Allen, P. C. Beard, Univ. College London (United Kingdom)

Lipid rich atheromatous plagues are of clinical importance because they can rupture leading to occlusive thrombus formation but can be difficult to identify using conventional methods such as intravascular ultrasound. Spectroscopic photoacoustic imaging using excitation wavelengths in the range 900nm-1400nm has the potential to identify such plaques on account of specific absorption features of lipids at 920nm and 1300nm. Furthermore, light in this spectral range can penetrate several mm of blood (thus obviating the need for a saline flush in endoscopic implementations) as well as the full thickness of the vessel wall in order to image the thickest plaques. In this study we investigated the possibility of

identifying regions of high lipid concentration from 2D multi-wavelength photoacoustic images of vascular tissue. A range of human aortic tissue samples were imaged at different wavelengths through several mm of blood using a line-scanned focused ultrasound transducer. A novel deconvolution routine was developed in order to improve the fidelity of the photoacoustic images by correcting for the instrument point spread function. Comparison of the reconstructed photoacoustic images with histology demonstrated that the lipid content of atheroma could be identified.

7564-12, Session 2

Volumetric photoacoustic endoscopy of internal organs

J. Yang, K. Maslov, Washington Univ. in St. Louis (United States); H. Yang, R. Chen, Q. Zhou, K. K. Shung, The Univ. of Southern California (United States); L. V. Wang, Washington Univ. in St. Louis (United States)

We have successfully implemented in-situ rectum imaging of a rat with our side-scanning photoacoustic endoscopic probe. After the probe was inserted into the intact rectum, a set of serial B-scan images was acquired with a pull-back motion of the probe (C-scan), and reconstructed as a three-dimensional image. The C-scan and exact three-dimensional reconstruction of the target tissue can be achieved by employing a motorized linear scanning system which is synchronized with a rotating mirror that performs circumferential sector scanning (B-scan). The probe's imaging range is determined by set data acquisition parameters, and usually exceeds 3 mm in radial depth and several centimeters in the translational direction. The B-scan frame rate is ~ 3 Hz, and is currently limited by the laser system's pulse repetition rate and the micromotor's rotation speed. The radial imaging resolution is $\sim 50 \, \mu m$, but the transverse resolution ranges from about 200 μm to 500 $\mu m,$ depending on the imaging depth. This system can perform multi-wavelength imaging through the selection of appropriate laser wavelengths. Hence, it provides diverse information on the functional features as well as the morphological structure of the target tissue, based on optical absorption contrast. Since conventional pulse-echo based ultrasound endoscopy is sensitive only to mechanical properties of tissue, photoacoustic endoscopy with spectral volumetric imaging is expected to be used as a new diagnostic tool for better characterization of tissue abnormalities at super-depths (depths beyond one transport mean free path).

7564-13, Session 3

Extracting quantitative information from photoacoustic images

B. T. Cox, J. G. Laufer, P. C. Beard, Univ. College London (United Kingdom)

In recent years, the ability of photoacoustic tomography to image sub-100 micron light-absorbing structures within biological tissue has been demonstrated both ex and in vivo. Many such images, while compelling and indeed useful, provide little in the way of accurate quantitative information about the tissue composition. Unsophisticated attempts to apply spectroscopic techniques to sets of images obtained at multiple-wavelengths, and thereby extract maps of the concentrations of chromophores or quantities of interest, eg. blood oxygenation, have been shown to fail, due to the nonuniformity of the fluence within the tissue as well as the nonlinear dependence of the fluence on the absorption coefficient. Furthermore, the photoacoustic images themselves often suffer from artifacts due either to the method of data acquisition, or the method of image reconstruction. Here, inversion schemes that attempt to overcome many of these difficulties, through the incorporation of prior information in the form of numerical models of acoustic and optical propagation, will be described and demonstrated on both simulated and measured data.



7564-14, Session 3

Monte Carlo modeling for photoacousticbased transport-regime optical property estimation

J. C. Ranasinghesagara, R. J. Zemp, Univ. of Alberta (Canada)

We developed a unique reflection-mode photoacoustic technique sensitive to optical scattering in turbid media. We focused a small laser spot on to the surface of a turbid medium and captured the photoacoustic signal by a focused ultrasound transducer. The amplitude of the photoacoustic signal for different surface illumination spot locations is an effective estimate of the Green's function of light transport in turbid media. Our results for different concentrations of Intralipid indicate that this method is capable of distinguishing small changes in the reduced scattering coefficient. In this work, we present experimental measurements for an Intralipid phantom with reduced scattering coefficients of 3, 4, and 5 cm-1, and show that Monte Carlo simulations of light transport accurately reproduce experimental curves. This means that we can estimate transport-regime optical properties of the media given a suitable fitting algorithm.

7564-15, Session 3

Photon propagation correction in 3D photoacoustic imaging using Monte Carlo simulation

K. M. Stantz, Purdue Univ. (United States)

Purpose: The purpose of this study is to develop a new 3-D iterative Monte Carlo algorithm to recover the heterogeneous distribution of molecular absorbers with a solid tumor.

Introduction: Spectroscopic imaging (PCT-S) has the potential to identify a molecular species and quantify its concentration with high spatial fidelity. To accomplish this task, tissue attenuation losses during photon propagation in heterogeneous 3D objects is necessary. An iterative recovery algorithm has been developed to extract 3D heterogeneous parametric maps of absorption coefficients implementing a MC algorithm based on a single source photoacoustic scanner and to determine the influence of the reduced scattering coefficient on the uncertainty of recovered absorption coefficient.

Material and Methods: This algorithm is tested for spheres and ellipsoids embedded in simulated mouse torso with optical absorption values ranging from 0.01-0.5/cm, for the same objects where the optical scattering is unknown (ms'=7-13/cm), and for a heterogeneous distribution of absorbers.

Results: Systemic and statistical errors in ma with a priori knowledge of ms' and g are <2% (sphere) and <4% (ellipsoid) for all ma and without a priori knowledge of ms' is <3% and <6%. For heterogenous distributions of ma, errors are <4% and <5.5% for each object with a prior knowledge of ms' and g, and to 7 and 14% when ms' varied from 7-13/cm.

Conclusions: A Monte Carlo code has been successfully developed and used to correct for photon propagation effects in simulated objects consistent with tumors.

7564-16, Session 3

Photoacoustic image reconstruction for linear scanning geometry using particle swarm optimization with a K-space simulation scheme

Y. Sheu, W. Wang, Y. Hung, P. Li, National Taiwan Univ. (Taiwan)

Photoacoustic reconstruction for linear scanning geometry is not fullview, causing distortion in the image. In this study, we demonstrate a reconstruction method by formulating reconstruction into an optimization problem, and solve the problem with the particle swarm optimization (PSO) method. First we guess the initial optical energy distribution. The generated photoacoustic wave for a time series can be computed. The k-space method and the time domain evolution is evaluated by an exact time propagator. Next we compare the collected signals generated from the guessed optical energy distribution with the measured signals. By minimizing the error, the initial optical energy distribution is obtained. This is an optimization problem in which the dimension of unknowns is the size of the initial optical energy distribution. High computational costs resulted from a large number of particles can be alleviated with the use of the GPUs. Numerical results will be presented.

7564-17, Session 3

k-Wave: a MATLAB toolbox for photoacoustic simulation and image reconstruction

B. E. Treeby, B. T. Cox, Univ. College London (United Kingdom)

Photoacoustic tomography as an imaging and visualisation tool is based on the reconstruction of embedded light absorbing structures from surface measurements of ultrasonic waves over time. The success of the modality is thus inherently linked to the quality and speed of the associated numerical computations. As in many areas of research computing, the complexity of many state-of-the-art algorithms means their use by the wider photoacoustics community can be limited. Here, the beta release of a new freely available MATLAB toolbox, k-Wave, is described. The toolbox has been designed to make simulations of photoacoustic imaging simple and fast. It consists of a set of functions for solving the acoustic (ultrasonic) forward and inverse problems in photoacoustic imaging. These include: an easy-to-use forward model of photoacoustic wave propagation in acoustically heterogeneous media (in one, two, and three dimensions); many simple-to-follow tutorial examples tailored towards getting started guickly; the option to make a wave propagation movie for use in presentations; the option to use the forward model as a flexible, time-reversal image reconstruction algorithm; and a fast, one-step, image reconstruction algorithm for data recorded on a line (2D) or planar (3D) measurement surface. This release of the k-Wave Toolbox is focussed on modelling and image reconstruction in photoacoustic imaging, as many of the functions have been tried and tested as research tools in this area. Future releases will incorporate additional functionality of use to the wider ultrasound community, as well as an expanded set of standard reconstruction algorithms.

7564-18, Session 3

Compressed sensing in photoacoustic tomography with in vivo experiments

Z. Guo, C. Li, L. Song, L. V. Wang, Washington Univ. in St. Louis (United States)

The data acquisition speed in photoacoustic computed tomography (PACT) is limited by the laser repetition rate and the number of parallel ultrasound detecting channels. Reconstructing PACT image with a less number of measurements can effectively accelerate the data acquisition and reduce the system cost. Recently emerged Compressed Sensing (CS) theory enables us to reconstruct a compressible image with a small number of projections. This paper adopts the CS theory for reconstruction in PACT. The idea is implemented as a non-linear conjugate gradient descent algorithm and tested with phantom and in vivo experiments.



7564-19, Session 3

Semi-analytical model-based inverse approach for quantitative optoacoustic imaging

A. Rosenthal, D. Razansky, V. Ntziachristos, Technische Univ. München (Germany) and Helmholtz Zentrum München GmbH (Germany)

For over a decade, there has been considerable research directed towards developing inversion methods that reconstruct the OAT images from the measured acoustic signals. Backprojection algorithms were the first to be demonstrated for OAT image reconstruction. These algorithms are based on closed-form inversion formulae that can be efficiently evaluated in 2- and 3D and are analogues to the Radon transform. Backprojection formulae currently exist for several detection geometries and are implemented either in the spatial domain or Fourier domain. A major disadvantage of conventional backprojection algorithms is that they are not exact, resulting in artifacts in the reconstructed image. Specifically, the reconstruction accentuates fast variation in the image and produces negative values. Although these artifacts have not prevented the use of backprojection algorithms for structural imaging, they limit its use for applications such as molecular imaging, in which well-quantified images are required. In this work we propose a novel semi-analytical model-based optoacoustic inversion scheme and compared it to the backprojection algorithm. We tested both types of algorithms on numerically simulated data as well as experimental data from several tissue mimicking phantoms and model animals. The results confirmed that although backprojection algorithm are very useful for visualization, they are limited when it comes to quantitative imaging. In contrast, the model-based approach produced quantitative artifact-free results.

7564-20, Session 3

Prediction of sensitivity thresholds in optoacoustic tomography

D. Razansky, J. Baeten, Technische Univ. München (Germany) and Helmholtz Zentrum München GmbH (Germany); V. Ntziachristos, Technische Univ. München (Germany) and Helmholtz Zentrum München, GmbH (Germany)

While the feasibility of different optoacoustic imaging implementations has been showcased and hypothetical assumptions have been reported in the literature predicting generally the potential sensitivity of the method, little is known on the sensitivity performance from a theoretical and systematic stand-point. For this reason, we investigated herein the theoretically predicted sensitivity of the method over wide range of imaging-related parameters and provided the necessary experimental reference measurements. Optoacoustic signals were simulated emanating from a target bio-marker, represented by an absorbing sphere, which was embedded in tissue-mimicking scattering and absorbing phantoms. By accounting for diffuse light distribution and ultrasound dispersion as it occurs in tissues, we removed system dependent characteristics to yield a better understanding of performance and physical limitations of target detection using optoacoustics. A range of clinically relevant bio-marker concentrations was examined, covering four orders of magnitude in target radii, embedded in different tissue dimensions. We find the optoacoustic detection limits as they are constrained by the interplay of light penetration and ultrasonic frequency-dependent attenuation (dispersion) and further observe a non-linear performance in the detection limit, which invalidates simplistic linear predictions of optoacoustic sensitivity typically assumed in the literature. We experimentally verify and reference our theoretical findings in tissue-mimicking phantoms, using a newly developed multispectral optoacoustic tomography (MSOT) system.

7564-21, Session 4

Polymer fiber detectors for photoacoustic imaging

H. Grün, T. Berer, RECENDT GmbH (Austria): G. Paltauf, Karl-Franzens-Univ. Graz (Austria); P. Burgholzer, RECENDT GmbH (Austria)

Photoacoustic Imaging is a novel imaging method which combines the advantages of Diffuse Optical Imaging (high contrast) and Ultrasonic Imaging (high spatial resolution). A short laser pulse excites the sample. The absorbed energy causes a thermoelastic expansion and thereby launches a broadband ultrasonic wave (photoacoustic signal). This way one can measure the optical contrast of a sample with ultrasonic resolution and therefore Photoacoustic Imaging is suitable for medical and biological applications. For collecting photoacoustic signals our group introduced so called integrating detectors a few years ago. Such integrating detectors integrate the pressure at least in one dimension e.g. a line detector. Thereby the three dimensional imaging problem is reduced to a two dimensional problem which allows a simpler setup with only one rotation axis. Recently we used fiber-based detectors made of polymer as such an integrating line detector. Fiber-based detectors are easy to use and possess a constant, high spatial resolution over their entire active length. Polymer fibers provide a better impedance matching and a better handling compared with glass fibers which was our first approach. First measurement results of simple structures using polymer fiber detectors and some details of the polymer line detector will be discussed. For example different types of interferometers which are possible as line detectors or various possibilities of stabilizing the operating point.

7564-22. Session 4

Novel Fiber Optic Interferometric Sensors for Optoaoustic Imaging

H. R. Lamela, D. Gallego, Univ. Carlos III de Madrid (Spain); A. A. Oraevsky, Fairway Medical Technologies, Inc. (United States)

Optoacoustic tomography is a promising non-invasive non-ionizing imaging technique to visualize biological soft tissues. It combines the advantages of optical absorption contrast and optical spectroscopy with the spatial resolution of ultrasound imaging techniques. The optical detection of ultrasound has been studied as an alternative to piezoelectric technology. Intrinsic fiber optic interferometric sensors contrary to piezoelectric transducers, are not affected by external electromagnetic disturbances or other artifacts like electrical noise and thermal signals produced by the direct laser pulse illumination. In this work we present for the first time results on the detection of optoacoustic signals using fiber optic interferometric sensors which are designed for the frequency range from 100 KHz to 5 MHz. In this line, we propose a novel fiber optic interferometric ultrasonic sensor with a finite aperture to reconstruct optoacoustic images and we have compared it with images obtained using a PVDF probe imaging system (LOIS).

7564-23, Session 4

Image reconstruction in photoacoustic tomography using integrating detectors accounting for frequency-dependent attenuation

P. Burgholzer, J. Bauer-Marschallinger, RECENDT GmbH (Austria); G. Paltauf, Karl-Franzens-Univ. Graz (Austria)

Photoacoustic Imaging (also known as thermoacoustic or optoacoustic imaging) is a novel imaging method which combines the advantages of Diffuse Optical Imaging (high contrast) and Ultrasonic Imaging (high



spatial resolution). A short laser pulse excites the sample. The absorbed energy causes a thermoelastic expansion and thereby launches a broadband ultrasonic wave (photoacoustic signal). This way one can measure the optical contrast of a sample with ultrasonic resolution. For collecting photoacoustic signals our group introduced so called integrating detectors a few years ago. Such integrating detectors integrate the pressure in one or two dimensions -a line or a plane detector, respectively. Thereby the three dimensional imaging problem is reduced to a two or a one dimensional problem for the projections and a two or three dimensional inverse radon transform as a second step to get the three dimensional initial pressure distribution. The integrating detectors are mainly optical detectors and thus can provide a high bandwidth up to several 100 MHz. Using these detectors the resolution is often limited by the acoustic attenuation in the sample itself, because attenuation increases with higher frequencies. Compensation of this frequency-dependent attenuation is an ill-posed problem and is limited by the thermodynamic fluctuation of the measured pressure around its mean value. These fluctuations are closely related to the dissipation caused by acoustic attenuation (fluctuation dissipation theorem) and therefore a theoretical resolution limit for photoacoustic attenuation can be derived. Experimental results will be compared with this theoretical

7564-24, Session 4

Compensation for transducer effects in optoacoustic tomography

K. Wang, M. A. Anastasio, Illinois Institute of Technology (United States); S. Ermilov, H. Brecht, R. Su, A. Oraevsky, Fairway Medical Technologies, Inc. (United States)

Optoacoustic Tomography (OAT) is a hybrid imaging modality that combines the advantages of optical and ultrasound imaging techniques. Most existing reconstruction algorithms for OAT assume point-like transducers, which can result in conspicuous image blurring and distortions in certain applications. In this work, an image reconstruction method for OAT that can compensate for the temporal and spatial responses of the ultrasound transducer is developed and investigated. To achieve this, a system matrix is employed that numerically models the relationship between a discrete representation of the optical absorption distribution and the pressure data measured by a real-world transducer. Based on this system matrix, an iterative conjugate gradient image reconstruction algorithm is developed. Computer-simulation studies are conducted to demonstrate the ability of the reconstruction algorithm to compensate for transducer effects and the effects of stochastic noise on image accuracy are quantified. These results are corroborated by use of experimental phantom data. We also consider different scanning geometries of practical interest, to identify situations where compensating for the transducer response in image reconstruction is particularly important. These studies confirm that it is more important to compensate for transducer effects when the scanning radius is small and/or the object is placed away from the center of the scanning system. Therefore, the proposed reconstruction method may facilitate the development of compact OAT imaging systems.

7564-25. Session 4

Using a phase contrast imaging method in photoacoustic tomography

R. Nuster, Karl-Franzens-Univ. Graz (Austria); M. Haltmeier, G. Zangerl, O. Scherzer, Univ. Innsbruck (Austria); G. Paltauf, Karl-Franzens-Univ. Graz (Austria)

To speed up the data acquisition in photoacoustic tomography full field detection can be used to avoid the time consuming scanning around the object. The full field detection can be realized using a phase contrast method like commonly used in optical microscopy. An expanded light beam considerably larger than the object size illuminates the sample

placed in the middle of the propagating light beam. Images obtained with a CCD-camera at a certain time show a projection of the instantaneous pressure field (phase object) in a given direction. A set of such projection images is taken while the object is rotated about an axis perpendicular to the probe beam direction. The reconstruction method is related to imaging with integrating line detectors, but has to be matched to the specific information in the recorded images, which is now purely spatially resolved as opposed to spatiotemporally for a single scanning detector.

The reconstruction of the initial three dimensional pressure distribution is a two step process. First of all projection images of the initial pressure distribution are acquired. This is done by back propagating the observed wave pattern either in frequency or Radon space. In the second step the inverse Radon transform is applied to the obtained projection dataset to reconstruct the initial three dimensional pressure distribution.

Simulations and experiments are performed to show the overall adaptability of this technique in photoacoustic tomography.

7564-26, Session 4

Improved contrast optoacoustic imaging of deep breast tumors using displacement-compensated averaging: Phantom studies

M. Jaeger, S. Preisser, M. Frenz, Univ. Bern (Switzerland)

For real-time optoacoustic imaging of the human body, a linear array transducer and reflection mode optical irradiation is usually preferred. Such a setup however results in significant image background, which prevents imaging structures at the ultimate depth limited only by the signal noise level. Therefore we previously proposed a method for image background reduction, based on displacement-compensated averaging (DCA) of image series obtained when the tissue sample under investigation is gradually deformed. Optoacoustic signals and background signals are differently affected by the deformation and can thus be distinguished. The proposed method has now been thoroughly applied to imaging artificial tumors embedded deep inside breast phantoms. Optoacoustic images are acquired alternately with pulse-echo images using a combined optoacoustic/ echo-ultrasound device. Tissue deformation is accessed via speckle tracking in pulse echo images, and optoacoustic images are compensated for the local tissue displacement. In that way optoacoustic sources are highly correlated between subsequent images, while background is decorrelated and can therefore be reduced by averaging. We show that breast image contrast is strongly improved and detectability of embedded tumors significantly increased, using the DCA method.

7564-27, Session 4

Sparse signal representation at the service of quantitative optoacoustic tomography

A. Rosenthal, D. Razansky, V. Ntziachristos, Technische Univ. München (Germany) and Helmholtz Zentrum München GmbH (Germany)

Although the enormous potential of optoacoustic imaging is well recognized, certain limitations currently hinder its effective implementation in many realistic imaging scenarios. Typically, simple photon propagation patterns are assumed or the issue of nonuniform distribution of illuminating photon field is completely disregarded. This in turn imposes variety of limitations on practical application, e.g. with respect to ability for accurate and quantitative imaging of endogenous tissue contrast and distribution of bio-markers and contrast agents. A common assumption is that broad illumination will result in a planewise uniform photon distribution in tissue, which is a very inaccurate assumption that has so far resulted in mostly superficial blood vessel images. Naturally, as light propagates in tissue, heterogeneous intrinsic tissue absorption and overall light propagation characteristics alter the propagation pattern, by creating a heterogenous deposition of energy in the various tissue elements. Herein we describe and implement a method





to perform high-fidelity opto-acoustic imaging, offering true quantitative imaging not only of superficial but also of deeper seated contrast. Instead of indirect photon propagation modeling, it is assumed that the photon fluence in tissue can be directly extracted from the recorded optoacoustic signals. Since the latter represent a product between the local light fluence and the local absorption coefficient, in most practical cases, it can be assumed that the fluence exhibits much slower spatial dependence as compared to more rapid absorption coefficient variations. We utilize this fact in order to effectively decompose these two contributions using sparse representation methods. This makes the final tomographic reconstruction independent from the particular experimental geometry and measurement conditions.

7564-28, Session 4

The integration of photoacoustic imaging and high intensity focused ultrasound

H. Cui, J. Staley, X. Yang, The Univ. of Kansas (United States)

We have developed an integrated photoacoustic imaging (PAI) and high intensity focused ultrasound (HIFU) system for solid tumor treatment. A single-element, spherically focused ultrasonic transducer, with a central frequency of 5MHz, was used to generate a HIFU field in soft tissue. The same ultrasonic transducer was also used as a detector during photoacoustic imaging before and after HIFU treatments. During each experiment, targeted soft tissue was first imaged by PAI. The resulted image was used for the planning of subsequent HIFU treatment. After HIFU treatment, targeted soft tissue was imaged again by PAI to evaluate the treatment result. Good contrast was obtained between photoacoustic images before and after HIFU treatment. It is concluded that PA imaging technology may potentially be combined with HIFU treatment for imaging-guided therapy.

7564-29, Session 5

Simultaneous photoacoustic tomography and microscopy based on Fabry-Perot polymer film ultrasound sensors

P. C. Beard, E. Zhang, Univ. College London (United Kingdom)

A novel dual mode photoacoustic tomography and microscopy system, based on a backward mode Fabry-Perot (FP) polymer film ultrasound sensor is proposed. The system can be operated in two distinct modes, each of which address a different spatial scale. In the tomography mode, a relatively large volume (~1cm2) of tissue is illuminated and the photoacoustic signals are mapped by scanning a focused interrogation laser beam over the surface of the sensor. A 3D image is then reconstructed using an acoustic backpropagation algorithm. In the microscopy mode, a fraction of the excitation laser beam is combined with the sensor interrogation beam so that it is focussed on to the tissue surface. The two beams are then scanned simultaneously over the sensor/tissue surface, one generating the photoacoustic signals, the other detecting them. The advantage of this dual mode approach is that it combines the relatively deep penetration depths (~10mm) and acoustically defined spatial resolution of photoacoustic tomography with the near optical diffraction limited lateral resolution to sub-mm depths of conventional light microscopy. The vertical resolutions of both modes are similar at approximately 10µm and depend on the the bandwidth of the FP sensor (300MHz) and the pulse duration of the excitation light (6ns). The lateral spatial resolution in microscopy mode is defined by the 5µm diameter of the excitation In the tomography mode, the lateral spatial resolution depends on the sensor bandwidth, the "element" size, the overall detection aperture and the depth. In the current setting, it ranges from 18µm at sub-mm depths to 30µm at a depth of 2mm in water.

7564-30, Session 5

Photoacoustic micro-tomography: system characterization and first results on biological specimens

G. Paltauf, R. Nuster, Karl-Franzens-Univ. Graz (Austria); M. Holotta, Innsbruck Medical Univ. (Austria); H. Grossauer, Leopold-Franzens-Univ. Innsbruck (Austria)

A photoacoustic tomography setup is presented that uses an optical interferometer as ultrasound sensor. Within the interferometer, a focused optical beam integrates the acoustic pressure over its propagation length in a water tank. Based on previous work, the ideal parameters for three-dimensional (3D) photoacoustic tomography of small biological specimens are determined. These include the optical beam characteristics, the way the acoustic field around the sample is scanned with the line detector and also the image reconstruction algorithm.

The optical beam forming the sensing element of the tomography setup is focused to a typical minimum diameter of 40 µm with a depth of field of about 20 mm. Scanning the beam across the sample along an arc- or box-shaped curve and rotating the sample gives data for 3D reconstruction. Used algorithms are time-domain back projection or frequency-domain reconstruction. The former method requires longer computation time but allows for implementation of special weight factors that improve the imaging result. Samples were irradiated with pulses from an optical parametric oscillator operating in the wavelength range from 420 to 2000 nanometers.

Experiments with phantoms consisting of arrangements of human hairs were performed to test the achievable spatial resolution with this setup. The results show that a constant spatial resolution over the entire imaging volume can be obtained, in accordance with theoretical predictions for imaging with line detectors. Biological specimens were isolated mouse hearts. Images taken at varying irradiation wavelengths show detailed structures near the surface and in the interior of the samples.

7564-31, Session 5

Photoacoustic microscopy with submicron resolution

K. Maslov, G. Ku, L. V. Wang, Washington Univ. in St. Louis (United States)

The lateral resolution of photoacoustic microscopy is limited only by ability to focus light or ultrasound either by a focusing device or virtually, through image reconstruction. However, detection of the acoustic wave generated by a small light absorber is a challenging problem because generated acoustic energy is proportional to the square of the size of the photoacoustic source, that is, the actual absorber size or the effective optical focus diameter, whichever is smaller. Additionally, the bandwidth of the acoustic pulse, and hence the thermal noise of the receiving transducer, is inversely proportional to the source size. Nevertheless, taking into account that a temperature rise in biological tissue as small as one degree produces acoustic pressure as high as several bars, we show that it is possible to obtain high optical contrast photoacoustic tissue images with 0.6 m transverse resolution. To achieve high sensitivity, we used a high NA (0.85), 125 MHz spherically focused ultrasonic transducer in confocal arrangement with high resolution optical objective (NA=0.65). A few nJ laser pulses with duration of 1.5 ns at a 20KHz pulse repetition rate were used to generate photoacoustic waves. Due to the short depth of focus, complete 3D mechanical scanning over the object was performed. Although the penetration depth of such a device is limited to hundreds of microns by both optical scattering and ultrasonic absorption, the developed technique can compete with optical microscopy, for example, in quantitative spectral measurements or nanoparticle detection.



7564-32, Session 5

High repetition rate passively Q-switched fiber and microchip lasers for optical resolution photoacoustic imaging

W. Shi, I. Utkin, J. Ranasinghesagara, L. Pan, Y. Godwal, R. J. Zemp, R. Fedosejevs, Univ. of Alberta (Canada)

Optical-resolution photoacoustic microscopy is a novel imaging technology for visualizing optically-absorbing superficial structures in vivo with lateral spatial resolution determined by the optical spot size rather than acoustic detection. Since scanning of the illumination spot is required, the imaging speed is limited by the scanning speed and the laser pulse repetition rate. Unfortunately, lasers with high-repetition rate and suitable pulse durations and energies are difficult to find. We are developing compact laser sources for this application. Passively Q-switched fiber and microchip lasers with pulse repetition rates up to 120 kHz are demonstrated. Using a diode-pumped microchip laser fiber-coupled to a large mode-area Yb-doped fiber amplifier we obtained 60 J 1-ns pulses at the frequency-doubled 532-nm wavelength. The pulse-repetition rate was determined by the power of the microchip laser pump source at 808nm and may exceed 10 kHz. Additionally, a passively Q-switched fiber laser utilizing a Yb-doped double-clad fiber and an external saturable absorber has shown to produce 100ns pulses at repetition rates of 120KHz. Using a fast-scanning mirror oscillating at 600 scan lines per second, this is being developed into a system capable of C-scan imaging at 5 frames per second. A photoacoustic probe enabling flexible scanning of the focused output of these lasers consisted of a 45-degree glass prism in an optical index-matching fluid. Photoacoustic signals exiting the sample are deflected by the prism to an ultrasound transducer. Phantom studies with a 15-micron carbon fiber demonstrate the ability to image with optical rather than acoustic resolution. We believe that the high pulse-repetition rates and the potentially compact and fiber-coupled nature of these lasers will prove important for clinical imaging applications where realtime imaging performance is essential.

Funding from MPB Technologies Inc., NSERC Canada, the Terry Fox Foundation via the Canadian Cancer Society, the Canada Foundation for Innovation, and the Alberta Cancer Board is gratefully acknowledged."

7564-33, Session 5

Fine-resolution photoacoustic imaging of the eye

R. H. Silverman, Weill Cornell Medical College (United States) and Riverside Research Institute (United States); Y. Chen, F. Kong, Hunter College, CUNY (United States); H. O. Lloyd, Weill Cornell Medical College (United States)

We developed a system for photoacoustic imaging of the eye utilizing a focused pulsed laser and single-element focused ultrasound transducers. The laser emitted 1 uJ pulses of 5-nsec duration at either 1064 nm or 532 nm at 500 Hz. The axis of the 35 MHz transducer was oriented so that its axis and that of the optical beam intersected at a common focus at a 30-degree angle. The 20 MHz transducer had a central aperture allowing the optical and acoustic beams to be coaxial and confocal.

After characterization of lateral resolution and depth-of-field using fine wire targets, we imaged ex vivo tissues of pig eyes, including the anterior segment (cornea, iris, lens) and posterior layers (retina, choroid). We also performed in vivo scans of anesthetized white mice.

Photoacoustic images demonstrated pigmented structures such as the iris, retinal pigment epithelium and choroid. The anterior surface of the lens also showed a clear photoacoustic signal at 532 nm. Scans of the anterior segment performed in excised eyes showed fine details of the ciliary body and zonules.

For clinical imaging of intact eyes, the cornea and lens may introduce small displacements due to refraction that will require compensation to maintain confocality of the optic and acoustic beams. Clinical application will also require compliance with ANSI maximum permissible exposure

standards. Fine-resolution photoacoustic imaging of the eye will provide clinically valuable information because the detected parameter, optical absorption, is independent of that detected by conventional imaging techniques (optical coherence tomography and pulse-echo ultrasound).

7564-34, Session 5

In vivo functional human imaging using photoacoustic microscopy

C. P. Favazza, K. Maslov, Washington Univ. in St. Louis (United States); L. A. Cornelius, Washington Univ. School of Medicine (United States); L. V. Wang, Washington Univ. in St. Louis (United States)

Recently, there has been tremendous growth in photoacoustic imaging research for biomedical applications. However, most studies have been limited to small animal and/or phantom imaging experiments. To date, the published reports on in vivo human imaging experiments are sparse; moreover, few, if any, of these involve functional measurements. We report results of two in vivo functional human imaging experiments using photoacoustic microscopy. In Experiment 1, the hemodynamic response to an ischemic event was measured. The palms of several volunteers were imaged and a single cross-section was monitored while periodic arterial occlusions were administered using a blood pressure cuff wrapped around the upper arm and inflated to ~280 mmHg. Significant relative decreases in oxygen saturation (sO2) and total hemoglobin (HbT) were observed during periods of ischemia. Upon release of the occlusion, significant relative increases in sO2 and HbT due to post-occlusive reactive hyperemia were recorded. Experiment 2 explored the vascular response to a local, external thermal stimulus. Thermal hyperemia is a common physiological phenomenon and thermoregulation function in which blood flow to the skin is increased to more efficiently exchange heat with the ambient environment. The forearms of volunteers were imaged and a single cross-section was monitored while the imaged surface was exposed to an elevated temperature of ~44°C. Due to thermal hyperemia, relative increases in sO2 and HbT were measured as the temperature of the surface was raised. These results may contribute as clinically relevant measures of vascular functioning for detection and assessment of vascular related diseases.

7564-35, Session 5

Off-axis photoacoustic microscopy

R. L. Shelton, B. E. Applegate, Texas A&M Univ. (United States)

Photoacoustic microscopy (PAM) is a high-contrast, high-resolution imaging modality used primarily for imaging hemoglobin and melanin. Important applications include mapping of the microvasculature and melanoma tumor margins. We have developed a novel photoacoustic microscope design, which substantially simplifies construction by enabling the use of unmodified commercial optics and ultrasonic transducers. Moreover, the simple design may be readily incorporated into a standard light microscope, thus providing a familiar imaging platform for clinical researchers. A proof-of-concept Off-Axis PAM system with a lateral resolution of 26 µm and a modest axial resolution of 410 µm has been assembled and characterized using tissue samples. We have derived the appropriate equations to describe the relevant design parameters and verified the equations via measurements made on our prototype Off-Axis PAM system. A consequence of the simple design is a reduction in axial resolution compared to coaxial designs. The reduction is inversely proportional to the cosine of the angle between excitation and detection and equal to 15% and 41% for angles of 30° and 45°, respectively. While resolution is negatively affected by off-axis detection, the ability to measure weak signals at depth is enhanced. Offaxis detection has an inherent dark-field quality; chromophores excited outside the numerical aperture of the ultrasonic detector will not be detected. The physical geometry of Off-Axis PAM enables the placement of the ultrasonic transducer at the minimum distance from the sample with no obstructions between the sample and transducer. This may



prove to be an additional advantage of Off-Axis PAM over designs that incorporate long working distance ultrasonic transducers and/or require the propagation of the acoustic wave through the laser excitation optics to achieve co-axial detection.

7564-36, Session 5

Gigahertz optoacoustic imaging for cellular imaging

S. Narasimhan, Ryerson Univ. (Canada); W. Bost, F. Stracke, Fraunhofer-Institut für Biomedizinische Technik (Germany); E. Weiss, Kibero GmbH (Germany); R. Lemor, Fraunhofer-Institut für Biomedizinische Technik (Germany); M. C. Kolios, Ryerson Univ. (Canada)

Photoacoustic imaging exploits contrast mechanisms that depend on optical and thermomechanical properties of endogenous or exogenous optical absorbers. Theoretical work has shown that the photoacoustic signal bandwidth is dictated by the absorber size and the laser pulse width. In this work we demonstrate that photoacoustic signals can be detected from micron and sub-micron particles when using high frequency ultrasound transducers with reception sensitivity up to Gigahertz frequencies. We anticipate applications to include cellular imaging with nanometer sized contrast agents such as gold nanoshells, nanorods, and nanocages.

An existing acoustic microscopy system was used (the SASAM 1000, kibero GmbH). This platform is developed on an Olympus IX81 optical microscope with a rotating column that has an optical condenser for transmission optical microscopy and an acoustic module for the acoustic microscopy. The adapted optoacoustic module consists of a Q-switched Nd:YAG solid-state-laser (Teem Photonics, France) generating subnanosecond pulses. Scans were acquired of microparticles (5 µm Fe3O4 and 1 µm black Toner particles) and other nanoparticles.

The confocal arrangement allowed high signal to noise ratio photoacoustic signals (>30 dB) to be detected at 400 MHz. The particles of various size sizes produced signals of different frequency content. In imaging mode, the full width half maximum (FWHM) was measured to be 3.6 μm for the 400 MHz transducer which is in general agreement theory for a 0.3 NA objective (4.3 μm).

We report the detection of > 400 MHz ultrasonic waves produced by the microparticles. Examples with nanoparticles will be presented, as well as imaging in cellular systems. Moreover, acoustic microscopy and photoacoustic microscopy of the same samples will be presented.

7564-37, Session 6

Quantitative photoacoustic measurement of blood oxygen saturation in vivo aided by an optical contrast agent

J. R. Rajian, P. L. Carson, X. Wang, Univ. of Michigan (United States)

The dissimilarities between the absorption spectra of the oxygenated and the deoxygenated hemoglobin enable one to image the distribution of blood oxygen saturation in biological tissues by using spectroscopic photoacoustic tomography (SPAT) technique. In photoacoustic imaging, the amplitude of photoacoustic signal induced by optical absorption in biological tissue is proportional to local light energy deposition that is the product of the optical absorption coefficient and the local light fluence at the imaging target. Since the optical properties of tissues are wavelength dependent, the spectrum of the local light fluence at a target tissue beneath the sample surface is different than the spectrum of the incident light fluence above the surface. An unknown spectrum of the light fluence at the target prevents us from obtaining a quantitative image of the distribution of optical properties by SPAT. We have presented a new technique of using a contrast agent with known optical properties to obtain the spectrum of the light fluence at a target within a scattering

medium. By using this technique, one could reproduce a more accurate optical absorption spectrum of the subsurface biological tissue without being affected by the strong light diffusion in the background tissue. In this work, we have explored the feasibility of in vivo application of this new SPAT technique. By performing photoacoustic measurements at 5 different wavelengths before and after injecting the contrast agent, we have achieved improved accuracy in measuring blood oxygen saturation in our experiments on a rat model.

7564-38, Session 6

Enhanced detection of circulating melanoma cells using gold nanoparticles as photoacoustic contrast agents

D. McCormack, K. Bhattacharyya, K. Katti, J. A. Viator, Univ. of Missouri, Columbia (United States)

Gold nanoparticles can provide optical contrast in imaging methods due to their surface plasmon resonance in the visible and infrared wavelengths. Researchers have investigated their use as targeting agents in tumor detection and therapy. We have used gold nanoparticles to enhance the photoacoustic effect induced in circulating melanoma cells in a photoacoustic flowmeter. Circulating melanoma cells are those cells that travel through the blood and lymph systems to create secondary tumors. We incubated gold nanoparticles into a pigmented melanoma cell line and tested the photoacoustic response. We determined the photoacoustic response from 410 to 610 nm for normally pigmented melanoma cells and nanoparticle enhanced melanoma cells. The absorption for melanoma cells corresponded to the melanin absorption spectrum, while the response of enhanced melanoma cells was closer to the spectrum of nanoparticles. Furthermore, we tested the melanoma cells in a photoacoustic flowmeter and showed a tenfold increase in the photoacoustic effect in nanoparticle enhanced melanoma cells over native melanoma cells. Nanoparticle enhancement may be used in future clinical tests to improve pigmented melanoma cell detection as well as to enable detection of amelanotic melanoma.

7564-39, Session 6

In vivo integrated photoacoustic diagnostic and photothermal therapy of lymphatic system using novel molecular contrast agents

E. I. Galanzha, Univ. of Arkansas for Medical Sciences (United States); J. Kim, Univ. of Arkansas (United States); E. V. Shashkov, V. P. Zharov, Univ. of Arkansas for Medical Sciences (United States)

The lymphatic system is currently under intense investigation for the assessment of cancer metastasis, immunity, and lymphatic malformations. Problems surrounding the molecular detection of lymphatic cells in vivo include low sensitivity of existing techniques and the risk of toxicity for radio- or fluorescent tags. Here, we present a diagnostic/therapeutic in vivo strategy for an advanced lymphatic assessment based upon the integration of multicolor photoacoustic (PA) diagnosis and photothermal (PT) therapy enhanced by multiplex molecular targeting with novel low-toxicity hybrid nanoparticles (NPs).

Time-resolved PA spectral identification of cells was achieved using multicolor labels, laser pulses of different wavelengths, and time delays. Multicolor NPs were conjugated with different lymphatic markers (e.g., folate, anti-LYVE-1 antibodies) and used as multiplex PA/PT contrast agents.

The capability of PA diagnosis and PT therapy was demonstrated in preclinical studies for multicolor molecular mapping of lymphatic system; for detecting immune-related, metastatic, and endothelial cells with unprecedented sensitivity (one tumor cell among millions of normal cells); and for targeted PT eradication of undesired cells (e.g., cancer metastatic cells) in lymph vessels and sentinel lymph nodes. The unique features of



novel NPs permitted identification of individual cells within standards of laser safety for humans.

Presented strategy can fill gaps in lymphatic research in vivo by monitoring immune status, establishing multi-correlations between primary tumor progression, metastatic cell production, lymph node status and lymphangiogenesis. Possible clinical benefits are the use of the techniques safely in humans, low-toxicity NPs, sterile fibers for diagnosing/purging metastasis within the lymphatic system, and for targeted destruction of defective tissue in lymphatic malformations.

7564-40, Session 6

Nanoparticle-targeted photoacoustic cavitation for tissue imaging

J. R. McLaughlan, R. A. Roy, T. W. Murray, Boston Univ. (United States)

Photoacoustic tomography is a non-invasive imaging technique based on the detection of broadband acoustic emissions generated by the absorption of light in tissue. This technique utilises the high contrast of optical imaging with high resolution from ultrasound imaging. However, the ability to detect these emissions above the noise level ultimately limits the depth to which imaging can be performed. Introduction of light-absorbing gold nanoparticles can improve the signal to noise ratio in tissue, through greater optical absorption and targeting specific cell populations, thereby enhancing contrast and the ability to delineate tissue types. For sufficiently high laser fluence incident on a nanoparticle, a transient vapour cavity is formed and undergoes inertial collapse, generating a broadband emission and possibly additional contrast. However, the laser fluence required to achieve this typically exceeds the maximum permissible exposure (MPE) for tissue. Through the combination of ultrasonic and optical pulses, the light and sound thresholds required to repeatedly generate inertial cavitation were reduced to 5mJ/cm2 and 1MPa respectively. Experiments employed a transparent acrylamide gel possessing a small (<600µm) spherical region doped with 80nm diameter gold nanoparticles and simultaneously exposed to pulsed laser light (532nm) and pulsed ultrasound (1.1MHz). The amplitude of broadband emissions induced by both light and sound exceeded that produced by light alone by almost two orders of magnitude, thereby facilitating imaging a deeper depth within tissue. 2D images of doped regions generated from conventional photoacoustic and ultrasound-enhanced emissions are presented and compared. [Work supported by a Boston University COE Dean's Catalyst Award and the Gordon Center for Subsurface Sensing and Imaging Systems (NSF ERC Award No. EEC-9986821).]

7564-41, Session 6

Contrast enhancement using magnetic-forceinduced motion in photoacoustic imaging

C. Jia, Univ. of Michigan (United States); S. Huang, Y. Jin, C. H. Seo, L. Huang, J. F. Eary, X. Gao, M. O'Donnell, Univ. of Washington (United States)

The specific contrast of photoacoustic (PA) imaging can be enhanced by molecular targeting using absorbing contrast agents such as gold nanoparticles. However, absorption in background tissue also generates a PA signal and limits contrast enhancement. To increase the linear range of molecular contrast agents, the background must be suppressed. In this study, we demonstrate that contrast can be increased by magnetomotive manipulation of Au-shell-encapsulated magnetic nanoparticles (MNPs). These nanoparticles are subjected to a time-varying magnetic field and exhibit much stronger optical absorption above 700-nm than pure MNPs. By magnetically moving the particles and estimating regional motion, PA contrast can be greatly enhanced. A 10% polyvinyl alcohol (PVA) disk with 2-mm thickness was constructed with two 3-mm diameter cylindrical inclusions made of 10% PVA mixed with 8% 15-um polymer beads: one containing black ink

serves as the background and the other containing 0.6mg/ml MNP-Au core-shell nanoparticles (~25-nm core size) serves as an object of interest. A solenoid with a cone-shaped iron core integrated with a DC power amplifier, current amplifier, and function generator generates 4.9-s 0.8-Tesla pulses. It was placed under a water tank holding the phantom. A 15-MHz single element transducer detected the PA signal created at 780-nm optical wavelength. Both inclusions generate PA signals but only the inclusion with MNP-Au core-shell nanoparticles was detected with 40-um displacement induced by magnetic force. Using this information, background PA signals from the ink inclusion were greatly suppressed.

7564-42, Session 6

Heating of nanoparticle thermal contrast agents at RF frequencies

D. Byrd, G. Hanson, S. Patch, Univ. of Wisconsin-Milwaukee (United States)

Thermoacoustic imaging can resolve the boundaries between different tissue types only if their electrical properties are sufficiently disparate. Controlled deposition of conducting materials can enhance TCT contrast, and allow the use of lower illumination frequencies, where tissue penetration is good but signal to noise ratios are poor. We will present theoretical results showing that at RF illumination frequencies nanospheres and nanotubes can enhance the heating of their host materials, and we will examine the effect of conductivity on absorption. For single-walled carbon nanotubes (SWNT's) whose length is small compared to the illumination wavelength, tubes with lower conductivities (e.g., semiconducting tubes) are predicted to be optimal. For SWNT's whose lengths are large compared to the illumination wavelength, absorption is optimized by maximizing conductivity. We also show that moderately low-conductivity nanospheres absorb energy better than conducting ones. However, a thin layer of dielectric coating on a conducting nanosphere can have a significant effect on the amount of energy the particle can absorb. We hope to present experimental corroboration with 108 MHz illumination.

7564-43, Session 7

In vivo photoacoustic and ultrasonic mapping of rat sentinel lymph nodes with a modified commercial ultrasound imaging system

T. N. Erpelding, Philips Research North America (United States); C. Kim, M. Pramanik, Washington Univ. in St. Louis (United States); Z. Guo, Washington University in St. Louis (United States); J. Dean, L. Jankovic, Philips Research North America (United States); K. Maslov, L. V. Wang, Washington Univ. in St. Louis (United States)

Sentinel lymph node biopsy (SLNB) has become the standard method for axillary staging in breast cancer patients, relying on invasive identification of sentinel lymph nodes following injection of blue dye and radioactive tracers. While SLNB achieves a low false negative rate (5-10%), it is an invasive procedure requiring ionizing radiation. As an alternative to SLNB, ultrasound-guided fine needle aspiration biopsy has been tested clinically. However, ultrasound alone is unable to accurately identify which lymph nodes are sentinel. Therefore, a non-ionizing and non-invasive detection method for accurate SLN mapping is needed.

In this study, we successfully imaged methylene blue dye accumulation in vivo in rat axillary lymph nodes using a Phillips iU22 ultrasound imaging system adapted for photoacoustic imaging with a Nd:YAG pumped, tunable dye laser. Photoacoustic images of rat SLNs clearly identify methylene blue dye accumulation within minutes following intradermal dye injection and co-registered photoacoustic/ultrasound images illustrate lymph node position relative to surrounding anatomy. To investigate clinical translation, the imaging depth was extended up to 2.5 cm by adding turkey breast on top of the rat skin surface. In addition, photoacoustic spectroscopy (606-678 nm) confirms methylene





blue accumulation in rat SLNs. Finally, three dimensional photoacoustic images, acquired by mechanically scanning, demonstrate dynamic imaging of methylene blue dye accumulation from lymph vessels to SLNs. These results raise confidence that photoacoustic imaging can be used clinically for accurate, non-invasive SLN mapping.

7564-44, Session 7

Imaging hypoxia using 3D photoacoustic spectroscopy

K. M. Stantz, Purdue Univ. (United States)

Purpose: The objective is to develop a multivariate in vivo hemodynamic model of tissue oxygenation (MiHMO2) based on 3D photoacoustic spectroscopy.

Introduction: Low oxygen levels, or hypoxia, deprives cancer cells of oxygen and confers resistance to irradiation, some chemotherapeutic drugs, and oxygen-dependent therapies (phototherapy) leading to treatment failure and poor disease-free and overall survival. For example, clinical studies of patients with breast carcinomas, cervical cancer, and head and neck carcinomas are more likely to suffer local recurrence and metastasis if their tumors are hypoxic. A novel method to noninvasively measure tumor hypoxia, identify its type, and monitor its heterogeneity is devised by measuring tumor hemodynamics, MiHMO2.

Material and Methods: Simulations are performed to compare tumor pO2 levels and hypoxia based on physiology - perfusion, fractional plasma volume, fractional cellular volume - and its hemoglobin status - oxygen saturation and hemoglobin concentration - based on in vivo measurements of breast, prostate, and ovarian tumors. Simulations of MiHMO2 are performed to assess the influence of scanner resolutions and different mathematical models of oxygen delivery.

Results: Sensitivity of pO2 and hypoxic fraction to photoacoustic scanner resolution and dependencies on model complexity will be presented using hemodynamic parameters for different tumors.

Conclusions: Photoacoustic CT spectroscopy provides a unique ability to monitor hemodynamic and cellular physiology in tissue, which can be used to longitudinally monitor tumor oxygenation and its response to anti-angiogenic therapies.

7564-45, Session 7

Multiwavelength photoacoustic imaging of vascular networks in transgenic mice

J. G. Laufer, J. O. Cleary, E. Z. Zhang, M. F. Lythgoe, P. C. Beard, Univ. College London (United Kingdom)

The preferential absorption of near infrared light by blood makes photoacoustic imaging well suited to visualising vascular structures in soft tissue. In addition, the spectroscopic specificity of tissue chromophores can be exploited by acquiring images at multiple excitation wavelengths. This allows the quantification of endogenous chromophores, such as oxy- and deoxyhaemoglobin, and the detection of exogenous chromophores, such as functionalised contrast agents. The measurement of chromophore concentrations typically requires the use of model-based inversion schemes which incorporate theoretical models of the photoacoustic signal generation and detection. From the determined oxy- and deoxyhaemoglobin concentrations, related functional haemodynamic parameters, such as blood oxygenation and total haemoglobin concentration can be then obtained. More importantly, this approach has the potential to visualise the spatial distribution of low concentrations of functionalised contrast agents against the strong background absorption of the endogenous chromophores. This has a large number of applications in the life sciences. One example is the structural and functional phenotyping of transgenic mice for the study of the genetic origins of vascular malformations, such as heart defects. In this study, photoacoustic images of mouse embryos have been acquired and correlated to structural microMRI images in order to study the development of the vasculature following specific genetic knockouts.

7564-46, Session 7

Optoacoustic imaging of a prostate cancer model

M. P. Patterson, M. Arsenault, Univ. of Prince Edward Island (Canada); C. Riley, Atlantic Veterinary College (Canada); M. Kolios, Ryerson Univ. (Canada); W. M. Whelan, Univ. of Prince Edward Island (Canada)

Prostate cancer is currently the most common cancer among Canadian men. Due to an increase in public awareness and screening, prostate cancer is being detected at earlier stages and in much younger men. This is raising the need for better treatment monitoring approaches. Optoacoustic (OA) imaging is being investigated as a guidance tool for monitoring prostate cancer treatments, including thermal therapies. OA is a new imaging technique that involves exposing tissues to pulsed light and detecting the tissue generated acoustic waves. Our backward-mode OA imaging system consists of a Nd:YAG pumped Ti:sapphire laser operating at 775 nm and 1064 nm and an 8 element annular transducer array with a central frequency of 4 MHz. Our initial phantom experiments show that India ink targets with absorption coefficients of 0.1cm-1 to 1.0 cm-1 can be clearly visualized at 775 nm. OA images of India ink targets embedded in a tissue equivalent, resin-based mouse phantom (optical absorption, 0.1 cm-1, and scattering, 20 cm-1) will be presented. A murine model of prostate cancer, TRAMP (transgenetic ardenocarcinoma of mouse prostate), is also being investigated. Around the age of 10 weeks, TRAMP mice spontaneously develop prostate cancer which closely mimics the progression of the human disease. OA images of wild type mouse prostate and TRAMP prostate at 16, 18, 20, 22 week time points acquired at 775 nm and 1064 nm will be presented.

7564-47, Session 7

Photoacoustic diagnosis of edema in rat burned skin

K. Yoshida, Keio Univ. (Japan); S. Sato, K. Hatanaka, D. Saitoh, H. Ashida, T. Sakamoto, National Defense Medical College Research Institute (Japan); M. Obara, Keio Univ. (Japan)

Diagnosis of edema in tissue is important for managing various traumatic injuries and diseases. In case of severe burn injuries, the permeability of blood vessels is increased due to thermal invasion, resulting in development of edema. The extent of edema reflects not only local but also systemic hemodynamics in a patient. However, there is no reliable method for real-time monitoring of edema. In this study, we examined photoacoustic (PA) monitoring of edema formed in burned skin in rats, for which a light wavelength of 1430 nm showing an absorption peak of water was used. Deep dermal burn with a 20% total body surface area was made in the dorsal skin of rats. The burn and its adjacent tissue was irradiated with 1430-nm, 6-ns light pulses and PA signals induced were measured with a piezoelectric transducer as a function of post-burn time. For the measurement, a dark field illumination technique was used to observe water in deep dermal tissue. The PA signal amplitude at 1430 nm was increased until 24 h post-burn and thereafter, signal amplitude was gradually decreased to its initial level at 72 h post-burn. There was a significant correlation between PA signal amplitudes and water contents in the tissue measured by wet/dry weight method. The measurement of urine volume showed that the phase of PA signal decrease, i.e., after 72 h post-burn, coincided with a diuretic phase for the rat. These findings demonstrate the validity of PA measurement for real-time, noninvasive monitoring of edema.



7564-48, Session 7

Detection and capture of single circulating melanoma cells using photoacoustic flowmetry

C. O'Brien, J. Mosely, J. A. Viator, Univ. of Missouri, Columbia (United States)

Photoacoustic flowmetry has been used to detect single circulating melanoma cells in vitro. Circulating melanoma cells are those cells that travel in the blood and lymph systems to create secondary tumors and are the hallmark of metastasis. This technique involves taking blood samples from patients, separating the white blood cells and irradiating them with pulsed laser in a flowmetry set up. Rapid, visible wavelength laser pulses on the order of 5 ns can induce photoacoustic waves in melanoma cells due to their melanin content, while surrounding white blood cells remain acoustically passive. We have developed a system that identifies rare melanoma cells and captures them in 10 microliter volumes using suction applied near the photoacoustic detection chamber. We have tested this system on dyed microspheres ranging in size from 50 to 500 microns. This system was also tested on single cultured melanoma cells spiked in a saline suspension of white blood cells. Capture of circulating melanoma cells may provide the opportunity to study metastatic cells for basic understanding of the spread of cancer and to optimize patient specific therapies.

7564-49, Session 7

Opto-acoustic 13C-breath test analyzer

H. Harde, G. Helmrich, Helmut-Schmidt Univ. (Germany); M. Wolff, Hamburg Univ. of Applied Sciences (Germany)

The composition and concentration of exhaled volatile gases well reflects the physical ability of a patient. Therefore, a breath analysis allows one to recognize an infectious disease in an organ or even to identify a tumor. One of the most prominent breath tests is the 13C-urea-breath test, applied to ascertain the presence of the bacterium helicobacter pylori in the stomach wall as an indication of a gastric ulcer.

After a patient has orally received an isotope-marked urea probe (the most common isotope 12C is replaced to a large extent by 13C), the substrate is metabolized in the stomach to isotope-marked carbon dioxide which in the presence of helicobacter bacteria is absorbed by the blood and finally released in the patient's breath. For a reliable diagnosis changes of the 13CO2 concentration of 1% have to be detected at a concentration level of this isotope in the breath of about 400 ppm.

In this contribution we present a new optical analyzer that employs a compact and simple set-up based on photoacoustic spectroscopy. It consists of two identical photoacoustic cells containing two breath samples, one taken before and one after capturing the isotope-marked substrate, and it measures simultaneously the relative CO2 isotopologue concentrations in both samples by exciting the molecules on specially selected absorption lines with a semiconductor laser operating at a wavelength of 2.744 μm .

7564-50, Session 7

Photoacoustic detection of hemozoin in human blood as an early indicator of malaria infection

J. Custer, M. Kariuki, B. Beerntsen, J. A. Viator, Univ. of Missouri, Columbia (United States)

Malaria is a blood borne infection affecting hundreds of millions of people worldwide. The disease usually progresses from an initial mosquito bite from which plasmodium parasites enter the bloodstream and embeds in the liver. The infection eventually reenters the bloodstream where

the parasites invade red blood cells. The parasites reproduce within the blood cells, eventually causing their death and lysis. This process releases the parasites into the blood, continuing the cycle of infection. Usually, malaria is diagnosed only after a patient presents symptoms, including high fever, naseau, and, in advanced cases, coma and death. While invading the bloodstream of a host, malaria parasites convert hemoglobin into an insoluble crystal, known as hemozoin. These crystals, approximately several hundred nanometers in size, are contained within red blood cells and those white blood cells that injest free hemozoin in the blood. Thus, infected red blood cells and white blood cells contain a unique optical absorber that can be detected in blood samples using photoacoustic flowmetry. We cultured and isolated 100 milligrams of hemozoin from malaria infected blood. Using a tunable laser system consisting of an optical parametric oscillator pumped by an Nd:YAG laser with a pulse duration of 5 ns, we determined the relative absorption spectrum of hemozoin from 410 to 640 nm. We then separated the white blood cells from malaria infected blood and tested it in a photoacoustic flowmetry set up. Our threshold of detection was 10 infected white blood cells per microliter, comparable to current tests using microscopic analysis of blood.

7564-51, Session 8

In vivo photoacoustic detection and photothermal eradication of circulating tumor cells

V. P. Zharov, E. I. Galanzha, E. V. Shashkov, D. Nedosekin, M. Sarimollaoglu, Univ. of Arkansas for Medical Sciences (United States); J. Kim, Univ. of Arkansas (United States)

This review summarizes recent advances in in vivo ultrasensitive photoacoustic (PA) detection and photothermal (PT) eradiation of circulating tumor cells (CTC) targeted directly in the bloodstream by multicolor nanoparticles. We discuss the application of advanced near infrared lasers with a pulse repetition rate up to 0.5 MHz, new fast software, a hybrid multicolor nanoparticles (e.g., golden carbon nanotubes), multiplex conjugation using antibodies, folate, and ATF to target simultaneously several CTC biomarkers, and real-time integration of PA diagnosis with PT treatment of CTCs. The study in vivo on tumorbearing mouse models and spiked human blood samples demonstrated specificity, sensitivity, and therapy efficiency for melanoma and breast cancer CTCs prior to the development of distant metastases that was unachievable with existing CTC assays. It may provide to use CTC as marker not only of metastasis progression, cancer recurrence or therapy efficiency, but also for metastasis prevention and early cancer diagnosis at parallel progression of primary tumor and CTCs.

7564-52, Session 8

Noninvasive optoacoustic monitoring platform: Clinical studies

R. O. Esenaliev, Y. Petrov, I. Y. H. Petrova, The Univ. of Texas Medical Branch (United States); C. S. Robertson, L. Ponce, Baylor College of Medicine (United States); M. Kinsky, R. Seeton, N. Henkel, D. Prough, The Univ. of Texas Medical Branch (United States)

Practical noninvasive monitors that could quickly provide continuous information in both high acuity and low acuity environments would greatly facilitate prompt recognition and treatment of a variety of life-threatening illnesses. Our long-term objective is to improve the patient care by developing a multiparameter, noninvasive, optoacoustic diagnostic platform that will accurately and continuously measure total hemoglobin concentration, venous oxyhemoglobin saturation (both cerebral and mixed), cardiac output, circulating blood volume, cardiac index, systemic oxygen delivery, hepatic function, and other important physiological parameters. Currently, invasive measurements of these



parameters are routinely used in the care of large populations of patients including anemic patients, patients with traumatic brain injury, critically ill patients, patients with circulatory shock, surgical patients. In addition, the optoacoustic technique can be used for measurement of blood pressure in vessels: arteries, arterioles, veins, and capillaries. We built optoacoustic systems for monitoring of these parameters and performed clinical tests of the systems. We developed patient interfaces that incorporate optoacoustic probes designed and built for these diagnostic applications. Our systems include highly-portable, light-weight, inexpensive, laser diode-based systems suitable for clinical applications. In this paper we report results of the clinical studies performed by our group at the University of Texas Medical Branch and at Baylor College of Medicine to demonstrate the capabilities of the optoacoustic platform for noninvasive monitoring of mulitple physiological parameters. Our data indicate that the accuracy of the optoacoustic measurements is approaching that of "gold standard" invasive techniques.

7564-53, Session 8

Novel, focused optoacoustic transducers for accurate monitoring of total hemoglobin concentration and oxyhemoglobin saturation: pre-clinical and clinical tests

E. Särchen, I. Y. H. Petrova, Y. Y. Petrov, D. Prough, R. O. Esenaliev, The Univ. of Texas Medical Branch (United States)

Measurement of total hemoglobin concentration is one of the most frequently performed blood tests. Monitoring of mixed venous oxyhemoglobin saturation is critically important for management of patients with circulatory shock and surgery patients. We have developed optoacoustic technquies for noninvasive, accurate, and continuous monitoring of these parameters by probing of specific blood vessels such as the radial artery and the internal jugular vein. Our initial studies were performed using non-focused optoacoustic transducers. In this work we report development and tests of novel, focused optoacoustic transducers that provide blood vessel probing with higher, sub-millimeter lateral resolution. The custom-made focused optoacoustic transducers combine sensitive piezoelectric polymer and acoustic lenses designed for probing these blood vessels. The focused transducers were incorporated into our highly portable, laser diode-based optoacoustic monitoring system for pre-clinical and clinical tests. First, we calibrated the transducers using sub-millimeter optoacoustic sources and measured the focal length and lateral resolution of the transducers. Then, we performed in vitro tests with blood at different hemoglobin concentrations (from 4 to 16 g/dL) in highly scattering phantoms simulating tissue with mm-sized arteries and veins. Finally, we tested the transducers in vivo in human subjects. In addition, we performed in vitro and in vivo comparative studies of the focused and non-focused optoacoustic transducers. Optimization of focal parameters and lens materials allowed for minimal insertion losses, while the sub-millimeter lateral resolution provided higher signal-to-noise ratio and higher accuracy of the measurements, in particular, from smaller blood vessels such as the radial artery (diameter 2-3 mm).

7564-54, Session 8

Effects of radiation on tumor hemodynamics and NF-kappaB in breast tumors

K. M. Stantz, B. Liu, Purdue Univ. (United States); M. Cao, Indiana Univ. School of Medicine (United States); N. Cao, Purdue Univ. (United States); H. Chin-Sinex, M. Mendonca, Indiana Univ. School of Medicine (United States); J. J. Li, Univ. of California-Davis (United States)

Purpose: The purpose of this study is to monitor in vivo the IR dose dependent response of NF-kappaB and tumor hemodynamics as a function of time.

Material and Methods: An MDA-231 breast cancer cell line was stably

transfected with a firefly luciferase gene within the NF-kappaB promoter. Tumors on the right flank irradiated with a single fractionated dose of 5Gy or 10Gy. Over two weeks, photoacoustic spectroscopy (PCT-S), bioluminescence imaging (BLI), and dynamic contrast enhanced CT (DCE-CT) was used to monitor hemoglobin status, NF-kappaB expression, and physiology, respectively.

Results: From the BLI, an increase in NF-kappaB expression was observed in both the right (irradiation) and left (non-irradiated) tumors, which peaked at 8-12 hours, returned to basal levels after 24 hours, and increased a second time from 3 to 7 days. This data identifies both a radiation-induced bystander effect and a bimodal longitudinal response associated with NF- B-controlled luciferase promoter. The physiological results from DCE-CT measured an increase in perfusion (26%) two days after radiation and both a decrease in perfusion and an increase in fp by week 1 (10Gy cohort). PCT-S measured increased levels of oxygen saturation two days post IR, which did not change after 1 week. Initially, NF- B would modify hemodynamics to increase oxygen delivery after IR insult. The secondary response appears to modulate tumor angiogenesis.

Conclusions: A bimodal response to radiation was detected with NFkappaB-controlled luciferase reporter with a concomitant hemodynamic response associated with tumor hypoxia. Experiments are being performed to increase statistics.

7564-55, Session 8

Broadband characterization of the ultrasonic attenuation in biological tissues using photoacoustics

B. E. Treeby, B. T. Cox, Univ. College London (United Kingdom)

Photoacoustic tomography as a biomedical imaging modality exploits the in vivo generation of ultrasonic waves via thermo-elastic expansion. If the skin is illuminated with nanosecond laser pulses of visible or near-infrared light, broadband ultrasonic waves are produced from light absorbing structures such as blood vessels. The propagation of these waves through tissue is accompanied by significant acoustic absorption, particularly at higher frequencies. Knowledge of the absorption characteristics of the propagation medium allows this effect to be partially mitigated using specialised image reconstruction techniques. However, the ultrasonic characterisation of biological materials has typically been limited to either diagnostic (1-10 MHz) or biomicroscopy (40-60 MHz) frequencies. The extrapolation of these results to other frequencies can be erroneous due to the unknown distribution of relaxation mechanisms responsible for the absorption. Here, broadband ultrasound transmission measurements (1-90 MHz) are made using a photoacoustic plane-wave source and an optical ultrasound sensor (a planar Fabry-Perot polymer film interferometer). The ultrasonic source is produced by illuminating a thin black paint layer on a polymethylmethacrylate (PMMA) substrate with nanosecond pulses of laser light. The system is used to measure the ultrasonic attenuation in human blood at both in vivo and ex vivo temperatures. Power law attenuation parameters are extracted by fitting the experimental attenuation data to a frequency power law while simultaneously fitting the dispersion data to the corresponding Kramers-Krönig relation. The effect of ultrasound contrast agents on the attenuation in human blood is described, and preliminary results from other tissue measurements including animal liver are also presented.

7564-56, Session 8

Effects of optical energy distribution on the frequency spectrum of laser-induced acoustic

A. Conjusteau, S. A. Ermilov, A. A. Oraevsky, Fairway Medical Technologies, Inc. (United States)

We have investigated the limitations of our laser ultrasonic plane wave

TEL: +1 360 676 3290 · +1 888 504 8171 · customerservice@spie.org



source. In theory, the device is capable of producing an acoustic impulse with a bandwidth exceeding 50 MHz. However, in practice, a bandwidth of 12 MHz is measured with a calibrated wideband hydrophone. We have investigated three experimental parameters that alter the generated acoustic impulse: laser pulse duration, laser spatial profile, and absorber opacity. Through numerical simulations, the effect of each individual parameter was quantified. Modifications to the experimental setup, along with corresponding experimental data, are presented.

7564-57, Session 8

Toward characterizing the size of microscopic optical absorbers using optoacoustic emission spectroscopy

A. G. Gertsch, N. L. Bush, D. C. Birtill, J. Bamber, Institute of Cancer Research (United Kingdom)

To assess the malignancy and progression of a tumour various parameters, e.g. the number, distribution and size of microvessels may be of importance. Optical absorption by the blood that fills microvessels can be visualised by optoacoustic imaging (OA), which thermoelastically generates ultrasound. We have previously reported that an inhomogeneous optical absorption within an object region produces an acoustic emission that has reduced acoustic coherence compared with that from a homogeneously absorbing region, which results in improved region contrast and boundary detectability. Here we propose that in addition to this, further analysis of the acoustic emission signals should permit a characterization of the optical inhomogeneity in terms of microscopic absorber size and density. Both ultrasound texture analysis and spectral analysis should have value but in this study the aim was to investigate the influence of the size of the absorbers on the frequency spectrum of the emitted optoacoustic signal. Cylindrical gelatine phantoms containing black absorbing polymer microspheres with different diameters (50 µm - 1 mm) for each phantom were measured in both water and an optically scattering (intralipid solution) background at various distances from a linear array probe, using pulsed illumination that had been adjusted for an optimal distribution of fluence with depth. Simulations were conducted using a combination of Monte Carlo photon transport and time domain acoustic propagation methods. Preliminary findings show that the size of the absorbers, rather than their distribution, is directly related to the average frequency spectrum of the optoacoustic signal.

7564-58, Session 8

Dynamics of thermoelastic expansion for native and coagulated ex vivo bovine liver tissues

B. Soroushian, Ryerson Univ. (Canada); W. M. Whelan, Univ. of Prince Edward Island (Canada); M. C. Kolios, Ryerson Univ. (Canada)

Optoacoustic imaging based on ultrasonic detection of the stresses generated by short laser pulses in tissues has been shown to be useful in monitoring of thermal therapies. The optoacoustic signal is sensitive to the changes in optical and thermoacoustic properties that occur after tissue coagulation. The mechanisms by which these changes affect the optoacoustic signal are however not well understood. In this study an interferometry system capable of measuring transient surface displacements of samples with a temporal resolution of less than 10 ns and spatial resolution of around 5 nm was used to measure dynamics of thermoelastic expansion for native and coagulated ex-vivo bovine liver tissues after their irradiation by 6 ns laser pulses at 750 nm. Significant differences were observed between the dynamics of thermoelastic expansion for native and coagulated liver tissues. Furthermore, the experimental data were used to estimate the changes that occur in the optical penetration depth and Gruneisen coefficient of ex vivo liver upon coagulation. This work demonstrates that the Gruneisen coefficient is an important thermacoustic property of tissues undergoing thermal therapy and it plays a key role in the differential optoacoustic signals observed between native and coagulated liver tissues.

7564-87, Poster Session

Novel laser-induced cavitation: the constrained ring bubble

P. A. Prentice, S. Zolotovskaya, E. Rafailov, Univ. of Dundee (United Kingdom)

Using high speed photography at sub-microsecond temporal resolution, we observed laser-induced cavitation within a thin film of liquid. In accordance with the literature, focussing a pulse of a gaussian-like intensity distribution into the liquid, instigated a disk-shaped cavity. The propagation of an acoustic transient, generated during the formation and expansion of the cavity, is evidenced by secondary cavitation stimulated in the surrounding liquid. Introducing a laguerre-gauss holographic diffractive optic element into the beam path, redistributes the optical energy into the so-called 'doughnut mode', with an axial intensity minimum. Focusing this modulated pulse into the liquid induced a ring-shaped cavity with a notably different dynamic to that of the disk cavity, due primarily to the encapsulated droplet, which is present from cavity inititation through expansion and subsequent deflation. In this paper we present initial observations on the novel dynamics of the ringshaped cavity and discuss several of the distinctive features. Particularly the secondary cavitation induced in the surrounding liquid, and the implicated multiplexing of the acoustic transient generated during the ring-cavity expansion, is of interest.

7564-88, Poster Session

Acousto-optical coherence tomography using random phase jumps on ultrasound and light

S. Farahi, M. Lesaffre, Ecole Supérieure de Physique et de Chimie Industrielles (France); M. Gross, Ecole Normale Supérieure (France); P. Delaye, Univ. Paris-Sud 11 (France); C. Boccara, F. Ramaz, Ecole Supérieure de Physique et de Chimie Industrielles (France)

The combination of light and ultrasound to measure local optical properties through thick and highly scattering media is a tantalizing approach for breast cancer detection. Light is highly scattered within biological tissues, while the ultrasounds are ballistic. Thus, thanks to the acousto-optic effect, we can get the optical contrast information given by light and get the spatial localization from the ultrasound longitudinal waves. However, resolution can remain poor along the ultrasounds axis.

To get a millimetric axial resolution, the most common configuration is to apply a microsecond pulse regime to the ultrasounds.

We introduce here a new technique called Acousto-Optical Coherence Tomography (AOCT) that enables to get this millimetric axial resolution with continuous US and light beams by applying random phase jumps on both of them. The set up we use is based on the photorefractive effect to perform a self-adaptive wavefront holography with a GaAs bulk crystal and a single large area photodetector.

This technique is performed by application of a stochastic phase modulation on light and ultrasounds. By this way, we get a short coherence length ultrasound source that explores the sample. A time delay between the ultrasound and light modulation enables to select the active zone along the ultrasound column, where the acousto optic interferometric signal remains coherent in time.

It is a low coherence imaging technique like OCT (Optical Coherence Tomography) that involves "low coherence acousto optic sources", i.e an optical source and an ultrasound source, which are both incoherent in time, but fully correlated together.



7564-89, Poster Session

Photoacoustic Correlation Technique for Low-speed Flow Measurement

S. Chen, T. Ling, Univ. of Michigan (United States); S. Huang, Univ. of Washington (United States); H. W. Baac, Univ. of Michigan (United States); Y. Chang, National Changhua Univ. of Education (Taiwan); L. J. Guo, Univ. of Michigan (United States)

We propose a photoacoustic correlation technique for the flow measurement for the first time. This principle of this technique is inspired by the well-studied fluorescence correlation spectroscopy, which is commonly used in the characterization of the dynamics of fluorescent species. The detected ultrasound signal strength in photoacoustic correlation experiment is the counterpart of the photon counts in the fluorescence correlation spectroscopy. Microcirculation is smallest functional unit of the cardiovascular system. Studying it provides a unique comprehension of disease processes. However, the study remains a challenge due to small vessel size, low blood flow speed, and large imaging depth (~5 mm). Photoacoustic correlation flow measurement holds the promise in acquiring low-speed blood flow with a proper design of probe volume. Previously we have demonstrated a highly sensitive polymer microring resonator based ultrasound detector. The use of such a low-noise device makes it possible to increase the imaging depth. Experiments of photoacoustic correlation were carried out on micrometer-scale microspheres illuminated by a millimeter-size pulsed laser beam. The correlation curves were calculated from the fluctuation of the detected signal strength due to the number and position variation of microspheres in the probe volume under the flow condition, and the resolution is mainly limited by the digital recording system, which is ~0.5 s. Our results show that flow speeds of less than 0.05 mm/s can be measured. This experiment serves as a basis for photoacoustic correlation spectroscopy, which can potentially be used for functional imaging, especially for detecting low-speed blood flow of relatively deep microcirculation in biological tissues.

7564-90, Poster Session

Stimulated Raman scattering based photoacoustic microscopy

H. Wang, N. Chai, Purdue Univ. (United States); S. Hu, L. V. Wang, Washington Univ. in St. Louis (United States); R. P. Lucht, J. Cheng, Purdue Univ. (United States)

We present a new photoacoustic imaging technique that is based on molecular vibration absorption in a stimulated Raman process. We use near-IR, nano-second laser beams from a Nd:YAG laser and an optical-parametric-oscillators (OPO) to generate Raman-induced acoustic waves. The ultrasound signals are detected by a focused type 20MHz transducer. Photoacoustic Raman imaging of lipids in sample phantoms and biological tissues are inspected.

7564-91, Poster Session

Evans blue dye-enhanced capillary-resolution photoacoustic microscopy in vivo

J. Yao, K. Maslov, S. Hu, L. V. Wang, Washington Univ. in St. Louis (United States)

Complete and continuous imaging of microvascular networks is crucial for a wide variety of biomedical applications. Photoacoustic tomography can provide high resolution microvascular imaging using hemoglobin within red blood cells (RBC) as an endogenic contrast agent. However, intermittent RBC flow in capillaries results in discontinuous and fragmentary capillary images. To overcome this problem, we used Evans Blue (EB) dye as a contrast agent for in vivo photoacoustic imaging. EB has strong optical absorption and distributes uniformly in the blood

stream by chemically binding to albumin. By intravenous injection of EB (6%, 200 μL), complete and continuous microvascular networksespecially capillaries-of the ears of nude mice were imaged. The diffusion of EB (3%, 100 μL) leaving the blood stream was monitored for 2 hours and an exponential recovery model was used to fit the passive diffusion dynamics. At lower administration dose of EB (3%, 50 μL), the clearance of the EB-albumin complex was imaged for 10 days and quantitatively investigated using a two-compartment model.

7564-92, Poster Session

Comparison of ultrasonic medical imaging and multiphoton laser scanning tomography

K. König, Saarland Univ. (Germany); M. Speicher, H. G. Breunig, JenLab GmbH (Germany); M. Kaatz, Univ. Hospital Jena (Germany)

Ultrasonic imaging and multiphoton laser scanning tomography are important methods for non-invasive medical investigations of skin. We report on a clinical study comparing ultrasound and multiphoton examinations which involved 47 patients with a variety of dermatological disorders. Ultrasound frequencies in the range 22 MHz to 100 MHz (Dub75 / Dub100- Taberna, Pro Medicum GmbH) were employed. The lower frequencies were used for skin imaging, whereas the use of 100-MHz ultrasound allowed lower range but higher resolution imaging (resolution of about 16 µm) of the uppermost skin layers. While ultrasound imaging provides fast wide-field cross-sectional (vertical) images of the tissue it does not achieve cellular resolution. In contrast to that, the clinical multiphoton tomograph Dermalnspect (JenLab GmbH), based on detecting autofluorescence from endogenous fluorophores such as NAD(P)H, flavoproteins, keratin, lipofuscin, elastin, collagen, melanin, and metal-free porphyrins as well as on second harmonic generation by collagen fibers, images horizontal optical sections with subcellular resolution up to 200 µm tissue depth however with a comparably smaller field of view. Thus, the combination of state-of-the art ultrasound and multiphoton systems provides both, the vertical widefield image and a stack of high-resolution horizontal multiphoton images of the same region. The study has been performed on 47 patients (31 males, 16 females, age range: 24 - 88 years) who gave written informed consent. The dermatological disorders include epithelial skin cancer, pigmented skin lesions, inflammatory skin disorders, autoimmune diseases, seborrheic keratosis, hemangioma and tattoo. In some cases, the diagnosis was confirmed by histopathological examination after surgical excision.

7564-95, Poster Session

Intravascular photoacoustic imaging of coronary artery stents

J. L. Su, B. Wang, S. Y. Emelianov, The Univ. of Texas at Austin (United States)

Coronary stents are the most widely used coronary intervention in the United States. While the procedures are more than 95% successful, stents have brought several issues including restenosis, hyperplasia and stent drift. The ability to visualize stents during the stenting procedure and during post-surgery follow-up is important to correctly assess the stent with respect to the plaques and vessel. Current imaging modalities suffer from low contrast, resolution depth penetration issues and/or unfavorable artifacts that can inhibit correct visualization of stents in

We introduce a combined intravascular photoacoustic (IVPA) and ultrasound (IVUS) method for imaging stents with sufficient contrast, resolution and depth penetration to visualize the stent with respect to the vessel wall. A commercial off-the-shelf stent was deployed in a 10 mm diameter vessel phantom which consisted of regions where the stent was embedded, adjacent and malapposed relative to the lumen wall. Photoacoustic signal from the stent was co-registered with the



ultrasound signal of the vessel allowing for quantitative measurements of stent position with respect to the vessel cross-section. Using IVUS pullback, the imaging method allowed for 3D reconstructions which accurately showed the stent in its entirety within the vessel. This combination of IVUS/IVPA has already been shown to be a powerful tool in the detection of atherosclerotic plaques which may require further treatment through stenting. Combined IVUS/IVPA imaging therefore may become a natural and feasible method for the diagnosis and treatment of atherosclerosis.

7564-96, Poster Session

Photo-acoustic concave transmitter for generating high frequency focused ultrasound

H. W. Baac, T. Ling, S. Ashekenazi, S. Huang, L. J. Guo, Univ. of Michigan (United States)

We present a photo-acoustic concave transmitter to generate and subsequently focus broadband ultrasound with clean waveform and sharp focusing for the high frequency components. The transmitter consists of a light-absorbing film coated on concave spherical glass lens. An estimated center frequency of the transmitter was approximately 67 MHz, which was obtained by taking the Fourier transform of the timederivative of 6-ns laser pulse waveform. In the proposed focal transmitter, an effective aperture is determined by the size of the laser beam. We investigate the relation of the laser beam size and the profile of focused ultrasound. Focal widths for different harmonic frequency components were extracted from the measured results. These agree with the calculated values. For ultrasound detection, we used an optical microring resonator which has a quality factor > 10000 in water and a broadband frequency response. Time-domain output waveforms of the transmitter were aberration-free and very clean without the complex oscillating tail typically observed in piezoelectric transducers. This is due to coherent summation of photo-acoustic signal at the focus, which is generated simultaneously across the spherical curvature of the lens. This property is a main advantage over conventional transducers, and is desirable for high resolution ultrasound microscopy. An axial profile of the focused ultrasound was also measured and compared with the simulated result.

7564-97, Poster Session

Design of acoustic 4f imaging system by using an optical microring ultrasound detector

H. W. Baac, T. Ling, L. J. Guo, Univ. of Michigan (United States)

We design an acoustic 4f imaging system by using an optical microring ultrasound detector (OMUD). The concept of 4f imaging system for photo-acoustic imaging was recently reported by using a piezoelectric transducer as a detector [Z. Chen et al., Optics Express 15, 4966 (2007)]. However, its resolution was severely limited due to detector's limited performance in terms of physical size and frequency response. As the 4f imaging system adopts a two focusing lenses and its imaging is based on the collection of point images in space, a small size acoustic detector is required to achieve high resolution. The OMUD platform is very attractive because of its small size, while maintaining high sensitivity and broadband response up to high frequency. Our OMUD sensor has a planar geometry with 100 µm in diameter and 2 µm in width. It becomes more promising since the quality factor of the microring resonator has been recently improved (Q >10000), which means the possibility of higher sensitivity. Our 4f imaging system also includes a pair of backto-back acoustic lenses, designed by considering boundary reflection, acoustic attenuation inside the material, and focal distance. Microring output signal and spatial image will be demonstrated. A preliminary data shows that images are blurred by aberration and diffraction from objects. This suggests that high frequency ultrasound is necessary to take full benefit of high resolution. Several factors important to image resolution

are discussed such as spatial and temporal aberrations, the detector bandwidth, and the detector's geometrical effect to high frequency ultrasound

7564-98, Poster Session

Frequency-selective multiphoton-excitationinduced photoacoustic imaging to visualize the cross sections of dense objects

Y. Yamaoka, M. Nambu, T. Takamatsu, Kyoto Prefectural Univ. of Medicine (Japan)

Multiphoton excitation-induced photoacoustic imaging can be used to investigate the interior of dense objects directly because the multiphoton excitation occurs only at the focal point. This method makes it possible to avoid the strong signal from the surface of dense objects. However, in the case of tissue imaging, one-photon photoacoustic signals affect the image constructed from the multiphoton-photoacoustic signals, owing to the smaller cross section of multiphoton absorption compared with that of one-photon absorption. Thus, in order to apply the multiphoton-photoacoustic imaging for precise investigation in living tissues, it is important to enhance (or extract) only the photoacoustic signals induced by multiphoton excitation.

In this study, we examined the use of frequency-selective detection in multiphoton-photoacoustic imaging. Because the multiphoton-photoacoustic signals are generated in a very small region, the multiphoton-photoacoustic signals include higher frequency components compared with one-photon photoacoustic signals. We measured the images at the cross sections of blood-vessel phantoms visualized by multiphoton-photoacoustic signals using the high frequency components. We found that the images visualized using only high frequency components showed better contrast compared with those visualized using all frequency components. We conclude that the combination of frequency-selective detection and multiphoton-photoacoustic imaging demonstrates great potential for precise observation of cross sections of blood vessels in living tissues.

7564-99, Poster Session

Photoacoustic and ultrasound imaging contrast enhancement using remotely triggered nanocarriers

K. E. Wilson, K. Homan, S. Emelianov, The Univ. of Texas at Austin (United States)

Ultrasound is a cost-effective and safe imaging modality used widely in clinical practice. However, due to limited resolution and contrast, ultrasound cannot image tissue at the cellular/molecular level. Recently, photoacoustic imaging has been introduced as a functional imaging technique given the large amplitude and spectral variations of optical absorption of tissues. Yet, some tissues do not exhibit sufficient optical absorption contrast. We have developed a novel contrast agent to seamlessly combine the functionality and molecular imaging of photoacoustics with the morphological imaging of ultrasound. Incorporation of optically absorbing nanoparticles inside a liquid perfluorocarbon nanocarrier provides contrast for both modalities, while also having the advantage of being able to be remotely triggered into its active state when it has reached the desired imaging site.

Gold nanospheres with an average diameter of 20 nm and optical absorption peak around 526 nm were encased in perfluorocarbon nanocarriers and placed into inclusions in 10% polyacrylamide phantoms. Ultrasound images before and after remote optical triggering using a 532 nm pulsed laser showed activation of these nanocarriers, as well as enhanced ultrasound contrast. Furthermore, during optical triggering, photoacoustic signal was shown in the inclusion. In vitro studies using the nanocarrier with incorporated plasmonic nanoparticles absorbing in the near infra-red (NR) spectral region were also performed.



These nanocarriers were imaged using a combined photoacoustic and ultrasound imaging system (PAUS). The developed agent strengthened both photoacoustic and ultrasound signals when optically triggered.

7564-100, Poster Session

Photoacoustic microscopy of collagenaseinduced Achilles tendinitis in a mouse model

P. Wang, National Tsing Hua Univ. (Taiwan); W. Chen, National Taiwan Univ. Hospital (Taiwan); M. Li, National Tsing Hua Univ. (Taiwan)

Assessments of vascularity are important when assessing inflammation changes in tendon injuries since Achilles tendinitis is often accompanied with neovascularization or hypervascularity. In this study, we have investigated the feasibility of photoacoustic imaging in noninvasive monitoring of morphological and vascular changes in Achilles tendon injuries. Collagenase-induced Achilles tendinitis model of mice was adopted here. During collagenase-induced tendinitis, a 25-MHz photoacoustic microscopy (PAM) was used to image micro-vascular changes in Achilles tendons longitudinally up to 23 days. The positions of vessels imaged by PAM were identified by co-registration of PAM B-mode images with 25-MHz ultrasound (USM) ones. Morphological changes in Achilles tendons due to inflammation and edema were revealed by the PAM and USM images. Proliferation of new blood vessels within the tendons was also observed. Observed micro-vascular changes during tendinitis were similar to the findings in the literatures. This study demonstrates that photoacoustic imaging, owning required sensitivity and penetration, has the potential for high sensitive diagnosis and assessment of treatment performance in tendinopathy.

7564-101, Poster Session

Tissue classification by wavelet modified generic Fourier descriptor and their recognition using hybrid correlator

R. B. Yadav, The Univ. of Electro-Communications (Japan); A. K. Gupta, Instruments Research and Development Establishment (India)

Segmentation in Magnetic resonance imaging (MRI) images is a widely studied problem, and techniques (supervised and unsupervised) are discussed in the literature. The basic approaches to image segmentation are based upon: (a) boundary representation, (b) regional characteristics and (c) a combination of boundary and region-based features. In this paper, we report retrieval and classification of brain tissue based objects employing one of combination of boundary and region-based features as wavelet modified generic Fourier descriptor (WGFD) technique.

This technique have been applied to a database consisting of 5 different class's tissues, each class consists of 20 shapes. The Euclidean distance has been calculated as a similarity measure parameter for shape classification. To study the effect of noise on the retrieval and classification of shapes of different objects, additive and multiplicative noise of various variances were applied to the database. The classification results have been compared and it is inferred that WGFD performs better than wavelet descriptor (WD) technique. For retrieved shape recognition, an optical experiment employing hybrid correlator architecture has been carried out. We have used Wavelet modified maximum average correlation hight (MACH) filter for hybrid correlator. To evaluate the correlation output, metrics such as correlation peak height, peak-to-correlation energy, and peak-to-side lobe ratio are calculated using the simulated results.

Key words: generic Fourier descriptor, wavelet transform, shape retrieval, classification, recognition, hybrid correlator, Wavelet modified MACH filter.

7564-102, Poster Session

Reconstruction of photoacoustic tomography with finite-aperture detectors: deconvolution of the spatial impulse response

M. Li, C. Cheng, National Tsing Hua Univ. (Taiwan)

In this study, we introduce a new reconstruction method developed to reduce the finite aperture effect in photoacoustic tomography with finite-aperture detectors. The finite aperture effect and degradation in tangential resolution result from the spatial impulse response of the finite-size flat transducer. The proposed method is based on a linear, discrete model of the photoacoustic tomography system in matrix formalism. Using this model, a spatiotemporal deconvolution filter designed in minimum mean square error sense is used to compensate the spatial impulse responses associated with a finite-size flat transducer at each imaging point; thus restoration of the tangential resolution can be achieved retrospectively. The performance of the proposed reconstruction method is verified using simulation data. Compared with that reconstructed by the backprojection algorithm, the proposed method provides uniform tangential resolution over the imaging area while retaining the radial resolution because the full geometry of the flat transducer, instead of the simplified point-detector approximation is taken into consideration. The effect of the signal-to-noise ratio on the proposed method is also discussed. In addition, by taking electrical impulse response of the transducer into account, the proposed method can potentially improve the radial resolution, too.

7564-103, Poster Session

Multispectral photoacoustic microscopy using a photonic crystal fiber supercontinuum source

Y. N. Billeh, Imperial College London (United Kingdom); M. Liu, T. Buma, Univ. of Delaware (United States)

Photoacoustic microscopy (PAM) provides excellent image contrast based on optical absorption. Spectroscopic imaging requires a wavelength tunable pulsed nanosecond laser, which can be expensive. Microchip lasers at 1064 nm are extremely compact and cost effective. The purpose of this work is to investigate the feasibility of multispectral PAM with a supercontinuum source based on a photonic crystal fiber (PCF) pumped with a microchip laser. To our knowledge, this is the first demonstration of spectroscopic PAM with a nanosecond pulsed supercontinuum source. The Q-switched Nd:YAG microchip laser produces 0.6 ns duration pulses at 1064 nm with 8 uJ of energy at a 6.6 kHz repetition rate. These pulses are sent through 7 meters of PCF with a 5 um diameter core and a zero dispersion wavelength of 1040 nm. The supercontinuum is sent through a long-pass filter of desired cut-off wavelength before coupling into a multi-mode fiber attached to a PAM system employing dark-field illumination. Detection is performed with a 25 MHz spherically focused f/4 transducer. Preliminary experiments were performed on phantoms containing regions of red, blue, and black dye. PAM images were acquired with no optical filtering as well as cut-off wavelengths of 540, 580, and 630 nm. Photoacoustic images in multiple spectral windows are obtained by processing appropriate image sets. Resulting images clearly distinguish the different absorbing regions of the test sample. These preliminary results suggest the potential of the supercontinuum PCF source for multispectral PAM.

7564-104, Poster Session

Photoacoustic micro-imaging of focusedultrasound induced blood-brain-barrier opening in a rat model

P. Wang, National Tsing Hua Univ. (Taiwan); P. Hsu, H. Liu, Chang

TEL: +1 360 676 3290 · +1 888 504 8171 · customerservice@spie.org



Gung Univ. (Taiwan); C. C. Wang, National Chung-Cheng Univ. (Taiwan); M. Li, National Tsing Hua Univ. (Taiwan)

Blood brain barrier (BBB) prevents most of the drug from transmitting into the brain tissue and decreases the treatment performance for brain disease. One of the methods to overcome the difficulty of drug delivery is to locally increase the permeability of BBB with high-intensity focused ultrasound. In this study, we have investigated the feasibility of photoacoustic microscopy of focused-ultrasound induced BBB opening in a rat model in vivo with gold nanorods (AuNRs) as a contrast agent. This study takes advantage of the strong near-infrared absorption of AuNRs and their extravasation tendency from BBB opening foci due to their nano-scale size. Before the experiments, craniotomy was performed on rats to provide a path for focused ultrasound beam. Localized BBB opening at the depth of about 3 mm from left cortex of rat brains was achieved by delivering 1.5 MHz focused ultrasound energy into brain tissue in the presence of microbubbles. PEGylated AuNRs with a peak optical absorption at ~800 nm were then intravenously administered. Pre-scan prior to BBB disruption and AuNR injection was taken to mark the signal background. After injection, the distribution of AuNRs in rat brains was monitored up to 2 hours. Experimental results show that imaging AuNRs reveals BBB disruption area in left brains while there are no changes observed in the right brains. From our results, photoacoustic imaging plus AuNRs shows the promise as a novel monitoring strategy in identifying the location and variation of focused-ultrasound BBB-opening in a rat model.

7564-105, Poster Session

Multicolor photoacoustic imaging by a single transducer with piezoelectric copolymer film in a wide frequency range

T. Ohmori, M. Ishihara, I. Bansaku, M. Kikuchi, National Defense Medical College (Japan)

Photoacoustic imaging can offer a tomographic image with resolution of sub-milimeters in depth of centimeters, and distinguish objectives by their absorption spectra. We focused on (1) frequency analysis of a photoacoustic image and (2) multi-color photoacoustic imaging. The former is important because frequency of generated acoustic wave is related to absorption length and the amplitude is more decayed with higher frequency. The aim of the latter is "spectral" diagnosis of cancer, oxygen saturation, and so on.

We performed a photoacoustic imaging measurement by scanning a single detector (Φ 5 mm) with copolymer P(VDF-TrFE) film which is sensitive from kHz to tens MHz. A sample phantom was made of 10% agar in which agarose gels stained by indocyanine green (ICG) and methylene blue (MB) were embedded within 1 cm depth. Laser pulses (685-900 nm) were used from a Ti:Sappire tunable laser.

Photoacoustic signals of the phantom excited by 687.5 nm pulses were obtained. Each of S/N was about 100 times larger compared with a PZT sensor (Olympus V309, 5 MHz, Φ 12.7 mm). A high-contrasted photoacoustic image was constructed by mapping these high S/N signals. This shows bright regions where MB and ICG were distributed. Frequency filtering of the high-contrast images to extract signals and exclude artifacts is in progress.

Two-color photoacoustic imaging was also achieved. The photoacoustic image of the phantom excited by 795 nm pulses shows strongly bright region due to ICG and does not show MB clearly. ICG molecules were extracted by excitation wavelength according to absorption spectra.

7564-106, Poster Session

In vivo dual-modality imaging of lymphatic systems using indocyanine green in rats: three-dimensional photoacoustic imaging and planar fluorescence imaging

C. Kim, K. H. Song, L. V. Wang, Washington Univ. in St. Louis (United States)

The purpose of this study is to map non-invasively sentinel lymph nodes (SLNs) and lymphatic vessels of rats in vivo using FDA-approved indocyanine green (ICG) and two non-ionizing imaging modalities: volumetric spectroscopic photoacoustic (PA) imaging, which measures optical absorption, and planar fluorescence imaging, which measures fluorescent emission. The spatial resolutions of both imaging techniques were compared at various imaging depths by layering additional biological tissue on top of the rats. SLNs and lymphatic vessels were clearly visible after a 0.2 ml-intradermal-injection of 1 mM ICG in both imaging systems. Moreover, the expansion and compression of lymphatic vessels were identified in both systems. Deeply positioned SLNs beneath additional biological tissue were clearly seen in PA images at high spatial resolution, whereas image degradation was obviously recognized in fluorescence images, owing to strong light scattering. Furthermore, SLNs were identified spectroscopically in PA images. These two modalities, when used together with ICG, have the potential to map SLNs in axillary staging and to study tumor metastasis in breast cancer patients.

7564-107, Poster Session

Monte Carlo simulations of acousto-optics with microbubbles

T. S. Leung, J. Honeysett, E. Stride, P. Beard, Univ. College London (United Kingdom)

Acousto-optic (AO) imaging is a promising technique with improved spatial resolution over optical imaging. The AO signal however is very weak which often hinders its use in biomedical applications. Various schemes have been proposed to enhance its detection including the use of intense acoustic bursts, parallel detection using a CCD camera, and a powerful long pulse laser. The aim of this work was to investigate the potential of using microbubbles to amplify the AO signals. Microbubbles are widely used contrast agents in ultrasound imaging to improve image contrast. A resonating microbubble produces varying optical scattering during an acoustic period due to changes in its surface area and internal refractive index. A resonating microbubble also radiates pressure leading to refractive index changes in the surrounding medium. Using Monte Carlo (MC) simulations, we investigate how these factors change the optical phase of a photon as it propagates through a turbid medium containing microbubbles. The scattering angle resulting from the collision between a photon and a microbubble is determined by the Mie scattering phase function. Parameters of the microbubble are derived using the Rayleigh-Plesset equation. We present the results in terms of the magnitude of the modulation depth of the AO signal as a function of the microbubble concentration, the ultrasound frequency, the ultrasound pressure, the optical absorption and scattering. The simulation results will be verified by experiments. The MC code has been implemented on a graphical processing unit (Nvidia) which is two to three orders of magnitude faster than its CPU-based counterpart.

7564-108, Poster Session

Photoacoustic tomography of pathological tissue in ex vivo mouse hearts

M. Holotta, Innsbruck Medical Univ. (Austria); H. Grossauer, Leopold-Franzens-Univ. Innsbruck (Austria); C. Kremser, P. Torbica, J. Völkl, R. Esterhammer, Innsbruck Medical Univ.



(Austria); R. Nuster, G. Paltauf, Karl-Franzens-Univ. Graz (Austria); W. Jaschke, Innsbruck Medical Univ. (Austria)

In the present study we evaluated the applicability of ex-vivo photoacoustic imaging (PAI) in organs of small animals. We used photoacoustic tomography (PAT) to visualize infarcted areas within mouse hearts and compared it to other imaging techniques (MRT, CT, US) and histological sections.

In order to induce ischemia an in-vivo ligation of the Ramus interventricularis anterior (RIVA, left anterior descending, LAD) was performed on three C57bl6 mice. Following a three day survival period the mice were sacrificed. The hearts were excised and immediately transferred into formaldehyde for conservation.

Various wavelengths in the visible and near infrared region (500nm - 1000nm) were tested to find the best representation of the ischemic regions. Samples were illuminated with nanosecond laser pulses delivered by a Nd:YAG pumped optical parametric oscillator. Ultrasound detection was achieved by an Mach-Zehnder interferometer working as an integrating line detector. For acoustic coupling the samples were located inside a water tank. The voxel data were computed from the measurement data by a Fourier domain based reconstruction algorithm, followed by a sequence of inverse Radon transforms.

Results clearly show the capability of PAI to detect pathological tissue and the possibility to produce three-dimensional images with resolutions well below 100 $\mu m.$ Different wavelengths allow the representation of structure inside an organ or on the surface even without contrast enhancing tracers.

7564-109, Poster Session

Ultrasound-modulated optical tomography using amplitude modulated ultrasound signals

R. Li, L. Song, D. Elson, C. Dunsby, R. Eckersley, M. Tang, Imperial College London (United Kingdom)

A significant challenge in current ultrasound modulated optical tomography (UOT) is the low signal to noise ratio of the optical measurement. This can be improved either by enhancing the sensitivity of the optical detection or by using a higher ultrasound pressure. When high pressure ultrasound is used, a significant acoustic radiation force (ARF) can be generated. This force may induce larger particle displacements, normally in the range of several micrometres, much higher than that due to ultrasonic vibration. In this study, the effect of a low frequency oscillating radiation force generated by an amplitude modulated ultrasound signal on the UOT signal was investigated. An experimental system was set up with a CW green laser (Excelsior 532) and CCD camera (QImaging Retiga EXi). Using a CCD-based speckle contrast detection scheme, signals were measured in both homogeneous and inhomogeneous phantoms. The apparatus was then used to investigate the effect of the acoustic radiation force on UOT image contrast. The oscillating acoustic radiation force was generated by using a functional generator to create an amplitude modulated ultrasound signal. The amplitude modulation frequency varied from 125 Hz to 1KHz. The results show large periodic variations of UOT signal contrast at the low modulation frequency. This is in contrast with unmodulated ultrasound excitation where the UOT signal contrast varies little over time. Further efforts are underway to confirm the role that radiation force plays in such periodic variations in UOT signal and to compare the system to conventional UOT system.

7564-110, Poster Session

Multiparametric optimization of multispectral opto-acoustic tomography for deep tissue imaging

N. C. Deliolanis, Helmholtz Zentrum München GmbH

(Germany) and Technische Univ. München (Germany); L. Ding, Helmholtz Zentrum München (Germany) and Technische Univ. München (Germany); A. Taruttis, A. Rosenthal, D. Razansky, V. Ntziachristos, Helmholtz Zentrum München GmbH (Germany) and Technische Univ. München (Germany)

Fluorescent reporter technologies (both fluorescent probes and proteins) have emerged as a very powerful imaging tool in biomedical research. They have been vastly exploited in established imaging modalities, such as fluorescence microscopy or epillumination imaging, though with limited penetration depth. Multispectral optoacoustic tomography (MSOT) is an emerging imaging technology that combines the advantage of the high optical contrast with the higher resolution of ultrasonic imaging. It can resolve fluorophore concentration in small animals situated in deep tissue by multispectral acquisition and processing of optoacoustic signals. The widely used NIR fluorescent probes, as well as the new generation of fluorescent proteins operating in the red and NIR part of the spectrum open exciting possibilities for deep-tissue imaging of fluorescent activities.

In this work, we study the optimum operating conditions of MSOT in imaging fluorescence activity in small animals. Optimization is performed against two parameters: First, we examine various fluorochromes/ fluorescent proteins and compare their optoacoustic signals when emanating from deep tissue. We also compare the significance of the various spectral measurements by means of principle component analysis in order to determine the optimal wavelengths and reduce the number of multispectral measurements. The study is based both in analytical calculations and in signal simulation and is verified by phantom experiments. It was found that the signal from the new infrared fluorescent protein is an order of magnitude brighter than the red ones and that reduction down to three wavelengths can accurately unmix and reconstruct the 3D distribution of fluorochromes in deep tissue.

7564-111, Poster Session

Photoacoustic quantification of the optical absorption cross-sections of gold nanostructures

C. Kim, E. C. Cho, Washington Univ. in St. Louis (United States); F. Zhou, Institute of Physics, CAS (China); C. M. Cobley, K. H. Song, J. Chen, Washington Univ. in St. Louis (United States); Z. Li, Institute of Physics, CAS (China); Y. Xia, L. V. Wang, Washington Univ. in St. Louis (United States)

This study demonstrates a method for measuring the optical absorption cross-sections (a) of Au-Ag nanocages and Au nanorods. The method is based on photoacoustic (PA) sensing where the detected signal is directly proportional to the absorption coefficient (µa) of the nanostructure. For each type of nanostructure, we first obtained μa from the PA signal by benchmarking against a linear calibration curve (PA signal vs. µa) derived from a set of methylene blue solutions with different concentrations. We then calculated a by dividing the µa by the corresponding concentration of the Au nanostructure. Additionally, we obtained the extinction cross-section (e, sum of absorption and scattering) from the extinction spectrum recorded using a conventional UV-vis-NIR spectrometer. From the measurements of a and e, we were able to easily derive both the absorption and scattering cross-sections for each type of gold nanostructure. The ratios of absorption to extinction obtained from experimental and theoretical approaches agreed well, demonstrating the potential use of this method in determining the optical absorption and scattering properties of gold nanostructures and other types of nanomaterials.



7564-112, Poster Session

Optimization of the acousto-optic signal detection in cylindrical and hemispherical geometries: from transmission to reflection

S. Gunadi, C. E. Elwell, P. C. Beard, T. S. Leung, Univ. College London (United Kingdom)

Ultrasonic waves had been used to tag multiple scattered photons in the region of interest within turbid media for tomographic imaging. In most experiments described in literature, the acousto-optic (AO) signal had been detected by aligning the optical detector to the optical source and performing measurements in transmission mode. However this setup was not viable for all clinical applications. Depending on the imaging targets (e.g. breasts, neonatal heads or small animals), the optical source, optical detector and ultrasound transducer assembly needed to adapt to a range of measurement geometries. This study aimed to optimize the detection of the AO signal in different geometries to accomodate various clinical scenarios. In our experiments, the optical detector was systematically repositioned at different angles relative to the optical source, from transmission to reflection modes. The focused ultrasound transducer was operating in tone burst mode so that a higher acoustic pressure could be used while keeping it within the safety limit. Two idealized anatomical geometries were considered, i.e. cylindrical and hemispherical. The optical detection setup consisted of a single photon counter and a digital correlator. The modulation depth was then derived from the normalized autocorrelation function and used to indicate the strength of the AO signal. The experimental results were further verified by Monte Carlo based computer simulations of optical and acoustic interactions.

7564-113, Poster Session

Characterization of a 2D sparse detector array for analysis via singular value decomposition

M. Roumeliotis, P. Ephrat, A. Immucci, J. J. Carson, Lawson Health Research Institute (Canada)

A photoacoustic tomography (PAT) approach, which employs an iterative reconstruction algorithm and incomplete measurement data, has been used in the reconstruction of simple objects [Ephrat, et al., JBO, 13(05), 054052]. The approach was made feasible by the use of a calibration scan of a PA point source through object space while recording the 3D spatio-temporal response of the detector array. Calibration scans have been completed in previous work [e.g. M. Roumeliotis et. al., SPIE BiOS, 7177 (2009)] in order to correct for acoustic wave interactions with transducers of finite dimension during image reconstruction. However, the previous scans were performed on a coarse grid of points within object space. The coarse grid spacing (5 mm) necessitated interpolation of calibration metrics during image reconstruction and was greater than the system resolution (~2 mm). To improve the imaging performance of PAT systems that utilize sparse array detection will require calibration on a finer grid spacing (~1 mm). This will also enable objective evaluation of the imaging system performance by singular value decomposition methods (see G. Chaudhary et. al. this volume). Here we report on a method that improves upon our previous gantry system, that enables the complete time series from 30 detectors to be recorded simultaneously at each point in object space with 1 mm step spacing. The calibration scan contains 17,576 individual scan points (as compared to 216 points reported previously). The method incorporates a Nd:YAG laser with 20 Hz pulse repetition rate for exciting the PA point source, a high-speed robotic arm (Epson model E2C351S-UL) for rapid and accurate translation of the PA source between grid locations, and USB2 communications between the data acquisition system and computer to facilitate rapid transfer of calibration time series data.

7564-114, Poster Session

Combined photoacoustic and magnetomotive ultrasound imaging

M. Qu, M. Mehrmohammadi, S. Mallidi, The Univ. of Texas at Austin (United States); P. Joshi, The Univ. of Texas Health Science Ctr. at Houston (United States); Y. Chen, K. Homan, S. Emelianov, The Univ. of Texas at Austin (United States)

Non-ionizing, cost-effective and portable ultrasound imaging is capable of excellent resolution at reasonable depth. However, contrast in ultrasound imaging is limited, and various ultrasound-based techniques such as integrated photoacoustic (PA) and ultrasound (US) imaging and magneto-motive ultrasound (MMUS) imaging have been developed. Photoacoustic imaging enhances ultrasound by visualizing optical absorption of either tissue or injected contrast agent (e.g., gold or silver nanoparticles). MMUS imaging enhances the sensitivity and specificity of ultrasound based on the detection of magnetic nanoparticles perturbed by an external magnetic field. This paper presents combined photoacoustic and magneto-motive ultrasound imaging - a fusion of complementary ultrasound-based techniques. To demonstrate the utility of PA/MMUS imaging, experiments were performed using a mixture of iron oxide (Fe3O4) nanoparticles and gold (Au) nanorods injected into a specimen of porcine tissue ex vivo. The sample was irradiated from the top using a tunable, nanosecond pulsed laser coupled with a fiber optical light delivery system. An external pulsed magnetic field was applied from the bottom of the sample. Using either a single element transducer or an array of ultrasound transducers, the spatially co-registered and temporally consecutive ultrasound, photoacoustic, and magneto-motive ultrasound images were obtained. The ultrasound image identified the morphological properties of the tissue. The photoacoustic and magnetomotive images showed the regions of nanoparticle accumulation based on optical absorption and the magnetic motion, respectively. Our results indicate that combined ultrasound, photoacoustic and magnetomotive ultrasound imaging can be used to detect magnetic/plasmonic nanoparticles with reliable resolution, sensitivity and contrast.

7564-115, Poster Session

Comparison of reconstruction algorithms for sparse-array detection photoacoustic tomography

G. Chaudhary, M. A. Anastasio, Illinois Institute of Technology (United States); M. Roumeliotis, J. J. L. Carson, The Univ. of Western Ontario (Canada)

A photoacoustic tomography (PAT) approach based on a sparse 2D array of detector elements and an iterative image reconstruction has been proposed [Ephrat, et al., JBO, 13(05), 054052], which opens the possibility for high frame-rate 3D PAT [Ephrat, et al. Optics Express, 16(26): 21570-21581 (2008)]. The efficacy of this PAT implementation is highly influenced by the choice of reconstruction algorithm. In recent years, a variety of new reconstruction algorithms have been proposed for medical image reconstruction that have been motivated by the emerging theory of compressed sensing. These algorithms have the potential to accurately reconstruct sparse objects from highly incomplete measurement data, and therefore may be highly suited for sparsearray PAT. In this context, a sparse object is one that is described by a relatively small number of voxel elements, such as typically arises in blood vessel imaging.

In this work, we investigate the use of a gradient projection-based iterative reconstruction algorithm for image reconstruction in sparse-array PAT. The algorithm seeks to minimize a L1-norm penalized least-squares cost function. By use of extensive computer-simulation studies and experimental data, the algorithm performance is compared to that of other traditional iterative reconstruction methods such as the algebraic reconstruction technique (ART) and penalized least-squares reconstruction algorithms employing quadratic penalties. Different noise



levels and sparse-array transducer configurations are considered. We demonstrate that, for sparse objects, the gradient projection algorithm outperforms these conventional algorithms in terms of image accuracy, and therefore may further improve the efficacy of sparse-array PAT.

7564-116, Poster Session

Evaluation of Her2 status using photoacoustic spectroscopic CT techniques

M. R. Shaffer, N. Cao, Purdue Univ. (United States); H. J. Chin-Sinex, M. S. Mendonca, Indiana Univ. School of Medicine (United States); R. Kruger, OptoSonics, Inc. (United States); K. Stantz, Purdue Univ. (United States)

Purpose: The purpose of this study is to evaluate Her2+ conjugated drug delivery utilizing photoacoustic spectroscopy techniques.

Introduction: Photoacoustic CT spectroscopy (PCT-S) has the potential to identify molecular properties of tumors and fluorescent dye conjugates, while overcoming the limited depth resolution associated with optical imaging modalities. Photoacoustics functions by pulsing laser light onto biological tissue, absorption occurs which in turn produces an acoustic wave due to the thermal volume expansion. The acoustic signal is proportional to the optical absorption properties of the tissue, which are wavelength dependent based on the molecular species within the tissue.

Material and Methods: An animal model bearing both Her2+ and Her2cell lines was developed for in vivo imaging of a herceptin receptor targeting drug conjugated with a LiCor IRDYE800. The drug conjugate is introduced intravenously (4mg/kg) then longitudinally imaged with the photoacoustic spectroscopic system and NIR optical imager over 1 week. Spectral deconvolution will allow for separating the signal from the drug conjugate from the surrounding tissue. Tumor to muscle ratios are plotted to assess tumor binding and uptake.

Results: The usage of photacoustic spectroscopy allows for the determination of in vivo tumor drug delivery. The Her2+ tumors showed significantly higher drug uptake than the control tumors with photoacoustic spectroscopy and NIR fluorescence values.

Conclusions: NIR conjugates used in conjunction with photacoustic spectroscopy allow for in vivo determination of Her2 status in tumors. This technique also allows for determining drug delivery within the tumor in relation to tumor vasculature and physiology.

7564-117, Poster Session

Fluorescence response to hydrostatic pressure using fluorophore-quencher labeled microbubbles

B. Yuan, P. M. Mehl, Y. Liu, The Catholic Univ. of America (United States)

Recently, microbubbles labeled with fluorophore and quenchers (F-Q microbubbles) have been proposed to increase the efficiency of ultrasound-modulated fluorescence. During our studies of characterizing the optical and acoustic properties of F-Q microbubbles, we found that the sensitivity of fluorescence to hydrostatic pressure can be significantly improved when adopting F-Q microbubbles. This result implies a possible technique to use F-Q microbubbles as a pressure sensor for in vivo hydrostatic pressure measurement in a tumor, such as tumor blood pressure and elevated interstitial fluid pressure. We present a system that is used to measure the response of fluorescence lifetime and intensity to the externally applied static pressure. The improvement of the sensitivity by adopting F-Q microbubbles to the applied pressure is experimentally quantified. A theoretical model for quantifying the sensitivity of F-Q microububbles is derived and the results show a pressure variation as low as 1 mm Hg may be resolved by using F-Q microbubbles. Important implications from the theoretical studies are provided.

7564-118, Poster Session

Biodegradable plasmonic nanoclusters as contrast agent for photoacoustic imaging

S. J. Yoon, J. Tam, J. Tam, A. Murthy, P. Joshi, S. Mallidi, K. Johnston, The Univ. of Texas at Austin (United States); K. Sokolov, The Univ. of Texas M.D. Anderson Cancer Ctr. (United States); S. Emelianov, The Univ. of Texas at Austin (United States)

Metallic nanoparticles have been widely used in a variety of imaging and therapeutic applications due to their unique optical properties in the visible and near-infrared (NIR) regions - for example, various plasmonic nanoparticles are considered for molecular photoacoustic imaging and photothermal therapy. However, there are concerns that these agents have not been proven to be safe in terms of accumulation and toxicity, because these nanoparticles are not biodegradable. In this paper, we investigate the feasibility of using biodegradable gold nanoclusters as a contrast agent for highly sensitive photoacoustic imaging. The size of biodegradable nanoclusters, consisting of sub-5 nm primary gold particles and polymer binder, was smaller than 100 nm. Due to plasmon coupling, these nanoclusters are characterized by a broad absorption spectrum extended to a near infrared (NIR) spectral range. First, the optical properties and the stability of the biodegradable nanoclusters were studied and compared to that of the gold nanorods. Aqueous solutions of nanoparticles were irradiated with 780 nm wavelength laser pulses of different (up to 30 mJ/cm2) energies, and the absorption spectra before and after the exposure were measured using a spectrophotometer. Furthermore, photoacoustic imaging of the tissue models containing inclusions with different concentration of nanoparticles was performed using a tunable pulsed laser system. The results indicate that the biodegradable nanoclusters of ultrasmall gold nanoparticles can be used as contrast agents in photoacoustic imaging.

7564-119, Poster Session

Characterization of sparse-array detection photoacoustic tomography using the singular value decomposition

G. Chaudhary, Illinois Institute of Technology (United States); M. Roumeliotis, P. Ephrat, R. Z. Stodilka, J. J. L. Carson, The Univ. of Western Ontario (Canada); M. A. Anastasio, Illinois Institute of Technology (United States)

Recently, a photoacoustic tomography (PAT) method that employs a sparse 2D array of detector elements [Ephrat, et al., JBO, 13(05), 054052] has been investigated and was employed to reconstruct images of simple objects from highly incomplete measurement data. However, there remains an important need to understand what type of object features can be reliable reconstructed from highly incomplete PAT measurement data. In this work, we numerically compute the singular value decomposition (SVD) of different system matrices that are relevant to implementations of sparse-array PAT. Our numerical analysis will be used to quantitatively characterize the null space of the PAT system matrix (i.e., imaging operator). For a given number and arrangement of measurement transducers, this will reveal the type of object features that can be reliably reconstructed as well as those that are invisible to the imaging system. By varying the number and arrangement of the transducers, we will investigate how the class of reconstructible object features changes. For each measurement configuration, the distribution of the singular values of the SVD will be analyzed to understand the numerical stability of the associated reconstruction problem. Our SVD analyses will reveal optimal system designs for reconstructing different types of objects. To our knowledge, this will represent the first application of the SVD to optimize a PAT imaging system.



7564-120, Poster Session

Monitor hemoglobin concentration and oxygen saturation in living mouse tail using Photoacoustic CT scanner

B. Liu, K. M. Stantz, Purdue Univ. (United States); R. Kruger, D. Reinecke, OptoSonics, Inc. (United States)

Purpose: The purpose of this study is to use PCT spectroscopy scanner to monitor the hemoglobin concentration and oxygen saturation change of living mouse by imaging the arteries and veins in a mouse tail.

Materials and Methods: The mouse tails of three mice were scanned at the isosbestic wavelength (796nm) to obtain their hemoglobin concentration. Immediately after the imaging, the mice were euthanized, their blood was extracted and the hemoglobin concentration was measured using a co-oximeter. A Monte Carlo algorithm and a forward projection routine were used to determine the photon and ultrasound attenuation based on the bone structure in the mouse tail and scanner geometry. After the correction, the hemoglobin concentrations calculated from the PCT images were compared with co-oximeter results. Next, five mice were immobilized and placed in the PCT scanner. Gas with different concentrations of oxygen was given to each mouse to change the oxygen saturation levels. PCT tail vessel spectroscopy scans were performed 15 minutes after the introduction of gas. The oxygen saturation values were then calculated to monitor the oxygen saturation change of mouse due to the various oxygen concentrations in the gas.

Results: The systematic error for hemoglobin concentration measurement was less than 5% after correction. Same correction technique was used for oxygen saturation calculation. After correction, the oxygen saturation level change matches the oxygen volume ratio change of the introduced gas.

Conclusion: This mouse tail experiment has shown that PCT-spectroscopy can be used to monitor the oxygen saturation status in living small animals.

7564-121, Poster Session

Ex vivo hemoglobin status study using photoacoustic computed tomography small animal scanner

B. Liu, K. M. Stantz, Purdue Univ. (United States); R. A. Kruger, D. R. Reinecke, OptoSonics, Inc. (United States)

Purpose: The purpose of this study is to calibrate the PCT scanner to quantify the hemoglobin status, concentration and oxygen saturation, utilizing a blood flow phantom.

Materials and Methods: India ink phantoms were used to validate the stability and reproducibility of the scanner over the near infrared range on a daily basis. A blood circulation system was designed and constructed to control the oxygen saturation and hemoglobin concentration of blood. As a part of the circulation system, a 1.1mm FEP tube was placed in the center of imaging tank of PCT scanner as the imaging object. Photoacoustic spectra (690-950 nm) was acquired for different concentrations of hemoglobin (CtHb) and oxygen saturation levels (0-100%). The CtHb and oxygen saturation values of each blood sample were obtained using co-oximeter. Monte Carlo simulations were performed to calculate the photon energy depositions in the phantom tube, taking into account photon losses in water, india ink, blood, as well as spectral variations in photon intensity and beam profile. A Kappa value which presents the energy transfer efficiency of hemoglobin molecule was calculated based on the PCT measurement and simulation result. The final SaO2 value of each blood sample was calculated based on the PCT spectrum and kappa value. These oxygen saturation results were compared with co-oximeter measurements to obtain the statistical and

Results and conclusion: The statistic and systematic errors of PCT blood measurements were within 5%. These calibration techniques were

used in hypoxia measurements in tumor s, as well as for endogenous biomarkers.

7564-122, Poster Session

In vivo multimodality photoacoustic tracking of prostate tumor growth using a window chamber

D. R. Bauer, R. Olaffson, The Univ. of Arizona (United States); L. G. Montilla, College of Optical Sciences, The Univ. of Arizona (United States); R. Witte, The Univ. of Arizona (United States)

The goal of this work was to establish an in vivo method for imaging the tumor microenvironment and monitoring tumor growth in mice using multiple modalities. Photoacoustic imaging, high-resolution pulse echo ultrasound and optical/fluorescent imaging were all used together to track growth and development of PC-3 prostate tumor cells injected into three mice implanted with a dorsal skin flap window chamber. The multiwavelength 3-D photoacoustic imaging system, consisting of a pulsed laser (5 nsec , 20 mJ, 20 Hz, tunable 680-1000nm) and 25 MHz focused ultrasound transducer, revealed near infrared absorbing regions, such as blood vessels. Simultaneously obtained pulse echo images provided details on the tumor microstructure and growth over three weeks with 100- m precision. Because the prostate cancer cell line was transfected with green fluorescing protein, fluorescent and optical images were also used for comparison and cross validation with the photoacoustic and pulse echo images. The size of the tumor of one representative mouse increased by 2.4 mm (lateral) and 0.95 mm (axial), as determined from pulse echo ultrasound. The photoacoustic images revealed an increase in blood vasculature near the border of the tumor coincident with tumor growth, suggesting the role of angiogenesis. Photoacoustic and pulse echo imaging are safe, noninvasive and complementary approaches. When combined, they may be ideal for diagnosing cancer and tracking effects of therapy. The mouse window chamber is an excellent model for developing ultrasound and photoacoustic techniques and potentially testing effects of drugs for cancer therapy.

7564-123, Poster Session

Real-Time Pulse Echo and Photoacoustic Imaging Using an Ultrasound Array and Inline Reflective Illumination

L. G. Montilla, College of Optical Sciences, The Univ. of Arizona (United States); R. Olafsson, R. Witte, The Univ. of Arizona (United States)

Photoacoustic imaging requires pulsed light to be absorbed by the area of interest and the induced acoustic waves detected by a distant ultrasound transducer. Difficulty exists in illuminating thick samples because light has to be directed around the transducer. Conventional photoacoustic imaging designs involve off-axis illumination or transillumination through the object in the direction of the transducer. Whereas transillumination works best with thin objects, off-axis illumination may not uniformly illuminate the region of interest. We present a method of efficiently delivering light around a linear array transducer similar to what has been described previously for a single element. The method exploits a prism to transmit light while reflecting the acoustic waves to and from the transducer. The illumination is symmetrical along each axis of the array, producing a pattern similar to the acoustic beam profile of the transducer. With this arrangement, we demonstrate realtime pulse echo and photoacoustic imaging integrated with a linear array (L10-5) and clinical ultrasound scanner (Zonare Medical Systems). To test the device, photoacoustic and pulse echo images were acquired of 0.5 mm graphite rods submerged in water. The measured pulse echo spatial dimensions (-6dB) with the device was .40 mm x .45 mm (axial x lateral). As this is close to the nominal spatial dimensions of .35 mm x



.45 mm, the introduction of the prism did not degrade the image quality significantly. A system with these capabilities may not only facilitate small animal photoacoustic imaging, but it may also promote transition of this modality into clinical practice.

7564-124, Poster Session

In vivo detection of amyloid-beta deposits by optical-resolution photoacoustic microscopy

S. Hu, P. Yan, K. Maslov, J. Lee, L. V. Wang, Washington Univ. in St. Louis (United States)

Advances in high-resolution imaging have permitted microscopic observations within the brains of living animals. Applied to Alzheimer's disease (AD) mouse models, multiphoton microscopy has opened a new window to study the real-time appearance and growth of amyloid plaques. However, available multiphoton excitation sources are expensive. Here, we report a cost-effective alternative technologyoptical-resolution photoacoustic microscopy (OR-PAM)-for in vivo imaging of amyloid plaques in a transgenic AD mouse model. In vitro and in vivo validations using conventional fluorescence microscopy and multiphoton microscopy show that OR-PAM has sufficient sensitivity and spatial resolution to identify amyloid plaques in living brains. In addition, with dual-wavelength OR-PAM, the three-dimensional morphology of amyloid plaques and the surrounding microvasculature are imaged simultaneously through a cranial window.

7564-125, Poster Session

In vivo photoacoustic microscopy of anterior ocular segment in small animals

B. Rao, S. Hu, L. Li, K. Maslov, L. Wang, Washington Univ. at St. Louis (United States)

Imaging modalities such as optical coherence tomography (OCT), fluorescein iris angiography (FIA), indocyanine green angiography (ICGA) and high frequency ultrasound microscopy (UBM) are used in eye clinic for diagnosing anterior segment of eye. In practice, both OCT and UBM can provide anatomical information of anterior segment of eye while FIA and ICGA can supply complement iris microvasculature information. A non-invasive, endogenous imaging modality is preferable for the monitoring of hemodynamics of iris microvasculature in normal and diseased conditions. We investigated the in vivo anterior ocular segment imaging with photo-acoustic microscopy (PAM) in mouse models. We demonstrated the unique advantage of combining high three-dimensional spatial resolution (5 µm x 5 µm x 15 µm) and endogenous contrast that is not available from both FIA and ICGA. Finer capillary network is observed from speckle-free PAM images comparing to OCT.

7564-126, Poster Session

In vivo functional photoacoustic microimaging of the electrically stimulated rat brain with multiwavelengths

L. Liao, National Chiao Tung Univ. (Taiwan); M. Li, National Tsing Hua Univ. (Taiwan); H. Lai, Y. Chen, P. C. Chao, National Chiao Tung Univ. (Taiwan); P. Wang, National Tsing Hua Univ. (Taiwan)

In this study, we report on using multi-wavelength photoacoustic microscopy to image hemodynamic changes of total hemoglobin concentration (HbT) (i.e., blood volume) and oxygenation (SO2) in rat brain cortex vessels with electrical stimulation. Electrical stimulation of the rat left forelimb was applied to evoke changes in vascular dynamics of the rat somatosensory cortex. The applied current pulses were with a pulse frequency of 3 Hz, pulse duration of 0.2 ms, and

pulse amplitude of 2, 5, and 10 mA, respectively. HbT changes were probed by images acquired at 570 nm, a hemoglobin isosbestic point while SO2 changes were imaged by those acquired at 560 nm or 600 nm and their derivatives, which were normalized to those with 570-nm wavelength. Correlation between the electrical stimulation paradigm and images acquired at 570, 560, and 600 nm in contralateral and ipsilateral vasculature was statistically analyzed, showing that the HbT and SO2 changes revealed by multi-wavelength photoacoustic images spatially correlated with contralateral vasculature. The corresponding changes in multi-wavelength photoacoustic images to stimulation with different current amplitude were also analyzed.

7564-127, Poster Session

Photoacoustic characterization of human ovarian tissue

A. Aguirre, Y. Ardeshirpour, Univ. of Connecticut (United States); M. M. Sanders, M. Brewer, Univ. of Connecticut Health Ctr. (United States); Q. Zhu, Univ. of Connecticut (United States)

Ovarian cancer has a five-year survival rate of only 30%, due to the fact that current imaging techniques are not capable of detecting ovarian cancer early. Hence, most diagnoses occur in later stages when the cancer has already become widely metastatic. On the other hand, while the majority of women with a detectable ultrasound abnormality do not harbor a cancer, they all undergo unnecessary oophorectomy. Therefore, new imaging techniques are needed for improving the specificity of ovarian cancer detection and characterization.

Last year we reported, for the first time, characterization results of normal ovarian tissue from pigs using a 3D co-registered ultrasound and photoacoustic imaging system. We demonstrated that photoacoustic imaging is capable of detecting highly vascularized structures otherwise not visible by ultrasound.

We have extended the study to ex-vivo human ovarian tissue. A total of twelve human ovaries, including normal and diseased, have been imaged to date. A new parameter from RF data has been derived to compare the photoacoustic imaging results from all the ovaries. The results show higher optical absorption for abnormal and premenopausal ovaries than for postmenopausal ones.

To estimate the quantitative optical absorption properties of the ovaries, additional ultrasound-guided diffuse optical tomography images were acquired. On average ovaries from premenopausal women show higher optical absorption coefficient than those from postmenopausal women. These results are comparable to photoacoustic results. However, local absorption changes from abnormal postmenopausal ovaries cannot be detected by diffused light due to its low resolution. Thus, our preliminary results suggest photoacoustic imaging has a potential to detect early ovarian cancer.

7564-128, Poster Session

Photoacoustic tomography of foreign bodies in soft biological tissue

X. Cai, C. Kim, M. Pramanik, L. V. Wang, Washington Univ. in St. Louis (United States)

Ultrasound imaging suffers from poor sensitivity (~50%) and specificity of detecting small foreign bodies. Hence, alternative imaging methods are needed. Photoacoustic (PA) imaging takes advantage of strong optical absorption contrast and high ultrasonic resolution. A PA imaging system was employed to detect foreign bodies in biological tissues. To achieve deep penetration, we used near-infrared light and a 5-MHz spherically focused ultrasonic transducer. PA images were obtained from objects (glass, wood, cloth, plastic, and metal) embedded in chicken tissue. The location and size of the targets from the PA images agreed well with those of actual samples. Objects were imaged more than 1 cm deep. Spectroscopic PA imaging was performed on the objects. These results



suggest PA imaging can potentially be a useful intraoperative imaging tool to identify foreign bodies and discriminate viable tissues in wounded patients.

7564-129, Poster Session

Optoacoustic visualization of HIFU-induced thermal lesions in live tissue

P. V. Chitnis, Riverside Research Institute (United States); H. Brecht, R. Su, A. A. Oraevsky, Fairway Medical Technologies, Inc. (United States)

A 3-D optoacoustic imaging system was used to visualize thermal lesions produced in vivo using high intensity focused ultrasound (HIFU). A 7.5 MHz surgical, focused transducer with a radius of curvature of 35 mm and an aperture diameter of 23 mm was used to generate HIFU. A pulsed laser which could operate 760 nm and 1064 nm was used to illuminate the specimens of study (excised tissue or mice) using a bifurcated fiber bundle resulting in two wide beams of light. The tomographic images were obtained while the specimens were rotated within a sphere outlined by a concave arc-shaped array of 64 piezo-composite transducers. These images were then combined to construct 3-D volume images (0.5 mm voxel) which were acquired before and after HIFU exposure. Images of excised tissue at both wavelengths and in vivo optoacoustic images acquired using 760 nm light did not adequately image HIFU-induced lesion; however, the images of mice acquired with the 1064 nm light provided visualization of HIFU-induced thermal lesion. In this case, the HIFU lesion was indicated by the low optical contrast associated with the reduction in the concentration of oxygenated blood in the necrotic tissue. These results demonstrate the ability of optoacoustic imaging to guide HIFU therapy and monitor the progress of the treatment.

7564-130, Poster Session

Effect of ultrasound transducer color on light fluence distribution in photoacoustic imaging

B. Tavakoli, P. D. Kumavor, A. Aguirre, Q. Zhu, Univ. of Connecticut (United States)

The front-surface color of ultrasound transducers used for photoacoustic imaging imposes different boundary conditions on the light fluence distribution. Additionally, many endoscopic, intravascular, and transvaginal clinical applications require light delivery through single or multiple optical fiber configurations in the reflection mode. Thus, depending on the boundary color of the transducer used, the light fluence distribution is different for each source fiber configuration. Understanding and characterizing the boundary effects on fluence distribution is critical for optimizing the light illumination and therefore signal-to-noise ratio of photoacoustic waves.

We have evaluated the effects of the boundary conditions imposed by different front-face colors (gray, white, red, and black) of the ultrasound transducers on the light fluence distributions in reflection mode using both simulations and experiments. The simulations were done using Monte Carlo (MC) technique. For the experiments a Ti:Sapphire pulsed laser coupled into a 1x7 optical power splitter made by OFS Inc. was used. The seven output arms of the splitter formed the light source fibers. The spatial light fluence distribution was measured inside the turbid medium by translating a 0.5 numerical aperture optical fiber coupled to a power meter.

Both simulation and experiments have demonstrated that the spatial light fluence distribution with the white probe boundary is more uniform and is 1.6 times higher in intensity than that of the other probes. The fluence is lowest with the black probe boundary due to the absorption of the photons by the probe. Angled fibers improve the fluence distribution at the lower depths compared to that obtained with normal incident source fibers.

7564-131, Poster Session

Background reduction in optoacoustic imaging based on tissue deformation: Quantitative analysis

M. Jaeger, S. Preisser, M. Frenz, Univ. Bern (Switzerland)

We previously proposed digital processing of images obtained from a gradually deformed tissue sample for reduction of echo and bulk tissue background in deep optoacoustic imaging. Optoacoustic signals and background are differently affected when the investigated tissue is gradually deformed, which enables background identification using digital processing. In displacement-compensated averaging (DCA), a local tissue displacement map is determined via speckle tracking in simultaneously acquired pulse-echo images. The optoacoustic images are then compensated for the local tissue displacement. In that way optoacoustic sources are highly correlated throughout the compensated image series, while background is decorrelated and can therefore be reduced by averaging. We quantitatively access the potential improvement in image contrast using DCA or related, improved processing methods. Based on simulations, we focus on the influence of image decorrelation and the accuracy of the speckle tracking algorithm on one hand, and on the influence of the sample geometry on the other

7564-144. Poster Session

Photothermoacoustic imaging comparison of pulsed laser and frequency-domain (radar) modalities: signal-to-noise ratio, contrast, and resolution enhancement using nonlinear chirp modulation

S. A. Telenkov, B. Lashkari, A. Mandelis, Univ. of Toronto (Canada)

The present study compares experimentally the two photoacoustic imaging modalities (pulsed laser and chirped (photothermoacoustic radar or sonar) with respect to the maximum imaging depth achieved in scattering media with optical properties similar to biological tissues. The obtained results demonstrate the capabilities of both techniques and can be used in specific PTA imaging applications for development of image reconstruction algorithms aimed at maximizing system performance. Distinct advantages of the PTA radar include superior signal-to-noise ratio and efficiently suppressed baselines underscoring the high potential of this technique for depth-selective imaging of deep lying tissue chromophores. Our results demonstrate that submillimeter depth-selective photoacoustic imaging can be achieved without nanosecond pulsed laser systems by appropriate modulation of a continuous laser source and a signal processing algorithm adapted to specific parameters of the photoacoustic response.

Furthermore, (PTA) imaging contrast is compared with the pulsed laser method. The application of nonlinear frequency modulation instead of the standard linear frequency chirps was investigated and its effects on signal to noise ratio (SNR), contrast and image resolution will be discussed. In addition to the image produced by the amplitude of the cross-correlation between input and detected signals, the phase of the correlation signal was used as a filter of the PTA amplitude combined with linear or nonlinear frequency chirps. It was demonstrated that the phase signal can effectively filter the amplitude image and greatly improve its contrast. The experimental results with a high-frequency transducer exhibit more than 10 and 8 times contrast enhancement using nonlinear and linear chirps, respectively. Concomitant improvements in SNR and image resolution were also observed.



7564-145, Poster Session

Wavelength-modulated differential photothermal radiometry for non-invasive blood glucose detection

X. Guo, A. Mandelis, A. Matvienko, K. Sivagurunathan, B. Zinman, Univ. of Toronto (Canada)

No abstract available.

7564-59, Session 9

Molecular imaging of NPR-1 using photoacoustic spectroscopy

K. M. Stantz, Purdue Univ. (United States); M. Cao, Indiana Univ. School of Medicine (United States); B. Liu, Purdue Univ. (United States); R. Kruger, OptoSonics, Inc (United States); K. D. Miller, Indiana Univ. School of Medicine (United States); L. Guo, Eli Lilly and Co. (United States)

Purpose: Our purpose is to develop and test a molecular probe that can detect the expression of neutropilin-1 receptor (NPR-1) in vivo using fluorescence imaging and photoacoustic spectroscopy.

Introduction: NPR-1 is expressed on endothelial cells and some breast cancer cells, and binds to vascular endothelial growth factor VEGF165, a growth factor associated with pathological tumor angiogenesis. This receptor is co-expressed with VEGFR2 and shown to enhance the binding of VEGF165; therefore, it has the potential to be used as a marker of angiogenic activity and targeted for therapy.

Material and Methods: A peptide specific to NPR-1 receptor was synthesized and conjugated to a NIR fluorochrome (IRDye800CW) and was intravenously injected into mice with breast tumors (MCF7VEGF). Probe kinetics was monitored in vivo via near infrared fluorescence (NIRF) within an optical imager for up to 72 hours within the tumor and compared to other organs (liver, muscle) for binding specificity. A multivariate fitting algorithm was used to spectrally deconvolve the IRDye800CW from endogenous hemoglobin signature (hemoglobin concentration and oxygen saturation).

Results: Dynamics of the NIR fluorescence signal within the first hour after injection indicates specific binding compared to muscle, with an average tumor-to-muscle ration of 2.00 (+/- 0.27). Spectral analysis clearly indentified the presence of the NPR-1 probe. Based on calibration data, the average tumor concentration from both NIRF and PCT-S was measured to be ~200-250nM.

Conclusion: These preliminary results show the capability of PCT to image an exogenous probe in vivo in addition to its hemoglobin state.

7564-60, Session 9

Multiwavelength approach to quantitative photoacoustic molecular imaging (PMI) using the Cramer-Rao lower bound

D. Modgil, P. J. La Riviere, The Univ. of Chicago (United States)

Several recent papers have addressed the issue of estimating chromophore concentration in photoacoustic imaging using a multi-wavelength acquisition strategy. The specific set of wavelengths chosen can, of course, influence the qualitative and quantitative accuracy of the resulting images. Previous work seeking to optimize wavelengths has generally considered only the wavelength dependence of the chromophore extinction coefficients. But the distribution of the incident light is also wavelength dependent and will influence the strength of the signal received from the various chromophores. In this paper, we propose a framework for optimizing wavelength choice considering both of these factors. The framework entails quantifying the estimation

accuracy of chromophore concentration using the so-called Cramer-Rao lower bound (CRLB). This lower bound on achievable variance estimate can be evaluated numerically for different wavelengths using a model of light distribution along with the variation of the extinction coefficients and scattering coefficients with wavelength. The set of wavelengths that gives the smallest CRLB for a chromophore of interest will be considered optimal. Building on work by Razansky et al., we show that the expression for CRLB can be derived analytically for the case of a single chromophore contained in a sphere within a spherical background solution. We also show that this approach can be readily extended numerically to optimizing wavelength choice for the estimation of concentrations of multiple chromophores and for other geometries.

7564-61, Session 9

Stability of molecular therapeutic agents for noninvasive photoacoustic and ultrasound image-guided photothermal therapy

Y. Chen, P. P. Joshi, S. Kim, K. Homan, W. Frey, The Univ. of Texas at Austin (United States); K. Sokolov, The Univ. of Texas at Austin (United States) and The Univ. of Texas M.D. Anderson Cancer Ctr. (United States); S. Emelianov, The Univ. of Texas at Austin (United States)

Image-guided molecular photothermal therapy using targeted gold nanoparticles acting as photoabsorbers can be used to noninvasively treat various medical conditions, including cancer. Among different types of gold nanoparticles, gold nanorods are attractive candidates for both photothermal therapy and photoacoustic imaging due to their high and tunable optical absorption cross-section. However, the nanorods are not thermodynamically stable - under laser exposure, the nanorods can easily transform to spheres thus changing their desired optical properties. In this study, we investigated the stability of gold nanorods. Specifically, we studied the stability of the nanorods under heat generated by the nanoparticle absorption and that of the chemical fractionalization under local heat at the particle surface. Various surfactants and surface coatings were investigated. For example, we synthesized gold-silica core-shell nanorods. The silica surface was then modified to contain amine groups for further bioconjugation with antibody. First, the thermal stability of nanorods was studied using the temperature controlled transmission electron microscopy (T-TEM). Furthermore, optical absorbance of the nanorods in aqueous solution under different ambient temperatures (25 to 50°C) was measured using a spectrophotometer. The samples were also exposed to up to 200 pulses (750 nm wavelength, 5 ns pulse duration, 10 Hz repetition rate) of variable fluences (0 to 20 mJ/cm2) and optical absorbance was measured before and after the exposure. Finally, the targeting stability of the nanorods was studied using normal and cancer cell cultures and tissue models. The results of our study suggest that gold-silica core-shell nanorods are good candidates for Image-guided molecular photothermal therapy.

7564-62, Session 9

Fluorescent protein imaging with multispectral optoacoustic tomography

D. Razansky, Technische Univ. München (Germany) and Helmholtz Zentrum München GmbH (Germany); M. Distel, Helmholtz Zentrum München GmbH (Germany); C. Vinegoni, Harvard Medical School (United States); R. Koester, Helmholtz Zentrum München (Germany); V. Ntziachristos, Technische Univ. München (Germany) and Helmholtz Zentrum München GmbH (Germany)

The ability to optically interrogate and visualize intact organisms is of high importance due to the great variety of intrinsic optical contrast and exogenous molecular probes available in the visible and near-



infrared spectra. In this work, a selective-plane illumination multispectral optoacoustic tomography technique was developed and applied for high-resolution whole-body visualization of intact optically diffusive organisms whose sizes may vary from sub-millimeter up to a centimeter range and more. The size of many relevant biological samples and model organisms, e.g. developing insects, small animals and their extremities, animal and fish embryos as well as of some adult organisms, lie in this range. However, due to the high optical diffusion and relatively small size, they are not accessible by existing optical microscopy nor by diffusion-based optical tomography methods. Although it is known that optoacoustic imaging is mostly sensitive to hemoglobin, we achieved good contrast also from other biological tissues like fat, bones, and other internal structures. By applying the multispectral imaging methodology, we further demonstrate that other molecularly-relevant information related to biodistribution and targeting of fluorescent biomarkers and fluorescent proteins, e.g. gene expression, morphogenesis, decease progression and many other targeted mechanisms, could now be visualized in whole bodies of opaque living objects with high sensitivity and spatial resolution close to a single cell dimensions.

7564-63, Session 9

Design and synthesis of new gold nanoparticles for enhanced photoacoustic response

C. Wei, National Taiwan Univ. (Taiwan); C. Poe, C. Chen, National Chung-Cheng Univ. (Taiwan); C. C. Wang, National Chung Cheng Univ. (Taiwan); P. Li, National Taiwan Univ. (Taiwan)

In this study, we aimed at design and synthesis of a new type of gold nanorods (AuNRs) for enhanced photoacoustic response. The key idea is to create nanostructure allowing anisotropic heat release. To achieve this, a layer of SiO2 was coated along the longer axis of the gold nanorods, but not covered both ends (AuNR@nu-SiO2). Photoacoustic measurements were conducted. The laser has a wavelength of 900 nm corresponding to the maximal absorption wavelength of test samples. A transducer with a center frequency of 20 MHz and focal depth of 10 mm detected the resulted acoustic signal. Each sample was measured for three times and the mean intensity clearly showed an increase in intensity about 5 dB was observed for AuNR@nu-SiO2, compared to bare AuNR. These particles are anticipated to enhance the contrast of photoacoustic imaging as well as to assist several previous proposed in vivo studies involved with cancer researches. It also implies that less toxicity in vivo can be expected.

7564-64. Session 9

In vitro imaging of a protease-sensitive optoacoustic molecular imaging agent

A. Green, The Univ. of Chicago (United States); Z. Xie, H. F. Zhang, Univ. of Wisconsin-Milwaukee (United States); P. J. La Riviere, The Univ. of Chicago (United States)

We have been developing a protease-sensitive molecular imaging agent for optoacoustic tomography that shifts its absorption peak upon cleavage by a protease of interest. This allows its uncleaved and cleaved forms to be detected and distinguished through a mutiwavelength optoacoustic imaging strategy. We have now performed preliminary in vitro optoacoustic microscopy imaging of the probe to characterize its spectral and optoacoustic properties and found that the absorption spectra of the uncleaved and cleaved versions of the probe are readily distinguishable.

Proteases are protein-cleaving proteins known to be overactive in a number of pathologies, including cancers and vascular disease. Protease-sensitive molecules based on fluorescence have been developed previously in the context of diffuse optical imaging, but diffuse optical imaging has limited resolution and sensitivity at depth in tissue.

We have been working to develop an analog more suitable for optoacoustics, which could overcome these limitations and be more readily translatable into human use. The molecule we have synthesized is based on chlorophyll a, a strong naturally occurring chromophore that absorbs strongly at 668 nm in its monomer form and at longer wavelengths when it aggregates. The current version of the molecule involves a chlorophyll molecule attached to a peptide sequence that is the target for a protease of interest. When the molecule is whole it tends to aggregate with chlorophylls stacking in dimmer and trimers. After cleavage, aggregation is disrupted, and the chlorophyll tends to remain free as a monomer, producing a markedly different absorption spectrum. A version based on bacteriochlorophyll a, which absorbs further in the near infrared, is also under development.

7564-65, Session 9

Multi-wavelength photoacoustic imaging for monitoring nano-molecular interactions invivo

S. Mallidi, A. Karpiouk, S. Kim, P. Joshi, K. Sokolov, S. Emelianov, The Univ. of Texas at Austin (United States)

Gold nanoparticles are excellent photoacoustic contrast agents because of their absorption properties at visible and near-infrared wavelengths. When gold nanoparticles are functionalized to specifically target cancer biomarkers such as epidermal growth factor receptor (EGFR), they undergo molecular specific aggregation leading to plasmon resonance coupling effect. The phenomena results in an optical red-shift of the plasmon resonance frequency of gold nanoparticles and an increase of optical absorption in the red region. In this study, we evaluated the feasibility of a multi-wavelength photoacoustic imaging technique in detecting plasmon resonance coupling phenomenon of gold nanoparticles in subcutaneous tumor xenografts in-vivo.

To grow the subcutaneous tumor, human epithelial cancer cells (A431 cells that overexpress EGFR) were implanted in immunodeficient mice. Either EGFR targeted or PEGylated gold nanospheres (20 nm diameter) were intravenously injected via the tail vein. To observe the accumulation and molecular interactions of gold nanoparticles in the tumor, 3-D ultrasound and photoacoustic imaging of the tumor region was performed at various time points.

The increase in the optical absorption of the tumor tissue in the near infrared optical region due to molecular interactions of EGFR targeted gold nanoparticles with A431 tumor cells was observed by analyzing the multi-wavelength (680-800 nm) photoacoustic images. On the other hand, PEGylated gold nanoparticles also accumulated in the tumor due to enhanced permeation and retention effect but did not enhance contrast in photoacoustic images since there were no interaction with tumor cells and, therefore, no plasmon resonance coupling. In conclusion, the multi-wavelength photoacoustic imaging technique together with EGFR targeted gold nanospheres has the ability to monitor fine molecular interactions that can aid in early detection and treatment of cancer.

7564-66, Session 9

Molecular photoacoustic imaging using targeted gold nanoparticles as a contrast agent

C. Kim, E. C. Cho, J. Chen, K. H. Song, L. Au, C. P. Favazza, Q. Zhang, C. M. Cobley, Y. Xia, L. V. Wang, Washington Univ. in St. Louis (United States)

Gold nanoparticles have received much attention due to their potential diagnostic and therapeutic applications. Gold nanoparticles are attractive to many biomedical applications because of biocompatibility, easily modifiable surfaces for targeting, lack of heavy metal toxicity, wide range of sizes (35-100 nm), tunable plasmonic resonance peak, encapsulated



site-specific drug delivery, and strong optical absorption in the near-infrared regime. Specifically due to their strong optical absorption, gold nanoparticles have been used as a contrast agent for molecular photoacoustic (PA) imaging of tumor. The plasmonic resonance peak of the gold nanoparticles was tuned to the near-infrared regime and the ratio of the absorption cross-section to the extinction cross-section was approximately ~80%, measured by PA sensing. An in-vitro study showed the uptake of targeted gold nanoparticles in a tumor cell was significantly more than that of untargeted (PEGylated) gold nanoparticles. Our in- vivo imaging experiments revealed a statistically significant enhancement of PA signals within tumors using targeted gold nanoparticles as compared to ones using untargeted nanoparticles. These results strongly suggest PA imaging paired with targeted gold nanoparticles is a promising diagnostic tool for early cancer detection.

7564-67, Session 10

Real-time optoacoustic imaging of breast cancer using an interleaved two laser imaging system coregistered with ultrasound

M. P. Fronheiser, Seno Medical Instruments, Inc. (United States); S. A. Ermilov, Fairway Medical Technologies (United States); H. Brecht, R. Su, A. Conjusteau, K. Mehta, Fairway Medical Technologies, Inc. (United States); P. Otto, The Univ. of Texas Health Science Ctr. at Houston (United States); A. A. Oraevsky, Fairway Medical Technologies, Inc. (United States)

We present results from a real-time interleaved two laser optoacoustic (OA) imaging system coregistered with ultrasound for purposes of breast cancer detection. The system utilizes a standard linear ultrasonic transducer array, which has been modified to include two parallel rectangular optical bundles, to operate in both ultrasonic and optoacoustic modes. In optoacoustic mode, we can display images from two optical wavelengths (755 nm and 1064 nm) simultaneously at a maximum rate of 20 Hz. The real-time aspect of the system permits probe manipulation to identify regions of high absorption within and near the lesion. Results collected during a clinical study have shown an ability to co-register regions of high absorption seen in OA images with ultrasonic images collected at same location with the dual modality probe. The dual wavelength results are compared to pathology results thereby associating tumor angiogenesis with optoacoustic images in an attempt to perform qualitative differentiation based upon OA image brightness at two laser wavelengths within the breast lesion correlated with the shape of the tumor as observed with ultrasound.

7564-68, Session 10

Fast-scanning ultrasonic-photoacoustic biomicroscope: in vivo performance

T. Harrison, H. Lu, J. Ranasinghesagara, R. J. Zemp, Univ. of Alberta (Canada)

The combination of ultrasonic and photoacoustic imaging modalities has yet to be realized in the high-frequency regime (>20MHz) where spatial resolution may permit visualization of the microvasculature. In this work, we characterize the in-vivo performance of a custom ultrasound-photoacoustic B-scanning imaging system. This system utilizes a combined ultrasound/photoacoustic probe attached to a voice-coil capable of approximately 1cm lateral translation at a rate of up to 15Hz. The probe is comprised of a 25MHz ultrasound transducer, configured confocally with a conical mirror-based dark-field laser delivery system. The fast-scanning mode permits real-time ultrasound imaging. The imaging speed of the photoacoustic mode is limited by the repetition rate of the 532nm laser (up to 100Hz). Signals from the transducer are amplified by a 39dB preamp with an additional time-gain compensation stage of up to 24dB. Control of the system is through a digital input-output PCI card, which acts as a pulse-sequencer and permits software

control of time-gain compensation. This setup permits interlaced pulse sequences for excellent registration of ultrasonic and photoacoustic data, as well as separate time-gain compensation curves for photoacoustic and ultrasound modalities. We have managed to achieve a lateral resolution of 155 microns and an axial resolution of 40 microns. The system is used to visualize the finger and palm of a hand to almost 1cm ultrasound depths and multiple millimeter-scale photoacoustic depths. Photoacoustic images are overlaid on the ultrasound images for simultaneous visualization of the microvasculature and surrounding tissue.

7564-69, Session 10

Tissue temperature monitoring using thermoacoustic and photoacoustic techniques

M. Pramanik, Washington Univ. in St. Louis (United States); T. N. Erpelding, L. Jankovic, Philips Research North America (United States); L. V. Wang, Washington Univ. in St. Louis (United States)

During thermotherapy it is necessary to monitor the temperature distribution in tissues for the safe deposition of heat energy in surrounding healthy tissue and efficient destruction of tumor and abnormal cells. Thus, real-time temperature monitoring with high spatial resolution (~1 mm) and high temperature sensitivity (1oC or better) is needed. A temperature sensing technique using thermoacoustic and photoacoustic measurements has been explored in this study. Using a tissue phantom, this noninvasive method has been demonstrated to have high temporal resolution and temperature sensitivity. Because both photoacoustic and thermoacoustic signal amplitudes depend on the temperature of the source object, the signal amplitudes can be used to monitor the temperature. The signal is proportional to the dimensionless Grueneisen parameter of the object, which in turn varies with the temperature of the object. With a single element ultrasonic transducer, a temperature sensitivity of 0.15oC was obtained at a temporal resolution as short as 2 sec with 20 signal averages. Two dimensional crosssectional images were obtained for thermal imaging using a clinical Philips ultrasound imaging system (iU22) adapted for thermoacoustic and photoacoustic tomography. The deep tissue imaging capability of this technique can potentially lead us to in vivo temperature monitoring with high temperature sensitivity.

7564-70, Session 10

Fast-scanning reflection-mode integrated optical-coherence and photoacoustic microscopy

L. Li, B. Rao, K. Maslov, L. V. Wang, Washington Univ. in St. Louis (United States)

We previously demonstrated that multimodal microscopy combining photoacoustic microscopy and optical coherence tomography can provide comprehensive insight into biological tissue at μm -level resolution by exploiting both optical absorption and scattering contrasts. Recently, we have developed a second-generation integrated photoacoustic and optical-coherence microscope, which can potentially be adapted for clinical applications. In this new system, we can perform photoacoustic and optical-coherence imaging simultaneously at a speed faster than 5,000 A-lines per second with real-time on-screen display. Also, both modalities now work in reflection mode instead of transmission mode, allowing easy access to various anatomical locations of interest. The imaging capabilities of the current system have been demonstrated in small animals.



7564-71, Session 10

Simultaneous photo- and thermoacoustic CT of mouse anatomy

R. A. Kruger, R. B. Lam, S. P. DelRio, D. R. Reinecke, OptoSonics, Inc. (United States)

We have constructed and tested a prototype test bed that allows us to form 3D, photoacoustic CT images using near-infrared (NIR) irradiation (700 - 900 nm) and 3D, thermoacoustic CT images using microwave irradiation (434 MHz). The device utilizes a vertically oriented, cylindrical array to capture the photo- and thermoacoustic data. Because the same detector array is used to form both types of images, both 3D images can be co-registered exactly.

NIR radiation is provided by a tunable, NIR laser coupled to a 1:2 fiber optic bundle. Microwave energy is delivered to the imaging volume via a pair of linearly polarized, horn antennae. Data are acquired as the object being imaged is rotated about its vertical axis through 96 discrete angles spanning 360°. Microwave and NIR data are acquired angle-by-angle. Image acquisition for both data sets takes 5 minutes per wavelength and angle of polarization.

The photoacoustic and thermoacoustic images formed in this way reveal complimentary anatomic information. Images of biologic tissue (beefsteak) and mouse anatomy are presented to illustrate the complementary nature of the images. The thermoacoustic images differentiate among muscle, fat and bone; whereas the photoacoustic images reveal the hemoglobin distribution, which is localized predominantly in the vascular space.

7564-72, Session 10

Integrated photoacoustic and oblique incidence diffuse reflectance for quantitative optical sensing in turbid media

J. C. Ranasinghesagara, R. J. Zemp, Univ. of Alberta (Canada)

The photoacoustic signal of an optical absorber in a turbid medium is proportional to local laser fluence, optical absorption coefficient and the Gruneisen parameter. The local fluence at a subsurface absorber is determined by the initial incident fluence and optical properties of the media. Knowledge of laser fluence at subcutaneous tissue locations will improve our ability to estimate local chromophore concentrations and will lead to more quantitative estimates of blood oxygen saturation with photoacoustics. By integrating an oblique incidence reflectance (OIR) system in a photoacoustic imaging system, we are able to estimate optical properties of the turbid medium. To do this, we use a unique photoacoustic probe consisting of a 45-degree optical prism in an optical index-matching fluid. An oblique CW-laser beam interrogates the tissue surface at the same location as a pulsed laser, used for photoacoustic interrogation. Photoacoustic signals collected from the tissue are deflected by the prism to a focused 25 MHz ultrasound transducer. Diffuse light from the CW-laser is collected by a CCD camera and analyzed to estimate the bulk absorption and scattering coefficients. We fixed a tube filled with known concentrations of an absorbing dye below the probe in an Intralipid bath. We obtained the OIR and photoacoustic measurements for different Intralipid concentrations (providing a mus' between 2 and 10 cm-1). The OIR measurements were used to estimate the bulk optical parameters. Using these values, models of light transport were then used to calculate local laser fluence to normalize the photoacoustic measurements. The corrected photoacoustic signals show direct proportionality to the tube dye concentrations irrespective of bulk turbid medium properties.

7564-02, Session 11

Pulsed photoacoustic Doppler flowmetry using a cross correlation method

J. Brunker, P. Beard, Univ. College London (United Kingdom)

The feasibility of making spatially resolved measurements of blood flow using pulsed photoacoustic Doppler techniques has been explored. Doppler time shifts were quantified via cross-correlation of pairs of photoacoustic waveforms generated within various blood-simulating phantoms using pairs of laser light pulses. The photoacoustic waves were detected using a focussed PZT ultrasound transducer. A range of different transducers, planar and focussed and of various frequencies, were evaluated. In addition, the effect of the time separation between the laser pulses on measurement resolution and the maximum measurable velocity was investigated. This approach was found to be effective for quantifying the linear motion of micron-scale absorbers imprinted on an acetate sheet moving with velocities in the range 0.2 to 1.5 metres per second. The technique was subsequently applied to a fluid phantom incorporating carbon particles (2 to 12 microns in diameter) flowing at rates less than 0.3 metres per second along an optically transparent tube. The distinguishing advantage of pulsed rather than continuous-wave excitation is that spatially resolved velocity measurements can be made. This offers the prospect of mapping flow within the microcirculation and thus providing insights into the perfusion of tumours and other pathologies characterised by abnormalities in flow status.

7564-73, Session 11

In vivo 3D visualization of peripheral circulatory system using linear optoacoustic array

S. A. Ermilov, Fairway Medical Technologies, Inc. (United States); M. P. Fronheiser, Seno Medical Instruments, Inc. (United States); R. Su, A. A. Oraevsky, Fairway Medical Technologies, Inc. (United States)

We used previously developed laser optoacoustic (OA) imaging system based on a linear commercial ultrasound probe to visualize vasculature of a human forearm in 3D. The experiments involved precise translation of the probe along a forearm during acquisition of OA data. The filtered radial backprojection was used for 2D tomographic reconstruction of OA images corresponding to individual positions of the probe along the arm. The resultant images were appropriately stacked and visualized using VolViewTM to yield spatial distribution of the forearm vasculature. We propose that this technique can be used during preoperative mapping of forearm vessels that is essential for hemodialysis treatment.

7564-74, Session 11

Functional Imaging using the Optoacoustic 3D Whole-Body Tomography system

H. F. Brecht, R. Su, A. Conjusteau, S. A. Ermilov, Fairway Medical Technologies, Inc. (United States); M. P. Fronheiser, Seno Medical Instruments, Inc. (United States); A. A. Oraevsky, Fairway Medical Technologies, Inc. (United States)

We recently developed a multi-wavelength 3D whole-body optoacoustic tomography system for applications in preclinical research on mice. The system is capable of generating images with resolution of better than 0.5 mm. We used the imaging system to perform quantitative experiments in phantoms using nickel and copper sulfate representing absorption coefficients found in the mouse. Pixel intensities of the reconstructed image were compared to each other as a function of absorption coefficient and wavelength.



7564-75, Session 11

A high-speed photoacoustic tomography system based on a commercial ultrasound and a custom transducer array

X. Wang, J. B. Fowlkes, P. Carson, D. Chamberland, Univ. of Michigan (United States); L. Mo, D. DeBusschere, ZONARE Medical Systems, Inc. (United States); C. Hu, J. Cannata, The Univ. of Southern California (United States)

Building photoacoustic imaging systems by using stand-alone ultrasound (US) units makes it convenient to take the advantages of the state-ofthe-art US image processing, management and display technologies. However, the limited receiving sensitivity and especially the comparatively narrow bandwidth of commercial US probes are not sufficient for the acquisition of high quality photoacoustic images. In this work, a highspeed photoacoustic tomography (PAT) data acquisition system has been developed using a commercial US unit and a custom designed 128-element PVDF array transducer. After some software modification, the US unit is synchronized with laser firing and acquires data with a frame rate at 10 Hz (i.e. laser repetition rate). Since the US unit supports simultaneous signal acquisition from 64 parallel receive channels, PAT data from a 64-element array aperture can be acquired after a single laser firing. The PVDF linear array with a center frequency of 8.5 MHz provides a broad detection bandwidth of >125% at -6 dB, which guarantees the satisfactory image quality for tomographic photoacoustic imaging. Other transducer parameters include 0.3-mm pitch, 6-mm elevational height, and 3 cm elevational focus through a curved surface. A custom designed 128-channel preamplifier circuit board (20 dB amplification) that connects the PVDF array directly without using any cable enables impedance match and further elevates the signal-to-noise ratio in detecting weak photoacoustic signals. To examine the performance of this imaging system, experiments have been conducted using micro-flow vessel phantoms and ex vivo tissue specimens. The performance of this system and the experimental results will be presented.

7564-76, Session 11

In Vivo optoacoustic 3D whole-body measurement using a commercial ultrasound scanner: Experiments in nude mice

S. Preisser, M. Jaeger, M. Frenz, Univ. Bern (Switzerland)

For in vivo optoacoustic imaging, a linear array transducer is preferable for the acquisition of 2D (B-mode) images in real time. The comparably low amount of B-mode data permits an entire optoacoustic image to be acquired with a single laser pulse, which eliminates the influence of motion artifacts. For 3D imaging, a stack of images is obtained perpendicular to the array line of the transducer. We show that it is not possible to precisely reconstruct a 3D volume from a single stack of B-mode images. We solved this problem by performing additional scans with various different angles between the transducer axis and scanned surface. In this way complete 3D volume reconstruction is possible. For this purpose we developed an optoacoustic imaging system based on a commercial ultrasound device for simultaneous pulse-echo and optoacoustic imaging. A comparison of multi-angle and single-angle measurements in mice demonstrates the advantage of multi-angle B-mode measurements for 3D whole-body.

7564-78, Session 11

Real-time monitoring of small animal cortex hemodynamics by photoacoustic tomography

C. Li, Washington Univ. in St. Louis (United States); A. Aquirre, J. Gamelin, Q. Zhu, Univ. of Connecticut (United States); L. V. Wang, Washington Univ. in St. Louis (United States)

Photoacoustic (PA) tomography (PAT) has successfully imaged the small animal cortex. However, most of the previous PAT brain studies were slow in the data acquisition, making it challenging to study fast hemodynamic changes in the entire cortex region. In this work, we presented that for the first time the hemodynamics within the entire cerebral cortex of a mouse were studied by PAT in real time. Our system is a 512-element full-ring array, with each element cylindrically focused. The PAT system received the PA signal primarily from a slice of about 2 mm thickness, and the field of view is about 1.2 cm in diameter. The spatial resolution within the imaging plane is less than 200 µm. The data acquisition speed is about 1s per full scan. We demonstrated that this system can provide high resolution brain vascular images in vivo without averaging. To demonstrate the capability of the real-time hemodynamics study by using this system, we recorded the wash-in process of a PA contrast agent in a mouse cerebral cortex. The contrast agent was administrated via the tail vein injection. We used the near infrared laser with the wavelength within the strong optical absorption spectrum of the contrast agent. By continuous imaging the entire cortex region before and soon after the administration, the experimental results demonstrated the quick increase in the magnitudes of PA images. Thus, PAT can be a powerful imaging modality to study real-time small animal neurofunctional activities that can cause changes in hemodynamics.

7564-79, Session 11

Point spread function of arc-array transducers in 2D optoacoustic tomography

I. M. Pelivanov, Lomonosov Moscow State Univ. (Russian Federation); T. D. Khokhlova, Univ. of Washington (United States); V. A. Simonova, A. A. Karabutov, Lomonosov Moscow State Univ. (Russian Federation)

One of the major characteristics of an array transducer is the spatial resolution it provides. This characteristic can be inferred from the point spread function of the array, namely, the reconstructed 2D image of a point optoacoustic source. The relation between the resolution and the array dimensions (aperture, element width, element spacing) can not be determined analytically in 2D optoacoustic tomography, because, unlike 3D optoacoustic tomography, there is no rigorous solution to the inverse problem. Thus, the goal of this study was to find an empirical relation between image resolution and array dimensions using numerical simulations of direct and inverse problems of OA tomography. The focused elements, which allow to achieve an acceptable resolution in the perpendicular to the imaging plane direction, and two array designs (the elements were located either along a straight line planar or along a curve) were considered.

First, the calculation of the output signals of the array elements detecting the OA pulse from the point source was performed. Each element was considered to have a limited frequency band. The number of elements, their width, the array aperture angle, were the variable parameters. For image reconstruction we employed the backprojection algorithm. Longitudinal and lateral sizes (at 1/2 level) of the obtained image corresponded to the in-depth and transverse spatial resolution, correspondingly.

The empirical relationships as the functions of the in-depth and transverse spatial resolution on transducer parameters were determined. These relationships permit to choose the array design so that the defined image resolution can be achieved.

7564-80, Session 11

Continuous acquisition scanner for wholebody multispectral optoacoustic tomography

R. Ma, V. Ntziachristos, D. Razansky, Helmholtz Zentrum München GmbH (Germany) and Technische Univ. München (Germany)



The main difficulty arising from three-dimensional optoacoustic imaging is the long acquisition times associated with recording signals from multiple spatial projections. The acquired signals are also generally weak and the signal-to-noise ratio is low, problems that are usually solved by multiple averaging, which only further complicates matters and makes imaging challenging for most applications, especially those dealing with living subjects. Finally, when considering multispectral data acquisition, in which the same tomographic data is recorded at several different wavelengths, the imaging times become unrealistic.

In this work we present instead a fast data acquisition approach that continuously records high quality tomographic data without averaging. In this way, two dimensional image acquisition having 270 angular projections only takes about 9 seconds, while full multispectral three-dimensional image can normally take about 15 minutes to acquire with a single ultrasonic detector.

The various performance characteristics were tested on tissue-mimicking phantoms containing known concentrations of fluorescent molecular agent as well as small animals. In-plane spatial resolution on the order of 50µm and vertical resolution of about 150µm were demonstrated in both phantom experiments and imaging of small animals. These initial results confirmed availability of the system for high resolution whole-body visualization of molecular probes and other biomarkers located deep in small animals with characteristic sizes of below mm up to several cm, including mice and many other biologically relevant organisms, in which pure optical methods are not able to provide an adequate penetration depth and/or spatial resolution.

7564-81, Session 12

Spatial resolution of ultrasound-modulated optical tomography used for the detection of absorbing and scattering objects in thick scattering media

G. Rousseau, A. Blouin, J. Monchalin, National Research Council Canada (Canada)

Ultrasound-modulated optical tomography combines the good spatial resolution of ultrasonic waves (sub-mm) and the spectroscopic properties of light to detect optically absorbing and scattering objects in thick (cm scale) highly scattering media. In this work, a double-pass confocal Fabry-Perot interferometer is used as a band-pass filter to selectively detect the ultrasound-tagged photons. The limited etendue of the confocal Fabry-Perot interferometer is compensated by using a single-frequency laser emitting powerful optical pulses. Compared to photoacoustic tomography, ultrasound-modulated optical tomography is not only sensitive to optical absorption but also to scattering properties. In this paper, we consider the detection of absorbing and scattering objects embedded in thick (30 to 60 mm) tissue-mimicking phantoms and biological tissues. The experimental evaluation of the spatial resolution of the technique is compared to that expected from the ultrasonic beam profile. Preliminary results indicate that the edge spread function is influenced by the level of absorption of the embedded object and the scattering properties of the surrounding medium.

7564-82, Session 12

Real-time monitoring of high intensity focused ultrasound therapy using acoustooptic imaging

P. Lai, A. Draudt, R. O. Cleveland, T. W. Murray, R. A. Roy, Boston Univ. (United States)

High intensity focused ultrasound (HIFU) is a powerful, noninvasive tool for targeted tissue ablation. Detection of the onset of lesion formation in real time, however, remains challenging. The tissue necrosis during the HIFU therapy leads to changes in optical properties. In this paper, we explore the use of acousto-optic (AO) imaging to sense the changes

in optical contrast at depth in turbid media associated with the onset formation of HIFU lesions. The tissue to be treated is illuminated with near-infrared light and a continuous, amplitude modulated, focused ultrasound beam. A single ultrasound source is used to induce HIFU related tissue changes and to drive the AO interaction. The AO signal is detected via a PRC-based interferometer, and then fed into a lock-in amplifier tuned to the ultrasound modulation frequency. As the thermal lesion forms in the ultrasound focal zone, which is also the zone of AO interaction, the AO signal is found to reduce. The evolution of AO signal as a function of exposure time under appropriate pressure amplitudes provides a means for continuous monitoring of HIFU treatment and detection of the initial stages of the lesion formation. Once formed, the lesion can also be imaged using short pulsed ultrasound beams to generate the AO response. [Work supported by the Gordon Center for Subsurface Sensing and Imaging Systems (NSF ERC Award No. EEC-9986821).]

7564-83, Session 12

Ultrasound-modulated fluorescence

B. Yuan, P. M. Mehl, Y. Liu, J. Vignola, The Catholic Univ. of America (United States)

Fluorescence techniques can provide unique tissue physiological information and is very sensitive to tissue microenvironments, such as tissue pH value and gas/ion concentrations. Recently, ultrasoundmodulated fluorescence attracts attention for early cancer detection and diagnosis because of its high spatial resolution and optical functional contrast. We developed a system based on a phase sensitive detection technique and successfully detected the ultrasoundmodulated fluorescence in water and Intralipid solution. Possible modulation mechanisms were discussed. To enhance the modulation efficiency, microbubbles labeled with fluorophore and quenchers (F-Q microbubbles) were adopted. Fluorescence resonance energy transfer (FRET) between the fluorophore and the quenchers was studied by observing the fluorescence lifetime and intensity variations. The improvements were quantified based on the data acquired from the system. A fluorescent target was imaged by three modalities (ultrasonic, optical and acousto-optical).

7564-84, Session 12

Polarization effects in thermoacoustic CT of biologic tissue at 434 MHz

R. A. Kruger, R. B. Lam, D. R. Reinecke, S. P. DelRio, OptoSonics, Inc. (United States)

Thermoacoustic image contrast depends on the dielectric and thermoacoustic properties of the tissue being imaged, its spatial distribution, and the polarization of the incident microwave radiation. We have designed and constructed a thermoacoustic computed tomography (CT) test bed to study these effects in phantoms, biologic tissue (beefsteak) and mice. The test bed consists of a pair of opposing horn antennas immersed in thermoacoustic coupling fluid to irradiate the volume between them. The horns produce linearly polarized radiation, and are rotated ±90 degrees to change their polarization angle from vertical to horizontal. A vertically-oriented, curved detector array, consisting of 128 ultrasound transducer elements, was used to capture 3D thermoacoustic data. This array was positioned 90 degrees to the colinear axes of the two horn antennas.

The sample to be imaged is positioned vertically within a 25-mm-diameter plastic tube. This tube is rotated 360 degrees during imaging to capture a nearly complete set of radial projections. Image acquisition is completed in 2 minutes. Full 3D images are formed using filtered backprojection, resulting in an isotropic spatial resolution of < 350 microns. For each phantom, we captured images using both vertical and horizontal polarization.





Our results indicate that muscle and fat are easily differentiated, but the relative thermoacoustic absorption is strongly dependent on the polarization angle of the microwaves and the morphology of the fat and muscle. Importantly, the differentiation of fatty tissue from muscle appears to be enhanced in the difference image between the images formed with horizontal and vertical polarization.

7564-85, Session 12

Femtosecond Photoacoustics

M. E. van Raaij, B. Stefanovic, F. S. Foster, Sunnybrook Health Sciences Ctr. (Canada)

Conventional photoacoustic imaging systems excite a photoacoustic wave by illuminating an area on the order of square centimeters with millijoule laser pulses. Spatial resolution is then determined by the ultrasound transducer and typically on the order of 100 micrometers. We report on a system that focuses femtosecond, nanojoule pulses to a spot with a diameter of 1 micrometer to perform laser-scanning photoacoustics with micrometer resolution.

Near-infrared femtosecond laser pulses with a pulse energy of 2.4 nanojoules excite a train of photoacoustic waves at the repetition rate of the pulsed laser (80 MHz). These photoacoustic waves are detected by an unfocused single-element ultrasound transducer tuned to 80 MHz. A radiofrequency lock-in amplifier recovers the amplitude of the frequency component of the photoacoustic signal at the pulse repetition frequency. This amplitude is an indicator of the absorption coefficient of the sample at the laser focus and at the laser wavelength.

Initial experiments using a graphite rod as absorber reproducibly yield signals in the 0.2 - 2 microvolt range with a signal-to-noise ratio of 18 dB, recovered from 10 mV of broadband noise.

The photoacoustic detection system is integrated in a commercial laserscanning two-photon fluorescence microscope, enabling simultaneous three-dimensional fluorescence- and photoacoustic imaging. One major application will be to measure both topology and oxygen saturation of microvessels in brain tissue of anesthetized rodents in vivo, allowing in situ assessment of the efficacy of antiangiogenic drugs.

In this paper we describe the physics of femtosecond photoacoustics and demonstrate initial results.

7564-86, Session 12

Photothermal phase imaging of semiconducting and metallic nanomaterials

Y. Jung, C. Yang, J. Cheng, Purdue Univ. (United States)

Photothermal heterodyne imaging has demonstrated a high sensitivity of seeing single metallic nanoparticles of diameter down to 5 nm. However, rare attention has been paid to the phase of the photothermal heterodyne signal relative to that of the modulated pump beam. We show that the phase of the photothermal heterodyne signal from semiconducting nanomaterials such as silicon and germanium nanowires is around 0 degree, while that from metallic nanomaterials such as silver and gold nanoparticles is around 180 degree. Using this property we have been able to distinguish semiconducting from metallic single walled carbon nanotubes (SWNTs) in a label-free and contact-free manner.



Monday 25 January 2010 • Part of Proceedings of SPIE Vol. 7565 Biophotonics and Immune Responses V

7565-01, Session 1

Tumor PDT-associated immune response: relevance of sphingolipids

M. Korbelik, S. Merchant, British Columbia Cancer Agency (Canada); D. Separovic, Wayne State Univ. (United States)

Sphingolipids are a family of membrane lipids with important structural roles in lipid bilayer that are now also recognized as essential effector molecules in signal transduction with links to various aspects of cell function, immune response, as well as cancer progression and treatment response. Sphingolipids (especially major representatives ceramide, sphingosine and sphingosine-1-phosphate (S1P)) have attracted interest in their relevance to tumor response to photodynamic therapy (PDT) because of their roles as enhancers of apoptosis and autophagy, mediators of cell growth and vasculogenesis, and regulators of immune response. From extensive in vitro studies, it is now clear that ceramide is involved in promotion of PDT-induced apoptosis of cancer cells and it was proposed that sensitivity to PDT can be regulated by targeting ceramide -metabolizing enzymes. Our recent in vivo studies with mouse tumor models have confirmed that PDT treatment has a pronounced impact on sphingolipid profile in the targeted tumor and that significant advances in therapeutic gain with PDT can be attained by combining this modality with adjuvant treatment with ceramide analog LCL29. Further investigation is warranted on i) the prospects for superior therapeutic gains with other types of sphingolipid agents, and ii) how to exploit immune response-modulating effects of sphingolipids for optimization of tumor response to PDT.

7565-02, Session 1

Photodynamic therapy for cancer and activation of immune response

M. R. Hamblin, P. Mroz, Massachusetts General Hospital (United States)

Anti-tumor immunity is stimulated after PDT for cancer due to the acute inflammatory response, exposure and presentation of tumor-specific antigens, and induction of heat-shock proteins and other danger signals. Nevertheless effective, powerful tumor-specific immune response in both animal models and also in patients treated with PDT for cancer, is the exception rather than the rule. Research in our laboratory and also in others is geared towards identifying reasons for this sub-optimal immune response and discovering ways of maximizing it. Reasons why the immune response after PDT is less than optimal include the fact that tumor-antigens are considered to be self-like and poorly immunogenic, the tumor-mediated induction of CD4+CD25+foxP3+ regulatory T-cells (T-regs), that are able to inhibit both the priming and the effector phases of the cytotoxic CD8 T-cell anti-tumor response. Moreover defects in dendritic cell maturation, activation and antigen-presentation may also

Strategies to overcome these immune escape mechanisms employed by different tumors include combination regimens using PDT and immunostimulating treatments such as products obtained from pathogenic microorganisms against which mammals have evolved recognition systems such as PAMPs and toll-like receptors (TLR). Data will be presented on the use of CpG oligonucleotides (a TLR9 agonist found in bacterial DNA) to reverse dendritic cell dysfunction. Methods to remove or inhibit the immune suppressor effects of T-regs are under active study worldwide and we will present data on the use of low-dose cyclophosphamide to accomplish this goal. Lastly it may be possible to increase expression of tumor antigens by reversing epigenetic silencing of the genes that encode them using demethylating agents and HDAC inhibitors.

7565-03, Session 1

Can the dendritic cells see light?

A. Chen, Wellman Ctr. for Photomedicine (United States); R. W. Sands, Harvard Univ. (United States); M. R. Hamblin, Wellman Ctr. for Photomedicine (United States) and Harvard Medical School (United States)

There are many evidences showing that the low level light/laser therapy (LLLT) can enhance wound healing, upregulate cell proliferation and have anti-apoptotic effects by activating intracellular protective genes. In the field of immune responsive study, there has not been conclusively addressed whether light/laser is pro-inflammatory or anti-inflammatory. With more and more study, dendritic cells have been found to play an important role in the inflammation and immunological response. In this study, we try to look at the impact of the low level near infrared light (810nm) on the murine bone-marrow derived dendritic cells. Changes in the surface markers, including MHC II, CD80 and CD86 and the secretion of interleukins induced by light may provide additional evidences to reveal the mystery of how light derives the maturation of the dendritic cells as well how these light induced mature dendritic cells would affect the activation of adaptive immune response.

7565-04, Session 2

In-situ photoimmunotherapy: a tumordirected approach to the treatment of advanced melanoma with cutaneous metastases: preliminary data

M. Alam, S. A. St. Pierre, J. Rommel, Northwestern Univ. (United States); A. M. Ciurea, The Univ. of Texas M.D. Anderson Cancer Ctr. (United States); D. Fife, M. Martini, S. S. Yoo, T. Kuzel, J. Wayne, A. Rademaker, D. P. West, Northwestern Univ. (United States)

Metastatic melanoma is associated with high mortality as there are few effective treatments. In situ photoimmunotherapy (ISPI), a combination of laser therapy and immunomodulation with pharmacologic agents, is a targeted approach designed to enhance tumor-specific immunity. The immune response provoked by photoimmunotherapy in situ may produce sufficient antigenic material to trigger immune recognition of distant metastases and hence reduction or elimination of tumor burden. This study assesses efficacy and tolerability of treatment, disease progression, and survival status of two subjects with advanced metastatic melanoma treated with ISPI. Two weeks of pretreatment with imiquimod (5% cream) applied to tumor sites was followed by a single session of phototherapy using an 810-nm diode laser to dermal metastases injected with indocyanine green 0.25% solution in order to enhance photosensitization. This 2-week regimen was repeated once and followed by a final 2-week course of imiguimod. Outcome measures included post-treatment tumor site biopsies and CT/MRI/PET imaging of chest/abdomen/pelvis. One subject remains free from detectable visceral metastases 14 months after initiation of ISPI, but with some local skin tumor recurrence. Eight months after initiation of ISPI, the second subject has had limited in-transit and lymphatic recurrence but remains alive and well. Treatment toxicities included local pain, ulceration, and wound infection that were all well-managed in these subjects. ISPI is a relatively non-invasive, minimally toxic approach to treatment of advanced melanoma with cutaneous metastases. There is preliminary indication that ISPI may prolong survival, but definitive assessment of efficacy awaits further long-term studies.



7565-05, Session 2

Preliminary results of a phase I/II clinical trial using in situ photoimmunothearpy combined with imiquimoid for metastatic melanoma patients

X. Li, Chinese PLA General Hospital (China) and Univ. of Central Oklahoma (United States); W. R. Chen, Univ. of Central Oklahoma (United States); M. F. Naylor, Univ. of Oklahoma (United States); R. E. Nordquist, Wound Healing of Oklahoma (United States)

In Situ Photoimmunothearpy (ISPI), a newly developed modality for cancer therapy, has been shown to be able to modulate the body's own immune response. This clinical trial was designed to evaluate the safety and therapeutic effect of ISPI, using imiquimod as its immunoadjuvant for metastatic melanoma patients. The modality consists of three main aspects: 1) Injection of 0.25% ICG to the local tumors for enhancement of light absorption, 2) Laser irradiation (805nm, 1.0 W/cm2, 10 min) of local tumors, 3) Local application of imiquimod (5% cream under plastic occlusion). Twelve patients with stage III and stage IV (American Joint Commission on Cancer) melanoma were enrolled in this study. Five patients had disease stage III (IIIB 2, IIIC3), and 7 patients had stage IV (Mla 1, Mlb 1, and M1c 5). All patients had undergone prior surgeries. Three patients had received prior systemic chemotherapy therapy for their metastatic disease, three patients had received radiation therapy, and two patients had been treated with isolated limb perfusion therapy. All the patients completed at least one cycle of treatments; one patient received 6 cycles. The most common adverse effect was rash, diarrhea/ colitis, and endocrinopathies. No grade 3 or 4 toxicity was observed. Six of the twelve patients are still alive at the time of this report. One patient died of progression of myelodysplasia to leukemia, which is unrelated to melanoma. Median overall survival of the 11 evaluated patients is 12.3 months. Treatment of ISPI using imiquimod was safe and well tolerant. Our preliminary clinical results suggest that this new method could be a promising modality for late stage, metastatic tumors.

7565-06, Session 2

Laser-assisted immunotherapy: initial results from a phase II human breast cancer trial

M. Guerra, Immunophotonics Inc. (United States); J. A. Lunn, International Strategic Cancer Alliance (United States); W. R. Chen, Univ. of Central Oklahoma (United States); T. Hode, Immunophotonics Inc. (United States); O. Adelsteinsson, International Strategic Cancer Alliance (United States); R. E. Nordquist, Immunophotonics Inc. (United States)

Laser-assisted Immunotherapy is an experimental immunotherapy for solid tumors that utilizes an autologous vaccine-like approach to stimulate immune responses. Specifically, laser-assisted immunotherapy combines laser-induced in situ tumor devitalization with an immunoadjuvant for local immunostimulation.

Here we report the initial results from a phase II human breast cancer trial with laser-assisted immunotherapy. The immediate goal of the trial is to determine the optimal dosage for the alteration of the course of the disease, and the reduction of the tumor burden. Each patient is individually evaluated for toxicity tolerance through physical exams and by appropriate supplemental and routine laboratory tests (CSC, UA and complete metabolic profile) before and during therapy. Observable tumors in patients are followed with physical examination and radiological evaluations. Treatment efficacy is judged by the size and number of local and systemic metastases before and after treatment when patients are evaluated with CT examinations. Secondary efficacy parameters include the values of the hematology and blood chemistry studies. Other immunological parameters are monitored that may reveal clues to the ultimate mechanism of action of this form of treatment.

7565-07, Session 3

Effect of laser immunotherapy and surgery in the treatment of mouse mammary tumors

V. A. Chen, H. Le, Univ. of Central Oklahoma (United States); X. Li, Chinese PLA General Hospital (China) and Univ. of Central Oklahoma (United States); A. Sarkar, H. Ferguson, Univ. of Central Oklahoma (United States); H. Liu, Univ. of Oklahoma (United States); R. E. Nordquist, Wound Healing of Oklahoma (United States); W. R. Chen, Univ. of Central Oklahoma (United States)

Laser immunotherapy (LI), using laser thermal therapy and immunological stimulation could achieve tumor-specific immune responses, as indicated by our previous pre-clinical and clinical studies. To further study the effect of the LI and to understand its mechanism, we conducted investigation combining LI and surgery. After LI, treated tumors were surgically removed at different time points. The survival rates of treated mice were compared among different groups. Furthermore, the cured mice were rechallenged to test the immunity induced by LI. Our results showed that the mice treated with surgical removal one week after LI had the higher survival rate (77%). When the tumors were removed immediately after LI treatment, the survival rate was 57%. In comparison, immunological stimulation without laser treatment and followed by immediate tumor removal resulted in the lowest survival rate (33%). Most cured mice withstood tumor rechallenge, indicating an induction of tumor immunity by LI. The differentiations between different surgery groups indicate that the treated tumors may have contributed to the immunological responses of the hosts.

7565-08, Session 3

Topical photosan-mediated photodynamic therapy for DMBA-induced hamster buccal pouch premaligant lesions: an in vivo study

Y. Hsu, Chung Yuan Christian Univ. (Taiwan); C. Chiang, National Taiwan Univ. (Taiwan); J. W. Chen, B. R. Budiarto, M. Tseng, Chung Yuan Christian Univ. (Taiwan); J. Lee, Tzu Chi Univ. (Taiwan)

In Taiwan, oral cancer has becomes the most prominent cancer disease in recent years. The reason is the betel nut chewing habit combing with smoking and alcohol-drinking lifestyle of people results in oral cancer becomes the fastest growth incident cancer amongst other major cancer diseases. In previous studies showed that photosan, haematoporphyrin derivative (HPD), has demonstrated effective PDT results on human head and neck disease studies. To avoid the systemic phototoxic effect of photosan, this study was designed to use a topical photosanmediated PDT for treatment of DMBA-induced hamster buccal pouch precancerous lesions. DMBA was applied to one of the buccal pouches of hamsters thrice a week for 8 to 10 weeks. Precancerous lesions of moderate to severe dysplasia were induced and proven by histological examination. These induced precancerous lesions were used for testing the efficacy of topical photosan-mediated PDT. Before PDT, fluorescence spectroscopy was used to determine when photosan reached its peak level in the lesional epithelial cells after topical application of photosan gel. We found that photosan reached its peak level in precancerous lesions about 13.5min (range, 0 to 30 hours) after topical application of photosan gel. The precancerous lesions in hamsters were then treated with topical photosan-mediated PDT (fluence rate: 200 mW/cm2; light exposure dose 100 J/cm2) using the portable WonderLight LED 635 nm fiber-quided light device once or twice a week. Visual and histological examination demonstrated that topical photosan-mediated PDT was a very effective treatment modality for DMBA-induced hamster buccal pouch precancerous lesions.



7565-09, Session 3

In-vivo targeted photothermal purging of metastasis in sentinel lymph nodes guided by fiber-based multicolor photoacoustic lymphography

E. I. Galanzha, Univ. of Arkansas for Medical Sciences (United States); J. Kim, Univ. of Arkansas (United States); V. Tuchin, N.G. Chernyshevsky Saratov State Univ. (Russian Federation); M. S. Kokoska, Indiana Univ. School of Medicine (United States); E. Shashkov, Z. Vladimir, Univ. of Arkansas for Medical Sciences (United States)

The significance of lymphatics as part of the immune system for diagnosis and therapy has already been emphasized for many diseases. In particular, cancer metastatic tumor cells can be disseminated through lymph vessels to sentinel lymph nodes (SLNs). The metastatic tumor cells have dual roles as the first metastatic place and the immune barrier for tumor cells. This makes the SLN status one of the crucial portent prognostic indicators for survival in cancer patients.

This report introduces a novel diagnostic and therapeutic platform for noninvasive rapid detection and treatment of metastases in SLNs at the single cell level. This platform integrates multicolor photoacoustic (PA) lymph flow cytometry, PA lymphography, absorption image cytometry, and photothermal (PT) therapy. We demonstrated the capability of this platform for real-time mapping of lymph vessels and SLNs, counting disseminated tumor cells in prenodal lymphatics, diagnosis of early micrometastasis in SLNs, and its purging. This technology overcomes the limitations of existing techniques and potentially permits prevention, or at least inhibition, of metastatic progression by noninvasive targeted PT therapy of early disseminated tumor cells and micrometastasis; precisely in SLNs.

Taking into account the successful clinical applications of PA techniques using the safe range of laser fluence, non-toxic (e.g., melanoma) or low toxic (e.g., gold nanoparticles) contrast agents, and sterile disposable fibers; we anticipate PA/PT technologies can be rapidly translated to the bedside through the use of a portable device.

7565-10, Session 3

Novel applications of diagnostic x-rays in activating photo-agents through x-ray induced visible fluorescence from rare-earth particles: an in-vitro study

D. B. Tata, R. W. Waynant, U.S. Food and Drug Administration (United States); J. E. Collins, J. S. Friedberg, Univ. of Pennsylvania (United States); A. Kumar, H. Bell, Sunstone Biosciences, Inc. (United States)

Photodynamic agents utilized in cancer therapy possess a remarkable property to become preferentially retained within the tumors and the tumor's immediate micro-vascular environment. Upon the photo agent's activation through visible light photon absorption, the photo agents exert their cytotoxicity through type I and type II mechanistic pathways through extensive generation of reactive oxygen species: such as Superoxide anions, hydrogen peroxide, and the dominant singlet oxygen molecules within the intratumoral environment. Unfortunately, due to very shallow visible light photon's penetration depth (~ 2mm to 5mm) in tissues, currently the photodynamic strategy has largely been confined to the treatments of surface tumors, such as the melanomas. Additional invasive strategies through optical fibers are currently utilized in getting the visible light photon's into the intended deep seated targets within the body for PDT. In this communication, we report on a novel strategy in utilizing "soft" diagnostic energy X-ray photons (~ 100 keV) to activate Photofrin II as the photo agent in the presence of engineered rare-earth particles.

7565-11, Session 3

The role of temperature increase rate in combinational hyperthermia chemotherapy treatment

Y. Tang, A. J. McGoron, Florida International Univ. (United States)

Hyperthermia in combination with chemotherapy has been widely used in cancer treatment. Our previous study has shown that rapid rate hyperthermia in combination with chemotherapy can synergistically kill cancer cells whereas a sub-additive effect was found when a slow rate hyperthermia was applied. In this study, we explored the molecular basis of this difference. For this purpose, in vitro cell culture experiments with a uterine cancer cell line (MES-SA) and its multidrug resistant (MDR) variant MES-SA/Dx5 were conducted. P-glycoprotein (P-gp) expression, Caspase 3 activity, and heat shock protein 70 (HSP 70) expression following the two different modes of heating were measured. Doxorubicin (DOX) was used as the chemotherapy drug. Indocyanine green (ICG), which absorbs near infrared light at 808nm (ideal for tissue penetration), was chosen for achieving rapid rate hyperthermia. A slow rate hyperthermia was provided by a cell culture incubator. Cells were subjected to different concentrations of DOX and either 60 minutes in a 43°C incubator or to one minute at 43°C using 5µM of ICG and an 808nm laser. HSP70 expression was highly elevated under incubator hyperthermia while maintained at the baseline level under laser-ICG hyperthermia. Cells expressed high levels of Caspase3 after incubator hyperthermia while necrotic cell death was found after laser-ICG hyperthermia. Neither incubator nor laser-ICG Hyperthermia changed P-gp expression compared to controls. In conclusion, slow rate hyperthermia induced HSP70 overexpression may be responsible for the subadditive effect found in the DOX-incubator hyperthermia treatment. However, further research has to be conducted to explain the synergistic cell killing achieved by DOX and laser-ICG hyperthermia.

7565-12, Session 4

Monitoring hepatocellular carcinoma metastasis by in-vivo flow cytometer

X. Wei, Y. Li, J. Guo, G. Liu, Y. Chen, Fudan Univ. (China)

Hepatocellular carcinoma (HCC) may metastasize to the lung, bones, kidney, and many other organs. Surgical resection, liver transplantation, chemotherapy and radiation therapy are the foundation of current HCC therapies. However the outcomes are poor: the survival rate is almost zero for metastatic HCC patients. Molecular mechanisms of HCC metastasis need to be understood better and new therapies must be developed to selectively target to unique characteristics of HCC cell growth and metastasis. We have developed the "in vivo microscopy" to study the mechanisms that govern liver tumor cell spread through the microenvironment in vivo in real-time confocal near-infrared fluorescence imaging. A recently developed "in vivo flow cytometer" and optical imaging are used to assess liver tumor cell spreading and the circulation kinetics of liver tumor cells. A real- time quantitative monitoring of circulating liver tumor cells by the in vivo flow cytometer will be useful to assess the effectiveness of the potential therapeutic interventions.

7565-13, Session 4

Differences in HMME-mediated photodynamic therapy sensitivity for C666-1 and CNE2 cells

B. Li, Z. Chen, H. Lin, L. Liu, S. Xie, Fujian Normal Univ. (China)

The nasopharyngeal carcinoma (NPC) cell lines that widely used for photodynamic therapy (PDT) studies, such as CNE1, CNE2 and HK1 were Epstein-Barr virus (EBV)-negative NPC cell lines. In fact, in greater than 95% NPC patients, the latent form of EBV is present in the NPC



cells. To date, C666-1 is the only EBV-positive NPC cell line after a long-term culture. The aim of this study was to compare the sensitivity of hematoporphyrin monomethyl ether (HMME) mediated PDT for the EBV-positive C666-1 and EBV-negative CNE2 cell lines. Laser-induced fluorescence and laser scanning fluorescence microscopy were used to study the cellular uptake and subcellular localization of HMME in C666-1 and CNE2 cells, respectively. The survival rate of C666-1 and CNE2 cells after HMME-mediated PDT was evaluated with colony-forming assay. As compared to the C666-1 cells, CNE2 cells had a higher intracellular uptake of HMME after 3 h incubation. HMME has a similar pattern of diffuse cytoplasmic distribution in C666-1 and CNE2 cells, and the confocal images show no significant differences between C666-1 and CNE2 cells. The obtained results indicate that the sensitivity of HMMEmediated PDT for CNE2 cells was higher than that for C666-1 cells. It was found that the HMME-mediated PDT sensitivity for C666-1 and CNE2 cells mainly depends on intracellular accumulation.

7565-14, Session 4

A fluorescence-based centrifugal microfluidic system for parallel detection of multiple allergens

Q. Chen, H. Ho, Y. Suen, S. Kong, K. Cheung, W. J. Li, C. Wong, The Chinese Univ. of Hong Kong (Hong Kong, China)

This paper reports a robust polymer based centrifugal microfluidic analysis system that can provide parallel detection of multiple allergens in vitro. Many commercial food products (milk, bean, pollen...) may introduce allergy to people. A low-cost device for rapid detection of allergens is highly desirable. With this as the objective, we have studied the feasibility of using a rotating disk device incorporating centrifugal microfluidics for performing actuation-free and multi-analyte detection of various allergen species with minimum sample usage and fast response time. We used Acridine Orange (AO) to demonstrate degranualtion of KU812 human basophils. It was found that the AO fluorescent signal decreased significantly when the granules were stimulated by ionomycin, thus signifying a 100% release of histamine which may induce allergy symptom. Within this rotating optical platform, major microfluidic components including sample reservoirs, reaction chambers, microchannel and flow-control compartments are integrated into a single polydimethylsiloxane (PDMS) substrate. The flow sequence and reaction time can be controlled precisely. Sequentially through varying the spinning speed, the disk may perform a variety of steps on the sample including loading, reaction, separation and detection. The device may be mass produced simply by a simple molding process. PDMS is a potential replacement for glass and silicon-glass in microfluidic systems if bio-compatibility, low-cost and mass fabrication are desired. Our work demonstrates the feasibility of using centrifugation as a possible immunoassay system for future.

7565-15, Session 4

Preliminary study of antibacterial effect of glycated chitosan

C. M. N. Yow, C. M. Cheung, Hong Kong Polytechnic Univ. (China); W. R. Chen, Univ. of Central Oklahoma (United States); Z. Huang, Univ. of Colorado Denver (United States)

Background and Objectives: Chitosan possesses various biological effects and can act as an antimicrobial agent against a wide range of microorganisms. Glycated chitosan (GC) shows potentials as an immunoadjuvant. It has been used in combination with selective photothermal interaction in treatment of cancer. In this research, the antibacterial potential of GC was studied. Methods and Materials: Both wild type Staphylococcus aureus (S. aureus) and methicillin resistant Staphylococcus aureus (MRSA) were used as model bacteria. Bacterial cells (10E5 to 10E6 cfu/ml) were incubated with 0.2944, 0.368 and 0.46 % (v/v) of GC. The numbers of viable cells were examined at pre-

determined time points between 2 - 6 h. Propidium iodide (PI) staining was performed to assess the membrane integrity of bacteria treated with GC. Results: In both wild type S. aureus and MRSA, 0.2944, 0.368 and 0.46% of GC exhibited 99.9% killing within 6 h of incubation, but it was more effective for the wild type. The membrane integrity assay showed that both wild type S. aureus and MRSA were stained with PI after being treated with GC, indicating membrane disruption. Conclusions: Preliminary results suggest that glycated chitosan possesses antibacterial potential and its bactericidal effect involves the disruption of cell membrane integrity.

7565-16, Session 4

Comparison of different light irradiation modalities in light intensity distribution in blood

X. Li, Chinese PLA General Hospital (China); G. Cheng, Beijing Institute of Technology (China); N. Huang, L. Wang, F. Liu, Y. Gu, Chinese PLA General Hospital (China)

To compare the differences of the light intensity distributions in blood with different light irradiation modalities, Monte Carlo simulation was used. Light distribution of He-Ne laser (632.8nm) in human whole blood was simulated. The diameter of the optic fiber is 400µm. We referred to the work done by other researchers to determine four major tissue optical parameters of blood. For the same output laser power of 5mW, our results showed that the highest power density could be more than 5000mW/cm2 using spot optic fiber. But when using cylinder optic fiber (the light emission length=3mm), the highest power density was less than 200mW/cm2. Increasing the light emission length of cylinder optic fiber could further reduce the highest power density. In summary, cylinder optic fiber is good modality for light irradiation in whole blood, which can decrease the light intensity and make it more uniformed distributed in blood. It is of great importance to choose the suitable light emission length of cylinder optic fiber for clinical applications.

7565-17, Poster Session

Artemisinin induces ROS-mediated caspase 3 activation in ASCT-a-1 cells

F. Xiao, South China Normal Univ. (China)

Artemisinin, an antimalarial phytochemical from the sweet wormwood plant or a naturally occurring component of Artemisia annua, has been shown have a potential anticancer activity, and to induce cell death by apoptotic pathways. Moreover, some reports have demonstrated that artemisinin and its derivatives inhibit the growth of a limited set of human cancer cell lines, such as leukemia cells, fibrosarcoma cells, ovarian cells, breast cancer cells and cervical cancer cells and so forth. However, the molecular mechanism of artemisinin-induced apoptosis has not been defined. Human lung adenocarcinoma (ASTC-a-1) cell is non-small-cell lung cancer (NSCLC cell line). In our report, cell counting kit (CCK-8) assay showed that treatment ASTC-a-1 cells with artemisinin effectively increase cell death by inducing apoptosis in a time- and dose-dependent fashion. Hoechst 33258 staining was used to detect apoptosis as well. Reactive oxygen species (ROS) generation was observed in cells exposed to artemisinin at concentrations of 400 µM for 48 h. N-acetyl-Lcysteine (NAC), an oxygen radical scavenger, suppressed the rate of ROS generation and inhibited the artemisinin-induced apoptosis. Moreover, AFC assay, (Fluorometric assay for Caspase-3 activity), showed that ROS was involved in artemisinin-induced caspase 3 acitvation. Taken together, our present results indicate that artemisinin induces ROS-mediated caspase 3 activation in a time-and dose-dependent way in ASCT-a-1



7565-18, Poster Session

Taxol induces concentration-dependent phosphatidylserine (PS) externalization and cell cycle arrest in ASTC-a-1 cells

W. Guo, South China Normal Univ. (China)

Taxol (Paclitaxel) is an important natural product for the treatment of solid tumors. Different concentrations of taxol can trigger distinct effects on both the cellular microtubule network and biochemical pathways. Apoptosis induced by low concentrations (5-30 nM) of taxol was associated with mitotic arrest, alteration of microtubule dynamics and/or G2/M cell cycle arrest, whereas high concentrations of this drug (0.2-30 M) caused significant microtubule damage, and was found recently to induce cytoplasm vacuolization in human lung adenocarcinoma (ASTC-a-1) cells. In present study, Cell counting kit (CCK-8) assay, Confocal Microscope, and flow cytometry analysis were used to analyze the cell death form induced by 35 nM and 70 M of taxol respectively in human lung adenocarcinoma (ASTC-a-1) cells. After treatment of 35 nM taxol for 48 h, the OD450 value was 0.80, and 35 nM taxol was found to induce dominantly cell death in apoptotic pathway such as phosphatidylserine (PS) externalization, G2/M phase arrest after treatment for 24 h, and nuclear fragmentation after treatment for 48 h. After 70 M taxol treated the cell for 24 h, the OD450 value was 1.01, and 70 M taxol induced cytoplasm vacuolization programmed cell death (PCD) and G2/M phase as well as the polyploidy phase arrest in paraptotic cell death. These findings imply that the regulated signaling pathway of cell death induced by taxol is dependent on taxol concentration in ASTC-a-1 cells.

7565-19. Poster Session

Bax translocation to mitochondria during curcumol-induced apoptosis in human lung adenocarcinoma cells

W. Zhang, South China Normal Univ. (China); Z. Wang, Guangzhou Univ. of TCM (China); T. Chen, South China Normal Univ. (China)

Curcumol is the main component of oil of zedoary turmeric isolated from Chinese herb Radices zedariae. Previous studies indicate that curcumol has good curative effect to some solid tumors such as cervical cancer and has no serious adverse effect. However, little is known about the molecular mechanism of curcumol-induced apoptosis. In this report, we analyzed the Bax translocation from cytoplasm to mitochondria during curcumol-induced apoptosis using Confocal microscopey in single living human lung adenocarcinoma (ASTC-a-1) cell. Cell counting kit (CCK-8) assay was used to assess the inhibition of curcumol on the cells viability. Apoptotic activity of curcumol in ASTC-a-1 cells was detected by Hoechst 33258 and PI staining as well as flow cytometry analysis. To monitor the dynamics of Bax translocation in single living cell, the cells were transfected with GFP-Bax plasmid. Our results indicated that 1) the growth inhibition of curcumol on ASTC-a-1 cells was in a dose-dependent manner, curcumol of 100 µM exerted potent inhibitory effect on ASTC-a-1 cells viability was observed 48 h post treatment and induced approximately 50% cell death; 2) Although chromatin condensation was observed in curcumol-treated ASTC-a-1 cells, DNA fragmentation as a hallmark of apoptosis was not observed; 3) Bax translocation to mitochondria was observed in curcumol-induced apoptosis.

7565-20, Poster Session

Involvement of ASK1 activation in apoptosis induced by NPe6-PDT

L. Liu, South China Normal Univ. (China)

Photodynamic therapy (PDT) employing photosensiter N-aspartyl chlorin e6 (NPe6) can induce lysosome disruption and initiate apoptotic pathway. Apoptosis signal-regulating kinase (ASK1) is an important regulator of apoptosis in response to various stresses, such as reactive oxygen species (ROS), endoplasmic reticulum (ER) stress, lipopolysaccharide (LPS) and calcium influx. In this study, we investigated the molecular mechanisms of apoptosis induced by NPe6-PDT in ASTC-a-1 cells. The results showed that the activities of ASK1 increased in response to NPe6-PDT. Overexpression of wild-type or activated mutant of ASK1 could obviously decrease cell viability and increase cell death; while inhibition of ASK1 significantly decreased cell apoptosis. These results suggested that ASK1 plays an important role in apoptosis induced by NPe6-PDT.

7565-21, Poster Session

Low-power laser irradiation inhibits cytosolic translocation of SIRT1

C. Meng, D. Xing, S. Wu, L. Huang, South China Normal Univ. (China)

Sirtuin type 1 (SIRT1), a NAD+-dependent histone deacetylases, plays a critical role in cellular senescence, aging and longevity. Low-power laser irradiation (LPLI) can induce cell proliferation, in which how SIRT1 activity was modulated is still not understood. In the present studies, using confocal microscopy, we investigated the activity of SIRT1 in response to LPLI (< 15 J/cm2) in African green monkey 4SV40-transformed kidney fibroblast cells (COS-7). Using a fluorescence reporter, GFP-SIRT1, we found that SIRT1 localized to nuclei in physiological conditions. We devised a model enabling cell senescence via growth factor deprivation. and we found that SIRT1 partially translocated to cytosol under the treatment, suggesting a reduced level of SIRT1's activity. LPLI inhibited cytosolic translocation of SIRT1 in senescent cells in a time- and dosedependent manner. PKCs and PI3K were involved in the inhibition of SIRT1's cytosolic translocation under LPLI treatment, because inhibition of these kinases significantly decreased the amount of SIRT1 maintained in nuclei. Taken together, we demonstrated that LPLI inhibited SIRT1's cytosolic translocation in cell senescence, providing a new insight for the mechanisms of LPLI.

7565-22, Poster Session

Spatial-temporal changes of cardiolipin subcellular localization at the early stage of apoptosis

Z. He, D. Xing, L. Liu, S. Yang, South China Normal Univ. (China)

Cardiolipin is a unique and ubiquitous diphosphatidylglycerol phospholipid, located exclusively in inner membrane of mitochondria and particularly intermembrane contact sites. Cardiolipin is essential for mitochondrial to maintain its function. Recent studies have confirmed that cardiolipin participates in several mitochondria-dependent apoptotic steps, such as interacting with cardiolipin, cytochrome c, Bid and caspase-8. These processes are associated with the redistribution of cardiolipin in mitochondria. However, the exact mechanism of its redistribution, which happens at the early stage of apoptosis, is still controversial. In this study, 10-N-nonyl acridine orange (NAO), a specific probe for cardiolipin, was used to monitor the spatial-temporal changes of cardiolipin subcellular localization during apoptosis. The results showed that cardiolipin moves to the outer leaflet of mitochondrial inner membrane from the inner leaflet, during apoptosis, reactive oxygen species (ROS) may involved in this process.



7565-23, Poster Session

Analysis of GFP-FOXO3a nuclear-cytoplasmic shuttling in ASTC-a-1 cells under growth factor stimulation

X. Wang, D. Xing, South China Normal Univ. (China); W. R. Chen, Univ. of Central Oklahoma (United States) and South China Normal Univ. (China); H. Li, South China Normal Univ. (China)

FOXO transcription factors are important regulators of cell survival in response to a variety of stimuli, among which are hypoxic stress, oxidative stress, and growth factor deprivation. Subcellular localization of FOXO proteins plays a major role in the regulation of their activity. In this study, using confocal imaging of the cells transfected with GFP-FOXO3a and fluorescence recovery after photobleaching technique, we visualized the dynamic nuclear translocation of GFP-FOXO3a in ASTC-a-1 cells under growth factor stimulus. In healthy cells, GFP-FOXO3a was well-distributed in the cytoplasm or widespread distributed in the cytoplasm and the nucleus but the cytoplasm was significantly more than the nucleus. Deprivation of growth factor, we monitored the nuclear localization of GFP-FOXO3a and the dynamic nuclear translocation of it from cytoplasm to nucleus. Interestingly, upon stimulation with growth factor in cells again, we visualized the dynamic nuclear exclusion of GFP-FOXO3a and cytoplasm distribution rapidly. In conclusion, these results demonstrated that FOXO3a can reversible shuttling between cytoplasm and nucleus upon stimulation with growth factor.

7565-24, Poster Session

Study of MR imaging in labeled human lung adenocarcinoma cells with ENDOREM in vivo

W. L. Chen, M. Yu, South China Normal Univ. (China)

To evaluate the optimal condition for labeling the human lung adenocarcinoma cell line (ASTC-a-1) with SPIO in vitro and the ASTC-a-1 magnetic resonance imaging, SINEREM, one kind of SPIO, was used in our study, labeled ASTC-a-1 by incorporating with Poly-1-lysine. The prush blue staining results indicated that ASTC-a-1 could be efectively labeled with $25\mu g/ml$ SPIO and the llabeling eficiency was more than 99 . MRI implied the signal intensity decrease for the labeled ASTC-a-1 with SPIO compared with that for unlabeled on T1WI , T2WI , and FGR/ 20° and FGR/ 70° sequences. CCK-8 showed the high concentration (200 $\mu g/ml$) SPIO-PLL increase in intracellular ROS level of ASTC-a-1 and cell activity decrease ,ROS Mitochondrial membrane potential decrease obviously after treating 4h,compared the unlabelle cells. All the results inferred that SPIO could label ASTC-a-1 efficient at appropriate condition without adverse effects.

7565-25, Poster Session

DC-mediated anti-tumor responses of NK cells

G. Chirico, M. Caccia, T. Gorletta, F. Granucci, M. Collini, Univ. degli Studi di Milano-Bicocca (Italy)

Recent Two Photon Laser Scanning Microscopy (TPLSM) studies have demonstrated that dendritic cells (DCs) play a crucial role in the activation process of Natural Killer cells (NKs): the lymphocytes of the innate immunity endowed with direct anti-tumor activity. In this report we want to focus on the role of Pathogen Associated Molecular Pattern (PAMP) activated-DCs in NK cell-mediated anti-tumor responses.

Our TPLSM set up is particularly suitable for intravital microscopy. Thanks to a femtosecond pulsed lasers coupled to a confocal scanning head we are able to simultaneously excite multiple dyes and to exploit Second Harmonic Generation (SHG) for imaging of the connective components of the tissues. A non descanned detection unit increases the detection efficiency and a home-made temperature controlled box surrounding the entire microscope together with a system for the flux of physiological fluids keeps the explanted organs very close to the condition they experience in live animals.

Mice previously injected with AK7 cells, a mesothelioma cell line sensitive to NK cell responses, are injected with labeled NK cells. After that different bacterial-derived stimuli are injected s.c. to induce labeled DC activation. Using 4 dimensional tracking we follow the kinetic behavior of NK cells both at the Draining Lymph-Node (DLN) and eventually at the tumor level.

Our preliminary data suggest that NK cells are recruited to the DLN where they can interact with activated-DCs in the periphery of the T cell area with a peculiar kinetic behavior. It seems that NK cells accumulated strongly also at the tumor site after treatment with activated-DC, suggesting that NK cells and activated-DCs might efficiently interact in the DLN, where NK cells could be activated and subsequently induced to reach the tumor site. Therefore, in our opinion, activated-DCs not only play a key role in the activation process of NK but seem to be also crucial for the control of their distribution at the DLN and at the tumor site.

Return to Contents TEL: +1 360 676 3290 · +1 888 504 8171 · customerservice@spie.org



Sunday 24 January 2010 • Part of Proceedings of SPIE Vol. 7566 Optics in Tissue Engineering and Regenerative Medicine IV

7566-01, Session 1

Monitoring adipose-derived stem cells within 3D carrier by combined dielectric spectroscopy and spectral domain optical coherence topography

P. Bagnaninchi, The Univ. of Edinburgh (United Kingdom)

Cell-therapy strategies make use of 3D carriers to deliver stem cells to a location of interest. There is a need to assess non-invasively, just before their implantation in vivo, the state of the cells within this 3D structure.

We propose to combine dielectric spectroscopy (DS) and spectral domain optical coherence tomography (SDOCT) to quality assess the cells to be delivered.

A SD-OCT (930nm FWHM 90nm) was built around a commercial spectrometer and laser source (Thorlabs), our custom Michelson interferometer accommodates a dielectric probe in the sample arm to make simultaneous DS measurements. Both spectrometer and material analyser were controlled through Labview allowing synchronized DS measurements between 20MHz and 3GHz and Ascan rate of 1.2KHz. Adiposed-derived stem cells (ADSC) were grown in alginate scaffolds (Algimatrix, invitrogent) and maintain in MesenPRO RS medium, while others were induced to differentiate towards osteoblasts.

The multimodality system has allowed us to monitor the distribution of the cells within the carrier as well as their specific dielectric spectra for high cell concentration. We demonstrated the advantages of combining DS and SOCT in terms of modelling and improving the DS data.

This multimodality technique could be advantageous to assess noninvasively cell loaded carriers for cell therapy.

7566-02, Session 1

Investigation of pore structure and cell distribution in EH-PEG hydrogel scaffold using optical coherence tomography and fluorescence confocal microscopy

C. Chen, M. Betz, J. Fisher, A. Paek, Univ. of Maryland, College Park (United States); J. Jiang, H. Ma, A. Cable, Thorlabs (United States); Y. Chen, Univ. of Maryland, College Park (United States)

Hydrogel scaffolds are of interest in the fields of tissue engineering, drug delivery, and stem-cell-based therapies, because of their capability to facilitating cellular activities such as attachment, matrix deposition, migration, and tissue ingrowth induction in the scaffold. Non-destructive characterization of scaffold structures in situ is important for optimization of scaffold designs for specific application. In this study, macroporous EH-PEG hydrogels fabricated by porogen-leaching method are characterized by optical coherence tomography (OCT). OCT allows for non-invasive cross-sectional imaging of material architecture, providing typical axial resolution of 8 um and depth of penetration of 2 mm. Due to its non-invasive nature, OCT images represent scaffolds in situ and therefore make subsequent image reconstruction and processing possible. Image processing algorithms to quantify the pore size, porosity, and pore connectivity are presented. Those parameters are key to designing scaffolds, and can be automatically quantified through our algorithm. The results indicated that pore connectivity highly depends on the porogen size. To investigate pore connectivity more directly, and to confirm the interaction between cells and the scaffold, fluorescence imaging using the confocal microscopy was conducted to monitor the population and distribution of labeled human mesenchymal stem cells (hMSCs) loaded on the surface of the scaffold. Fluorescence images

revealed that hMSCs distribute themselves more evenly in the scaffolds with larger pore sizes than those with smaller pore sizes. This supports both hMSCs viability in EH-PEG hydrogels and cells' utilization of scaffolds, in accordance with the result from pore connectivity analysis.

7566-03, Session 1

Combined optical coherence phase microscopy and impedance sensing measurements of differentiating adipose derived stem cells

P. Bagnaninchi, Univ. of Edinburgh (United Kingdom)

There is a growing interest in monitoring differentiating stem cells in 2D culture without the use of labelling agents. In this study we explore the feasibility of a multimodality method that combines impedance sensing (IS) and optical coherence phase microscopy (OCPM) to monitor the main biological events associated with adipose derived stem cells differentiation into different lineages.

Adipose derived stem cells were cultured in Mesenpro RS medium on gold electrode arrays. The system (Applied biophysics) is connected to a lock-in amplifier connected to a computer, and the impedance is derived from the in-phase and out of phase voltages. Multi-frequency measurement spanning from 1kHz to 100 kHz are recorded every 2 minutes. The Optical coherence phase microscope is build around a Thorlabs engine (930nm FWHM: 90nm) and connected to a custom build microscope probe.

The IS and OCPM were successfully integrated. The electrode area (250um) was imaged with a lateral resolution of 1.5um during impedance measurements. Impedance sensing gave an average measurement of differentiation, as a change in impedance over the electrode area, whereas OCPM provides additional information on the cellular events occurring on top of the electrode. The information retrieved from OCPM was used to feed the mathematical model correlating cellular differentiation and impedance variation.

In this study we have demonstrated the feasibility of integrating two non-invasive monitoring techniques that will be instrumental in designing stem cell based screening assays and enable quality assessment for cell replacement therapies.

7566-04, Session 1

Noninvasive system for the evaluation of bioengineered tissue constructs combining time-resolved fluorescence and ultrasound imaging

B. Z. Fite, M. Decaris, Y. Sun, Y. Sun, C. Ki Lok Ho, K. Leach, L. Marcu, Univ. of California, Davis (United States)

Fluorescence Lifetime Imaging Microscopy (FLIM), Time Resolved Laser Induced Fluorescence Spectroscopy (TR-LIFS), and Ultrasound Backscatter Microscopy (UBM) are shown here to noninvasively track the production of chondrogenic extracellular matrix produced by equine adipose-derived mesenchymal stem cells (eASCs) grown on biodegradable, biomimetic scaffolds. Chondrogenic cells exhibited increases in both fluorescence intensity, and average fluorescence lifetime during a 7 week period of differentiation. For chondrogenic differentiation, average lifetimes were 1.19 \pm 0.05 ns, 1.38 \pm 0.09 ns, 1.94 \pm 0.11 ns, 2.18 \pm 0.14 ns for weeks 1, 3, 5, and 7 post-induction for 430 - 490 nm compared to 0.98 \pm 0.08 ns, 0.97 \pm 0.09 ns, 0.97 \pm 0.07 ns, 0.99 \pm 0.1 ns for control, while fluorescence intensity was 9.79, 13.67,



29.72, 52.67 versus 6.21, 6.77, 6.46, 6.65 for control. The combination of FLIM, TR-LIFS and UBM tracks eASC chondrogenic differentiation. The fluorescence and ultrasound based results are validated against those acquired via conventional techniques. FLIM, TR-LIFS and UBM demonstrated promise in evaluating the expression of structural proteins in tissue constructs and have possible applications in the nondestructive evaluation of structural protein expression.

7566-05, Session 2

Development of the hyperspectral cellular imaging system to apply to regenerative medicine

M. Ishihara, National Defense Medical College (Japan) and Tokai Univ. (Japan); M. Sato, Tokai Univ. (Japan); K. Matsumura, National Defense Medical College (Japan); J. Toguchida, Kyoto Univ. (Japan); J. Mochida, Tokai Univ. (Japan); M. Kikuchi, National Defense Medical College (Japan)

Regenerative medicine by the transplantation of differentiated cells or tissue stem cells has been clinically performed, particularly in the form of cell sheets. To ensure the safety and effectiveness of cell therapy, the efficient selection of desired cells with high quality is a critical issue, which requires the development of new evaluation method to discriminate cells non-invasively with high throughput. There were many ways to characterize cells and their components, among which the optical spectral analysis has a powerful potential for this purpose. We developed a hyperspectral imaging system, which captured both spatial and spectral information in a single pixel. Hyperspectral data are composed of continual spectral bands, whereas multispectral data are usually composed of about 5 to 10 discrete bands of large bandwidths. The hyperspectral imaging system which we developed was set up by a commonly-used inverted light microscope for cell culture experiments, and the time-lapse imaging system with automatic focus correction was attached. Spectral line imaging device with EMCCD was employed for spectral imaging. The system finally enabled to acquire 5 dimensional (x, y, z, time, wavelength) data sets. In this study, the illuminating condition of light/laser source was optimized in the case of cells regulated by cell-cycle and cell sheets were used as sample. We recognized individual spectrum of arbitrary intracellular and/or extracellular regions, which will be useful to discriminate cells.

7566-06, Session 2

Raman spectroscopy as a noninvasive analysis tool for living cells

M. Pudlas, Fraunhofer-Institut für Grenzflächen- und Bioverfahrenstechnik (Germany) and Univ. of Stuttgart (Germany); S. Koch, Univ. of Stuttgart (Germany); H. Mertsching, Fraunhofer Institute for Interfacial Engineering and Biotechnology (Germany)

In the field of cell culture and tissue engineering there is an increasing need for non-invasive methods that are able to analyze living cells under in vivo conditions. Raman spectroscopy is a purely optical, laser-based, and non-contact technique which allows a characterization of cells without lysis, fixation or the use of any chemicals. This method overcomes limitations of common cell analysis methods and probes cells without any cell damage. Raman spectra of cells contain typical fingerprint regions and information about the cell type and cell status. Characteristic peaks in Raman spectra could be assigned to biochemical molecules like proteins, nucleic acid or lipids. Due to its non-invasive properties, short integration times of only a few minutes and an easy sample preparation Raman spectroscopy is a promising technology for the quality control of cells in tissue engineering applications.

The distinction between Raman spectra of several cell types and the determination of variances during dedifferentiation of cells was shown and confirmed by immunohistological staining. Furthermore a discrimination of vital, apoptotic and necrotic cells by its Raman spectra is possible. Further work needs to be done on the analysis of cells embedded in a scaffold to characterize cells in tissue engineering products.

7566-07, Session 2

Using PS-OCT to investigate regional properties of peripheral nerve

J. Harle, The Open Univ. (United Kingdom) and Univ. of Liverpool (United Kingdom); S. Mason, J. Phillips, The Open Univ. (United Kingdom); Y. Yang, Keele Univ. (United Kingdom)

Peripheral nerves must bend and stretch around joints to accommodate normal body movement. Previous studies have demonstrated that the joint and non joint regions of rat peripheral nerve are biomechanically diverse (Phillips et al., 2004) with the structural features mediating this mechanical heterogeneity poorly understood. Characterisation of region-specific mechanical architecture, alongside the development of a real time imaging technique with appropriate spatial and contrast resolution, would enable development of novel clinical techniques to enhance peripheral nerve repair and monitor the healing process.

This study used Polarisation Sensitive-Optical Coherence Tomography (PS-OCT) to image the joint and non joint regions of sciatic nerves which were resected post mortem from 250-350 g rats. The nerves were maintained at their in situ tension and stored in Phosphate Buffered Saline prior to immersion in an appropriate optical clearing agent for PS-OCT. Contralateral joint and non joint regions of rat nerve were fixed and processed for investigation by electron microscopy and histological staining using established protocols.

PS-OCT images from joint and non joint regions were analysed and correlated to quantitative measurements of nerve architecture, including perineurial thickness, collagen fibril diameter and elastin content, using ImageJ software. Preliminary results show that the size distribution of collagen fibrils varied at joint and non joint regions. These regions also showed characteristic different birefringence patterns in transverse and longitudinal PS-OCT images. These preliminary results demonstrate that PS-OCT could be a powerful tool to reveal the spatial internal arrangement of peripheral nerves, in particular the collagen fibril organization.

7566-08, Session 2

Spectral imaging polarimetry to assess structural organization in biological tissue

J. C. Gladish, D. D. Duncan, Oregon Health & Science Univ. (United States)

Changes in the structural organization of biological tissue can be indicative of disease. The ability to measure and associate changes in structural organization with disease-related cellular architecture has significant diagnostic value. Here we present a spectral imaging polarimeter to probe the local structural organization of tissue. The system is based on liquid crystal technology, and is comprised of two modules, a Stokes generator and a polarimeter. The Stokes generator uses a pair of Liquid Crystal Variable Retarders to generate a set of Stokes vectors incident on a sample, while the polarimeter utilizes a separate pair to analyze the scattered Stokes vectors. A CCD camera is employed to image the illuminated region, thus providing spatially resolved estimates of the complete Mueller matrix. Characterization of the system is in terms of a data reduction matrix that relates the polarimeter measurements to the incident Stokes vector. Calibration of the polarimeter (calculation of the elements of this data reduction matrix) is performed by presenting a series of known Stokes vectors to the device. The resulting over-determined system of equations is solved using the Singular Value Decomposition. We discuss the construction and calibration of the system and present data on a variety of biological media.



7566-09, Session 2

Investigation of a tissue engineered tendon model by PS-OCT

Y. Yang, M. Ahearne, I. Wimpenny, J. Guijarro-Leach, Keele Univ. (United Kingdom); J. Torbet, Grenoble High Magnetic Field Lab. (France)

A few native tissues, such as tendon, skin, retinal tissues possess highly organized collagenous structures. In particular, the collagen fibers in tendon are organized into hierarchical and unidirectional format, which gives the tissue high mechanical properties and this has been clearly revealed by a conventional polarized light microscope. The newly developed polarization-sensitive optical coherence tomography (PS-OCT) technique allows non-invasive visualization of the birefringence images due to orientated structures in three dimensional format. Our previous studies of native tendon and tissue engineered tendon by PS-OCT demonstrate that tissue engineered tendon has a far less perfect collagen fiber organization than native tendon even under dynamic culture condition. The purpose of this study is to use PS-OCT to assess the relationship between the degree of birefringence and collagen concentration and fiber density in a model tendon tissue. The model tendon tissue is constructed from aligned collagen hydrogel and aligned polyester nanofibers. The effects of the diameter and density of nanofiber and the collagen concentration in the model have been investigated. The alignment of collagen fibrils is induced by high magnetic field during the fibrillogenesis and aligned nanofibers are manufactured by electrospinning technique. It is found that collagen concentration and nanofiber density are the key parameters controlling the birefringence in OCT images. The perfectly aligned collagen hydrogel with concentration as high as 4 mg/ml does not exhibit birefringence image until the hydrogel has been compressed and concentrated. Aligned nano-fiber bundle has demonstrated marginal birefringence image without matrix. These studies enhance our understanding of how to control and optimize the parameters in tendon tissue engineering.

7566-10, Session 3

Multiphoton fabrication of crosslinked fibronectin for tissue engineering applications

P. J. Campagnola, Y. Su, X. Chen, Univ. of Connecticut Health Ctr. (United States)

The ability to fabricate concentration gradients of extracellular matrix (ECM) proteins in vitro to induce haptotaxis (i.e. migration towards attractive surfaces) would have great benefit for tissue engineering applications as differentiation and migration are necessary precursor steps for new collagen synthesis for repair/regeneration. A drawback of most previous efforts is that proteins are typically physisorbed rather than covalently linked and such devices may have insufficient stability with respect to surface desorption for long term applications. To improve upon this situation, we present our efforts using multiphoton excited (MPE) photochemistry to fabricate covalently crosslinked gradients with nanostructured topography. Using Rose Bengal photochemistry and a novel galvo scanning control, we fabricate gradients of fibronectin consisting of a series of individual parallel linear gradients 1 mm in length with slope of 0.1 µM/100 µm. Using these structures we show the morphology of 3T3 fibroblasts respond strongly to the concentration gradient. Over 3 days the cells become increasingly aligned with respect to the gradient direction of increasing fibronectin concentration and similarly the cells become increasingly elongated. The cytoskeletal properties are also highly controlled by the gradient. Using circular statistics, we show differences in the direction of the stress fiber distribution for different concentration ranges, where at high concentration the stress fibers are nearly axially aligned with the gradient direction. Similarly, the focal adhesion expression increases with fibronectin concentration. These results demonstrating the ability to control adhesion and differentiation suggest that the method would be applicable to enhancing differentiation of stem cells for regeneration/ repair.

7566-11, Session 3

Concentration distribution of nanoparticles in biological tissues measured with Schlieren visualization technique

A. I. Omelchenko, E. N. Sobol, Institute on Laser and Information Technologies (Russian Federation)

Development of the new medical methods of healing with nanoparticles demands new diagnostic techniques. However, a high quality result in imaging of nanoparticles in pathological tissues could be obtained using the simple methods of visualization. One of these methods is a shlieren visualization of the phase objects caused by laser heating of small heterogeneities in refraction index of low absorbing media.

This paper presents the results of measurement of axial symmetric distribution of concentration of photo absorbing nanoparticles in hydrated biological tissues with digital image processing of shadowgraph.

These shadowgraphs occurred in the space of laser-tissue interaction illuminated with the probe radiation.

It has been studied the laser-induced process of shadowgraph formation in the visco-elastic and low scattering biological medias and the influence of concentration of photo absorbing nanoparticles in the tissue on their image contrast, as well.

Image processing was carried out by means of solution of reverse problem for restoration of spatial distribution of absorbers on the shadowgraph profiles.

It was obtained the simple expression for absorbers concentration distribution in the tissues in case of thermal action of cylindrical laser beam on hydrated tissue with the limited hydraulic conductivity.

Concentration distributions of nanoparticles of -Fe3O4 in cartilage and hydro gel were determined by data obtained with Schlieren visualization technique.

7566-12, Session 3

Confocal mosaicing of engineered tissues

A. Ardeshiri, D. Levitz, D. Gareau, S. Jacques, Oregon Health & Science Univ. (United States)

Characterization of engineered tissues using optical methods often involves tradeoff between the fraction of total volume that is imaged and the spatial resolution. The limitation is not technological but rather practical, having more to do with effective probe designs and computer memory storage for large datasets.

In this paper, we propose using multimodal confocal mosaicing, a technique used to characterize wide areas of excised biopsies from Mohs surgeries, to characterizing collagen gels. This technique stitches together high-resolution 2D images of a series adjacent 0.5mm square fields-of-view that collectively make up areas that are up to 2 cm2 square. The step-and-capture image acquisition time is approximately 5 min.

Using digital staining technique, we are able to false color the reflectance signal that represents the collagen matrix in pink, and the fluorescence from acridine orange or eosin staining of nuclei or cytoplasm (respectively) in purple. The resulting high-resolution images closely resemble hematoxylin and eosin histological sections, only obtained without the time-consuming embedding and sectioning steps and captured on biologically viable samples.

Disk-shaped collagen gels of 1 ml volume and ~1.5 cm diameter were prepared with smooth muscle cells and imaged at 1 and 5 days. Using the digital staining technique, we were able to survey the spatial distribution of cells in the hydrogel and assess spatial heterogeneity in 3D from the fluorescence data. The reflectance data provided information on collagen fibril structure and matrix remodeling by the cells. Digital staining presented the data in a way that is easily interpreted by tissue engineers. We conclude that multimodal confocal mosaicing in



combination with digital staining represents an important technological novelty that significantly advances non-destructive optical evaluation of engineered tissues.

7566-13, Session 3

HMC and fibroblast illuminating experiments using microdisplay

C. Ou, Hsiuping Institute of Technology (Taiwan)

Techniques like optical neural guiding, photodynamic therapy and photosynthesis of the cell all required specific spatial energy distribution. For the past few years, the optical neural/cell guiding experiment become a promising technique. It required producing a small light spot close to the neuron tip, and the photo-chemical effects callused by the illumination condition will results in the neural growth. Influences factors like the wavelength, polarization, spatial intensity distribution are all required. Most of these results are using the laser diode to complete this task. However, during the cell culturing, appropriate illumination condition for the cells inside the incubator are required to meet more complicated conditions. Therefore, the multipoint illuminating techniques and related apparatus becomes a reasonable next step. In this paper, we report the system that using of the spatial light modulator to provide a multipoints control for the cell culturing. This system is modified from the commercialized projection system to reduce the cost. It is now possible to apply it to other bio-culturing related applications. Results for Human Melanocyte (HMC) and fibroblast cell are discussed.

7566-14, Session 3

Improvement of the frequency domain inverse **Monte Carlo simulation**

H. Zhao, S. Zhang, J. Liang, Z. Qin, X. Zhou, Tianjin Univ. (China)

This article aims at the optical property (absorption coefficient and scatter coefficient) reconstruction from the frequency- domain (FD) near-infrared diffuse measurement on small tissues, for which inverse Monte Carlos (MC) simulation is the suitable choice. To achieve the fast and accurate reconstruction based on the inverse Monte Carlo simulation, following techniques were adopted. First, in the forward calculation, a database, which include the frequency-domain information calculated from MC simulation for a series of optical parameters of tissue, were established with fast methods. Then, in the reconstruction procedure, Levenberg-Marguardt (L-M) optimization was adopted and Multiple Polynomial Regression method was used to rapidly get the FD information at any optical properties by best fitting the curved surface formed by the above database. At Last, in the reconstruction, to eliminate the influence of the initial guess of optical properties on the reconstruction accuracy, cluster analysis method was introduced into L-M reconstruction algorithm to determine the region of the initial guess. The reconstruction algorithm was demonstrated with simulation and experimental data. The results showed that it takes less than 0.5s to reconstruction one set of optical properties. The average relative error from the reconstruction algorithm joined with cluster analysis is 5% lower than that without cluster analysis.

7566-15, Session 4

Doppler optical micro-angiography improves the quantification of local fluid flow and shear stress within 3D porous constructs

Y. Jia, R. K. Wang, Oregon Health & Science Univ. (United States)

Traditional phase-resolved Doppler optical coherence tomography (PRDOCT) has been reported to have potential to characterize local fluid flow within microporous scaffold. In this work, we apply Doppler optical micro-angiography (DOMAG), a new imaging technique that

was developed by combining optical micro-angiography (OMAG) and phase-resolved method, for improved assessment of local fluid flow and its derived parameters, shear stress and interconnectivity, within highly scattering porous constructs. Compared with PRDOCT, we demonstrate a dramatic improvement of DOMAG in quantifying flow-related properties within scaffolds in situ for functional tissue engineering.

7566-16, Session 4

Optical coherence tomography investigation of growth cycles of engineered skin tissue

R. Schmitt, U. Marx, Fraunhofer-Institut für Produktionstechnologie (Germany); H. Mertsching, A. Heymer, Fraunhofer-Institut für Grenzflächen- und Bioverfahrenstechnik (Germany)

Engineered tissues are widely used in dermatological, pharmacological and toxicological studies and as autologous transplants in wound healing. To improve the successful imitation of humanoid tissue the challenge is to find ideal growth parameters for the cultivation process. Thus, non-invasive monitoring of engineered tissue during the growth cycles is of major significance to understand and consequently improve the growth characteristics of in vitro tissue. Prior to the framework of the automation of artificial humanoid 3d - skin tissue engineering, optimal growth parameters need to be determined. The successful engineering of humanoid tissue is strongly coupled to the composition and structure of the upper epidermal and dermal skin layers. The layers are based on primary humanoid keratinocytes and a collagen - fibroblasts matrix. We applied optical coherence tomography as tissue imaging technology, which offers great potential to detect and characterize the layer structure of engineered skin. OCT provides a high resolution in the micron range with an imaging depth of about 1.5mm in semitransparent tissue and therefore is particularly suitable for the imaging of the layer structure of artificial skin with thicknesses between 20 - 100µm. Due to a high quality signal to noise ratio, even small changes in signal at the boundary of the skin layers are detectable. To achieve satisfying results, we processed OCT images to reduce the speckle characteristics of the interferometric tomograms. By monitoring the growth cycle of the artificial skin tissue, we detected and analysed the changes in structure and homogeneity over the course of time.

7566-17, Session 4

Using swept source optical coherence tomography to monitor wound healing in tissue engineered skin

L. E. Smith, The Univ. of Sheffield (United Kingdom); M. Bonesi, The Medical Univ. of Vienna (Austria); R. Smallwood, S. J. Matcher, S. MacNeil, The Univ. of Sheffield (United Kingdom)

There is an increasing need for a robust simple to use non-invasive imaging technology to follow tissue engineered constructs as they develop. Our aim was to evaluate the use of swept-source optical coherence tomography (SS-OCT) to image tissue engineered skin as it developed over several weeks. Two tissue engineered skin models were produced either using de-epithelialised acellular dermis (DED) or amorphous collagen gels. In both cases the epidermis could be readily distinguished from the neodermis based on a comparison with standard destructive histology of samples. Constructs produced with DED showed more epidermal/dermal maturation than those produced using collagen. The development of tissue engineered skin based on DED was accurately monitored with SS-OCT over three weeks and confirmed with conventional histology. Furthermore it was possible to image the constructs healing after wounding with a scalpel, with or without the addition of a fibrin clot.

OCT is being used increasingly to non-invasively image tissue engineered constructs. Previous reports have shown that OCT can be used



successfully to image tissue engineered tendon and skin reconstructed from amorphous collagen gels. However to the best of our knowledge this is the first time OCT has been used to image tissue engineered skin based on DED. This is despite OCT being used increasingly in dermatology. In conclusion we would suggest that OCT shows great promise for the non-invasive imaging of optically turbid tissue engineered constructs, including tissue engineered skin.

7566-18, Session 4

The study of effects of pore architecture in chitosan scaffolds on the fluid flow pattern by Doppler OCT

Y. Yang, A. Iftimia, Keele Univ. (United Kingdom); Y. Jia, Oregon Health & Science Univ. (United States); A. El Haj, T. Gould, Keele Univ. (United Kingdom); R. Wang, Oregon Health & Science Univ. (United States)

Optimizing and fully understanding the dynamic culture conditions in tissue engineering technique will accelerate exploration of this new technique into a promising therapy in the medical field. Scaffolds used in tissue engineering usually are highly porous with various pore architecture depending on manufacture techniques. Perfusing culture fluid through a scaffold in a bioreactor has proved to be an efficient method to enhance exchanging of nutrients and gas within cell-scaffold constructs. Upon the perfusion, flowing fluid in pores inevitably produces shear stress on the wall of the pores, which will induce cellular response for the cells possessing mechanotransducers. Thus, establishing a relationship between perfusion rate, fluid shear stress and pore architecture in a 3-dimensional cell culture environment is a challenging task faced by tissue engineers because the same inlet flow rate could induce local variation of flow rate within the pores. Until present, there is no proper non-destructive monitoring technique capable of measuring flow rate in opaque thick objects. In this study, chitosan scaffolds with altered pore architectures were manufactured by freeze-drying or alkaline gelation techniques. Doppler optical coherence tomography (DOCT) has been used to differentiate the flow rate pattern within scaffolds which have either lamellar pore structure or homogeneous spherical pore structure. The structural and flow images have been obtained for the scaffolds. It is found that pore interconnectivity is critically important in obtaining a steady flow under a given inlet flow rate. In addition, different internal pore structures affect local flow rate pattern.

7566-19, Session 4

Understanding the nature of optical coherence tomography images using Monte Carlo modeling

P. H. Tomlins, National Physical Lab. (United Kingdom) and Univ. of Birmingham (United Kingdom); A. Beaumont, National Physical Lab. (United Kingdom)

Optical coherence tomography has generated substantial interest within the research community and this is now beginning to translate into clinical applications, beyond ophthalmology. The development of technologies to increase imaging speed and sensitivity is well established, to the point that commercial exploitation is increasingly widespread.

However, there are still fundamental questions regarding OCT image formation and interpretation. This is of particular importance in tissue engineering and regenerative medicine, where the quality control afforded by quantitative analysis is of great value.

In this study, we have chosen to implement a Monte Carlo simulation of an OCT system in order to investigate elements of the underlying physics of OCT images. Of particular interest is the signal decay primarily attributable to optical scattering, refractive index variations, including

index matching, and how these are affected by the inherent broadband nature of light-sources employed in OCT imaging. We present clinical results from oral soft tissue in which the simulated phenomena are observed and discuss the potential implications for regenerative medicine and tissue engineering.

7566-20, Session 4

Common-path endoscopic Fourier domain OCT with a reference Michelson interferometer

R. Wang, J. Zinkovich, X. Yuan, Clemson Univ. (United States); R. Goodwin, Univ. of South Carolina (United States); R. R. Markwald, Medical Univ. of South Carolina (United States); H. Yao, B. Z. Gao, Clemson Univ. (United States)

Endoscopy and catheter-based optical coherence tomography (OCT) has enabled high resolution imaging in deep tissue regions. In conventional endoscopic OCT, motion of the sample-arm fiber leads to polarization mismatch between the reference and the sample beams, resulting in fading signals. (CPOCT) is able to remove this mismatch as both beams share the same physical path. Typical CPOCT uses a precisely aligned cover glass in the sample arm to provide reference beam or a conicaltip of the optical fiber to serve both as reference mirror and focusing lens. Those configurations require that the sample is very close to the reference mirror, and is thus not suitable when circumferential scanning is needed, especially for large lumens such as the gastrointestinal tract.

Here we report a common-path OCT for endoscopic application that uses the distal end surface of the fiber as reference mirror, which is self-aligned. In the miniaturized probe of this OCT system, the transmission light was focused into the tissue sample by a grin lens. To compensate the optical path difference between the reference and the sample beams, an outside reference Michelson interferometer was used to offset the optical path. This configuration avoided attaching the sample very close to the reference mirror, allowed enough space for imaging optics and package, and was suitable for OCT imaging of various types of lumens.

With high speed spectrometer, our system could achieve 18,000 lines/s scanning speed. A SLD source was used and provided a spectrum with 40nm bandwidth centered at 850nm after filter group, and 6µm axial resolution was achieved.



Conference 7567: Design and Performance Validation of Phantoms used in Conjunction with **Optical Measurement of Tissue**

Saturday 23 January 2010 • Part of Proceedings of SPIE Vol. 7567 Design and Performance Validation of Phantoms Used in Conjunction with Optical Measurement of Tissue II

7567-01, Session 1

The need for validation standards in medical imaging

R. J. Nordstrom, L. Clarke, National Institutes of Health (United States)

Imaging as a biomarker is becoming a motivating factor in imaging research. By replacing disease or drug intraction outcome, imaging can serve as a surrogate endpoint, thus offering more rapid knowledge to the researcher. However, this function must be validated in order to determine whether imaging is indeed able to perform this task. Optical methods for imaging generally fall into two categories; those that record the field of view photographically, and those that require reconstruction of the final image from intermediate signals. Tomography is an example of the latter, while methods of confocal microscopy are examples of the former. Validation of data collection, instrument performance and reproducibility, and image information content are all required for proper validation. Tissue phantoms can play an important role in this procedure. An overview of the role of phantoms and the types of phantoms needed in optical measurements will be presented.

7567-02, Session 1

Quality control and assurance for validation of DOS/I measurements

W. W. Mantulin, B. J. Tromberg, A. Durkin, T. Quang, R. Kwong, Univ. of California, Irvine (United States); N. MacKinnon, OneLight Corp. (Canada); A. Cerussi, Univ. of California, Irvine (United States)

Ongoing multi-center clinical trials are crucial for Biophotonics to gain acceptance in medical imaging. In these trials, quality control (QC) and assurance (QA) are key to success and provide "data insurance." Quality control and assurance deal with standardization, validation, and compliance of procedures, materials and instrumentation. Specifically, QC/QA involves systematic assessment of testing materials, instrumentation performance, standard operating procedures, data logging, analysis, and reporting. QC/QA are important for FDA accreditation and acceptance by the clinical community. Our Biophotonics research in the Network for Translation in Optical Imaging (NTROI) program focuses on QA/QC issues primarily related to the broadband Diffuse Optical Spectroscopy and Imaging (DOS/I) instrumentation, because this is an emerging technology with limited standardized QC/QA in place. In the multi-center trial environment, we implement QA/QC procedures: 1. Standardize and validate calibration standards and procedures. (DOS/I technology requires both frequency domain and spectral calibration procedures using tissue simulating phantoms and reflectance standards, respectively.) 2. Standardize and validate data acquisition, processing and visualization (optimize instrument software-EZDOS; centralize data processing) 3. Monitor, catalog and maintain instrument performance (document performance; modularize maintenance; integrate new technology) 4. Standardize and coordinate trial data entry (from individual sites) into centralized database 5. Monitor, audit and communicate all research procedures (database, teleconferences, training sessions) between participants ensuring "calibration." Our presentation will detail our ongoing efforts, successes and challenges to implement these strategies.

7567-03, Session 1

Contrast phantoms for optical coherence tomography

P. H. Tomlins, P. D. Woolliams, R. Ferguson, C. Hart, National Physical Lab. (United Kingdom)

As optical coherence tomography (OCT) matures into a viable clinical imaging technology, serious questions are now being asked regarding its ability to provide contrast between features of clinical relevance.

In this work we present a series of contrast phantoms and their use to quantitatively determine the 'contrast' performance of an OCT instrument. In this initial study of contrast, we have produced resin based, solid, bi-layer phantoms, each layer doped with a different density of titanium dioxide to provide scattering contrast. The phantom refractive index was held constant with only the relative scattering coefficient between the two layers being varied. The relative scattering coefficient was varied over a number of samples to provide a graded contrast test. By choosing scattering properties close to those reported in the literature for various tissue types, we have determined a contrast metric to specify the ability of OCT to discriminate between tissue types. This has important implications from a quality control perspective as well as providing a quantitative method for the inter-comparison of OCT instrumentation operating in different wavebands, a subject of current interest to the OCT community.

7567-04, Session 1

Characterizing deep optical-sectioning microscopy performance with scattering phantoms and numerical simulations

J. T. C. Liu, M. J. Mandella, G. S. Kino, C. H. Contag, Stanford Univ. (United States)

Microscopes are being developed for use in living animals, and even humans, to image microanatomical changes and molecular markers that are associated with disease. Phantoms that can be used to evaluate the performance characteristics of these systems have not been well described or standardized. We have been developing the tools to evaluate a dual-axis confocal (DAC) microscope design to optimize the features required for in vivo diagnosic imaging, and these may have features that are useful for evaluation of other such devices. We have performed diffraction-theory modeling, Monte-Carlo scattering simulations, reflectance experiments in tissue phantoms, and tissueimaging. First, we determined how scattering from tissue deteriorates the diffraction-limited transverse and vertical responses in reflectance DAC imaging. Specifically, the vertical and transverse responses of the DAC to a plane reflector and a knife edge, respectively, were measured at various depths in an Intralipid scattering phantom. Comparisons were made with both diffraction-theory and Monte-Carlo scattering simulations. Secondly, as a practical demonstration of deep-tissue fluorescence microscopy, three-dimensional fluorescence images were obtained in thick human biopsy samples. These results demonstrate that the efficient rejection of scattered light in a DAC microscope enables deep optical sectioning in tissue. Finally, we will discuss our needs and plans for similar tissuephantom experiments to validate the performance of multimodal opticaland ultrasound-imaging platforms under development. As devices are developed for the imaging of epithelial surfaces and substructures, standardized phantoms that represent the multilayered anatomical features of these tissues will need to be developed.

TEL: +1 360 676 3290 · +1 888 504 8171 · customerservice@spie.org

Conference 7567: Design and Performance Validation of Phantoms used in Conjunction with Optical Measurement of Tissue



7567-05, Session 2

Multilayer silicone phantoms for the evaluation of quantitative optical techniques in skin imaging

R. B. Saager, C. Kondru, K. Au, K. Sry, F. Ayers, A. J. Durkin, Univ. of California, Irvine (United States)

With the development of multilayer models for the analysis of quantitative spectroscopic techniques, there is a need to generate controlled and stable phantoms capable of validating these new models specific to the particular instrument performance and/or probe geometry. Direct applications for these multilayer phantoms include characterization or validation of depth penetration for specific probe geometries or describing layer specific sensitivity of optical instrumentation.

We will present a method of producing interchangeable silicone phantoms that vary in thickness from 90 microns up to several millimeters which can be combined to produce multilayered structures to mimic optical properties of physiologic tissues such as skin. The optical properties of these phantoms are verified through inverse adding-doubling methods and the homogeneous distribution of optical properties will be discussed.

Initial investigations into instrument validation employing these phantoms, such as characterizing depth penetration of a combined Steady State and Frequency Domain (SSFDPM) superficial diffusing probe or the effectiveness of melanin compensating models for quantitative spatial frequency domain wide-field functional imaging techniques, will be discussed.

7567-06, Session 2

Development of an autofluorescent probe designed to help brain tumour removal: preliminary phantom and simulation studies

B. Leh, Univ. Paris-Sud 11 (France); R. Siebert, CNRS, Univ. Paris-Sud 11 (France); Y. Charon, Univ. Paris 7 (France); M. Duval, Univ. Evry P6 (France); F. Lefebvre, CNRS, Univ. Paris-Sud 11 (France); L. Menard, Univ. Paris 7 (France)

The success of chirurgical treatment of brain tumours, e.g. Glioblastoma, is directly related to the precision of the tumour resection and thus influences life quality and prognosis of the patient. Autofluorescence spectroscopy is one possible way to discriminate cancerous from healthy brain tissues and we are developing a new fibre probe for this issue.

To evaluate the sensitivity of such a probe as a function of different optical and geometrical parameters each related to cancerous or healthy tissues, optical calibrated phantom measurements are essential. Our phantoms are made of gel (gelatine of porcine skin, 10%), India ink (absorber), microparticles of glass (scatterer), and fluorophores (RhB or FITC). Thus the optical properties of our phantoms can be adapted to those found in literature for healthy and cancerous brain tissues. Various phantom geometries have been used: bi-layered phantoms for checking the impact of different thicknesses of the upper layer; phantoms with cylindrical inclusions of different depths and diameters. Methods to minimise boundary issues between the different layers and inclusions will be shown and remaining influence on the results will be discussed.

A Monte Carlo based program has been developed too to simulate the fluorescence detection. It first models the propagation and absorption of the excitation light in the tissue and, subsequently, simulates the propagation and detection of the fluorescence photons. Experimental results of the probe sensitivity are shown and compared to the simulated data.

7567-07, Session 2

Correlation between collagen phantoms and skin containing methylene blue

E. Morandé Sales, Univ. de São Paulo (Brazil); N. A. Daghastanli, Univ. Federal do ABC (Brazil); D. F. Teixeira da Silva, Univ. Nove de Julho (Brazil); M. d. S. Baptista, R. Itri, Univ. de São Paulo (Brazil)

Phantoms do not possess the complex structures of the biological tissues and can be used in comparison those tissues and provide a qualitative means of testing the parameters and assumptions made with mathematical or optical parameters. Thus we measured the transmittance of red laser light, P= 40mW, wavelength of 664nm, through collagen phantoms containing methylene blue (MB) and Intralipid to compare with the results carried out in vitro with fresh skin samples containing MB obtained from post-mortem of Wistar rat. Light scattered at 90° from the direction of the laser beam was collected with an Electron Multiplying CCD camera to analyze its distribution and inferred about how penetration depth and maximum intensity position changed with time. For the collagen samples with low concentrations or without Intralipid, the effective attenuation coefficient (µeff) was 7.5x10-4cm-1M-1, while for samples containing higher concentrations of Intralipid μeff was 15x10-4cm-1M-1. Even thought it wasn't possible to measure the µeff for skin, our results indicated that the transmitted light through skin is compatible with the value measured for phantoms with the highest concentration of Intralipid. Our results indicate that the predominating effect in the light transmittance is the scattering, even at the presence of the cromophore. It was possible to observe that the distribution in skin was not homogeneous as one could see in the phantoms and maximum intensity position in skin was 1.6mm, while in the phantoms was 1mm.

7567-08, Session 2

Monte Carlo simulations combined with experimental measures: a new possibility of study of the light distribution in fat emulsions

A. L. Ramos, M. Souza, A. C. Magalhães, M. Saito, M. C. Chavantes, E. Yoshimura, Univ. de São Paulo (Brazil)

Monte Carlo Simulations (MCS) has become an important tool for dosimetry.

We used the code MCML(1.2.2-2000) to simulate light distribution in Lipovenos® 10%(Lp) layers with various thicknesses illuminated by a red laser beam. With the results, the light fluence distribution at the bottom of the layer and profile of light fluence along a plane distant 5.8mm from the laser beam were calculated. The results show that the light transmitted to the bottom of the sample has a Gaussian distribution with widths that increase linearly with the thickness. Also, the maximum light intensity and the total fluence transmitted across the sample have an exponential decay behavior with the thickness.

To validate the simulation an experiment has been carried out, acquiring pictures with a CCD camera of the light transmitted and the light scattered at 90° from a PMMA cuvette containing different quantities of Lp, illuminated from the top with He-Ne laser. The experimental result showed a maximum intensity of light transmitted curve with an asymptotic exponential coefficient of 9.05cm-1, very similar to the simulation result. The variation of the Gaussian widths of the simulated and experimental results were basically the same, with compatible angular coefficients. The simulated light profile at 5.8mm from the incidence plane are very similar to the experimental curve of light intensity with depth, whose maximum occurs at 3.0mm with asymptotic exponential coefficient of 3.9cm-1.

These results show that images of illuminated tissue combined with MCS can contribute with the evaluation of light intensity distribution inside injured tissue.

Conference 7567: Design and Performance Validation of Phantoms used in Conjunction with Optical Measurement of Tissue



7567-09, Session 2

Uncertainty analysis of time resolved transmittance characterization of solid tissue phantom

J. Bouchard, I. Noiseux, S. Leclair, M. Fortin, O. Mermut, INO (Canada)

Solid tissue phantom are the preferred tool for the development, validation, testing and calibration of photon migration instrument. Accuracy, or trueness, of the optical properties of reference phantoms is of the utmost importance as they will be used as the conventional true value against which instrument errors will be evaluated. A comparative analysis of error sources of time resolved transmittance (reflectance), frequency resolved transmittance (reflectance) and continuous wave total transmittance and reflectance will be presented. Time resolved transmittance is shown to be less error prone and to have random error sources that are easier to model. A detailed quantitative analysis of the uncertainty of time-resolved transmittance characterization of solid optical tissue phantom is then presented. The terminology and methodology for uncertainty evaluation follows the directive of the International Committee for Weight and Measures (CIPM). Random error sources taken into account are Poisson noise of the photon counting process and additive dark count noise. Systematic error sources taken into account are: phantom dimension uncertainty, instrument response function stability, refractive index uncertainty, anisotropy factor uncertainty, time correlated single photon counting system time base calibration uncertainty and linearity. Correction procedure for these systematic errors will be presented whenever a correction is possible.

7567-10, Session 3

Development of optical phantoms for use in fluorescence-based imaging

I. Noiseux, M. Fortin, S. Leclair, J. Osouf, O. Mermut, INO (Canada)

In the field of fluorescence-based molecular imaging, development of optical standards and imaging phantoms with stable fluorescence properties and accurately characterized optical properties are necessary. Phantoms are used in systems calibration, inter-system comparisons, instrument development and methodology implementation. The optical parameters of tissues, specifically their absorbance, luminescence and scattering properties, are mimicked by phantoms. In fluorescence imaging of tissues, the determination of optical properties is a critical step for retrieving the concentration of fluorophores in vivo. Currently, there are no fluorescent phantoms standards with controlled scattering properties available.

We fabricated solid polyurethane-based phantoms in which Cy5 and quantum dot (QD) fluorophores were homogeneously incorporated in the phantoms. Fluorescent inclusions are incorporated into a matrix for which scattering and absorbance properties are well characterized and mimic the optical properties and luminescence of tissues. The casting of fluorophores in a matrix affects the molecular extinction coefficient and the resultant fluorescence intensity. We measured both the molecular extinction coefficient and fluorescence intensity of both Cy5 and QD in solution and in polyurethane matrix in order to evaluate the impact of the casting process on the optical properties of the dyes. Since the fluorescence intensity of dyes in solution decrease over the time, we also compared the intensity of dyes in the matrix vs. that in solution over a period - than 3 months. It was observed that the incorporation of dyes permit long-term stability of the fluorescence signal compared to what was observed in solution..

7567-11, Session 3

Lateral scattered light used to study laser light propagation in turbid media phantoms

C. Valdes, E. Solarte, Univ. del Valle (Colombia)

Laser light propagation in soft tissues is a problem of great interest because of the growing biomedical applications of lasers and the need to optically characterize the biological media. In order to determine appropriate doses and the intensities of radiation required to achieve a desired effect carefully measurements and modeling of light propagation in such media must be done. Following previous developments of the group, we have developed low cost models, Phantoms, of the soft tissue. The process was developed in a clean room to avoid the medium contamination. Each model was first characterized by measuring the refractive index with a standard Abbe refractometer, and by spectral reflectance and transmittance measurements. To study the propagation of laser light, each model was illuminated with a clean beam of laser light, using sources such as He-Ne (632nm) and DPSSL, (532 and 473 nm). The light intensity was controlled for the diverse LED sources. The laterally scattered light was imaged and the images were processed digitally to gray scale. We analyzed the intensity distribution of the scattered radiation in order to obtain details of the beam evolution in the medium. Line profiles taken from the intensity distribution surface allow measuring the beam spread, and to find expressions for the longitudinal (along the beam incident direction) and transversal (across the beam incident direction) intensities distributions. From these behaviors, the radiation penetration depth and the total coefficient of extinction have been determined. The multiple scattering effects were remarkable, especially for the low wavelength laser beams.

7567-12, Session 3

Polyurethane phantoms with homogeneous and nearly homogeneous optical properties

V. T. Keränen, Oregon Health and Science Univ. (United States) and Univ. of Oulu (Finland); A. J. Mäkynen, Univ. of Oulu (Finland); A. L. Dayton, S. A. Prahl, Oregon Health and Science Univ. (United States)

Phantoms with controlled optical properties are often used for calibration and standardization. The phantoms are typically prepared by adding absorbers and scatterers to a clear host material. It is usually assumed that the scatterers and absorbers are uniformly dispersed within the medium. To explore the effects of this assumption, we prepared paired sets of polyurethane phantoms (both with identical masses of absorber, india ink and scatterer, titanium dioxide). Polyurethane phantoms were made by mixing two polyurethane parts (a and b) together and letting them to cure in the polypropylene container. The mixture was degassed before curing to ensure sample without bubbles. The optical properties were controlled by mixing titanium dioxide or india ink into polyurethane part (a or b) before blending the parts together. By changing the mixing sequence, we could change the aggregation of the scattering and absorption particles. Each set had one sample with homogeneously dispersed scatterers and absorbers, and a second sample with slightly aggregated scatterers or absorbers. We found that the measured transmittance could easily vary by a factor of twenty. The estimated optical properties (using the inverse adding-doubling method) indicate that when aggregation is present, the optical properties are no longer proportional to the concentrations of absorbers or scatterers.

TEL: +1 360 676 3290 · +1 888 504 8171 · customerservice@spie.org

Conference 7567: Design and Performance Validation of Phantoms used in Conjunction with Optical Measurement of Tissue



7567-13, Session 3

Development and validation of multilayered scattering and absorbing polyurethane phantoms

S. Ruderman, V. Stoyneva, J. D. Rogers, A. J. Gomes, V. Backman, Northwestern Univ. (United States)

Calibration standards are needed for evaluation of fiber-optic probe performance used for testing and measurements of tissues with polarization-gated spectroscopy. We describe a method for the preparation of a novel multi-layered polyurethane phantom that replicates the optical properties of stratified biological tissue. The absorption properties are controlled through the addition of Epolin 5532 (absorption peak at 500 nm), and the scattering properties are controlled by the addition of titanium dioxide particles to the polyurethane. An ideal phantom incorporates multiple layers with independently determined scattering and absorption. The resulting phantom possesses quantified absorption coefficients and reduced scattering coefficients that can mimic different characteristics within tissue, including epithelial, connective tissue and microvasculature layers. The optical properties of the constructed phantoms were validated with an integrating sphere and tested with our previously designed fiber-optic probes. Varying the thickness of a non-absorbing top layer between 0 and 500 microns allows for characterization of the scattered signal as a function of depth. The ability to measure this signal profile enables optimization of the design for fiber-optic probes that can target specific depths within a sample. We demonstrate that the optical properties of the multi-layered phantom can be simulated from the characterization and quantification of thin single-layered phantoms. We show the results of experimental measurements and compare to the predicted characteristics.

7567-14, Session 3

Tissue-mimicking optical phantoms for validation and multi-center standardization of spectroscopic devices: the Ramanujam lab experience

J. Q. Brown, N. Ramanujam, Duke Univ. (United States)

Tissue-mimicking phantoms play a critical role in the development and validation of optical tissue-interrogation modalities. Furthermore, tissue-mimicking phantoms which allow for standardization of optical measurements across institutions are of extreme importance. In the Ramanujam laboratory at Duke University, liquid phantoms are used extensively for validation of developing technologies. However, they are also used for standardization of measurements across various instruments and clinical sites in a number of clinical studies currently underway at Duke University Hospital, Duke University Ambulatory Surgery Center, and the VA Hospital-Durham. The design of optical tissue phantoms may vary according to application. For instance, for technology validation, the most important aspect of the phantom may be to achieve a phantom which most closely approximates the optical properties (i.e., scattering, absorption, fluorescence) of the tissue of interest. This leads to the selection of chromophores and scatterers which closely mimic the properties of tissue, but are not necessarily stable with respect to time, temperature, or other factors. However, for standardization or calibration of measurements across instruments or institutions, the materials used for phantom construction must be carefully chosen to provide phantoms which are stable and resistant to drift, or which are otherwise amenable to reproducible construction in the field. Here, the most important requirement is that the optical properties of the phantom are known exactly, which dictates that they be carefully characterized once and remain stable over time, or that methods for reliable characterization in the field are also available. In this presentation, we will discuss the use of phantoms in our laboratories for technology development and standardization, and will share the methods, techniques, and technologies we have developed to address these challenges.

7567-15, Session 4

Spectral imaging of a simple tissue phantom for re-projection in the NIST hyperspectral image projector

M. Litorja, E. L. Shirley, D. W. Allen, National Institute of Standards and Technology (United States)

The NIST Hyperspectral Image Projector (HIP) was developed to enable system-level evaluation of field hyperspectral imagers for environmental remote sensing. These imagers are currently evaluated using spatially uniform radiance and reflectance standards while data retrieval algorithms are evaluated independently through simulations. Similarly, optical imagers for biomedical use can be calibrated and validated using the HIP system, which can re-project complex images with spectral information. The conventional method of preparing tissue phantoms in the laboratory to mimic the in vivo scene which the optical system views during use, is here updated using the HIP system. A simple tissue phantom is prepared, imaged using a laboratory hyperspectral imager and re-projected by the HIP. Projection of images of various modifications of the tissue phantom will demonstrate the utility of the digital tissue phantom.

7567-16, Session 4

Design of a multimodality breast-like phantom for combined optical tomography and ultrasound measured in transmission geometry

M. T. Ghijsen, B. Unlu, O. Nalcioglu, G. Gulsen, Univ. of California, Irvine (United States)

In this project, we seek to create a multimodality imaging phantom meant to mimic the optical and acoustic properties of breast tissue for near infrared light and ultrasound in the vicinity of 2 MHz. This multimodality phantom will be used to take measurements in DOT and ultrasound in transmission mode and will prospectively simulate tissue in studies of a combined DOT-US system.

The phantom must imitate the optical and acoustic properties of breast tissue. The key will be to find a material capable of modeling proper acoustic attenuation without adversely affecting the optical properties; a few materials are currently being explored. Once a material is selected and its attenuation is characterized, a heterogeneous phantom will be created. This phantom will have several inclusions meant to model glandular and adipose tissues in addition to tumors.

In order to validate the phantom, a DOT system will test the optical properties of the phantom to ensure their integrity in comparison to more conventional optical phantoms. The frequency domain DOT system we use takes data at multiple wavelengths. To test the acoustic attenuation, the phantom will be placed in a water bath where dual transducers will measure the ultrasound signal in transmission mode.

7567-17, Session 4

Multilayer tubular phantoms for optical coherence tomography

C. Bisaillon, G. Campbell, C. deGrandpré, M. L. Dufour, G. Lamouche, National Research Council Canada (Canada)

Many medical applications of optical coherence tomography (OCT), target tissue structures with tubular shapes (i.e. blood vessels). These tissues are often composed of one or more tissue layers. We previously reported a method to produce tubular phantoms composed of multiple layers to mimic these tissues. Calibrated concentrations of alumina and carbon black are mixed with silicone to replicate the OCT signal of each

Conference 7567: Design and Performance Validation of Phantoms used in Conjunction with Optical Measurement of Tissue



tissue layer for a specific structure. With specific formulations of silicone, the elasticity of soft tissue is also mimicked, but for small deformations. For high deformations, most tissues show a strain hardening effect (or elastic "J" curve) that is not mimicked by this method. Furthermore, the field of use for these phantoms is limited to the OCT imaging technique.

In this presentation, these two issues of optical and elastic properties are addressed. Materials and formulations are being investigated to mimic the mechanical properties soft tissues and to target additional imaging techniques like Magnetic Resonance Imaging (MRI) or Ultrasound imaging.

7567-18, Session 4

Design of a dynamic optical tissue phantom to model extravasation pharmacokinetics

J. Y. Zhang, A. Ergin, K. L. Andken, Boston Univ. (United States); C. Sheng, East Carolina Univ. (United States) and Brody School of Medicine (United States); I. J. Bigio, Boston Univ. (United States)

We describe an optical tissue phantom that enables the simulation of drug extravasation from microvessels. The phantom consists of a microdialysis tubing bundle to simulate the permeable blood vessels, immersed in either an aqueous suspension of titanium dioxide (TiO2) or an agarose scattering medium. The intent is to facilitate testing of optical pharmacokinetics (OP) methods for monitoring local drug delivery to tissues in vivo, and to validate computational compartmental models of drug delivery. Our dynamic tissue phantom implements OP to monitor the vessel diffusivity and extravasation kinetics. To simulate drug administration, an optical dye is circulated through the porous microdialysis tubing bundle. OP spectroscopy is used to measure changes in the absorption coefficient of the scattering medium due to the arrival and diffusion of the dye. We have established time and particle size dependent concentration profiles to compare the phantom simulation of drug delivery by intravenous (IV) and intra-arterial (IA) routes. Additionally, pharmacokinetic compartmental models are implemented in computer simulations of drug extravasation from the blood vessels, for the conditions studied with the phantom. The simulated concentration-time profiles agree well with measurements from the phantom. The results are encouraging for future optical pharmacokinetic method development, both physical and computational, to understand drug extravasation under various physiological conditions.

7567-19, Session 4

Developing multifunctional tissue simulating phantoms for quantitative biomedical optical imaging

R. X. Xu, J. S. Xu, J. Huang, R. Qin, J. Ewing, The Ohio State Univ. (United States)

Background:

Major advantages of biomedical optical imaging modalities include low cost, portability, no radiation hazard, molecular sensitivity, and real-time non-invasive measurements of multiple tissue parameters. However, clinical acceptance of optical imaging is hampered by the lack of calibration standards and validation techniques.

Method:

Over the years, we have developed various tissue simulating phantoms for validation and calibration of biomedical optical devices. These phantoms fall into three categories: (1) liquid phantoms with embedded heterogeneities and controlled optical properties to simulate various tissue physiologic conditions, (2) portable solid phantoms to simulate tissue structural and functional characteristics, (3) multifunctional phantoms with concurrent contrast in multiple imaging modalities.

Results:

- (1) Several optical imaging and spectroscopic devices have been validated on liquid phantoms containing Intralipid, blood, and India ink, with oxygenation levels controlled by a membrane oxygenator.
- (2) Compression induced tissue structural, functional, and optical property changes have been studied on tissue-simulating gel wax phantoms at different dynamic loading condition.
- (3) Multifunctional microbubbles have been used to fabricate phantoms with strong contrast in multiple imaging modalities such as ultrasound, fluorescence, and photoacoustic imaging.

Conclusion:

The phantom systems developed in our lab have the potential to provide standardized traceable tools for quantitative optical imaging and multimodal image co-registration.

7567-20, Session 4

Fabricating multifunctional microbubbles and nanobubbles for concurrent ultrasound and photoacoustic imaging

R. Qin, J. S. Xu, R. X. Xu, The Ohio State Univ. (United States); C. Kim, L. V. Wang, Washington Univ. in St. Louis (United States)

Background: Clinical ultrasound (US) uses ultrasonic scattering contrast to characterize subcutaneous anatomic structures. Photoacoustic (PA) imaging detects the functional properties of thick biological tissue with high optical contrast. In the case of image-guided surgical oncology, simultaneous US and PA imaging can be useful for intraoperative assessment of tumor boundaries and therapeutic margins. In this regard, accurate co-registration between imaging modalities and high sensitivity to cancer cells are important.

Methods: We synthesized poly-lactic-co-glycolic acid (PLGA) microbubbles (MBs) and nanobubbles (NBs) encapsulating India ink or indocyanine green (ICG). Multiple tumor simulators were fabricated by entrapping ink MBs or NBs at various concentrations in gelatin phantoms for simultaneous US and PA imaging. MBs and NBs were also conjugated with CC49 antibody to target TAG-72, a human glycoprotein complex expressed in many epithelial-derived cancers.

Results: Accurate co-registration and intensity correlation were observed in US and PA images of MB and NB tumor simulators. MBs and NBs conjugating with CC49 effectively bound with over-expressed TAG-72 in LS174T colon cancer cell cultures. We also encapsulated ICG in MBs and demonstrated concurrent contrast in US and fluorescence imaging modalities

Conclusions: Multifunctional MBs and NBs can be potentially used as a general contrast agent for multimodal intraoperative cancer imaging.

Return to Contents TEL: +1 360 676 3290 · +1 888 504 8171 · customerservice@spie.org



Saturday-Monday 23-25 January 2010 • Part of Proceedings of SPIE Vol. 7568 *Imaging, Manipulation, and Analysis of Biomolecules, Cells, and Tissues VIII*

7568-04, Session 1

Gold nanorods for cell imaging with confocal reflectance microscopy and two-photon fluorescence microscopy

J. Y. Chen, P. Wang, Fudan Univ. (China)

Due to the characteristics of biosafety, high reflection coefficients and high two-photon absorption cross sections, gold nanorods have been considered as agents for cell imaging. In this report, two methods, twophoton fluorescence microscopy and confocal reflectance microscopy, were comparatively studied to detect cellular gold nanorods in living rat basophilic leukemia (RBL-2H3) cells. Two-photon photoluminescence (TPL) images of gold nanorods in living cells can be acquired by the 800 nm femto-second (fs) laser in mW level with the advantages of high spacial resolution and low background. This high power was necessary for the TPL acquiring, but the cell damaging appeared after 30 times continuous scanning of fs laser demonstrating that the seriously photothermal effect occurred. The remarkable photothermal effect is probably the disadvantage of TPL for cell imaging with gold nanorods, because the cell damaging is unwanted and the original distribution of cellular gold nanorods may be changed. The 3-D images of cellular gold nanorods were also achieved with this fs laser of 50 µW in confocal reflectance microscopy, avoiding the serious photothermal effect, but the imaging resolution was relatively poor. Therefore, by combining the TPL and confocal reflectance images with the same 800 nm fs laser, gold nanorods could be the flexible agents for cell imaging.

7568-33, Session 1

Two-photon microscopy of living cells by simultaneously exciting multiple endogenous fluorophores and fluorescent proteins

W. Zheng, D. Li, J. Y. Qu, Hong Kong Univ. of Science and Technology (Hong Kong, China)

Endogenous fluorophpores, such as reduced nicotinamide adenine dinucleotide (NADH), keratin, and tryptophan, have been used as contrast agents for imaging metabolism and morphology of living cells and tissue. Multilabeling which maps the distribution of different targets is an indispensable technique in many biochemical and biophysical studies. Therefore, two-photon excitation fluorescence (TPEF) microscopy of endogenous fluorophores combining with in vivo fluorescence labeling techniques such as genetically encoded fluorescent protein (FP) could be a powerful tool for imaging living cells and tissue. However, the challenge is that the excitation and emission wavelength of these endogenous fluorophore and fluorescence labels are very different. A multi-color ultrafast source is required for the excitation of multiple fluorescence molecules. In this study, we developed a two-photon imaging system with excitations from the pump femtosecond laser and the selected supercontinuum generated from a photonic crystal fiber (PCF), Multiple endogenous fluorophore and fluorescent proteins such as NADH, green fluorescent protein, yellow fluorescent protein and red fluorescent protein were excited in their optimal wavelengths simultaneously. A time- and spectral-resolved detection system was used to record the TPEF signals. This detection technique separated the TPEF signals from multiple sources in time and wavelength domains. Cellular organelles such as nucleus, mitochondria, microtubule and endoplasmic reticulum, were clearly revealed in the TPEF images. Finally, we use the two-photon microscopy system to image transgenic animals and produce coregistered images of endogenous and FP fluorescence.

7568-38, Session 1

The fluorescence lifetime of BRI1-GFP as probe for the noninvasive determination of the membrane potential in living cells

K. Elgass, K. Casear, Eberhard Karls Univ. Tübingen (Germany); Z. Chen, Univ. of Glasgow (United Kingdom); F. Schleifenbaum, A. J. Meixner, Eberhard Karls Univ. Tübingen (Germany); M. R. Blatt, Univ. of Glasgow (United Kingdom); K. Harter, Eberhard Karls Univ. Tübingen (Germany)

As the excited state lifetime of a fluorescent molecule depends on its environment, it is possible to use it as a probe for physico-chemical parameters of the surrounding medium. Whereas this is well known for organic dyes, only few reports of quantitative, temporal resolved in vivo studies to monitor a chromophoric nano-environment are known from literature. Here we present a novel method to determine the membrane potential of living cells based on the fluorescence lifetime analysis of membrane-located GFP.

By using confocal sample scanning microscopy (CSSM) combined with fluorescence lifetime (FLT) imaging microscopy, we recently showed that brassinolide (BL) induces cell wall expansion and a decrease in the FLT of BRI1-GFP in living cells of Arabidopsis thaliana seedlings. Although the dependence of the GFP FLT on its physico-chemical environment e.g. pH-value, refractive index and pressure has been reported, the observed FLT decrease of BRI1-GFP in the case of BL addition could not be explained by these parameters.

Remarkably, our in vivo FLT and CSSM data indicate that the decrease in the FLT of BRI1-GFP is caused by a BL-induced and BRI1-GFP-dependent activation of the plasma membrane P-ATPase resulting in an alteration of the membrane potential (Em). Thus, our results suggest that BRI1-GFP can serve as sensitive and non-invasive probe for recording the Em of the plasma membrane in living plant cells with high spatio-temporal resolution.

7568-48, Session 1

Nanoprocessing and targeted transfection of stem cells

K. König, JenLab GmbH (Germany); Z. Földes-Papp, ISS, Inc. (United States); H. Studier, R. Bückle, H. G. Breunig, JenLab GmbH (Germany); A. Uchugonova, Saarland Univ. (Germany); G. M. Kostner, Medical Univ. of Graz (Austria)

Multiphoton microscopes have become important tools for noncontact sub-wavelength three-dimensional nanoprocessing of living biological specimens based on multiphoton ionization and plasma formation. The novel ultracompact multiphoton sub-20 femtosecond near infrared 85 MHz laser scanning microscope Femtogene havs been used to perform high spatial resolution two-photon imaging of stem cell clusters as well as selective intracellular nanoprocessing and knock out of living single stem cells within an 3D microenvironment without any collateral damage.

Single point illumination of the cell membrane was performed to induce a transient nanopore for the delivery of extracellular green fluorescent protein plasmids and SQMB-probes as well

Mean powers of less than 7mW (<93 pJ) and low millisecond exposure times were found to be sufficient to transfect human pancreatic and salivary gland stem cells in these preliminary studies. Also lethal cell exposure of large parts of cell clusters was successfully probed while maintaining single cells of interest alive. Furthermore the binding of superquencher molecular beacon (SQMB) probes to human single-



stranded cellular miRNA-122 targets was detected in various single live cells with femtosecond laser microscope. In single cells of the human liver cell lines Huh-7D12 and IHH that expressed miRNA-122, we measured target binding in the cytoplasm by two-photon fluorescence imaging.

The mean power could be kept in the milliwatt range for 3D nanoprocessing and even in the microwatt range for two-photon imaging. Ultracompact low power sub-20 fs laser systems may become interesting tools for optical nanobiotechnology such as optical cleaning of stem cell clusters as well as optical transfection.

7568-58, Session 1

Total internal reflection holographic microscopy for quantitative phase characterization of cellular adhesion

W. M. Ash III, D. Clark, L. Krzewina, M. K. Kim, Univ. of South Florida (United States)

A new form of near-field microscopy is presented using digital holography for quantitative phase imagery and characterization of cell-substrate interfaces. This imaging technique, termed total internal reflection holographic microscopy (TIRHM), utilizes an evanescent wave phase shift from the presence of cellular organisms, membranes, adhesions, and tissue structures on a prism face in order to modulate an object beam wavefront in a digital holographic microscope. Quantitative phase images of live cellular specimens are presented.

7568-62, Session 1

Quantification of optical disorder due to nanoscale density fluctuations in biological tissue: inverse participation ratio (IPR) analysis of transmission electron microscopy images for early-stage cancer detection

P. Pradhan, D. Damania, Northwestern Univ. (United States); H. Roy, Univ. of Chicago (United States); V. Backman, Northwestern Univ. (United States)

Recent studies suggest that there are nano-architectural changes occurring within cells during early carcinogenesis which precede the microscopically evident changes at tissue level. Most cancers are curable only if they are diagnosed and treated at the early stages. Therefore, the ability to comprehensively interrogate the nanoarchitecture (e.g., DNA, RNA, proteins, lipids, etc.) of single cells is critical to study early carcinogenesis. Nanoscale changes in cells lead to mass density variations contributing to the refractive index fluctuations. Hence, the pre-cancerous changes in tissues can be considered to be on the nanoscale. The optical disorder properties of nanoscale mass density fluctuations of biological cells/tissues are studied by quantifying their nanoscale light localization properties. TEM images of human tissues and cell lines (HT29) are used to construct corresponding effective disordered optical lattices. Light localization properties are studied by the statistical analysis of the inverse participation ratio (IPR) of the eigenfunctions of these optical lattices at the nanoscales. Our experimental results from genetically modified HT29 cell lines show a statistically significant increase of the average IPR value parallel to the increase in aggressive growth of these cell-lines. Similar trend of the average IPR values is obtained from tissues of control and adenoma (precancerous) patients. These results indicate elevation of nanoscale optical disorder strength (refractive index fluctuations) in early carcinogenesis. Importantly, our results demonstrate that the increase in the nanoscale disorder represents the earliest structural alteration in cells undergoing carcinogenesis known to date. Experiments with dielectric nanoparticles to calibrate the technique will also be discussed.

7568-72, Session 1

Effects of oxytocin on the cytoskeletal changes of human umbilical cord blood derived mesenchymal stem cells revealed by phase retardation imaging techniques

S. Shin, I. H. Shin, H. M. Park, Gwangju Institute of Science and Technology (Korea, Republic of); Y. S. Kim, Y. Ahn, Chonnam National Univ. Hospital (Korea, Republic of)

The effects of oxytocin on the cytoskeletal changes of human umbilical cord blood derived mesenchymal stem cells have been investigated using both the conventional molecular biology techniques and phase retardation imaging techniques. Oxytocin has been known to enhance the differentiation of mouse embryonic stem cells and cardiomyocytes, and migration and invasion of human endothelial cells. Oxytocin was applied to human umbilical cord blood derived mesenchymal stem cells. The conventional molecular biology techniques revealed several effects of the oxytocin treatment. Oxytocin receptors increased, tube formation was delayed, angiopoietin-1 mRNA was reduced, and transmigration activity was dramatically increased. However, the conventional technique only showed the result of the oxytocin effects. The phase retardation imaging technique clearly and vividly showed in real time the effects of oxytoin on the dynamically changing cytoskeletal structures of the mesenchymal stem cells. It will be shown that how multiple focal adhesion points in the cell are coordinating during migration and that how cells continuously reorganizing the focal adhesion points even while the cells are not migrating.

7568-76, Session 1

Three-dimensional morphologies of human breast cancer cell lines obtained using FF-OCT and confocal microscopy

S. Shin, I. H. Shin, H. M. Park, B. H. Lee, W. J. Choi, C. Jun, Gwangju Institute of Science and Technology (Korea, Republic of)

Three dimensional morphologies of human breast cancer cell lines cultured in vitro were investigated using FF-OCT and confocal microscopy. The cell lines investigated were: normal MCF 10A, weakly invasive MCF 7, highly invasive MDA MB 231 and MDA MB 435S. Conventional optical microscopy of biological cells confined to two dimensional plane views could not reveal three dimensional morphologies. Three dimensional morphologies of cells could reveal new information of the cells under study, which could lead into the discovery of new scientific aspects of cell biology and the development of new cell diagnostic methods utilizing the information from the three dimensional morphologies. The only three dimensional imaging technique currently available to biomedical researchers is confocal microscopy. However, the confocal microscopy has some drawbacks. Cells have to be stained with fluorescent dyes, and the confocal microscopy is not fast enough for imaging dynamically changing morphologies. Both the dyes and the focused scanning laser beam could adversely affect the livelihood of the cells under study. In contrast, FF OCT imaging technique is comparatively rather fast and non destructive and does not require the use of fluorescent dyes. The FF OCT images clearly showed that the cell lines have distinctive three dimensional morphological differences. Especially, the highly invasive cell lines, MDA MB 231 and 435S, were much thinner compared to the other normal and weakly invasive cell lines. Fluorescence images also showed that the thin morphologies reflected well developed actin and tubulin networks. The thinness of the highly invasive cell lines could be related in future studies to high motilities of invasive cancer cells. The images from the FF OCT were compared to those from the confocal microscope.



7568-79, Session 1

Dynamic phase imaging of host cells attacked by vibrio vulnificus using quantitative phase microscopy

S. R. Lee, W. Yang, J. Y. Lee, Gwangju Institute of Science and Technology (Korea, Republic of); M. H. Cha, Dongshin Univ. (Korea, Republic of); Y. R. Kim, Clinical Vaccine R&D Center (Korea, Republic of); D. Y. Kim, Gwangju Institute of Science and Technology (Korea, Republic of)

Vibrio vulnificus is a species of halophilic estuarine bacteria in the genus vibrio which can cause an acute cell death and a fatal septicaemia. In this study, we present the dynamic phase imaging and volume change of RBL-2H3 cells attacked by V. vulnificus for 90 minutes by using quantitative phase microscopy. For a live cell phase imaging in transparent cells, we propose quantitative phase microscopy (QPM) with a live cell incubator system to allow continuous flow input from a syringe pump. The quantitative phase microscopy is based on a common path interferometer. Two bacterial strains of V. vulnificus, wild type (MO6-24/O) and mutant type (rtxA1-), are used to study the interaction between V. vulnificus and RBL-2H3 cells. The real-time change of RBL-2H3 cells shape is observed with QPM and the cell volume is calculated during the 90 minutes. RBL-2H3 cells shape undergoes four stages such as ellipse, round, irregular and cell membrane broken after wild type V. vulnificus addition. However, cells incubated with mutant V. vulnificus for 90 minutes have no significant change. The volume of RBL-2H3 cells incubated with wild V. vulnificus remains unchanged during the first 70 minutes, but sharply decreases after another 20 minutes of treatment. Then, the cell volume reaches to a new constant level, which corresponding to the fourth stage of phase image. No any significant change of the cell volume is observed during the 90 minutes of incubation with mutant V. vulnificus. The cytotoxicity of V. vulnificus is also measured by using LDH release method. During the 60 minutes, the cytotoxicity of wild V. vulnificus has no significant difference compared with mutant, but there is considerably difference between wild and mutant at 90 minutes.

7568-03, Session 2

Resources from the National Cancer Institute to support your innovative analytical technologies for cancer

M. D. Lim, National Cancer Institute, NIH (United States)

With the rapid advance of translational medicine, progress towards a more personalized level of cancer care becomes increasingly dependent on innovative methods and technologies that can be applied across clinical and research laboratory settings. The NCI created the Innovative Molecular Analysis Technologies (IMAT, http://innovation.cancer.gov) program in 1998 to drive the inception and development of creative analytical methods and tools in support of cancer research in the area of detection, epidemiology, prevention, diagnosis, treatment and surveillance, with the goals of strengthening and catalyzing the pipeline of innovation. By taking risks on early-stage transformative tools, IMAT has been instrumental in the inception and development of many blockbuster technologies that are used universally across the cancer research and clinical communities. This IMAT support allows innovators to obtain necessary feasibility data to secure larger sources of funding from other federal agencies, venture capitalists, and NIH R01 grants. This presentation will discuss opportunities from IMAT and other resources from the NCI for innovators willing to help reduce the burden of cancer.

7568-06, Session 2

Plant abiotic stress diagnostic by laser induced chlorophyll fluorescence spectral analysis of in vivo leaf tissue of biofuel spieces

A. S. Gouveia-Neto, E. A. Silva, E. B. Costa, L. A. Bueno, L. M. H. Silva, M. M. C. Granja, M. J. Medeiros, T. J. R. Câmara, L. G. Willadino, Univ. Federal Rural de Pernambuco (Brazil)

Laser induced fluorescence(LIF) is exploited to evaluate the effect of abiotic stresses(salt stress) upon the evolution and characteristics of in vivo chlorophyll emission spectra of leaves tissues of brazilian biofuel plants species(Saccharum officinarum RB863129 and Jatropha curcas). The chlorophyll fluorescence emission spectra of the 20 min predarkened intact leaves were studied employing several excitation wavelengths in the UV-VIS spectral region. Red(Fr) and far-red (FFr) chlorophyll fluorescence emission signals around 685 nm and 735 nm, respectively, were observed and analyzed as a function of the stress intensity and the time of illumination(Kautsky effect). The Chl fluorescence ratio Fr/FFr which is a valuable nondestructive indicator of the chlorophyll content of leaves was investigated. The dependence of the Chl fluorescence ratio Fr/FFr upon the intensity of the abiotic stress(salinity) was examined. The results indicated that the salinity plays a very important hole in the chlorophyll concentration of leaves tissues in both plants spieces, with a significant reduction in the ChI content for NaCl concentrations around and beyond 100 mM. Our results agreed guite well with those obtained using conventional in vitro spectrophotometric methods. The laser induced ChI fluorescence analysis allowed detection of damage caused by salinity in the early stages of the plants growing process, and as consequence can be used as an early-warning indicator of salinity stress

7568-11, Session 2

Use of optical micro-angiography to compare pharmacological effects of tPA on reperfusion in a mouse model of ischemic injury

S. Hurst, Y. Jia, A. Lin, E. Tucker, A. Gruber, R. K. Wang, Oregon Health & Science Univ. (United States)

Optical microangiography (OMAG) is a novel noninvasive imaging technique that is capable of resolving 3D distribution of dynamic blood perfusion in real time, in vivo, at 10 micron resolution at 2 mm depth from the tissue surface. OMAG is based on the differential analysis of the Doppler effect on light scattering by moving blood cells within vessels versus stationary tissues. By using OMAG, we compared the effect of early treatment of reversible intraluminal middle carotid artery occlusion (MCAO) with tissue plasminogen activator (tPA) to vehicle (saline) on the cortical blood perfusion in a mouse model of ischemic stroke. Infusion of tPA both inhibited progressive cortical blood vessel occlusions due to thrombogenesis during MCAO, and enhanced post-MCAO reperfusion of the parietal cortex compared to saline infusion. This is the first report to demonstrate, in vivo, that the profibrinolytic agent, tPA, may act in part by reducing spatial extension of the ischemic region during occlusion of the MCA. This study validates OMAG as a useful research tool that could provide information about the mechanism of action of drugs, including tPA that has been used to treat ischemic stroke. OMAG thus has potential applications in pharmacological studies of cerebrovascular perfusion in real time, during and after MCAO-induced stroke in a mouse model without the need for tissue sampling.



7568-15, Session 2

A comparative study of different instrumental concepts for spectrally and lifetime-resolved multiphoton intravital tomography (5D-IVT) in dermatological applications

M. Schwarz, I. Riemann, F. Stracke, Fraunhofer-Institut für Biomedizinische Technik (Germany); V. Huck, Univ. of Muenster (Germany); C. Gorzelanny, S. W. Schneider, Heidelberg Univ. (Germany); S. Puschmann, V. Lutz, N. Sommer, C. Rahn, S. Gallinat, H. Wenck, K. Wittern, F. Fischer, Beiersdorf AG (Germany)

Multiphoton optical tomography or intravital tomography (IVT) provides non-invasive optical sectioning of skin with high spatial and subcellular resolution without the need for contrast agents. It can be used to distinguish between normal and diseased tissue due to the differences in morphological appearance. Additional information beyond morphology can be obtained by analyzing the collected fluorescence light spectroscopically and by means of its fluorescence decay curve. This is frequently termed spectral lifetime imaging (SFLIM) or 5D-intravital tomography (5D-IVT). Spectral and temporal resolution scales with the number of detection increments (i.e. spectral channels and time bins). This enables us to detect new physiological parameters, however accompanied with a decrease in intensity per channel. Moreover, the increase of data requests a higher need of software skills.

In this study we investigate and evaluate different technical modes of 5D-IVT with respect to their clinical relevance: (1) a 16-channel PMT array coupled to a diffraction grating, each channel being analyzed by time correlated single photon counting (TCSPC), (2) three separate PMTs in spectral separation path using dichroic mirrors, each channel being analyzed by TCSPC and (3) a single PMT TCSPC setup in combination with a high resolution CCD-spectrograph for point-wise microspectroscopy.

The study is performed on artificial and natural samples and evaluated according to clinical criteria like physiological selectivity, information content, acquisition time, and applied energy doses.

This work has been funded by the german federal ministry for education & research BMBF (grant no. 13N8292)

7568-23, Session 2

Optical coherence tomography imaging of engineered skin tissue

R. Schmitt, U. Marx, Fraunhofer-Institut für Produktionstechnologie (Germany); H. Mertsching, A. Heymer, Fraunhofer-Institut für Grenzflächen- und Bioverfahrenstechnik (Germany)

Engineered skin tissues are widely used in dermatological, pharmacological and toxicological studies and as autologous transplants in wound healing. Production processes for engineered tissue are in a high demand for automated monitoring techniques to image the internal structure and consistency of in vitro tissue products. We applied Optical Coherence Tomography OCT in tissue engineering, which offers great potential for non-invasive inline quality control. This imaging technology is based on an interferometric setup operating with low coherent near infrared NIR light to detect the inner structure of semitransparent media. OCT offers a high resolution in the micron range with an imaging depth of about 1.5mm in semitransparent tissue and therefore is particularly suitable for the imaging of engineered skin tissue. To automate the monitoring process, we processed the OCT images to detect significant characteristics in the tomograms e.g. shape, defects, homogeneity, density. The determined parameters provide information to characterize the condition and quality of the tissue. This will allow the automated exclusion of deficient tissue products and determination of ideal growth parameters for the tissue cultivation process. A great challenge lies in the automated processing of speckles, noise and varying image contract to achieve a reliable image processing. Further the parameterisation of the detected characteristics is essential to achieve comparable values. As a result, the application of optical coherence tomography in automated tissue engineering processes allows a distinct evaluation of tissue to guarantee a high quality production process.

7568-46, Session 2

Fluorescence tomography based on dispersion of biotissue absorption for small animal imaging

M. S. Kleshnin, I. V. Turchin, Institute of Applied Physics (Russian Federation); M. V. Shirmanova, Nizhny Novgorod State Medical Academy (Russian Federation); I. V. Balalaeva, N.I. Lobachevsky State Univ. of Nizhniy Novgorod (Russian Federation); V. A. Kamensky, Institute of Applied Physics (Russian Federation)

Traditionally different types of fluorescence diffuse tomography utilize many different projections: fluorescence and excitation signals propagated through an investigated object collected from different source and detector positions. The efficacy of reconstruction can be significantly increased if one uses additional information about spectral changes of light propagation in biotissue. Absorption and reduced scattering coefficients are the basic parameters describing propagation of light radiation in biotissues. Scattering coefficient weakly depends on wavelength, but absorption coefficient has a strong dispersion in the range of wavelengths of 500-650 nm. Absorption dispersion causes spectral shape changes of the optical radiation propagating through biological tissues. This phenomenon can be used for 3-D reconstruction of the fluorophore concentration. The experimental setup for fluorescence tomography based on dispersion of biotissue absorption has been created. An animal is scanned in the transilluminative configuration by a single source-detector pair. The spectrum of optical radiation propagated through the investigated object is registered by a spectrometer in each position. In our experiment we scanned experimental animal with RFP-marked tumor. We used the white light source which gives the information about biotissue absorption and scattering and the laser source which excites RFP. The obtained results have shown a basic opportunity of fluorescence tomography based on dispersion of biotissue absorption. If optical parameters of a biological tissue are well-known it is possible to make 3-D reconstruction of spatial distribution of fluorophore concentration without angular resolution in 2-D images of the examined object by changing the spectral shape of the registered fluorescence.

7568-56, Session 2

Remodeling of texture in physiological and pathological healing

D. P. Ferro, G. Vieira, A. A. de Thomaz, A. L. Randall, C. L. Cesar, K. Metze, Univ. Estadual de Campinas (Brazil)

Keloid and hypertrophic scars are abnormally healed skin wounds formed by excessive accumulation of connective tissue, especially, collagen. Hypertrophic scars form completely within the boundary of the original wound and may spontaneously regress over time while keloids extend beyond the wound boundary and tend to remain elevated. Other differences between keloids and hypertrophic scars include histologic morphology. The diagnosis is made by the follow-up of the patient and the only way to differentiate between these wounds is to monitor if the scar regress within time or not. But this process can last for a year or more. The purpose of this work was to analyze the process of healing in physiological and pathological routine histological blade and make the diagnosis promptly. Therefore we created a system based on the computerized analysis of large confocal fluorescence images. The full image of the whole sample (2 or 3mm long) was composed by several 220x220µm frames with 512x512 pixels. Then a gliding box of 128x128 pixels ran in 1-pixel steps along a predefined axis in parallel to



the bottom line of the image. For every new box, texture features were calculated and plotted in diagrams, where the position on the x-axis was equivalent to the topography in the histologic picture. For texture analysis we applied features of the co-occurence matrix, Fast-Fourier-transformed (FFT) images or the fractal dimensions. With these images we were able to make the diagnosis as soon as the blades were prepared.

7568-57, Session 2

Confocal microscopy for automatic measurement of the density and distance between elastin fibers of histologic preparations of normotensive and hipertensive patients

G. Vieira, D. P. Ferro, A. L. Randall, A. A. Thomaz, C. L. Cesar, K. Metze, Univ. Estadual de Campinas (Brazil)

Elastic fibers are essential components of the human aorta, and there is an association between elastin fibers remodeling and several diseases. Hypertension is one such example of a disease leading to elastin fibers remodeling. These fibers can be easily seen in eosin-hematoxilin (HE) stained histologic sections when observed by UV-excited fluorescence microscopy or by a much more precise Laser Scanning Confocal Microscope (LSCM). In order to study the effect of the hypertension on the elastin fibers pattern we developed an automatic system (software and hardware) to count the number of elastin fibers and to measure the distance between them in a LSCM and used it compare the statistical distribution of the distance between these fibers in normotensive and hypertensive patients. The full image of the whole sample (2 or 3mm long) was composed by several 220x220µm frames with 512x512 pixels. The software counters fiber and distance between fibers. We compared the elastic fiber texture in routinely HE-stained histologic slides of the aorta ascendens in 24 normotensive and 30 hypertensive adult patients of both sexes and of similar age from our autopsy files. Our results show that the average number of fibers is the same for both cases but the distance between the fibers are larger for hypertensive patients than for normotensive ones.

7568-74, Session 2

Specific binding of molecularly targeted agents to pancreas tumors and impact on observed optical contrast

K. S. Samkoe, O. Pardesi, J. A. O'Hara, B. Pogue, Dartmouth College (United States)

In optical imaging it is thought that optimum tumor contrast can be achieved with the use of small labeled molecular tracers that have high affinity to their targets and fast clearance rates from the blood stream and healthy tissues. An example of this is fluorescently tagged EGF to monitor the molecular activity of tumors, such as pancreatic cancer. Extensive fluorescence contrast analysis for fluorescence molecular tomography has been performed on the AsPC-1 pancreas tumor, grown orthotopically in mice; yet, the binding dynamics of the EGFfluorescent agent in vivo is not completely known. The bulk pancreatic tumor displays 3:1 contrast relative to the normal pancreas at long times after injection; however, even higher levels of fluorescence in the liver, kidney and intestine suggest that molecular specificity for the tumor may be low. Mice were administered a fluorescently labeled EGF agent and were sacrificed at various time points post-injection. To analyze the amount of specific binding at each time point frozen tissue samples were fluorescently imaged, washed with saline to remove the interstitially distributed contrast agent, and then imaged again. This technique demonstrated that approximately ~10% of the molecular target was firmly bound to the cell, while 90% was mobile or unbound. This low binding ratio suggests that the contrast observed is from inherent properties of the tumor (i.e. enhanced permeability and retention effect)

and not from specific bound contrast as previously anticipated. The use of EGF contrast agents in MRI-guided fluorescence tomography and the impact of low binding specificity are discussed.

7568-75, Session 2

Spectral ophthalmoscopy based on supercontinuum

Y. Cheng, Graduate Institute of Applied Physics, National Taiwan Univ. (Taiwan); J. Yu, H. Wu, National Taiwan Univ. (Taiwan); B. Huang, Graduate Institute of Applied Physics, National Taiwan Univ. (Taiwan); J. M. Stone, J. C. Knight, Univ. of Bath (United Kingdom); S. Chu, National Taiwan Univ. (Taiwan)

Reflectance and fluorescence spectrum play important roles in biomedical researches as fingerprints of local chemical composition inside a cell. By combining reflectance and fluorescence spectrum with imaging, also called spectral imaging, molecule contrast will be uncovered and the biochemical function can be investigated. Spectral imaging is crucial for early diagnosis of dysplastic and malignant pigmented lesions, and is also useful for blood oxygenation level monitoring as well as photoreceptor recognition.

Confocal retina spectral imaging possesses capability of acquiring metabolic and physiologic information of fundus, which is valuable to ophthalmic researches. However, current subcellular-resolution ophthalmoscopes require complicated design for only 3 to 5 spectral bands, which is quite limited for clinical application nowadays. Furthermore, inhabited off-axis aberration of spherical mirror restrains the resolution of the mirror-based scanning system.

To achieve high speed retinal spectral imaging, we demonstrate an adaptive optics scanning laser ophthalmoscope combined with an acousto-optic tunable filter (AOTF), a diffraction-limited-performance mirror-based broadband scanning system and a supercontinuum laser source. AOTF is highly attractive to spectral sensing applications owing to its high switching speeds of wavelength and random spectral access without moving mechanical parts. The mirror-based scanning system and the supercontinuum laser altogether ensure the broadband capability. Non-linear effects are observable with short pulsewidth and high intensity of supercontinuum. With this system we can attain images with 30 bands within visible spectral region and we demonstrate hyperspectral images of the cone cells of zebrafish.

7568-83. Session 2

Estrogen receptor-targeted optical imaging of breast cancer cells with near-infrared fluorescent dye

I. Jose, Biral Institute of Technology and Sciences, Pilani (India); K. D. Deodhar, Indian Institute of Technology (India); S. Chiplunkar, M. Patkar, Advanced Ctr. for Treatment, Research & Education in Cancer (India)

As a first step, the objective of this work was to synthesize and characterize one such NIR fluorescent dye conjugate, which could potentially be used to detect estrogen receptors (ER). The excitation and emission peaks for the conjugate were recorded in the NIR region as 750nm and 788nm respectively. The ester was found nontoxic on adenocarcinoma breast cancer cell lines MCF-7/MDA-MB-231. Specific binding and endocytosis of the estrogen-labeled conjugate was studied on the MCF-7 (ER positive) and MDA-MB-231 (ER negative). Conjugate staining of MCF-7 cells showed ~ 4-fold increase in signal intensity compared to MDA-MB-231. Further, estrogen molecules were found to be specifically localized to the nuclear region of MCF-7 cells, whereas MDA-MB-231 showed plasma membrane staining.



7568-88, Session 2

Selective excitation light fluorescence (SELF) imaging

M. Khojasteh, C. E. MacAulay, British Columbia Cancer Agency (Canada)

Fluorescence imaging is a potential candidate for tissue diagnostics in a wide variety of clinical situations. In order to extract diagnostic information using fluorescence, different approaches may be used. Typically, fluorescence imaging is performed by illuminating the sample at a single excitation wavelength and detecting the emissions at one or more wavelengths.

There are alternative fluorescence imaging techniques available to extract the relevant diagnostic information, and perhaps additional information. In many of the potential applications, it is not yet clear which will be optimal.

We have built a prototype system for a new fluorescence imaging technique denoted Selective Excitation Light Fluorescence (SELF) Imaging. In this technique, the sample is illuminated with multiple excitation wavelengths, and one or more emitted wavelength images are detected. The different emitted images for the different excitation wavelengths are then combined into a single three-color representation using principle component decomposition where the three presented colors are the three first principle components.

Some potential advantages of this imaging technique are: detection of multiple labeled objects in microscopy using only a single filter cube, increasing the number of simultaneous labels which can be used on a single slide since labels are separated by their absorption spectra not just their emission spectra, detection of different components of tissue based on different excitation spectra, etc.

Examples of applying this technique to in-vivo and ex-vivo microscopy and macroscopy using a spectrally programmable light engine, OneLight Spectra system, are presented in the paper that clearly demonstrate that this technique is capable of detecting different structures in the tissue.

7568-02. Session 3

Decoding gene regulatory networks using microfluidics: NF- B signaling and dynamic range

S. Tay, Stanford Univ. (United States) and Howard Hughes Medical Institute (United States); R. Gomez-Sjoberg, Stanford Univ. (United States) and Lawrence Berkeley National Lab. (United States); A. Leyrat, J. Hughey, T. K. Lee, M. Covert, S. R. Quake, Stanford Univ. (United States)

Cells sense their environment via surface receptors, process biochemical information using genetic circuitry, and mount specific responses to external stimuli by activating gene expression programs. Transcription factors are mediators of biological information processing: their cooperative dynamic properties determine the gene expression

We have adopted high-throughput microfluidic cell culture in order to decode network properties of transcriptional and signaling pathways in mammalian cells. Using a fully automated cell culture system comprising a three-layer microfluidic chip capable of running 96 different culture conditions in parallel, an inverted microscope and custom software for control and image processing, we are able to simultaneously monitor fluorescently labeled protein activity in tens of thousands of mammalian cells under identical external conditions for durations up to a weeks with a temporal resolution of 3 minutes. We investigate dynamic activity of the transcription factor nuclear factor-KB (NF-KB) under stimulation of different signaling molecules in order to completely map its network properties. NF-KB is innate immune system mediator involved in inflammation and a multitude of diseases including cancer and autoimmune diseases. We investigate NF-KB response to a wide

range of doses of the inflammatory cytokine TNF and bacterial product LPS using high-throughput microfluidic cell-culture and fluorescent time-lapse microscopy, and identify its signaling characteristics. Our data reveals the activation thresholds for both inputs and shows that the cells can respond to nearly 4 orders of magnitude difference in the dose. We observe stochastic switching near threshold and show, using mathematical modeling, that stochasticity can be explained by small fluctuations in key protein expression levels. The nuclear localization response time for both ligands depends strongly on the dose, with higher doses triggering a significantly faster response than the lower doses. The amplitude shows a striking difference: while the response to the inflammatory input (TNF) is graded and depends on the dose, the amplitude in response to LPS is independent of the stimulation $\,$ dose, indicative of analog vs. digital signaling. Our results, in addition to their biological significance, underscore the importance of high-quality, single-cell data in understanding and modeling biological systems, and demonstrate the efficiency of microfluidic techniques in obtaining such data easily and reproducibly.

7568-29, Session 3

Temporal and spatial in vivo optical analysis of microtubules in neurospora crassa

M. Held, C. Edwards, D. V. Nicolau, Univ. of Liverpool (United Kingdom)

Microtubules are a crucial part of the fungal cytoskeleton and the long-distance vesicle transport along these tracks is believed to be one of the driving forces of polarized growth. Common approaches to determine the role of the microtubules in fungal growth is to inhibit the filaments by chemical agents or genetic mutation. This study focuses on the observation of the spatial and temporal distribution of microtubules in viable fungi in two and three dimensions. The fungal strain used expressed a normal growth pattern combined with the expression of green fluorescent protein (GFP) along the microtubules enabling their direct study with fluorescence and confocal microscopy. Timelapse imaging revealed that the microtubules are very dynamic, being assembled and disassembled at high rates as well as moving with the cytoplasmic flow. In the apical compartment, the filaments are arranged mostly parallel but not helical to the growth axis and appear to determine the growth direction in close interaction with the Spitzenkörper. The microtubule distribution in subapical compartments is more random and the motility is predominantly driven by the cytoplasmic flow. However, this flow is affected by hyphal septa that act as partition walls with small connecting pores. Three-dimensional imaging shows that in order to pass through a septum, the filaments have to align parallel to the growth axis. The aim of this study was to attempt to reveal deeper insight into the role of microtubules in fungal growth thus confirming and challenging some suggestions proposed in previous literature.

7568-41. Session 3

Confocal fluorescence detection for 3D cultured mammalian cells in a microfluidic cell culture system

J. Choi, Yonsei Univ. (Korea, Republic of); J. H. Sung, M. L. Shuler, Cornell Univ. (United States); D. Kim, Yonsei Univ. (Korea, Republic of)

We investigate a confocal fluorescence detection system for 3D cultured mammalian cells in a microfluidic cell culture analog system. A microfluidic cell culture system is a device consisting of multiple cell culture chambers, connected by microfluidic channels, which simulate key organs in an animal body according to physiologically-based pharmacokinetic models. Based on the designs of microfluidic cell culture systems, 3D cell cultures were established to provide a microenvironment that is close to in vivo conditions and thus are useful to better mimic animal physiology. For direct measurement of metabolic changes in the



microfluidic cell culture analogs using 3D cell cultures, we constructed a compact and portable confocal fluorescence detection system that uses discrete optical components. The confocal detection system was designed to provide a depth scan in situ without lateral images for fast scanning and acquisition of average fluorescence variation associated with a large number of cells in 3D cultures of the microfluidic device. Specifically, using Calcein AM as a fluorescence indicator, we studied the effect of diffusion of toxins on the 3D cell cultures in extracellular matrix. Also, we present the data that we observed regarding cellular activities such as cell growth and death in the depth dimension.

7568-42, Session 3

High-throughput in vivo on-chip subcellular imaging and femtosecond-laser nanosurgery screen for neuro-regenerative compounds

M. F. Yanik, Massachusetts Institute of Technology (United States)

Therapeutic treatment of spinal cord injuries, brain trauma, stroke, and neurodegenerative diseases, will greatly benefit from the discovery of compounds that enhance neuronal regeneration. In recent years, the advantages of using small animals as models for human diseases have become increasingly apparent, and resulted in Nobel Prizes in 2002, 2006 and 2008 for the discoveries made using nematode C. elegans. We previously demonstrated femtosecond laser nanosurgery as a precise and reproducible injury method, which allowed the first study of neuronal regeneration in the optically transparent C. elegans. Wild type animals move constantly, and to perform subcellular-resolution imaging and laser surgery, animals must be immobilized. Therefore, we also developed microfluidic on-chip technologies that allow automated and rapid manipulation, orientation, and non-invasive immobilization of animals for sub-cellular resolution two-photon imaging and femtosecondlaser nanosurgery. Our technologies include microfluidic whole-animal sorters, as well as integrated chips containing multiple addressable incubation chambers for exposure of individual animals to compounds and sub-cellular time-lapse imaging of hundreds of animals on a single chip. Our devices also allow delivery of compound libraries from standard multi-well plates to microfluidic chips, and rapid dispensing of screened animals into multi-well plates. These technologies can be used for a variety of highly sophisticated in vivo high-throughput compound and genetic screens, and we performed the first in vivo screen for compounds enhancing neuronal regrowth after injury. We discovered highly potent compounds with a wide variety of cellular targets, such as cytoskeletal components, vesicle trafficking, and protein kinases that enhance neuronal regeneration. www.rle.mit.edu/Yanik

7568-50, Session 3

Mechanical anisotropy and adaptation of metastatic cells probed by magnetic microbeads

Z. Zhang, Y. Shi, S. M. Jhiang, C. Menq, The Ohio State Univ. (United States)

Metastatic cells have the ability to break through the basal lamina, enter the blood vessels, circulate through the vasculature, exit at distant sites, and form secondary tumors. This multi-step process, therefore, clearly indicates the inherent ability of metastatic cells to sense, process, and adapt to the mechanical forces in different surrounding environments. We describe a magnetic probing device that is useful in characterizing the mechanical properties of cells along arbitrary two-dimensional directions. Magnetic force, with the advantages of biocompatibility and specificity, was produced by four magnetic poles placed in a quadrupole configuration and applied to fibronectin-coated magnetic microbeads attached on cell membrane. Cell deformation in response to the applied force was then recorded through the movement of the microbeads. The motion of the beads was measured by computer processing the

video images acquired by a high-speed CMOS camera at up to 1000 frames per second. Rotating force vectors with constant magnitude while pointing to directions of all 360 degrees were applied to study the mechanical anisotropy of metastatic breast cancer cells MDA-MB 231. The temporal changes in magnitude and directionality of the viscoelastic modulus were then analyzed to investigate the cellular adaptation to force stimulation. This probing technology has the potential to provide us a better understanding of the mechano-signatures of metastatic cells, which may eventually lead to the development of new strategies for cancer prevention and/or therapy.

7568-52, Session 3

Nonresonant femtosecond laser vaporization and mass analysis of solid state biomolecules at atmospheric pressure

J. Brady, E. Judge, R. J. Levis, Temple Univ. (United States)

The detection of large, nonvolatile molecules with minimal sample preparation is important for biochemistry assays and forensic investigation. Matrix-assisted laser desorption ionization is one standard method for such analysis, and the laser always couples resonantly into the matrix molecule. However, the number of suitable matrix molecules is limited and this restricts the applicability of the technique. The new method of non-resonant, intense femtosecond laser vaporization can be universally used to transfer intact, nonvolatile, molecules directly from the solid state into the gas phase, in ambient air, for subsequent electrospray ionization (ESI) mass spectral analysis. This contribution will present the methods and apparati necessary to perform rapid, no work up mass analysis from sample at atmospheric pressure. Mass spectral measurements for neat samples, including a drugs, and biologically relevant molecules, such as dipeptide, protoporphyrin IX, vitamin B12 and hemoglobin, adsorbed on glass surface were obtained using an 800 nm, 70 fs laser having intensity of 1013 W cm-2.

7568-59, Session 3

Studying chemotaxis in real time using optical tweezers: applications for interactions study in rhodnius prolixus-trypanosoma cruzi/trypanosoma rangeli

A. A. de Thomaz, Univ. Estadual de Campinas (Brazil); C. V. Stahl, Fundacao Oswaldo Cruz (Brazil); D. Burigo Almeida, Univ. Estadual de Campinas (Brazil); A. Fontes, Univ. Federal de Pernambuco (Brazil); J. Santos-Mallet, Fundacao Oswaldo Cruz (Brazil); C. L. Cesar, Univ. Estadual de Campinas (Brazil); D. Feder, Univ. Federal Fluminense (Brazil); S. A. O. Gomes, Fundacao Oswaldo Cruz (Brazil)

Chagas disease caused by Trypanosoma cruzi (parasite) is transmitted to humans either by blood-sucking triatomine vectors (insect), blood transfusion or congenital transmission. The closely related but nonpathogenic to humans, Trypanosoma rangeli, has a sympatric distribution with T. cruzi, and is carried by the same vectors. Antigenic similarity between T. cruzi and T. rangeli has shown a serological crossreactivity in human infection leading a misdiagnosis of Chagas disease. Rhodnius prolixus is the second most important triatomine vector of the Chagas parasite due to its efficient adaptation to the human domicile. T. rangeli and T. cruzi are both morphologically similar with overlapping geographical distribution and hosts. Both whole cycles starts when the parasite detects the target cell, intestine (T cruzi) or salivary gland (T rangeli) and moves towards it. We have used an optical tweezers setup to quantitatively study the force and movement of T. cruzi/T rangeli towards the midgut wall cells/salivary gland respectively in order to understand its chemotaxis and the interaction process. A quadrant detector allowed us to measure not only the intensity of the parasite force but its sense



and direction. The measurements were made with the parasites alone and in the presence of midgut/salivary gland cells in different conditions. Parasites trapped were brought to different parts of intestine/salivary gland and changes of behavior were quantified. Optical tweezers are the ideal tool to perform observations of chemotaxis response of cells and microorganisms with high sensitivity to capture instantaneous responses to a given stimulus.

7568-68, Session 3

Fast optical protein patterning

J. M. Belisle, D. Kunik, S. Costantino, Maisonneuve-Rosemont Hospital (Canada) and Univ. de Montréal (Canada)

Spatial distributions of proteins are crucial for the development, growth and normal life of living organism. The position of cells in a morphogen gradient determines their differentiation in a specific manner. Neutrophils are the initial responders to bacterial infection or other inflammatory stimuli and have the ability to migrate rapidly up shallow gradients of attractants in vivo. Moreover, for the correct wiring of the nervous system, axonal growth cones detect specific proteins called guidance cues in order to navigate and reach their targets. Guidance cues can either be chemoattractive or chemorepulsive, and the same protein can act successively as both depending on the time point in development or the simultaneous presence of other guidance cues. A prerequisite to understand chemotaxis in a precise manner is the availability of a method able to reproduce in vitro the spatial distributions of proteins found in vivo. We recently introduced LAPAP, an optical method to produce substrate-bound protein patterns with micron resolution (Laserassisted protein adsoption by photobleaching). Here, we present key improvements in terms of simplicity and patterning time. We replaced the laser scanning required in LAPAP by widefield illumination, therefore considerably reducing the time spent to produce a pattern. Furthermore, this illumination scheme can be implemented on a standard inverted microscope. Moreover, the use of secondary antibodies as first binding molecules now allows producing patterns combining multiple proteins. We will present a full characterization of widefield illumination LAPAP, examples of multicomponent patterns and of axonal guidance by patterns produced with this method.

7568-73, Session 3

High-throughput magnetic sorting of human stem cell subsets for autologous transplantation in regenerative medicine

L. M. Reece, Purdue Univ. (United States); L. Sanders, Purdue Univ. (United States) and IKOTECH. LLC (United States); B. K. Guernsey, D. J. Kennedy, IKOTECH, LLC (United States); J. F. Leary, Purdue Univ. (United States)

Human stem cell subsets from peripheral blood were magnetically separated by continuous flow in a commercial prototype Quadrupole Magnetic cell Sorter (QMS). Cells were labeled with anti-CD34 magnetic beads and the relative binding distributions of magnetic particles per cell were determined using a Magnetic Cell Tracking Velocimeter (MCTV). QMS sorted cells were analyzed for purity by flow cytometry.

In QMS sorting a sample stream enters a vertical annular flow channel near the channel's interior wall. A sheath flow enters near the exterior wall. The two flows are initially separated by a flow splitter. They pass through the bore of a Halbach permanent quadrupole magnet assembly, which draws magnetized cells outward and deflects them into a positive outflow while negative cells continue straight out via the inner flow lamina. QMS sorts cells based upon their magnetophoretic mobility, the velocity of a cell per unit ponderomotive force, the counterpart of fluorescence intensity in flow cytometry. The magnetophoretic mobility distribution of a cell population, measured by automated MCTV is used as input data for the algorithmic control of sample, sheath and outlet flow velocities.

The purpose of this closed system for sorting cells is to sterilely isolate large numbers of human stem cells directly from a donor's blood for subsequent manipulation in tissue culture for regenerative medicine within that same patient. This will eliminate the need for immune suppressive drugs in an autologous transplantation procedure.

7568-86, Session 3

Incoherent on-chip cell holography for subcellular imaging and point-of-care diagnostics

S. O. Isikman, S. Seo, I. Sencan, D. Tseng, O. Mudanyali, T. Su, A. F. Erlinger, A. Ozcan, Univ. of California, Los Angeles (United

Development of a cost-effective, compact and light-weight microscopy and diagnostic platform has paramount importance for point-of-care and telemedicine applications. To address this need, we illustrate a lensfree on-chip holographic microscope that may provide a powerful solution for various global-health problems in resource-poor settings. This lensfree cell holography platform is composed of an incoherent light source (such as an LED) emanating through a large aperture (e.g., 50-100um) and it records the holographic diffraction pattern of each cell individually on a sensor-array such as a CMOS chip. Through digital holographic processing of these cell holograms, microscopic images of the cells can be reconstructed with a sub-cellular resolution sufficient to differentiate granulocytes, monocytes and lymphocytes from each other, permitting cytometry of dense blood samples up to ~0.4 million cells/µL with a counting accuracy of >95%. Employing a large incoherent aperture not only lowers the device cost significantly, making it highly suitable for resource-limited-settings, but also eliminates coherent speckle noise as well as multiple reflection artifacts observed in conventional coherent holography platforms. Further, the light-throughput of this lensfree platform is increased by orders-of-magnitude, achieving a mechanically robust assembly, tolerant to misalignments as desired for point of care operation. Placing the cell-plane close to the sensor-array also increases the field-of-view making it significantly higher throughput. Because this lensfree holography platform utilizes compact and cost-effective components that are also misalignment tolerant, it may provide an important toolset for telemedicine based cytometry and diagnostics applications especially in resource-poor settings for various global-health problems such as malaria and HIV.

7568-90, Session 3

MICAO: first universal all-in-the-box adaptive optics plug in accessory for standard highresolution microscopes

J. Andilla, X. Levecq, Imagine Optic SA (France)

Adaptive optics has been a critical component of developments in astronomy over the past 3 decades. The next generation of extremely large telescopes, dedicated to searching for life and habitable new planets in the universe, will benefit tremendously from the technology's corrective abilities.

The past several years have seen adaptive optics adapted to applications with more down-to-earth results, one of which is its ability to correct for specimen induced image degradation in life sciences microscopy. As many scientific publications have demonstrated, the technology enables researchers to improve both the transverse and axial resolutions of nearly all optical and non-linear imaging techniques.

In this paper, Imagine Optic will present MICAO™. The device, based on the company's proprietary electromagnetic deformable mirror technology, is designed to enable a wider range of scientists to benefit from microscopy enhanced with adaptive optics. MICAO hardware is an accessory that is easily adaptable to any standard microscope frame and compatible with most microscope lenses. Its software component

TEL: +1 360 676 3290 · +1 888 504 8171 · customerservice@spie.org



features all the necessary functionalities for image correction and control in fluorescence, confocal, spinning disk confocal and structured light microscopy.

Imagine Optic will demonstrate how the accessory is adapted to a microscope and display images obtained using the technology

7568-08, Session 4

Ultrasensitive detection and quantitation of DNA hybridization via terahertz spectrometry

A. Rahman, Applied Research & Photonics, Inc. (United States); B. Stanley, The Pennsylvania State Univ. College of Medicine (United States); A. K. Rahman, Applied Research & Photonics, Inc. (United States)

Terahertz (THz) spectrometry has been used to analyze DNA hybridization state and its quantitation in a label-free manner. Time-resolved THz signal (or temporal signal) converted to frequency domain constitutes a signature of a given molecular "event" (e.g., a vibrational state or bond position or bending, or a conformational state, etc.). The temporal signal provides a means of probing a molecular event in an appropriate time window. This is a unique ability of this technique because different molecular events exhibit different time response based on their physical and chemical nature. For example, compositional or conformational difference of a given molecule results in different signatures with an appropriate time response that can be accurately probed by a terahertz temporal signal. In this work we discriminate between single stranded and double stranded 25-mer oligonucleotides via spectral signature, where the spectra were acquired with a terahertz spectrometer designed at ARP. For each species, different peaks were identified; however, the peaks are distinctly different for each species allowing an easy comparison. Additionally, temporal transmission spectra of the specimens were collected at normal temperature and atmosphere. The peak value extracted from the temporal spectra exhibit a power law behavior over a region spanning from 27.2 femto-moles to 0.272 nanomoles. The results clearly demonstrate the ability of the spectrometer to discern a minute amount of biomolecules in a label-free fashion. This capability can be used as a diagnostic tool, as well as for studying molecular reactions such as mutation. Exemplary data will be presented.

7568-10, Session 4

High-speed fluorescence lifetime imaging microscope by analog mean-delay (AMD) method

Y. J. Won, D. Kim, W. Yang, D. Y. Kim, Gwangju Institute of Science and Technology (Korea, Republic of)

We have demonstrated high-speed fluorescence lifetime imaging microscopy (FLIM) by analog mean-delay (AMD) method. The AMD method is a new signal processing technique for measurement of fluorescence lifetime. The fluorescence lifetime can be perfectly extracted by the difference between the mean arrival time of the analog photonelectronic pulse of fluorescence signal and the mean arrival time of the signal for slow instrumental response function (IRF) of the system. Since the AMD method is based on an analog signal that contains a number of fluorescence photons in a pulse, the measurement speed is not limited by the single-photon constraint and can increase up to the excitation repetition rate, while only a single photon is permitted for a fluorescence photon by the conventional time-correlated single-photon counting (TCSPC). In addition, the AMD method can be applied in confocal imaging system for the good spatial resolution, and it provides good accuracy and precision for measurement of fluorescence lifetime. To set up the high-speed FLIM, resonant galvanometer scanner with a scan rate of 4 KHz for x-direction and non-resonant galvanometer scanner for y-direction were used. Fluorescence pulse signals were acquired by highspeed digitizer with voltage resolution of 8-bits and a sampling rate of

100 MS/s. Adding the Gaussian low pass filter (GLPF) is required to have the highest frequency of pulse signals less than 50 MHz according to the Nyquist-Shannon sampling theorem. Based on our high-speed FLIM system, we successfully obtained the sequence of confocal fluorescence lifetime images of RBL-2H3 cell labeled with Fluo-3/AM and excited by 4 PDD (TRPV channel agonist) within one second.

7568-51, Session 4

High-throughput vibrational cytometry based on nonlinear Raman microspectroscopy

V. V. Yakovlev, Univ. of Wisconsin-Milwaukee (United States)

Flow cytometry is a technology that allows a single cell or particle to be measured for a variety of characteristics, determined by looking at their properties while they flow in a liquid stream. High speed of flow and huge number of objects to be analyzed imposed some strict criteria on which methods can be used for analysis. All the known commercial instruments are currently using light scattering for particle sizing and fluorescence detection for chemical recognition. However, vibrational spectroscopy is the only non-invasive optical spectroscopy tool, which has proven to provide chemically-specific information about the interrogated sample. It is proposed that vibrational spectroscopy, based on nonlinear Raman scattering can be used to serve as an analytical tool for cytometry by providing rapid and accurate chemical recognition of flowing materials.

To achieve a desired speed (>10,000 cell/particles per second), we have substantially upgraded our previous system for nonlinear Raman microspectroscopy [1-2]. By increasing the size of the excitation volume to the size of a cell and by keeping the incident intensity at the same level, a dramatic increase of the nonlinear Raman signal is achieved. This allows high-quality vibrational spectra to be acquired within 10-100 microsecond from a single yeast cell without any observable damage to the irradiated cell. This is four orders of magnitude better than any previous attempts involving Raman microspectroscopy.

In the talk, the design principles and the outline of a new instrument will be presented. The challenges, such as obtaining the highest signal-to-noise ratio with the currently commercially available technology and avoiding non-resonant background will be discussed in details. Potential applications and possible further improvements will be discussed.

References:

[1] G. I. Petrov, R. Arora, V. V. Yakovlev, X. Wang, A. V. Sokolov, and M. O. Scully, Proc. Natl. Acad. Sci. USA 104, 7776-7779 (2007).

[2] V. V. Yakovlev, "Biochemical applications of nonlinear optical spectroscopy", CRC Press (2009).

7568-61, Session 4

The use of time-resolved fluorescence in gelbased proteomics for improved biomarker discovery

A. Sandberg, Karolinska Institutet (Sweden); V. Buschmann, P. Kapusta, R. Erdmann, PicoQuant GmbH (Germany); A. M. Wheelock, Karolinska Institutet (Sweden)

This paper describes a new platform for quantitative intact proteomics, entitled Cumulative Time-resolved Emission 2-Dimensional Gel Electrophoresis (CuTEDGE). The CuTEDGE technology utilizes differences in fluorescent lifetimes to subtract the confounding background fluorescence from the fluorescence originating from specific protein labels during in-gel detection and quantification of proteins, resulting in a drastic improvement in both sensitivity and dynamic range compared to existing technology. The platform is primarily designed for image acquisition in 2-dimensional gel electrophoresis (2-DE), but is also applicable to e.g. 1-dimensional gel electrophoresis, and proteins electroblotted to PVDF membranes. In a set of proof-of-principle measurements, we have evaluated the performance of the novel technology using the MicroTime 100 instrument (PicoQuant



GmbH, Berlin, Germany) in conjunction with the CyDye minimal labeling fluorochromes (GE Healthcare, Uppsala, Sweden) to perform differential gel electrophoresis (DIGE) analyses. The results indicate that the CuTEDGE technology provides an improvement in the dynamic range as well as the sensitivity of detection of 3-4 orders of magnitude as compared to current state-of-the-art image acquisition instrumentation available for 2-DE (Typhoon 9400, GE Healthcare). Given the resulting dynamic range of 7-8 orders of magnitude and sensitivities in the attomol range, the described invention represents a technological leap in detection of low abundance cellular proteins, which is desperately needed in the field of biomarker discovery.

7568-63, Session 4

Evaluation of interventional lipid nanoparticlecarried drug delivery for cancer therapy using fluorescence imaging

X. Jin, The Univ. of Texas Health Science Ctr. at San Antonio (United States); W. Yan, The Univ. of North Texas Health Science Ctr. at Fort Worth (United States); M. Saenz, B. A. Goins, A. Bao, The Univ. of Texas Health Science Ctr. at San Antonio (United States)

Minimally invasive interventional drug delivery with nanoparticle carrier has the advantages of high intratumoral drug retention and low normal tissue toxicity. It provides an alternative treatment plan in applications when the traditional systemic drug delivery fails to transfer the drug from the blood circulation into solid tumor efficiently. To treat the solid tumor effectively, a broad coverage of the tumor is necessary. There is, however, a lack of a detailed study on drug retention and distribution in tumor with interventional drug delivery. In this research, we studied the distribution of drug-carrying lipid nanoparticles (liposomes) in tumors with different drug delivery schemes by using fluorescence imaging. Two fluorophores, Rhadamine B and Fluorescein, were used to label liposomes, which were then directly injected into rat tumors in vivo. The rats were later sacrificed and the tumors were removed for further study. We calculated the liposome distributions based on the fluorescence images of tumor slices. The interferences between the two fluorophores were corrected for to make the computation more accurate. Histological data were further obtained to provide structure information on the tumor extracellular matrixes, which were later co-registered with the fluorescence images to verify the results obtained with fluorescence imaging. This study provides important information for pre-treatment evaluation for a safe, predictable, and effective patient treatment.

7568-64, Session 4

Spectroscopic microscopy using a stretched supercontinuum source

H. Song, D. Y. Kim, Gwangju Institute of Science and Technology (Korea, Republic of)

We present a measurement method for determining scatterer size through elastic scattering properties. Scatterer size is determined by analyzing the interferogram which is obtained with a stretched pulse source (SPS) and self-referenced interferometer. SPS is easily obtained with a supercontinuum source and a dispersive medium such as a conventional single mode fiber (SMF), a dispersion compensating fiber (DCF). As the pulse propagates through the dispersive fiber, the spectral information in the wavelength domain is converted to the amplitude in the time domain with help of the group-velocity dispersion in the dispersive fiber. Therefore, SPS enables us to measure the spectral information in time-domain. We also measured 2D scanned image with galvano scanning system. To demonstrate the feasibility of our system, we used a polystyrene microsphere as a test sample. We also measured nanometerscale motions in living cells by using a phase-sensitive technique. The stability, spatial resolution and measurement speed of the system has been also characterized.

7568-66, Session 4

Spectroscopic phase microscopy for quantifying hemoglobin concentrations in intact red blood cells

Y. Park, T. Yamauchi, W. Choi, R. Dasari, K. Badizadegan, M. S. Feld, Massachusetts Institute of Technology (United States)

Molecular concentrations are important indicators in assessing physiological conditions of biological cells and tissues. Here, we present spectroscopic phase microscopy (SPM), a practical method for label-free quantification of specific molecules in a single living cell using spectroscopic imaging of sample-induced phase shifts. Diffraction phase microscopy, a common-path interferometric microscopy, with various wavelengths of light source enables to acquire wavelength-dependent phase images. With the calibration of molecular specific dispersion, the concentration of the molecule of interest is quantified.

Using SPM we have quantitatively measured phase dispersion for PDMS polymer, bovine serum albumin solution (BSA), and hemoglobin (Hb) solution over the range of 440 - 760 nm. We demonstrate the extraction of hemoglobin concentration and cytoplasmic volume in individual red blood cells simultaneously. This study will lead to non-invasive monitoring of physiological states of individual living cells.

7568-67, Session 4

Denoising of single scan Raman spectroscopy signals

S. D. Hunt, L. Quintero, Univ. de Puerto Rico Mayagüez (United States)

Noise reduction algorithms for improving Raman spectroscopy signals while preserving signal information were implemented. Algorithms based on Wavelet denoising and Kalman filtering are presented in this work as alternatives to the well-known Savitky-Golay algorithm. The Wavelet and Kalman algorithms were designed based on the noise statistics of real signals acquired using CCD detectors in dispersive spectrometers. Experimental results show that the random noise generated in the data acquisition is governed by sub-Poisson statistics. The proposed algorithms have been tested using both real and synthetic data, and were compared using Mean Squared Error (MSE) and Infinity Norm (L ∞) to each other and to the standard Savitky-Golay algorithm. Results show that denoising based on Wavelets performs better in both the MSE and L ∞ the sense.

7568-70, Session 4

Label-free quantitative detection of biomarkers

D. Dave, S. Chirvi, The Univ. of Texas at Arlington (United States)

We report an optical technique for label free detection of large biomolecules. The optical technique is based on phase sensitive spectral interferometry to detect and quantify binding of target biomolecules on functionalized surfaces. The described technique measures change in optical path length due to the binding of the target biomolecules to the functionalized surfaces with a sensitivity of less than 50 pM Results are presented that demonstrate quantitative detection of EGFR and IgG. The potential applications of the label free technique include point-of-care screening of cancer biomarkers and tumor cell adhesion analysis.

Return to Contents TEL: +1 360 676 3290 · +1 888 504 8171 · customerservice@spie.org



7568-82, Session 4

Intravital real-time study of tissue response to controlled laser-induced cavitation using 500-ps UV laser pulses focused in murine gut mucosa under online dosimetry and spectrally resolved 2-photon microscopy

R. B. Orzekowsky-Schroeder, A. Klinger, A. Schüth, S. Freidank, G. Hüttmann, A. Gebert, A. Vogel, Univ. zu Lübeck (Germany)

We present a novel experimental setup to induce and monitor tissue lesions intravitally down to a subcellular level in murine gut mucosa. Using single 355-nm, 500-ps laser pulses coupled to a two-photon microscope, we induced optical breakdown with subsequent cavitation bubble formation in the tissue. Imaging was based on spectrally resolved two-photon excited tissue autofluorescence. Online-dosimetry of the induced microbubbles was done by a cw probe-beam scattering technique. From the scattering signal, bubble size and dynamics were deduced on a ns time scale. In turn, this signal can be used to control the bubble size and, thus, the severity of the damage. This is important for reproducible generation of minute effects in the tissue, despite strong biological variation in tissue response to pulsed laser irradiation.

After producing local UV damage, cells appeared dark, probably due to destruction of mitochondria and loss of NAD(P)H fluorescence. Within 10 min after cell damage, epithelial cells adjacent to the injured area migrated into the wound to cover the denuded area, resulting in extrusion of the damaged cells from the epithelial layer. Using the nuclear acid stain propidium iodide, we showed that UV pulses induced cell membrane damage with subsequent necrosis. For all observed lesions, no immune cells migrated toward the injured area within observation periods of up to 5 hours.

This model will be used in further studies to investigate the intrinsic repair system and immune response to laser-induced lesions of intestinal epithelium in vivo.

7568-13, Session 5

Image processing techniques in computerassisted patch clamping

M. Azizian, R. V. Patel, Univ. of Western Ontario (Canada) and Canadian Surgical Technologies and Advanced Robotics (Canada); M. Poulter, Univ. of Western Ontario (Canada) and Robarts Research Institute (Canada)

Patch clamping is used in electrophysiology to study single or multiple ion channels in cells. Multiple micropipettes are used as electrodes to collect data from multiple nerve cells. Placement of these electrodes is a time consuming and complicated task due to the lack of depth perception, limited view through the microscope lens and the possibility of collision between micropipettes. To aid in this process a computerassisted approach was developed using image processing techniques applied to images obtained through the microscope. Image processing algorithms were applied to perform autofocusing, relative depth estimation, distance estimation and tracking of the micropipettes in the images. The software does not require any changes in the existing patch clamp equipment or microscope controllers. Autofocusing is performed based on maximization of the sharpness of the acquired images. Several sharpness measures was studied and the best one was selected based on unimodality, repeatability, reduced sensitivity to noise and illumination changes, also computational efficiency. An optimization technique was used to achieve fast convergence while avoiding local maxima. As a result, autofocusing of 1.0 micrometer precision was achieved. Relative depth estimation is performed based on autofocusing. Three dimensional distance estimation with an overall accuracy of approximately 2.4 micrometers was achieved; This accuracy has the potential to be further improved if a higher magnification lens is used. An image-based tracking algorithm was developed to track a micropipette tip at a rate of 30Hz;

the algorithm is based on an optical flow tracking approach. A temporal frequency domain filtering approach was also used to detect the tip of a micropipette based on vibrating micropipettes with a frequency of 5 to 10Hz, which is used before tracking starts or whenever image-based tracking fails. Manual registration of micropipette coordinates to the microscope coordinates is also performed and used to validate the micropipette tip detection and tracking results. An accuracy of 1.57 micrometer and a precision of less than 1.0 micrometer have been achieved for tracking results.

7568-16, Session 5

Label-free single cell analysis with a chipbased impedance flow cytometer

A. Pierzchalski, Univ. Leipzig (Germany); M. Hebeisen, Leister Process Technologies (Switzerland); A. Mittag, Univ. Leipzig (Germany); M. Di Berardino, Leister Process Technologies (Switzerland); A. Tarnok, Univ. Leipzig (Germany)

Label-free identification of phenotype and physiology of a large number of individual cells is a requirement in clinical research and cell therapy. Impedance flow cytometry (IFC) (Leister/Axetris) is a promising label-free alternative to fluorescence-based flow cytometry (FCM).

IFC measures impedance of up to 300 single cells /sec simultaneously at various frequencies. The frequencies used for signal acquisition range from 0.1 to 20 MHz. The impedance signal provides information about cell volume (<1 MHz), membrane capacitance (~1-4 MHz) and cytoplasmic conductivity (4-10 MHz), parameters directly related to the physiological conditions of single cells.

Hybridoma cell viability detection by IFC was tested after treatment with cell death inducers. Impedance analysis showed discrimination between viable and dead cells. This was clearly visible at 4 MHz suggesting that differentiation was possible based on cell membrane capacitance. IFC results were confirmed by FCM measurement of aliquots after AnnexinV/PI labelling.

Also changes in cell membrane potential and [Ca2+]i are detectable by IFC. Peripheral blood mononuclear cells were loaded with membrane potential sensitive dye (DiBAC4) or with calcium sensitive dye (Fluo-3). The cells were then treated with the ionophores: valinomycin or A23187, respectively. Changes in membrane potential and [Ca2+] i were detectable at the level of cytoplasm conductivity (>4 MHz) and membrane capacitance (1-4 MHz), respectively.

IFC can be a valuable alternative to conventional FCM. In combination with cell sorting IFC may gain additional relevance in stem cell isolation for therapeutic use. The work will be extended to address further applications in biotechnology and biomedical cell analysis.

7568-17, Session 5

Practical way to develop 10-color flow cytometry protocols for the clinical laboratory

A. Tarnok, J. Bocsi, Univ. Leipzig (Germany)

The latest development of commercial flow cytometers (FCM) is their equippment with three (blue, red, violet) or more lasers and many PMT detectors. Nowadays, routine clinical instruments are capable of detecting 10 or more fluorescence colors simultaneously. Thereby, they present opportunities for getting detailed cell-population information on the single-cell level for cytomics and systems biology to improve diagnosis, enable predictive medicine and monitoring of patients.

University Leipzig (Germany) recently started a cluster-of-excellence to study the molecular background of life style and environment associated diseases, enrolling 25.000 healthy and diseased individuals. To this end the most comprehensive FCM protocol for characterizing peripheral blood leukocytes has to be developed.

For this clinical setting we aimed to optimize fluorochrome and antibody



combinations to the characteristics of our instrument (Navios, Beckman-Coulter) for successful routine 10-color FCM. Systematic review of issues related to sampling, preparation, instrument settings, spillover and compensation matrix, reagent performance, and general principles of panel construction was performed.

10-color FCM enables for increased accuracy in cell subpopulation identification, the ability to obtain detailed information from blood specimens, improved laboratory efficiency, and the means to consistently detect and characterize major and rare cell populations. Careful attention to details of instrument and reagent performance allows for the development of panels suitable for screening of samples from healthy and diseased donors.

The characteristics of this technique are particularly well suited to the analysis in large human population cohorts and have the potential to become everyday practice on standardized way in the clinical laboratory.

7568-20, Session 5

An integrated approach to human carcinogenicity testing based on image analysis and automatic classification of foci

C. Urani, G. F. Crosta, C. Procaccianti, P. Melchioretto, Univ. degli Studi di Milano-Bicocca (Italy); F. M. Stefanini, Univ. degli Studi di Firenze (Italy)

Chemical carcinogenesis in live animals as well as in cultured cells is a multistep process, divided broadly into initiation, promotion and

The Cell Transformation Assay (CTA) is one of the promising in vitro methods used as predictor of human carcinogenicity. The neoplastic phenotype is monitored in suitable cells by foci formation, showing typical transformed morphological features.

At present, the classification of transformed foci, performed by a trained human expert, relies on scoring under light microscopy. Three types of morphologically altered foci have been described: Type I, characterized by partially transformed cells, Type II and Type III, considered to have undergone neoplastic transformation. The method of visual classification, although widely accepted, is time-consuming, and, in some cases, prone to subjectivity, leading to possible over/under-estimation of carcinogenic potential of chemical or physical agents. Due to these disadvantages, the CTA has not yet been accepted by regulatory Authorities.

Herewith we outline an integrated approach aimed at objectively classifying foci images. Implementation consists of: 1) performing in vitro CTAs; 2) processing images for the extraction of morphological descriptors of foci; 3) submitting said descriptors to a trainable classifier for recognition.

Morphological descriptors, e.g., structure, texture, edge profiles, fractal dimensions, capable (in principle) of representing the transformed phenotype, are extracted by a variety of image analysis algorithms, including "spectrum enhancement". Different classification algorithms, including principal components analysis and kernel machines, are applied and their effectiveness compared.

New schemes emerged for automatic classification of foci, with possible feedback on CTA protocol.

7568-21, Session 5

Fluorescence diffuse tomography setup with a single source-detector pair for small-animal imaging

I. V. Turchin, A. Orlova, M. Kleshnin, I. Fiks, Institute of Applied Physics (Russian Federation); I. Balalaeva, M. Shirmanova, Nizhny Novgorod State Univ. (Russian Federation); A. Savitsky, A.N. Bach Institute of Biochemistry (Russian Federation)

Fluorescence diffuse tomography (FDT) setup for different applications of small-animal imaging has been created. An animal is scanned in transilluminative plane geometry by a single source and detector pair. An experimental animal was scanned using the following algorithm: (1) large-step scanning to obtain a general view of the animal (source and detector move synchronously); (2) selection of the fluorescing region; and (3) small-step scanning of the selected region and different relative shifts between the source and detector to obtain sufficient information for 3D reconstruction. If the 3D reconstruction is not available only the (1) step of scanning process is used. In this case DFT setup operates as a projection method. In order to increase the precision of reconstruction we developed the analytical hybrid model of light propagation in tissue based on the small-angle approximation of the RadiativeTransfer Equation and the diffusion approximation. The results of in vivo experiments with mice carrying human carcinoma expressing red fluorescent proteins with 3D reconstruction of the tumor will be presented. We will also present the results of employing DFT in applications of preclinical study of new photosensitizers for fluorescent diagnostics and photodynamic therapy and visualization of the drug delivery process using quantum dots. In these applications DFT is used as a projection technique and 3D reconstruction is not available, because the ratio of the fluophore concentration between tumor and surrounding tissues is not enough high. Nevertheless, the results of the experiments show good efficacy of the presented DFT technique in mentioned applications.

7568-27, Session 5

Automatic image analysis system for networks formed by endothelial cells in vitro

D. Chen, P. Gudla, J. Collins, SAIC-Frederick, Inc. (United States); E. Zudaire Ubani, C. Fang, F. Cuttitta, National Cancer Institute (United States); S. Lockett, SAIC-Frederick, Inc. (United States)

Tumor angiogenesis is the stage of cancer development, in which tumors become vascularized and malignancy and metastasis established. In efforts to understand the mechanisms of tumor induced angiogenesis, various in vitro models have been developed to explore the fundamentals of the early network formed by endothelial cells with controllable parameters to simulate the in vivo situations, while excluding other undefined factors in the real environment.

Effective analysis of the network system extracted from fluorescence microscopy images obtained from the in vitro culture model system is an important issue. Therefore it is extremely desirable to have a computerized system that automatically does quantitative analysis of images of early network formed by endothelial cells in in vitro culture for the understanding of the biology that regulates vasculogenesis in the culture models.

We propose an automatic image analysis system to comprehensively and quantitatively describe the network formed by endothelial cells in culture. The analysis system starts with segmentation by a Hessian matrix based multi-scale vessel enhancement scheme, followed by a skeletonization and pruning process to generate the binary skeleton image of the network. Quantitative analysis is then performed with the metrics defined and developed for this system, such as fractal dimension, network entropy, lacunarity, total number of network nodes, edges, chord length and average chord length, etc.; the quantitative values of these quantities are the output of the analysis system, which provides comprehensive evaluation of the network formed in culture, and the quantification and characterization of the network is automatic.

Project funded by NCI Contract No. HHSN261200800001E

TEL: +1 360 676 3290 · +1 888 504 8171 · customerservice@spie.org



7568-36, Session 5

Time-gated real-time bioimaging system using multicolor microsecond-lifetime silica nanoparticles

D. Jin, J. Piper, Macquarie Univ. (Australia); J. Yuan, Dalian Univ. of Technology (China); R. C. Leif, Newport Instruments (United States)

A real-time time-gated luminescence microscope system has been constructed by adding a pulsed excitation source and a synchronized time-gated shutter to a conventional epi-fluorescence microscope. The solid-state excitation source can be either a 365nm 250mW LED (100 microsecond pulse) or a diode-pumped 355 nm laser or a recently developed tunable ultraviolet cerium laser. A signal-delay generator is used to synchronize the pulsed excitation and a super-fast optical chopper to produce time-gated detection (up to 2500 Hz repetition rate with a close-to-open duty ratio of 25%:75%) after the eyepiece. An additional eyepiece behind the optical chopper is used for real-time cell imaging either by a colour digital camera or naked eyes.

A covalent binding nano-encapsulation method is used for synthesizing stable ultra-bright lanthanide-containing silica nanoparticles. The method is based on introduction of an active group, such as 3-aminopropyl) triethoxysilane (APS), to the existing microsecond-lifetime dyes, such as europium (BHHCT) and terbium (BPTA) complexes. By varying the ratio of europium to terbium, the synthesized nanoparticles appear to differ in colour from green, orange to red. By reacting with different antibodies, a variety of labelling kits was prepared for multi-color detection of several waterborne pathogens.

Results: Nanoparticles with differing luminescence emissions (617nm Red and 545nm Green) and specificities were used to stain to several waterborne pathogens, e.g. Giardia cyts and Cryptosporidium oocysts. Background-free images of these labelled target micro-organisms were obtained by the true-colour time-gated luminescence microscopy. The photo-bleaching process over 10 mins was recorded by a video camera.

7568-44, Session 5

Fiber-based microflow cytometer

M. Fortin, P. Grenier, P. Gallant, O. Mermut, F. Emond, I. Noiseux, INO (Canada)

In the context of measuring living cells properties, flow cytometry is considered the preferred technique to evaluate the expression of a number of biochemical markers. Flow cytometers (FCs) are highly performing devices, offering unique and advanced features.

Traditional system designs are based on the principle of hydrodynamic focusing. In this approach, a sheath liquid is filling the flow chamber surrounding the pipe bringing the analyte in the interrogation volume. However, such FCs are bulky devices with a complex optical system. Furthermore, the sheath fluid requirements imply a large volume and impose a problem of biohazardous waste management.

INO developed a new fiber-optic flow cell (FOFC) technology for portable FC, base on a special optical fiber with a square cross-section through which a hole is transversally bored by laser micromachining. This new technology is potentially capable of achieving flow cytometry with comparable performances to current commercial systems, and providing several advantages such as: sheathless flow, low cost, reduced number of optical components, no need for alignment, ease-of-use, miniaturization, portability and robustness.

This paper presents developments and recent results for this FOFC. This special fiber optic provides the capability to illuminate a large surface with a uniform intensity distribution, independently of the initial shape originating from the light source and without loss of optical power. The integration of LED sources presents several advantages in cost, compactness, and wavelength availability. Finally, the measured CVs and sensitivity of this FOFC are compared to industry benchmarks.

7568-55, Session 5

Cyto IQ: an adaptive cytometer for extracting the noisy dynamics of molecular interactions in live cells

D. A. Ball, Virginia Polytechnic Institute and State Univ. (United States); S. E. Moody, Orca Photonic Systems, Inc. (United States); J. Peccoud, Virginia Polytechnic Institute and State Univ. (United States)

We have developed a fundamentally new type of cytometer to track the statistics of dynamic molecular interactions in hundreds of individual live cells in a single experiment. This entirely new high-throughput experimental system, which we have named Cyto IQ, reports statistical, rather than image-based data for a large cellular population. Like a flow cytometer, Cyto IQ rapidly measures several fluorescent probes in a large population of cells to give a reduced statistical model that is matched to the experimental goals set by the user. However, Cyto IQ moves beyond flow cytometry by tracking multiple probes in individual cells over time. Using adaptive learning algorithms, we process data in real time to maximize the convergence of the statistical model parameter estimators.

By using a tunable pulsed laser as the light source for fluorescence measurement, Cyto IQ can detect, in individual cells, at least 10 different RNAs and/or protein probes with single-molecule sensitivity. Software controlling Cyto IQ integrates existing open source applications to interface hardware components, process images, and adapt the data acquisition strategy based on previously acquired data. These innovations allow the study of larger populations of cells, and molecular interactions with more complex dynamics than is possible with traditional microscope-based approaches.

Cyto IQ supports research to characterize the noise affecting biological processes. Our current prototype serves as a test-bed to validate new imaging and machine learning algorithms.

7568-69, Session 5

Impulsive noise reduction in Raman spectroscopy images

S. D. Hunt, L. Quintero, Univ. de Puerto Rico Mayagüez (United States)

Charge-Coupled Device (CCD) detectors are becoming more popular in spectroscopy instrumentation. In spite of technological advances, spurious signals and noise are unavoidable in Raman spectroscopes. In general, the noise comes from two major sources [1], impulsive noise caused by high energy radiation from local or extraterrestrial sources (cosmic rays), and noise produced in Raman backscattering estimation. In this work, two algorithms for impulsive noise removal are presented, based in spectral and spatial features of the noise. The algorithms combine pattern recognition and classical filtering techniques to identify the impulses. Once an impulse has been identified, it is removed and substituted with data points having similar statistical properties as the surrounding data.

7568-91, Session 5

An analog method to produce time-gated images

R. C. Leif, Newport Instruments (United States); S. Yang, Newport Instruments (United States) and Phoenix Flow Systems (United States)

Problem: Previous images of time-gated luminescence have been obtained with a cooled CCD camera by digitally summing a series of sequential images. The data acquisition rate of approximately 10 one



millisecond images per second was too slow for standard research and clinical use. With one millisecond each acquisition and exposure periods, and a required 50% duty cycle for 2,500 images, 500 seconds were required for a total exposure of 2.5 seconds.

Solution: An analog approach is to use an interline transfer, electronically shuttered camera. After each exposure, the storage line is not readout; instead, the electrons from the acquisition pixels are transferred to the storage pixels and thus are added to those previously stored. The length of the exposure is limited by the capacity of the storage pixels and the rate of generation of background (noise) electrons. This electronic concept was tested with a Point Grey Dragonfly 2 640 by 480, monochrome camera equipped with a Sony 1/3" progressive interline scan, electronically shuttered CCD, which since it did not have any cooling, was operated at room temperature. Pulsed excitation was used with a Nichia UV LED.

Results: Five micron uniform europium complex stained beads could at room temperature be time-gated imaged with excitation and acquisition times of 1 millisecond each and the analog summation of 50 images.

Conclusion: The analog integration solution apparently works; however, a cooled scientific grade camera with the same capacity for multiple transfers into storage pixels would be better suited for use with dimmer objects.

7568-12, Session 6

Fluorescence intensity decay shape analysis microscopy (FIDSAM) for quantitative and sensitive live-cell imaging

F. Schleifenbaum, K. Elgass, M. Sackrow, S. Peter, K. Caesar, K. Harter, A. J. Meixner, Eberhard Karls Univ. Tübingen (Germany)

Quantitative live-cell fluorescence microscopy and imaging is regularly confronted with the problem of background autofluorescence, which is inherent in many biological samples. This background emission strongly reduces the image contrast, or requires high fluorescence label concentrations, which are most often achieved by cells overexpressing a autofkluorescent fusion protein.

Here, we present a novel technique to enhance the contrast of fluorescence images by over at least one order of magnitude by fluorescence intensity decay analysis (FIDSAM). Our method bases on the analysis of the shape of the fluorescence intensity decay (fluorescence lifetime curve) and benefits from the fact that the decay patterns of typical fluorescence label dyes strongly differ from emission decay curves of autofluorescent sample areas. By recording a fluorescence lifetime microscopy (FLIM) image and comparing the shape of the spatially recorded intensity decays with the decay shape of the pure label dye, we obtain a robust coefficient, which describes the fraction of autofluorescent background to the recorded signal. This approach avoids the possibility that autofluorescence interferes with the desired target signal and results in fluorescence images which are no longer adulterated by background artefacts. Our method, therefore, reduces the necessity for the over-expression of fluorophore-tagged proteins and enables the quantitative and highly sensitive fluorescence imaging of low-expressed proteins, especially in background-afflicted

7568-34, Session 6

Angular domain spectroscopic imaging of turbid media using silicon micromachined microchannel arrays

F. Vasefi, Simon Fraser Univ. (Canada) and Lawson Health Research Institute (Canada); E. Ng, Univ. of Western Ontario (Canada); M. Najiminaini, Simon Fraser Univ. (Canada); G. Albert, Lawson Health Research Institute (Canada); B. Kaminska, G. H. Chapman, Simon Fraser Univ. (Canada); J. J. L. Carson, Lawson

Health Research Institute (Canada) and Univ. of Western Ontario (Canada)

We experimentally characterized a novel Angular Domain Spectroscopic Imaging (ADSI) technique for the detection and characterization of optical contrast abnormalities in turbid media. The new imaging system employs silicon micromachined angular filtering methodology, which has high angular selectivity for photons exiting the turbid medium. The angular filter method offers efficient scattered light suppression at moderate levels of scattering (i.e. up to 20 mean free paths).

An ADSI system was constructed from a wideband QTH light source, an Angular Filter Array (AFA), and an imaging spectrometer. The collimated broadband light source was used to trans-illuminate a turbid sample over a wide range of wavelengths in the near infrared region of the spectrum. The AFA rejected nearly all scattered light exiting the turbid sample and selected the imaging forming quasi-ballistic light. The imaging spectrometer decomposed the output of the AFA into hyperspectral images representative of spatial location and wavelength. It collected and angularly filtered a line image from the object onto the CCD camera with the spatial information displayed along one axis and wavelength information along the other.

The ADSI system was tested on tissue-mimicking phantoms including a gel phantom with thickness of 7 mm (1% Intralipid) representative of the turbid medium and 3 mm diameter spheres (oxygenated blood) as absorption targets at three different depths hidden in the turbid medium. The contrast and resolution of the ADSI system was characterized for different absorption levels of the target along with different scattering levels of the turbid medium.

7568-43, Session 6

Difference Raman for enhancing image resolution by modulating tip of atomic force probe that enhances or shadows Raman signal

R. Dekhter, H. Taha, A. Israel, D. Lewis, Nanonics Imaging Ltd. (Israel); A. Lewis, Hebrew Univ. of Jerusalem (Israel)

Tip enhanced Raman scattering (TERS) has been shown as a potential technique for overcoming limitations of conventional micro Raman spatial resolution and for other apertureless near-field optical measurements based on plasmonic interactions. In this talk we will compare the resolutions obtainable by such plasmonic enhancement techniques as compared to a method we have developed based on the ultra-sensitive nature of difference Raman. In this latter technique an AFM probe with an exposed tip geometry that is optimized to block a nanometric region of a sample will be used in conjunction with difference Raman to obtain significant improvements in Raman image resolution over conventional far-field scattering. For this new imaging protocol one has to have not only exposed tip geometries but also an AFM system that can modulate and scan the probe independently of the sample scanning required for Raman imaging systems. The tip scanning is required for optimizing the position of the probe tip for maximizing the shadow effect on the sample in the near-field. The tip modulation is required for bringing the probe in and out of the near-field of the sample so that a difference Raman can be recorded at each pixel and an image formed as the sample is scanned point by point. All of the above in terms of the Shadow protocol are predicated by having an AFM system that has a completely free optical axis from above and is completely independent from the lens of the micro-Raman. Results will be shown on structured thin films of strained silicon on silicon to show the relative fidelity of these imaging modalities.



7568-47, Session 6

Multi-color digital holographic microscope (DHM) for biological, bio-medical purposes

S. Tokes, Computer and Automation Institute (Hungary) and PPKE The Faculty of Information Technology (Hungary)

Our digital holographic (DH) approach can be used to study tissue structures both in vitro and in vivo. This transmissive or reflective DHM architecture can produce white light microscopic 3D and 4D images. Different holographic setups and reconstruction algorithms are presented with demonstrative simulations and experimentally captured and numerically reconstructed images. Comparing the individually reconstructed color images with each other we can add information both for recognition of different types of cells or microorganisms and for diagnostic purposes.

7568-54, Session 6

Enhanced transverse resolution through polarization switching

O. Masihzadeh, D. Kupka, P. Schlup, R. A. Bartels, Colorado State Univ. (United States)

In optical microscopy, the polarization state of the focal field strongly influences formed images due to its impact on effective focal spot size, and interactions with the sample. We demonstrate control over focal field spatial polarization state improves spatial resolution in laserscanning third harmonic generation (THG) microscopy. The focal field is manipulated by imaging a spatial light modulator to the focal plane of a moderate numerical aperture microscope. The resolution enhancement arises as THG is quenched for circularly-polarized fundamental field in isotropic media. In this approach, the polarization state of the focal field is linear at the beam center out to radius rs, and converted to circular outside rs, so THG beyond rs is suppressed. A transverse spatial resolution of up to 2 times is demonstrated. Moreover, two non-iterative algorithms are developed for characterization of the polarization state at the focus under moderate and tight focusing: Under moderate focusing where recorded THG signal is dominated by the incident paraxial polarization component, the spatial polarization state is determined non-iteratively via three linear-polarization projection THG images. Under tight focusing conditions, polarization scrambling occurs such that the input and focal fields are not similar. We introduce an algorithm for focal field retrieval through far field THG collection. A nano-particle with known third-order susceptibility localizes THG scattering to a small focal volume. Scanning this nano-probe through the focal volume allows for complete reconstruction of the vector point spread function, yielding longitudinal and transverse field components from the focal volume.

7568-60, Session 6

Real-time megapixel multispectral bioimaging

J. M. Eichenholz, N. Barnett, Ocean Optics, Inc. (United States)

Spectral imaging involves capturing images over multiple discrete wavelength bands and extracting spectral content from that data. The resulting 3D data cube (x, y,) allows materials to be identified by the spectral signature at each pixel. The most common tool, the hyperspectral imager is very useful for researchers who are looked at the unknown. However hyperspectral imagers have major drawbacks such as cost, size, need for scanning, and the copious amount of data generated per image that limits the widespread commercial and clinical acceptance. Getting an answer from this data cube is computationally intensive and in many cases the complete hyperspectral data cube provides little additional information compared to just a few (typically 3-8) multispectral imaging bands. A new class of multispectral imaging systems has been developed that utilizes lithographically patterned dichroic filter arrays integrated with standard CCD and CMOS detector

imagers. The imagers offer the unique advantage of scalability to tens of Megapixel resolutions, compact size, and no moving parts, while simultaneously measuring each spectral channel. Our multispectral imagers are much simpler to manufacture because the complexity is in the lithographically patterned dichroics rather than in the bulk optical system. The patterned dichroic filter arrays are fabricated utilizing standard microlithography techniques and can incorporate up to 10 different wavelength bands deposited onto a single substrate. Our filter array approach takes a different path for multispectral imaging, from a science experiment to a commercial product. Recent developments of these cameras will be discussed.

7568-65, Session 6

Speckle-field digital holographic microscopy

Y. Park, W. Choi, Z. Yaqoob, R. Dasari, K. Badizadegan, M. S. Feld, Massachusetts Institute of Technology (United States)

The use of coherent light in conventional holographic phase microscopy (HPM) poses three major drawbacks: poor spatial resolution, weak depth sectioning, and fixed pattern noise due to unwanted diffraction. Here, we report a technique which can overcome these drawbacks, but maintains the advantage of phase microscopy - high contrast live cell imaging and 3D imaging. A speckle beam of a complex spatial pattern is used for illumination to reduce fixed pattern noise and to improve optical sectioning capability. By recording of the electric field of speckle, we demonstrate high contrast 3D live cell imaging without the need for axial scanning - neither objective lens nor sample stage. This technique has great potential in studying biological samples with improved sensitivity, resolution and optical sectioning capability.

7568-87, Session 6

Macroscopic rasterscanning as a tool for fluorescence lifetime based proteomics or μ -well plate based assays

V. Buschmann, F. Koberling, M. Patting, PicoQuant GmbH (Germany); A. Sandberg, Karolinska Institutet (Sweden); M. Wahl, PicoQuant GmbH (Germany); Å. Wheelock, Karolinska Institutet (Sweden); R. Erdmann, PicoQuant GmbH (Germany)

Fluorescence Lifetime Imaging (FLIM) based on Time-Correlated Single Photon Counting (TCSPC) is nowadays a well established technique that is very often realised as an add-on for confocal laser scanning microscopes. However, the standard laser scanning technique limits the maximum scan range in these setups to a few millimeter, making it therefore unusable for macroscopic material science studies on e.g. semiconductor materials or for fluorescence lifetime studies on e.g. $\mu\text{-well}$ plate based assays or in 2D gel electrophoresis.

In order to also realize larger scanning ranges, we have developed a sample scanning approach based on a xy-cross stage equipped with piezo linear motors. Using online position monitoring, this approach permits fast acceleration and scanning as well as precise positioning and features scan ranges from 100x100 microns up to 80x80 mm with sub micron positioning accuracy. Standard upright and inverse microscope bodies can easily be equipped with this scanning device. Along with the necessary excitation and detection components "large-area" FLIM thus becomes possible.

We will show new results illustrating the system capabilities for lifetime based imaging in macroscopic samples such as the improvement of the fluorescence sensitivity in 2D gel electrophoresis or the possibility to perform lifetime based fluorescence multiplexing in $\mu\text{-well}$ plate based assays.



7568-14, Poster Session

Evaluation of human serum of severe rheumatoid arthritis by confocal Raman spectroscopy

C. S. Carvalho, L. J. Raniero, A. M. Espirito Santo, Univ. do Vale do Paraíba (Brazil); M. M. Pinheiro, L. E. C. Andrade, Univ. Federal de São Paulo (Brazil); M. A. G. Cardoso, Univ. do Vale do Paraiba (Brazil); J. S. Junior, Biomed Lab. (Brazil); A. A. Martin, Univ. do Vale do Paraiba (Brazil)

Rheumatoid Arthritis is a chronic inflammatory disease, recurrent and systemic, initiated by autoantibodies and maintained by inflammatory mechanisms cellular applicants. The evaluation of this disease to promote early diagnosis, need an associations of many tools, such as clinical, physical examination and thorough medical history. However, there is no satisfactory consensus due to its complexity. In the present work, confocal Raman spectroscopy was used to evaluate the biochemical composition of human serum of 40 volunteers, 20 patients with rheumatoid arthritis presenting clinical signs and symptoms, and 20 healthy donors. The technique of latex agglutination for the polystyrene covered with human immunoglobulin G was performed for confirmation of possible false-negative results within the groups, facilitating the statistical interpretation and validation of the technique. This study aimed to verify the peak absorption of biomolecules such as immunoglobulins (1400-1450 cm-1 for IgG1, IgM and IgA 1550-1650cm -1 for IgG4, IgG3 and IgG2) amides (1250-1280 cm-1 and 1600-1480 cm-1) and protein (1450-1453 cm-1). The results were highly significant with a good separation between groups mentioned. The discriminant analysis was performed through the principal components and correctly identified 98% of the donors. Loading plot and Boxplot were used to observe changes in the spectra regions. The area under curves were calculated and compared and the results were statistically significant with an r2> 98% coefficient with p <0.005. Based on these results, we observed the behavior of arthritis autoimmune, evident in certain spectral regions that characterize the serological differences between the groups.

7568-25, Poster Session

Development of in vivo confocal microscope for reflection and fluorescence imaging simultaneously

M. Ahn, C. Song, B. Chun, D. Gweon, Korea Advanced Institute of Science and Technology (Korea, Republic of)

In-vivo confocal microscope has various capabilities which are the acquisition of non-invasive, three dimensional and high resolved images. This technology can be applied to the medical imaging diagnosis, bioengineering and new drug development.

To obtain confocal reflection images, we used a linearly polarized diode laser with the wavelength of 830 nm. To acquire confocal fluorescence images, we used two diode lasers with the wavelength of 488 nm and 660 nm, respectively. By using two detectors, we can acquire a confocal reflection image and a confocal fluorescence image independently. Two diode lasers are combined with a fiber-coupler-typed wavelength combiner. Emission signals from a fluorescent specimen are selectively chosen by several band-pass filters. Near infra-red light and visible light are combined or separated with a customized dichroic mirror. With two mirror scanners which consist of a resonant mirror and a galvano mirror, we can achieve high-speed image acquisition rate. By using an objective PZT scanner, optical sectioning images are able to be acquired. This hybrid system has a broad spectrum from 488 nm to 830 nm. Therefore, optics should correct various optical aberrations. We designed and optimized relay optics with an optical design software (ZEMAX). In the near future, we will make some basic experiments with bio-specimens. From these experiments, we will acquire various reflection and fluorescence images.

7568-26, Poster Session

Effects of Nacl on photosynthesis in arabidopsis and thellungiella leaves based on the fluorescence spectra, the fast chlorophyll fluorescence induction dynamics analysis, and the delayed fluorescence technique

W. L. Chen, Z. Chen, South China Normal Univ. (China)

Wild type Arabidopsis thaliana (ecotype Columbia) and Thellungiella were used as experimental material in this artile. The leaves of the Arabidopsis and the Thellungiella were treated with different concentrations of Nacl. The fluorescence emission spectra, the chlorophyll fluorescence and the delayed fluorescence were detected respectively. We found that there was an obvious change in the photosynthetic efficiency of PS and the DF intensity of the Arabidopsis leaves with different concentrations of Nacl treatment. However, there wasnot an obvious change in the photosynthetic efficiency of PS and the DF intensity of the Thellungiella leaves with 100µmol/L and 200µmol/L Nacl treatment. While it also showed that there came to be an obvious stress of the leaves of Thellungiella with 300µmol/L Nacl treatment. The fast chlorophyll fluorescence induction dynamics analysis revealed that the photosynthetic efficiency of PS of the Arabidopsis leaves had a sharp decline along with the 100-200 mmol/L Nacl treatmen, While the Thellungiella leaves showed a strong tolerances to salt stress.

7568-30, Poster Session

Programmed cell death-involved cadmium toxicity in arabidopsis thaliana is associated with the production of reactive oxygen species

W. L. Chen, W. Zhang, South China Normal Univ. (China)

Cadmium (Cd) is a highly toxic heavy metal mainly as a result of pollution from industrial processes and phosphate fertilizers. Cd causes various effects in plants, such as inhibiting photosynthesis, respiration and decreasing water and mineral uptake. Those changes in plant metabolism can ultimately inhibit plant growth. Potential mechanisms of Cd toxicity measured as Cd-induced inhibition of growth in the root and shoot in barley seedlings and maize plants were investigated. Compared with the control treatment without Cd, the accumulation of Cd in protoplast of Arabidopsis thaliana triggered reactive oxygen species (ROS) production. Recent studies have described Cd-induced apoptosis-like cell death in plant and animal cells. In this study, we show that protoplast of Arabidopsis thaliana exposed to low concentrations of Cd for short times undergoes slightly changes in a manner that is dose and cell density dependent. At higher concentrations of Cd or longer exposure times, Cd induces cell death and ROS production. Several apoptotic features appear during Cd treatment, including cell shrinkage, vacuolation, nuclear fragmentation, as well as DNA ladder. The data presented suggest that Cd toxicity resulting in programmed cell death (PCD) in Arabidopsis thaliana is associated with the production of ROS.

7568-31, Poster Session

The effects of salicylic acid and methyl salicylate on the early growth of arabidopsis

W. L. Chen, L. Yun, South China Normal Univ. (China)

Salicylic acid (SA) and methyl salicylate (MeSA) are important plant signaling molecules. The current study shows that, SA can alleviate the abiotic stress. SA can be transformed into MeSA largely in plants, which have a variety of physiological functions. We studied the effects of different SA concentrations and different MeSA saturated solution treatment times on Arabidopsis seed germination and some indicators

Return to Contents TEL: +1 360 676 3290 · +1 888 504 8171 · customerservice@spie.org



of early growth with the wild-type (WT) and the lack of SA accumulation capacity NahG transgenic plants (NahG) as our experimental materials. The results showed that low concentration of SA (500µM) to promote seed germination and early WT growth, while high concentration (800µM) showed inhibitory effects. In NahG, low concentration of SA had no significant effects while the high one showed promote effects. The treatment of MeSA saturated solution for six hours to promote seed germination and early WT growth, and had no significant effects for 12 hours, while showed inhibitory effects for18 hours. In NahG, the treatment of MeSA saturated solution had no significant effect for 6 hours, and showed promote effects for 12 hours while showed inhibitory effect for 18 hours. We conclued that: SA and MeSA which under a certain dose play a promoting role in the germination and early growth of Arabidopsis.

7568-32, Poster Session

Combined optical coherence tomography based on the extended Huygens-Fresnel principle and histology of mouse skin

S. Wu, H. Li, Fujian Normal Univ. (China)

With the development laser technology, the laser cosmetology is more paid attention by human kind. So aging skin is more studied, Skin is a nontransparent medium due to absorption and scattering. Absorption depends on the concentration of melanin and hemoglobin and scattering on difference in refractive index. The skin structure changes with aging. In the past, age-related changes in skin have extensively been studied by histological sectioning. And the optical parameters got from scattering medium usually in vitro. In this study, we development a noninvasive measurement technique to obtain tissue optical properties such as the scattering coefficientµs and the anisotropy factor g using optical coherence tomography (OCT) model which based on the Extended Huygens-Fresnel principle. Here, we used older and younger mouseskin to compare its scattering coefficientus and the anisotropy factor g, then got the outcome that scattering coefficientµs was increased with the age of mouse-skin. Furthermore, we made ages mouse-skin into H.E stain slices, from which we observed the morphologic of all mouse-skin and got the changes of collagen and elastic in dermal from younger to older mouse-skin, the result of which is correlated with the OCT imaging and matched with result of OCT-EHF principle. All of that have provided the theoretical basis to the research on photo-aging skin and photoreiuvenation.

7568-40. Poster Session

Tomographic imaging system using digital holograpic technique based on integrating four buckets phase shifting interferometry

G. Min, J. W. Kim, W. J. Choi, Gwangju Institute of Science of Technology (Korea, Republic of); E. S. Choi, Chosun Univ. (Korea, Republic of); B. H. Lee, Gwangju Institute of Science of Technology (Korea, Republic of)

We propose the three-dimensional tomographic imaging system that is based on the phase shifting digital holography microscopy (DHM) using the integrating bucket methods. DHM is the biomedical imaging tool that uses the hologram recorded on a charge-coupled device (CCD), and enables to get refocused images. In order to obtain the refocusing, we need to have the complex field, the field having amplitude and phase, at least on the out of focal plane at the location of CCD. From the complex field on the out of focal plane, the field at the focal plane can be obtained by using diffraction theory in general. In the proposed system, the complex field is acquired from the integrating buckets method as distinct from a existing phase shifting DHM that uses phase stepping methods. The interference fringe is integrated at the CCD during at each quarter period of phase modulation but at four different phases. From four integrated images, the amplitude and the phase at the CCD plane are

extracted. The phase modulation is induced by a piezoelectric transducer (PZT), which vibrates the mirror attached on the reference arm. The proposed system is composed of a white light Michelson interferometer, which uses an incoherence light source as the illuminator. The white light interferometer enables the system to have a high axial resolution in getting the depth information of a sample. Therefore, the proposed system is expected to be a powerful imaging tool owing to its dynamic focusing ability and allow a high resolution tomographic imaging system.

7568-45, Poster Session

Optical modulation of smooth muscle cell contraction

J. Yoon, C. Choi, H. Choi, Korea Advanced Institute of Science and Technology (Korea, Republic of)

Even though electrical stimulation is generally used for induction of smooth muscle cell contraction, it is very hard to obtain fine control and also very invasive for using electrode. Herein, we developed a new optical technology to control smooth muscle cell contraction. This optical method using femtosecond pulsed laser (FSPL) has advantage of focused stimulation and fine control of stimulation intensity. Upon brief exposure to FSPL, primary cultured human and rat vascular and urinary bladder smooth muscle cells showed a rapid increase of intracellular calcium levels followed by cell contraction. We also found that exposure to high-intensity lasers caused a rapid mitochondrial fragmentation and robust retraction of smooth muscle cells. With high-intensity laser stimulation, smooth muscle cells became refractory to further stimulations; however, stimulation with lower intensity FSPL permitted repetitive contraction and calcium waves inside the cells. Collectively, we suggest that FSPL can be a useful tool for control of smooth muscle cell contraction.

7568-49, Poster Session

Development of bioluminescent probe for in vivo imaging of reactive oxygen species

H. Takakura, Y. Urano, T. Nagano, The Univ. of Tokyo (Japan)

Bioluminescent assay system using luciferase and a functional bioluminescence probe is known as one of the most highly sensitive systems for detecting target analytes. So far, several functional bioluminescence probes have been developed, however, a limited range of analytes could be assayed by using these probes due to the design strategy based only on caged luciferin. Recently, we have established novel rational design strategy for fluorescence probes based on the photoinduced electron transfer (PeT) process. Then, we proposed that the concept of PeT could be applied to bioluminogenic substrates.

For the scaffold of tunable luminophore, we selected aminoluciferin as a core structure and synthesized various derivatives bearing benzene ring in the vicinity to examine whether they exhibit luminescence or not. Upon reaction with luciferase almost all the derivatives emitted light, however, the derivatives bearing the benzene moiety of high electron density emitted little luminescence. Therefore it was proved that luciferase-dependent luminescence could be controlled by the concept of electron transfer. By applying the design strategy of guenching by electron transfer, a novel bioluminescence probe, APL, for highly reactive oxygen species (hROS) was developed. APL bears an aryloxyaniline moiety as a moiety of high electron density which is O-dearylated in the ipso-substitution manner by hROS. APL did not emit light even in the presence of luciferase before reaction with hROS, whereas the reaction product of APL and hROS strongly emitted. Further, APL could detect hROS dose-dependently, and it might be powerful tool to observe the formation of hROS in vivo.



7568-53, Poster Session

Quantitative measurement of cerebral perfusion using time-series analysis of indocyanine green molecular dynamics imaging

T. Ku, H. Jeong, C. Choi, Korea Advanced Institute of Science and Technology (Korea, Republic of)

Accurate measurement of cerebral perfusion is important for study of various brain disorders such as stroke, epilepsy, and vascular dementia; however, quantitative and convenient methods which can provide sensitive cerebral perfusion images are not developed. Here we propose a novel optical imaging method using time-series analysis of dynamics of indocyanine green (ICG) fluorescence to generate cerebral perfusion maps. In scalp-removed mice, ICG was injected intravenously, and 740nm LED light was illuminated for fluorescence emission signals around 820nm acquired by cooled-CCD. Time-lapse 2D images were analyzed by custom-built software, and the maximal time point of fluorescent influx in each pixel was processed as a perfusion-related parameter. The generated perfusion map exactly reflected the shape of the brain without any interference of the skull, the dura mater, and other soft tissues. The perfusion map in mice whose scalp was not removed also showed comparable results in both white and black mice. We also confirmed that our method can detect decreased cerebral perfusion in murine cerebral ischemia models. This method may be further applicable for study of other disease models in which the cerebral hemodynamics is changed either acutely or chronically.

7568-77, Poster Session

Detecting biomarkers of disease using carbone-fluorine spectroscopy

F. Menaa, Fluorotronics, Inc. (United States); A. Boucharaba, Ecole Polytechnique Fédérale de Lausanne (France); B. Menaa, C. A. Guimaraes, Fluorotronics, Inc. (United States); L. Avakyants, Lomonosov Moscow State Univ. (Russian Federation); O. N. Sharts, Fluorotronics, Inc. (United States)

The specific detection of markers of disease from biological samples is possible by our patented Carbon-Fluorine Spectroscopy technology (www.fluorotronics.com). A single type of fluoro-modified amino-acid (e.g., 4-Fluoro-L-phenyalanine) was added to the medium-containing cells at the final concentration of 10 mM. The corresponding nonmodified amino-acid (L-phenylalanine) was used as control. The cells (e.g., cancer ones) incorporated naturally the amino-acid during the natural occurring protein synthesis process without interfering with the activity or the conformation of the proteins of interest. After C-F labelling, the biomarker (e.g., p21) was isolated and enriched by immunoprecipitation using a specific antibody. Eventually, the enriched fluoro-labelled protein and the corresponding non-fluoro-labelled protein were comparatively analysed by FRS. A 532 nm DPSS Q-switched laser (Sierra, General Atomics, USA) with 20 kHz repetition rate and 10 ns pulse duration was used to deliver 10 mW of average power to a small amount of the sample. The Raman spectra of the F-labelled protein were specifically and more sensitively detected than the corresponding non-labelled protein. The vibrational assignments of the main spectral regions were identified. Because the C-F signal is directly proportional to the concentration of the analyte, it was also possible to quantify the protein amount. Thus, we show that our non-destructive technology can be routinely used to selectively, sensitively and rapidly detect F-labeled biological molecules in vitro, ex-vivo or in vivo.

Eventually, our emerging fluoro-imaging Raman spectrometry device, using stable and non-fluorescent or radioactive labelling, will definitively offer advantages in terms of health safety (prevention, diagnostics, therapeutics) and cost-effectiveness.

7568-81, Poster Session

Topography, biomechanics, and chemical components of cancer cell membranes exploited by combined atomic force microscopy and Raman microspectroscopy

Y. Wu, G. D. McEwen, S. Baker, T. Yu, T. A. Gilbertson, D. B. DeWald, A. Zhou, Utah State Univ. (United States)

The investigation of the hydrophobic properties of cancer cell membrane is of importance in elucidating cell membrane roles in membrane protein folding, membrane fusion, and cell adhesion that are directly related to cancer cell biophysical behaviors such as aggression and migration. On the other hand, the chemical component analysis of cancer cell membrane could be potentially applied in the clinical diagnosis of cancer by the identification of specific biomarker receptors expressed on cancer cell surfaces. In the present work, a combined atomic force microscopy (AFM) and Raman microspectroscopy technique was applied to detect the difference in hydrophobicity and membrane chemical components between two cancer cell lines, human lung carcinoma cells (A549) and human breast cancer cells (MDA-MB-435 with and without BRMS1 metastasis suppressor). The AFM results indicated that membrane surface adhesion forces for these cancer cells acquired in culture medium were measured at 0.684±0.355 nN for lung cancer A549 cell, and 0.600±0.237 nN for breast cancer MDA-MB-435 cell. Furthermore, Raman spectral analysis indicated similar peaks between two breast cancer cell lines including ~856 cm-1 (ring breathing Tyrosine), 1006 cm-1 (symmetric ring breathing Phenylalanine), and 1455 cm-1 (CH deformation). Slight variations were detected between ~620 - 830 cm-1 (DNA/RNA and proteins) and 1035 - 1210 cm-1 (lipid and proteins). In conclusion, this study demonstrated the capability of using this combined AFM/Raman technique to visualize and localize particular receptors or biomarker molecules expressed on single cancer cell.

7568-89. Poster Session

Novel and facile design of photo-caged bioluminescent probes for noninvasive imaging of firefly luciferase expression

T. Jiang, Nanyang Technological Univ. (Singapore)

Firefly luciferase (fLuc) has been widely utilized for optical reporter gene imaging in biochemical assays, cell culture and living animals. fLuc can catalyze the oxidation of its substrate D-luciferin to generate bioluminescent signal that can be viewed by a charge coupled device camera. Although luciferase based bioluminescence imaging technique displays low background and high sensitivity compared to fluorescence imaging, some challenges still exist, for example, how to precise tracking the dynamic properties of cellular functions and repetitive monitoring the reporter genes at a desired time and/or location in intact cells, tissues or living animals. In order to address these issues, we designed a set of stable and novel photo-releasable luciferin derivatives, which consist of D-Luciferin covalently modified at the 6- hydroxyl position. These "caged" luciferin derivatives display rapid photo release of D-luciferin and confer robust fluorescent and bioluminescent signals with minimum background after brief UV irradiation. Moreover, they also show good membrane permeability, low cytotoxicity within living cell assays and successfully monitor the luciferase activity in living animal. We hope these probes could be used to solve current issues in biological tomography, allowing the visual monitoring of biochemical responses within intact cells.

In addition, we are also currently working on improving the platform from UV uncaging to two-photon IR photolysis, which means a longer excitation could be capable to release the D-luciferin. Compared to UV excitation, this two-photon photolysis will bring up more advantages, such as far less cell or tissue damaging and better tissue penetration. The excellent properties would offer this optical probe a bright future for dynamical or spatiotemporal imaging in living cells and small animals.

BIOS ** SPIE Photonics Wes

Conference 7568: Imaging, Manipulation, and Analysis of Biomolecules, Cells, and Tissues VIII

7568-93, Poster Session

Immersion Mirau Interferometry for labelfree live cell imaging in an epi-illumination geometry

O. V. Lyulko, G. Randers-Pehrson, D. J. Brenner, Columbia Univ. (United States)

In cell biology studies it is often important to avoid the damaging effects caused by fluorescent stains or UV-light. Immersion Mirau Interferometry (IMI) is an epi-illumination label-free imaging technique developed at Columbia University Radiological Research Accelerator Facility. It is based on the principles of phase-shifting interferometry (PSI) and represents a novel approach for interferometric imaging of living cells in medium.

To accommodate the use of medium, a custom immersion Mirau interferometric attachment was designed and built in-house. The space between the reference mirror and the beamsplitter is filled with liquid to ensure identical optical paths in the test and reference arms. The interferometer is mountable onto a microscope objective.

The largest limitation of standard PSI is the sensitivity to environmental vibrations, because it requires consecutive acquisition of several interferograms. We are developing Simultaneous Immersion Mirau Interferometry (SIMI), which facilitates simultaneous acquisition of all interferograms and eliminates vibration effects.

Polarization optics, incorporated into the design, introduces a phase delay to one of the components of the test beam. This enables simultaneous creation and spatial separation of two interferograms, which, combined with the background image, are used to reconstruct the intensity map of the specimen.

Preliminary results show that this system produces images of quality, sufficient to perform targeted cellular irradiation experiments.

This work was supported by the National Institute of Biomedical Imaging and Bioengineering under Grant: NIBIB 2 P41 EB002033-14





Sunday-Tuesday 24-26 January 2010 • Part of Proceedings of SPIE Vol. 7569 Multiphoton Microscopy in the Biomedical Sciences X

7569-01, Session

Plasmon-controlled fluorescence: applications to sensing and single molecule detection

J. R. Lakowicz, K. Ray, M. H. Chowdhury, Y. Fu, J. Zhang, H. Szmacinski, K. Nowaczyk, Univ. of Maryland School of Medicine (United States)

Fluorescence detection has been a valuable tool in the biosciences for several years. In recent years there has been a growing interest in studying the interactions of fluorophores with metallic surfaces or particles. The spectral properties of fluorophores can dramatically be altered by near-field interactions with the electron clouds present in metals. These interactions modify the emission in ways not seen in classical fluorescence experiments. Fluorophores in the excited state can create plasmons that radiate into the far-field and that fluorophores in the ground state can interact with and be excited by surface plasmons. These reciprocal interactions suggest that the novel optical absorption and scattering properties of metallic nanostructures can be used to control the decay rates and direction of fluorophore emission. We refer to these phenomena as plasmon-controlled fluorescence (PCF). Our studies on the effects of metallic surfaces and nanostructures on nearby fluorophores showed significant increase in brightness and photostability both at the ensemble and single molecule level. We believe including metallic nanostructures and nanoparticles offer unique opportunities to further expand the scope of single molecule detection (SMD) and fluorescence correlation spectroscopy (FCS). Recent research combining plasmonics and fluorescence suggest that it is possible to control the migration of electromagnetic energy across and through metal surfaces, and to control where the energy is converted back into light. We believe that metal-fluorophore interactions will result in new approaches for sensing, diagnostics and molecular imaging and in a new generation of ultra-bright probes.

7569-02, Session

Nanoscopy with focused light

S. W. Hell, Max-Planck-Institut für biophysikalische Chemie (Germany)

For a long while, to apply microscopy with focused light meant that details smaller than half the wavelength of light (200 nm) could not be resolved. Today it is know that using conventional optics it is possible to image at least fluorescent samples with a level of detail far below the diffraction limit. Stimulated Emission Depletion (STED) microscopy and newer far-field optical approaches can provide resolutions better than 20 nm, and in principle are able to resolve molecular detail. Thus far-field optical nanoscopy ushers in non-invasive access to the nanoscale of the living cell.

7569-03, Session

Label-free nonlinear optical imaging for biology and medicine

S. X. Xie, Harvard Univ. (United States)

Our group has recently developed several label-free microscopy techniques for imaging living cells and organisms. The contrast mechanisms are stimulated Raman scattering, stimulated emission, and near-degenerate four-way mixing. Unlike fluorescence, they arise from coherent nonlinear responses from a sample, which provide molecular

specificity and high sensitivity for optical imaging. The principles and applications of these new imaging modalities will be discussed.

7569-04, Session 1

Coherent Raman scattering microscopy: current status and new advances

J. Cheng, Purdue Univ. (United States)

Laser-scanning coherent anti-Stokes Raman scattering (CARS) imaging on a confocal microscope platform has become a robust imaging tool. Multimodality on a CARS microscope further permits imaging of complex tissue samples. Stimulated Raman scattering (SRS) microscopy has allowed vibrational imaging with fingerprint Raman band. Fingerprint spectral information is attainable by coupling spontaneous Raman microspectroscopy and coherent Raman imaging using a picosecond laser source. CARS microscopy has shown great potential in areas of single cell profiling, white matter injury, lipid metabolism, cancer, and vascular biology. Although in an early phase, SRS microscopy has opened up exciting opportunities in pharmaceutical research.

7569-05, Session 1

CARS and SHG microscopy of artificial bioengineered tissues

A. M. Enejder, C. Brackmann, J. Dahlberg, P. Gatenholm, Chalmers Univ. of Technology (Sweden)

Major efforts are presently made to develop artificial replacement tissues with optimal architectural and material characteristics, mimicking those of their natural correspondents. Encouraged by the readiness with which cellulose woven by the bacteria Acetobacter xylinum form different macroscopic geometries and microscopic textures, it has immense potential to develop into a multipurpose tissue scaffold. However, systematic studies on how the microstructure of the cellulose network influences its macroscopic properties in terms of strength, elasticity and endurance are not available. Neither on how it can be controlled for the integration and proliferation of native, functional cells. The morphology has been characterized by means of Scanning Electron Microscopy, though limited to gold-coated, freeze-dried samples. This raises the question to which extent the natural morphology was studied. As a promising alternative, we have developed a protocol employing simultaneous CARS and SHG microscopy for monitoring the formation of the cellulose fibrils in vivo and during cell integration in vitro, as well as in situ as implants. The impact of various growth parameters and addition of porogens on fiber density/thickness, degree of branching/ orientation, and layer formation were studied and compared with the characteristics of native tissue matrices. The integration and functionality of a wide range of cells were studied; smooth muscles cells, osteoblasts, and endothelial cells toward fully functional artificial blood vessels, bone tissue, and articular cartilage. We hereby intend to form the fundamental knowledge required for full-scale production of bioengineered tissues, eventually available for clinical use.

7569-06, Session 1

Stimulated Raman scattering (SRS) microscopy: label-free imaging with improved sensitivity and specificity

C. W. Freudiger, W. Min, B. G. Saar, S. X. Xie, Harvard Univ. (United States)

TEL: +1 360 676 3290 · +1 888 504 8171 · customerservice@spie.org



We recently developed a new multiphoton imaging technique, stimulated Raman scattering (SRS) microscopy, which allows imaging based on vibrational spectroscopy without the need for staining or fluorescent labeling. Chemical specificity of the technique is achieved by probing the vibrational frequencies of the molecules. Superb sensitivity is achieved by implementation of a high-frequency phase-sensitive detection scheme and surpasses that of other label-free imaging techniques, such as spontaneous Raman scattering and coherent anti-Stokes Raman scattering (CARS) microscopy. Compared to CARS, SRS microscopy does not suffer from the unwanted nonresonant background signal that distorts vibrational spectra and is thus advantages for applications that require exact spectroscopic identification. We present recent technical advances towards a higher specificity of SRS imaging as well as a variety of applications in lipid metabolism, drug development and understanding of diseases.

7569-07, Session 1

Multimodal CARS microscopy using femtosecond lasers

A. F. Pegoraro, National Research Council Canada (Canada) and Queen's Univ. (Canada); A. Ridsdale, D. J. Moffatt, National Research Council Canada (Canada); B. K. Thomas, L. Fu, L. Dong, M. E. Fermann, IMRA America, Inc. (United States); A. Stolow, National Research Council Canada (Canada) and Queen's Univ. (Canada)

Picosecond laser CARS microscopy has been very successfully applied to a wide range of problems. Such lasers, however, are generally expensive and require an environmentally stable lab environment. In our work, we demonstrate multimodal CARS microscopy using a single femtosecond oscillator combined with a photonic crystal fiber (PCF) and an optimal chirping method. This provides a simple, inexpensive, versatile, broadly and rapidly tuneable source that facilitates multimodal (simultaneous CARS plus SHG plus TPF) imaging. We demonstrate that our optimal chirping approach also permits very facile extension to other techniques such as high speed multiplex CARS and spectral scanning FM CARS imaging. A key point in optimally chirped femtosecond CARS is that the pump-Stokes delay variation corresponds to spectral scanning and allows rapid modulation of the resonant CARS signal. The combination of a femtosecond oscillator with a PCF leads to a natural extension based on fiber oscillators to construct an all fiber source for multimodal multiphoton CARS microscopy. An all fiber system will be compact, highly stable and robust against environmental fluctuations as compared to free space systems. We demonstrate use of an all-fiber based source for simultaneous CARS, TPF and SHG imaging. This simple proof-of-concept system is capable of imaging live tissue samples and live cell cultures with 4 us/pixel dwell time at low average powers.

7569-08, Session 1

Frequency modulation coherent anti-Stokes Raman scattering (FM-CARS) microscopy based on spectral focusing of chirped laser pulses

S. Lim, J. Sung, B. Chen, The Univ. of Texas at Austin (United States)

We demonstrate a new approach to CARS microscopy based on fast switching of effective vibrational excitation frequency generated by chirped broadband laser pulses. Broadband pump and Stokes pulses can excite a single vibrational mode with a high spectral resolution when the two pulses are identical chirped and their pulse durations are approaching the dephasing time of the excited vibrational state. This "spectral focusing" concept is applied to CARS microscopy with a single broadband Ti:Sapphire laser (bandwidth > 1800 cm-1). The vibrational excitation frequency is controlled by the time delay between the pump

and Stokes pulses and fast switching of the excitation frequency (~100 kHz) is achieved with a Pockels cell and polarization optics. Lock-in detection of the difference between the CARS signals at two frequencies separated by the natural Raman linewidth eliminates the non-resonant background and enables highly selective vibrational detection. We also show that the theoretical sensitivity of this technique is comparable to the CARS method with two synchronized narrowband lasers. We demonstrate both micro-spectroscopy and chemical imaging at the fingerprint region of the vibrational spectrum of various biological samples. Selectivity, sensitivity, available CARS vibrational window and application to cell biology are discussed.

7569-09, Session 1

Hyperspectral CARS imaging: label-free and quantitative mapping of cholesterol in lipid mixtures

A. Volkmer, G. Hehl, Univ. Stuttgart (Germany)

By accessing the full wealth of the spectroscopic information content in Coherent Raman Scattering (CRS) microscopy, we report on the hyperspectral coherent anti-Stokes Raman scattering (CARS) imaging of specific lipid molecules in biological systems. Here, CARS microspectroscopy is used for spatially and frequency resolved spectroscopic measurements with sub-micron and 5-cm-1 resolution, respectively. And, phase retrieval using the maximum entropy method (E. Vartiainen, K.-E. Peiponen, T. Asakura, Applied Spectroscopy, 50, 1283-1289 (1996)) is applied to reconstruct linear Raman spectra from recorded CARS spectra. As an example, we demonstrate the quantitative identification of cholesterol, and the formation of cholesterol-rich domains in different lipid structures, such as ternary lipid mixtures and tissues.

7569-10. Session 2

Femtosecond pulse shaping for the enhancement of nonlinear microscopy in tissue

W. S. Warren, M. C. Fischer, Duke Univ. (United States)

Nonlinear optical interactions offer several advantages for molecular imaging in highly scattering tissue. The localized nature of the interaction leads to high spatial resolution, optical sectioning, and larger possible imaging depth than linear methods. However, nonlinear contrast (other than fluorescence) is generally difficult to measure because it is overwhelmed by the large background of detected illumination light. This background can be suppressed by using femtosecond pulse shaping to encode nonlinear interactions in background-free regions of the frequency spectrum. Using these pulse shaping techniques we have been able to detect non-fluorescent metabolic markers and functional processes in tissue (e.g. the imaging of different types of melanin in pigmented lesions, the mapping of oxygenation content in blood vessels, or even the optical recording of electrical activity in live neurons).

Our pulse shaping technique can also be beneficial to the detection of vibrational Raman signatures. The major challenge in coherent Raman detection is the ubiquitous non-resonant contribution to the nonlinear susceptibility. Various way have been devised to either enhance the molecularly specific resonant contributions or to suppress the unwanted non-resonant ones. We will describe a technique to utilize the omnipresent non-resonant component in order to interferometrically enhance the smaller resonant signatures.



7569-11, Session 2

Background-free CARS microscopy at interfaces

H. Rigneault, G. David, Institut Fresnel (France); F. Billard, Institut Carnot de Bourgogne (France); S. Brustlein, Institut Fresnel (France)

Gaussian focused beams exhibit specific properties that drive the emitted fields in nonlinear optical microscopy. We discuss here how the basic field and CARS object symmetry properties can be favorably used to obtain background-free spectra in third-order nonlinear optical processes. We concentrate here on coherent anti-Stokes Raman scattering (CARS) spectra. In CARS microscopy, the vibrational related (resonant) signal is often overwhelmed by a nonresonant background. Various strategies have been implemented to circumvent the undesirable effects of this nonresonant background: picosecond pulse excitation, time resolved, polarization sensitive and epi detections, signal processing, interferometry, spectral or spatial phase control. Among them, the efficient background suppression methods always require complex technical implementation (interferometry, phase mask...). We suggest here a new simple method to obtain pure Raman spectrum in CARS microscopy in a collinear configuration when the resonant medium is forming an arbitrary interface with a nonresonant medium. This is done by the subtraction of two consecutively obtained CARS spectra at interfaces where the roles of the resonant and nonresonant media are inverted. This simple operation cancels the nonresonant background detected in the forward direction and uses the nonresonant medium as a local oscillator with which the Raman spectrum is measured in heterodyne detection. Such a scheme is useful when the sample nonresonant background is stronger than the resonant signal as usually found in CARS microscopy and spectroscopy. Experimental demonstration is conducted on test samples and living cells.

7569-12, Session 2

CARS endoscopy

B. G. Saar, Harvard Univ. (United States); R. S. Johnston, Univ. of Washington (United States); M. B. J. Roeffaers, ; E. J. Seibel, Univ. of Washington (United States); X. S. Xie, Harvard Univ. (United States)

We report an endoscope used to perform in situ imaging based on coherent anti-Stokes Raman scattering (CARS). The imaging is performed with a scanning fiber endoscope (SFE) in combination with a miniature gradient index objective lens. The system produces images at 5 frames per second or better with high spatial resolution and chemical specificity without the use of labels. Details of the design and construction of the device, together with images of test objects and animal tissues are presented. The demonstration of CARS endoscopy is expected to open the door to a range of clinical applications that require high resolution, label-free chemical imaging for diagnosis of disease and surgical guidance.

7569-13, Session 2

Chemistry in confinement: using CARS for quantitative monitoring of chemical processes

M. Bonn, K. Domke, G. Rago, J. Day, FOM Institute for Atomic and Molecular Physics (Netherlands); M. Kox, B. Weckhuysen, Utrecht Univ. (Netherlands)

One of the main advantages of multiplex CARS in combination with maximum entropy method (MEM) data analysis [1] is the possibility to monitor and quantify small changes in the local chemical composition of a sample with submicron resolution.

We have used multiplex CARS to investigate (i) fast chemical reactions occurring in microfluidic reactors and (ii) precursor states of the catalytic polymerisation in the nanometer pores of single- crystal zeolite crystals.

For microfluidics, we extend earlier work on a model acid-base reaction [2], to gather kinetic information on Pt-catalyzed hydrosilation reactions. CARS in conjunction with microfluidics provide a unique means of determining reaction rates and mechanisms.

For the zeolites, differences in the CARS spectra of pure and adsorbed 2-chlorothiophene illustrate the interaction of the reactant with the zeolite pore network. 3D CARS maps of individual (~10 µm size) zeolite crystals reveal that the molecules are distributed rather evenly throughout the crystal prior to polymerisation, with slightly higher local concentrations in the center of the crystal and along defect sites.

The versatile multiplex CARS/MEM tool enables us to detect changes in local chemical composition even in highly congested spectral regions.

[1] E.M. Vertiainen; H.A. Rinia; M. Muller, and M. Bonn, Optics Express 14 (8), 3622 (2006).

[2] D. Schafer, J. Squier, J. Maarseveen, D. Bonn, M. Bonn, and M. Muller, J. Am. Chem. Soc. 130, 115932 (2008).

7569-14, Session 2

Vibrational phase contrast CARS microscopy for quantitative analysis

M. Jurna, E. T. Garbacik, J. P. Korterik, C. Otto, J. L. Herek, H. L. Offerhaus, Univ. Twente (Netherlands)

In biological samples the resonant CARS signal of less abundant constituents can be overwhelmed by the non-resonant background, preventing detection of those molecules. Using a cascaded phasepreserving chain, we obtain the phase of the oscillators in the focal volume that allows discrimination of those hidden molecules. The novelty here lies in the fact that the phase is measured with respect to the local excitation fields. It is measured point-by-point and takes into account refractive index changes in the sample, phase curvature over the fieldof-view and interferometric instabilities. The detection of the phase of the vibrational motion can be regarded as a vibrational extension of the linear (refractive index) phase contrast microscopy. The local phase detection does not require additional sources or wavelengths.

The combination of phase and amplitude information allows for the discrimination of multiple constituents that are simultaneously resonant. By plotting the image in a complex plane based on the detected phase and amplitude, the position of the resonances are separated. Mixing of constituents can be observed as connecting lines between points in the complex plane that represent the pure constituents. We demonstrate vibrational phase contrast CARS microscopy on multiple compound analysis.

7569-16, Session 2

A novel hands-free and compact picosecond CARS light source based on OPO technology

I. Rimke, D. Neumeyer, R. Bressel, E. Büttner, APE GmbH (Germany)

Fast and sensitive imaging with Coherent Anti-Stokes RAMAN (CARS) microscopy requires 3 photons at 2 different tuneable wavelengths perfectly synchronized in time and space, ideally as picosecond pulse trains with around 100 MHz repetition rate and power levels of several hundred milliwatts. In the past few years synchronously pumped picosecond Optical Parametric Oscillators have proven their capability and reliability as light sources in CARS microscopy. But still the systems consisted of separate boxes: pump laser and OPO, with the need of overlapping Pump and Stokes pulses in time and space on the optical



Here we present a novel generation of light sources that is integrating the pump laser and the OPO into one housing and taking care of the spatial and temporal overlap of the pulses. As a pump laser a 7 ps mode locked Nd:VAN laser is used. 1 W of the pump can be used as Stokes pulses and are combined internally with the Signal pulses of the OPO to achieve an energy difference of 700 to 4500 cm-1. Alternatively Signal and Idler of the OPO can be used as Pump and Stokes pulses. Power levels of the 1064 nm and the OPO can be set independently up to 750 mW. Sensors for the temporal and spatial overlap are included. The whole system is completely computer controlled and truly hands free in operation.

To allow for new techniques in suppressing the non-resonant background in CARS such as stimulated RAMAN scattering (SRS) or heterodyne CARS, an acousto-optical modulator with modulation frequencies up to 10 MHz can be integrated into the 1064 nm arm.

7569-21, Session 2

Broadband CARS microscopy: noninvasive chemical imaging for biology

M. T. Cicerone, Y. J. Lee, S. Parekh, National Institute of Standards and Technology (United States)

Several distinct characteristics make coherent anti-Stokes Raman scattering (CARS) microscopy potentially ideal for non-invasively imaging chemically complex systems such as materials and biological cells and tissues. These characteristics include high spatial resolution, high sensitivity, and label-free chemical specificity. Use of vibrational spectroscopy for chemically sensitive imaging of complex samples, such as the intracellular medium, requires spectral sensitivity over the "fingerprint" frequency range of 500 - 1800 cm-1. While broadband CARS microscopy presents the promise of great chemical resolving power, Raman peaks are often crowded and weak in the fingerprint region of biological systems, so can be obscured by noise associated with the nonresonant background (NRB), which normally accompanies the CARS signal. I will discuss CARS signal generation, and methods of extracting quantitative and qualitative chemical information from broadband CARS spectral images of materials and biological systems. I will also discuss application of broadband CARS microscopy to labelfree, noninvasive phenotype determination, with an example of cancer detection in thyroid tissues.

7569-15, Session 3

Nonlinear Raman microscopy: improving detection through nonlinear optical interaction

V. V. Yakovlev, Univ. of Wisconsin-Milwaukee (United States)

Raman spectroscopy based on spontaneous scattering cannot compete with nonlinear Raman spectroscopy, when the sample volume is large enough to take advantage of the coherent nature of nonlinear optical interactions. However, when the interaction volume is small, the number of optical photons generated through spontaneous Raman scattering can be larger than the number of photons generated by coherent Raman process. Nevertheless, for practical reasons, coherent Raman spectroscopies are employed, since they provide a better overall signal-to-noise-ratio.

Why is it happening? Nonlinear Raman microscopy based on CARS or SRS imaging has an obvious advantage over conventional spontaneous Raman spectroscopy on the detection part of the system. Spontaneous Raman spectroscopy suffers from a fluorescence background and a substantial noise associated with the read-out noise of a silicon-based CCD detector. The later also limits the spectral range of the excitation wavelength. Partially, the above problems are addressed with EM-CCD detectors, which allow quality spectral acquisition with 1-ms exposure times [1].

We further improve this concept by providing signal amplification prior

to detection. To achieve this goal we use an optical parametric amplifier, which provides a factor of 1000 gain over a short period of time (4-5 ps) [2-3]. It allows to get rid of fluorescence background, which lasts for several nanoseconds, and allows bringing the number of photons well above the noise level of a typical CMOS linear array detector. As a result, background-free Raman spectra can be acquired in less than 0.1-ms.

In my talk, I will discuss the major design principles and will demonstrate different modes of operation of the new nonlinear microscopic Raman imaging system, which results in substantial simplification of the overall system and allows kHz rate spectral imaging.

References

[1] http://www.witec.de/en/download/Raman/ImagingMicroscopy4_07.

[2] G. I. Petrov, A. Saha, R. Arora, and V. V. Yakovlev, Nature Photonics (2009) Submitted.

[3] V. V. Yakovlev, US Patent Pending (2009).

7569-17, Session 3

Short-pulse fiber lasers for coherent Raman microscopies

F. W. Wise, Cornell Univ. (United States)

The recent emergence of new concepts in pulse-shaping has allowed the development of femtosecond- and picosecond-pulse fiber lasers that offer performance comparable to standard solid-state lasers, but with the practical benefits of fiber devices. This work will be summarized briefly, and applications to Raman microscopies will be described.

7569-18, Session 3

Leica TCS CARS: a CARS commercial solution with high temporal resolution

V. Lurquin, W. C. Hay, V. Krishnamachari, Leica Microsystems CMS GmbH (Germany)

Confocal and multiphoton microscopy are powerful fluorescence techniques for morphological and dynamics studies of labeled elements. For non-fluorescent components, CARS (Coherent Anti-Stokes Raman Scattering) microscopy can be used for imaging various elements of cells such as lipids, proteins, DNA, etc. This technique is based on the intrinsic vibrational properties of the molecules. Leica Microsystems has combined CARS technology with its TCS SP5 II confocal microscope to provide several advantages for CARS imaging. The Leica TCS SP5 II combines two technologies in one system: a conventional scanner for maximum resolution and a resonant scanner for high time resolution. For CARS microscopy, two picosecond near-infrared lasers are tightly overlapped spatially and temporally and sent directly into the confocal system. The conventional scanner can be used for morphological studies and the resonant scanner for following dynamic processes of unstained living cells. The fast scanner has several advantages over other solutions. First, the sectioning is truly confocal and does not suffer from spatial leakage. Second, the high speed (25 images/sec @ 512x512 pixels) provides fast data acquisition at video rates, allowing studies at the subcellular level. In summary, CARS microscopy combined with the tandem scanner makes the Leica TCS CARS a powerful tool for multi-modal and three-dimensional imaging of chemical and biological samples. We will present our solution and show results from recent studies with the Leica TCS CARS instrument to illustrate the high flexibility of our system.



7569-19, Session 3

Coherent Raman imaging of chemical compounds in human hair

E. O. Potma, M. Zimmerley, Univ. of California, Irvine (United States)

Many hair care products claim to improve the health of hair fibers, however, it has been difficult to quantitatively determine what the active components of hair care products actually do to the hair. One important parameter that has remained elusive is to what extent the molecular agents penetrate into the hair. Questions like how fast does penetration occur, how deep, and how much, are still left unanswered. Our study attempts to answer these questions by directly visualizing the molecular agents in the hair. We apply a special optical imaging technique, called coherent Raman scattering microscopy, to visualize applied molecular agents in the hair. Our work shows this maging approach is extremely successful: a series of key molecular agents have now been successfully mapped out in human hair fibers for the first time, providing clues to the functional chemistry and physics of several hair care products.

7569-20, Session 3

Minimally invasive coherent Raman clinical diagnostic microscopy

G. S. Young, Brigham and Women's Hospital (United States); S. Xie, C. Freudiger, B. Saar, Harvard Univ. (United States); S. Kesari, X. Xu, Q. Zeng, Brigham and Women's Hospital (United States)

Despite advances in CT, MRI and PET, (i) definitive differential diagnosis of mass-like brain lesions caused by primary brain tumor (malignant diffuse glioma - MDG), metastases, lymphoma, demyelination, stroke and other disorders, and (ii) pathological subtyping and (iii) grading of primary brain tumors remains impossible prior to brain surgical biopsy in many cases. Minimally invasive, needle guided optical diagnosis could eliminate the need for conventional brain surgery in patients whose mass-like lesions on MRI are not due to primary brain tumor, shorten surgeries for patients with high grade glioma, reduce need for re-operation, improve extent of resection, and thus substantially reducing risks, discomfort, delay and cost of diagnosis of mass-like brain lesions. The novel coherent Raman microscopy techniques Coherent anti-Stokes Raman Scattering (CARS) and Stimulated Raman Scattering (SRS) microscopy, produce chemical contrast derived from intrinsic molecular vibrational spectra specific for lipids, water and protein. Because this does not require staining, it can in principle be applied in vivo, on unfrozen and unfixed tissue. Our goal is to develop a fiberoptic micro-endoscope system for insertion into living brain through a small hollow needle as part of a conventional stereotactic CT or MRI guided core biopsy procedure prior to and/or during brain surgery. We present preliminary data to demonstrate the potential diagnostic efficacy of coherent Raman microscopy for this application, and discuss the fiber-optic, image guidance and stereotactic technologies existing and under development that will be required for ongoing proof of principle experiments.

7569-21, Session 3

High-speed CARS spectral imaging using acousto optic tunable filter

M. Hashimoto, T. Minamikawa, T. Araki, Osaka Univ. (Japan)

We have developed high speed CARS (coherent anti-Stokes Raman scattering) spectral-imaging system using an acousto optic tunable filter and multi-focus excitation system. The highly synchronized ps Ti:Sapphire mode-locked laser and fs Ti:Sapphire mode-locked laser were used for the light source. For detection of high speed CARS

imaging, multi-focus CARS system using a microlens array scanner was used. We compared two methods of CARS emission filtering and CARS excitation filtering. For CARS emission filtering, the generated CARS excited with narrow band ps laser and broad band fs laser was filtered by an AOTF. On the other hand, for excitation filtering the broad band fs laser pulse were filtered before excitation. The experimental result indicated that the CARS emission filtering was suitable for CARS microscopy.

7569-22, Session 3

Stain-free histopathology using nonlinear interferometric vibrational imaging and spectroscopy

P. D. Chowdary, Z. Jiang, W. Benalcazar, A. Ahmad, E. Chaney, M. Gruebele, S. Boppart, Univ. of Illinois at Urbana-Champaign (United States)

Nonlinear interferometric vibrational imaging (NIVI) uses the chemical sensitivity of coherent anti-Stokes Raman scattering (CARS) for endogenous vibrational contrast. By combining chirped-CARS with Fourier transform spectral interferometry, NIVI extracts the complex third order nonlinear susceptibility (3). This helps retrieve the Raman lineshape by eliminating the nonresonant background that plagues CARS. Here, we present proof of the principle results identifying the diagnostic potential of NIVI for breast cancer diagnosis. In particular, we present a diagnostic algorithm, trained to predict the pathological state of rat breast tissue with < 1% classification error. We also discuss the uniqueness of NIVI in combining structural information with spatial texture analysis, which makes it a sensitive clinical diagnostic tool for real time stain- or label-free histopathological studies.

We have imaged normal and tumor tissue sections (30 - 100 µm thick) in the C-H stretch (2800 - 3100 cm-1) vibrational spectral range. The normal and tumor tissue spectra differ in a very reproducible manner for tumors of different size and location from multiple animals. The primary reason for these differences is identified as the relative abundance of lipid (fat) and protein (collagen) domains in the tissue composition. This is consistent with a morphological model for human breast cancer identifying the fat to collagen ratio as a diagnostic parameter. The normal mammary tissue is rich in fat leading to prominent peaks at 2855 cm-1 (C-H2 stretch) and 3015 cm-1 (=C-H stretch). Tumor leads to an attrition of fat thus switching the composition scale towards collagen leading to absence of the above spectral features. We used logistic regression to classify the tissue pathology with < 1% classification error in the reduced dimensional space of just two principal components of spectra from multiple tissue sections. By mapping back the appropriate mix of principal component scores we reconstruct tissue maps for spatial texture analysis. Preliminary studies show substantial promise for the NIVI reconstructed tissue maps to have comparable value to the stained histological images, with added information on spatially-dependent molecular composition.

7569-23, Session 3

Comparing coherent and spontaneous Raman scattering signals for biological imaging and biosensing applications

J. P. Ogilvie, B. R. Bachler, S. R. Nichols, M. Cui, Univ. of Michigan (United States)

Coherent anti-Stokes Raman scattering (CARS) microscopy is an active field of research due to its ability to provide intrinsic molecular contrast. Under some experimental conditions, CARS can provide orders of magnitude higher signal than spontaneous Raman scattering. In biological imaging, potentially higher signals permit faster acquisition times and reduced incident power, limiting the possibility of sample damage. As a multiphoton microscopy, CARS facilitates 3D imaging



due to the inherent localization of the signal to small focal volumes. In addition, the higher frequency of the scattered CARS signal is readily separated from fluorescence produced by many biological samples. A drawback of CARS compared to spontaneous Raman scattering is that its implementation is more complex, and it produces a nonresonant background signal that can distort Raman line shapes and reduce chemical contrast. To date there have been few reports in the literature that compare coherent and spontaneous Raman signals under conditions that are relevant to biological imaging. In a recent comparison study, we found that the signal strengths are comparable for the coherent and spontaneous methods in many potential imaging applications.[1] Our comparison employed a time-delayed three-color coherent Raman method. Here we discuss the relevance of our work to other widelyused approaches to CARS imaging. We also present a preliminary comparison of surface-enhanced coherent and spontaneous Raman scattering signals from plasmonic substrates for use in biological sensing applications.

1. M. Cui, B. R. Bachler, and J. P. Ogilvie, Optics Letters 34, 773-775 (2009).

7569-96, Session 3

Polarization-resolved coherent anti-Stokes Raman scattering microscopy

F. Munhoz, S. Brustlein, Institut Fresnel (France); P. A. Agaskar, Spherosils LLC (United States); S. Brasselet, H. Rigneault, Institut Fresnel (France)

Coherent anti-Stokes Raman scattering (CARS) microscopy is a nonlinear optical technique that provides label-free imaging thanks to its resonant nature. The interaction of the incident fields with the sample induces a third-order nonlinear polarization whose properties depend on the structure of the medium, characterized by a fourth-rank susceptibility tensor, Chi(3). This tensor contains rich information on (1) the microscopic-scale vibrational symmetry properties in isotropic media such as solutions; (2) the macroscopic-scale structural information in ordered media, from highly organized crystals to statistical orientational distributions in biomolecular assemblies.

In this work we investigate polarization-resolved CARS microscopy by continuously varying the incident linear polarizations at the pump and Stokes wavelengths in a pico/pico CARS forward-detection microscope. The emitted signal is furthermore analyzed using a polarized detection.

We show theoretically and experimentally that polarization-resolved CARS applied to a solution (isotropic symmetry) is a powerful way to determine the microscopic Raman depolarization ratio of the probed molecular bonds.

We have furthermore extended the polarimetric CARS technique to ordered crystalline media. Theoretical investigations show that this method is highly sensitive to both the symmetry and the orientation of the structure. First investigations on crystalline H8Si8012 samples (Oh symmetry) show that the measured signals are in good agreement with the corresponding structure symmetry group, and allow retrieving information on the unit-cell orientations in 3D.

This technique can be further applied to biological samples, showing the potential of CARS for conformational investigation. Several pathologies are related to collagen disorder, which can be potentially probed using this method.

7569-24, Session 4

Time-resolved anisotropy imaging enables quantification of protein cluster sizes with sub-cellular resolution

H. C. Gerritsen, A. Bader, E. Hofman, P. van Bergen en Henegouwen, G. van Meer, Utrecht Univ. (Netherlands) Fluorescence anisotropy based homo-FRET imaging methods can be employed to visualize clustering of identical proteins in cells. In this work the potential of steady-state and time-resolved anisotropy detection methods combined with both one- and two photon excitations was investigated for the quantitative imaging of protein clusters with sub cellular resolution. The methods were evaluated on cells expressing green fluorescent protein (GFP) constructs that contain one or two FK506-binding proteins (FKBP12). This allows controlled dimerization and oligomerization of the constructs. Both two-photon excitation and time resolved detection offer a larger dynamic anisotropy range than one photon steady state measurements, resulting in a more accurate discrimination between cluster sizes. The relation between anisotropy and cluster size was established experimentally by the controlled dimerization and oligomerization of the FBPK12 fused GFP. The results show that, independent of the experimental method, the commonly made assumption of complete depolarization after a single energy transfer step is not valid here. This is likely due to a non-random relative orientation of the fluorescent proteins. The experimental relation between anisotropy and cluster size was employed in quantitative cluster size imaging experiments on GPI-anchored proteins and epidermal growth factor receptors (EGFR). The experiments on the GPI-anchored proteins revealed that GPI forms clusters with an average size of more than two subunits. For the epidermal growth factor receptor (EGFR), timeresolved anisotropy imaging reveals that small clusters are present before activation. After activation, the cluster size increases dramatically: anisotropy decreases to a level that corresponds to oligomerization.

7569-25, Session 4

Better FLIM and FCS data by GaAsP hybrid detectors

W. Becker, Becker & Hickl GmbH (Germany)

The principle of the hybrid PMT is known for about 15 years: Photoelectrons emitted by a photocathode are accelerated by a strong electrical field, and directly injected into an avalanche diode chip. Until recently, the gain of hybrid PMTs was too low for picosecond-resolution photon counting. Now devices are available that reach a total gain of a few 100,000, enough to detect single photons at ps resolution. Compared with conventional PMTs, multi-channel PMTs, and SPADs (single-photon avalanche photodiodes) hybrid PMTs have a number of unique features: With a modern GaAsP cathode the detection quantum efficiency reaches the efficiency of a SPAD. However, the active area is on the order of 5 mm2, compared to 2.5 10-3 mm2 for a SPAD. A hybrid PMT can therefore be used for non-descanned detection in a multiphoton microscope. The TCSPC response is clean, without any bumps typical for PMTs, and without the diffusion tail typical for SPADs. Most important, the hybrid PMT is free of afterpulsing. So far, afterpulsing has been present in all photon counting detectors. It causes a signal-dependent background in FLIM measurements, and a typical afterpulsing peak in FCS. With a hybrid PMT, FLIM measurements reach a much higher dynamic range. Clean FCS data are obtained from a single detector. Compared to cross-correlation of the signals of two detectors an increase in FCS efficiency by a factor of four is obtained. We demonstrate the performance of the new detector for a number of applications.

7569-26, Session 4

Seamless integration of FLIM and FCS for confocal laser scanning microscopy

L. Kuschel, Leica Microsystems CMS GmbH (Germany); B. Krämer, U. Ortmann, F. Koberling, M. Wahl, M. Patting, R. Erdmann, PicoQuant GmbH (Germany); C. Kappel, Leica Microsystems CMS GmbH (Germany)

Confocal laser scanning microscopes (CLSM) are an essential tool in biological and biomedical research. Their functionality can be further enhanced by adding highly sensitive time-resolved data acquisition



capabilities, enabling Fluorescence Lifetime Imaging (FLIM) and Fluorescence (Lifetime) Correlation Spectroscopy (F(L)CS) down to the single molecule level.

However, the measurements were up to now relatively tedious because the user had to operate two systems at the same time.

Based on a recently added network interface the FLIM and FCS data acquisition can now be directly accessed from the CLSM computer. This unique integration together with the specialized FLIM and FCS application wizards in the confocal software LAS AF from Leica allows for a seamless workflow recording FLIM volume stacks or for the investigation of the dependence of FLIM images onto the detection wavelengths band (FLIM lambda stacks).

One example for this technique is the spectral and time resolved fingerprinting of pathogenic fungus invading a tomato fruit. The huge information inherent in a lambda - FLIM stack allows to unambiguously identify different autofluorescent structures like chloroplasts, fungal hyphae and putative parenchyma, as to name only a few.

In addition with F(L)CS, diffusion coefficients or sample concentrations can be automatically measured at different preprogrammed locations inside the sample. Single molecule sensitive photon detectors are applied which can also be used for imaging. F(L)CS can therefore be used to calibrate the image intensity in order to display the concentration of the probe molecule investigated.

7569-27, Session 4

Comparison of FRET microscopy imaging techniques for studying protein-protein interactions in living cells using FRET standards

Y. Sun, S. Seo, A. Periasamy, Univ. of Virginia (United States)

Förster resonance energy transfer (FRET) methodology is a powerful tool to localize protein-protein interactions in living specimens. Various FRET microscopy imaging techniques have been established and are generally categorized into intensity-based and lifetime-based methods. Based on the detection of the sensitized emission of acceptor, we have developed the processed FRET (PFRET) method for wide-field, confocal and spectral FRET microscopy. All these FRET microscopy methods have the capability to interpret the change in proximity between donor and acceptor through measuring the apparent FRET efficiency (E%). However, to answer what subtle change can be detected, the imaging techniques have to be well calibrated. Here, we compared the E% measured using various FRET microscopy methods. Their utilities were assessed using several genetic ("FRET standard") constructs where Cerulean and Venus fluorescent proteins are tethered by different amino acid linkers. We also compared the E% results for live and fixed specimens using FLIM-FRET microscopy.

7569-28, Session 4

Time-resolved fluorescence microscopy using TCSPC and multifrequency techniques

L. Chandler, HORIBA Jobin Yvon Inc. (United States)

Time-resolved fluorescence microscopy is the ultimate tool for investigating dynamic events in cellular/sub-cellular structures and nanomaterials. This paper describes a fully automated filter-based confocal system (the DynaMic) to measure fluorescence lifetimes and intensity directly under the microscope. The DynaMic system features time-correlated single photon counting (TCSPC) for sensitive and rapid acquisition. By virtue of its ability to measure multiple frequencies simultaneously, the novel Horiba Jobin Yvon frequency domain system exhibits ultra-fast data acquisition over a broad dynamic range. In contrast to single frequency measurements that provide average lifetime information, the multiple frequency measurements allow accurate resolution of individual lifetimes for complex decays in a single

acquisition. A high speed UV-NIR frequency domain time-resolved system will be introduced as the basis of a future HJY microscope system.

7569-29, Session 4

Regulatory assembly of the vacuolar proton pump VoV1-ATPase in yeast by FLIM-FRET

S. Ernst, Univ. Stuttgart (Germany); C. Batisse, EMBL Heidelberg (Germany); N. Zarrabi, Univ. Stuttgart (Germany); B. Böttcher, EMBL Heidelberg (Germany); M. Börsch, Univ. Stuttgart (Germany)

We investigate the reversible disassembly of VoV1-ATP synthase in life yeast cells by confocal FRET imaging with single-molecule detection methods. During starvation, the ATP-driven vacuolar proton pump disassembles and different diffusion constants of the labeled subunit complexes indicate sizes of single subunits or of fragments of V1. Using a multi color autofluorescent protein fusion system for labeling, tagging different V-ATPase subunits simultaneously allowed for life cell colocalization analyses by fluorescence lifetime imaging (FLIM). Based on the combination of several pulsed lasers at different wavelengths, which can be driven in optimized alternating pulse schemes, the conformation and intramolecular arrangement of subunits C and E are unraveled by fluorescence resonance energy transfer (FRET). Additionally, fluorescence anisotropy revealed large conformational changes in the proton channel which accompany the regulation process.

7569-105, Session 4

Molecular order imaging in lipid membranes by polarimetric two-photon fluorescence microscopy

A. Gasecka, T. Han, C. Favard, H. Rigneault, S. Brasselet, Institut Fresnel (France)

Molecular order is a key parameter in a large variety of biological phenomena. Imaging such molecular organizations quantitatively using optical microscopy remains however a challenge. This issue has been essentially addressed by fluorescence anisotropy, which is however only successful in cases restricted to cylindrical-symmetry distributions with an average orientation known a priori. We present a polarimetric two-photon microscopy technique to image the local static molecular orientational behavior in lipid and cell membranes in the most general configuration. This approach, based on a tuneable excitation polarization state complemented by a polarized read-out, is easily implementable and does not require hypotheses on the molecular angular distribution such as its mean orientation. In particular, it allows retrieving complete information on the molecular distribution shape and orientation in samples that can be strongly heterogeneous. Our experiments are complemented by a model which introduces the effects of distinct absorption and emission angles of the molecular transition dipoles, as well as the presence of fluorescence resonance energy transfer (homo-FRET). The method is applied to the imaging of the molecular angular distribution in Giant Unilamellar Vesicles formed by liquid ordered and liquid disordered micro-domains, and in COS-7 cell membranes. This study is performed on different fluorescent labels that show that the highest order contrast between domains is obtained for dyes locating within the membrane acyl chains. This technique can be extended to other nonlinear imaging processes, as well as in complex geometries such as cells of any shape or biomolecular assemblies of a priori unknown nature.



7569-30, Session 5

Spectral resolved fluorescence lifetime imaging: new developments and applications

A. C. Rueck, F. Dolp, B. v. Einem, C.A.F. v. Arnim, and D. Strat, Univ. Ulm (Germany)

The fluorescence decay of a fluorophore in many cases does not show a simple monoexponential profile. A very complex situation arises, when more than one compound has to be analyzed. This could be the case when endogenous fluorophores of living cells and tissues have to be discriminated to identify oxidative metabolic changes (reviewed in [1]). Other examples are FRET (resonant energy transfer) measurements, when different donor/acceptor pairs are observed simultaneously. In those cases a considerable improvement could be achieved when time-resolved and spectral-resolved techniques are simultaneously incorporated. SLIM (spectral fluorescence lifetime imaging) is a new technique, which combines both. SLIM is working in the time domain employing excitation with short light pulses and detection of the fluorescence intensity decay in many cases with time-correlated single photon counting (TCSPC). Spectral resolved detection is achieved by a polychromator in the detection path and a 16-channel multianode photomultiplier tube with the appropriate routing electronics.

The various possibilities which SLIM offers to improve molecular imaging in living cells will be discussed as well as successfully realized applications [2]. Special attention will be focused on FRET measurements with respect to protein interactions involved in Alzheimer's disease [3]. Improvement of FRET calculations will be presented using global analysis as the phasor plot approach or new algorithms taking into account the multidimensional datasets which results from the kinetic equations in every spectral channel.

[1] D. Chorvat, Jr. and A. Chorvatova, "Multi-wavelength fluorescence lifetime spectroscopy: a new approach to the study of endogenous fluorescence in living cells and tissues," Laser Phys. Lett., 6(3), 175-193 (2009).

[2] A. Rück, C.H. Hülshoff, I. Kinzler, W. Becker, R. Steiner, SLIM: A new method for molecular imaging," Micr. Res. Tech., 70, 485-492 (2007).

[3] A. Rück, F. Dolp, R. Steiner, C. Steinmetz, B. v. Einem, C.A.F. v. Arnim, SLIM for multispectral FRET imaging," SPIE Proceedings, Photonics West, 6860, 68601F-1 (2008).

7569-31, Session 5

Dynamics of celluar energy metabolism during cell culture growth measured with fluorescence lifetime and anisotropy imaging

V. Ghukasyan, T. Buryakina, C. Hsu, F. Kao, National Yang-Ming Univ. (Taiwan)

Energy metabolism rate is an important parameter of cells physiology. The rate values change significantly in a range of diseases, such as cancer, Parkinson's disease, various mitochondrial dysfunctions, etc. and this served as a basis for the development of new diagnostic techniques. Autofluorescence lifetime and anisotropy imaging (AFLAIM) techniques have been demonstrated as the most advantageous for the metabolic mapping of cells as of their noninvasiveness and sensitivity. Mainly based on the measurement of lifetime and anisotropy of coenzyme nicotinamide adenine dinucleotide reduced (NADH), one of the key molecules in energy turnover in cells, they provide with the relative concentrations of free and bound forms of this compound. When bound, NADH donates an electron to the so called electron transfer chain in mitochondria, launching the synthesis process of adenosine triphosphate, the main repository and transporter of energy in cells, so that free/bound ratio of NADH is an indicator of metabolic activity of cells. In order to properly characterize the NADH dynamics in normal state, which is important for thorough discrimination from pathologies, we have applied AFLAIM for the metabolic mapping of cells growing in culture, revealing the changes in initial, exponential and confluency stages, and showing the dependence of the metabolism rate on cells density.

7569-32, Session 5

Pulsed excitation is not just TPE and FLIM: lifetime weighted FCS (FLCS) and laser cutting with confocal laser scanning microscopes

V. Buschmann, B. Kraemer, PicoQuant GmbH (Germany); S. Fore, PicoQuant Photonics North America, Inc. (United States); I. Raabe, J. Peychl, Max-Planck-Institut für molekulare Zellbiologie und Genetik (Germany); U. Ortmann, F. Koberling, P. Kapusta, PicoQuant GmbH (Germany); I. M. Tolic-Nørrelykke, Max-Planck-Institut für molekulare Zellbiologie und Genetik (Germany); R. Erdmann, PicoQuant GmbH (Germany)

In recent years the upgrade of confocal laser scanning microscopes (CLSM) towards time-resolved measurements have become very popular. Today such upgrades are readily available for all major CLSM manufacturers and are usually based on the Time-Correlated Single Photon Counting (TCSPC) technique. The required pulsed excitation is conveniently generated by picosecond pulse diode lasers, which cover a broad spectral range between 375 nm and the infrared. Even the formerly problematic green excitation around 532nm has become available recently.

Besides the "classical" applications such as FLIM, FLIM-FRET or FCS, upgraded CLSMs offer even more possibilities, exploiting the benefits of pulsed excitation:

(a) By using in addition also lifetime information of the measurement data, classical intensity based FCS can be improved by sorting and weighting the detected photons. We will show how Fluorescence Lifetime Correlation Spectroscopy (FLCS) can be used to suppress detector afterpulsing or to separate up to four signal components in a single detector setup. We will also show how FLCS enables a significant background reduction in cellular environments and present examples of FLCS used as an alternative to dual color FCCS using only a single laser and detector setup.

(b) A picosecond pulsed diode laser at 405nm can also be used as a tool for intracellular nanosurgery. We will show examples of cutting of fluorescently labelled microtubules and mitotic spindles in fission yeast. Various effects from photo-bleaching to partial and complete breakage are obtained by varying the exposure time, while simultaneously imaging the structures of interest. Such a setup can even be used to generate enucleated cells without perturbing the distribution of other organelles.

7569-33, Session 5

Total internal reflection fluorescence lifetime imaging microscope to probe FRET in neurobiology

V. Devauges, LPPM-CNRS, Univ. Paris-Sud 11 (France); P. Blandin, LPPM-CNRS, Ecole Supérieure de Physique et de Chimie Industrielles (France); J. Cossec, CRICM, Ecole Supérieure de Physique et de Chimie Industrielles (France); S. Lécart, CPBM, Univ. Paris-Sud 11 (France); C. Marquer, M. Potier, CRICM, Ecole Supérieure de Physique et de Chimie Industrielles (France); F. Druon, P. Georges, Institut d'Optique Graduate School (France); S. Leveque-Fort, LPPM-CNRS, Univ. Paris-Sud 11 (France)

In order to follow dynamic biological processes at the plasma membrane, we combined Total Internal Reflection Microscopy with Fluorescence Lifetime Imaging Microscopy (FLIM). Thanks to the supercontinuum laser source, this TIRFLIM set-up allows us to perform wide-field imaging with sub-wavelength axial resolution for a large range of fluorophores and probe the cells' environment. To achieve real time FLIM, we are currently testing different approaches to optimize fluorescence decay sampling but



also processing.

This set-up is currently dedicated to the study of the homodimerization of the amyloid precursor protein (APP), a membrane protein involved in Alzheimer's disease (AD). It is cleaved by two enzymes (the -secretase BACE1 and the -secretase complex) to release the A peptide, which accumulates in senile plaques, one of the major hallmarks of AD. It was shown that the addition of cholesterol at the plasma membrane leads to a higher production of $\ensuremath{\mathsf{A}}$, related to an increase of APP homodimerization. We are following FRET efficiency (between GFP and mCherry) using FLIM to study the APP homodimerization. These FRET measurements are made in parallel on living HEK-293 cells and on embryonic rat's hippocampal neurons. We're also implementing time resolved fluorescence anisotropy measurements in TIRF configuration to evidence HomoFRET and so probe more efficiently homodomerization. Likewise, we want to underline the cholesterol's action on the heterodimerization of APP with its -site cleaving enzyme (BACE1).

Performances of the set-up will be fully described, as well as our first results on homodimerization and heterodimerization of APP in living neurons and cells.

7569-34, Session 5

In vivo stoichiometry monitoring of G protein coupled receptor oligomers using spectrally resolved two-photon microscopy

M. R. Stoneman, D. R. Singh, V. Raicu, Univ. of Wisconsin-Milwaukee (United States)

Resonance Energy Transfer (RET) between a donor molecule in an electronically excited state and an acceptor molecule in close proximity has been frequently utilized for studies of protein-protein interactions in living cells. Typically, the cell under study is scanned a number of times in order to accumulate enough spectral information to accurately determine the RET efficiency for each region of interest within the cell. However, the composition of these regions may change during the course of the acquisition period, limiting the spatial determination of the RET efficiency to an average over entire cells. By means of a novel spectrally resolved two-photon microscope, we are able to obtain a full set of spectrally resolved images after only one complete excitation scan of the sample of interest (Raicu, Stoneman, et al, Nat. Photonics, 3, 2009). From this pixel-level spectral data, a map of RET efficiencies throughout the cell is calculated. By applying a simple theory of RET in oligomeric complexes to the experimentally obtained distribution of RET efficiencies throughout the cell, a single spectrally resolved scan reveals stoichiometric and structural information about the oligomer complex under study. This presentation will describe our experimental setup and data analysis procedure, as well as an application of the method to experiments involving the determination of RET efficiencies throughout yeast cells (S. cerevisiae) expressing a G-protein-coupled receptor, Sterile 2 factor protein (Ste2p), in the presence and absence of -factor, a yeast mating pheromone.

7569-35, Session 5

New strategies to measure sodium concentrations in living cells.

S. Dietrich, B. Hoffmann, S. E. Stanca, C. Cranfield, K. Benndorf, C. U. Biskup, Univ. Hospital Jena (Germany)

Fluorescent ion indicators are widely used to measure ion concentrations in living cells. However, despite considerable efforts in synthesizing new compounds, no ratiometric sodium indicator is available that can be excited at visible wavelengths. Using non-ratiometric indicators may result in artifacts that are caused by inhomogeneities of the indicator concentration or the illumination path: Measured high fluorescence signals are not necessarily due to a high sodium concentration but can also be caused by accumulation of the indicator dye in certain regions of a cell or a higher illumination intensity. It is difficult to disentangle

these effects. As a consequence, it is almost impossible to measure sodium concentrations reliably. One way to circumvent this problem is to measure fluorescence lifetimes, which are independent of these factors. Another way is to embed the indicator dye and a reference dye in the polymer matrix of nanoparticles. By relating the indicator fluorescence to the fluorescence of the reference dye, inhomogeneities in the nanosensor concentration can be cancelled out reliably. This approach has the additional advantage that the indicator dye is protected by the polymer matrix from interactions with intracellular proteins, whereas it is still freely accessible to sodium ions. In this study we compare the benefits and drawbacks of both approaches.

7569-36, Session 6

Current developments in clinical multiphoton tomography

K. König, Univ. Saarbrücken (Germany) and JenLab GmbH (Germany)

This review focuses on applications of in vivo clinical multiphoton tomography of hundreds of patients and volunteers in Europe, Asia, and Australia. The femtosecond laser scanning multiphoton tomographs DermaInspect and MPT flex provide fluorescence and SHG images with submicron spatial resolution, picosecond temporal resolution as well as spectral resolution (spectral FLIM). Two-photon high NA microendoscopes (1.7 mm outer diameter) can be attached to the systems. The major application field is the human skin. The tomographs are in clinical use for early diagnosis of melanoma (sensitivity 95%, specificity 97%) and Atopic Dermatitis as well as to optimize PDT and other treatment modalities. Characteristic FLIM patterns in dependence on the disease were found.

Another major application field is the testing of cosmetical products by French, German, and Japanese companies such as the intratissue distribution of sunscreen nanoparticles, the determination of the skin age by the spatially resolved measurement of the ratio of elastin to collagen, the interaction of agents with intracellular coenzymes as well as the biosynthesis of collagen by anti-aging products.

Current developments include the combination of OCT, ultrasound, confocal reflectance, and Raman/CARS with multiphoton tomography.

7569-37. Session 6

Long-term marker-free multiphoton imaging, targeted transfection, optical cleaning of stem cell clusters, and optical transport of microRNA with extreme ultrashort laser pulses

A. Uchugonova, Univ. Saarland (Germany); K. König, H. Studier, JenLab GmbH (Germany); G. M. Kostner, Medizinische Univ. Graz (Austria); Z. Földes-Papp, ISS, Inc. (United States)

The novel utrashort femtosecond laser scanning microscope FemtOgene (JenLab GmbH, Germany) with 12 femtoseconds at the focal plane have been employed in marker-free imaging and optical manipulation of stem cells as well as fort he non-contact introduction of microRNA in cancer cells.

Human adult pancreatic stem cells, salivary gland stem cells, and human dental pulp stem cells have been investigated by femtosecond laser multiphoton microscopy. Autofluorescence based on NAD(P) H and flavoproteins and second harmonic generation due to collagen have been imaged with submicron spatial resolution, 270 ps temporal resolution, and 10 nm spectral resolution. Major emission peaks at 460 nm and 530 nm with typical mean fluorescence lifetimes of 1.8 ns and 2.0 ns, respectively, were measured in a variety of stem cells using spectral imaging and time-correlated single photon counting. During differentiation, the ratios of bound to free NAD(P)H and NAD(P)



H/flavoproteins changed. In addition, the biosynthesis of lipids and collagen was detected over a long period of time of up to 5 weeks. Nanoprocessing was performed with 12 femtosecond laser pulses and low picojoule pulse energies to realize targeted transfection and optical cleaning of human adut stem cell populations.

Multiphoton sub-20fs microscopes may become novel non-invasive tools for marker-free optical stem cell characterization, for on-line monitoring of differentiation within a three-dimensional microenvironment, and for optical manipulation.

7569-38, Session 6

Arbitrary-scan imaging for two-photon microscopy

E. J. Botcherby, C. W. Smith, M. J. Booth, R. Juskaitis, T. Wilson, Univ. of Oxford (United Kingdom)

The standard approach for imaging volume specimens in multiphoton microscopy is to record a through-focus stack of images, from a volumetric specimen. Focusing to different depths in the specimen is usually done by physically changing the distance between the objective lens and specimen, a process that is relatively slow. We have recently built a two-photon microscope based on a different refocusing architecture that overcomes this speed limitation. In our system, refocusing is carried out remotely and rapidly - at least an order of magnitude faster than existing methods based on mechanical movement of the specimen. In addition to acquiring traditional through-focus image stacks of a specimen our system is also capable of scanning userdefined paths and imaging specific features of a specimen directly. Due to the refocusing method used, images can be obtained at far greater speeds than previously from curved surfaces, complex linear trajectories or from discrete points in three-dimensional space. In this paper, we will present experimental results from studies that use these different scan modes and demonstrate the potential use our system in biology.

7569-39, Session 6

Multiphoton microscopy as a diagnostic imaging modality for lung cancer

I. P. Pavlova, K. R. Hume, S. A. Yazinski, R. M. Peters, R. S. Weiss, W. W. Webb, Cornell Univ. (United States)

Lung cancer is the leading killer among all cancers for both men and women in the US, and is associated with one of the lowest 5-year survival rates. Current diagnostic techniques, such as histopathological assessment of tissue obtained by computed tomography guided biopsies, have limited accuracy, especially for small lesions. Early diagnosis of lung cancer can be improved by introducing a real-time, optical guidance method based on the in vivo application of multiphoton microscopy (MPM). In particular, we hypothesize that MPM imaging of living lung tissue based on two-photon excited intrinsic fluorescence and second harmonic generation can provide sufficient morphologic and spectroscopic information to distinguish between normal and diseased lung tissue. Here, we used an experimental approach based on MPM with multichannel fluorescence detection for initial discovery that MPM spectral imaging could differentiate between normal and neoplastic lung in ex vivo samples from a murine model of lung adenocarcinoma. Current results indicate that MPM imaging can directly distinguish normal and neoplastic lung tissues based on their distinct morphologies and fluorescence emission properties in non-processed lung tissue. Moreover, we found initial indication that MPM imaging differentiates between normal alveolar tissue, inflammatory foci, and neoplasms at various stages of malignant progression. Our long-term goal is to apply results from ex vivo lung specimens to aid in the development of multiphoton endoscopy for in vivo imaging of lung abnormalities in various animal models, and ultimately for the diagnosis of human lung cancer.

7569-40, Session 6

Controllable infrared continuum source for multiphoton imaging

C. de Mauro, D. Alfieri, Light4Tech Firenze S.r.I. (Italy); M. Arrigoni, D. Armstrong, Coherent, Inc. (United States); F. S. Pavone, Univ. of Florence (Italy)

Light sources obtained via nonlinear broadening in photonic crystal fibers (PCFs) have been demonstrated to be suitable for different biological imaging techniques, ranging from multiphoton microscopy to optical coherence tomography as examples. A high degree of spatial coherence and a controllable spectrum are very important for high resolution imaging and to achieve a great versatility in a compact source.

Usually the spectrum from a PCF can cover the range from ultraviolet up to 2 microns, with hundreds of milliwatts of total power. Instead, we choose to pump in the normal dispersion region, limiting the non-linear interaction and favouring a greater power density (above 2 mW/nm) only in the 700-1000 nm range. Indeed, the two-photon absorption cross sections of most common dyes, lie in this spectral region. Moreover, the typical power densities used in most microscopy systems are of the order of a few milliwatts per nanometer. While the spectral coverage of the broadened spectra is lower than the overall coverage of the pump laser, advantages of using the fiber are the generation of the larger spectrum simultaneously and the rapid switching between portions of the spectrum, using a dedicated spectral shaper. The continuum beam has been coupled into a scanning microscope system. Spatial resolution close to theoretical limit has been measured as well as autocorrelation trace of the pulse at fiber output for time distribution characterisation. Spectral selectivity of different dyes in the same sample and high image resolution are demonstrated at tens of microns in depth.

7569-41, Session 6

What can jumping optical tweezers offer in probing the cell mechanics of red blood cells?

Y. Wu, C. Ho, M. Wei, A. E. T. Chiou, National Yang-Ming Univ. (Taiwan)

In jumping optical tweezers, a laser beam, diffracted by an acoustooptic modulator (AOM), was coupled into a high NA objective lens via appropriate optics to serve as the trapping beam. The focal spot was scanned discretely (or jumped) between two points by controlling the voltage of the radio-frequency (RF) driving the AOM. At a scanning frequency ~1kHz, the jumping focal spots served as a pair of parallel laser tweezers. With appropriate laser power and jumping distance, individual erythrocytes were trapped in the focal plane and stretched along the scanning direction. We measured under different environmental conditions not only the steady-state deformation of individual erythrocytes as a function of jumping distance (in the range of 3.1µm to 7.3µm) but also the deformation dynamics, in terms of the deformation time constant and the recovery time constant, by switching the jumping distance back and forth between 3.8µm and 5.9µm. Simple theoretical models were applied to correlate the deformability and the deformation time constant with the viscoelastic properties of the cell. The viscoelastic properties of individual erythrocytes under different environments, such as temperature, osmotic pressure, pH, and the oxidative stress will be reported.

7569-42, Session 6

Latest advances in ultrafast laser sources for multiphoton microscopy

P. G. Smith, Newport Spectra-Physics (United States)



The advent of compact, fully automated, and widely wavelength-tunable ultrafast oscillators has triggered an explosive growth in their use in a broad array of multiphoton imaging techniques. Over the past decade laser manufacturers have constantly improved the performance characteristics of these sources to meet the requirements of the user community. We will review the latest advances at Newport / Spectra-Physics in this field and discuss new ways of optimizing key parameters for efficient deep-tissue fluorescence generation, including turn-key, automated second order dispersion compensation that allows for optimization of the pulse width at the sample over a wide wavelength range, without compromising beam pointing and other critical beam parameters.

7569-43, Session 6

Nonlinear fs-laser scanning microscopy with broadband and ultrabroadband pulses

H. Studier, H. G. Breunig, K. König, JenLab GmbH (Germany)

Non-linear microscopy of human skin and of differently colored nanobeads was carried out using two different excitation fs-lasers: a spectrally tunable 80-MHz-Ti:sapphire oscillator which produced 100-fs pulses (spectral width ~10 nm) and an 1-GHz-Ti:sapphire oscillator generating ultra broadband 6-fs pulses. The lasers were combined with a laser scanning microscope (TauMap, Jenlab GmbH), a system for high resolution three-dimensional fluorescence imaging with submicron resolution, to excite various naturally endogenous fluorophors of the skin at different depths. The non-linearly induced autofluorescence arises mainly from the proteins NADH, flavins, elastin, melanin and porphyrins. Additionally, second harmonic generation (SHG) was exploited to detect collagen fibers. While the ultra broadband pulses enable simultaneous excitation of several fluorophors at once due to the overlap of the pulse spectrum and the two-photon absorption spectra, the 100 fs pulses are spectrally selective and require wavelength tuning for covering the same absorption range. This wavelength selectivity was confirmed in measurements with nanobeads with absorption maxima in the red, green and blue spectral region. In the skin measurements in particular, the strength of the collagen SHG signal in dependence on the spectral excitation width was investigated. The influence of the 12.5 times higher pulse repetition rate under the condition of same average laser power at the target will be discussed. In order to examine the impact of pulse duration on the autofluorescence and SHG signals as well as on the depth of maximal signal strength a dispersion precompensation was assembled.

7569-44, Session 6

Wavefront correction in two-photon microscopy using a nematic liquid crystal modulator

G. Hall, J. G. White, K. Eliceiri, Univ. of Wisconsin-Madison (United States)

A novel approach to correct wavefront aberrations in two-photon microscopy is proposed. Previously, deformable mirrors have been used to correct for optical aberrations thereby facilitating imaging at increased depths within the specimen. However, these devices generally have a limited stroke and resolution.

We have used a nematic liquid crystal spatial light modulator (NLC-SLM, Boulder Nonlinear Systems) with a high resolution (512x512 pixels) and a stroke of 2pi which makes it possible to correct large aberrations. In particular by taking the modulo 2pi of the wavefront to correct even larger aberrations.

In order to evaluate the potential of the device, the correction range and accuracy of the NLC-SLM is estimated using a Shack-Hartmann wavefront sensor at a conjugate plane.

Aberrations introduced by a refractive-index mismatch at the sample-

immersion medium interface are predicted theoretically and compared with experimental data. In particular, we consider the practical case of imaging with a high numerical-aperture oil immersion lens into an aqueous medium as well as into other media with different refractive indices. In addition we consider the effects of imaging depth and numerical aperture.

Our theoretical results have shown that quite a large stroke is required to correct for aberrations due to refractive-index mismatch, in particular at increasing depths. Initial experimental results have shown an improvement in image intensity using wavefront correction. Work is in progress to quantify and compare the theoretical and experimental results.

7569-45, Session 6

Two-photon excited photothermal lens microscopy for label free imaging of heme proteins

S. Lu, W. Min, S. Chong, G. R. Holtom, X. S. Xie, Harvard Univ. (United States)

Heme proteins, such as hemoglobins and cytochromes, play important roles in various biological processes. To be able to image these protein in their intrinsic physiological environment could greatly facilitate biomedical studies such as tumor angiogenesis, cerebral oxygen delivery in brain and apoptosis signaling.

In this work, we employ the two-photon excited photothermal effect as a new contrast mechanism to map heme proteins distribution. Particularly, both a thermal lens scheme and a high-frequency modulation are utilized to enhance the signal-to-noise ratio. Compared with one-photon excited photothermal microscopy, two-photon excited photothermal effect concentrates excitation field in the z-axis and offers better signal, 3D sectioning and spatial resolution. Using NIR laser beam for two-photon excitation also minimizes scattering and photodamage in thick biological samples. We demonstrate label-free imaging of individual red blood cells, mitochondria in live mammalian cells and the micro-vascular networks in mouse ear tissue and in a zebrafish gill.

7569-46, Session 6

Imaging skin mast cells in vivo with twophoton autofluorescence microscopy

C. Li, Massachusetts General Hospital (United States); R. K. Pastila, Radiation and Nuclear Safety Authority (Finland) and Massachusetts General Hospital (United States); C. P. Lin, Massachusetts General Hospital (United States)

We report in vivo mouse skin mast cells imaging with two-photon fluorescence microscopy by using endogenous tryptophan as the fluorophore. Mast cells are widely recognized as the effector cells in allergic diseases. Recently their roles both as effector and as immunoregulatory cells in certain immune responses are being actively investigated. Newly identified functions of mast cells in neural system, cardiovascular disease, and tumor biology include neuroimmune links, anti-inflammatory and immunosuppressive effects. No in vivo method exists to perform functional imaging of mast cells in real-time to our knowledge. Therefore an in vivo mast cell imaging modality will not only greatly improve the quality and quantity of in vivo murine mast cell data but also introduce a new way of conducting human mast cell research. We have developed two-photon microscopy for mast cell imaging in vivo with endogenous tryptophan fluorescence, where the pre-stored granules in mast cells act as the source of the tryptophan fluorescence. Mast cell degranulation is the first step in the mast cell activation process in which the granules are released into peripheral tissue to trigger downstream reactions. In vivo imaging of the mast cell exocytosis process will give insight into the dynamics of mast cells reactions to the specific stimulation. We have also monitored mast cell degranulation process in



vivo upon immune stimulation by quantifying the tryptophan fluorescence intensity change with two-photon microscopy. The results indicate quick release of granules by mast cells upon immune stimulation.

7569-103, Session 6

Advances in lasers for biological imaging

D. P. Armstrong, Coherent, Inc. (United States)

Biological imaging techniques such as multiphoton excitation and fluorescence lifetime imaging have become important techniques, enabling the study of dynamic processes in living cells and tissues without causing significant damage. These techniques can produce high-resolution, three-dimensional images, and primarily rely on the use a tunable, ultrafast laser to excite highly specific fluorophores in order to follow specific biochemical processes. Key to future advances in multiphoton biological imaging is the ability to work with a wider range of fluorophores, to increase data acquisition speed, and to improve data signal-to-noise ratio. In terms of laser characteristics, these requirements translate into wider tuning range, faster tuning speeds, and higher peak power delivered to the sample. This paper explores the advances in tunable ultrafast laser and amplifier technology currently under development to meet these goals and thus power the next generation of MPE instrumentation.

7569-70, Poster Session

Real-time molecular imaging of organelles in living cell by multifocus excitation CARS microscope

T. Minamikawa, T. Araki, M. Hashimoto, Osaka Univ. (Japan)

We demonstrated real-time imaging of organelles in a living HeLa cell with a multi-focus excitation CARS (coherent anti-Stokes Raman scattering) microscope. By the multi-focus excitation, image exposure time is prolonged proportionally to number of the foci, and thus a high signal-to-noise ratio imaging will achieved comparing with a single beam scanning method. Two ps Ti:sapphire lasers were used as light source. Laser pulse duration was automatically minimized and the two lasers were synchronized within 30 fs with the bandwidth of 150 Hz. The multiple foci were formed with a microlens array disk scanner. We observed a living HeLa cells at 2840 cm-1 which originates in CH2 stretching vibration. The image acquisition rate of 10 frames per second was achieved. We also obtained z-sectioned images of living HeLa cells with 80 sections over 8 micrometers, and three-dimensional distribution of lipid rich organelles, such as mitochondria, lipid rich vesicles, and nucleolus, was visualized within 16 s.

7569-71, Poster Session

In situ observation of collagen thermal denaturation by second harmonic generation

C. S. Liao, Z. Y. Zhuo, J. Y. Yu, P. H. Chao, S. W. Chu, National Taiwan Univ. (Taiwan)

Recently, laser thermal therapies have been increasingly applied to treatment of tumor and other diseases. For example, by heating cornea with radio frequency waves, the shrinkage of collagen fibers provides a precise means to correct hyperopia, astigmatism, or presbyopia. Since collagen is the most abundant protein in human tissues, it is of vital importance to characterize heat-induced collagen denaturation processes for clinical practice.

Here we use second harmonic generation microscopy (SHGM) to study collagen denaturation in situ. The technique provides noninvasive, in vivo observation with optical sectioning capability. It has been shown that SHG intensity is strongly related with the molecular conformation of type

I collagen; thus it may be the only way to reveal both the shrinkage and denaturation of collagen.

We heated tendon collagen from 30°C to 60°C with 2°C step for 30 minutes every step and simultaneously imaged the denaturation progress by SHGM. Below 56°C, there was no shrinkage and SHG intensity unchanged. At 56°C the denaturation started and we found that the process could be classified to three stages. First, the crimp pattern of collagen became straight and then the straight collagen fibrils started to shrink. Because the overall SHG intensity remained unchanged, the changes in the first two stages arose mainly from the break of interconnecting hydrogen bond between collagen molecules. At the third stage, the SHG intensity became weaker, indicating the denaturation of triple-helical structure inside collagen molecules. This three-stage process may only be revealed by SHG imaging technique.

In conclusion, we investigate the heat-induced denaturation in molecular level, which provides detailed understanding of the biothermal-mechanics

7569-72, Poster Session

Spatio-temporal control in multiphoton fluorescence laser-scanning microscopy

A. K. De, D. Roy, D. Goswami, Indian Institute of Technology Kanpur (India)

Multiphoton fluorescence laser-scanning microscopy (LSM), one of the modern day imaging techniques, relies on the non-linear photon absorption of fluorophores. However, due to the broad spectral window of an ultra-short laser pulse and the broad overlapping multiphoton absorption spectra of common fluorophores restrict selective excitation of one fluorophore in presence of others. This can be taken care of by controlling the optical field in time-frequency domain. Starting with the pulse train modulation (PTM) technique [1, 2], the use of pulse-pair excitation [3] along with some recent work on high-speed laser pulseshaping (using a concave grating based programmable pulse shaper with acousto-optic spatial light modulator (AO-SLM) acting as a spectral phase modulator) compatible with LSM will be addressed. In addition, the combination of spatial beam shaping with pulse-shaping in time frequency domain will be discussed. 1. De, A. K. and Goswami, D., "Exploring the Nature of Photo-Damage in Two-Photon Excitation by Fluorescence Intensity Modulation", J. Fluorescence 19, 381-386 (2009). 2. De, A. K. and Goswami, D., "A Simple Twist for Signal Enhancement in Non-linear Optical Microscopy", J. Microscopy in press (2009). 3. De, A. K. and Goswami, D., "Coherent Control in Multiphoton Fluorescence Imaging, Proc. SPIE 7183, 71832B: 1-6 (2009).

7569-73, Poster Session

Discrimination the collagen in normal and pathological dermis through polarization second harmonic generation

P. Su, W. Chen, National Taiwan Univ. (Taiwan); J. Hong, National Taiwan Univ. Hospital (Taiwan); T. Li, R. Wu, C. Chou, National Taiwan Univ. (Taiwan); S. Lin, National Taiwan Univ. Hospital (Taiwan) and Biomedical Engineering Institute, National Taiwan Univ. (Taiwan); C. Dong, National Taiwan Univ. (Taiwan)

Polarization-resolved, second harmonic generation (P-SHG) microscopy at single pixel resolution is utilized for medical diagnosis of pathological skin dermis. In analyzing the large area, pixel by pixel, second order susceptibility of normal and pathological skin dermis, we found that P-SHG can be used to distinguish normal and dermal pathological condition of keloid, morphea, and dermal elastolysis. Specifically, we found that the second order susceptibility tensor ratio of d33/d31 for normal skins is 1.27±0.20, while the corresponding values for keloid, morphea, and dermal elastolysis are respectively 1.67±0.29, 1.79±0.30, and 1.75±0.31. We also observe that the histogram distributions of the



d33/d31 ratio for the pathological skins are 1.5 times wider than that of the normal case, suggesting that the pathological dermal collagen fibers tend to be more structurally heterogeneous. Our work demonstrates that pixel-resolved, second-order susceptibility microscopy is effective for detecting heterogeneity in spatial distribution of collagen fibers and maybe used for future clinical diagnosis of collagen pathological

7569-74, Poster Session

Multispectral autofluorescence lifetime imaging of RPE cells using two-photon

J. Qu, L. Zhao, D. Chen, H. Niu, Shenzhen Univ. (China)

The retinal pigment epithelium (RPE) cell is one of the most important functional cell types in the retina. Its metabolic state is related to the causes of many retinal diseases, such as diabetic retinopathy, glaucoma and age-related macular degeneration (AMD) etc. In this paper, we present our investigation on multispectral autofluorescence lifetime imaging of RPE cells in four emission bands (500-550nm, 550-600nm, 600-700nm, and 500-700nm) using two-photon excitation fluorescence microscopy. Morphological characters of RPE cells have been obtained with high spatial resolution. Different autofluorescence lifetime parameters, such as m, 1, 2, 1, 1/2, q1, have been compared in different emission channels. Spatial distribution of dominant endogenous fluorophores in RPE cells, such as FAD, A2E and AGE etc have been obtained by the analysis of m and 1/2 ratio in the whole emission spectrum (500-700nm). Our experimental results show that the fluorophore with Ops < m < 300 ps, 1/2 > 19,95 < 1 < 100 and emission spectrum of 600-700nm is distributed in the whole cell but is concentrated in the juxtamembrane region, which is corresponding to A2E; the fluorophore with 0ps \leq m \leq 300ps, 0 \leq 1/2 \leq 9, 0 \leq 1 \leq 80 and emission spectrum of 500-550nm is concentrated in cytoplasm region, which is corresponding to AGE; a small quantity of fluorophores with $300ps \le m \le 800ps$, $0 \le 1/2 \le 9$, $0 \le 1 \le 80$, and emission spectrum of 500-550nm is distributed in the outermost area of the cell, and in the membrane, the fluorophore may originate from FAD; the fluorophore with 300ps≤ m≤800ps,9≤ 1/ 2≤19, 80≤ 1≤95 and emission spectrum of 550-600nm is distributed in juxtamembrane region, which may originate from one or several fluorophores.

7569-75, Poster Session

In vivo multiphoton imaging of metabolic dynamics of obstructive cholestasis in mice

F. Li, C. Dong, National Taiwan Univ. (Taiwan)

We tried to image obstructive cholestasis by using a newly developed imaging system to measure the alterations of hepatobiliary function in living mice with ligated bile ducts. A hepatic imaging window was installed on the upper abdomen soon after the mice underwent ligation of common bile duct. On the next day, the mice received intravenous injection of rhodamine B isothiocyanate-dextran and carboxyfluorescein diacetate (CFDA). The later would be transformed into fluorogenic carboxyfluorescein (CF) by hepatocytes and then excreted into bile canaliculi. By time-lapsed, multiphoton imaging, fluorescence intensities within hepatocytes and sinusoids were measured. In mice with bile duct ligation, bile canaliculi failed to appear during the observation period of around 100 minutes post-carboxyfluorescein diacetate injection. Furthermore, CF fluorescence intensities in sinusoids were persistently higher and longer retained than in hepatocytes. Bile duct ligation impedes hepatocyte excretion of CF into bile canaliculi. Our results show that intrvital multiphoton microscopy can be used to image and characterize metabolic changes in diseased liver. Such studies can lead to an improved understanding of hepatobiliary diseases.

7569-77, Poster Session

Versatile photonic crystal fiber-enabled source for multi-modality biophotonic imaging beyond conventional multiphoton microscopy

H. Tu. S. Boppart, Univ. of Illinois at Urbana-Champaign (United States)

An ultrafast Ti:sapphire laser, due to its wide wavelength tunabilty across 690-1040 nm, has become the most popular light source for multiphoton microscopy (MPM). While such source is very useful, there are a significant number of fluorescent agents which can only be multiphotonexcited in the visible (<690 nm) and the infrared (>1100 nm). Thus, it will be desirable to convert some energy of the near-infrared Ti:sapphire beam into a visible and/or an infrared beam by nonlinear frequencyconversion techniques. This does not affect the normal operation of the Ti:sapphire laser since the laser typically possesses an average power more than adequate for MPM. Also, the generation of such additional excitation wavelengths is essential for Coherent anti-Stokes Raman scattering. Optical parametric oscillators (OPO) are most popular for this purpose, but they introduce significantly higher costs and experimental complexity. Also, one OPO can only generate one additional excitation wavelength.

We present an alternative nonlinear frequency-conversion technique based on Cherenkov radiation from photonic crystal fibers pumped under a short nonlinear-interaction condition, which is a simple and costeffective method. This process allows spectrally-isolated narrowband (~10 nm) Cherenkov radiation with a typical average power of 10 mW to be generated across 485-690 nm, and spectrally-isolated Raman solitons having a typical average power of 30 mW to be simultaneously generated across 1100-1400 nm. The wavelength of the frequencyshifted components can be tuned by varying the wavelength of the Ti:sapphire laser. Thus, this technique adds to the near-infrared source laser the capability of a picosecond (or femtosecond) visible laser and a femtosecond infrared laser, and should therefore considerably expand its capability for MPM.

7569-78, Poster Session

Ultrasensitive Raman imaging in living monocytes using doubly-resonant four-wave mixina

T. J. Weeks, Lawrence Livermore National Labs. (United States) and Univ. of California, Davis (United States); T. R. Huser, S. Wachsmann-Hogiu, Univ. of California, Davis (United States)

Trialyceride-rich lipoproteins (TGRL) distribute lipids and energy to cells through the vascular system. TGRL particle size and their chemical composition and structure are all implicated in the development of atherosclerotic cardiovascular disease (ASCVD). Recent work has shown that monocytes treated with TGRL lipolysis products form lipid droplets in their cytoplasm. Live cells treated directly with free fatty acids, such as oleic acid also form similar lipid droplets. By directly labeling fatty acids with small molecule markers with unique Raman-spectral signatures this process can be directly visualized with high contrast and high specificity in live cells by coherent Raman scattering (CRS) microscopy. To further increase the sensitivity of CRS, we have developed a new approach called doubly-resonant four-wave mixing (DR-FWM) microscopy, which exploits interferences between two Raman resonances. Here, we will discuss the mechanisms leading to the formation of lipid droplets in monocytes as well as the sensitivity limits of DR-FWM and how such label free imaging techniques may contribute to biomedical research.



7569-79, Poster Session

Multiplex coherent anti-Stokes Raman scattering flow cytometry for real-time classification of particles in a microfluidic channel

C. H. Camp, Jr., S. Yegnanarayanan, A. A. Eftekhar, Georgia Institute of Technology (United States); H. Sridhar, Harvard Univ. (United States); A. Adibi, Georgia Institute of Technology (United States)

Multiplex anti-Stokes Raman scattering (MCARS) is applied to differentiating particles within a microfluidic channel. As opposed to fluorescent techniques, MCARS does not require the addition of endogenous fluorophores, which may disrupt or discontinue normal biological processes. Additionally, as MCARS is a broadband Raman technique, it can collect much or all of the vibrational spectrum simultaneously; thus, cytometric analysis is not limited to just a single wavelength, and allows the analysis of not only particle presence and size, but also chemical composition in real-time. In our work, the particles were fed into a glass microfluidic chip through a syringe pump that provided a controllable, constant flow of the particles as well as confined their location within the channel by hydrodynamic focusing. An MCARS microscope focused on the center portion of the channel recorded broadband spectra covering approximately 1450 - 3300 cm-1. The MCARS microscope used a femtosecond Ti:sapphire laser as the pump/ probe source and to feed a length of photonic crystal fiber that produced a supercontinuum Stokes source. The resultant CARS spectrum from a sample is collected into a cooled-CCD spectrometer. Using this system, spectra were recorded of passing particles and subsequently registered based on their spectral features. Using the methyl-stretch region of the Raman spectra, 9 um diameter polystyrene (PS) and Poly(methyl methacrylate) (PMMA) microspheres were successfully differentiated.

7569-80, Poster Session

Quantitative analysis of biological tissues using Fourier transform-second-harmonic generation imaging

R. Ambekar Ramachandra Rao, Univ. of Illinois, Urbana-Champaign (United States); M. R. Mehta, S. M. Leithem, K. C. Toussaint, Jr., Univ. of Illinois at Urbana-Champaign (United States)

We demonstrate the use of Fourier transform-second-harmonic generation (FT-SHG) imaging of collagen fibers as a means of performing quantitative analysis of obtained images of selected spatial regions in porcine trachea, ear, and cornea. Three quantitative markers that determine preferred fiber orientation, minimum feature size, and spacing between periodic fiber structures are proposed for differentiating structural information between various regions of interest in the specimens. In the spatial frequency domain, the estimated minimum feature size (or maximum spatial frequency) and orientation in the ear does not exhibit any spatial variation, as is confirmed in its real-space image. Conversely, for the trachea, there are observable changes in the orientation and minimum feature size, indicating a more random organization. Finally, the analysis is applied to a 3D image stack of the cornea. It is shown that the standard deviation of the orientation is sensitive to the randomness in fiber orientation. Regions with variations in the maximum spatial frequency, but with relatively constant orientation, suggest that this is useful as an independent quantitative marker. Also, select regions exhibit many periodic arrays of fibers of various spacings. We emphasize that FT-SHG is a simple, yet powerful, tool for extracting information from images that is not obvious in real space. This technique can be used as a quantitative biomarker to assess the structure of collagen fibers that may change due to damage from disease or physical injury.

7569-81, Poster Session

NIR Luminescence Microscopy for Nano- and PV-Material Characterization

L. Chandler, HORIBA Jobin Yvon Inc. (United States)

NIR luminescence spectroscopy is an essential technique for biomedical imaging and material characterization. Because of the low absorption coefficient of human tissue in the NIR region (>700nm), the background interference is significantly reduced, which makes it possible for deep tissue imaging in in vivo imaging applications. Significant effort has been made toward developing NIR emissive nano-materials including quantum dots, single walled carbon nanotubes, and Groupings of Uniform Materials Based on Organic Salts (GUMBOS). The latest developed NIR quantum dots, such as PbS, have its emission extended beyond 1000nm, and shown much improved stability. The GUMBOS is a new class of nano-material with single step preparation and much improved uniformity, and is an ideal candidate as a leakage free probe for in vivo imaging. In the recent solar cell development, time-resolved NIR spectroscopy is proven to be an important tool for solar cell process control process. This paper describes an advanced NIR luminescent instrument for characterizing these new NIR nano-materials and solar cells, and the fluorescence life mapping and hyper-spectral imaging results will be presented.

7569-82, Poster Session

Fluorescence standards for confocal microscopy

S. Ruettinger, Physikalisch-Technische Bundesanstalt (Germany); P. Kapusta, V. Voellkopf, F. Koberling, R. Erdmann, PicoQuant GmbH (Germany); R. Macdonald, Physikalisch-Technische Bundesanstalt (Germany)

Confocal laser scanning microscopes are broadly used in biological and biomedical studies.

State of the art confocal microscopes offers, diffraction limited (or even better) spatial resolution, single molecule sensitivity and ps-fluorescence lifetime measurement accuracy. However, even for the manufactures it is difficult to assign numbers to these qualities. For the user it is not easy to ascertain that the instrument is properly aligned as a large number of factors might influence resolution or sensitivity. Therefore we aspire to design a set of standard samples to be deployed on a day-to-day fashion in order to check the instruments characteristics.

The main quantities such standards must address are:

spatial resolution (in confocal microscopy this is the confocal volume) sensitivity (molecular brightness)

fluorescence lifetime

To facilitate the deployment and thus promote wide range adoption in day-to-day performance testing the standard samples have to be ready made, easy to handle and to store. The measurement procedures necessary should be available on as many different setups as possible and the procedures involved in their deployment should be as easy as possible

To this end, we developed two standard samples to accomplish the mentioned goals:

Resolution standard

Combined molecular brightness and fluorescence lifetime standard

The first one is based on the imaging of the confocal volume with subresolution sized Tetra-Speck fluorescent beads or alternatively on the imaging of single molecules on a glass surface, while the latter is a liquid sample containing fluorescent dyes of different concentrations and spectral properties.

Both samples are sealed in order to ease their use and prolong their storage life.



Currently long term tests are performed to ascertain durability and road capabilities.

sensitivity over spontaneous emission and absorption contrast, allowing more reporters for molecular imaging.

7569-83, Poster Session

Fiber-based multiphoton system

G. Liu, Beckman Laser Institute and Medical Ctr. (United States); K. Kieu, Cornell Univ. (United States); L. Yu, Beckman Laser Institute and Medical Ctr. (United States); F. W. Wise, Cornell Univ. (United States); Z. Chen, Beckman Laser Institute and Medical Ctr. (United States)

Multiphoton microscopy (MPM) is an important technology for in vivo imaging of cells, embryos and organisms. MPM has been introduced into the clinic (Dermalnspect, JenLab GmbH, Germany). Ti:Sapphire femtosecond laser is currently widely used as the dominate light source for MPM due to its high power output, short pulse and broad wavelength tunability. However, there are several drawbacks of this laser including its bulky size, high cost, and the need for maintenance. Recent advancement in the development of fiber laser has made cheap, portable and maintenance-free laser sources available. We designed an ultrafast, all normal dispersion (ANDi)fiber laser with central wavelength of around 1.06uµm, 125 femtosecond pulse width and watt-level average output power. The ANDi fiber laser is simple in structure. Laser mode locking is easily obtained through turning of the waveplates and the mode locking is quite stable.

We designed and integrated a handheld probe with double cladding photonic crystal fiber (DCPCF), a galvanometer based scanner, and a half-inch-diameter lens system. The DCPCF works in both excitation pulse delivery and multiphoton signal collection. The DCPCF have a large core (16 μm) diameter and a high numerical aperture (0.65) inner cladding. The lens system includes a beam expander and a focusing lens. The lateral resolution of the system was found to be less than 2 μm by imaging fluorescence beads. Second harmonic generation and two photon excited fluorescence images of biological sample were demonstrated with our system.

7569-84, Poster Session

Biological chromophore imaging with stimulated emission microscopy

W. Min, S. Lu, S. Chong, R. Roy, G. Holtom, S. X. Xie, Harvard Univ. (United States)

While fluorescence, i.e., spontaneous emission, has long been considered to be the most sensitive contrast mechanism in optical bioimaging, many chromophores do not have detectable fluorescence because their spontaneous emission are dominated by the fast nonradiative decay and hence overwhelmed by various background signals. Here we report the use of stimulated emission as a contrast mechanism for imaging of chromophores. In a pump-probe experiment, upon photoexcitation by a ~200fs (FWHM) pump pulse, the sample is stimulated down to the ground state by a time-delayed ~200fs probe pulse, whose intensity is concurrently increased. By intensity modulation of the pump beam at a high megahertz-frequency and using a lock-in amplifier for phase-sensitive detection, we extract the miniscule intensity increase with shot-noise limited sensitivity. Due to its nonlinear dependence on the input intensities, the signal is generated only at the laser foci, which offers intrinsic three-dimensional optical sectioning capability. In contrast, conventional one beam absorption measurement suffers from poor sensitivity, lack of 3D sectioning capability, and complication by sample scattering. We demonstrate a variety of applications of stimulated emission microscopy, including visualizing chromoproteins, non-fluorescent variants of the green fluorescent protein, monitoring lacZ gene expression with a chromogenic reporter, mapping transdermal drug distribution, and label-free microvascular imaging based on endogenous contrast from hemoglobin. In all these cases, stimulated emission microscopy offers orders of magnitude improvement in detection

7569-85, Poster Session

Advances in complex monolithic optics for optical tagging in multi-wavelength fluorescence microscopy

A. Graham, G. P. Tsai, J. Dow, Agilent Technologies, Inc. (United States)

Fluorescent tagging of biological cell structures, organelles, and proteins is a common research tool in many academic and government laboratories. Commercial interest for pharmaceutical discovery and clinical diagnostics is hindered by the lack of reliable, robust tools for certain processes. In particular, though significant progress has been made improving microscopy techniques and fluorescent reagents over the last few years, little improvement has been made to the light sources necessary to stimulate the substantial Stokes shifts required.

Initially, fluorescent illumination utilized HeNe and Ar+ laser lines. Later, monochromator-based light sources were used to address the diversity of wavelengths enabled by newly developed reagents; but low-power, off-wavelength light-leakage, and low sensitivity limited application to commercial requirements.

More recently, advancements in solid-state laser technology enable sufficient diversity of wavelengths to largely eliminate the need for monochromator-based illumination instrumentation. Today, a series of discrete optics and optomechanical mounts with precision adjustment enable combination of up to five lasers in a single instrument. However, the alignment freedom of each optomechanical mount results in a highly-random assembly process that is less robust in the laboratory where temporal and environmental instabilities require frequent realignment and cleaning for optimal performance.

Complex Monolithic Optic (CMO) design uses external assembly tooling to control and lock alignment tolerances such that alignment and other instabilities are eliminated. A CMO-designed combiner achieves an accuracy that can be maintained over a wide variety of shipping, storage, and operating conditions with no ongoing alignment maintenance required.

7569-86, Poster Session

Fiber optic two-photon fluorescence endomicroscope with dynamic focus tracking

Y. Wu, L. Huo, J. Xi, X. Li, The Johns Hopkins Univ. (United States)

A miniature fiber-optic endomicroscope probe with dynamic focus tracking was developed for three-dimensional two-photon fluorescence (TPF) imaging of biological samples. A double-clad fiber was used for both single-mode fs laser delivery and efficient large-area collection of the nonlinear optical signals. Fast two-dimensional lateral beam scanning was realized by resonantly vibrating the double-clad fiber with a tubular piezo actuator. Slow axial scanning was achieved by moving the probe or the miniature objective lens with an electrically driven shape memory alloy (SMA) which is extremely compact. The SMA allowed maximally ~3% contraction of the length (e.g. ~300 µm contraction with 1 cm long SMA) with a driving voltage varying from 50 mV to 100 mV. A depth scanning accuracy of 10 µm could be easily achieved. The response of the SMA contraction with the applied voltage was nonlinear and could be accurately calibrated. Three-dimensional two-photon fluorescence imaging was performed on fluorescent phantoms, unstained white paper, and biological tissue samples stained with acriflavine. The depth-resolved imaging results strongly suggest the potential of this novel nonlinear optical endomicroscope probe with shape memory alloy for in vivo threedimensional assessment of internal organs.



7569-87, Poster Session

Nonlinear phase contrast imaging in tissue

P. Samineni, H. C. Liu, Duke Univ. (United States); R. Yasuda, Duke Univ. Medical Ctr. (United States); W. S. Warren, M. C. Fischer, Duke Univ. (United States)

Nonlinear microscopy can achieve high spatial resolution and optical sectioning even in thick scattering samples. The most widely used nonlinear contrast is two-photon fluorescence; however, its use is restricted to fluorescent markers (in the near-IR region these are mostly exogenous dyes). Here we investigate nonlinear phase modulation as a contrast mechanism in tissue. Nonlinear phase contrast is an intrinsic material property and can depend on molecular structure, local anisotropy and chemical environment.

We have developed a spectral hole refilling measurement technique for self-phase modulation (SPM) measurements using shaped ultrafast laser pulses. With this technique we can extract nonlinear phase contrast in tissue with very modest laser power levels. As an important application of this technique we have demonstrated strong intrinsic SPM signatures of glutamate induced neuronal activity in ex vivo hippocampal rat brain slices. Recently we have been able to show that SPM changes occur in individual neurons during electrically stimulated trains of action potential firing.

We will describe the dual-color extension of our nonlinear phase modulation measurement. While in the single color case (self-phase modulation) the phase of the propagating pulse is modified by the pulse itself, in the dual-color case (cross-phase modulation, XPM) one pulse affects the phase of the other. We have independent control of both colors, which offers a much better background suppression and a larger parameter space to explore. We will describe our experimental implementation of the measurement technique based on femtosecond pulse shaping, and discuss potential applications.

7569-88, Poster Session

Nonlinear microscopy with wavelength swept pulsed laser delivered by single-mode fiber

J. W. Kang, P. Kim, S. Yun, Massachusetts General Hospital (United States) and Harvard Medical School (United States)

Since multiphoton microscopy was invented, there has been much effort to translate it into clinic. Multiphoton imaging can excite common UV fluorephores without damaging UV illumination and the use of infrared laser makes deep imaging possible. Furthermore, many intricsic molecules can be imaged by multiphoton fluorescence without labeling. Comprehensive multiphoton microscopic imaging of internal organ can reduce sampling error, costs, risk and time compared to random biopsy.

Nonlinear microscope is implemented based on wavelength swept pulsed laser delivered by single mode fiber. Sweeping source is made by filtering broadband mode-locked titanium: sapphire laser using galvano mirror, grating, and single mode fiber. The instantaneous power and linewidth of the source are 3mW and 1.1nm at the central wavelength. This sweeping picosecond pulse is delivered through 5m single mode fiber without precompensation.

At the end of the fiber, fast scanning is done by combining sweeping laser and dispersive optics. Swept pulsed laser is diffracted by grating and makes focus on sample plane by single aspheric lens.

Comprehensive image of internal tubular organ can be done by combining fast scanning with slow spiral scanning. To mimic spiral scanning in tubular organ, slow axis scanning is done by one dimensional motorized stage.

Two photon fluorescence image of stained lens tissue and the second harmonic generation image of mouse tail tendon are successfully obtained. Combined with spiral scanning, this can be applied for endoscopy system in the near future.

7569-89, Poster Session

Line scanning multiphoton modulation microscopy with a single element detector

S. S. Howard, A. Straub, C. Xu, Cornell Univ. (United States)

Conventional imaging microscopy with a multi-element detector generates high quality, high speed images of biological samples. Image quality is subsequently reduced in scattering media as points within the sample are not faithfully mapped to the detector. Point scanning microscopy allows for imaging in scattering media by illuminating a single diffraction limited point in the sample at a time, allowing for a single-element large-area detector to be used with no loss in resolution. However, the image is generated serially, introducing an inherent speed limitation.

In this presentation, we demonstrate a novel line scanning multiphoton microscope with parallel acquisition of pixels using a single element detector, potentially allowing fast imaging deep into scattering tissue by illuminating several hundred diffraction limited points in a sample at one time, each modulated at a unique RF frequency. The sample response is measured by a single-element detector (PMT) and demodulated to reconstruct the diffraction limited image. The excitation light is modulated by a custom-built spatial light modulator that can modulate 5 micrometer x 5 micrometer pixels at rates over 1 MHz by scanning a focused line across a lithographically patterned reflective surface. We characterized the system in transmission mode with a 1951 USAF Resolution Test Chart target generating a 115 x 374 pixel diffraction limited image with modulation rates from 150 to 300 kHz. Additionally, the intrinsic second harmonic generation from tendons extracted from the tail of a rat was imaged ex vivo by epi-collecting the signal through the objective and detected by a PMT.

7569-90, Poster Session

Microprisms for in vivo multiphoton microscopy of mouse cortex

T. Chia, M. J. Levene, Yale Univ. (United States)

Fluorescence microscopy of cortical slices, yielding ready access to all six layers of cortex, has proven to be a powerful technique in neurophysiology, however it lacks the context of in vivo experiments. In vivo microscopy, primarily multiphoton microscopy, provides this context but without ready access to deeper layers and typically involves imaging of a field-of-view that is roughly parallel to the cortical layers. Needle-like gradient index (GRIN) lenses have been used as invasive relay lenses to access deeper brain structures, however these lenses damage the apical dendrites of the neurons of interest during insertion into the cortex, and are therefore of limited use for functional cortical imaging.

We present here the use of micro-prisms for performing in vivo multiphoton microscopy of mouse cortex. Small (~1 mm) prisms with a reflective coating on the hypotenuse act as a miniature periscope, rotating the image plane from one parallel to the cortical layers to one that is perpendicular to the layers. This enables simultaneous imaging of the entire thickness of cortex, much as is done it cortical slice preparations, while maintaining a large degree of the in vivo context.

7569-91, Poster Session

Two-photon imaging of partial pressure of oxygen in small animal brain tissue and vasculature

S. Sakadzic, Massachusetts General Hospital (United States) and Harvard Medical School (United States); M. A. Yaseen, Massachusetts General Hospital (United States); V. J. Srinivasan, E. T. Mandeville, Massachusetts General Hospital (United States) and Harvard Medical School (United States); A. Devor,



Massachusetts General Hospital (United States) and Harvard Medical School (United States) and Univ. of California, San Diego (United States); E. Roussakis, Univ. of Pennsylvania (United States); E. H. Lo, Massachusetts General Hospital (United States) and Harvard Medical School (United States); S. A. Vinogradov, Univ. of Pennsylvania (United States); D. A. Boas, Massachusetts General Hospital (United States) and Harvard Medical School (United States)

Non-invasive monitoring of brain vascular and tissue partial pressure of oxygen (pO2) is of crucial importance for understanding brain metabolism in normal and diseased brains. Two-photon imaging of pO2 based on oxygen-quenching of phosphorescence offers the unique potential to provide high spatial resolution pO2 imaging of both cortical tissue and vasculature deep within brain tissue.

We have developed a two-photon microscopy system for measuring pO2 using oxygen dependent quenching of phosphorescence. In order to increase the detection sensitivity, a custom-built two-photon microscope was designed with the large etendue four-channel fluorescence detector, in which one channel was equipped with the photon counting PMT for collection of phosphorescence decays. Imaging was performed using a recently developed oxygen-sensitive probe with large two-photon absorption cross section. The Pt porphyrin core in the probe is well protected from interactions with the proteins in the probe environment - an important characteristics for application of the dye in both tissue and blood. Demonstrations of in vivo pO2 heterogeneity in mice cortical microvasculature and brain tissue pO2 responses during hypoxia and cortical spreading depression are presented.

The developed system is a novel tool for quantitative analysis of the dynamic delivery of oxygen and brain tissue functions and metabolism on a microscopic scale, which will lead to a greater understanding of neurovascular coupling in normal and diseased brain.

7569-92, Poster Session

In vivo deep tissue imaging with long wavelength two-photon excitation

D. Kobat, M. E. Durst, N. Nishimura, A. W. Wong, C. B. Schaffer, C. Xu, Cornell Univ. (United States)

As a result of the large difference between scattering mean free paths and absorption lengths in brain tissue, scattering dominates over absorption by water and intrinsic molecules in determining the attenuation factor for wavelengths between 350 nm and 1300 nm. We propose using longer wavelengths for two-photon excitation, specifically the 1300-nm region, in order to reduce the effect of scattering and thereby increase imaging depth. In this study, we demonstrate the advantages of using the excitation spectral window around 1300 nm for two-photon excitation over the conventional excitation window around 800 nm in in vivo mouse brain. A calibrated imaging depth comparison reveals that high contrast imaging of in vivo cortical vasculature can be achieved at approximately twice the depth with 1280-nm excitation as with 775-nm excitation. An imaging depth of 1 mm can be achieved in in vivo imaging of adult mouse brains at 1280 nm with approximately 1-nJ pulse energy at the sample surface. Our imaging depth is comparable to that of the previous record by Theer et al. using nearly 200-nJ excitation pulses at the sample surface. As an illustration of the capability of twophoton microscopy to measure deep tissue physiological dynamics, blood flow speed measurements at a depth of 900 µm are performed. Furthermore, we observed an increased capability to image through blood vessels and a greater ability to suppress endogenous fluorescence background with 1280-nm excitation.

7569-93, Poster Session

Coherent anti-Stokes Raman scattering microscopy using photonic crystal fiber

M. Naii, S. Murugkar, K. Khan, H. Anis, Univ. of Ottawa (Canada)

Broadband multiplex coherent anti Stokes Raman scattering (CARS) microscopy using a single femtosecond laser (pump beam) and the supercontinuum (Stokes beam) generated in a photonic crystal fiber (PCF) has been recently gaining in popularity. An ideal Stokes beam derived from the PCF would provide sufficient power and broad tunability in order to access the fingerprint region (800 - 1800 cm-1) as well as the vibrations due to lipid and water molecules.

We compare the performance of two different PCF's of identical lengths, but different spacing between the zero dispersion wavelengths (200 nm and 500 nm), for implementation of the Stokes source in a multimodal microscopy and spectroscopy setup. The CARS imaging of lipid- rich biological samples is demonstrated. Relative intensity noise (RIN) measurements are performed to determine the noise in the supercontinuum from the two fibers as well as in the CARS signal under similar excitation conditions of the input pulse into the PCF. We show that the RIN of the PCF with further zero dispersion wavelengths (500nm) is higher than that of the closer one (200 nm). Moreover, our results indicate a correlation between the spacing of the two zero dispersion wavelengths and the strength of the CARS signal. Simulations are employed to understand the physical process underlying the experiments.

7569-94, Poster Session

Ex vivo second and third harmonic generation imaging of cornea by epi-detection on a whole eye

L. Jay, C. Dion, A. Brocas, K. Singh, J. Kieffer, Institut National de la Recherche Scientifique (Canada); I. Brunette, Univ. de Montréal (Canada); T. Ozaki, Institut National de la Recherche Scientifique (Canada)

We have previously shown that the simultaneous use of second harmonic generation (SHG) and third harmonic generation (THG) imaging can clearly distinguish the different corneal layers, even on the posterior side of this tissue. This is a unique capability, which is difficult by other imaging methods. For example, THG can reveal the Stroma/ Descemet membrane interface, which has not been imaged using autofluorescence. However, it is important to demonstrate the application of this technique to a whole eye, which requires both signals to be detected in the backward (epi-) direction.

The laser source used for harmonic generation imaging was a solid-state mode-locked Yb:KGW oscillator (t-Pulse 20: 1030nm, 1000mW, 200fs. 50MHz; Amplitude-Systemes). The nonlinear optical imaging system consisted of an upright microscope built using opto-mechanical parts. Fresh ex vivo eyes (pig or rabbit) were obtained from a farm within 6 hours of death and kept in a humid chamber at 4 degrees C until the experiments.

SHG/THG signals are combined to image cornea at the macroscale providing OCT-like picture, to precisely determine the position of the corneal layers. At the microscale, the technique can reveal morphologic details in the different layers (e.g. endothelial cells and keratocytes). Recently, we have demonstrated that these images can be obtained on the whole eye by epi-detection on full thickness corneas. This new ability, when added to the intrinsic possibility of nonlinear optical microscopy to allow 3D reconstruction, results in a promising tool for future clinical application.



7569-97, Poster Session

CARS microscopy in a microcavity

H. Rigneault, D. Gachet, Institut Fresnel (France); F. Billard, Institut Carnot de Bourgogne (France)

For more than two decades there has been a tremendous work devoted to the understanding of atom-like emitters located in photonics structures whose spatial dimensions are of the order of the wavelength. Both radiation patterns and lifetime are affected and demonstrations have been reported in atomic and solid state physics. In principle biomolecules could profit from these discoveries to improve the detection sensitivity limit. Demonstrations have been reported in fluorescence but few works have considered contrast mechanisms that belong to nonlinear optics. We focus here on Coherent anti-Stokes Raman scattering (CARS) which requires ~10^6 molecular bonds per cubic micron to give a viable signal and still suffers from a lack of sensitivity. Several strategies have been proposed to enhance the CARS signal and most of them are based on heterodyne detection. Improving the local density of states have been also reported with tip enhanced CARS. In this talk we report theoretical and experimental investigations of CARS in a Fabry-Perot microcavity. We focus on design where the microcavity is transparent for pump and Stokes beams but reflective for the generated anti-Stokes beam. We show that the CARS radiation can be concentrated in a single direction and generates a strong Epi (backward) CARS signal. Such a cavity opens potential applications in microscopy combined with microfluidics to improve signal collection or to work with Epi detection. Moreover, this study illustrates the influence of electromagnetic environment on CARS, to potentially take advantage of surface enhanced substrates such as the ones found in SERS.

7569-98, Poster Session

Polarized broadband multiplex CARS in the picosecond regime

S. Michel, F. Munhoz, Institut Fresnel (France); A. Courjaud, E. Mottay, Amplitude-Systèmes (France); J. Dudley, Femto-ST (France); H. Rigneault, Institut Fresnel (France)

Coherent AntiStokes Raman Scattering (CARS) is a non-invasive, fluorescence free, and high-spatial-resolution technique to probe chemical bounds in a living cell. Most experiments in CARS spectroscopy and microscopy need two synchronized laser sources or optical parametric oscillators in order to product the Pump and Stokes beams used in CARS process. Nevertheless, by pumping a photonic crystal fiber (PCF), CARS processes is excited from only one primary source by combining spatially and temporally the pump and the long wavelength part of a supercontinuum (SC) generated in the PCF. Previously reported work has used femtosecond (fs) lasers for efficient SC generation, but this approach requires spectral filtering or pulse shaping to improve the poor spectral resolution achievable with fs pulses. In this paper, we demonstrate a compact picosecond CARS laser source in the wavenumber range 500-2000cm-1 by pumping a highly-non linear PCF with a 6 ps oscillator (Nd:Vanadate, rep rate 35MHz). The spectral resolution obtained is 2cm-1, and the SC (together with the CARS signal) stability is ensured by an active feedback on the coupling into the PCF, avoiding thus thermal and mechanical drifts. The efficiency of this feedback is evaluated and we successfully obtain CARS spectra in test samples. We also show that such a multiplex CARS setup is suitable to perform a polarized multiplex CARS analysis on bio-samples. Such an analysis is important in biology because it yields orientational or conformational information; we demonstrate here its ability in the multiplex scheme by measuring the Raman depolarization ratio of test samples.

7569-99, Poster Session

Polarization second harmonic generation (PSHG) imaging of neurons: estimating the effective orientation of the SHG source in axons

S. Psilodimitrakopoulos, Instituto de Ciencias Fotónicas (Spain); V. Petegnief, G. Soria, Consejo Superior de Investigaciones Cientícas (Spain); I. Amat-Roldan, Instituto de Ciencias Fotónicas (Spain); D. Artigas, Univ. Politècnica de Catalunya (Spain) and Instituto de Ciencias Fotónicas (Spain); A. M. Planas, Consejo Superior de Investigaciones Cientícas (Spain); P. Loza-Alvarez, Instituto de Ciencias Fotónicas (Spain)

Polarization sensitive second harmonic generation (PSHG) imaging can provide information unreachable by intensity only SHG imaging. Specifically, it can provide the effective orientation of the SHG source. The information is obtained by analysing the SHG intensity variation on the incoming polarization. The experimental data is fitted into a biophysical model that assumes cylindrical symmetry in the x2 tensor of the SHG source structures. This allows calculating the ratios of the non-vanishing tensor elements. By assuming a single-axis source, its SHG effective orientation can be estimated.

Here, we developed and used this technique to retrieve submicron structural information and to estimate the effective orientation of the SHG source in cultured neurons. The PSHG images of axons were fitted pixel by pixel using an algorithm based on the above mentioned model, where a coefficient of determination of $\rm r2 > 90\%$ was chosen as a filtering mechanism. For selected ROIs we then retrieved the pixels' values histograms of the harmonophores' effective orientations, e. The histograms were centered at $\rm e=33.96^\circ$, and had a bandwidth of $\rm \Delta~e=12.85^\circ$. This angle value coincides with the diagonal of the rectangle containing the tubulin heterodimmer with respect to the long axis of the microtubule. Modifications on tubulin dimers may alter $\rm e~or~\Delta~e$, thus the PSHG optical technique may be used to characterize neurons' plasticity as well as disease progression.

7569-100, Poster Session

Multiphoton microscopy for in situ investigations of cryopreserved samples

D. Dörr, A. Beier, M. Schwarz, H. Zimmermann, I. Riemann, J. Schulz, F. Stracke, Fraunhofer-Institut für Biomedizinische Technik (Germany)

Cryopreservation of biological specimen in the regenerative medicine demands a continuous monitoring of the samples during the whole freezing and thawing processes. Currently used techniques to examine the specimens during the freezing process are electron microscopy and optical transmission microscopy. Whereas optical transmission microscopy suffers from strong scattering and does not provide highly resolved access to the samples. This is only ensured by cryo electron microscopy, which requires a complex sample preparation and leads to the loss of vitality of the sample.

Here we demonstrate the application of a non-linear microscopy technique for the investigation of cryoinjury mechanisms and their correlation to established methods for determination of survival rates under various freezing conditions of biological and medically relevant specimen. This non-invasive imaging method based on the non-linear absorption of two or more photons is a key feature for cryo-imaging due to the spatial sectioning caused by the fact, that scattered photons do not contribute to excitation and all fluorescence photons reaching the detector can unambiguously be attributed to the location of the focal plane. This offers the possibility to monitor morphological changes during the preservation process even after the phase transition from liquid to solid, e.g. the formation of intracellular ice crystals. Furthermore the two-photon fluorescence signal of the femtoliter sized focal volume enables



a tomographic imaging of frozen samples at sub micrometer resolution with penetration depths similar to the liquid phase.

assay, comet assay, and histology. Preliminary experiments determining the mechanisms by which the benefits occur are underway.

7569-101, Poster Session

Complementary equipment for controlling multiple laser beams on single scanner **MPLSM** systems

P. J. Helm, G. Nase, CMBN & LRC, Univ. of Oslo (Norway); P. Heggelund, T. Reppen, Univ. of Oslo (Norway)

Multi-Photon-Laser-Scanning-Microscopy (MPLSM) now stands as one of the most powerful experimental tools in biology. Specifically, MPLSM based in-vivo studies of structures and processes in the brains of small rodents and imaging in brain-slices have led to considerable progress in the field of neuroscience.

Equipment allowing for independent control of two laser-beams, one for imaging and one for photochemical manipulation, strongly enhances any MPLSM platform, provided sufficiently high spatial and temporal resolution. Some industrial MPLSM producers have introduced double scanner options in MPLSM systems.

Here we describe the upgrade of a single scanner MPLSM system with equipment that is suitable for independently controlling the beams of two Titanium Sapphire lasers. The upgrade is compatible with any actual MPLSM system and can be combined with any commercial or self assembled system.

Making use of the pixel-clock, frame-active and line-active-signals provided by the scanner-electronics of the MPLSM, the user can, by means of an external unit, select individual pixels or rectangular ROIs within the field of view of an overview-scan to be exposed, or not exposed, to the beam(s) of one or two lasers during sub-sequent scans. The switching processes of the laser-beams during the subsequent scans are performed by means of Electro-Optical-Modulators (EOMs).

While this system does not provide the flexibility of two-scanner modules, it strongly enhances the experimental possibilities of onescanner systems provided a second laser and two independent EOMs are available.

Even multi-scanner-systems can profit from this development, which can be used to independently control any number of laser beams.

7569-102, Poster Session

Investigating the protective effects of milk phospholipids against ultraviolet exposure in a skin equivalent model using multiphoton microscopy

A. Russell, A. Laubscher, R. Jimenez-Flores, L. H. Laiho, California Polytechnic State Univ., San Luis Obispo (United States)

Current research on bioactive molecules in milk have documented health advantages of bovine milk and its components. Milk phospholipids, selected for this study, represent molecules with great potential benefit in human health and nutrition. In this study we used multiphoton microscopy to monitor changes in skin morphology upon exposure to ultraviolet light and evaluate the potential of milk phospholipids in preventing photodamage to skin. We imaged skin equivalent models based on human keratinocytes and dermal fibroblasts cultured in a collagen matrix. We compared images from skin equivalent models with (a) no exposure to UV light, (b) exposure to a dose of 60 mJ/cm2 of UVB exposure, triple the minimal erythema dose, (c) exposure to milk phospholipids in the media, and (d) exposure to milk phospholipids in the media followed by exposure to UV light. The results suggest that milk phospholipids act upon skin cells in a protective manner against the effect of ultraviolet radiation. Similar results were obtained from MTT

7569-104, Poster Session

In vivo tissue imaging using a compact mobile nonlinear microscope

R. Cicchi, D. Kapsokalyvas, D. Stampouli, V. De Giorgi, S. Sestini, D. Massi, T. Lotti, F. S. Pavone, Univ. degli Studi di Firenze (Italy)

We have built a compact mobile multidimensional non-linear microscope equipped with a combination of different non-linear laser imaging techniques including two-photon fluorescence (TPEF), second-harmonic generation imaging (SHG), fluorescence lifetime imaging microscopy (FLIM), and multispectral two-photon emission detection (MTPE). The system is composed of a microscope head, containing both scanning and detection system, as well as the electronic and electro-mechanical devices, optically relayed to the laser source with a seven-mirror articulated arm. The particular mirror positioning inside the arm allows to move the microscope head maintaining the optical alignment of the system. The microscope head is composed by two ErGaAl anodized boards, mounted one over the other. The former board is hosting galvoscanners, beam expander, objective lens and fluorescence dichroic; whereas in the latter board we have placed blocking filter, collection optics, and detectors with their electronics. This experimental setup, offering high spatial (sub-cellular) and temporal (sub-nanosecond) resolution, has been used to image both ex-vivo and in-vivo biological samples, including cells, tissues, and living patients. Here we present the capability of the system in imaging skin. In particular we present the ex-vivo imaging of both epidermal (BCC, MM) and dermal (keloids, tumour stroma) diseases, as well as an in-vivo application where the reorganization of collagen in human dermis after a laser treatment has been monitored.

7569-106, Poster Session

Fast rasterscanning enables FLIM in macroscopic samples up to several centimeter

F. Koberling, V. Buschmann, PicoQuant GmbH (Germany); C. Hille, Univ. Potsdam (Germany); M. Patting, M. Wahl, PicoQuant GmbH (Germany); C. Dosche, Univ. Potsdam (Germany); R. Erdmann, PicoQuant GmbH (Germany); S. Fore, PicoQuant Photonics North America, Inc. (United States)

Fluorescence Lifetime Imaging (FLIM) based on Time-Correlated Single Photon Counting (TCSPC) is nowadays a well established technique that is very often realised as an add-on for confocal laser scanning microscopes. However, the standard laser scanning technique limits the maximum scan range in these setups to a few millimeter, making it therefore unusable for e.g. fluorescence multiplexing in multi well plate based assays or for macroscopic material science studies on solar cells, wafers and similar material.

In order to also realize larger scanning ranges, we have developed a sample scanning approach based on a xy-cross stage equipped with piezo linear motors. Using online position monitoring, this approach permits fast acceleration and scanning as well as precise positioning and features scan ranges from 100x100 microns up to 80x80 mm with sub micron positioning accuracy. Standard upright and inverse microscope bodies can easily be equipped with this scanning device. Along with the necessary excitation and detection components "large-area" FLIM thus becomes possible.

We will show new results illustrating the system capabilities for lifetime based imaging in macroscopic samples such as the improvement of the fluorescence sensitivity in 2D gel electrophoresis or the possibility to perform lifetime based fluorescence multiplexing in µ-well plate based assays. Even Two Photon Excitation (TPE) imaging is possible



with this widerange sample scanning approach and first FLIM results on cockroach salivary glands, loaded with a chloride sensitive dye (MQAE) will be presented.

7569-107, Poster Session

pH and chloride recordings in living cells using two-photon fluorescence lifetime imaging microscopy

M. Lahn, C. Hille, Univ. of Potsdam (Germany); F. Koberling, P. Kapusta, PicoQuant GmbH (Germany); C. Dosche, Univ. of Potsdam (Germany)

Today fluorescence lifetime imaging microscopy (FLIM) has become established as an extremely powerful technique in life sciences. The independency of the fluorescence decay time on fluorescence dye concentration and emission intensity circumvents many artefacts arising from intensity based measurements. To minimise cell damage and improve scan depth a combination with two-photon (2P) excitation is quite promising.

Here, we describe the implementation of a 2P-FLIM setup for biological applications. For that we used a commercial fluorescence lifetime microscope system. 2P-excitation at 780nm was generated by a nontuneable, but inexpensive and easily manageable mode-locked fs-fiber laser. Time-resolved fluorescence image acquisition was performed by objective-scanning with the reversed time-correlated single photon counting (TCSPC) technique.

We analysed the suitability of the pH-sensitive dye BCECF and the chloride-sensitive dye MQAE for recordings in an insect tissue. Both parameters are quite important, since they affect a plethora of physiological processes in living tissues. We performed a straight forward in situ calibration method to link the fluorescence decay time with the respective ion concentration and carried out spatially resolved measurements under resting conditions. BCECF still offered only a limited dynamic range regarding fluorescence decay time changes under physiologically pH values. However, MQAE proofed to be well suited to record chloride concentrations in the physiologically relevant range. Subsequently, several chloride transport pathways underlying the intracellular chloride homeostasis were investigated pharmacologically.

In conclusion, 2P-FLIM is well suited for ion detection in living tissues due to precise and reproducible decay time measurements in combination with reduced cell and dye damages.

7569-108, Poster Session

Extracellular oxygen concentration mapping with a confocal multiphoton laser scanning microscope and TCSPC card

N. A. Hosny, M. M. Knight, D. A. Lee, Queen Mary Univ. of London (United Kingdom)

Extracellular oxygen concentrations influence cell metabolism and tissue function. Fluorescence Lifetime Imaging Microscopy (FLIM) offers a non-invasive method for quantifying local oxygen concentrations. However, existing methods show limited spatial resolution, require custom made systems, and have only explored intracellular oxygen.

This study describes a new optimised approach for quantitative extracellular oxygen detection, providing an off-the-shelf system with high lifetime accuracy and spatial resolution down to 0.34 µm, while avoiding systematic photon pile-up. Excitation used a multi-photon 80 MHz Mai-Tai Sapphire laser, pulse-picked to 500 kHz, coupled to a Leica confocal laser scanning microscope. Fluorescence lifetime detection of an oxygen sensitive fluorescent dye, tris(2,2 -bipyridyl)ruthenium(II) chloride hexahydrate [Ru(bipy)3]2+, was measured using a Becker&Hickl time-correlated single photon counting (TCSPC) card.

Lifetime images (256 x 256 pixels) captured extracellular oxygen

concentrations around isolated chondrocytes, seeded in threedimensional agarose gel. Ethidium homodimer staining confirmed cellular viability was maintained 24 hours post acquisition. Systematic photon pile-up was avoided by examining the effects caused by dye concentration, oxygen levels, and laser power. In determining an optimised chi-square cut-off point and photon collection rate, speed and accuracy of lifetime acquisitions were maximised.

With increasing time in culture, oxygen gradients were established, lower oxygen concentrations were seen at the cell periphery. This could reflect the presence of pericellular matrix and/or oxygen consumption. The technique provides a powerful tool for quantifying spatial oxygen gradients within three-dimensional cellular models. In addition, the system has the potential for investigating intra and extracellular information using longer lifetime dyes not affected by autofluorescence.

7569-109, Poster Session

A multimodal multiphoton microscope for biological imaging

R. Mouras, A. Downes, G. Rischitor, M. Mari, A. Elfick, Univ. of Edinburgh (United Kingdom)

We have constructed a highly flexible system for advanced biological imaging, where all the following imaging techniques are integrated into the same microscope: CARS, TPF, SHG, sum frequency generation (SFG), fluorescence lifetime imaging (FLIM) and differential interference contrast (DIC). Raman spectroscopy and fluorescence correlation spectroscopy are also available. The system employs a Nd:YVO4 laser as pump (7 ps, 1064 nm), and two tunable OPOs (6 ps, 700 - 1000 nm). Beams are focused onto a single mode fiber for ease of alignment, which is connected to the input of a confocal inverted optical microscope. Such a set-up can also be converted to heterodyne CARS with the addition of a phase modulator, and stimulated Raman scattering microscopy by adding an amplitude modulator.

Three external photomultiplier detectors (Hamamatsu R3896, Shizuoka, Japan) were used to detect the signals in the forward as well as in the backscattered (epi-) direction. The epi-detected NLO signal can be sent either through a spectrometer (or via filters) to the photomultipliers or an avalanche photodiode (Perkin Elmer SPCM-AQR-14, Vaudreuil, Canada). This allows all relevant CARS wavenumbers to be imaged, and simultaneous detection of three imaging modes.

Our microscope comprises a heater stage and perfusion cell for imaging of live cells, and features an atomic force microscope (AFM) which enables optical imaging at 10 nm resolution. The versatility of our system has been demonstrated by imaging breast cancer cells and tissue using CARS, 2PF and SHG and by imaging anti-cancer drugs in live cells using CARS and 2PF.

7569-110, Poster Session

Chitin SHG and its organization in the squid pen

A. A. de Thomaz, C. Lenz Cesar, H. F. Carvalho, Univ. Estadual de Campinas (Brazil)

SHG microscopy allows high-resolution, high-contrast, three-dimensional studies of live cell and tissue architectures. Collagen, elastin, myosin and cellulose fibrils are among the biological structures producing SHG signals. We became interested in investigating whether chitin, a N-acetyl-glucosamine polymer found in arthropods, mollusks and fungi, emits SHG signal and explore it for the determination of chitin fibrils in the Loligo pen. To the best of our knowledge, this is the first description of SHG by chitin. Examination of the squid pen also showed that the alkali-treated pen is composed of aligned fibrils with a mean thickness of 0.78 micrometers and a long pitch wavy pattern. These fibers were not resolved in the native pen, showing that the protein moiety keeps the chitin in microfibril organization and that its removal allows further aggregation of the microfibrils. These results confirm previous



observation by polarization microscopy (Zool Jarhb Anat 121:39, 1991) and along with atomic force and electron microscopy data, allowed the proposition of a molecular model for the organization of chitin fibrillar structures in the squid pen.

7569-111, Poster Session

Patterns of second harmonic generation in human ovarian tissues

L. Pietro, C. Lenz Cesar, L. Lamonier, L. A. Andrade, A. A. de Thomaz, C. L. Machado, F. Bottcher-Luiz, Univ. Estadual de Campinas (Brazil)

Collagen is the major component of ECM in human tissues, providing structural organization and mechanical strength for cell phenotype maintenance and proliferation. Recent data have suggested that collagen fibers alterations are frequently linked to neoplasias, in order to facilitate tumor invasion and metastasis liberation. Nevertheless, the principal alterations published are related to breast and prostate tumors. Considering that ovarian cancer is the second most common and the highest mortality tumor among the gynecological cancers, this study aimed to identify the pattern of collagen fibers distribution and organization in ovarian tissues. The sample was composed by biopsies from non tumoral specimens and benign ovarian tumors. The slides were obtained without dyes and excited by a Ti:Sapphire laser. The images were recorded at triplets, corresponding to clear field, normal fluorescence and SHG. Data showed some variations of collagen type I, characterized by uniform layer with high structured collagen restrict to the stroma. Surprisingly, the benign tumors exhibited some dense and shortened fibers, with some angle deviation in relation to the cell disposition. At the moment, we are investigating the relations between this data and other phenotypes related to the tissue architecture. We believe to contribute with the knowledge about SHG properties of ovarian tissues, in order to promote comparison with the malignant ones.

7569-112, Poster Session

Wavefront optimized multiphoton microsocpy of ex vivo ocular tissues

E. Gualda, J. M. Bueno, P. Artal, Univ. de Murcia (Spain)

Non-linear microscopy techniques such as two-photon autofluorescence (TPEF) and second harmonic generation (SHG) are becoming important tools in areas of medical and biological science. These techniques might be significantly improved when combined with wavefrontassisted approaches, reducing the required excitation power levels and minimizing phototoxicity side-effects. The aim of this work was to investigate the impact of the aberrations of the illuminating laser beam on imaging ex-vivo ocular tissues of several species. For this purpose, we developed an improved version of a multiphoton microscope with optimized wavefront of the laser beam. The multiphoton imaging system combines an ultrafast high-power laser, a scanning unit, a motorized Z-scan device and a photon-counting detector. A Hartmann-Shack wavefront sensor was included in the illumination pathway to measure the aberrations of the incoming beam in real time. These wavefront aberrations were fairly constant over time and the main contribution is due to low order aberrations (defocus and astigmatism). This indicates that simple static correction of low-order aberrations would produce a significant increase in the detected nonlinear signal. The dynamic correction of higher-order aberrations with a deformable mirror produced an additional benefit. TPEF and SHG images of ex-vivo corneal and retinal tissues were recorded for different beam wavefronts. Results show that an accurate control of the illuminating beam wavefront increases the contrast and resolution in nonlinear microscope images of ocular tissues. This indicated the potential of this approach for the development of new clinical tools for diagnosis of ocular pathologies or in the improvement of laser ablation surgery techniques.

7569-113, Poster Session

Nonlinear 3D microscopy of ex vivo corneas

J. M. Bueno, E. J. Gualda, P. Artal, Univ. de Murcia (Spain)

Multiphoton microscopy is a non-invasive technique which provides high resolution imaging without using exogenous dyes with intrinsic sectioning capabilities. A research prototype multiphoton microscope has been developed to investigate the sources of non-linear signals (two-photon emission fluorescence -TPEF-, and second harmonic generation -SHG-) in corneas from different species, including human. The instrument combines a mode-locked Ti:Sapphire laser as excitation source, a photon-counting detection unit and an inverted microscope. A set of two galvanometric mirrors (XY scanning) and Z-scan motor allowed the recording of stacks of images to reconstruct 3D volume images of the corneal samples. TPEF-SHG pairs of images were also combined to obtain 3D volume images with complementary information. Corneal samples were neither fixed nor stained. All images were registered in the backward direction since this configuration is more similar to a possible implementation for future in-vivo experiments. Results show that both, epithelium and endothelium provide TPEF signal arising from the mytochondrial NAD(H)P. The only source of SHG was the stroma, due to the non-centrosymmetric organization of type I collagen. Within the stroma, TPEF signal from keratocytes were also observed. The arrangement of the stromal lamellae was clearly different among especies and changed with depth within each especimen. This indicates that different organization of collagen fibres within the stroma provides similar conditions of corneal tissue transparency. The instrument and procedure are a powerful tool to obtain new relevant information of corneal structures that could be used for future early diagnosis of pathologies or for the follow-up of different corneal refractive approaches.

7569-114, Poster Session

Comparison of double- and single-pass adaptive optics configuration in an optical sectioning microscope

M. C. Muellenbroich, S. P. Poland, Univ. of Strathclyde (United Kingdom); K. Buttenschoen, J. M. Girkin, Durham Univ. (United Kingdom); A. J. Wright, Univ. of Strathclyde (United Kingdom)

Adaptive Optics (AO) has been demonstrated to overcome system and sample aberrations, to bring back signal strength and resolution to surface quality, when imaging at depth in biological tissue with optical sectioning microscopes. When designing an "Adaptive Microscope" a decision has to be made as to where the AO device should be placed in the optical setup, specifically in relation to the beam scanning system. Depending on where the AO device is situated, additional optics will need to be introduced to expand or reduce the size of the beam according to the limiting apertures of the system, typically, the scanner, the active aperture of the AO device and the back aperture of the microscope objective. This decision can also impact on whether the light passes off the AO device once or twice before it reaches the detector, referred to as single-pass or double-pass respectively. It has been argued that a double-pass configuration could potentially increase the maximum correction obtainable but place a restriction on the Zernike aberrations which can be corrected. Concerns have been raised that a double-pass setup might not be able to correct for circularly asymmetric aberrations, for example, astigmatism. Using an electrostatic deformable membrane mirror and a genetic algorithm to rapidly alter the shape of this mirror to optimise on signal intensity, we have examined both the single- and double-pass options. We report on the merits of different AO integration in an optical sectioning microscope and on how this pertains to confocal and non-linear microscopy.



7569-126, Poster Session

Annular-aperture detection scheme in radially polarized coherent anti-Stokes Raman scattering (RP-CARS) microscopy for vibrational contrast enhancement

J. Lin, F. Lu, H. Wang, W. Zheng, Z. Huang, National Univ. of Singapore (Singapore)

We report on a unique annular aperture detection scheme in radially polarized coherent anti-Stokes Raman scattering (RP-CARS) microscopy to effectively remove the solvent background for high contrast vibrational imaging. Our finite-difference time-domain (FDTD) calculations show that the far-field RP-CARS radiation from the scatterer with size comparable to the excitation wavelength is stronger than that from the solvent at large cone angles (around 45° to 150°). The annular detection provides about one order higher contrast for both forward and backward detected RP-CARS microscopy. These results are proved by imaging water-immersed polystyrene beads.

7569-130, Poster Session

Fiber delivered probe for efficient CARS imaging of tissues

M. Balu, G. Liu, Beckman Laser Institute and Medical Ctr. (United States); E. O. Potma, Univ. of California, Irvine (United States); B. J. Tromberg, Beckman Laser Institute and Medical Ctr. (United States)

We demonstrate a fiber-based probe for maximum collection of the Coherent anti-Stokes Raman Scattering (CARS) signal in biological tissues. We discuss the design challenges including capturing the back-scattered forward generated CARS signal in the sample and the effects of fiber nonlinearities on the propagating pulses. Three different biological tissues were imaged in vitro in order to assess the performance of our fiber-delivered probe for CARS imaging, a tool which we consider an important advance towards label-free, in vivo probing of superficial tissues.

7569-47, Session 7

Alterations of the extracellular matrix in ovarian cancer studied by second harmonic generation imaging microscopy

P. J. Campagnola, O. Nadiarnykh, R. B. LaComb, M. A. Brewer, Univ. of Connecticut Health Ctr. (United States)

For this investigation we use Second Harmonic Generation (SHG) imaging microcopy to study changes in the structure of the ovarian ECM in human normal and malignant ex vivo biopsies. The normal and diseased tissues have highly different collagen fiber assemblies, where the latter are characterized by homogenous fiber shape and size, more densely packed collagen, and low cellular density. To quantify these changes in collagen morphology we utilize an integrated approach of 3D SHG imaging measurements, bulk optical parameter measurements, and Monte Carlo simulations. Through this approach we find quantitative discrimination using small patient data sets. Specifically the SHG creation attributes (i.e. emission directionality and relative SHG intensity) and bulk optical parameters, both of which are related to the tissue structure, are significantly different in the malignant biopsies in a manner that is consistent with the change in collagen assembly. Monte Carlo simulations of the axially dependent directional and attenuation data quantitatively reproduce the experimental data. Collectively, these findings show that the malignant ovaries are characterized by higher regularity at both the fibril and fiber levels. In addition the increased

scattering and relative SHG intensity also suggests that desmoplasia occurs during ovarian carcinogenesis. The increased regularity and collagen density further suggest the assembly may be comprised of newly synthesized collagen as opposed to modification of existing fibers. This issue will be further examined through comparisons with protease degradations of self-assembled fibrillar collagen gels. Ultimately these measurements may be developed as intrinsic biomarkers for use in clinical applications.

7569-48, Session 7

Adaptive multiphoton and harmonic generation microscopy for developmental biology

M. J. Booth, A. Thayil, A. Jesacher, T. Wilson, Univ. of Oxford (United Kingdom)

Specimen-induced aberrations are frequently encountered in high resolution microscopy, particularly when high numerical aperture lenses are used to image deep into biological specimens. These aberrations distort the focal spot causing a reduction in resolution and, often more importantly, reduced signal level and contrast. This is particularly problematic in multiphoton microscopy, where the non-linear nature of the signal generation process means that the signal level is strongly affected by changes in the focal spot intensity. We have applied the techniques of adaptive optics to measure and correct the aberrations, restoring image quality. This has been demonstrated in two-photon fluorescence and harmonic generation microscopes. As aberration correction leads to more efficient signal generation, the illumination laser power can be reduced. The energy absorbed by the sample is therefore lower leading to reduced phototoxic effects when imaging living specimens. This in turn could permit an increase in the period over which specimens could be observed. To this end, we have developed efficient adaptive optics schemes for multiphoton microscopes that minimize the specimen exposure. In combination with novel culture methods, these adaptive microscope systems have been used in the long term imaging of early stage mouse embryos. We present three-dimensionally resolved, time-lapse data showing developmental processes in these specimens.

7569-49, Session 7

Longitudinal study of multiphoton autofluorescence microscopy and second harmonic generation microscopy during oral carcinogenesis

T. Shilagard, S. R. L. Rudrabhatla, N. Patrikeeva, V. Resto, S. McCammon, S. Qiu, G. Vargas, The Univ. of Texas Medical Branch (United States)

The objective of this research is to evaluate the nonlinear optical microscopy techniques of multiphoton autofluorescence microscopy (MPAM) and second harmonic generation microscopy (SHGM) for noninvasive imaging of oral epithelial carcinogenesis. In vivo imaging is performed in a hamster model for oral carcinogenesis to characterize optical and morphometric alterations during neoplastic transformation. In this study, a longitudinal study of MPAM and SHGM was employed and the time course of optical changes were correlated to the time course of biological markers of carcinogenesis.

Oral carcinogenesis was induced in the buccal mucosa of hamsters using a thrice weekly application of DMBA. Imaging was performed at three sites per animal at weekly intervals for a period of seven weeks when early carcinoma is evident. Changes in autofluorescence and SHG as well as morphometry using texture metrics were employed to characterize the optical changes over the course of the longitudinal study. In a parallel study biopsies were obtained from hamsters treated in the same manner in order to characterize samples for expression of molecular markers suspected to alter epithelial and stromal changes.



Data is presented showing alterations in morphometry and collagen density during the precancerous phase of neoplastic transformation. Immunohistofluorescence of DMBA treated hamsters revealed changes in proteins associated with stromal restructuring, one such marker being MMP-7.

7569-50, Session 7

Digital holography for second harmonic microscopy

E. Shaffer, C. Depeursinge, Ecole Polytechnique Fédérale de Lausanne (Switzerland)

Quantitative phase images make digital holographic microscopy (DHM) an excellent instrument for metrological, but also for biological applications, where it can reveal deformations and morphological details at ultrahigh resolution in the order of a few nanometers only, while also precisely determining the refractive index across a sample (e.g. cell or neuron). On the other hand, non-linear light-matter interactions have also proved very useful in microscopy. For instance, second harmonic generation (SHG) allows marker-free identification of cell structures, tubulin or membranes and, because of its coherent nature, SHG is very sensitive to the local sample structure and to the direction of the laser polarization. In addition, since SHG does not result from light absorption and subsequent re-emission, in opposition to fluorescence, photobleaching of the studied material can be avoided by a judicious selection of the laser wavelength. These characteristics make SHG very interesting for biomedical imaging.

We have designed and built a microscope that combines the fast and precise DHM imaging with tagging capabilities of non-linear lightmatter interactions. Here, we present the technique and look into its possible applications to biological and life sciences. Among promising applications is the 3D tracking of colloidal gold nanoparticles.

7569-51, Session 7

Video-rate higher-harmonic-generation fiber-endoscope with a submicron spatial resolution

C. Yu, S. Chia, T. Liu, N. Cheng, M. Chan, I. Chen, National Taiwan Univ. (Taiwan); C. Sun, National Taiwan Univ. (Taiwan) and Research Ctr. for Applied Sciences, Academia Sinica (Taiwan)

We successfully developed the first-ever higher-harmonic generation (HHG) fiber-endoscope with a sub-micron spatial resolution and a video frame rate. A compact, high-power, and fiber-delivered femtosecond Cr:forsterite laser was setup and used as our light source. The video frame rate was achieved by the two-dimensional (2D) asynchronous scanning of a micro-electro-mechanical system (MEMS) mirror with a 9.8KHz resonant frequency. In order to minimize the spherical aberration and coma induced by oblique incidence, the radius of curvature of two miniaturized tube lenses were carefully designed, and no image distortion was found on the boundary of the acquired 2D HHG images. Through the use of a high numerical aperture objective and high nonlinearity. the corresponding transverse resolution can be down to sub-micron. With fiber-delivered short excitation pulses, a high-speed MEMS mirror, well-designed tube lenses, and high optical nonlinearity, the sub-micron spatial resolution and the video-rate movies of in vivo clinical HHG biopsy imaging can be obtained for the first time through this HHG fiberendoscope system.

7569-52, Session 7

Two-photon and second harmonic generation microscopy for dynamic investigation of skin morphogenesis

C. Wang, Y. Chen, P. Su, C. Dong, S. Lin, National Taiwan Univ. (Taiwan)

The development of skin appendage involves a complex interaction between the epidermis and mesenchyme with dynamic remodeling of the extracellular matrix. For feather morphogenesis, the dermal papilla cells have a vital role in guiding the epidermis to differentiate into feather epithelium and the dynamic remodeling of extracellular matrix is believed to have an important role for the appropriate spacing and segregation of dermal papilla cells from the non-follicular dermal cells. Up to date, the dynamic cell behavior and the extracellular remodeling during feather morphogenesis have not been characterized. In this study, we utilized multiphoton microscopy for imaging and evaluating feather morphogenesis of embryonic skin. To investigate the interaction between cells and ECM during feather buds formation, we labeled the nuclei of cells by the use of fluorescent probe of Hoechst. We found that cells are highly motile during the formation of feather bud and dermal cell aggregation can be observed in different stages of the developing embryonic skin. Though it is believed that collagen first form a tract before the formation of dermal papilla to instruct the self-aggregation of dermal papilla cells, backscattered SHG signal cannot be detected until later stages in the chick embryo when aggregates of dermal papilla cells already form. We demonstrate that, dynamic cell behavior and structural information from two-photon and SHG, we create a minimally invasive system for studying feather morphogenesis.

7569-53, Session 7

Second harmonic generation microscopy detection of individual hybrid nanoprobes

S. Brasselet, Institut Fresnel (France); N. Sandeau, Univ. Pierre et Marie Curie Paris VI (France); E. Delahaye, R. Clément, Institut de Chimie Moléculaire et des Matériaux d'Orsay, Univ. Paris-Sud 11 (France)

Nonlinear nanoparticles active for Second Harmonic Generation (SHG) are interesting potential candidates for localization imaging and tracking in biological samples. Indeed SHG radiation is by nature stable and not affected by photobleaching, and allows the use of a tuneable excitation wavelength. We show that inorganic, organic and hybrid nanoparticles fabrication routes can lead to efficient nonlinear emitters. We have developed a dedicated SHG microscopy technique to study individual nonlinear nano-objects and molecular nano-assemblies, which combines polarization-dependence and defocused radiation-imaging SHG. Indeed contrary to fluorescence which is an incoherent optical process, the coherent nature of SHG makes it highly sensitive to the structure of a nano-object, as well as its size and shape. We illustrate the application of this technique to the investigation of the structure of hybrid nanoparticles based on the insertion of the push-pull 4-[2-(4-dimethylaminophenyl) azo]-1-methylpyridinium (DAZOP) chromophore in the manganese hexathiohypodiphosphate MnPS3 inorganic matrix. The included chromophores form J-Aggregates responsible for efficient SHG in 10-20nm size nano-objects. The SHG efficiency of the particles is studied by Hyper Rayleigh Scattering in solution and polarized nonlinear microscopy in a polymer thin film, which permits to probe the intrinsic molecular order in individual immobilized particles. When diluted in a polymer film, they are seen to assemble in hundreds nanometers size agglomerates whose morphology, can lead to a collective optimal one-dimensional arrangement resulting from inter-particles interactions. We show that polarimetric and radiation imaging SHG can potentially be applied to any nonlinear active nano-object, including biomolecular assemblies.



7569-95, Session 7

Differential nonlinear microscopy for biomedical imaging

V. Barzda, D. Sandkuijl, A. Tuer, R. Cisek, S. Musikhin, Univ. of Toronto Mississauga (Canada)

In vivo biological samples often have tendency to change due to intracellular dynamics, or experience bleaching when imaged with nonlinear microscopy. If different excitation conditions are used to create differential contrast in the microscopic in vivo imaging, almost simultaneous scanning with the different excitation conditions is required. Interlaced laser pulses with different spectral, temporal, and polarization properties have been used for the in vivo differential microscopy. The detection electronics demultiplexed photon counts originating from the different excitation pulses. This way only one scan was required to obtain two images at different excitation conditions, and create the differential image. The differential microscopy technique is demonstrated by imaging multiphoton excitation fluorescence, second and third harmonic generation of biological tissue.

7569-54, Session 8

Second-order susceptibility imaging with polarization-resolved second harmonic generation microscopy

W. Chen, T. Li, P. Su, C. Chou, P. T. Fwu, National Taiwan Univ. (Taiwan); S. Lin, National Taiwan Univ. Hospital (Taiwan) and National Taiwan Univ. (Taiwan); D. Kim, P. T. So, Massachusetts Institute of Technology (United States); C. Dong, National Taiwan Univ. (Taiwan)

Second harmonic generation (SHG) microscopy has become an important tool for minimally invasive biomedical imaging. Bio-molecules such as collagen and myosin are strong second harmonic generators. However, differentiation of different second harmonic generating species is mainly provided by morphological features. In this work, we used excitation polarization-resolved SHG microscopy to determine the ratios of the second-order susceptibility tensor elements at single pixel resolution. Mapping the resultant ratios for each pixel onto an image provides additional contrast for the differentiation of different sources of SHG. We demonstrate this technique by imaging collagen-muscle junction of chicken wing and the dermis of human skin.

7569-55, Session 8

In vivo optical virtual biopsy of human oral cavity with harmonic generation microscopy

M. Tsai, S. Chen, National Taiwan Univ. (Taiwan); D. Shieh, National Cheng-Kung Univ. (Taiwan); P. Lou, National Taiwan Univ. Hospital (Taiwan); C. Sun, National Taiwan Univ. (Taiwan)

Oral cancers are among the ten most common cancers in the world. The development of an oral cancer is a sequential result that arises from the initial presence of a pre-cancerous lesion that subsequently develops into cancer. Because the oral cavity is easily assessable, cancers of the oral cavity could thus be detected by an optical biopsy system, theoretically, at the earliest stage of development. In this research, we perform the in vivo optical virtual biopsy of human oral cavity with harmonic generation microscopy (HGM) and modify the original scanning system to adapt to the application. No energy release is required during the harmonic generation processes, thus the HGM can serve as a noninvasive tool for the inner mucosal surface of the volunteer's lower lip. HGM can provide high spatial resolution dynamic images of oral mucosa in all three dimensions without complex physical biopsy procedures. The second harmonic generation (SHG) contrasts can provide the collagen structure

in the lamina propria. The cell morphology in the epithelial layer and blood flow of the capillary can be revealed by third harmonic generation (THG) signals. Moreover, we applied 4% acetic acid on the oral mucosa before the examination to study the possibility of using acetic acid as an in vivo contrast enhancing agent and found that the THG contrasts in epithelial layer were greatly enhanced. The first in vivo optical virtual biopsy of human oral cavity is successfully demonstrated by utilizing HGM that promises for future noninvasive in vivo diseases examinations.

7569-56, Session 8

Polarization and phase pulse shaping applied to structural contrast in nonlinear microscopy imaging

P. Schön, M. Behrndt, D. Aït-Belkacem, H. Rigneault, S. Brasselet, Institut Fresnel (France)

Second Harmonic Generation (SHG) microscopy has been introduced a decade ago to image biological samples. We propose a new SHG imaging technique that yields information on the structure of molecular assemblies. We show that spectral polarization shaping of ultrashort laser pulses allows direct individual retrieval of all 2D tensorial components of the second-order nonlinear susceptibility that governs the SHG of molecular samples. This cannot be achieved by traditional polarization controlled excitation due to the mixing of SHG signals arising from different tensorial components while they can be easily separated in our excitation scheme. Applied to nonlinear microscopy imaging, we demonstrate that this technique provides a new structural contrast with sub-micrometric resolution that can be directly related to information on the local symmetry and orientational order in molecular assemblies. So far our technique requires a spectral measurement of the SHG signal but by additional spectral phase shaping of the pulse we can avoid the need for a spectrometer to gain our contrast which allows for the use of more sensible and faster detectors, thus greatly increasing the imaging speed. For this we tune the positions of symmetric and anti-symmetric points in the spectral phase to only create a SHG signal arising from one desired tensorial component. The success of this procedure depends strongly on the careful characterization and compensation of all phase distortions introduced by all optical elements in the beam path.

7569-57, Session 8

Nonlinear optical response of the collagen triple helix and second harmonic microscopy of collagen liquid crystals

A. Deniset-Besseau, P. De Sa Peixoto, Ecole Polytechnique (France); J. Duboisset, C. Loison, E. Benichou, Univ. Lyon I (France); F. Hache, Ecole Polytechnique (France); P. Brevet, Univ. Lyon I (France); G. Mosser, M. Schanne-Klein, Ecole Polytechnique (France)

Collagen is characterized by triple helical domains and plays a central role in the formation of fibrillar and microfibrillar networks, basement membranes, as well as other structures of the connective tissue. Remarkably, fibrillar collagen exhibits efficient Second Harmonic Generation (SHG) and SHG microscopy proved to be a sensitive tool to score fibrotic pathologies [Strupler et al, Opt. Express 2007 and JBO 2008].

However, the nonlinear optical response of fibrillar collagen is not fully characterized yet and quantitative data are required to further process SHG images. We therefore performed Hyper-Rayleigh Scattering (HRS) experiments and measured a second order hyperpolarisability of 1.25 10-27 esu for rat-tail type I collagen [Deniset-Besseau et al, submitted]. This value is surprisingly large considering that collagen presents no strong harmonophore in its amino-acid sequence. In order to get insight into the physical origin of this nonlinear process, we performed HRS measurements after denaturation of the collagen triple helix and for a



collagen-like short model peptide [(Pro-Pro-Gly)10]3. It showed that the collagen large nonlinear response originates in the tight alignment of a large number of weakly efficient harmonophores, presumably the peptide bonds, resulting in a coherent amplification of the nonlinear signal along the triple helix. To illustrate this mechanism, we successfully recorded SHG images in collagen liquid solutions by achieving liquid crystalline ordering of the collagen triple helices. Large SHG signals were also consistently observed in biomimetic fibrillar matrices [Deniset-Besseau et al, in preparation].

7569-58, Session 8

MMP-2 silencing by siRNA inhibits morphogenesis of the rat ventral prostate in vitro studied by SHG microscopy

A. Cardoso, A. A. de Thomaz, C. Lenz Cesar, H. F. Carvalho, Univ. Estadual de Campinas (Brazil)

The rodent ventral prostate (VP) undergoes significant growth and development immediately after birth. In this period, the epithelial structures undergo growth, branching, and canalization. We have hypothesized that these events would require ECM remodeling, and hence matrix metaloproteinase (MMP) activity. The aim of this work was to evaluate the impact of blocking MMP-2 using whole organ culture by detecting the presence of collagen by SHG microscopy. Male Wistar rats were decapitated on the day of delivery and had their ventral prostate removed. The VPs were cultured for a week on PTFE membranes floating on DMEM/Ham's F-12 (1:1; vol:vol) supplemented with 10 nM of testosterone and ITS. siRNA was employed to inhibit MMP-2 expression, and GM6001 (a broad-spectrum MMP inhibitor) to inhibit general MMP activity. These blocks affected VP branching and growth negatively. Furthermore, SHG analysis revealed that MMP-2 silencing affected the gland archicteture by interfering in the lumen formation and cellular organization of both epithelium and stroma, besides intense accumation of collagen fibers. Taken together, these data suggest that MMPs in general, and MMP-2 in particular play an important role in prostatic growth, being directly involved with epithelial morphogenesis.

7569-59, Session 8

Second harmonic generation in human ovarian neoplasias

L. Lamonier, A. A. de Thomaz, F. Bottcher-Luiz, L. Pietro, L. A. Andrade, C. L. Machado, C. Lenz Cesar, Univ. Estadual de Campinas (Brazil)

Metastasis is the principal cause of death in cancer patients that requires a complex process of tumor cell dissemination, extra cellular matrix (ECM) remodeling, cell invasion and tumor-host interactions. Collagen is the major component of ECM, which fibers polymerization or degradation is paralleled altered with evolution of the cancerous lesions. As the collagen fiber structure has the ideal properties required for the second harmonic generation (SHG) signal, this study aimed to identify the collagen content, spatial distribution and fibers organization from paraffin embedded biopsies of human ovarian tissues. The specimens included were benign and malignant tumors with their respective histological subtypes. Biopsies were prepared in slides without dyes and were excited by Ti:Sapphire laser. The images were recorded at triplets, corresponding to clear field, normal fluorescence and SHG. Data showed considerable anisotropy in malignant tissues, with regions of dense collagen arranged as individual fibers or in combination with immature segmental filaments. Radial fibers alignment or regions with minimal signal were observed in the high clinical grade tumors, suggesting effective degradation of original fibers or altered polymerization state of them. At the moment, we are investigating if these alterations are independent or are associated with the histological subtypes. These findings allow us to assume that the collagen signature will be reliable and a promising marker for diagnosis and prognosis in human ovarian cancers.

7569-60, Session 9

High-throughput three-dimensional (3D) lithographic microfabrication in biomedical applications

D. Kim, P. T. C. So, Massachusetts Institute of Technology (United States)

In the past two decades, microfabrication based on two-photon absorption process has found applications in photonics and biomedicine by building tissue scaffold for organ regeneration, integrated optical circuit with photonic crystal, microfluidic device, and optical data storage with petabyte scale in 3D. By utilizing the highly nonlinear kinetic process of photopolymerization, it can also achieve fabrication resolution beyond the diffraction limit. However, two-photon microfabrication is based on sequentially scanning a spatially focused spot over the specimen in 3D that is inherently slow. Therefore, its applications are limited to prototyping. There is a demand for a 3D microfabrication system that enables mass production.

In this paper, we propose high-throughput 3D lithographic microfabrication system based on two-photon depth-resolved wide field illumination using a temporal focusing approach. The concept of depth-resolved wide-field illumination has proven to be useful for developing scanningless imaging system. The same concept can be applied to produce 3D microstructures. Its depth discrimination capability is evaluated by photobleaching 2D patterns at different depths in the fluorescence microsphere. In addition, 3D microstucture is fabricated through the photopolymerization process with potential applications in manufacturing tissue scaffold for regenerative medicine research.

7569-61, Session 9

Assessment of fibrotic liver disease with multimodal nonlinear optical microscopy

F. Lu, W. Zheng, National Univ. of Singapore (Singapore); D. C. S. Tai, Institute of Bioengineering and Nanotechnology (Singapore); J. Lin, H. Yu, Z. Huang, National Univ. of Singapore (Singapore)

Liver fibrosis is the excessive accumulation of extracellular matrix proteins such as collagen that occurs in most types of chronic liver diseases. Advanced liver fibrosis results in cirrhosis, liver failure, and portal hypertension. In this study, we apply a multimodal nonlinear optical microscopy platform developed to investigate the fibrotic liver diseases in mice models established by performing bile duct ligation (BDL) surgery. The three nonlinear microscopy imaging modalities are implemented on the same sectioned tissues of diseased model sequentially: i.e., Second harmonic generation (SHG) imaging quantifies the growing of the collagens, the two-photon excited fluorescence (TPEF) imaging reveals the morphology of hepatic cells, while coherent anti-Stokes Raman scattering (CARS) imaging maps the distributions of fats or lipids quantitatively across the tissue. Our imaging results show that during the development of liver fibrosis (collagens) in BDL model, fatty liver disease also occurs, however the aggregated concentrations of collagen and fat constituents in liver fibrosis model do not show a high correlationship between each other.

7569-62. Session 9

Two-photon autofluorescence imaging deep in human epithelial tissue down to the out-offocus background limit

N. J. Durr, C. T. Weisspfennig, B. A. Holfeld, The Univ. of Texas at Austin (United States); L. Zachariah, A. M. Gillenwater, The Univ. of Texas M. D. Anderson Cancer Ctr. (United States); A. Ben-Yakar, The Univ. of Texas at Austin (United States)



Endogenous fluorescence provides morphological, spectral, and lifetime contrast that can indicate disease state in tissues. Previous experimental studies have demonstrated that two-photon imaging (TPI) can be used for non-invasive, three-dimensional sampling of autofluorescence in epithelial tissues down to 200 µm beneath the skin surface. In this paper, we report autofluorescence TPI of human epithelial tissue from a tongue biopsy down to approximately 350 µm below the surface. Beyond this maximum imaging depth, the collected fluorescence emission from the focal volume becomes less than the fluorescence generated outside the focal volume. With appropriate objective lens, collection optics, and detector choice, this imaging depth can be reached with 2 nJ excitation pulses available from 80 MHz repetition rate ultrafast laser oscillators at 760 nm. Using optical properties extracted from our biopsy measurements, we compare this maximum imaging depth limit to an analytical model, a time-dependant Monte Carlo simulation, and experiments using tissue phantoms. Results from these studies suggest that the low staining inhomogeneity and large scattering coefficient associated with visible-wavelength autofluorescence contrast precludes conventional TPI from imaging greater than approximately 4-5 mean free scattering lengths deep, or approximately 400 µm, in epithelial tissue.

7569-63, Session 9

Multiphoton microscopy of entire intact mouse organs

M. J. Levene, S. Parra, Yale Univ. (United States)

Three-dimensional datasets from tissue biopsies may provide critical morphological information that is not readily obtained from traditional approaches to histology using thin physical sections of tissue. Multiphoton microscopy (MPM) provides optical sectioning with penetration into highly scattering materials, ready excitation of intrinsic tissue fluorescence, and access to nonlinear signals such as second harmonic generation (SHG). However, the penetration depth of MPM is typical limited to ~200 microns in many tissues. We present MPM of entire intact, fixed and optically cleared mouse organs. Clearing of tissue is typically incomplete for large tissue samples, however, MPM has sufficient tolerance to scattering to image entire mouse organs. Using macro lenses with 5x magnification and 0.5 numerical aperture enables the generation of high resolution, large field-of-view datasets with imaging depths of several millimeters, sufficient to generate 3D image sets of mouse intestine, heart, lung, brain and other organs.

7569-64, Session 9

Multimodal multiphoton microscopy at 1.5 µm

C. Zhan, C. Joo, S. Yazdanfar, GE Global Research (United States); M. Berezin, W. Akers, Y. Ye, S. Achilefu, Washington Univ. School of Medicine in St. Louis (United States)

We describe multimodal multiphoton fluorescence microscopy at an excitation wavelength near 1550 nm with a compact, turnkey femtosecond fiber laser. Shifting the laser wavelength to this spectral range allows the instrument to simultaneously excite near infrared (NIR) and visible contrast agents, through two- (2P) and three-photon (3P) excitation, respectively. This system offers advantages in penetration depth, contrast, and simplicity as compared to conventional two-photon microscopy. Furthermore, by harnessing the visible and NIR spectra, the system facilitates multiplexing of contrast agents by allowing for large separation between emission spectra.

Using this instrument, we have demonstrated improved imaging depth in a scattering phantom (Intralipid) and ex vivo mouse kidneys with two-photon microscopy of NIR contrast agents. Renal tubules were visualized at depths greater than 160 microns below the renal capsule. This represents >2x improvement over conventional 2P microscopy with excitation near 800 nm, owing to the lower attenuation of both the excitation and emission wavelengths.

We have also implemented three-photon excitation fluorescence microscopy near 1550 nm using the same instrument. Since 3P microscopy is a complementary imaging modality to 2P imaging, this multimodal instrument allows for imaging of a wider selection of fluorescent labels with visible and NIR emission.

7569-65, Session 9

Microscope lens for multiphoton endoscopy

H. Lim, Cornell Univ. (United States) and City Univ. of New York (United States); C. Xu, W. W. Webb, Cornell Univ. (United States)

Medical-Multiphoton Microscopic-Endoscopy (M-MPM-E) can enable real-time diagnosis of diseases by visualizing subcellular features and fluorescenct tissue patterns in vivo. Creation of the necessary miniature probe optics presents technical challenges. Furthermore, it is crucial that M-MPM-E provide efficient signal collection, in order to achieve adequate image quality without exogenous agents or photodamage. Here, we describe the design of new microscope lenses for M-MPM-E. Unlike confocal microscopy, multiphoton microscopy resolution is determined solely by the excitation focus. A separate emission imaging pathway can substantially enhance efficient image collection in deep tissue. Our lens designs include dichroic reflection surfaces, implementing co-axial dual imaging systems for two different wavelengths of excitation and broad emission. The lens is so designed that the numerical aperture for near infrared point scanned excitation is 0.56, whereas the fluorescence in the visible range undergoes low magnification to facilitate fluorescence collection from a larger tissue surface area. The field viewed is approximately 200um X 200um. The outer diameter of the lenses is 3.2 mm. We present experimental results on the performance of the lenses in two-photon excited fluorescence. Preliminary data demonstrates the depth-sectioning capability with < 1-micron resolution. We also address other considerations for microscope objective lenses desirable in multiphoton microscopy.

7569-66, Session 9

The analysis of fluorophore orientation by multiphoton fluorescence microscopy

J. Leeder, D. L. Andrews, Univ. of East Anglia Norwich (United Kingdom)

The accessibility of tunable, ultrafast laser sources has spurred the development and wide application of specialized microscopy techniques based on chromophore fluorescence following two- and three-photon absorption. The attendant advantages of such methods, which have led to a host of important applications including three-dimensional biological imaging, include some features that have as yet received relatively little attention. In the investigation of cellular or sub-cellular processes, it is possible to discern not only on the location, concentration, and lifetime of molecular species, but also the orientations of key fluorophores. Detailed information can be secured on the degree of orientational order in specific cellular domains, or the lifetimes associated with the rotational motions of individual fluorophores; both are accessible from polarizationresolved measurements. This paper reports the equations that are required for any such investigation, determined by robust quantum electrodynamical derivation. The general analysis, addressing a system of chromophores oriented in three dimensions, determines the fluorescence signal produced by the nonlinear polarizations that are induced by multiphoton absorption, allowing for any rotational relaxation. The results indicate that multiphoton imaging can be further developed as a diagnostic tool, either to selectively discriminate micro-domains in vivo, or to monitor dynamical changes in intracellular fluorophore orientation.



7569-67, Session 9

3D resolved two-photon microscopy with liquid lens

K. Lee, P. Vanderwall, The Institute of Optics, Univ. of Rochester (United States); S. Murali, CREOL, The College of Optics and Photonics, Univ. of Central Florida (United States); K. P. Thompson, Optical Research Associates (United States); J. Y. Qu, Hong Kong Univ. of Science and Technology (Hong Kong, China); J. P. Rolland, The Institute of Optics, Univ. of Rochester (United States)

The most common method for axial focusing within the sample in two photon microscopy is through mechanical motion of either the objective lens or the sample. This motion limits the speed at which a depth scan can be accomplished. As an alternative, a variable focus microscope without moving parts can provide a faster, more robust, and cost-effective solution for biomedical systems such as 3D two photon and optical coherence microscopes. We fabricated a custom dynamic focusing objective that incorporates a liquid lens within the optical design of the microscope with a focus change of over 2mm depth that is generated over 100 ms. This is achieved through a curvature change controlled by a applied external voltage. The dynamic focusing objective is incorporated in a widefield two photon microscope to achieve a 3D resolved fluorescence image at video frame rates. We use a Ti:sapphire laser with ultrashort laser pulses (<10 fs) and high average power (~100mW) for efficient excitation of two photon fluorescence using the invariant 0.2 numerical aperture dynamic focusing custom objective. The excited fluorescence is collected and collimated in the backward direction by the objective and then separated from the light source by a dichroic mirror before being focused on a Electron Magnifying CCD camera to produce images. The 3D sample image is acquired through successive focus changes in depth. The field of view, resolution, and imaging speed are demonstrated with images of 5 µm polystyrene microspheres immersed in a Rhodamine B solution.

7569-68, Session 9

Maximizing signals from in vivo multiphoton microscopy: noncontact total emission detection (TEDII)

A. V. Smirnov, J. Knutson, National Institutes of Health (United States)

The generation of a privileged focal volume for two-photon excitation of fluorophores within living tissue is an imaging event. The scanned collection of fluorescence emission is incoherent; i.e., no real image needs to be formed on a detector plane. Thus, new schemes that efficiently funnel all attainable photons to detector(s) become tenable. We previously showed (JOM v.228, p.330-7, 2007) that parabolic mirrors and condensers could be combined to collect the totality of solid angle around the spot for tissue blocks, leading to ~8-fold signal gain.

We now show a new version of this Total Emission Detection instrument modified to make non-contact images inside tissue in vivo. The device is mounted on a periscope (LSM Tech) to facilitate approach to live animals. We find that blood vessels tagged with DsRed-actin ~100 mm deep within an exposed mouse brain provide over 2.5X more light in the TED-II device (compared to light collected by the 20X water 0.95NA dipping objective alone).

Thus, scanning with the same SNR could occur at more than twice the normal rate. Alternatively, one could reduce laser power 60% to reduce photodamage. We have also designed a smaller version to directly replace an objective.

7569-69, Session 9

Fiber optic endomicroscopy for intrinsic nonlinear optical imaging of biological tissues

Y. Wu, J. Xi, L. Huo, The Johns Hopkins Univ. (United States); M. Li, Corning Inc. (United States); X. Li, The Johns Hopkins Univ. (United States)

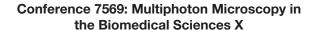
A scanning fiber-optic endomicroscopy system has been developed with the ability of intrinsic two-photon fluorescence (TPF) and second harmonic generation (SHG) imaging of biological tissues for the first time. In the endomicroscope, a customized double-clad fiber (DCF) was employed for single-mode fs pulse delivery and multimode TPF/SHG collection. The new DCF has a larger inner-clad diameter and numerical aperture to effectively suppress the background TPF/SHG signal and improve the TPF/SHG collection efficiency, thus greatly improving the signal-to-background ratio by a factor ~100. The DCF also served as a resonant cantilever driven by a PZT actuator for fast two-dimensional lateral beam scanning. A miniature compound lens was developed to achieve a tight excitation focus, reduce chromatic aberration and improve the TPF/SHG excitation and collection efficiency. These technological innovations have made it possible to perform intrinsic nonlinear optical imaging (auto-fluorescence and SHG) of biological tissues for the first time with a single fiber based endomicroscope. The preliminary experimental results show strong promise of the fiber-optic endomicroscopy technology for translating TPF/SHG microscopy to in vivo studies and clinical applications.

7569-76, Session 9

Multicolor excitation two-photon microscopy: in vivo imaging of cells and tissues

D. Li, W. Zheng, J. Y. Qu, Hong Kong Univ. of Science and Technology (Hong Kong, China)

Two-photon excitation fluorescence (TPEF) microscopy based on endogenous fluorescence provides non-invasive imaging of living biological system. Reduced nicotinamide adenine dinucleotide (NADH), flavin adenine dinucleotide (FAD), keratin, collagen and elastin are the endogenous fluorophores widely used as the contrast agents for imaging metabolism and morphology of living cells and tissue. The fluorescence of tryptophan, a kind of essential amino acid, conveys the information on cellular protein content, structure and microenvironment. However, it can't be effectively excited by the commonly used Ti:sapphire femtosecond laser. Because each endogenous fluorophore provides limited information, it is desirable to simultaneously excite fluorescence from as many fluorophores as possible to obtain accurate biochemical and morphological information on biomedical samples. In this study, we demonstrate that the supercontinuum generation from a photonic crystal fiber (PCF) excited by an ultrafast source can be used to excite multiple endogenous nonlinear optical signals simultaneously. By employing the spectral lifetime detection capability, this technology provides a unique approach to sense the fine structure, protein distribution and cellular metabolism of cells and tissues in vivo. In particular, with application of acetic acid, a safe contrast agent used for detection cervical cancer for many years, the tryptophan signals reveal cellular morphology and even cell-to-cell junctions clearly. Moreover, it was found that the pH value dependent lifetime of tryptophan fluorescence could provide the qualitative information on the gradient of pH value in epithelial tissue. Finally, we will demonstrate the potential of our multi-color TPEF microscopy to investigate the early development of cancer in epithelial





7569-125, Session 9

Pulse shaping for reducing photodamage in multiphoton microscopy

D. Pestov, Y. Andegeko, V. V. Lozovoy, M. M. Dantus, Michigan State Univ. (United States)

Deleterious effects of the laser radiation on the imaged sample, especially if the imaging is done in vivo, have always been an outstanding concern in microscopy. It is well-known that the laser power for damage-free imaging can be limited by either linear or nonlinear damage mechanisms. For a conventional two-photon microscope with a 100-200 fs laser source, the major contributors towards photodamage in cells, e.g., are two-to-three photon absorption processes that trigger formation of reactive oxygen radicals, direct DNA damage, intracellular optical breakdown and plasma formation, etc. The linear damage mechanism (heating), however, is deemed dominant for pigment-rich tissues, such as skin and retina. Our simple model analysis of photodamage dependence on laser parameters suggests that by adjusting both the laser pulse duration and the average laser power at the sample, one can balance between the linear and nonlinear contributions into photodamage. It will allow optimizing two-photon excited fluorescence and/or secondharmonic generation while retaining the laser-induced damage at tolerable level. We formulate the strategy for mitigation of laser-induced damage and optimization of two-photon excited signal by means of pulse shaping and follow up with an experimental study based on these guidelines. We use a broadband Ti:Sapphire laser source aided with a 4f pulse shaper and featuring pulses as short as 12-13 fs. To gain control over the temporal pulse shape at the microscope focal plane, we first pre-compensate for spectral phase distortions using multiphoton intrapulse interference phase scan (MIIPS) and then apply various phase masks to alter the optical waveform.



Monday-Thursday 25-28 January 2010 • Part of Proceedings of SPIE Vol. 7570 Three-Dimensional and Multidimensional Microscopy: Image Acquisition and Processing XVII

7570-40, Poster Session

Two and three-dimensional refractive index measurements of biological samples

G. R. Erry, M. Tedaldi, P. Tomlins, National Physical Lab. (United Kingdom)

Refractive index values in tissues are a promising diagnostic for discriminating between normal and abnormal tissues samples. By measuring the optical path difference within the sample using optical coherence tomography (OCT) or by other techniques such as phase contrast microscopy the refractive index can be inferred, however this reconstruction is difficult due to nature of the measurement. We have demonstrated that using a reference flat and applying some weak assumptions at the boundary of the sample the two-dimensional refractive index can be calculated with high spatial resolution. Results from measurement of sample tissues have been obtained, showing the variation of refractive index within the sample.

Modification of the measurement system enables optical path difference as a function of angle to be recorded, from which it is possible to obtain three-dimensional measurements of refractive index. Reconstruction of the refractive index using data involving a reflective geometry using incomplete and noisy data requires an inversion algorithm that is designed to cope with such deficiencies. These algorithms will be described, and examples showing the reconstruction technique on simple phantoms will be presented.

Other techniques for data collection have been investigated to improve the speed and accuracy of the measurement. One promising technique based on phase contrast microscopy measures out-of-focus intensity planes to infer the optical path difference in the sample. By using a direct solution to the intensity transport equation the optical path difference in the sample can be calculated quickly with high spatial resolution.

7570-41, Poster Session

Return to Contents

Fully automated data acquisition and fast interpretation in a customized multimodal multiphoton microscope

C. Rahn, Beiersdorf AG (Germany); H. Meine, Univ. Hamburg (Germany); S. Gallinat, H. Wenck, K. Wittern, F. Fischer, Beiersdorf AG (Germany)

Examining a volunteer or patient in vivo usually is a strictly time-constrained process. When complex (custom) multi-component, multi-modal imaging devices are involved, an examination session can become significantly stressful for the experimenter. This is especially true when many parameters, several different devices or several different software applications are to be controlled during a single session.

In order to ease image acquisition, we developed a new intuitive and interactive software application that integrates control of all hardware components, guides the experimenter through customizable acquisition workflows, presents the recorded data ready for facilitated interpretation using state-of-the-art image processing algorithms and thus supports the experimenter in acquiring optimized and highly valuable image data. Our software combines many functions into one single application, that were previously performed by several different programs. It allows linking together the functionalities, it allows automation, and it adds several convenience and safety features.

At the moment, the new software is evaluated in our daily image acquisition work. First impressions show a significant improvement for

the experimenter during in vivo imaging sessions with volunteers over the previous heterogeneous software environment.

7570-42, Poster Session

Low-cost two-photons microscope with fully customized trajectories

S. Lodo, A. Tomaselli, C. Vacchi, E. Ugolotti, Univ. degli Studi di Pavia (Italy)

We have developed a modular and efficient two photons scanning microscope using a Nd:Glass ultrashort pulses laser source in order to excite nonlinear fluorescence and second harmonic in a sample.

The system is fully controlled with an ad-hoc electronic system based on FPGA: the board manages all the operations required by the microscope. The sample is scanned using fully customizable trajectories, in order to find best performances of the mechanical system. Standard linear trajectories are ready on powerup while other trajectories, like Lissajous ones, can be loaded quickly. Digital zoom and positioning in the scanning area are provided. The scanning can be done in a closed-loop way, collecting instant positions of the scanning galvomotors in order to process and remove image distortions due to misalignment of electronic and mechanical systems.

The electronic system is also characterized by the management of the target focusing on different focal planes and automatic research of the best focal plane. This is done by moving the sample along in the direction of the laser beam with a linear travel stage and a stepper motor.

The electronic board hosts the power controller for the stepper motor and a standard USB interface to a PC. An ad-hoc software has been developed to simplify the control of the system and to save images in BMP format. It is possible to program automatic acquisitions of images on different focal planes to allow an offline 3D reconstruction.

7570-43, Poster Session

The photobleaching property of confocal laser scanning microscopy with masked illumination

D. Kim, S. Moon, H. Song, W. Yang, D. Y. Kim, Gwangju Institute of Science and Technology (Korea, Republic of)

Confocal and two-photon excitation laser scanning microscopy has become the tool of choice for 3D fluorescence imaging in thick samples. One of the essential components in these microscopes is the high speed scanner for fast 3D image formation. Resonant galvanometer scanners at several KHz are commonly used for the fast x-axis scan. However, during the repeated observation for 3D image formation, phototoxicity and photobleaching may largely occur at both edges than the center of the scan range due to an inherent property (e.g. sinusoidal angular displacement) of the scanner mirror. Usually, no data is acquired at both edges due to large scan distortion even though excitation beam is still illuminated. Here we present confocal laser scanning microscopy with the masked illumination, a simple and low cost method, to exclude the unwanted excitation illumination at both edges. Moreover, the excluded illumination is used as the zero level of the detected signals for a signal quantizing step. The mask with a square hole in its center is set at the image plane for the low diffraction and is slightly tilted by a central vertical axis in combination with a confocal pinhoing method to remove back-reflection scanning beams. The size of the square hole depends on

301

TEL: +1 360 676 3290 · +1 888 504 8171 · customerservice@spie.org



an active scan range. Finally the evidence of reduced photobleaching at both edges with the masked illumination method is also presented with a single layer of fluorescent polymer beads.

7570-44, Poster Session

Self-reference extended depth-of-field quantitative phase microscopy

J. Jang, J. Ye, Korea Advanced Institute of Science and Technology (Korea, Republic of)

Recently, quantitative phase microscopy has been extensively investigated as a tool to visualize the function of bio-samples without staining. For example, FPM (fourier phase microscopy) is based on the principle of phase contrast microscopy and phase shifting interferometery using scattered and unscattered lights from a sample as object and reference fields, respectively. In the case of HPM (hilbert phase microscopy), one reference and object fields are propagated by optical fibers, and the phase image is obtained from a single shot image using Hilbert transform. The FPM and HPM employed complicated commonpath propagation and optical fiber to minimize phase aberration. Here, we propose a novel quantitative phase microscopy based on a very simple and intuitive self-referencing scheme. More specifically, the system consists of EDOF (extended depth-of-field) and Michelson interferometer. Using a pair of objective lenses, the phase aberration by one objective can be corrected by another objective. Furthermore one beam is split onto an SLM (spatial light modulator), which provides a reference field with controlled phase shifts. In order to achieve the homogeneous reference field for accurate phase measurement, the imaging field-of-view is split into specimen and homogenous background. Then, the reference arm optics switches the relative position of homogenous background and specimen, which facilitates the high quality homogeneous reference field. Furthermore, due to the symmetric role of reference and specimen, two distinct phase shifted interference images can be obtained simultaneously. Experimental results using various samples such as micro-patterning poly(dimethylsiloxane) from photomask film, red blood cell and neuron confirm the accuracy and stability of the proposed system.

7570-45, Poster Session

An improvement based on FDK reconstruction algorithm for cone-beam CT

H. Miao, T. Wang, H. Zhao, F. Gao, Tianjin Univ. (China)

As a typical 3D image algorithm, Feldkamp-David-Kress reconstruction algorithm is a filtered backprojection very similar to the 2D algorithm. However, with FDK algorithm only the midplane can be exactly reconstructed, and the reconstruction exactness of other planes decreases with the distance from the midplane increases. In the article, we use an improved method based on FDK algorithm. We reconstructed the object with data we acquired in FDK algorithm and our improved FDK method, the quality of the image using the new method is better than the traditional one in the same reconstruction time.

7570-01, Session 1

Fluorescence fluctuation analysis of mixed chromophores from a line-scanning hyperspectral imager

R. W. Davis, J. S. Aaron, M. B. Sinclair, J. A. Timlin, Sandia National Labs. (United States)

Fluorescence fluctuation analysis provides a powerful method for fast and accurate determination of diffusion dynamics, local concentrations, and aggregation states of biomolecules in cellular environments.

However, spectral overlap among multiple fluorescent constructs and autofluorescence and background inhomogeneities can compromise the quantitative accuracy and constrain useful biological implementation in complex systems. In order to better understand these limitations and expand the utility of correlation methods in general, fluorescence auto- and cross-correlation analyses were performed on high spectral resolution line-scanned images. The parallel pixel streams of the image data provide correlations of mixed and interacting fluorophores in a density gradient polyacrylamide gel. Comparison of the results from integrating spectral windows found in commercial fluorescence microscopes and those from spectral pure components generated by multivariate curve resolution (MCR) reveal potential misinterpretations of data. These are predicated by spectral crowding, environmentally sensitive fluorescence, and inhomogeneous autofluorescence, and are exacerbated at the low concentrations typical of single molecule studies. The described experimental platform and analytical approach provide unique implications for field-free and multiplexed microfluidic and gel separations at sub-nanomolar analyte concentrations, and allow diffusion based identification of non-denatured, and neutrally charged biomolecules. Additionally, because neither MCR nor line-scan fluorescence correlation spectroscopy require prior calibration, in tandem they offer a method which is insensitive to common optical artifacts, detector saturation, and laser focusing errors which can prevent quality data extraction from standard image processing routines. Finally, we discuss the trade-off implications between image acquisition speed and spectral resolution in correlation studies of increasing spectral complexity.

7570-02, Session 1

Quantitative depth-variant imaging for fluorescence microscopy using the COSMOS software package

C. Preza, V. Myneni, The Univ. of Memphis (United States)

The previously developed depth-variant maximum-likelihood restoration DVEM algorithm for fluorescent microscopy [1] has been implemented as part of the computational optical sectioning microscopy open source (COSMOS) software package [2]. COSMOS has facilitated the performance analysis of the DVEM algorithm as well as other algorithms developed for computational optical sectioning microscopy. The COSMOS package has four platform-independent graphical user interfaces (GUIs) developed using a visualization tool kit for point-spread function (PSF) generation, intensity estimation, image visualization and performance analysis. In the PSF generation GUI two PSF models for widefield (nonconfocal) microscopy are currently available [3, 4]. In the estimation GUI there are currently 5 different algorithms for data processing: an expectation maximization algorithm [5], a linear least square algorithm [6], a linear maximum a posteriori algorithm [7], the Jansen-van Cittert algorithm [8], and the DVEM algorithm. The first 3 algorithms and the PSF generation software are available in the original XCOSM package[9].

The DVEM algorithm addresses depth-variant imaging due to spherical aberration only. The algorithm is based on an imaging model that approximates space-variant imaging by modeling only depth variability using a small number of depths (strata) within the sample which is represented by non-overlapping strata. Interpolation of PSFs defined at depths bounding a stratum characterizes the PSF associated with each stratum which is then utilized to predict the image of a stratum. The choice for the number of strata used provides a tradeoff between accuracy of the model and the computational complexity of the algorithm. The performance of the DVEM algorithm is affected by this tradeoff. Physical parameters such as the lens used, the size of the object and its refractive index contribute to the amount of spherical aberration present in the PSF. In this paper we show results obtained from studies in which different parameters that contribute to depth variability are investigated with noisy simulations. The main conclusion from these studies is that a small number of PSFs can be used for the estimation without a significant loss in algorithm performance. The DVEM algorithm does not address specimen-induced aberrations, rendering it best suited for only imaging homogeneous samples.



References:

- [1] Preza, C. and Conchello, J-A., "Depth-variant maximum-likelihood restoration for three-dimensional fluorescence microscopy," JOSA A, 21:1593-1601, (2004).
- [2] COSMOS Software Package, http://cirl.memphis.edu/cosmos/index.html
- [3] Gibson, S. F. and Lanni, F., "Experimental test of an analytical model of aberration in an oil-immersion objective lens used in three-dimensional light microscopy," J. Opt. Soc. Am. A., 9:54-66, 1992.
- [4] O. Haeberlé, "Focusing of light through a stratified medium: a practical approach for computing microscope point spread functions. Part I: Conventional microscopy," Opt. Commun. 216, 55-63, 2003.
- [5] Conchello, J.-A., "Super-resolution and convergence properties of the expectation-maximization algorithm for maximum-likelihood deconvolution of incoherent images", J. Opt. Soc. Am. A, 15:2609-2620, 1998
- [6] Preza, C., Miller, M. I., Thomas, Jr., L. J., and McNally, J. G., "Regularized linear method for reconstruction of three dimensional microscopic objects from optical sections," J. Opt. Soc. Am. A., 9(2):219 228, 1992.
- [7] Preza, C., Miller, M. I., and Conchello, J. A., "Image reconstruction for 3 D light microscopy with a regularized linear method incorporating a smoothness prior," in Biomedical Image Processing and Biomedical Visualization, R. S. Acharya and D. B. Goldgof, Eds., Proc. SPIE 1905:129 139, 1993.
- [8] Agard, D. A., ''Optical sectioning microscopy," Annu. Rev. Biophys. Bioeng., 13:191-219, 1984.
- [9] XCOSM software package, URL: http://www.essrl.wustl.edu/~preza/xcosm/.

7570-03, Session 1

Comparison of estimation algorithms in single-molecule localization

A. V. Abraham, S. Ram, The Univ. of Texas Southwestern Medical Ctr. at Dallas (United States); J. Chao, The Univ. of Texas at Dallas (United States); E. S. Ward, The Univ. of Texas Southwestern Medical Ctr. at Dallas (United States); R. J. Ober, The Univ. of Texas at Dallas (United States) and The Univ. of Texas Southwestern Medical Ctr. at Dallas (United States)

Different techniques have been advocated for estimating the location of single molecules from microscopy images, and the question arises as to which produces the most accurate results. The accuracy of an estimation technique is measured by the standard deviation of its estimates. Various factors, e.g. the stochastic nature of the photon emission/detection process, extraneous additive noise, pixelation, etc., results in the estimated location of a single molecule deviating from its true location. Here, we compare the performance of the maximum likelihood and non-linear least squares estimators for estimating single molecule locations in different scenarios. Our results show that on average both estimators recover the true location of the single molecule in all scenarios. Comparing the standard deviations of the estimates from both estimators, we find that in the absence of noise and modeling inaccuracies, the maximum likelihood estimator is more accurate than the non-linear least squares estimator, and attains the best possible accuracy achievable [1] for the sets of experimental and imaging conditions tested. Even in the presence of noise and modeling inaccuracies, the maximum likelihood estimator produces results with consistent accuracy across various model mismatches and misspecifications. At high noise levels, neither estimator provides an accuracy advantage over the other. Comparisons were also carried out between two localization accuracy measures derived previously. Software packages with userfriendly graphical interfaces were developed for single molecule location estimation (EstimationTool) and limit of the localization accuracy calculations (FandPLimitTool).

1. Ober, R. J., Ram, S., Ward, E. S. (2004) Biophys. J. 86, 1185-1200

7570-04, Session 1

Reconstructing features of thick objects from phase images

H. Sierra, C. A. DiMarzio, D. H. Brooks, Northeastern Univ. (United States)

Phase microscopy modalities are extensively used to image unstained transparent biological samples because of their ability to obtain high contrast images without exogenous agents. Quantitative phase techniques in particular provide valuable information that can be interpreted easily when the imaged object is optically thin, that is, when the thickness of the object is much less than the depth of field of the imaging system. However, many biological objects of interest have thicknesses comparable to or larger than the depth of field. This work focuses on the initial development of inversion techniques for phase images, in order to reconstruct features of thick transparent samples. We use a shape-based iterative approach that assumes that the index of refraction inside the object can be approximated as piecewise constant. The cases of thick homogeneous and inhomogeneous objects are examined. We assume that the boundary location of all inhomogeneities is known or can be obtained by pre-processing the image. Our goal here is to estimate their unknown indices of refraction. We analyze the performance of the reconstructions for objects with thickness that range from 1 to 20 illumination wavelengths (0.633 micrometers). We simulate experiments using a 10x objective lens and a numerical aperture of 0.5. Results for objects with optical properties similar to real transparent biological samples are presented. The reconstructed indices of refraction have an error less than 5% compared to the true value.

7570-05, Session 1

Closed-loop adaptive optics for microscopy without a wavefront sensor

P. A. Kner, The Univ. of Georgia (United States); L. Winoto, Univ. of California, San Francisco (United States); D. A. Agard, Univ. of California, San Francisco (United States) and Howard Hughes Medical Institute (United States); J. W. Sedat, Univ. of California, San Francisco (United States)

A three-dimensional wide-field image of a small fluorescent bead contains more than enough information to accurately calculate the wavefront in the microscope objective back pupil plane using the phase retrieval technique. The phase-retrieved wavefront can then be used to set a deformable mirror to correct the point-spread function (PSF) of the microscope without the use of a wavefront sensor. This technique will be useful for aligning the deformable mirror in a widefield microscope with adaptive optics and could potentially be used to correct aberrations in samples where small fluorescent beads or other point sources are used as reference beacons. Another advantage is the high resolution of the retrieved wavefont as compared with current Shack-Hartmann wavefront sensors. Here we demonstrate effective correction of the PSF in 3 iterations. Starting from a severely aberrated system, we achieve a Strehl ratio of 0.78 and a greater than 10-fold increase in maximum intensity.

7570-06, Session 1

Increasing precision of lifetime determination in fluorescence lifetime imaging

C. Chang, M. Mycek, Univ. of Michigan (United States)

The interest in fluorescence lifetime imaging is increasing, as commercial lifetime sensing modules become available for confocal and multi-photon microscopy, as well as small animal macroscopic and human endoscopic lifetime imaging in vivo. Lifetime imaging can be employed to remove fluorescence intensity-based artifacts for accurate and quantitative sensing of fluorophore environment. However, in biological applications,

Return to Contents TEL: +1 360 676 3290 · +1 888 504 8171 · customerservice@spie.org



low fluorescence signals from samples can be a challenge, causing poor precision in fluorophore lifetime measurements.

In this report, for the first time, we compare wavelet-based and total variation denoising methods that were developed, optimized, and applied to time-domain fluorescence lifetime imaging data. The methods were first tested using artificial fluorescence lifetime images with features and specifications commonly found in live-cell microscopy. We then applied the methods to experimentally measured images of fluorescence standards acquired under low-light imaging conditions. The methods developed could improve lifetime precision in fluorescence lifetime imaging by 5-to-10-fold in low-light imaging. These promising results should be generally applicable to precision enhancement for different types of fluorescence lifetime imaging, but are especially useful for low-light and/or fast, video-rate imaging, including live-cell microscopy, in vivo small animal imaging, and endoscopic lifetime imaging.

7570-07, Session 2

Gabor wavelet transform for dynamic analysis in digital holographic microscopy

J. Zhong, J. Weng, C. Hu, Jinan Univ. (China)

Real time dynamic analysis of micro-object is one of the significant advantages of the digital holographic microscopy with its power of obtaining quantitative phase information from the hologram. In order to achieve the dynamic analysis, lots of holograms should be recorded and every hologram should be numerical reconstructed. In order to filter out the zero-order term, the twin image term and the parasitic interferences, the process of the spatial filtering must be carried out in the well-known Fresnel diffraction integral method and the angular spectrum method. But when some noises and parasitic interferences are introduced into the hologram, the spectrum of the virtual image would be disturbed by the other spectrum. It brings difficulties to define the spatial filter because of the blurry boundary and non-regular distribution of the spectrum. Manual spatial filters are often used. However, defining different manual spatial filters would consume plenty of time for dynamic analysis. In this paper, a numerical reconstruction technique by means of Gabor wavelet transform (GWT) is presented for real time dynamic analysis. Appling the GWT, the object wave can be reconstructed by calculating the wavelet coefficients of the hologram at the ridge of the GWT automatically and the quantitative phase image of the micro-object is obtained. It provides a way for real time dynamic analysis without the process of the spatial filtering. An experiment with a sequence of holograms of an animalcule is proposed for the dynamic and automatic analysis by employing the GWT method.

7570-08, Session 2

A wide field-of-view microscope based on holographic focus grid

J. Wu, X. Cui, G. Zheng, C. Yang, California Institute of Technology (United States)

Conventional microscope usually has limited field-of-view (FOV), especially for high magnification objective. The requirement for high quality objective lenses also increases the cost for conventional microscope. We have developed a novel microscope technique that can achieve wide FOV imaging and yet possess resolution that is comparable to conventional microscope. The principle of wide FOV microscope system breaks the link between resolution and FOV magnitude of traditional microscopes. Furthermore, by eliminating bulky optical elements from its design and utilizing holographic optical elements, the wide FOV microscope system is more cost-effective.

In the wide FOV microscope system, a hologram was made to focus incoming collimated beam into a focus grid. The sample is put in the focal plane and the transmissions of the focuses are detected by an imaging sensor. By scanning the incident angle of the incoming beam, the focus grid will scan across the sample and the time-varying

transmission can be detected. We can then reconstruct the transmission image of the sample. The resolution of microscopic image is limited by the size of the focus formed by the hologram. The scanning area of each focus spot is determined by the separation of the focus spots and can be made small for fast imaging speed.

We have fabricated a prototype system with a 2.4-mm FOV and 1- μ m resolution. The prototype system was used to image onion skin cells for a demonstration. The preliminary experiments prove the feasibility of the wide FOV microscope technique, and the possibility of a wider FOV system with better resolution.

7570-09, Session 2

Dual-mode digital holographic and fluorescence microscopy for the study of morphological changes in cells under simulated microgravity

M. F. Toy, J. Parent, J. Kühn, Ecole Polytechnique Fédérale de Lausanne (Switzerland); M. Egli, ETH Zürich (Switzerland); C. Depeursinge, Ecole Polytechnique Fédérale de Lausanne (Switzerland)

Continuous exposure to weightlessness causes physiological alterations in living organisms (i.e. orthostatic intolerance, muscle atrophy, cardiac susceptibility to ventricular arrhythmias). Long duration manned space missions require preventive measures for these alterations. Cellular and subcellular imaging of live cells during the exposure can extend the understanding of mechanisms behind these modifications. A dual mode microscope is developed to study morphological evolution of mouse myoblast cells under simulated microgravity in real time. Microscope operates in Digital Holographic Microscopy (DHM) and widefield epifluorescence microscopy modes in a time sequential basis. DHM offers real time quantitative phase information which can be deduced as cellular morphology. EGFP transfected actin filaments in mouse myoblast cells function as the reporter for the fluorescence microscopy mode. A Light Emitting Diode (LED) provides the excitation signal for the fluorescence microscopy mode. DHM and fluorescence microscopy modes share a common microscope objective and CCD camera. Dichroic filter of the fluorescence microscopy mode also serves as a beam splitter to combine reference and object waves in DHM mode. Microgravity condition is simulated by a Random Positioning Machine (RPM). Independently rotating two orthogonal frames of the RPM average the g-vector to microgravity conditions in time. Experimental setup is fixed in the RPM to observe microgravity induced dynamic changes in live cells. Initial results revealed two different modifications. Disorganized structures become visible in the formed lamellipodia, and actin filaments accumulate in the perinuclear region. Future work involves miniaturization of the microscope and experimentation during a space flight.

7570-10, Session 3

Full-field quantitative differential interference contrast microscopy based on 2D structured-aperture wavefront sensor

X. Cui, C. Yang, California Institute of Technology (United States)

We report a full-field quantitative differential interference contrast (DIC) microscope based on a 2D structured-aperture (SA) wavefront sensor. Progressing from our previous proof-of-concept experiment, we implemented a fully integrated 2D SA wavefront sensor on a commercially available CMOS image sensor. By simply adding the wavefront sensor to the camera port of a standard bright-field optical microscope, we can turn it into a full-field quantitative DIC microscope. Unlike the qualitative nature and the enhanced contrast only in a shear direction at a time of a conventional DIC microscope, the new microscope can separate the amplitude and differential phase information of a sample image, and generate one bright-filed image and



two DIC images along two orthogonal shear directions simultaneously. The 2D SA wavefront sensor is the key component in the microscope. It consists of $350\times280~5~\mu m$ circular apertures with 11 μm spacing defined on a 150 nm thick aluminum coated CMOS image sensor. A 10 μm thick SU8 resin was spun-on to separate the apertures away from the image sensor. When a sample image is projected on the wavefront sensor by a microscope, the total transmission of each aperture's diffraction pattern is proportional to the average image intensity at the aperture; the offsets of the diffraction pattern are directly related to the two orthogonal differential phase gradient components of the sample wavefront at the aperture. Our invention can greatly reduce the cost and complexity of building a DIC microscope, and we anticipate it will become a widely accessed unstained live cell imaging technique.

7570-11, Session 3

Differential interference contrast microscopy for the quantitative assessment of tissue organization

D. D. Duncan, Oregon Health & Science Univ. (United States); D. G. Fischer, NASA Glenn Research Ctr. (United States); M. Daneshbod, The Univ. of New Mexico (United States); S. Prahl, Oregon Health and Science Univ. (United States)

The propagation of light through complex structures, such as biological tissue, is a poorly understood phenomenon. Typically the tissue is envisioned as an effective medium, and Monte Carlo techniques are used to solve the radiative transport equation. In such an approach the medium is characterized in terms of a limited number of physical scatter and absorption parameters, but is otherwise considered homogeneous. For exploration of propagation phenomena such as spatial coherence, however, a physical model of the tissue medium having a multiscale structure is required.

We present a particularly simple means of establishing such a multiscale tissue characterization based on measurements using a differential interference contrast (DIC) microscope. This characterization is in terms of spatially resolved maps of the (polar and azimuthal) angular ray deviations. With such data, tissues can be characterized in terms of their first and second order scatter properties. We discuss a simple means of calibrating a DIC microscope, the measurement procedure and quantitative interpretation of the ensuing data, and give example characterizations for a number of different tissue types. These characterizations are in terms of the scatter phase function and the spatial power spectral density.

7570-12, Session 3

Differential interference contrast with spatial light modulator

C. Maurer, S. Fassl, R. Steiger, Innsbruck Medical Univ. (Austria); T. McIntyre, The Univ. of Queensland (Australia); S. Bernet, M. Ritsch-Marte, Innsbruck Medical Univ. (Austria)

Different applications of spatial light modulators (SLM) in optical microscopy are presented. The applications range from high contrast coherent imaging over artefact reduction in partial coherent phase contrast to phase gradient measurements with spatial incoherent illumination. A SLM operates as a Fourier filter to enhance the contrast of phase images or, if a series of images is recorded, to calculate the complex field distribution within the object. Partial coherent illumination can increase the signal to noise ratio, allowing although a spatial dependent filter. We have enhanced the Zernike phase contrast filter to reduce effectively artefacts like the halo effect, when we spread randomly the illumination over the whole numerical aperture of the condenser.

At last an incoherent illumination excludes a spatial dependent filter. We have adopted the concept of Differential Interference Contrast (DIC) to the SLM based setup. A diffraction pattern displayed at the

SLM diffracts the incoming light into two close-by directions. The two generated images are therefore separated and the interference of them can be observed. The shear distance, orientation and relative phase of the two images can be modulated at video rate. The method is demonstrated with different biological samples. A quantitative phase calculation of polystyrene beads completes the description SLM based DIC microscope.

7570-13, Session 3

Measurement of phase resolution

Y. Cotte, C. Depeursinge, Ecole Polytechnique Fédérale de Lausanne (Switzerland)

We present a simple method of directly determining the resolution in phase imaging. The setup is based on Digital Holographic Microscopy (DHM), an interferometric method providing access to the complex wave front. In off-axis transmission configuration, a sub-wavelength nanometric hole on metallic films acts as a complex point source emitter.

The thin film is evaporated on the substrate. A conventional microscope slide, common in bio microscopy with nominal thickness of 0.15 mm is used to model realistic experimental circumstances. Subsequently, focused ion beam (FIB) graving and scanning electron microscopy (SEM) allows creating and characterizing well defined structures in the nanometric scale.

The slides are investigated by a commercial optical microscope combined with DHM. Thus, the phase of known sub-resolution structures can be measured in resolution limited imaging system. Film materials, film thickness and hole structures are varied to access different phase imaging aspects. Rayleigh's classical two point resolution condition can be rebuilt by interfering complex fields emanated from multiple single circular apertures on an opaque metallic film. Similarly, the phase resolution capacity is assessed by measuring the complex point spread function (PSF) of sub-resolution pure phase objects on transparent films.

The amplitude and phase of the point spread function is extracted from holograms, through which point spread functions of different configurations of holes are. In the same way, the complex PSF is compared to simulations from the Debye theory.

7570-14, Session 3

Quantitative phase microscopy by QWLSI wavefront sensing: applications to long-duration imaging

P. Bon, PHASICS S.A. (France) and Institut Fresnel (France); B. F. Wattellier, PHASICS S.A. (France); S. Monneret, Institut Fresnel (France)

Marker-free cell visualization requires a specific setup as Zernike phase contrast or Nomarski-DIC equipments. Those techniques implicitly use the fact that light passing through a sample accumulates phase shift. Accessing to the actual value of this phase shift is very difficult, explaining that such techniques are commonly used as contrast enhancer only. We describe here the use of quadri-wave lateral shearing interferometry (QWLSI) [1] for wavefront sensing, in order to measure quantitatively the local phase shift within a sample.

We use a SID4-HR wavefront sensor (Phasics) and we get a 300x400 sampling points on the sample, with both phase and intensity information. The method is easy to implement on a conventional microscope: it requires only a bright-field illumination and a wavefront sensor in the microscope image plane.

The study of transparent adherent COS-7 cells is considered. The visualization of intracellular elements is clearly possible with a high contrast. Cellular dynamic study -such as particle tracking- is also demonstrated as the acquisition time is only depending on the frame rate of the camera.

305

Return to Contents TEL: +1 360 676 3290 · +1 888 504 8171 · customerservice@spie.org



This paper will present the measurement principle. This will be illustrated by the study of COS-7 cell division under white-light illumination and intracellular particle tracking.

[1] Bon, Maucort, Wattellier, and Monneret, "Quadriwave lateral shearing interferometry for quantitative phase microscopy of living cells," Opt. Express 17, 13080-13094 (2009)

7570-15, Session 4

Applying optical Fourier filtering to standard optical projection tomography

R. Lorbeer, H. Meyer, M. Heidrich, H. Lubatschowski, A. Heisterklamp, Laser Zentrum Hannover e.V. (Germany)

Advances in biology are often based on new microscopy techniques which reveal previously unseen details. One quite young technique is the so called optical projection tomography (OPT), using algorithms and methods well established in X-Ray computer tomography in the filed of optical microscopy. In contrast to most other three-dimensional microscopy techniques it is able to create three-dimensional data-sets of specimen absorption and non fluorescent staining. Additionally it still can be used for fluorescence microscopy and samples with dimensions in the millimeter range can be imaged. These advantages are certainly accompanied by a lower resolution, reconstruction artifacts, and a relatively high loss of light. In our approach, we want to reduce several of these disadvantages and therefore apply optical filters in the fourier plane of the image path, which - by its nature - is not possible in X-Ray imaging. Several filtering techniques are tested. A Ram-Lak filter as used in the filtered back projection algorithms for instance can be implemented physically. Since the phase information cannot be recorded, it is not equivalent to the usual filtered back projection. Furthermore even more restrictive filters suppressing the low spatial frequencies can be used to raise the imaging resolution or focal length. Our simulations already show a multiple fold better resolution respectively to the usual OPT.

7570-16, Session 4

tomoFLIM: fluorescence lifetime projection tomography

J. A. McGinty, Imperial College London (United Kingdom); D. W. Stuckey, Imperial College Healthcare NHS Trust (United Kingdom); K. B. Tahir, R. Laine, Imperial College London (United Kingdom); J. V. Hajnal, A. Sardini, Imperial College Healthcare NHS Trust (United Kingdom); P. M. W. French, Imperial College London (United Kingdom)

Optical Projection Tomography (OPT) is a wide-field technique for measuring the three-dimensional distribution of absorbing/fluorescing species in non-scattering (optically cleared) samples up to ~1cm in size, and as such is the optical analogue of X-ray computed tomography. We have extended the intensity-based OPT technique to measure the three-dimensional fluorescence lifetime distribution (tomoFLIM) in samples. Due to its inherent ratiometric nature, fluorescence lifetime measurements are robust against intensity-based artefacts as well as producing a quantitative measure of the fluorescence signal, making it particularly suited to Förster Resonance Energy Transfer (FRET) measurements.

In tomoFLIM a series of wide-field time-gated images at different relative time delays with respect to a train of excitation pulses is acquired at a range of projection angles. For each time delay the three-dimensional time-gated intensity distribution is reconstructed using a filtered back projection algorithm and the fluorescence lifetime subsequently determined for each reconstructed horizontal plane by iterative fitting of an appropriate decay model.

We will present autofluorescence and labelled tomoFLIM reconstructions of chick embryos, including a FRET-based calcium sensor. This genetically encoded sensor, TN-L15, comprises the calcium-binding

domain of Troponin-C, flanked by the fluorophores cyan fluorescent protein and citrine. In the presence of calcium ions TN-L15 changes conformation bringing the two fluorophores into close proximity, and resulting in FRET. The sensor was electroporated in ovo into the neural tube of the embryos, which were subsequently dissected 1-3 days post-electroporation, fixed in ethanol and embedded in agarose before being optically cleared ready for acquisition by tomoFLIM.

7570-17, Session 4

Dual-modal optical projection tomography microscopy for cancer diagnosis

Q. Miao, Univ. of Washington (United States); J. Yu, M. G. Meyer, J. R. Rahn, T. Neumann, A. C. Nelson, VisionGate Inc. (United States); E. J. Seibel, Univ. of Washington (United States)

A dual-modal optical projection tomography microscope (OPTM) is presented, which can take three-dimensional (3D) images of single cells with isometric high resolution both in fluorescence and absorption modes. Depth of field (DOF) of a high numerical aperture (NA) objective is extended by scanning the focal plane through the sample in order to enable reconstruction by tomography. This extended DOF image is called pseudoprojection. Pseudoprojections from different perspectives are taken by rotating the cells in a microcapillary rotation stage. Cells are fixed, stained, and mixed with optical gel and injected into the capillary for imaging. The optical gel, capillary, and surrounding immersion oil have the same refractive index, thus minimizing the optical distortion caused by the curvature of the capillary. This technique improves resolution by viewing samples from different angles, thus it can provide isometric high resolution both in absorption and fluorescence modes. Absorption images can provide cellular structural information. Fluorescence images can provide molecular-specific contrast. Combining these two modes allows us to image different aspects of the disease process. The 3D absorption image can help to localize the molecular changes. The 3D fluorescence molecular image can help to understand the underlying cause of cellular morphological changes. Images of cells stained with both hematoxylin and fluorescence probes are shown. Registrations between two modes are discussed. When samples rotate around the axis of the capillary, the position of the samples' centroid can be described as a sinusoidal wave. This property is used to register images in absorption and fluorescence modes.

7570-18, Session 4

Computational model of OCT in lung tissue

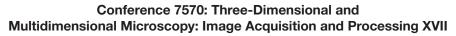
D. C. Reed, C. A. DiMarzio, Northeastern Univ. (United States)

Lung research may have significant impact on human health. As two examples, recovery from collapse of the alveoli and the severe post surgery declines in forced vital capacity in patients involving anesthesia are both poorly understood. Optical imaging is important to lung research for its inherently high resolution. Microscopy and color imaging are fundamentals of medicine, but interior lung tissue is usually viewed either endoscopically or in ex vivo, stained slices.

Techniques such as confocal microscopy and optical coherence tomography (OCT) have become increasing popular because of their improved sectioning and depth penetration. Since OCT has the ability to achieve higher depth penetration than confocal it is more widely used, despite the difficulty of interpreting the images.

To understand light propagation through the highly reflective and refractive surfaces of the lung, we developed a Finite--Difference Time Domain (FDTD) simulation. FDTD solves a discrete approximation to Maxwell's equations.

Initial simulations have shown that structure up to ten micrometers below the surface is clearly visible. Deeper structures are hard to interpret, because of light scattering, compounded by speckle associated with coherent detection. Further simulations and experimental imaging may lead to improved collection and processing of images at deeper levels.





7570-19, Session 4

Integrated optical coherence tomography (OCT)/optical coherence microscopy imaging of pathology

H. Lee, C. Zhou, Massachusetts Institute of Technology (United States); Y. Wang, Beth Israel Deaconess Medical Ctr. (United States); A. D. Aquirre, Massachusetts Institute of Technology (United States) and Harvard-MIT Div. of Health Sciences and Technology (United States); T. Tsai, Massachusetts Institute of Technology (United States); D. W. Cohen, J. L. Connolly, Beth Israel Deaconess Medical Ctr. (United States); J. G. Fujimoto, Massachusetts Institute of Technology (United States)

Excisional biopsy is the gold standard in disease diagnosis; however, it requires processing specimens and can have unacceptable false negative rates because of sampling errors. Optical coherence tomography (OCT) is a promising imaging technique that can provide real-time, high resolution and three dimensional (3D) images of the tissue morphology. Optical coherence microscopy (OCM) is an extension of OCT technology, which integrates the coherence gating of OCT with confocal gating of confocal microscopy. OCM can provide cellular resolution imaging with better imaging depth compared to confocal microscopy. An integrated OCT/OCM imaging system can provide multiscale imaging of tissue morphology. 3D-OCT provides architectural information with a large field of view and can be used to find the regions of interest, while OCM provides high magnification enabling cellular images which are coregistered with OCT images. The integrated OCT/OCM system provides images with axial resolution <4 um for both 3D-OCT and OCM modalities and transverse resolutions of 14 um and <2 um for 3D-OCT and OCM, respectively. In this study, we imaged a wide variety of human specimens including colon (58), thyroid (43), breast (34), and kidney (19). Freshly excised human specimens were imaged within 2 to 4 hours and images were compared with histology. The feasibility of visualizing pathology using an integrated OCT/OCM system was demonstrated and the possibility of using real time optical imaging methods in the pathology laboratory was investigated.

7570-20, Session 4

Snapshot spectral imaging system

T. Arnold, M. De Biasio, R. Leitner, Carinthian Tech Research AG (Austria)

Spectral imaging is the combination of spectroscopy and imaging. Each of these fields is well developed and is being used intensively in many application fields including industry and life sciences. The classical approach to acquire hyper-spectral data is to sequentially scan a sample in space or wavelength. These acquisition methods are time consuming because only two spatial dimensions or a spatial and the spectral dimension can be acquired simultaneously. With a computed tomographic imaging spectrometer (CTIS) it is possible to acquire two spatial dimensions and a spectral dimension during a single integration time, without scanning neither in spatial nor in spectral dimensions. This makes it possible to acquire dynamic image scenes without spatial registration of the hyper-spectral data which is advantageous compared to tunabele filter based systems which need sophisticated image registration techniques. While tunable filters provide full spatial and spectral resolution, for CTIS systems there is always a tradeoff between spatial and spectral resolution as the spatial and spectral information corresponding to an image cube is squeezed onto a 2D camera frame.

The presented CTIS system utilizes a computer generated hologram to project the spectral and spatial image information at once on a 2D CCD camera array. The current system is designed for a microscopy application for the analysis of fixed specimens in pathology and cytogenetics, cell imaging and material analysis. The CTIS approach is generally not limited to microscopy applications, thus it would be possible to implement it in a hand-held device for e.g. real-time, intrasurgery tissue classification.

7570-21, Session 4

Compressed sensing in optical coherence tomography

N. Mohan, I. Stojanovic, W. C. Karl, Boston Univ. (United States); B. Saleh, CREOL, The College of Optics and Photonics, Univ. of Central Florida (United States); M. C. Teich, Boston Univ. (United States)

Optical coherence tomography (OCT) is a valuable technique for non-invasive imaging in medicine and biology. In some applications, conventional time-domain OCT (TD-OCT) has been supplanted by spectral-domain OCT (SD-OCT); the latter uses an apparatus that contains no moving parts and can achieve orders of magnitude faster imaging. This enhancement comes at a cost, however: the CCD array detectors required for SD-OCT are more expensive than the simple photodiodes used in TD-OCT. We explore the possibility of extending the notion of compressed sensing (CS) to SD-OCT, potentially allowing the use of smaller detector arrays. CS techniques can yield accurate signal reconstructions from highly undersampled measurements, i.e., data sampled significantly below the Nyquist rate. The Fourier relationship between the measurements and the desired signal in SD-OCT makes it a good candidate for compressed sensing. Fourier measurements represent good linear projections for the compressed sensing of sparse point-like signals by random under-sampling of frequency-domain data, and axial scans in OCT are generally sparse in nature. This sparsity property has recently been used for the reduction of speckle in OCT images. We have carried out simulations to demonstrate the usefulness of compressed sensing for simplifying detection schemes in SD-OCT. In particular, we demonstrate the reconstruction of a sparse axial scan by using fewer than 10 percent of the measurements required by standard SD-OCT.

7570-22, Session 5

Multifocal imaging of retinal activation

J. Wang, X. Yao, The Univ. of Alabama at Birmingham (United States)

Because of delicate structure of the retina, high resolution evaluation of retinal neural dysfunction is important for improved disease diagnosis and treatment evaluation. Fast intrinsic optical signals (IOSs) hold potential application for high resolution examination of retinal neural function. Our recent investigation suggested that high spatial resolution is essential to separate localized IOSs with opposite, i.e., positive (increasing) and negative (decreasing), polarities. However, practical resolution of reflected light imaging has been challenged by high transparency of the retina. In order to achieve high resolution imaging of reflected IORs in the retina, a microlens array (MLA) and virtual pinholes based parallel confocal imager was constructed. While the MLA based illuminator could provide parallel illumination foci at retina, a fast (1000 Hz) digital camera allowed simultaneous recording of fast IORs from these multiple (60 x 60) retinal points. For the multifocal imager, lateral and axial dimensions of each sampling volume were estimated to 1 and 10 μm , respectively. In coupling with concurrent electrophysiological measurement, multifocal imaging of fast IOSs in stimulus activated frog retinas was demonstrated. Because of effective reduction of background light due to the virtural pinhole confocal imaging mechanism, rapid multifocal imaging disclosed fast IOSs with magnitude peak as large as 40% &I/I, where &I was dynamic optical change and I was background light intensity. Both positive and negative IOSs were consistently observed associated with retinal stimuli.

Return to Contents TEL: +1 360 676 3290 · +1 888 504 8171 · customerservice@spie.org



7570-23, Session 5

Confocal microscope with enhanced lateral resolution using engineered illumination pupil

B. R. Boruah, Indian Institute of Technology Guwahati (India)

The maximum lateral resolution achievable with a confocal microscope is twice that of a wide field microscope. However, the spatial frequency content in the confocal image near the cutoff has very poor signal to noise ratio and is hardly of any practical use. Barring in the fluorescence mode, no technique can provide significant resolution enhancement simultaneously both in the reflection and fluorescence mode of the confocal microscope. This paper proposes a technique based on aperture engineering that can significantly enhance the high spatial frequency content in the image of a confocal microscope working either in the reflection or the fluorescence mode. In the proposed scheme two confocal images, using two separate vectorially engineered illumination pupils, are recorded. Each illumination pupil has four symmetrically arranged circular sub apertures, with the two pairs of diametrically opposite sub apertures having orthogonal polarizations. The polarizations in the sub apertures are arranged in such a way that, at the centre of the focal spot, the first illumination pupil produces constructive interference and the second illumination pupil produces destructive interference. By subtractive the cofocal image obtained with the second illumination pupil from that with the first one, spatial frequency content near the cut off in the resultant image can be significantly enhanced. Using the scheme, theoretical best lateral resolution gain relative to a conventional confocal system is 78%, without severely compromising the axial resolution. This paper presents an analytical treatment to the technique and implementation results in an open frame confocal microscope.

7570-24, Session 5

Coherent pupil engineered scanning reflectance confocal microscope (SRCM) for turbid imaging

C. Glazowski, J. Zavislan, Univ. of Rochester (United States)

The turbidity of an object influences the collected light in ways that can lead to unwanted artifact. It is well known that use of laser illumination in microscopic imaging can lead to speckle in the resultant images. The influence of speckle artifact is more pronounced particularly when investigating deep regions of biological samples. Furthermore, the regions of turbid media above the focal plane of interest impart statistical modifications to the resulting background and focal signal, which then coherently interfere at the pinhole plane. Through a novel coherent model of imaging in a SRCM and subsequent experimental evidence, we have shown that engineering the electric field distribution in the system's pupils can influence the resulting information to the user. As such, this research has direct implications for clinical use of SRCM systems. In this model, the problem at hand is framed in the sense of two-beaminterference of the focal signal and background light. With this model we have theoretically studied the effect of two spatially non-symmetric electric field distributions and their effect on resultant images for turbid media in a moderately high NA (0.9) SRCM system. These distributions are TEM10 and a novel Nomarski DIC. Signal and background (speckle) statistics were parameterized against these pupil distributions and compared to standard TEM00 pupil illumination. To model the influence of a turbid media, skin tissue was mathematically modeled and statistically characterized in terms of the aggregate wavefront deformation and its respective RMS and correlation length. This data will be used to engineer a realistic and repeatable tissue phantom using standard glass fabrication techniques.

7570-25, Session 5

Optimal pupil design for confocal microscopy

Y. G. Patel, C. A. DiMarzio, Northeastern Univ. (United States); M. Rajadhyakshay, Memorial Sloan-Kettering Cancer Ctr. (United States)

Confocal reflectance microscopy may enable screening and diagnosis of skin cancers noninvasively and in real-time, as an adjunct to biopsy and pathology. Current instruments are large, complex, and expensive. A simpler, confocal line-scanning microscope may accelerate the translation of confocal microscopy in clinical and surgical dermatology. A confocal reflectance microscope may use a beamsplitter, transmitting and detecting through the pupil, or a divided pupil, or theta configuration, with half used for transmission and half for detection. The divided pupil may offer better sectioning and contrast.

We present a Fourier optics model and compare the on-axis irradiance of a confocal point-scanning microscope in both pupil configurations, optimizing the profile of a Gaussian beam in a circular or semicircular aperture. We repeat both calculations with a cylindrical lens which focuses the source to a line. The variable parameter is the fill-factor, h, the ratio of the 1/e^2 diameter of the Gaussian beam to the diameter of the full aperture. The optimal values of h, for point scanning are 0.90 (full) and 0.66 for the half-aperture. For line-scanning, the fill-factors are 1.02 (full) and 0.52 (half).

Additional parameters to consider are the optimal location of the point-source beam in the divided-pupil configuration, the optimal line width for the line-source, and the width of the aperture in the divided-pupil configuration. Additional figures of merit are field-of-view and sectioning. Use of optimal designs is critical in comparing the experimental performance of the different configurations.

7570-26, Session 5

Real-time focal modulation microscopy

N. Chen, C. Wong, S. Chong, C. J. R. Sheppard, National Univ. of Singapore (Singapore)

Focal modulation microscopy is a novel microscopy method that can achieve a large penetration depth with single photon excited fluorescence. In this method, excitation intensity within the focal volume is modulated by the use of a time dependent spatial phase modulator. The resultant fluorescence emission is filtered by the spatial gating provided by the pinhole and demodulated with a lock-in amplifier. Previous implementation of the spatial modulator is realised through a mechanical tilt plate phase modulator. This mechanical implementation affords stable modulation and provides satisfactory image quality. However, the slow modulation rate(in kHz range) depreciates the prospect of its employment in real time imaging. A new modulation scheme is proposed in which an acoustic optical modulator(AOM) is utilised. This new arrangement boost the modulation speed and makes real time imaging possible. We report on the development of such a modulation system together with the accompanying electronics. Images obtained with this new modulation system will also be presented

7570-27, Session 5

Parametric spatio-temporal control of focusing laser pulses

M. A. Coughlan, M. Plewicki, R. J. Levis, Temple Univ. (United States)

Optical systems having multiple foci are useful for biological imaging applications. Acquiring a high spatial resolution scan of a sample area can be generated by multiplexing multiple foci, in addition to increasing raster scan rate and signal to noise level. Our method employs simultaneous spatial and temporal focusing pulses and parametric pulse



shaping with characterization performed using scanning SEA TADPOLE. Multiple foci are created with optically-controlled longitudal and transverse spatial positions from pulse shapes generated in the temporal domain. The characterized foci are in agreement with the predictions of a Fourier optics model. The measurements reveal significant pulse front tilt resulting from the simultaneous spatial and temporal focusing optics. Application of complex phase and amplitude functions to a femtosecond pulse allows for control of both the number of spatio-temporal foci and the corresponding longitudal and transverse position of each focus. This control is achieved using simultaneous spatial and temporal focusing optics in conjunction with phase and amplitude laser pulse shaping. The driving pulses are designed using a parametric pulse-shaping algorithm combined with the standard 1 dimensional 256-element pixilated liquid crystal modulator. The evolution of the spatio-temporal intensities along the focusing beam path are characterized using scanning SEA TADPOLE measurements This characterization reveals several new features including pulse front tilt and the ability to control both longitudinal and lateral focal spot position. The absolute positions of the foci can be controlled using parametric pulse shaping. Multiple temporal foci produced through parametric pulse shaping provide longitudinal and transverse scanning capabilities without the need for mechanical motion.

7570-28, Session 6

Extended depth-of-field microscopy

E. J. Botcherby, C. W. Smith, M. J. Booth, R. Juskaitis, T. Wilson, Univ. of Oxford (United Kingdom)

The imaging properties of both conventional and confocal optical microscopes may be tuned in a variety of ways by tailoring the form of the electric field in the pupil plane of the objective lens. A particular example of importance is the ability to dramatically extend the depth of focus by the use of an annular pupil plane aperture without compromising lateral resolution. However the use of such a physical stop is optically very inefficient since most of the incident light is blocked by the annular filter and so cannot contribute to the image signal. This paper describes an alternative method of generating extended focus point spread functions efficiently without compromising the overall light budget of the system. Experimental results and images will be presented.

7570-29, Session 6

Image-based adaptive optics and acoustooptic depth-of-field switching for nonlinear microscopy

N. Olivier, D. Débarre, Ecole Polytechnique (France); A. Mermillod-Blondin, C. B. Arnold, Princeton Univ. (United States); E. Beaurepaire, Ecole Polytechnique (France)

We present two experiments involving wavefront control in nonlinear microscopy.

First, we adapt image-based (wavefront sensorless) aberration correction strategies[1] to the specific case of third-harmonic generation (THG) microscopy[2]. We describe a correction scheme relying on measured aberration modes produced by a deformable mirror and on the relative influence of these modes in THG images. We find an appropriate quality metric for estimating the impact of aberration in this context, given the complexity of the TH imaging process. We achieve a robust correction of N non-orthogonal aberration modes using 2(2N+1) measurements in various samples, and we report aberration correction in multiharmonic-multiphoton fluorescence experiments. We apply this approach to adaptive THG imaging in developing embryonic tissue.

Second, we describe a simple setup that allows depth of field switching at kilohertz rates in a non-linear microscope[3]. Beam profile is modulated using a tunable acoustically-driven gradient-index (TAG) fluid lens[4]. We implement two modulation strategies, one based on fast varifocus scanning during each pixel and the other based on pseudo-Bessel beam excitation. Average beam shape is switched every line during scanning,

resulting in the interlaced acquisition of two different images. We apply this approach to the simultaneous standard and 4.5times-extended depth of field imaging of biological samples.

7570-30, Session 6

Highly parallel CMOS lock-in optical sensor array for hyperspectral recording in scanned imaging systems

R. A. Light, N. S. Johnston, R. J. Smith, S. D. Sharples, M. G. Somekh, M. C. Pitter, The Univ. of Nottingham (United Kingdom)

Many optical measurements that are subject to high levels of background illumination rely on phase sensitive lock-in detection to extract the useful signal. By modulating the portion of the signal that contains information, phase sensitive or lock-in detection can be employed to achieve a very narrowband and low noise detection away from drift, 1/f and other low frequency noise sources. Lock-in detection is therefore widely used in optical imaging and measurement, including optical coherence tomography, heterodyne interferometry, optoacoustic tomography and a range of pump-probe techniques.

Phase sensitive detection is generally performed sequentially with a single photodetector and a lock-in amplifier and this can severely limit the rate of multi-dimensional image acquisition. We present a novel complimentary metal oxide semiconductor (CMOS) linear array chip that can perform phase sensitive, shot-noise limited optical detection in up to 256 parallel channels. This has been achieved by employing four independent wells in each pixel, and massively enhancing the intrinsic well depth with supplementary capacitance to reduce the effect of optical shot noise. Because of the linear architecture of the sensor, these enhancements do not come at the cost of fill factor, which is 88%.

The array can reduce the number of dimensions that need to be sequentially scanned and greatly speed up acquisition. Results demonstrating spatial and spectral parallelism in pump-probe experiments are presented where the a.c. amplitude to background ratio approaches 1 part in one million.

7570-31, Session 6

Scientific CMOS (sCMOS) technology for ultralow-light quantitative calcium flux microscopy

C. G. Coates, D. Denvir, M. Barszczewski, Andor Technology plc (Ireland); N. McHale, K. Thornbury, G. Sergeant, M. Hollywood, Dundalk Institute of Technology (Ireland)

Ultrasensitive detection of low photon flux signals from dynamic calcium microscopy protocols has been performed using a Scientific CMOS (sCMOS) camera. sCMOS is a new high-performance imaging technology that can be considered unique in its ability to simultaneously offer low noise, rapid frame rates, wide dynamic range, high resolution and a large field of view, without the performance compromises that are commonly associated with other scientific detection standards. The 5.5 megapixel sensor used in this study offered < 3 e- rms read noise at 100 frames/s (full frame), whilst maintaining > 16,000:1 dynamic range.

For these experiments, smooth muscle cells were loaded with calcium binding fluorophore and dynamically imaged by either a spinning disk (Nipkow) laser confocal microscopy set-up, or a conventional widefield fluorescence configuration. Each modality incorporated Andor Technology's prototype sCMOS camera operating in excess of 100 fps. At this speed, camera exposure times were sufficiently short such that photon fluxes available to the sensor during a given exposure were very low. Furthermore, the enhanced detector sensitivity afforded significant attenuation of laser powers (thus prolonging cell/dye lifetimes), lower dye concentrations, and minimal exposures, enabling the full frame rate of the camera to be harnessed. Such demonstrations of sensitivity at high-speed operation, particularly over an extended field of view, suggest that

309

Return to Contents TEL: +1 360 676 3290 · +1 888 504 8171 · customerservice@spie.org



sCMOS holds potential to become a breakthrough enabling technology across many strands of quantitative multi-dimensional live cell analysis.

7570-32, Session 7

Practical optical quality assessment and correction of a nonlinear microscope

R. Aviles-Espinosa, ICFO-The Institute of Photonic Sciences (Spain); J. Andilla, Imagine Optic (France); R. Porcar-Guezenec, Imagine Optic (France) and ICFO-The Institute of Photonic Sciences (Spain); O. Olarte, S. I. Santos, ICFO-The Institute of Photonic Sciences (Spain); X. Levecq, Imagine Optic (France); D. Artigas, Univ. Politècnica de Catalunya (Spain) and ICFO-The Institute of Photonic Sciences (Spain); P. Loza-Alvarez, ICFO-The Institute of Photonic Sciences (Spain)

Nonlinear microscopy (NLM) has covered the requirement for higher contrast and resolution compared with other microscopy techniques, however, the optical quality of this imaging apparatus and the sample structure can compromise its capabilities. Here, we show that the imaging capabilities of a NLM can be affected by the aberrations produced by the setup optical elements alignment, the materials from which they are fabricated and more importantly by the sample. To overcome this, a Shack-Hartman Wavefront sensing scheme has been implemented for characterizing: 1) the whole NLM setup and, 2) the sample induced aberrations. The first part includes all the aberrations introduced by the optical elements, starting from the laser and until the microscope objective. Having these information, aberrations can be compensated in a closed-loop configuration resulting in the system calibration. Then the remaining aberrations (microscope objective and sample) are recorded. This is done employing the sample nonlinear fluorescence signal collected at one point (keeping the excitation beam static) in the imaging plane. Given that this emission is an incoherent process, it can be considered as a point source. Therefore its wavefront will contain the sample and the objective aberrations. Using the wavefront sensor the information is recorded and passed to the deformable mirror which will compensate the aberrations in a "single shot" (open-loop configuration). This compared with other adaptive optics strategies (i.e. iterative algorithms) results in a reduced sample exposure, and greatly decreases sample damage. Importantly the application of both corrections (system and sample) enables a significant signal intensity and contrast improvement.

7570-33, Session 7

Label-free classification of cell types by imaging of cell membrane fluctuations using low-coherent full-field quantitative phase microscopy

T. Yamauchi, Hamamatsu Photonics K.K. (Japan) and Massachusetts Institute of Technology (United States); N. Sugiyama, Hamamatsu Photonics K.K. (Japan); T. Sakurai, Hamamatsu Univ. School of Medicine (Japan); H. Iwai, Y. Yamashita, Hamamatsu Photonics K.K. (Japan)

We recently developed low-coherent full-field quantitative phase microscopy for obtaining images of cell membrane morphology. Our setup is based on a Linnik-type phase-shifting interferometric microscope with a coherence length of 1.5 micrometer. This setup is able to quantitatively measure the three-dimensional topography of a cell membrane without a priori assumption of the cell's refractive index. In addition, stabilization of the optical path difference between the sample and the reference arm is introduced to realize 1.2-nanometer long-term stability of the height measurement over 500 seconds. In this presentation we report our analysis of membrane fluctuations of different types of cells and of cells under different conditions in a recording

that lasts several minutes. Spontaneous membrane fluctuations of cultured cells are assessed in a human breast cancer cell line and a rat pancreatic beta cell line. In terms of the amplitude and vibration spectra of the membrane fluctuations, those two cell types exhibit different characteristics, with the pancreatic beta cells showing three times more vibration than breast cancer cells. We also treat the cells with a 2% formalin solution, and the pancreatic beta cells show a significant reduction in fluctuations from 200 nm to 70 nm. The breast cancer cells show relatively mild change, but the difference can be observed in the vibration spectra. We believe that these results imply the feasibility of the low-coherent quantitative phase microscope for cell classification without fluorescent labeling.

7570-34, Session 7

Image correlation spectroscopy for the assessment of fiber networks

U. Utzinger, S. M. Mir, B. K. Baggett, The Univ. of Arizona (United States)

Summary: Image Correlation Spectroscopy (ICS) is a tool well suited for analyzing images of fibrous networks such as the Extracellular Matrix (ECM). Images of the ECM are preferably generated using confocal reflectance or SHG microscopy.

Approach: From a universal Gaussian fit to data around the origin of an image's auto correlation function it is possible to extract parameters which describe average fiber orientation, fiber thickness, fiber length and fiber content; all parameters that describe the mechanical properties of the FCM

Sensitivity analyses were conducted on simulated fiber networks. In addition, collagen gels reconstituted under various conditions such as pH other than neutral and non physiologic temperatures, confirm the techniques ability to characterize fiber networks effectively.

We will also present results on the techniques ability to determine fiber network pore size, an important parameter affecting amoeboid cell migration.

7570-35, Session 7

High-resolution image slicing spectrometer (ISS) for hyperspectral microscopy

L. Gao, R. Kester, T. Tkaczyk, Rice Univ. (United States)

Hyperspectral microscopy (HM) is emerging technique in biological research. It can capture the whole spectrum within its 2D FOV, and build a 3D datacube (x, y, λ) which can provide accurate information on fluorescent probe distributions and relative concentrations over the whole specimen. Most current available HMs need some kind of scanning, either in spatial domain or spectral domain. This limits their potential use in real-time imaging. A high resolution Image Slicing Spectroscopy (ISS) is developed for HM. ISS is a spectral imaging technique that is compatible with many biomedical imaging instruments, e.g. microscope and endoscope. It is a snapshot technique without scanning. Spatial and spectral information can be obtained simultaneously by slicing and dispersing the field. The critical component of the ISS is a customfabricated micro-scale facet mirrors termed image slicer. It plays the role of integrate field unit in astronomical optics, but has many improvements over its comparative. Proof-of-concept instrument has been realized at the sampling of $100\times100\times25$ (x, y, λ) in the datacube. Spatial and spectral resolution is determined by the choice of microscope objective and dispersive prism. The result presented in the prototype is about 0.5µm and 6nm respectively. High sampling (250×250×25) ISS system is currently being developed in the group. It enjoys larger field of view (~100µm) and high light throughput. It is expected to have the capability to capture the image with integration time ~200ms. System design and preliminary test results in fluorescent microscopy will be presented.



311

7570-36, Session 7

Wide-field supercritical fluorescence microscopy: real-time live cell membrane imaging

 K. Balaa, Ecole Supérieure de Physique et de Chimie Industrielles (France);
 S. Lévêque-Fort, Univ. Paris-Sud 11 (France);
 J. Delahaye,
 E. Fort, Ecole Supérieure de Physique et de Chimie Industrielles (France)

Numerous cell mechanisms involve membrane processes. The understanding of such processes is thus of crucial importance in biomedical applications. It explains the spectacular development of specific fluorescence imaging techniques like TIRFM.

Here, we present an alternative wide field imaging technique based on supercritical emission of particular interest for cell membrane studies. This technique is based on selecting the fluorescence emission at supercritical angles (also called forbidden light). When fluorescent emitters are placed in the vicinity of the glass slide, their near-field components become propagative. This supercritical emission decays sharply the fluorophore/surface distance d (as d-6) with a characteristic decay length of about 100 nm. Selecting the supercritical emission thus provides an efficient mean of spatial filtering. This can be obtained simply with a mask placed in the back focal plane of a high numerical microscope objective.

This technique has numerous advantages over techniques based on excitation confinement like TIRFM. In particular, it avoids the major drawbacks of the loss of confinement due to light scattering. Standard light sources, with a homogeneous lighting, can be used instead of the usually required lasers.

We will show wide field real-time images of live cell membrane activity using this technique. We will give the measured high performances of this technique in terms of image quality, sensibility and resolution. Moreover, we will show that simultaneously standard epifluorescence images can be acquired to give precious complementary information on inner cell activity and membrane events.

7570-37, Session 7

Pupil polarimetry using stress-engineered optical elements

T. G. Brown, A. M. Beckley, Univ. of Rochester Medical Ctr. (United States)

No abstract available.

7570-38, Session 7

Hyper-NA imaging with solid-immersion optics and induced polarization imaging

J. Zhang, T. D. Milster, College of Optical Sciences, The Univ. of Arizona (United States); S. Yang, Samsung Electronics Co., Ltd. (Korea, Republic of); W. L. Bletscher, D. Hansen, College of Optical Sciences, The Univ. of Arizona (United States)

No abstract available.

7570-39, Session 7

Real-time, extended depth DIC microscopy

I. E. Beckers, Technische Fachhochschule Berlin (Germany); R. H. Cormack, C. J. Cogswell, Univ. of Colorado at Boulder (United States)

No abstract available.

Return to Contents TEL: +1 360 676 3290 · +1 888 504 8171 · customerservice@spie.org



Saturday-Monday 23-25 January 2010 • Part of Proceedings of SPIE Vol. 7571 Single Molecule Spectroscopy and Imaging III

7571-01, Session 1

Photon statistics and hydrodynamic properties of fluorescently labeled DNA helices

S. Pallikkuth, A. Volkmer, Univ. Stuttgart (Germany)

We report the high-time resolution measurement of photon statistics and hydrodynamic properties of fluorescently labeled DNA helices freely diffusing in solution at room temperature. By calculating the full second-order correlation function from picoseconds to seconds from the recorded photon detection time traces, we observe photon bunching on time scales of tens of nanoseconds to several milliseconds, in addition to the quantum optical photon antibunching at shorter time scales. A complete theoretical analysis of the measured correlation reveals information about the fluorophore stoichiometry, both the rotational and translational Brownian diffusion of the biopolymer along with the triplet kinetics of the attached fluorophore. We believe this technique could provide a unique tool for studying simultaneously the hydrodynamic and photophysical properties of fluorophore-DNA complexes occurring on time scales covering more than twelve orders of magnitude.

7571-02. Session 1

Understanding enzyme activity using single molecule spectroscopy

Y. Liu, Y. Zeng, Y. Luo, Q. Xu, M. Himmel, National Renewable Energy Lab. (United States); S. Smith, South Dakota School of Mines and Technology (United States); H. Wei, S. Ding, National Renewable Energy Lab. (United States)

To develop more cost-effective approaches to liberate fermentable sugars from recalcitrant biomass, the enzyme cocktail used for saccharification must be improved. We have developed a single-molecule technique based on fluorescence imaging to track the binding orientation and the motion of cellulase components with spatial resolution at several nanometers. We used single molecule spectroscopy to study the behavior of carbohydrate-binding modules (CBMs) labeled with quantum dots (QDs) or green fluorescence protein (GFP) while bound to cellulose crystals. These bio-assembles were subjected to total internal reflection fluorescence (TIRF) microscopy. The concentrations of the CBMs and fluorophores (QDs, GFP) were optimized to achieve single molecule resolution. This technique revealed a confined nanometerscale movement of the CBMs bound to cellulose with preferred binding orientation. Although the mechanism of CBM motion is still unknown, the single molecule approach used here offers new opportunities to guide us toward a fundamental understanding of cellulase function, especially the mechanism of the "processivity" of exoglucanse.

7571-03, Session 1

Solvent relaxation studies applied to stimuliresponsive core-shell nanoparticles

K. Prochazka, P. Matejicek, M. Stepanek, Charles Univ. in Prague (Czech Republic); M. Hof, J. Humpolickova, R. Sachl, Czech Academy of Sciences (Czech Republic); J. Schroeder, Georg-August Univ. of Gottingen (Germany)

The self-assembled amphiphilic block copolymer micelles containing hydrophobic cores (e.g., polystyrene, polycaprolactone, etc.) and

water-soluble shells formed either be neutral chains, e.g., poly(ethylene oxide), or by electricaly charged polyelectrolytes, e.g., poly(methacrylic acid) have been amply studied as models - and in the case of their full biocompatibility and biodegradability - as components of real systems for the targetted drug delivery. A suitable behavior of water-soluble shell-forming chains is a crucial condition for the stability and hence for applicability of such systems in medicine. The shells formed by weak polyelectrolytes (such as polymethacrylic acid) offer a number of advantageous features, because their behavior is stimuli-responsive and can be tuned by pH, ionic strength and temperature.

However, this behavior is fairly complex and difficult to study experimentaly in detail. There exists a strong gradient in the properties across the shell and the density of polymer segments, degree of dissociation, polarity, etc. change considerably in the radial direction.

Advanced fluorescence studies with polarity-sensitive fluorophores can reveal important details of the shell structure, providing that their localization is sufficiently known. The fluorescent surfactants composed of a polar fluorescent head-group and a long aliphatic chain are suitable probes for such studies. We have been studying aqueous micellar systems and the behavior of their shells by a combination of light scattering and fluorescence for almost two decades. In this communication we report on solvent relaxation studies on aqueous micelles using patman as a polarity-sensitive probe.

7571-04, Session 1

Near-field scanning optical microscopy as a new tool to study the kinetics of single proteins at a biological membrane

A. Naber, N. Neuberth, M. Herrmann, J. Wissler, J. Pérez, D. Gradl, Univ. Karlsruhe (Germany)

Over the last years the demand for high-resolving imaging techniques capable of observing kinetic processes on a nanometric scale has considerably grown. Optical fluorescence techniques have been proven to be most useful due to advanced preparation methods and unmatched sensitivity. In contrast to common far-field optical methods, near-field scanning optical microscopy (NSOM) features a spatial resolution down to 10 nm without compromising temporal resolution. Using a NSOM probe based on a triangular aperture, single fluorescent molecules could be imaged at a resolution of ~30 nm with excellent signal-to-noise ratio. In biology, NSOM has been used mainly on dried samples but progress regarding probe-sample distance control recently allowed also imaging of unfixed membranes in liquid.

We will present a novel technique which enabled us to reliably image functionally intact nuclear pore complexes (NPCs) embedded in a freestanding native nuclear envelope (NE) at high optical resolution. NPCs are highly differentiated macromolecular assemblies of ring-like structure that regulate the exchange of molecules between nucleus and cytoplasm. Since the transport channel of the NPC was no longer obstructed by a support, we could observe the translocation of fluorescence-labeled proteins (NTF2) through the pore by placing the NSOM probe over a NPC and detecting the fluorescence of NTF2 as a function of time. The strong fluorescence fluctuations generated during the translocation were analyzed by means of fluorescence correlation spectroscopy (FCS). Thereby we obtained previously inaccessible kinetic information about the still unknown mechanism of the NPC as gated permeability barrier.

7571-05, Session 1

Single molecule study on cardiac muscle

J. Borejdo, P. Mettikolla, P. Muthu, R. Luchowski, I. Gryczynski,



Z. Gryczynski, Univ. of North Texas Health Science Ctr. at Fort Worth (United States)

Single molecule detection technique was applied to study the mechanism of the heart muscle. We compare the environments of a single cross-bridge of transgenic wild-type heart and transgenic heart carrying disease-causing mutations in the regulatory light chain of myosin, as it undergoes cycle of binding and dissociating from actin. These experiments measure environment of a cross-bridge by monitoring fluorescent lifetime. The lifetime is different when cross-bridge is bound to actin and when it is dissociated from it. From independent measurements we proved that mutated muscle exhibits pronounced decrease in the cross-bridge turnover rate. The fact that duty cycle remains constant suggests that mutation causes cross-bridges to spend more time detached from thin filaments.

7571-06, Session 2

Design and application of single fluorophore dual-view imaging system

H. Zhang, D. Shu, Univ. of Cincinnati (United States); M. Browne, Andor Technology (United States); W. Wang, R. Petrenko, T. Lee, J. Meller, P. Guo, Univ. of Cincinnati (United States)

Simultaneous detection of two fluorescent markers is important in determination of distance, relative motion and conformational change of nanoparticles or nanodevices. We constructed an imaging system with single fluorophore sensitivity and multicolor detection ability. The system combines deep-cooled sensitive EMCCD camera, prism-type TIRF, and objective-type TIRF. A laser combiner was introduced to facilitate simultaneous dual-channel imaging by deliver lasers with different wavelength synchronically via an optic fiber to the sample. The system produces stable signal with extremely low background for studies on structures, stoichiometry, distances and function of the phi29 DNA packaging motor. Single-molecule photobleaching combined with binomial distribution analysis clarified the stoichiometry of pRNA on the motor and elucidated the mechanism of pRNA hexamer assembly. The feasibility of single-molecule FRET analysis with this system was demonstrated. Distance rulers of dual-labeled dsDNA and RNA/DNA hybrids were used to evaluate the system. Eight dimer pairs of phi29 motor pRNA were assembled with single donor or acceptor at various locations. FRET were detected for six dimers and utilized to assess the distance between each donor/acceptor pair. The results provide the distance constraints for 3D computer modeling of phi29 DNA packaging motor. We have also re-engineered the energy conversion protein, gp16, of phi29 motor for single fluorophore labeling to facilitate the singlemolecule studies of motor mechanism. The potential applications of single-molecule high-resolution imaging with photobleaching (SHRImP) and single molecule high resolution with co-localization (SHREC) approaches to the study of the nanomotor were also investigated.

7571-07, Session 2

The electrostatic corral: a new approach for nanoscale trapping of single molecules

J. C. Woehl, C. A. Carlson, Univ. of Wisconsin-Milwaukee (United States)

It is well established that larger dielectric particles can be trapped free in solution by steep electromagnetic field gradients produced by a strongly focused laser beam. However, such techniques have failed to trap molecular-scale objects because of fundamental limitations related to the high beam intensities that would be required.

More recently, a 2D electrophoretic trap has been developed for trapping nanoparticles and even single fluorescent molecules by applying quasi-DC fields in a feedback loop to counteract Brownian motion. The trap, however, can only operate when the particle is located, which is problematic in the case of single molecules which often exhibit

intermittent fluorescence emission.

In this contribution, we will discuss a new approach for the trapping and manipulation of single molecules, which has great potential for new types of measurements at the molecular scale. The proposed trapping scheme has distinct characteristics which set it apart from other trapping techniques, such as a trapping efficiency that scales favorably with particle size (down to the single molecule level and a stable potential well that does not require any imaging for particle trapping, and multiparticle trapping capabilities. The feasibility of the new approach will be discussed and first results of nanoparticle trapping with a microscale implementation of the new trapping scheme will be presented.

7571-08, Session 2

Simultaneous single molecule atomic force and fluorescence lifetime imaging

O. Schulz, Arizona State Univ. (United States); F. Koberling, M. Koenia, PicoQuant GmbH (Germany); D. Walters, J. Viani, Asylum Research (United States); R. Ros, Arizona State Univ. (United States)

The combination of atomic force microscopy (AFM) with singlemolecule-sensitive confocal fluorescence microscopy enables a fascinating investigation into the structure, dynamics and interactions of single biomolecules or their assemblies. AFM reveals the structure of macromolecular complexes with nanometer resolution, while fluorescence can facilitate the identification of their constituent parts. In addition, nanophotonic effects, such as fluorescence quenching or enhancement due to the AFM tip, can be used to increase the optical resolution beyond the diffraction limit, thus enabling the identification of different fluorescence labels within a macromolecular complex.

We present a novel setup consisting of two commercial, state-of-the-art microscopes. A sample scanning atomic force microscope is mounted onto an objective scanning confocal fluorescence lifetime microscope. The ability to move the sample and objective independently allows for precise alignment of AFM probe and laser focus with an accuracy down to a few nanometers. Time correlated single photon counting (TCSPC) gives us the opportunity to measure single-molecule fluorescence lifetimes. We will be able to study molecular complexes in the vicinity of an AFM probe on a level that has yet to be achieved. With this setup we simultaneously obtained single molecule sensitivity in the AFM topography and fluorescence lifetime imaging of YOYO-1 stained lambda-DNA samples.

7571-09, Session 2

Dielectric microspheres to enhance single molecule fluorescence detection

H. Aouani, J. Wenger, Institut Fresnel, Aix-Marseille Univ. (France); D. Gérard, Institut Charles Delaunay, Univ. de Technologie Troyes (France); H. Rigneault, A. Devilez, N. Bonod, Institut Fresnel, Aix-Marseille Univ. (France)

Fluorescence Correlation Spectroscopy (FCS) is a powerful technique used for the detection and characterization of fluorescent single molecules. Based on the statistical analysis of fluorescence intensity fluctuations, FCS can provide informations about translational and rotational diffusion, molecular concentrations, chemical kinetics, and biding reactions. FCS is commonly implemented on a confocal microscope with a high numerical aperture (NA) objective to define a small observation volume and maximize the detected photons from each molecule. However, this approach is limited by the optical diffraction and the low fluorescence signal. To overcome these limits, we propose the use of a single dielectric microsphere illuminated by a tightly focused Gaussian beam to focus light on a spot with three-axis subwavelenght confinement and enhance the fluorescence of a single emitter. FCS measurement performed by positioning a 2 µm sphere at the focus



of a high NA objective showed a 10x reduced observation volume together with a 5x fluorescence enhancement. Since the electromagnetic enhancement is maximum at the microsphere top surface, the present technique can be straightforwardly extended to the detection of luminescent probes bound to the functionalized sphere surface. Furthermore, microspheres can be combined with low NA objectives to form high performance optical systems, as an alternative to the expensive and complex high NA objectives. This offers new opportunities for reducing the bulky microscope setup and extending FCS applications. Young Investigator best paper competition BO130

7571-10, Session 2

Nonlinear optical techniques for improved data capture in fluorescence microscopy and imaging

D. S. Bradshaw, J. Leeder, D. L. Andrews, Univ. of East Anglia Norwich (United Kingdom)

Multiphoton fluorescence microscopy is now a well-established technique, currently attracting much interest across all fields of biophysics - especially with regard to enhanced focal resolution. The fundamental mechanism behind the technique, identified and understood through the application of quantum theory, reveals new optical polarization features that can be exploited to increase the information content of images from biological samples. In another development, based on a newly discovered, fundamentally related mechanism, it emerges the passage of off-resonant probe laser pulses may characteristically modify the intensity of single-photon fluorescence, and its associated optical polarization and temporal behavior. Here, the probe essentially confers optical nonlinearity on the decay transition, affording a means of optical control over the fluorescent emission. Compared to a catalogue of other laser-based techniques widely used in the life sciences, including FRET, FLIP/FRAP and STED, most suffer limitations reflecting the exploitation of specifically lifetime-associated features; the new optical control mechanism promises to be more generally applicable for the determination of kinetic data. Again, there is a prospect of improving spatial resolution, non-intrusively. It is anticipated that tight directionality can be imposed on single-photon fluorescence emission, expediting the development of new imaging applications. In addition, varying the optical frequency of the probe can add another dimension to the experimental parameter space. This affords a means of differentiating between molecular species with strongly overlapping fluorescence spectra, on the basis of their differential nonlinear optical properties. Such techniques significantly extend the scope and the precision of spatial and temporal information accessible from fluorescence studies.

7571-11, Session 2

Bimodal single molecule microscopy: multiparameter spectroscopy gives insight into photodegradation processes

F. Schleifenbaum, S. Peter, A. J. Meixner, Eberhard Karls Univ. Tübingen (Germany)

The triumphal course of optical single molecule studies mainly focuses on fluorescence based techniques. However, the structural insight, which can be gained by these methods, is often rather limited due to the broad and unstructured fluorescence spectra. This restriction may be overcome by surface enhanced Raman spectroscopy (SERS), which provides a chemical fingerprint of the investigated species. Nevertheless, for complex systems such as e. g. proteins, the interpretation of the obtained spectra is often too intricate. We present a novel bimodal microscopy approach to correlate the information content of the two spectroscopic modes on the single molecule level. By performing both, fluorescence and SERS spectroscopy on the same individual bichromophoric autofluorescent protein, we are able to assign distinct Raman bands

to isolated fluorescence forms. On basis of these data we compare Raman spectra of native and photobleached proteins independently for the two distinct spectral forms. This in turn enables us to study the individual photoegradation processes and to open the field of elucidating the chemical structure of the generated compounds by spectroscopic methods on the single molecule level.

7571-12, Session 3

Single-molecule studies of gene expression in living cells

X. S. Xie, Harvard Univ. (United States)

Our group has achieved imaging single fluorescent proteins with millisecond time resolution and nanometer spatial precision [1], and applied the method to the study of gene expression and regulation. We reported the first movie of protein production one molecule at a time in a single live E. coli cell, providing a quantitative description of transcription and translation [2]. We directly monitored binding and unbinding of single lac repressors on DNA, and studied how the repressor finds its specific binding sites [3]. We demonstrated that a stochastic event of complete dissociation of a single repressor is solely responsible for the life changing decision of a cell, switching from one phenotype to another [4]. We will also report our latest work which combines single-molecule biology with systems biology.

- 1. Xie et al. 2008, Ann. Rev. Biophys. 37, 417
- 2. Yu et al. 2006, Science 311, 1600
- 3. Elf et al. 2007, Science 316, 1191
- 4. Choi et al. 2008, Science 322, 442

7571-13, Session 4

Concepts and components for time-resolved single molecule microscopy

F. Koberling, B. Kraemer, P. Kapusta, PicoQuant GmbH (Germany); S. Ruettinger, Physikalisch Technische Bundesanstalt (Germany); V. Buschmann, M. Koenig, S. Tannert, M. Wahl, R. Erdmann, PicoQuant GmbH (Germany); D. A. Walters, J. A. Viani, Asylum Research (United States); S. Fore, PicoQuant Photonics North America Inc. (United States)

Modern time-resolved measurements permit to follow fluorescence dynamics from the sub-nanosecond range up to fluctuations in the second range and even beyond. The underlying data acquisition technique (Time-Tagged Time-Resolved (TTTR) recording) allows to store for every photon individually timing as well as spectral and polarisation information, based on a multichannel detection. To exploit the full photon information and overcome the routing bottleneck we offer now a true multichannel photon timing instrumentation (HydraHarp 400) with up to 8 independent detection channels (1).

By exploiting the full information content of such a multi-dimensional measurement, classical intensity based analysis schemes like FCS and FRET can be significantly improved by sorting and weighting the detected photons. This approach is for example used in Fluorescence Lifetime Correlation Spectroscopy (FLCS), which allows to study diffusion properties of different species which just differ in their fluorescence lifetime without the need for multicolour labeling (2).

The single photon data format enables also easily the incorporation of spatial information, generated by point scanning imaging devices. The whole TTTR data acquisition can be operated as a slave and integrated into homebuilt or commercial imaging devices. We will present recent results towards a seamless integration into laser scanning microscopes, paving the way for time-resolved methods like FCS and FLIM to become standard tools in biological microscopy.

Based on the same principle we set up a straightforward combination of a sample scanning Atomic Force Microscope (AFM) with a single-



molecule-sensitive confocal fluorescence microscope in order to record simultaneously fluorescence and topographic information. This will also enable force studies on a single particle whilst simultaneously monitoring its response using fluorescent probes.

7571-14, Session 4

Binding studies of G-protein coupled receptor associated nanolipoproteins using fluorescence correlation spectroscopy

T. Gao, M. Coleman, T. Huser, J. Voss, W. He, Univ. of California, Davis (United States); F. Bourguet, C. Blanchette, Lawrence Livermore National Lab. (United States); S. Ly, Univ. of California, Davis (United States); F. Katzen, W. A. Kudlick, Life Technologies Corp. (United States)

Nanolipoprotein particles (NLPs) represent a unique nanometer-sized scaffold for supporting membrane proteins. G-coupled protein receptors (GPCRs) comprise an important class of membrane-associated proteins, and represent 60% of current drug discovery targets. However, characterization of the dynamic shape and association of NLPs with GPCRs remains a challenging endeavor. Here we present a rapid method of GPCR production coupled with fluorescent correlation spectroscopy to characterize the NLP-GPCR complex association as well as size. FCS provided an in situ measurement for both qualitative and quantitative assessment of NLP formation in solution that has never before been obtained using other techniques. The resulting bR-loaded NLPs were dynamically discoidal in solution with diameter around 7.79 nm. Its insertion rate (percentage of bR-loaded NLPs versus the total number of NLPs including the empty NLPs) was about 55%. The function of bR was confirmed by the color change of the co factor all-trans retinal from light yellow to purple. The second GPCR model is the neurokinin receptor NK1. The preliminary result from electron paramagnetic resonance (EPR) showed a clear difference due to this positive binding compared with that of NK1 inserted NLPs without ligand in the expression reaction. We are currently working on using FCS to characterize the competitive binding assay for the interaction between substance P and the NK1.

7571-15, Session 5

High-throughput multispot single-molecule spectroscopy

R. A. Colyer, G. Scalia, Univ. of California, Los Angeles (United States): T. Kim. Nesher Technologies (United States): I. Rech. D. Resnati, S. Marangoni, M. Ghioni, S. Cova, Politecnico di Milano (Italy); S. Weiss, X. Michalet, Univ. of California, Los Angeles (United States)

Solution-based single-molecule spectroscopy and fluorescence correlation spectroscopy (FCS) are powerful techniques to access a variety of molecular properties such as size, brightness, conformation, and binding constants. However, this is limited to low concentrations, which results in long acquisition times in order to achieve good statistical accuracy. Data can be acquired more quickly by using parallelization. We present a new approach using a multispot excitation and detection geometry made possible by the combination of three powerful new technologies: (i) a liquid crystal spatial light modulator to produce multiple diffraction-limited excitation spots; (ii) a multipixel detector array matching the excitation pattern and (iii) a low-cost reconfigurable multichannel counting board. We demonstrate the capabilities of this technique by reporting FCS measurements of various calibrated samples as well as single-molecule burst measurements.

7571-16, Session 5

Fluorescence lifetime correlation spectroscopy resolves EGFR interaction in live cells

J. M. Irudayaraj, J. Chen, Purdue Univ. (United States)

Binding of antagonist to epidermal growth factor receptor (EGFR) in cancer cells was studied using fluorescence lifetime correlation spectroscopy (FLCS) at single molecule precision. An antagonist (EGFR neutralizing antibody) was labeled with Alexa 488, and HEK293 cells were transiently transfected with EGFR-EGFP. The binding specificity of EGFR neutralizing antibody was confirmed by fluorescence cross-correlation spectroscopy (FLCS) measurements where FLCS with picosecond timeresolution could separate the autocorrelation contributions from Alexa 488 labeled antibody and EGFR-EGFP with respect to their lifetimes. Compared to dual-color cross-correlation FCS experiments, FLCS is much simpler because it requires only a single wavelength excitation and detection optics and could also be used as a cross validation for dual color FCS. With proper choice of fluorophores a tri-color FLCS could be done using one laser line. This study may have significant applications in pharmacological studies as it provides evidence that FLCS can be used as a powerful technique for studying antagonist-receptor interactions in live cells.

7571-17. Session 5

Measuring rotational diffusion of proteins with pulsed interleaved excitation fluorescence correlation spectroscopy (PIE-FCS)

A. Loman, I. Gregor, J. Enderlein, Georg-August-Univ. Göttingen (Germany)

We describe a novel method for measuring rotational diffusion of large biomolecules in solution based on fluorescence correlation on the nanosecond time scale. In contrast to conventional fluorescence anisotropy measurements, a correlation-based method will work also if the rotational diffusion time is much longer than the fluorescence decay time. Thus, the method is suited to study the rotational diffusion of macromolecules having rotational diffusion times of dozen to hundred nanoseconds, which is considerably larger than the fluorescence lifetime of most commercially available dyes or autofluorescent proteins. A pulsed interleaved excitation scheme with crossed excitation polarization maximizes the temporal dynamics of the measured correlation curve as caused by rotational diffusion. Using the determined rotational diffusion coefficient, precise values of the hydrodynamic radius can be obtained. The method is exemplified on sizing globular proteins.

7571-18, Session 5

Extending coincidence analysis to count fluorescent molecules

H. Ta, A. Kiel, Ruprecht-Karls-Univ. Heidelberg (Germany); M. Wahl, PicoQuant GmbH (Germany); D. Herten, Ruprecht-Karls-Univ. Heidelberg (Germany)

Acquisition of quantitative information from microscopic biological samples is highly desirable in the context of the emerging field of systems biology. Photon-antibunching has been used in singlemolecule fluorescence spectroscopy to prove the occurrence single fluorophores. To a limited extent it was also applied to determine the number of fluorophores in the diffraction limited observation volume of a confocal microscope. However, the ability to count fluorophores is so far limited to ~3 molecules due to saturation of the respective calibration curve with increasing number of fluorophores. Recently, we introduced the theoretical framework for analyzing the photon-distribution in a



confocal four-detector setup and thereby extend the range for counting fluorophores. We derived a statistical approach to estimate the number of fluorescent molecules in the observation volume based on a confocal microscope for single-molecule detection. The method employs pspulsed lasers sources for excitation and time-correlated single-photon counting with 4 avalanche photon diodes (APDs) for detection of individual photons. The feasibility for estimating the number of molecules is shown based on simultaneous emission and detection of multiple photons under realistic experimental conditions. Here, we present the experimental realization of the proposed scheme in a confocal four-detector setup using a novel single-photon counting module with 4 fully independent channels and a biotinylated DNA construct that was labeled DNA constructs we were able to identify up to 15 molecules.

7571-20, Session 6

Single molecule detection of biomolecules in the ultraviolet region

J. R. Lakowicz, K. Ray, M. H. Chowdhury, Univ. of Maryland School of Medicine (United States)

Fluorescence detection has been a valuable tool in the biosciences for several years. During the past several years we have studied the effects of metallic surfaces and nanostructures or nearby fluorophores. These studies have shown dramatic increases in brightness and photostability, especially for low quantum yield fluorophores. Much of this work was performed using visible or NIR fluorophores. However, we have recently extended our studies to UV wavelengths and have shown that silver and aluminum nanoparticles can enhance the emission of UV fluorophores including intrinsic protein fluorescence from 300 to 420 nm. We believe metallic nanostructures offer unique opportunities to develop SMD and FCS using intrinsic fluorescence from biomolecules. We performed finite-difference time domain (FDTD) calculations to explore the possibility of enhancing the intrinsic fluorescence of biomolecules with metal nanoparticles in the ultraviolet region.

7571-21, Session 6

Enhanced single molecule detection on plasmonic nanostructures

R. Luchowski, Univ. of North Texas Health Science Ctr. at Fort Worth (United States); T. Shtoyko, The Univ. of Texas at Tyler (United States); P. Sarkar, E. G. Matveeva, Univ. of North Texas Health Science Ctr. at Fort Worth (United States); T. Sorensen, Univ. of Copenhagen (Denmark); N. Calander, I. Gryczynski, Z. Gryczynski, Univ. of North Texas Health Science Ctr. at Fort Worth (United States)

We developed metallic nanostructures which show ~1000 fold enhancements of fluorescence emission in "hot spots". Such strong enhancement in the brightness of fluorophore allows significant reduction in the excitation power which in turn reduces the substrate background. We demonstrate single molecule detection study on self assembled colloidal structures (SACS) substrates can be done using such low laser power that is extremely difficult/impossible to perform on glass substrates.

7571-22, Session 6

Multiparametric single molecule fluorescence spectroscopy studies of photo-induced charge transfer between CdSe/ZnS quantum dots and fullerene

Z. Xu, M. Cotlet, Brookhaven National Lab. (United States)

The potential application of semiconductor quantum dots in solar cells has recently attracted more and more attention. Their size-dependent optical band gap can be utilized to improve the capability of light harvesting. Multiple exciton generation by one absorbed photon in some quantum dots offers the possibility to greatly enhance the efficiency of photon-to-electron conversion. A common approach to apply quantum dots in solar cells is to couple them with another semiconducting material which can form efficient donor-acceptor interaction with them. Following photon absorption in quantum dots, photo-induced charge transfer resulted in separated charge carriers in donor and acceptor respectively, and collection of the separated charge carriers forms photocurrent.

The inhomogeneous dynamics of photo-induced charge transfer processes due to the complexity of local interfacial environment is difficult to be analyzed by the traditional ensemble measurements. In this paper, multi-parametric single-molecule confocal microscope is used to study the photo-induced charge transfer processes between CdSe/ZnS quantum dots and a well-known electron acceptor fullerene (C60) in single molecule level. The size and distance dependence of charge transfer rate between quantum dots and fullerene have been studied by combining single-molecule fluorescence trajectories, lifetime and spectra measurements. Furthermore, statistical analysis of the multi-parametric fluorescence properties from quantum dots provides detailed information about the spatial inhomogeneity and temporal fluctuation of charge transfer rate.

7571-23, Session 6

Metal nanoparticle fluorophore: a powerful fluorescence probe in single cell imaging

J. Zhang, Univ. of Maryland School of Medicine (United States)

Metal nanoparticle fluorophores have been developed using metal-enhanced fluorescence (MEF) principle. Compared with the conventional organic fluorophores, the metal fluorophores display the increasing brightness and shortening lifetime as well as the lengthening photostability and reducing photoblinking. Conjugated the metal fluorophores on the surfaces of cell lines, the cell images were recorded on a scanning confocal microscopy in the either emission intensity or lifetime. The emission spots by the conjugated metal fluorophores were isolated distinctly from the cell images because of their brighter signals and shorter lifetimes. Collected in the three-dimension, the total number of emission spot could be counted quantitatively and the distribution could be described on the cell surfaces. It was noticed that the emission intensity over the cell image was increased with an increase of the number of metal fluorophore on the cell surface but the lifetime was decreased. A quantitative regression curve was achieved between the amount of metal fluorophore on the cell surface and the emission intensity or lifetime over the entire cell image. Based on this regression curve, the target molecules on the cell surfaces could be quantified readily through the cell intensity and/or lifetime at the single cell level instead of the direct count to the emission spots. As novel molecule imaging agents, these metal fluorophores are being applied in the quantification and distribution of target molecule on the cell surface for the clinical diagnostic research.

Keywords: metal-enhanced fluorescence (MEF), metal nanoparticle fluorophore, emission intensity, lifetime, cell imaging, emission spot, and clinical diagnosis.



7571-24, Session 7

Monitoring the catalytic mechanism of P-glycoprotein by single-molecule fluorescence resonance energy transfer

S. Ernst, Univ. Stuttgart (Germany); B. Verhalen, Upstate Medical Univ. (United States); N. Zarrabi, Univ. Stuttgart (Germany); S. Wilkens, Upstate Medical Univ. (United States); M. Börsch, Univ. Stuttgart (Germany)

We monitor the catalytic mechanism of P-glycoprotein (Pgp) using single-molecule fluorescence resonance energy transfer (FRET). Pgp, a member of the ATP binding cassette family of transport proteins, is found in the plasma membrane of animal cells where it is involved in the ATP hydrolysis-driven export of hydrophobic molecules. When expressed in the plasma membrane of cancer cells, the transport activity of Pgp can lead to the failure of chemotherapy by excluding the mostly hydrophic drugs from the interior of the cell. Despite ongoing effort, the catalytic mechanism by which Pgp couples MgATP binding and / or hydrolysis to translocation of drug molecules across the lipid bilayer is poorly understood. Using site directed mutagenesis, we have introduced cysteine residues for fluorescence labeling into different regions of the nucleotide binding domains of Pgp. Double-labeled single Pgp showed fluctuating FRET efficiencies during ATP-driven transport as expected from the distinct recent X-ray crystallographic structures. Duty cycleoptimized pulsed alternating laser excitation (DCO-ALEX) is applied to minimize FRET artifacts and to select the appropriate transporters. Hidden-Markov-Models (HMM) provide the objective way of analyzing the fluorescence time trajectories of Pgp. Thus we report on the dynamics of individual Pgp molecules as well as the effects of different hydrophobic drugs and inhibitors.

7571-25, Session 7

Super-resolved position and orientation estimation of fluorescent dipoles using 3D steerable filters

S. Geissbuehler, F. Aguet, I. Märki, T. Lasser, École Polytechnique Fédérale de Lausanne (Switzerland)

The diffraction patterns of fixed fluorophores are characteristic of the orientation of the molecules' underlying dipole. Fluorescence localization microscopy techniques such as PALM and STORM achieve superresolution by sequentially imaging sparse subsets of fluorophores, which are localized by means of Gaussian-based localization. This approach is based on the assumption of isotropic emitters, where the diffraction pattern corresponds to a section of the point spread function. Applied to fixed fluorophores, it can lead to an estimation bias in the range of 5-20nm.

We introduce a method for the joint estimation of position and orientation of single fluorophores, based on an accurate image formation model expressed as a 3-D steerable filter. We establish the theoretical limits on estimation accuracy using Cramér-Rao bounds and demonstrate experimental estimation accuracies of 5 nm for position and 2 degrees for orientation.

Knowledge of the orientation or rotational freedom of molecules may provide valuable information for understanding biological structures and processes at the molecular scale. In single molecule fluorescence resonance energy transfer (smFRET), the ambiguity of the orientation factor limits the interpretation of measurements and makes it difficult to deduce the inter-dye distance in dipole-dipole interactions. Based on the results obtained, we believe that by applying our algorithm to estimate the orientation factor, the distance measurements with smFRET can be significantly improved.

7571-26, Session 7

Quantitative FRET measurement by highspeed fluorescence excitation and emission spectrometer

J. Yuan, Wellman Ctr. for Photomedicine, Massachusetts General Hospital (United States) and Huazhong Univ. of Science & Technology (China); L. Peng, Wellman Ctr. for Photomedicine, Massachusetts General Hospital (United States) and College of Optical Sciences, The Univ. of Arizona (United States); B. E. Bouma, G. J. Tearney, Wellman Ctr. for Photomedicine, Massachusetts General Hospital (United States)

We report a novel instrument for observing dynamic macromolecule interaction via Förster resonance energy transfer (FRET). The instrument is a high-speed Fourier Fluorescence Excitation Emission spectrometer, which simultaneously measures excitation and emission spectral properties of FRET signals at high speed. It employs a scanning interferometer, which uses an all-reflective optical delay line in which delay scans are created by a galvanometer driven tilting mirror. The broadband excitation light is modulated by interference scanning before being sent to excite FRET donors and acceptor simultaneously. The acceptor emission light is transmitted back into the excitation interferometer in a double-passed interferometer configuration, and detected by a photomultiplier after filtering. The instrument measures both excitation and emission spectral properties by fast Fourier transform spectrograph at up-to 500 measurements per second. In this paper, we describe the use of this device for monitoring FRET signal changes during immunoreactions. By exciting donors and acceptors simultaneously, the instrument can provide quantitative FRET in the presence of free donors and acceptors, which enables real time immunoreactions kinetics studies. Research on improving the instrument sensitivity so that it can make single molecule measurements is underway and will be presented at the meeting.

7571-27, Session 7

Diffusion spFRET reveals nanoscopic cardiac reserve

M. Chinnaraj, H. C. Cheung, J. M. Robinson, The Univ. of Alabama at Birmingham (United States)

The cardiac myofilament is a protein assembly that provides the Ca-regulated force development that enables the heart to undergo alternating periods of contraction and relaxation. Troponin (Tn), a threemember protein assembly within the myofilament, acts as a Ca-sensitive switch. Tn is prototype for studying ligand-regulated allosteric signaling in macromolecular assemblies, the most common form of information processing in biology (Robinson, Phys Rev Lett (2008) 101, 178104). Here, using single pair FRET in freely diffusing Tn assemblies, we show that Tn incompletely activates after binding regulatory Ca. In Ca-bound Tn, we observe approximately equally weighted subpopulations of active and inactive Tn. The reserved population of inactive Tn appears to function as a nanoscopic form of cardiac reserve that can be can be manipulated by cell signaling mechanisms to fine-tune cardiac contractility.

7571-28, Session 7

Quantitative analysis using imaging mode single particle detection

D. Brouard, M. Lessard-Viger, G. Bracamonte, F. Magnan, H. Poirier-Richard, D. Boudreau, Univ. Laval (Canada)

Recent advances in the field of biosensing and nanomaterials have led to the development of super-luminescent systems in which the optical



signal generated upon a biorecognition event is high enough to allow analyte detection at the single target molecule level using an optical detection scheme adapted to this task. , , The main objective of this work is to achieve absolute molecular detection efficiency, in effect to count all target analyte molecules from a defined sample volume, in an analogy to photon counting technology. To reach this objective, our group has been working on the synthesis of functionalized superluminescent coreshell nanoparticles and on the development of a single particle optical detection scheme inspired from the capillary-based single DNA fragment imaging strategy described by Van Orden et al. in 2000.

This paper will present a technical overview of the optical detection technique in development in our lab, as well as recent results in terms of analytical performance, detection efficiency and sample throughput. For example, sample volumes as large as 100 µL were efficiency probed within 5 minutes and the analyte-bearing particles counted with good accuracy and reproducibility. Analytical results obtained with our coreshell nanoparticles in the context of single DNA target detection from aqueous samples will be presented. Furthermore, since our detection system can capture single particle images from a given analyte population and simultaneously obtain valuable wavelength-resolved photophysical information by integrating signal intensity from each luminescent particle, it can be used as a powerful and fast diagnostic tool for the characterization of superluminescent nanosensors. Therefore, the use of this optical detection scheme for the study of Resonance Energy Transfer (RET) within individual multilayer core-shell nanoparticles will be presented.

- 1 Ho, HA; Dore, K; Boissinot, M; Boivin, G; Bergeron, MG; Tanguay, RM; Boudreau, D; Leclerc, M (2005), J. Am. Chem. Soc. 127, 12673-12676.
- 2 Lessard-Viger, M; Rioux, M; Rainville, L; Boudreau, D (2009), Nano Letters (ASAP july 15).
- 3 Jarvius, J; Melin, J; Goransson, J; Stenberg, J; Fredriksson, S; Gonzalez-Rey, C; Bertilsson, S; Nilsson, M (2006), Nature Meth. 3, 725-727.
- 4 Van Orden, A; Keller, RA; Ambrose, WP (2000), Anal. Chem. 72, 37-41.

7571-29, Session 8

Far-field optical nanoscopy

S. W. Hell, Max-Planck-Institut für biophysikalische Chemie (Germany)

For a long while, to apply microscopy with focused light meant that details smaller than half the wavelength of light (200 nm) could not be resolved. Today it is know that using conventional optics it is possible to image at least fluorescent samples with a level of detail far below the diffraction limit. Stimulated Emission Depletion (STED) microscopy and newer far-field optical approaches can provide resolutions better than 20 nm, and in principle are able to resolve molecular detail. Thus far-field optical nanoscopy ushers in non-invasive access to the nanoscale of the living cell.

7571-30. Session 9

dSTORM: real-time subdiffraction-resolution fluorescence imaging with organic fluorophores

M. Schüttpelz, S. Wolter, S. van de Linde, M. Heilemann, M. Sauer, Univ. Bielefeld (Germany)

In the recent past, a variety of methods have been developed to circumvent the diffraction barrier of light which restricts optical resolution to about 200 nm. Single-molecule based localization or photoswitching microscopy methods such as direct stochastic optical reconstruction microscopy (dSTORM) or photoactivated localization microscopy (PALM) have been successfully implemented for subdiffraction-resolution fluorescence imaging. Generally, subdiffraction-resolution imaging requires the acquisition of several thousand images entailing

hundreds of thousands of localizations with nanometer accuracy. The major drawback of this technique is that the computational effort for the image reconstruction process is tremendous. Reconstruction of a subdiffraction-resolution image from experimental data measured typically within minutes can take up to several hours and, thus, limits the applicability of this technique.

Here we present a new computational algorithm for data processing that consists of noise-reduction, detection of likely fluorophore positions, high-precision fluorophore localization and subsequent visualization of found fluorophore positions in a subdiffraction-resolution image. We find that even real-time data processing is possible and that subdiffraction-resolution imaging with organic fluorophores of cellular structures with ~20 nm optical resolution can be achieved in less than 10 seconds.

7571-31, Session 9

Dual excitation image-scanning microscopy

C. Mueller, J. Enderlein, Georg-August-Univ. Göttingen (Germany)

We present a new method of super-resolution fluorescence microscopy, which is based on two apporaches: taking two pictures of the same sample but at two different excitation intensities, and using a scanning focused excitation but recording at each scan position a whole wide-field image of the resulting fluorescence. By applying a rather straightforward image analysis, it is possible to achieve superresolution with a standard confocal microscope equipped with a wide-field imaging CCD. The method works with any kind of fluorescing labeling and does not require special dyes or equipment. We give a presentation of the basic principles of our method and present first experimental results.

7571-32, Session 9

Superresolution microscopy of viral infection pathways

D. L. Thompson, G. P. McNerney, T. Huser, Univ. of California, Davis (United States) and NSF Ctr. for Biophotonics Science and Technology (United States)

A major, but poorly understood pathway for viral infections is the direct transmission of virus from an infected cell to an uninfected cell. We study this mechanism on the example of the human immunodeficiency virus-1 (HIV-1). Here, viral proteins accumulate at the point of contact between two immune cells, which may lead to the highly localized assembly of new viral particles that are then directly passed along to the uninfected cell. Due to the very high viral load at the synapse between cells as well as the small size of viruses it is extremely difficult to dynamically follow the assembly process and the exact transmission pathway in this spatially constrained region. We have used 3D structured illumination microscopy (SIM) to analyze virological synapses in fixed cells, as well as stimulated emission depletion (STED) microscopy to analyze them in living cells. STED provides rapid 2D resolution of live cells well below the diffraction limit, but is typically limited to a single excitation wavelength. SIM, on the other hand, can be conducted at multiple excitation and emission colors with ~ 100 nm lateral and 200 nm vertical resolution. Here, we compare results obtained with both techniques and demonstrate how these allow us to dissect viral transmission pathways between cells.



7571-44, Session 9

Fast, background-free, 3D superresolution optial fluctuation imaging (SOFI)

T. Dertinger, R. A. Colyer, R. Vogel, G. Iyer, S. Weiss, Univ. of California, Los Angeles (United States); J. Enderlein, Georg-August Univ. Göttingen (Germany)

No abstract available.

7571-33, Session 10

In vivo three-dimensional superresolution fluorescence tracking using a double-helix point spread function

M. D. Lew, M. A. Thompson, M. Badieirostami, W. E. Moerner, Stanford Univ. (United States)

The point spread function (PSF) of a widefield fluorescence microscope is not suitable for three-dimensional super-resolution imaging. We characterize the localization precision of a unique method for 3D superresolution imaging featuring a double-helix point spread function (DH-PSF) developed at the University of Colorado. The DH-PSF is designed to have two lobes that rotate about their midpoint in any transverse plane as a function of the axial position of the emitter. In effect, the PSF appears as a double helix in three dimensions. By comparing the Cramer-Rao bound of the DH-PSF with the standard PSF as a function of the axial position, we show that the DH-PSF has higher and more uniform localization precision than the standard PSF throughout a 2 µm depth of field. We then measure the localization precision of our method with 200 nm fluorescent beads, which serve as diffraction- and photon-limited point sources. With 5000-7000 photons detected on top of background noise of ~5 photons/pixel, the localization precision for the DH-PSF is 8-15 nm in the x-y directions and 10-20 nm in the axial direction. Comparisons between the DH-PSF and other methods for 3D super-resolution are briefly discussed. We also illustrate the applicability of the DH-PSF for imaging biological systems by tracking the movement of ParB-fluorescent protein fusions in live Caulobacter crescentus cells in three dimensions with precision beyond the diffraction limit.

7571-34, Session 10

STED nanoscopy and single molecule tracking map the nanoscale dynamics of plasma membrane lipids

S. J. Sahl, M. Leutenegger, C. Ringemann, V. Müller, S. Hell, C. Eggeling, Max Planck Institute for Biophysical Chemistry (Germany)

Far-field fluorescence microscopy of single molecules can provide detailed insights into molecular characteristics in biological and nonbiological materials. However, due to its limited spatial resolution, conventional far-field microscopy can often not solve prominent problems in biology. For example, cholesterol-assisted lipid interactions such as the integration into lipid nanodomains ('rafts') are considered to play a functional part in a whole range of membrane-associated processes, but their direct and non-invasive observation in living cells is impeded by the resolution limit of >200nm. Using the superior spatial resolution of stimulated emission depletion (STED) microscopy as well as the exceeding spatial localization accuracy of single-molecule tracking, we report the direct and non-invasive detection of single diffusing lipid molecules in nano-sized areas in the plasma membrane of living cells and obtain new details of molecular membrane dynamics. Specifically, we combine a (tunable) resolution of down to 30nm with tools such as fluorescence correlation spectroscopy (FCS), or implement a simple

optical method capable of tracking a fluorescent molecule in two dimensions, with high fidelity and currently unrivaled spatiotemporal resolution. As a result, we demonstrate that certain lipids or other 'raft'-associated molecules are transiently (~10ms) trapped on the nanoscale (<20nm areas) in cholesterol-mediated molecular complexes.

7571-35, Session 10

Three-dimensional localization of single particles at the nanoscale

I. Märki, N. Bocchio, S. Geissbühler, F. Aguet, A. Bilenca, T. Lasser, Ecole Polytechnique Fédérale de Lausanne (Switzerland)

Typically, nanoscopy approaches have been focused on the manipulation and detection of the intensity of fluorescence light leading to lateral accuracy of a few nanometers. Example techniques include STED microscopy and localization microscopy (PALM, STORM). Axial accuracy of the same order providing three-dimensional nanometer precision remains a challenge. Several studies have shown that the axial localization accuracy can be improved to a few 10's of nanometers by introducing optical astigmatism or engineered excitation patterns, without substantially comprising the lateral accuracy. In addition, the phase of fluorescence light has shown to be valuable for axial measurements at the nano-scale.

We present a combination of self-interference microscopy at the single-molecule level with lateral super resolution microscopy and demonstrate a novel approach for localizing a single nano-object to within a few nanometers in all three dimensions. For lateral localization, we consider the complex emission pattern of a single fluorescent object, which yields not only an improved estimation of the axial position but also an improved lateral accuracy as well as information on the orientation of the fluorescent emitter. As a proof of principle we demonstrate the measurement of a nanometer displacement of quantum dots placed on polymer bilayers that undergo swelling when changing from an air environment to a water environment. A standard deviation for the lateral and axial localization in the order of 6 nm and 4 nm, respectively, has been achieved. We expect that this technique will open up new possibilities for biological investigations with three-dimensional molecular resolution.

7571-36, Session 10

Four-focus single-particle position determination and fluorescence cross-correlation spectroscopy

L. M. Davis, B. K. Canfield, J. A. Germann, J. K. King, W. N. Robinson, The Univ. of Tennessee Space Institute (United States); A. D. Dukes III, S. J. Rosenthal, P. C. Samson, J. P. Wikswo, Vanderbilt Univ. (United States)

The location of a single molecule can be measured to within tens of nanometers by imaging the point spread function and finding the center of the image. Methods for 3-D localization include multi-focal-plane imaging, astigmatic imaging or engineering the 3-D point spread function combined with fitting the shape of the image, and interferometric widefield imaging. However, for many applications, confocal microscopy is preferable as it can provide improved signal-to-noise ratio, is necessary for two-photon excitation, and facilitates monitoring of sub-millisecond dynamics and fluorescence lifetimes by use of a single-photon avalanche diode for time-resolved single-photon detection. We discuss the capabilities for sub-diffraction, single-nanoparticle position determination in a confocal one- or two-photon microscope with four-focus pulseinterleaved excitation and time-gated single-photon counting. As the technique is scalable to multiple detectors for multi-color observations, it can be used to find the separations of differently colored molecules over a distance range that is complementary to that achievable by FRET. Also, there is a possibility for improved spatial localization by using the non-



linearity of saturation of the excitation. Applications of two experimental set-ups to four-focus fluorescence cross-correlation spectroscopy, studies of quantum dots, and single-particle manipulation and trapping are also discussed.

7571-37, Session 10

The mathematical nanoscope: obtaining sub-diffraction-limited resolution by multiple hypothesis testing

F. Ma, A. Bilenca, Lehigh Univ. (United States)

Recent fluorescence microscopy techniques such as STORM (STochastic Optical Reconstruction Microscopy) and PALM (PhotoActivated Localization Microscopy) have achieved optical resolution beyond the diffraction limit (or, super-resolution) by repeatedly localizing single photoactivatable molecules with nanometer-level precision. Yet, these techniques suffer from a major tradeoff between localization accuracy and image acquisition rate - A tradeoff that particularly limits their capabilities for live-cell imaging.

Typically, super-resolution localization microscopy utilizes rejection algorithms that accept only image data containing at most one activated molecule within a single diffraction-limited spot while discarding all other data to obtain high localization accuracy; however, this comes at the expense of imaging speed. In this talk, we will present a novel method that speeds up the imaging process by reducing the total number of imaging cycles required to produce a super-resolved image. The key to this unique ability is multiple hypothesis testing, which is a powerful mathematical tool for detecting multiple signals embedded in noise.

We will show that unlike conventional rejection algorithms our appraoch uses all measured image data to determine with high probability the exact number (which is unknown a-priori) of a few molecules activated simultaneously within one diffraction-limited area and to produce highly accurate estimates of the molecules' transversal locations. In addition, we will discuss the performance of the algorithm and its dependence on the detected signal-to-noise ratio and the number and proximity of the activated molecules.

7571-38, Session 10

Fluorescence correlation spectroscopy on nanofakir surfaces

J. Delahaye, S. Gresillon, Ecole Supérieure de Physique et de Chimie Industrielles (France); S. Lévêque-Fort, Univ. Paris-Sud 11 (France); N. Sojic, Univ. Bordeaux 1 (France); E. Fort, Ecole Supérieure de Physique et de Chimie Industrielles (France)

Single biomolecule behaviour can reveal crucial information about processes not accessible by ensemble measurements. It thus represents a real biotechnological challenge. Common optical microscopy approaches require pico- to nano-molar concentrations in order to isolate an individual molecule in the observation volume. However, biologically relevant conditions often involve micromolar concentrations which impose a drastic reduction of the conventional observation volume by at least three orders of magnitude. This confinement is also crucial for mapping subwavelength heterogeneities in cells which play an important role in many biological processes.

We propose an original approach which couples Fluorescence Correlation Spectroscopy (FCS), a powerful tool to retrieve essential information on single molecular behaviour, and nanostructured plasmonic substrates with strong field enhancements and confinements at their surface. These electromagnetic singularities at nanometer scale, called "hotspots", are the result of the unique optical properties of surface plasmons. They provide an elegant means for studying single-molecule dynamics at high concentrations by reducing dramatically the excitation volume and enhancing the fluorophore signal by several orders of magnitude.

The nano-fakir substrates used are obtained from etching optical fiber bundles followed by sputtering of a gold thin-film. It allows one to design reproducible arrays of nanotips with curvature radius ≤ 10 nm. We present two-photon FCS results on these nano-fakir substrates using fluorescent nanobeads. We show i) a dramatic reduction of the observation volume and ii) the ability to perform at high concentration measurements which is promising biological applications.

7571-39, Poster Session

Single-molecule photoswitching microscopy using only a single excitation wavelength

V. Buschmann, PicoQuant GmbH (Germany); S. van de Linde, M. Sauer, S. Wolter, Univ. of Bielefeld (Germany); R. Erdmann, F. Koberling, PicoQuant GmbH (Germany)

Super-resolution microscopy techniques offer unprecedented insight into cellular structure1. In Stochastical Optical Reconstruction Microscopy (STORM) and Photo-activation light microscopy (PALM), the dyesensor-molecules are switched using 2 different excitation wavelengths. Recently, it has been shown that certain dye labels exhibit intrinsic dark states with a lifetime which can be tuned by adjusting the level of oxidants and reductants in the buffer2,3. We have built an instrument based on a standard inverse microscope using TIRF excitation and ultrasensitive CCD camera detection to exploit these redox-level adjusted photoswitching behaviour for high resolution imaging. We achieved a lateral resolution of approx. 100nm when imaging ATTO655-molecules, which had been immobilized via a Biotin/Streptavdin-tag. As just a single wavelength is used for one dye, the method has the potential to image several labels with different absorption properties in parallel.

7571-41, Poster Session

High-speed multipoint patch clamp fluorometry system for the real-time monitoring of calcium-activated potassium (BKca) channels in a cell

W. Song, B. Lee, C. Park, D. Y. Kim, Gwangju Institute of Science and Technology (Korea, Republic of)

High speed multi point patch clamp fluorometry using basic image shifting method and commercial multi mode fiber is presented in this paper. Using a singlet lens, the original fluorescence image of a sample is shifted to another plane, and a fiber tip in an xyz stage delivers the fluorescent single at a specific sample position to a spectrometer system with an electron multiplying charge coupled device (EMCCD). The spectrometer is composed with a prism and an EMCCD, which can measure optical spectrum between 450 and 650 nm wavelength. We have measured spectrum changes in calcium activated potassium (BKca) channels in a cell utilizing Lanthanide-binding tag (LBT) and green fluorescence protein (GFP). We expect that ion currents and fluorescence changes in a cell can be monitored simultaneously by using a conventional patch clamp method combined with our proposed fluorometry system. Experimental results about calcium activated potassium channel are presented to illustrate the performance and the flexibility as well as the robustness of our system with respect to background noises.



7571-42, Poster Session

Near-field optical fluorescence correlation spectroscopy

J. Pérez, M. Herrmann, D. Gradl, A. Naber, Univ. Karlsruhe (Germany)

Near field Scanning Optical Microscopy (NSOM) is a well established technique to image fluorescent stained samples with sub-diffraction limited resolution. To achieve this, the excitation light can be squeezed through a tiny transparent aperture of a few tenth nanometers in an opaque film. The lateral dimension of these so called aperture probes sets the highest achievable resolution. In axial direction evanescent fields provide a high intensity decaying exponentially within a few nanometers at the aperture. Our triangular aperture probes offer a high detectivity with their wide taper angle of about 90° and allowed us previously to image single molecules at a resolution down to 30nm. So far NSOM was rather used only in ambient conditions. But we showed that the ultra small excitation volume (3 to 4 orders of magnitude smaller than in confocal microscopy) at the aperture probe can be used in solution in combination with Fluorescence Correlation Spectroscopy (FCS) to study the kinetics of processes at a biological membrane on the nanometer scale.

We will present the application of FCS to NSOM on diffusing molecules in solution. The ultra small excitation volume in such a technique allows measurements with fluorophore concentrations of up to 100 micro Molar. The very small measured correlation times confirm the size of the excitation volume. The presented measurements will give more insight in the modelisation of the excitation volume for FCS measurement.



Conference 7572: Optical Diagnostics and Sensing X: Toward Point-of-Care Diagnostics

Monday-Tuesday 25-26 January 2010 ● Part of Proceedings of SPIE Vol. 7572 Optical Diagnostics and Sensing X: Toward Point-of-Care Diagnostics

7572-15. Poster Session

Evaluation of the cell depleted layer of blood flow in vitro using confocal microscopic PIV method

C. Park, S. H. Lim, H. Lee, C. Lee, G. Kim, Kyungpook National Univ. (Korea, Republic of)

When blood flow is presented below 300-micron inner diameter blood vessel, there exists a regime with no red blood cells (RBCs) around the blood vascular wall, the cell depleted layer. The presence of cell depleted layer is of very importance in hemorheology and it is closely related to peculiar characteristics of RBCs. Concerning this kind of cell migration feature, many studies have been performed by using optical imaging methods including in vivo case. It is known that the lower the hematocrit ratio is, the greater the cell free layer thickness is. In the present study, we employed the laser scanning confocal microscope to image entire blood flow with accurate red blood cell imaging of 0.001 mm spatial resolution. In vitro blood flow of rat with a hematocrit ratio of 20% was simulated inside a 300-micron opaque tube. The scanning rate of confocal microscope was 30 fps with 500 x 500 pixels of image. As a result, we can obtain clear images of RBCs to define the thickness of cell depleted layer by detecting distance from cell edge to wall surface. In addition, the RBCs can be used as tracer particles to get the velocity field of blood flow by performing particle image velocimetry (PIV) technique non-invasively. Based on the present novel optical application, we can easily indicate the presence of cell depleted layer of blood flow in vitro and its boundaries.

7572-16, Poster Session

Monte Carlo simulation of ZPP fluorescence in the retina

X. Chen, S. Lane, Univ. of California, Davis (United States)

We have used Monte Carlo simulation of autofluorescence in the retina to determine that noninvasive detection of nutritional iron deficiency is feasible. Nutritional iron deficiency (which leads to iron deficiency anemia) affects more than 2 billion people worldwide, and there is an urgent need for a simple, noninvasive diagnostic test. Zinc protoporphyrin (ZPP) is a fluorescent compound that accumulates in red blood cells and is used as a biomarker for nutritional iron deficiency. To determine whether ZPP fluorescence can be measured directly in tissue, we developed a computational model of the eye, using parameters that were identified either by literature search, or by direct experimental measurement. By incorporating fluorescence into Steven Jacques' original code for multilayered tissue, we performed Monte Carlo simulation of fluorescence in the retina to determine that if the beam is not focused on a blood vessel in neural retina layer or part of light is hitting the vessel, ZPP fluorescence will be 10-20 times higher than background lipofuscin fluorescence coming from the retinal pigment epithelium (RPE) layer directly below. If, however, light can be focused entirely onto a blood vessel in the neural retina layer, the fluorescence signal only comes from ZPP. The fluorescence from layers below does not contribute to the signal. Therefore, a device could potentially be built and detect ZPP fluorescence.

7572-17. Poster Session

Research on the NIR spectroscopy of turbid media with optical-length resolved detection

Z. Du, C. Li, F. Chen, K. Xu, Tianjin Univ. (China)

The technologies of high sensitivity optical spectroscopy analysis on turbid media play an important part in scientific research and biomedical applications. The optical path in which photons travel inside the turbid media generally brings information of the components of the media. This paper introduces a novel method to study some of the properties of turbid media by measuring and analyzing the differences of optic paths of wavelength modulated laser beams experienced in the media. The outputs of DFB lasers with different center wavelengths are combined and wavelength modulated further by means of current induced wavelength shifting. The combined laser output is divided into reference beam and measuring beam. The signal light, which is sourced by the measuring beam and has been propagated inside the turbid media for a short distance, interferes with the reference beam at the receiver or inside an optic fiber. The frequency of the interference beat signal carries information of the optical path the laser beam experienced inside the media. A high resolution absorbing spectrum is obtained by studying the absorption amplitude of the same optical path undertaken by laser beams with different wavelength. Experiments and measurements on air, water and simulation tissue fluid are reported in the paper as well.

7572-18, Poster Session

Feasibility of analyte prediction in phantoms using a theoretical model of near-infrared spectra

F. Zou, B. Peshlov, Univ. of Massachusetts Medical School (United States); R. Ross, College of the Holy Cross (United States); G. Ellerby, P. Scott, Y. Yang, B. Soller, Univ. of Massachusetts Medical School (United States)

Near-infrared (NIR) spectroscopic measurement of blood and tissue chemistry often requires a large set of subject data for training a prediction model. We have previously developed the principal component analysis loading correction (PCALC) method to correct for subject related spectral variations. In this study we tested the concept of developing PCALC factors from simulated spectra. Methods: Thirty, two -layer solid phantoms were made with 5 ink concentrations (0.004%-0.02%), 2 µs' levels, and 3 fat thicknesses. Spectra were collected in reflectance mode and converted to absorbance by referencing to a 99% reflectance standard. Spectra (5733) were simulated using Kienle's two-layer turbid media model encompassing the range of parameters used in the phantoms. PCALC factors were generated from the simulated spectra at one ink concentration. Simulated spectra were corrected with the PCALC factors and a PLS model was developed to predict ink concentration from spectra. The measured phantom spectra were corrected with the PCALC factors derived from the simulated spectral set. The bestmatched simulated spectrum was identified for each corrected phantom spectrum and used in the PLS model to predict ink concentration. Results & Conclusion: The ink concentrations were predicted with an R2=0.89, and an estimated error (RMSEP) of 0.0037%. This study demonstrated the feasibility of using simulated spectra to correct for inter-subject spectral differences and accurately determine analyte concentrations in turbid media.

Conference 7572: Optical Diagnostics and Sensing X: Toward Point-of-Care Diagnostics



7572-19, Poster Session

An integrated CMOS dual lock-in amplifier for optoelectronic antigens detection

N. Hong, D. Kim, I. Jung, H. Son, H. Kim, T. Chung, Y. Choi, Y. Choi, Chung-Ang Univ. (Korea, Republic of)

Recently, a number of portable optoelectronic sensors have been developed to monitor the health condition of human beings regardless of time and place. For convenient measurement of health status, we need portable sensors that can detect low-level signals under noisy environments with low energy consumption. Also a suitable signal processing is required to obtain relevant information. Hence, especially for point of case portable sensors, a special technique is essentially required to detect concealed weak signal in intensive noisy environment. It has been known that lock-in detection method is able to minimize the effect of noises by using modulation technique between signal and reference. Previously, we reported hybrid-type highly sensitive lock-in detection system. Most of commercial photoelectron sensor systems employ band pass filters for signal detection. However, this method has a point of issue on minimum detection range. In this work, we design and fabricate a CMOS dual lock-in amplifier for antibody-antigens (IgG) detection using optoelectronics. The lock-in architecture is designed for 1.8 V supply voltage and input signal frequency of 5 kHz. The proposed lock-in amplifier is compensated phase error by using dual channel detection method. The simulation results show that the power consumption is 5.4 mW, the output noise is 304 nV/Hz1/2 at the input frequency, and the gain is 80 dB. More detailed experimental results on optoelectronic sensors and discussions will be presented.

7572-20, Poster Session

A fast imaging system and algorithm for monitoring microlymphatics

T. J. Akl, E. Rahbar, Texas A&M Univ. (United States); D. Zawieja, A. Gashev, Texas A&M Univ. Health Science Ctr. (United States); J. Moore, Jr., G. Cote, Texas A&M Univ. (United States)

The lymphatic system is not well understood and tools to quantify aspects of its behavior are needed. A technique to monitor lymph velocity that can lead to flow, the main determinant of transport, in a near real time manner can be extremely valuable. We recently built a new system that measures lymph velocity, vessel diameter and contractions using optical microscopy digital imaging with a high speed camera (500fps) and a complex processing algorithm. The processing time for a typical data period was significantly reduced to less than 3 minutes in comparison to our previous system in which readings were available 30 minutes after the vessels were imaged. The processing was based on a correlation algorithm in the frequency domain, which, along with new triggering methods, reduced the processing and acquisition time significantly. In addition, the use of a new data filtering technique allowed us to acquire results from recordings that were irresolvable by the previous algorithm due to their high noise level. The algorithm was tested by measuring velocities and diameter changes in rat mesenteric micro-lymphatics. We recorded velocities of 0.25mm/s on average in vessels of diameter ranging from 54um to 140um with phasic contraction strengths of about 6 to 40%. In the future, this system will be used to monitor acute effects that are too fast for previous systems and will also increase the statistical power when dealing with chronic changes. Furthermore, we plan on expanding its functionality to measure the propagation of the contractile activity.

7572-21, Poster Session

Oblique-incidence spatially resolved diffuse reflectance spectroscopic diagnosis of skin cancer

A. Garcia-Uribe, Washington Univ. in St. Louis (United States); J. Zou, Texas A&M Univ. (United States); M. Duvic, V. Prieto, The Univ. of Texas M. D. Anderson Cancer Ctr. (United States); L. V. Wang, Washington Univ. in St. Louis (United States)

This paper presents the use of spatially resolved oblique-incidence diffuse reflectance spectroscopy for skin cancer diagnosis. Spatiospectral data from 400 pigmented and 269 non-pigmented skin lesions were collected in the clinic in the wavelength range from 455 to 765 nm. The skin lesions were initially divided into pigmented and non-pigmented groups based on their melanocytic conditions. A set of classifiers separates the pigmented malignant melanomas from the benign and dysplastic subgroups. A total of 145 lesions were used as the training set and 255 lesions were used as the testing set. This classifier for the training data set performs with an overall 91% sensitivity and 89% specificity. The second classifier separates the benign common nevi from the dysplastic subgroups. A total of 130 lesions were used as the training set and 240 lesions were used as the testing set. The overall classification rates are 80% for common nevi and 85% for the dysplastic group. A third classifier distinguishes the severe dysplastic subgroup from mild and moderate dysplastic nevi with overall classification rates of 86% for common nevi and 82% for the dysplastic group. A second set of classifiers were developed for the non-pigmented group to separate basal cell and squamous cell carcinomas from actinic and seborrheic keratosis. A total of 130 lesions were used to train the classifiers and 139 lesions were used for testing. The designed classifier generated 88% sensitivity and 85% specificity.

7572-22, Poster Session

Comparison of different kinds of skin using Raman spectroscopy

A. Villanueva-Luna, J. Castro-Ramos, S. Vazquez-Montiel, Instituto Nacional de Astrofísica, Óptica y Electrónica (Mexico)

In this work we developed a novel technique to remove the fluorescence background in the Raman spectrum. This technique permit us to obtain better accuracy in the spectrum peaks, it is based in the wavelets theory, using symlets and biothogonals wavelets. Therefore it is adapting with the Raman Spectrum. We use a spectral range between 300-1800(cm-1), 785 nm laser excitation source and Oceans optics spectrometer. The experimental samples were people with different kinds of skin, like brown, black and white. We use 5 brown persons, 6 dark brown persons and 4 white persons. We compare differences between Raman spectra. It is permit us to identified persons due to accuracy of Raman spectroscopy. This results shows that Raman spectroscopy has greatly precision in this field of biomedical optics.

7572-24, Poster Session

The velocity profile measurement of the blood flow in the micro-channel using the confocal laser scanning microscope based on particle image velocimetry

W. H. Kim, H. Lee, H. C. Choi, C. W. Park, S. H. Lim, Kyungpook National Univ. (Korea, Republic of)

The blood flow in the circulation is considered as one of the main factors to determine the risk of the circulatory diseases. The in vivo and in vitro measurement of the blood velocity, blood volume and the profile is

Return to Contents TEL: +1 360 676 3290 · +1 888 504 8171 · customerservice@spie.org

Conference 7572: Optical Diagnostics and Sensing X: Toward Point-of-Care Diagnostics



helpful for the better and earlier diagnosis of the circulatory diseases. In order to measure the characteristics of the blood flow in the capillary or the capillary size channel, it is required to detect the micro-scale motion of the blood cells. The Particle Imaging Velocimetery (PIV) has been used to study the flow in the micro-channel by tracking the trajectory of the exogenous micro/nano scale particles in the flow.

In this study, we used the video rate of confocal laser scanning microscopy (CLSM) to observe the motion of the red blood cells (RBC) in the micro channel. By tracking the trajectory of the blood cell in the blood stream, we were able to acquire the velocity profile in the microchannel without using the exogenous particles that are essential in the conventional PIV.

The blood sample was harvested from the rat and diluted to the hematocrit value of 50%. The diluted blood sample was injected into the 80um square channel using the syringe based pump. The motion of the red blood cell in the channel was recorded using the CLSM with the frame rates of 30 frames per second. (Fig. 1) The PIV was performed using the red blood cells instead of the exogenous particles. The Gaussian like velocity profiles were acquired in the various section of the micro-channel. (Fig. 2) The developed CLSM based PIV using the blood cells is expected to be applied for the blood flow measurement in vivo animal models.

Fig. 1 The motion of the red blood cell in 80um square channel by being recorded from ${\rm CLSM}$

Fig. 2 Gaussian velocity profiles of blood stream based on PIV

7572-25, Poster Session

A minimally invasive human glucose detection instrument by surface plasmon resonance

D. Li, J. Zhang, P. Wu, K. Xu, Tianjin Univ. (China)

Diabetes is a frequently encountered disease for old folks, dynamic, continuous and accurate detection of human blood glucose concentration is the key for prevention and treatment of the diabetes. A portable minimally-invasive human glucose detection instrument was studied in this paper. This instrument is based on surface plasmon resonance (SPR) technology. Through immobilizing D-galactose/D-glucose Binding Protein (GGBP) on the SPR sensor surface, which can absorb the glucose specially, it can estimate the blood glucose concentration through detecting glucose concentration in the interstitial fluid. The instrument contains interstitial fluid extractive unit, liquid flow pipeline unit, SPR sensor unit and control processing unit.

Based on minimally-invasive human glucose detection instrument, the experiments of immobilizing GGBP and measuring glucose concentration were carried out. Quick and precise glucose detection results without the extraction of human blood which can bring infective risk were obtained. Twenty-four-hour continuous glucose detection was achieved and it can satisfy the clinical requirement on dynamic, continuous and accurate detection of human blood glucose concentration. The experimental results show that: through GGBP immobilized on the SPR sensor surface, the glucose detection resolution could reach 0.5mg/L, and it has good linearity relationship when the glucose concentration is around 0.05mg/dL to 0.5mg/dL. It shows the SPR technology with immobilized GGBP will obtain a wide application in the field of minimally-invasive glucose measurement.

7572-26, Poster Session

Adulteration detection in milk using nearinfrared spectroscopy combined with twodimensional correlation analysis

B. He, R. Liu, R. Yang, K. Xu, Tianjin Univ. (China)

Adulteration of milk and dairy products has brought serious threats to human health as well as enormous economic losses to the food

industry. Considering the diversity of adulterants possibly mixed in milk, such as melamine, urea, vegetable oil, sugar/salt and so forth, a rapid, widely available, high-throughput, cost-effective method is needed for detecting each of the components in milk at once. In this paper, a method using Fourier Transform Infrared spectroscopy (FTIR) based on two-dimensional (2D) correlation spectroscopy is established for the discriminative analysis of adulteration in milk. Firstly, the characteristic peaks of fresh milk are found in the 1000-2500 nm region by its synchronous and asynchronous 2D correlation spectra which have higher spectral resolution and can provide information about concentrationdependent intensity changes not readily accessible from one-dimensional spectra. Secondly, the possible adulterants are respectively detected with the same method to establish a spectral database for subsequent comparison. Then, the suspected milk sample is detected and the characteristic peaks of its synchronous 2D correlation spectrum are compared with those of fresh milk. The differences between the two kinds of synchronous spectra imply that the suspected milk sample must contain some kinds of adulterants and the source of correlative peaks can be provided after further investigation of the asynchronous spectra of fresh milk. Prediction results for the best classification models achieved an overall correct classification rate of 95.9, 94.2, 97.3 and 91.6% for melamine, urea, vegetable oil and sugar adulterants, respectively. This nondestructive method can be used for a correct discrimination on whether the milk and dairy products are adulterated with deleterious substances and provides a new simple and cost-effective alternative to test the components of milk.

7572-01, Session 1

Development of a real-time closed-loop dualwavelength optical polarimeter for glucose monitoring

B. H. Malik, G. L. Coté, Texas A&M Univ. (United States)

Over the last decade, noninvasive glucose sensors based on optical polarimetry have been proposed to probe the anterior chamber of the eye. Such sensors would ultimately be used to measure the aqueous humor glucose concentration which is correlated with blood glucose concentration. Although the effect of other chiral components in the eye has been minimized, the time-variant corneal birefringence due to motion artifact is still a limiting factor preventing the realization of such a device. Here we present the development of a real-time dual wavelength optical polarimetric system employing a classical three-term feedback controller. Our dual wavelength system utilizes real-time closed-loop feedback based on proportional-integral-derivative (PID) control, which effectively reduced the time taken by the system to stabilize to less than 300 ms while minimizing the effect of motion artifact, which appears as common noise source for both wavelengths. Measurements in the presence of time-variant test cell birefringence demonstrate the sensitivity of the current system to measure glucose within the range of 0-600 mg/dL with a standard error of less than 13 mg/dL using the dual wavelength information. We also present a geometric ray-tracing scheme of light coupling through the eye, modeled using optical design software. Performance of this system along with the ray tracing model for a multiple wavelength polarimeter will be analyzed and possible approaches to maximize the efficiency of the system including the coupling shall be discussed.

7572-02, Session 1

Multivariate image processing technique for noninvasive glucose sensing

A. J. Webb, B. D. Cameron, The Univ. of Toledo (United States)

A potential noninvasive glucose sensing technique was investigated for application towards in vivo glucose monitoring in individuals afflicted with diabetes mellitus. Three dimensional ray tracing simulations using an advanced human eye model are reported for physiological glucose concentrations ranging between 100 to 700 mg/dL. The anterior chamber

Conference 7572: Optical Diagnostics and Sensing X: Toward Point-of-Care Diagnostics



of the human eye contains a clear fluid known as the aqueous humor. This fluid's optical refractive index varies on the order of 1.5x10-4 for a change in glucose concentration of 100 mg/dL. A pseudo iris pattern was imaged at varying refractive indices that correspond to a specific aqueous humor glucose concentration. The simulation data was analyzed by means of a developed multivariate chemometrics procedure that utilizes the images to form a calibration model. Results from these simulations show considerable potential for use of the developed method in the prediction of glucose. For further demonstration, an in vitro eye model was then created in order to validate the computer based modeling technique. In these experiments, the eye model had a pseudohuman iris which was placed in an analog eye model in which the glucose concentration within the fluid representing the aqueous humor was varied. A of series high resolution digital images were acquired using a near infrared optical imaging system. The images were then used to form an in vitro calibration model utilizing the multivariate chemometric technique. In general, the developed method exhibits considerable applicability towards its use as an in vivo platform for the noninvasive monitoring of physiological glucose concentration.

7572-03, Session 1

New scheme for polarimetric glucose sensing without polarization optics

A. M. Winkler, The Univ. of Arizona (United States); G. T. Bonnema, D4D Technologies, LLC (United States); J. K. Barton, The Univ. of Arizona (United States)

Polarimetric glucose sensing is a promising method for noninvasive estimation of tissue glucose concentration. Published methods of polarimetric glucose sensing generally rely on measuring the rotation of light as it traverses the aqueous humor of the eye. This method requires precise control of the light source polarization and polarization analyzing elements to achieve the necessary sensitivity. Additionally, the measurement is complicated by a number of confounders, most notably linear retardance of the cornea. In this article, an interferometer is described that can detect polarization changes due to glucose without the use of polarization control or polarization analyzing elements. Also, the interferometer responds differently to linear retardance, such as that induced by the cornea, and circular retardance, which is induced by the presence of glucose. Therefore, this instrument may be less sensitive to confounding effects from the cornea. A simple prototype has been built and has measured a circular retardance of 8 nm at 1300 nm wavelength, equivalent to a change in refractive index difference in the eye of 8.0e-7. A new design is proposed to achieve the necessary sensitivity for in vivo applications (Dn ~ 1e-10).

7572-04, Session 1

Dynamic testing and in-vivo evaluation of dermally implantable luminescent microparticle glucose sensors

R. Long, B. Collier, M. J. McShane, Texas A&M Univ. (United States)

We have been developing dermally-implantable microparticle glucose sensors to monitor interstitial glucose levels. For these sensors to be deployed in vivo, a matched opto-electronic system to interrogate implanted sensors has been designed and constructed. We have developed several hardware designs intended to excite and collect ratiometric luminescence intensity as well as lifetime data. Furthermore, an approach based on combining oxygen and glucose probes to compensate for local oxygen variability was developed. The aim of this study is to test the capability of the sensor system including in vivo sensor performance, hardware efficiency and finally the hardware will be optimized based on test results. Skin phantoms were developed to test the operational characteristics of microsensors, optical hardware, and software, and experimental data were compared with theoretical

simulations made using 3D statistical ray-tracing software. This paper will report the results of dynamic in vitro tests of sensor performance and the results of preliminary experiments of implants in animal models.

7572-05, Session 1

Accurate glucose detection in a small etalon

J. Martini, S. Kuebler, M. I. Recht, F. E. Torres, J. Roe, P. Kiesel, R. H. Bruce, Palo Alto Research Center, Inc. (United States)

We are developing a continuous glucose monitor for subcutaneous long-term implantation. This detector contains a double chamber Fabry-Perot-etalon that measures the differential refractive index (RI) between a reference and a measurement chamber at 850nm. The etalon chambers have wavelength dependent transmission maxima which are linearly dependent on the RI of their contents. An RI difference of $\Delta n=1.5\,$ 10-6 changes the spectral position of a transmission maximum by 1pm in our measurement. By sweeping the wavelength of a single-mode vertical-cavity-surface-emitting-laser linearly in time and detecting the maximum transmission times of the etalon, we measure the RI with an accuracy of $n=\pm3.5\,$ 10-6 over a Δn - range of 0 to 1.75 10-4 and with an accuracy of 2% over a Δn -range of 1.75 10-4 to 9.8 10-4. The accuracy is primarily limited by the reference measurement.

The RI difference between the etalon chambers is made specific to glucose by the competitive, reversible release of Concanavalin A (ConA) from an immobilized dextran matrix. The matrix and ConA bound to it, is positioned outside the optical detection path. ConA is released from the matrix by reacting with glucose and diffuses into the optical path to change the RI in the etalon. Factors such as temperature affect the RI in measurement and detection chamber equally but do not affect the differential measurement. A typical standard deviation in RI is ±1.4 10-6 over the range 32°C to 42°C. The detector enables an accurate glucose specific concentration measurement. We will present our current results including response times of the measurement, sensitivity and specificity.

7572-06, Session 1

Challenge for spectroscopic tomography of biomembrane using imaging type twodimensional Fourier spectroscopy

I. Ishimaru, Kagawa Univ. (Japan)

We propose an image-producing Fourier spectroscopic technology that enables two-dimensional spectroscopic images to be obtained within the focusing plane alone. This technology incorporates auto-correlational phase-shift interferometry that uses only object light generated by the bright points that optically make up the object.

We are currently involved in studies of non-invasive technologies used to measure blood components such as glucose and lipids, which are measured for use in daily living. Previous studies have investigated non-invasive technologies that measure blood glucose levels by utilizing near-infrared light that permeates the skin well. It has been confirmed that subtle changes in the concentration of a glucose solution, a sample used to measure the glucose level, can be measured by analyzing the spectroscopic characteristics of near-infrared light; however, when applied to a biomembrane, technology such as this is incapable of precisely measuring the glucose level because light diffusion within the skin disturbs the measurement. Our proposed technology enables two-dimensional spectroscopy to a limited depth below the skin covered by the measurement. Specifically, our technology concentrates only on the vascular territory near the skin surface, which is only minimally affected by light diffusion, as discussed previously; the spectroscopic characteristics of this territory are obtained and the glucose level can be measured with good sensitivity.

In this paper we propose an image-producing Fourier spectroscopy method that is used as the measuring technology in producing a three-dimensional spectroscopic image.

Conference 7572: Optical Diagnostics and Sensing X: Toward Point-of-Care Diagnostics



7572-07, Session 2

Wireless near-infrared spectroscopy of skeletal muscle oxygenation and hemodynamics during exercise and ischemia

B. Shadgan, D. Reid, Univ. of British Columbia (Canada); M. Taghavi, IRI National Olympic & Paralympic Academy (Iran, Islamic Republic of); A. J. Macnab, Univ. of British Columbia (Canada)

Monitoring of local muscle oxygenation and perfusion during and after exercise is of great importance in the investigation of muscle performance. Using a wireless continuous wave near-infrared spectroscope (NIRS) instrument with spatially resolved configuration we studied skeletal muscle oxygenation and hemodynamics during isometric contraction and ischemia induction. In ten healthy subjects comparable patterns of change in chromophore concentration (O2Hb, HHb), total hemoglobin (tHb) and muscle tissue oxygen saturation index (TSI) were observed during 3 sets of isometric voluntary forearm muscle contraction at 10, 30 and 50% of maximum voluntary contractions (MVC), and a period of ischemia generated subsequently. A significant decrease in tHb and O2Hb accompanied by an increase in HHb occurred in each subject during isometric contraction, and the magnitude of change became larger as the percentage of MVC increased. During the period of induced forearm ischemia all subjects showed a similar pattern of increase in HHb and decrease in O2Hb. Following sustained muscle contraction above 10% MVC, tissue muscle oxygen saturation declined. The pattern and magnitude of change in chromophore concentrations and the value of muscle TSI in response to incremental isometric contraction and subsequent arterial obstruction was consistent in all subjects. Variation in the values obtained was somewhat greater during isometric contraction at 10% MVC than during ischemia. This small series indicates that data with good reproducibility can be obtained with the wireless NIRS technology. Having access to reliable telemetric NIRS technology will increase the practicality of this biomedical monitoring technique in clinical settings.

7572-08, Session 2

Optical sensor technology for a noninvasive continuous monitoring of blood components

J. Kraitl, S. Andruschenko, H. Koroll, H. Ewald, Univ. Rostock (Germany)

NIR-spectroscopy and Photoplethysmography is used for a measurement of blood components. The fact that the absorption-coefficient for blood differs at different wavelengths is used for calculation of the optical absorbability characteristics of blood yielding information on blood components like Haemoglobin, Carboxyhaemoglobin, Oxygen saturation and tissue water. The measured PPG time signals and the ratio between the peak to peak pulse amplitudes are used for a measurement of these parameters. A newly developed sensor device has been introduced. The non-invasive in-vivo multi-spectral method is based on the radiation of monochromatic light, emitted by laser diodes. The objective of this development is to reduce the dependence on measurement techniques which require that a sample of blood be withdrawn from the patient for in-vitro analysis. The absorption and scattering of whole blood in the visible and near infrared range is dominated by the red blood cells, the different Haemoglobin derivates and the blood plasma that consists mainly of water. The Photometric Sensor Device is basically a main box of electronic components, a light probe and a Laptop or PC for display and data storing. The probe is attached to the patient's body usually the finger. Orange to Near Infrared light is then shone sequentially through the body tissue via fast -switching laser diodes and special driver circuits. Results with this photometric method to measure changes in the CO-Hb, SpO2 and Haemoglobin concentration were demonstrated during measurements with a hemodynamic model and healthy subjects.

7572-09, Session 2

Measurement of blood flow rate in hemodialysis shunts using self-mixing laser diode

S. Cattini, Univ. degli Studi di Modena (Italy); M. Norgia, A. Pesatori, Politecnico di Milano (Italy); L. Rovati, Univ. degli Studi di Modena (Italy)

The measurement of blood flow in hemodialysis systems is essential to control the quality of the treatment. Moreover, in line monitoring of the flow is useful for the detection of impending access failure and the prevention of underdialysis [1]. However, the blood flow measurements recovered from the dialysis blood roller-pump angular velocity is affected by large measuring uncertainty and errors. Commercial sensors are generally based on the ultrasound sensors technique, but they are bulky and expensive thus limiting the potential economical advantages. Also optical sensors have been proposed on the market for flow measurements, but they are still bulky and expensive, or requires contact-sensing.

To measure blood flow rate in hemodialysis systems, we propose an optical Doppler flowmeter based on the self-mixing effect within a laser diode (SM-LD). Advantages in adopting such techniques derive from reduced costs, ease of implementation and limited size. Moreover, the SM-LD technique offers the advantage to have the excitation and measurement beams spatially overlapped, thus it is well suitable with the limited aperture offered by the standard cuvettes. Preliminary measurements have been performed on both optical phantom i.e. Intralipid® solution, and bovine blood. The first and second order momentum of the Doppler band obtained from the SM-LD measurements have been show to be related to the local flow velocity, thus to the blood flow in the cuvette under test.

Bibliography

[1] Depner, Thomas A.; Krivitski, Nikolai M., "Clinical Measurement of Blood Flow in Hemodialysis Access Fistulae and Grafts by Ultrasound Dilution," ASAIO Journal, 41(3),pp M745-M749, 1995.

7572-10, Session 2

Detection range analysis of pulse oximetry based on phase sensitive detection method

K. Kim, H. Son, I. Jung, Y. Choi, Chung-Ang Univ. (Korea, Republic of)

The pulse oximetry, which is a noninvasive method for monitoring the oxygen saturation of blood, has been used to check the health condition of human beings regardless of time and place. The principle of pulse oximetry is based on the detection of absorption difference between oxygenated hemoglobin and deoxygenated hemoglobin at 660 nm and 940 nm wavelength, respectively. However, the sensitivity of the system is limited by background noises which are generated by photodetector, environment, and so on. In current technology of the pulse oximetry, minimum detectable level would be a critical factor. The sensitivity of commercial pulse oximetry system is poor because the band pass filter applied for signal detection can not satisfactorily block the in-band noise. Therefore, most of the pulse oximetry controls the input current of LED for enhancement of detection range, though it induces high current consumption. In this work, for low power consumption and wide detection range, we applied a phase sensitive detection method to the pulse oximetry. The phase sensitive detection method is special technique for weak signal near background noises. In the proposed pulse oximetry, lightwaves of 660 nm and 940 nm are modulated by frequencies of f1 and f2, respectively, and the modulated signals are transmitted to finger's blood in which oxygenated hemoglobin and deoxygenated hemoglobin are. Wide detection range with low power consumption can be achieved in our novel system of oximetry by carrying out the phase sensitive detections. It is believed that our novel method enables oximetry system to be in point-of-care applications.

Conference 7572: Optical Diagnostics and Sensing X: Toward Point-of-Care Diagnostics



7572-11, Session 3

Low-cost fluorescence microscopy for pointof-care cell imaging

M. J. Lochhead, J. Ives, M. Givens, M. Delaney, K. Moll, C. Myatt, Precision Photonics Corp. (United States)

Fluorescence microscopy has long been a standard tool in laboratory medicine. Implementation of fluorescence microscopy for near-patient diagnostics, however, has been limited due to cost and complexity associated with traditional fluorescence microscopy techniques. There is a particular need for robust, low-cost imaging in high disease burden areas in the developing world, where access to central laboratory facilities and trained staff is limited. Here we describe a point-of-care assay system that combines a disposable plastic cartridge with an extremely low cost fluorescence imaging instrument. Based on a novel, multi-mode planar waveguide configuration, the system capitalizes on advances in volume-manufactured consumer electronic components to deliver an imaging system with minimal moving parts and low power requirements. A two-color cell imager will be presented, with magnification optimized for enumeration of immunostained human T cells. To demonstrate the system, peripheral blood mononuclear cells were stained with anti-CD4-Alexa647 and anti-CD45-Alexa790 antibodies. Registered images were used to generate fractional CD4/ CD45 staining results that show excellent correlation with flow cytometry. The cell imager is under development as a very low cost CD4+ T cell counter for HIV disease management in limited resource settings.

7572-12, Session 3

Tumor specific lung cancer diagnostics with multiplexed FRET immunoassays

D. Geißler, D. Hill, H. Löhmannsröben, Univ. Potsdam (Germany); E. Thomas, A. Lavigne, B. Darbouret, E. Bois, Cezanne (France); L. Charbonnière, R. Ziessel, CNRS, Univ. Louis Pasteur (France); N. Butlin, Lumiphore Inc. (United States); N. Hildebrandt, Fraunhofer-Institut für Angewandte Polymerforschung (Germany)

Survival rates of lung cancer are closely related to the histological types, namely small and non-small cell lung cancer (SCLC and NSCLC). NSCLC requires surgery whereas SCLC needs chemo or radiotherapy treatment. Unfortunately lung cancer patients often do not show early stage symptoms, so that diagnosis is late in most cases. An effective early stage screening is not available and lung biopsy is required to diagnose suspected lung cancer. In this contribution we present an optical multiplexed immunoassay for early stage diagnosis of SCLC and NSCLC specific tumor markers (TM - CEA, SCC, CYFRA21-1 and NSE). The assay principle is based on Förster resonance energy transfer (FRET) from a Terbium-complex (TC) to a fluorescent dye. Both compounds are labeled to two different antibodies (AB) within an "AB1-TM-AB2" immunocomplex. The time-gated intensity ratio of TC and dye luminescence is directly proportional to the TM concentration. We achieved parallel detection of CEA, SCC, CYFRA and NSE within a single homogeneous assay. Moreover, FRET is demonstrated from TC to eight different commercially available dyes measured on a commercial immuno-analyzer (KRYPTOR®) with detection limits in the ng/ml range. Multiplexed detection of five wavelength-separated emissions within the different acceptor combinations suggests the feasibility of including another TM (e.g. ProGRP) if even better diagnostic accuracy or selectivity are required. Due to multiplexed optical detection within one single homogeneous (liquid phase) assay the method is perfectly suited for fast and low-cost miniaturized point-of-care testing as well as for highthroughput screening in a broad range of in-vitro diagnostic applications.

7572-13, Session 3

Guided-mode resonance biochip system for early detection of ovarian cancer

D. D. Wawro, Resonant Sensors (United States); P. Koulen, Univ. of Missouri, Kansas City (United States); Y. Ding, R. Magnusson, Resonant Sensors (United States)

A high-accuracy, sensor system has been developed that provides near-instantaneous detection of biomarker proteins as indicators of ovarian serous papillary carcinoma. Based upon photonic guidedmode resonance technology, these high-resolution sensors employ multiple resonance peaks to rapidly test for relevant proteins in complex biological samples. This label-free sensor approach requires minimal sample processing and has the capability to measure multiple agents simultaneously and in real time. In this work, a sensor system that uses a fixed-wavelength source with a shaped input wavefront to auto-scan in angle has been developed. As binding events occur at the sensor surface, resonance reflection peak shifts are tracked as a function of incident angle on an integrated CMOS detector. The amount of angular shift is linearly correlated to the quantity of biomarker protein in a biological sample. Multiple resonance peaks provide increased detection information about the binding dynamics occurring at the sensor surface, thus decreasing false detection readings. Simultaneous detection of multiple biomarker proteins in parallel with sensitivities in the pM range contributes to the potential for differential real-time data analysis. A biochip system prototype has been developed and the system performance characterized. Identification and quantification of protein biomarkers that are up- or down- regulated in blood and serum as indicators of ovarian cancer will be presented.

7572-14, Session 3

Multi-wavelength spectroscopy of oriented erythrocytes

Y. Serebrennikova, Univ. of South Florida, College of Public Health (United States); L. Garcia-Rubio, D. Huffman, J. Smith, Claro Scientific (United States)

Accurate characterization of the optical properties of erythrocytes is essential for the applications in optical biomedicine, in particular, for diagnosis of blood related diseases. These optical properties strongly depend on the erythrocyte's size, hemoglobin composition and orientation relative to the incident light. We explored the effect of orientation on the absorption and scattering properties of erythrocytes suspended in saline using UV-visible spectroscopy and theoretical predictive modeling based on anomalous diffraction approximation. We demonstrate that the orientation of erythrocytes in dilute saline suspensions is not random and produces consistent spectral pattern. Numerical analysis showed that the multi-wavelength absorption and scattering properties of erythrocytes in dilute suspensions can be accurately described with two orientation populations. These orientation populations with respect to the incident light are face-on incidence and edge-on incidence. The variances of the orientation angles for each population are less than 15 degrees and the relative proportions of the two populations strongly depend on the number density of the erythrocytes in suspensions. Further, the identified orientation populations exhibit different sensitivities to the changes in the compositional and morphological properties of erythrocytes. The anomalous diffraction model based on these orientation populations predicts the absorption and scattering properties of erythrocytes with accuracy greater than 99%. Establishment of the optical properties of normal erythrocytes allows for detection of the disease induced changes in the erythrocyte spectral signatures.



Saturday-Monday 23-25 January 2010 • Part of Proceedings of SPIE Vol. 7573 Biomedical Applications of Light Scattering IV

7573-01, Session 1

Simulating the optical phase conjugation phenomenon of light multiply scattered through a macroscopic random medium

S. H. Tseng, National Taiwan Univ. (Taiwan)

The light scattering effects of turbid media causing opacity may be undone via Optical Phase Conjugation (OPC). Here we rigorously simulate light scattering through a macroscopic random using the pseudospectral time-domain (PSTD) technique. The OPC phenomenon of multiply scattered light can be quantitatively analyzed which is not feasible otherwise. Specifically, factors affecting the electromagnetic energy propagation and refocusing phenomenon is analyzed. The reported simulation study allows accurate characterization of the optical properties of the OPC phenomenon for practical biomedical applications.

7573-02, Session 1

Origin of partial wave spectroscopic signals in a weak refractive index medium

H. Subramanian, D. Damania, P. Pradhan, L. Cherkezyan, I. R. Capoglu, A. Taflove, V. Backman, Northwestern Univ. (United States)

Recent thrust to understand biological processes at the nanoscale has been stymied by the lack of practical means of analysis of cell architecture at the nanoscale level. We recently developed an optical technique, partial-wave spectroscopic (PWS) microscopy that allows the quantification of the statistical properties of cell nanostructure. We had earlier demonstrated the nanoscale sensitivity of PWS in experiments with nanostructure models which showed that PWS microscopy is sensitive to structures that are less than ~ 40nm. This was further reaffirmed by our studies on HT29 cancer cell lines that demonstrated the capability of PWS to differentiate cells of different genetic knockdowns that are otherwise similar under a conventional microscope. In this paper, we study the origin of these PWS signals in a medium with weak refractive index fluctuations. We first elucidate the role of numerical aperture (NA) in determining the origin of PWS signals by varying the input and the output NA of the objective lens used in the PWS experiment. We also calculate the optimal input and output NA necessary to maximise the sensitivity of nanoscale refractive index fluctuations by performing experiments with nanostructure model. Using this optimal NA of the objective, we show that PWS can be used to study the effects of molecular crowding in biological cells that are treated with external crowding agents such as sucrose solution.

7573-03, Session 1

The limits of multimode fibers and dispersion in the frequency domain

A. L. Dayton, N. Chourdhury, S. A. Prahl, Oregon Health & Science Univ. (United States)

In practice, complete removal of lesions during a lumpectomy is difficult. Positive margins following lumpectomy range from 10% to 50% and are likely to locally recur. To provide for uniformly wide negative margins and acceptable cosmesis, a spherical specimen centered around the lesion is desired. We have demonstrated the use of an optical wire to remove breast lesions in eight patients. The surgeon used an optical wire, which was an optical fiber attached to the standard metal wire used to localize

breast lesions. The optical wire emitted light from the center of the lesion and successfully guided the surgeries. However, a more quantitative way to orient the surgeon to the lesion was needed. To accomplish this, the proposed optical wire emits sinusoidally modulated visible light through a 195µm multimode fiber into a scattering medium. An optical probe collects the light and the phase lag is measured with a network analyzer. The distance from the emitting fiber tip to the probe is calculated based on the phase lag. One significant source of error arrises from the dispersion of light through the fiber and the medium. Furthermore, both scattering and absorption can be quite low in breast tissue, which increases this type of error. The accuracy of this technique was modeled using multimode fibers with Monte Carlo. In addition, the phase lag was measured for source detector separation distances up to 40 mm in an array of polyurethane phantoms. The phantoms had absorption coefficients of 0.05-0.1 [1/mm] and reduced scattering coefficients of 0.5-2 [1/mm].

7573-04, Session 1

A new approach to SVM model selection for pre-cancerous and cancerous tissue diagnosis using elastic scattering spectroscopy

Y. Jiao, Univ. College London (United Kingdom); W. K. Jerjes, Univ. College Hospital (United Kingdom); M. R. Austwick, Univ. College London (United Kingdom); C. Hopper, Univ. College London Hospitals NHS Foundation Trust (United Kingdom); L. B. Lovat, S. G. Bown, J. Shawe-Taylor, D. R. Hardoon, Univ. College London (United Kingdom)

The aim of this study is to improve on the current diagnostic accuracy by adopting a new approach to support vector machine (SVM) model selection. In this study, rather than selecting, during training, a single model to be used, we demonstrate that it is possible to choose different models for different test subjects. The performance of SVM is heavily dependent on the choices of kernel parameters and penalty coefficient C. Currently the most popular techniques for tuning these parameters are using cross-validation, which is time consuming and data dependent. The method we propose generates a series of candidate models, and selects the model with the highest confidence estimate (smallest nonconformity measure) which measures how different a test sample is from calibration data given a label.

This will give us not only the class the test samples belong to, but also the rate of confidence for the prediction.

We apply the above methods to three independent dataset (High Grade Dysplasia in Barrett's Oesophagus (BE), metastastic breast cancer in lymph nodes, and malignancy in skin lesions), the method predicts with an sensitivity of 70% with specificity of 78%, competitive with conventional SVM and LDA.

7573-05, Session 2

Quantitative blood flow imaging using multiexposure laser speckle contrast imaging

A. K. Dunn, The Univ. of Texas at Austin (United States)

Laser speckle contrast imaging has become a widely used method for imaging blood flow due to its high spatial and temporal resolution and its relatively simple instrumentation. However, most speckle contrast imaging applications are limited to measures of relative blood flow changes due to a combination of instrumentation artifacts



and incomplete understanding of the underlying physics. This talk will describe how multi-exposure laser speckle contrast imaging can overcome many of the existing limitations of traditional single exposure speckle approaches.

7573-06, Session 2

Real-time laser speckle imaging

O. Yang, Beckman Laser Institute and Medical Ctr., Univ. of California, Irvine (United States); B. Choi, Beckman Laser Institute, Univ. of California, Irvine (United States); D. J. Cuccia, Modulated Imaging, Inc. (United States)

Laser speckle imaging is a technique in which coherent light incident on a surface produces a reflected speckle pattern. The spatio-temporal statistics of this pattern is related to the underlying movement of optical scatterers , such as blood, and image processing algorithms can be applied to produce speckle flow index (SFI) maps, which are representative of blood flow. This information, if obtained in real time, has significant clinical application, especially in image-guided surgery or as a first response tool for tissue viability.

Currently, we employ a CPU-based algorithm integrated into LabVIEW that can process frames at approximately 1.5 frames per second (fps). This algorithm requires intense CPU calculations and is slow. Therefore, there is a critical need for a real-time image processor that can keep up with the camera frame rate.

We present a novel algorithm that employs the NVIDIA's Compute Unified Device Architecture (CUDA) platform to perform processing on the graphics processing unit (GPU), which allows parallel processing on the multiplexed GPU thread processors. Software written in C was integrated with CUDA extensions to perform speckle contrast analysis on the GPU and then compiled into a Dynamic Link Library (DLL) to be called from LabVIEW. To validate the software, a LabVIEW VI was interfaced with a QImaging Retiga EXi monochrome CCD camera [1392x1040] acquiring raw speckle images at 10 fps. With the fully functional LabVIEW VI, the processing and display of SFI images are capable of up to 15 fps at full resolution, demonstrating our ability to perform real-time laser speckle imaging.

7573-07, Session 2

Probing light fluctuations with wide-field interferometry: application to blood flow imaging in vivo

M. Atlan, Ecole Supérieure de Physique et de Chimie Industrielles (France); M. Gross, Ecole Normale Supérieure (France); I. Ferezou, Ecole Supérieure de Physique et de Chimie Industrielles (France)

The development of parallel optical Doppler blood flow imaging tools faces a major technological challenge. A detection sensitivity high enough to assess optical spectrum dispersion from momentum transfer between scattered light and biological tissues in the low radiofrequencies range is critical. We demonstrate here the performance of an original wide-field interferometric method enabling optical Doppler imaging with cameras. We report images of mice cerebral cortex illuminated with near infrared laser light in reflection, bringing local motion contrasts from blood flow down to the smallest capillaries. In our approach, a camera is turned into a parallel detector for laser Doppler imaging in heterodyne configuration. Wide-field imaging of the Doppler spectrum of near infrared laser light is achieved by mixing the backscattered beam with a separate local oscillator beam. High sensitivity scattered light fluctuations probing with a charge-coupled device (CCD) or complementary metaloxide semiconductor (CMOS) camera is enabled by a highly efficient noise rejection scheme involving a double modulation of the signal. In our experiments, the cerebral cortex is illuminated over the whole region to be imaged. The local oscillator beam is frequency-shifted with respect

to the illumination field to enable tunable detection of radiofrequencyselective optical fluctuations images. Our approach enables imaging of the optical Doppler spectrum in vivo in low-light conditions. It is potentially suited to the design of wide-field microrheology imaging tools.

7573-08, Session 2

Application of a novel wide-field functional imaging (WiFI) instrument to a mammary window chamber preclinical model of breast cancer

A. J. Moy, J. G. Kim, Beckman Laser Institute and Medical Ctr., Univ. of California, Irvine (United States); E. Y. H. P. Lee, Univ. of California, Irvine (United States); B. Choi, Beckman Laser Institute, Univ. of California, Irvine (United States)

Current imaging modalities allow precise visualization of tumors but do not enable quantitative characterization of the tumor metabolic state. Such quantitative information would enhance our understanding of tumor progression, response to treatment, and to our overall understanding of tumor biology. To address this problem, we have developed a wide-field functional imaging (WiFI) instrument which combines two optical imaging modalities, spatially modulated imaging (MI) and laser speckle imaging (LSI).

Using MI, optical property maps of the tissue are estimated by applying a Monte Carlo model to the measured spatially-resolved reflectance of projected sinusoidal patterns onto the tissue. Tissue composition is then extracted from the optical property maps in the form of oxy-, deoxy-, and total hemoglobin concentrations, and percentage of lipid and water. Using LSI, the reflectance of a 785 nm laser speckle pattern on the tissue is acquired and analyzed to compute maps of blood perfusion in the tissue. Tissue metabolism state is estimated from the values of blood perfusion, volume and oxygenation state.

We are currently employing the WiFI instrument to study tumor development and response to chemotherapy in a mammary window chamber mouse breast tumor model. In this model, a tumor is implanted into the mammary tissue and covered with an acrylic window. This technique allows for direct visualization of the tumor and eliminates back-scattering of laser light from the skin, allowing detailed blood perfusion maps to be generated while maintaining the fidelity of the tissue composition information. At present, preliminary WiFI studies using the mammary window chamber model have been initiated and we report on the progress of these studies.

7573-09, Session 2

Fluctuation spectroscopy in low-coherence dynamic light scattering of tissue responding to pharmacologicals

D. D. Nolte, Purdue Univ. (United States); K. Jeong, Korea Military Academy (Korea, Republic of); J. J. Turek, Purdue Univ. (United States)

Motility contrast imaging uses subcellular motion as a fully-endogenous contrast agent for functional imaging. We perform fluctuation spectroscopy of the dynamic speckle in low-coherence digital holography arising from membrane fluctuations and organelle motion in multicellular tumor spheroids. The differential spectral time-response to environmental pertubations and pharmcologicals separates into frequency bands between 0.01 Hz to 1 Hz and show specific responses to temperature and osmolarity, to metabolic drugs that affect ATP synthesis, or to cytoskeletal anti-cancer drugs such as taxol or cytochalasin.

Depth-gated dynamic light scattering is performed using low-coherence Fourier-domain digital holography. Backscattering from full-field illumination shows rich dynamic speckle structure selected from a target

Return to Contents TEL: +1 360 676 3290 · +1 888 504 8171 · customerservice@spie.org



depth inside tissue. The power spectrum of the fluctuations is nearly 1/f between 0.01 Hz to 1 Hz. However, with the application of physiological or pharmcological perturbations, three distinct frequency bands appear that respond differently to different types of perturbations. The lowest frequency band responds directly to the actin drug cytochalasin corresponding to membrane fluctuations, while the highest frequency band responds directly to the metabolic drug iodoacetate (that inhibits anaerobic glycolysis) corresponding to mitochondrial motions. By applying physiological perturbations (temperature and osmolarity) and pharmacological perturbations (metabolic and anti-mitotic drugs) we separate out distinct fingerprints of the different drug actions on different frequency bands. This has potential importance for fully-endogenous high-throughput screening technology.

7573-10, Session 3

A statistical model of light scattering in biological continuous random media based on the Born approximation

I. R. Capoglu, J. D. Rogers, A. Taflove, V. Backman, Northwestern Univ. (United States)

A comprehensive three-parameter statistical model based on the Whittle-Matern family of functions is described for the refractive index fluctuations in continuous homogeneous random media. This model encompasses different types of correlation functions including exponential, stretched exponential, Gaussian, Kolmogorov, and fractal correlations. Using the Born (or single-scattering) approximation, lightscattering parameters for these media such as the scattering coefficient, mean free path and anisotropy factor are derived and investigated. The dependences of these parameters to random medium properties such as the correlation length the refractive index fluctuations are explained, and the spectral behaviors of the same parameters are discussed in detail. The effects of polarization on the scattering properties are examined and a comparison to scalar theory is given. Next, a rigorous numerical error analysis is presented for the scattering coefficient under the Born approximation in a biologically-relevant, albeit more simplified geometry. Results of previous investigations on refractive indices of biological media are used to construct a statistical model for the random medium. This statistical model is then used as an input to the finite-differencetime-domain (FDTD) computational method, which provides numerical solutions to light scattering problems via the spatial and temporal discretization of basic electromagnetic equations. Using these exact results, the ranges for the correlation length and the refractive index fluctuation strength under which Born approximation is valid are clearly identified.

7573-11, Session 3

Extracting intrinsic optical properties using the 400/200 elastic scattering spectroscopy geometry

M. R. Austwick, J. Brunker, C. A. Mosse, Y. Jiao, L. B. Lovat, S. G. Bown, J. C. Hebden, Univ. College London (United Kingdom)

Elastic Scattering Spectroscopy (ESS) is a point-measurement, broadband optical scattering technique. In our geometry, a 400 μm optical fibre injects light from a Xenon arc lamp, and an adjacent 200 μm fibre collects the back-scattered light. Using this "400/200" geometry, we have had significant successes using statistical methods to detect cancer and pre-cancer, including metastatic breast cancer in the axillary lymph nodes, and high grade dysplasia in Barrett's Oesophagus. Other groups have succeeded in extracting tissue optical absorption (μa) and scattering (μs ') properties from similar ESS geometries and single-fibre ESS, and we apply these methods to our geometry.

We demonstrate the modifications required to extract optical properties from our 400/200 geometry using Monte Carlo simulations, and

experimentally using phantoms. For these small fibre separations it is likely that the propagation of light is sensitive to the scattering anisotropy term (g) as well as the scattering coefficient (µs). With this in mind, we constructed our phantoms using polystyrene microspheres, which have known g values in the range 0.92-0.95, similar to that of tissue. Evans Blue dye provided the non-scattering absorber, and in combination with varying concentrations of polystyrene spheres, provided values of µa and µs' to span the range encountered in most biological tissues (0.01-1 cm-1 and 5-20 cm-1 respectively). Existing Monte Carlo code [Wang et al, Comput. Methods Programs Biomed. 1995] was adapted by co-workers in Rotterdam to simulate our geometry, and the results compared and contrasted with phantom results.

Our work is supported by the CRUK project grant "Elastic Scattering Spectroscopy for diagnosis of dysplasia and aneuploidy in Barrett's oesophagus".

7573-12, Session 3

Stochastic Huygens and partial coherence propagation through thin tissues

S. Prahl, Providence St. Vincent Medical Ctr. (United States); D. G. Fischer, NASA Glenn Research Ctr. (United States); D. D. Duncan, Oregon Health & Science Univ. (United States)

Stochastic Huygens describes a method of propagating a partially coherent source by sampling the Huygens wavelets that evolve from each point of the wavefront. The amplitude and phase of each wavelet is tracked as the light passes through the optical system. We have previously described how a partially coherent wavefront may be simulated by propagating an ensemble of wavefronts with specified first and second-order statistics through simple optical systems. In this work we extend the modeling effort to include an ensemble of phase (or scattering) screens that characterize thin microscope tissue samples in the optical path.

In this paper, we demonstrate a Stochastic Huygens approach for propagating partially coherent fields through stochastic optical systems. Random sources with specific spatial coherence properties are generated using a Gaussian copula. Similar techniques are used to generate phase screens that characterize thin tissue slices. Physical optics and Stochastic Huygens predictions of the first and second-order statistics of the field are compared for coherent sources passing through tissue samples. Finally, partially coherent (Gauss-Schell) sources are propagated through an optical system with an ensemble of phase screens to study the interaction of the properties of the phase screen with the cross spectral density.

7573-13, Session 3

Investigating the spectral characteristics of backscattering from heterogeneous spheroidal nuclei using broadband finite-difference time-domain simulations

G. Chao, K. Sung, National Taiwan Univ. (Taiwan)

Backscattered light spectra have been used to extract size distribution of cell nuclei in epithelial tissues for non-invasive detection of precancerous lesions. In existing experimental studies, size estimation is achieved by assuming nuclei and other scatterers as homogeneous spheres and fitting the measured data with results of models based on Mie theory. However, the validity of simplifying nuclei as homogeneous spheres has not been fully explored. In order to address the limitation of Mie theory, we implement a three-dimensional finite-difference time-domain (FDTD) simulation tool using a Gaussian pulse as the light source to obtain backscattering spectra from models of spherical nuclei consisting of a nucleolus and randomly distributed chromatin condensation in homogeneous nucleoplasm. The results show that the oscillating patterns of backscattering spectra from spherical heterogeneous nuclei



are similar to those from homogeneous spheres. Heterogeneity in nuclei results in increased backscattering as compared to homogeneous nuclei and the difference is more pronounced in models of dysplastic nuclei due to higher relative refractive indices between chromatin/nucleolus and nucleoplasm. The degree of which the backscattering spectra of heterogeneous nuclei deviate from Mie theory is highly dependent on the distribution of chromatin/nucleolus in the simulated nuclei but not sensitive to nucleolar size, refractive index fluctuation and chromatin density. Preliminary results of simulated backscattering spectra from spheroidal nuclei show similar oscillating patterns to those from homogeneous spheres, with the diameter equal to the projective length of the major axis of a spheroidal nucleus along the propagation direction.

7573-14, Session 3

Bayesian variable selection for pre-cancerous versus cancerous tissue diagnosis using elastic scattering spectra

Y. Jiao, T. Diethe, M. R. Austwick, Univ. College London (United Kingdom); C. Hopper, Univ. College London Hospitals NHS Foundation Trust (United Kingdom); L. B. Lovat, S. G. Bown, D. Barber, Univ. College London (United Kingdom)

The aim of this study is to improve on the current diagnostic accuracy of elastic scattering spectroscopy by adopting an approach based on Bayesian linear methods, in particular Bayesian variable selection methods in logistic regression. The method attempts to automatically identify a small number of wavelengths that are most informative of the cancerous/pre-cancerous class label. This is potentially useful since rather than using a broadband spectrum, small groups of selected wavelengths bands as can be produced by LED's may be used without significant loss of diagnostic accuracy, simplifying the data collection as only a simple photodetector and not a spectrometer is required.

We apply the method to three independent dataset (High Grade Dysplasia in Barrett's Oesophagus (BE), metastatic breast cancer in lymph nodes, and malignancy in skin lesions) and compare the diagnosis accuracy with conventional SVM and LDA techniques. The technique selects around 10 critical wavelengths, without significant degradation in test performance compared to using all wavelengths. For Barrett's Oesophagus, based on a balanced test dataset of equal numbers of pre-cancerous and cancerous samples, the method predicts with an accuracy of 74% (this would give a specificity 87% and sensitivity 60%), competitive with conventional state-of-the-art techniques.

As a separate study we penalized large local changes on the linear weight factors of neighbouring wavelengths help more robustly understand the physical correlation and interpretation as to which components of the signals are important for diagnosis. This results in bands of wavelengths grouped according to their positive or negative effect on the likelihood of the sample being cancerous.

7573-15. Session 4

Tomographic imaging of Förster resonance energy transfer in highly light scattering media

V. Y. Soloviev, Univ. College London (United Kingdom); J. A. McGinty, K. B. Tahir, R. Laine, D. W. Stuckey, J. V. Hajnal, A. Sardini, P. M. W. French, Imperial College London (United Kingdom); S. R. Arridge, Univ. College London (United Kingdom)

Three-dimensional localization of protein conformation changes in turbid media using Förster Resonance Energy Transfer (FRET) was investigated by tomographic fluorescence lifetime imaging (FLIM). FRET occurs when a donor fluorophore, initially in its electronic excited state, transfers energy to an acceptor fluorophore in close proximity through non-radiative dipole-dipole coupling. An acceptor effectively behaves

as a quencher of the donor's fluorescence. The quenching process is accompanied by a reduction in the quantum yield and lifetime of the donor fluorophore. Therefore, FRET can be localized by imaging changes in the quantum yield and the fluorescence lifetime of the donor fluorophore. Extending FRET to diffuse optical tomography has potentially important applications such as in vivo studies in small animal. We show that FRET can be localized by reconstructing the quantum yield and lifetime distribution from time-resolved non-invasive boundary measurements of fluorescence and transmitted excitation radiation. Image reconstruction was obtained by an inverse scattering algorithm. Thus we report, to the best of our knowledge, the first tomographic FLIM-FRET imaging in turbid media. The approach is demonstrated by imaging a highly scattering cylindrical phantom concealing two thin wells containing cytosol preparations of HEK293 cells expressing TN-L15, a cytosolic genetically-encoded calcium FRET sensor. A 10mM calcium chloride solution was added to one of the wells to induce a protein conformation change upon binding to TN-L15, resulting in FRET and a corresponding decrease in the donor fluorescence lifetime. The resulting fluorescence lifetime distribution, the quantum efficiency, absorption and scattering coefficients were reconstructed.

7573-16, Session 4

Optical narrow-band frequency analysis of polystyrene bead mixtures

K. A. Popov, T. P. Kurzweg, Drexel Univ. (United States)

Early pre-cancerous conditions in tissue are often characterized by an increase in the nuclei size of surface epithelium cells. Thus the skin tissue can be studied as mixture of cancerous and healthy cells. Using white light spectroscopy, it is well known that a specific sized scatterer contributes to a specific oscillation pattern, as a function of the wavelength and scatterer diameter. This pattern can be used to determine the scatterer size, by counting the number of peaks in this signature. However, when examining a mixture of scatterers, the spatial oscillation pattern is not easily analyzed, making it difficult to determine the individual components of the mixture. We have found by converting this spatial oscillation pattern into the Fourier domain, many complex and noisy signature frequency peaks exist, however, characteristic peaks for individual scatterers are still hard to determine. In order to confine the frequency signatures of each scatterer, we interrogate the sample using a narrow band pass optical filter during data collection. With this approach, the frequency content in the Fourier domain is substantially reduced, isolating a single signature frequency for each scatterer in the mixture. We also experimentally show a linear relationship between the particle concentration and the resulting amplitude of the signature frequency peak in the Fourier domain. In addition, we provide theoretical amplitude dependence analysis of the frequency peaks among the scatterers both individually and when in mixtures, based on the Tyndall Effect when particles aggregate into colloidal clusters

7573-17, Session 4

Spatially modulated quantitative spectroscopy (SMoQS): determination of optical properties of turbid media spanning visible and near-infrared regimes

R. B. Saager, D. J. Cuccia, A. J. Durkin, Univ. of California, Irvine (United States)

We present a novel, non-contact method for the determination of quantitative optical properties of turbid media from 430-1050 nm. Through measuring the broadband reflectance from an unknown sample as a function of the spatial frequency of the projected illumination patterns, the absolute absorption and reduced scattering coefficients can be calculated without any a priori assumptions of the chomophores present. This technique, which is called Spatially Modulated Quantitative Spectroscopy (SMoQS), was validated through the quantification



of optical properties of homogenous liquid phantoms with known concentrations of absorbers and scatterers. The properties of the phantoms were recovered across the range of values prepared with R2 values of 0.985 and 0.996 for absorption and reduced scattering, respectively. A measurement was also performed on skin tissue as a cursory in-vivo test of the performance of the method. The resultant absorption spectrum was well described by a multi-chromophore fit, and the quantitative values for oxy- and deoxy hemoglobin, water and melanin were within published ranges for skin.

7573-18, Session 4

Scanning fiber angle-resolved lowcoherence interferometry for light-scattering measurement of cell morphology

Y. Zhu, N. G. Terry, M. G. Giacomelli, A. P. Wax, Duke Univ. (United States)

Light scattered by tissues carries morphological and spectroscopic information regarding cell structure and composition. Angle-resolved low coherence interferometry (a/LCI) collects angular light scattering to measure the morphology of biological scatterers, and achieves depth sectioning with low coherence interferometry. It has been demonstrated capable of obtaining quantitative nuclear structural information from epithelial and sub-epithelial sites in studies of cells, animals and human tissues, and has been successfully applied to diagnose intraepithelial neoplasia.

We present a novel fiber-optic probe for Fourier-domain angle-resolved low coherence interferometry for the determination of depth-resolved scatterer size. The probe employs a scanning singlemode fiber to collect the angular scattering distribution of the sample, which is analyzed using Mie theory or T-matrix to obtain the average size of the scatterers. Depth-sectioning is achieved with low coherence Mach-Zehnder interferometry. A delivery fiber illuminates the specimen and a scanning collection fiber samples the backscattering to obtain either one- or two- dimensional angular distribution. We characterize the probe's optical performance and demonstrate its depth-resolved sizing capability with high sensitivity and subwavelength accuracy using phantoms composed of microspheres or spheroids. In addition, its application for biological samples is demonstrated in studies of cells and ex vivo animal tissues.

7573-19, Session 5

A fiber-coupled microfluidic cytometer for the obtaining of nanostructural mitochondria information in single cells

X. Su, W. Rozmus, Y. Y. Tsui, Univ. of Alberta (Canada)

The ability to characterize single live cells is of particular interest to researchers in biophotonics, cell biology and medicine. Light scattering has been used as a label-free, non-invasive technique for the studying of biological cells. Here we explore a two-dimensional (2D) microfluidic light scattering cytometry for the potential detection of mitochondrial components in single biological cells.

A wide angle 2D light scattering microfluidic cytometer has been developed. Laser light is coupled into a microfluidic channel via an optical fiber to illuminate a single scatterer in a fluidic flow. The single scatterer can be imaged by using a microscope located on top of the microfluidic channel. While the wide angle 2D light scattering patterns are obtained using a charge-coupled device (CCD) located beneath the microfluidic chip. Experiments on THP-1 cells are performed using the 2D microfluidic cytometer, and cell scatter patterns are studied by finite-difference time-domain (FDTD) simulations of light scattering from non-homogeneous cell models.

The FDTD 2D light scattering patterns have similar structures as those patterns obtained experimentally from THP-1 cells. The 2D scatter patterns are dominated by many small scale 2D structures. This may

be due to that the THP-1 cells have rich mitochondrial components. Representative FDTD study of the mitochondrial contribution on the 2D light scattering patterns is performed. The analysis of the 2D light scattering patterns may help to understand mitochondrial components in biological cells independent of fluorescence or electron microscope. This may have potential applications for the study of many mitochondria related diseases.

7573-20, Session 5

Quantification of colloidal and intracellular gold nanomarkers down to the single particle level using confocal microscopy

S. Klein, Friedrich-Loeffler-Institut (Germany); S. Petersen, Laser Zentrum Hannover e.V. (Germany); U. Taylor, D. Rath, Friedrich-Loeffler-Institut (Germany); S. Barcikowski, Laser Zentrum Hannover e.V. (Germany) and Excellence Cluster Rebirth (Germany)

Gold nano particles are bio-inert nano markers with exclusively high stability of excitation characteristics of the absorption cross section in comparison to fluorescent dyes and quantum dots. To investigate cellular functions it is necessary to quantify the nano markers in minute amounts within biological materials. The aim of the study was to evaluate gold nano particles size-dependently in dispersion and in cells after co-incubation. We show the quantification of colloidal gold particles down to the single particle level by standard confocal microscopy. A calibration is demonstrated for pixel numbers and reflecting areas in number and mass based dilution series of uncoated gold nano particles. We give implications for practical use of advanced cellular imaging by quantification of cellular uptake of gold nanoparticles in bovine immortalised cells.

7573-21, Session 5

Detecting the role of cytoskeleton in nanoscale alterations of biological cells using partial wave spectroscopic microscopy

D. Damania, H. Subramanian, Northwestern Univ. (United States); A. K. Tiwari, NorthShore Univ. HealthSystem (United States); Y. Stypula, P. Pradhan, Northwestern Univ. (United States); H. K. Roy, Evanston Hospital (United States); V. Backman, Northwestern Univ. (United States)

Light microscopy has long been used to study tissue and cell architecture. However, due to the diffraction-limit, this technique cannot capture the nano-architectural alterations which precede microscopically detectable cellular changes in carcinogenesis. We had earlier reported the development of partial wave spectroscopic microscopy (PWS) technique to measure the nano-scale morphological changes that occur during early cancerization within cells. Based on the mesoscopic light transport theory, PWS offers sub-diffractional sensitivity to quantify the nanoscale refractive index fluctuations within cells in terms of intracellular disorder strength where the disorder strength depends on variance of refractive index fluctuations and correlation length of these fluctuations. Herein, we report the development of second generation guasi real time PWS system (rt-PWS). The experiments performed on HT29 celllines confirm that an increase in the degree-of-disorder in cell nanoarchitecture parallels genetic events in the early stages of carcinogenesis. Furthermore, we demonstrate that cytoskeleton is one of the contributors to these disorder strength changes in HT29 cell-lines. We investigated this dependence by performing treatments on the cytoskeletal components. We targeted the rupture of actin micro-filaments (present in nucleus and cytoplasm) using the drug, Cytochalasin D, which brings the difference of the genetically modified HT29 cell-lines nearly equal. We also performed the rupture of microtubules (present predominantly



in cytoplasm) using the drug, Colchicine, which nullifies the difference of disorder strength in cytoplasm but the changes in nucleus remain significant. Moreover, preliminary clinical results from colon cancer studies emphasizing the capability of rt-PWS to detect phenomena of field-effect will be discussed.

7573-22, Session 6

Spectral scatter imaging of breast cancer tumors

B. W. Pogue, Dartmouth College (United States)

Recovering a scatter spectrum from tissue ideally could be used to differentiate different types of tumors and tumor heterogeneity. Applications could ideally be non-invasive, invasive or as a surgical adjuvant. Scatter spectroscopy non-invasively through bulk tissue offers the largest challenge, because of partial volume averaging, and the illposedness of the spectrum recovery with diffuse light. In comparison, direct measurements from non-diffuse light have considerably higher fidelity and hold more promise for a useful information to aid the physician. The data obtained with deep tissue tomography will be compared to the data obtained on ex vivo samples, illustrating the areas of similarity and of difference. Comparison of the in vivo measurements to ex vivo histopathology analysis is also a critical part of this, and correlation is seen between in situ measurements and estimates of epithelial to stromal ratio, as well as other structural and molecular features of the tumor. The areas where pathology can confirm the accuracy of in situ imaging offer the most potential for validated in vivo imaging.

7573-23, Session 6

Assessment of breast tumor margins via quantitative spectral reflectance imaging

J. Q. Brown, T. M. Bydlon, S. A. Kennedy, L. M. Richards, M. Junker, L. Wilke, J. Geradts, N. Ramanujam, Duke Univ. (United States)

Diffuse reflectance spectroscopy of tissue allows quantification of underlying physiological and morphological changes associated with cancer, provided that the absorption and scattering properties of the tissue can be effectively decoupled. A particular application of interest for tissue reflectance spectroscopy in the UV-Visible is intraoperative detection of residual cancer at the margins of excised breast tumors, which could prevent costly and unnecessary repeat surgeries. Our multi-disciplinary group has developed an optical imaging device, which employs a model-based algorithm for quantification of tissue optical properties, and is capable of surveying the entire specimen surface down to a depth of 1-2mm, all within a short time as required for intraoperative use. In an IRB-approved study, reflectance spectral images were acquired from 136 margins in 107 patients. Conversion of the spectral images to quantitative tissue parameter maps was facilitated by a fast scalable inverse Monte-Carlo model. Data from margin parameter images were reduced to image-descriptive scalar values and compared to goldstandard margin pathology. The utility of the device for classification of margins was determined via the use of a conditional inference tree modeling approach. The sensitivity of the device for detecting positive margins was assessed both as a function of type of disease present at the margin, as well as a function of distance of disease from the issue surface. Current efforts are aimed at increasing the speed of the device as well as the tissue coverage area to enhance the practical clinical utility of the device.

7573-24, Session 6

In-vivo clinical Fourier-domain angle resolved low-coherence interferometry for dysplasia detection

N. G. Terry, Y. Zhu, M. T. Rinehart, Duke Univ. (United States); S. C. Gebhart, W. J. Brown, Oncoscope, Inc. (United States) and Duke Univ. (United States); S. Bright, E. Carretta, R. Madanick, The Univ. of North Carolina School of Medicine (United States); J. T. Woosley, The Univ. of North Carolina at Chapel Hill (United States); N. J. Shaheen, The Univ. of North Carolina School of Medicine (United States); A. P. Wax, Duke Univ. (United States)

Improved methods for detecting dysplasia, or pre-cancerous growth are a current clinical need, particularly in the esophagus. The currently accepted method of random biopsy and histological analysis provides only a limited examination of tissue in question while being coupled with a long time delay for diagnosis. Light scattering spectroscopy, in contrast, allows for inspection of the cellular structure and organization of

Fourier-domain angle-resolved low-coherence interferometry (a/ LCI) is a novel light scattering spectroscopy technique that provides quantitative depth-resolved morphological measurements of the size and optical density of the examined cell nuclei, which are characteristic biomarkers of dysplasia. Previously, clinical viability of the a/LCI system was demonstrated through analysis of ex vivo human esophageal tissue in Barrett's esophagus patients using a portable a/LCI, as was the development of a clinical a/LCI system. Data indicating the feasibility of the technique in other organ sites (colon, oral cavity) will be presented.

We present the results of a clinical in vivo study of Barrett's esophagus patients using the a/LCI system. Subjects (n = 27) were selected from a pool of patients enrolled in routine Barrett's esophagus (BE) surveillance and scanned with the clinical a/LCI device in parallel with the standard biopsy collection procedure. Following pathological examination, the results of the a/LCI technique were compared to traditional diagnosis for each study biopsy (n = 95). These results indicate detection of dysplasia by the a/LCI technique with a sensitivity and specificity of 100% and 84.1% respectively.

7573-25, Session 6

Detection of dysplasia in Barrett's esophagus with endoscopic polarized spectroscopic scanning (EPSS) instrument

L. Qiu, D. Pleskow, R. Chuttani, E. Vitkin, J. Leyden, N. Ozden, S. Itani, A. Sacks, J. Goldsmith, M. D. Modell, E. B. Hanlon, I. Itzkan, L. T. Perelman, Harvard Medical School (United States)

We have recently developed an endoscopic polarized spectroscopic scanning (EPSS) instrument. The EPSS instrument gives real time, in vivo information on the location of high grade dysplasia, a traditional predictor of adenocarcinoma in Barrett's esophagus. This instrument, compatible with existing commercial endoscopes, is based on the technique of polarized light scattering spectroscopy. It can scan large areas of the esophagus chosen by the physician, and has the software and algorithms necessary to obtain quantitative, objective data about tissue structure and composition, which can be translated into diagnostic information in real time. This enables the physician to take confirming biopsies at suspicious sites and minimize the number of biopsies taken at nondvsplastic sites.



7573-26, Session 7

Measurements of clinically relevant in-vivo concentration of a photosensitizer using optical pharmacokinetics and correlations with PDT necrosis

M. R. Austwick, J. H. Woodhams, C. A. Mosse, Univ. College London (United Kingdom); V. Chalau, Univ. College London (United Kingdom) and Research Institute of Oncology and Medical Rad (Belarus); Y. Jiao, L. B. Lovat, A. J. MacRobert, Univ. College London (United Kingdom); I. J. Bigio, Boston Univ. (United States); S. G. Bown, Univ. College London (United Kingdom)

Optical Pharmacokinetics (OP) is a point-contact diffuse reflectance spectroscopy technique. One 400-micron fibre injects white light from a Xenon arc lamp, and a 200-micron collection fibre, located 2mm from the source fibre, also on the surface, collects the diffusely scattered light. We demonstrate in-vivo detection of the photosensitizing drug Aluminium Disulphonated Phthalocyanine (AlS2Pc) in rats. The OP demonstrates a sensitivity which is limited by the lower limit of quantitation (LLQ) of the gold standard chemical extraction (CE) technique (~0.3µg/g). In phantom experiments, OP can detect signals from 0.025µg/g of AlS2Pc, and so it would be necessary to increase the sensitivity of our gold standard technique before the LLQ of OP is well-characterized.

Different methods of data extraction from the spectra were assessed. At higher concentrations, the area of the AlS2Pc spectral peak correlated linearly with CE with a zero intercept, in contrast with previous reports. Peak-fitting methods established a bimodal shape, with a 12-15nm red-shifted peak joining the aqueous signal. Using this fit as an alternative measure gave a power-law behaviour in the OP/CE relationship in the mouth and colon, with a power similar to phantom experiments.

Finally, correlating the necrosis extent with drug concentration using a simple model for diffuse light propagation, and incorporating the shadowing effect of the chromophore, yielded plausible results for PDT necrosis in the liver and colon.

This project was supported by the NIH/NCI Network for Translational Research: Optical Imaging (NTROI, U54 CA104599).

7573-27, Session 7

In-vivo time course studies of site specific inflammation using microneedle array fiduciary markings

K. G. Phillips, N. Choudhury, Oregon Health & Science Univ. (United States); H. Singh, Texas Tech Univ. (United States); P. Thuillier, S. L. Jacques, Oregon Health & Science Univ. (United States)

The characterization of cutaneous disease formation and abatement in murine models has traditionally been carried out through exposure of animal models to damaging agents with subsequent excision of affected tissues. Changes in tissue morphology are studied with immunohistological examination- such as hematoxylin and eosin staining. While a ubiquitous tool, immunohistology provides only a limited twodimensional presentation of tissue morphology at the cost of halting disease progression at a single time point. Additionally, histological techniques applied in animal studies often lack site specificity: the exposure and response of tissues are assumed uniform over the area of interest. Using optical coherence tomography, we perform in vivo time course imaging of mice with epidermal inflammation induced by topical application of 12-O-tetradecanoylphorbol-13-acetate (TPA). Cutaneous fiduciary markings by carbon nanoparticles delivered by a microneedle array are employed to co-register agent delivery and tissue imaging. The degree of inflammation over a 24 hour period is inferred from the attenuation rate of the ensemble average of A-scans performed in the

region of interest. This method provides a means of studying the time dependence of disease progression and abatement with a high degree of site specificity without recourse to invasive histological based methods which require halting the biological state of the tissue.

7573-28, Session 7

Dependence of the hemoglobin spectrum on lateral scattering in reflectance oximetry

T. Ririe, K. Sieluzycka, College of Optical Sciences, The Univ. of Arizona (United States); K. Denninghoff, The Univ. of Arizona (United States); L. W. Hillman, The Univ. of Alabama in Huntsville (Deceased) (United States); R. A. Chipman, College of Optical Sciences, The Univ. of Arizona (United States)

Fiberoptic reflectometers provide one method for investigating blood reflectance by using one fiber to deliver light to the blood and another to collect light that has been laterally backscattered. In this study, a modified reflectometer, which also allowed for collection of directly backscattered light, was used to probe whole blood samples with oxygen saturations of 48.1%, 53.8%, 60.6% and 99.6%. Laser wavelengths of 514.5, 501.7, 496.6, 488.0, 476.5 and 472.4 nm were used to illuminate the medium as the blood was pumped past the probe tip. The detector signals were normalized to the relative laser powers and the spectra from the directly and laterally back-scattered light were compared. It was found that while the laterally scattered light signal contained a strong hemoglobin signature, the directly back-scattered light showed no discernable hemoglobin signature. Oximetric analysis of the blood using the blue-green minima technique yielded an accurate oxygenation reading only when the laterally scattered light signal was used for the analysis.

7573-29, Session 7

Correlation between light scattering signal and tissue reversibility in rat brain exposed to hypoxia

S. Kawauchi, S. Sato, Y. Uozumi, H. Nawashiro, M. Ishihara, M. Kikuchi, National Defense Medical College (Japan)

Light scattering signal is a potential indicator of tissue viability in brain because cellular and subcellular structural integrity should reflect energy metabolism in the tissue. We previously performed multiwavelength diffuse reflectance measurement for a rat global ischemic brain model and observed a unique triphasic change in light scattering at a certain time after oxygen and glucose deprivation. This triphasic scattering change (TSC) was shown to precede cerebral ATP exhaustion, suggesting that loss of brain tissue viability can be predicted by detecting scattering signal. In the present study, we examined correlation between light scattering signal and tissue reversibility in rat brain in vivo. We performed transcranial diffuse reflectance measurement with a broadband tungsten lamp for rat brain; hypoxia was induced for the rat by nitrogen gas inhalation and reoxygenation was started at various time points. The body temperature of rats was kept at 32 ± 0.5 °C. We observed TSC to start at 198 ± 14 s after starting nitrogen gas inhalation (mean \pm SD, n=18). When reoxygenation was started before TSC, all rats survived (n=4), while no rats survived when reoxygenation was started after TSC (n=6). When reoxygenation was started during TSC, some rats survived; survival rate depended on the phase of starting reoxygenation. These results indicate that TSC can be used as an indicator of tissue reversibility in brains, providing useful information on the critical time point for rescuing the brain by appropriate treatments.



7573-31, Session 7

Ex-vivo elastic light single-scattering measurements to differentiate precancerous tissue from normal cervical tissue

M. Canpolat, T. Denkceken, Ş. Karaveli, E. Peştereli, G. Erdoğan, D. Özel, U. Bilge, T. Şimşek, Akdeniz Üniv. (Turkey)

We have investigated the potential application of elastic light singlescattering spectroscopy (ELSSS) as an adjunctive tool for screening of cervical precancerous lesions non-invasively and real time. Ex-vivo measurements were performed on 95 cervix biopsy material of 60 patients. Normal cervix tissues of 10 patients after hysterectomy were used as a control group. From each patient, one to four biopsy materials obtained and within five minutes at least 16 spectra have been taken randomly on the epithelial surface of each biopsy material and then the biopsy materials have been sent for histopathological examination. Correlation between ELSSS spectra and results of the histopathology has been investigated. It has been found that sign of the spectral slope is positive for all the spectra taken on normal cervix tissues of the control group. Sign of the spectral slope of at least one biopsy material was found negative for Pap smear positive patients. It shows that Pap smear and ELSSS results are in good agreement. Most of the biopsy material had both positive and negative sign of the spectral slopes. Therefore, we have calculated percentage of the spectral slopes with negative sign and assumed that it is correlated to dysplastic percentage of the epithelial tissue of the biopsy material. Mann-Whitney U Test was used to differentiate normal from LSIL and HSIL tissue using dysplastic percentage obtained from ELSSS measurements. Sensitivity and specificity of the ELSSS system in differentiation normal from LSIL and HSIL tissues are 70.4% and %66.7 respectively with p < 0.05.

7573-32, Session 8

High anisotropy utilized diffuse light suppression for large area spectroscopic imaging

Z. Xu, J. Liu, Y. L. Kim, Purdue Univ. (United States)

A unique optical property of biological tissue is high anisotropy so that light is scattered in the same direction with respect to the incident direction. For example, most biological tissue including major organs is highly anisotropic with anisotropy factor > 0.8 - 0.95, indicating that the light scattered from biological tissue will slightly deviate from its original incident direction. We demonstrate that simple back-directional gating allows us to take advantage of such an intrinsic property of biological tissue to significantly suppress unwanted diffuse light which otherwise deteriorates the image contrast. In back-directional gated imaging, the high anisotropic property of the surrounding medium can serve as a waveguide to deliver the incident light to the embedded object and to isolate the ballistic or snake-like light backscattered from the object in a moderate depth. Although this idea is straightforward, it has not been utilized for diffuse light suppression and imaging depth improvement in large-area imaging of biological tissue. We further show that by combining a spectral analysis with back-directional gated imaging, image contrast and depth can be enhanced to visualize microvascular blood content in relatively deep tissue up to optical thickness ~ 15 - 20. Given that microvasculature is typically heterogeneous, our imaging approach also permits representative visualization of microvascularity in a relatively large area up to 15 mm x 15 mm. In several animal studies, we demonstrate the utility of our imaging approach for noninvasively assessing the temporal and spatial extents of microvascularity alterations.

7573-33, Session 8

Probing turbid medium structure using ultralow coherence enhanced backscattering spectroscopy

B. DeAngelo, G. Arzumanov, C. Matovu, P. Shanley, M. Xu, Fairfield Univ. (United States)

Backscattering of light has been widely used in optical probing of tissue. To probe the superficial layer of tissue which is of most interest in, for example, sensing the epithelium for potential pathological changes, the detector must be placed close to the source. To the same end, spatially low coherence light may be used to limit the penetration depth via detecting enhanced backscattering light. We have developed an ultra low coherence enhanced backscattering spectroscopy (ULEBS) system using a line source generated by a Xenon lamp. The spatial coherence length of the incident beam is not greater than 25 µm, much smaller than either scattering or transport mean path in typical biological tissue. ULEBS signal can be detected in four different pairs of linear polarization (ss, sp, ps, and pp) of the incident and scattering light.

ULEBS is used to exam enhanced backscattering from tissue phantoms and ex vivo tissue samples. Both intralipid-20% suspensions and a set of suspensions of polystyrene spheres with diameters of 0.19 $\mu m, 0.49 \ \mu m, 4.19 \ \mu m,$ and 8.31 μm are first investigated. A periodic structure is found to be contained in the low coherence enhanced backscattering spectrum whose period is proportional to the scatterer size. The spectral slope of the low coherence enhanced backscattering spectrum is found to be related to the fractal dimension of the turbid medium. A theoretical model is proposed to explain the experimental observations. Electric field Monte Carlo simulations are used to verify the proposed model. ULEBS is then used to exam ex vivo tissue samples to access its potential in tissue diagnosis. The results on both phantom systems and ex vivo tissues will be presented and the potential application of ULEBS in tissue diagnosis is discussed.

7573-34, Session 8

Measurement of optical and physical properties with low-coherence enhanced backscattering spectroscopy

V. M. Turzhitsky, J. D. Rogers, N. N. Mutyal, V. Backman, Northwestern Univ. (United States)

Low-coherence enhanced backscattering is a technique that has recently shown promise for the characterization of pre-cancerous changes in tissue. This novel method employs partial spatial coherence illumination coupled with spectrally resolved detection to obtain wavelengthdependent enhanced backscattering information. The use of partial spatial coherence acts to broaden the peak and limit the penetration depth. The resulting signal is sensitive to the scattering coefficient and the anisotropy coefficient of the scattering media when the transport mean free path (ls*) is much greater than the spatial coherence length (Lsc). When Is* is less than Lsc, a model based on the diffusion approximation accurately characterizes the peak properties. In this highly scattering regime, LEBS is only characterized by Is*. We present experimental results from polystyrene microsphere suspensions and Polarized light Monte Carlo simulations to support these conclusions. We also emphasize that the choice of the phase function in the Monte Carlo significantly impacts the accuracy of the results. In the case of weakly fluctuating continuous refractive index media, the Fractal dimension can also be calculated from the wavelength-dependence of the signal by applying the Born approximation. The optical properties can also be converted to physical properties including the variance of the refractive index fluctuation and the correlation length. Finally, we show that the LEBS Fourier transform relationship can be used to calculate p(r), the probability distribution of directly backscattered light. These results suggest that LEBS is a powerful tool that can be used to non-invasively and comprehensively characterize light scattering.

TEL: +1 360 676 3290 · +1 888 504 8171 · customerservice@spie.org



7573-35, Session 8

Helicity flip of backscattered circularly polarized light

I. Meglinski, Univ. of Otago (New Zealand); V. L. Kuzmin, St. Petersburg Institute of Commerce and Economics (Russian Federation)

We study coherent and non-coherent backscattering of circularly polarized light from a turbid medium. We find that the sign of helicity of circular polarized light does not change for a medium of point-like scatterers and can change significantly for the medium with high scattering anisotropy. The helicity flip is observed when the light scattering is described in terms of the Henyey-Greenstein scattering phase function. The angular dependence of the sum of coherent and non-coherent parts of backscattering also exhibits a helicity flip.

7573-36, Session 9

Measuring structural features using a dual window method for light scattering spectroscopy and Fourier-domain low coherence interferometry

F. E. Robles, A. P. Wax, Duke Univ. (United States)

Light scattering spectroscopy (LSS) and Fourier-domain low coherence interferometry (fLCI) use spectral information to measure the enlargement of the cell nucleus associated with precancerous development. A similar approach is used in spectroscopic optical coherence tomography (SOCT), which provides the same excellent cross-sectional tomographic imaging capabilities of OCT with the added benefit of spectroscopic based contrast, thereby providing an additional dimension for viewing and classifying images. In SOCT, short time Fourier transforms (STFTs) or wavelet transforms are used to obtain spectroscopic information. Unfortunately, the windowing process of these techniques introduces an inherent trade off between spatial and spectral resolution, which prohibits further quantitative processing of the depth resolved spectra. Recently, we have introduced the dual window (DW) method for processing SOCT signals achieving both high spectral and spatial resolution, ultimately allowing for a more thorough quantitative treatment of the depth-resolved spectroscopic information. The DW method decomposes each A-scan from the OCT signal into a time frequency distribution (TFD) allowing for a self-registered quantitative spectral analysis. Here, we demonstrate the use of the DW method for obtaining fLCI and LSS measurements from any region of interest in an OCT image by using a white light parallel frequency domain OCT system that provides access to the visible region of the spectrum and an axial resolution of 1.22µm. The results presented will include imaging of a two-layer phantom, with each layer containing a suspension of different sized polystyrene beads, and measuring scattering structures within using LSS and fLCI. Also, results from ex-vivo tissue samples drawn from the hamster cheek pouch carcinogenesis model will be presented and a discussion of future implementation of the system for probing cell nuclear morphology in-vivo will be included.

7573-37, Session 9

Detection of biofilms in middle ear by low coherence interference data

C. T. Nguyen, H. Tu, E. J. Chaney, Univ. of Illinois at Urbana-Champaign (United States); C. N. Stewart, Blue Highway, LLC (United States); S. A. Boppart, Univ. of Illinois at Urbana-Champaign (United States)

Chronic Otitis Media (OM) is a common illness in children which leads to their hearing loss and communication difficulties. Recent researches have considered that bacteria biofilm is the cause of chronic OM. However

biofilms are thin (10-100 m), low optical contrast, and therefore cannot be distinguished from tympanic membrane by standard otoscope or ultrasound. Low coherent interference (LCI)/Optical Coherence Tomography (OCT) with high depth resolution has been applied to image these microstructures. We present a specific algorithm to classify one dimensional LCI data (axial scans) of middle ears and detect the presence of biofilms. Based on biological and optical study of middle ear, the LCI data are characterized by three features scattering intensity, structure thickness and attenuation slope. A set of signal models representing different states of OM is established from training data. Each axial scan is subsequently classified to the most fitted signal model. The core of classification is implemented first by a linear discriminant analysis (LDA) of scattering intensity and structure thickness, then a linear minimum distance (LMD) of normalized signals. For each patient, the statistic result of axial scans' classification give final decision of OM diagnosis. The algorithm are demonstrated in OM of rat model and

7573-40, Poster Session

Anisotropic optical property of a bio-medium with highly photon-scattering anisotropic biomolecules

T. Nee, S. F. Nee, National Yang-Ming Univ. (Taiwan)

The optical scattering and absorption coefficients have been measured in many biological tissues. The scattering coefficient is usually much larger than the absorption coefficient. Tissues are optically anisotropic and highly photon scattering media. Using a simple ellipsoid model of bio-molecule, we have recently shown that the photon is highly depolarized as it passes the bio-medium, such as the cell membrane, due to the strong scattering with the anisotropic bio-molecules. The medium molecular density dependence of the scattering cross section was quantitatively demonstrated. This theory is extended to investigate the anisotropic optical property of the bio-medium. Using an effective mean-field theory, the anisotropic optical constants N(j) = n(j) + i ktot(j), (j = x, y, z) is derived for a bio-medium with anisotropic bio-molecules. Numerically fitting results of the existing experimental tissue scattering and absorption data, will be reported.

References:

- [1] "Scattering polarization by anisotropic biomolecules", T. W. Nee et. al., JOSA-A, 25, 1030-1038 (2008); VJBIO 3, Issue 6 (2008).
- [2] "Optical scattering depolarization in a bio-medium with anisotropic bio-molecules", T. W. Nee et. al., JOSA-A, 26, 1101-1108 (2009); VJBPR Vol.17, Issue 10 (2009); VJBIO, Vol. 4, Issue 7 (2009).
- [3] "Theory of dielectric relaxation in polar liquids", T. W. Nee and R. Zwanzig, J. Chem. Phys. 52, 6353 (1970).

7573-41, Poster Session

Spatially resolved 2-D attenuation image of a semi-infinite non-homogeneous tissue from diffuse reflectance

J. Tse, L. Chen, The Chinese Univ. of Hong Kong (Hong Kong, China)

Optical properties of biological tissue such as reduced scattering and absorption coefficients can be determined from the temporal or spatial reflectance curve of the diffusion process. Owing to its non-homogenous nature, the assumption of uniform optical parameters may not be valid in practice. We propose a new scheme to resolve the optical effective attenuation profile from the spatial reflectance curve of a non-homogeneous tissue. The algorithm reconstructs the linear attenuation profile along the line of measurement, rather than giving one single value for the coefficient for each reflectance curve. The technique was applied to the reconstruction of a 2-dimensional attenuation image.



7573-42, Poster Session

Non-negative matrix factorization: a blind sources separation method applied to optical fluorescence spectroscopy and multiplexing

A. Montcuguet, Lab. d'Electronique de Technologie de l'Information (France) and GIPSA-Lab, (France); L. Hervé, L. Guyon, J. Dinten, Lab. d'Electronique de Technologie de l'Information (France); J. I. Mars, Univ. Joseph Fourier (France) and GISPA-Lab. (France)

Fluorescent imaging in diffusive media is an emerging imaging modality for medical applications: injected fluorescent markers (in multiplexing, several fluorophores are used) bind specifically to carcinoma. The region of interest is illuminated with near infrared light and the emitted back fluorescence is analyzed to localize the fluorescence sources. To investigate thick medium for medical diagnostic application, as the fluorescence signal gets exponentially weak with the light travel distance, any disturbing signal, such as biological tissues intrinsic fluorescence, may be a limiting factor. To remove these unwanted contributions, or separate different fluorophores, a spectroscopic approach is explored.

Capillary tubes filled with fluorophores (ICG and Alexa750) are used to simulate marked tumors, and inserted in mice or inside optical phantoms, then illuminated at 785 nm along a line with a planar laser. Translation stages are used to get a scan of the whole object. The fluorescence signal emitted back is collected by an imaging spectrometer coupled with a CCD camera.

The fluorescence acquisition is processed with Non-negative matrix factorization (NMF) algorithm which approximates the acquisition image as the product of two non negative matrices i.e. the spectra and the weighting factors of the fluorescence sources. Spectroscopic measurements being the sum of nonnegative components, the method is suitable for spectroscopic measurements.

We found that in vivo spectrally resolved acquisition combined to NMF processing successfully separates different fluorophores or filters different fluorescence contributions of interest from measurements impaired by unwanted signals and allows performing a more accurate 3D reconstruction of the whole object.

7573-43, Poster Session

Angular dependence of blood spectrum using scattering spectroscopy in reflection

K. Sieluzycka, T. Ririe, College of Optical Sciences, The Univ. of Arizona (United States); K. Denninghoff, The Univ. of Arizona (United States); R. Chipman, College of Optical Sciences, The Univ. of Arizona (United States)

Determining how the angle of light scattered from a turbid medium such as blood or tissue affects the measured spectrum is significant for many biomedical techniques such as light scattering spectroscopy and diffuse reflectance spectroscopy. In this study, scattering spectroscopy in reflection was used on swine blood to analyze the angular dependence of measured spectra. An Argon ion laser (514.5, 496.5, 488, 476.5, 457.9 nm) illuminated blood and a laterally scanning pinhole in the imaging pathway confined each measurement to a small range of angles. The spectrum of blood was measured for scatter angles ranging from 0 to 7°. We found that the variance of the spectrum was larger when calculated from greater scatter angles. This suggests that higher spectral resolution might be obtained in scattering spectroscopy by detecting larger angles of scatter.

7573-44, Poster Session

Photon-cell interactive Monte Carlo simulation for quantification of MCV and MCHC of RBCs

D. Sakota, S. Takatani, Tokyo Medical and Dental Univ. (Japan)

A 3-dimensional biconcave RBC model together with photon-cell interaction computer program has been developed to study effects of mean cell volume (MCV) and mean cell hemoglobin concentration (MCHC) on the optical propagation through whole blood. The Monte Carlo program (MCP) was modified to include cell and photon interaction reflecting variations in MCV, MCHC and refractive indices.

The modified MCP first defines random orientation of a biconcave RBC with respect to incident photon direction divided from 0 degree flat-on to 90 degree edge-on incidence into 100 steps, followed with placement of photon on the selected RBC cross section divided into 1000 nodes. The scattering angle is thereafter defined using Gegenbaur-Kernel phase function to determine reflection, diffraction, or propagation through a cell. The photon energy propagating through the cell is expressed by Beer-Lambert law. After repeated interaction of the photon with RBCs, the total energy received by the detector and propagation time are recorded.

The optical density and propagation time through the medium containing old and young RBCs separately were measured using a time and space resolved optical spectrometer. The mean error between the experimental and MCP for OD and propagation time were minimized when the MCV and MCHC of 65.5 fL and 28.8 g/dL for young and 54.5 fL and 28 g/dL $\,$ for old were used in the model, while experimentally they were 64.2 and 28.4 for young and 55.1 and 29.3 for old, respectively. The modified MCP can provide MCV and MCHC of RBCs with accuracy of less than 3.0%.

7573-45, Poster Session

Comparison of the performance of two depth-resolved optical imaging systems: laminar optical tomography and spatially modulated imaging

E. Guevara, M. Abran, S. Bélanger, N. Ouakli, F. Lesage, Ecole Polytechnique de Montréal (Canada)

The objective of this research is to compare quantitatively the imaging capabilities of a laminar optical tomography (LOT) system with those of a spatially modulated imaging (SMI) system. LOT is a three dimensional optical imaging technique that achieves depth sensitivity by measuring multiple-scattered light at different source-detector separations. The SMI method is based on spatially modulated illumination-detection patterns, which encode both optical properties and depth information. In this work, simulation studies are carried out at different noise levels, to obtain the figures of merit of tomographic reconstructions for both systems. Experiments on phantoms are performed to demonstrate the validity of the method.

7573-46. Poster Session

Surface effect measurement of a small scattering object in highly scattering medium by use of diffuse photon-pairs density wave

C. Chou, Chang Gung Univ. (Taiwan); L. Yu, National Yang Ming Univ. (Taiwan): J. Wu. National Central Univ. (Taiwan)

The surface effect occurred at the boundaries of a scattering object in a highly scattering medium has a potential to increase the spatial resolution of inverse algorithms. Theoretically, the surface effect becomes dominated when the size of the object decreases (an object with a surface-to-volume ratio > 1 mm^-1). The ability to detect the surface

TEL: +1 360 676 3290 · +1 888 504 8171 · customerservice@spie.org



effect implies the ability to resolve small scattering objects in a highly scattering medium. However, the surface effect is difficult to detect because it only happens near the boundaries of the object. Few studies have reported on the importance of the surface effect. Moreover, to our knowledge, there is no available experimental data to demonstrate the surface effect of a small scattering object in a highly scattering medium. In the paper, we measure the surface effect of a small scattering object by using the amplitude and phase signal of diffuse photon-pairs density wave (DPPDW). DPPDW theory has been developed in our laboratory in recent years. The results demonstrate that DPPDW has high sensitivity for resolving the surface effect of a small object. Imaging in highly scattering media with the developed DPPDW method can potentially increase the spatial resolution of small scattering inclusions.

7573-47, Poster Session

Study on dynamics of photon migration in human breast based on three-dimensional Monte Carlo modeling

C. Chuang, C. Chen, J. Tsai, National Taiwan Univ. (Taiwan); C. Lu, Industrial Technology Research Institute (Taiwan); C. Sun, National Yang-Ming Univ. (Taiwan)

The scattering and absorption properties of human breast are very important for cancer diagnosis based on diffuse optical tomography (DOT). In this study, the dynamics of photon migration in threedimensional human breast model with various source-detector separations is simulated based on a Monte Carlo algorithm. The threedimensional human breast structure is obtained from in-vivo MRI image. The breast model consists of epidermis, fatty, glandular, sternum, and ribcage. The backscattered diffuse photons from each layer in breast are recorded by marking the deepest layer which every photon can reach. The experimental results indicate that the re-emitted photons contain more information from the deep tissue regions when the source-detector separations are increased. The geometric position is optimized with the source-detector separations because of the strong dependence to the resolution and sensitivity in DOT imaging. Besides, the different sizes of breast tumor are modeled for further analysis of optical image characterizations.

7573-48. Poster Session

Exploration of the influence of the spectrometer sensitivity on optical cancer diagnosis using elastic scattering spectroscopy

Y. Jiao, J. M. Dunn, M. R. Austwick, C. A. Mosse, Univ. College London (United Kingdom); M. R. Novelli, Univ. College Hospital (United Kingdom); M. R. Banks, S. G. Bown, L. B. Lovat, Univ. College London (United Kingdom)

Elastic Scattering Spectroscopy (ESS) is an emerging optical diagnostic technique for the detection of high grade dysplasia in Barrett's oesophagus. We have previously demonstrated sensitivity of 92% using principle component analysis (PCA) followed by linear discriminant analysis (LDA), Briefly, white light is delivered via a 400micron optical fibre placed in contact with the tissue to be investigated, and undergoes multiple scattering events before collection.

The acquired spectra reflect both the scattering and absorptive properties of the tissue, influenced by both vascular and morphological changes. Absorption of the oxy and deoxy hemoglobin mainly affect the spectra in the range 400nm-500nm. Above this scattering effects dominate, which may more accurately reflect sub-cellular structural changes.

For this in vivo study the influence of the spectral range and sensitivity of the spectrometer on accuracy of diagnosis was investigated. The

previous spectrometer and a red enhanced spectrometer, more sensitive in the range 500nm-800nm, were compared. Spectral data for each spectrometer was collected at matched sites in vivo. A biopsy of the site was then taken and histopathology reviewed. The diagnostic algorithm was generated using the previously described dataset (Lovat GUT 2006) and tested on the histology data. To further enhance accuracy support vector machine analysis was used, which had given higher accuracy on the published dataset. This work should confirm the robustness of the technique and indicate whether SVM or LDA analysis is more effective.

7573-49, Poster Session

Combining finite element and propagation methods for scattering simulations of biological nanoparticles

M. Kuhn, LightTrans GmbH (Germany); J. Schoeberl, RWTH Aachen Univ. (Germany); T. Untermann, LightTrans GmbH (Germany); F. Wyrowski, Friedrich-Schiller-Univ. Jena (Germany)

The analysis of scattering problems involving nano-particles requires rigorous simulation techniques as Finite Element Methods (FEM). These methods ensure that the physical error of the simulation model is small. Other methods, as geometrical optics are not applicable if the particle size or other length scales are close to the wavelength.

On the other hand, FEM is still restricted to rather small domains since the complexity (memory requirements and CPU time) increases with the inverse of the wavelength.

In this talk we present the concept of Unified Optical Modeling that allows to combine different simulation techniques within a single modeling task.

In particular we focus on the combination of FEM with classical propagation techniques including free space and geometrical optics propagation.

We show that using locally adapted simulations techniques can speed up calculations considerably or can make them feasible at all.

The described methods are especially useful in biological applications that are characterized by different length scales, e.g. if the scattered field of cell structures is to be analyzed in the far field or behind a lens.

Results obtained by the optical simulation software VirtualLab(TM) (www. lighttrans.com) are presented.



Conference 7574: Nanoscale Imaging, Sensing, and Actuation for Biomedical Applications VII

Wednesday-Thursday 27-28 January 2010 • Part of Proceedings of SPIE Vol. 7574 Nanoscale Imaging, Sensing, and Actuation for Biomedical Applications VII

7574-30, Poster Session

Biofilms of chitosan-gold nanorods as a novel composite for the laser welding of biological tissue

P. Matteini, F. Ratto, F. Rossi, R. Pini, Istituto di Fisica Applicata Nello Carrara (Italy)

Gold nanorods (GNRs) exhibit intense localized plasmon resonances at optical frequencies in the near infrared (NIR), which is the window where the penetration of light into the body is maximal. Upon excitation with a NIR laser, a strong photothermal effect is produced, which can be exploited to develop minimally invasive therapies. Here we show the efficiency of chitosan-GNRs films as a novel nanocomposite for the photothermal transduction of NIR laser light during surgical interventions of tissue welding. Chitosan is an attractive biomaterial due to its biodegradability, biocompatibility, hemostatic, antimicrobial and wound healing-promoting activity. Colloidal GNRs were embedded in polysaccharide chitosan, which enwrapped them in highly stabilized, flexible and easy-to-handle films, which were stored in physiological buffer until the time of surgery. The films were positioned on freshly explanted rabbit tendon samples in which a 3 mm-incision was previously produced by using a pre-calibrated knife. Then by administration of single pulses of 40-80 ms and 1 W of power delivered by a 300-um optic fiber and produced by a 810 nm diode laser, we achieved spots of local thermally-induced adhesion, which resulted into a very satisfactory weld. The histological analysis depicted a structural remodelling of the fibrillar collagen located beneath the laser-activated film and probably associated with its denaturation and noncovalent interactions with the chitosan strands. The present results are very encouraging for the development of a novel minimally-invasive technology based on the application of bioderived nanophotonic structures to biomedical optics.

7574-31, Poster Session

Depolarized scattering of silver nanostructures in dye-less sensing

P. Sarkar, Univ. of North Texas Health Science Ctr. at Fort Worth (United States); T. Shtoyko, The Univ. of Texas at Tyler (United States); R. Luchowski, N. Calander, Z. K. Gryczynski, I. Gryczynski, Univ. of North Texas Health Science Ctr. at Fort Worth (United States)

Scattering from noble metallic nanoparticles with specific structures are strongly depolarized in contrast to dielectric particles. The effect depends on the shape and symmetry of the nanoparticles and can be explained by induced plasmonic multi-resonances along different axes of symmetry. In our experiments we found that the scattering from 'nanorod' structures of silver is more polarized than globular colloidal silver nanostructures.

The depolarized scattering can be tuned to the near-infrared region by using proportionate mixture of the colloids and nanorods. We demonstrate this effect in solution as well as in polymer films where nanoparticles were immobilized.

This phenomenon of depolarized scattering is promising for designing dye-less sensing devices useful in diagnostics. We show scattering polarization profile from asymmetric nanostructures changes during their aggregation. Modulating the rate of aggregation of these nanostructures by 'receptor -ligand'-like interactions can be successfully utilized for sensitive'dye-less' diagnostics.

7574-32, Poster Session

Limit of detection for a bead-based diffraction biosensor

Y. Lim, D. D. Nolte, K. M. Arif, C. A. Savran, Purdue Univ. (United States)

Diffraction-based biosensors that rely on optical scattering are a sensitive approach for biomolecular detection. The development of robust and fluorescence-free diffraction biosensors is important for early diagnosis of disease because it makes detection processes rapid and inexpensive. A diffraction grating can be self-assembled by biconjugated beads captured to target molecules, and the surface-captured beads enhance diffraction signal intensities.

The approach we take to simulate the operation of our system is based on Mie scattering, which is an exact formalism to give accurate results quickly. Although Mie scattering easily handles spherical particles, the scattering by spherical particles on surface is more complicated. Our code is based on the MSDI (Mie surface double-interaction) model to simulate our system of beads on the in situ assembly of diffraction gratings where coherent light beams are reflected from beads on a gold substrate. The current model is in the first Born approximation in which light scattered by the bead does not deplete the light incident upon the bead. This approach is physically acceptable when the beads are small and dilute. However, extension to GMT (Generalized Mie Theory) is necessary in the dense bead limit for which multiple scattering is not negligible. The LOD (Limit of Detection) for a system having 26 stripes is calculated to be approximately 25 beads in total, or approximately one bead per stripe in an immunoassay experiment. This sensitivity limit is orders of magnitude better than label-free molecular sensors, and is furthermore consistent with high-speed scanning for high-throughput assavs.

7574-02, Session 1

In-vitro and in-vivo detection of p53 by fluorescence lifetime on a hybrid FITC-gold nanosensor

G. Chirico, Univ. degli Studi di Milano-Bicocca (Italy); L. Sironi, S. Freddi, L. D'Alfonso, Univ. degli Studi di Milano Bicocca (Italy); M. Collini, Univ. degli Studi di Milano-Bicocca (Italy); T. Gorletta, Univ. degli Studi di Milano Bicocca (Italy); S. Soddu, Regina Elena Cancer Institute (Italy)

We have studied constructs based on gold nanoparticles (NPs) functionalized with specific anti-p53 antibodies and with a fluoresceine derivative, FITC. The FITC excited state lifetime follows linearly the p53 concentration in solutions up to 200 - 400 pM, depending on the size of the NP, with an uncertainty about 5 pM. We have evaluated the specificity of the nanosensor for p53 by testing it against bovine serum albumine, beta-lactolglobulin and lysozyme solutions. The titration of total cell extracts from p53+/+ or p53-/- cells with the p53antibody decorated gold NPs, indicates that this construct will be a valuable tool also for in vivo screening.

Contents TEL: +1 360 676 3290 · +1 888 504 8171 · customerservice@spie.org

Conference 7574: Nanoscale Imaging, Sensing, and Actuation for Biomedical Applications VII



7574-03, Session 1

SPR tuning by pH-controlled reversible assembly of polyelectrolyte-coated gold nanorods

D. Zheng, Y. Chen, X. Li, The Johns Hopkins Univ. (United States)

We report the development of pH sensitive nanocomposites with a large surface plasmon resonance (SPR) tuning range. The nanocomposites are made of polyelectrolyte-coated gold nanorods. Half of the nanorods are coated with poly styrene sulfonate (PSS) and the other half are coated with poly styrene sulfonate (PSS) followed by poly allylamine hydrochloride (PAH). The electrostatic attraction between the two types of coated nanorods in aqueous solution is highly sensitive to the pH value, PSS-nanorods and PAH-nanorods can self-assemble into nanocomposites through the electrostatic interaction. The size of the nanocomposites can be sensitively tuned by the solution pH within the physiological range. The resulted SPR peak shift of the nanocomposites is fairly large and the SPR peak tuning is reversible controlled by the solution pH. Nearly uniform nanoasseblies of a quasi-spherical shape can be achieved by controlling the NaCl concentration in solution during synthesis. The large SPR peak shift of the nanoassemblies is due to both the surface plasmon coupling between the neighboring nanorods and the variation of the local dielectric constant inside of the PSS/PAH assembly. Our experimental results show that the reversible nanoassembly of Polyelectrolyte-coated gold nanorods is a promising pH sensitive sensor and can be potentially used as a contrast agent for molecular optical and photo acoustic imaging.

7574-04, Session 1

Combined photothermal therapy and magneto-motive ultrasound imaging using multifunctional nanoparticles

M. Mehrmohammadi, M. Qu, K. A. Homan, The Univ. of Texas at Austin (United States); P. Joshi, The Univ. of Texas Health Science Ctr. at Houston (United States); Y. Chen, S. Y. Emelianov, The Univ. of Texas at Austin (United States)

Photothermal therapy is a promising non-invasive technique for cancer treatment. Photothermal therapy can be enhanced by employing metal nanoparticles that absorb the radiant energy from the laser leading to localized thermal damages. More efficient and localized targeting of photo absorbers increases the effectiveness of the treatment. Moreover, efficient targeting can reduce the required dosage of photo absorbers; thereby reducing the side effects associated with general systematic administration of photo absorbers. Magnetic nanoparticles, due to their small size and response to an external magnetic field gradient have been proposed for targeted drug delivery. In this study, we propose multifunctional nanoparticles (e.g., nanoparticles with magnetic core and gold nanorods absorbing at near-infrared spectrum) for photothermal therapy.

The presence of photo absorbers is a key to ensure the success of photothermal therapy. Therefore, there is a need for an imaging technique to detect the presence of optical absorbers. Magneto-motive ultrasound (MMUS) imaging is an ultrasound based imaging technique capable of detecting magnetic nanoparticles indirectly by utilizing a focused high strength magnetic field to induce motion within the magnetically labeled tissue. The ultrasound imaging is used to detect the internal tissue motion. Due to presence of the magnetic component, the proposed multifunctional nanoparticles along with MMUS imaging can be used to detect the presence of the photo absorbers. Clearly the higher concentration of magnetic carriers leads to a monotonic increase in MMUS signal. Thus, MMUS can determine the presence of the hybrid agents and provide information about their concentration.

7574-05, Session 1

From circulation to tumor cells in living subjects: the sub-microscale journey of targeted carbon nanotubes in living subjects imaged using intravital microscopy

B. R. Smith, C. L. Zavaleta, Z. Liu, H. Dai, S. S. Gambhir, Stanford Univ. (United States)

While nanoparticles have become invaluable in the molecular imaging toolkit, little is known about the mechanisms by which they target disease. To overcome this obstacle, we visualized targeted single-walled carbon nanotubes (SWNTs) entering tumor vasculature, specifically binding luminal targets, extravasating from vessels, and binding to tumor cells. To understand the fundamental mechanisms underlying SWNT tumor uptake, we confirmed and correlated our intravital microscopy (IVM) results with macroscopic Raman imaging, which quantitatively detects the SWNTs' intrinsic Raman signal.

We prepared targeted SWNTs by conjugating RGD peptides (targeting v 3-integrins expressed on tumor neovasculature and some tumor cells) and Cy5.5 dye. Dorsal chambers were surgically implanted into mice and EGFP-U87MG tumor cells (expressing v 3-integrins) or EGFP-SKOV3 were inoculated. 25 mice (U87MG, SKOV-3, no tumor) were imaged with RGD-SWNTs (~60 pmol) and controls. Mice were imaged during injection and frequently during the following month with Raman and IVM. Unlike controls, RGD-SWNTs were observed to bind tumor blood vessels. Within hours, SWNTs extravasated in U87MG tumor beds, but not SKOV-3. While both RGD and control SWNTs were observed associated with some tumor cells in U87MG tumors, RGD-SWNTs not only bound more (P<0.0001), but they differentially bound tumor cells over time compared with controls (P<0.007) and they persisted in tumor for more than month. Control SWNTs cleared within ~1 week.

In summary, IVM allowed detailed exploration of the mechanisms of SWNT uptake in tumor. This work offers unprecedented understanding of the mechanisms/temporal framework of nanoparticle tumor uptake, which will translate into superior properties for pre-clinical/clinical utility.

7574-06, Session 1

Single molecule tracking by spatially resolved single photon counting as a tool for far-field optical nanoscopy

S. J. Sahl, M. Leutenegger, M. Hilbert, C. Eggeling, S. Hell, Max Planck Institute for Biophysical Chemistry (Germany)

Much can be learned from observing the behavior of single molecules in biological and non-biological materials when ensemble averaging is absent. We report the implementation of a simple optical method capable of tracking a fluorescent molecule in two dimensions, with high fidelity and currently unrivaled spatiotemporal resolution. The fluorescence signal during individual passages of just one molecule through a spot of excitation light allows for the sequential localization, and thus lateral tracking, if its fluorescence is collected on at least three separate point detectors arranged in close proximity. To demonstrate the potential of this non-correlation-based single molecule method, we show trajectories of individual membrane lipids diffusing in the plasma membrane of living mammalian cells. In particular, the influence of trapping interactions becomes obvious, notably for sphingolipids, as identified in a recent report. Further applications include the assembly of maps of molecular distributions and dynamics with nanoscale resolution.

Conference 7574: Nanoscale Imaging, Sensing, and **Actuation for Biomedical Applications VII**



7574-07, Session 1

Tracking of optically trapped particle in three dimensions using off-axis digital holographic microscopy

Y. Bae, S. Lee, Gwangju Institute of Science and Technology (Korea, Republic of); W. Yang, Gwangju Institute of Science and Technolgy (Korea, Republic of); D. Y. Kim, Gwangju Institute of Science and Technology (Korea, Republic of)

Three dimensional particle tracking is very useful technology to characterize live cell or surrounding environment by tracing the small particle such as fluorescence or polystyrene bead which adhered to the objective sample. In microscopy imaging system, the longitudinal(z axis) tracking of the bead is essential for implementation of 3 dimensional particle tracking, however it's been still challenging topic to find out exact position of the particle in z axis with high precision.

In this study, we present how to find out the longitudinal position of the bead, as well as transverse position(x,y axis) by applying the numerical focusing method and peak detection with digital holographic microscope.

Transmission type off-axis digital holographic microscope is implemented based on Mach-Zehnder interferometer and 3µm polystyrene beads embedded in water is investigated for this experiment. 632.8nm HeNe laser is used as a coherent light source of the microscope and highspeed CMOS camera is utilized for acquiring the hologram of the trapped

Digital holographic microscope makes it possible to record and reconstruct the phase and amplitude image of the sample.

Once the phase and the amplitude are reconstructed, we apply the numerical focusing algorithm, which enables translation of the imaging focus without actual longitudinal movement of the sample, to find out z axis position of the bead, where it is sharply imaged.

We demonstrated this method by applying to investigate the 3 dimensional motion of the trapped polystyrene bead.

7574-08, Session 1

Nanoplatforms for biomedical imaging

S. Sridhar, Northeastern Univ. (United States)

The plasmon resonance conditions in nano-sized materials leads to local field enhancement resulting in amplified response of various linear and nonlinear optical processes at the nano-scale. In this paper, metallic nanoparticles are imaged using several modalities - brightfield, confocal reflectance, two-photon, and second harmonic generation. Several examples are discussed - Au nanoparticles in embryonic stem cells and the zebrafish spinal column, and Ag nanoparticles in fresh skin excisions. We show that the optical properties of noble-metal nanoparticles offer an attractive alternative to the fluorophore-based staining and labeling of biological samples.

Magnetic nanoparticles in lipid packages were characterized extensively for their physical, electric, magnetic properties and in in vitro and in vivo studies. In vivo MRI imaging on melanoma tumor bearing animal models demonstrated superior T2 contrast enhancement, long circulation properties, accumulation in tumors, and direct visualization of magnetic guidance of nanoparticles into tumors. These nanolatforms have important potential applications in monitoring therapeutic benefit of drug

In collaboration with E.Gultepe, F.Reynoso, D.Tada, D.Nagesha, Y.Patel, C.diMarzio, R.Campbell, A.Jhaveri, R.Sawant, V.Torchilin, M.Amiji, S.Saha and D.O'Malley. This work was supported by the National Science Foundation through NSF-0504331 IGERT Nanomedicine Science and Technology and by the Electronic Materials Research Institute, Northeastern University.

7574-09, Session 1

A nonlinear theory for the optical property of gold nanorods

J. Lin, Jr., New Vision Inc. (Taiwan) and National Taiwan Univ. (Taiwan); Y. Hong, C. Chang, National Taiwan Univ. (Taiwan)

Gold nanoparticles (GNPs) have been extensively studied for their applications in both imaging(sensing) and therapy. These GNPs include nanospheres, nanorods, nanshells, nanostars, nanotubes and other shapes. Theoretical studies for the surface plasmon resonance (SPR) properties of GNPs have focused on the key parameters of: the maximum absorption wavelength (W), the extinction coefficients, the refractive index sensitivity (RIS), the resonance line width (RLW, FWHM), and the figure of merit (FOM) defined by RIS/RW. For gold nanorods (GNR), Gans theory was used for the above-described key parameters which, however, are limited to the linear approximation (LA) for both the gold real dielectric constant and the polarization factor (P) defined by the aspect ratio(R). The LA suffers huge errors particularly for small R<2 and large R>5.

This study presents a nonlinear theory for more accurate results covering a wide range of R=(1.0 -10). Our calculated results show the following important features: (a) the LA underestimates W and overestimates RIS; (b) The RIS is an increasing function of R, W and the medium index (n); (c) the range of RIS is (100-1000) nm/RIU for R=(1-10); (d) for FWHM=(30-120) nm, the corresponding FOM=(1-12) with maximum value at optimum R=(3.5-4.5) depending on n=(1.33-1.5); where the optimum FOM of gold nanorod is about 5 times of nanoshell showing huge potential for biosensing applications...

7574-10, Session 1

Dependence of numerical aperture on sizes of subwavelength circular apertures

Y. M. Wang, G. Zheng, C. Yang, California Institute of Technology (United States)

Optofluidic microscopy (OFM) is a compact lensless imaging technique developed by our group. Image formation is based on projection images of objects microfluidically moved across a 1D array of micrometersized apertures on a metal-coated CMOS. Intuitively, resolution of the system depends on aperture size. In this work, we characterize this dependence by theoretical model and experimental measurements of acceptance angles of sub-micrometer circular apertures in metal films. Acceptance angles directly relate to numerical aperture (NA) and image resolution. We model a plane wave incident at varying angles on a subwavelength aperture in a PEC film. In the current model, total power transmitted is detected by a large NA detector. Simulation results show at large aperture limit (~ 3 wavelengths), acceptance angle approaches 60 degrees, as expected. Acceptance angle falls to approximately 40 degrees as aperture size approach zero mode cutoff. Decreasing aperture diameter below this results in an increase in acceptance angle. This trend closely agrees with data obtained from experiments where light incident at varying angles transmitted through circular apertures in 200nm thick titanium films is collected by a 100x oil immersion objective and detected by a CCD camera. Notably, the point of inflexion in the trend found experimentally is accurately predicted by the model. Reduction of discrepancies in exact values of the acceptance angle is expected with an improved theoretical model incorporating a limited NA detector. These experiments help to determine the optimal aperture size for the OFM and provide an estimation of achievable resolution for the system.

Conference 7574: Nanoscale Imaging, Sensing, and Actuation for Biomedical Applications VII



7574-11, Session 2

Modified multi-walled carbon nanotubes potentially suitable for intracellular pH measurements

F. Baldini, Istituto di Fisica Applicata Nello Carrara (Italy); G. Giambastiani, Consiglio Nazionale delle Ricerche (Italy); A. Giannetti, G. Ghini, Istituto di Fisica Applicata Nello Carrara (Italy); G. L. Puleo, Consiglio Nazionale delle Ricerche (Italy); C. Trono, Istituto di Fisica Applicata Nello Carrara (Italy)

Multi-walled carbon nanotubes (MWCNTs) are proposed as macromolecular carriers for pH detection inside cells. A bis-ethylen glycol fluorescein derivate was covalently bound to carboxyl functionalized MWCNTs. Ether chains were bound in the correspondence of the carboxylic group of the dye, paying attention not to affect its fluorescence properties and its pH dependence. The ether spacers have a twofold function: i) to separate the dye from the nanotube in order to prevent the fluorescence quenching; ii) to provide a better water solubility to the final product. The presence of the dye bound on MWCNTs was demonstrated by infrared spectra that show the characteristic absorption bands of the carboxyl ester groups and of the ether chain of the dye. Elementary analysis performed on the achieved samples revealed a ratio of 0.018mmol of dye per 100mg of sample. The pH dependence of the modified nanotubes was investigated interrogating, after suitable sonication, a solution of MWCNTs the pH of which was adjusted in the range 4-9 pH units by adding drops of hydrochloric acid and sodium hydroxide. Light from a halogen lamp was suitably filtered at 480 nm with a high pass-band filter and coupled to an optical fibre which illuminates the solution. A second optical fibre, at 90° with the respect to the first one, is connected with a Hamamtsu spectrum analyzer for the recording of the fluorescence spectra. The modified MWCNTs exhibited a linear pH dependence in the range between 6 and 8 pH units with a sensitivity less than 0.1 pH units.

7574-12, Session 2

AFM imaging and manipulation of cytoskeleton proteins on surfaces

S. Dobroiu, Univ. of Liverpool (United Kingdom); M. Naldi, V. Andrisano, Univ. of Bologna (Italy); D. V. Nicolau, Univ. of Liverpool (United Kingdom)

No abstract available.

7574-13, Session 2

Plasmon-enhanced near-field detection and imaging with metal nanostructures

K. Kim, D. Kim, Yonsei Univ. (Korea, Republic of)

Evanescent field-based imaging techniques, such as total internal reflection fluorescence microscopy, are widely used to observe molecular events near cell membranes. Fluorescence agents such as dyes or quantum dots are excited in the penetration depth of an evanescent field, which is typically smaller than 100 nm. This provides an extremely high depth resolution difficult to achieve in epifluorescence or confocal imaging microscopy. The characteristics of an evanescent field can be easily modified by depositing metal thin films and exciting surface plasmons. In this paper, we explore the imaging characteristics when evanescent fields are excited, modified, and localized by surface nanostructures and present significant enhancement of field intensity and spatial resolution based on the coupled localized plasmon excitation using various nanostructures. We first calculated near-field intensity and plasmon resonance conditions using finite-difference time-domain method and rigorous coupled-wave analysis to find an optimum

design. Various nanostructures, such as nanogratings, nanoholes, and nanoisland patterns were fabricated and characterized using electron beam lithography. The field enhancement was verified on a quantitative basis by exciting and imaging fluorescent beads and qualitatively using biological targets eg. cells. The enhancement was also confirmed by label-free measurements of various biomolecular processes including SAM formation and DNA hybridization.

7574-14, Session 2

Modeling of biological nanostructured surfaces

P. D. A. Cristea, R. A. Tuduce, O. Arsene, A. Dinca, D. I. Nastac, Polytechnical Univ. of Bucharest (Romania); D. V. Nicolau, F. Fulga, Univ. of Liverpool (United Kingdom)

The paper presents a methodology using atoms and amino acid hydrophobicity describing the surfaces properties of proteins in view of predicting of interactions with artificial nanostructured surfaces and with other proteins. A local standardized pattern is built around each atom from the surface of the molecule for a radius scalable in terms of its type and size A clustering algorithm has been developed to classify the resulting patterns and to identify possible interactions. The methodology is implemented in a software package based on Java technology deployed in a Linux environment.

7574-15, Session 3

Optofluidic biochemical sensor based on antiresonant optical waveguides

R. Biswas, Univ. at Buffalo (United States); E. P. Furlani, Univ. at Buffalo (United States) and Eastman Kodak Inc. (United States); N. M. Litchinitser, Univ. at Buffalo (United States)

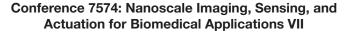
We propose a novel optofluidic biochemical sensor wherein detection is based on the contrast between the refractive index of the target material and the ambient carrier fluid. The sensor consists of multiple parallel fluidic microchannels that have a periodic spacing, and run normal to the surface of a substrate. The central microchannel is illuminated with a focused beam of light, and the transmission spectra through the substrate depend on the dimensions and refractive index of both the carrier fluid and the substrate material. Sensing is achieved via accumulation of a thin layer of target material on the surface of the microchannel walls, which are functionalized to bind with the material as it flows through the system. The presence of the layer causes a shift in the transmission spectrum of the sensor due to the contrast between the refractive index of the target material and the ambient carrier fluid. We use analytical predictions based on antiresonant reflecting optical waveguide model and 2D full-wave time-harmonic field analysis to design the device and to study the field distribution and transmission spectrum of the sensor. Our analysis demonstrates that detectable shifts in transmission can be accurately predicted and achieved and that the sensor hold potential for compact and low-cost biochemical sensing applications.

7574-16, Session 3

Detecting protein on a diffractive optical balance

X. Wang, M. Zhao, D. D. Nolte, Purdue Univ. (United States)

Diffraction-based biosensors detect diffracted light from protein patterned on a solid substrate. The sensitivity of these biosensors is due to the separation of the weak off-axis diffracted protein signal from the noise of the probe light. However, printing proteins in a micro-pattern can be difficult and with inconsistent quality. We have fabricated a novel





diffractive biosensor in which the substrate, rather than the protein, is patterned into a diffraction grating using photolithography. The protein can be easily printed or immobilized over the grating in an arbitrary pattern and size without compromising the sensitivity. The key feature of the fabricated grating that gives it high sensitivity to captured protein is its performance as an optical balance, composed of two opposite interferometric guadratures with equal but opposite protein response.

This biosensor is called a diffraction land-contrast BioCD (DLC BioCD) analogous to a conventional BioCD which detects protein with interferometry. In the DLC BioCD, gratings consisting of grooves 65 nm deep with an 8 µm periodicity are etched into 200 nm SiO2 on a silicon wafer. The first-order diffraction is proportional to |r1-r2|^2 where r1 and r2 are the reflection coefficients on 200 nm SiO2/Si and 135 nm SiO2/Si. r1≈r2 for 488 nm wavelength light at normal incidence, so the grating generates nearly zero first-order diffraction. After applying a protein layer on the SiO2, the complex values of r1 and r2 change oppositely on the complex plane. Therefore the change of |r1-r2|^2 caused by protein is maximized while the near-zero background significantly improves the sensitivity for protein detection. Experiments show that signal-to-noise ratio of the protein signals is improved by a factor of 4 compared to a conventional BioCD, with further improvements possible.

7574-17. Session 3

Label-free detection of biomolecules using LED technology

N. Wu, W. Wang, Y. Ling, L. Farris, B. Kim, M. J. McDonald, X. Wang, Univ. of Massachusetts Lowell (United States)

This paper presents a label-free biosensor using two Light Emitting Diodes (LEDs) as light sources and a photo detector as a receiver. The sensor uses a silica-on-silicon wafer with PMMA (Poly[methyl methacrylate]) as the functional layer. The principle of this biosensor is based on the Fabry Perot (FP) interferometer. A thickness of a 100 nm PMMA layer is spin-coated on the silicon wafer, which has a thin thermal oxide layer of a 500 nm. In such a configuration, the PMMA layer and silica layer function as an FP cavity. When a light illuminates the surface of the sensor, the reflections from the PMMA-air and silica-silicon interfaces will interfere with each other. Consequently, the change of the cavity length, which is caused by biomaterial binding on the PMMA layer, will result in a red shift in the reflection spectrum. An intensity change of the reflection light will be observed on an individual wavelength. In order to eliminate environment noise and to enhance the sensitivity of the sensor, two LEDs, whose center wavelength is chosen on both sides of the spectrum notch, are introduced in the system. A photo detector will obtain the intensities of the two individual reflected lights alternatively and transduce the signal into a data acquisition system. Long-term tests have shown that the sensor is resistant to environmental fluctuation. Biolinker ProteinG was used for binding tests. The sensor shows great potential in biotest applications due to its compact size and low cost.

7574-18, Session 3

Fluorine surface modification of organosilica nanoporous sol-gel glasses host matrices enhance the protein folding process

F. Menaa, B. Menaa, C. A. Guimaraes, Fluorotronics, Inc. (United States); L. Avakyants, Lomonosov Moscow State Univ. (Russian Federation); O. N. Sharts, Fluorotronics, Inc. (United States)

Organic-inorganic nanoporous silica sol-gel glasses constitute the ideal support for protein bioencapsulation and for studying the different factors influencing the protein folding process in a crowded environment. The enhancement of the protein folding in such host matrices is important to develop efficient bionanodevices (e.g., biocatalysts, sensors) and find novel therapies against diseases that are due to protein misfolding (e.g. Alzheimer). Modified "wet-aged" silica-based glasses, obtained via solgel process, can be used to mimic the protein local micro-environment

and tune the properties (e.g., surface hydration, crowding, hydrophobicity etc.) influencing the protein folding. The incorporation of fluorine into amino-acids became a prominent strategy to enhance the structural stability of peptides and proteins [1]. Numerous studies showed that silica-based nanoporous glasses can stabilize bioactive proteins due to the hydrophobic effect [2]. For instance, the increase of ellipticity and folding of apomyoglobin encapsulated or adsorbed in fluorinated sol-gel glasses (e.g., fluorinated silica matrix trifluoropropyltrimethoxysilane) has been enlightened using CD Spectroscopy with signals observable at 222 nm characterizing the secondary structure at the far UV [3]. The results demonstrated the critical effect of fluorine on the protein folding near to its native state. Following our statements on the role of fluorine, its incorporation to new sol-gel glass systems might bring both steric and hydrophobic effects to enhance the protein folding.

Eventually, the precise role of fluorine on the protein folding enhancement is further investigated by our group at Fluorotronics, Inc. (www. fluorotronics.com) using a patented technology known as Carbone-Fluorine Raman Spectroscopy [4].

7574-19, Session 4

Tuning the feature size of nanostructured materials for improved infiltration and detection of small molecules

S. M. Weiss, Y. Jiao, J. L. Lawrie, G. Gaur, J. D. Ryckman, D. S. Koktysh, Vanderbilt Univ. (United States)

Nanostructured materials offer several advantages for biosensing applications. In particular, nanoscale porous materials possess a very large reactive surface area to facilitate the capture of small molecules, and they have the capability to selectively filter out contaminant molecules by size. In this work, we address the issues of efficient molecule infiltration and immobilization inside nanoscale pores and the influence of nanostructured feature size on small molecule detection sensitivity. Porous silicon with variable porosity and pore sizes between 10nm and 100nm are used as the model system. DNA oligos of different lengths and quantum dots of different sizes are selected to evaluate infiltration into the porous silicon samples. The role of surface functionalization will also be discussed.

7574-20, Session 4

Electrophoretic entrapment of nano particles into a size-dependent-nanoarray for optical immunosensing

J. Han, S. Lakshmana, H. Kim, S. J. Gee, B. D. Hammock, I. M. Kennedy, Univ. of California, Davis (United States)

A nanoarray, integrated with an electrophoretic system, was developed to detect multiple biological reagents. This nanoarray overcomes the complications of losing the function and activity of the protein binding to the surface in conventional microarrays by using nano-scale-amounts of sample. The nanoarray is also superior to other biosensors that use immunoassays in terms of lowering the limit of detection to the femtoor atto-molar level. In addition, our nanoarray is able to simultaneously detect two different kinds of targets on a single chip by maneuvering trapping locations of antibody-immobilized-nanoparticles with different physical sizes. The channels were patterned onto a PMMA coating on conductive indium tin oxide (ITO)-coated glass slide by using e-beam lithography. Two hundred nm or 100 nm-carboxylated-fluorescentnanoparticles were conjugated with mouse IgG or rabbit IgG respectively. The suspensions of 200 nm nanoparticles then were added to the glass chip followed by adding 100 nm nanoparticles with a droplet. On top of the droplet, another ITO-coated-glass slide was covered. Negatively charged fluorescent nanoparticles were selectively trapped onto the positively charged ITO surface at the bottom of the channel, based on the size of the particle and channel. The anti-rabbit or anti-mouse IgG

Conference 7574: Nanoscale Imaging, Sensing, and Actuation for Biomedical Applications VII



conjugated with fluorescent labels (Alexa 350 and FITC) were then added to the chip. A confocal laser scanning microscope was employed to observe fluorescent images of the nanoarray. Quantification of secondary antibody bound to primary antibody was performed by using optical fibers for excitation and collection of emission. The intrinsic fluorescent signals from 200 nm-fluorescent nanoparticles (blue emission) or 100 nm-fluorescent nanoparticles (green emission) trapped on the nanoarray were used as internal standard signals for the assay.

7574-21, Session 4

Optimum time and space resolution for tracking motile nano-objects

F. Fulga, Univ. of Liverpool (United Kingdom)

No abstract available.

7574-22, Session 4

New directions in AFM bio-imaging in liquids

D. Lewis, R. Dekhter, G. Fish, S. Kokotov, M. Kokotov, H. Taha, Nanonics Imaging Ltd. (Israel); A. Lewis, Hebrew Univ. of Jerusalem (Israel) and Nanonics Imaging Ltd. (Israel)

Atomic force microscopy with tuning fork feedback is the best method of AFM imaging known today. We now report the operation of this feedback mechanism in liquids. This allows for liquid cell AFM and NSOM operation in physiological media without optical or mechanical constraints or interference. The use of this feedback mechanism in liquids for scanned probe microscopy liquid cell imaging permits working transparently with any optical microscope including upright, 4 pi or standard Raman microprobes. It will be shown that water immersion objectives can also be used with multiprobe atomic force microscopy for imaging in physiological media and transparently integrating with nanopipette SPM probes, for conductance and futuristic structurally correlated patch clamp applications.

7574-23, Session 4

Plasmonic optical antennas excited by guided mode resonance for SERS applications

J. Li, D. A. Fattal, Z. Li, Hewlett-Packard Labs. (United States)

To use periodic structures for Raman spectrocopy applications possesses at least two distinctive advantages over the conventional rough-surface based surface enhanced Raman spectroscopy. Firstly, the position of the high field intensity and the exact field magnitude is well controlled by the design, rather than randomly distributed over the surface of the device. Secondly, the constructive interference from the elements placed in periodic array may form a collective resonance and provide a further enhancement to the field intensity. In this paper we present a design of SERS substrates by integrating the guided mode resonance (GMR) of a dielectric grating with optical nano-antennas made of plasmonic materials. The GMR of the grating provides a spatially confined, enhanced electromagnetic (EM) field which is weakly coupled with the localized surface plasmon resonance of the optical nanoantennas that are also field-enhancing devices. A field intensity much higher than that of a similar optical antenna on a bare substrate (i.e. no gratings) can be achieved, as demonstrated by numerical simulation. We also perform a rigorous numerical analysis to simulate the influence of the device to the radiation of an excited molecule. By this means we achieve not only the enhancement of the device to the radiation process of the Raman scattering, but also a knowledge about the angular distribution of the radiated Raman signal into the space, and the portion of the Raman signals that is coupled to the guided mode of the grating.

7574-24, Session 4

Photo-driven nano-impellers and nanovalves for on-command drug release

J. I. Zink, J. F. Stoddart, E. Choi, Univ. of California, Los Angeles (United States)

Mesostructured silica thin films and particles prepared by surfactanttemplated sol-gel techniques are highly versatile substrates for the formation of functional materials. The ability to deliberately place molecules possessing desired activities in specific spatially separated regions of the nanostructure is an important feature of these materials. Such placement utilizes strategies that exploit the physical and chemical differences between the silica framework and the templated pores, and enables molecular machines to be synthesized. Three types of molecular machines that are based on molecules that undergo large amplitude motion when attached to mesoporous silica are described: impellers, valves and snap-tops. Derivatized azobenzene molecules, attached to pore walls by using one of the placement strategies, function as impellers that can move other molecules through the pores. Nanoparticles containing anticancer drugs in the mesopores are taken up by cancer cells. These systems are the first examples of artificial molecular machines operating under remote control inside of living cells. Rotaxanes and pseudorotaxanes, placed at pore entrances, function as gatekeepers or valves that can trap and release molecules from the pores when stimulated. Examples of these machines and their operation are discussed. A new type of biocompatible nanodevice based on mesoporous silica nanoparticles with pore openings controlled by "snaptop" covers will be introduced. When closed the snap-top contains the guest molecules but releases them following cleavage of the stopper. Snap-tops that are responsive to light and to specific enzymes for selfopening operation inside of cells is described in detail.

7574-25, Session 4

Dry etched nanoporous silicon substrates for optical biosensors

M. Hajjhassan, M. Cheung, T. Gonzalez, V. P. Chodavarapu, M. P. Andrews, McGill Univ. (Canada)

Porous nanostructured materials such as Porous silicon offer an attractive platform for the encapsulation of chemical and biological recognition elements. Porous silicon is a crystalline material with large internal surface area consisting of nanometer to micron-sized pores in a silicon matrix. To date, porous silicon based chemical and biological sensors have been developed using a variety of optical platforms including waveguides, filters, microcavities, and Bragg mirrors. For these applications, porous silicon is fabricated either by electrochemical etching using hydrofluoric acid or wet photolithographic processing techniques. Here, we demonstrate the fabrication of porous silicon using a simple dry etching technique. The Xenon Difluoride (XeF2) etching technique allows selective formation of porous silicon where a standard hard baked photoresist layer can serve as a masking layer. The pore size, morphology, and thickness of the fabricated porous silicon layer can be easily controlled in the etching process. Using the XeF2 etching technique, we demonstrate free standing ultra-thin films of porous silicon that are only 5µm thick and used for biological sample filtering. Further, we employ the porous silicon as a substrate for the immobilization of sol-gel derived xerogel thin films that encapsulate specific analyte responsive luminophores in their nanostructured pores. The porous silicon layers behave as an optical interference filter which allows efficient and selective detection of the wavelengths of interest. Specifically, we demonstrate a gaseous oxygen sensor by encapsulating a rutheniumbased luminophore within the xerogel material.

Conference 7574: Nanoscale Imaging, Sensing, and Actuation for Biomedical Applications VII



345

7574-26, Session 4

CMOS camera-on-a-chip for fluorescence life-time imaging

M. M. Eldesouki, M. J. Deen, Q. Fang, McMaster Univ. (Canada)

Fluorescence optical imaging is becoming a very important technique for in-vivo imaging and characterization of biological tissues. In order to add more contrast to the fluorescence image, fluorescence life-time imaging (FLIM) can be used, making it possible to differentiate between molecules with overlapping spectra, such as cancerous and noncancerous cells. However, designing FLIM imaging systems in a compact, complete camera-on-chip solution is a very challenging task and has led to significant research efforts in designing high-speed and high sensitivity imagers.

Such high-speed imaging has become possible with the significant advances in deep submicron CMOS technologies. Since there is a practical limit on the minimum pixel size, CMOS technology scaling can allow for an increased number of transistors to be integrated. Such smart pixels truly show the potential of CMOS technology for imaging applications allowing CMOS imagers to achieve the image quality and global shuttering performance necessary to meet the demands of ultrahigh speed applications.

This research work focuses on designing low-light level imagers in CMOS technology for biomedical applications that can be suitable for extremely high-speed applications, such as fluorescence lifetime imaging (FLIM) that is used for cancer diagnosis. This work will discuss the design and implementation of an ultrahigh speed active-pixel sensor CMOS imager that can capture 8 frames at an acquisition rate of 1.25 billion fps. This work also discusses the design and implementation of single-photon avalanche-photodiode based complete camera-on-a-chip with a low dead time.

7574-27, Session 4

Neuromorphic optical sensor chip with color change-intensity change disambiguation

A. H. Titus, Univ. at Buffalo (United States)

No abstract available.

7574-28, Session 4

Applications and developments of carbonefluorine spectroscopy

F. Menaa, B. Menaa, C. A. Guimaraes, Fluorotronics, Inc. (United States); L. Avakyants, Lomonosov Moscow State Univ. (Russian Federation); O. N. Sharts, Fluorotronics, Inc. (United States)

Carbon-Fluorine Spectroscopy is a patented platform technology using various methods and a family of devices called PLIRFATM ("Pulsed Laser Isochronic Raman and Fluorescence Apparatus") developed by Fluorotronics, Inc. (www.fluorotronics.com). The key feature of this technology is based on the discovery of a characteristic optical signature of carbon-fluorine bond(s) in the fingerprint spectral area of 550 cm-1 and 950 cm-1 allowing detection, characterization, imaging. and measurement of fluoroorganics. The FRS method is ultra-specific, ultra-sensitive, non-destructive, rapid, require no sample preparation, easy to use and therefore cost effective. Furthermore, the C-F bond signal is directly proportional to the concentration of the analyte, allowing a quantitative determination of F-labelled compounds. Since the C-F bond is unique in its character, it can be used as an external or internal chemical tag/molecular marker. Furthermore, the C-F label is efficient, soluble, cheaper, smaller, more stable and less toxic than fluorescent dyes, nanoparticles or quantum dot materials. Consequently, FRS can be used for numerous applications. For instance, C-F bonds are often incorporated into pharmaceutical, agrochemical and biological molecules as well as in polymers and nano-materials to achieve special properties (e.g. molecular stability, tracing a compound during the production or the synthesis cycle). FRS is applicable for multiplexing, high throughput analysis of any type of fluoroorganics in various media, in any physical state as well as in cells.

Eventually, Fluoro-Raman spectroscopy represents a powerful and flexible technology. We will present some of our promising data and review the most important applications of our patented technology.

Return to Contents TEL: +1 360 676 3290 · +1 888 504 8171 · customerservice@spie.org



Saturday-Monday 23-25 January 2010 • Part of Proceedings of SPIE Vol. 7575 Colloidal Quantum Dots for Biomedical Applications V

7575-01, Session 1

Plasmon rulers for measuring dynamical distance changes in biological macromolecular assemblies (Keynote Presentation)

A. P. Alivisatos, Lawrence Berkeley National Lab. (United States) and Univ. of California, Berkeley (United States)

The intensity and spectral signature of light scattering from Au nanocrystals depends strongly upon their separation. This phenomenon can be used to construct a spectroscopic ruler for monitoring the assembly and deformations of macromolecular complexes. The ruler consists of two particles joined by an oligonucelotide or peptide. The oligo or peptide motion changes the distance between the particles resulting in a change in the light scattering. These plasmon rulers can be used to study the mechanisms of DNA cleavage by restriction enzymes. A second application involves the study of protease activity and caspase 3 activation in apoptosis. New nanocrystal molecules consisting of pyramidal and chiral arrangements of metallic and semiconductor nanocrystals will also be described.

7575-02, Session 2

Rare earth doped oxide nanoparticles for biomedical imaging: development of particles with enhanced properties

T. Gacoin, G. Mialon, S. C. Türkcan, A. Alexandrou, J. Biolot, Ecole Polytechnique (France)

Rare earth doped oxides represent a well known class of phosphor materials with many applications in light emitting devices. For several years, our two groups have been involved in researches concerning the application of these systems as nanoparticles for biological imaging. The objective was to take advantage of the original optical properties of rare earth emission, and interesting results have been obtained so far [1-4]. We here describe a detailed investigation of the emission properties of nanoparticles, with the aim to understand their commonly observed altered properties as compared to the bulk reference materials. This is usually attributed to the detrimental effect of surface states that quench the excited states involved in the emission process. We study the influence of crystalline defects that are present due to the low temperature synthesis of 30-nm sized YVO4:Eu nanoparticles. Annealing treatments up to 1000°C in a porous silica matrix allow the recovery of perfectly crystalline particles as colloidal suspensions. Emission properties of pristine and annealed particles are compared with those of the bulk material. A simple model of the emission process allows an accurate fit of the luminescence decay and of the dependence of the quantum yield on europium content. Our results show that pristine particles exhibit altered emission properties mainly due to quenching from defects, among which surface OH groups, and altered energy transfers within the particle. Annealed particles exhibit properties that are almost the same as those of the bulk material, except that the emission yield for the optimum Eu content is limited to 40% instead of 70% for the bulk material. We show that the difference may be simply explained by the difference of radiative lifetime that results from the lower effective refractive index in the case of the particles. This effect then seems to be the ultimate limitation for the emission properties of perfectly well crystallized nanoparticles as compared to the bulk material. This work provides an example of a general strategy toward the investigation of the physical properties of nanocrystals which physical properties may be altered by crystalline defects.

- [1] Buissette, V.; Giaume, D.; Gacoin, T.; Boilot, J.-P. J. Mater. Chem. 2006, 16, 529-539.
- [2] Casanova, D.; Giaume, D.; Beaurepaire, E.; Gacoin, T.; Boilot, J.P.; Alexandrou, A. Appl. Phys. Lett. 2006, 89, 253103.
- [3] Casanova, D.; Giaume, D.; Gacoin, T.; Boilot, J.P.; Alexandrou, A. J. Phys. Chem. B 2006, 110, 19264-19270.
- [4] Casanova, D.; Giaume, D.; Moreau, M.; Martin, J.L.; Gacoin, T.; Boilot, J.-P.; Alexandrou, A. J. Am. Chem. Soc. 2007, 129, 12592-12593.

7575-04, Session 2

Silica capped CdS/Cd(OH)2 quantum dots for biological applications

C. R. Chaves, Univ. Federal de Pernambuco (Brazil); D. Almeida, Univ. Estadual de Campinas (Brazil); A. Fontes, Univ. Federal de Pernambuco (Brazil); C. Lenz Cesar, Univ. Estadual de Campinas (Brazil); B. S. Santos, P. M. A. Farias, Univ. Federal de Pernambuco (Brazil)

Nanoparticles of fluorescent semiconductor, quantum dots (QDs), are a promising class of materials in the labeling of biological systems. They have been increasingly used in biolabeling recently as their advantages over molecular fluorophores have become clear. Even though they have several advantages over the conventional biolabels, the presence of elements as cadmium, tellurium and selenium is still a concern and so efforts are being made in order to prevent the release of these substances in the biological media. One solution proposed is the SiO2 coating. The silica is an extremely stable and resistant material, providing a good isolation between the quantum dot and the media. In this work we report the production of silica coated core/shell CdS/Cd(OH)2 QDs for biological applications. The silanization process was adapted from processes described in the literature for II-VI semiconductor nanoparticles. In the quantum dot formation step a cadmium hydroxide shell is formed and this passivation layer serves as a surface nucleating agent, enabling the silanization process directly in the quantum dot without the need of any further surface preparation. The silanized CdS QDs (5-7 nm) were characterized by optical spectroscopies (absorption, excitation and emission) and by transmission electronic microscopy showing good emission properties potentializing its use as biocompatible fluorescent probes.

7575-05, Session 3

One-sided growth of large plasmonic gold domains on CdS quantum rods observed on the single particle level

C. Sönnichsen, L. Carbone, A. Jakab, Y. Khalavka, Johannes Gutenberg Univ. Mainz (Germany)

Until now, it has not been possible to control the metal size in hybrid semiconductor-metal nanoparticles. The gold domains were typically in the order of 2.0 nm in diameter when reacting CdS nanorods in anaerobic condition and eventually just overcame 10 nm when ripened for 3 days in the presence of oxygen for nanorods longer than 50 nm. Since plasmons in gold nanoparticles are strongly damped for particle diameters below 10-20 nm by surface scattering and the size dependent d-band-Fermilevel offset, the poorly understood interaction between plasmons and excitons could not be studied in detail in such hybrid particles.

Here, we provide a strategy for creating large gold domains of controlled size (up to 15 nm) on CdS or CdSe/CdS quantum rods through the photo-reduction of gold ions. The metal deposition is promoted and



controlled by UV light irradiation under anaerobic conditions. The large gold domain supports efficient plasmon oscillations with a light scattering cross section large enough to visualize single hybrid particles in a dark-field microscope during the particle growth in real time.

7575-06, Session 3

Synthesis and surface modification of highly fluorescent gold nanoclusters and their exploitation for cellular labeling

C. J. Lin, C. Lee, J. Hsieh, W. Yu, Chung Yuan Christian Univ. (Taiwan); R. Sperling, Philipps-Univ. Marburg (Germany); H. Wang, H. Yeh, Mackay Memorial Hospital (Taiwan); W. J. Parak, Philipps-Univ. Marburg (Germany); W. H. Chang, Chung Yuan Christian Univ. (Taiwan)

We introduce a general approach to make small gold nanoclusters (NCs) in organic phase. For this purpose gold nanoparticles prepared from a one-phase reaction either with or without purification by methanol precipitation are etched into small NCs by the gold precursor solution. The etched gold NCs lose their surface plasmon properties and lead to a yellowish or even colorless transparent solution, whereas the original larger gold nanoparticles possess strong surface Plasmon absorption around 520~530 nm. The addition of freshly reduced lipoic acid can replace the surfactants on the etched gold NCs via the formation of strong dithiol-Au bonds, whereby the acid headgroup points towards the solution. Upon such ligand exchange with lipoic acid the gold NCs become red-emitting fluorophores. By deprotonization under basic buffer, the etched gold NCs become water-soluble and form a monodispersion stabilized by electrostatic repulsion. The fluorescent gold nanoclusters can perform a variety of bioconjugation process such as PEGylation, biotinylation as well as forming complex nanobioconjugates with streptavidins. The brightening effects under proper surface modification are also reported. The clusters have a decent quantum yield, high colloidal stability, and can be readily conjugated with biological molecules. Specific staining of cells and nonspecific uptake by living cells is demonstrated. C.-A. J. Lin, T. Y. Yang, C. H. Lee, S. H. Huang, R. A. Sperling, M. Zanella, J. K. Li, J. L. Shen, H. H. Wang, H. I. Yeh, W. J. Parak, W. H. Chang, (2009). "Synthesis, Characterization, and Bioconjugation of Fluorescent Gold Nanoclusters toward Biological Labeling Applications." ACS Nano 3(2): 395-401.

7575-07, Session 3

Biocompatible water soluble UV-blueemitting ZnSe quantum dots for biomedical applications

J. Andrade, A. G. Brasil, Jr., C. Azevedo, B. Barbosa, P. Farias, A. Fontes, B. S. Santos, Univ. Federal de Pernambuco (Brazil)

ZnSe quantum dots (QDs) are wide-band gap materials suitable for UV-blue-emitting applications like laser diode or biolabeling probes. They are also appropriate as passivating agents for luminescence enhancement of core-shell nanocrystals and host for the formation of doped nanostructures. Organometallic approaches have been proposed for preparing these kinds of QDs with high quantum yield (QY), high crystallinity and monodispersity. However, chemicals used in these procedures are toxic, expensive and pyrophoric. Aiming to develop a more simple and applicable methodology many research groups are working in alternative methods to synthesize blue-emitting ZnSe nanocrystals in aqueous media. This work shows a new experimental methodology for obtaining water soluble colloidal synthesis and postpreparative treatment of thiol-stabilized ZnSe QDs for application as biophotonic probes. In additional, zinc based QDs are less toxic than cadmium QDs for in vivo assays. These nanoparticles were synthesized by a simple methodology based on the arrested precipitation of ZnSe. The structural characterizations, performed by X-Ray diffraction and

Transmission Electron Microscopy, show that QDs are in a strong confinement regime, with diameters in the range of 2.5 nm, and have a characteristic zinc blend crystalline structure. QDs optical properties present a large Stokes's shift between the absorption band (360 nm) and the emission peak (420 nm) with a half-media peak enlargement of about 30 nm. The post UV-irradiation treatment of ZnSe QDs improved their luminescence properties leading to a high blue band gap emission.

7575-08, Session 4

Fabrication of biocompatible nanoparticles for molecular imaging and drug delivery

H. Weller, Univ. Hamburg (Germany)

The talk describes recent advances in the synthesis of highly luminescent and magnetic nanoparticles. It is shown that preparing the particles under continuous flow conditions allows reproducibility far beyond the limits of batch synthesis.

Special emphasis is put on the development of a protocol for ligand exchange against alpha-omega-substituted polyethylene-oxide containing ligands. It is shown that small changes in the composition result in tremendous differences in stability against serum and buffer solutions and fluorescence quantum efficiencies in the biological environment. We present various types of ligands allowing reproducible and stable fluorescence properties of quantum dot systems.

We further present in-vitro and in-vivo data on cell toxicity and molecular imaging with such modified quantum dots and superparamagnetic iron oxide nanoparticles. Examples for in vivo tumor targeting are given.

7575-09, Session 4

Taking advantage of unspecific interactions to orient antibodies on magnetic nanoparticles

J. Martinez de la Fuente, P. del Pino, S. Puertas, Univ. de Zaragoza (Spain); P. Batalla, R. Fernandez-Lafuente, J. M. Guisan, Instituto de Catálisis y Petroleoquímica (CSIC) (Spain); V. Grazu, Univ. de Zaragoza (Spain)

There is a growing interest in the use of magnetic nanoparticles (MNps) for applications in drug delivery, MRI contrast agents and biosensors. In turn, it is necessary to develop strategies for the adequate biofunctionalization of these nanoparticles to be used in biotechnological and biomedical applications. Different biomolecules have been used to provide specificity and bioactivity to MNps but the stars among them are antibodies. This is due the high efficiency of antigen-antibody interaction plus to their high diversity that allows detecting a wide range of analytes (from big pathogens to small allergens).

All reported protocols used to immobilize antibodies by their constant (Fc) region leaving free the site where the antigen recognition take place (Fab regions) are more or less sophisticated. Thus, there is a need to develop very easy methodologies for the immobilization of non modified antibodies in an oriented way onto MNps. Here, we report a simple way to functionalize MNps via a two step strategy that involves a first ionic adsorption of the antibody followed by its further covalent attachment. The biological activity of antiperoxidase anchored to Nps by this two steps way was similar to those immobilized in an oriented form through their carbohydrate moieties. This implies that the Fab regions of the antibody are not involved during the attachment. This easy new functionalization technique is applicable to carboxilated or aminated Nps and almost all antibodies. Its potential is huge as it will be very useful for the development of more bioactive nanoparticles for diagnostic applications.



7575-10, Session 4

Interactions between a colloidal CdTe quantum dot and distinct functionalizer compounds

E. Leite, Univ. Federal de Pernambuco (Brazil); J. Sousa, Univ. Federal do Ceará (Brazil); K. Carvalho, A. G. Brasil, Jr., A. Fontes, P. Farias, B. S. Santos, Univ. Federal de Pernambuco (Brazil)

Biological applications of semiconductor quantum dots (QDs) are intrinsically related to QDs biocompatibility. In general, this condition is achieved by recovering QDs' surface with layers of organic compounds, such as mecapto acetic acid (MAA). This work presents and discusses the results obtained by using quantum mechanical calculations in order to investigate the interaction between colloidal cadmium telluride (CdTe) QDs and distinct functionalizer agents, which have been used in our experimental procedures. We studied the complexation interaction between simplified models of CdTe with the functionalizers mercaptoacetic acid (MAA), mercaptopropionic acid (MPA), trimetoxi mercapto silane (TMS) and cysteine (CYS). Small clusters with different numbers of Cd2+ and Te2- ions were used as models to describe the QD. Initially, we performed geometry optimization for isolated molecules of functionalizers as well as for isolated CdTe pairs. Then, each QDfunctionalizer was optimized by using a density functional approach via the GAUSSIAN 03 program package (B3LYP/LANL2DZ/6-31G* method). The results indicate that the stability increasing order between the QD and the functionalizers is the following: TMS < MPA < MAA < CYS. As another approach to study the same systems, we plan to use a better basis set including corrections for the basis set superposition errors to estimate more accurate energy values, to improve the QD model using a nanoparticle of 1.6 nm with an ONIOM methodology and finally to perform experiments to corroborate the theoretical results.

7575-11, Session 5

Energy conversion within the hybrid materials engineered from the nanocrystals quantum dots and photochromic membrane proteins

A. Sukhanova, CIC nanoGUNE Consolider Research Ctr. (Spain) and Univ. de Reims Champagne-Ardenne (France); A. Rakovich, Trinity College Dublin (Ireland); C. Mendicute, CIC nanGUNE Consolider Research Ctr. (Spain); N. Bouchonville, Univ. de Reims Champagne-Ardenne (France); Y. P. Rakovich, Trinity College Dublin (Ireland); M. Molinary, M. Troyon, Univ. de Reims Champagne-Ardenne (France); J. F. Donegan, Trinity College Dublin (Ireland); A. O. Govorov, Ohio Univ. (United States); I. Nabiev, CIC nanGUNE Consolider Research Ctr. (Spain) and Univ. de Reims Champagne-Ardenne (France)

Most photosensitive integral membrane proteins are not able to deal with the excess energy of photons from UV to blue region and normally do not absorb them at all. If high-energy photons were absorbed, they might destroy the light-harvesting chromophores or even induce apoptotic-like cell death. Thus, the energy efficiency of green plants is less than 5% and the energy-producing membrane protein bacteriorhodopsin (bR) not possessing specific light-harvesting system utilizes less than 0.5% of solar light. Nanotechnology opens the way to increase performances of biological functions. Summarizing the sources of energy losses provides an idea to optimization through the engineering of a built-on-the-membrane light-harvesting antenna from photoluminescent (PL) quantum dots (QDs) which might be able (1) to harvest light from deep UV to blue region, (2) to convert this energy to photons that can be absorbed by bR or photosynthetic reaction centers (RC), (3) to transfer this additional energy to proteins' chromophores thus effecting biological function.

Here we show that the combination of nanotechnology and genetic engineering permits developing hybrid materials build from QDs specifically selected to be optically coupled with the photochromic membrane proteins and with surfaces functionalized to be covalently tagged with desired amino acid residues of bR or RC membrane proteins. Such optical and spatial coupling forms efficient energy transfer donor / acceptor pairs operating in the FRET-regime and providing new hybrid materials with improved biological functions and advantages of stability and efficiency of light-controlled operation.

7575-12, Session 5

A quantum dot-fluorescent protein FRET probe for imaging intracellular pH

A. M. Dennis, W. J. Rhee, D. Sotto, G. Bao, Georgia Institute of Technology (United States)

Fluorescent resonance energy transfer (FRET) is the non-radiative transfer of energy from one molecule to another based on the proximity of the two molecules and their spectral overlap. This phenomenon has been harnessed to develop a sensitive fluorescent probe for measuring pH. A quantum dot (QD) is utilized as the donor, while the pH-sensitive fluorescent protein mOrange is used as the FRET acceptor. mOrange is a particularly useful FRET acceptor not only because of its high molar extinction coefficient and quantum yield, but also because the molar extinction coefficient of mOrange, not its quantum yield, changes with pH. Thus, both the QD quenching and mOrange emission are modulated by changes in pH. We found that at low pHs mOrange does not absorb or emit at its characteristic wavelengths, so the QD emission is high when excited at 400 nm. As the molar extinction coefficient of mOrange increases with pH, it quenches some of the QD emission through FRET and the ratio of the mOrange emission to the QD emission (FA/FD) increases more than 10-fold between pH 4.5 and 7.5. Using QDs as donors has added advantage of low photobleaching; QDs are inherently more photostable than organic dyes or fluorescent proteins and as mOrange absorbs light minimally at the excitation wavelength of 400 nm, the lifetime of the fluorescent protein is extended in this probe format as well. This probe holds great promise for applications in fluorescence imaging, including the tracking of molecules through endocytic pathways.

7575-13, Session 5

Energy transfer from terbium complexes to quantum dots: the advantage of independent donor and acceptor decay time analysis for investigations on FRET distance dependence

N. Hildebrandt, Fraunhofer-Institut für Angewandte Polymerforschung (Germany)

The efficient use of luminescent semiconductor quantum dots (QDs) as energy transfer (ET) acceptors can be accomplished with terbium complexes (TCs) as donors. TCs exhibit long excited state lifetimes (in the millisecond range) up to 105 times longer than typical QD lifetimes. When ET occurs from TCs to QDs the measured TC luminescence decay times decrease (ET quenching), whereas the QD decay times increase (ET sensitization). Although ET was demonstrated for the TC-QD donoracceptor pair it is doubtable that it is of Förster Resonance Energy Transfer (FRET) type. The mechanisms considered for the luminescent TC quintet-septet transitions are magnetic dipole and induced electric dipole transitions both not covered by FRET theory. As the relatively large QDs cannot be considered as point dipoles they do not match FRET theory either. We analyzed 10 different TC-to-QD donor acceptor systems with varying separation distances using the biological binding system of biotin (biotinylated QDs - Biot-QD) and streptavidin (TCs labeled to streptavidin - TC-sAv). By analyzing both donor and acceptor decay times we received an independent control of the assumed theoretical model of distance dependence. The acceptor luminescence decay curves of each FRET pair were fitted using the Förster type distance dependence assumption (r^-6), and the donor decay traces were fitted without assumptions concerning distance dependence. Both procedures lead to similar luminescence decay times and the resulting distances are in very



good agreement with the actual QD sizes. Therefore, our comprehensive data set gives good evidence for Förster type (r^-6) TC-to-QD energy transfer

7575-14, Session 5

Optical size determination of quantum dots using FRET with terbium complexes as donors

D. Geißler, H. Löhmannsröben, Univ. Potsdam (Germany); L. J. Charbonnière, R. F. Ziessel, Univ. Louis Pasteur (France); N. G. Butlin, Lumiphore Inc. (United States); I. L. Medintz, U.S. Naval Research Lab. (United States); H. Mattoussi, Florida State Univ. (United States): N. Hildebrandt. Fraunhofer-Institut für Angewandte Polymerforschung (Germany)

Due to their strong absorption over a broad wavelength range, luminescent semiconductor quantum dots (QDs) are, in principle, well suited as Förster Resonance Energy Transfer (FRET) acceptors in biomedical applications. However, as they are directly excited along with the donor when using steady-state fluorescence techniques, their use as acceptors has been limited. The use of lanthanide complexes (LCs) as FRET donors in combination with time-resolved detection effectively circumvents these issues. LCs exhibit long luminescence decay times up to five orders of magnitude longer than the QD decay times. Thus, directly excited QD luminescence can be efficiently suppressed by timegating (measuring after the complete decay of QD luminescence). We demonstrate the use of terbium complexes (TCs) as FRET donors and QDs as FRET acceptors for spectroscopic ruler measurements. The TCs were labeled to polyhistidine-appended peptides which self-assembled onto three different QDs emitting at 530, 578 and 635 nm, respectively. The QD emissions show very weak overlap with the Tb luminescence spectrum, making multiplexed detection possible. Förster distances of the TC-to-QD FRET systems were in the range of 60-75 and FRET efficiencies of up to 97 % were realized. Time-resolved analysis of donor and acceptor decay times allowed the determination of donoracceptor separation distances. The results are in good agreement with size estimations for the QD core-shell systems and peptide lengths. This suggests the efficient use of our TC-to-QD FRET systems for multiplexed optical size determination, molecular ruler measurements and multiparameter diagnostics.

7575-15, Session 6

Immobilization of quantum dots in multiple responsive microgels for biomedical applications

S. Zhou, W. Wu, T. Zhou, M. Aiello, College of Staten Island (United States)

We report a general and facile method for in-situ immobilization of QDs in smart microgels for multiple optical sensing with a high sensitivity. The thermal- and pH-dual responsive copolymer microgel of poly(Nisopropylacrylamide-acrylamide-acrylic acid) [p(NIPAM-AAm-AA)] was firstly synthesized, which could be further functionalized with a glucosesensitive phenylboronic acid (PBA) moiety to produce a glucose sensitive p(NIPAM-AAm-PBA) microgels. The amino groups of pAAm segments are designed to sequester the precursor Cd2+ ions for in situ formation of CdS QDs in the interior of microgels and stabilize the CdS QDs embedded in the microgels. The external stimuli such as temperature, pH, and glucose concentration change can induce a reversible swelling/shrinkage of the hybrid microgels, which can further modify the physicochemical environment of the QDs immobilized inside the microgels, resulting in a reversible photoluminescence (PL) quenching/ antiquenching. The temperature, pH, and glucose sensitivity of the PL intensity can be tuned through the composition and structure control of the template microgels. The method is extendable to other QDs with

specific emission wavelengths and other targeting ligands, thus it is possible to develop multifunctional hybrid micro-/nano-gels for additional important biomedical applications.

7575-16, Session 6

Ion and pH sensing with colloidal nanoparticles: the influence of surface charge on sensing and colloidal properties

W. J. Parak, F. Zhang, A. Ali Zulqurnain, F. Amin, Philipps-Univ. Marburg (Germany); M. Oheim, Paris Descartes (France); A. Feltz, Ecole Normale Supérieure de Cachan (France)

Ion sensors based on colloidal nanoparticles (NPs), either as actively ion-sensing NPs or as nanoscale carrier systems for organic ion-sensing fluorescent chelators typically require a charged surface in order to be colloidally stable. We demonstrate that this surface charge can significantly impact on ion binding and thus affect the read-out. Sensor read-out is thus not determined by the bulk ion concentration, but by the local ion concentration in the nano-environment of the NP surface. We present a conclusive model corroborated by experimental data that reproduces the strong distance-dependence of the effect.

7575-17, Session 6

Whispering-gallery mode based biosensing using quantum dot-embedded microspheres

H. T. Beier, G. L. Coté, K. E. Meissner, Texas A&M Univ. (United States)

Highly sensitive, miniature biosensors are desired for the development of new techniques for biological and environmental analyte sensing. One potential approach uses the detection of optical resonances, known as Whispering Gallery Modes (WGMs), from quantum dot embedded polystyrene microspheres. These modes arise from the total internal reflection of the quantum dot emission light within the high index polystyrene microsphere, to produce narrow spectral peaks, which are sensitive to refractive changes in the immediate vicinity of the microsphere surface. The high refractometric sensitivity of the WGMs in these microspheres offers potential for remote detection of molecules adsorbed onto or bound to the microsphere surface without the need for direct coupling of the light via an optical fiber. The sensitivity of these modes has been shown to exceed the theoretical sensitivity of a homogeneous microsphere, using a Mie theory model. This enhancement is believed to be due to the embedded layer of quantum dots at the surface of the microspheres. Thus, the model was extended to compare the sensitivity to a microsphere containing a thin, high index outer layer to examine this phenomenon. Additionally, analyte sensitivity and the potential for targeted sensing has been verified through adsorption of thrombin and detection of myoglobin to anti-myoglobin antibodies bound to the microsphere surface.

7575-18, Session 7

Superparamagnetic nanoparticles as platforms for studying protein-carbohydrate interactions

J. Martinez de la Fuente, M. Moros, B. Pelaz, V. Grazu, Univ. de Zaragoza (Spain)

It is known that complex oligosaccharides conjugated to the surface of mammalian cells via proteins or lipids are involved in the control of many normal and pathological processes. In turn, there are targets of many pathogenic viruses and bacteria in their initial infection cycles, and also certain diseases cause changes in the glycosilation pattern of cells.



However the study of these interactions is still tedious as there is a need of multivalent presentation to overcome their low affinity.

Nps are good platforms to be used in these studies, as they permit a multivalent presentation of the ligands. We report the synthesis and characterization of glyco-magnetic nanoparticles (GMNps) with an excellent size control and high stability in physiological media. These GMNps were used for studying carbohydrate-protein interactions by observing changes in their aggregation state due to the addition of a target molecule, in this case Concanavalin A lectin. This aggregation provokes changes in the relaxation time of water protons, allowing us its monitorization using a tabletop MR relaxometer. When Con A was added to a solution containing glucose-NPs, agglutination of NPs took place even using extreme low concentrations of ConA (7 picomols). Controls performed with galactose-NPs and heat inactivated ConA did not lead to any significant change in T2 values, showing again the specificity of the interactions. Thus, all these results make us conclude that very sensitive aggregation-based sensors of carbohydrate binding proteins could be designed using these kind of Nps.

7575-19, Session 7

3D single molecule tracking of quantum-dot labeled antibody molecules using multifocal plane microscopy

R. J. Ober, The Univ. of Texas at Dallas (United States) and The Univ. of Texas Southwestern Medical Ctr. at Dallas (United States); S. Ram, The Univ. of Texas Southwestern Medical Ctr. at Dallas (United States); P. Prabhat, J. Chao, The Univ. of Texas at Dallas (United States) and The Univ. of Texas Southwestern Medical Ctr. at Dallas (United States); E. S. Ward, The Univ. of Texas Southwestern Medical Ctr. at Dallas (United States)

No abstract available.

7575-20, Session 7

Synthesis and manipulation of multifunctional, fluorescent-magnetic nanoparticles for single molecule tracking

J. O. Winter, G. Ruan, D. Thakur, S. Hawkins, The Ohio State Univ. (United States)

Heterogeneous nanostructures that possess multiple properties as a result of their differing constituent materials have attracted significant interest in the last few years. In particular, fluorescent-magnetic nanostructures have potential applications in imaging, separations, and single molecule tracking as a result of their fluorescent and magnetic properties. Here we report the synthesis of fluorescent-magnetic nanocomposites composed of fluorescent semiconductor quantum dots or graphitic carbon nanoparticles and magnetic iron oxide nanoparticles. We have developed synthetic strategies using either micellular or polymer encapsulation, yielding composites from ~10 - 100s of nms. Composites maintain the fluorescent and magnetic properties of their constituent materials. These composites can be used for in vitro and in vivo imaging using fluorescent or magnetic (e.g., MRI) modalities. Additionally, we describe the manipulation of these composites using magnetic instrumentation. In particular, we have designed a magnetic needle that can be used to manipulate nanocomposites. Particles as small as 30 nm can be manipulated while simultaneous observed through their fluorescent property. Single particle status can be confirmed through quantum dot blinking, demonstrating the potential of these composites for single molecule tracking.

7575-21, Session 7

Ultrasensitive western immunoblot detection using single quantum dot imaging

T. Q. Vu, Oregon Health & Science Univ. (United States)

No abstract available.

7575-22, Session 8

Biomedical application of fluorescent gold nanoclusters

W. H. Chang, Chung Yuan Christian Univ. (Taiwan); H. Wang, Mackay Memorial Hospital (Taiwan); C. J. Lin, C. Lee, Chung Yuan Christian Univ. (Taiwan); Y. Lin, C. Hsieh, Y. Tseng, C. Chen, C. Tsai, H. Yeh, Mackay Memorial Hospital (Taiwan)

We have developed a facile method of water-soluble fluorescent Au nanoclusters (FANCs) which the fluorescent spectrum is located between red to near infrared range, possessing better signal intensity in tissue samples. The modification and biocompatibility test of FANCs toward biomedical application are also presented. To be close to the requirement of clinical medicine, general labeling techniques of FANCs is utilized under useful carrier system design to give a stable anchorage within cytosol. FANCs-labeled human endothelial progenitor cells are introduced to evaluate the cell therapeutic role of hind limb ischemia. We focus on the imaging including fluorescence, confocal laser scanning microscopy as well as investigating cellular function using real-time PCR, western blot and gap junction communication. The effects of FANCs probing on the progenitor cells and its tracking in vivo are investigated to understand how these cells repare the ischemic tissues.

7575-23, Session 8

Quantum dot, a versatile probe for exo-/ endocytosis and beyond

Q. Zhang, Y. Li, R. W. Tsien, Stanford Univ. (United States)

Semiconduct nanocrystal, also known as quantum dot (Qdot), possesses unique photoproporties that render it to be ideal probe for biomedical research, such as single molecule imaging. Here we take the advantage of its nanometer size as well as photoluminescence to study the behavior of presynaptic vesicles (PSVs) in live neurons.

The PSVs are lipid membrane compartments packed with neurotransmitters. The secretion of neurotransmitters from PSVs allows one neuron talk to another. As the essential component for neuronal network, PSVs have been one of the main focus in Neuroscience research for decades. Despite intensive studies, the coupling of PSV release and retrieval, particularly in mammalian central nerve system, is still controversial.

Using commercially available Qdots, we were able to visualize different routes of PSV release and retrieval at single vesicle level with high spatiotemporal resolution. This is because their high quantum yield results in great signal-to-noise ratio, their extreme photostability allows long-term imaging, their wide absorbance and narrow emission spectrum permit multicolor labeling, and most importantly, their size makes one-Qdot-one-vesicle loading possible.

By monitoring hundreds of vesicles simultaneously, we found that (1) PSVs with different release probability exhibit different preference on fast and slow recycling routes, (2) recycled PSVs are available for reuse as short as 3 seconds after their original exocytosis, (3) the overall recycling of PSVs is tightly coupled with neuronal activity, (4) the fusion duration but not the refilling of PSVs is regulated by neuronal activity and (5) PSVs retain their identity after rounds of fusion with plasma membrane.

With the various options of surface conjugation, we are making different Qdot conjugates that have better pH-sensitivity, selectivity and



stability. Furthermore, we expend our work on to tracking endocytotic vesicles containing specific cell surface receptors. We envision that the development of new Qdots in combination with creative application will speed up the quest of deciphering our own mind.

Acknowledgement

This work is supported by Grass Foundation and NIDA to QZ and NIMH to RWT

7575-24, Session 8

Biocompatible water soluble quantum dots as new biophotonic tools for hematologic cells: applications for flow cell cytometry

A. Sales Neto, R. Lira, A. G. Brasil, Jr., D. Azevedo, K. Carvalho, M. Cavalcanti, A. Amaral, P. Farias, B. Santos, A. Fontes, Univ. Federal de Pernambuco (Brazil)

Quantum dots (QDs) are a promising class of fluorescent probes that can be conjugated to a variety of specific cell antibodies. For this reason, simple, cheap and reproducible routes of QDs's syntheses are the main goal of many researchs in this field. The main objective of this work was to demonstrate the ability of QDs as biolabels for flow cell cytometry analysis. We have synthesized biocompatible water soluble CdS/ Cd(OH)2 and CdTe/CdS QDs and applied them as fluorescent labels of hematologic cells. CdTe/CdS QDs was done using mercaptoacetic acid and mercaptopropionic acid as stabilizing agents. The resulting CdTe/CdS QDs can target biological membrane proteins and can also be internalized by cells. We applied the CdTe/CdS QDs as biolabels of human lymphocytes and compared the results obtained for lymphocytes treated and non-treated with permeabilizing agents for cell membranes. Permeabilized cells present higher fluorescence pattern than non permeabilized ones. We covered CdS/Cd(OH)2 QDs with antibody A to label red blood cell (RBC) membrane antigen A. In this case, the O erythrocytes were used as negative control. The results demonstrate that QDs were successfully functionalized with antibody A. There was a specific binding of QDs-antibody A to RBC membrane antigen only for A RBCs. We have also monitored QDs-hematologic cell interaction by using fluorescence microscopy. Our method shows that QDs can be conjugated to a variety of specific cell antibodies and can become a potential, highly efficient and low cost diagnostic tool for flow cell cytometry, very compatible with the lasers and filters used in this kind of equipments.

7575-44, Session 8

Return to Contents

Quantum-dot-based quantitative identification of pathogens in complex mixture

S. H. Lim, F. Bestwater, Institut Pasteur Korea (Korea, Republic of); P. Buchy, S. Mardy, Institut Pasteur Cambodia (Cambodia); A. D. C. Yu, Institut Pasteur Korea (Korea, Republic of)

In the present study we describe sandwich design hybridization probes consisting of magnetic particles (MP) and quantum dots (QD) with target DNA, and their application in the detection of avian influenza virus (H5N1) sequences. Hybridization of 25-, 40-, and 100-mer target DNA with both probes was analyzed and quantified by flow cytometry and fluorescence microscopy on the scale of single particles. The following steps were used in the assay: (i) target selection by MP probes and (ii) target detection by QD probes. Hybridization efficiency between MP conjugated probes and target DNA hybrids was controlled by a fluorescent dye specific for nucleic acids. Fluorescence was detected by flow cytometry to distinguish differences in oligo sequences as short as 25-mer capturing in target DNA and by gel-electrophoresis in the case of QD probes. This report shows that effective manipulation and control of micro- and nanoparticles in hybridization assays is possible.

7575-26, Session 9

Delivery of quantum dot bioconjugates to the cellular cytosol: release from the endolysosomal system

J. B. Delehanty III, C. Bradburne, K. Boeneman, I. Medintz, D. Farrell, T. Pons, B. Mei, Naval Research Lab. (United States); J. Blanco-Canosa, P. Dawson, Scripps Research Institute (United States); H. Mattoussi, Naval Research Lab. (United States)

To realize their full potential as intracellular imaging and sensing reagents, robust and efficient methods for the targeted cellular delivery of luminescent semiconductor quantum dots (QDs) must be developed. We have previously shown that QDs decorated with histidine-terminated polyarginine cell-penetrating peptides (CPP) are rapidly and specifically internalized via endocytosis by several mammalian cell lines with no cytotoxicity (1). Here we demonstrate the long-term intracellular stability and fate of these QD-peptide conjugates. We found that the QD-peptide conjugates remain sequestered within endolysosomal vesicles for up to three days after delivery. However, the CPP appeared to remain stably associated with the QD within these acidic vesicles over this time period. Hence, we explored a number of techniques to either actively deliver QDs directly to the cytosol or to facilitate the endosomal release of endocytosed QDs to the cytosol. Active methods (electroporation, nucleofection) delivered only modest amounts of QDs to the cytosol that appeared to form aggregates. Delivery of QDs using polymer-based transfection reagents resulted primarily in the endosomal sequestration of the QDs, although one commercial polymer tested delivered QDs to the cytosol but only after several days in culture and with a considerable degree of polymer-induced toxicity. Finally, a modular, amphiphilic peptide containing functionalities designed for cell penetration and vesicular membrane interaction demonstrated the ability to deliver QDs in a well-dispersed manner to the cytosol. This peptide mediated rapid QD uptake followed by a slower efficient endosomal release of the QDs to the cytosol that peaked at 48 hours post-delivery. Importantly, this QDpeptide conjugate elicited minimal cytotoxicity in two cell lines tested. A more detailed understanding of the mechanism of the peptide's uptake and endosomal escape attributes will lead to the design of further QD conjugates for targeted imaging and sensing applications.

7575-27, Session 9

Cellular uptake of conjugated InP quantum dots

L. Carlini, K. Ntumba, J. L. Nadeau, McGill Univ. (Canada) No abstract available.

7575-28, Session 9

Cell uptake of magnetic nanoparticles functionalized with penetratin

P. del Pino, J. Martinez de la Fuente, Univ. de Zaragoza (Spain); C. Berry, T. Dejardin, Univ. of Glasgow (United Kingdom)

Syntheses of hybrid materials involving inorganic nanoparticles and biomolecules have found a great deal of interest in many recent studies. Merging the particular properties of nanoparticles with biomolecules of interest at the nanoscale level have many applications in a wide variety of areas like cell and molecular biology, biosensing, bioimaging, masking of immunogenic moieties to targeted drug delivery and for interaction studies. In particular, biocompatible magnetic nanoparticles are commonly used in fields like MRI, and more recently, targeted magnetic drug delivery and cell transfection magnetofection.

In this study we investigate the cell uptake of magnetic nanoparticles against those derivatized with Penetratin, a cell penetrating peptide

TEL: +1 360 676 3290 · +1 888 504 8171 · customerservice@spie.org



derived from the homeodomain of Antennapedia protein. Cell uptake of plane nanoparticles and those derivatized with Penetratin was investigated in the presence and absence of an 8mT magnetic field by fluorescence microscopy and SEM. Cell inmunostaining and Western Blots were used to assess whether cell uptake of nanoparticles can be clathrin and/or caveolin mediated endocytosis.

Application of the magnetic field produced a strong influence on particle uptake, particularly on plain nanoparticles, without which uptake was negligible. Penetratin clearly enhanced cell specific uptake, both in the presence and absence of magnetic field. Interestingly, uptake appeared to be mediated by both clathrin and caveolin. Results clearly indicate that whilst magnetic fields promote uptake, that is random. The use of a cell penetrating peptide such as Penetratin effectively enhanced cell specific uptake with no effect on cell viability. It is thus suggested that the use of such peptides should be adopted in future magnetic targeting and magnetofection bioapplications

7575-45, Session 9

Reactive oxygen species detection in living cells by nanoparticle imaging: application to PDGF dignaling

C. Bouzigues, T. L. Nguyen, D. Casanova, R. Ramodiharilafy, T. Gacoin, J. Biolot, A. Alexandrou, Ecole Polytechnique (France)

No abstract available.

7575-46, Session 9

In vitro imaging of cells using peptideconjugated quantum dots

M. Ishikawa, V. P. Biju, National Institute of Advanced Industrial Science and Technology (Japan)

The delivery of colloidal particles such as quantum dots (QDs) into cells is an important and emerging area of biological research in itself because it also relates to the cell-to-cell communication with the outside cells, the delivery and processing of nutrients, and the delivery of viruses. Delivery of materials bound on the surface of a cell can be nonspecific or specific in terms of the type of binding to cell surface. Also, clathrindependent and - independent pathways are discriminated in terms of the cellular molecules involved in endocytosis. Nonspecific binding is easily accomplished with positively charged materials due to the negative charge on the cell surfaces.

Specific binding is characterized by receptor-mediated endocytosis, in which transport vesicles coated by clathrin protein are typically involved. A representative example, also clathrin-dependent endocytosis, is the delivery of transferrin by transferrin receptor. Nonspecific and specific delivery of materials motivate us to consider that natural transport processes can and should be exploited for delivery of QDs to cells in a manner analogous to natural transport.

A key challenge in the use of QDs for intracellular tracking is the delivery of QDs to the cytoplasma and organelles, such as nucleus and mitochondria. Although certain organic dyes are able to permeate cell and nucleous membranes, the size and surface properties of QDs prevent passive diffusion across the lipid bilayer. Several groups demonstrated the use of receptor-mediated endocytosis of QDs. They found that majority of QDs entering cells by this pathway form large aggregates in endosomal compartments where they are unavailable for subsequent intracellular assays. Thus, QDs were less used to be targeted to specific organelles including nucleous and mitochondria, proteins, or nucleic acids into living cells. To fully exploit the potential of intracellular QD labeling, we require QDs highly permeable to subcellular organelles.

In our previous work1 we have achieved remarkable observations that QDs conjugated with insect neuropeptide allatostatin (AST1) are delivered into cytoplasm and even in the nuclei of cells. To explore possible mechanisms underlying the delivery of the QDs into cytoplasm we carried

out experiment using a combination of flow cytometry and fluorescence microscopy enabling us the qualitative and quantitative analysis of QD delivery mechanism. We conclude that clathrin-mediated endocytosis is dominant pathway for the delivery of AST1-conjugated QDs.2 Experimental evidence for the conclusion was obtained by inhibiting the formation of clathrin coats on the transport vesicles and colocalization experiment using the antibody of clathrin. Involving endocytosis itself in the delivery of AST1-conjugated QDs was also supported by cooling the cells to 4 oC, a technique known to block endocytosis.

[References]

- (1) V. Biju, D. Muraleedharan, K. Nakayama, Y. Shinohara, T. Itoh, Y. Baba, M. Ishikawa Langmuir 2007, 23, 10254-10261.
- (2) A. Anas, T. Okuda, N. Kawashima, K. Nakayama, T. Itoh, M. Ishikawa, V. Biju ACS Nano 2009, 3, 2419-2429.

7575-47, Session 9

Quantum dots and supermagnetic iron oxide nanocrystals for systemic investigation of lipoprotein metabolism by correlative in vivo imaging

O. T. Bruns, Univ. Medical Ctr. Hamburg-Eppendorf (Germany); R. Reimer, Univ. Hamburg (Germany); C. Waurisch, Technische Univ. Dresden (Germany); U. I. Tromsdorf, H. weller, Univ. Hamburg (Germany); A. Eychmüller, Technische Univ. Dresden (Germany); J. Heeren, Univ. Medical Ctr. Hamburg-Eppendorf (Germany); H. Hohenberg, Univ. Hamburg (Germany)

No abstract available.

7575-31, Session 10

Visualizing the influx of various nanoparticle types from blood vessels into tumor interstitium in multiple animal models and tumor varieties using intravital microscopy

B. R. Smith, Z. Cheng, Z. Liu, H. Dai, S. S. Gambhir, Stanford Univ. (United States)

Nanoparticles comprising various materials, shapes, and sizes are becoming ubiquitous within molecular imaging, particularly for cancer diagnosis/treatment. Predominantly intended for parenteral administration, deeper understanding of how and why these nanoparticles extravasate from tumor neovasculature into interstitium is critical. It is essential to the field to characterize shape- and size-dependent nanoparticle behavior in addition to tumor- and site-dependent behavior in order to take diagnostic/therapeutic nanoparticles from lab-to-clinic and to optimize their design.

We probed the extravasational behavior of two nanoparticle types (each with/without ligand) in two different animal models with three different tumor types using intravital microscopy. In particular, we employed near-infrared (800nm) emitting quantum dots (qdots) (~20-25nm diameter) and single-walled carbon nanotubes (SWNTs, to which were conjugated fluorophores) both with/without surface-conjugated RGD peptides (targeting v 3-integrins) using intravital microscopy on ~50 living mice. We employed both nude mice, in which tumors were inoculated in the ear, and C.B-17 SCID mice into which dorsal skinfold chambers were implanted for direct visualization. Three different tumor cell lines were employed in these models, all transduced with EGFP for visualization: SKOV3, LS174T, and U87MG cells. 100µl of long-circulating dye was injected to visualize the tumor and its vasculature prior to injection of the respective nanoparticle.

No extravasation occurred in SKOV-3, while all nanoparticles extravasated from U87MG (though at different rates); however,



extravasation in LS174T was highly nanoparticle-dependent. We thus directly visualized nanoparticle extravasation from tumor blood vessels and demonstrated highly nanoparticle- and tumor-dependent differences, which will facilitate in-depth exploration of nanoparticle behavior in living subjects.

7575-32, Session 10

Semiconductor nanoparticles produced by femtosecond laser ablation as photosensitizer for photodynamic therapy

D. Rioux, Ecole Polytechnique de Montréal (Canada); L. Lilge, Ontario Cancer Institute (Canada); M. Meunier, Ecole Polytechnique de Montréal (Canada)

Photodynamic therapy is a cancer treatment where singlet oxygen is produced in order to kill cancer cells. Singlet oxygen production requires the use of a photosensitizer that is conventionally an organic molecule. However, these molecules are prone to photobleaching upon illumination, limiting the efficiency of the treatment. Inorganic semiconductor nanoparticles, on the other hand, show excellent resistance to photobleaching as well as good potential for singlet oxygen generation. The synthesis of these nanoparticles by chemical and electrochemical methods raises questions of biocompatibility because of the use of toxic materials and chemistry. We present the production of ultrapure nanoparticles such as Si, TiO2 and Ge by femtosecond laser ablation in liquid environment. Because they are produced by laser ablation, these nanoparticles are free of any toxic material. Control of the laser parameters, mainly the laser fluence, can be used to tune the size of the nanoparticles between 5 to 100 nm and hence their optical absorption and emission properties, and possibly also their singlet oxygen quantum yield. These nanoparticles produce singlet oxygen upon illumination, resulting in cell kill. We have investigated the effect of laser parameters and oxygen content in the solvent on the size and composition of these nanoparticles. Singlet oxygen generation efficiency from these nanoparticles and their resistance to photobleaching were also measured. We will also present results of in vitro cell survival experiments with different efficiencies depending on the nanoparticle production parameters in a variety of cancerous mammalian cell lines. These nanoparticles show great potential for their use in photodynamic therapy as well as disinfecting agents of bacteria because of their ability to generate singlet oxygen.

7575-33, Session 10

Radiation sensitivity enhancement in cells using high-Z nanoparticles

N. J. Withers, J. B. Plumley, B. A. Akins, G. Medina, G. Timmons, G. A. Smolyakov, M. Osinski, The Univ. of New Mexico (United States)

No abstract available.

7575-34, Session 10

Whole-body imaging of HER2/neuoverexpressing tumors using scFv-antibody conjugated quantum dots

I. V. Balalaeva, Nizhny Novgorod State Univ. (Russian Federation) and Institute of Applied Physics RAS (Russian Federation); T. A. Zdobnova, Shemyakin and Ovchinnikov Institute of Bioorganic Chemistry RAS (Russian Federation) and Institute of Applied Physics RAS (Russian Federation); A. A. Brilkina, Nizhny Novgorod State Univ. (Russian Federation) and Institute of

Applied Physics RAS (Russian Federation); I. M. Krutova, M. V. Shirmanova, Nizhny Novgorod State Univ. (Russian Federation); O. A. Stremovskiy, E. N. Lebedenko, Shemyakin and Ovchinnikov Institute of Bioorganic Chemistry RAS (Russian Federation); V. V. Vodeneev, Nizhny Novgorod State Univ. (Russian Federation); I. V. Turchin, Institute of Applied Physics RAS (Russian Federation); S. M. Deyev, Shemyakin and Ovchinnikov Institute of Bioorganic Chemistry RAS (Russian Federation)

Semiconductor quantum dots (QDs) are widely used in different fields of bioscience and biotechnology due to their unique optical properties. QDs can be used as fluorescent markers for optical detection and monitoring of deeply located tumors in vivo after specific labeling achieved by conjugating of QDs with targeting molecules.

In this work the possibilities of intravital tumor labeling with QDs and subsequent in vivo tumor imaging were estimated. The experiments were run on immunodeficient nu/nu mice bearing human breast carcinoma SKBR-3, overexpressing surface protein HER2/neu. We used quantum dots Qdot 705 ITK (Invitrogen, USA) linked to anti-HER2/ neu 4D5 scFv antibody. Antibody scFv fragments as a targeting agent for directed delivery of fluorophores possess significant advantages over full-size antibodies due to their small size, lower cross-reactivity and immunogenicity. QDs were bound to 4D5 scFv by barnase-barstar system (bn-bst) analogous to the streptavidin-biotidin system. Wholebody images were obtained using diffuse fluorescence tomography (DFT) setup with low-frequency modulation and transilluminative configuration of scanning, created at the Institute of Applied Physics of RAS (Russia). DFT-results were confirmed post mortem by confocal microscopy.

We have demonstrated effective application of modular barnase-barstar system and 4D5 scFv antibodies for target delivery of QDs to HER2/neuoverexpressing cancer cells. We report the results of in vivo whole-body tumor imaging with QDs complexes as contrasting agents. Intravital images of QDs-labeled tumors were obtained using specific tumor cells targeting and fluorescence transilluminative imaging method, while "passive" QD-labeling failed to mark effectively the tumor.

7575-48, Session 10

Targeting cell surface proteins in breast cancer cell lines and tumor mice models using ImmunoQDots

G. Iyer, J. Xu, S. Sirk, J. Li, A. Wu, S. Weiss, Univ. of California, Los Angeles (United States)

No abstract available.

7575-35, Session 11

Nanoparticle-modified polymer capsules as carrier systems for biosensing and drug delivery

L. L. del Mercato, A. A. Zahoor, M. Ochs, A. Muñoz Javier, P. del Pino, W. J. Parak, Philipps-Univ. Marburg (Germany)

One of the possible contributions of nanomedicine consists in building biocompatible multifunctional carrier systems that are able to navigate within living organisms using remote guidance and activation for the local release of their cargo. Such carrier systems can be used to improve cargo stability, to sustain and control their release rates, to increase the bioavailability of cargo substances, and to target them to specific sites

Multilayer polyelectrolyte capsules are spherical microcontainers based on layer-by-layer adsorption of oppositely charged polyelectrolyte polymers onto a sacrificial template followed by the decomposition of this template. Compared to other systems (such as liposomes, block



copolymers, and dendrimer polymers) polymer capsules have many advantageous properties which make them attractive candidates for medical applications including biosensing and drug delivery. Firstly, they can be synthesized under mild conditions by using numerous different materials. Secondly, their functional properties can be well-defined by embedding different nanoscale building blocks (as colloidal inorganic nanoparticles or biomolecules) within and on top of their wall. Thirdly, they can efficiently host (biological) macromolecules within their cavity for numerous biomedical applications. Finally, they can be composed of biocompatible materials for the delivery of encapsulated materials into cells.

In this work the main concepts concerning the fabrication of polyelectrolyte capsules are described and their applications for delivery and sensing in cells are showed. The use of these systems is envisioned to open new ways in a broad range of disciplines since their properties may be promptly tailored to specific applications by varying the nature of the encapsulated material and the polymer shell composition.

7575-36, Session 11

Intracellular processing of proteins mediated by biodegradable polyelectrolyte capsules

P. Rivera Gil, Philipps-Univ. Marburg (Germany); S. De Koker, B. G. De Geest, Univ. Gent (Belgium); W. J. Parak, Philipps-Univ. Marburg (Germany)

Multilayer polyelectrolyte capsules made by layer-by-layer assembly of oppositely charged biodegradable polyelectrolytes were filled with a model of a non-active pro-drug, a self-quenched fluorescence-labeled protein. After capsule uptake by living cells the walls of the capsules were actively degraded and digested by intracellular proteases. Upon capsule wall degradation intracellular proteases could reach the protein cargo in the cavity of the capsules. Enzymatic fragmentation of the self-quenched fluorescence-labeled protein by proteases led to individual fluorescencelabeled peptides and thus revoked self-quenching of the dye. In this way non-active (non-fluorescent) molecules were converted into active (fluorescent) molecules. The data demonstrate that biodegradable capsules are able to convert non-active molecules (pro-drugs) to active molecules (drugs) specifically only inside cells where appropriate enzymes are at hand. In this way only cargo inside the capsules reaching cells is activated, but not the one in capsules which are remaining extracellularly. The peptide fragments undergo further processing inside the cells, leading ultimately to exocytosis.

7575-37, Session 11

Studying nanotoxic effects of CdTe quantum dots in Trypanosoma cruzi

C. Vieira Stahl, Fundacao Oswaldo Cruz (Brazil); D. Burigo Almeida, A. A. de Thomaz, Univ. Estadual de Campinas (Brazil); A. Fontes, Univ. Federal de Pernambuco (Brazil); J. R. Santos-Mallet, Fundacao Oswaldo Cruz (Brazil); C. Lenz Cesar, Univ. Estadual de Campinas (Brazil); S. A. O. Gomes, Fundacao Oswaldo Cruz (Brazil); D. Feder, Univ. Federal Fluminense (Brazil)

Protozoan pathogens as Trypanosoma cruzi, etiologic agent of Chagas disease, is transmitted to humans either by blood-sucking triatomine vectors (insect), blood transfusion, organs transplantation or congenital transmission. It is present in 18 countries, with prevalence of 16 millions of human cases. The study of the life cycle, biochemical, genetics, morphology and others aspects of the T. cruzi is very important to better understand the interactions with its hosts and the disease evolution on humans. One of the fundamental goals in biology has been the understanding cellular interactions. In this context quantum dot, nanocrystals, highly luminescent can be used as tool for experiments in vitro and in vivo T. cruzi life cycle development in real time. Many studies have been done in order to verify the possible nanotoxicity of quantum

dots in cells and we are investigating this on T. cruzi parasite cells. In vitro experiments were been done in order to test the interference of this nanoparticle on parasite development, parasite morphology and reactive oxygen species generation from this parasite. Ours previous results demonstrated that T. cruzi QDs labeling did not effect: (i) on parasite integrity, at least until 14 days; (ii) parasite cell dividing and (iii) parasite motility. This fact confirms the low level of cytotoxicity of these QDs on this parasite cell. We are now investigating if T. cruzi QDs labeling would to present any molecular changes. In summary our results is showing T. cruzi QDs labeling could be used for in vivo cellular studies in Chagas disease.

7575-38, Poster Session

Re-dispersion of aggregated colloidal quantum dots using small needle valve with pinhole auto regulation

N. Manabe, S. Hanada, Y. Futamura, A. Hoshino, International Medical Ctr. of Japan (Japan); T. Adschiri, Tohoku Univ. (Japan); K. Yamamoto, International Medical Ctr. of Japan (Japan)

Nanoparticles, whose size is $1\sim100$ nm, easily aggregate as their size becomes smaller. Therefore, it is difficult to produce solution in which nanoparticles are dispersed. We have, as a way to disperse aggregated particles, for example, a media-typed disperse machine. During the procedures, however, we have to deal with some complicating operations; separation of the media from the solution, washing the media, avoiding the defacement of the media into the solution, and so on. Furthermore, it is not an effective method for particles whose size is less than 100nm.

We tried to find an easier and more effective method for producing solution in which we re-disperse aggregated nanoparticles to still smaller particles.

The aggregated particles were put into a machine with a pinhole auto regulation small needle valve, and they were re-dispersed by "sheering stress". The estimation of re-dispersion was carried out by the measurement of their size distribution and surface z-average.

With the utility of the machine, the re-dispersions of aggregated particles were observed. Furthermore, the increase of the pressure and of the velocity of the flow caused the decrease of particle size, which makes the surface area larger and therefore the surface z-average larger.

It become clear that it is possible to re-disperse aggregated nanoparticles by adding shearing stress. We can regulate shearing stress by controlling the pressure and flow, and therefore we can control the effectiveness and the yield.

7575-40, Poster Session

Silver nanoparticle-induced degranulation observed with quantitative phase microscopy

W. Yang, S. Lee, J. Lee, Y. Bae, D. Kim, Gwangju Institute of Science and Technology (Korea, Republic of)

The use of AgNP is becoming more and more widespread in biomedical field. But compared with the promising bactericidal function, other physiological effects of AgNP on cells are relatively scant. In this research, we propose quantitative phase microscopy (QPM) as a new method to study the degranulation, and AgNP-induced RBL-2H3 cell degranulation is studied as well. Firstly, the validity of QPM is manifested by the volume increment of RBL-2H3 cell exerted with compound 48/80. RBL-2H3 cell volume increased immediately after the Compound 48/80 treatment. Ten minutes later, the volume began to decrease but it was still lager than that of the beginning. PBS has no such effect. Furthermore, Hela cell was used as a cell control and Compound 48/80 has no effect on the Hela cell volume either. Secondly, AgNP (ABC Nanotech, SARPU 50KW, diameter of 30 nm.) can increase RBL-2H3 cell volume but has no effect on the volume of Hela cell. RBL-2H3 cell volume increased



significantly along with the addition of AgNP. Several minutes later, it recovered to the baseline level. Phase images obviously indicate the RBL-2H3 cell deformation. Especially within the first 6 minutes of AgNP addition, the periphery of cell became granulated, rather than smooth in the resting state, with the major axis of cell shortened and minor axis lengthened. Ten minutes later, the cell shape recovered. Thirdly, degranulation of RBL-2H3 cell induced by AgNP is further confirmed by the increment of intracellular calcium and extracellular histamine. Compared with that of Hank's group, histamine in either Compound 48/80 or AgNP treated group increased significantly (p<0.01).

7575-41, Poster Session

Photochemical nitric oxide delivery using semiconductor quantum dots

A. D. Ostrowski, P. C. Ford, Univ. of California, Santa Barbara (United States)

The long-term goal of our research is to synthesize materials that are capable of releasing nitric oxide (NO) after light irradiation. Such materials could be used in a new type of photodynamic therapy (PDT), where site-specific irradiation can cause NO release. NO plays an important role in blood pressure regulation, neural transmission, immune response, cell apoptosis, and radiation sensitization [1]. In this context, we are designing new systems that selectively release NO upon photoexcitation.

One such NO precursor is trans-Cr(cyclam)(ONO)2+. We have now demonstrated that photoexcitation leads to sufficient NO release, even at μM concentrations, to activate the enzyme soluble guanylate cyclase (sGC). We are also investigating the photosensitization of trans-Cr(cyclam)(ONO)2+using semi-conductor quantum dots (QDs). We have previously demonstrated that water-soluble CdSe/ZnS core/shell QDs form electrostatic assemblies with trans-Cr(cyclam)(ONO)2+ complexes and act as antenna for photosensitized release of nitric oxide (NO) [2]. Energy transfer behavior is consistent with a Förster resonance energy transfer (FRET) mechanism, it is proportional to the overlap between the QD (donor) emission and the Cr(III) complex (acceptor) absorbance [3]. These results provide a guideline for the design of other QD-based materials and devices that rely on photosensitized energy transfer.

References:

- 1. Nitric Oxide: Biology and Pathobiology, Ignarro, L. J., ed. Academic Press, San Diego (2000) and references therein
- 2. Neuman, D; Ostrowski, A. D.; Absalonson, R. O.; Strouse, G. F.; Ford, P. C. J. Amer. Chem. Soc., 2007, 129, 4146-4147
- 3. Neuman, D; Ostrowski, A. D.; Mikhailovsky, A. A.; Absalonson, R. O.; Strouse, G. F.; Ford, P. C. J. Amer. Chem. Soc., 2008, 130, 168 -17

Conference 7576: Reporters, Markers, Dyes, Nanoparticles, and Molecular Probes for Biomedical Applications

BIOS *
SPIE Photonics West

Monday-Wednesday 25-27 January 2010 • Part of Proceedings of SPIE Vol. 7576

Reporters, Markers, Dyes, Nanoparticles, and Molecular Probes for Biomedical Applications II

7576-01, Session 1

Targeted theranostic nanoparticles for biomedical applications

T. Hasan, P. Rai, L. Z. Zheng, Z. Mai, R. Rahmanzadeh, X. Zheng, Wellman Ctr. for Photomedicine (United States)

Nanomedicine is beginning of impact the treatment of several diseases and current research efforts include development of integrated nanoconstructs (theranostics) which serve as probes for diagnosis, detection, and therapy monitoring in addition to delivering high payload of therapeutic agents. Optical theranostics have potential due to high sensitivity and minimally invasive nature of optical methods and the availability of optical fibers to access many anatomical sites. We have investigated several such constructs in cancer and noncancer applications in combination with Photodynamic Therapy (PDT). Using models of ovarian and pancreatic cancers, we find that generally, these constructs deliver high concentrations of therapeutic and diagnostic agents, and also result in increased therapeutic efficacy. PDT also sensitizes cancer cells to treatment with biologics so that including these biologics within the nanoconstructs, specifically tailored to the molecular mechanisms being targeted, enhances the treatment outcome significantly. Results from our initial studies and clinical implications of these results will be discussed in this presentation.

7576-02, Session 1

Two different approaches in skin cancer therapy in vivo using a photosensitizer/a natural product

A. Abraham, G. Devi, T. R. Cibin, Univ. of Kerala (India); D. Ramaiah, National Institute of Interdisciplinary Science and Technology, CSIR (India)

Developing novel strategies to prevent/cure skin cancer represents a desirable goal due to increasing rise in the incidence of skin cancer patients throughout the world. The major arenas dealt within this study are two potential modes for the treatment of skin cancer-one a novel approach-photodynamic therapy (PDT) - using a squaraine dye and the other using a natural product- the flavonoid fraction of Saraca asoka. Bis (3, 5-diiodo-2, 4, 6-trihydroxyphenyl) squaraine is a photosensitizing agent, which is preferentially taken up and retained by the tumor cells and when irradiated with high power visible light results in the selective destruction of the tumor cells. The uniqueness of this mode of treatment lies in the selective destruction of tumor cells without affecting the neighbouring normal cells, which is much advantageous over radiation therapy now frequently used. The chemopreventive and therapeutic effects of the plant component are explored as well. The experimental models were Swiss albino mice in which skin tumor was induced by 7, 12-Dimethyl Benz(a)anthracene-DMBA. Marked reduction in tumor volume and burden in the treated groups were observed. The reversal of biochemical enzyme markers like rhodanese, myeloperoxidase, β-D glucuronidase, lactate dehydrogenase, hexokinase and sialic acid to near normal levels were observed in the PDT and flavonoid fraction treated groups. The live photographs of the experimental animals and histopathological data further support the obtained results. The study assumes importance as it combines a traditional treatment mode and a novel aspect in cancer therapy using the same experimental models.

7576-03, Session 1

Microdistribution of fluorescently-labeled monoclonal antibody in a peritoneal dissemination model of ovarian cancer

N. Kosaka, M. Ogawa, D. S. Paik, C. H. Paik, P. L. Choyke, H. Kobayashi, National Institutes of Health (United States)

Detailed evaluation of the microdistribution of injected monoclonal antibody within tumor nodules is important for antibody-targeted therapy, because nonuniform microdistribution is known to be a reason for therapy failure. In this study, we developed a semiquantitative approach for measuring microdistribution of an antibody using in situ fluorescence microscopy, and evaluated the microdistribution of a fluorescentlylabeled monoclonal antibody, (trastuzumab 50-µg intraperitoneal injection (i.p.), 150-µg i.p., and 100-µg intravenous injection (i.v.)) in a peritoneal dissemination mouse model of human ovarian cancer. Furthermore, we evaluated the microdistribution of concurrently-injected (i.p.and i.v. antibody 30 µg i.p. and 100 µg i.v.) trastuzumab or serial injections of i.p. trastuzumab (30 µg each) using in situ multicolor fluorescence microscopy. Fluorescence images after the administration of 50-µg i.p. and 100-µg i.v. trastuzumab showed no significant difference in the ratio of central to peripheral signal (C/P ratios) and demonstrated a peripheral-dominant antibody accumulation, whereas administration of 150-uq i.p. trastuzumab showed relatively uniform, central dominant accumulation. The concurrent-injection study demonstrated that i.v. trastuzumab distributed more centrally than concurrently-injected i.p. trastuzumab. Moreover, after a 19-h interval, the 2nd injection of trastuzumab distributed more centrally than the first injection, while no difference was observed in the control mixed-injection group. Our results suggest that increasing the dose results in a more uniform antibody distribution within peritoneal nodules. Furthermore, the concurrent injection of i.p. and i.v. antibody or the serial i.p. injection of antibody can modify the microdistribution within tumor nodules and has the potential for preferential delivery of anti-cancer drugs to either the tumor periphery or center.

7576-04, Session 1

Reporters to monitor cellular MMP12 activity

C. Schultz, A. Cobos-Correa, European Molecular Biology Lab. Heidelberg (Germany); M. Mall, Children's Hospital, Univ. Clinic Heidelberg (Germany)

Macrophage elastase (MMP-12) belongs to a family of proteolytic enzymes known to remodel the extracellular matrix. Under certain pathological conditions, including inflammation, overexpression of MMP-12 has been observed and its elevated proteolytic activity has been suggested to be the cause of emphysema. Therefore, imaging MMP-12 activity would give an insight into the development of lung inflammation and help to find better treatments. Our approach to visualize MMP-12 activity is based on FRET (Foerster Resonance Energy Transfer). We have generated two different types of reporters. The soluble reporter (LaRee5) is suitable to measure extracellular MMP-12. It consists of a MMP-12specific amino acid sequence flanked by two fluorophores that form a FRET pair and PEG linkers for improved solubility. Labeling of the probe with different fluorophore pairs has been optimized in order to increase sensitivity and MMP-12 activity is detectable in the subnanomolar range. The membrane targeted reporter (LaRee1) has been modified by the introduction of palmitic acid. This moiety leads the reporter to the outer side of the plasma membrane and measures MMP-12 at the pericellular milleu. Upon MMP-12 cleavage, the acceptor fluorophore and the charged part of the molecule are released with the consequent loss of FRET and internalization of the donor fluorophore. We combined both

Conference 7576: Reporters, Markers, Dyes, Nanoparticles, and Molecular Probes for Biomedical Applications



sensors to study MMP-12 activity in a mouse model of lung inflammation caused by inhalation of particulate matter. Results demonstrating the suitability of the probes in in vitro and ex vivo experiments will be presented.

allowing for imaging applications. Examples for cell imaging using hydrophobic dyes and charged dyes will be given demonstrating the importance of net charge as well dye hydrophobicity.

CE using NIR LIF detection. Certain NIR dyes accumulate in live cells

7576-05, Session 1

Bio-luminescent imaging and characterization of organ-specific metastasis of human cancer in NOD/SCID mice

T. Murakami, Jichi Medical Univ. (Japan)

Cancer metastasis is the end result of a complex series of biological events that leads to the formation of clinically significant secondary tumors at distant sites. Many clinical evidences demonstrate that the sites of distant metastasis are not random and certain malignant tumors show a tendency to develop metastases in specific organs (e.g., brain, liver and lungs). However, an appropriate animal model to characterize the metastatic nature of transplantable human cancer cell lines has not been adequately reported. Recent advances in bio-luminescent imaging (BLI) technologies have facilitated the quantitative analysis of various cellular processes in vivo. To visualize the fate of tumor progression in living mice, we are constructing a luciferase-expressing human cancer cell library (including melanoma, colon, breast and prostate cancer). Herein, we demonstrate that use of BLI technology coupled with a fine ultrasonic guidance detects cancer cell-type dependent metastasis to specific organs. For example, some melanoma cell lines showed frequent metastasis to the brain, lungs, and lymph nodes in the mouse model. Notably, some of the cell lines showed preferential metastasis to the brain, reflecting the clinical features of melanoma, breast and prostate cancer. Moreover, these cellular resources for BLI allow a high throughput screening for potential anti-cancer drugs. Thus, the use of this BLImediated additional strategy with luciferase-expressing cancer cell resources should promote many translational studies for human cancer therapy.

7576-06. Session 2

Near-infrared fluorophores as biomolecular probes and tracers

G. Patonay, G. Beckford, L. Strekowski, M. Henary, Georgia State Univ. (United States)

Near-Infrared (NIR) fluorescence has been valuable in analytical and bioanalytical chemistry. NIR probes and labels have been used for several applications, including hydrophobicity of protein binding sites, DNA sequencing, immunoassays, CE separations, etc. The NIR region (700-1100 nm) has advantages for the spectroscopist due to the inherently lower background interference from the biological matrix and the high molar absorptivities of NIR chromophores. During the studies we report here several NIR dyes were prepared to determine the role of the hydrophobicity of NIR dyes and their charge in binding to amino acids and proteins e.g., serum albumins. We synthesized NIR dye homologs containing the same chromophore but substituents of varying hydrophobicity. Hydrophobic moieties were represented by alkyl and aryl groups and hydrophilic moieties were polyethylene glycols (PEG). NIR dyes of varying hydrophobicity exhibited varying degrees of H-aggregation in aqueous solution; PEGylated NIR dyes had very little aggregation and their binding constants were smaller as well, indicating that the degree of H-aggregation could be used as an indicator to predict binding characteristics to serum albumins. Typical dye structures that exhibit large binding constants to biomolecules were compared in order to optimize applications utilizing non-covalent interactions. The importance of net charge of the NIR dye was studied by synthesizing dyes having net charge from -3 to +3. The binding characteristics of these dyes have been investigated to determine their utility as reporters and markers. The utility of NIR dyes as tracers for measuring small molecule binding to biomolecules (e.g., HSA) was demonstrated via

7576-07, Session 2

In vivo photoconversion for cell tracking in live animals

A. L. Carlson, Massachusetts General Hospital (United States); W. Zhao, Harvard Stem Cell Institute (United States); J. Fujisaki, Massachusetts General Hospital (United States); S. Schaefer, J. Karp, Harvard Stem Cell Institute (United States); C. P. Lin, Massachusetts General Hospital (United States)

To advance therapies associated with cell transplantation, better understanding of cell homing and engraftment is needed. The ability to track cells and identify sites where infiltration, proliferation, and differentiation occur is an essential component in the study of cell transplantation, engraftment, and reconstitution. Optical photoconversion is a technique that allows donor cells to be tracked in vivo over time in their host environment, enabling the study of cell homing, infiltration, and proliferation.

We report two methods of photoconversion used with in vivo videorate confocal microscopy to track cells in live mice. In both cases, fluorescence images are acquired before and after photoconversion for ratiometric imaging. The first method uses a FRET pair consisting of Cy3 and Cy5 dyes. Photoconversion was induced by FRET acceptor photobleaching, changing the dominant fluorophore from Cy5 to Cy3. The second method takes advantage of the optical properties of a lipophilic membrane dye, DiR, that fluoresces in the near infrared at 780nm initially, but can be photoconverted using 750nm light, causing it to fluoresce in the red region at approximately 670nm.

The fluorescence ratio before and after photoconversion was then used to distinguish between infiltrating and proliferating cells within an area of tissue. Cells that infiltrated the tissue were photoconverted; at a later time point, the same area of tissue was imaged. Cells that infiltrated the tissue after photoconversion yielded a different fluorescence ratio than cells that were photoconverted, yielding information about the infiltration and proliferation rates of the cells of interest.

7576-08, Session 2

In vivo investigation of pharmacokinetics of model drug: comparison of near infrared technique with high-performance liquid chromatography

Y. Gu, China Pharmaceutical Univ. (China); F. Liu, China pharmaceutical Univ. (China); Z. Qian, Nanjing Univ. of Aeronautics and Astronautics (China); S. Achilefu, Washington Univ. in St. Louis (United States)

Near infrared spectroscopy possess great potential for in vivo quantitative monitoring of drugs in animal subject. The accuracy of the measurements by near infrared technique should be evaluated by an established method. In this study, a near infrared fluorescence dye, cypate and its conjugation cypate-PEG were used as model drug for in vivo dynamic study. The pharmacokinetics of the model drug in mice subjects were investigated by near infrared spectroscopy and high performance liquid chromatography, respectively. The results from the two techniques were compared. The pharmacokinetic parameters calculated based on the acquired data by DAS software showed that there were no statistical differences between the two methods.

TEL: +1 360 676 3290 · +1 888 504 8171 · customerservice@spie.org

Conference 7576: Reporters, Markers, Dyes, Nanoparticles, and Molecular Probes for Biomedical Applications



7576-71, Session 2

Single dose intravenous toxicity study of IRDye 800CW in Sprague-Dawley rats

D. M. Olive, LI-COR Biosciences (United States)

No abstract available.

7576-75, Session 2

Phosphorescent light-emitting iridium complexes serve as a hypoxia-sensing probe for tumor imaging in living animals

T. Takeuchi, S. Zhang, K. Negishi, T. Yoshihara, M. Hosaka, S. Tobita, Gunma Univ. (Japan)

Iridium complex, a promising organic light-emitting diode material for next generation television and computer displays, emits phosphorescence. Phosphorescence is quenched by oxygen. We used this oxygen-quenching feature for imaging tumor hypoxia. Red light-emitting iridium complex Ir(btp)2(acac) (BTP) presented hypoxiadependent light emission in culture cell lines, whose intensity was in parallel with hypoxia-inducible factor (HIF)-1 expression. BTP was further applied to imaging five nude mouse-transplanted tumors: human oral squamous carcinoma-derived SCC-9, human glioma-derived U87, human lymphoma-derived RAMOS, human colon carcinoma-derived HT-29, and mouse lung cancer-derived LL-2. All tumors presented a bright BTP-emitting image as early as 5 min after the injection. The BTP-dependent tumor image peaked at 1 to 2 h after the injection, and was then removed from tumors within 24 h. The minimal BTP image recognition size was at least 2 mm in diameter. By morphological examination and phosphorescence lifetime measurement, BTP is presumed to localize to the tumor cells, not to stay in the tumor microvessels by binding to albumin. The primary problem on suse of luminescent probe for tumor imaging is its weak penetrance to deep tissues from the skin surface. Since BTP is easily modifiable, we made BTP analogues with a longer excitation/emission wavelength to improve the tissue penetrance. One of them, BTPHSA, displayed 560/720 wavelength, and depicted its clear imaging from tumors transplanted over 6-7 mm deep from the skin surface. We suggest that BTP analogues have a vast potential for imaging hypoxic lesions such as tumor tissues.

7576-09, Session 3

Intraoperative detection of tiny tumors in living mice with novel, fast-responding, and highly activatable fluorescence probes

Y. Urano, M. Sakabe, D. Asanuma, M. Kamiya, T. Nagano, The Univ. of Tokyo (Japan); M. Ogawa, N. Kosaka, P. L. Choyke, H. Kobayashi, National Cancer Institute, National Institutes of Health (United States)

Nowadays, several tumor imaging modalities such as MRI, radionuclide including PET and fluorescence imaging techniques have been extensively investigated. One of the central problems associated with these conventional tumor-targeted imaging methods, however, is the fact that the signal contrast between tumor and surrounding tissues relies on the efficient targeting to the tumor and the rapid sequestration or excretion of unbound agent. Among these modalities, only fluorescence imaging technique has a significant feature, in that great signal activation could be achieved which potentially leads to the selective imaging of cancer with higher tumor-to-background ratio. In this symposium, I will present a novel technique of fluorescence cancer imaging based on highly activatable strategies with using precisely designed novel fluorescence probes.

Recently, we have succeeded in developing novel and highly sensitive

fluorescence probes for various hydrolases which were applicable for living cell system. By utilizing these probes, we could establish a novel and highly activatable strategy for sensitive and fast-responding fluorescence imaging of disseminated tumors in the peritoneum. These probes were reactive to cancer-related hydrolases to yield highly fluorescent products in higher rate than those we have developed. With using these probes, we could detect tiny tumors quite sensitively and rapidly, i.e. within 1 min after the drug administration, which means intraoperative diagnosis of tiny tumors can be accomplished with fluorescence endoscopes.

7576-10, Session 3

Hydrocyanines: a new family of leucodyes that can image reactive oxygen species in vitro, in cell culture, and in vivo

N. Murthy, Georgia Tech (United States)

In this presentation we will discuss a new family of leucodyes recently developed in our laboratory termed the hydrocyanines, which can image reactive oxygen species (ROS) in vitro, in cell culture and in vivo. The hydrocyanines and are sythesized via sodium borohydride reduction of the cyanine dyes. The cyanine dyes comprise a large and diverse family of dyes and it appears that most cyanine dyes can be coverted into ROS sensors via sodium borohydride reduction. The hydrocyanines have numerous useful properties for imaging ROS, such as nanomolar sensitivity, tunable emission wavelengths ranging from 570-810 nm, and accumulation within cells after oxidation. We have been to image ROS in a variety of animal models using the hydrocyanines, such as in hind limb ischemia, arthritis and LPS induced inflammation. We will also discuss recent improvements of the hydrocyanines based on explication of the kinetic isotope effect.

7576-11, Session 3

Near-infrared molecular imaging probes based on chlorin-bacteriochlorin dyads

M. Ptaszek, North Carolina State Univ. (United States); H. L. Kee, Washington Univ. in St. Louis (United States); C. Muthiah, North Carolina State Univ. (United States); R. Nothdurft, W. Akers, S. Achilefu, J. P. Culver, Washington Univ. School of Medicine in St. Louis (United States); D. F. Bocian, Univ. of California, Riverside (United States); D. Holten, Washington Univ. in St. Louis (United States)

Chlorin-bacteriochlorin dyads were synthesized and spectroscopically characterized in order to examine their potential as a new class of near-infrared fluorophores for molecular imaging applications. Each dyad is comprised of a chlorin macrocycle (free base or zinc chelate) as an energy donor and a free base bacteriochlorin as an energy acceptor. Excitation of the chlorin (650 nm, zinc chelate; 675 nm, free base) results in fast (5 ps) and nearly quantitative (>99%) energy transfer to the adjacent bacteriochlorin moiety and consequently bacteriochlorin fluorescence (760 nm). Thus, each chlorin-bacteriochlorin dyad behaves as a single chromophore, with a large Stokes shift (85 or 110 nm), a significant fluorescence quantum yield (0.19), long excited-state lifetime (5.4 ns), narrow excitation and emission bands (fwhm < 20 nm), as well as high chemical stability.

Imaging experiments performed using phantoms show that the chlorin-bacteriochlorin dyads exhibit a range of superior properties compare to commercially available imaging dyes. While the latter are often brighter the chlorin-bacteriochlorin dyads exhibit narrower excitation and emission bands and larger Stokes shift, therefore allowing more efficient and selective excitation and detection of fluorescence. This high selectivity is further demonstrated with in vivo imaging studies of mice.

The narrow absorption bands of chlorins allow selective excitation, whereas sharp emission bands of bacteriochlorins enable selective,

Conference 7576: Reporters, Markers, Dyes, Nanoparticles, and Molecular Probes for Biomedical Applications



simultaneous multichannel detection of fluorescence from several different dyads. This selectivity together with the tunability of absorption and emission wavelengths using substituent effects under synthetic control make the chlorin-bacteriochlorin dyads ideal candidates for multicolor imaging applications. In addition, the long fluorescence lifetimes make those probes suitable for lifetime imaging applications.

The results presented here constitute a foundation for the development of a new class of tunable fluorophores for near-infrared multicolor bioimaging.

7576-12, Session 3

Strategy for developing pH sensitive NIR probes

M. Y. Berezin, H. Lee, Washington Univ. School of Medicine in St. Louis (United States); K. Guo, Washington Univ. in St. Louis (United States); W. J. Akers, S. Achilefu, Washington Univ. School of Medicine in St. Louis (United States); O. Vasalatiy, A. H. Gandjbakhche, G. Griffiths, National Institutes of Health (United States); A. Almutairi, J. M. J. Frechet, Univ. of California, Berkeley (United States)

Many physiological processes function efficiently within a well-controlled pH range. Higher acidity level (acidemia and acidosis) has been implicated with a number of systemic pathologies, such as renal acidosis, metabolic disorders, intoxications, diabetes and emphysema, as well as localized hyperacidity such as infections, inflammation and cancer. The potential of pH sensitive fluorescent probes for reporting on biological environments has been widely utilized on a variety of cell studies and has been recently recognized as a powerful approach for in vivo imaging of diseases associated with elevated acidity level. We present several strategies aiming on the development of pH sensitive probes suitable for in vivo imaging. The strategies include incorporation of pH sensitive functionalities in known fluorophores, synthesis of novel pH sensitive skeletons and design of pH sensitive nanoparticles using acid-degradable polymers.

7576-13, Session 4

Fluorescence lifetime imaging spectroscopy in living cells with particular regards to pH dependence and electric field effect

N. Ohta, T. Nakabayashi, S. Oshita, M. Kinjo, Hokkaido Univ. (Japan)

Intracellular pH is one of the most important factors to understand physiological states of cells because significant changes in intracellular pH occur in a close relationship with many cellular functions, and pH-sensitive fluorescent dyes have been widely used to monitor intracellular pH. Fluorescence microscopy with pH-sensitive dyes offers a method for pH imaging in cells and tissues. However, fluorescence intensity is not easy to be analyzed with a microscope because it depends on excitation intensity, photobleaching of fluorescent chromophores, and absorption by the sample. Fluorescence lifetime imaging spectroscopy (FLIM) solves these problems, since fluorescence lifetime is independent of photobleaching, excitation power, and other factors that limit intensity measurements.

In the present study, we have shown that the intracellular pH of a single cell can be imaged using FLIM of green fluorescent proteins (GFPs). The correlation between the intracellular pH and the fluorescence lifetime of EGFP is well explained by considering the pH-dependent ionic equilibrium of the p-hydroxybenzylidene-imidazolidinone structure of the chromophore of EGFP. The equilibrium constant between the neutral and anionic EGFP chromophores in HeLa cells is obtained by analyzing the fluorescence lifetimes observed with different values of intracellular pH. The equilibrium between these chromophore forms depends on pH of the

medium.

It is also discussed how fluorescence lifetime in living cells is affected by the electric fields surrounding the chromophore.

7576-14, Session 4

Modeling structure and spectra of red fluorescent proteins

J. Collins, I. Topol, SAIC- Frederick Inc., NCI-Freder (United States); A. Savitsky, A.N. Bach Institute of Biochemistry (Russian Federation); A. V. Nemukhin, M.V. Lomonosov Moscow State Univ. (Russian Federation)

Photosensing proteins which contain organic chromophores with extended π -conjugated systems play a crucial role in living organisms. They include the light converters which emit light as a consequence of the primary photoexcitation as in Green Fluorescent Protein (GFP) like proteins, widely used in biology and medicine as in vivo biomarkers. Red fluorescent proteins (RFP) which are able to emit light in the far red range are more favorable in actual applications to living cells. To assist rational design of novel efficient biomarkers, the modern tools of molecular modeling are being used for predictions of structures and optical spectra of different variants of RFPs. We apply quantum mechanical approaches to estimate equilibrium geometry configurations as well as positions and intensities of spectral bands of the chromophore containing regions for a number of RFPs, including the kindling version of the chromoprotein from the sea anemone Anemonia sulcata, asFP595, DsRed (or drFP583) from Discosoma coral, and its artificial mutants of the so-called mFruits series. As demonstrated in previous simulations for GFP and blue fluorescent proteins, the following practical strategy can be used for modeling. A model system is designed as a molecular cluster constructed on the basis of available crystal structures of the related protein. The equilibrium geometry parameters of the cluster are optimized with the density functional theory approximation. The vertical excitation energies corresponding to the S0-S1 transitions are computed by using the semiempirical ZINDO technique. Effects of protein environment on the optical properties of the chromophore containing domain are taken into account by using a quantum mechanical - molecular mechanical approach. Mechanisms of photoexcitation, identification of the functional states of the chromophores, elucidation of the role of point mutations in the photoreceptor proteins are considered on the basis of simulations.

7576-15, Session 4

Strong local electric fields in red fluorescent proteins result in quadratic Stark shifts of their absorption peaks

M. A. Drobizhev, S. E. Tillo, N. S. Makarov, T. E. Hughes, A. Rebane, Montana State Univ. (United States)

Intrinsically fluorescent proteins (FPs) exhibit broad variations of absorption and emission colors and are available for different imaging applications. The physical cause of the absorption wavelength change from 540 nm to 590 nm in the Fruits series of red FPs has been puzzling because the mutations that cause the shifts do not disturb the piconjugation pathway of the chromophore. Here we use two-photon absorption (2PA) measurements to obtain all-optically the value of the permanent dipole moment difference (deltamu) between the excited and the ground states in a series of 9 different FPs of the Fruits series. Large variations of deltamu within the series (1 - 4D) are explained by a guite large contribution from an induced part of the permanent dipole moment change. Since deltamu is sensitive to internal electric field, the latter can be extracted from one- and two-photon absorption measurements. Our approach presents the first purely experimental (and purely optical) method of assessing internal electric fields inside proteins. Furthermore, we observe that in the Fruits FP series, large shifts in absorption peak (corresponding to different hues) can be explained by a quadratic Stark

Return to Contents TEL: +1 360 676 3290 · +1 888 504 8171 · customerservice@spie.org

Conference 7576: Reporters, Markers, Dyes, Nanoparticles, and Molecular Probes for Biomedical Applications



effect due to large variations (10 - 100 MV/cm) of the strong internal electric field within the beta barrel. The understanding of the role of local field in photophysical properties of FPs, such as absorption peak position, 2PA brightness, photostability, and sensitivity to local intracellular fields and ion concentration provides new guidelines for smart mutations, potentially capable to dramatically improve the above mentioned properties.

7576-16, Session 4

A quantitative nanoplatform for receptormediated amplification of gene silencing

M. A. McDonald, J. T. Elliott, M. Halter, A. L. Plant, National Institute of Standards and Technology (United States)

RNA interference, a powerful molecular analysis tool which permits targeted inhibition of gene expression, has tremendous potential in medical diagnostics and in vivo therapeutics. Protein nanospheres represent a versatile and quantitative nanoplatform for the targeted delivery of plasmid DNA encoding siRNA to specific cells. Some advantages of protein nanospheres include 1) the ability to convert apparently any protein into a nanosphere, 2) retention of receptormediated uptake, and 3) encapsulation of nanoparticles, genes and drugs. Transferrin protein nanospheres encapsulating a plasmid construct containing eGFP inhibiting siRNA and transferrin receptor expressing genes were evaluated for amplification of gene silencing in eGFP stably transfected NIH-3T3 fibroblast cells. Our aim was to correlate concentration of nanospheres with the efficiency of three simultaneous outcomes in cells: eGFP inhibition through siRNA transfection, TfR upregulation via delivery of the TfR coding sequence and cell viability. Monodisperse < 100 nm nanospheres were evaluated via ZetaPALS analysis and electron microscopy. eGFP inhibition was determined by flow cytometry, fluorescence microscopy and immunohistochemistry. Receptor-specific binding, up-regulation, and receptor-mediated endocytosis were analyzed using FACS and pulsing studies conducted at 4°C with intermittent freeze-thaw cycles. We will also present preliminary data on amplifying probe signal by nanospheres encapsulating a plasmid which contains both reporter genes (eGFP and TfR) and metal nanoparticles. It is hoped that a receptor-mediated positive feedback model for amplification of probe signal and gene transfection will eventually prove useful in the treatment of disorders of receptor function, such as severe forms of hemochromatosis and familial hypercholesterolemia.

7576-52, Poster Session

Aqueous synthesis of PbS quantum dots for noninvasive near-infrared fluorescence imaging in a mouse model

D. Deng, X. Chen, J. Zhang, F. Liu, J. Cao, Y. Gu, China Pharmaceutical Univ. (China)

In recent years, the syntheses and bio-applications of water-soluble near-infrared(NIR)-emitting quantum dots (QDs) have received an increasing attention. To date, various kinds of aqueous NIR-emitting QDs, including CdTe, CdHgTe, HgTe and so on have been synthesized. However, to our knowledge, these Cd-, Hg-, and Te-, Se-based quantum dots all are highly toxic; the commonly used stabilizers are volatile effluvial liquids with the carcinogenic properties; and the synthetic conditions are also complicated, needing high reaction temperature (≥100), long refluxing time and the protection of inert atmosphere. These shortcomings will limit their applications in biomedical fields.

As a member of the important and classical group of IV-VI semiconductors, PbS now has been widely used in many fields, such as infrared (IR) detection, photography, optical switching, and solar absorption. Due to the rather small band gap (0.41 eV) and the large exciton Bohr radius (18 nm), PbS should be a very ideal material for the synthesis of NIR-emitting nanocrystals. In this study, water-soluble

dihydrolipoic acid (DHLA)-capped PbS QDs were prepared by using a new facile and environmental friendly method. The resulting QDs show a strong near-infrared fluorescence. The photoluminescence quantum yield (QY) of ~10% was achieved under optimized conditions without any post-preparative treatment. We further investigated the cytotoxicity and in vivo toxicity of PbS QDs. The preliminary results indicated that these QDs are lowly toxic, compared to the above existing aqueous NIR-emitting QDs. In addition, the produced DHLA-capped PbS QDs were tried to use for the NIR fluorescence imaging in a mouse model.

7576-53, Poster Session

Photodynamic/photocatalitic effects on microorganisms, processed by nanodyes

E. Tuchina, V. V. Tuchin, Saratov State Univ. (Russian Federation)

Photodynamic therapy uses laser, LED or lamp light sources in combination with dyes - photosensitizers for the enhancement and localization of effects within the human body. We are developing a new approach of improvement of the efficiency of antimicrobial phototherapy via combined application of photosensitizers and the photocatalysts to pathogenic microorganisms. The main goal of the paper is to conduct experiments to study the action of nanodyes, based on mixtures of nanoparticles and photosensitizers, in combination with LED irradiation of pathogens.

Materials and methods

An object of the study used is a culture of Staphylococcus aureus, Escherichia coli, Candida albicans.

Source of red light is LED with a maximum radiance in the range around 625 nm and the emission power density of 33 mW/sq.cm; the source of blue light is LED with a maximum radiance in the range around 405 nm and the emission power density of 31.5 mW/sq.cm. The light exposure was ranged from 5 to 30 min. As photosensitizers 0.0025%-aqueous solution of methylene blue was used. As a photocatalyst 0.02%-suspension of nanoparticles of titanium dioxide (TiO2) was used.

The method of consecutive cultivations of initial concentration of a microbial suspension of 1000 microbial cells per ml was applied. Solutions of photosensitizers were added to a suspension of the microorganisms, the received mixture was remained in darkness during 10 min. Then the suspension was placed to sections of experimental ditch of volume of 0.2 ml for light exposure. After exposure to light culture was distributed to Petry dishes with a dense nutrient medium. The account of results was provided by calculation of colony forming units (CFU) in 5 days after incubation at 37°. As the control accepted colony forming ability values of bacteria not subjected to an irradiation and not processed by dyes. Each experiment has been made in tenfold frequency

Application of nanodye with combined blue-red radiation (405, 625 nm) to S. aureus was very effective. Reduction of the number of CFU occurred after 5 min of irradiation by blue-red light was of 25%; after 10 min - 40%; after 15 min - 65%; and after 30 min - 90%. Application of nanodye led to a substantial reduction in bacterial populations. After 10 min of irradiation, the use of nanodye 2-4 times increased the antibacterial effect of phototreatment.

Exposure of cells E.coli to combined light (405, 625 nm) did not significantly affect the development of these microorganisms. The observed reduction of the number of CFU was in average of 2 - 8% to the control that is not a valid value. Using nanodye (nanoparticles + methylene blue) light action led to a more pronounced effect: after 30 min-exposure the reduction of CFU was of 18%.

Treatment of cells C. albicans by combined radiation (405, 625 nm) caused a significant reduction of the number of these microorganisms after 30 min of exposure (19 - 93%.). Using nanodye as a photosensitizer has the overwhelming effect after 10 min of exposure. Reduction of the number of CFU of microorganisms, incubated with nanodye, with variation of exposure time from 5 to 30 min occurred in the range of 33 - 97%

We assume that differences in the sensitivity of the investigated



microorganism to radiation can be explained by differences in the structure of their cell walls.

S. aureus is a gram-positive microorganism with a cell wall composed mainly of peptidoglycan. Several differencies has a cell wall of C. albicans, but in the overall structure is similar. The interaction of photosensitizers, nanoparticles and radiation activate a number of radicals, which damage peptidoglycan and kill these microorganisms.

E. coli is a gram-negative microorganism with a cell wall, the main feature of which is the presence of LPS layer (the so-called outer membrane). The efficiency of interaction of photosensitizers with the cell wall is low. The active radicals over the course of time not able to overcome many layers. Lesions arising in cells of E.coli via the photodynamic/ photocatalitic effects are of less significance, the cell remains alive.

7576-54, Poster Session

Development of highly sensitive novel fluorescence probes to detect activity of protease based on unique intramolecular spirocyclization

M. Sakabe, The Univ. of Tokyo (Japan); H. Kobayashi, National Institutes of Health (United States); T. Nagano, Y. Urano, The Univ. of Tokyo (Japan)

Proteases play essential roles in cancer and immune disease, as well as in the generation of amino acids for protein synthesis. Sensitive and accurate protease detection systems become a crucial tool for the early diagnosis of diseases. To detect activity of protease, rhodamine110 derivatives based fluorescence probes have been widely used. However, since these substrates have two reactive sites, two enzymatic reactions are necessary to become strongly fluorescent, decreasing the rate of fluorescence manifestation and limiting the linear range of assays.

Recently, we reported that a series of tetramethylrhodamine derivatives bearing a hydroxymethyl or mercaptomethyl group instead of original carboxy group showed unique intramolecular spirocyclization. Based on these findings, we synthesized a series of new hydroxymethylrhodamine110 (RhoHM) derivatives. RhoHM was strongly fluorescent in aqueous solution at pH7.4, while a compound that one of the amino groups of RhoHM is acetylated, was colorless and nonfluorescent. This result suggests that we can regulate fluorescence by controlling intramolecular spirocyclization at one reactive site. Next, we developed fluorescent probes for leucine aminopeptidase and gammaglutamyltranspeptidase based on this approach. With our probes, the activity of these proteases could be detected sensitively, quickly and quantitatively. Finally, we applied them to various living cells and imaged activity of proteases. We will present their properties in detail in this symposium.

7576-55, Poster Session

Fluorescence emission and polarization analyses for evaluating binding of ruthenium metalloglycocluster to lectin and tetanus toxin C-fragment

T. Okada, N. Minoura, Tokyo Univ. of Technology (Japan)

We have confirmed a fluorescent ruthenium metalloglycocluster as a powerful molecular probe for evaluating a binding event between carbohydrates and lectins by fluorescence emission (FE) and fluorescence polarization (FP) analysis. The fluorescent ruthenium metalloglycoclusters designed in this study, [Ru(bpy-2Gal)3] and [Ru(bpy-2Glc)3], possess clustered galactose and glucose surrounding the ruthenium center. Changes in FE and FP of these metalloglycoclusters were measured by adding each lectin (Peanut agglutinin (PNA), Ricinus communis agglutinin 120 (RCA), Concanavalin A (ConA), or Wheat germ agglutinin (WGA)) or tetanus toxin c-fragment (TCF). Following

the addition of PNA, the FE spectrum of [Ru(bpy-2Gal)3] showed new emission peak and the FP value of [Ru(bpy-2Gal)3] increased. Similarly, the FE spectrum of [Ru(bpy-2Glc)3] showed new emission peak and the FP value increased following the addition of ConA. Since other combinations of the metalloglycoclusters and lectin caused little change, specific bindings of galactose to PNA and glucose to ConA were proved by the FE and FP measurement. Dissociation constants (Kd) of [Ru(bpy-2Gal)3] to PNA and [Ru(bpy-2Glc)3] to ConA were calculated from the changes in FP values following addition of each lectin. From nonlinear least-squares fitting, Kd of [Ru(bpy-2Gal)3] and PNA was 6.1 × 10-6 M, and Kd of [Ru(bpy-2Glc)3] and ConA was 1.8 × 10-5 M. Furthermore, the FP measurements proved specific binding of [Ru(bpy-2Gal)3] to TCF. The results obtained in this study ensure that the FP analysis using the ruthenium metalloglycocluster is useful for evaluating interactions between carbohydrate and toxins.

7576-56, Poster Session

Tissue distribution, toxicity assessment, and oxidative profile of squaraine-based photosensitizer

G. Devi, D. Ramaiah, T. R. Cibin, A. Abraham, Univ. of Kerala (India)

Photodynamic therapy is an investigational anti-cancer therapy that involves the usage of photosensitizers and visible light. Measuring the fluorescence intensity of squaraine dyes-one of the newly developed photosensitizers-localized within different organs has not previously been described. The present study confirms the selective uptake of bis (3, 5-diiodo-2, 4, 6-trihydroxyphenyl) squaraine within tumor tissues compared to adjacent normal tissues. 7, 12-Dimethyl Benz(a) anthracene was used for the induction of skin tumor in Swiss albino mice. Concentration of the dye in different organs and tumor tissue was determined fluorimetrically at different intervals of time after administration. It was found to be maximal at 6h (both in the normal and tumor-induced animals) after administration and there is no indication of the dye in other parts of the body after 24h, except in the tumor site. The toxicity assessments and analysis of oxidative stress were carried out in normal healthy Swiss albino mice at 6h and 24h post injection of the dye. The biochemical markers of toxicity (alkaline phosphatase, acid phosphatase, serum glutamate oxaloacetate transaminase serum glutamate pyruvate transaminase, lactate dehydrogenase and creatine kinase) were assayed. Since the photosensitizers induce photo-killing of malignant cells by the formation of reactive oxygen species, the oxidative profile of the normal tissues should be checked. The study thus involves the assessment of oxidative status (Thiobarbituric acid reactive substance, Superoxide dismutase, catalase, Glutathione peroxidase, Glutathione reductase and Reduced Glutathione content) of the dye-injected mice. The results reveal that the dye is absolutely non-toxic and the animals did not show any symptoms of toxicity. The oxidative profile of the normal tissues is not altered significantly by the dye. Taken together, the observed data show that bis (3, 5-diiodo-2, 4, 6-trihydroxyphenyl) squaraine provides impetus for further experimental investigations and possible clinical applications.

7576-57, Poster Session

Squaraine PDT induces oxidative stress in skin tumor of swiss albino mice

T. R. Cibin, G. Devi, D. Ramaiah, A. Abraham, Univ. of Kerala (India)

Photodynamic Therapy (PDT) using a sensitizing drug is recognized as a promising medical technique for cancer treatment. It is a two step process that requires the administration of a photosensitizer followed by light exposure to treat a disease. Following light exposure the photosensitizer is excited to a higher energy state which generates free radicals and singlet oxygen. The present study was carried out

TEL: +1 360 676 3290 · +1 888 504 8171 · customerservice@spie.org



to assess the oxidative damage induced by bis (3, 5-diiodo-2, 4, 6-trihydroxyphenyl) squaraine in skin tumor tissues of mice with/ without light treatment. Skin tumor was induced using 7, 12-Dimethyl Benz(a) anthracene and croton oil. The tumor bearing mice were given an intraperitoneal injection with the squaraine dye. After 24h, the tumor area of a few animals injected with the dye, were exposed to visible light from a 1000 W halogen lamp and others kept away from light. All the mice were sacrificed one week after the PDT treatment and the oxidative profile was analyzed (Thiobarbituric acid reactive substance, Superoxide dismutase, catalase, Glutathione peroxidase, Glutathione reductase and Reduced Glutathione content) in tumor/ skin tissues. The dye induces oxidative stress in the tumor site only on illumination and the oxidative status of the tumor tissue was found to be unaltered in the absence of light. The results of the study clearly shows that the tumor destruction mediated by PDT using bis (3, 5-diiodo-2, 4, 6-trihydroxyphenyl) squaraine as a photosensitizer is due to the generation of reactive oxygen species, produced by the light induced changes in the dye.

7576-58, Poster Session

Cellular uptake of polymeric nanocapsules loaded with ICG by human blood monocytes and endothelial cells

B. Bahmani, B. Jung, S. Gupta, B. Anvari, Univ. of California, Riverside (United States)

Indocyanine green (ICG) is an FDA approved near infrared dye used in assessment of hepatic function and ophthalmological vascular imaging. However, given the rapid clearance of ICG from the blood stream, its imaging and phototherapeutic applications remain very limited. As a potential method to increase circulation time of ICG, and extend its clinical applications, we have encapsulated ICG within polymeric based nanoconstructs whose surface can be coated with various materials including polyethylene glycol (PEG) and dextran. ICG-containing nanocapsules (ICG-NCs) can be constructed in various diameters ranging from approximately 80 nm to 1 µm. To gain an understanding of the interaction between ICG-NCs and vascular cells, we are characterizing the uptake of the nanocapsules coated with various materials by peripheral blood monocytes and endothelial cells using fluorescence microscopy. Results of these studies will be useful in identifying the appropriate diameter and coating material that will result in increased circulation time of ICG-NCs within the vasculature.

7576-59, Poster Session

Organically modified silica nanoparticles entrapping hydrophobic two-photon absorbing squaraine dye as probes for twophoton optical imaging

X. Wang, C. O. Yanez, S. Yao, S. A. Coombs, C. L. Arnett, K. D. Belfield, Univ. of Central Florida (United States)

Nanomaterials have revolutionized the fields of medicine, bioimaging, and photonics due to their chemical and biological resilience, safety, and multimodality of the surface. Ceramic-based nanomaterials have proven to be innocuous and have been widely used in drug delivery and bioimaging technologies. We report the synthesis and characterization of organically modified silica (ORMOSIL) nanoparticles, entrapping a hydrophobic squaraine-based dye, which can provide a stable aqueous dispersion of the flourophore. Monodispersed organically modified silica nanoparticles (ca. 20 nm diameter), entrapping hydrophobic two-photon absorbing squaraine dye 2,4-bis (4-(dibutyliminio)-2-hydroxycyclohexa-2, 5-dienyl)-3-oxocyclobut-1-enolate (SQ44OH) have been synthesized in the nonpolar core of Pluronic F 87 micelles by hydrolysis of triethoxyvinylsilane. After TEM characterization of the nanoparticles, spectroscopy was used to demonstrate that the optical properties of the incorporated dye were retained. In vitro studies using HCT-116

cells revealed cellular uptake of the nanoparticles. The ease of surface functionalization of a variety of biotargeting molecules, which can deliver the probes to specific cancer cells, makes these two-photon fluorescent organically modified silica (ORMOSIL) nanoparticles potential candidates as efficient probes for optical bioimaging.

7576-60, Poster Session

Fluorescence Imaging of Peritoneal Metastases of Ovarian tumors in Mouse Models with beta-Galactosidase Targeted Fluorescence Activatable Probes

D. Asanuma, M. Kamiya, The Univ. of Tokyo (Japan); M. Ogawa, N. Kosaka, Y. Hama, Y. Koyama, P. L. Choyke, H. Kobayashi, National Cancer Institute, National Institutes of Health (United States); T. Nagano, Y. Urano, The Univ. of Tokyo (Japan)

Peritoneal metastases are an important cause of morbidity and mortality especially in ovarian cancer patients. The majority of patients with ovarian cancer have a poor prognosis because they already have advanced-stage disease with peritoneal metastasis at the time of diagnosis. Cytoreductive surgery followed by systemic or peritoneal chemotherapy is the standard of care for the initial management of patients with advanced-stage ovarian cancer. However, cytoreduction is often suboptimal due to the small size and location of the metastases and the poor visual contrast between tumor and normal tissue under the white-light conditions. For such operations, fluorescence activatable probes that become highly fluorescent to realize facile detection of lesions after their target reaction have been attracting much attention. In several ovarian tumor cells, we found high enzymatic activities of betagalactosidase that is often used as a reporter enzyme and is believed not to be expressed so much in normal mammalian cells. Therefore, we tried to visualize peritoneal metastases in mouse models by intraperitoneal injection of our developed fluorescence activatable probe, HMRB-betaGal, for beta-galactosidase based on the rhodol fluorophore (30 nmol/mouse). At 1 hr post-injection, peritoneal metastases were successfully visualized in vivo as small as submillimeter in size by laparoscopic or endoscopic fluorescence imaging in all tested mouse models with ovarian tumor cells including SHIN3, OVCAR3 or SKOV3. Furthermore, unlike other fluorescence activatable probes such as 5-aminolevulinic acid, our activatable strategy targets rapid enzymatic reaction. Therefore, visualization of the lesions with HMRB-betaGal in the mouse models was achieved even at 10 min post-injection, indicating that our strategy realizes early fluorescence detection of peritoneal metastases in the imaging time course.

7576-61. Poster Session

Characterization of surface enhanced Raman scattering (SERS) substrates fabricated from colloidal printing inks

M. A. Figueroa, W. Stephenson, Drexel Univ. (United States); S. D. Park, Univ. of California, Berkeley (United States); K. Pourrezaei, S. D. Tyagi, Drexel Univ. (United States)

Fabrication of surface enhanced Raman scattering (SERS) substrates to detect trace concentrations of biological molecules has been vigorously studied for the past few decades. A variety of fabrication methods exists including electron beam lithography, vapor deposition and sputter coating. These methods typically involve multiple steps that significantly add to the production costs of SERS substrates. Although colloidal suspensions of metallic nanoparticles have been extensively used for SERS applications, there are few published accounts of using colloidal nanoparticle thin films as SERS substrates. Here we discuss an inexpensive and reproducible fabrication method for SERS substrates using colloidal silver nanoparticle inks. We show that when thermally treated the silver particles in the nanoparticle based inks arrange into



fractal clusters creating an environment ideal for localizing optical excitations that results in very high SERS amplification. By varying the temperature and heating time after printing it is possible to tune the interparticle spacing to optimize the SERS effect. Typically, heating the as-deposited colloidal nanoparticle films in the 80 - 100oC range for 10 - 30 seconds was found adequate to yield SERS amplification factors exceeding 106. We have also studied the effect of thermal annealing on the microwave conductivity of the nanoparticle films at approximately 10 GHz. The microwave losses predominantly occur at the weak links between the silver nanoparticles during the pre-sintering stage. This makes the microwave conductivity a sensitive measure of the degree of sintering and hence can be correlated to the SERS performance of the substrates.

7576-72, Poster Session

Dual near-infrared optical/MRI organic probe sensitive to protein binding

K. Guo, Washington Univ. in St. Louis (United States); M. Berezin, Washington Univ. School of Medicine in St. Louis (United States); J. Zheng, Washington Univ. in St. Louis (United States); W. J. Akers, Washington Univ. School of Medicine in St. Louis (United States); F. Lin, Washington Univ. in St. Louis (United States); O. Vasalatiy, A. H. Gandjbakhche, G. Griffiths, National Institutes of Health (United States); S. Achilefu, Washington Univ. School of Medicine in St. Louis (United States)

No abstract available.

7576-17, Session 5

Multifunctional inorganic nanoparticles for imaging, targeting, and drug delivery

J. I. Zink, M. Liong, A. Nel, F. Tamanoi, Univ. of California, Los Angeles (United States)

The synthesis of multifunctional inorganic nanoparticles with a coreshell structure that have dual-imaging capability and are capable of cancer cell-specific delivery of anticancer drugs is described. Superparamagnetic Fe3O4 nanocrystals were incorporated in the nanoparticles as the core materials for the magnetic functionality and MR imaging. The ionic surfactants were used to solubilize the hydrophobic nanocrystals in water and also served as the structure directing agents for the mesoporous silica shell formation. A mild ion-exchange procedure was used in removing the surfactant templates from the mesopores to avoid dissolution of the iron oxide core and to prevent particle aggregation. An additional surface coating with hydrophilic groups increased the stability of the nanoparticle dispersion in aqueous solution. The mesoporous silicate shell was further modified with fluorescent molecules and targeting ligands, and the pores were filled with chemotherapeutic drug molecules. These nanoparticles were monitored inside the cells by both MR and fluorescence imaging methods, and were used as drug delivery vehicles. The targeting ligand modification increased the drug payload delivery into human cancer cells, but not into non-cancerous cells. The potential to simultaneously monitor and deliver molecules to the targeted tissue region will be highly beneficial for both imaging and therapeutic purposes.

7576-18, Session 5

Sustained and observable oxidation-triggered release of therapeutics using porous Si particles

E. Wu, J. Andrew, J. Park, J. Park, E. Segal, L. Cheng, W. Freeman, M. Sailor, Univ. of California, San Diego (United States)

There is a need for a controlled and observable drug delivery system, enabling long acting local treatment of cancer, ocular diseases, and other diseases in which recurring drug administration is necessary. To address challenges in the delivery of drugs with narrow therapeutic indices, we have developed biodegradable and biocompatible porous Si microparticles with tunable photonic properties. The molecules are bound to the Si matrix by covalent attachment using a Si-C linker. Oxidation of the underlying Si matrix in aqueous solutions results in conversion to silicon oxide, allowing a slow release of the linker-molecule complex by hydrolysis of the Si-O attachment points. In addition, the porous structure of the particles gives rise to an optical reflectance spectrum that allows for monitoring of drug release. As drugs are released or as the particles degrade, the optical reflectance spectrum changes, resulting in an observable color change. The potential for intraocular drug delivery was tested using daunorubicin-loaded particles. Daunorubicin release from porous Si particles was observed for up to 30 days in vitro. Compared to free daunorubicin, the residence time of daunorubicin attached to porous Si particles is significantly prolonged. The optical spectra of the particles were monitored and a correlation was observed between daunorubicin release and the color change of the particles. The unique optical properties of porous Si allow for a simple and non-invasive method of monitoring the extent of drug release in the vitreous during the treatment of ocular diseases.

7576-19, Session 5

Novel remotely triggered nanocarrier for imaging and therapy applications

K. E. Wilson, K. Homan, S. Emelianov, The Univ. of Texas at Austin (United States)

Nanoparticles that can act as multifunctional carriers for imaging contrast and therapy agents can provide unique solutions for effective disease detection, diagnosis and treatment. We introduce one such injectable, biocompatible, and targetable nanocarrier that is multifaceted. To fabricate these multifunctional nanocarriers, the desired nanoparticles (e.g., gold nanospheres or nanorods, silver nanospheres, nanotriangles, or nanodiscs, iron oxide nanospheres, etc.) and therapeutic agents (e.g., chemotherapeutic drugs, etc.) are incorporated in organic liquid perfluorocarbon droplet nanocarriers in an aqueous environment. After intravenous injection, these particles accumulate in diseased tissues due to targeting and the enhanced permeability and retention effect. The delivery and accumulation of nanocarriers within tissue can be visualized since the nanocarrier can act as an imaging contrast agent in photoacoustic, ultrasound, thermal or magneto-motive imaging. Once accumulated, among many other possibilities, the nanocarrier can provide optically triggered or radio frequency controlled release of drug encapsulated within the droplet. Furthermore, the nanocarrier can be used to facilitate photomechanic, photothermal, and microwave ablation therapy, etc. Overall, the remote triggering of the nanocarrier is critical for its functionality ranging from an imaging contrast agent to various forms

In this paper, the development of nanocarriers containing optically absorbing metal nanoparticles is described. Imaging and therapeutic applications of the developed nanocarriers will be demonstrated. Overall, our studies indicate that the developed multi-functional nanocarriers can house a wide variety of nanoparticles and therapeutic agents. Furthermore, these nanocarriers have high potential in many applications including diagnostic multi-modal imaging, image-guided therapies, drug delivery and release, etc.



7576-20, Session 5

Photophysical characterization of fluorescent metal nanoclusters synthesized using oligonucleotides, proteins and small reagent molecules

H. Yeh, J. Sharma, Los Alamos National Lab. (United States); Y. Bao, Univ. of Alabama (United States); J. H. Werner, J. S. Martinez, Los Alamos National Lab. (United States)

Noble metal nanoclusters are composed of only a few metal atoms and are typically less than 1nm in size. With dimensions close to the Fermi wavelength, these nanoclusters demonstrate molecular-like properties distinct from bulk metals or atoms, such as discrete and size-tunable electronic transitions which lead to photoluminescence. In contrast to semiconductor quantum dots, which are often larger and contain toxic metal cores, noble metal nanoclusters show substantial promise as new fluorescent labels and have many advantages in biological imaging and detection due to their size and bio-compatibility. Current research aims to elucidate the fundamental photophysical properties of the existing metal nanoclusters made by different means and based on different templates. Here, we report the study of the photophysical properties, including quantum yields, lifetimes, synthetic yields, and sizes, of gold or silver nanoclusters synthesized from templates such as an oligonucleotide (CCCTTAATCCCC), a protein (bovine serum albumin) and a Good's buffer molecule (MES, 2-(N-morpholino)ethanesulfonic acid). Size, particle concentration, and brightness per cluster were determined by fluorescence correlation spectroscopy, with fluorescence lifetime measured by time-correlated single photon counting. From ensemble fluorescence and lifetime measurements, we found multiple fluorescent species are generated from silver templated with DNA, while single fluorescent species are formed when gold is templated by the protein and MES. We also explore the possibility to use these fluorescent metal clusters as a donor or an acceptor in forming resonance energy transfer pairs with commercial quantum dots and common organic dyes.

7576-21, Session 6

Enzymatic generation of quantum dots: activity assay for acetylcholine esterase with exponential evolution of fluorescence

V. Pavlov, CIC BiomaGUNE (Spain)

Inorganic semiconductor nanoparticles have been extensively studied due to their electronic and optical properties and employed as probes for biosensing in bioanalytical chemistry. Their emission properties are a consequence of quantum effects, hence they are frequently called quantum dots (QDs). QDs have been generally used as fluorescent labels in immunoassays and as energy-transfer donors in assays based on fluorescence resonance energy transfer (FRET).

In the present work, we report the first example of enzymatic generation of quantum dots in vitro with a bioanalytical application for the detection of the enzymatic activity of acetylcholine esterase (AChE) and its inhibition by 1,5-bis(4-allyldimethylammoniumphenyl) pentan-3-one dibromide (BW284c51). We have developed a new method for the synthesis of CdS nanoparticles in the presence of cadmium sulfate, sodium thiosulfate and the thiol-bearing compound thiocholine. Anions of thiosulfate, S2O32- are hydrolyzed to S2- which in the presence of Cd2+ cations form nanocrystals of CdS. The rate of this reaction is low, but thiol-containing organic compounds decompose S2O32- to S2-. Thiocholine is produced by the hydrolysis of acetylthiocholine mediated by acetylcholine esterase and enhances the rate of decomposition of sodium thiosulfate into S2- anions which in the presence of cadmium sulfate yield fluorescent CdS quantum dots. The formation of the enzimatically produced CdS QDs was followed by fluorescence spectroscopy. We have been able to modulate the formation of CdS nanoparticles by varying the activity of acetylthiocholine esterase. Here, we introduce a new approach for the detection of enzymatic activities using biocatalytic generation of quantum dots.

7576-22, Session 6

Design of PEGylated rare-earth doped ceramic nanophosphors for near-infrared bioimaging

Y. Nagasaki, Univ. of Tsukuba (Japan) and International Ctr. for Materials Nanoarchitectonics, National Institute for Materials Science (Japan); M. Kamimura, Univ. of Tsukuba (Japan); K. Soga, Tokyo Univ. of Science (Japan) and Ctr. for Tsukuba Advanced Research Alliance, Univ. of Tsukuba (Japan)

Fluorescence biolabeling is a technique for visualizing biological events and can be applied in medical sensing and diagnosis using fluorescence materials. Most of current fluorescence bioimaging materials such as organic dyes, fluorescence protein and quantum dot require ultraviolet (UV) light as the excitation source. However, UV damage to the observed object, biomolecules in the observation object generate autofluorescence. Furthermore, UV light cannot penetrate deep in to the specimen. To solve these problems, we focused on the rare-earth ion doped ceramic nanophosphors (RED-CNP) applied in fluorescence bioimaging. RED-CNP are known to show near-infrared (NIR)-to-visible upconversion emission and NIR-to-NIR emission. NIR excitation light does not excited biomolecules, the emission of RED-CNP can be measured with less autofluorescence and scattering of the excitation light as compared with UV excitation. NIR excitation and emission light also can penetrate deeply into tissues in vivo.

In this study, poly(ethylene glycol) (PEG)/polyanion block copolymer was introduced on the surface of ytterbium and erbium ion co-doped yttrium oxide nanoparticles (YNP) to improve dispersing stability. The PEGylated YNPs were dispersed over 1week under physiological conditions as a result of the steric repulsion between the PEG chains on the YNP surface. Moreover, streptavidin installed YNP were prepared by the co-immobilization of PEG/polyamion and streptavidin. The PEG/streptavidin co-immobilized YNP specifically recognized biotinylated antibodies and emitted strong upconversion emission and NIR emission upon NIR excitation. The obtained complex is a promising as NIR bioimaging materials with high performances.

7576-23, Session 6

Nanocrystalline rare-Earth oxides for use as a novel multifunctional biological probe

R. C. Dennis, K. L. Nash, J. B. Gruber, D. K. Sardar, M. G. Zhang, W. Gorski, The Univ. of Texas at San Antonio (United States)

Nanocrystalline rare earth (RE) oxides exhibit both strong absorption and fluorescence ranging from the visible to the near IR region and have long fluorescent lifetimes on the order of milliseconds. The rare earths have an advantage over fluorescent labeling organic dyes and quantum dots (QD) that have the potential of being toxic to cells. We investigate the application of nanocrystalline RE3+:Y2O3 as a novel biosensor by exploiting both the emission and photoacoustic response of these materials in the near infrared (NIR). Two of the rare earths oxides that are ideal for this biosensor applications are Ho3+:Y2O3 and Nd3+:Y2O3, which have characteristic emission at 1.2 m and 0.9 to 1.1 m, respectively. Both Ho3+ and Nd3+ have strong absorption that overlaps well with the absorption of gold nanoshells, which is relatively strong and broad, ranging from 0.6 to 1.0 m. A comparative photoacoustic study is performed on RE3+:Y2O3/Au core/shell nanoparticles, 2-hydroxylmethacrylate (HEMA) coated RE3+:Y2O3 and pure nanocrystalline RE3+:Y2O3. The successful excitation of the nanocrystals yields a novel multifunctional probe for potential use in immunoassays and in vivo studies. This work was supported in part by the NSF sponsored Center for Biophotonics Science and Technology (CBST) at UC Davis under Cooperative Agreement No. PHY 0120999.



7576-24, Session 6

Rapid conjugation of nucleic acids to gold nanoparticles for cancer cell targeting

T. A. Larson, N. Li, A. Ellington, K. Sokolov, The Univ. of Texas at Austin (United States)

Plasmonic metal nanoparticles are of great interest to the biomedical community due to their strong optical properties and their ease of conjugation. Nucleic acids are routinely attached to gold nanoparticle surfaces, but published protocols are lengthy and involve slowly increasing salt concentrations over a period of 24 - 48 hours. We have developed a rapid conjugation protocol that can be finished in 1 hour by separately heating a solution of gold nanoparticles and a solution of thiol-terminated oligonucleotide handles to 80 C and then mixing rapidly at 80C. The kinetics of the thiol-gold interaction were explored and the reaction was found to be sufficient for gold nanoparticle stability in higher salt concentrations by 10 minutes. After washing away excess oligonucleotide handle via centrifugation, aptamers were conjugated to the oligonucleotide handles via an extension off the aptamer 3' end. The extent of aptamer loading was characterized and the nanoparticles were then incubated with A431 cells. The degree of labeling was determined via darkfield and confocal fluorescence microscopy. As the aptamer loading approached 200 aptamers per particle, the binding affinity towards A431 cells was lost. This was surprising given that other aptamers have been used at higher concentrations on gold nanoparticles, and work is ongoing to determine whether this is a general characteristic of all aptamer-conjugated gold nanoparticles or restricted to certain aptamers. These improvements and characterizations of aptamer-nanoparticle conjugates are a necessary next step in applying these particles to in vivo delivery of nucleic acids for molecular specific therapeutic and imaging applications.

7576-25, Session 6

Synthesis and characterization of upconversion emission on lanthanides doped ZrO2 nanocrystals coated with SiO2 for biological applications

T. López Luke, Ctr. de Investigaciones en Optica (Mexico); E. De La Rosa, Ctr. de Investigaciones en Óptica (Mexico); C. Angeles Chavez, Instituto Mexicano del Petroleo (Mexico); P. Salas, CFATA, Univ. Nacional Autónoma de México (Mexico)

Recently, upconversion fluorescence from lanthanide-doped nanocrystals have attracted much attention due to the potential applications as sensitive biolabelings, as improved alternatives to fluorophores and Quantum Dots (QD's). The main advantage of this approximation is the absence of absorption by tissue avoiding the self-fluorescence. In this work, funtionalization with SiO2 and bioconjugation of lanthanide doped ZrO2 nanocrystals to attach some specific protein is presented. The studied nanocrystals have different average size from 20 nm to 70 nm. These nanoparticles were coated with Silica with various thicknesses. The silica shell can prevent possible toxic effects of nanocrystals and provide better surface to facilitate conjugation with biomolecules. Fluorescence was obtained by up conversion processes after excitation with an LD at 970 nm. Luminescence properties were studied as a function of silica-shell thickness and biomolecules used. These bioconjugated nanoparticles are ready to be used in cancer detection research for both diagnostic and imaging.

7576-74, Session 6

Multicolor lymphatic optical imaging using nanoparticles

H. Kobayashi, National Institutes of Health (United States) No abstract available.

7576-26, Session 7

Dynamic molecular imaging using nanoparticle plasmon resonance coupling

K. V. Sokolov, The Univ. of Texas M.D. Anderson Cancer Ctr. (United States); J. Aaron, K. Travis, N. Harrison, The Univ. of Texas at Austin (United States)

Distance dependant coupling of plasmon resonances between closely spaced metal nanoparticles offers an attractive alternative for the imaging of molecular interactions. Here we analyzed interactions between molecular specific gold nanoparticles and live cells using a combination of dark-field reflectance and hyperspectral imaging. The results of optical imaging were correlated with transmittance electron microscopy of cell slices and theoretical simulations of optical properties of gold aggregates. We showed that nanoparticles targeted to growth factor receptors (epidermal growth factor receptor, EGFR - an important cancer biomarker) form closely spaced assemblies in the presence of the target molecule. Our experiments with living cells showed that receptor mediated assembly and plasmon coupling of gold bioconjugates result in a spectral shift of more than 100 nm in plasmon resonance frequency of the nanoparticles giving a very bright red signal. We demonstrated that plasmon coupling can be used for imaging of EGFR activation and trafficking as formation of EGFR dimers and further intracellular uptake in early and late endosomes is associated with progressive color changes from green to red, respectively, with each stage of EGFR cycle being associated with a distinct color of EGFR bound nanoparticles. This approach can allow imaging of molecular interactions ranging from protein pairs to multi-protein complexes with sensitivity and SNR that cannot be currently achieved with any other method.

7576-27, Session 7

Gold nanoparticle bioconjugates by laser ablation: a novel method aiming at pure nanomarkers for biomedical applications

S. Petersen, S. Barcikowski, Laser Zentrum Hannover e.V. (Germany)

Bioconjugated gold nanoparticles are of increasing interest for biomedical applications such as gene- and drug delivery, therapy and diagnostics. But each biological or medical application demands a tailored design of the nanoparticulate carrier system. Since the relationship between design and function is often not predictable, a screening method providing various bioconjugates is required. Conventionally, the generation of nanoparticles is well established by chemical synthesis methods. The molecular design of the nanoparticulate carrier with required functions for targeting, enhanced cellular uptake etc. is enabled in a successive surface functionalization (after the nanoparticle generation). However, application prospects might be restricted due to possible impurities resulting from the use of surfactants, chemical precursors or reducing agents.

We have established an in-situ bioconjugation during ultrashort pulsed laser ablation in liquids allowing both the generation of pure stable nanoparticles and their bioconjugation, demonstrated at the example of nucleic acids and a cell penetrating peptide. Besides functionality the in-situ conjugation provides the laser generated nanoparticles with a second prerequisite for application in biomedical assays, which is a

365

Return to Contents TEL: +1 360 676 3290 · +1 888 504 8171 · customerservice@spie.org



high stability in saline solutions. Furthermore the tunability of the process is discussed concerning surface coverage values, surface charge and conjugate size.

Since the mechanism of the in-situ bioconjugation during laser ablation is based on fundamental electron donor (biomolecule) - electron acceptor (nanoparticle) attraction, a huge variety of materials bearing these basic properties should be conjugable in future.

7576-28, Session 7

Biodegradable near-infrared plasmonic nanoclusters for biomedical applications

J. O. Tam, J. M. Tam, A. Murthy, L. L. Ma, K. A. Travis, K. P. Johnston, K. V. Sokolov, The Univ. of Texas at Austin (United States)

Nanoparticles such as gold and silver with plasmonic resonances in the near-infrared (NIR) optical region, where soft tissue is the most transparent, are of great interest in the biomedical applications. A major roadblock in translation of inorganic nanoparticles to clinical practice for systemic targeting of disease is their non-biodegradable nature. In addition, gold nanoparticles that absorb in the NIR are typically greater than 50 nm, which is above the threshold size of 5.5 nm required for effective excretion from the body. Here we describe a new class of biodegradable gold nanoparticles with plasmon resonances in the NIR region. The synthesis is based on controlled assembly of very small (less than 5 nm) primary gold particles into nanoclusters with approximately 50 nm overall diameter and an intense NIR absorbance. The assembly is mediated by biodegradable polymers, polyethylene glycol (PEG) and polylactic acid (PLA) copolymer, and small capping ligands on the constituent nanoparticles. Nanoclusters deaggregate into sub-5nm primary gold particles upon biodegradation of the polymer binder in live cells over 1 week, as shown by darkfield reflectance and hyperspectral imaging. This result was further verified using direct observation of nanocluster sizes by transmittance electron microscopy (TEM) of cell slices. We also demonstrated that plasmonic biodegradable nanoclusters provide high contrast in reflectance optical and photoacoustic imaging. The assembly of hybrid polymer/ionorganic nanoclusters provides a platform that combines advantages of the biodegradability of the polymer/stabilizer with the strong imaging contrast and NIR absorbance of an assembly of closely-spaced gold nanoparticles.

7576-30, Session 8

Gold nanoprobes for multi-modality tumor imaging

D. Davé, J. Nyagilo, The Univ. of Texas at Arlington (United States)

We report the development of gold nanoparticle based probes (nanotags) for combined optical and X-ray computed tomography (CT). The nanotags are quasi-spherical gold nanoparticles coated with a Raman reporter dye (color) encapsulated by a monolayer of polyethylene glycol (PEG) molecules with carboxylate functional group for bioconjugation with a ligand. The synthesized nanotags exhibit large surface enhanced Raman scattering (SERS) cross-section and X-ray absorption that is larger than the iodinated compounds that are clinically used as CT contrast agents. Dual-modality in vivo imaging of orthotopic prostate tumor metastasis in an animal model with the nanotags is demonstrated which correlates very well with FDG-PET imaging.

7576-31, Session 8

Luminescent resonance energy transfer measurements from a novel core-shell nanoparticle

S. Lakshmana, J. Han, I. M. Kennedy, Univ. of California, Davis (United States)

Core-shell nanoparticles (NP) with a phosphorescent, lanthanide core and plasmonic, gold shell are employed for Luminescent Resonance Energy Transfer (LRET) measurements in a nanoarray. The LRET is demonstrated from a highly efficient fluoride NP doped with Ytterbium (Yb) and Erbium (Er) ions to a Streptavidin conjugated with Alexa fluorophore. The nanoparticles can also function as up-conversion markers. The choice of the Alexa dye was based on the efficient emission of Er3+ ion at 545 nm. Based on the affinity of the gold towards thiol, thiol substituted Biotin was employed as the linker to trap Streptavidin. The LRET measurements were performed in water solution to demonstrate the feasibility of the concept. For demonstrating immunoassay device based on the core-shell NP with LRET, we prepared an 80 nm nanoarrays, as the nanoparticles had an average diameter around 50 nm. The nanoarrays were prepared by electron beam etching of polymethyl-methacrylate (PMMA) that was coated on to the thin film of a conductive indium tin oxide (ITO) containing glass slide. The trapping of the nanoparticle was performed by applying electric field to the ITO surface. The LRET was visualized using a confocal fluorescent microscopy.

7576-32, Session 8

Gold nanorods for optical contrast in two photon microscopy of oral carcinogenesis

G. Vargas, S. R. L. Rudrabhatla, S. Motamedi, T. Shilagard, S. Qiu, The Univ. of Texas Medical Branch (United States)

Gold nanorods have been shown to be effective contrast agents for two photon luminescence in that powers required for imaging are very low compared to traditional fluorophores and endogenous (autofluorescent) fluorophores. In this study they are investigated for use in two photon microscopy of lesions in an oral carcinogenesis model.

Oral carcinogenesis was induced in the buccal mucosa of hamsters using a thrice weekly application of DMBA for 9 weeks. Commercially available nanorods were injected i.v. (n=5) after baseline two-photon microscopy was performed and oral lesions of interest were identified. Immediately after injection, two-photon microscopy was performed in the lesion regions of interest including associated microvasculature to confirm presence of the nanorods in the circulation. Imaging in the same animal was again performed after 24 hours. In supporting trials, average incident power responses in tissues with and without nanorods was quantified and together with microspectroscopy was used to quantitatively describe the signal to background of nanorods over traditional fluorophores. Biopsies were obtained of imaged areas and processed for histology and staging

Gold nanorods were confirmed to be immediately present in the microvasculature surrounding dysplastic and early cancer lesions of interest in the in vivo buccal pouch. Additionally, nanorods were present in a variety of oral lesions using incident powers that were many times smaller than required for autofluorescence or using traditional fluorophores such as acridine orange (0.2 mW vs >10 mW using a 40x 1.2 N.A. objective) and through volume analysis the amount present was consistent for a given timepoint following injection.



7576-33, Session 8

Three-dimensional imaging of living cells labeled with gold nanobiomarkers using phase shifting heterodyne digital holographic microscopy

F. Joud. Lab. Kastler Brossel. Ecole Normale Superieure (France): N. Warnasooriya, Lab. d'Optique, École Supérieure de Physique et de Chimie Industrielles (France); P. Bun, Institut Jacques Monod (France); G. Tessier, M. Atlan, Lab. d'Optique, École Supérieure de Physique et de Chimie Industrielles (France); P. Desbiolles, Lab. Kastler Brossel, Ecole Normale Superieure (France): M. Coppey-Moisan, Institut Jacques Monod (France): M. Abboud, Univ. Saint-Joseph (Lebanon); M. Gross, Lab. Kastler Brossel, Ecole Normale Superieure (France)

In most optical microscopic techniques, imaging an object moving in a 3D space requires permanent position adjustment of both the focal plane and the sample. Digital holography allows overcoming this difficulty by giving access to different planes of the sample from a single recorded hologram. Moreover, holographic holograms contain both amplitude and phase information thus allowing a complete reconstruction of the whole object without the need of any contrast techniques.

In this communication we present a new phase-shifting digital holographic microscopy technique with shot noise limited sensitivity in a total internal reflection configuration for biological imaging. For the first time to our knowledge, Gold nanoparticles in live cells environments are imaged with significant acquisition times of the order of 50 ms.

The experimental setup is a Mach-Zehnder interferometer where a CCD camera records the interference pattern of a reference laser beam and the light scattered by the sample and collected by a microscope objective. Phase-shifting is obtained by the use of two Acousto-optic modulators that shifts both beams' frequencies. The recorded hologram is then numerically treated and reconstructed using Fourier optics based algorithm giving intensity images of the object in virtually any z-plane. Our sample consists of NIH 3T3 mouse fibroblasts tagged with 40 nm Streptavidin-coated Gold particles functionalized in a way to stick onto the cellular surface via the Integrin membrane receptor. We proved the ability of our method to accurately detect Gold nanoparticles contained in living cells and distinguish their corresponding signal from the parasitic cellular signal.

7576-73, Session 8

Multipurpose mode of heating nanoparticles by nanosecond, picosecond, and femtosecond pulses

R. R. Letfullin, Rose-Hulman Institute of Technology (United States)

No abstract available.

7576-34. Session 9

Biological applications of fluorescence lifetime imaging beyond microscopy

W. J. Akers, M. Berezin, H. Lee, Washington Univ. School of Medicine in St. Louis (United States); K. Guo, Washington Univ. in St. Louis (United States); A. Almutairi, J. M. J. Frechet, Univ. of California, Berkeley (United States); G. M. Fischer, E. Daltrozzo, A. Zumbusch, Univ. Konstanz (Germany); S. Achilefu, Washington Univ. School of Medicine in St. Louis (United States)

Fluorescence lifetime is a relatively new contrast mechanism for optical imaging in living subjects that relies on intrinsic properties of fluorophores rather than concentration dependent intensity. Drawing upon the success of fluorescence lifetime imaging microscopy (FLIM) for investigation of protein-protein interactions and intracellular physiology, in vivo fluorescence lifetime imaging (FLI) promises to dramatically increase the utility of fluorescence-based imaging in preclinical and clinical applications. Intrinsic fluorescence lifetime measurements in living tissues can distinguish pathologies such as cancer from healthy tissue. Unfortunately, intrinsic FLT contrast is limited to superficial measurements. Conventional intensity-based agents have been reported for measuring these phenomena in vitro, but translation into living animals is difficult due to optical properties of tissues. For this reason, contrast agents that can be detected in the near infrared (NIR) wavelengths are being developed by our lab and others to enhance the capabilities of this modality. FLT is less affected by concentration and thus is better for detecting small changes in physiology, as long as sufficient fluorescence signal can be measured. FLT can also improve localization of signals for improved deep tissue imaging. Examples of the utility of exogenous contrast agents will be discussed, including applications in monitoring physiologic functions, controlled drug release and cancer biology. Instrumentation for FLI will also be discussed, including planar and diffuse optical imaging in time and frequency domains. Future applications will also be discussed that are being developed in this exciting field that complement other modalities.

7576-35, Session 9

Targeted multi-functional multi-modal microspheres as optical contrast agents for cardiovascular disease and cancer

R. John, F. T. Nguyen, E. J. Chaney, M. Marjanovic, K. Suslick, S. A. Boppart, Univ. of Illinois at Urbana-Champaign (United States)

Recently, there has been increasing interest in the development of molecular imaging techniques by the intelligent design and application of contrast agents. A large number of agents have been developed, including engineered microspheres, plasmon-resonant nanoparticles, near-infrared absorbing dyes, and magnetomotive agents. In this study, we demonstrate the use of protein microspheres of size from 2 to 5 µm filled with oil suspensions of iron oxide nanoparticles as multimodal contrast agents in ultrasound, magnetic resonance, and magnetomotive optical coherence tomography (MM-OCT) imaging

The study reported in this paper focuses on the development, characterization and use of multi-functional multi-modal microspheres as targeted contrast and therapeutic agents. These engineered protein microspheres are made through the use of high-frequency ultrasound. The sonication process creates a fluid mixing state allowing the protein to form a shell encapsulating the oil and hydrophobic nanoparticles. Traditionally, similar microspheres have been filled with perfluorocarbon and used for ultrasound imaging. However, the introduction of an oil or liquid as the solvent of the inner core has resulted in a much more stable and longer lasting contrast agent, extending its lifetime from days to several months. It is possible to replace this liquid core with a drug, and the relatively large volume of the encapsulating microsphere offers the potential as a targeted drug-delivery vehicle. These microspheres containing iron oxide nanoparticles in their cores have been demonstrated as unique contrast agents in MM-OCT. We have functionalized our microspheres with the RGD peptide ligand, and have demonstrated targeting of these microspheres in carcinogen-induced rat mammary tumors and in the aorta of a hyperlipidemic rat model. Preliminary results demonstrate tracking in vivo dynamics of these functionalized microspheres in real-time using a small ultrasound imaging



7576-36, Session 9

Colon cancer targeting and screening with an enhanced contrast dual modality imaging system

N. V. Iftimia, M. Mujat, D. Hammer, Physical Sciences Inc. (United States); Y. Ye, S. Achilefu, Washington Univ. School of Medicine in St. Louis (United States); S. Gunta, M. Amiji, Northeastern Univ. (United States)

An advanced imaging system for colon cancer screening and its preliminary testing on a mouse model of colon cancer will be discussed. This system is based on a combined Optical Coherence Tomography (OCT) and fluorescence imaging approach. While OCT offers tremendous potential as a diagnostic tool for detection and characterization of epithelial cancer, it is associated with a limited field of view, on the order of millimeters, and thus scanning of large organs is not very practical because involves the time-consuming analysis of very large data sets. The use of a guidance tool, like fluorescence imaging, can more efficiently highlight the presence of suspicious lesions and perform OCT imaging only on those lesions as a confirmatory tool. However, while endogenous and exogenous fluorescence has shown to be relatively sensitive to cancer, its specificity is still limited when no targeting contrast agents are used. Therefore, enhanced contrast fluorescence imaging markers are used to target cancer cells. Our preliminary combined OCT-fluorescence imaging technique in conjunction with tumor-targeted delivery of contrast agents (RGD functionalized nanoparticles) seems to be a more attractive approach for large organ cancer screening. A very preliminary testing of this technology is currently being performed on an orthotopic human colon cancer nude mice model. The results will be discussed in detail in this paper.

7576-37, Session 9

Photoacoustic tomography offers simultaneous vasa vasorum and ruptured plaque assessments of atherosclerotic plaque with targeted gold nano beacons

D. Pan, M. Pramanik, A. Senpan, M. Scott, Washington Univ. School of Medicine in St. Louis (United States); P. J. Gaffney, St. Thomas Hospital (United Kingdom); S. A. Wickline, L. V. Wang, G. M. Lanza, Washington Univ. School of Medicine in St. Louis (United States)

Background: Unstable atherosclerotic plaque is characterized by vasa vasorum expansion and microintimal rupture. Photoacoustic (PA) tomography (PAT) can enhance traditional ultrasound assessments of carotid disease by affording noninvasive microvasculature visualization based on circulating hemoglobin.

Objective This research further extends the capability of PAT atherosclerotic imaging to include the potential concomitant molecular imaging of microthrombus in ruptured plaque using a novel fibrin-specific near-infrared (NIR) gold nanobeacon.

Methods and Results: Gold nanoparticles (2-4 nm) were synthesized and incorporated into the core of lipid-encapsulated nanoparticles (GNB) (~140 nm), providing 1080 µg gold/g of 20% colloid suspension. GNB provided 15-fold increase (p<0.05) in PA signal over blood in vitro (Fig 1a). PAT signal from human fibrin-rich clot was increased significantly with the fibrin-targeted GNB versus control (p<0.05) (Fig 1b). As a nontargeted, blood pool agent, GNB increased microcirculatory contrast 60% (p<0.05) above the background hemoglobin signal. Pharmacokinetics of GNB PAT signal, monitored from femoral vein, revealed an expected decay that decreased to background signal level within 60 min to afford imaging without circulatory background.

Conclusions: PAT could enhance clinical assessment of carotid arteries in patients presenting with neurological symptoms by providing

concomitant assessments of plaque vasa vasorum and intimal microthrombus in addition to standard Doppler measurements of stenosis.

7576-38, Session 9

Single fluorescent gold nanoclusters and its possible biomedical application

C. Yuan, Academia Sinica (Taiwan); W. Chou, National Chiao Tung Univ. (Taiwan); J. Tang, Academia Sinica (Taiwan); C. J. Lin, J. Shen, Chung Yuan Christian Univ. (Taiwan); D. Chuu, National Chiao Tung Univ. (Taiwan); W. H. Chang, Chung Yuan Christian Univ. (Taiwan)

Both ensemble and single-molecule measurements were performed to explore the fluorescence properties of Au nanoclusters (NCs). Photoinduced fluorescence enhancement was observed for ensemble NCs in solution, but photobleaching was found at ambient environments. At the single-molecule level, fluorescence blinking and single-step photobleaching were observed. Furthermore, their time-resolved fluorescence shows a single exponential decay with a lifetime of ~7 ns and is insensitive to changes in fluorescence intensity. The lifetime distribution is more homogeneous within ensemble Au NCs as compared to CdSe QDs. Therefore, Au NCs have potential applications as nontoxic fluorescent labels for lifetime-based imaging microscopy. We have also demonstrated the efficient labeling of Au NCs in both fixed and living cells. However, their low quantum yields (compared to quantum dots) and poor photostability are disadvantageous factors, which require further improvement. Related Reference: [1] C. T. Yuan, C. Chou, J. Tang, C. A. Lin, W. H. Chang, J. L. Shen, and D. S. Chuu, (2009) "Single fluorescent gold nanoclusters", Optics Express, in press. [2] C.-A. J. Lin, T. Y. Yang, C. H. Lee, S. H. Huang, R. A. Sperling, M. Zanella, J. K. Li, J. L. Shen, H. H. Wang, H. I. Yeh, W. J. Parak, W. H. Chang, (2009). "Synthesis, Characterization, and Bioconjugation of Fluorescent Gold Nanoclusters toward Biological Labeling Applications." ACS Nano 3(2): 395-401.

7576-39, Session 10

Applications of fluorescence spectroscopy to problems of food safety: detection of fecal contamination and of the presence of central nervous system tissue and diagnosis of neurological disease

J. W. Petrich, Iowa State Univ. (United States); T. A. Casey, National Animal Disease Ctr., USDA (United States); A. Gapsch, TECHnical SOLutions Group, Inc. (United States); M. A. Rasmussen, Ctr. for Veterinary Medicine, US Food & Drug Administration (United States)

Applications of fluorescence spectroscopy that enable the real-time or rapid detection of fecal contamination on beef carcasses and the presence of central nervous system tissue in meat products are discussed. The former is achieved by employing spectroscopic signatures of chlorophyll metabolites; the latter, by exploiting the characteristic structure and intensity of lipofuscin in central nervous system tissue. The success of these techniques has led us to investigate the possibility of diagnosing scrapie in sheep by obtaining fluorescence spectra of the retina. Crucial to this diagnosis is the ability to obtain baseline correlations of lipofuscin fluorescence with age. A murine model was employed as a proof of principle of this correlation.



7576-40, Session 10

Characterization of the drug-binding site (subdomain IIA) of human serum albumin using 7-hydroxyquinoline as a molecular probe

O. K. Abou-Zied, N. Al-Lawatia, Sultan Qaboos Univ. (Oman)

7-hydroxyguinoline (7-HQ) shows unique absorption and fluorescence features that are sensitive to the presence of water which make it a water-sensitive probe to explore the local environment of the binding sites in proteins. We used 7-HQ in this work as a molecular probe to characterize the drug-binding site (subdomain IIA) of human serum albumin (HSA) in its native, unfolded and refolded states. The study was carried out by measuring the changes in the spectra of 7-HQ and of HSA in the frequency domain and time domain. After probe binding, resonance energy transfer from the fluorescence of the Trp-214 residue of HSA to 7-HQ was measured, and the distance between the donor and acceptor was calculated using Förster theory. The results point to a static quenching mechanism. Unfolding of HSA in the presence of guanidine hydrochloride (GdnHCl) starts at [GdnHCl] > 1.0 M and is complete at [GdnHCl] = 6.0 M. Unfolding of HSA results in fluorescence from the Tyr-263 residue which was confirmed by its fluorescence quenching by 7-HQ. Refolding of the denatured HSA was induced by buffer dilution. Both unfolding and refolding processes were found to be unaffected by the presence of the probe. The latter results rule out any possible structural deformation of the protein by the presence of the 7-HQ molecule in the binding site.

7576-41, Session 10

Time-resolved fluorescence measurements of cyanine dyes in biomimetic systems

F. Luschtinetz, C. Dosche, M. Kumke, Univ. Potsdam (Germany)

Cyanine dyes are widely used in sensing applications. Because of their red excitation wavelength (> 600nm) these dyes are especially suited for applications in fluorescence spectroscopy of biological samples. In this spectral range autofluorescence background signal and cell damage are significantly reduced.

The photo physical characteristics of cyanine dyes are highly influenced by their microenvironments. Self-aggregation and rotation hindrance of the probes can take place in biological systems (e.g. after binding onto proteins or in the cell membrane). These matrix effects are not fully understood yet and interfere with the data interpretation.

Non-ionic surfactants are often used in pharmaceutical and bioanalytical applications, such as drug delivery systems. Micelles and vesicles can also be used as biomimetic systems, e.g. as model systems for biological membranes.

The objective of this study was to investigate environment effects on the mobility and aggregation behavior of new fluorescence probes of the cyanine-type, their biotin derivates and the corresponding biotin-streptavidin-complexes. The influence of detergents on the photophysics of the dyes was investigated by using fluorescence correlation spectroscopy (FCS) and time-resolved anisotropy measurements.

FCS is a powerful technique for the investigation of intra-molecular and diffusion-controlled processes on a μs to ms time scale in biological and colloidal systems. Time-resolved anisotropy measurements were used to describe the rotational dynamics of the fluorescence probes. The application of an associated anisotropy model allows us to describe the contributions from fluorescing species in different microenvironments.

7576-42, Session 10

Smart pH cuvette for optical monitoring of pH of biological samples

D. A. Guenther, M. R. Shahriari, Ocean Optics, Inc. (United States)

A Smart pH Cuvette is developed by coating the inner surface with pH sensitive thin film. The coating is a hydroscopic sol-gel material doped with colorimetric pH indicator dye sensitive to the pH of analyte solutions in biological range. Ocean Optics miniaturized spectrometers are used for signal detection and analysis, along with multimode optical fibers. This new pH sensing arrangement yields an inexpensive solution for monitoring the pH of samples for biological applications. The Smart pH Cuvettes provide a resolution of 0.01 pH units, an accuracy of 1% of the reading, and 90% response in less than 10 seconds.

7576-43, Session 10

Smart oxygen cuvette for optical monitoring of dissolved oxygen in biological samples

H. Dabhi, Ocean Optics Inc (United States)

A smart Oxygen Cuvette is developed by coating a cuvette with oxygen sensitive thin film material. The coating is a sol-gel matrix encapsulated with Ru compound. The fluorescence of the ruthenium is quenched depending on the oxygen level. Ocean Optics NeoFox phase fluorometer is used for signal processing. Optical fibers are used for light transportation between cuvette and NeoFox. The Smart Oxygen Cuvettes provide a resolution of 4 PPB units, an accuracy of less than 5% of the reading, and 90% response in less than 10 seconds.

7576-44, Session 11

New fluorescent nucleosides for real-time exploration of nucleic acids

Y. Tor, Univ. of California, San Diego (United States)

Biologically relevant nucleic acids experience a variety of structural perturbations while performing their essential "everyday" functions. These may include strand cleavage and ligation, local conformational changes, base flipping, as well as structural and environmental perturbations that are induced upon protein and low MW ligand binding. Fluorescent nucleosides analogs that are sensitive to their local environment have therefore become powerful tools for investigating nucleic acids structure, dynamics and recognition. In addition, fluorescence-based methods have become instrumental in advancing high throughput screening techniques, particularly in the context of drug discovery.

The following represent our criteria for "ideal" fluorescent nucleoside analogs: (a) high structural similarity to the native nucleobases to faithfully mimic their size and shape, as well as hybridization and recognition properties; (b) red shifted absorption to minimize overlap with the absorption of the natural bases; (c) red shifted emission band (preferably in the visible); (d) a reasonable emission quantum efficiency; and, importantly, (e) sensitivity/responsiveness of photophysical parameters (λ em and/or ϕ F, τ) to changes in the microenvironment.

Our program, aimed at the implementation of these design criteria for the development of new emissive isosteric/isomorphic nucleoside analogs, has yielded several useful nucleobases. The lecture will present the design and synthesis of fluorescent isosteric nucleobase analogs and their utilization for the fabrication of "real-time" fluorescence-based biophysical assays as well as the detection of protein toxins.

369

Return to Contents TEL: +1 360 676 3290 · +1 888 504 8171 · customerservice@spie.org



7576-45, Session 11

Sequence-dependent photophysical properties of Cy3-labeled DNA

M. Levitus, Arizona State Univ. (United States)

Cyanine dyes are among the most popular fluorescent probes used in the investigation of the structure and dynamics of nucleic acids. In particular, Cy3 has been widely used in biophysical studies of nucleic acids, often in combination with the structurally-related red-absorbing fluorophore Cy5 acting as an acceptor in FRET experiments.

We have investigated the photophysical properties of Cy3 covalently attached to DNA, and found that its fluorescence efficiency and lifetime depend strongly on the microenvironment sensed by the fluorophore. Large variations were observed depending on DNA sequence, the chemistry used for the conjugation, and whether the probe was attached to single-stranded or duplex DNA.

We interpreted this behavior in terms of a photoisomerization mechanism that deactivates the singlet excited state with an efficiency that depends strongly on the local microscopic friction. Our results are consistent with a model in which Cy3-DNA interactions increase the energetic barrier for photoisomerization, increasing the fluorescence lifetime and quantum yield. These interactions are stronger for single-stranded DNA than for duplex DNA, and as a consequence the fluorescence efficiency of the probe decreases by a factor of more than 2 (depending on sequence) when a Cy3-labeled oligo is hybridized to its complementary strand. The study of the properties of Cy3 covalently attached to DNA oligos revealed that the extent of the Cy3-DNA interaction is determined by the flexibility of the chain and the presence of purines. These factors are responsible for the dramatic variations in fluorescence efficiency (0.18-0.38) measured for Cy3 on different DNA sequences.

7576-46, Session 11

Synthesis and characterization of new aminereactive fluorene probes for two-photon bioimaging

A. R. Morales, C. O. Yanez, K. D. Belfield, Univ. of Central Florida (United States)

The great advantages of two-photon fluorescence microscopy (2PFM) imaging include extended sample penetration and lower damage on specimen and fluorophore. Although biomedical applications of 2PFM are steadily increasing, the technique still suffers from the lack of efficient two-photon absorbing fluorescence probes highly specific for a target. Introduction of new fluorescent compounds possessing enhanced nonlinearities are essential for advancing the utility of two-photon absorption (2PA) processes in the biological sciences. We reported herein the synthesis of fluorophores tailored for multiphoton imaging. incorporating the succinimidyl ester functionality as reactive linker for further coupling with a wide variety of biologically relevant molecules. These fluorophores are based on the fluorene ring system, known to exhibit high fluorescence quantum yield and high photostability. The succinimidyl ester amine reactive probes were conjugated with the amine functions of cyclic peptide RGDfK and polyclonal anti-rat IgG IgG protein. Upon conjugation, the basic molecular architecture and photophysical properties of the active 2PA chromophore remain unchanged. Finally, conventional and 2PFM imaging of COS-7 and HeLa cells, incubated with fluorene-RGD peptide conjugate and fluorene-IgG conjugate, respectively, was demonstrated.

7576-47, Session 11

Lysome-specific fluorene dyes for confocal and two-photon fluorescence microscopy

C. O. Yanez, C. D. Andrade, X. Wang, S. Yao, S. A. Coombs, C. L. Arnett, K. D. Belfield, Univ. of Central Florida (United States)

Lysosomes contain enzymes capable of digesting proteins, nucleic acids, lipids and carbohydrates. Lysosomal enzymes have been reported to be involved in important processes such as cell death (apoptosis) in cancer cells, neurological disease (developmental axon pruning), and cardiovascular affections. Studying lysosomal activity requires organelle specific dyes or stains. Fluorescent lysosome-selective dyes, such as acrydine, are frequently used for fluorescence imaging purposes. However, few of these dyes have been developed for more recent, higher resolution microscopic techniques such as two-photon fluorescence microscopy (2PFM) and stimulated emission depletion (STED) microscopy. Among the advantages of 2PFM are the possibility of using longer wavelengths to excite the fluorescent dye, which ultimately translates in better tissue penetration and safer radiation energies. We report a series fluorescent dyes that exhibit lysosomal-affinity in HCT-116 cells. These dyes were specifically developed to have high two-photon absorption cross sections at wavelengths attainable by a tunable Ti:sapphire laser (700-1000 nm). These fluorene-based hydrophobic dyes showed good two-photon absorption cross sections and excellent fluorescence quantum yields upon photophysical characterization. Furthermore, some of these have excellent one- and two-photon STED properties, making them promising probes for super resolution fluorescence microscopy.

7576-48, Session 11

Inhibition study of the oncogenic functionality of STAT3 at single molecule level

B. Liu, D. Badali, M. Avadisian, S. Fletcher, P. T. Gunning, C. Gradinaru, Univ. of Toronto Mississauga (Canada)

Signal-Transducer-and-Activator-of-Transcription 3 (STAT3) protein plays an important role in the onset of cancers such as leukemia and lymphoma. In this study, we tested the effectiveness of a novel peptide drug designed to tether STAT3 to the phospholipid bilayer of the cell membrane and thus inhibit unwanted transcription. A newly developed fluorescein derivative label (F-NAc) has been designed to be incorporated into the structure of the peptide drug so that peptide-STAT3 interactions are examined at single molecule level via single molecular fluorescence energy transfer. This dye is spectrally characterized and is found to be well suited for its application to this project, as well as other singlemolecule studies. The membrane localization via high-affinity cholesterolbound small-molecule binding agents is demonstrated by encapsulating TMR-labeled STAT3 and inhibitors within a vesicle model cell system. Preliminary results of the efficiency and stability of the STAT3 anchoring in lipid membranes obtained via quantitative confocal imaging and singlemolecule spectroscopy using a custom-built multiparameter fluorescence microscope are reported here.





7576-49, Session 12

Lipid nanoparticles (LNP): a new technology for fluorescence contrast agents with improved properties

J. J. Gravier, T. Delmas, A. Couffin, F. Navarro Y Garcia, E. Heinrich, Commissariat à l'Énergie Atomique (France); S. Dufort, J. Coll, INSERM, Institut Albert Bonniot (France); F. Vinet, I. Texier-Nogues, Commissariat à l'Énergie Atomique (France)

Several new approaches have been developed lately for the in vivo delivery and targeting in diseased area of poorly soluble active ingredients, such as drugs or contrast agents. Among them, lipid-based particles are showing promising properties. We developed new lipid nanoparticles (LNP, 25-200 nm diameter), composed of a lipid core stabilized by phospholipids and PEGylated surfactants. LNP display numerous advantages: these particles are mostly composed of low-cost and biocompatible lipids; they can be stored in injection-ready forms for long duration; their manufacturing process is versatile and up-scalable.

Different lipophilic fluorescent dyes have been successfully loaded in the oily LNP core: DiO (484 nm / 501 nm), DiD (646 nm / 668 nm), DiR (748 nm / 775 nm), ICG (798 nm / 820 nm). Dye loaded LNP display an excellent colloidal stability, as well as outstanding optical properties: high fluorescence quantum yield, long fluorescence lifetime, reduced photobleaching rate. Therefore, they constitute contrast agents of choice for performing in vitro or in vivo fluorescence imaging studies. The in vivo fate of these new contrast agents has been assessed in different Nude mice models bearing sub-cutaneous xenografts. Passive accumulation of LNP in different tumor models due to the Enhanced Permeability and Retention effect has been demonstrated. cRGD grafting onto the nanoparticles allows their specific selectivity towards v 3 integrins expressing tumours, both in vitro and in vivo in Nude mice.

7576-50, Session 12

Bioconjugated ICG-micelles as translational fluorescence agents for optical molecular imaging

Y. Chen, X. Li, Johns Hopkins Univ. (United States)

Near infrared (NIR) fluorescence imaging has become a powerful molecular imaging tool for studying various disease models, screening new drugs and monitoring therapeutic outcomes. However, clinical translation of this powerful technique has been hindered by the lack of appropriate fluorescent contrast agents. In addition to excitation and fluorescence in the NIR wavelength range which enables deep tissue imaging, the ideal properties of fluorescent contrast agents also include biocompatibility, long-term fluorescence stability, high fluorescence quantum yield, and convenient biofunctionalization. Indocyanine green (ICG) is the only NIR fluorescent dye approved by FDA for routine clinical use. However, ICG suffers chemical degradation, optical/thermal instability, nonspecific binding to blood proteins, and rapid circulation kinetics and clearance. Recently we have proposed and successfully demonstrated that the previous limitations of ICG can be effectively overcome by encapsulating ICG molecules into polymeric micelles that are formed by FDA approved polymers. This ICG-micelle nanocapsule approach dramatically improves the stability of ICG fluorescence (up to more than 3 weeks even under body temperature), and exhibit a very low critical micelle concentration and cytotoxicity. To enable bioconjugation for tumor targeting and molecular imaging, the (PEO)-OH terminals on the corona of the ICG-micelles are pre-activated and then conjugated with antibodies. In vitro experiments have demonstrated strong molecularly specific enhancement in fluorescence imaging of cancer cells with bioconjugated ICG-micelles. The bio-functionalized ICG-nanocapsules hold strong promise for translating optical molecular imaging to in vivo clinic practice.

7576-51, Session 12

Evaluation of arsenazo III as a contrast agent for photoacoustic imaging of calcium transients in glial cells

E. J. Cooley, Sandia National Labs. (United States); P. Kruizinga, The Univ. of Texas at Austin (United States); T. C. Monson, Sandia National Labs. (United States); S. Emelianov, The Univ. of Texas at Austin (United States); D. W. Branch, Sandia National Labs. (United States)

Elucidating the role of calcium fluctuations in neuronal tissues at the cellular level is essential to gain insight into the complex signaling and metabolic activity within the brain. Recent developments in optical monitoring of calcium suggest that glial cells, though electrically inactive, integrate and transmit information through networks similar to neurons. Thus, monitoring calcium transients in glial cells is important for identifying normal and pathological states of these networks. Though imaging of calcium flux can be achieved using fluorescent probes, photobleaching often occurs, resulting in degradation of the optical signal. Alternatively, the widely used metallochromic dye, Arsenazo III, does not suffer from photobleaching, and is useful for optical techniques that rely on differential absorption of light rather than fluorescence. We report on the use of Arsenazo III as a contrast agent for imaging of calcium transients using photoacoustics, a technique in which an ultrasound signal is generated from localized absorption of modulated light. Tissue-like phantoms were used to monitor the change in absorbance of Arsenazo III at 660 nm in the presence of calcium. Subsequent results demonstrated a linear relationship between photoacoustic signal and the amount of calcium introduced. For in vivo experiments, Arsenazo III was encapsulated within a liposomal carrier for cellular uptake and imaging. This work demonstrates the feasibility of using a strongly absorbing calcium sensitive dye for photoacoustic monitoring of glial activity in vivo.

Sandia is a multi-program laboratory operated by Sandia Corporation, a Lockheed Martin Company, for the United States Department of Energy under contract DE-AC04-94AL85000.

TEL: +1 360 676 3290 · +1 888 504 8171 · customerservice@spie.org



Wednesday-Thursday 27-28 January 2010 • Part of Proceedings of SPIE Vol. 7577 Plasmonics in Biology and Medicine VII

7577-40, Poster Session

Ultrathin silver coated gold nanoparticles in solution as suitable substrates for surface-enhanced Raman scattering

C. Domingo, L. Guerrini, S. Sanchez-Cortez, J. V. Garcia-Ramos, Instituto de Estructura de la Materia, CSIC (Spain)

Au and Ag colloids are metallic systems largely employed in Surfaceenhanced Raman spectroscopy. Despite of their easy preparation, these systems are rather difficult to control and characterize because of the wide range of nanoparticle morphologies. Although gold shows a lower enhancement factor in the visible in comparison to silver, Au colloids have many advantages, including an easier preparation and a higher homogeneity in the distribution of diameters. For this reason, several attempts to obtain composite particles by depositing Ag on preformed Au nanoparticles have been carried out in order to get more homogeneous Ag surfaces, as well as a greater SERS enhancement of the Au colloids. Nevertheless, such methods produce bimetallic nanoparticles with plasmonic properties very different from the corresponding to the core, whereas, for some technological applications, it could be interesting to preserve these original plasmonic properties. Besides, and related to the design of SERS-based sensors, it is necessary to consider the chemical properties of the metal surfaces.

We here report an easy method for the self-deposition of silver on gold nanoparticles, in solution, where the resulting Au/Ag systems keep the plasmonic properties of gold and have the chemical surface affinity of silver. SERS spectra on these bimetallic systems of three probe molecules which present different spectral pattern on both metals (luteolin, thiophenol and lucigenin), allow to demonstrate the progressive Ag enrichment of the outer part of the gold nanoparticles in the colloidal suspension, as well as to propose a model for the growing process of the Ag shell.

7577-41, Poster Session

SERS+MEF of the anti tumoral drug emodin adsorbed on silver nanoparticles.

P. Sevilla, Univ. Complutense de Madrid (Spain) and Instituto de Estructura de la Materia, CSIC (Spain); R. De LLanos, C. Domingo, S. Sanchez-Cortez, J. V. Garcia-Ramos, Instituto de Estructura de la Materia, CSIC (Spain)

The possibility of combining localized surface plasmon (LSP) enhancement in metallic nanoparticles has opened the way to new and powerful tools. Silver nanoparticles have become efficient vehicles to store and deliver "magic bullets" to achieve cancer targeting. They avoid the undesirable side-effects inherent to conventional cancer therapy. Our goal is to develop systems for the release of probes in order to exploit the effects of LSP. Emodin is a natural anthraquinone dye that has an anti tumoral effect and binds different albumins, forming a complex that is important to ensure the drug delivery. We use Raman and fluorescence spectroscopy to study emodin molecules and albumin-emodin complexes in the presence of silver nanoparticles, with pharmaceutical interest. Aggregation of emodin at certain pHs gives rise to SERS and MEF effects. The binding of emodin to bovine serum albumin undergoes changes when metal nanoparticles are present in solution affecting not only the structure of the protein but also the binding of the emodin. The secondary structure of the protein is modified by the absorption on nanoparticles. Analysis of the binding saturation curve allows us to determine a single binding site for emodin. This differs from previous results obtained for the complex in aqueous solution and in the absence of silver nanoparticles. Furthermore, fluorescence lifetime studies have

been carried out for the protein-emodin complex, in absence and presence of nanoparticles. Results indicate small decrease in protein fluorescence lifetime when nanoparticles are present and also when drug concentration increases.

7577-42, Poster Session

Spectroscopic and microscopic characterization of albumin / porous silica / gold nanorods

F. Ratto, P. Matteini, F. Rossi, R. Pini, Istituto di Fisica Applicata Nello Carrara, CNR (Italy)

We have engineered aqueous colloids of hybrid nanoparticles composed of a gold nanorod inner core, a porous silica middle shell and a bovine serum albumin outer shell, which are of great interest to test innovative concepts at the crossroad of biomedical optics and nanomedicine. These nanoparticles display intense plasmon resonances in the window of the near infrared (700 - 1000 nm) of principal interest to develop minimally invasive concepts of laser assisted diagnoses and therapies. The interplay of the various functional layers gives enhanced light absorption and scattering in the near infrared, excellent photo- and thermo- stability, drug / gene delivery capacity, as well as cell membrane affinity. Here we report on the self assembly of these nanoparticles, which is surprisingly facile, rapid and sustainable. As a model of drug carrier with immediate potential for controlled release e.g. on remote laser activation, we loaded the pores of the silica layer with the cationic surfactant cetrimonium, which exerts cytotoxic activity. Then this drug carrier was passivated and encapsulated within the albumin layer. The formation of the various shells was followed by the combination of spectroscopic (light absorption and scattering) and microscopic (transmission electron microscopy and atomic force microscopy) techniques. Future developments will include a characterization of the interaction between these nanoparticles, cell cultures and near infrared light to explore a variety of novel opportunities for cell diagnoses and therapies.

7577-43, Poster Session

Stability of silica and polyethylene glycol modified gold nanorods upon near infrared laser excitation

F. Ratto, P. Matteini, F. Rossi, R. Pini, Istituto di Fisica Applicata Nello Carrara, CNR (Italy)

Metal nanoparticles with plasmon resonances in the near infrared such as gold nanorods and gold nanodogbones are receiving much attention as versatile tools for a variety of minimally invasive diagnostic and therapeutic applications based on laser activation. Their extreme efficiencies of photothermal conversion challenge their morphological stability upon laser excitation, which may drive processes of coagulation, partial reshaping, complete melting and fragmentation. Whether or not these processes may be functional to the specific requirements of the biomedical application, their characterization is critical. Here we compare the photo-stability of different solutions of gold nanorods and gold nanodogbones dispersed in semi-solid films of polyvinyl alcohol, which is taken as a rude model of a biological membrane. In particular we place particular emphasis on the dependence of the photo-stability on the average size and shell modification of the nanoparticles. We confront two shell modifications of special interest in the scientific literature, i.e. silica and polyethylene glycol. We investigate a range of laser excitations (pulses of ~ 10 msec - 10 sec duration, ~ 100 W cm-2 fluence, 810 nm wavelength) useful for the development of minimally



invasive photothermal microsurgeries, such as the hyperthermia of cancer and the welding of ophthalmic tissues. The damage induced in the gold nanoparticles and the polymer films is investigated by optical spectromicroscopy and transmission electron microscopy. Our results give new insight into the opportunities and limitations behind the use of laser activated gold nanorods and gold nanodogbones in biomedicine.

7577-44, Poster Session

Nanowire-enhanced localized surface plasmon resonance sensor for a detection of avian-influenza DNA hybridization

S. A. Kim, Seoul National Univ. (Korea, Republic of); K. M. Byun, Kyung Hee Univ. (Korea, Republic of); K. Kim, D. Kim, Yonsei Univ. (Korea, Republic of); S. J. Kim, Seoul National Univ. (Korea, Republic of)

Surface plasmon resonance (SPR) is known as a simple optical technique with no labeling procedure for detecting DNA hybridization at a metaldielectric interface. To improve the SPR characteristics, various efforts employing colloidal nanoparticles have been made. However, tagging target molecules with metallic nanoparticles requires a complex and target-specific modification in binding events and thus, the advantage of label-free SPR detection is inevitably transformed into a labeled one. In this study, we used an alternative structure with gold nanowires directly deposited on a gold film, which can yield a large SPR angle shift and therefore enhance the sensitivity without modifying the target DNA probes. In theoretical calculation based on rigorous coupled-wave analysis (RCWA), the resonance angle shift of a gold nanowire sample was considerably increased compared with the case of a bare gold film without nanowires. Since an introduction of gold nanowires enables an efficient excitation of localized surface plasmons and an increase of surface reaction area, the sensor performance can be improved significantly. Moreover, the experimental results of avian-influenza DNA hybridization showed a notable sensitivity enhancement and were consistent with the RCWA calculation. As a result, we confirmed that the use of gold nanowires may provide a highly sensitive detection of DNA hybridization and a precise analysis of the binding kinetics.

7577-45. Poster Session

The plasmonic Raman sensor using periodic nanofocusing arrays

K. Yamaguchi, Toyohashi Univ. of Technology (Japan); M. Fujii, Toba National College of Maritime Technology (Japan); M. L. Kurth, S. J. Goodman, D. K. Gramotnev, P. Fredericks, Queensland Univ. of Technology (Australia); M. Fukuda, Toyohashi Univ. of Technology (Japan)

Recently, biosensors exploring the surface plasmon resonance have received a lot of attention. Using this approach, binding reaction of the molecule can be detected in real time with high sensitivity. However, to achieve this, large enhancements of the electromagnetic field and Raman are required.

Structures with plasmon nano-focusing could present a break-through in achieving both nano-scale confinement of the electromagnetic energy (for achieving nano-scale resolution) and major highly controlled local field enhancement (i.e., hot spots) required for efficient surface-enhanced Raman spectroscopy (SERS). Therefore the combination of SERS in plasmonic nano-structures with plasmon nano-focusing for producing controlled hot-spots presents a unique opportunity for the design of a new generation of nano-sensors with unique characteristics, operational capabilities and sensitivity.

In this paper, we investigate theoretically and experimentally a new sensor for the detection of Raman-sensitive molecules and substances, which uses hole arrays and periodic nano-focusing structures in a thin metal film on a dielectric substrate. We investigate the expected capabilities of this sensor, including the achievable local field enhancements and typical sensitivities. The expected local filed enhancements are determined and optimized numerically using the finite element analysis for the consideration of plasmonic resonance effects and nano-focusing in periodic hole arrays and tapered nano-structures in thin metal films. The analyzed hole arrays are then fabricated by means of focused ion beam lithography. Experimental investigation of the Raman signal is then conducted for the hole arrays with different periodicity and hole/taper dimensions. Optimized structures are determined and compared with the theoretical predictions.

7577-47, Poster Session

Momentum mismatch for improved plasmon enhanced fluorescence emission

Y. Oh, K. Kim, K. Ma, E. Sim, D. Kim, Yonsei Univ. (Korea, Republic of)

Near-field photonics have been rapidly developed in recent times for imaging molecular events. One of the techniques based on near-field photonics is imaging through plasmon enhanced fluorescence emission, where fluorescence is excited in the evanescent fields created by the formation of plasmons. The peak intensity of localized fields, thus the largest emission of fluorescence, has been presumed occurring at SPR. In this paper, however we confirm that this is generally not true for plasmonic emission of fluorescence in metallic thin films and nanostructures. In particular, we explore the degree of field localization near resonance condition, whereby plasmon-enhanced fluorescence emission is optimized. We have calculated plasmon-associated nearfields and far-field resonance characteristics using rigorous coupledwave analysis. Near-field intensity was experimentally measured with fluorescent microbeads of various sizes using Ag thin films and nanostructures. The results indicate that momentum mismatching when exciting plasmons can increase the consequent emission of fluorescence. While the improvement in the emission is approximately 10% for metallic thin films, it can be much more significant with plasmons excited in nanostructures. Finally, we discuss the impact of the results on biosensing applications, as they suggest that sensitivity of near-field fluorescence imaging can be enhanced simply by adjusting momentum matching conditions.

7577-48, Poster Session

Novel multilayer core-shell nanoprobes based on metal-enhanced FRET for biosensing applications

M. Rioux, M. Lessard-Viger, A. Bracamonte, D. Boudreau, Univ. Laval (Canada)

Our research group is working on the development of multilayer coreshell nanoparticles (NPs) featuring a metal core surrounded by concentric silica layers containing fluorophores positioned at precise distances from the core. Recent results show that the controlled geometry of these core-shell NPs enhances fluorescence intensity and photostability several-fold through plasmonic coupling with the core and improves Förster Resonant Energy Transfer (FRET) efficiency and range between donor-acceptor pairs.1 These enviable characteristics make such multilayer core-shell NPs a promising alternative to improve detection sensitivity, photostability as well as FRET range and efficiency in a variety of applications.

In this poster presentation, we will describe the progress accomplished in three projects related to the tailoring of multilayer luminescent NPs for biosensing applications: i) The identification of blood genotypes using bioconjugated fluorescent silica-coated silver nanoparticles grafted with probe oligonucleotides and complexed with an optical polymeric hybridization transducer. The capture of human genomic DNA onto the surface of the NP allows the excitation light to be coupled to the



FRET acceptors immobilized in the silica shell, resulting in enhanced detection sensitivity; ii) The detection of intracellular Ca2+ using a nanosensor based on the Fluo-4 Ca2+-specific indicator grafted onto small fluorescent silica-coated gold nanoparticles. Excitation of the calcium-complexed Fluo-4 molecules leads to metal-enhanced FRET to the acceptors immobilized in the silica shell; and iii) Application of the above scheme to the development of optically-traceable drug delivery nanocarriers, where the amplitude of Metal-Enhanced FRET is modulated by the release of fluorescent molecules hosted by cyclodextrin-grafted nanoparticles.

1. M.L.-Viger et al., Nano Letters, ASAP July 15 2009.

7577-49, Poster Session

Sensitivity enhancement in rotated-gratingcoupled surface plasmon resonance based bio-detection of amyloid-beta labeled by colloidal gold particles

M. Csete, University of Szeged, Department of Optics and Quantum Electronics (Hungary) and MIT, RLE, Nanostructures Laboratory (United States); A. Sipos, A. Mathesz, A. Szalai, University of Szeged, Department of Optics and Quantum Electronics (Hungary); Z. Bozsó, L. Fülöp, University of Szeged, Department of Medical Chemistry (Hungary); A. Kőházi-Kis, University of Szeged, Department of Optics and Quantum Electronics (Hungary); M. Deli, Biological Research Center of Hungarian Academy of Sciences, Laboratory of Molecular Neurobiology (Hungary); Z. Bor, University of Szeged, Department of Optics and Quantum Electronics (Hungary); B. Penke, University of Szeged, Department of Medical Chemistry (Hungary)

Novel plasmonic sensing chips are prepared by fabricating submicrometer gratings on polymer-bimetal multi-layers via UV laser-based two-beam interference lithography. Amyloid-beta oligomer populations of specific aggregation grade, which are markers for early diagnosis of Alzheimer disease, are covalently conjugated with suspensions of 1.4 nm, 10 nm and 20 nm diameter colloidal gold particles. Tapping Mode AFM investigations prove that all types of amyloid-beta-gold conjugates prefer to attach into the valleys, according to the large periodic adhesion modulation on laser-generated gratings. The size distribution of the developed peptide-gold-complexes is influenced by the diameter of the gold-particle, indicating that processes depending on conjugates surface chemistry govern the adherence. Polar and azimuthal angle dependent surface plasmon resonance spectroscopy is performed in modified Kretschmann arrangement collecting information regarding the secondary peaks appeared on the resonance curves caused by rotated-grating-coupling phenomenon. The comparison of the measured and theoretical plasmon resonance curves determined by Scattering Matrix Method taking the gold-protein ratio of different solvents into account indicate that the shift and the FWHM of the secondary minima are strongly influenced by the size of the labeling gold nano-particles. Numerical simulations prove that the grating-coupled plasmons propagating in the valleys and the localized plasmons excited with high efficiency in the gold colloid particles at the optimal azimuthal orientation cause strong field confinement around the amyloid-beta molecules to be detected. Utilization of colloidal gold nano-particles in bio-detection of the amyloid-beta oligomers based on rotated-grating-coupled SPR phenomenon is proposed, due to the demonstrated improved sensitivity and decreased limit of detection.

7577-01, Session 1

Plasmonic nanostructures for biophotonic applications

J. Popp, Institute of Photonic Technology Jena e.V. (Germany) and Friedrich-Schiller Univ. Jena (Germany)

Metal nanostructures represent ideal systems for light management in dimensions well below the illumination wavelength. This phenomenon originates in the excitation of collective carrier oscillations resulting in highly localized enhanced evanescent fields. Such drastic electromagnetic field-enhancements have been shown to be the source of increased Raman scattering intensities for analyte molecules in close contact to a metal nanostructure (SERS) with an increase of Raman scattering intensities of up to 15 orders of magnitude.

Despite the widespread use of SERS as a biomedical analytical tool, still a major challenge is the requirement of reproducible experimental conditions. For the production of reproducible SERS substrates we applied different technological approaches like e.g.: (1) lithographically produced nanostructured gold surfaces for quantitative and reproducible SERS applications or (2) the defined deposition of silver nanoparticles through an enzymatic reaction for a microarray-based detection of dye-labeled DNA by means of SERRS (surface enhanced resonance Raman scattering). Furthermore we will demonstrate the methodological power of combining SERS with microfluidic devices in order to develop novel lab-on-a-chip devices with promising applications in clinical or pharmaceutical research. Finally we will report the first applications of tip-enhanced Raman spectroscopy (TERS) for bio-diagnostics. In doing so we succeeded in recording Raman spectra of the surface of a single microorganism or even on a single virus.

The presented examples convincingly demonstrate that the enhancement of the intrinsically weak Raman signals through utilizing the unique optical properties of nanostructures is an extremely potent tool in bioanalytical science offering high sensitivity as well as molecular specificity.

7577-02, Session 1

Thermal therapy and optimization of EGFR over-expression imaging using surface-enhanced Raman spectroscopy

L. Lucas, P. Lee, K. C. Hewitt, Dalhousie Univ. (Canada)

Our research aims to image Epidermal Growth Factor receptor (EGFR) distribution in cancer cells and to destroy those cancer cells using laser heating. Many cancers and pre-cancers over-express EGFR, a cell surface receptor. A431 cancer cells are targeted by attaching ligands specific to HER1 (EGF protein or anti-EGFR antibody) or HER2 (Herceptin antibody) receptors to gold or silver nanoparticles (Au/AgNPs) of 5, 30, 50, 60, and 70 nm sizes. Normal human bronchial epithelial (NHBE) cells are used as controls. By tuning the 632.8 nm He-Ne laser excitation frequency to the nanoparticle surface plasmon, we create an enhancement effect called SERS. Raman spectroscopy (Horbia Jobin Yvon T64000) measurements are obtained with a Raman point-mapping scheme (0.3 µm step size, ~40 x 40 µm map) and snapshot Raman. These techniques map the distribution or the distribution over time, respectively. Previous research showed signal intensities of 850:1 at 1583 cm-1 and 107 orders of magnitude enhancement with anti-EGFR antibody tagged 30 nm AuNPs on A431 cells. We report on our recent efforts to achieve greater enhancement, as the increase in scattering to absorption cross-section for large nanoparticles should maximize SERS intensity. Since EGFR is engulfed by the cell through endocytosis, we expect that this will be captured by our snapshot Raman images. The low scattering to absorption cross-section of the small nanoparticles is ideal for the destruction of the cancer using thermal heating effects. This yields a simple and effective way to map EGFR over-expression and destroy cancers.



7577-03, Session 1

Shape-dependent effect of surface-enhanced Raman scattering on gold nanostructured arrays

H. Lin, C. Huang, C. Chang, Y. Lan, H. Chui, National Cheng Kung Univ. (Taiwan)

Surface-enhanced Raman scattering (SERS) on gold nanostructured arrays with precisely controlled size, spacing and shape fabricated via focused ion beam was investigated. The nanostructured arrays with the maintained edge-to-edge distance, size, but nanodisk shapes of rod, circle, triangle, and those inverted nanoholes were individually excited by 632- and 785-nm lasers. Results demonstrate that three distinct nanodisk and nanohole structures exhibit strong SERS signals at 632-nm excitation, but only triangular nanoholes present obvious SERS signals at 785-nm excitation. The collected normal incidence transmission spectrum of three nanohole structures shows the wavelength range extends to longer wavelengths as compared with that of three nanodisk structures. The most effective enhancement of SERS signal is presented in the triangular nanoholes, due to the possession of multi-mode surface plasmon resonance, leading to the resonance wavelength extends to the near-infrared regime. The broadband wavelength of localized surface plasmon resonance and the empty space confined by the triangular nanoholes suggest promise for the application of being a functional component in biosensing, Raman spectroscopy, and photonic devices.

7577-04, Session 2

Functionalized nanoparticles for measurement of biomarkers using a SERS nanochannel platform

M. E. Benford, M. Wang, J. Kameoka, G. Cote, Texas A&M Univ. (United States)

The overall goal of this research is to develop a new point-of-care system for early detection and characterization of cardiac markers to aid in diagnosis of acute coronary syndrome. The envisioned final technology platform incorporates functionalized gold colloidal nanoparticles trapped at the entrance to a nanofluidic device providing a robust means for analyte detection at trace levels using surface enhanced Raman spectroscopy (SERS). To discriminate a specific biomarker, we designed an assay format analogous to a competitive ELISA. Notably, the biomarker would be captured by an antibody and in turn displace a peptide fragment, containing the binding epitope of the antibody labeled with a Raman reporter molecule that would not interfere with blood serum proteins. To demonstrate the feasibility of this approach, we used C-reactive protein (CRP) as a surrogate biomarker. We functionalized agarose beads with anti-CRP that were placed outside the nanochannel, then added either Rhodamine-6-G (R6G) labeled-CRP and gold (as a surrogate of a sample without analyte present), or R6G labeled CRP, gold, and unlabeled CRP (as a surrogate of a sample with analyte present). Analyzing the spectra we see an increase in peak intensity in the presence of analyte at characteristic peaks for R6G specifically, 1284 and 1567 cm-1. Further, our results illustrate the reproducibility of the Raman spectra collected for R6G-labeled CRP in the nanochannel. Overall, we believe that this method will provide the advantage of sensitivity and narrow line widths characteristic of SERS as well as the specificity toward the biomarker of interest.

7577-05, Session 2

Polarization selective optical antennas for Raman spectroscopy applications

J. Li, W. Wu, Z. Li, Hewlett-Packard Labs. (United States)

Using plasmonic structures to enhance the Raman scattering has been of constant research interests. In a typical Raman scattering process, a molecule is first excited into a virtual energy state by the local electromagnetic field, then radiates as a dipole source at a frequency that may be relatively low (Stokes scattering) or high (anti-Stokes scattering) compared to the excitation signal. In order to amplify the Raman scattering process, optical antennas are often designed to maximize the local electromagnetic field where the molecules reside. Ideally, such an antenna should also resonant at both the incident (the excitation) and the radiation (the scattered) frequency of a Raman process. Depend on the frequency shift of the specific molecular vibration modes, it may be difficult to achieve such properties with a single optical antenna.

In this paper we show a design of optical antenna system for Raman spectroscopy applications that makes use of not only the field enhancement capability, but also the polarization selective property of an optical antenna. Two linear antennas of perpendicular polarizations are crossed to each other with a common hot spot area, and are designed to resonant at different frequencies. Incident excitation of only certain polarization is enhanced by the system, and the Raman scattering of either Stokes or anti-Stokes type will be greatly enhanced. The radiated Raman signal is at the polarization perpendicular to that of the incidence. We believe such a polarization selective device can be of great interest in various applications beyond Raman spectroscopy.

7577-06, Session 2

Large-area plasmonics-active SERS substrates for chem-bio detection

A. Dhawan, H. Wang, Duke Univ. (United States); Y. Du, North Carolina State Univ. (United States); M. D. Gerhold, U.S. Army Research Office (United States); V. Misra, North Carolina State Univ. (United States); T. Vo-Dinh, Duke Univ. (United States)

No abstract available.

7577-07, Session 3

High sensitivity of SPR with microplasmonic structures

J. Masson, L. S. Live, Univ. de Montréal (Canada)

Plasmonic microstructures such as triangles and holes exhibit high sensitivity with a Kretschmann SPR instrument to refractive index and formation of a monolayer. Triangles of sizes ranging from 200 nm to 1.8 µm were prepared using nanosphere lithography (NSL). Each Au triangle displays characteristic LSPR properties in transmission spectroscopy. Excitation of the smallest triangles (200-300 nm edge length) with Kretschmann SPR results in no response. However, larger triangle exhibits two absorption peaks and a transmission maximum. These peaks were attributed to SPR on microstructures, as verified with the positive response from Au and Ag triangles and the null response from TiOxNy and Ag2O triangles. Sensitivity of these triangles is between 1000 and 2000 nm/RI depending on physical parameters and formation of a monolayer results in a SPR response 5 times greater than for SPR on a thin film. Nano and microhole arrays were also prepared with NSL with periodicities of 650 nm to 3 µm. SPR excitation of the nano and microhole arrays resulted in a spectra composed of a superposition of the SPR response for microtriangles and for thin films. With increasing periodicity, the transition from a short range propagating SPR mode to propagating SPR has been mapped. This provides a complete structure/optical properties study for the size range between LSPR and



propagating SPR. Construction of a biosensor with these structures will also be presented. Thus, improved plasmonic materials for SPR sensing could be emerging from micron scale structures.

7577-08, Session 3

Quantitative analysis of calcification in MC3T3-e1 cells using surface plasmon resonance sensor

S. A. Kim, Seoul National Univ. (Korea, Republic of); K. M. Byun, Kyung Hee Univ. (Korea, Republic of); S. J. Kim, Seoul National Univ. (Korea, Republic of)

Many investigations have been attempted to promote calcification as applications to orthopedic and dental implants. To date, several methods have been developed with an aim of controlling the calcification via extracellular matrix of osteoblast cells. However, there has been no efficient quantitative analysis technique that measures the calcification in real-time without any labeling process. In this study, a simplified and improved surface plasmon resonance (SPR) biosensor is proposed for an accurate quantified measure of calcification in MC3T3-e1 cells. We implement an optimized SPR system for calcification via osteogenesis of the cells so that calcified volume could be detected rapidly. To facilitate the calcified velocity, we used biphasic electrical stimulation. We controlled two stimulation parameters of duration and starting time in order to optimize a stimulation condition in calcification. In the electrical stimulation, the resonance angle shift induced by calcification is greater than that of control group. The amount of calcification is sufficient to induce the dose-dependent SPR angle shift and the shift of SPR angle shows a more subtle change than the results of conventional analysis techniques, such as staining or cell counting. This study reveals that SPR detection is an accurate and effective way for the application to calcification measure and we believe that the developed SPR biosensor is feasible in other clinical areas based on surface reactions.

7577-09. Session 3

The detection of small organic molecules based on a novel functionalized surface plasmon resonance sensor

R. Zheng, B. D. Cameron, Univ. of Toledo (United States)

The development of rapid, inexpensive, and accurate in vivo detection of small organic molecules, such as theophylline, glucose and caffeine, would be very beneficial for a variety of applications. For example, the detection of theophylline can be used as a probe for cytochrome P450 (CYP450) enzyme activity which is very important for characterizing drug-metabolizing phenotypes. Current techniques used to assess CYP450 activity involve complex solid phase extraction and liquid chromatography/mass spectrometry, which are time consuming and expensive. In this study, two types of specific and sensitive functionalized surface plasmon resonance (SPR) sensors which are coupled with planar SPR (PSPR) and localized SPR(LSPR) are developed for theophylline. Although SPR by itself is a quick, convenient, and label-free technique, it is neither selective nor sensitive for detection of low concentration and molecular weight compounds. These problems can be simultaneously addressed by combining the sensing area with an appropriate molecular imprinted polymer (MIP) as a receptor. Results will be presented demonstrating the ability of the developed sensor to effectively detect theophylline at low concentrations in the presence of other confounding components, such as, caffeine which has a very similar chemical structure.

7577-10, Session 3

The ITO-based circular polarization interferometer via fault tolerance algorithm for surface plasmon biosensor

C. Jan, Y. Lee, C. Lee, National Taiwan Univ. (Taiwan)

The newly developed surface plasmon based instrument utilized the scheme of circular polarization interferometry, which combined P-S common beam, to pursue bio-molecule detection. The instrument named "OBMorph" includes a light source, a powerful variation incident angle scheme with parabolic and spherical mirrors, and sample stage utilizing the prism coupling. The sensitivity is restricted by optimal incident angle, so we use precise step-motor with 0.12406 um per count and parabolic mirror to control incident angle accurately from 18° to 78°. Compared with mechanical arm, it is possible to apply personal medical device while the system volume would be reduced in our scheme. OBMorph allows mapping of thin film over the sensing area, with information available at 633nm. By use of faulty tolerance algorithm, the imperfect adjustment of circular polarization interferometer is eliminated to obtain its higher resolution 4.92×10-6 RIU. A few studies have been made on the refractive index change of ITO thin film by applying varied voltages. We design a ITO thin film on chip to change different surface plasmon resonance angle shift and extend wide dynamic range for phase interrogation via tunable characteristics of refractive index of dielectric materials. The OBMorph covers the diversity of thin film applications, in the fields of flat panel displays, optical coating, and drug delivery. We successfully measured CRP and anti-CRP specific interaction. In addition, the concentrations of tuberculosis inhibitor - DHFR and compound Mg2P4O7 that can interact with CYP450 are quantified successfully.

7577-11, Session 3

Development of plasmonic substrates for surface plasmon resonance imaging

A. Dhawan, Duke Univ. (United States); M. T. Canva, Lab. Charles Fabry (France); H. Wang, T. Vo-Dinh, Duke Univ. (United States)

7577-12, Session 4

No abstract available.

Surface plasmon effects induced by uncollimated emission of semiconductor microstructures

D. Lepage, J. J. Dubowski, Univ. de Sherbrooke (Canada)

The inherent surface sensitivity of the surface plasmon resonance (SPR) effect has made it highly attractive for biochemical analysis of processes localized on metal surfaces. Many devices have been developed commercially for that purpose within the past 20 years. However, a monolithically integrated SPR microchip, which could be easily integrated with specimen processing hardware for a wholly automated analysis, has yet to be demonstrated. We have recently proposed an innovative microstructure for a monolithically integrated SPR device comprising a metal coated SiO2 layer deposited atop a photoluminescence emitting quantum well (QW) wafer. The functioning of such a device is based on the uncollimated and incoherent emission of semiconductors. Therefore, any given point of the metal-dielectric interface is exposed to the whole range of wavevector spectra and thus, coupling of all the SPR modes supported by the architecture is expected to take place. We discuss the results of our calculations and measurements aimed at the description of SPs coupling in QW semiconductor-based SPR architectures designed for biosensing applications. Dispersion (kll) maps (angular frequency versus in-plane wavevector) of the analytical far-field dispersion relation for the investigated microstructure are studied using hyperspectral



luminescence mapping. These maps determine experimentally the spectro-angular properties of studied SPR systems. Two SPs modes could be coupled in the 0th diffraction order where the injected in-plane wavevectors from the QW structures can always meet SPR conditions. This results in increasing the SPs coupling efficiency up to 100 times higher than in case of indirect SPs injection.

7577-14, Session 4

Integrated chip-level surface plasmon resonance biochemical sensors using patterned metallic nanostructures

J. Guo, H. Leong, Y. Lin, R. Lindquist, The Univ. of Alabama in Huntsville (United States); J. Wei, CFD Research Corp. (United States); D. J. Brady, Duke Univ. (United States)

Periodic metallic nanostructures such as nanohole and nano-dot arrays exhibit localized surface plasmon resonance (SPR) phenomena, which has been widely investigated for biological and chemical sensing applications. The principle of localized surface plasmon sensors is that the plasmon resonance frequency shifts when target biochemical agents bind to the near surface of the metallic nanostructures. The frequency shift is measured by a separate spectrometer. The current sensing platform is difficult to integrate in chip-level devices. Using e-beam lithography, we created super-periodic microscopic patterns of metallic nanostructures. Surface plasmon resonance sensing and resonance frequency resolving can be integrated on the single sensor chip. In this talk, we will present the design, fabrication and the results of an integrated chip-level SPR biochemical sensor.

7577-15, Session 4

Surface plasmon resonance in effective nanostructured metal films

H. Leong, J. Guo, R. Lindquist, The Univ. of Alabama in Huntsville (United States); Q. H. Liu, Duke Univ. (United States)

We investigated the surface plasmon resonances in deep subwavelength nanostructured metal films at the Kretschmann configuration. The deep subwavelength nanostructured metal films can be thought as an effective metal films with different optical property. We calculated the reflectance, transmittance, and absorption for varying dielectric fill factor, metal film thickness, as well as the period of the nanostructure. We found that enhanced surface plasmon resonance and electromagnetic field can be achieved by using the nanostructured metal films. The introduction of nanostructure in the metal film provides a freedom in controlling the material property and the surface plasmon resonance, which can help to make high sensitivity biological and chemical sensors.

7577-16, Session 4

Miniature surface plasmon resonance fiber biosensor for in vitro diagnostics

Y. Y. Shevchenko, T. Francis, M. Dakka, M. C. DeRosa, J. Albert, Carleton Univ. (Canada)

SPR sensors implemented in optical fibers are preferred over other sensor designs because it is possible to design a very compact label-free sensor that is also capable of remote sensing and sensing in small closed volumes. The SPR sensor presented here employs a single mode fiber that allows monitoring biomolecular interactions occurring on the surface of the cladding in aqueous solutions at sub-µM concentrations.

Excitation of SPR on the surface of the fiber is made possible by using a Tilted Fiber Bragg Grating (TFBG), which acts as a coupling element to excite a set of cladding modes; each of those excited modes probes

the gold coated surface of the fiber for SPR resonances1. The use of the TFBG instead of other types of fiber coupling mechanisms (such as Fiber Bragg Grating and Long Period Grating) provides the sensor with a wide operating range allowing work in solutions with various refractive indexes.

The experimental results indicate that the sensor can be used for characterizing the formation of self-assembled monolayer of short DNA sequences on the surface of the gold coating as well as their hybridization with complementary DNA strands. Short DNA sequences used in those tests (aptamers) were synthesized to selectively bind to molecules of alpha-thrombin protein. The sensor is able to distinguish the attachment of protein at various concentrations as small as several hundreds of nM. Attachment of biomolecules is confirmed with fluorescence confocal imaging and AFM.

7577-17, Session 4

Novel CMOS modulated light cameras for sensitive surface plasmon resonance imaging

N. S. Johnston, R. Light, Univ. of Nottingham (United Kingdom); C. Stewart, Univ. of Exeter (United Kingdom); M. Somekh, M. Pitter, Univ. of Nottingham (United Kingdom)

Novel complimentary metal oxide semiconductor (CMOS) cameras that can measure the phase and amplitude of periodically modulated optic signals have been developed. The cameras use a modified active pixel architecture incorporating four independent wells in each pixel, and a phase stepping algorithm is applied to demodulate the four acquired intensities. By integrating the wells into each pixel, the camera can obtain four synchronous images in less than one microsecond. In addition, supplementary capacitance results in a much greater well depth which reduces the effect of optical shot noise. These features allow parallel lock-in imaging without the need for mechanical scanning at 256 x 256 pixel resolution and modulation frequencies of greater than one MHz.

Differential phase surface plasmon resonance (DP-SPR) is a very sensitive interrogation technique for detecting tiny changes in refractive index, for example, corresponding to binding of molecules to a sensor surface. Polarization modulation and lock-in detection are used in DP-SPR to achieve extremely high refractive index sensitivity, but lock-in acquisition has previously limited the technique to point and two-channel measurements. However in conjunction with the modulated cameras described above, spatially resolved SPR imaging has been achieved with sensitivities of better than 10 microRIU per pixel per second. This allows the possibility of label-free multi-analyte array reading and functional imaging of live cells. Results demonstrating the performance of modulated light cameras for DP-SPR imaging and high resolution SPR imaging microscopy are presented and discussed.

7577-18, Session 4

Biosensing with surface plasmon resonance polarimetry

S. V. Patskovsky III, A. Blanchard-Dionne, L. Guyot, M. Maisonneuve, O. D. Kelly, M. Meunier, Ecole Polytechnique de Montréal (Canada)

Providing more information and higher sensitivity, optical phase sensitive biosensing schemes are now the focus of intensive research as a promising tool to upgrade the performance of conventional intensity-sensitive biosensing technologies. In Surface Plasmon Resonance (SPR) polarimetry, phase difference between s- and p- polarized light, combined with their amplitude, could provide a detection limit up to two orders of magnitude lower compared to the conventional SPR technique, while providing a sufficient dynamic range. We have performed the theoretical calculation and experimental tests to obtain the optimal spectral, angular and metal film parameters that provide high sensitivity and reproducibility of the biosensing results. We propose a polarimetric system based on a sinusoidal temporal phase modulation of s- and p- polarized beam components by using a photoelastic modulation and



a synchronous detection of the reflected light. Using different signal harmonics and optimizing initial phase retardance and modulation amplitude, we can enhance signal-to-noise ratio in phase measurements and improve phase-sensitive sensor dynamic range.

To further enhance the sensing response, significant research efforts are currently undertaken on the excitation of propagating and/or localized surface plasmons through the interaction of light with nanofabricated plasmonic structures. Here we propose to use the phase of the light reflected or refracted by the nanoplasmonic structure at different angles and wavelengths as the transducer principle in label-free gas and biosensing. Polarization state and phase characteristics of light at the resonance conditions for excitation of surface plasmons are very sensitive to changes in the interfacial refractive index and could be used as an efficient sensing parameter.

Applications of SPR polarimetry scheme for the planar, micro and nanofabricated plasmonic structures in different interrogation schemes and sensing geometry for the detection of proteins and drugs are considered.

7577-19, Session 5

Nanoapertures to enhance single molecule fluorescence detection

H. Aouani, J. Wenger, Institut Fresnel, CNRS, Univ. Aix-Marseille (France); D. Gérard, Institut Charles Delaunay, Univ. de Technologie Troyes (France); H. Rigneault, Institut Fresnel, CNRS, Univ. Aix-Marseille (France); E. Devaux, T. Ebbesen, Institut de Science et d'Ingénierie Supramoléculaires, CNRS, Univ. Louis Pasteur (France); S. Blair, The Univ. of Utah (United States)

Plasmonic nanostructures offers new opportunities for controlling the emission of single emitters. Especially, a subwavelength aperture milled in a metallic film can significantly increase the fluorescence emission rate of molecule diffusing inside of them. This phenomenon stems from the electromagnetic field enhancement inside the aperture but also from modifications of the emission properties of the molecule. Thanks to these devices, fast enzymatic cleavage reaction at micromolar concentrations can be efficiently monitored with integration times less than one second. We also discuss the design of the optimum nanoaperture structures to enhance the fluorescence emission of single molecules. These investigations include the aperture diameter, the nature of the metal used, the influence of the supplementary adhesion layer used to maintain contact between the metal and the glass substrate, and lastly the shape of the aperture. We show that the nanoapertures are very sensitive to the nature of the adhesion layer (permittivity and thickness) and we demonstrate the largest enhancement factor reported to date (x25) by using a TiO2 adhesion layer. Clearly, one has to consider the role of the adhesion layer while designing plasmonic structures for high-efficiency single-molecule analysis. Last, we compare the properties of different aperture shapes: circular, rectangular, triangular and co-axial. For the specific application of plasmonic-enhanced FCS, we show that circular apertures are the design to be preferred.

7577-20. Session 5

Metal-enhanced intrinsic fluorescence of proteins and label-free bioassays

K. Ray, H. Szmacinski, M. H. Chowdhury, J. R. Lakowicz, Univ. of Maryland School of Medicine (United States)

Most of the applications of fluorescence require the use of labeled drugs and labeled biomolecules. Due to the need of labeling biomolecules with extrinsic fluorophores, there is a rapidly growing interest in methods which provide label-free detection (LFD). Proteins are highly fluorescent, which is due primarily to tryptophan residues. However, since most proteins contain tryptophan, this emission is not specific for proteins of interest in a biological sample. This is one of the reasons of not

utilizing intrinsic tryptophan emission from proteins to detect specific proteins. Here, we present the intrinsic fluorescence for several proteins bound to the silver or aluminum metal nanostructured surfaces. We demonstrate the metal enhanced fluorescence (MEF) of proteins with different numbers of tryptophan residues. Large increases in fluorescence intensity and decreases in lifetime provide the means of direct detection of bound protein without separation from the unbound. We present specific detection of individual types of proteins and measure the binding kinetics of proteins such as IgG and streptavidin. Additionally, specific detection of IgG and streptavidin has been accomplished in the presence of large concentrations of other proteins in sample solutions. These results will allow design of surface-based assays with biorecognitive layer that specifically bind the protein of interest and thus enhance its intrinsic fluorescence. The present study demonstrates the occurrence of MEF in the UV region and thus opens new possibilities to study tryptophancontaining proteins without labeling with longer wavelength fluorophores and provides an approach to label-free detection of biomolecules.

7577-21, Session 5

Numerical and experimental study of fluorescence enhancement and quenching with SiO2 encapsulated metallic nanospheres and nanorods

J. B. Zhang, L. Chen, Q. Q. Teo, National Univ. of Singapore (Singapore); J. Y. Sze, A*STAR Data Storage Institute (Singapore); B. Lukiyanchuk, National Univ. of Singapore (Singapore)

A combination comprising of an excitation light and one or more fluorophore molecules (fluo-molecules) in the vicinity of one metallic NP is a complicated system. Numerical modeling for each individual system is desired for optimization of NP's size and shape. As only limited publications have addressed the physical origins of one NP and one fluo-molecule system, there is large room for further in-depth study on individual fluo-molecules-laser-NPs systems.

We will first present an analytical study of the interaction between one metallic nanosphere/nanorod and one fluo-molecule which is initially approximated as a point dipole, followed by FDTD modeling of such a system with two orientations for a fluo-molecule dipole close to a nanosphere, and five orientation-position geometries for a fluo-molecule close to a nanorod. The FDTD simulation is performed on the trends of the radiative decay rate and the quantum yield of fluo-molecules versus SiO2 shell thickness, which functions to prevent energy from direct transfer from fluo-molecules to NPs. Next, we will present the chemical fabrication processes and results for controlling the SiO2 shell thickness from 6 nm to 50 nm and the aspect ratio of Au nanorods from 1.7 to 3.3. We will also describe our efforts on SiO2 encapsulation of nanorods, where positvely charged rod surface has to be converted to negatively charged surface. The test results of Metal-Enhanced Fluorescence (MEF) and fluorescence quenching with Au and Ag colloids are demonstrated with some protein-dye conjugates and pure fluorophores such as BSA-Rhodamine B, BSA-FITC and CY3.

7577-22, Session 5

FRET enhancement in multilayer core-shell nanoparticles

M. Lessard-Viger, M. Rioux, L. Rainville, D. Boudreau, Univ. Laval (Canada)

Förster resonance energy transfer (FRET) is a powerful tool used in several fields of science. However, its usefulness is sometimes hindered by the limited photostability of current fluorophores and by the limited range over which this intermolecular energy transfer process can occur. Interestingly, the efficiency and range of FRET can be significantly increased by placing the donor-acceptor pairs in proximity to metal nanoparticles and exploiting the phenomenon called metal-enhanced



fluorescence, which affects the emission of nearby fluorophores by enhancing excitation and emission rates, and improves FRET efficiency by increasing the strength of donor-acceptor interactions.

In this work, we synthesized, using a versatile, simple and reproducible procedure, multilayer core-shell nanoparticles (NP) featuring a metal core surrounded by concentric silica layers containing fluorophores positioned at precise distances from the core. This controlled geometry allows us to study the role of plasmon resonance on fluorescence and FRET. Our experiments revealed that the luminosity and photostability of the fluorophores in these nanocomposites are increased several-fold by the presence of the metal core, and it shows that the range and efficiency of FRET is increased in these multilayer core-shell fluorescent NPs. Given these enviable characteristics, these composite NPs could therefore provide increased detectability, range and efficiency of FRET in a variety of applications such as ultrasensitive DNA detection, long exposure FRET imaging studies, and the study of long-range extracellular protein-protein, cell-protein and cell-cell interactions.

Viger et al. Nano Letters, ASAP july 15 2009.

7577-23, Session 5

ICG fluorescence enhancement by layer-bylayer assembly of polyelectrolytes between ICG molecules and gold nanorods

Y. Chen, X. Li, Johns Hopkins Univ. (United States)

Near infrared (NIR) fluorescence imaging has emerged as a new modality for deep tissue molecular imaging. Biocompatible, stable and high quantum yield fluorescent contract agents are the integral part of the NIR fluorescence imaging technology, in particular for in vivo applications. This paper reports a promising and convenient approach to enhance the fluorescence yield of NIR fluorescent dyes by using metal nanoparticles as "nanoantenna" and by controlling the distance between the dye molecules and nanoparticles. Indocyanine green (ICG), the only NIR fluorescent dye approved by FDA for routine clinical use, is chosen for this study, aiming to improve the relatively low quantum yield of ICG which is ~0.016 in solution. Gold nanorods of a dimension ~48±3 nm (length) and ~15±2 nm (diameter) are used as the nanoantenna and their surface are coated with layer-by-layer assembly of PSS/PAH polyelectrolytes. The number of layers can be accurately controlled during the assembly process to reach a desired coating thickness. ICG molecules are then absorbed to the outer surface of the coating through electrostatic interaction. Our experimental results show a ~9-fold of fluorescence yield enhancement can be achieved for ICG when ICG molecules are spaced by ~8 nm from the surface of gold nanorods. Furthermore, our results reveal that the presence of gold nanorods also dramatically improves the fluorescence stability of ICG in addition to the fluorescence yield enhancement.

7577-24. Session 5

The use of aluminum nanostructures as platforms for metal enhanced fluorescence of the intrinsic emission of biomolecules in the ultra-violet

M. H. Chowdhury, K. Ray, Univ. of Maryland School of Medicine (United States); S. K. Gray, Argonne National Lab, (United States); J. Pond, Lumerical Solutions Inc. (Canada); J. R. Lakowicz, Univ. of Maryland School of Medicine (United States)

Fluorescence today is one of the most widely used technologies in biomedical sciences where the target biomolecules are ususally tagged with external fluorescent probes that emit in the visible. This is because the intrinsic emission of biomolecules occur in the ultra-violet (UV) where there are problems associated with high background and expensive optical components. A major disadvantage of externally tagging

biomolecules is that it requires chemical modification and washing steps which are cumbersome and can potentially perturb the native functionality of biomolecules. In this study we use the finite-difference time-domain (FDTD) method to predict that aluminum nanoparticles can be used as efficient substrates for metal-enhanced fluorescence in the UV region for the label free detection of biomolecules. Our calculations focus on the fluorophore emission in the range of 300-420 nm which is typical of the intrinsic biomolecule emission. We show that fluorophores next to aluminum nanoparticles display strongly enhanced emission which is dependent on the nanoparticle size, fluorophore-nanoparticle spacing, fluorophore orientation and the presence of dimers. We also examine the effect of the incident excitation and excited fluorophores on the near-fields around the nanoparticles. Finally we present experimental evidence showing that a thin film of amino acids show significant emission enhancements in close proximity to aluminum nanostructures. Our results suggest that the interaction of aluminum nanostructures with biomolecules can be exploited to device numerous strategies for the label free detection of biomolecules.

7577-25, Session 6

Plasmon resonance gold nanoparticles for improving optical diagnostics and photothermal therapy of tumor

E. V. Zagainova, M. A. Sirotkina, M. V. Shirmanova, V. Elagin, Nizhny Novgorod State Medical Academy (Russian Federation); M. Kirillin, P. Agrba, V. Kamensky, Institute of Applied Physics, RAS (Russian Federation); V. Nadtochenko, N.N. Semenov Institute of Chemical Physics, RAS (Russian Federation)

There are quite a number of problems of nanoparticles assisted diagnostics and treatment that have not been solved yet. These include noninvasive control of nanoparticles accumulation in tumor, targeting these agents to the lesion, their influence on biological objects, control of tumor inner temperature during hyperthermia, and others.

In our investigations we considered different types of gold nanoparticles with plasmon resonance in the near infrared spectrum: bipyramids, rods, branches, shells with different biocompatible coatings such as polyethilenglycol and chitosan.

Optical coherence tomography (OCT) and optical diffuse tomography (ODT) were used for in vivo imaging and control of nanoparticles accumulation in tumor, crafted in mice. Lasers with different wavelengths (810-1500 nm) were employed for photothermolysis of tumor lesions. Temperature increase during photothermolysis was controlled by means of a standard thermograph and an original setup comprising two acoustic thermometers.

Accumulation of gold nanoparticles in tumors was traced by means of OCT and ODT. OCT images at maximum accumulation of nanoparticles in tumors demonstrated increasing signal intensity and visualization of some internal tumor structures. ODT revealed accumulation of gold nanoparticles deep in tumors in case of passive delivery, as well as in case of targeting of these agents by specific tumor antibodies. When gold nanoparticle-antibody conjugates were used, ODT detected longer accumulation (up to 4 days) of this structure in tumor tissue.

Laser hyperthermia of tumor was three times faster when gold nanoparticles were used and laser power was to be decreased to maintain the temperature near 43-45 Co .

Plasmon resonance gold nanoparticles with unique optical properties in the near infrared can be successfully used as contrast agents for optical bioimaging and as thermosensitizers for guided photothermolysis.



7577-26, Session 6

Sub-wavelength plasmonic readout for direct linear analysis of optically tagged DNA

J. J. Bernstein, The Charles Stark Draper Lab., Inc. (United States); J. Varsanik, Massachusetts Institute of Technology (United States) and The Charles Stark Draper Lab., Inc. (United States); W. Teynor, J. LeBlanc, H. A. Clark, The Charles Stark Draper Lab., Inc. (United States); J. R. Krogmeier, U.S. Genomics (United States); T. Yang, K. Crozier, Harvard Univ. (United States)

This work describes the development and fabrication of a novel nanofluidic flow-through sensing chip that utilizes a plasmonic resonator to excite fluorescent tags with sub-wavelength resolution. We cover the design of the microfluidic chip and simulation of the plasmonic resonator using Finite Difference Time Domain (FDTD) software. The fabrication methods are presented, with testing procedures and preliminary results.

This research is aimed at improving the resolution limits of the Direct Linear Analysis (DLA) technique developed by US Genomics [1]. In DLA, intercalating dyes which tag a specific 8 base-pair sequence are inserted in a DNA sample. This sample is pumped though a channel, where it is stretched into a linear geometry and interrogated with laser light which excites the fluorescent tags. The resulting sequence of optical pulses produces a characteristic "fingerprint" of the sample which uniquely identifies any sample of DNA. Plasmonic confinement of light to a 100 nm wide metallic nano-stripe enables resolution of a higher tag density compared to free space optics.

Nanofluidic chips were fabricated using BK7 glass wafers and cover slips. Optical waveguides were diffused using an ion-exchange process. Plasmonic resonators were fabricated using e-beam lithography and metal liftoff, followed by anodic bonding, dicing, edge polishing and fiber attach.

Prototype devices have been fabricated and are being tested with tagged DNA. Preliminary results show evanescent coupling to the plasmonic resonator is occurring with high resolution, but that light scattering limits the S/N of the detector. Methods to reduce scattering, currently being implemented, are discussed.

7577-27, Session 6

Cell membrane imaging using time-resolved surface plasmon-mediated fluorescence microscopy

K. Balaa, Ecole Supérieure de Physique et de Chimie Industrielles (France); V. Devauges, CNRS, Unv. Paris-Sud 11 (France); S. Lévêque-Fort, CNRS, Univ. Paris-Sud 11 (France); E. Fort, Ecole Supérieure de Physique et de Chimie Industrielles (France)

Surface Plasmon-Mediated Fluorescence Microscopy (SPMFM) is a new imaging technique which takes the advantage of surface plasmon (SP) properties of a metallic thinfilm to selectively excite and detect fluorophores in a restricted specimen region immediately adjacent to the metallic/sample interface. This technique is particularly suitable for cell membrane imaging. SP mediated excitation and emission provide many advantages over other competing techniques. When compared to standard TIRF microscopy, the molecular detection efficiency is enhanced and the confinement is increased. Besides, the additional distance dependant emission filter resulting from the near-field coupling of the fluorophore emission to the SP, provides an enhanced signal to noise ratio. In cell imaging, it limits the background noise resulting from the scattering effect of the excitation light by the sample.

The presence of the metallic surface in the vicinity of the fluorophores induces modifications of the fluorescence lifetime. The coupling to the metallic surface provides additional relaxation processes which decrease the fluorescence lifetime by several orders of magnitude. These variations depend strongly on the fluorophore/metal distance d and on the molecular orientation of the emission dipole in the range d<200

nm. Since the orientation of the fluorophores can be controlled in the membrane, it is thus possible to use this dependence to image, with a nanometric axial-resolution, the local topography of cell membranes.

We will present results on live cell membrane topography using time resolved SPMFM. In particular, we will show that membranes undergo strong local deformation during exocytosis events.

7577-28, Session 6

Plasmon resonant gold-coated liposomes for spectrally controlled content release

S. J. Leung, M. Romanowski, The Univ. of Arizona (United States)

We recently demonstrated that liposome-supported plasmon resonant gold nanoshells are degradable into components of a size compatible with renal clearance, potentially enabling their use as multifunctional agents in applications in nanomedicine, including imaging, diagnostics, therapy, and drug delivery (Troutman et al., Adv. Mater. 2008, 20, 2604-2608). These liposomes can be used to encapsulate substances, including therapeutic and diagnostic agents. Laser light illumination causes gold-coated, thermosensitive liposomes with a plasmon resonance band matching the laser wavelength to rapidly release their encapsulated substances. Alternatively, gold-coated liposomes with a resonance band not corresponding to the laser wavelength exhibit minimal content release. In this work, we seek to optimize conditions for controlled release to produce rapid release with minimal energy input. The present research demonstrates that such photothermal release of encapsulated agents from gold-coated liposomes depends on the pulse width of the illuminating laser, with the most efficient release (i.e., highest release per cumulative energy) obtained for pulse widths in the single microsecond range. These observations are discussed in the context of the theory of thermal confinement (Jacques, Appl. Opt. 1993, 32(3), 2447-2454). By adjusting the pulse width, the zone of thermal changes can be restricted to the size of thermosensitive, gold-coated liposome, resulting in a lower energy required for liposome content release and less global heating. Spatial control of heating is especially important in drug delivery applications, to help achieve spatial and spectral control of delivery and minimize thermal damage to tissue.

7577-29, Session 6

Photodynamic activity of gold nanorods on human erythrocytes

P. G. Gananathan, S. Ganesan, P. Aruna, Anna Univ. (India)

The conventional organic photosensitisers are having absorption at wavlenths lesser than 700 nm and has limitation in their penetration. In this context, photosensitisers with NIR absorption is of current interest for effective Photodynamic therapy (PDT), in particular for treating deep seated tumours. In the present study, Au nanorods were synthesized at various sizes to have absorption ranging from 680 to 900nm and they were characterised by UV-Visible absorption spectrometry. The spectra of Au Nanorods have two peaks correspond to Transverse Surface Plasmon Resonance (TSPR) and Longitudinal Surface Plasmon Resonance (LSPR). The primary peak at 530 corresponds to TSPR and the secondary peak varies with respect to size of nanorod ranging from 680-900nm. This secondary peaks may be due to LSPR. This confirms the formation of nanorods and size dependant characteristics. The stability of rods were also studied as the function of pH. At pH above seven, it is found that the nanorods are highly stable, confirming the potential of using them for PDT applications. The Photodynamic Activity (PDA) of Au Nanorods was also carried out in human erythrocytes. The nature of PDA was also analysed using different scavengers. The details of results will be discussed



7577-30, Session 7

Polarization effect of coupled gold nanorods and their use for contrast mechanism

K. B. Mehta, N. Chen, National Univ. of Singapore (Singapore)

Light interaction with metal nano-particles changes the property of the incident light in several unique ways, detection of them can be used to generate contrast in biomedical imaging. Enhancement of the scattering and absorption cross-section due to Plasmon resonance in metallic structure has been widely used for the contrast mechanisms in several imaging modalities. Depolarization effects from asymmetrical particles have also been tried in polarization sensitive microscopy as a contrast agent. Various shapes of the nano-particles have been studied to understand their scattering properties. With the advancement in the nanofabrication technology, it is now possible to fabricate novel nanometalic structures. In this work, we have studied various polarization effects by coupled nano-rod structure, which can be used to get the contrast in polarization sensitive microscopy. We have used the finite difference time domain (FDTD) method to study the polarization effects.

7577-31, Session 7

Optical characterization for nearly spherical gold colloidals via their polarization response

B. Al-Qadi, T. Saiki, Keio Univ. (Japan)

Polarization anisotropy is investigated for colloidal gold nanoparticles with different aspect ratios using polarized light scattering. Our model is a dilute suspension of gold nanoparticles with typical dimension of 50nm ~100nm illuminated with a laser light wavelength of 532nm. The scattered light was split into two orthogonal components having similar intensities. When an isotropic particle comes into the observation volume, the difference between both components is minimal while it becomes noticeable when the particle has some sort of anisotropy.

By monitoring the time-trace of polarized scattering from a particle, the maximum value of the particle's anisotropy can be detected due to its rotational diffusion in the observation volume. We could observe rotational dynamics of the particle as a fluctuation in the measured anisotropy time-trace.

Analytically, each particle was modeled as a prolate spheroid, for which we calculated the maximum anisotropy, aspect ratio, and rotational dynamics based on the data obtained from the transmission electron microscope (TEM) images. Quantitative determination of the particle anisotropy permits precise determination of their geometrical properties in excellent agreement with TEM measurements.

The high contrast, photochemical stability and high biocompatibility make polarized scattering as an alternative to fluorescence and can be utilized in an ultrasensitive molecular sensing applications such as bioconjugated nanoparticle probes. Nanoparticle anisotropy causes a fluctuation in both scattering intensity and polarization and this is a crucial point in biosensing applications which raise the necessity to study the optical anisotropy of nanoparticles.

7577-32, Session 7

Second harmonic generation enhancement in isolated metal nano-apertures

S. Brasselet, P. Schoen, N. Bonod, Institut Fresnel, CNRS, Univ. de St. Jérôme (France); T. Ebbesen, Lab. des Nanostructures, Univ. Louis Pasteur (France): J. Wenger, H. Rigneault, Institut Fresnel, CNRS, Univ. de St. Jérôme (France)

Metallic nano-apertures are able to create sub-wavelength electric fields localization, which leads to a considerable sensitivity improvement of single molecules and biomolecules detection, such as already

demonstrated in Fluorescence Correlation Spectroscopy. Two-photon optical processes are expected to be even further enhanced in such structures, due to the nonlinear nature of the excitation. In this work, we investigate the capacity of gold nano-apertures to enhance two-photon processes using Second Harmonic Generation (SHG) as a probe. SHG is a two-photon excitation process highly sensitive to the local structure of the investigated object. In the present case SHG originates from the asymmetry at the interface between the metal and its surrounding medium. The polarization dependence of SHG is moreover a sensitive reporter of the local structure of the object down to the nanometric scale. We have developed a polarization-sensitive SHG microscopy technique to investigate the local field spatial repartition and magnitude in metallic nano-apertures. We show that while volumic field enhancement can be probed by fluorescence detection, SHG is able to report local surface field enhancements in such structures. We demonstrate SHG enhancement in non-centrosymmetric triangular apertures, as well as in circular centrosymmetric nano-aperture, with a significant size dependence between 80nm and 400nm sizes. The observed effects are supported by numerical calculations that account for the structure geometry and the microscopy optical fields focusing. This study demonstrates the potential of such nano-apertures as nonlinear nanosources which characteristics can be ultimately controlled to probe twophoton processes down to the single molecule level.

7577-33, Session 7

Extraction of complex refractive index dispersion from SPR data

M. Nakkach, M. Julien, M. Canva, Institut d'Optique (France)

Surface Plasmon Resonance (SPR) is a boundary wave propagating at the interface between a metallic and a dielectric layer. Recently SPR technique was used to study absorbing mediums, but under monochromatic light only. In this communication we present an angular and spectral SPR sensor. A white light illuminates the sensor and the reflectivity spectrum in TE and TM polarization is measured with a spectrometer. By changing the coupling conditions, a complete reflectivity surface R(,) can be measured, allowing the determination of the variation of the complex refractive index of the dielectric layer in the visible range. The resonant wavelength absorbed by the dielectric medium is observed through a valley in the reflected spectrum. According to the Kramers-Kronig relations, the refractive index imaginary part of an absorbing medium is proportional to the absorption while the real part presents a large dispersion around the absorption wavelength. In this work we reconstruct the whole complex refractive index of a dye above the gold surface, with an absorption band around 630 nm, from the SPR reflectivity experimental data. The reflectivity surface R(,) was measured from 580 nm to 700 nm. To extract the refractive index of the dyee, we have developed a program based on extended Rouard method to fit the experimental angular plasmon data for each wavelength. These results show that the classical SPR technique can be extended to acquire precise spectral information about biomolecular interactions occurring on the metallic layer.

7577-34, Session 7

Aperiodic photonic-plasmonic structures for radiative rate enhancement and biosensing

S. V. Boriskina, C. Forestiere, G. Walsh, A. Gopinath, B. M. Reinhard, L. Dal Negro, Boston Univ. (United States)

Based on the generalized Mie theory and the coupled-dipole simulations, we demonstrate how subtle interplay between diffractive and nearfield coupling in metal nanoparticle arrays with deterministic aperiodic morphologies can be used to achieve broadband light scattering [1], enhancement [2] and localization [2,3]. Our simulations predict that control of diffraction coupling and multiple scattering in aperiodic plasmonic arrays offers the way to increase the hot-spots intensities by scaling the array size, thus providing larger electric field enhancement



with respect to nanoparticle dimers and periodic structures [2]. We also show that performance of plasmonic arrays can be further optimized by tuning the radii and shapes of individual nanoparticles [2,3]. We have exploited the ability of aperiodic plasmonic arrays to generate highly localized intense hot-spots in the design of robust and efficient substrates for Surface Enhanced Raman Scattering, and measured spatially-averaged reproducible 107 SERS enhancement factors using pMA (para-mercaptoaniline) as Raman marker [2]. We also discuss potential use of intense localized electromagnetic fields in aperiodic plasmonic structures for the enhancement of the efficiency of light emission from low-quantum yield systems such as fluorescent molecules, silicon quantum dots and erbium doped silicon structures. Finally, photonic-plasmonic array morphology can be engineered to provide focusing in sub-wavelength hot spots at several pre-defined wavelengths paving the way for the design of multi-wavelength broadband plasmonic nano-antennas.

- [1]. A. Gopinath, et al, Nano Lett. 8, 2423, 2008.
- [2]. A. Gopinath, et al, Opt. Express, 17, 3741, 2009.
- [3]. C. Forestiere, et al, Opt. Express, 17, 9648, 2009.

7577-35, Session 8

Experimental and numerical analysis of extraordinary optical transmission through nano-hole arrays in a thick metal film

M. Najiminaini, Simon Fraser Univ. (Canada); F. F. Vasefi, Simon Fraser Univ. (Canada) and Lawson Health Research Institute (Canada); J. Carson, Lawson Health Research Institute (Canada) and Univ. of Western Ontario (Canada); B. Kaminska, Simon Fraser Univ. (Canada)

Extraordinary Optical Transmission (EOT) through nano-hole arrays constructed from thick metal films may provide a means to enhance the detection performance of fluorescence optical microscopy. To enhance detection performance, the optical properties related to EOT of the nano-hole array such as wavelength, transmission, and spectral bandwidth need to be matched and optimized to the emission characteristics of the fluorophore. In the case of nano-hole arrays, the process of matching and optimization can be accomplished by adjusting the geometrical parameters of the nano-hole array and dielectric constants of the metal film and the dielectric substrate.

In this paper, we present experimental and numerical analysis on EOT through various nano-hole arrays constructed from a thick metal film within the visible spectrum of light. Various large nano-hole arrays with different designs and geometrical parameters (hole shape, hole periodicity, and dielectric and metal thickness) were fabricated using Electron Beam Lithography (EBL). In EBL, the fabrication parameters (such as beam current and dose area) must be determined for each nano-hole array with respect to its geometrical design parameters. The optical transmission properties (wavelength, peak, and spectral bandwidth of transmission resonances) of the fabricated nano-hole arrays were characterized by using a microscope equipped with a photometer, monochromator, and a PMT detector. The optical transmission results were validated by numerical analysis based on Finite Difference Time Domain (FDTD). Finally, the experimental and numerical results were analyzed to determine the dependencies and discrepancies between EOT properties for various nano-hole arrays.

7577-36, Session 8

Thermal analysis of gold nanostructures heated by pulsed laser irradiation

D. S. Eversole, S. Haering, The Univ. of Texas at Austin (United States); O. Ekici, Turkish Aerospace Industries (Turkey); R. Harrison, N. Durr, A. Ben-Yakar, The Univ. of Texas at Austin (United States)

We present a two-temperature computational module including thermal interference conductance to study the heating processes of gold nanostructures in aqueous medium by femtosecond laser pulses. The peak fluences necessary for particle melting and bubble formation in the surrounding liquid, characteristic time scales of the system, the effect of multiple laser pulses, and orientational dependence of anisotopic particle energy absorption are studied.

We studied the heating properties of two fundamental shapes to biological applications (48 x 14 nm rod and 50 nm sphere) upon irradiation by 250 fs, 760 nm laser light. For rods, results show that the water temperature at the surface of a particle reaches 90% of its critical value with the application of a single fs laser pulse having 9.2 J m^(-2) peak fluence and the particle reaches the melt temperature of 1337 K at a peak fluence of 10.2 J m^(-2) when the laser polarization and nanorod axis are parallel. Nanorod melting requires approximately two orders of magnitude less fluence than is necessary with spherical particles. For both shapes, multiple pulse irradiation at 80 MHz resulted in negligible temperature increases of only a few Kelvins, which bodes well for multiphoton imaging, since particles will not accumulate heat during imaging. Additionally, it was found that the heating properties of anisotropic particle shapes were strongly dependent upon their orientation with respect to the incident laser polarization. The melting fluence is found to increase by almost three orders of magnitude from nanorods aligned along the polarization to those aligned perpendicularly.

7577-38, Session 8

Combined AFM and multiphoton luminescence imaging of single gold nanoparticles

M. Ruosch, D. Marti, J. Ricka, M. Frenz, Univ. Bern (Switzerland)

Gold nanoparticles have gained importance in life science, especially as contrast agents for tracking and biomedical imaging, since they offer interesting plasmonic and luminescence properties. Gold nanoparticles can be conjugated to molecules, cells or proteins and feature a high multiphoton luminescence cross section. Due to this nonlinear excitation process, the luminescence only occurs in the focal spot of a tightly focused femtosecond laser enabling a 3-dimensional localization. The multiphoton luminescence signal of gold nanoparticles has been believed to be photostable, a crucial condition for 3-d tracking. However, we recently found that upon strong femtosecond laser irradiation gold nanoparticles can suffer from temporal fluctuations in the multiphoton luminescence signal namely by blinking, bleaching and "switching on". Bleaching is observed for any incident laser irradiance. In contrast, blinking is only observed when exceeding a threshold of 800 GW/cm2. Furthermore initially non-luminescent particles could be "switched on" by increasing the incident laser irradiance. The same particles then exhibited luminescence even at lower irradiance, suggesting laser induced permanent changes in terms of the particle structure. By combining AFM and multiphoton luminescence imaging of single gold nanoparticles we visualize how the particles change upon laser irradiation. We present a study on how the structural changes depend on the incident laser irradiance and how the particle morphology correlates with the exhibited temporal fluctuations in the multiphoton luminescence signal.

7577-39, Session 8

Biodegradable Polymer/Inorganic Nanoclusters for NIR Imaging

J. O. Tam, J. M. Tam, A. Murthy, D. Ingram, L. L. Ma, K. A. Travis, K. P. Johnston, K. V. Sokolov, The Univ. of Texas at Austin (United States)

No abstract available.